

These are unabridged paperback reprints of established titles  
widely used by universities and colleges throughout the world.

Prentice Hall International publishes these lower-priced  
editions for the benefit of students.

This edition may be sold only in those countries  
in which it is consigned by Prentice Hall  
International. It is not to be re-exported, and is  
not for sale in the U.S.A., Mexico, or Canada.

ISBN 0-13-599028-9



9 780135 990285

90000

DIGITAL AND ANALOG  
COMMUNICATION SYSTEMS

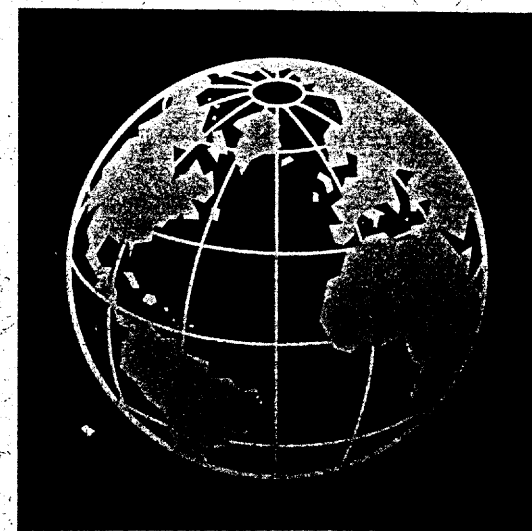
FIFTH  
EDITION

PHIPI



PRENTICE  
HALL

# DIGITAL AND ANALOG COMMUNICATION SYSTEMS



LEON W. COUCH III

Prentice Hall International Editions

Fifth Edition

---

# DIGITAL AND ANALOG COMMUNICATION SYSTEMS

**LEON W. COUCH II**

*Professor of Electrical and Computer Engineering  
University of Florida, Gainesville*



PRENTICE-HALL INTERNATIONAL, INC.

# Abbreviations

ac	alternating current	LO	local oscillator
ADC	analog-to-digital conversion	LOS	line of sight
ADM	adaptive delta modulation	LPF	low-pass filter
AM	amplitude modulation	LSSB	lower single sideband
ANSI	American National Standards Institute	MAP	maximum a posteriori (criterion)
APLL	analog phase-locked loop	MPSK	<i>M</i> -ary phase shift keying
ASCII	American Standard Code for Information Interchange	MQAM	<i>M</i> -ary quadrature amplitude modulation
ATM	Asynchronous transfer mode	MSK	minimum-shift keying
AT&T	American Telephone and Telegraph	NBFM	narrowband frequency modulation
AWGN	additive white Gaussian noise	NCS	National Communications System of the federal government
BER	bit error rate	NRZ	nonreturn-to-zero
BISYNC	binary synchronous communication protocol	OOK	on-off keying
BPSK	binary phase shift keying	OQPSK	offset quadrature phase shift keying
CATV	cable antenna television system	OSI	open system interconnection protocol model
CCITT	Consultative Committee for International Telephone and Telegraph	PAM	pulse amplitude modulation
CDMA	code-division multiple access	PCM	pulse code modulation
CFT	continuous Fourier transform	PD	phase detection
CMOS	complementary metal oxide conductor	PDF	probability density function
CO	central telephone office	PEP	peak envelope power
CRT	cathode ray tube	PLL	phase-locked loop
dB	decibel	PM	phase modulation
dc	direct current	PPM	pulse position modulation
DCE	data communications equipment	PSD	power spectral density
DFT	discrete Fourier transform	PSK	phase shift keying
DM	delta modulation	PTM	pulse time modulation
DPCM	differential pulse code modulation	PWM	pulse width modulation
DSB-SC	double-sideband suppressed carrier	QAM	quadrature amplitude modulation
DTE	data terminal equipment	QPSK	quadrature phase shift
EIRP	effective isotropic radiated power	rms	root-mean-square
EIA	Electronics Industries Association	RT	remote telephone terminal
ERP	effective radiated power	RZ	return-to-zero
FCC	Federal Communications Commission (United States)	SAW	surface acoustics wave
FDM	frequency-division multiplexing	SDLC	synchronous data link control protocol
FET	field effect transistor	S/N or SNR	signal-to-noise ratio
FFT	fast Fourier transform	SS	spread spectrum (system)
FM	frequency modulation	SSB	single sideband
FSK	frequency shift keying	TDM	time-division multiplexing
HDLC	high-level data link control protocol	TDMA	time-division multiplex access
HDTV	high-definition television	TELCO	telephone company
HF	high frequency	THD	total harmonic distortion
IEEE	Institute of Electrical and Electronics Engineers	TTL	transistor transistor logic
IF	intermediate frequency	TV	television
IMD	intermodulation distortion	TVRO	TV receive only terminal
ISDN	integrated service digital network	TWT	traveling-wave tube
ISI	intersymbol interference	UHF	ultra high frequency
ISO	International Organization for Standardization	USSB	upper single sideband
ITU	International Telecommunications Union of the United Nations	VCO	voltage-controlled oscillator
LED	light-emitting diode	VF	voice frequency
		VHF	very high frequency
		VSB	vestigial sideband
		WBFM	wideband frequency modulation

---

# CONTENTS

PREFACE	xvii
LIST OF SYMBOLS	xxi
1 INTRODUCTION	1
1-1 Historical Perspective	2
1-2 Digital and Analog Sources and Systems	2
1-3 Deterministic and Random Waveforms	6
1-4 Organization of This Book	6
1-5 Use of a Personal Computer and MATLAB	7
1-6 Block Diagram of a Communication System	8

1-7	Frequency Allocations	9
1-8	Propagation of Electromagnetic Waves	10
1-9	Information Measure	16
	<i>Example 1-1 Evaluation of Information and Entropy,</i>	17
1-10	Channel Capacity and Ideal Communication Systems	18
1-11	Coding	19
	<i>Block Codes,</i>	21
	<i>Convolutional Codes,</i>	21
	<i>Code Interleaving,</i>	23
	<i>Code Performance,</i>	24
	<i>Trellis-Coded Modulation,</i>	27
1-12	Preview	30
1-13	Study-aid Examples	30
	Problems	31

**2 SIGNALS AND SPECTRA**

33

2-1	Properties of Signals and Noise	33
	<i>Physically Realizable Waveforms,</i>	34
	<i>Time Average Operator,</i>	35
	<i>Dc Value,</i>	36
	<i>Power,</i>	37
	<i>Example 2-1 Evaluation of Power,</i>	38
	<i>Rms Value and Normalized Power,</i>	39
	<i>Energy and Power Waveforms,</i>	40
	<i>Decibel,</i>	40
	<i>Phasors,</i>	42
2-2	Fourier Transform and Spectra	43
	<i>Definition,</i>	43
	<i>Example 2-2 Spectrum of an Exponential Pulse,</i>	45
	<i>Properties of Fourier Transforms,</i>	46
	<i>Parseval's Theorem and Energy Spectral Density,</i>	47
	<i>Example 2-3 Spectrum of a Damped Sinusoid,</i>	49
	<i>Dirac Delta Function and Unit Step Function,</i>	50
	<i>Example 2-4 Spectrum of a Sinusoid,</i>	52
	<i>Rectangular and Triangular-Pulses,</i>	54
	<i>Example 2-5 Spectrum of a Rectangular Pulse,</i>	54
	<i>Example 2-6 Spectrum of a Triangular Pulse,</i>	57
	<i>Convolution,</i>	58
	<i>Example 2-7 Convolution of a Rectangle with an Exponential,</i>	58
	<i>Example 2-8 Spectrum of a Triangular Pulse by Convolution,</i>	59
	<i>Example 2-9 Spectrum of a Switched Sinusoid,</i>	60

2-3	Power Spectral Density and Autocorrelation Function	62
	<i>Power Spectral Density,</i>	62
	<i>Autocorrelation Function,</i>	63
	<i>Example 2-10 PSD of a Sinusoid,</i>	63
2-4	Orthogonal Series Representation of Signals and Noise	65
	<i>Orthogonal Functions,</i>	65
	<i>Example 2-11 Orthogonal Complex Exponential Functions,</i>	66
	<i>Orthogonal Series,</i>	66
2-5	Fourier Series	68
	<i>Complex Fourier Series,</i>	68
	<i>Quadrature Fourier Series,</i>	70
	<i>Polar Fourier Series,</i>	71
	<i>Line Spectra for Periodic Waveforms,</i>	73
	<i>Example 2-12 Fourier Coefficients for a Rectangular Wave,</i>	75
	<i>Power Spectral Density for Periodic Waveforms,</i>	76
	<i>Example 2-13 PSD for a Square Wave,</i>	77
2-6	Review of Linear Systems	78
	<i>Linear Time-Invariant Systems,</i>	78
	<i>Impulse Response,</i>	79
	<i>Transfer Function,</i>	79
	<i>Example 2-14 RC Low-Pass Filter,</i>	81
	<i>Distortionless Transmission,</i>	83
	<i>Example 2-15 Distortion Caused by a Filter,</i>	83
2-7	Bandlimited Signals and Noise	84
	<i>Bandlimited Waveforms,</i>	86
	<i>Sampling Theorem,</i>	86
	<i>Impulse Sampling,</i>	89
	<i>Dimensionality Theorem,</i>	92
2-8	Discrete Fourier Transform	93
	<i>Using the DFT to Compute the Continuous Fourier Transform,</i>	94
	<i>Example 2-16 DFT for a Rectangular Pulse,</i>	97
	<i>Using the DFT to Compute the Fourier Series,</i>	100
	<i>Example 2-17 Use the DFT to Compute the Spectrum of a Sinusoid,</i>	100
2-9	Bandwidth of Signals	101
	<i>Example 2-18 Bandwidths for a BPSK Signal,</i>	105
2-10	Summary	109
2-11	Study-Aid Examples	110
	Problems	113

**BASEBAND PULSE AND DIGITAL SIGNALING**

- 3-1 Introduction 127
- 3-2 Pulse Amplitude Modulation 128  
*Natural Sampling (Gating), 129*  
*Instantaneous Sampling (Flat-Top PAM), 133*
- 3-3 Pulse Code Modulation 136  
*Sampling, Quantizing, and Encoding, 137*  
*Practical PCM Circuits, 140*  
*Bandwidth of PCM, 141*  
*Effects of Noise, 143*  
**Example 3-1 Design of a PCM System, 145**  
*Nonuniform Quantizing:  $\mu$ -Law and A-Law Companding, 146*
- 3-4 Digital Signaling 148  
*Vector Representation, 150*  
**Example 3-2 Vector Representation of a Binary Signal, 151**  
*Bandwidth Estimation, 151*  
*Binary Signaling, 152*  
**Example 3-3 Binary Signaling, 153**  
*Multilevel Signaling, 154*  
**Example 3-4  $L = 4$  Multilevel Signal, 155**
- 3-5 Line Codes and Spectra 157  
*Binary Line Coding, 157*  
*Power Spectra for Binary Line Codes, 159*  
*Differential Coding, 166*  
*Eye Patterns, 167*  
*Regenerative Repeaters, 168*  
*Bit Synchronization, 170*  
*Power Spectra for Multilevel Signals, 173*  
*Spectral Efficiency, 175*
- 3-6 Intersymbol Interference 176  
*Nyquist's First Method (Zero ISI), 179*  
*Raised Cosine-Rolloff Filtering, 180*  
**Example 3-1 (continued), 182**  
*Nyquist's Second and Third Methods for Control of ISI, 184*
- 3-7 Differential Pulse Code Modulation 185
- 3-8 Delta Modulation 189  
*Granular Noise and Slope Overload Noise, 190*  
**Example 3-5 Design of a DM System, 191**  
*Adaptive Delta Modulation and Continuously Variable Slope Delta Modulation, 193*  
*Speech Coding, 194*

**Contents**

127

**Contents**

- 3-9 Time-Division Multiplexing 196  
*Frame Synchronization, 196*  
*Synchronous and Asynchronous Lines, 200*  
**Example 3-6 Design of a Time-Division Multiplexer, 201**  
*TDM Hierarchy, 203*  
*The T1 PCM System, 205*
- 3-10 Pulse Time Modulation: Pulse Width Modulation and Pulse Position Modulation 209
- 3-11 Summary 210
- 3-12 Study-Aid Examples 214  
 Problems 217

**4 BANDPASS SIGNALING PRINCIPLES AND CIRCUITS**

- 4-1 Complex Envelope Representation of Bandpass Waveforms 226  
*Definitions: Baseband, Bandpass, and Modulation, 227*  
*Complex Envelope Representation, 228*
- 4-2 Representation of Modulated Signals 229
- 4-3 Spectrum of Bandpass Signals 230
- 4-4 Evaluation of Power 233  
**Example 4-1 Amplitude-Modulated Signal, 234**
- 4-5 Bandpass Filtering and Linear Distortion 236  
*Equivalent Low-Pass Filter, 236*  
*Linear Distortion, 238*
- 4-6 Bandpass Sampling Theorem 240
- 4-7 Received Signal Plus Noise 241
- 4-8 Classification of Filters and Amplifiers 242  
*Filters, 242*  
*Amplifiers, 246*
- 4-9 Nonlinear Distortion 247
- 4-10 Limiters 252
- 4-11 Mixers, Up Converters, and Down Converters 253
- 4-12 Frequency Multipliers 259
- 4-13 Detector Circuits 261  
*Envelope Detector, 261*  
*Product Detector, 262*  
*Frequency Modulation Detector, 264*

4-14	Phase-Locked Loops and Frequency Synthesizers	269
4-15	Direct Digital Synthesis	276
4-16	Transmitters and Receivers	277
	Generalized Transmitters,	277
	Generalized Receiver: The Superheterodyne Receiver,	279
	<b>Example 4-2</b> AM Broadcast Superheterodyne Receiver,	281
4-17	Summary	283
4-18	Study-Aid Examples	283
	Problems	288

## 5 AM, FM, AND DIGITAL MODULATED SYSTEMS

### Contents

295

### Contents

5-10	Multilevel Modulated Bandpass Signaling	345
	Quadrature Phase-Shift (QPSK) Keying and M-ary Phase-Shift Keying (MPSK),	345
	Quadrature Amplitude Modulation (QAM),	346
	Power Spectral Density for MPSK and QAM,	349
5-11	Minimum-Shift Keying (MSK)	352
5-12	Spread Spectrum Systems	357
	Direct Sequence,	358
	Frequency Hopping,	364
5-13	Summary	366
5-14	Study-Aid Examples	366
	Problems	369

5-1	Amplitude Modulation	296
	<b>Example 5-1</b> Power of an AM Signal,	299
5-2	AM Broadcast Technical Standards	301
5-3	Double-Sideband Suppressed Carrier	302
5-4	Costas Loop and Squaring Loop	303
5-5	Asymmetric Sideband Signals	304
	Single Sideband,	304
	Vestigial Sideband,	308
5-6	Phase Modulation and Frequency Modulation	311
	Representation of PM and FM signals,	311
	Spectra of Angle-Modulated Signals,	315
	<b>Example 5-2</b> Spectrum of a PM or FM Signal with Sinusoidal Modulation,	316
	Narrowband Angle Modulation,	321
	Wideband Frequency Modulation,	322
	<b>Example 5-3</b> Spectrum for WBFM with Triangular Modulation,	323
	Preemphasis and Deemphasis in Angle-Modulated Systems,	325
5-7	Frequency-Division Multiplexing and FM Stereo	326
5-8	FM and Noise Reduction Standards	329
	FM Broadcast Technical Standards,	329
	Dolby and DBX Noise Reduction Systems,	329
5-9	Binary Modulated Bandpass Signaling	332
	On-Off Keying (OOK),	332
	Binary-Phase Shift Keying (BPSK),	336
	Differential Phase-Shift Keying (DPSK),	337
	Frequency-Shift Keying (FSK),	338
	<b>Example 5-4</b> Spectrum of the Bell-Type 103 FSK Modem,	339

## 6 RANDOM PROCESSES AND SPECTRAL ANALYSIS

381

6-1	Some Basic Definitions	382
	Random Processes,	382
	Stationarity and Ergodicity,	383
	<b>Example 6-1</b> First-Order Stationarity,	383
	<b>Example 6-2</b> Ergodic Random Process,	385
	Correlation Functions and Wide-Sense Stationarity,	386
	Complex Random Processes,	390
6-2	Power Spectral Density	391
	Definition,	391
	Wiener-Khintchine Theorem,	392
	Properties of the PSD,	395
	<b>Example 6-3</b> Evaluation of the PSD for a Polar Baseband Signal,	395
	General Formula for the PSD of Digital Signals,	399
	White Noise Processes,	402
	Measurement of PSD,	403
6-3	Dc and Rms Values for Ergodic Random Processes	404
6-4	Linear Systems	406
	Input-Output Relationships,	406
	<b>Example 6-4</b> Output Autocorrelation and PSD for an RC Low-Pass Filter,	409
	<b>Example 6-5</b> Signal-to-Noise Ratio at the Output of an RC Low-Pass Filter,	410
6-5	Bandwidth Measures	411
	Equivalent Bandwidth,	411
	Rms Bandwidth,	411
	<b>Example 6-6</b> Equivalent Bandwidth and Rms Bandwidth for an RC LPF,	413

6-6	The Gaussian Random Process	413
	<i>Properties of Gaussian Processes,</i>	415
	<i>Example 6-7 White Gaussian Noise Process,</i>	417
6-7	Bandpass Processes	418
	<i>Bandpass Representations,</i>	418
	<i>Properties of WSS Bandpass Processes,</i>	421
	<i>Example 6-8 Spectra for the Quadrature Components of White Bandpass Noise,</i>	424
	<i>Example 6-9 PSD for a BPSK Signal,</i>	424
	<i>Proofs of Some Properties,</i>	425
	<i>Example 6-10 PDF for the Envelope and Phase Functions of a Gaussian Bandpass Process,</i>	428
6-8	Matched Filters	430
	<i>General Results,</i>	430
	<i>Results for White Noise,</i>	433
	<i>Example 6-11 Integrate-and-Dump (Matched) Filter,</i>	434
	<i>Correlation Processing,</i>	437
	<i>Example 6-12 Matched Filter for Detection of a BPSK Signal,</i>	437
	<i>Transversal Matched Filter,</i>	438
6-9	Summary	441
6-10	Appendix: Proof of Schwarz's Inequality	443
6-11	Study-Aid Examples	446
	Problems	448

## 7 PERFORMANCE OF COMMUNICATION SYSTEMS CORRUPTED BY NOISE

458

7-1	Error Probabilities for Binary Signaling	459
	<i>General Results,</i>	459
	<i>Results for Gaussian Noise,</i>	461
	<i>Results for White Gaussian Noise and Matched-Filter Reception,</i>	463
	<i>Results for Colored Gaussian Noise and Matched-Filter Reception,</i>	464
7-2	Performance of Baseband Binary Systems	465
	<i>Unipolar Signaling,</i>	465
	<i>Polar Signaling,</i>	467
	<i>Bipolar Signaling,</i>	468
7-3	Coherent Detection of Bandpass Binary Signals	470
	<i>On-Off Keying,</i>	470
	<i>Binary-Phase-Shift Keying,</i>	472
	<i>Frequency-Shift Keying,</i>	473
7-4	Noncoherent Detection of Bandpass Binary Signals	476
	<i>On-Off Keying,</i>	477
	<i>Frequency-Shift Keying,</i>	480
	<i>Differential Phase-Shift Keying,</i>	482

7-5	Quadrature Phase-Shift Keying and Minimum-Shift Keying	484
7-6	Comparison of Digital Signaling Systems	487
	<i>Bit Error Rate and Bandwidth,</i>	487
	<i>Synchronization,</i>	489
7-7	Output Signal-to-Noise Ratio for PCM Systems	490
7-8	Output Signal-to-Noise Ratios for Analog Systems	495
	<i>Comparison with Baseband Systems,</i>	496
	<i>AM Systems with Product Detection,</i>	497
	<i>AM Systems with Envelope Detection,</i>	498
	<i>DSB-SC Systems,</i>	499
	<i>SSB Systems,</i>	500
	<i>PM Systems,</i>	501
	<i>FM Systems,</i>	505
	<i>FM Systems with Threshold Extension,</i>	508
	<i>FM Systems with Deemphasis,</i>	509
7-9	Comparison of Analog Signaling Systems	511
	<i>Ideal System Performance,</i>	514
7-10	Summary	515
7-11	Study-Aid Examples	515
	Problems	524

## 8 CASE STUDIES OF COMMUNICATION SYSTEMS

533

8-1	Telecommunication Systems	534
	<i>Time-Division Multiplexing,</i>	534
	<i>Frequency-Division Multiplexing,</i>	534
8-2	Telephone Systems	536
	<i>Historical Basis,</i>	536
	<i>Modern Telephone Systems and Remote Terminals,</i>	536
8-3	Integrated Service Digital Network	543
8-4	Capacities of Public Switched Telephone Networks	547
8-5	Satellite Communication Systems	547
	<i>Digital and Analog Television Transmission,</i>	551
	<i>Data and Telephone Signal Multiple Access,</i>	553
	<i>Example 8-1 Fixed Assigned Multiple-Access Mode Using an FDMA Format,</i>	554
	<i>Example 8-2 SPADE System,</i>	555
	<i>Personal Communications via Satellite,</i>	559
8-6	Link Budget Analysis	560
	<i>Signal Power Received,</i>	561
	<i>Thermal Noise Sources,</i>	563

<i>Characterization of Noise Sources</i> , 564	
<i>Noise Characterization of Linear Devices</i> , 565	
<b>Example 8-3</b> $T_e$ and $F$ for a Transmission Line, 569	
<i>Noise Characterization of Cascaded Linear Devices</i> , 570	
<i>Link Budget Evaluation</i> , 572	
<b><math>E_b/N_0</math> Link Budget for Digital Systems</b> , 574	
<b>Example 8-4</b> <i>Link Budget Evaluation for a Television Receive-Only Terminal for Satellite Signals</i> , 575	
8-7 Fiber Optic Systems 580	
<b>Example 8-5</b> <i>Link Budget for a Fiber Optic System</i> , 581	
8-8 Cellular Telephone Systems 582	
8-9 Television 589	
<i>Black-and-White Television</i> , 589	
<i>MTS Stereo Sound</i> , 596	
<i>Color Television</i> , 596	
<i>Standards for TV and CATV Systems</i> , 601	
<i>HDTV</i> , 605	
8-10 Summary 609	
8-11 Study-Aid Examples 609	
Problems 614	

## APPENDIX A MATHEMATICAL TECHNIQUES, IDENTITIES, AND TABLES

620

A-1 Trigonometry 620	
<i>Definitions</i> , 620	
<i>Trigonometric Identities</i> , 620	
A-2 Differential Calculus 621	
<i>Definition</i> , 621	
<i>Differentiation Rules</i> , 621	
<i>Derivative Table</i> , 622	
A-3 Indeterminate Forms 623	
A-4 Integral Calculus 623	
<i>Definition</i> , 623	
<i>Integration Techniques</i> , 623	
A-5 Integral Tables 623	
<i>Indefinite Integrals</i> , 623	
<i>Definite Integrals</i> , 626	
A-6 Series Expansions 627	
<i>Finite Series</i> , 627	
<i>Infinite Series</i> , 628	

A-7 Hilbert Transform Pairs 629	
A-8 The Dirac Delta Function 629	
<i>Properties of Dirac Delta Function</i> , 630	
A-9 Tabulation of $Sa(x) = (\sin x)/x$ 631	
A-10 Tabulation of $Q(z)$ 632	

## APPENDIX B PROBABILITY AND RANDOM VARIABLES

634

B-1 Introduction 634	
B-2 Sets 635	
B-3 Probability and Relative Frequency 636	
<i>Simple Probability</i> , 636	
<i>Joint Probability</i> , 637	
<b>Example B-1</b> <i>Evaluation of Probabilities</i> , 637	
<b>Example B-1</b> <i>(Continued)</i> , 638	
<i>Conditional Probabilities</i> , 638	
<b>Example B-1</b> <i>(Continued)</i> , 638	
B-4 Random Variables 639	
<b>Example B-2</b> <i>Random Variable</i> , 639	
B-5 Cumulative Distribution Functions and Probability Density Functions 639	
<b>Example B-2</b> <i>(Continued)</i> , 641	
<i>Properties of CDFs and PDFs</i> , 642	
<i>Discrete and Continuous Distributions</i> , 642	
<b>Example B-3</b> <i>A Continuous Distribution</i> , 642	
<b>Example B-3</b> <i>(Continued)</i> , 644	
B-6 Ensemble Average and Moments 646	
<i>Ensemble Average</i> , 646	
<b>Example B-4</b> <i>Evaluation of an Average</i> , 647	
<i>Moments</i> , 647	
B-7 Examples of Important Distributions 649	
<i>Binomial Distribution</i> , 649	
<i>Poisson Distribution</i> , 652	
<i>Uniform Distribution</i> , 652	
<i>Gaussian Distribution</i> , 653	
<i>Sinusoidal Distribution</i> , 657	
B-8 Functional Transformations of Random Variables 658	
<b>Example B-5</b> <i>Sinusoidal Distribution</i> , 659	
<b>Example B-6</b> <i>PDF for the Output of a Diode Characteristic</i> , 660	
B-9 Multivariate Statistics 663	
<i>Multivariate CDFs and PDFs</i> , 663	
<i>Bivariate Statistics</i> , 665	

<i>Gaussian Bivariate Distribution</i> , 666
<i>Multivariate Functional Transformation</i> , 666
<b>Example B-7 PDF for the Sum of Two Random Variables</b> , 667
<i>Central Limit Theorem</i> , 669
<b>Example B-8 PDF for the Sum of Three Independent Uniformly Distributed Random Variables</b> , 669
Problems 670

## APPENDIX C STANDARDS AND TERMINOLOGY FOR COMPUTER COMMUNICATIONS

677

C-1 Codes 677
<i>Baudot</i> , 677
<i>ASCII</i> , 678
C-2 DTE/DCE and Ethernet Interface Standards 678
<i>Current Loop</i> , 680
<i>RS-232C, RS-422A, RS-449, and RS-530 Interfaces</i> , 680
<i>Centronics Parallel Interface</i> , 681
<i>IEEE-488 Interface</i> , 681
<i>Ethernet (IEEE 802.3) Interface</i> , 684
C-3 The ISO OSI Network Model 686
C-4 Data Link Control Protocols 690
<i>BISYNC</i> , 690
<i>SDLC</i> , 690
<i>HDLC</i> , 690
<i>CCITT X.25 Protocol</i> , 691
<i>Asynchronous Transfer Mode (ATM)</i> , 692
C-5 Modem Standards 693
C-6 Brief Computer Communications Glossary 698

## REFERENCES

703

## ANSWERS TO SELECTED PROBLEMS

714

## INDEX

720

## FRONT ENDPAPERS

Abbreviations

## BACK ENDPAPERS

*Fourier Transform Theorems**Fourier Transform Pairs**Q(z) Function*

## PREFACE

Continuing the tradition of the first to fourth editions of this book, this new edition provides the latest up-to-date treatment of digital and analog communication systems. It includes a significant number of new study-aid examples and homework problems, many of which require solutions via a personal computer. It is written as a textbook for junior or senior engineering students and is also appropriate for an introductory graduate course or as a modern technical reference for practicing electrical engineers. It covers *practical aspects* of communication systems developed from a sound *theoretical basis*.

## THE THEORETICAL BASIS

- Representation of digital signals
- Representation of analog signals
- Magnitude and phase spectra
- Fourier analysis
- Modulation theory
- Random variables
- Probability density
- Random processes

- Orthogonal function theory
- Power spectral density
- Linear systems
- Nonlinear systems
- Intersymbol interference
- Calculation of (SNR)
- Calculation of BER
- Optimum systems
- Block codes
- Convolutional codes

## THE PRACTICAL APPLICATIONS

- PAM, PCM, DPCM, DM, PWM, and PPM baseband signaling
- OOK, BPSK, QPSK, MPSK, MSK, and QAM bandpass digital signaling
- AM, DSB-SC, SSB, VSB, PM, and FM bandpass analog signaling
- Time-division multiplexing and the standards used
- Digital line codes and spectra
- Circuits used in communication systems
- Bit synchronizers
- Frame synchronizers
- Carrier synchronizers
- Frequency-division multiplexing and the standards used
- Telecommunication systems
- Telephone systems
- ISDN
- Satellite communication systems
- Effective input-noise temperature and noise figure
- Link budget analysis
- SNR at the output of analog communication systems
- BER for digital communication systems
- Fiber optic systems
- Spread spectrum systems
- Cellular radio telephone systems
- Television systems
- Technical standards for AM, FM, TV, HDTV, and CATV
- Computer communication systems
- Protocols for computer communications
- Technical standards for computer communications
- Math tables
- Study-aid examples
- More than 550 homework problems with selected answers
- More than 60 computer-solution homework problems with solution templates
- Extensive references
- Emphasis on design of communication systems

Many of the equations and homework problems are marked with a personal computer symbol,  , which indicates that there is a MATLAB and MATHCAD solution for this equation or problem on an available floppy disk or via Internet, <http://www.eel.ufl.edu/~lcouc>.

This book is an outgrowth of my teaching of graduate as well as undergraduate communication courses at the University of Florida and is tempered by my experiences as an amateur radio operator (K4GWQ). I believe that the reader does not fully understand the technical material unless he or she has the opportunity to work on problems. Consequently, more than 550 problems have been included. (Personal computer solutions are provided for more than 60 of these problems on a floppy disk.) Some of them are easy, so that the beginning student will not become frustrated, and some are difficult enough to challenge the more advanced students. All the problems are designed to provoke thought about, and understanding of, communication systems.

This book is written to be applicable to many different course structures. Some of these are summarized in the accompanying table.

Course Length	Chapters Covered	Course Title and Comments
<b>Short Courses</b>		
3 days	1, 3 (partially), 7 (partially)	Digital Communications and Coding
3 days	3, 8	Telecommunications
3 days	4, 5	Modulation, Transmitters, and Receivers
3 days	1, 8	Survey of Communication Systems
3 days	Appendix B	Probability and Random Variables
3 days	6	Random Processes
1 day	8	Case Studies of Communication Systems
<b>Undergraduate</b>		
1 term	1, 2 (rapidly), 3–5, 8	Introduction of Digital and Analog Communication Systems (deterministic approach)
1 term	1, Appendix B, 6–8	Noise in Digital and Analog Communication Systems (a course in probability, random variables, random processes, and applications to communication systems)
1 term	1, Appendix B, 3, 6, 7–1 to 7–8	Noise in Digital Communication Systems
1 term	1, 2 (rapidly), 3–5, 7	Digital and Analog Communication Systems (prior course in random processes required)
<b>Two terms</b>	1st term	1, 2 (rapidly), 3–5
	2nd term	Appendix B, 6–8
<b>Graduate</b>		
1 term	1, Appendix B, 6–8	Introduction to Communication Systems (some undergraduate knowledge of communications required)

I appreciate the help of the many persons who contributed to this book and the helpful comments that have been provided by the reviewers, in particular Marvin Siegel, Department of Electrical Engineering, University of Michigan, and J. B. O'Neal, North Carolina State University. I also appreciate the assistance of my colleagues at the University of Florida. I thank my wife, Dr. Margaret Couch, who typed the original and revised manuscripts.

LEON W. COUCH II  
*Gainesville, Florida*  
*lcouch@admin.ee.ufl.edu*

## LIST OF SYMBOLS

There are not enough symbols in the English and Greek alphabets to allow the use of each letter only once. Consequently, some symbols may be used to denote more than one entity, but their use should be clear from the context. Furthermore, the symbols are chosen to be generally the same as those used in the associated mathematical discipline. For example, in the context of complex variables,  $x$  denotes the real part of a complex number (i.e.,  $c = x + jy$ ), whereas in the context of statistics  $x$  might denote a random variable.

### Symbols

$a_n$	a constant
$a_n$	quadrature Fourier series coefficient
$A_c$	level of modulated signal of carrier frequency $f_c$
$A_e$	effective area of an antenna
$b_n$	quadrature Fourier series coefficient
$B$	baseband bandwidth

$B_p$	bandpass filter bandwidth
$B_T$	transmission (bandpass) bandwidth
$c$	a complex number where $c = x + jy$
$c$	a constant
$c_n$	complex Fourier series coefficient
$C$	channel capacity
$C$	capacitance
$^{\circ}\text{C}$	degrees Celsius
$\text{dB}$	decibel
$D$	dimensions/s, symbols/s ( $D = N/T_0$ ), or baud rate
$D_f$	frequency modulation gain constant
$D_n$	polar Fourier series coefficient
$D_p$	phase modulation gain constant
$e$	error
$e$	the natural number, 2.7183
$E$	modulation efficiency
$E$	energy
$\mathcal{E}(f)$	energy spectral density (ESD)
$E_b/N_0$	energy per bit/noise power spectral density ratio
$f$	frequency (Hz)
$f(x)$	probability density function (PDF)
$f_c$	carrier frequency
$f_i$	instantaneous frequency
$f_0$	a (frequency) constant; the fundamental frequency of a periodic waveform
$f_s$	sampling frequency
$F$	noise figure
$F(a)$	cumulative distribution function (CDF)
$g(t)$	complex envelope
$g(t)$	corrupted complex envelope
$G$	power gain
$G(f)$	power transfer function
$h$	Planck's constant, $6.2 \times 10^{-34}$ joule-s
$h(t)$	impulse response of a linear network
$h(x)$	mapping function of $x$ into $h(x)$
$H$	entropy
$H(f)$	transfer function of a linear network
$i$	an integer
$I_j$	information in the $j$ th message
$j$	the imaginary number $\sqrt{-1}$
$j$	an integer
$k$	Boltzmann's constant, $1.38 \times 10^{-23}$ joule/K
$k$	an integer
$k(t)$	complex impulse response of a bandpass network
$K$	number of bits in a binary word that represents a digital message

$K$	degrees Kelvin ( $^{\circ}\text{C} + 273$ )
$l$	an integer
$\ell$	number of bits per dimension or bits per symbol
$L$	inductance
$L$	number of levels permitted
$m$	an integer
$m$	mean value
$m(t)$	message (modulation) waveform
$\tilde{m}(t)$	corrupted (noisy received) message
$M$	an integer
$M$	number of messages permitted
$n$	an integer
$n$	number of bits in message
$n(t)$	noise waveform
$N$	an integer
$N$	number of dimensions used to represent a digital message
$N$	noise power
$N_0$	level of the power spectral density of white noise
$p(t)$	an absolutely time-limited pulse waveform
$p(t)$	instantaneous power
$p(m)$	probability density function of frequency modulation
$P$	average power
$P_e$	probability of bit error
$P(C)$	probability of correct decision
$P(E)$	probability of message error
$\mathcal{P}(f)$	power spectral density (PSD)
$Q(z)$	integral of Gaussian function
$Q(x_k)$	quantized value of the $k$ th sample value, $x_k$
$r(t)$	received signal plus noise
$R$	data rate (bits/s)
$R$	resistance
$R(t)$	real envelope
$R(\tau)$	autocorrelation function
$s(t)$	signal
$\tilde{s}(t)$	corrupted signal
$S/N$	signal power/noise power ratio
$t$	time
$T$	a time interval
$T$	absolute temperature (Kelvin)
$T_b$	bit period
$T_e$	effective input-noise temperature
$T_0$	duration of a transmitted symbol or message
$T_0$	period of a periodic waveform
$T_0$	standard room temperature (290 K)

$T_s$	sampling period
$u_{11}$	covariance
$v(t)$	a voltage waveform
$v(t)$	a bandpass waveform or a bandpass random process
$w(t)$	a waveform
$W(f)$	spectrum (Fourier transform) of $w(t)$
$x$	an input
$x$	a random variable
$x$	real part of a complex function or a complex constant
$x(t)$	a random process
$y$	an output
$y$	an output random variable
$y$	imaginary part of a complex function or a complex constant
$y(t)$	a random process
$\alpha$	a constant
$\beta$	a constant
$\beta_f$	frequency modulation index
$\beta_p$	phase modulation index
$\delta$	step size of delta modulation
$\delta_{ij}$	Kronecker delta function
$\delta(t)$	impulse (Dirac delta function)
$\Delta F$	peak frequency deviation (Hz)
$\Delta\theta$	peak-phase deviation
$\epsilon$	a constant
$\epsilon$	error
$\eta$	spectral efficiency [(bits/sec)/Hz]
$\theta(t)$	phase waveform
$\lambda$	dummy variable of integration
$\lambda$	wavelength
$\Lambda(r)$	likelihood ratio
$\pi$	3.14159
$\rho$	correlation coefficient
$\sigma$	standard deviation
$\tau$	independent variable of autocorrelation function
$\tau$	pulse width
$\varphi_j(t)$	orthogonal function
$\phi_n$	polar Fourier series coefficient
$\omega_c$	radian carrier frequency, $2\pi f_c$
$\equiv$	mathematical equivalence
$\triangleq$	mathematical definition of a symbol

**Defined Functions**

$J_n(\cdot)$	Bessel function of the first kind $n$ th order
$\ln(\cdot)$	natural logarithm

$\log(\cdot)$	base 10 logarithm
$\log_2(\cdot)$	base 2 logarithm
$Q(z)$	integral of a Gaussian probability density function
$\text{Sa}(z)$	$(\sin z)/z$
$u(\cdot)$	unit step function
$\Lambda(\cdot)$	triangle function
$\Pi(\cdot)$	rectangle function

**Operator Notation**

$\text{Im}\{\cdot\}$	imaginary part of
$\text{Re}\{\cdot\}$	real part of
$\overline{[\cdot]}$	ensemble average
$\langle [\cdot] \rangle$	time average
$[\cdot] * [\cdot]$	convolution
$[\cdot]^*$	conjugate
$/[\cdot]$	angle operator or angle itself, see (2-108)
$ [\cdot] $	absolute value
$[\hat{\cdot}]$	Hilbert transform
$\mathcal{F}[\cdot]$	Fourier transform
$\mathcal{L}[\cdot]$	Laplace transform
$[\cdot] \cdot [\cdot]$	dot product

---

## INTRODUCTION

What is a communication system? To put the answer to this question in perspective, it is useful to ask a more fundamental question. What is electrical engineering (EE)? If one poses this question to 50 electrical engineers, one will probably get 50 different answers. However, it is clear that EE is concerned with solving problems of two types:

- Production and transmission of electrical energy
- Transmission of information

Communications systems are systems designed to transmit information.

Many areas within EE are needed to solve communication and electric energy problems. Some examples of these areas are computers, electrical and electronic circuits, electronic devices, digital signal processing, electromagnetics, and photonics.

It is important to realize that communication systems and electric energy systems have distinctly different sets of constraints. In electric energy systems, the waveforms are usually *known*, and one is concerned with designing the system for *minimum energy loss*.

In communication systems, the waveform present at the sink (user) is *unknown* until after it is received—otherwise, no information would be transmitted, and there would be no need for the communication system. More information is communicated to the sink when the user at the sink is “surprised” by the message that was transmitted. That is, the transmission of information implies the communication of messages that are not known ahead of time (*a priori*). Conversely, in energy or power systems, it is known *a priori* what the received waveform will be, and it is the energy imparted by the received waveform that is the desired quantity.

Noise limits our ability to communicate. If there were no noise, we could communicate messages electronically to the outer limits of the universe using an infinitely small amount of power. This has been obvious on an intuitive basis since the early days of radio. However, the theory that describes noise and the effect of noise on the transmission of information was not developed until the 1940s by such persons as D. O. North [1943], S. O. Rice [1944], C. E. Shannon [1948], and N. Wiener [1949].

## 1-1 HISTORICAL PERSPECTIVE

A time chart showing the historical development of communications is given in Table 1-1. The reader is encouraged to spend some time studying this table to obtain an appreciation for the chronology of communications. Note that although the telephone was developed late in the nineteenth century, the first transatlantic telephone cable was not completed until 1954. Previous to this date, transatlantic calls were handled via shortwave radio. Similarly, although the British began television broadcasting in 1936, transatlantic television relay was not possible until 1962 when the *Telstar 1* satellite was placed into orbit. Digital transmission systems—embodied by telegraph systems—were developed in the 1850s before analog systems—the telephone—in the twentieth century.

This book provides technical details for most of the communication inventions listed in the table. For example, pulse code modulation—used for modern digital transmission of telephone voice signals—was invented by Alex Reeves in 1937 and is described in detail in Chapter 3. Superheterodyne receivers and frequency modulated (FM) systems are discussed in Chapters 4 and 5. The effects of noise on communications systems are covered in Chapters 6 and 7. Recent developments in cellular mobile telephone, satellite, and personal communication systems (PCS) are given by case studies in Chapter 8. Computer communication standards are tabulated in Appendix C.

## 1-2 DIGITAL AND ANALOG SOURCES AND SYSTEMS

**DEFINITION.** A *digital information source* produces a finite set of possible messages.

A typewriter is a good example of a digital source. There is a finite number of characters (messages) that can be emitted by this source.

**DEFINITION.** An *analog information source* produces messages that are defined on a continuum.

TABLE 1-1 IMPORTANT DATES IN COMMUNICATIONS

Year	Event
Before 3000 b.c.	Egyptians develop a picture language called <i>hieroglyphics</i> .
A.D. 800	Arabs adopt our present number system from India.
1440	Johannes Gutenberg invents movable metal type.
1752	Benjamin Franklin's kite shows that lightning is electricity.
1827	Georg Simon Ohm formulates his law ( $I = E/R$ ).
1834	Carl F. Gauss and Ernst H. Weber build the electromagnetic telegraph.
1838	William F. Cooke and Sir Charles Wheatstone build the telegraph.
1844	Samuel F. B. Morse demonstrates the Baltimore, MD, and Washington, DC, telegraph line.
1850	Gustav Robert Kirchhoff first publishes his circuit laws.
1858	The first transatlantic cable is laid, and fails after 26 days.
1864	James C. Maxwell predicts electromagnetic radiation.
1871	The Society of Telegraph Engineers is organized in London.
1876	Alexander Graham Bell develops and patents the telephone.
1883	Thomas A. Edison discovers flow of electrons in a vacuum, called the “Edison effect,” the foundation of the electron tube.
1884	The American Institute of Electrical Engineers (AIEE) is formed.
1887	Heinrich Hertz verifies Maxwell's theory.
1889	The Institute of Electrical Engineers (IEE) forms from the Society of Telegraph Engineers in London.
1894	Oliver Lodge demonstrates wireless communication over a distance of 150 yards.
1900	Guglielmo Marconi transmits the first transatlantic wireless signal.
1905	Reginald Fessenden transmits speech and music by radio.
1906	Lee deForest invents the vacuum-tube triode amplifier.
1907	The Society of Wireless Telegraph Engineers is formed in the United States.
1909	The Wireless Institute is established in the United States.
1912	The Institute of Radio Engineers (IRE) is formed in the United States from the Society of Wireless Telegraph Engineers and the Wireless Institute.
1915	Bell System completes a U.S. transcontinental telephone line.
1918	Edwin H. Armstrong invents the superheterodyne receiver circuit.
1920	KDKA, Pittsburgh, PA, begins the first scheduled radio broadcasts.
1920	J. R. Carson applies sampling to communications.
1923	Vladimir K. Zworykin devises the “iconoscope” television pickup tube.
1926	J. L. Baird, England, and C. F. Jenkins, United States, demonstrate television.
1927	The Federal Radio Commission is created in the United States.
1927	Harold Black develops the negative-feedback amplifier at Bell Laboratories.
1928	Philo T. Farnsworth demonstrates the first all-electronic television system.
1931	Teletypewriter service is initiated.
1933	Edwin H. Armstrong invents FM.
1934	The Federal Communication Commission (FCC) is created from the Federal Radio Commission in the United States.
1935	Robert A. Watson-Watt develops the first practical radar.
1936	The British Broadcasting Corporation (BBC) begins the first television broadcasts.

TABLE 1-1 (cont.)

Year	Event
1937	Alex Reeves conceives pulse code modulation (PCM).
1941	John V. Atanasoff invents the computer at Iowa State College.
1941	The FCC authorizes television broadcasting in the United States.
1945	The ENIAC electronic digital computer is developed at the University of Pennsylvania by John W. Mauchly.
1947	Walter H. Brattain, John Bardeen, and William Shockley devise the transistor at Bell Laboratories.
1947	Steve O. Rice develops statistical representation for noise at Bell Laboratories.
1948	Claude E. Shannon publishes his work on information theory.
1950	Time-division multiplexing is applied to telephony.
1950s	Microwave telephone and communication links are developed.
1953	NTSC color television is introduced in the United States.
1953	The first transatlantic telephone cable (36 voice channels) is laid.
1957	First Earth satellite, <i>Sputnik 1</i> , is launched by USSR.
1958	A. L. Schawlow and C. H. Townes publish the principles of the laser.
1958	Jack Kilby of Texas Instruments builds the first germanium integrated circuit (IC).
1958	Robert Noyce of Fairchild produces the first silicon IC.
1961	Stereo FM broadcasts begin in the United States.
1962	The first active satellite, <i>Telstar 1</i> , relays television signals between the United States and Europe.
1963	Bell System introduces the touch-tone phone.
1963	The Institute of Electrical and Electronic Engineers (IEEE) is formed by merger of IRE and AIEE.
1963–66	Error-correction codes and adaptive equalization for high-speed error-free digital communications are developed.
1964	The electronic telephone switching system (No. 1 ESS) is placed into service.
1965	The first commercial communications satellite, <i>Early Bird</i> , is placed into service.
1968	Cable television systems are developed.
1971	Intel Corporation develops the first single-chip microprocessor, the 4004.
1972	Motorola demonstrates the cellular telephone to the FCC.
1976	Personal computers are developed.
1979	64-kb random access memory ushers in the era of very large-scale integrated (VLSI) circuits.
1980	Bell System FT3 fiber optic communication is developed.
1980	Compact disk is developed by Philips and Sony.
1981	IBM PC is introduced.
1982	AT&T agrees to divest its 22 Bell System telephone companies.
1984	Macintosh computer is introduced by Apple.
1985	FAX machines become popular.
1989	"Pocket" cellular telephone is introduced by Motorola.
1990-present	Era of digital signal processing with microprocessors, digital oscilloscopes, digitally tuned receivers, megaflop workstations, spread spectrum systems, integrated service digital networks (ISDNs), digital satellite systems and high-definition television (HDTV).

## Sec. 1-2 Digital and Analog Sources and Systems

A microphone is a good example of an analog source. The output voltage describes the information in the sound, and it is distributed over a continuous range of values.

**DEFINITION.** A *digital communication system* transfers information from a digital source to the sink.

**DEFINITION.** An *analog communication system* transfers information from an analog source to the sink.

Strictly speaking, a *digital waveform* is defined as a function of time that can have only a discrete set of values. If the digital waveform is a binary waveform, only two values are allowed. An *analog waveform* is a function of time that has a continuous range of values.

An electronic *digital communication system* usually has voltages and currents that have digital waveforms; however, it *may* have analog waveforms. For example, the information from a binary source may be transmitted to the sink by using a sine wave of 1000 Hz to represent a binary 1 and a sine wave of 500 Hz to represent a binary 0. Here the digital source information is transmitted to the sink by use of analog waveforms, but this is still called a digital communication system. From this viewpoint, we see that a *digital communication engineer* needs to know how to analyze analog circuits as well as digital circuits.

Digital communication has a number of advantages:

- Relatively inexpensive digital circuits may be used.
- Privacy is preserved by using data encryption.
- Greater dynamic range (the difference between largest and smallest value) is possible.
- Data from voice, video, and data sources may be merged and transmitted over a common digital transmission system.
- In long-distance systems, noise does not accumulate from repeater to repeater.
- Errors in detected data may be small, even when there is a large amount of noise on the received signal.
- Errors may often be corrected by the use of coding.

Digital communication also has disadvantages:

- Generally, more bandwidth is required than that for analog systems.
- Synchronization is required.

The advantages of digital communication systems usually outweigh their disadvantages. Consequently, digital systems are becoming more and more popular.

In this book we emphasize the *theory* of communication systems and the corresponding mathematical concepts because these ideas are basic to the understanding of future as well as present systems. This approach gives the graduate engineer a set of working tools that will be invaluable throughout his or her professional career and will not be hardware dependent. Conversely, we will strive not to get bogged down in mathematical complexity. Optimum analog communication systems are often impossible to obtain, whereas it is possible

to obtain and analyze some optimum digital communication systems without too much difficulty.

*Practical applications* are also of prime importance. These not only provide motivation and ease of understanding of theoretical concepts, but also give the young engineer a working knowledge of communication systems. We think that this approach provides an excellent basis for the development of future communication systems as well as an understanding of present systems.

### 1-3 DETERMINISTIC AND RANDOM WAVEFORMS

In communication systems, we are concerned with two broad classes of waveforms: deterministic and random (or stochastic).

**DEFINITION.** A *deterministic waveform* can be modeled as a completely specified function of time.

For example, if

$$w(t) = A \cos(\omega_0 t + \varphi_0) \quad (1-1)$$

describes a waveform where  $A$ ,  $\omega_0$ , and  $\varphi_0$  are known constants, this waveform is said to be deterministic.

**DEFINITION.** A *random waveform* (or stochastic waveform) cannot be completely specified as a function of time and must be modeled probabilistically.<sup>†</sup>

Here we are faced immediately with a dilemma when analyzing communication systems. We know that the waveforms that represent the source cannot be deterministic. For example, in a digital communication system we might send information corresponding to any one of the letters of the English alphabet. Each letter might be represented by a deterministic waveform, but when we examine the waveform that is emitted from the source, we find that it is a random waveform because we do not know exactly which characters will be transmitted. Consequently, we really need to design the communication system using a random signal waveform, and any noise that is introduced would also be described by a random waveform. This technique requires the use of probability and statistical concepts (covered in Chapters 6 and 7) that make the design and analysis procedure more complicated. Fortunately, if we represent the signal waveform by a "typical" deterministic waveform, we can obtain most, but not all, of the results we are seeking. This is the approach taken in the first part of this book.

### 1-4 ORGANIZATION OF THIS BOOK

Chapters 1 to 5 use a deterministic approach in analyzing communication systems. This approach allows the reader to grasp some important concepts without the complications of sta-

<sup>†</sup>A more complete definition of a random waveform, also called a *random process*, is given in Chapter 6.

tistical analysis. It also allows the reader who is not familiar with statistics to obtain a basic understanding of communication systems. However, the important topic of performance of communication systems in the presence of noise cannot be analyzed without the use of statistics. These topics are covered in Chapters 6 and 7, and Appendix B.<sup>†</sup> Chapter 8 gives practical case studies of communication systems.

This textbook is designed to be reader friendly. To aid the student in problem solving, several study-aid problems with abbreviated solutions are included at the end of each chapter. In addition, the personal computer (PC) is used to solve problems as appropriate.

This book is also useful as a reference source for mathematics (Appendix A), statistics (Appendix B and Chapter 6), computer communication systems (Appendix C), and as a reference listing communication systems standards that have been adopted (Chapters 3, 4, 5, and 8, and Appendix C).

Communications is an exciting area in which to work. There are the traditional areas, such as AM radio, FM stereo, TV, and shortwave (around the world) radio. There are fast-developing areas, such as computer communications, satellite systems, cellular telephone, spread spectrum, personal communication systems (PCSs), high-definition television (HDTV), and intelligent telecommunication networks. These topics and others are covered in this book. The reader is urged to browse through Chapter 8, looking at case-study topics that are of special interest, such as telephone systems.

### 1-5 USE OF A PERSONAL COMPUTER AND MATLAB

The PC is a modern device that helps communication engineers analyze and design communication systems. This textbook is designed so that a PC may be used as a tool to plot waveforms; compute spectra (using the fast Fourier transform); evaluate integrals; and, in general, help the reader to understand, analyze, and design. When one investigates the available software for use with the PC, one is faced with programming in C, Pascal, Basic, or FORTRAN; or one can select a software package that solves a particular class of problems, such as mathematical problems. For use with this textbook, the author has chosen to use MATLAB, which is available in student versions (for Windows and the MAC) at a reasonable price.

PC solutions via MATLAB M files are provided for selected equations and study-aid problems that are marked with a PC (□) symbol. Table 2-3 shows an example of a MATLAB M file. An IBM compatible floppy disk with the MATLAB M files may be obtained by returning the request card that is included at the end of this book. MATHCAD as well as MATLAB files can also be obtained via the Internet. Anonymous file transfer protocol (FTP) to [ftp.eel.ufl.edu/pub/COUCH/5ed](ftp://ftp.eel.ufl.edu/pub/COUCH/5ed). (Additional MATLAB and MATHCAD files for homework problems marked with the □ symbol are made available to the instructor on a floppy disk that is included with the *Solutions Manual*.)

<sup>†</sup>Appendix B covers the topic of probability and random variables, and is a complete chapter in itself. This allows the reader who has not had a course on this topic to learn this material before Chapters 6 and 7 are studied.

## 1-6 BLOCK DIAGRAM OF A COMMUNICATION SYSTEM

Communication systems may be described by the block diagram shown in Fig. 1-1. Regardless of the particular application, all communications systems involve three main subsystems: the *transmitter*, the *channel*, and the *receiver*. Throughout this book, we use the symbols as indicated in this diagram so that the reader will not be confused about where the signals are located in the overall system. The message from the source is represented by the information input waveform  $m(t)$ . The message delivered to the sink is denoted by  $\tilde{m}(t)$ . The  $[ \sim ]$  indicates that the message received may not be the same as that transmitted. That is, the message at the sink,  $\tilde{m}(t)$ , may be corrupted by noise in the channel or there may be other impairments in the system, such as undesired filtering or undesired nonlinearities. The message information may be in analog or digital form, depending on the particular system, and it may represent audio, video, or some other type of information. In multiplexed systems, there may be multiple input and output message sources and sinks. The spectra (or frequencies) of  $m(t)$  and  $\tilde{m}(t)$  are concentrated about  $f = 0$ ; consequently, they are said to be *baseband* signals.

The signal-processing block at the transmitter conditions the source for more efficient transmission. For example, in an analog system, the signal processor may be an analog low-pass filter that is used to restrict the bandwidth of  $m(t)$ . In a hybrid system, the signal processor may be an analog-to-digital converter (ADC). This produces a “digital word” that represents samples of the analog input signal (as described in Chapter 3 in the section on Pulse Code Modulation). In this case, the ADC in the signal processor is providing *source coding* of the input signal. In addition, the signal processor may also add parity bits to the digital word to provide *channel coding* so that error detection and correction can be used by the signal processor in the receiver to reduce or eliminate bit errors that are caused by noise in the channel. The signal at the output of the transmitter signal processor is a baseband signal because it has frequencies concentrated near  $f = 0$ .

The transmitter carrier circuit converts the processed baseband signal into a frequency band that is appropriate for the transmission medium of the channel. For example, if the channel consists of a fiber optic cable, the carrier circuits convert the baseband input (i.e., frequencies near  $f = 0$ ) to light frequencies, and the transmitted signal,  $s(t)$ , is light. If the channel propagates baseband signals, no carrier circuits are needed, and  $s(t)$  can be the output of the processing circuit at the transmitter. Carrier circuits are needed when the transmission channel is located in a band of frequencies around  $f_c$  where  $f_c \gg 0$ . (The subscript denotes “carrier” frequency.) In this case,  $s(t)$  is said to be a *bandpass* because it is designed to have frequencies located in a band about  $f_c$ . For example, an amplitude modulated (AM)

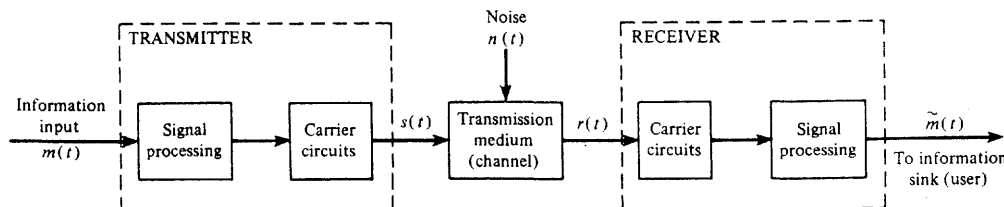


Figure 1-1 Communication system.

broadcasting station with an assigned frequency of 850 kHz has a carrier frequency of  $f_c = 850$  kHz. The mapping of the baseband input information waveform  $m(t)$  into the bandpass signal  $s(t)$  is called *modulation*. [ $m(t)$  is the audio signal in AM broadcasting.] In Chapter 4, it will be shown that any bandpass signal has the form

$$s(t) = R(t) \cos[\omega_c t + \theta(t)] \quad (1-2)$$

where  $\omega_c = 2\pi f_c$ . If  $R(t) = 1$  and  $\theta(t) = 0$ ,  $s(t)$  would be a pure sinusoid of frequency  $f = f_c$  with zero bandwidth. In the modulation process provided by the carrier circuits, the baseband input waveform  $m(t)$  causes  $R(t)$  and/or  $\theta(t)$  to change as a function of  $m(t)$ . These fluctuations in  $R(t)$  and  $\theta(t)$  cause  $s(t)$  to have a nonzero bandwidth that depends on the characteristics of  $m(t)$  and on the mapping functions used to generate  $R(t)$  and  $\theta(t)$ . In Chapter 5, practical examples of both digital and analog bandpass signaling are presented.

Channels may be classified into two categories: hardwire and softwire. Some examples of *hardwire* channels are twisted-pair telephone lines, coaxial cables, waveguides, and fiber optic cables. Some typical *softwire* channels are air, vacuum, and seawater. It should be realized that the general principles of digital and analog modulation apply to all types of channels, although channel characteristics may impose constraints that favor a particular type of signaling. In general, the channel medium attenuates the signal so that the noise level of the channel and/or the noise introduced by an imperfect receiver causes the delivered information  $\tilde{m}$  to be deteriorated from that of the source. The channel noise may arise from natural electrical disturbances (e.g., lightning) or from man-made sources, such as high-voltage transmission lines, ignition systems of cars, or even switching circuits of a nearby digital computer. The channel may contain active amplifying devices, such as repeaters in telephone systems or satellite transponders in space communication systems. These devices are necessary to help keep the signal above the noise level. In addition, the channel may provide *multiple paths* between its input and output that have different time delays and attenuation characteristics. Even worse, these characteristics may vary with time. This variation produces signal fading at the channel output. You have probably observed this type of fading when listening to distant shortwave stations.

The receiver takes the corrupted signal at the channel output and converts it to a baseband signal that can be handled by the receiver baseband processor. The baseband processor “cleans up” this signal and delivers an estimate of the source information  $\tilde{m}(t)$  to the communication system output.

The goal of the engineer is to design communication systems so that the information is transmitted to the sink with as little deterioration as possible while satisfying design constraints, such as allowable transmitted energy, allowable signal bandwidth, and cost. In digital systems, the measure of deterioration is usually taken to be the *probability of bit error* ( $P_e$ )—also called *bit error rate* (BER)—of the delivered data  $\tilde{m}$ . In analog systems, the performance measure is usually taken to be the signal-to-noise ratio at the receiver output.

## 1-7 FREQUENCY ALLOCATIONS

In communication systems that use the atmosphere for the transmission channel, interference and propagation conditions are strongly dependent on the transmission frequency. Theoret-

ically, any type of modulation (e.g., amplitude modulation, frequency modulation, single sideband, phase-shift keying, frequency-shift keying, etc.) could be used at any transmission frequency. However, to provide some semblance of order and for political reasons, government regulations specify the modulation type, bandwidth, and type of information that can be transmitted over designated frequency bands.

On an international basis, frequency assignments and technical standards are set by the International Telecommunications Union (ITU). The ITU is a specialized agency of the United Nations, and the ITU administrative headquarters are located in Geneva, Switzerland, with a staff of 700 persons. This staff is responsible for administering the agreements that have been ratified by the 184 member nations of the ITU. In 1992, the ITU was restructured into three sectors. The Radiocommunication Sector (ITU-R) provides frequency assignments and is concerned with the efficient use of the radio frequency spectrum. The Telecommunications Standardization Section (ITU-T) examines technical, operating, and tariff questions. It recommends worldwide standards for the public telecommunications network (PTN) and related radio systems. The Telecommunication Development Sector (ITU-D) provides technical assistance, especially for developing countries. This encourages a full array of telecommunication services to be economically provided and integrated into the worldwide telecommunication system. Before 1992, the ITU was organized into two main sectors: the International Telegraph and Telephone Consultative Committee (CCITT) and the International Radio Consultative Committee (CCIR).

Each member nation of the ITU retains sovereignty over the spectral usage and standards adopted in its territory. However, each nation is expected to abide by the overall frequency plan and standards that are adopted by the ITU. Usually, each nation establishes an agency that is responsible for administration of the radio frequency assignments within its borders. In the United States, the FCC regulates and licenses radio systems for the general public, and state and local government. In addition, the National Telecommunication and Information Administration (NTIA) is responsible for U.S. government and U.S. military frequency assignments. The international frequency assignments are divided into subbands by the FCC to accommodate 70 categories of services and 9 million transmitters. Table 1-2 gives a general listing of frequency bands, their common designations, typical propagation conditions, and typical services assigned to these bands.

## 1-8 PROPAGATION OF ELECTROMAGNETIC WAVES

The propagation characteristics of electromagnetic waves used in softwire channels are highly dependent on the frequency. This situation is shown in Table 1-2, where users are assigned frequencies that have the appropriate propagation characteristics for the coverage needed. The propagation characteristics are the result of changes in the radio-wave velocity as a function of altitude and boundary conditions. The wave velocity is dependent on air temperature, air density, and levels of air ionization.

Ionization (i.e., free electrons) of the rarified air at high altitudes has a dominant effect on wave propagation in the medium-frequency (MF) and high-frequency (HF) bands. The ionization is caused by ultraviolet radiation from the sun, as well as cosmic rays. Consequently, the amount of ionization is a function of the time of day, season of the year, and

TABLE 1-2 FREQUENCY BANDS

Frequency Band <sup>a</sup>	Designation	Propagation Characteristics	Typical Uses
3–30 kHz	Very low frequency (VLF)	Ground wave; low attenuation day and night; high atmospheric noise level	Long-range navigation; submarine communication
30–300 kHz	Low frequency (LF)	Similar to VLF, slightly less reliable; absorption in daytime	Long-range navigation and marine communication radio beacons
300–3000 kHz	Medium frequency (MF)	Ground wave and night sky wave; attenuation low at night and high in day; atmospheric noise	Maritime radio, direction finding, and AM broadcasting
3–30 Mhz	High frequency (HF)	Ionospheric reflection varies with time of day, season, and frequency; low atmospheric noise at 30 Mhz	Amateur radio; international broadcasting, military communication, long-distance aircraft and ship communication, telephone, telegraph, facsimile
30–300 MHz	Very high frequency (VHF)	Nearly line-of-sight (LOS) propagation, with scattering because of temperature inversions, cosmic noise	VHF television, FM two-way radio, AM aircraft communication, aircraft navigational aids
0.3–3 GHz	Ultra high frequency (UHF)	LOS propagation, cosmic noise	UHF television, cellular telephone, navigational aids, radar, microwave links, personal communication systems
<i>Letter designation</i>			
1.0–2.0	L		
2.0–4.0	S		
3–30 GHz	Super high frequency (SHF)	LOS propagation; rainfall attenuation above 10 GHz, atmospheric attenuation because of oxygen and water vapor, high water vapor absorption at 22.2 GHz	Satellite communication, radar microwave links
<i>Letter designation</i>			
2.0–4.0	S		
4.0–8.0	C		
8.0–12.0	X		
12.0–18.0	Ku		
18.0–27.0	K		
27.0–40.0	Ka		
26.5–40.0	R		

<sup>a</sup> kHz =  $10^3$  Hz; MHz =  $10^6$  Hz; GHz =  $10^9$  Hz.

TABLE 1-2 FREQUENCY BANDS (cont.)

Frequency Band <sup>a</sup>	Designation	Propagation Characteristics	Typical Uses
30–300 GHz	Extremely high frequency (EHF)	Same; high water vapor absorption at 183 GHz and oxygen absorption at 60 and 119 GHz	Radar, satellite, experimental
	<i>Letter designation</i>		
27.0–40.0	Ka		
26.5–40.0	R		
33.0–50.0	Q		
40.0–75.0	V		
75.0–110.0	W		
110–300	mm (millimeter)		
$10^3$ – $10^7$ GHz	Infrared, visible light, and ultraviolet	LOS propagation	Optical communications

<sup>a</sup> kHz =  $10^3$  Hz; MHz =  $10^6$  Hz; GHz =  $10^9$  Hz.

the sun activity (sunspots). This results in several layers of varying ionization density located at various heights surrounding the Earth.

The dominant ionized regions are D, E, F<sub>1</sub>, and F<sub>2</sub> layers. The D layer is located closest to the Earth's surface at an altitude of about 45 or 55 miles. For  $f > 300$  kHz, the D layer acts as a radio-frequency (RF) sponge to absorb (or attenuate) these radio waves. The attenuation is inversely proportional to frequency and becomes small for frequencies above 4 MHz. For  $f < 300$  kHz, the D layer provides refraction (bending) of RF waves. The D layer is most pronounced during the daylight hours, with maximum ionization when the sun is overhead, and almost disappears at night. The E layer has a height of 65 to 75 miles, has maximum ionization around noon (local time), and practically disappears after sunset. It provides reflection of HF frequencies during the daylight hours. The F layer ranges in altitude between 90 and 250 miles. It ionizes rapidly at sunrise, reaches its peak ionization in early afternoon, and decays slowly after sunset. The F region splits into two layers, F<sub>1</sub> and F<sub>2</sub>, during the day and combines into one layer at night. The F region is the most predominant medium in providing reflection of HF waves. As shown in Fig. 1-2, the electromagnetic spectrum may be divided into three broad bands that have one of three dominant propagation characteristics: ground wave, sky wave, and line of sight (LOS).

Ground-wave propagation is illustrated in Fig. 1-2a. It is the dominant mode of propagation for frequencies below 2 MHz. Here the electromagnetic wave tends to follow the contour of the Earth. That is, diffraction of the wave causes it to propagate along the surface of the Earth. This is the propagation mode used in AM broadcasting, where the local coverage follows the Earth's contour, and the signal propagates over the visual horizon. The question is often asked: What is the lowest radio frequency that can be used? The answer is that the value of the lowest useful frequency depends on how long you want to make the antenna. For efficient radiation, the antenna needs to be longer than  $\frac{1}{10}$  of a wavelength. For example, for signaling with a carrier frequency of  $f_c = 10$  kHz, the wavelength is

## Sec. 1-8 Propagation of Electromagnetic Waves

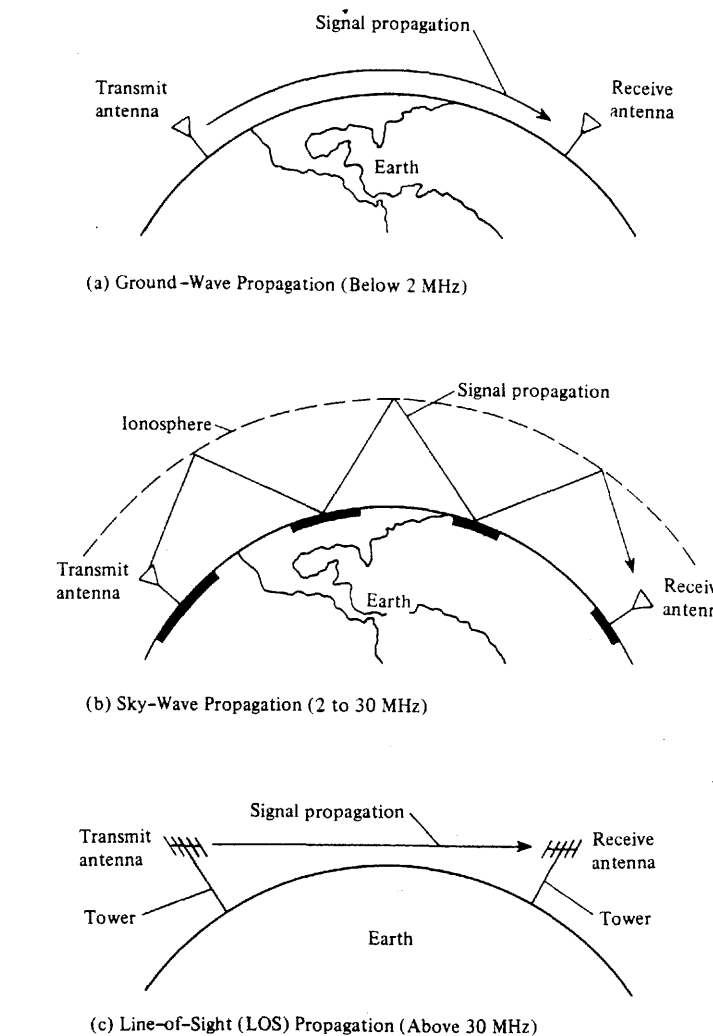


Figure 1-2 Propagation of radio frequencies.

$$\lambda = \frac{c}{f_c}$$

$$\lambda = \frac{(3 \times 10^8 \text{ m/s})}{10^4} = 3 \times 10^4 \text{ m} \quad (1-3)$$

where  $c$  is the speed of light. (The formula  $\lambda = c/f_c$  is distance = velocity  $\times$  time, where the time needed to traverse one wavelength is  $t = 1/f_c$ .) Thus an antenna needs to be at least 3000 m in length for efficient electromagnetic radiation at 10 kHz.

Sky-wave propagation is illustrated in Fig. 1-2b. It is the dominant mode of propagation in the 2- to 30-MHz frequency range. Here long-distance coverage is obtained by reflecting the wave at the ionosphere and at the Earth's boundaries. Actually, in the ionosphere the waves are refracted (i.e., bent) gradually in an inverted U shape because the index of refraction varies with altitude as the ionization density changes. The refraction index of the ionosphere is given by [Griffiths, 1987; Jordan and Balmain, 1968]

$$n = \sqrt{1 - \frac{81N}{f^2}} \quad (1-4)$$

where  $n$  is the refractive index,  $N$  is the free electron density (number of electrons per cubic meter), and  $f$  is the frequency of the wave (in hertz). Typical  $N$  values range between  $10^{10}$  and  $10^{12}$  depending on the time of day, season, and the number of sunspots. In an ionized region  $n < 1$  because  $N > 0$  and outside the ionized region  $n \approx 1$  because  $N \approx 0$ . In the ionized region, because  $n < 1$ , the waves will be bent according to Snell's law:

$$n \sin \varphi_r = \varphi_i \quad (1-5)$$

where  $\varphi_i$  is the angle of incidence (between the wave direction and vertical) measured just below the ionosphere and  $\varphi_r$  is the angle of refraction for the wave (from vertical) measured in the ionosphere. Furthermore, the refraction index will vary with altitude within the ionosphere because  $N$  varies. For frequencies selected from the 2- to 30-MHz band, the refraction index will vary with altitude over the appropriate range so that the wave will be bent back to Earth. Consequently, the ionosphere acts as a reflector. The transmitting station will have coverage areas as indicated in Fig. 1-2b by heavy black lines along the Earth's surface. The coverage near the transmit antenna is due to the ground-wave mode, and the other coverage areas are due to sky wave. Notice that there are areas of no coverage along the Earth's surface between the transmit and receive antennas. The angle of reflection and the loss of signal at an ionospheric reflection point depend on the frequency, the time of day, the season of the year, and the sunspot activity of the sun [Jordan, 1985, Chap. 33].

During the daytime (at the ionospheric reflection points), the electron density will be high so that  $n < 1$ . Consequently, sky waves from distant stations on the other side of the world will be heard on the shortwave bands. However, the D layer is also present during the day. This absorbs frequencies below 4 MHz. This is the case for AM broadcast stations, where distant stations cannot be heard during the day, but at night the layer disappears and distant AM stations can be heard via sky-wave propagation.

Sky-wave propagation is caused primarily by reflection from the F layer (90 to 250 miles in altitude). Because of this layer, international broadcast stations in the HF band can be heard from the other side of the world at almost any time during the day or night.

LOS propagation is illustrated in Fig. 1-2c. This is the dominant mode for frequencies above 30 MHz. Here the electromagnetic wave propagates in a straight line. In this case,  $f^2 \gg 81N$ , so that  $n \approx 1$ , and there is very little refraction by the ionosphere. In fact, the signal will propagate *through* the ionosphere. This property is used for satellite communications.

The LOS mode has the disadvantage that for communication between two terrestrial (Earth) stations, the signal path has to be above the horizon. Otherwise, the Earth will block

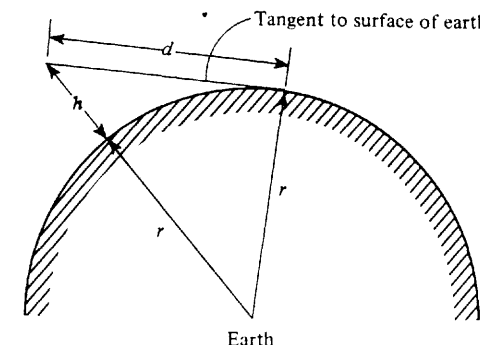


Figure 1-3 Calculation of distance to horizon.

the LOS path. Thus antennas need to be placed on tall towers so that the receiver antenna can "see" the transmitting antenna. A formula for the distance to the horizon,  $d$ , as a function of antenna height can be easily obtained by the use of Fig. 1-3. From this figure,

$$d^2 + r^2 = (r + h)^2$$

or

$$d^2 = 2rh + h^2$$

where  $r$  is the radius of the Earth and  $h$  is the antenna height above the Earth's surface. In this application  $h^2$  is negligible with respect to  $2rh$ . The radius of the Earth is 3960 statute miles. However, at LOS radio frequencies the effective Earth radius<sup>†</sup> is  $\frac{4}{3}$  (3960) miles. Thus, the distance to the radio horizon is



$$d = \sqrt{2h} \text{ miles} \quad (1-6)$$

where conversion factors have been used so that  $h$  is the antenna height measured in feet, and  $d$  is in statute miles. For example, television stations have assigned frequencies above 30 MHz in the VHF or UHF range (see Table 1-2), and the fringe-area coverage of high-power stations is limited by the LOS radio horizon. For a television station with a 1000-ft tower,  $d$  is 44.7 miles. For a fringe-area viewer who has an antenna height of 30 ft,  $d$  is 7.75 miles. Thus, for these transmitting and receiving heights, the television station would have fringe-area coverage out to a radius of  $44.7 + 7.75 = 52.5$  miles around the transmitting tower.

In addition to the LOS propagation mode, it is possible to have *ionospheric scatter propagation*. This mode occurs over the frequency range of 30 to 60 MHz, when the radio frequency signal is scattered because of irregularities in the refractive index of the lower ionosphere (about 50 miles above the Earth's surface). Because of this scattering, communications can be carried out over path lengths of 1000 miles even though this is beyond the LOS distance. Similarly, *tropospheric scattering* (within 10 miles above the Earth's sur-

<sup>†</sup>The refractive index of the atmosphere decreases slightly with height, which causes some bending of radio rays. This effect may be included in LOS calculations by using an effective Earth radius that is four-thirds of the actual radius.

face) can propagate radio frequency signals that are in the 40-MHz to 4-GHz range over paths of several hundred miles.

For more technical details about radio-wave propagation, the reader is referred to textbooks that include chapters on ground-wave and sky-wave propagation [Griffiths, 1987; Jordan and Balmain, 1968] and to a radio engineering handbook [Jordan, 1985]. A very readable description of this topic is also found in the ARRL handbook [ARRL, 1994], and personal computer programs, MINIMUF, and PropMan, are available that predict sky-wave propagation conditions [Rose, 1982, 1984; Rockwell, 1995].

## 1-9 INFORMATION MEASURE

As we have seen, the purpose of communication systems is to transmit information from a source to a sink. However, what exactly is information, and how do we measure it? We know qualitatively that it is related to the surprise that is experienced when we receive the message. For example, the message “The ocean has been destroyed by a nuclear explosion” contains more information than the message “It is raining today.”

**DEFINITION.** The *information* sent from a digital source when the  $j$ th message is transmitted is given by

$$I_j = \log_2 \left( \frac{1}{P_j} \right) \text{ bits} \quad (1-7a)$$

where  $P_j$  is the probability of transmitting the  $j$ th message.<sup>†</sup>

From this definition, we see that messages that are less likely to occur (smaller value for  $P_j$ ) provide more information (larger value of  $I_j$ ). We also observe that this information measure depends on only the likelihood of sending the message and does not depend on possible interpretation of the content as to whether or not it makes sense.

The base of the logarithm determines the units used for the information measure. Thus for units of “bits,” the base 2 logarithm is used. If the natural logarithm is used, the units are “nats”; and for base 10 logarithms, the unit is the “hartley,” named after R. V. Hartley, who first suggested using the logarithm measure in 1928 [Hartley, 1948].

In this section, the term *bit* denotes a unit of information as defined by (1-7a). In later sections, particularly in Chapter 3, *bit* is also used to denote a unit of binary data. Please do not confuse these two different meanings for the word *bit*. Some authors use *binit* to denote units of data and use *bit* exclusively to denote units of information. However, most engineers use the same word (*bit*) to denote both kinds of units, with the particular meaning understood from the context in which the word is used. This book follows that industry custom.

For ease of evaluating  $I_j$  on a calculator, (1-7a) can be written in terms of the base 10 logarithm or the natural logarithm.

<sup>†</sup>The definition of probability is given in Appendix B.

$$I_j = -\frac{1}{\log_{10} 2} \log_{10} P_j = -\frac{1}{\ln 2} \ln P_j \quad (1-7b)$$

In general, the information content will vary from message to message because the  $P_j$  will not be equal. Consequently, we need an average information measure for the source, considering all the possible messages we can send.

**DEFINITION.** The *average information* measure of a digital source is



$$H = \sum_{j=1}^m P_j I_j = \sum_{j=1}^m P_j \log_2 \left( \frac{1}{P_j} \right) \text{ bits} \quad (1-8)$$

where  $m$  is the number of possible different source messages, and  $P_j$  is the probability of sending the  $j$ th message ( $m$  is finite because a digital source is assumed). The average information is called *entropy*.

### Example 1-1 EVALUATION OF INFORMATION AND ENTROPY

Find the information content of a message that consists of a digital word 12 digits long in which each digit may take on one of four possible levels. The probability of sending any of the four levels is assumed to be equal, and the level in any digit does not depend on the values taken on by previous digits.

In a string of 12 symbols (digits) where each symbol consists of one of four levels, there are  $4 \cdot 4 \cdots 4 = 4^{12}$  different combinations (words) that can be obtained. Because each level is equally likely, all the different words are equally likely. Thus,

$$P_j = \frac{1}{4^{12}} = \left( \frac{1}{4} \right)^{12}$$

or

$$I_j = \log_2 \left( \frac{1}{\left( \frac{1}{4} \right)^{12}} \right) = \log_2(4) = 24 \text{ bits}$$

In this example we see that the information content in *any* of the possible messages equals that in any other possible message (24 bits). Thus, the average information  $H$  is 24 bits.

Suppose that only two levels (binary) had been allowed for each digit and that all the words were equally likely. Then the information would be  $I_j = 12$  bits for the binary words, and the average information would be  $H = 12$  bits. Here, all the 12-bit words gave 12 bits of information because the words were equally likely. If they had not been equally likely, some of the 12-bit words would contain more than 12 bits of information and some would contain less, and the average information would have been less than 12 bits.

The rate of information is also important.

**DEFINITION.** The *source rate* is given by

$$R = \frac{H}{T} \text{ bits/s} \quad (1-9)$$

where  $H$  is evaluated using (1-8), and  $T$  is the time required to send a message.

The definitions previously given apply to digital sources. The definitions for continuous sources are not presented here because the mathematics becomes more complicated, and the physical meanings are more difficult to interpret. However, we do not need to be too concerned about the continuous case because, from a microscopic viewpoint, communication is inherently a discrete process, as pointed out by Shannon in 1948 and mentioned by Hartley in 1928. From a macroscopic viewpoint, analog sources can be approximated by digital sources with as much accuracy as we desire.

## 1-10 CHANNEL CAPACITY AND IDEAL COMMUNICATION SYSTEMS

Many criteria can be used to measure the effectiveness of a communication system to see if it is ideal or perfect. Some of these criteria are cost, channel bandwidth used, required transmitter power, signal-to-noise ratios at various points of the system, probability of bit error for digital systems, and time delay through the system.

In digital systems, the optimum system might be defined as the system that minimizes the probability of bit error at the system output subject to constraints on transmitted energy and channel bandwidth. Thus, bit error and signal bandwidth are of prime importance and are covered in subsequent chapters. This raises the question: Is it possible to invent a system with no bit error at the output even when we have noise introduced into the channel? This question was answered by Claude Shannon in 1948–1949 [Shannon, 1948, 1949]. The answer is yes, under certain assumptions. Shannon showed that (for the case of signal plus white Gaussian noise) a channel capacity  $C$  (bits/s) could be calculated such that if the rate of information  $R$  (bits/s) was less than  $C$ , the probability of error would approach zero. The equation for  $C$  is



$$C = B \log_2 \left( 1 + \frac{S}{N} \right) \quad (1-10)$$

where  $B$  is the channel bandwidth in hertz (Hz), and  $S/N$  is the signal-to-noise power ratio (watts/watts, not dB) at the input to the digital receiver. Shannon does not tell us how to build this system, but he proves that it is theoretically possible to have such a system. Thus, Shannon gives us a theoretical performance bound that we can strive to achieve with practical communication systems. Systems that approach this bound usually incorporate error-correction coding. The channel noise still causes errors at the input to the receiver decoder; however, enough redundancy has been added in the transmitted signal so that the decoder can detect and correct errors with its processing circuits.

In analog systems, the optimum system might be defined as the one that achieves the largest signal-to-noise ratio at the receiver output subject to design constraints, such as chan-

nel bandwidth and transmitted power. Here, the evaluation of the output signal-to-noise ratio is of prime importance. We might ask the question: Is it possible to design a system with infinite signal-to-noise ratio at the output when noise is introduced by the channel? The answer is no. The performance of practical analog systems with respect to that of Shannon's ideal system is illustrated in Chapter 7 (see Fig. 7-27).

Other fundamental limits for digital signaling were discovered by Nyquist in 1924 and Hartley in 1928. If a pulse represents one bit of data, Nyquist showed that noninterfering pulses could be sent over a channel no faster than  $2B$  pulses/s, where  $B$  is the channel bandwidth in hertz. This is now known as the dimensionality theorem and is discussed in Chapter 2. Hartley generalized Nyquist's result for the case of multilevel pulse signaling as discussed in Chapters 3 and 5.

The following section describes the improvement that can be obtained in digital systems when coding is used and how these coded systems compare with Shannon's ideal system.

## 1-11 CODING

If the data at the output of a digital communication system have errors that are too frequent for the desired use, the errors can often be reduced by the use of either of two main techniques.

- Automatic repeat request (ARQ)
- Forward error correction (FEC)

In an ARQ system, when a receiver circuit detects errors in a block of data, it requests that the data block be retransmitted. In an FEC system, the transmitted data are encoded so that the receiver can correct as well as detect errors. These procedures are also classified as *channel coding* because they are used to correct errors caused by channel noise. This is different from *source coding*, described in Chapter 3, where the purpose of the coding is to extract the essential information from the source and encode it into digital form so that it can be saved or transmitted using digital techniques.

The choice between using the ARQ or the FEC technique depends on the particular application. ARQ is often used in computer communication systems because it is relatively inexpensive to implement, and there is usually a duplex (two-way) channel so that the receiving end can transmit back an acknowledgment (ACK) for correctly received data or a request for retransmission (NAC) when the data are received in error. (See Appendix C, Section C-4, for examples of ARQ signaling.) FEC techniques are used to correct errors on simplex (one-way) channels where returning of an ACK/NAC indicator (required for the ARQ technique) is not feasible. FEC is preferred on systems with large transmission delays because if the ARQ technique were used, the effective data rate would be small; the transmitter would have long idle periods while waiting for the ACK/NAC indicator, which is retarded by the long transmission delay. Because ARQ systems are covered in Appendix C, we concentrate on FEC techniques in the remainder of this section.

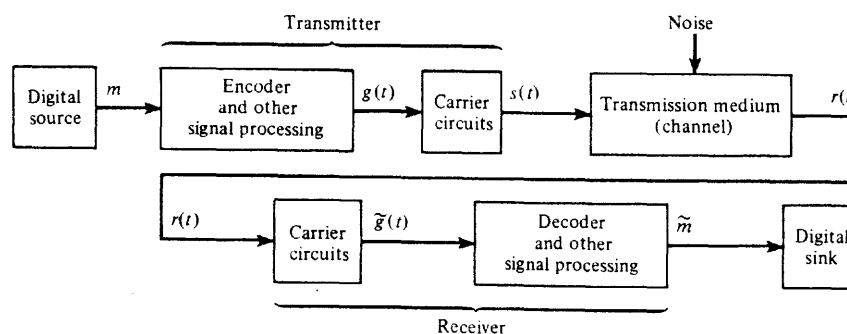


Figure 1-4 General digital communication system.

Communication systems with FEC are illustrated in Fig. 1-4, where encoding and decoding blocks have been designated. From a *theoretical viewpoint*, Shannon's channel capacity theorem states that a finite value for S/N limits only the *rate* (bits/s) of transmission. That is, the probability of error,  $P(E)$ , can approach zero provided the information rate is less than the channel capacity. This theorem implies that coding is needed to make  $P(E) \rightarrow 0$ . The question is: *What P(E) can be achieved when practical coding is used?*

The topic of coding is immense, and we will not even attempt to give an introduction to the numerous coding techniques that have been developed. However, we will summarize some of the basic concepts involved and cite results that indicate the practical improvement that can be achieved when coding is used.

Coding involves adding extra (redundant) bits to the data stream so that the decoder can reduce or correct errors at the output of the receiver. However, these extra bits have the disadvantage of increasing the data rate (bits/s) and, consequently, increasing the bandwidth of the encoded signal.

Codes may be classified into two broad categories:

- *Block codes*. A block code is a mapping of  $k$  input binary symbols into  $n$  output binary symbols. Consequently, the block coder is a *memoryless* device. Because  $n > k$ , the code can be selected to provide redundancy, such as *parity bits*, which are used by the decoder to provide some error detection and error correction. The codes are denoted by  $(n, k)$ , where the code rate  $R^+$  is defined by  $R = k/n$ . Practical values of  $R$  range from  $\frac{1}{4}$  to  $\frac{7}{8}$ , and  $k$  ranges from 3 to several hundred [Clark and Cain, 1981].
- *Convolutional codes*. A convolutional code is produced by a coder that has *memory*. The convolutional coder accepts  $k$  binary symbols at its input and produces  $n$  binary symbols at its output, where the  $n$  output symbols are affected by  $v + k$  input symbols. Memory is incorporated because  $v > 0$ . The code rate is defined by  $R = k/n$ . Typical values for  $k$  and  $n$  range from 1 to 8, and the values for  $v$  range from 2 to 60. The range of  $R$  is between  $\frac{1}{4}$  and  $\frac{7}{8}$  [Clark and Cain, 1981]. A small value for code rate  $R$  indicates a high degree of redundancy, which should provide more effective error control at the expense of increasing the bandwidth of the encoded signal.

<sup>†</sup>Do not confuse the code rate (with units of bits/bits) with the data rate or information rate (that have units of bits/s).

## Block Codes

Before discussing block codes, several definitions are needed. The *Hamming weight* of a code word is the number of binary 1 bits. For example, the code word 110101 has a Hamming weight of 4. The *Hamming distance* between two code words, denoted by  $d$ , is the number of positions by which they differ. For example, the code words 110101 and 111001 have a distance of  $d = 2$ . A received code word can be checked for errors. Some of the errors can be detected and corrected if  $d \geq s + t + 1$ , where  $s$  is the number of errors that can be detected, and  $t$  is the number of errors that can be corrected ( $s \geq t$ ). Thus, a pattern of  $t$  or fewer errors can be both detected and corrected if  $d \geq 2t + 1$ .

A general code word can be expressed in the form

$$i_1 i_2 i_3 \cdots i_k p_1 p_2 p_3 \cdots p_r$$

where  $k$  is the number of information bits,  $r$  is the number of parity check bits, and  $n$  is the total word length in the  $(n, k)$  block code, where  $n = k + r$ . This arrangement of the information bits at the beginning of the code word followed by the parity bits is most common. Such a block code is said to be *systematic*. Other arrangements with the parity bits interleaved between the information bits are possible and are usually considered to be equivalent codes.

Hamming has given a procedure for designing block codes that have single error-correction capability [Hamming, 1950]. A Hamming code is a block code having a Hamming distance of 3. Because  $d \geq 2t + 1$ ,  $t = 1$ , and a single error can be detected and corrected. However, only certain  $(n, k)$  codes are allowable. These allowable Hamming codes are

$$(n, k) = (2^m - 1, 2^m - 1 - m) \quad (1-11)$$

where  $m$  is an integer and  $m \geq 3$ . Thus, some of the allowable codes are  $(7, 4)$ ,  $(15, 11)$ ,  $(31, 26)$ ,  $(63, 57)$ , and  $(127, 120)$ . The code rate  $R$  approaches 1 as  $m$  becomes large.

In addition to Hamming codes, there are many other types of block codes. One popular class consists of the cyclic codes. *Cyclic codes* are block codes, such that another code word can be obtained by taking any one code word, shifting the bits to the right, and placing the dropped-off bits on the left. These types of codes have the advantage of being easily encoded from the message source by the use of inexpensive linear shift registers with feedback. This structure also allows these codes to be easily decoded. Examples of cyclic and related codes are Bose-Chaudhuri-Hocquenhem (BCH), Reed-Solomon, Hamming, maximal-length, Reed-Müller, and Golay codes. Some properties of block codes are given in Table 1-3 [Bhargava, 1983].

## Convolutional Codes

A convolutional encoder is illustrated in Fig. 1-5. Here  $k$  bits (one input frame) are shifted in each time, and, concurrently,  $n$  bits (one output frame) are shifted out, where  $n > k$ . Thus,

TABLE 1-3 PROPERTIES OF BLOCK CODES

Property	Code <sup>a</sup>			
	BCH	Reed-Solomon	Hamming	Maximal Length
Block length	$n = 2^m - 1$ $m = 3, 4, 5, \dots$	$n = m(2^m - 1)$ bits	$n = 2^m - 1$	$n = 2^m - 1$
Number of parity bits		$r = m2t$ bits	$r = m$	
Minimum distance	$d \geq 2t + 1$	$d = m(2t + 1)$ bits	$d = 3$	$d = 2^m - 1$
Number of information bits	$k \geq n - mt$		$k = m$	

<sup>a</sup> $m$  is any positive integer unless otherwise indicated;  $n$  is the block length;  $k$  is the number of information bits.

every  $k$ -bit input frame produces an  $n$ -bit output frame. Redundancy is provided in the output, because  $n > k$ . Also, there is memory in the coder, because the output frame depends on the previous  $K$  input frames where  $K > 1$ . The *code rate* is  $R = k/n$ , which is  $\frac{3}{4}$  in this illustration. The *constraint length*,  $K$ , is the number of input frames that are held in the  $kK$ -bit shift register.<sup>†</sup> Depending on the particular convolutional code that is to be generated, data from the  $kK$  stages of the shift register are added (modulo 2) and used to set the bits in the  $n$ -stage output register.

For example, consider the convolutional coder shown in Fig. 1-6. Here  $k = 1$ ,  $n = 2$ ,  $K = 3$ , and a commutator with two inputs performs the function of a two-stage output shift register. The convolutional code is generated by inputting a bit of data and then giving the commutator a complete revolution. This process is repeated for successive input bits to produce the convolutionally encoded output. In this example, each  $k = 1$  input bit produces  $n = 2$  output bits, so the code rate is  $R = k/n = \frac{1}{2}$ . The code tree of Fig. 1-7 gives the encoded sequences for the convolutional encoder example of Fig. 1-6. To use the code tree, one moves up if the input is a binary 0 or down if the input is a binary 1. The corresponding encoded bits are shown in parentheses. For example, if the input sequence  $x_{11} = 1010$  is fed into the input (most recent input bit on the right), the corresponding encoded output sequence is  $y_{11} = 11010001$ , as shown by path A in Fig. 1-7.

A convolutionally encoded signal is decoded by “matching” the encoded received data to the corresponding bit pattern in the code tree. In sequential decoding (a suboptimal technique), the path is found like that of a car driver who occasionally makes a wrong turn at a fork in a road but discovers the mistake, goes back, and tries another path. For example, if  $y_{11} = 11010010$  was received, path A would be the closest match and the decoded data would be  $x_{11} = 1010$ . If noise was present in the channel, some of the received encoded bits might be in error, and then the paths would not match exactly. In this case, the match

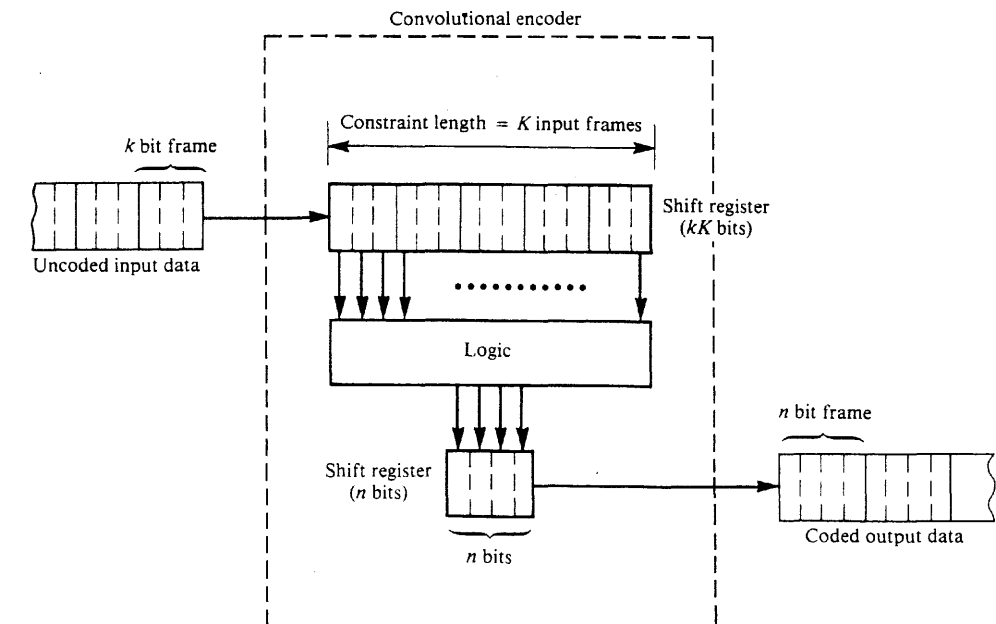


Figure 1-5 Convolutional encoding ( $k = 3$ ,  $n = 4$ ,  $K = 5$ , and  $R = \frac{3}{4}$ ).

is found by choosing a path that will minimize the Hamming distance between the selected path sequence and the received encoded sequence.

An optimum decoding algorithm, called *Viterbi decoding*, uses a similar procedure. It examines the possible paths and selects the best ones based on some conditional probabilities [Forney, 1973]. The Viterbi procedure can use either soft or hard decisions. A *soft decision* algorithm first decides the result based on the test statistic<sup>‡</sup> being above or below a decision threshold and then gives a “confidence” number that specifies how close the test statistic was to the threshold value. In *hard decisions* only the decision output is known, and it is not known if the decision was almost “too close to call” (because the test value was almost equal to the threshold value). The soft decision technique can translate into a 2-dB improvement (decrease) in the required receiver input  $E_b/N_0$  [Clark and Cain, 1981].  $E_b$  is the received signal energy over a 1-bit time interval, and  $N_0/2$  is the power spectral density (PSD) of the channel noise at the receiver input. Both  $E_b$  and  $N_0$  will be defined in detail in later chapters—for example, see (7-24b) or (8-44).

## Code Interleaving

In the previous discussion, it was assumed that if no coding was used, the channel noise would cause random bit errors at the receiver output that are more or less isolated, that is,

<sup>†</sup> Several different definitions for constraint length are used in the literature [Blahut, 1983; Clark and Cain, 1981; Proakis, 1995].

<sup>‡</sup> The test statistic is a value that is computed at the receiver based on the receiver input during some specified time interval, see (7-4).

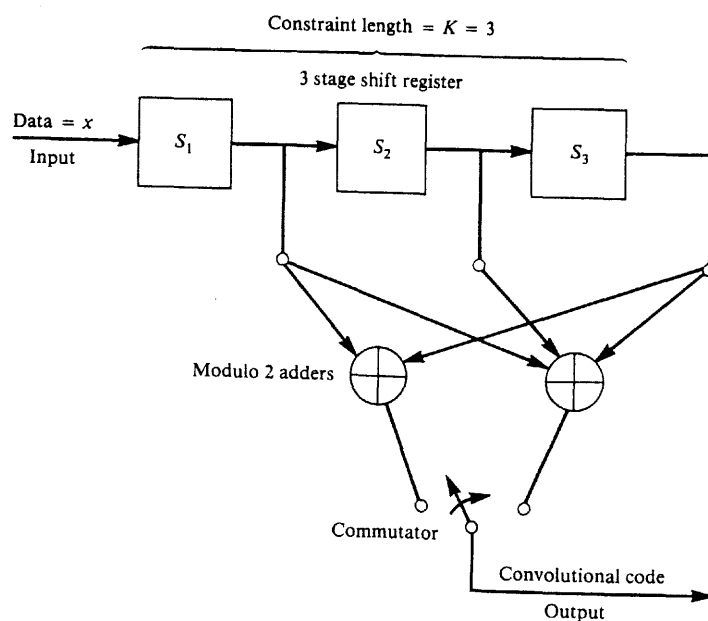


Figure 1-6 Convolutional encoder for a rate  $\frac{1}{2}$ , constraint length 3 code.

not adjacent. When coding was added, the code redundancy allowed the receiver decoder to correct the errors so that the decoded output was almost error free. However, in some applications, large wide pulses of channel noise occur. If the usual coding techniques are used in these situations, bursts of errors will occur at the decoder output because the noise bursts are wider than the “redundancy time” of the code. This situation can be ameliorated by the use of code interleaving.

At the transmitting end, the coded data are interleaved by shuffling (i.e., like shuffling a deck of cards) the coded bits over a time span of several block lengths (for block codes) or several constraint lengths (for convolutional codes). The required span length is several times the duration of the noise burst. At the receiver, before decoding, the data with error bursts are deinterleaved to produce coded data with isolated errors. The isolated errors are then corrected by passing the coded data through the decoder. This produces almost error-free output even when noise bursts occur at the receiver input. These are two classes of interleavers—block interleavers and convolutional interleavers [Sklar, 1988].

### Code Performance

The improvement in the performance of a digital communication system that can be achieved by the use of coding is illustrated in Fig. 1-8. It is assumed that a digital signal plus channel noise is present at the receiver input. The performance of a system that uses binary-phase-shift-keyed (BPSK) signaling is shown both for the case when coding is used and for the case when there is no coding. For the no code case, the optimum (matched filter) detec-

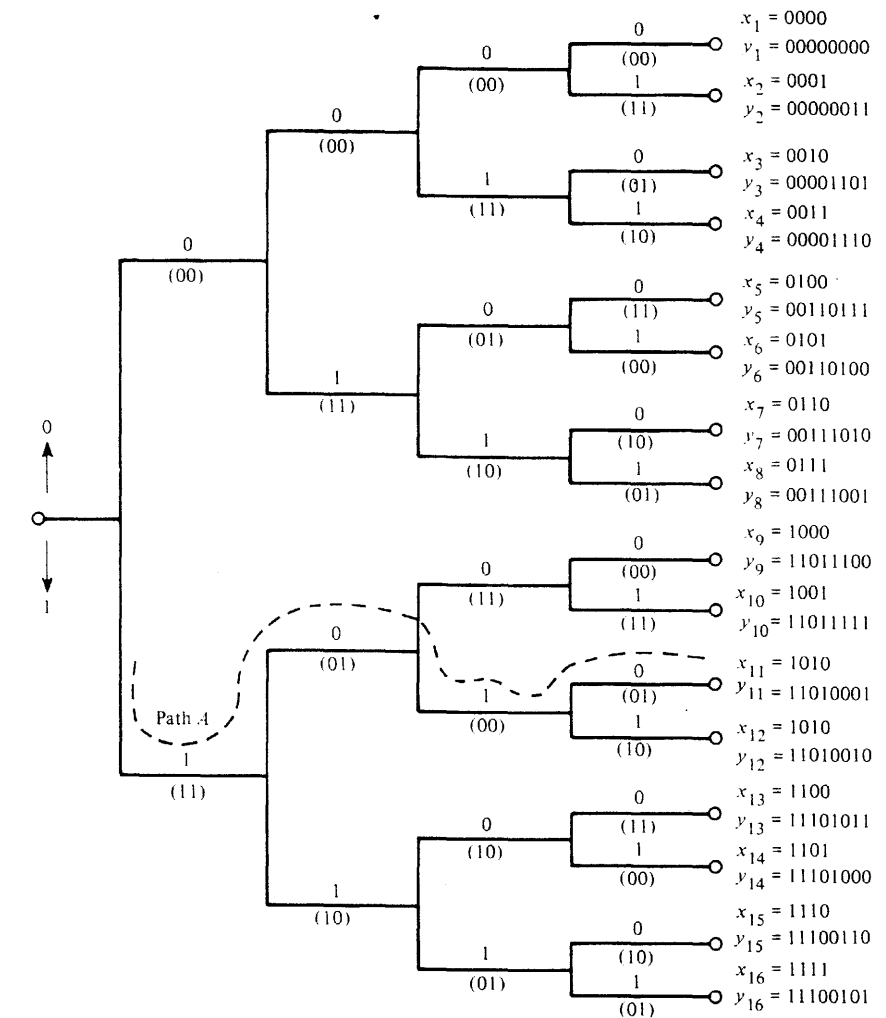


Figure 1-7 Code tree for convolutional encoder of Figure 1-6.

tor circuit is used in the receiver as derived in Chapter 7 and described by (7-38). For the coded case a (23,12) Golay code is used.  $P_e$  is the probability of bit error—also called the bit error rate (BER)—that is measured at the receiver output.  $E_b/N_0$  is the energy-per-bit/noise-density ratio at the receiver input (as described in the preceding section). The coding gain is defined as the reduction in  $E_b/N_0$  (in decibels) that is achieved when coding is used when compared with the  $E_b/N_0$  required for the uncoded case at some specific level of  $P_e$ . For example, as can be seen in the figure, a coding gain of 1.33 dB is realized for a BER of  $10^{-3}$ . The coding gain increases if the BER is smaller so that a coding gain of 2.15 dB is achieved when  $P_e = 10^{-5}$ . This improvement is significant in space communication applications where every decibel of improvement is valuable. It is also noted that there is a

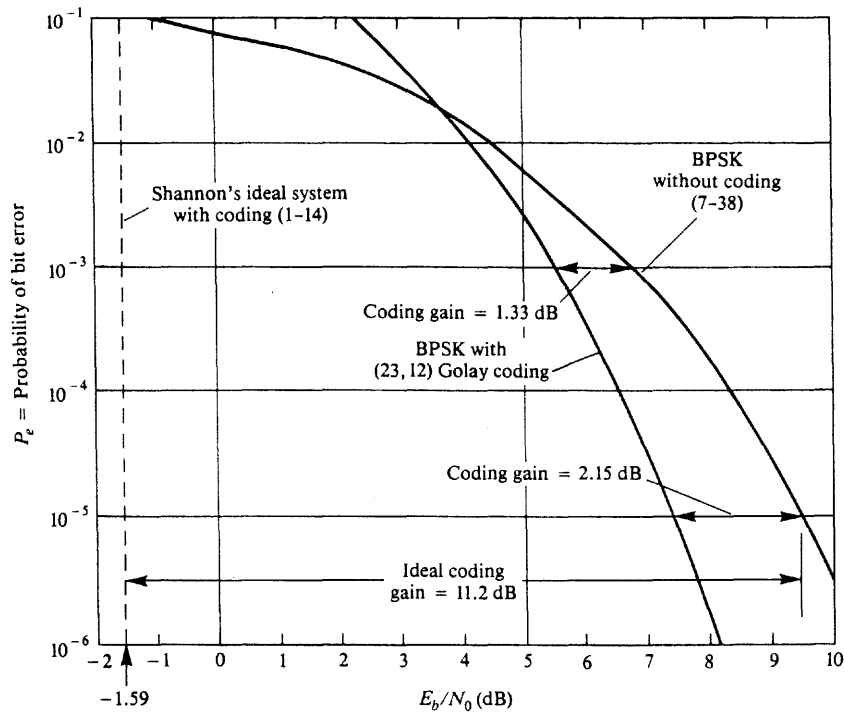


Figure 1-8 Performance of digital systems—with and without coding.

*coding threshold* in the sense that the coded system actually provides *poorer* performance than the uncoded system when  $E_b/N_0$  is less than the threshold value. In this example the coding threshold is about 3.5 dB. A coding threshold is found in all coded systems.

For optimum coding, Shannon's channel capacity theorem, (1-10), gives the  $E_b/N_0$  required. That is, if the source rate is below the channel capacity, the optimum code will allow the source information to be decoded at the receiver with  $P_e \rightarrow 0$  (i.e.,  $10^{-\infty}$ ) even though there is some noise in the channel. We will now find the  $E_b/N_0$  required so that  $P_e \rightarrow 0$  with the optimum (unknown) code. The optimum encoded signal is not restricted in bandwidth, so, from (1-10),

$$\begin{aligned} C &= \lim_{B \rightarrow \infty} \left\{ B \log_2 \left( 1 + \frac{S}{N} \right) \right\} = \lim_{B \rightarrow \infty} \left\{ B \log_2 \left( 1 + \frac{E_b/T_b}{N_0 B} \right) \right\} \\ &= \lim_{x \rightarrow 0} \left\{ \log_2 [1 + (E_b/N_0 T_b)x] \right\} \end{aligned}$$

where  $T_b$  is the time that it takes to send one bit, and  $N$  is the noise power that occurs within the bandwidth of the signal. The power spectral density (PSD) is  $\mathcal{P}_n(f) = N_0/2$ , and, as shown in Chapter 2, the noise power is

$$N = \int_{-B}^B \mathcal{P}_n(f) df = \int_{-B}^B \left( \frac{N_0}{2} \right) df = N_0 B \quad (1-12)$$

where  $B$  is the signal bandwidth. L'Hospital's rule is used to evaluate this limit.

$$C = \lim_{x \rightarrow 0} \left\{ \frac{1}{1 + (E_b/N_0 T_b)x} \left( \frac{E_b}{N_0 T_b} \right) \log_2 e \right\} = \frac{E_b}{N_0 T_b \ln 2} \quad (1-13)$$

If we signal at a rate approaching the channel capacity,  $P_e \rightarrow 0$  and we have the maximum information rate allowed for  $P_e \rightarrow 0$  (i.e., the optimum system). Thus,  $1/T_b = C$ , or, using (1-13),

$$\frac{1}{T_b} = \frac{E_b}{N_0 T_b \ln 2}$$

or

$$E_b/N_0 = \ln 2 = -1.59 \text{ dB} \quad (1-14)$$

This minimum value for  $E_b/N_0$  is  $-1.59$  dB and is called *Shannon's limit*. That is, if optimum coding/decoding is used at the transmitter and receiver, error-free data will be recovered at the receiver output provided that the  $E_b/N_0$  at the receiver input is larger than  $-1.59$  dB. This "brick wall" limit is shown by the dashed line in Fig. 1-8, where  $P_e$  jumps from  $0$  ( $10^{-\infty}$ ) to  $\frac{1}{2}(0.5 \times 10^0)$  as  $E_b/N_0$  becomes smaller than  $-1.59$  dB, assuming that the ideal (unknown) code is used. Any practical system will perform worse than this ideal system described by Shannon's limit. Thus, the goal of digital system designers is to find practical codes that approach the performance of Shannon's ideal (unknown) code.

When the performance of the optimum encoded signal is compared to that of BPSK without coding ( $10^{-5}$  BER), it is seen that the optimum (unknown) coded signal has a coding gain of  $9.61 - (-1.59) = 11.2$  dB. Using Fig. 1-8, compare this to the coding gain of 2.15 dB that is achieved when a (23,12) Golay-encoded BPSK signal is used. Table 1-4 shows the coding gains that can be obtained for some other codes [Bhargava, 1983].

All of the codes described earlier achieve their coding gains at the expense of *bandwidth expansion*. That is, when redundant bits are added to provide coding gain, the overall data rate and, consequently, the bandwidth of the signal are increased by a multiplicative factor that is the reciprocal of the code rate; the bandwidth expansion of the coded system relative to the uncoded system is  $1/R = n/k$ . Thus, if the uncoded signal takes up all of the available bandwidth, coding cannot be added to reduce receiver errors because the coded signal would take up too much bandwidth. However, this problem can be ameliorated by using trellis-coded modulation (TCM).

### Trellis-Coded Modulation

Gottfried Ungerboeck has invented a technique called *trellis-coded modulation* (TCM) that combines multilevel modulation with coding to achieve coding gain without bandwidth expansion [Benedetto, Mondin, and Montorsi, 1994; Biglieri, Divsalar, McLane, and Simon,

TABLE 1-4 CODING GAINS WITH BPSK OR QPSK

Coding Technique Used	Coding Gain (dB) at $10^{-5}$ BER	Coding Gain (dB) at $10^{-8}$ BER	Data Rate Capability
Ideal coding	11.2	13.6	
Concatenated <sup>a</sup> Reed-Solomon and convolution (Viterbi decoding)	6.5–7.5	8.5–9.5	Moderate
Convolution with sequential decoding (soft decisions)	6.0–7.0	8.0–9.0	Moderate
Block codes (soft decision)	5.0–6.0	6.5–7.5	Moderate
Concatenated <sup>a</sup> Reed-Solomon and short block	4.5–5.5	6.5–7.5	Very high
Convolutional with Viterbi decoding	4.0–5.5	5.0–6.5	High
Convolutional with sequential decoding (hard decisions)	4.0–5.0	6.0–7.0	High
Block codes (hard decisions)	3.0–4.0	4.5–5.5	High
Block codes with threshold decoding	2.0–4.0	3.5–5.5	High
Convolutional with threshold decoding	1.5–3.0	2.5–4.0	Very high

<sup>a</sup>Two different encoders are used in series at the transmitter (see Fig. 1-4), and the corresponding decoders are used at the receiver.

Source: Bhargava [1983].

1991; Ungerboeck, 1982, 1987]. The trick is to add the redundant coding bits by increasing the number of levels (amplitude values) allowed in the digital signal without changing the pulse width. This technique is called multilevel signaling and is introduced at the beginning of Chapter 3. It is later generalized to complex-valued multilevel signaling at the end of Chapter 5 where digital modulation is described. As discussed earlier by (1-2), modulation is the process of mapping the baseband source information into amplitude and phase variations— $R(t)$  and  $\theta(t)$ , respectively—of a bandpass sinusoidal carrier signal,  $s(t)$ , which has a spectrum that is concentrated about the carrier frequency,  $f_c$ . The variations can be expressed mathematically as the complex envelope,  $g(t)$ , where complex-valued multilevels are

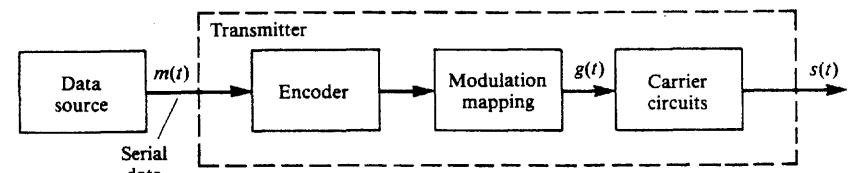
$$g(t) = R(t)e^{j\theta(t)} \quad (1-15)$$

as illustrated in Chapter 5. (The complex envelope is indicated on the communication sys-

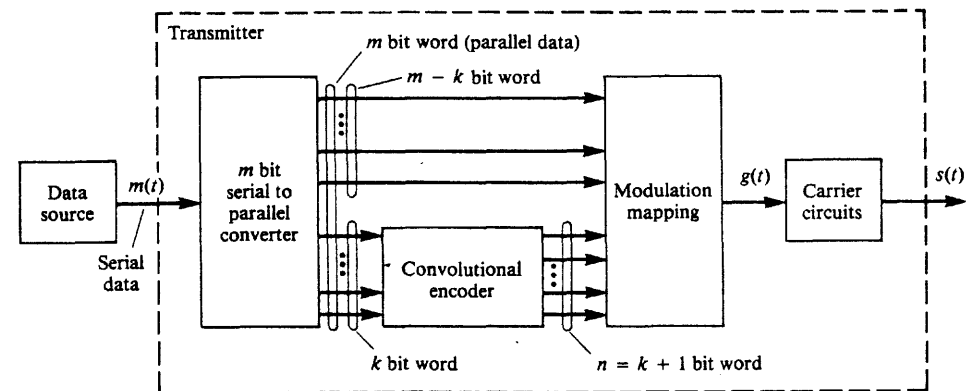
tem block diagram in Fig. 1-4.) As seen in Fig. 1-9a, which describes conventional coded systems, the coding and modulation operations are carried out separately by first encoding the baseband data to produce a coded baseband waveform and then modulating this onto the carrier as amplitude and phase variations.

The combined modulation and coding operation of TCM is shown in Fig. 1-9b. Here, the serial data from the source,  $m(t)$ , are converted into parallel ( $m$ -bit) data, which are partitioned into  $k$ -bit and  $(m - k)$ -bit words where  $k \leq m$ . The  $k$ -bit words (frames) are convolutionally encoded into  $(n = k + 1)$ -bit words so that the code rate is  $R = k/(k + 1)$ . The amplitude and phase are then set jointly on the basis of the coded  $n$ -bit word and the uncoded  $(m - k)$ -bit word. When a convolutional code of constraint length  $K = 3$  is implemented, this TCM technique produces a coding gain of 3 dB relative to an uncoded signal that has the same bandwidth and information rate. Almost 6 dB of coding gain can be realized if coders of constraint length 9 are used. The larger constraint length codes are not too difficult to generate, but the corresponding decoder for a code of large constraint length is very complicated. However, very-high-speed integrated circuits (VHSIC) are making this feasible.

The 9600-bit/s CCITT V.32 (Table C-9), 14,400-bit/s CCITT V.33bis (Table C-10), and 28,800-bit/s CCITT V.34 (Table C-7) computer modems use TCM. The CCITT V.32 modem has a coding gain of 4 dB and is described by Example 4 of Wei's paper [Wei, 1984; CCITT Study Group XVII, 1984].



(a) Conventional Coding Technique



(b) Trellis-Coded Modulation Technique

Figure 1-9 Transmitters for conventional coding and for TCM.

For further study about coding, the reader is referred to several excellent books on the topic [Blahut, 1983; Clark and Cain, 1981; Gallagher, 1968; Lin and Costello, 1983; McEliece, 1977; Peterson and Weldon, 1972; Sweeney, 1991; Viterbi and Omura, 1979].

## 1-12 PREVIEW

From the previous discussions, we see the need for some basic tools to understand and design communication systems. Some prime tools needed are mathematical models to represent signals, noise, and linear systems. Chapter 2 provides these tools. It is divided into the broad categories of properties of signal and noise, Fourier transforms and spectra, orthogonal representations, bandlimited representations, and descriptions of linear systems. Measures of bandwidth are also defined.

## 1-13 STUDY-AID EXAMPLES

**SA1-1** The antenna for a television (TV) station is located at the top of a 1500-foot transmission tower. Compute the LOS coverage for the TV station if the receiving antenna (in the fringe area) is 20 feet above ground.

**Solution.** Using (1-6), the distance from the TV transmission tower to the radio horizon is

$$d_1 = \sqrt{2h} = \sqrt{2(1500)} = 54.8 \text{ miles}$$

The distance from the receiving antenna to the radio horizon is

$$d_2 = \sqrt{2(20)} = 6.3 \text{ miles}$$

Then, the total radius for the LOS coverage contour (which is a circle around the transmission tower) is

$$d = d_1 + d_2 = 61.1 \text{ miles}$$

**SA1-2** A telephone touch-tone keypad has digits 0 to 9 plus the \* and # keys. Assume that the probability of sending \* or # is 0.005 and the probability of sending 0 to 9 is 0.099 each. If the keys are pressed at a rate of 2 keys/s, compute the data rate for this source.

**Solution.** Using (1-8)

$$\begin{aligned} H &= \sum P_j \log_2 \left( \frac{1}{P_j} \right) \\ &= \frac{1}{\log_2(2)} \left[ 10(0.099) \log_{10} \left( \frac{1}{0.099} \right) + 2(0.005) \log_{10} \left( \frac{1}{0.005} \right) \right] \end{aligned}$$

or

$$H = 3.38 \text{ bits/key}$$

Using (1-9) where  $T = 1/(2 \text{ keys/s}) = 0.5 \text{ s/key}$

$$R = \frac{H}{T} = \frac{3.38}{0.5} = 6.76 \text{ bits/s}$$

**SA1-3** A computer user plans to buy a higher-speed modem for sending data over his or her analog telephone line. The telephone line has a signal-to-noise ratio (SNR) of 25 dB and passes audio frequencies over the frequency range from 300 to 3200 Hz. Calculate the maximum data rate that could be sent over the telephone line for the case of no errors at the receiving end.

**Solution.** In terms of a power ratio, the SNR is  $S/N = 10^{(25/10)} = 316.2$  (see dB in Chapter 2), and the bandwidth is  $B = 3200 - 300 = 2900 \text{ Hz}$ . Using (1-10),

$$R = B \log_2 \left( 1 + \frac{S}{N} \right) = 2900 [\log_{10}(1 + 316.2)] / \log_{10}(2)$$

or

$$R = 24,097 \text{ bits/s}$$

Consequently, a 28.8-kbit/s modem signal would not work on this telephone line; however, a 14.4-kbit/s modem signal should transmit data without error.

## PROBLEMS

- 1-1** A high-power FM station of frequency 96.9 MHz has an antenna height of 1800 ft. If the signal is to be received 75 miles from the station, how high does a prospective listener need to mount his/her antenna in this fringe area?
- 1-2** Using geometry, prove that (1-6) is correct.
- 1-3** A terrestrial microwave system is being designed. The transmitting and receiving antennas are to be placed at the top of equal-height towers, with one tower at the transmitter site and one at the receiving site. The distance between the transmitting and receiving sites is 30 miles. Calculate the minimum tower height required for a LOS transmission path.
- 1-4** A cellular telephone cell site has an antenna located at the top of a 75-ft tower. A typical cellular telephone user has his/her antenna located 4 ft above the ground. What is the LOS radius of coverage for this cell site to a distant user?
- 1-5** A digital source emits -1.0- and 0.0-V levels with a probability of 0.2 each and +3.0- and +4.0-V levels with a probability of 0.3 each. Evaluate the average information of the source.
- 1-6** Prove that base 10 logarithms may be converted to base 2 logarithms by using the identity  $\log_2(x) = [1/\log_{10}(2)] \log_{10}(x)$ .
- 1-7** If all the messages emitted by a source are equally likely (i.e.,  $P_j = P$ ), show that (1-8) reduces to  $H = \log_2(1/P)$ .
- 1-8** For a binary source:
  - (a) Show that the entropy,  $H$ , is a maximum when the probability of sending a binary 1 is equal to the probability of sending a binary 0.
  - (b) Find the value of maximum entropy.
- 1-9** A single-digit, seven-segment liquid crystal display (LCD) emits a 0 with a probability of 0.25; a 1 and a 2 with a probability of 0.15 each; 3, 4, 5, 6, 7, and 8 with a probability of 0.07 each; and a 9 with a probability of 0.03. Find the average information for this source.



- 1-10** (a) A binary source sends a binary 1 with a probability of 0.3. Evaluate the average information for the source.  
 (b) For a binary source find the probability for sending a binary 1 and a binary 0, such that the average source information will be maximized.
- 1-11** A numerical keypad has the digits 0, 1, 2, 3, 4, 5, 6, 7, 8, and 9. Assume that the probability of sending any one digit is the same as that for sending any of the other digits. Calculate how often the buttons must be pressed in order to send out information at the rate of 2 bits/s.
- 1-12** Refer to Example 1-1 and assume that words, each 12 digits in length, are sent over a system and that each digit can take on one of two possible values. Half of the possible words have a probability of being transmitted that is  $(\frac{1}{2})^{13}$  for each word. The other half have probabilities equal to  $3(\frac{1}{2})^{13}$ . Find the entropy for this source.
- 1-13** Evaluate the channel capacity for a teleprinter channel that has a 300-Hz bandwidth and a SNR of 30 dB.
- 1-14** Assume that a computer terminal has 110 characters (on its keyboard) and that each character is sent using binary words.  
 (a) What are the number of bits needed to represent each character?  
 (b) How fast can the characters be sent (characters/s) over a telephone line channel having a bandwidth of 3.2 kHz and a SNR of 20 dB?  
 (c) What is the information content of each character if each is equally likely to be sent?
- 1-15** An analog telephone line has a SNR of 45 dB and passes audio frequencies over the range of 300 to 3200 Hz. A modem is to be designed to transmit and receive data simultaneously (i.e., full duplex) over this line without errors.  
 (a) If the frequency range 300 to 1200 Hz is used for the transmitted signal, what is the maximum transmitted data rate?  
 (b) If the frequency range 1500 to 3200 Hz is used for the signal being simultaneously received, what is the maximum received data rate?  
 (c) If the whole frequency range of 300 to 3200 Hz is used simultaneously for transmitting and receiving (by use of a Hybrid circuit as described in Chapter 8; Fig. 8-5), what are the maximum transmission and receiving data rates?
- 1-16** Using the definitions for terms associated with convolutional coding, draw a block diagram for a convolutional coder that has rate  $R = \frac{2}{3}$  and constraint length  $K = 3$ .
- 1-17** For the convolutional encoder shown in Fig. P1-17, compute the output coded data when the input data is  $x = [10111]$ . (The first input bit is the leftmost element of the  $x$  row vector.)

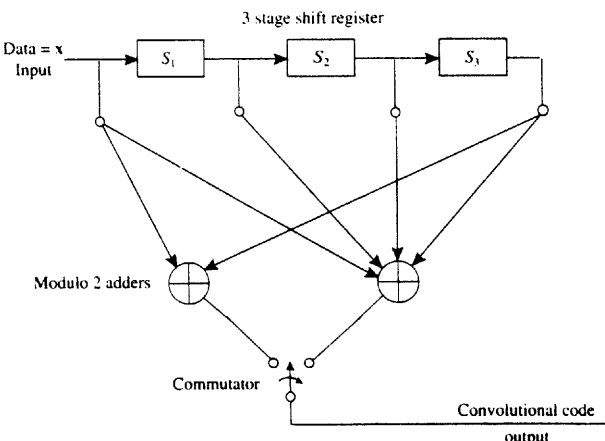


Figure P1-17

## CHAPTER 2

SIGNALS  
AND SPECTRA

## 2-1 PROPERTIES OF SIGNALS AND NOISE

In communication systems, the received waveform is usually categorized into the desired part containing the information, and the extraneous or undesired part. The desired part is called the *signal* and the undesired part is called *noise*.

This chapter develops mathematical tools that are used to describe signals and noise from a deterministic waveform point of view. (The random waveform approach is given in Chapter 6.) The waveforms will be represented by direct mathematical expressions or by the use of orthogonal series representations such as the Fourier series. Properties for characterizing these waveforms such as dc value, root mean square (rms) value, normalized power, magnitude spectrum, phase spectrum, power spectral density, and bandwidth will also be developed. In addition, effects of linear filtering will be studied.

The waveform of interest may be the voltage as a function of time,  $v(t)$ , or the current as a function of time,  $i(t)$ . Often the same mathematical techniques can be used when

working with either type of waveform. Thus, for generality, waveforms will be denoted simply as  $w(t)$  when the analysis applies to either case.

### Physically Realizable Waveforms

Practical waveforms that are *physically realizable* (i.e., measurable in a laboratory) satisfy several conditions<sup>†</sup>:

1. The waveform has significant nonzero values over a composite time interval that is finite.
2. The spectrum of the waveform has significant values over a composite frequency interval that is finite.
3. The waveform is a continuous function of time.
4. The waveform has a finite peak value.
5. The waveform has only real values. That is, at any time, it cannot have a complex value  $a + jb$  where  $b$  is nonzero.

The first condition is necessary because systems (and their waveforms) appear to exist for a finite amount of time. Physical signals also produce only a finite amount of energy. The second condition is necessary because any transmission medium—such as wires, coaxial cable, waveguides, or fiber optic cable—has a restricted bandwidth. The third condition is a consequence of the second, as will become clear from spectral analysis as developed in Sec. 2-2. The fourth condition is necessary because physical devices are destroyed if voltage or current of infinite value is present within the device. The fifth condition follows from the fact that only real waveforms can be observed in the real world, although *properties* of waveforms, such as spectra, may be complex. Later, in Chapter 4, it will be shown that complex waveforms can be very useful in representing real bandpass signals mathematically.

Mathematical models that violate some or all of the conditions listed previously are often used, and for one main reason—to simplify the mathematical analysis. In fact, we often have to use a model that violates some of these conditions in order to calculate any type of answer. However, if we are careful with the mathematical model, the correct result can be obtained when the answer is properly interpreted. For example, consider the digital waveform shown in Fig. 2-1. The mathematical model waveform has discontinuities at the switching times. This situation violates the third condition—the physical waveform is continuous. The physical waveform is of finite duration (decays to zero before  $t = \pm\infty$ ), but the duration of the mathematical waveform extends to infinity.

In other words, this mathematical model assumes that the physical waveform existed in its steady-state condition for all time. Spectral analysis of the model will approximate the correct results except for the extremely high-frequency components. The average power that is calculated from the model will give the correct value for the average power of the physical signal that is measured over an appropriate time interval. The total energy of the mathematical model's signal will be infinity because it extends to infinite time, whereas that of the physical signal will be finite. Consequently, this model will not give the correct value

<sup>†</sup> For an interesting discussion relative to the first and second conditions, see the paper by Slepian [1976].

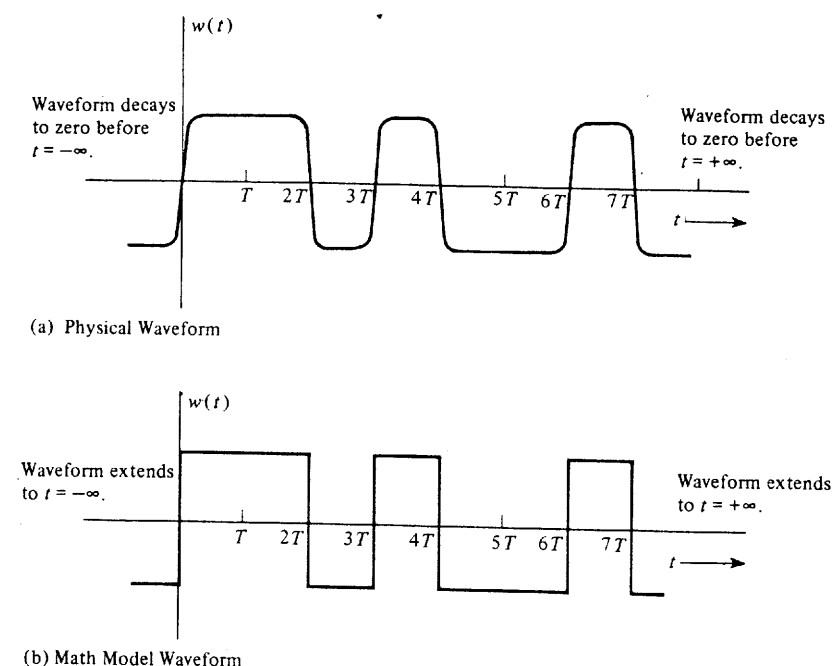


Figure 2-1 Physical and mathematical waveforms.

for the total energy of the physical signal without using some additional information. However, the model can be used to evaluate the energy of the physical signal over some finite time interval of the physical signal. This mathematical model is said to be a *power signal* because it has the property of finite power (and infinite energy), whereas the physical waveform is said to be an *energy signal* because it has finite energy. (Mathematical definitions for power and energy signals will be given in a subsequent section.) All physical signals are energy signals, although we generally use power signal mathematical models to simplify the analysis.

In summary, waveforms may often be classified as signals or noise, digital or analog, deterministic or nondeterministic, physically realizable or nonphysically realizable, and belonging to the power or energy type. Additional classifications, such as periodic and nonperiodic, will be given in the next section.

### Time Average Operator

Some useful waveform characteristics are dc (direct "current") value, average power, and rms (root mean square) value. Before these concepts are reviewed, the time average operator needs to be defined.

**DEFINITION.** The *time average operator*<sup>†</sup> is given by

$$\langle [\cdot] \rangle = \lim_{T \rightarrow \infty} \frac{1}{T} \int_{-T/2}^{T/2} [\cdot] dt \quad (2-1)$$

It is seen that this operator is a *linear* operator since, from (2-1), the average of the sum of two quantities is the same as the sum of their averages<sup>‡</sup>:

$$\langle a_1 w_1(t) + a_2 w_2(t) \rangle = a_1 \langle w_1(t) \rangle + a_2 \langle w_2(t) \rangle \quad (2-2)$$

Equation (2-1) can be reduced to a simpler form if the operator is operating on a *periodic* waveform.

**DEFINITION.** A waveform  $w(t)$  is *periodic* with period  $T_0$  if

$$w(t) = w(t + T_0) \quad \text{for all } t \quad (2-3)$$

where  $T_0$  is the smallest positive number that satisfies this relationship.<sup>§</sup>

For example, a sinusoidal waveform of frequency  $f_0 = 1/T_0$  hertz is periodic since it satisfies (2-3). From this definition it is clear that a periodic waveform will have significant values over an infinite time interval  $(-\infty, \infty)$ . Consequently, physical waveforms cannot be truly periodic, but they can have periodic values over a finite time interval. That is, (2-3) can be satisfied for  $t$  over some finite interval but not for all values of  $t$ .

**THEOREM.** If the waveform involved is periodic, the time average operator can be reduced to

$$\langle [\cdot] \rangle = \frac{1}{T_0} \int_{-T_0/2+a}^{T_0/2+a} [\cdot] dt \quad (2-4)$$

where  $T_0$  is the period of the waveform and  $a$  is an arbitrary real constant, which may be taken to be zero.

Eq. (2-4) readily follows from (2-1) because, referring to (2-1), integrals over successive time intervals  $T_0$  seconds wide have identical areas because the waveshape is periodic with period  $T_0$ . As these integrals are summed, the total area and  $T$  are proportionally larger, resulting in a value for the time average that is the same as just integrating over one period and dividing by the width of that interval,  $T_0$ .

In summary, (2-1) may be used to evaluate the time average of any type of waveform, whether or not it is periodic. Equation (2-4) is valid only for periodic waveforms.

### Dc Value

**DEFINITION.** The *dc (direct "current")* value of a waveform  $w(t)$  is given by its time average,  $\langle w(t) \rangle$ .

<sup>†</sup> In Appendix B, the ensemble average operator is defined.

<sup>‡</sup> See (2-130) for the definition of linearity.

<sup>§</sup> Nonperiodic waveforms are called *aperiodic* waveforms by some authors.

Thus,

$$W_{dc} = \lim_{T \rightarrow \infty} \frac{1}{T} \int_{-T/2}^{T/2} w(t) dt \quad (2-5)$$

For any physical waveform, we are actually interested in evaluating the dc value only over a finite interval of interest, say from  $t_1$  to  $t_2$ , so that the dc value is

$$\frac{1}{t_2 - t_1} \int_{t_1}^{t_2} w(t) dt$$

However, if we use a mathematical model with a steady-state waveform of infinite extent, we will obtain the correct result by using our definition (2-5), which involves the limit as  $T \rightarrow \infty$ . This will be demonstrated subsequently by Example 2-1. Moreover, as will be shown in Chapter 6, for the case of ergodic stochastic waveforms the time-averaging operator  $\langle [\cdot] \rangle$  may be replaced by the ensemble average operator  $\bar{[\cdot]}$ .

### Power

In communication systems, if the received (average) signal power is sufficiently large compared to the (average) noise power, information may be recovered. This concept was demonstrated by the Shannon channel capacity formula, (1-10). Consequently, average power is an important concept that needs to be clearly understood. From physics it is known that power is defined as work per unit time, voltage is work per unit charge, and current is charge per unit time. This is the basis for the definition of power in terms of electrical quantities.

**DEFINITION.** Let  $v(t)$  denote the voltage across a set of circuit terminals and let  $i(t)$  denote the current into the terminal, as shown in Fig. 2-2. The *instantaneous power* (incremental work divided by incremental time) associated with the circuit is given by



$$p(t) = v(t)i(t) \quad (2-6)$$

where the instantaneous power flows into the circuit when  $p(t)$  is positive and flows out of the circuit when  $p(t)$  is negative. The *average power* is given by

$$P = \langle p(t) \rangle = \langle v(t)i(t) \rangle \quad (2-7)$$

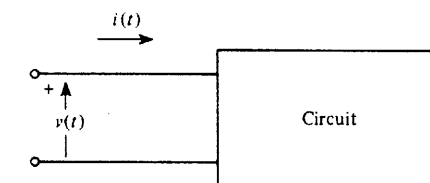


Figure 2-2 Polarity convention used for voltage and current.

**Example 2-1 EVALUATION OF POWER**

Let the circuit of Fig. 2-2 contain a 120-V, 60-Hz fluorescent lamp wired in a high-power-factor configuration. Assume that the voltage and current are both sinusoids and in phase (unity power factor), as shown in Fig. 2-3.<sup>†</sup> The dc value of this (periodic) voltage waveform is

$$\begin{aligned} V_{dc} &= \langle v(t) \rangle = \langle V \cos \omega_0 t \rangle \\ &= \frac{1}{T_0} \int_{-T_0/2}^{T_0/2} V \cos \omega_0 t \, dt = 0 \end{aligned} \quad (2-8)$$

where  $\omega_0 = 2\pi/T_0$  and  $f_0 = 1/T_0 = 60$  Hz. Similarly,  $I_{dc} = 0$ . The instantaneous power is

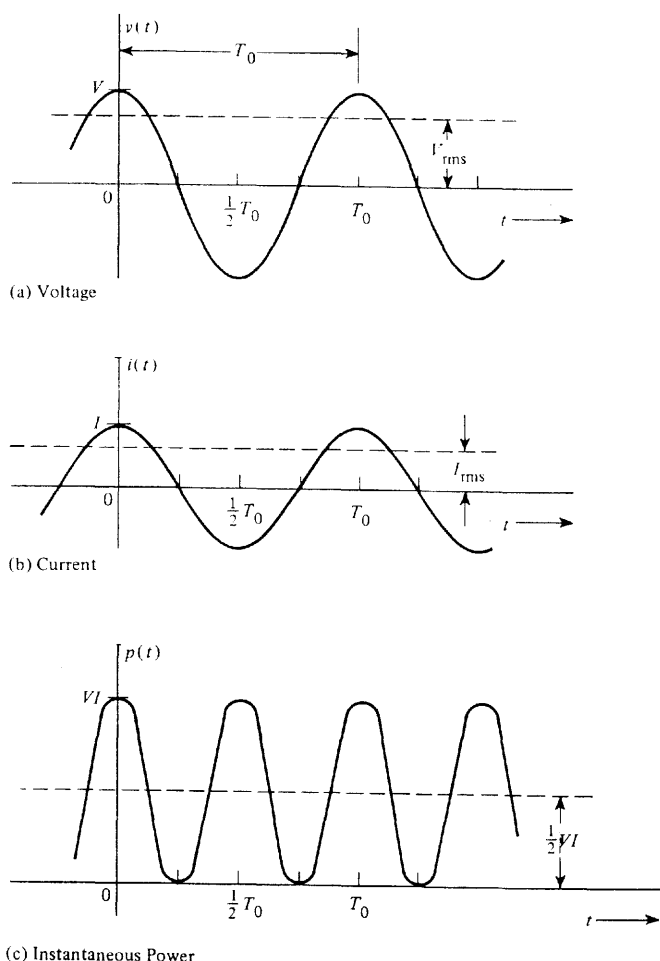


**Figure 2-3** Steady state waveshapes for Example 2-1.

<sup>†</sup> Two-lamp fluorescent circuits can be realized with a high-power-factor ballast that gives an overall power factor greater than 90% [Fink and Beatty, 1978].

$$p(t) = (V \cos \omega_0 t)(I \cos \omega_0 t) = \frac{1}{2}VI(1 + \cos 2\omega_0 t) \quad (2-9)$$

The average power is

$$\begin{aligned} P &= \langle \frac{1}{2}VI(1 + \cos 2\omega_0 t) \rangle \\ &= \frac{VI}{2T_0} \int_{-T_0/2}^{T_0/2} (1 + \cos 2\omega_0 t) \, dt \\ &= \frac{VI}{2} \end{aligned} \quad (2-10)$$

As can be seen from (2-9) and Fig. 2-3c, the power (i.e., light emitted) occurs in pulses at a rate of  $2f_0 = 120$  pulses per second. (In fact, this lamp can be used as a stroboscope to "freeze" mechanically rotating objects.) The peak power is  $VI$ , and the average power is  $\frac{1}{2}VI$ , where  $V$  is the peak voltage and  $I$  is the peak current. Furthermore, for this case of sinusoidal voltage and sinusoidal current we see that the average power could be obtained by multiplying  $V/\sqrt{2}$  with  $I/\sqrt{2}$ .

**Rms Value and Normalized Power**

**DEFINITION.** The root mean square (rms) value of  $w(t)$  is given by

$$W_{rms} = \sqrt{\langle w^2(t) \rangle} \quad (2-11)$$

**THEOREM.** If a load is resistive (i.e., unity power factor), the average power is given by

$$\begin{aligned} P &= \frac{\langle v^2(t) \rangle}{R} = \langle i^2(t) \rangle R = \frac{V_{rms}^2}{R} \\ &= I_{rms}^2 R = V_{rms} I_{rms} \end{aligned} \quad (2-12)$$

where  $R$  is the value of the resistive load.

Equation (2-12) follows from (2-7) by the use of Ohm's law, which is  $v(t) = i(t)R$ , and (2-11).

Continuing Example 2-1,  $V_{rms} = 120$  V. It is seen from (2-11), when sinusoidal waveforms are used, that  $V_{rms} = V/\sqrt{2}$  and  $I_{rms} = I/\sqrt{2}$ . Thus, using (2-12), we see that the average power is  $\frac{1}{2}VI$ , which is the same value that was obtained in the previous discussion.

The concept of *normalized* power is often used by communications engineers. In this concept,  $R$  is assumed to be  $1 \Omega$ , although it may be another value in the actual circuit. Another way of expressing this concept is to say that the power is given on a per-ohm basis. In the signal-to-noise power ratio calculations  $R$  will automatically cancel out, so that normalized values of power may be used to obtain the correct ratio. If the actual value for the power is needed, say at the end of a long set of calculations, it can always be obtained by "denormalization" of the normalized value. From (2-12) it is also realized that the square root of the normalized power is the rms value.

**DEFINITION.** The *average normalized power* is given by

$$P = \langle w^2(t) \rangle = \lim_{T \rightarrow \infty} \frac{1}{T} \int_{-T/2}^{T/2} w^2(t) dt \quad (2-13)$$

where  $w(t)$  represents a real voltage or current waveform.

### Energy and Power Waveforms<sup>†</sup>

**DEFINITION.**  $w(t)$  is a *power waveform* if and only if the normalized average power,  $P$ , is finite and nonzero (i.e.,  $0 < P < \infty$ ).

**DEFINITION.** The *total normalized energy* is given by

$$E = \lim_{T \rightarrow \infty} \int_{-T/2}^{T/2} w^2(t) dt \quad (2-14)$$

**DEFINITION.**  $w(t)$  is an *energy waveform* if and only if the total normalized energy is finite and nonzero (i.e.,  $0 < E < \infty$ ).

From these definitions it is seen that if a waveform is classified as either one of these types, it cannot be of the other type. That is, if  $w(t)$  has finite energy, the power averaged over infinite time is zero, and if the power (averaged over infinite time) is finite, the energy is infinite. Moreover, mathematical functions can be found that have both infinite energy and infinite power and, consequently, cannot be classified into either of these two categories. One example is  $w(t) = e^{-t}$ . Physically realizable waveforms are of the energy type, but we will often model them by infinite-duration waveforms of the power type. Laboratory instruments that measure average quantities—such as dc value, rms value, and average power—average over a finite time interval. That is,  $T$  of (2-1) remains finite instead of approaching some large number. Thus nonzero average quantities for finite energy (physical) signals can be obtained. For example, when the dc value is measured with a conventional volt-ohm-milliamp meter containing a meter movement, the time-averaging interval is established by the mass of the meter movement that provides damping. Thus the average quantities calculated from a power-type mathematical model (averaged over infinite time) will give the results that are measured in the laboratory (averaged over finite time).

### Decibel

The *decibel* is a base 10 logarithmic measure of power ratios. For example, the ratio of the power level at the output of a circuit compared to that at the input is often specified by the decibel gain instead of the actual ratio.

<sup>†</sup> This concept is also called *energy signals* and *power signals* by some authors, but it applies to noise as well as signal waveforms.

**DEFINITION.** The *decibel gain* of a circuit is given by<sup>†</sup>

$$\text{dB} = 10 \log \left( \frac{\text{average power out}}{\text{average power in}} \right) = 10 \log \left( \frac{P_{\text{out}}}{P_{\text{in}}} \right) \quad (2-15)$$

This definition gives a number that indicates the *relative* value of the *power out* with respect to the *power in* and does not indicate the actual magnitude of the power levels involved. If resistive loads are involved, (2-12) may be used to reduce (2-15) to

$$\text{dB} = 20 \log \left( \frac{V_{\text{rms out}}}{V_{\text{rms in}}} \right) + 10 \log \left( \frac{R_{\text{in}}}{R_{\text{load}}} \right) \quad (2-16)$$

or

$$\text{dB} = 20 \log \left( \frac{I_{\text{rms out}}}{I_{\text{rms in}}} \right) + 10 \log \left( \frac{R_{\text{load}}}{R_{\text{in}}} \right) \quad (2-17)$$

Note that the same value for decibels is obtained regardless of whether power, voltage, or current [(2-15), (2-16), or (2-17)] was used to obtain that value. That is, decibels are defined in terms of the logarithm of a power ratio but may be evaluated from voltage and/or current ratios.

If normalized powers are used,

$$\text{dB} = 20 \log \left( \frac{V_{\text{rms out}}}{V_{\text{rms in}}} \right) = 20 \log \left( \frac{I_{\text{rms out}}}{I_{\text{rms in}}} \right) \quad (2-18)$$

This equation does not give the true value for decibels unless  $R_{\text{in}} = R_{\text{load}}$ ; however, it is common engineering practice to use (2-18) even if  $R_{\text{in}} \neq R_{\text{load}}$  and even if the number that is obtained is not strictly correct. Engineers understand that if the correct value is needed, it may be calculated from this pseudovalue if  $R_{\text{in}}$  and  $R_{\text{load}}$  are known.

If the dB value is known, the power ratio or the voltage ratio can be easily obtained by inversion of the appropriate equations just given. For example, if the power ratio is desired, (2-15) can be inverted to obtain

$$\frac{P_{\text{out}}}{P_{\text{in}}} = 10^{\text{dB}/10} \quad (2-19)$$

The decibel measure can also be used to express a measure of the signal power to noise power ratio, as measured at some point in a circuit.

<sup>†</sup> Logarithms to the base 10 will be denoted by  $\log(\cdot)$ , and logarithms to the base  $e$  will be denoted by  $\ln(\cdot)$ . Note that both dB and the ratio  $(P_{\text{out}}/P_{\text{in}})$  are dimensionless quantities.

**DEFINITION.** The *decibel signal-to-noise ratio* is<sup>†</sup>

$$(S/N)_{\text{dB}} = 10 \log \left( \frac{P_{\text{signal}}}{P_{\text{noise}}} \right) = 10 \log \left( \frac{\langle s^2(t) \rangle}{\langle n^2(t) \rangle} \right) \quad (2-20)$$

Because the signal power is  $\langle s^2(t) \rangle / R = V_{\text{rms signal}}^2 / R$ , and the noise power is  $\langle n^2(t) \rangle / R = V_{\text{rms noise}}^2 / R$ , this definition is equivalent to

$$(S/N)_{\text{dB}} = 20 \log \left( \frac{V_{\text{rms signal}}}{V_{\text{rms noise}}} \right) \quad (2-21)$$

The decibel measure may also be used to indicate absolute levels of power with respect to some reference level.

**DEFINITION.** The *decibel power level* with respect to 1 mW is given by

$$\begin{aligned} \text{dBm} &= 10 \log \left( \frac{\text{actual power level (watts)}}{10^{-3}} \right) \\ &= 30 + 10 \log [\text{actual power level (watts)}] \end{aligned} \quad (2-22)$$

where the "m" in the dBm denotes a milliwatt reference.

Laboratory RF signal generators are usually calibrated in terms of dBm.

Other decibel measures of absolute power levels are also used. When a 1-W reference level is used, the decibel level is denoted dBW; when a 1-kW reference level is used, the decibel level is denoted dBk. For example, a power of 5 W could be specified as +36.99 dBm, 6.99 dBW, or -23.0 dBk. The telephone industry uses a decibel measure with a "reference noise" level of 1 picowatt ( $10^{-12}$  W) [Jordan, 1985]. This decibel measure is denoted dBn. A level of 0 dBn corresponds to -90 dBm. The cable television (CATV) industry uses a 1-millivolt rms level across a  $75\Omega$  load as a reference. This decibel measure is denoted dBmV, and it is defined as follows:

$$\text{dBmV} = 20 \log \left( \frac{V_{\text{rms}}}{10^{-3}} \right) \quad (2-23)$$

0 dBmV corresponds to -48.75 dBm.

It should be emphasized that the general expression for evaluating power is given by (2-7). That is, (2-7) can be used to evaluate average power for any type of waveshape and load condition, whereas (2-12) is useful only for resistive loads. In other books, especially in the power area, equations are given that are valid only for sinusoidal waveshapes.

## Phasors

Sinusoidal test signals occur so often in electrical engineering problems that a shorthand notation called *phasor notation* is often used.

<sup>†</sup> This definition involves the ratio of the *average signal power* to the *average noise power*. An alternative definition that is also useful for some applications involves the ratio of the *peak signal power* to the *average noise power*—see Sec. 6-8.

**DEFINITION.** A complex number  $c$  is said to be a *phasor* if it is used to represent a *sinusoidal waveform*. That is,

$$w(t) = |c| \cos[\omega_0 t + \angle c] = \text{Re}\{ce^{j\omega_0 t}\} \quad (2-24)$$

where the phasor  $c = |c|e^{j\angle c}$  and  $\text{Re}\{\cdot\}$  denotes the real part of the complex quantity  $\{\cdot\}$ .

We will refer to  $ce^{j\omega_0 t}$  as the *rotating phasor*, as distinguished from the phasor  $c$ . When  $c$  is given to represent waveform, it is *understood* that the actual waveform that appears in the circuit is a sinusoid as specified by (2-24). Because the phasor is a complex number, it can be written in either Cartesian form or polar form:

$$c \triangleq x + jy = |c|e^{j\phi} \quad (2-25)$$

where  $x$  and  $y$  are real numbers along the Cartesian coordinates and  $|c|$  and  $\angle c = \phi = \tan^{-1}(y/x)$  are the length and angle (real numbers) in the polar coordinate system. Shorthand notation for the polar form on the right-hand side of (2-25) is  $|c| \angle \phi$ .

For example,  $25 \sin(2\pi 500t + 45^\circ)$  could be denoted by the phasor  $25 \angle -45^\circ$  since

$$25 \sin(\omega_0 t + 45^\circ) = 25 \cos(\omega_0 t - 45^\circ) = \text{Re}\{(25e^{-j\pi/4})e^{j\omega_0 t}\}$$

where  $\omega_0 = 2\pi f_0$  and  $f_0 = 500$  Hz. Similarly,  $10 \cos(\omega_0 t + 35^\circ)$  could be denoted by  $10 \angle 35^\circ$ .

Some other authors may use a slightly different definition for the phasor. For example,  $w(t)$  may be expressed in terms of the imaginary part of a complex quantity instead of the real part as defined in (2-24). In addition, the phasor may denote the rms value of  $w(t)$  instead of the peak value [Kaufman and Seidman, 1979]. In this case,  $10 \sin(\omega_0 t + 45^\circ)$  should be denoted by the phasor  $7.07 \angle 45^\circ$ . However, throughout this book, the definition as given by (2-24) will be used, and phasors can represent only *sinusoidal* waveshapes.

## 2-2 FOURIER TRANSFORM AND SPECTRA

### Definition

In electrical engineering problems the signal, the noise, or the combined signal plus noise usually consists of a voltage or current waveform that is a function of time. Let  $w(t)$  denote the waveform of interest (either voltage or current). If desired, we could look at the waveform on an oscilloscope. The value of the voltage (or current) fluctuates as a function of time; consequently, certain frequencies or a frequency range is one of the main properties of interest to the electrical engineer. Theoretically, to evaluate the frequencies that are present, one needs to view the waveform over all time (i.e.,  $-\infty < t < \infty$ ) to be sure that the measurement is accurate and to guarantee that none of the frequency components is neglected. The relative level of one frequency as compared to another is given by the *voltage* (or *current*) *spectrum*. This is obtained by taking the *Fourier transform* of the voltage (or current) waveform.

**DEFINITION.** The *Fourier transform* (FT) of a waveform  $w(t)$  is

$$W(f) = \mathcal{F}[w(t)] = \int_{-\infty}^{\infty} [w(t)]e^{-j2\pi ft} dt \quad (2-26)$$

where  $\mathcal{F}[\cdot]$  denotes the Fourier transform of  $[\cdot]$  and  $f$  is the frequency parameter with units of Hz (i.e., 1/s).<sup>†</sup> This defines the term *frequency*; frequency is the parameter  $f$  in the Fourier transform.

This is also called a *two-sided spectrum* of  $w(t)$  because both positive and negative frequency components are obtained from (2-26).

In general, because  $e^{-j2\pi ft}$  is complex,  $W(f)$  is a complex function of frequency.  $W(f)$  may be decomposed into two real functions  $X(f)$  and  $Y(f)$  such that

$$W(f) = X(f) + jY(f) \quad (2-27)$$

This is identical to writing a complex number in terms of pairs of real numbers that can be plotted in a two-dimensional Cartesian coordinate system. For this reason, (2-27) is sometimes called the *quadrature form* or *Cartesian form*. Similarly, (2-26) can be written equivalently in terms of a polar coordinate system where the pair of real functions denotes the magnitude and phase

$$W(f) = |W(f)|e^{j\theta(f)} \quad (2-28)$$

where

$$|W(f)| = \sqrt{X^2(f) + Y^2(f)} \quad \text{and} \quad \theta(f) = \tan^{-1}\left(\frac{Y(f)}{X(f)}\right) \quad (2-29)$$

This is called the *magnitude-phase* form or *polar form*. To determine if certain frequency components are present, one would examine the magnitude spectrum  $|W(f)|$ , and sometimes engineers loosely call this just the *spectrum*.

It should be clear that the spectrum of a voltage (or current) waveform is obtained by a mathematical calculation and that it does not appear physically in an actual circuit.  $f$  is just a parameter (called *frequency*) that determines which point of the spectral function is to be evaluated. For example, the frequency  $f = 10$  Hz is present in the waveform  $w(t)$  if and only if  $|W(10)| \neq 0$ . From (2-26) it is realized that an exact spectral value can be obtained only if the waveform is observed over the infinite time interval  $(-\infty, \infty)$ . However, a special instrument called a *spectrum analyzer* may be used to obtain an approximation (i.e., finite time integral) for the magnitude spectrum  $|W(f)|$ .

The time waveform may be calculated from the spectrum by using the inverse Fourier transform

$$w(t) = \int_{-\infty}^{\infty} W(f)e^{j2\pi ft} df \quad (2-30)$$

<sup>†</sup> Some authors define the FT in terms of the frequency parameter  $\omega$  (radians per second), where  $\omega = 2\pi f$ . That definition is identical to (2-26) when  $\omega$  is replaced by  $2\pi f$ . I prefer (2-26) because spectrum analyzers are usually calibrated in units of hertz, not radians per second.

The functions  $w(t)$  and  $W(f)$  are said to constitute a *Fourier transform pair* where  $w(t)$  is the time domain description and  $W(f)$  is the frequency domain description. In this book, the time domain function is usually denoted by a lowercase letter and the frequency domain function by an uppercase letter. Shorthand notation for the pairing between the two domains will be denoted by a double arrow:  $w(t) \leftrightarrow W(f)$ .

The waveform  $w(t)$  is Fourier transformable (i.e., sufficient conditions) if it satisfies both *Dirichlet conditions*:

- Over any time interval of finite width, the function  $w(t)$  is single valued with a finite number of maxima and minima and the number of discontinuities (if any) is finite.
- $w(t)$  is absolutely integrable. That is,

$$\int_{-\infty}^{\infty} |w(t)| dt < \infty \quad (2-31)$$

Although these conditions are sufficient, they are not necessary. In fact, some of the examples given subsequently do not satisfy the Dirichlet conditions and yet the Fourier transform can be found.

A weaker sufficient condition for the existence of the Fourier transform is

$$E = \int_{-\infty}^{\infty} |w(t)|^2 dt < \infty \quad (2-32)$$

where  $E$  is the normalized energy [Goldberg, 1961]. This is the finite energy condition that is satisfied by all physically realizable waveforms. Thus all physical waveforms encountered in engineering practice are Fourier transformable.

It should also be noted that mathematicians sometimes use other definitions for the Fourier transform rather than (2-26). However, in these cases, the corresponding inverse transforms, equivalent to (2-30), would also be different, so that when the transform and its inverse are used together, the original  $w(t)$  would be recovered. This is a consequence of the Fourier integral theorem, which is

$$w(t) = \int_{-\infty}^{\infty} \int_{-\infty}^{\infty} w(\lambda)e^{j2\pi f(t - \lambda)} d\lambda df \quad (2-33)$$

Equation (2-33) may be decomposed into (2-26) and (2-30), as well as other definitions for Fourier transform pairs. The Fourier integral theorem is strictly true only for well-behaved functions (i.e., physical waveforms). For example, if  $w(t)$  is an ideal square wave, then at a discontinuous point of  $w(\lambda)$ , denoted by  $\lambda_0$ ,  $w(t)$  will have a value that is the average of the two values that are obtained for  $w(\lambda)$  on each side of the discontinuous point  $\lambda_0$ .

### Example 2-2 SPECTRUM OF AN EXPONENTIAL PULSE

Let  $w(t)$  be a decaying exponential pulse that is switched on at  $t = 0$ .

$$w(t) = \begin{cases} e^{-t}, & t > 0 \\ 0, & t < 0 \end{cases}$$

The spectrum of this pulse is given by the Fourier transform

$$W(f) = \int_0^{\infty} e^{-t} e^{-j2\pi ft} dt$$

or

$$W(f) = \frac{1}{1 + j2\pi f}$$

In other words, this Fourier transform pair is

$$\left\{ \begin{array}{ll} e^{-t}, & t > 0 \\ 0, & t < 0 \end{array} \right\} \leftrightarrow \frac{1}{1 + j2\pi f} \quad (2-34)$$

The spectrum can also be expressed in terms of the quadrature functions by rationalizing the denominator of (2-34); thus,

$$X(f) = \frac{1}{1 + (2\pi f)^2} \quad \text{and} \quad Y(f) = \frac{-2\pi f}{1 + (2\pi f)^2}$$

The magnitude-phase form is

$$|W(f)| = \sqrt{\frac{1}{1 + (2\pi f)^2}} \quad \text{and} \quad \theta(f) = -\tan^{-1}(2\pi f)$$

More examples will be given after some helpful theorems are developed.

### Properties of Fourier Transforms

Many useful and interesting theorems follow from the definition of the spectrum as given by (2-26). One of particular interest is the consequence of working with real waveforms. In any physical circuit that can be built, the voltage (or current) waveforms are real functions (as opposed to complex functions) of time.

**THEOREM.** *Spectral symmetry of real signals. If  $w(t)$  is real, then*

$$W(-f) = W^*(f) \quad (2-35)$$

The asterisk superscript denotes the conjugate operation.

**Proof.** From (2-26),

$$W(-f) = \int_{-\infty}^{\infty} w(t) e^{j2\pi ft} dt \quad (2-36)$$

and taking the conjugate of (2-26) yields

$$W^*(f) \int_{-\infty}^{\infty} w^*(t) e^{j2\pi ft} dt \quad (2-37)$$

But because  $w(t)$  is real,  $w^*(t) = w(t)$  and (2-35) follows because the right sides of (2-36) and (2-37) are equal. It can also be shown that if real  $w(t)$  happens to be an even function of  $t$ ,  $W(f)$  is *real*. Similarly, if real  $w(t)$  is an odd function of  $t$ ,  $W(f)$  is *imaginary*.

Another useful corollary of (2-35) is that for  $w(t)$  real, the magnitude spectrum is even about the origin (i.e.,  $f = 0$ ):

$$|W(-f)| = |W(f)| \quad (2-38)$$

and the phase spectrum is odd about the origin:

$$\theta(-f) = -\theta(f) \quad (2-39)$$

This can easily be demonstrated by writing the spectrum in polar form:

$$W(f) = |W(f)| e^{j\theta(f)}$$

Then

$$W(-f) = |W(-f)| e^{j\theta(-f)}$$

and

$$W^*(f) = |W(f)| e^{-j\theta(f)}$$

Using (2-35), we see that (2-38) and (2-39) are true.

In summary, from the previous discussion, some properties of the Fourier transform are

- $f$ , called frequency and having units of hertz, is just a parameter of the FT that specifies what frequency we are interested in looking for in the waveform  $w(t)$ .
- The FT looks for the frequency  $f$  in the  $w(t)$  over all time, that is, over  $-\infty < t < \infty$
- $W(f)$  can be complex even though  $w(t)$  is real.
- If  $w(t)$  is real, then  $W(-f) = W^*(f)$ .

### Parseval's Theorem and Energy Spectral Density

#### Parseval's Theorem.

$$\int_{-\infty}^{\infty} w_1(t) w_2^*(t) dt = \int_{-\infty}^{\infty} W_1(f) W_2^*(f) df \quad (2-40)$$

If  $w_1(t) = w_2(t) = w(t)$ , this reduces to<sup>†</sup>

$$E = \int_{-\infty}^{\infty} |w(t)|^2 dt = \int_{-\infty}^{\infty} |W(f)|^2 df \quad (2-41)$$

<sup>†</sup> This is also known as Rayleigh's energy theorem.

**Proof.** Work with the left side of (2-40), using (2-30) to replace  $w_1(t)$ .

$$\begin{aligned} \int_{-\infty}^{\infty} w_1(t)w_2^*(t) dt &= \int_{-\infty}^{\infty} \left[ \int_{-\infty}^{\infty} W_1(f)e^{j2\pi ft} df \right] w_2^*(t) dt \\ &= \int_{-\infty}^{\infty} \int_{-\infty}^{\infty} W_1(f)w_2^*(t)e^{j2\pi ft} df dt \end{aligned}$$

Interchanging the order of integration on  $f$  and  $t$ <sup>†</sup>

$$\int_{-\infty}^{\infty} w_1(t)w_2^*(t) dt = \int_{-\infty}^{\infty} W_1(f) \left[ \int_{-\infty}^{\infty} w_2(t)e^{-j2\pi ft} dt \right]^* df$$

Using (2-26) produces the result of (2-40). Parseval's theorem gives an alternative method for evaluating the energy by using the frequency domain description instead of the time domain definition. This leads to the concept of the energy spectral density function.

**DEFINITION.** The *energy spectral density (ESD)* is defined for energy waveforms by

$$\mathcal{E}(f) = |W(f)|^2 \quad (2-42)$$

where  $w(t) \leftrightarrow W(f)$ .  $\mathcal{E}(f)$  has units of joules per hertz.

By using Parseval's theorem, we see that the total normalized energy is given by the area under the ESD function:

$$E = \int_{-\infty}^{\infty} \mathcal{E}(f) df \quad (2-43)$$

For power waveforms, a similar function called the *power spectral density (PSD)* can be defined. This is developed in Sec. 2-3 and in Chapter 6. Later we will find that the PSD function is a very useful tool for solving communication problems.

There are many other Fourier transform theorems in addition to Parseval's theorem. Some are summarized in Table 2-1. These theorems can be proved by substituting the corresponding time function into the definition for the Fourier transform and reducing the result to that given in the rightmost column of the table. For example, the scale change theorem is proved by substituting  $w(at)$  into (2-26). We get

$$\mathcal{F}[w(at)] = \int_{-\infty}^{\infty} w(at)e^{-j2\pi ft} dt$$

Letting  $t_1 = at$  and assuming that  $a > 0$ , we get

$$\mathcal{F}[w(at)] = \int_{-\infty}^{\infty} \frac{1}{a} w(t_1)e^{-j2\pi(f/a)t_1} dt_1 = \frac{1}{a} W\left(\frac{f}{a}\right)$$

<sup>†</sup> Fubini's theorem states that the order of integration may be exchanged if all of the integrals are absolutely convergent. That is, these integrals are finite valued when the integrands are replaced by their absolute values. We assume that this condition is satisfied.

For  $a < 0$  this becomes

$$\mathcal{F}[w(at)] = \int_{-\infty}^{\infty} \frac{-1}{a} w(t_1)e^{-j2\pi(f/a)t_1} dt_1 = \frac{1}{|a|} W\left(\frac{f}{a}\right)$$

Thus, for either  $a > 0$  or  $a < 0$ , we get

$$w(at) \leftrightarrow \frac{1}{|a|} W\left(\frac{f}{a}\right)$$

The other theorems in Table 2-1 are proved in a similar straightforward manner, except for the integral theorem. The integral theorem is more difficult to derive since the transform result involves a Dirac delta function,  $\delta(f)$ . This theorem may be proved by the use of the convolution theorem, as illustrated by Prob. 2-36. The bandpass signal theorem will be discussed in more detail in Chapter 4. It is the basis for the digital and analog modulation techniques covered in Chapters 4 and 5. In Sec. 2-8 the relationship between the Fourier transform and the discrete Fourier transform (DFT) will be studied.

As we will see in the following examples, these theorems can greatly simplify the calculations required to solve Fourier transform problems. The reader should study Table 2-1 and be prepared to use it when needed. After the Fourier transform is evaluated, one should check to see that the easy-to-verify properties of Fourier transforms are satisfied; otherwise, there is a mistake. For example, if  $w(t)$  is real,

- $W(-f) = W^*(f)$ , or  $|W(f)|$  is even and  $\theta(f)$  is odd.
- $W(f)$  is real when  $w(t)$  is even.
- $W(f)$  is imaginary when  $w(t)$  is odd.

### Example 2-3 SPECTRUM OF A DAMPED SINUSOID

Let the damped sinusoid be given by

$$w(t) = \begin{cases} e^{-ut} \sin \omega_0 t, & t > 0, T > 0 \\ 0, & t < 0 \end{cases}$$

The spectrum of this waveform is obtained by evaluating the Fourier transform. This is easily accomplished by using the result of the previous example plus some of the Fourier theorems. From (2-34), and using the scale change theorem, where  $a = 1/T$ ,

$$\begin{cases} e^{-ut}, & t > 0 \\ 0, & t < 0 \end{cases} \leftrightarrow \frac{T}{1 + j(2\pi fT)}$$

Using the real signal frequency translation theorem with  $\theta = -\pi/2$ , we get

$$W(f) = \frac{1}{2} \left\{ e^{-j\pi/2} \frac{T}{1 + j2\pi T(f - f_0)} + e^{j\pi/2} \frac{T}{1 + j2\pi T(f + f_0)} \right\}$$

$$= \frac{T}{2j} \left\{ \frac{1}{1 + j2\pi T(f - f_0)} - \frac{1}{1 + j2\pi T(f + f_0)} \right\} \quad (2-44)$$



TABLE 2-1 SOME FOURIER TRANSFORM THEOREMS<sup>a</sup>

Operation	Function	Fourier Transform
Linearity	$a_1 w_1(t) + a_2 w_2(t)$	$a_1 W_1(f) + a_2 W_2(f)$
Time delay	$w(t - T_d)$	$W(f) e^{-j\omega T_d}$
Scale change	$w(at)$	$\frac{1}{ a } W\left(\frac{f}{a}\right)$
Conjugation	$w^*(t)$	$W^*(-f)$
Duality	$W(t)$	$w(-f)$
Real signal frequency translation [ $w(t)$ is real]	$w(t) \cos(\omega_c t + \theta)$	$\frac{1}{2}[e^{j\theta} W(f - f_c) + e^{-j\theta} W(f + f_c)]$
Complex signal frequency translation	$w(t) e^{j\omega_c t}$	$W(f - f_c)$
Bandpass signal	$\operatorname{Re}\{g(t) e^{j\omega_c t}\}$	$\frac{1}{2}[G(f - f_c) + G^*(-f - f_c)]$
Differentiation	$\frac{d^n w(t)}{dt^n}$	$(j2\pi f)^n W(f)$
Integration	$\int_{-\infty}^t w(\lambda) d\lambda$	$(j2\pi f)^{-1} W(f) + \frac{1}{2} W(0) \delta(f)$
Convolution	$w_1(t) * w_2(t) = \int_{-\infty}^{\infty} w_1(\lambda) \cdot w_2(t - \lambda) d\lambda$	$W_1(f) W_2(f)$
Multiplication <sup>b</sup>	$w_1(t) w_2(t)$	$W_1(f) * W_2(f) = \int_{-\infty}^{\infty} W_1(\lambda) W_2(f - \lambda) d\lambda$
Multiplication by $t^n$	$t^n w(t)$	$(-j2\pi)^{-n} \frac{d^n W(f)}{df^n}$

<sup>a</sup>  $\omega_c = 2\pi f_c$ .<sup>b</sup> \* denotes convolution as described in detail by (2-62).

where  $e^{\pm j\pi/2} = \cos(\pi/2) \pm j \sin(\pi/2) = \pm j$ . This spectrum is complex (i.e., neither real nor imaginary) because  $w(t)$  does not have even or odd symmetry about  $t = 0$ .

As expected, (2-44) shows that the peak of the magnitude spectrum for the damped sinusoid occurs at  $f = \pm f_0$ . Compare this to the peak of the magnitude spectrum for the exponential decay (Example 2-2) that occurs at  $f = 0$ . That is, the  $\sin \omega_0 t$  factor caused the spectral peak to move from  $f = 0$  to  $f = \pm f_0$ .

### Dirac Delta Function and Unit Step Function

Another type of function that often occurs in communication problems is the Dirac delta function.

**DEFINITION.** The *Dirac delta function*  $\delta(x)$  is defined by

$$\int_{-\infty}^{\infty} w(x) \delta(x) dx = w(0) \quad (2-45)$$

where  $w(x)$  is any function that is continuous at  $x = 0$ .

In this definition the variable  $x$  could be time or frequency depending on the application. An alternative definition for  $\delta(x)$  is

$$\int_{-\infty}^{\infty} \delta(x) dx = 1 \quad (2-46a)$$

and

$$\delta(x) = \begin{cases} \infty, & x = 0 \\ 0, & x \neq 0 \end{cases} \quad (2-46b)$$

where both (2-46a) and (2-46b) need to be satisfied. The Dirac delta function is not a true function, so it is said to be a singular function. However,  $\delta(x)$  can be defined as a function in a more general sense and treated as such in a branch of mathematics called *generalized functions* and the *theory of distributions*.

From (2-45), the *sifting property* of the  $\delta$  function is

$$\int_{-\infty}^{\infty} w(x) \delta(x - x_0) dx = w(x_0) \quad (2-47)$$

That is, the  $\delta$  function sifts out the value  $w(x_0)$  from the integral.

In some problems it is also useful to use the equivalent integral for the  $\delta$  function, which is

$$\delta(x) = \int_{-\infty}^{\infty} e^{\pm j2\pi xy} dy \quad (2-48)$$

where either the + or the - sign may be used as needed. This assumes that  $\delta(x)$  is an even function:  $\delta(-x) = \delta(x)$ . Equation (2-48) may be verified by taking the Fourier transform of a delta function

$$\int_{-\infty}^{\infty} \delta(t) e^{-j2\pi ft} dt = e^0 = 1$$

and then taking the inverse Fourier transform of both sides of this equation; (2-48) follows. For additional properties of the delta function, see Appendix A.

Another function that is closely related to the Dirac delta function is the unit step function.

**DEFINITION.** The *unit step function*  $u(t)$  is

$$u(t) = \begin{cases} 1, & t > 0 \\ 0, & t < 0 \end{cases} \quad (2-49)$$

Because  $\delta(\lambda)$  is zero except at  $\lambda = 0$ , the Dirac delta function is related to the unit step function by

$$\int_{-\infty}^{\infty} \delta(\lambda) d\lambda = u(t) \quad (2-50)$$

and consequently,

$$\frac{du(t)}{dt} = \delta(t) \quad (2-51)$$

#### Example 2-4 SPECTRUM OF A SINUSOID

Find the spectrum of a sinusoidal voltage waveform that has a frequency  $f_0$  and a peak value of  $A$  volts.

$$v(t) = A \sin \omega_0 t \text{ where } \omega_0 = 2\pi f_0$$

From (2-26), the spectrum is

$$\begin{aligned} V(f) &= \int_{-\infty}^{\infty} A \left( \frac{e^{j\omega_0 t} - e^{-j\omega_0 t}}{2j} \right) e^{-j\omega_0 t} dt \\ &= \frac{A}{2j} \int_{-\infty}^{\infty} e^{-j2\pi(f-f_0)t} dt - \frac{A}{2j} \int_{-\infty}^{\infty} e^{-j2\pi(f+f_0)t} dt \end{aligned}$$

By (2-48), these integrals are equivalent to Dirac delta functions. That is,

$$V(f) = \frac{A}{2} [\delta(f + f_0) - \delta(f - f_0)]$$

Note that this spectrum is imaginary, as expected, because  $v(t)$  is real and odd. In addition, a meaningful expression was obtained for the Fourier transform, although  $v(t)$  was of the infinite energy type and not absolutely integrable. That is, this  $v(t)$  does not satisfy the sufficient (but not necessary) Dirichlet conditions as given by (2-31) and (2-32).

The magnitude spectrum is

$$|V(f)| = \frac{A}{2} \delta(f - f_0) + \frac{A}{2} \delta(f + f_0)$$

where  $A$  is a positive number. Because only two frequencies ( $f = \pm f_0$ ) are present,  $\theta(f)$  is strictly defined only at these two frequencies. That is,  $\theta(f_0) = \tan^{-1}(-1/0) = -90^\circ$  and  $\theta(-f_0) = \tan^{-1}(1/0) = +90^\circ$ . However, because  $|V(f)| = 0$  for all frequencies except  $f = \pm f_0$  and  $V(f) = |V(f)| e^{j\theta(f)}$ ,  $\theta(f)$  can be taken to be any convenient set of values for  $f \neq \pm f_0$ . Thus the phase spectrum is taken to be

$$\theta(f) = \begin{cases} -\pi/2, & f > 0 \\ +\pi/2, & f < 0 \end{cases} \text{ radians} = \begin{cases} -90^\circ, & f > 0 \\ 90^\circ, & f < 0 \end{cases}$$

Plots of these spectra are shown in Fig. 2-4. It is seen that the magnitude spectrum is even and the phase spectrum is odd, as expected from (2-38) and (2-39).

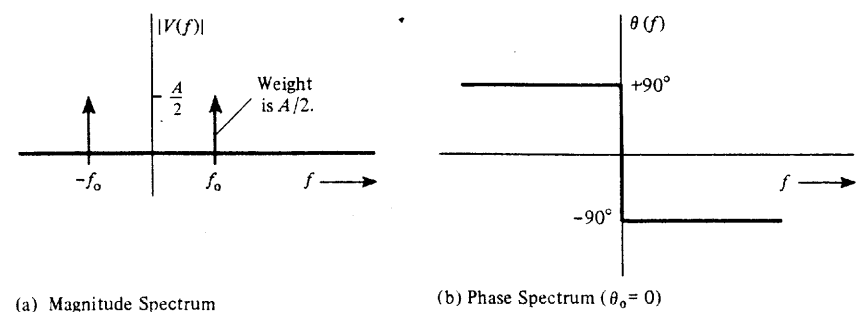


Figure 2-4 Spectrum of a sine wave.

Now let us generalize the sinusoidal waveform to one with an arbitrary phase angle  $\theta_0$ . Then

$$w(t) = A \sin(\omega_0 t + \theta_0) = A \sin[\omega_0(t + \theta_0/\omega_0)]$$

and, by using the time delay theorem, the spectrum becomes

$$W(f) = j \frac{A}{2} e^{j\theta_0(f/f_0)} [\delta(f + f_0) - \delta(f - f_0)]$$

The resulting magnitude spectrum is the same as that obtained before for the  $\theta_0 = 0$  case. The new phase spectrum is the sum of the old phase spectrum plus the linear function  $(\theta_0/f_0)f$ . However, since the overall spectrum is zero except at  $f = \pm f_0$ , the value for the phase spectrum can be arbitrarily assigned at all frequencies except  $f = \pm f_0$ . At  $f = f_0$  the phase is  $(\theta_0 - \pi/2)$  radians, and at  $f = -f_0$  the phase is  $-(\theta_0 - \pi/2)$  radians.

From a mathematical viewpoint, Fig. 2-4 demonstrates that two frequencies are present in the sine wave, one at  $f = +f_0$  and another at  $f = -f_0$ . This can also be seen from the time waveform; that is,

$$v(t) = A \sin \omega_0 t = \frac{A}{j2} e^{j\omega_0 t} - \frac{A}{j2} e^{-j\omega_0 t}$$

which implies that the sine wave consists of two rotating phasors, one rotating with a frequency  $f = +f_0$  and another rotating with  $f = -f_0$ . From the engineering point of view it is said that one frequency is present, namely,  $f = f_0$ , because for any physical (i.e., real) waveform, (2-35) shows that for any positive frequency present, there is also a mathematical negative frequency present. The phasor associated with  $v(t)$  is  $c = 0 - jA = A / -90^\circ$ . Another interesting observation is that the magnitude spectrum consists of lines (i.e., Dirac delta functions). As shown by (2-109), the lines are a consequence of  $v(t)$  being a periodic function. If the sinusoid is switched on and off, then the resulting waveform is not periodic and its spectrum is continuous as demonstrated by Example 2-9. A damped sinusoid also has a continuous spectrum, as demonstrated by Example 2-3.

## Rectangular and Triangular Pulses

Some additional waveshapes frequently occur in communications problems, so some special symbols will be defined to shorten the notation.

**DEFINITION.** Let  $\Pi(\cdot)$  denote a single rectangular pulse

$$\Pi\left(\frac{t}{T}\right) \triangleq \begin{cases} 1, & |t| \leq \frac{T}{2} \\ 0, & |t| > \frac{T}{2} \end{cases} \quad (2-52)$$

**DEFINITION.** Let  $\text{Sa}(\cdot)$  denote the function<sup>†</sup>

$$\text{Sa}(x) = \frac{\sin x}{x} \quad (2-53)$$

**DEFINITION.** Let  $\Lambda(\cdot)$  denote the triangular function

$$\Lambda\left(\frac{t}{T}\right) \triangleq \begin{cases} 1 - \frac{|t|}{T}, & |t| \leq T \\ 0, & |t| > T \end{cases} \quad (2-54)$$

These waveshapes are shown in Fig. 2-5. A tabulation of  $\text{Sa}(x)$  is given in Sec. A-9 (Appendix A).

### Example 2-5 SPECTRUM OF A RECTANGULAR PULSE

The spectrum is obtained by taking the Fourier transform of  $w(t) = \Pi(t/T)$ .

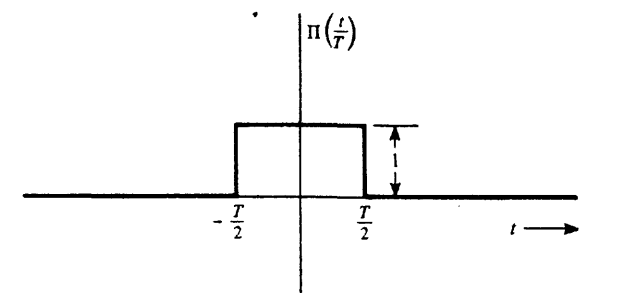
$$\begin{aligned} W(f) &= \int_{-T/2}^{T/2} 1 e^{-j\omega t} dt = \frac{e^{-j\omega T/2} - e^{j\omega T/2}}{-j\omega} \\ &= T \frac{\sin(\omega T/2)}{\omega T/2} = T \text{Sa}(\pi f T) \end{aligned}$$

Thus,

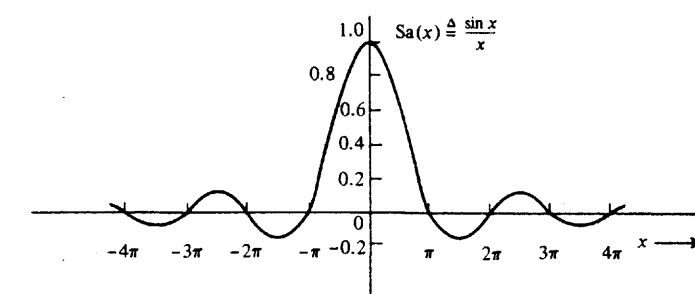
$$\Pi\left(\frac{t}{T}\right) \leftrightarrow T \text{Sa}(\pi f T) \quad (2-55)$$

This Fourier transform pair is shown in Fig. 2-6a. Note the inverse relationship between the pulse width  $T$  and the spectral zero crossing  $1/T$ . Also, by use of the duality theorem, the spectrum of a  $(\sin x)/x$  pulse is a rectangle. That is, realizing that  $\Pi(x)$  is an even function, and applying the duality theorem to (2-55), we get

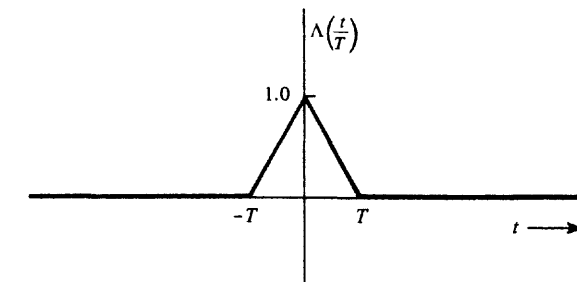
<sup>†</sup> This is related to the sinc function by  $\text{Sa}(x) = \text{sinc}(x/\pi)$  because  $\text{sinc}(\lambda) \triangleq (\sin \pi\lambda)/\pi\lambda$ . The notation  $\text{Sa}(x)$  and  $\text{sinc}(x)$  represent the same concept but can be confused because of scaling. In this book  $(\sin x)/x$  will often be used because it avoids confusion and does not take much more text space.



(a) Rectangular Pulse



(b) Sa(x) Function



(c) Triangular Function

Figure 2-5 Waveshapes and corresponding symbolic notation.

$$T \text{Sa}(\pi f T) \leftrightarrow \Pi\left(-\frac{f}{T}\right) = \Pi\left(\frac{f}{T}\right)$$

Replacing the parameter  $T$  by  $2W$ , we obtain the following Fourier transform pair.

$$2W \text{Sa}(2\pi f t) \leftrightarrow \Pi\left(\frac{f}{2W}\right) \quad (2-56)$$

where  $W$  is the absolute bandwidth in hertz. This Fourier transform pair is also shown in Fig. 2-6b.

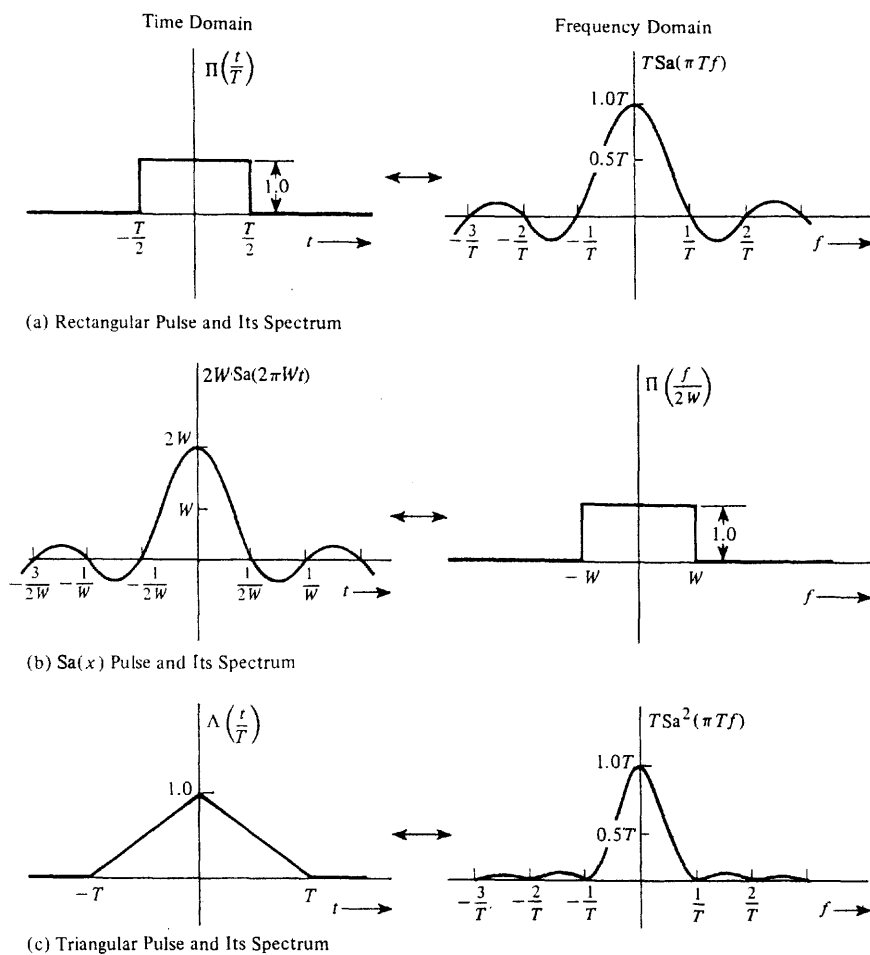


Figure 2-6 Spectra of rectangular,  $(\sin x)/x$ , and triangular pulses.

The spectra shown in Fig. 2-6 are real because the time domain pulses are real and even. If the pulses are offset in time to destroy the even symmetry, the spectra will be complex. For example, let

$$v(t) = \begin{cases} 1, & 0 < t < T \\ 0, & \text{elsewhere} \end{cases} = \Pi\left(\frac{t-T/2}{T}\right)$$

Then, using the time delay theorem and (2-55), we get the spectrum

$$V(f) = Te^{-j\pi fT} \text{Sa}(\pi fT) \quad (2-57)$$

In terms of quadrature notation, (2-57) becomes

$$V(f) = \underbrace{[T \text{Sa}(\pi fT) \cos(\pi fT)]}_{X(f)} + j \underbrace{[-T \text{Sa}(\pi fT) \sin(\pi fT)]}_{Y(f)} \quad (2-58)$$

Examining (2-57), the magnitude spectrum is

$$|V(f)| = T \left| \frac{\sin \pi fT}{\pi fT} \right| \quad (2-59)$$

and the phase spectrum is

$$\theta(f) = \underline{e^{-j\pi fT}} + \underline{\text{Sa}(\pi fT)} = -\pi fT + \begin{cases} 0, & \frac{n}{T} < |f| < \frac{n+1}{T}, & n_{\text{even}} \\ \pi, & \frac{n}{T} < |f| < \frac{n+1}{T}, & n_{\text{odd}} \end{cases} \quad (2-60)$$

### Example 2-6 SPECTRUM OF A TRIANGULAR PULSE

The spectrum may be evaluated directly by taking the Fourier transform of  $\Lambda(t/T)$  where the triangle is described by piecewise linear lines as shown in Fig. 2-6c. Another approach is to use the integral theorem. We will take the latter approach to demonstrate this technique. Let

$$w(t) = \Lambda(t/T)$$

Then

$$\frac{dw(t)}{dt} = \frac{1}{T} u(t+T) - \frac{2}{T} u(t) + \frac{1}{T} u(t-T)$$

and

$$\frac{d^2w(t)}{dt^2} = \frac{1}{T} \delta(t+T) - \frac{2}{T} \delta(t) + \frac{1}{T} \delta(t-T)$$

Consequently, we have the Fourier transform pair

$$\frac{d^2w(t)}{dt^2} \leftrightarrow \frac{1}{T} e^{j\omega T} - \frac{2}{T} + \frac{1}{T} e^{-j\omega T}$$

or

$$\frac{d^2w(t)}{dt^2} \leftrightarrow \frac{1}{T} (e^{j\omega T/2} - e^{-j\omega T/2})^2 = \frac{-4}{T} (\sin \pi fT)^2$$

Applying the integral theorem twice, we get

$$w(t) \leftrightarrow \frac{-4}{T} \frac{(\sin \pi fT)^2}{(j2\pi f)^2}$$

Thus

$$w(t) = \Lambda\left(\frac{t}{T}\right) \leftrightarrow T \text{Sa}^2(\pi fT) \quad (2-61)$$

This is illustrated in Fig. 2-6c.

## Convolution

The convolution operation, as first described in Table 2-1, is very useful. Later, we will show that the convolution operation can be used to describe the waveform at the output of a linear system.

**DEFINITION.** The *convolution* of a waveform  $w_1(t)$  with a waveform  $w_2(t)$  to produce a third waveform  $w_3(t)$  is

$$w_3(t) = w_1(t) * w_2(t) \triangleq \int_{-\infty}^{\infty} w_1(\lambda) w_2(t - \lambda) d\lambda \quad (2-62a)$$

where  $w_1(t) * w_2(t)$  is shorthand notation that delineates this integral operation and  $*$  is read "convolved with."

When this integral is examined, we realize that  $t$  is a parameter and  $\lambda$  is the variable of integration.

If discontinuous waveshapes are to be convolved, it is usually easier to evaluate the equivalent integral

$$w_3(t) = \int_{-\infty}^{\infty} w_1(\lambda) w_2(-(\lambda - t)) d\lambda \quad (2-62b)$$

Thus, the integrand for (2-62b) is obtained by

1. Time reversal of  $w_2$  to obtain  $w_2(-\lambda)$
2. Time shifting of  $w_2$  to obtain  $w_2(-(\lambda - t))$
3. Multiplying this result by  $w_1$  to form the integrand  $w_1(\lambda) w_2(-(\lambda - t))$

These three operations are illustrated in the following examples.

### Example 2-7 CONVOLUTION OF A RECTANGLE WITH AN EXPONENTIAL

Let

$$w_1(t) = \Pi\left(\frac{t - \frac{1}{2}T}{T}\right) \quad \text{and} \quad w_2(t) = e^{-t/T} u(t)$$

as shown in Fig. 2-7. Implementing step 3 above with the help of the figure, the convolution of  $w_1(t)$  with  $w_2(t)$  is 0 if  $t < 0$  because the product  $w_1(\lambda) w_2(-(\lambda - t))$  is zero for all values of  $\lambda$ . If  $0 < t < T$ , (2-62b) becomes

$$w_3(t) = \int_0^t 1 e^{+(\lambda-t)/T} d\lambda = T(1 - e^{-t/T})$$

If  $t > T$ , then (2-62b) becomes

$$w_3(t) = \int_0^T 1 e^{+(\lambda-t)/T} d\lambda = T(e - 1) e^{-t/T}$$

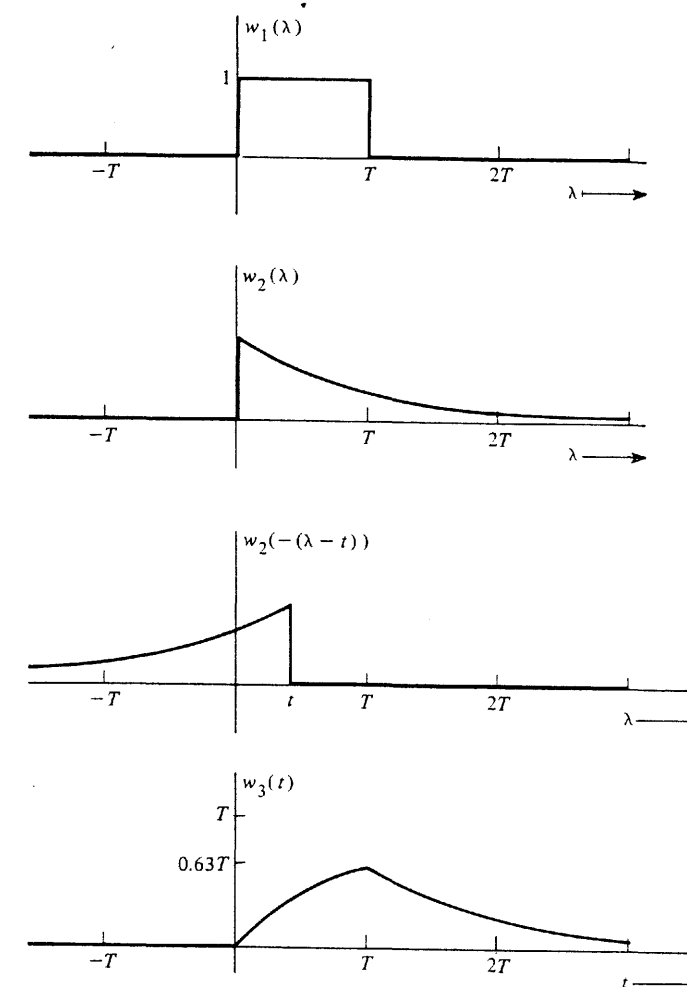


Figure 2-7 Convolution of a rectangle and an exponential.

Thus,

$$w_3(t) = \begin{cases} 0, & t < 0 \\ T(1 - e^{-t/T}), & 0 < t < T \\ T(e - 1)e^{-t/T}, & t > T \end{cases}$$

This result is plotted in Fig. 2-7.

### Example 2-8 SPECTRUM OF A TRIANGULAR PULSE BY CONVOLUTION

In Example 2-6 the spectrum of a triangular pulse was evaluated by using the integral theorem. The same result can be obtained by using the convolution theorem of Table 2-1. If the rectan-

angular pulse of Fig. 2-6a is convolved with itself and then scaled (i.e., multiplied) by the constant  $1/T$ , the resulting time waveform is the triangular pulse of Fig. 2-6c. Applying the convolution theorem, we obtain the spectrum for the triangular pulse by multiplying the spectrum of the rectangular pulse (of Fig. 2-6a) with itself and scaling with a constant  $1/T$ . As expected, the result is the spectrum shown in Fig. 2-6c.

### Example 2-9 SPECTRUM OF A SWITCHED SINUSOID

In Example 2-4 a continuous sinusoid was found to have a line spectrum with the lines located at  $f = \pm f_0$ . In this example we will see how the spectrum changes when the sinusoid is switched on and off. The switched sinusoid can be represented by

$$w(t) = \Pi\left(\frac{t}{T}\right) A \sin \omega_0 t = \Pi\left(\frac{t}{T}\right) A \cos\left(\omega_0 t - \frac{\pi}{2}\right)$$

Using (2-55) and the real signal translation theorem of Table 2-1, we see that the spectrum of this switched sinusoid is

$$W(f) = j \frac{A}{2} T[\text{Sa}(\pi T(f + f_0)) - \text{Sa}(\pi T(f - f_0))] \quad (2-63)$$

This spectrum is continuous and imaginary. The magnitude spectrum is shown in Fig. 2-8. Compare this continuous spectrum of Fig. 2-8 with the discrete spectrum obtained for the continuous sine wave, as shown in Fig. 2-4a. In addition, note that if the duration of the switched sinusoid is allowed to become very large (i.e.,  $T \rightarrow \infty$ ), the continuous spectrum of Fig. 2-8 becomes the discrete spectrum of Fig. 2-4a by the use of (A-103) in Appendix A.

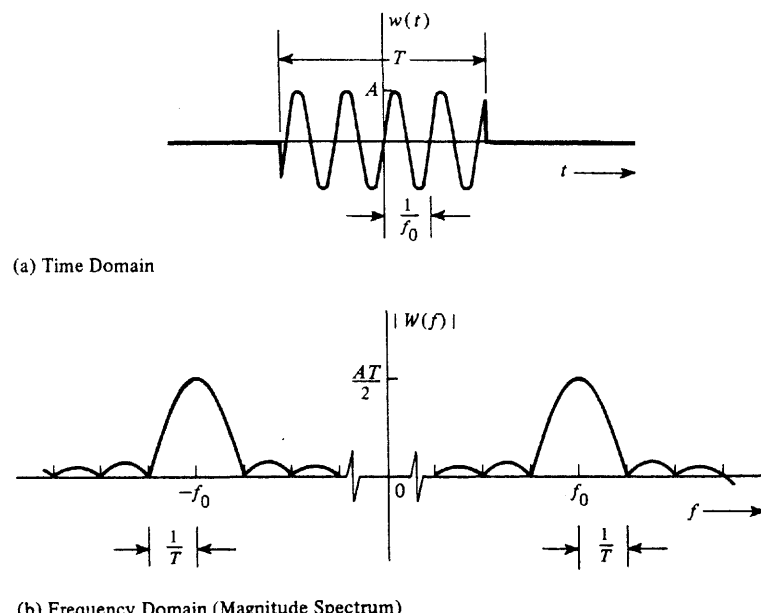


Figure 2-8 Waveform and spectrum of a switched sinusoid.

The spectrum for the switched sinusoid may also be evaluated using a different approach. The multiplication theorem of Table 2-1 may be used where  $w_1(t) = \Pi(t/T)$  and  $w_2(t) = A \sin \omega_0 t$ . Here the spectrum of the switched sinusoid is obtained by working a convolution problem in the frequency domain:

$$W(f) = W_1(f) * W_2(f) = \int_{-\infty}^{\infty} W_1(\lambda) W_2(f - \lambda) d\lambda$$

This convolution integral is easy to evaluate because the spectrum of  $w_2(t)$  consists of two delta functions. The details of this approach are left as a homework exercise for the reader.

A summary of Fourier transform pairs is given in Table 2-2. Numerical techniques using the discrete Fourier transform are discussed in Sec. 2-8.

TABLE 2-2 SOME FOURIER TRANSFORM PAIRS

Function	Time Waveform $w(t)$	Spectrum $W(f)$
Rectangular	$\Pi\left(\frac{t}{T}\right)$	$T[\text{Sa}(\pi f T)]$
Triangular	$\Lambda\left(\frac{t}{T}\right)$	$T[\text{Sa}(\pi f T)]^2$
Unit step	$u(t) \triangleq \begin{cases} +1, & t > 0 \\ 0, & t < 0 \end{cases}$	$\frac{1}{2} \delta(f) + \frac{1}{j2\pi f}$
Signum	$\text{sgn}(t) \triangleq \begin{cases} +1, & t > 0 \\ -1, & t < 0 \end{cases}$	$\frac{1}{j\pi f}$
Constant	1	$\delta(f)$
Impulse at $t = t_0$	$\delta(t - t_0)$	$e^{-j2\pi f t_0}$
Sinc	$\text{Sa}(2\pi Wt)$	$\frac{1}{2W} \Pi\left(\frac{f}{2W}\right)$
Phasor	$e^{j(\omega_0 t + \varphi)}$	$e^{j\varphi} \delta(f - f_0)$
Sinusoid	$\cos(\omega_0 t + \varphi)$	$\frac{1}{2} e^{j\varphi} \delta(f - f_0) + \frac{1}{2} e^{-j\varphi} \delta(f + f_0)$
Gaussian	$e^{-\pi(t/t_0)^2}$	$t_0 e^{-\pi(f/f_0)^2}$
Exponential, one-sided	$\begin{cases} e^{-tf}, & t > 0 \\ 0, & t < 0 \end{cases}$	$\frac{T}{1 + j2\pi f T}$
Exponential, two-sided	$e^{- t /T}$	$\frac{2T}{1 + (2\pi f T)^2}$
Impulse train	$\sum_{k=-\infty}^{k=\infty} \delta(t - kT)$	$f_0 \sum_{n=-\infty}^{n=\infty} \delta(f - nf_0),$ where $f_0 = 1/T$

## 2-3 POWER SPECTRAL DENSITY AND AUTOCORRELATION FUNCTION

### Power Spectral Density

The normalized power of a waveform will now be related to its frequency domain description by the use of a function called the *power spectral density (PSD)*. The PSD is very useful in describing how the power content of signals and noise is affected by filters and other devices in communication systems. In (2-42) the energy spectral density (ESD) was defined in terms of the magnitude squared version of the Fourier transform of the waveform. The PSD will be defined in a similar way. The PSD is more useful than the ESD since power-type models are generally used in solving communication problems.

First, define the truncated version of the waveform by

$$w_T(t) = \begin{cases} w(t), & -T/2 < t < T/2 \\ 0, & \text{elsewhere} \end{cases} = w(t)\Pi\left(\frac{t}{T}\right) \quad (2-64)$$

Using (2-13), we obtain the average normalized power

$$P = \lim_{T \rightarrow \infty} \frac{1}{T} \int_{-T/2}^{T/2} w^2(t) dt = \lim_{T \rightarrow \infty} \frac{1}{T} \int_{-\infty}^{\infty} w_T^2(t) dt$$

By the use of Parseval's theorem, (2-41), this becomes

$$P = \lim_{T \rightarrow \infty} \frac{1}{T} \int_{-\infty}^{\infty} |W_T(f)|^2 df = \int_{-\infty}^{\infty} \left( \lim_{T \rightarrow \infty} \frac{|W_T(f)|^2}{T} \right) df \quad (2-65)$$

where  $W_T(f) = \mathcal{F}[w_T(t)]$ . The integrand of the right-hand integral has units of watts/hertz (or, equivalently, volts<sup>2</sup>/hertz or amperes<sup>2</sup>/hertz, as appropriate) and can be defined as the PSD.

**DEFINITION.** The *power spectral density (PSD)* for a deterministic power waveform is<sup>†</sup>

$$\mathcal{P}_w(f) \triangleq \lim_{T \rightarrow \infty} \left( \frac{|W_T(f)|^2}{T} \right) \quad (2-66)$$

where  $w_T(t) \leftrightarrow W_T(f)$  and  $\mathcal{P}_w(f)$  has units of watts per hertz.

Note that the PSD is always a real nonnegative function of frequency. In addition, the PSD is not sensitive to the phase spectrum of  $w(t)$  because that is lost because of the absolute value operation used in (2-66). From (2-65), the normalized average power is<sup>‡</sup>

<sup>†</sup> Equations (2-66) and (2-67) give normalized (with respect to  $1 \Omega$ ) PSD and average power, respectively. For unnormalized (i.e., actual) values,  $\mathcal{P}_w(f)$  is replaced by the appropriate expression as follows. If  $w(t)$  is a voltage waveform that appears across a resistive load of  $R$  ohms, the unnormalized PSD is  $\mathcal{P}_w(f)/R$  W/Hz, where  $\mathcal{P}_w(f)$  has units of volts<sup>2</sup>/Hz. Similarly, if  $w(t)$  is a current waveform passing through a resistive load of  $R$  ohms, the unnormalized PSD is  $\mathcal{P}_w(f)R$  W/Hz, where  $\mathcal{P}_w(f)$  has units of amperes<sup>2</sup>/Hz.

$$P = \langle w^2(t) \rangle = \int_{-\infty}^{\infty} \mathcal{P}_w(f) df \quad (2-67)$$

That is, the area under the PSD function is the normalized average power.

### Autocorrelation Function

A related function called the *autocorrelation*,  $R(\tau)$ , can also be defined.<sup>†</sup>

**DEFINITION.** The *autocorrelation* of a real (physical) waveform is<sup>‡</sup>

$$R_w(\tau) \triangleq \langle w(t)w(t + \tau) \rangle = \lim_{T \rightarrow \infty} \frac{1}{T} \int_{-T/2}^{T/2} w(t)w(t + \tau) dt \quad (2-68)$$

Furthermore, it can be shown that the PSD and the autocorrelation function are Fourier transform pairs.

$$R_w(\tau) \leftrightarrow \mathcal{P}_w(f) \quad (2-69)$$

where  $\mathcal{P}_w(f) = \mathcal{F}[R_w(\tau)]$ . This is called the *Wiener-Khintchine theorem*. This theorem, along with properties for  $R(\tau)$  and  $\mathcal{P}(f)$ , are developed in detail in Chapter 6 using the more general theory of random processes that is applicable to nondeterministic waveforms.

In summary, the PSD can be evaluated by either of the two following methods:

1. Direct evaluation using the definition, (2-66)<sup>§</sup>
2. Indirect evaluation by first evaluating the autocorrelation function and then taking the Fourier transform,  $\mathcal{P}_w(f) = \mathcal{F}[R_w(\tau)]$

Furthermore, the total average normalized power for the waveform  $w(t)$  can be evaluated using any of the following four techniques:

$$P = \langle w^2(t) \rangle = W_{\text{rms}}^2 = \int_{-\infty}^{\infty} \mathcal{P}_w(f) df = R_w(0) \quad (2-70)$$

### Example 2-10 PSD OF A SINUSOID

Let

$$w(t) = A \sin \omega_0 t$$

<sup>†</sup> Here a time average is used in the definition of the autocorrelation function. In Chapter 6 an ensemble (statistical) average is used in the definition of  $R(\tau)$ . As shown in Chapter 6, these two definitions are equal if  $w(t)$  is ergodic.

<sup>‡</sup> The autocorrelation of a complex waveform is  $R_w(\tau) \triangleq \langle w^*(t)w(t + \tau) \rangle$ .

<sup>§</sup> Direct evaluation is usually more difficult than indirect evaluation.

The PSD will be evaluated using the indirect method. The autocorrelation is

$$\begin{aligned} R_w(\tau) &= \langle w(t)w(t + \tau) \rangle \\ &= \lim_{T \rightarrow \infty} \frac{1}{T} \int_{-T/2}^{T/2} A^2 \sin \omega_0 t \sin \omega_0(t + \tau) dt \end{aligned}$$

Using a trigonometric identity, (A-12), we obtain

$$R_w(\tau) = \frac{A^2}{2} \cos \omega_0 \tau \lim_{T \rightarrow \infty} \frac{1}{T} \int_{-T/2}^{T/2} dt - \frac{A^2}{2} \lim_{T \rightarrow \infty} \frac{1}{T} \int_{-T/2}^{T/2} \cos(2\omega_0 t + \omega_0 \tau) dt$$

which reduces to

$$R_w(\tau) = \frac{A^2}{2} \cos \omega_0 \tau \quad (2-71)$$

The PSD is then

$$\mathcal{P}_w(f) = \mathcal{F}\left[\frac{A^2}{2} \cos \omega_0 \tau\right] = \frac{A^2}{4} [\delta(f - f_0) + \delta(f + f_0)] \quad (2-72)$$

as shown in Fig. 2-9. It may be compared to the "voltage" spectrum for a sinusoid that was obtained in Example 2-4 and shown in Fig. 2-4.

The average normalized power may be obtained by using (2-67):

$$P = \int_{-\infty}^{\infty} \frac{A^2}{4} [\delta(f - f_0) + \delta(f + f_0)] df = \frac{A^2}{2} \quad (2-73)$$

This value,  $A^2/2$ , checks with the known result for the normalized power of a sinusoid:

$$P = \langle w^2(t) \rangle = W_{\text{rms}}^2 = (A/\sqrt{2})^2 = A^2/2 \quad (2-74)$$

It is also realized that  $A \sin \omega_0 t$  and  $A \cos \omega_0 t$  have exactly the same PSD (and autocorrelation function) because the phase has no effect on the PSD. This can be verified by evaluating the PSD for  $A \cos \omega_0 t$ , using the same procedure that was used earlier to evaluate the PSD for  $A \sin \omega_0 t$ .

Thus far, properties of signals and noise such as spectrum, average power, and rms value have been studied, but how do we represent the signal or noise waveform itself? The direct approach is to write a closed-form mathematical equation for the waveform itself. Other equivalent ways of modeling the waveform are often found to be very useful. One, which

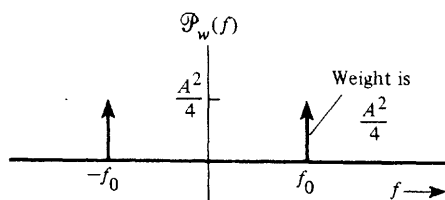


Figure 2-9 Power spectrum of a sinusoid.

the reader has already studied in calculus, is to represent the waveform by the use of a Taylor series (i.e., power series) expansion about a point  $a$ :

$$w(t) = \sum_{n=0}^{\infty} \frac{w^{(n)}(a)}{n!} (t - a)^n \quad (2-75)$$

where

$$w^{(n)}(a) = \left. \frac{d^n w(t)}{dt^n} \right|_{t=a} \quad (2-76)$$

In this case, if the derivatives at  $t = a$ ,  $\{w^{(n)}(a)\}$ , are known, this algorithm can be used to reconstruct the waveform. Another type of series representation that is especially useful in communication problems is the orthogonal series expansion, which is discussed in the next section.

## 2-4 ORTHOGONAL SERIES REPRESENTATION OF SIGNALS AND NOISE

An orthogonal series representation for signals and noise has many significant applications in communication problems such as Fourier series, sampling function series, and representation of digital signals. Because these specific cases are so important, they will be studied in some detail in sections that follow.

### Orthogonal Functions

Before the orthogonal series is studied, a definition for orthogonal functions is needed.

**DEFINITION.** Functions  $\varphi_n(t)$  and  $\varphi_m(t)$  are said to be *orthogonal* with respect to each other over the interval  $a < t < b$  if they satisfy the condition

$$\int_a^b \varphi_n(t) \varphi_m^*(t) dt = 0 \quad \text{where } n \neq m \quad (2-77)$$

Furthermore, if the functions in the set  $\{\varphi_n(t)\}$  are orthogonal, then they also satisfy the relation

$$\int_a^b \varphi_n(t) \varphi_m^*(t) dt = \begin{cases} 0, & n \neq m \\ K_n, & n = m \end{cases} = K_n \delta_{nm} \quad (2-78)$$

where

$$\delta_{nm} \triangleq \begin{cases} 0, & n \neq m \\ 1, & n = m \end{cases} \quad (2-79)$$

$\delta_{nm}$  is called the *Kronecker delta function*. If the constants  $K_n$  are all equal to 1, the  $\varphi_n(t)$  are said to be *orthonormal functions*.<sup>†</sup>

In other words, (2-77) is used to test pairs of functions to see if they are orthogonal. They are orthogonal over the interval  $(a, b)$  if the integral of their product is zero. The zero result implies that these functions are “independent” or in “disagreement.” If the result is not zero, they are not orthogonal, and consequently, the two functions have some “dependence” or “alikeness” to each other.

### Example 2-11 ORTHOGONAL COMPLEX EXPONENTIAL FUNCTIONS

Show that the set of complex exponential functions  $\{e^{jn\omega_0 t}\}$  are orthogonal over the interval  $a < t < b$  where  $b = a + T_0$ ,  $T_0 = 1/f_0$ ,  $\omega_0 = 2\pi f_0$  and  $n$  is an integer.

**Solution.** Substitute  $\varphi_n(t) = e^{jn\omega_0 t}$  and  $\varphi_m(t) = e^{jm\omega_0 t}$  into (2-77). We get

$$\begin{aligned} \int_a^b \varphi_n(t) \varphi_m^*(t) dt &= \int_a^{a+T_0} e^{jn\omega_0 t} e^{-jm\omega_0 t} dt = \int_a^{a+T_0} e^{j(n-m)\omega_0 t} dt \\ &= \int_a^{a+T_0} \end{aligned} \quad (2-80)$$

For  $m \neq n$  this becomes

$$\int_a^{a+T_0} e^{j(n-m)\omega_0 t} dt = \frac{e^{j(n-m)\omega_0 a} [e^{j(n-m)\omega_0 2T_0} - 1]}{j(n-m)\omega_0} = 0 \quad (2-81)$$

since  $e^{j(n-m)\omega_0 2T_0} = \cos[2\pi(n-m)] + j \sin[2\pi(n-m)] = 1$ . Thus (2-77) is satisfied and, consequently, the complex exponential functions are orthogonal to each other over the interval  $a < t < a + T_0$  where  $a$  is any real constant.

Also, for the case  $n = m$ , (2-80) becomes

$$\int_a^{a+T_0} \varphi_n(t) \varphi_n^*(t) dt = \int_a^{a+T_0} 1 dt = T_0 \quad (2-82)$$

Using this in (2-78), we find that  $K_n = T_0$  for all (integer) values of  $n$ . Because  $K_n \neq 1$ , these  $\varphi_n(t)$  are not orthonormal (but they are orthogonal). An orthonormal set of exponential functions is obtained by scaling the old set, where the functions in the new set are

$$\varphi_n(t) = \frac{1}{\sqrt{T_0}} e^{jn\omega_0 t}$$

### Orthogonal Series

Assume that  $w(t)$  represents some practical waveform (signal, noise, or signal-noise combination) that we wish to represent over the interval  $a < t < b$ . Then we can obtain an equivalent orthogonal series representation by using the following theorem.

<sup>†</sup> To normalize a set of functions, take each old  $\varphi_n(t)$  and divide it by  $\sqrt{K_n}$  to form the normalized  $\varphi_n(t)$ .

**THEOREM.**  $w(t)$  can be represented over the interval  $(a, b)$  by the series

$$w(t) = \sum_n a_n \varphi_n(t) \quad (2-83)$$

where the orthogonal coefficients are given by

$$a_n = \frac{1}{K_n} \int_a^b w(t) \varphi_n^*(t) dt \quad (2-84)$$

and the range of  $n$  is over the integer values that correspond to the subscripts that were used to denote the orthogonal functions in the complete orthogonal set.

For (2-83) to be a valid representation for any physical signal (i.e., one with finite energy), the orthogonal set has to be complete. This implies that the set  $\{\varphi_n(t)\}$  can be used to represent any function with an arbitrarily small error [Wylie, 1960]. In practice, it is usually difficult to prove that a given set of functions is complete. It can be shown that the complex exponential set and the harmonic sinusoidal sets that are used for the Fourier series in Sec. 2-5 are complete [Courant and Hilbert, 1953]. Many other useful sets are also complete such as Bessel functions, Legendre polynomials, and the  $(\sin x)/x$ -type sets [described by (2-161)].

**Proof of Theorem.** Assume that the set  $\{\varphi_n(t)\}$  is sufficient to represent the waveform. Then in order for (2-83) to be correct, we only need to show that we can evaluate the  $a_n$ . Using (2-83), we operate on both sides of this equation with the integral operator

$$\int_a^b [\cdot] \varphi_m^*(t) dt \quad (2-85)$$

obtaining

$$\begin{aligned} \int_a^b [w(t)] \varphi_m^*(t) dt &= \int_a^b \left[ \sum_n a_n \varphi_n(t) \right] \varphi_m^*(t) dt \\ &= \sum_n a_n \int_a^b \varphi_n(t) \varphi_m^*(t) dt = \sum_n a_n K_n \delta_{nm} \\ &= a_m K_m \end{aligned} \quad (2-86)$$

Thus (2-84) follows.

The orthogonal series is very useful in representing a signal, noise, or a signal-noise combination. The orthogonal functions  $\varphi_j(t)$  are deterministic. Furthermore, if the waveform  $w(t)$  is deterministic, the constants  $\{a_j\}$  are also deterministic and may be evaluated using (2-84). In Chapter 6 we will see that if  $w(t)$  is stochastic (e.g., in a noise problem), the  $\{a_j\}$  are a set of random variables that give the desired random process  $w(t)$ .

It is also possible to use (2-83) to generate  $w(t)$  from the  $\varphi_j(t)$  functions and the coefficients  $a_j$ . In this case  $w(t)$  is approximated by using a reasonable number of the  $\varphi_j(t)$

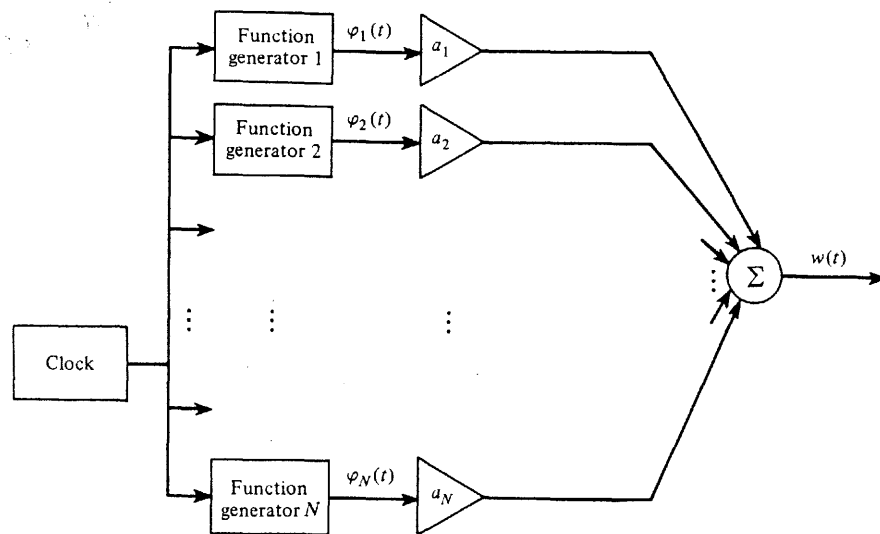


Figure 2-10 Waveform synthesis using orthogonal functions.

functions. As shown in Fig. 2-10, for the case of real values for  $a_j$  and real functions for  $\varphi_j(t)$ ,  $w(t)$  can be synthesized by adding up weighted versions of  $\varphi_j(t)$  where the weighting factors are given by  $\{a_j\}$ . The summing and gain weighting operation may be conveniently realized by using an operational amplifier with multiple inputs.

## 2-5 FOURIER SERIES

The Fourier series is a particular type of orthogonal series representation that is very useful in solving engineering problems, especially communication problems. The orthogonal functions that are used are either sinusoids, or, equivalently, complex exponential functions.<sup>†</sup>

### Complex Fourier Series

The complex Fourier series uses the orthogonal exponential functions.

$$\varphi_n(t) = e^{jn\omega_0 t} \quad (2-87)$$

where  $n$  ranges over all possible integer values, negative, positive, and zero;  $\omega_0 = 2\pi/T_0$ , where  $T_0 = (b - a)$  is the length of the interval over which the series, (2-83), is valid; and from Example 2-11,  $K_n = T_0$ . Using (2-83), the Fourier series theorem follows.

**THEOREM.** A physical waveform (i.e., finite energy) may be represented over the interval  $a < t < a + T_0$  by the complex exponential Fourier series

<sup>†</sup> Mathematicians generally call any orthogonal series a Fourier series.

$$w(t) = \sum_{n=-\infty}^{\infty} c_n e^{jn\omega_0 t} \quad (2-88)$$

where the complex (phasor) Fourier coefficients  $c_n$  are given by

$$c_n = \frac{1}{T_0} \int_a^{a+T_0} w(t) e^{-jn\omega_0 t} dt \quad (2-89)$$

and  $\omega_0 = 2\pi f_0 = 2\pi/T_0$ .

If the waveform  $w(t)$  is periodic with period  $T_0$ , this Fourier series representation is valid over all time (i.e., over the interval  $-\infty < t < +\infty$ ) because the  $\varphi_n(t)$  are periodic functions that have a common fundamental period  $T_0$ . For this case of periodic waveforms, the choice of a value for the parameter  $a$  is arbitrary, and it is usually taken to be  $a = 0$  or  $a = -T_0/2$  for mathematical convenience. The frequency  $f_0 = 1/T_0$  is said to be the fundamental frequency, and the frequency  $nf_0$  is said to be the  $n$ th harmonic frequency, when  $n > 1$ . The Fourier coefficient  $c_0$  is equivalent to the dc value of the waveform  $w(t)$ , because the integral is identical to that of (2-4) when  $n = 0$ .

$c_n$  is, in general, a complex number. Furthermore, it is a phasor since it is the coefficient of a function of the type  $e^{jn\omega_0 t}$ . Consequently, (2-88) is said to be a complex or phasor Fourier series.

Some properties of the complex Fourier series are as follows.

1. If  $w(t)$  is real,

$$c_n = c_{-n}^* \quad (2-90)$$

2. If  $w(t)$  is real and even [i.e.,  $w(t) = w(-t)$ ],

$$\text{Im}[c_n] = 0 \quad (2-91)$$

3. If  $w(t)$  is real and odd [i.e.,  $w(t) = -w(-t)$ ],

$$\text{Re}[c_n] = 0$$

4. Parseval's theorem is

$$\frac{1}{T_0} \int_a^{a+T_0} |w(t)|^2 dt = \sum_{n=-\infty}^{\infty} |c_n|^2 \quad (2-92)$$

See (2-125) for the proof.

5. The complex Fourier series coefficients of a real waveform are related to the quadrature Fourier series coefficients by

$$c_n = \begin{cases} \frac{1}{2} a_n - j \frac{1}{2} b_n, & n > 0 \\ a_0, & n = 0 \\ \frac{1}{2} a_{-n} + j \frac{1}{2} b_{-n}, & n < 0 \end{cases} \quad (2-93)$$

See (2-96), (2-97) and (2-98).

6. The complex Fourier series coefficients of a real waveform are related to the polar Fourier series coefficients by

$$c_n = \begin{cases} \frac{1}{2} D_n \angle \varphi_n, & n > 0 \\ D_0, & n = 0 \\ \frac{1}{2} D_{-n} \angle -\varphi_{-n}, & n < 0 \end{cases} \quad (2-94)$$

See (2-106) and (2-107).

Note that these properties for the complex Fourier series coefficients are similar to those of the Fourier transform as given in Sec. 2-2.

### Quadrature Fourier Series

The *quadrature* form of the Fourier series representing any physical waveform  $w(t)$  over the interval  $a < t < a + T_0$  is

$$w(t) = \sum_{n=0}^{n=\infty} a_n \cos n\omega_0 t + \sum_{n=1}^{n=\infty} b_n \sin n\omega_0 t \quad (2-95)$$

where the orthogonal functions are  $\cos n\omega_0 t$  and  $\sin n\omega_0 t$ . Using (2-77), we find that these Fourier coefficients are given by

$$a_n = \begin{cases} \frac{1}{T_0} \int_a^{a+T_0} w(t) dt, & n = 0 \\ \frac{2}{T_0} \int_a^{a+T_0} w(t) \cos n\omega_0 t dt, & n \geq 1 \end{cases} \quad (2-96)$$

and

$$b_n = \frac{2}{T_0} \int_a^{a+T_0} w(t) \sin n\omega_0 t dt, \quad n > 0 \quad (2-97)$$

Once again, because these sinusoidal orthogonal functions are periodic, this series is periodic with the fundamental period  $T_0$ , and if  $w(t)$  is periodic with period  $T_0$ , the series will represent  $w(t)$  over the whole real line (i.e.,  $-\infty < t < \infty$ ).

The complex Fourier series, (2-88), and the quadrature Fourier series, (2-95), are equivalent representations. This can be demonstrated by expressing the complex number  $c_n$  in terms of its conjugate parts,  $x_n$  and  $y_n$ . That is, using (2-89),

$$\begin{aligned} c_n &= x_n + jy_n \\ &= \left[ \frac{1}{T_0} \int_a^{a+T_0} w(t) \cos n\omega_0 t dt \right] + j \left[ \frac{-1}{T_0} \int_a^{a+T_0} w(t) \sin n\omega_0 t dt \right] \end{aligned} \quad (2-98)$$

for all integer values of  $n$ . Thus,

$$x_n = \frac{1}{T_0} \int_a^{a+T_0} w(t) \cos n\omega_0 t dt \quad (2-99)$$

and

$$y_n = \frac{-1}{T_0} \int_a^{a+T_0} w(t) \sin n\omega_0 t dt \quad (2-100)$$

Using (2-96) and (2-97), we obtain the identities

$$a_n = \begin{cases} c_0, & n = 0 \\ 2x_n, & n \geq 1 \end{cases} = \begin{cases} c_0, & n = 0 \\ 2 \operatorname{Re}\{c_n\}, & n \geq 1 \end{cases} \quad (2-101)$$

and

$$b_n = -2y_n = -2 \operatorname{Im}\{c_n\}, \quad n \geq 1 \quad (2-102)$$

where  $\operatorname{Re}\{\cdot\}$  denotes the real part of  $\{\cdot\}$  and  $\operatorname{Im}\{\cdot\}$  denotes the imaginary part of  $\{\cdot\}$ .

### Polar Fourier Series

The quadrature Fourier series, (2-95), may be rearranged and written in a polar (amplitude-phase) form. The *polar* form is

$$w(t) = D_0 + \sum_{n=1}^{n=\infty} D_n \cos(n\omega_0 t + \varphi_n) \quad (2-103)$$

where  $w(t)$  is real and

$$a_n = \begin{cases} D_0, & n = 0 \\ D_n \cos \varphi_n, & n \geq 1 \end{cases} \quad (2-104)$$

$$b_n = -D_n \sin \varphi_n, \quad n \geq 1 \quad (2-105)$$

The latter two equations may be inverted, and we obtain

$$D_n = \begin{cases} a_0, & n = 0 \\ \sqrt{a_n^2 + b_n^2}, & n \geq 1 \end{cases} = \begin{cases} c_0, & n = 0 \\ 2|c_n|, & n \geq 1 \end{cases} \quad (2-106)$$

and

$$\varphi_n = -\tan^{-1} \left( \frac{b_n}{a_n} \right) = \angle c_n, \quad n \geq 1 \quad (2-107)$$

where the angle operator is defined by

$$\angle [\cdot] = \tan^{-1} \left( \frac{\operatorname{Im}[\cdot]}{\operatorname{Re}[\cdot]} \right) \quad (2-108)$$

It should be clear from the context whether  $\angle$  denotes the angle operator or the angle itself. For example,  $\angle 90^\circ$  denotes an angle of  $90^\circ$ , but  $\angle [1+j2]$  denotes the angle operator and is equal to  $63.4^\circ$  when evaluated.

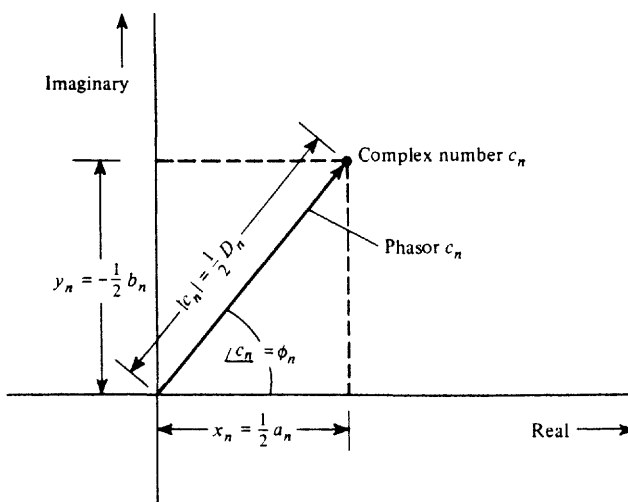


Figure 2-11 Fourier series coefficients,  $n \geq 1$ .

The equivalence between the Fourier series coefficients is demonstrated geometrically in Fig. 2-11. It is seen that, in general, when a physical (real) waveform  $w(t)$  is represented by a Fourier series,  $c_n$  is a complex number with a real part  $x_n$  and an imaginary part  $y_n$  (which are both real numbers) and, consequently,  $a_n$ ,  $b_n$ ,  $D_n$ , and  $\phi_n$  are real numbers. In addition,  $D_n$  is a nonnegative number for  $n \geq 1$ . Furthermore, all of these coefficients describe the amount of frequency component contained in the signal at the frequency of  $nf_0$  Hz.

In practice the Fourier series (FS) is often *truncated* to a finite number of terms. For example, 5 or 10 harmonics might be used to approximate the FS series for a square wave. Thus, an important question arises: For the finite series, are the optimum values for the series coefficients the same as those for the corresponding terms in the infinite series, or should the coefficients for the finite series be adjusted to some new values to give the best finite-series approximation? The answer: The optimum values for the coefficients of the truncated FS are the same as those for the corresponding terms in the nontruncated FS.<sup>†</sup>

As we have seen, the complex, quadrature, and polar form of the Fourier series are all equivalent, but the question is: *Which is the best form to use?* The answer is that it depends on the particular problem being solved! If the problem is being solved analytically, the complex coefficients are *usually* easier to evaluate. On the other hand, if measurements of a waveform are being made in a laboratory, the polar form is usually more convenient since measuring instruments, such as voltmeters, scopes, vector voltmeters, and wave analyzers, usually give magnitude and phase readings. Using the laboratory results, engineers often draw *one-sided* spectral plots where lines are drawn corresponding to each  $D_n$  value at  $f = nf_0$ , where  $n \geq 0$  (i.e., positive frequencies only). Of course, this one-sided spectral plot may be converted to the two-sided spectrum given by the  $c_n$  plot by using (2-94). It is understood that the actual spectrum is defined to be the Fourier transform of  $w(t)$  and consists

<sup>†</sup> For a proof of this statement see [Couch, 1995].

of two two-sided plots, one plot for  $|c_n|$  and the other for  $\angle c_n$ .

### Line Spectra for Periodic Waveforms

For *periodic* waveforms, the Fourier series representations are valid  $-\infty < t < \infty$ . Consequently, the (two-sided) spectrum, which depends from  $t = -\infty$  to  $t = \infty$ , may be evaluated in terms of Fourier coefficients.

**THEOREM.** *If a waveform is periodic with period  $T_0$ , the spectrum of the waveform  $w(t)$  is*

$$W(f) = \sum_{n=-\infty}^{n=\infty} c_n \delta(f - nf_0) \quad (2-109)$$

where  $f_0 = 1/T_0$  and  $c_n$  are the phasor Fourier coefficients of the waveform as given by (2-89).

*Proof.*

$$w(t) = \sum_{n=-\infty}^{n=\infty} c_n e^{jn\omega_0 t}$$

Taking the Fourier transform of both sides, we obtain

$$\begin{aligned} W(f) &= \int_{-\infty}^{\infty} \left( \sum_{n=-\infty}^{n=\infty} c_n e^{jn\omega_0 t} \right) e^{-j\omega t} dt \\ &= \sum_{n=-\infty}^{n=\infty} c_n \int_{-\infty}^{\infty} e^{-j2\pi(f-nf_0)t} dt = \sum_{n=-\infty}^{n=\infty} c_n \delta(f - nf_0) \end{aligned}$$

where the integral representation for a delta function, (2-48), was used.

This theorem indicates that a periodic function *always* has a line (delta function) spectrum with the lines being at  $f = nf_0$  and having weights given by the  $c_n$  values. An illustration of this property was given by Example 2-4, where  $c_1 = -jA/2$  and  $c_{-1} = jA/2$  and the other  $c_n$ 's were zero. It is also obvious that there is no dc component since there is no line at  $f = 0$  (i.e.,  $c_0 = 0$ ). Conversely, if a function does not contain any periodic component, the spectrum will be continuous (no lines) except for a line at  $f = 0$  when the function has a dc component.

It is also possible to evaluate the Fourier coefficients by sampling the Fourier transform of a pulse corresponding to  $w(t)$  over a period. This is shown by the following theorem.

**THEOREM.** *If  $w(t)$  is a periodic function with period  $T_0$  and is represented by*

$$w(t) = \sum_{n=-\infty}^{n=\infty} h(t - nT_0) = \sum_{n=-\infty}^{n=\infty} c_n e^{jn\omega_0 t} \quad (2-110)$$

where

$$h(t) = \begin{cases} w(t), & |t| < \frac{T_0}{2} \\ 0, & t \text{ elsewhere} \end{cases} \quad (2-111)$$

then the Fourier coefficients are given by

$$c_n = f_0 H(nf_0) \quad (2-112)$$

where  $H(f) = \mathcal{F}[h(t)]$  and  $f_0 = 1/T_0$ .

*Proof.*

$$w(t) = \sum_{n=-\infty}^{\infty} h(t - nT_0) = \sum_{n=-\infty}^{\infty} h(t) * \delta(t - nT_0) \quad (2-113)$$

where  $*$  denotes the convolution operation. Thus,

$$w(t) = h(t) * \sum_{n=-\infty}^{\infty} \delta(t - nT_0) \quad (2-114)$$

But the impulse train may itself be represented by its Fourier series<sup>†</sup>

$$\sum_{n=-\infty}^{\infty} \delta(t - nT_0) = \sum_{n=-\infty}^{\infty} c_n e^{jn\omega_0 t} \quad (2-115)$$

where all the Fourier coefficients are just  $c_n = f_0$ . Substituting (2-115) into (2-114), we obtain

$$w(t) = h(t) * \sum_{n=-\infty}^{\infty} f_0 e^{jn\omega_0 t} \quad (2-116)$$

Taking the Fourier transform of both sides of (2-116), we have

$$\begin{aligned} W(f) &= H(f) \sum_{n=-\infty}^{\infty} f_0 \delta(f - nf_0) \\ &= \sum_{n=-\infty}^{\infty} [f_0 H(nf_0)] \delta(f - nf_0) \end{aligned} \quad (2-117)$$

Comparing (2-117) with (2-109), we see that (2-112) follows.

This theorem is useful for evaluating the Fourier coefficients  $c_n$  when the Fourier transform of the fundamental pulse shape  $h(t)$  for the periodic waveform is known or can be obtained easily (such as from a Fourier transform table, e.g., Table 2-2).

<sup>†</sup> This is called the Poisson sum formula.

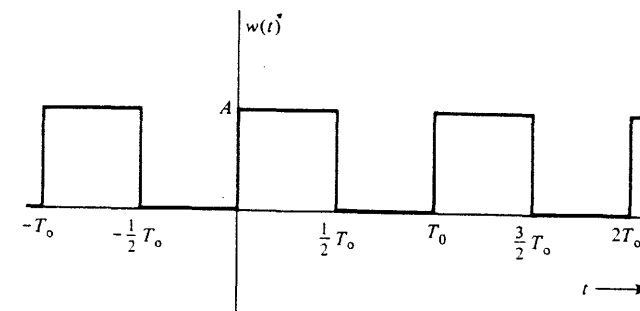


Figure 2-12 Periodic square wave used in Example 2-12.

### Example 2-12 FOURIER COEFFICIENTS FOR A RECTANGULAR WAVE

Find the Fourier coefficients for the periodic square wave shown in Fig. 2-12. The complex Fourier coefficients, using (2-89), are

$$c_n = \frac{1}{T_0} \int_0^{T_0/2} A e^{-jna\omega_0 t} dt = j \frac{A}{2\pi n} (e^{-jna\pi} - 1) \quad (2-118)$$

which reduce, using l'Hospital's rule for evaluating the indeterminant form for  $n = 0$ , to



$$c_n = \begin{cases} \frac{A}{2}, & n = 0 \\ -j \frac{A}{n\pi}, & n = \text{odd} \\ 0, & n \text{ otherwise} \end{cases} \quad (2-119)$$

This result may be verified by using (2-112) and the result of Example 2-5, where  $T_0 = 2T$ . That is,

$$c_n = \frac{A}{T_0} V(nf_0) = \frac{A}{2} e^{-jna/2} \frac{\sin(n\pi/2)}{n\pi/2} \quad (2-120)$$

which is identical to (2-119). It is realized that the dc value of the waveform is  $c_0 = A/2$ , which checks with the result by using (2-4). The spectrum of the square wave is easily obtained by using (2-109).

The other types of Fourier coefficients may also be obtained. Using (2-101) and (2-102), we obtain the quadrature Fourier coefficients

$$a_n = \begin{cases} \frac{A}{2}, & n = 0 \\ 0, & n > 0 \end{cases} \quad (2-121a)$$

$$b_n = \begin{cases} \frac{2A}{\pi n}, & n = \text{odd} \\ 0, & n = \text{even} \end{cases} \quad (2-121b)$$

Here all the  $a_n = 0$ , except for  $n = 0$ , because, if the dc value were suppressed, the waveform would be an odd function about the origin. Using (2-106) and (2-107), we find that the polar Fourier coefficients are

$$D_n = \begin{cases} \frac{A}{2}, & n = 0 \\ \frac{2A}{n\pi}, & n = 1, 3, 5, \dots \\ 0, & n \text{ otherwise} \end{cases} \quad (2-122)$$

and

$$\varphi_n = -90^\circ \text{ for } n \geq 1 \quad (2-123)$$

In communication problems the normalized average power is often needed, and, for the case of periodic waveforms, it can be evaluated using Fourier series coefficients.

**THEOREM.** For a periodic waveform  $w(t)$ , the normalized power is given by

$$P_w = \langle w^2(t) \rangle = \sum_{n=-\infty}^{n=\infty} |c_n|^2 \quad (2-124)$$

where  $\{c_n\}$  are the complex Fourier coefficients for the waveform.

**Proof.** For periodic  $w(t)$ , the Fourier series representation is valid over all time and may be substituted into (2-12) to evaluate the normalized (i.e.,  $R = 1$ ) power.

$$P_w = \left\langle \left( \sum_n c_n e^{jn\omega_0 t} \right)^2 \right\rangle = \left\langle \sum_n \sum_m c_n c_m^* e^{jn\omega_0 t} e^{-jm\omega_0 t} \right\rangle$$

$$= \sum_n \sum_m c_n c_m^* \langle e^{j(n-m)\omega_0 t} \rangle = \sum_n \sum_m c_n c_m^* \delta_{nm} = \sum_n |c_n|^2$$

or

$$P_w = \sum_n |c_n|^2 \quad (2-125)$$

Equation (2-124) is a special case of Parseval's theorem, (2-40), as applied to power signals.

### Power Spectral Density for Periodic Waveforms

**THEOREM.** For a periodic waveform, the power spectral density (PSD) is given by

$$\mathcal{P}(f) = \sum_{n=-\infty}^{n=\infty} |c_n|^2 \delta(f - nf_0) \quad (2-126)$$

where  $T_0 = 1/f_0$  is the period of the waveform and the  $\{c_n\}$  are the corresponding Fourier coefficients for the waveform.

**Proof.** Let  $w(t) = \sum_{n=-\infty}^{\infty} c_n e^{jn\omega_0 t}$ . Then the autocorrelation function of  $w(t)$  is

$$R(\tau) = \langle w^*(t)w(t + \tau) \rangle$$

$$= \left\langle \sum_{n=-\infty}^{\infty} c_n^* e^{-jn\omega_0 t} \sum_{m=-\infty}^{\infty} c_m e^{jm\omega_0(t+\tau)} \right\rangle$$

or

$$R(\tau) = \sum_{n=-\infty}^{\infty} \sum_{m=-\infty}^{\infty} c_n^* c_m e^{jm\omega_0 \tau} \langle e^{j\omega_0(m-n)\tau} \rangle$$

But  $\langle e^{j\omega_0(n-m)\tau} \rangle = \delta_{nm}$ , so this reduces to

$$R(\tau) = \sum_{n=-\infty}^{\infty} |c_n|^2 e^{jn\omega_0 \tau} \quad (2-127)$$

The PSD is then

$$\begin{aligned} \mathcal{P}(f) &= \mathcal{F}[R(\tau)] = \mathcal{F}\left[\sum_{n=-\infty}^{\infty} |c_n|^2 e^{jn\omega_0 \tau}\right] \\ &= \sum_{-\infty}^{\infty} |c_n|^2 \mathcal{F}[e^{jn\omega_0 \tau}] = \sum_{-\infty}^{\infty} |c_n|^2 \delta(f - nf_0) \end{aligned} \quad (2-128)$$

Equation (2-126) not only gives a way to evaluate the PSD for periodic waveforms but also can be used to evaluate the bandwidths of the waveforms. For example, the frequency interval could be found where 90% of the waveform power was concentrated.

### Example 2-13 PSD FOR A SQUARE WAVE

The PSD for the periodic square wave shown in Fig. 2-12 will be found. Because the waveform is periodic, (2-126) can be used to evaluate the PSD. Consequently this problem becomes one of evaluating the FS coefficients. Furthermore, the FS coefficients for a square wave are given by (2-120). Thus,

$$\mathcal{P}(f) = \sum_{-\infty}^{\infty} \left(\frac{A}{2}\right)^2 \left(\frac{\sin(n\pi/2)}{n\pi/2}\right)^2 \delta(f - nf_0) \quad (2-129)$$

This PSD is shown by the solid lines in Fig. 2-13 where the delta functions (which have infinite amplitudes) are represented with vertical lines that have length equal to the weight (i.e., area) of the corresponding delta function.

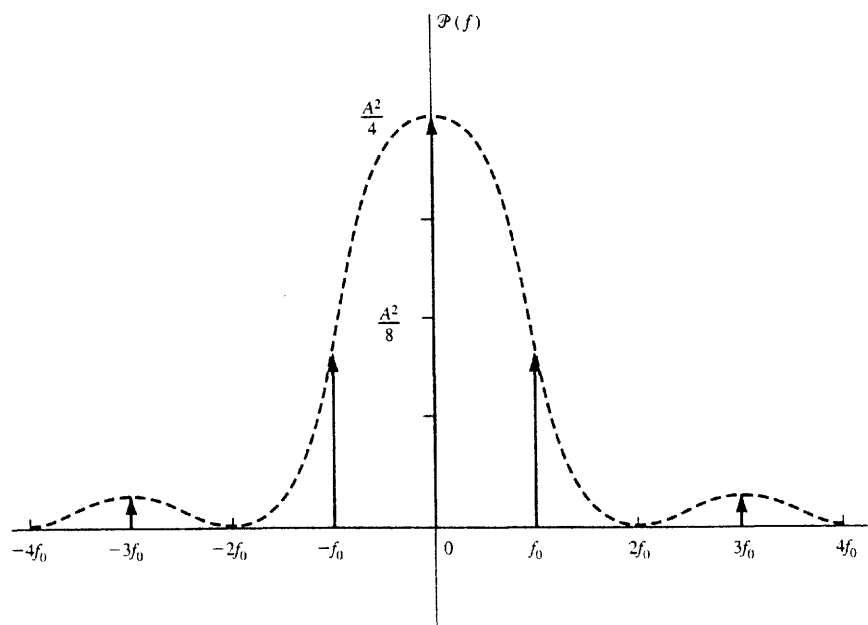


Figure 2-13 PSD for a square wave used in Example 2-13.

## 2-6 REVIEW OF LINEAR SYSTEMS

### Linear Time-Invariant Systems

An electronic filter or system is *linear* when *superposition* holds. That is,

$$y(t) = \mathcal{L}[a_1x_1(t) + a_2x_2(t)] = a_1\mathcal{L}[x_1(t)] + a_2\mathcal{L}[x_2(t)] \quad (2-130)$$

where  $y(t)$  is the output and  $x(t)$  is the input as shown in Fig. 2-14.  $\mathcal{L}[\cdot]$  denotes the linear (differential equation) system operator acting on  $[\cdot]$ . The system is said to be *time invariant* if, for any delayed input  $x(t - t_0)$ , the output is just delayed by the same amount  $y(t - t_0)$ .

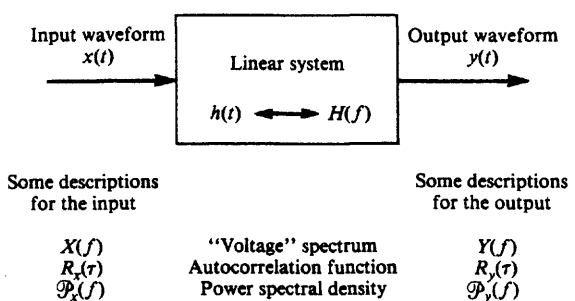


Figure 2-14 Linear system.

That is, the *shape* of the response is the same no matter when the input is applied to the system.

A detailed discussion of the theory and practice of linear systems is beyond the scope of this book. That would require a book in itself [Irwin, 1984, 1987, or 1993]. However, some basic ideas that are especially relevant to communication problems will be reviewed here.

### Impulse Response

The linear time-invariant filter or system without delay blocks is described by a linear ordinary differential equation with constant coefficients and may be characterized by its impulse response,  $h(t)$ . The *impulse response* is the solution to the differential equation when the forcing function is a Dirac delta function. That is,  $y(t) = h(t)$  when  $x(t) = \delta(t)$ . In physical networks the impulse response has to be *causal*. That is,  $h(t) = 0$  for  $t < 0$ .<sup>†</sup>

This impulse response may be used to obtain the system output when the input is *not* an impulse. In this case, a general waveform at the input may be approximated by<sup>‡</sup>

$$x(t) = \sum_{n=0}^{\infty} x(n \Delta t)[\delta(t - n \Delta t)] \Delta t \quad (2-131)$$

which indicates that samples of the input are taken at  $\Delta t$ -second intervals. Then using the time-invariant and superposition properties, the output is approximately

$$y(t) = \sum_{n=0}^{\infty} x(n \Delta t)[h(t - n \Delta t)] \Delta t \quad (2-132)$$

This expression becomes the exact result as  $\Delta t$  becomes zero. Letting  $n \Delta t = \lambda$ , we obtain

$$y(t) = \int_{-\infty}^{\infty} x(\lambda)h(t - \lambda) d\lambda \equiv x(t) * h(t) \quad (2-133)$$

An integral of this type is called the *convolution* operation, as first described by (2-62) in Sec. 2-2. That is, the output waveform for a time-invariant network can be obtained by convolving the input waveform with the impulse response for the system. Consequently, the impulse response can be used to characterize the response of the system in the time domain (see Fig. 2-14).

### Transfer Function

The spectrum of the output signal is obtained by taking the Fourier transform of both sides of (2-133). Using the convolution theorem of Table 2-1, we get

<sup>†</sup> The Paley-Wiener criterion gives the frequency domain equivalence for the causality condition of the time domain. It is that  $H(f)$  must satisfy the condition

$$\int_{-\infty}^{\infty} \frac{|\ln |H(f)||}{1 + f^2} df < \infty$$

<sup>‡</sup>  $\Delta t$  corresponds to  $dx$  of (2-47).

$$Y(f) = X(f)H(f) \quad (2-134)$$

or

$$H(f) = \frac{Y(f)}{X(f)} \quad (2-135)$$

where  $H(f) = \mathcal{F}[h(t)]$  is said to be the *transfer function* or *frequency response* of the network. That is, the impulse response and frequency response are a Fourier transform pair:

$$h(t) \leftrightarrow H(f)$$

Of course, the transfer function  $H(f)$  is, in general, a complex quantity and can be written in polar form

$$H(f) = |H(f)| e^{j\angle H(f)} \quad (2-136)$$

where  $|H(f)|$  is the *amplitude* (or *magnitude*) response and

$$\theta(f) = \angle H(f) = \tan^{-1} \left[ \frac{\text{Im}\{H(f)\}}{\text{Re}\{H(f)\}} \right] \quad (2-137)$$

is the phase response of the network. Furthermore, since  $h(t)$  is a real function of time (for real networks), it follows from (2-38) and (2-39) that  $|H(f)|$  is an even function of frequency and  $\angle H(f)$  is an odd function of frequency.

The transfer function of a linear time-invariant network can be measured by using a sinusoidal testing signal (that is swept over the frequency of interest) since the spectrum of a sinusoid is a line at the frequency under test. For example, if

$$x(t) = A \cos \omega_0 t$$

then the output of the network will be

$$y(t) = A |H(f_0)| \cos[\omega_0 t + \angle H(f_0)] \quad (2-138)$$

where the amplitude and phase may be evaluated on an oscilloscope or by the use of a vector voltmeter.

If the input to the network is a periodic signal with a spectrum given by

$$X(f) = \sum_{n=-\infty}^{n=\infty} c_n \delta(f - nf_0) \quad (2-139)$$

where, using (2-109),  $\{c_n\}$  are the complex Fourier coefficients of the input signal, the spectrum of the periodic output signal, using (2-134), is

$$Y(f) = \sum_{n=-\infty}^{n=\infty} c_n H(nf_0) \delta(f - nf_0) \quad (2-140)$$

We can also obtain the relationship between the power spectral density (PSD) at the input,  $\mathcal{P}_x(f)$ , and the output,  $\mathcal{P}_y(f)$  of a linear time-invariant network.<sup>†</sup> From (2-66) we know that

$$\mathcal{P}_y(f) = \lim_{T \rightarrow \infty} \frac{1}{T} |Y_T(f)|^2 \quad (2-141)$$

Using (2-134) in a formal sense, we obtain

$$\mathcal{P}_y(f) = |H(f)|^2 \lim_{T \rightarrow \infty} \frac{1}{T} |X_T(f)|^2$$

or

$$\mathcal{P}_y(f) = |H(f)|^2 \mathcal{P}_x(f) \quad (2-142)$$

Consequently, the *power transfer function* of the network is

$$G_h(f) = \frac{\mathcal{P}_y(f)}{\mathcal{P}_x(f)} = |H(f)|^2 \quad (2-143)$$

A rigorous proof of this theorem is given in Chapter 6.

#### Example 2-14 RC LOW-PASS FILTER

An *RC* low-pass filter is shown in Fig. 2-15, where  $x(t)$  and  $y(t)$  denote the input and output voltage waveforms, respectively. Using Kirchhoff's law for the sum of voltages around a loop, we get

$$x(t) = Ri(t) + y(t)$$

where  $i(t) = C dy(t)/dt$  or

$$RC \frac{dy}{dt} + y(t) = x(t) \quad (2-144)$$

Using Table 2-1, we find that the Fourier transform of this differential equation is

$$RC(j2\pi f)Y(f) + Y(f) = X(f)$$

Thus, the transfer function for this network is

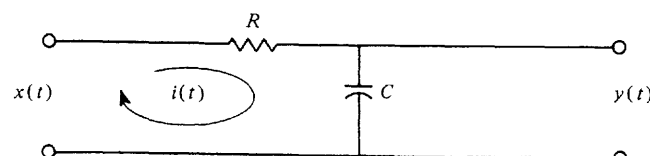
$$H(f) = \frac{Y(f)}{X(f)} = \frac{1}{1 + j(2\pi RC)f} \quad (2-145)$$

Using the Fourier transform Table 2-2, we obtain the impulse response

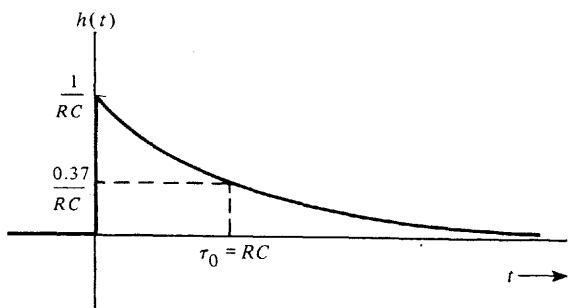


$$h(t) = \begin{cases} \frac{1}{\tau_0} e^{-t/\tau_0}, & t \geq 0 \\ 0, & t < 0 \end{cases} \quad (2-146)$$

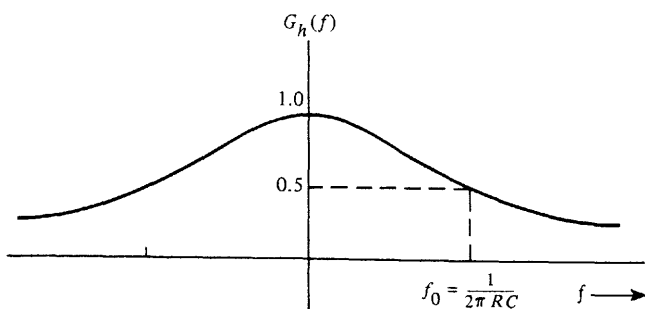
<sup>†</sup> The relationship between the input and output autocorrelation functions  $R_x(\tau)$  and  $R_y(\tau)$  can also be obtained as shown by (6-82).



(a) RC Low-Pass Filter



(b) Impulse Response



(c) Power Transfer Function

**Figure 2-15** Characteristics of an RC low-pass filter.

where  $\tau_0 = RC$  is called the *time constant*. When we combine (2-143) and (2-145), the power transfer function is

$$G_h(f) = |H(f)|^2 = \frac{1}{1 + (f/f_0)^2} \quad (2-147)$$

where  $f_0 = 1/(2\pi RC)$ .

The impulse response and the power transfer function are shown in Fig. 2-15. Note that the value of the power gain at  $f = f_0$  (called the 3 dB frequency) is  $G_h(f_0) = \frac{1}{2}$ . That is, the frequency component in the output waveform at  $f = f_0$  is attenuated by 3 dB compared with

that at  $f = 0$ . Consequently,  $f = f_0$  is said to be the 3-dB bandwidth of this filter. The topic of bandwidth is discussed in more detail in Sec. 2-9.

### Distortionless Transmission

In communication systems a *distortionless channel* is often desired. This implies that the channel output is just proportional to a delayed version of the input

$$y(t) = Ax(t - T_d) \quad (2-148)$$

where  $A$  is the gain (which may be less than one) and  $T_d$  is the delay.

The corresponding requirement in the frequency domain specification is obtained by taking the Fourier transform of both sides of (2-148).

$$Y(f) = AX(f)e^{-j2\pi f T_d}$$

Thus, for distortionless transmission, we require that the transfer function of the channel be given by

$$H(f) = \frac{Y(f)}{X(f)} = Ae^{-j2\pi f T_d} \quad (2-149)$$

This implies that for no distortion at the output of a linear time-invariant system, two requirements must be satisfied:

1. The amplitude response is flat. That is,

$$|H(f)| = \text{constant} = A \quad (2-150a)$$

2. The phase response is a *linear* function of frequency. That is,

$$\theta(f) = \angle H(f) = -2\pi f T_d \quad (2-150b)$$

When the first condition is satisfied, it is said that there is no *amplitude distortion*. When the second condition is satisfied, there is no *phase distortion*. For distortionless transmission both conditions must be satisfied.

The second requirement is often specified in an equivalent way using the time delay. Define the *time delay* of the system by

$$T_d(f) = -\frac{1}{2\pi f} \theta(f) = -\frac{1}{2\pi f} \angle H(f) \quad (2-151)$$

By (2-149), it is required that

$$T_d(f) = \text{constant} \quad (2-152)$$

for distortionless transmission. If  $T_d(f)$  is not a constant as a function of frequency, there is phase distortion because the phase response,  $\theta(f)$ , is not a linear function of frequency.

### Example 2-15 DISTORTION CAUSED BY A FILTER

Let us examine the distortion effect caused by the RC low-pass filter studied in Example 2-14. From (2-145) the amplitude response is

$$|H(f)| = \frac{1}{\sqrt{1 + (f/f_0)^2}} \quad (2-153)$$

and the phase response is

$$\theta(f) = \angle H(f) = -\tan^{-1}(f/f_0) \quad (2-154)$$

The corresponding time delay function is

$$T_d(f) = \frac{1}{2\pi f} \tan^{-1}(f/f_0) \quad (2-155)$$

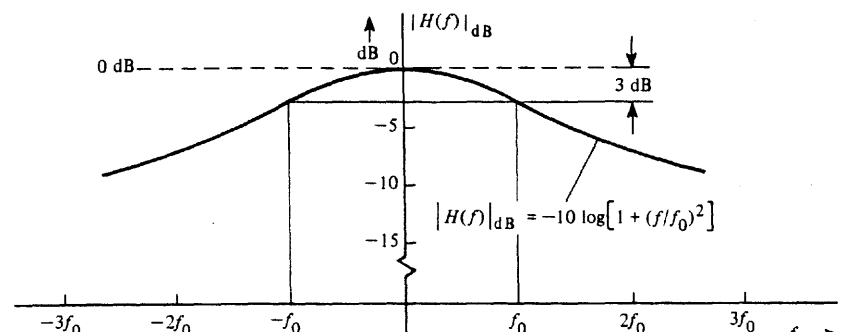
These results are plotted in Fig. 2-16, as indicated by the solid lines. This filter will produce some distortion since (2-150a) and (2-150b) are not satisfied. The dashed lines give the equivalent results for the distortionless filter. Several observations can be made. First, if the signals involved have spectral components at frequencies below  $0.5f_0$ , the filter will provide almost distortionless transmission since the error in the magnitude response (with respect to the distortionless case) is less than 0.5 dB and the error in the phase is less than  $2.1^\circ$  (8%). For  $f < f_0$ , the magnitude error is less than 3 dB and the phase error is less than  $12.3^\circ$  (27%). In engineering practice, this type of error is often considered to be tolerable. Waveforms with spectral components below  $0.50f_0$  would be delayed by  $1/(2\pi f_0)$  s. That is, if the cutoff frequency of the filter was  $f_0 = 1$  kHz, the delay would be 0.2 ms. For wideband signals the higher-frequency components would be delayed less than the lower-frequency components.

The distortion effects previously discussed were based on the assumption that the system was linear and time invariant. A linear time-invariant system will produce amplitude distortion if the amplitude response is not flat and it will produce phase (i.e., time delay) distortion if the phase response is not a linear function of frequency. Moreover, if the system is nonlinear and/or time varying, other types of distortion will be produced. As a result, there are new frequency components at the output that are not present at the input. In some communication applications, these new frequencies are actually a desired result and, consequently, might not be called distortion. The reader is referred to Sec. 4-3 for a study of these effects.

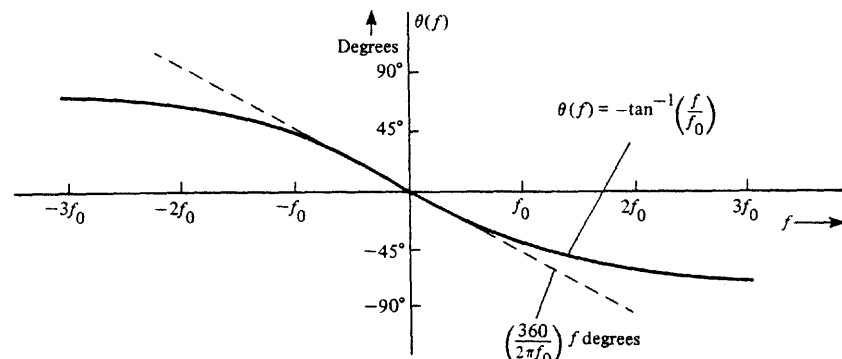
## 2-7 BANDLIMITED SIGNALS AND NOISE

Often we deal with signal and noise waveforms that may be considered to be *bandlimited*, which implies that their spectra are nonzero only within a certain frequency band. In this case we can apply some powerful theorems, namely, the sampling theorem to process the waveform. As we will show in Chapter 3, these ideas are *especially applicable to digital communication* problems.

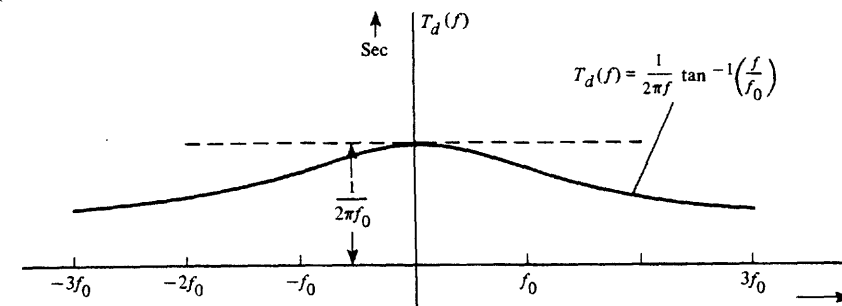
First, we examine some properties of bandlimited signals. Then the sampling and dimensionality theorems are developed.



(a) Magnitude Response



(b) Phase Response



(c) Time Delay

Figure 2-16 Distortion caused by an RC low-pass filter.

## Bandlimited Waveforms

**DEFINITION.** A waveform  $w(t)$  is said to be (absolutely) *bandlimited* to  $B$  hertz if

$$W(f) = \mathcal{F}[w(t)] = 0 \quad \text{for } |f| \geq B \quad (2-156)$$

**DEFINITION.** A waveform  $w(t)$  is (absolutely) *time limited* if

$$w(t) = 0 \quad \text{for } |t| > T \quad (2-157)$$

**THEOREM.** An absolutely bandlimited waveform cannot be absolutely time limited, and vice versa.

The result of this theorem is illustrated by examining the spectrum for the rectangular pulse waveform of Example 2-5. This time-limited waveform is shown to have a spectrum that is not bandlimited. A relatively simple proof of this theorem can be obtained by contradiction [Wozencraft and Jacobs, 1965].

This theorem raises an engineering paradox. If we observe that a waveform is bandlimited, for example, by viewing its spectrum on a spectrum analyzer, the waveform cannot be time limited. However, we believe that this physical waveform is time limited because the device that generates the waveform was built at some finite past time and the device will decay at some future time (thus producing a time-limited waveform). This paradox is resolved by realizing that we are modeling a physical process with a mathematical model and perhaps the assumptions in the model are not satisfied, although we believe them to be satisfied. That is, there is some uncertainty as to what the actual time waveform and corresponding spectrum look like, especially at extreme values of time and frequency, owing to the inaccuracies of our measuring devices. This relationship between the physical process and our mathematical model is discussed in an interesting paper by David Slepian [1976]. Although the signal may not be absolutely bandlimited, it may be bandlimited for all practical purposes in the sense that the amplitude spectrum has a negligible level above a certain frequency.

Another interesting theorem states that if  $w(t)$  is absolutely *bandlimited*, it is an *analytic* function. An analytic function is a function that possesses finite valued derivatives when they are evaluated for any finite value of  $t$ . This theorem may be proved by using a Taylor series expansion [Wozencraft and Jacobs, 1965].

## Sampling Theorem

The sampling theorem is one of the most useful theorems since it applies to digital communication systems. The sampling theorem is another application of an orthogonal series expansion.

**SAMPLING THEOREM.** Any physical waveform may be represented over the interval  $-\infty < t < \infty$  by

$$w(t) = \sum_{n=-\infty}^{n=\infty} a_n \frac{\sin(\pi f_s[t - (n/f_s)])}{\pi f_s[t - (n/f_s)]} \quad (2-158)$$



where

$$a_n = f_s \int_{-\infty}^{\infty} w(t) \frac{\sin(\pi f_s[t - (n/f_s)])}{\pi f_s[t - (n/f_s)]} dt \quad (2-159)$$

and  $f_s$  is a parameter that is assigned some convenient value greater than zero. Furthermore, if  $w(t)$  is bandlimited to  $B$  hertz and  $f_s \geq 2B$ , then (2-158) becomes the sampling function representation, where

$$a_n = w(n/f_s) \quad (2-160)$$

That is, for  $f_s \geq 2B$ , the orthogonal series coefficients are simply the values of the waveform that are obtained when the waveform is sampled every  $1/f_s$  seconds.

The series given by (2-158) and (2-160) is sometimes called the *cardinal series*. It has been known by mathematicians since at least 1915 [Whittaker, 1915] and to engineers since the pioneering work of Shannon, who connected this series with information theory [Shannon, 1949]. An excellent tutorial paper on this topic has been published in the *Proceedings of the IEEE* [Jeri, 1977].

**Proof.** We need to show that

$$\varphi_n(t) = \frac{\sin(\pi f_s[t - (n/f_s)])}{\pi f_s[t - (n/f_s)]} \quad (2-161)$$

form a set of the orthogonal functions. From (2-77) we need to demonstrate that (2-161) satisfies

$$\int_{-\infty}^{\infty} \varphi_n(t) \varphi_m^*(t) dt = K_n \delta_{nm} \quad (2-162)$$

Using Parseval's theorem, (2-40), we see that the left side becomes

$$\int_{-\infty}^{\infty} \varphi_n(t) \varphi_m^*(t) dt = \int_{-\infty}^{\infty} \Phi_n(f) \Phi_m^*(f) df \quad (2-163)$$

where

$$\Phi_n(f) = \mathcal{F}[\varphi_n(t)] = \frac{1}{f_s} \Pi\left(\frac{f}{f_s}\right) e^{-j2\pi(nf/f_s)} \quad (2-164)$$

We have

$$\begin{aligned} \int_{-\infty}^{\infty} \varphi_n(t) \varphi_m^*(t) dt &= \frac{1}{(f_s)^2} \int_{-\infty}^{\infty} \left[ \Pi\left(\frac{f}{f_s}\right) \right]^2 e^{-j2\pi(n-m)f/f_s} df \\ &= \frac{1}{(f_s)^2} \int_{-f_s/2}^{f_s/2} e^{-j2\pi(n-m)f/f_s} df = \frac{1}{f_s} \delta_{nm} \end{aligned} \quad (2-165)$$

Thus,  $\varphi_n(t)$  as given by (2-161) are orthogonal functions with  $K_n = 1/f_s$ . Using (2-84), we see that (2-159) follows. Furthermore, we will show that (2-160) follows for the case of  $w(t)$  being absolutely bandlimited to  $B$  hertz with  $f_s \geq 2B$ . Using (2-84) and Parseval's theorem, (2-40), we get

$$\begin{aligned} a_n &= f_s \int_{-\infty}^{\infty} w(t) \varphi_n^*(t) dt \\ &= f_s \int_{-\infty}^{\infty} W(f) \Phi_n^*(f) df \end{aligned} \quad (2-166)$$

Substituting (2-164),

$$a_n = \int_{-f_s/2}^{f_s/2} W(f) e^{-j2\pi f(n/f_s)} df \quad (2-167)$$

But because  $W(f)$  is zero for  $|f| > B$ , where  $B \leq f_s/2$ , the limits on the integral may be extended to  $(-\infty, \infty)$  without changing the value of the integral. This integral with infinite limits is just the inverse Fourier transform of  $W(f)$  evaluated at  $t = n/f_s$ . Thus  $a_n = w(n/f_s)$ , which is (2-160).

From (2-167) it is obvious that the minimum sampling rate allowed to reconstruct a bandlimited waveform without error is given by

$$(f_s)_{\min} = 2B \quad (2-168)$$

This is called the *Nyquist frequency*.

Let us now examine the problem of reproducing a bandlimited waveform by using  $N$  sample values. Suppose that we are interested in reproducing the waveform over a  $T_0$ -s interval as shown in Fig. 2-17a. Then we can truncate the sampling function series of (2-158) so that we include only  $N$  of the  $\varphi_n(t)$  functions that have their peaks within the  $T_0$  interval of interest. That is, the waveform can be approximately reconstructed using  $N$  samples:

$$w(t) \approx \sum_{n=n_1}^{n=n_1+N} a_n \varphi_n(t) \quad (2-169)$$

where the  $\{\varphi_n(t)\}$  are described by (2-161). Figure 2-17b shows the reconstructed waveform (solid line) which is obtained by the weighted sum of time-delayed  $(\sin x)/x$  waveforms (dashed lines), where the weights are the sample values,  $a_n = w(n/f_s)$ , denoted by the dots. The waveform is bandlimited to  $B$  hertz with the sampling frequency  $f_s \geq 2B$ . The sample values may be saved, for example, in the memory of a digital computer, so that the waveform may be reconstructed at a later time or the values may be transmitted over a communication system for waveform reconstruction at the receiving end. In either case, the waveform may be reconstructed from the sample values by the use of the equation above. That is, each sample value is multiplied by the appropriate  $(\sin x)/x$  function, and these weighted  $(\sin x)/x$  functions are summed to give the original waveform. This procedure is

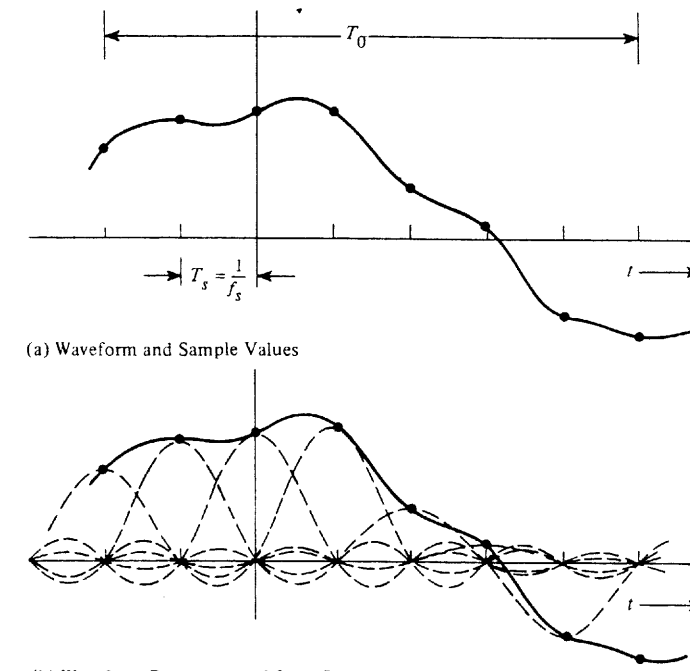


Figure 2-17 Sampling theorem.

illustrated in Fig. 2-17b. The minimum number of sample values that are needed for waveform reconstruction is

$$N = \frac{T_0}{1/f_s} = f_s T_0 \geq 2BT_0 \quad (2-170)$$

and there are  $N$  orthogonal functions in the reconstruction algorithm. We can say that  $N$  is the number of dimensions needed to reconstruct the  $T_0$ -second approximation of the waveform.

### Impulse Sampling

If one wants to reconstruct a waveform on a real-time basis, an alternative approach, called *impulse sampling*, is often used. The waveform is sampled with a unit-weight impulse train. This is accomplished by multiplying the waveform with a unit-weight impulse train. The resulting sampled waveform is

$$\begin{aligned} w_s(t) &= w(t) \sum_{n=-\infty}^{\infty} \delta(t - nT_s) \\ &= \sum_{n=-\infty}^{\infty} w(nT_s) \delta(t - nT_s) \end{aligned} \quad (2-171)$$

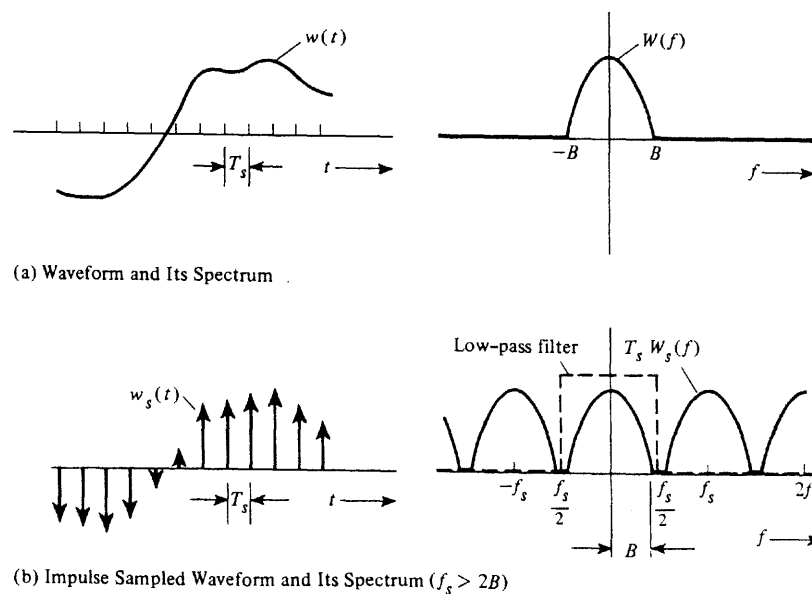


Figure 2-18 Impulse sampling.

where  $T_s = 1/f_s$ . This situation is illustrated in Fig. 2-18.<sup>†</sup> In the figure the weight (area) of each impulse,  $w(nT_s)$ , is indicated by the height. The spectrum for the impulse sampled waveform,  $w_s(t)$ , can be evaluated by substituting the Fourier series of the (periodic) impulse train into (2-171).

$$w_s(t) = w(t) \sum_{n=-\infty}^{\infty} \frac{1}{T_s} e^{jn\omega_s t} \quad (2-172)$$

Taking the Fourier transform of both sides of this equation, we get

$$\begin{aligned} W_s(f) &= \frac{1}{T_s} W(f) * \mathcal{F} \left[ \sum_{n=-\infty}^{\infty} e^{jn\omega_s t} \right] = \frac{1}{T_s} W(f) * \sum_{n=-\infty}^{\infty} \mathcal{F}[e^{jn\omega_s t}] \\ &= \frac{1}{T_s} W(f) * \sum_{n=-\infty}^{\infty} \delta(f - nf_s) \end{aligned}$$

or

$$W_s(f) = \frac{1}{T_s} \sum_{n=-\infty}^{\infty} W(f - nf_s) \quad (2-173)$$

<sup>†</sup> For illustrative purposes, assume that  $W(f)$  is real.

The spectrum of the impulse sampled waveform consists of the spectrum of the unsampled waveform that is replicated every  $f_s$  Hz.<sup>‡</sup> This is shown in Fig. 2-18b. Note that this technique of impulse sampling may be used to translate the spectrum of a signal to another frequency band that is centered on some harmonic of the sampling frequency. A more general circuit that can translate the spectrum to any desired frequency band is called a mixer. Mixers are discussed in Sec. 4-11.

If  $f_s \geq 2B$ , as illustrated in Fig. 2-18, the replicated spectra do not overlap and the original spectrum can be regenerated by chopping  $W_s(f)$  off above  $f_s/2$ . Thus  $w(t)$  can be reproduced from  $w_s(t)$  by simply passing  $w_s(t)$  through an ideal low-pass filter that has a cutoff frequency of  $f_c = f_s/2$  where  $f_s \geq 2B$ .

If  $f_s < 2B$  (i.e., the waveform is undersampled), the spectrum of  $w_s(t)$  will consist of overlapped, replicated spectra of  $w(t)$ , as illustrated in Fig. 2-19.<sup>§</sup> The spectral overlap or tail inversion is called *aliasing* or *spectral folding*.<sup>¶</sup> In this case, the low-pass filtered ver-

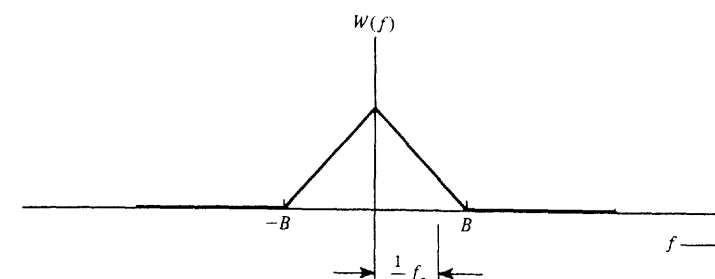


Figure 2-19 Undersampling and aliasing.

<sup>†</sup> In Chapter 3 this result is generalized to that of instantaneous sampling with a pulse train consisting of pulses with finite width and arbitrary shape (instead of impulses). This is called pulse amplitude modulation (PAM) of the instantaneous sample type.

<sup>‡</sup>For illustrative purposes, assume that  $W(f)$  is real.

<sup>§</sup> $f_s/2$  is the folding frequency where  $f_s$  is the sampling frequency. For no aliasing,  $f_s > 2B$  is required, where  $2B$  is the Nyquist frequency.

sion of  $w_s(t)$  will not be exactly  $w(t)$ . The recovered  $w(t)$  will be distorted because of the aliasing. The alias distortion can be eliminated by *prefiltering* the original  $w(t)$  before sampling so that the prefiltered  $w(t)$  has no spectral components above  $|f| = f_s/2$ . The prefiltering still produces distortion on the recovered waveform because the prefilter chops off the spectrum of the original  $w(t)$  above  $f = f_s/2$ . However, from Fig. 2-19, it can be shown that if a prefilter is used, the recovered waveform obtained from the low-pass version of the sample signal will have one half of the error energy compared to the error energy that would be obtained without using the presampling filter.

A physical waveform,  $w(t)$ , has finite energy. From (2-42) and (2-43) it follows that the magnitude spectrum of the waveform,  $|W(f)|$ , has to be negligible for  $|f| > B$  where  $B$  is an appropriately chosen positive number. Consequently, from a practical standpoint, the physical waveform is essentially bandlimited to  $B$  Hz where  $B$  is chosen to be large enough so that the error energy is below some specified amount.

### Dimensionality Theorem

The sampling theorem may be restated in a more general way called the *dimensionality theorem*.

**THEOREM.** A real waveform may be completely specified by

$$N = 2BT_0 \quad (2-174)$$

independent pieces of information that will describe the waveform over a  $T_0$  interval.  $N$  is said to be the number of dimensions required to specify the waveform, and  $B$  is the absolute bandwidth of the waveform.

The  $N$  sample values do not necessarily have to be periodic samples; they just have to be independent quantities. This can be demonstrated for the case of nonperiodic sampling by use of the complex Fourier series. We will represent the real  $w(t)$  over a  $T_0$ -s interval by the Fourier series

$$w(t) = \sum_n c_n e^{jn\omega_0 t}$$

where  $\omega_0 = 2\pi/T_0$ , and it is known that  $c_n^* = c_{-n}$  for any real signal. If  $w(t)$  is bandlimited to  $B$  hertz, the range of  $n$  needed to represent  $w(t)$  is  $-B \leq nf_0 \leq B$ , and because  $f_0 = 1/T_0$ , we have<sup>†</sup>

$$w(t) = \sum_{n=-BT_0}^{n=BT_0} c_n e^{jn\omega_0 t}$$

The  $c_0$  term is the dc level for  $w(t)$ , and a dc level does not impart any information (see Chapter 1). Since  $c_n = |c_n| e^{j\frac{\omega_0}{2}n}$  and  $c_{-n} = c_n^*$ , there are  $N = 2BT_0$  independent (real) val-

<sup>†</sup> Actually, for  $-B \leq nf_0 \leq B$  to hold with equality, we need an integer multiple of  $f_0$  equal to  $B$  (which may be any real positive number). Thus, in general,  $T_0$  needs to be large.

ues required. Note that the  $c_n$ 's in this example are not time samples of  $w(t)$ , and each  $c_n$  depends on the waveshape of  $w(t)$  over the whole  $T_0$  interval, as seen from (2-89).

The dimensionality theorem, (2-174), says simply that the information that can be conveyed by a bandlimited waveform or a bandlimited communication system is proportional to the product of the bandwidth of that system and the time allowed for transmission of the information. The *dimensionality theorem has profound implications in the design and performance of all types of communication systems*. For example, in radar systems it is well known that the time-bandwidth product of the received signal needs to be large for superior performance.

There are two distinct ways in which the dimensionality theorem can be applied. First, if any bandlimited waveform is given and we want to store some numbers in a table (or a computer memory bank) that could be used to reconstruct the waveform over a  $T_0$ -s interval, at least  $N$  numbers must be stored and, furthermore, the average sampling rate must be at least the Nyquist rate. That is,<sup>‡</sup>

$$f_s \geq 2B \quad (2-175)$$

Thus, in this first type of application, the dimensionality theorem is used to calculate the number of storage locations (amount of memory) required to represent a waveform.

The second type of application is the inverse type of problem. Here the dimensionality theorem is used to estimate the bandwidth of waveforms. This application is discussed in detail in Chapter 3 Sec. 3-4, where the dimensionality theorem is used to give a lower bound for the bandwidth of digital signals.

### 2-8 DISCRETE FOURIER TRANSFORM

With the convenience of personal computers and the availability of digital signal processing integrated circuits, the spectrum of a waveform can be easily approximated by using the discrete Fourier transform (DFT). Here we show briefly how the DFT can be used to compute samples of the continuous Fourier transform (CFT), (2-26), and values for the complex Fourier series coefficients (2-94).

**DEFINITION.** The *discrete Fourier transform (DFT)* is defined by

$$X(n) = \sum_{k=0}^{k=N-1} x(k) e^{-j(2\pi/N)nk} \quad (2-176)$$

where  $n = 0, 1, 2, \dots, N - 1$ , and the *inverse discrete Fourier transform (IDFT)* is defined by

<sup>‡</sup> If the spectrum of the waveform being sampled has a line at  $f = \pm B$ , there is some ambiguity as to whether or not the line is included within bandwidth  $B$ . The line is included by letting  $f_s > 2B$  (i.e., dropping the equality sign).

$$x(k) = \frac{1}{N} \sum_{n=0}^{n=N-1} X(n) e^{j(2\pi/N)nk} \quad (2-177)$$

where  $k = 0, 1, 2, \dots, N - 1$ .

Time and frequency do not appear explicitly because (2-176) and (2-177) are just definitions implemented on a digital computer to compute  $N$  values for the DFT and IDFT, respectively. Please be aware that other authors may use different (equally valid) definitions. For example, a  $1/\sqrt{N}$  factor could be used on the right side of (2-176) if the  $1/N$  factor of (2-177) is replaced by  $1/\sqrt{N}$ . This produces a different scale factor when the DFT is related to the CFT. Also, the signs of the exponents in (2-176) and (2-177) could be exchanged. This would reverse the spectral samples along the frequency axis.

MATLAB uses the DFT and IDFT definitions that are given by (2-176) and (2-177) except that the elements of the vector are indexed 1 through  $N$  instead of 0 through  $N - 1$ . Thus, the MATLAB FFT algorithms are related to (2-176) and (2-177) by<sup>†</sup>

$$\mathbf{X} = fft(\mathbf{x}) \quad (2-178)$$

and

$$\mathbf{x} = ifft(\mathbf{X}) \quad (2-179)$$

where  $\mathbf{x}$  is an  $N$ -element vector corresponding to samples of the waveform and  $\mathbf{X}$  is the  $N$ -element DFT vector.  $N$  is chosen to be a power of 2 (i.e.,  $N = 2^m$ , where  $m$  is a positive integer). If other FFT software is used, the user should be aware of the specific definitions that are implemented so that the results can be interpreted properly.

### Using the DFT to Compute the Continuous Fourier Transform

The relationship between the DFT, as defined by (2-180), and the CFT will now be examined. It involves three concepts: windowing, sampling, and periodic sample generation. These are illustrated in Fig. 2-20, where the left side is time domain and the right side is the corresponding frequency domain. Suppose that the CFT of a waveform  $w(t)$  is to be evaluated by use of the DFT. The time waveform is first windowed (truncated) over the interval  $(0, T)$  so that only a finite number of samples,  $N$ , are needed. The windowed waveform, denoted by a  $w$  subscript, is

$$w_w(t) = \begin{cases} w(t), & 0 \leq t \leq T \\ 0, & t \text{ elsewhere} \end{cases} = w(t) \Pi\left(\frac{t - (T/2)}{T}\right) \quad (2-180)$$

The Fourier transform of the windowed waveform is

$$W_w(f) = \int_{-\infty}^{\infty} w_w(t) e^{-j2\pi f t} dt = \int_0^T w(t) e^{-j2\pi f t} dt \quad (2-181)$$

<sup>†</sup>The MATHCAD algorithms are related to (2-176) and (2-177) by  $\mathbf{X} = \sqrt{N} icfft(\mathbf{x})$  and  $\mathbf{x} = (1/\sqrt{N}) cfft(\mathbf{X})$ .

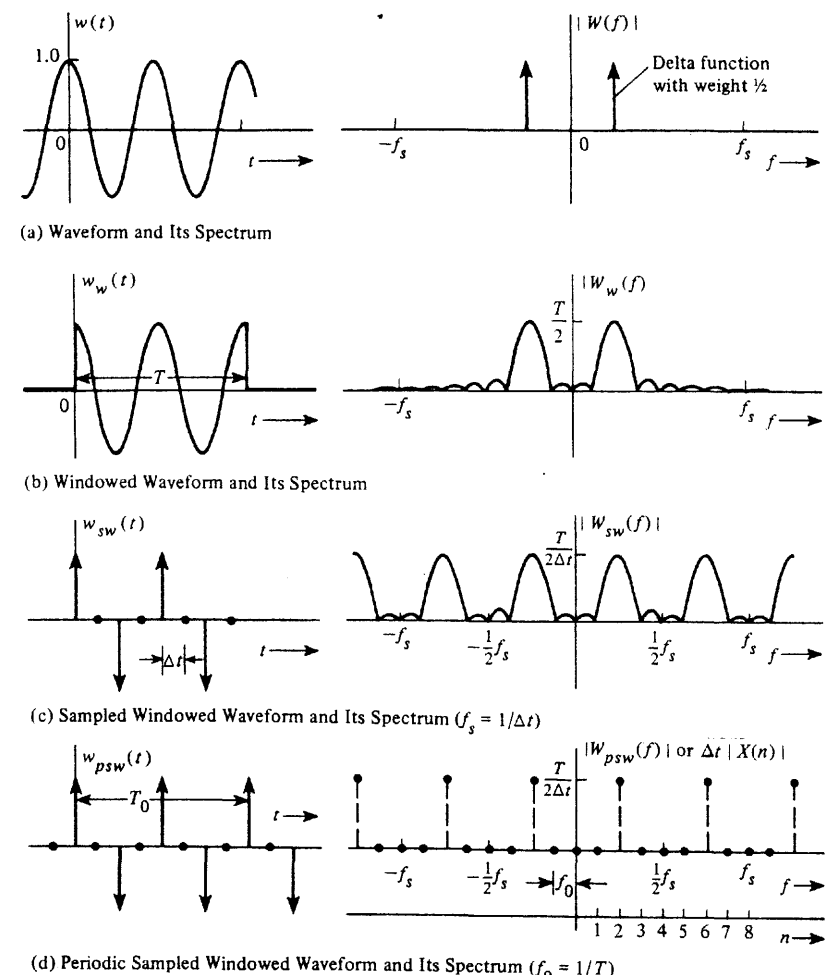


Figure 2-20 Comparison of CFT and DFT spectra.

Now approximate the CFT by using a finite series to represent the integral where  $t = k \Delta t$ ,  $f = n/T$ ,  $dt = \Delta t$ , and  $\Delta t = T/N$ . Then,

$$W_w(f)|_{f=n/T} \approx \sum_{k=0}^{N-1} w(k \Delta t) e^{-j(2\pi/N)nk} \Delta t \quad (2-182)$$

Comparing this with (2-176), the relation between the CFT and DFT is obtained:

$$W_w(f)|_{f=n/T} \approx \Delta t X(n) \quad (2-183)$$

where  $f = n/T$  and  $\Delta t = T/N$ . The sample values used in the DFT computation are  $x(k) = w(k \Delta t)$ , as shown in the left part of Fig. 2-20c. Also, since  $e^{-j(2\pi/N)nk}$  of (2-176) is peri-

odic in  $n$ —that is, the same values will be repeated for  $n = N, N + 1, \dots$  as were obtained for  $n = 0, 1, \dots$ —then  $X(n)$  is periodic (although only the first  $N$  values are returned by DFT computer programs since the others are just repetitions). Another way of seeing that the DFT (and the IDFT) are periodic is to recognize that since samples are used, the discrete transform is an example of impulse sampling, and consequently, the spectrum must be periodic about the sampling frequency,  $f_s = 1/\Delta t = N/T$  (as illustrated in Fig. 2-18 and again here in Fig. 2-20c and d). Furthermore, if the spectrum is desired for negative frequencies—the computer returns  $X(n)$  for the positive  $n$  values of  $0, 1, \dots, N - 1$ —(2-183) must be modified to give spectral values over the entire fundamental range of  $-f_s/2 < f < f_s/2$ . Thus, for positive frequencies, we use

$$W_w(f)|_{f=n/T} \approx \Delta t X(n), \quad 0 \leq n < \frac{N}{2} \quad (2-184a)$$

and for negative frequencies we use

$$W_w(f)|_{f=(n-N)/T} \approx \Delta t X(n), \quad \frac{N}{2} < n < N \quad (2-184b)$$

Figure 2-20 illustrates that if one is not careful, the DFT may give significant errors when used to approximate the CFT. The errors are due to a number of factors that may be categorized into three basic effects: *leakage*, *aliasing*, and the *picket-fence effect*.

The first effect is caused by windowing in the time domain. In the frequency domain this corresponds to convolving the spectrum of the unwindowed waveform with the spectrum (Fourier transform) of the window function. This spreads the spectrum of the frequency components of  $w(t)$ , as illustrated in Fig. 2-20b, and causes each frequency component to “leak” into adjacent frequencies. The leakage may produce errors when the DFT is compared with the CFT. This effect can be reduced by increasing the window width  $T$  or, equivalently, increasing  $N$  for a given  $\Delta t$ . Window shapes other than the rectangle can also be used to reduce the sidelobes in the spectrum of the window function [Harris, 1978; Ziemer, Tranter, and Fannin, 1989]. Large periodic components in  $w(t)$  cause more leakage, and if these components are known to be present, they might be eliminated before evaluating the DFT to reduce leakage.

From our previous study of sampling, it is known that the spectrum of a sampled waveform consists of replicating the spectrum of the unsampled waveform about harmonics of the sampling frequency. If  $f_s < 2B$ , where  $f_s = 1/\Delta t$  and  $B$  is the highest significant frequency component in the unsampled waveform, aliasing errors will occur. The aliasing error can be decreased by using a higher sampling frequency or a presampling low-pass filter. Note that the highest frequency component that can be evaluated with an  $N$ -point DFT is  $f = f_s/2 = N/(2T)$ .

The third type of error, the *picket-fence effect*, occurs because the  $N$ -point DFT cannot resolve the spectral components any closer than the spacing  $\Delta f = 1/T$ .  $\Delta f$  can be decreased by increasing  $T$ . If the data length is limited to  $T_0$  seconds, where  $T_0 \leq T$ ,  $T$  may be extended by adding additional zero-value sampling points. This is called *zero-padding* and will reduce  $\Delta f$  to produce better spectral resolution.

The computer cannot compute values that are infinite; therefore, the DFT will approximate Dirac delta functions by finite-amplitude pulses. However, the weights of the delta functions can be computed accurately by using the DFT to evaluate the Fourier series coefficients. This is demonstrated in Example 2-17.

In summary, several fundamental concepts need to be remembered when evaluating the CFT by use of the DFT. First, the waveform is windowed over a  $(0, T)$  interval so that a *finite* number of samples is obtained. Second, the DFT and the IDFT are periodic with periods  $f_s = 1/\Delta t$  and  $T$ , respectively. The parameters  $\Delta t$ ,  $T$ , and  $N$  are selected using the following considerations.

- $\Delta t$  is selected to satisfy the Nyquist sampling condition,  $f_s = 1/\Delta t > 2B$ , where  $B$  is the highest frequency in the waveform.  $\Delta t$  is the time between samples and is also called the *time resolution*. Also,  $t = k\Delta t$ .
- $T$  is selected to give the desired *frequency resolution*, where the frequency resolution is  $\Delta f = 1/T$ . Also,  $f = n/T$ .
- $N$  is the number of data points and is determined by  $N = T/\Delta t$ .

$N$  depends on the values used for  $\Delta t$  and  $T$ . The computation time increases as  $N$  is increased.<sup>†</sup> The  $N$  point DFT gives the spectra of  $N$  frequencies over the frequency interval  $(0, f_s)$  where  $f_s = 1/\Delta t = N/T$ . Half of this frequency interval represents positive frequencies and half represents negative frequencies as described by (2-184). This is illustrated in the following example.

### Example 2-16 DFT FOR A RECTANGULAR PULSE

Table 2-3 lists a MATLAB file that calculates the spectrum for a rectangular pulse using the DFT algorithm. The computed results are shown in Fig. 2-21. Note that (2-178) and (2-183) are used to relate the DFT results to the spectrum (i.e., the CFT). The parameters  $M$ ,  $t_{end}$ , and  $T$  are selected so that the computed magnitude and phase-spectral results compare favorably (i.e., little error) with the true spectrum of the rectangular pulse as given by (2-59) and (2-60) of Example 2-5. ( $T$  in Example 2-5 is equivalent to  $t_{end}$  in Table 2-3.)

The rectangular pulse is not absolutely bandlimited. However, for a pulse width of  $t_{end} = 1$ , the magnitude spectrum becomes relatively small at  $5/t_{end} = 5\text{Hz} = B$ . Thus, we need to sample the waveform at a rate of  $2B = 10\text{ Hz}$  or greater. For  $T = 10$  and  $N = 128$ ,  $\Delta t = 0.08$  or  $f_s = 1/\Delta t = 12.8\text{ Hz}$ . Therefore, the values of  $T$  and  $N$  have been selected to satisfy the Nyquist rate of  $f_s > 2B$ . The frequency resolution is  $\Delta f = 1/T = 0.1\text{ Hz}$ . Consequently, a good spectral representation is obtained using the DFT.

In the bottom plot of Fig. 2-21, the magnitude spectrum is shown over the whole range of the FFT vector, that is, for  $0 < f < f_s$ , where  $f_s = 12.8\text{ Hz}$ . Because (2-184b) was not used

<sup>†</sup> The Fast Fourier Transform (FFT) algorithms are fast ways of computing the DFT. The number of complex multiplications required for the DFT is  $N^2$ , whereas the FFT (with  $N$  selected to be a power of 2) requires only  $(N/2) \log_2 N$  complex multiplications. Thus, the FFT provides an improvement factor of  $2N/(\log_2 N)$  when compared to the DFT. This is an improvement of 113.8 for a  $N = 512$  point FFT.



TABLE 2-3 MATLAB LISTING FOR CALCULATING THE SPECTRUM OF A RECTANGULAR PULSE USING THE DFT

```
% File: FIG2_21.M
% Calculate the FFT for a truncated step
% Let tend be the end of the step.

M = 7;
N = 2^M;
n = 0:1:N-1;
tend = 1;
T = 10;
dt = T/N;
t = n*dt;
% Creating time waveform
w = zeros(length(t),1);
for (i = 1:length(w))
    if (t(i) <= tend)
        w(i) = 1;
    end;
end;
% Calculating FFT
W = dt*fft(w);
f = n/T;
% Calculating position of 4th NULL
pos = index(f,4/tend);
plot_pr(2);
plot(t,w);
axis([0 T 0 1.5]);
xlabel('t (sec) -->');
ylabel('w(t)');
title('Time Waveform');
pause;
subplot(311);
plot(f(1:pos),abs(W(1:pos)));
xlabel('f (Hz) -->');
ylabel('|W(f)|');
title('MAGNITUDE SPECTRUM out to 4th Null');
subplot(312);
plot(f(1:pos),180/pi*angle(W(1:pos)));
xlabel('f (Hz) -->');
ylabel('theta(f) (degrees)');
title('PHASE SPECTRUM out to 4th Null');
grid;
subplot(313);
plot(f,abs(W));
xlabel('f (Hz) -->');
ylabel('|W(f)|');
title('MAGNITUDE SPECTRUM over whole FFT frequency range');
```

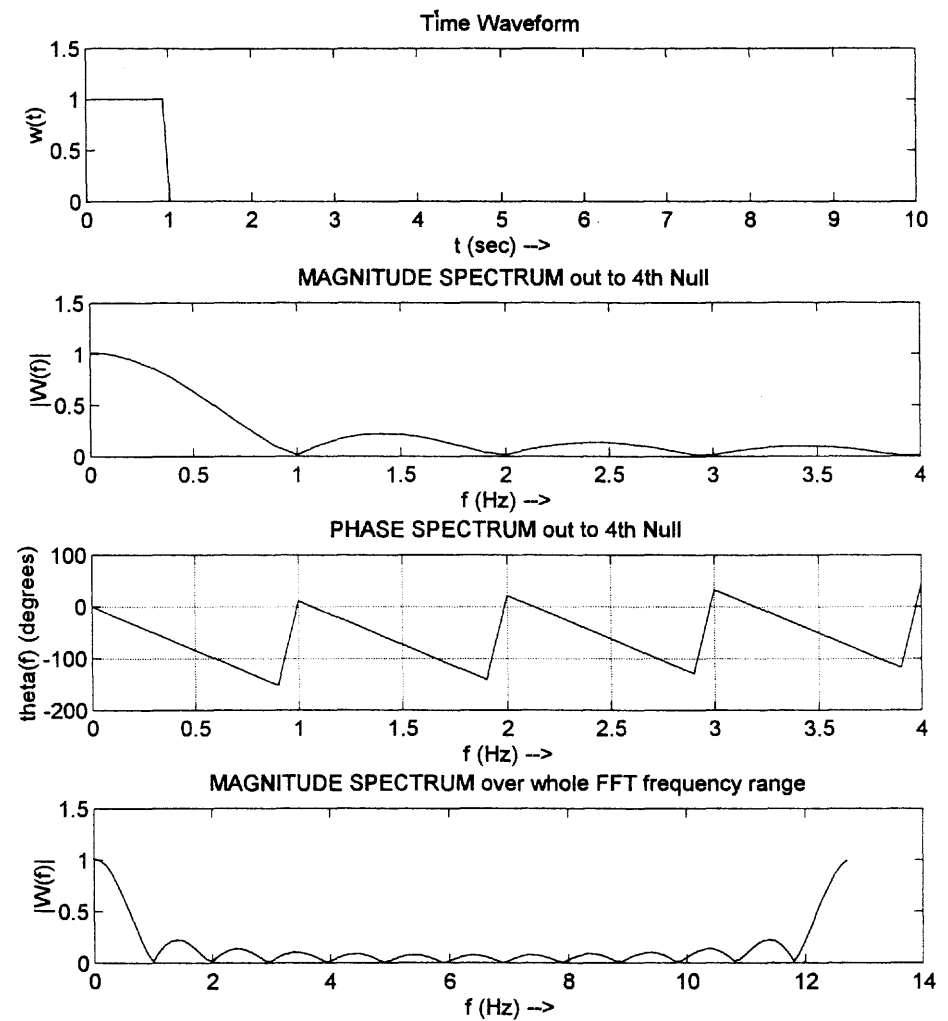


Figure 2-21 Spectrum for a rectangular pulse using the MATLAB DFT.



in the MATLAB program, the plot for  $0 < f < 6.8$  ( $f_s/2 = 6.8$  Hz) corresponds to the magnitude spectrum of the CFT over positive frequencies, and the plot for  $6.4 < f < 12.8$  corresponds to the negative frequencies of the CFT. The MATLAB program shown in Table 2-3 may be found on the computer disk for this book (as described in Chapter 1). The reader should try other values of  $M$ ,  $tend$ , and  $T$  to see how leakage, aliasing, and picket-fence errors become large if the parameters are not carefully selected. Also, note that significant errors occur if  $tend = T$ . Why?

### Using the DFT to Compute the Fourier Series

In a similar way the DFT may be also used to evaluate Fourier series coefficients. Using (2-89) yields

$$c_n = \frac{1}{T} \int_0^T w(t) e^{-j2\pi n f_0 t} dt$$

Approximate this integral by using a finite series where  $t = k \Delta t$ ,  $f_0 = 1/T$ ,  $dt = \Delta t$  and  $\Delta t = T/N$ . Then

$$c_n \approx \frac{1}{T} \sum_{k=0}^{N-1} w(k \Delta t) e^{-j(2\pi/N)nk} \Delta t \quad (2-185)$$

Using (2-176), the Fourier series coefficient is related to the DFT by

$$c_n \approx \frac{1}{N} X(n) \quad (2-186)$$

The DFT returns  $X(n)$  values for  $n = 0, 1, \dots, N - 1$ . Consequently, (2-186) must be modified to give  $c_n$  values for negative  $n$ . For positive  $n$ , we use

$$c_n = \frac{1}{N} X(n), \quad 0 \leq n < \frac{N}{2} \quad (2-187a)$$

and for negative  $n$  we use

$$c_n = \frac{1}{N} X(N + n), \quad -\frac{N}{2} < n < 0 \quad (2-187b)$$

#### Example 2-17 USE THE DFT TO COMPUTE THE SPECTRUM OF A SINUSOID

Let

$$w(t) = 3 \sin(\omega_0 t + 20^\circ) \quad (2-188)$$

where  $\omega_0 = 2\pi f_0$  and  $f_0 = 10$  Hz.

Because  $w(t)$  is periodic, (2-109) is used to obtain the spectrum

$$W(f) = \sum c_n \delta(f - nf_0)$$

where  $\{c_n\}$  are the complex Fourier series coefficients for  $w(t)$ . Furthermore, because  $\sin(x) = (e^{jx} - e^{-jx})/(2j)$ ,

$$3 \sin(\omega_0 t + 20^\circ) = \left(\frac{3}{2j} e^{j20}\right) e^{j\omega_0 t} + \left(\frac{-3}{2j} e^{-j20}\right) e^{-j\omega_0 t}$$

Consequently, the FS coefficients are known to be

$$c_1 = \left(\frac{3}{2j} e^{j20}\right) = 1.5 \angle +70^\circ \quad (2-189a)$$

$$c_{-1} = \left(\frac{-3}{2j} e^{-j20}\right) = 1.5 \angle -70^\circ \quad (2-189b)$$

and the other  $c_n$ s are zero. Now, see if this known correct answer can be computed by using the DFT. Referring to Table 2-4 and Fig. 2-22, MATLAB computes the FFT and plots the spectrum. The computed result checks with the known (correct) analytical result.

Note that  $\delta$  functions cannot be plotted because  $\delta(0) = \infty$ . Consequently, the weights of the  $\delta$  functions are plotted instead to indicate the magnitude spectra. Also at frequencies where  $|W(f)| = 0$ , any value may be used for  $\theta(f)$  because  $W(f) = |W(f)| / \theta(f) = 0$ .

These results can also be compared with those of Example 2-4 where the spectrum for a sinusoid was obtained by the direct evaluation of the Fourier transform integral.

### 2-9 BANDWIDTH OF SIGNALS

Spectral width of signals and/or noise in communication systems is a very important concept, for two main reasons. First, more and more users are being assigned to increasingly crowded RF bands, so that the spectral width required for each one needs to be considered carefully. Second, the spectral width of signals/noise is important from the equipment design viewpoint since the circuits need to have enough bandwidth to accommodate the signal but reject the noise. The question is: What is *bandwidth*? As we will see, there are numerous definitions for bandwidth.

As long as we use the same definition when working with several signals and noise, we can compare their spectral widths by using the particular bandwidth definition that was selected. If we change definitions, "conversion factors" will be needed to compare the spectral widths that were obtained by using different definitions. Unfortunately, the conversion factors usually depend on the type of spectral *shape* involved [e.g.,  $(\sin x)/x$  type of spectrum or rectangular spectrum].

In engineering definitions, the bandwidth is taken to be the width of a *positive* frequency band. (We are describing the bandwidth of real signals or the bandwidth of a physical filter that has a real impulse response; consequently, the magnitude spectra of these waveforms are even about the origin  $f = 0$ .) In other words, the bandwidth would be  $f_2 - f_1$ , where  $f_2 > f_1 \geq 0$  and  $f_2$  and  $f_1$  are determined by the particular definition that is used. For baseband waveforms or networks,  $f_1$  is usually taken to be zero since the spectrum extends down to dc ( $f = 0$ ). For bandpass signals,  $f_1 > 0$  and the band  $f_1 < f < f_2$  encompasses the carrier frequency  $f_c$  of the signal. It is recalled that as we increase the "signaling speed" of a signal (i.e., decrease  $T$ ) the spectrum gets wider (see Fig. 2-6). Consequently, for engineering definitions of bandwidth, we require the bandwidth to vary as  $1/T$ .

We will give six engineering definitions and one legal definition of bandwidth that are often used.

1. *Absolute bandwidth* is  $f_2 - f_1$ , where the spectrum is zero outside the interval  $f_1 < f < f_2$  along the positive frequency axis.
2. *3-dB bandwidth* (or half-power bandwidth) is  $f_2 - f_1$ , where for frequencies inside the band  $f_1 < f < f_2$ , the magnitude spectra, say  $|H(f)|$ , fall no lower than  $1/\sqrt{2}$  times



**TABLE 2-4** MATLAB LISTING FOR CALCULATING THE SPECTRUM OF A SINUSOID USING THE DFT

```
% File: TABLE2_4.M
% Calculate the spectrum for a sinusoid using the FFT.
M = 4;
N = 2^M;
fo = 10;
wo = 2*pi*fo;
n = 0:1:N-1;
T = 1/fo;
dt = T/N;
t = n*dt;
% Creating time waveform
w = 3*sin(wo*t + (pi/180*20));
% Compute the FFT data points.
W = fft(w);
W = W(:);
% SINCE THE WAVEFORM IS PERIODIC,
% USE COMPLEX FOURIER SERIES TO GET SPECTRUM.
% ==> Compute the FS coefficients from the FFT data using (2-186).
% Then use (2-109) to get the spectrum.
n1 = -N/2:1:N/2;
fn1 = n1/T;
fs = 1/dt;
% Generating complex fourier series coefficients
cn = 1/N * W;
% Generating Phase
Theta = (180/pi)*angle(cn + 0.001);
% Converting samples 0,1,2,3,...,N-1 to a positive and negative
% Note that (2-187) is a built in command: fftshift
cn = fftshift(cn)';
Theta = fftshift(Theta)';
cn = [cn cn(1)];
Theta = [Theta Theta(1)];
cn = cn(:);
Theta = Theta(:);
% Plotting results
plot_pr(4);
plot(t,w);
xlabel('t (sec) -->');
ylabel('w(t)');
title('Time Waveform');
pause;
plot(n,abs(W), 'o');
for (i = 1:1:length(n))
    line([n(i) n(i)], [0 abs(W(i))]);
end;
xlabel('n');
ylabel('|W(n)|');
title('FFT Data Points');
axis([0 16 0 25]);
pause;
subplot(211)
```

**TABLE 2-4** MATLAB LISTING FOR CALCULATING THE SPECTRUM OF A SINUSOID USING THE DFT (cont.)

```
plot(fn1,abs(cn), 'o');
for (i = 1:1:length(n1))
    line([fn1(i) fn1(i)], [0 abs(cn(i))]);
end;
xlabel('f (Hz) -->');
ylabel('|c(n)|');
title('MAGNITUDE SPECTRUM, |W(f)|');
axis([-80 80 0 2]);
subplot(212)
plot(fn1,zeros(length(fn1),1), 'w', fn1,Theta, 'o');
for (i = 1:1:length(n1))
    line([fn1(i) fn1(i)], [0 Theta(i)]);
end;
xlabel('f (Hz) -->');
ylabel('theta(f) (degrees)');
title('PHASE SPECTRUM, Theta(f)');
```

the maximum value of  $|H(f)|$ , and the maximum value falls at a frequency inside the band.

3. *Equivalent noise bandwidth* is the width of a fictitious rectangular spectrum (height specified below) such that the power in that rectangular band is equal to the power associated with the actual spectrum over positive frequencies. For example, from (2-142), the PSD is proportional to the magnitude squared of the spectrum. Let  $f_0$  be the frequency where the magnitude spectrum has a maximum; then the power in the equivalent rectangular band is proportional to

$$\text{equivalent power} = B_{\text{eq}} |H(f_0)|^2 \quad (2-190)$$

where  $B_{\text{eq}}$  is the equivalent bandwidth that is to be determined. The actual power for positive frequencies is proportional to

$$\text{actual power} = \int_0^\infty |H(f)|^2 df \quad (2-191)$$

Setting (2-190) equal to (2-191), we have the formula that gives the *equivalent noise bandwidth*,

$$B_{\text{eq}} = \frac{1}{|H(f_0)|^2} \int_0^\infty |H(f)|^2 df \quad (2-192)$$

4. *Null-to-null bandwidth* (or zero-crossing bandwidth) is  $f_2 - f_1$ , where  $f_2$  is the first null in the envelope of the magnitude spectrum above  $f_0$  and, for bandpass systems,  $f_1$  is the first null in the envelope below  $f_0$ , where  $f_0$  is the frequency where the magnitude spectrum is a maximum.<sup>†</sup> For baseband systems  $f_1$  is usually zero.

<sup>†</sup> In cases where there is no definite null in the magnitude spectrum, this definition is not applicable.

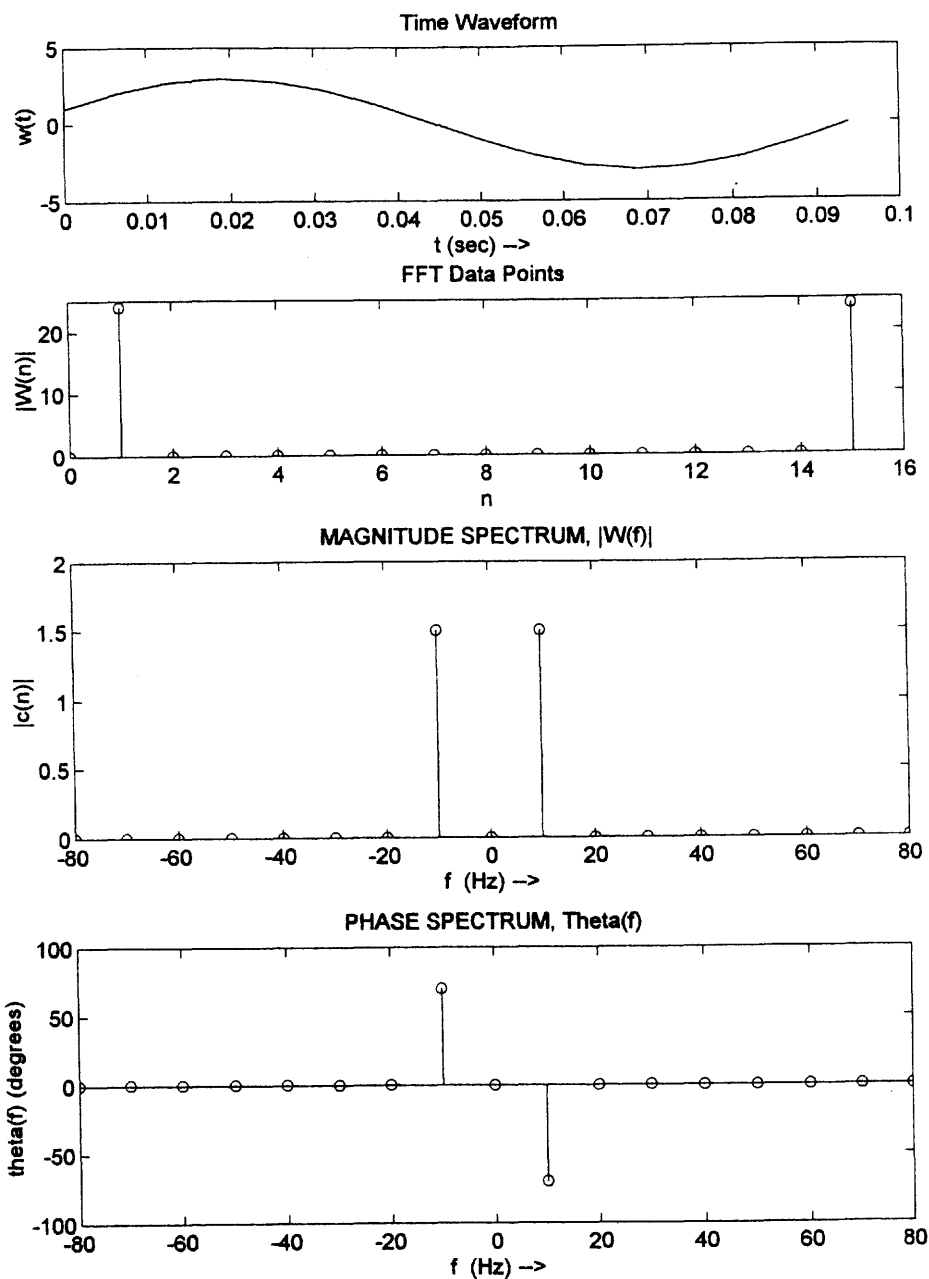


Figure 2-22 Spectrum of a sinusoid using the MATLAB DFT.



5. *Bounded spectrum bandwidth* is  $f_2 - f_1$  such that outside the band  $f_1 < f < f_2$ , the PSD, which is proportional to  $|H(f)|^2$ , must be down by at least a certain amount, say 50 dB, below the maximum value of the power spectral density.
6. *Power bandwidth* is  $f_2 - f_1$ , where  $f_1 < f < f_2$  defines the frequency band in which 99% of the total power resides. This is similar to the FCC definition of *occupied bandwidth*, which states that the power above the upper band edge  $f_2$  is  $\frac{1}{2}\%$  and the power below the lower band edge is  $\frac{1}{2}\%$ , leaving 99% of the total power within the occupied band (FCC Rules and Regulations, Sec. 2.202).
7. *FCC bandwidth* is an authorized bandwidth parameter assigned by the FCC to specify the spectrum allowed in communication systems. When the FCC bandwidth parameter is substituted into the FCC formula, the minimum attenuation is given for the power level allowed in a 4-kHz band at the band edge with respect to the total average signal power. Quoting Sec. 21.106 of the FCC Rules and Regulations: "For operating frequencies below 15 GHz, in any 4 kHz band, the center frequency of which is removed from the assigned frequency by more than 50 percent up to and including 250 percent of the authorized bandwidth, as specified by the following equation, but in no event less than 50 dB":

$$A = 35 + 0.8(P - 50) + 10 \log_{10}(B) \quad (2-193)$$

(attenuation greater than 80 dB is not required) where

- $A$  = attenuation (in decibels) below the mean output power level
- $P$  = percent removed from the carrier frequency
- $B$  = authorized bandwidth in megahertz

The FCC definition (as well as many other legal rules and regulations) is somewhat obscure, but it will be interpreted in Example 2-18. It actually defines a spectral mask. That is, the spectrum of the signal must be less than or equal to the values given by this spectral mask at all frequencies. The FCC bandwidth parameter  $B$  is not consistent with the other definitions that are listed in the sense that it is not proportional to  $1/T$ , the "signaling speed" of the corresponding signal [Amoroso, 1980]. In this sense the FCC bandwidth parameter  $B$  is a *legal* definition instead of an engineering definition. The *rms bandwidth*, which is very useful in analytical problems, is defined in Chapter 6.

#### Example 2-18 BANDWIDTHS FOR A BPSK SIGNAL

A binary-phase-shift-keyed (BPSK) signal will be used to illustrate how the bandwidth is evaluated for the different definitions just given.

The BPSK signal is described by

$$s(t) = m(t) \cos \omega_c t \quad (2-194)$$

where  $\omega_c = 2\pi f_c$ ,  $f_c$  being the carrier frequency (hertz), and  $m(t)$  is a serial binary ( $\pm 1$  values) modulating waveform originating from a digital information source such as a digital computer as illustrated in Fig. 2-23a. Let us evaluate the spectrum of  $s(t)$  for the worst case (widest bandwidth).

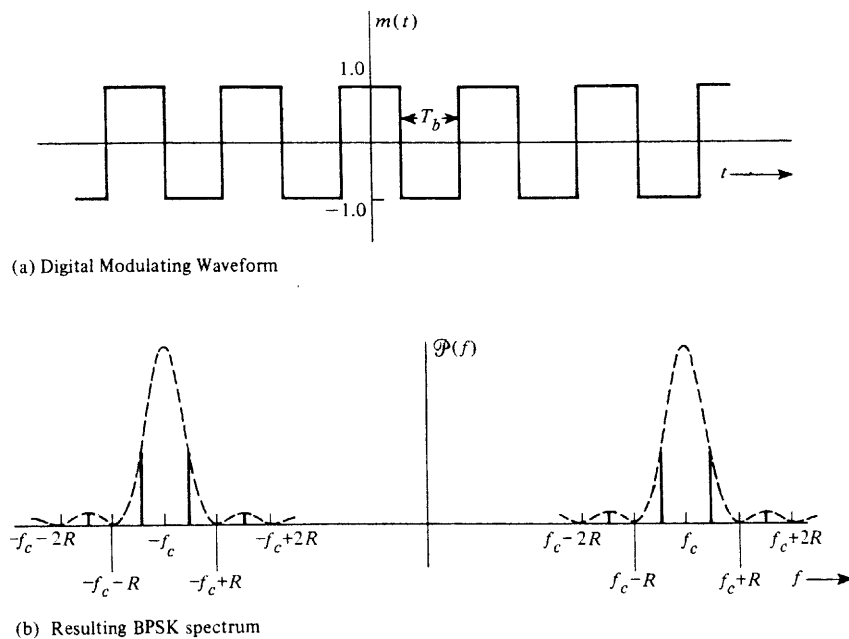


Figure 2-23 Spectrum of a BPSK signal.

The worst-case (widest-bandwidth) spectrum occurs when the digital modulating waveform has transitions that occur most often. In this case  $m(t)$  would be a square wave, as shown in Fig. 2-23a. Here a binary 1 is represented by a +1 V level and a binary 0 by a -1 V level, and the signaling rate is  $R = 1/T_b$  bits/s. The power spectrum of the square-wave modulation can be evaluated using Fourier series analysis. Using (2-126) and (2-120),

$$\mathcal{P}_m(f) = \sum_{n=-\infty}^{\infty} |c_n|^2 \delta(f - nf_0) = \sum_{n=-\infty, n \neq 0}^{\infty} \left[ \frac{\sin(n\pi/2)}{n\pi/2} \right]^2 \delta\left(f - n\frac{R}{2}\right) \quad (2-195)$$

where  $f_0 = 1/(2T_b) = R/2$ . The PSD of  $s(t)$  can be expressed in terms of the PSD for  $m(t)$  by evaluating the autocorrelation of  $s(t)$ .

$$\begin{aligned} R_s(\tau) &= \langle s(t)s(t+\tau) \rangle \\ &= \langle m(t)m(t+\tau) \cos \omega_c t \cos \omega_c(t+\tau) \rangle \\ &= \frac{1}{2} \langle m(t)m(t+\tau) \rangle \cos \omega_c \tau + \frac{1}{2} \langle m(t)m(t+\tau) \cos(2\omega_c t + \omega_c \tau) \rangle \end{aligned}$$

or

$$R_s(\tau) = \frac{1}{2} R_m(\tau) \cos \omega_c \tau + \frac{1}{2} \lim_{T \rightarrow \infty} \frac{1}{T} \int_{-T/2}^{T/2} m(t)m(t+\tau) \cos(2\omega_c t + \omega_c \tau) dt \quad (2-196)$$

The integral is negligible because  $m(t)m(t+\tau)$  is constant over small time intervals, but  $\cos(2\omega_c t + \omega_c \tau)$  has many cycles of oscillation since  $f_c \gg R$ .<sup>†</sup> Any small area that is accumulated by the integral becomes negligible when divided by  $T$ ,  $T \rightarrow \infty$ . Thus,

<sup>†</sup> This is a consequence of the Riemann-Lebesgue lemma from integral calculus [Olmsted, 1961].

$$R_s(\tau) = \frac{1}{2} R_m(\tau) \cos \omega_c \tau \quad (2-197)$$

The PSD is obtained by taking the Fourier transform of both sides of (2-197). Using the real-signal frequency transform theorem (Table 2-1), we get

$$\mathcal{P}_s(f) = \frac{1}{4} [\mathcal{P}_m(f - f_c) + \mathcal{P}_m(f + f_c)] \quad (2-198)$$

Substituting (2-195) into (2-198), we obtain the PSD for the BPSK signal:

$$\begin{aligned} \mathcal{P}_s(f) &= \frac{1}{4} \sum_{n=-\infty, n \neq 0}^{\infty} \left[ \frac{\sin(n\pi/2)}{n\pi/2} \right]^2 \\ &\times \{ \delta[f - f_c - n(R/2)] + \delta[f + f_c - n(R/2)] \} \end{aligned} \quad (2-199)$$

This spectrum is shown in Fig. 2-23b.

The spectral shape that results from using this worst-case deterministic modulation is essentially the same as that obtained when random data are used; however, for the random case, the spectrum is continuous. The result for the random data case, as worked out in Chapter 3 where  $\mathcal{P}_m(f)$  is given by (3-41), is

$$\mathcal{P}_s(f) = \frac{1}{4} T_b \left[ \frac{\sin \pi T_b(f - f_c)}{\pi T_b(f - f_c)} \right]^2 + \frac{1}{4} T_b \left[ \frac{\sin \pi T_b(f + f_c)}{\pi T_b(f + f_c)} \right]^2 \quad (2-200)$$

when the data rate is  $R = 1/T_b$  bits/sec. This is shown by the dotted curve in Fig. 2-23b.

This demonstrates that we can often use (deterministic) square-wave test signals to help us analyze a digital communication system instead of using a more complicated random data model.

The bandwidth for the BPSK signal will now be evaluated for each of the bandwidth definitions given previously. To accomplish this, the shape of the PSD for the positive frequencies is needed. From (2-200), it is

$$\mathcal{P}_s(f) = \left[ \frac{\sin \pi T_b(f - f_c)}{\pi T_b(f - f_c)} \right]^2 \quad (2-201)$$

Substituting this equation into the definitions, we obtain the resulting BPSK bandwidths as shown in Table 2-5, except for the FCC bandwidth.

The relationship between the spectrum and the FCC bandwidth parameter is a little more tricky to evaluate. We need to evaluate the decibel attenuation

TABLE 2-5 BANDWIDTHS FOR BPSK SIGNALING WHERE THE BIT RATE IS  $R = 1/T_b$  BITS/S.

Definition Used	Bandwidth (kHz) for $R = 9600$ bits/s
1. Absolute bandwidth	$\infty$
2. 3-dB bandwidth	$0.88R$
3. Equivalent noise bandwidth	$1.00R$
4. Null-to-null bandwidth	$2.00R$
5. Bounded spectrum bandwidth (50 dB)	$201.04R$
6. Power bandwidth	$20.56R$

$$A(f) = -10 \log_{10} \left[ \frac{P_{4\text{kHz}}(f)}{P_{\text{total}}} \right] \quad (2-202)$$

where  $P_{4\text{kHz}}(f)$  is the power in a 4-kHz band centered at frequency  $f$  and  $P_{\text{total}}$  is the total signal power. The power in a 4-kHz band (assuming that the PSD is approximately constant across the 4-kHz bandwidth) is

$$P_{4\text{kHz}}(f) = 4000 \mathcal{P}(f) \quad (2-203)$$

and, using the definition of equivalent bandwidth, we find that the total power is

$$P_{\text{total}} = B_{\text{eq}} \mathcal{P}(f_c) \quad (2-204)$$

where the spectrum has a maximum value at  $f = f_c$ . Using these two equations, (2-202) becomes

$$A(f) = -10 \log_{10} \left[ \frac{4000 \mathcal{P}(f)}{B_{\text{eq}} \mathcal{P}(f_c)} \right] \quad (2-205)$$

where  $A(f)$  is the decibel attenuation of power measured in a 4-kHz band at frequency  $f$  compared to the total average power level of the signal. For the case of BPSK signaling, using (2-201), we find that the decibel attenuation is

$$A(f) = -10 \log_{10} \left\{ \frac{4000}{R} \left[ \frac{\sin \pi T_b(f - f_c)}{\pi T_b(f - f_c)} \right]^2 \right\} \quad (2-206)$$

where  $R = 1/T_b$  is the data rate. If we attempt to find the value of  $R$  such that  $A(f)$  will fall below the specified FCC spectral envelope shown in Fig. 2-24 ( $B = 30$  MHz), we will find that  $R$  is so small that there will be numerous zeros in the  $(\sin x)/x$  function of (2-206) within the desired frequency range,  $-50$  MHz  $< (f - f_c) < 50$  MHz. This is difficult to plot, so we plot the envelope of  $A(f)$  instead, by replacing  $\sin \pi T_b(f - f_c)$  with its maximum value (unity). The resulting BPSK envelope curve for the decibel attenuation is shown in Fig. 2-24, where  $R = 0.0171$  Mbit/s.

It is obvious that the data rate allowed for a BPSK signal to meet the FCC  $B = 30$  MHz specification is ridiculously low. This is because the FCC bandwidth parameter specifies an almost absolutely bandlimited spectrum. To signal with a reasonable data rate, the pulse shape used in the transmitted signal must be modified from a rectangular shape (that gives the BPSK signal) to a rounded pulse such that the bandwidth of the transmitted signal will be almost absolutely bandlimited. Recalling our study of the sampling theorem, we realize that  $(\sin x)/x$  pulse shapes are prime candidates since they have an absolutely bandlimited spectrum. However, the  $(\sin x)/x$  pulses are not absolutely timelimited, so that this exact pulse shape cannot be used. Frank Amoroso and others have studied this problem, and a quasi-bandlimited version of the  $(\sin x)/x$  pulse shape has been proposed [Amoroso, 1980]. The decibel attenuation curve for this type of signaling, shown in Fig. 2-24, is seen to fit very nicely under the allowed FCC spectral envelope curve for the case of  $R = 25$  Mbit/s. This allowable data rate of 25 Mbit/s is a fantastic improvement over the  $R = 0.0171$  Mbit/s that was allowed for BPSK. It is also interesting to note that analog pulse shapes [ $(\sin x)/x$  type] are required instead of a digital (rectangular) pulse shape. *This is another way of saying that it is vital for digital communication engineers to be able to analyze and design analog systems as well as digital systems.*

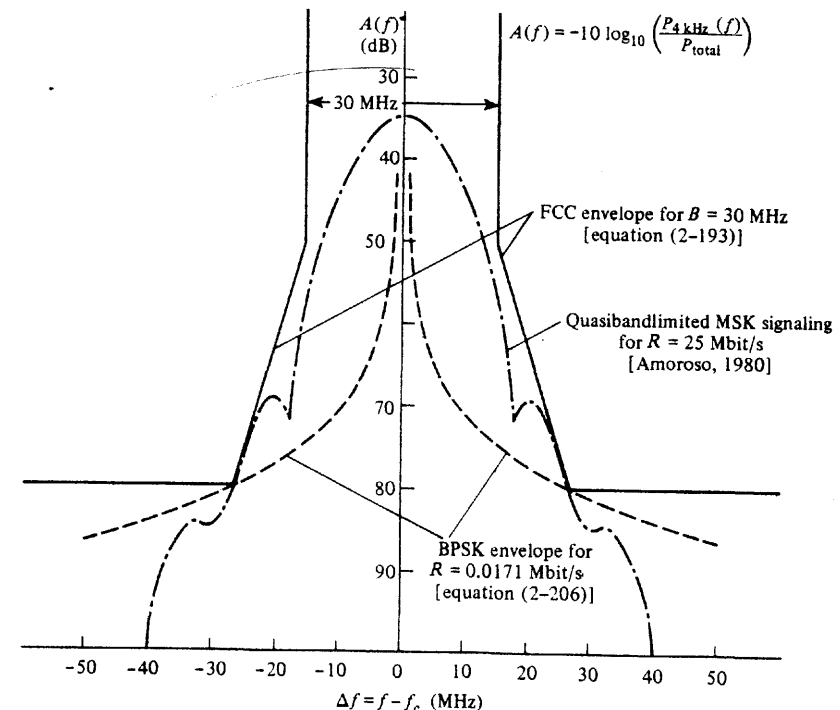


Figure 2-24 FCC-allowed envelope for  $B = 30$  MHz.

## 2.10 SUMMARY

Signals and noise may be deterministic (waveform known), where the signal is the desired part and noise is the undesired part; or they may be stochastic (waveform unknown but statistics of waveform known). Several useful properties of signals and noise are their spectra, dc value, rms value, and associated power.

The properties of Fourier transforms and spectra were studied in detail. The autocorrelation function and the PSD were defined and examined.

Signals and noise may be represented by orthogonal series expansions. Illustrations were given for digital and analog signals. The Fourier series and sampling function series were found to be especially useful.

Linear systems were reviewed, and the condition for distortionless transmission was found.

The properties of bandlimited signals and noise were developed. This resulted in the sampling theorem and the dimensionality theorem. The DFT was studied.

The concept of bandwidth was discussed, and seven popular definitions were given. An example of a BPSK signal was used to illustrate how different measures of bandwidth resulted from the same signal.

In Chapter 3, we will study how baseband analog waveforms are converted into baseband digital waveforms for transmission over digital communication systems.

## 2-11 STUDY-AID EXAMPLES

**SA2-1** Assume that  $v(t)$  is a periodic voltage waveform as shown in Fig. 2-25. Over the time interval  $0 < t < 1$ ,  $v(t)$  is described by  $e^t$ . Find the dc value and the rms value of this voltage waveform.

**Solution.** For periodic waveforms, the dc value is

$$V_{dc} = \langle v(t) \rangle = \frac{1}{T_0} \int_0^{T_0} v(t) dt = \int_0^1 e^t dt = e^1 - e^0$$

or

$$V_{dc} = e - 1 = 1.72 \text{ V}$$

Likewise,

$$V_{rms}^2 = \langle v^2(t) \rangle = \int_0^1 (e^t)^2 dt = \frac{1}{2} (e^2 - e^0) = 3.19$$

Thus,

$$V_{rms} = \sqrt{3.19} = 1.79 \text{ V}$$

**SA2-2** The periodic voltage waveform as shown in Fig. 2-25 appears across a  $600 \Omega$  resistive load. Calculate the average power dissipated in the load and the corresponding dBm value.

**Solution.**

$$P = V_{rms}^2 / R = (1.79)^2 / 600 = 5.32 \text{ mW}$$

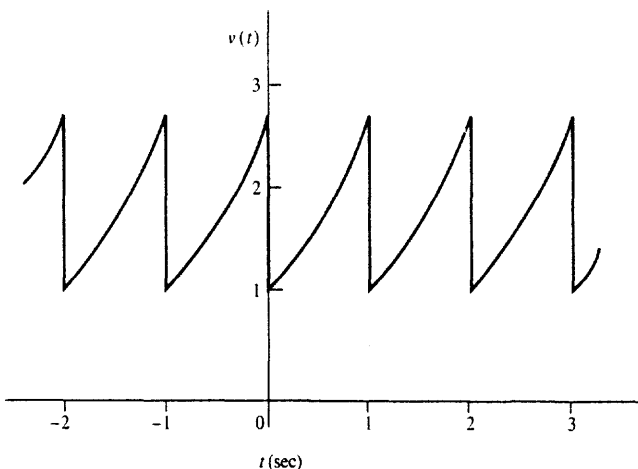


Figure 2-25

## Sec. 2-11 Study-Aid Examples

and

$$10 \log\left(\frac{P}{10^{-3}}\right) = 10 \log\left(\frac{5.32 \times 10^{-3}}{10^{-3}}\right) = 7.26 \text{ dBm}$$

**Note:** The peak instantaneous power is

$$\begin{aligned} \max [p(t)] &= \max [v(t) i(t)] = \max[v^2(t)/R] \\ &= \frac{(e)^2}{600} = 12.32 \text{ mW} \end{aligned}$$

**SA2-3** Find the spectrum for the waveform

$$w(t) = \Pi\left(\frac{t-5}{10}\right) + 8 \sin(6\pi t)$$

**Solution.** The spectrum of  $w(t)$  is the superposition of the spectrum for the rectangular pulse and the spectrum for the sinusoid. Using Tables 2-1 and 2-2,

$$\mathcal{F}\left[\Pi\left(\frac{t-5}{10}\right)\right] = 10 \frac{\sin(10\pi f)}{10\pi f} e^{j2\pi f 5}$$

and using the result of Example 2-4,

$$\mathcal{F}[8 \sin(6\pi t)] = j\frac{8}{2} [\delta(f+3) - \delta(f-3)]$$

Thus,

$$W(f) = 10 \frac{\sin(10\pi f)}{10\pi f} e^{j10\pi f} + j4[\delta(f+3) - \delta(f-3)]$$

**SA2-4** Find the spectrum for  $w(t) = 5 - 5e^{-2t} u(t)$ .

**Solution**

$$\begin{aligned} W(f) &= \int_{-\infty}^{\infty} w(t) e^{-j\omega t} dt \\ &= \int_{-\infty}^{\infty} 5e^{-j2\pi f t} dt - 5 \int_0^{\infty} e^{-2t} e^{-j\omega t} dt \\ &= 5\delta(f) - 5 \frac{e^{-2(1+j\pi f)t}}{-2(1+j\pi f)} \Big|_0^{\infty} \end{aligned}$$

or

$$W(f) = 5\delta(f) - \frac{5}{2 + j2\pi f}$$

**SA2-5** Show that  $\varphi_1(t) = \Pi(t)$  and  $\varphi_2(t) = \sin 2\pi t$  are orthogonal functions over the interval  $-0.5 < t < 0.5$ .

**Solution**

$$\begin{aligned} \int_a^b \varphi_1(t) \varphi_2(t) dt &= \int_{-0.5}^{0.5} 1 \sin 2\pi t dt = -\frac{\cos 2\pi t}{2\pi} \Big|_{-0.5}^{0.5} \\ &= \frac{-1}{2\pi} [\cos \pi - \cos(-\pi)] = 0 \end{aligned}$$

Because this integral is zero, (2-77) is satisfied. Consequently,  $\Pi(t)$  and  $\sin 2\pi t$  are orthogonal over  $-0.5 < t < 0.5$ . Note:  $\Pi(t)$  and  $\sin 2\pi t$  are not orthogonal over the interval  $0 < t < 1$  because  $\Pi(t)$  is zero for  $t > 0.5$ . That is, the integral is  $1/\pi$  (which is not zero).

**SA2-6** Find the Fourier series and the PSD for the waveform shown in Fig. 2-25. Over the time interval  $0 < t < 1$ ,  $v(t)$  is described by  $e^t$ .

**Solution.** Using (2-88) and (2-89), where  $T_0 = 1$  and  $\omega_0 = 2\pi/T_0 = 2\pi$

$$\begin{aligned} c_n &= \int_0^1 e^t e^{-jn2\pi t} dt = \frac{e^{(1-j2\pi n)t}}{1-j2\pi n} \Big|_0^1 \\ &= \frac{e-1}{1-j2\pi n} = 1.72 \frac{1}{1-j6.28n} \end{aligned}$$

Thus,

$$v(t) = 1.72 \sum_{n=-\infty}^{\infty} \frac{1}{1-j6.28n} e^{j2\pi nt}$$

Because  $v(t)$  is periodic, the PSD consists of delta functions as given by (2-126), where  $f_0 = 1/T_0 = 1$

$$\mathcal{P}(f) = \sum_{-\infty}^{\infty} |c_n|^2 \delta(f - nf_0)$$

or

$$\mathcal{P}(f) = \sum_{-\infty}^{\infty} \frac{2.95}{1 + (39.48)n^2} \delta(f - n)$$

**SA2-7** Let  $w(t)$  be a periodic function with period  $T_0$ , and let  $w(t)$  be *rotationally symmetric*. That is,  $w(t) = -w(t \pm T_0/2)$ . Prove that  $c_n = 0$  for even harmonics.

**Solution.** Using (2-89), and  $w(t) = -w(t - T_0/2)$

$$c_n = \frac{1}{T_0} \int_0^{T_0/2} w(t) e^{-jn\omega_0 t} dt - \frac{1}{T_0} \int_{T_0/2}^T w(t - T_0/2) e^{-jn\omega_0 t} dt$$

Make a change in variables. Let  $t_1 = t$  in the first integral and  $t_1 = t - T_0/2$  in the second integral. Then,

$$c_n = \frac{1}{T_0} \int_0^{T_0/2} w(t_1) e^{-jn\omega_0 t_1} dt_1 - \frac{1}{T_0} \int_0^{T_0/2} w(t_1) e^{-jn\omega_0(t_1 + T_0/2)} dt_1$$

or

$$= \frac{1}{T_0} \int_0^{T_0/2} w(t_1) e^{jn\omega_0 t_1} (1 - e^{-jn\pi}) dt_1$$

But  $(1 - e^{jn\pi}) = 0$  for  $n = \dots, -2, 0, 2, \dots$ . Thus,  $c_n = 0$  if  $n$  is even and  $w(t) = -w(t - T_0/2)$ . Similarly, it can be shown that  $c_n = 0$  if  $n$  is odd and  $w(t) = -w(t + T_0/2)$ .

## PROBLEMS

**2-1** For a sinusoidal waveform with a peak value of  $A$  and a frequency of  $f_0$ , use the time average operator to show that the rms value for this waveform is  $A/\sqrt{2}$ .

**2-2** A function generator produces a periodic voltage waveform as shown in Fig. P2-2.

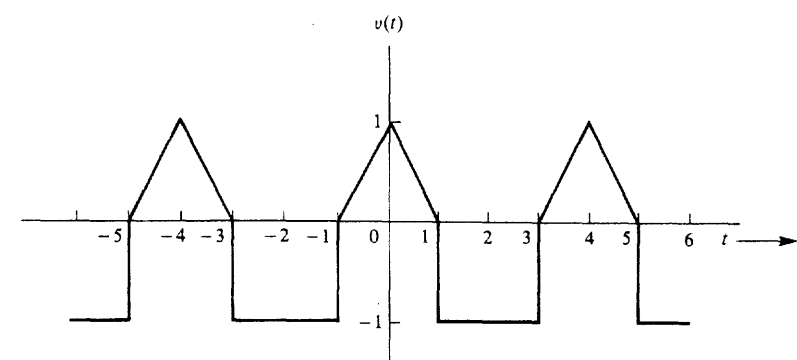


Figure P2-2

**(a)** Find the value for the dc voltage.

**(b)** Find the value for the rms voltage.

**(c)** If this voltage waveform is applied across a  $1000\text{-}\Omega$  load, what is the power dissipated in the load?

**2-3** The voltage across a load is given by  $v(t) = A_0 \cos \omega_0 t$ , and the current through the load is a square wave.

$$i(t) = I_0 \sum_{n=-\infty}^{\infty} \left[ \Pi\left(\frac{t - nT_0}{T_0/2}\right) - \Pi\left(\frac{t - nT_0 - (T_0/2)}{T_0/2}\right) \right]$$

where  $\omega_0 = 2\pi/T_0$ ,  $T_0 = 1$  sec,  $A_0 = 10$  V, and  $I_0 = 5$  mA.

**(a)** Find the expression for the instantaneous power and sketch this result as a function of time.

**(b)** Find the value of the average power.

- 2-4 The voltage across a  $50\Omega$  resistive load is the positive portion of a cosine wave. That is,

$$v(t) = \begin{cases} 10 \cos \omega_0 t, & |t - nT_0| < T_0/4 \\ 0, & \text{elsewhere} \end{cases}$$

where  $n$  is any integer.

- (a) Sketch the voltage and current waveforms.
- (b) Evaluate the dc values for the voltage and current.
- (c) Find the rms values for the voltage and current.
- (d) Find the total average power dissipated in the load.

- 2-5 For Prob. 2-4, find the energy dissipated in the load during a 1-hr interval if  $T_0 = 1$  sec.

- 2-6 Determine whether each of the following signals is an energy signal or a power signal and evaluate the normalized energy or power, as appropriate.

- (a)  $w(t) = \Pi(t/T_0)$ .
- (b)  $w(t) = \Pi(t/T_0) \cos \omega_0 t$ .
- (c)  $w(t) = \cos^2 \omega_0 t$ .

- 2-7 An average reading power meter is connected to the output circuit of a transmitter. The transmitter output is fed into a  $75\Omega$  resistive load and the wattmeter reads 67 W.

- (a) What is the power in dBm units?
- (b) What is the power in dBk units?
- (c) What is the value in dBmV units?

- 2-8 Assume that a waveform with a known rms value,  $V_{\text{rms}}$ , is applied across a  $50\Omega$  load. Derive a formula that can be used to compute the dBm value from  $V_{\text{rms}}$ .

- 2-9 An amplifier is connected to a  $50\Omega$  load and driven by a sinusoidal current source, as shown in Fig. P2-9. The output resistance of the amplifier is  $10\Omega$  and the input resistance is  $2\text{k}\Omega$ . Evaluate the true decibel gain of this circuit.

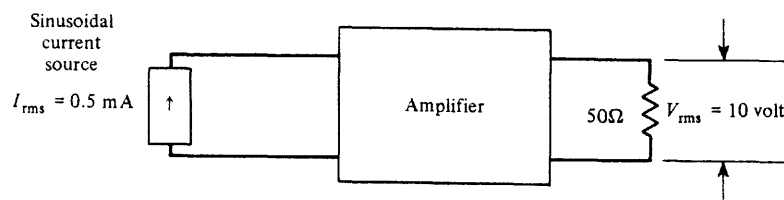


Figure P2-9

- 2-10 The voltage (rms) across the  $300\Omega$  antenna input terminals of an FM receiver is  $3.5\mu\text{V}$ .

- (a) Find the input power (watts).
- (b) Evaluate the input power as measured in decibels below 1 mW (dBm).
- (c) What would be the input voltage (in microvolts) for the same input power if the input resistance were  $75\Omega$  instead of  $300\Omega$ ?

- 2-11 What is the value for the phasor that corresponds to the voltage waveform  $v(t) = 12 \sin(\omega_0 t - 25^\circ)$ , where  $\omega_0 = 2000\pi$ ?

- 2-12 A signal is  $w(t) = 3 \sin(100\pi t - 30^\circ) + 4 \cos(100\pi t)$ . Find the corresponding phasor.

- 2-13 Evaluate the Fourier transform of

$$w(t) = \begin{cases} e^{-at}, & t \geq 1 \\ 0, & t < 0 \end{cases}$$

- 2-14 Find the spectrum for the waveform  $w(t) = e^{-\pi(t/T)^2}$  in terms of the parameter  $T$ . What can we say about the width of  $w(t)$  and  $W(f)$  as  $T$  increases? [Hint: Use (A-75).]

- 2-15 Using the convolution property, find the spectrum for

$$w(t) = \sin 2\pi f_1 t \cos 2\pi f_2 t$$

- 2-16 Find the spectrum (Fourier transform) of the triangle waveform

$$s(t) = \begin{cases} At, & 0 < t < T_0 \\ 0, & \text{elsewhere} \end{cases}$$

in terms of  $A$  and  $T_0$ .

- 2-17 Find the spectrum for the waveform shown in Fig. P2-17.

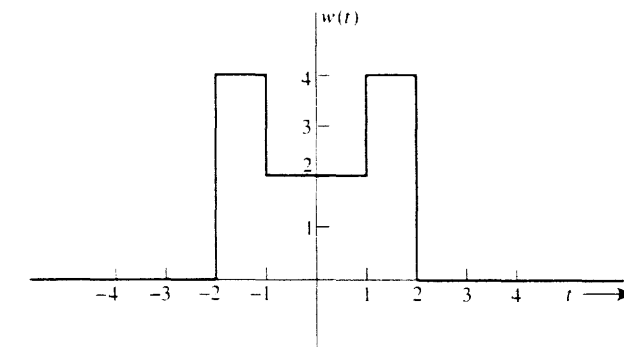


Figure P2-17

- 2-18 If  $w(t)$  has the Fourier transform

$$W(f) = \frac{j2\pi f}{1 + j2\pi f}$$

find  $X(f)$  for the following waveforms.

- (a)  $x(t) = w(2t + 2)$ .
  - (b)  $x(t) = e^{-jt}w(t - 1)$ .
  - (c)  $x(t) = 2 \frac{dw(t)}{dt}$ .
  - (d)  $x(t) = w(1 - t)$ .
- 2-19 Using (2-30), find  $w(t)$  for  $W(f) = A\Pi(f/2B)$  and verify your answer using the duality property.
- 2-20 Find the quadrature spectral functions  $X(f)$  and  $Y(f)$  for the damped sinusoidal waveform

$$w(t) = u(t)e^{-at} \sin \omega_0 t$$

where  $u(t)$  is a unit step function,  $a > 0$ , and  $W(f) = X(f) + jY(f)$ .

- 2-21 Derive the spectrum of  $w(t) = e^{-|t|/T}$ .



- 2-22 Find the Fourier transforms for the following waveforms. Plot the waveforms and their magnitude spectra. [Hint: Use (2-184).]

$$(a) \Pi\left(\frac{t-3}{4}\right).$$

(b) 2.

$$(c) \Lambda\left(\frac{t-5}{5}\right).$$



- 2-23 Find the approximate Fourier transform for the following waveform using (2-184)

$$x(t) = \begin{cases} \sin(2\pi t/512) + \sin(70\pi t/512), & 5 < t < 75 \\ 0, & \text{elsewhere} \end{cases}$$

- 2-24 Evaluate the spectrum for the trapezoidal pulse shown in Fig. P2-24.

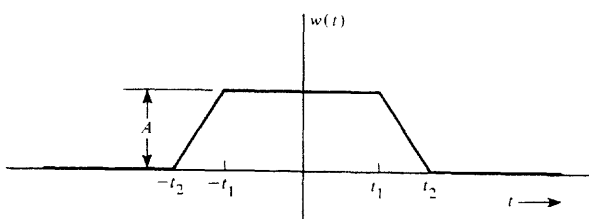


Figure P2-24

- 2-25 Show that

$$\mathcal{F}^{-1}\{\mathcal{F}[w(t)]\} = w(t)$$

[Hint: Use (2-33).]

- 2-26 Using the definition of the inverse Fourier transform, show that the value of  $w(t)$  at  $t = 0$  is equal to the area under  $W(f)$ . That is, show that

$$w(0) = \int_{-\infty}^{\infty} W(f) df$$

- 2-27 Prove that:

- (a) If  $w(t)$  is real and an even function of  $t$ ,  $W(f)$  is real.
- (b) If  $w(t)$  is real and an odd function of  $t$ ,  $W(f)$  is imaginary.

- 2-28 Suppose that the spectrum of a waveform as a function of frequency in hertz is

$$W(f) = \frac{1}{2} \delta(f - 4) + \frac{1}{2} \delta(f + 4) + \frac{j\pi f}{2 + j2\pi f} e^{j\pi f}$$

Find the corresponding spectrum as a function of radian frequency,  $W(\omega)$ .

- 2-29 The unit impulse can also be defined as follows:

$$\delta(t) = \lim_{a \rightarrow \infty} \left[ K_a \left( \frac{\sin at}{at} \right) \right]$$

Find the value of  $K$  needed, and show that this definition is consistent with those given in the text. Give another example of an ordinary function such that in the limit of some parameter, the function becomes a Dirac delta function.

- 2-30 Use  $v(t) = ae^{-at}$ ,  $a > 0$ , to approximate  $\delta(t)$  as  $a \rightarrow \infty$ .

- (a) Plot  $v(t)$  for  $a = 0.1, 1$ , and  $10$ .

- (b) Plot  $V(f)$  for  $a = 0.1, 1$ , and  $10$ .

- 2-31 Show that

$$\operatorname{sgn}(t) \leftrightarrow \frac{1}{j\pi f}$$

[Hint: Use (2-30) and  $\int_0^\infty (\sin x)/x dx = \pi/2$  from Appendix A.]

- 2-32 Show that

$$u(t) \leftrightarrow \frac{1}{2} \delta(f) + \frac{1}{j2\pi f}$$

[Hint: Use the linearity (superposition) theorem and the result of Prob. 2-31.]

- 2-33 Show that the sifting property of  $\delta$  functions, (2-47), may be generalized to evaluate integrals that involve derivatives of the delta function. That is, show that

$$\int_{-\infty}^{\infty} w(x) \delta^{(n)}(x - x_0) dx = (-1)^n w^{(n)}(x_0)$$

where the superscript  $(n)$  denotes the  $n$ th derivative. (Hint: Use integration by parts.)

- 2-34 Let  $x(t) = \Pi\left(\frac{t-0.05}{0.1}\right)$ . Plot the spectrum of  $x(t)$  using MATLAB with the help of (2-59) and (2-60). Check your results by using the FFT and (2-184).

- 2-35 If  $w(t) = w_1(t)w_2(t)$ , show that

$$W(f) = \int_{-\infty}^{\infty} W_1(\lambda)W_2(f - \lambda) d\lambda$$

where  $W(f) = \mathcal{F}[w(t)]$ .

- 2-36 Show that:

- (a)  $\int_{-\infty}^t w(\lambda) d\lambda = w(t) * u(t)$ .
- (b)  $\int_{-\infty}^t w(\lambda) d\lambda \leftrightarrow (j2\pi f)^{-1} W(f) + \frac{1}{2} W(0) \delta(f)$ .
- (c)  $w(t) * \delta(t - a) = w(t - a)$ .

- 2-37 Show that

$$\frac{dw(t)}{dt} \leftrightarrow (j2\pi f)W(f)$$

[Hint: Use (2-26) and integrate by parts. Assume that  $w(t)$  is absolutely integrable.]

- 2-38 As discussed in Example 2-8, show that

$$\frac{1}{T} \Pi\left(\frac{t}{T}\right) * \Pi\left(\frac{t}{T}\right) = \Lambda\left(\frac{t}{T}\right)$$

**2-39** Given the waveform  $w(t) = A\Pi(t/T) \sin \omega_0 t$ . Find the spectrum of  $w(t)$  by using the multiplication theorem as discussed in Example 2-9.

**2-40** Evaluate the following integrals.

(a)  $\int_{-\infty}^{\infty} \frac{\sin 4\lambda}{4\lambda} \delta(t - \lambda) d\lambda$ .

(b)  $\int_{-\infty}^{\infty} (\lambda^3 - 1) \delta(2 - \lambda) d\lambda$ .

**2-41** Prove that

$$M(f) * \delta(f - f_0) = M(f - f_0)$$

**2-42** Evaluate  $y(t) = w_1(t) * w_2(t)$ , where

$$w_1(t) = \begin{cases} 1, & |t| < T_0 \\ 0, & \text{elsewhere} \end{cases}$$

$$w_2(t) = \begin{cases} [1 - 2|t|], & |t| < \frac{1}{2}T_0 \\ 0, & \text{elsewhere} \end{cases}$$

**2-43** Given  $w(t) = 5 + 12 \cos \omega_0 t$  where  $f_0 = 10 \text{ Hz}$ :

- (a) Find  $R_w(\tau)$ .
- (b)  $\mathcal{P}_w(f)$ .

**2-44** Given the waveform

$$w(t) = A_1 \cos(\omega_1 t + \theta_1) + A_2 \cos(\omega_2 t + \theta_2)$$

where  $A_1, A_2, \omega_1, \omega_2, \theta_1$ , and  $\theta_2$  are constants.

- (a) Find the autocorrelation for  $w(t)$  as a function of the constants.
- (b) Find the PSD function for  $w(t)$ .
- (c) Sketch the PSD for the case of  $\omega_1 \neq \omega_2$ .
- (d) Sketch the PSD for the case of  $\omega_1 = \omega_2$  and  $\theta_1 = \theta_2 + 90^\circ$ .
- (e) Sketch the PSD for the case of  $\omega_1 = \omega_2$  and  $\theta_1 = \theta_2$ .

**2-45** Given the periodic voltage waveform shown in Fig. P2-45:

- (a) Find the dc value for this waveform.
- (b) Find the rms value for this waveform.

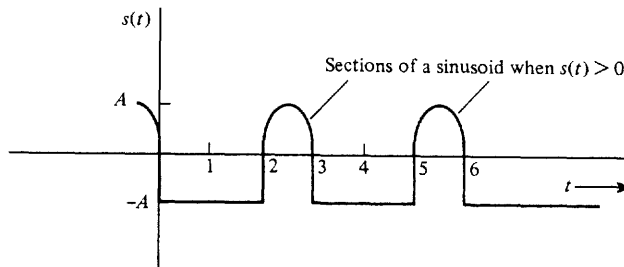


Figure P2-45

(c) Find the complex exponential Fourier series.

(d) Find the voltage spectrum for this waveform.

**2-46** Determine if  $s_1(t)$  and  $s_2(t)$  are orthogonal over the interval  $(-\frac{5}{2}T_2 < t < \frac{5}{2}T_2)$ , where  $s_1(t) = A_1 \cos(\omega_1 t + \varphi_1)$ ,  $s_2(t) = A_2 \cos(\omega_2 t + \varphi_2)$ , and  $\omega_2 = 2\pi/T_2$  for the following cases.

- (a)  $\omega_1 = \omega_2$  and  $\varphi_1 = \varphi_2$ .
- (b)  $\omega_1 = \omega_2$  and  $\varphi_1 = \varphi_2 + \pi/2$ .
- (c)  $\omega_1 = \omega_2$  and  $\varphi_1 = \varphi_2 + \pi$ .
- (d)  $\omega_1 = 2\omega_2$  and  $\varphi_1 = \varphi_2$ .
- (e)  $\omega_1 = \frac{1}{2}\omega_2$  and  $\varphi_1 = \varphi_2$ .
- (f)  $\omega_1 = \pi\omega_2$  and  $\varphi_1 = \varphi_2$ .

**2-47** Let  $s(t) = A_1 \cos(\omega_1 t + \varphi_1) + A_2 \cos(\omega_2 t + \varphi_2)$ . Determine the rms value of  $s(t)$  in terms of  $A_1$  and  $A_2$  for the following cases.

- (a)  $\omega_1 = \omega_2$  and  $\varphi_1 = \varphi_2$ .
- (b)  $\omega_1 = \omega_2$  and  $\varphi_1 = \varphi_2 + \pi/2$ .
- (c)  $\omega_1 = \omega_2$  and  $\varphi_1 = \varphi_2 + \pi$ .
- (d)  $\omega_1 = 2\omega_2$  and  $\varphi_1$  and  $\varphi_2$ .
- (e)  $\omega_1 = 2\omega_2$  and  $\varphi_1 = \varphi_2 + \pi$ .

**2-48** Show that

$$\sum_{k=-\infty}^{\infty} \delta(t - kT_0) \leftrightarrow f_0 \sum_{k=-\infty}^{\infty} \delta(f - kf_0)$$

where  $f_0 = 1/T_0$ . [Hint: Expand  $\sum_{k=-\infty}^{\infty} \delta(t - kT_0)$  into a Fourier series and then take the Fourier transform.]

**2-49** Three functions are shown in Fig. P2-49.

- (a) Show that these functions are orthogonal over the interval  $(-4, 4)$ .

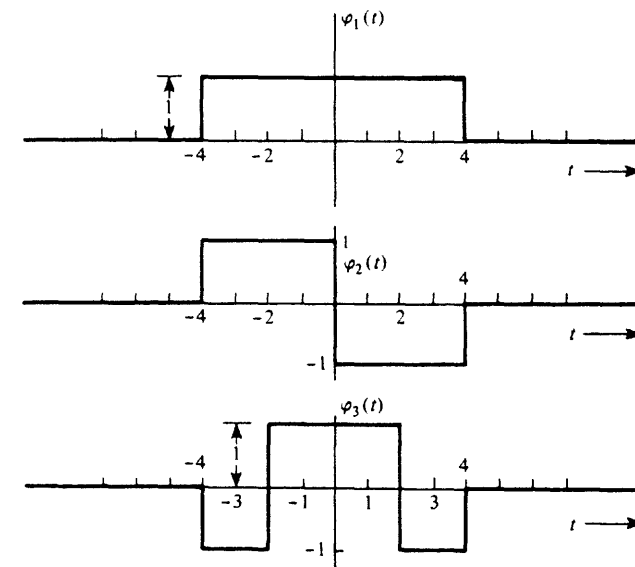


Figure P2-49

- (b) Find the corresponding orthonormal set of functions.  
 (c) Expand the waveform

$$w(t) = \begin{cases} 1, & 0 \leq t \leq 4 \\ 0, & \text{elsewhere} \end{cases}$$

into an orthonormal series using this orthonormal set.

- (d) Evaluate the mean square error for the orthogonal series obtained in part (c) by evaluating

$$\epsilon = \int_{-4}^4 \left[ w(t) - \sum_{j=1}^3 a_j \varphi_j(t) \right]^2 dt$$

- (e) Repeat parts (c) and (d) for the waveform

$$w(t) = \begin{cases} \cos(\frac{1}{4}\pi t), & -4 \leq t \leq 4 \\ 0, & \text{elsewhere} \end{cases}$$

Are the three orthonormal functions a complete orthonormal set?

- 2-50 Show that the quadrature Fourier series basis functions  $\cos(n\omega_0 t)$  and  $\sin(n\omega_0 t)$  as given in (2-95) are orthogonal over the interval  $a < t < a + T_0$  where  $\omega_0 = 2\pi/T_0$ .  
 2-51 Find expressions for the complex Fourier series coefficients that represent the waveform shown in Fig. P2-51.

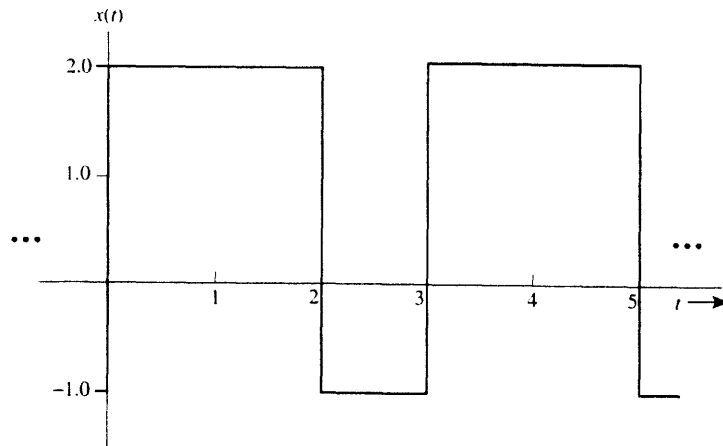


Figure P2-51

- 2-52 The periodic signal as shown in Fig. P2-51 is passed through a linear filter having the impulse response  $h(t) = e^{-\alpha t}u(t)$ , where  $t > 0$  and  $\alpha > 0$ .  
 (a) Find expressions for the complex Fourier series coefficients associated with the output waveform  $y(t) = x(t) * h(t)$ .  
 (b) Find an expression for the normalized power of the output,  $y(t)$ .  
 2-53 Find the complex Fourier series for the periodic waveform given in Figure P2-2.  
 2-54 Find the complex Fourier series coefficients for the periodic rectangular waveform shown in Fig. P2-54 as a function of  $A$ ,  $T$ ,  $b$ , and  $\tau_0$ . [Hint: The answer can be reduced to a  $(\sin x)/x$  form multiplied by a phase-shift factor,  $e^{j\theta_n(\tau_0)}$ .]

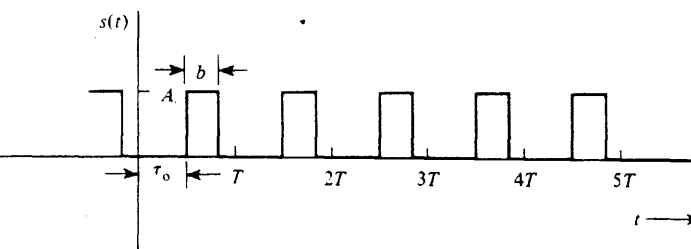


Figure P2-54

- 2-55 For the waveform shown in Fig. P2-55, find:

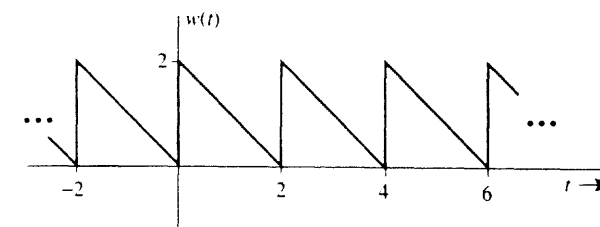


Figure P2-55

- (a) The complex Fourier series.  
 (b) The quadrature Fourier series.

- 2-56 Given a periodic waveform  $s(t) = \sum_{n=-\infty}^{\infty} p(t - nT_0)$ , where

$$p(t) = \begin{cases} At, & 0 < t < T \\ 0, & \text{elsewhere} \end{cases}$$

and  $T \leq T_0$ .

- (a) Find the  $c_n$  Fourier series coefficients.  
 (b) Find the  $\{x_n, y_n\}$  Fourier series coefficients.  
 (c) Find the  $\{D_n, \varphi_n\}$  Fourier series coefficients.

- 2-57 Prove that the polar form of the Fourier series, (2-103), can be obtained by rearranging the terms in the complex Fourier series, (2-88).

- 2-58 Prove that (2-93) is correct.

- 2-59 Let two complex numbers  $c_1$  and  $c_2$  be represented by  $c_1 = x_1 + jy_1$  and  $c_2 = x_2 + jy_2$ , where  $x_1, x_2, y_1$  and  $y_2$  are real numbers. Show that  $\operatorname{Re}\{\cdot\}$  is a linear operator by demonstrating that

$$\operatorname{Re}\{c_1 + c_2\} = \operatorname{Re}\{c_1\} + \operatorname{Re}\{c_2\}$$

- 2-60 Assume that  $y(t) = s_1(t) + 2s_2(t)$ , where  $s_1(t)$  is given by Fig. P2-45 and  $s_2(t)$  is given by Fig. P2-54.  $T = 3$ ,  $b = 1.5$ , and  $\tau_0 = 0$ . Find the complex Fourier coefficients  $\{c_n\}$  for  $y(t)$ .



- 2-61 Evaluate the PSD for the waveform shown in Fig. P2-2.

- 2-62 Assume that  $v(t)$  is a triangular waveform, as shown in Fig. P2-62.  
 (a) Find the complex Fourier series for  $v(t)$ .  
 (b) Calculate the normalized average power.

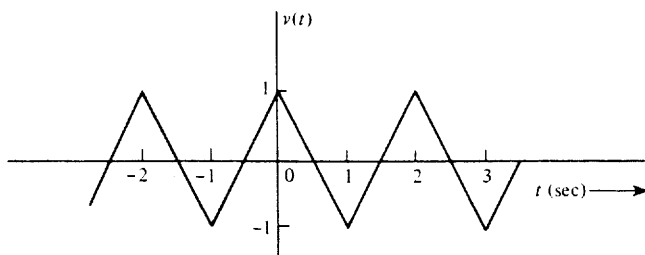


Figure P2-62

- (c) Calculate and plot the voltage spectrum.  
 (d) Calculate and plot the PSD.

**2-63** Let a complex number  $c$  be represented by  $c = x + jy$  where  $x$  and  $y$  are real numbers. Show that

$$(a) \operatorname{Re}\{c\} = \frac{1}{2}c + \frac{1}{2}c^*$$

$$(b) \operatorname{Im}\{c\} = \frac{1}{2j}c - \frac{1}{2j}c^*$$

where  $c^*$  is the complex conjugate of  $c$ . Note that when  $c = e^{jz}$ , (a) gives the definition of  $\cos z$  and (b) gives the definition of  $\sin z$ .



**2-64** Calculate and plot the PSD for the half-wave rectified sinusoid described by P2-4.

**2-65** The basic definitions for sine and cosine waves are

$$\sin z_1 \triangleq \frac{e^{iz_1} - e^{-iz_1}}{2j} \quad \text{and} \quad \cos z_2 \triangleq \frac{e^{iz_2} + e^{-iz_2}}{2}$$

Show that

$$(a) \cos z_1 \cos z_2 = \frac{1}{2} \cos(z_1 - z_2) + \frac{1}{2} \cos(z_1 + z_2).$$

$$(b) \sin z_1 \sin z_2 = \frac{1}{2} \cos(z_1 - z_2) - \frac{1}{2} \cos(z_1 + z_2).$$

$$(c) \sin z_1 \cos z_2 = \frac{1}{2} \sin(z_1 - z_2) + \frac{1}{2} \sin(z_1 + z_2).$$

**2-66** Let two complex numbers  $c_1$  and  $c_2$  be represented by  $c_1 = x_1 + jy_1$  and  $c_2 = x_2 + jy_2$ , where  $x_1, x_2, y_1$ , and  $y_2$  are real numbers. Show that

$$\operatorname{Re}\{c_1\} \operatorname{Re}\{c_2\} = \frac{1}{2} \operatorname{Re}\{c_1 c_2^*\} + \frac{1}{2} \operatorname{Re}\{c_1 c_2\}$$

Note that this is a generalization of the  $\cos z_1 \cos z_2$  identity of Prob. 2-65, where for the  $\cos z_1 \cos z_2$  identity,  $c_1 = e^{jz_1}$  and  $c_2 = e^{jz_2}$ .

**2-67** Prove that the Fourier transform is a linear operator. That is, show that

$$\mathcal{F}[ax(t) + by(t)] = a\mathcal{F}[x(t)] + b\mathcal{F}[y(t)]$$



**2-68** Plot the amplitude and phase response for the transfer function

$$H(f) = \frac{j10f}{5 + jf}$$



**2-69** Given the filter shown in Fig. P2-69.

- (a) Find the transfer function for this filter.

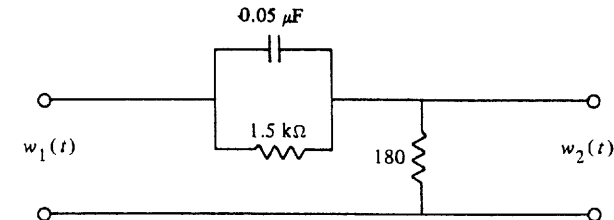


Figure P2-69

- (b) Plot the magnitude and phase response.  
 (c) Find the power transfer function for this filter.  
 (d) Plot the power transfer function.

**2-70** A signal with a PSD of

$$\mathcal{P}_x(f) = \frac{2}{(1/4\pi)^2 + f^2}$$

is applied to the network shown in Fig. P2-70.

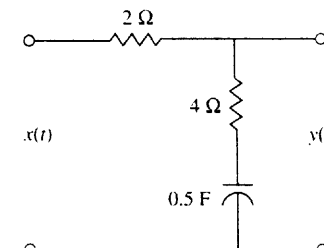


Figure P2-70

- (a) Find the PSD for  $y(t)$ .  
 (b) Find the average normalized power for  $y(t)$ .

**2-71** A signal  $x(t)$  has a PSD

$$\mathcal{P}_x(f) = \frac{K}{[1 + (2\pi f/B)^2]^2}$$

where  $K > 0$  and  $B > 0$ .

- (a) Find the 3-dB bandwidth in terms of  $B$ .  
 (b) Find the equivalent noise bandwidth in terms of  $B$ .

**2-72** The signal  $x(t) = e^{-400\pi t}u(t)$  is applied to a brick-wall low-pass filter where the transfer function of the filter is

$$H(f) = \begin{cases} 1, & |f| \leq B \\ 0, & |f| > B \end{cases}$$

Find the value of  $B$  such that the filter passes one-half the energy of  $x(t)$ .

- 2-73** Show that the average normalized power of a waveform can be found by evaluating the auto-correlation  $R_w(\tau)$  at  $\tau = 0$ . That is,  $P = R_w(0)$ .  
*Hint:* See (2-69) and (2-70).

- 2-74** The signal  $x(t) = 0.5 + 1.5 \cos[(\frac{2}{3})\pi t] + 0.5 \sin[(\frac{2}{3})\pi t]$  V is passed through an  $RC$  low-pass filter (see Fig. 2-15a) where  $R = 1 \Omega$  and  $C = 1 \text{ F}$ .

- (a) What is the input PSD,  $\mathcal{P}_x(f)$ ?
- (b) What is the output PSD,  $\mathcal{P}_y(f)$ ?
- (c) What is the average normalized output power,  $P_y$ ?

- 2-75** The input to the  $RC$  low-pass filter shown in Fig. 2-15 is

$$x(t) = 0.5 + 1.5 \cos \omega_x t + 0.5 \sin \omega_x t$$

Assume that the cutoff frequency is  $f_0 = 1.5f_c$ .

- (a) Find the input PSD,  $\mathcal{P}_x(f)$ .
- (b) Find the output PSD,  $\mathcal{P}_y(f)$ .
- (c) Find the normalized average power of the output,  $y(t)$ .

- 2-76** Using MATLAB, plot the frequency magnitude response and phase response for the low-pass filter shown in Fig. P2-76, where  $R_1 = 7.5 \text{ k}\Omega$ ,  $R_2 = 15 \text{ k}\Omega$ , and  $C = 0.1 \mu\text{F}$ .

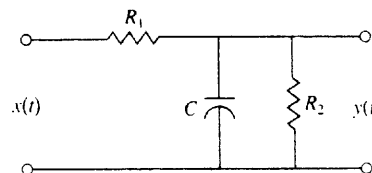


Figure P2-76

- 2-77** A comb filter is shown in Fig. P2-77. Let  $T_d = 0.1$ .

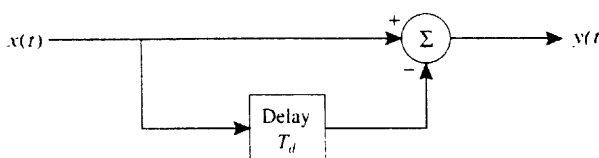


Figure P2-77

- (a) Plot the magnitude of the transfer function for this filter.
  - (b) If the input is  $x(t) = \Pi(t/T)$ , where  $T = 1$ , plot the spectrum of the output  $|Y(f)|$ .
- 2-78** A signal  $x(t) = \Pi(t - 0.5)$  passes through a filter that has the transfer function  $H(f) = \Pi(f/B)$ . Plot the output waveform when:
- (a)  $B = 0.6 \text{ Hz}$ .
  - (b)  $B = 1 \text{ Hz}$ .
  - (c)  $B = 50 \text{ Hz}$ .
- 2-79** Examine the distortion effect of an  $RC$  low-pass filter. Assume that a unity-amplitude periodic square wave with a 50% duty cycle is present at the filter input and that the filter has a 3dB bandwidth of 1500 Hz. Using a computer or a programmable calculator, find and plot the output waveshape if the square wave has a frequency of:

- (a) 300 Hz.
- (b) 500 Hz.
- (c) 1000 Hz.

*Hint:* Represent the square wave with a Fourier series.

- 2-80** Given that the PSD of a signal is flat [i.e.,  $\mathcal{P}_s(f) = 1$ ], design an  $RC$  low-pass filter that will attenuate this signal by 20 dB at 15 kHz. That is, find the value for the  $RC$  of Fig. 2-15 such that the design specifications are satisfied.

- 2-81** The bandwidth of  $g(t) = e^{-0.1t}$  is approximately 0.5 Hz; thus it can be sampled with a sampling frequency of  $f_s = 1 \text{ Hz}$  without significant aliasing. Take samples  $a_n$  over the time interval (0,14). Use the sampling theorem, (2-158), to reconstruct the signal. Plot and compare the reconstructed signal with the original signal. Do they match? What happens when the sampling frequency is reduced?

- 2-82** A waveform,  $20 + 20 \sin(500t + 30^\circ)$ , is to be sampled periodically and reproduced from these sample values.

- (a) Find the maximum allowable time interval between sample values.
- (b) How many sample values need to be stored in order to reproduce 1 sec of this waveform?

- 2-83** Using a computer program, calculate the DFT of a rectangular pulse,  $\Pi(t)$ . Take five samples of the pulse and pad it with 59 zeros so that a 64-point FFT algorithm can be used. Sketch the resulting magnitude spectrum. Compare this result with the actual spectrum for the pulse. Try other combinations of number of pulse samples and zero-pads to see how the resulting FFT changes.

- 2-84** Using the DFT, compute and plot the spectrum of  $\Lambda(t)$ . Check your results with those given in Fig. 2-6c.

- 2-85** Using the DFT, compute and plot  $|W(f)|$  for the pulse shown in Fig. P2-24, where  $A = 1$ ,  $t_1 = 1 \text{ s}$ , and  $t_2 = 2 \text{ s}$ .

- 2-86** Given the waveform

$$w(t) = 4 \sin(2\pi f_1 t + 30^\circ) + 2 \cos(2\pi f_2 t - 10^\circ)$$

where  $f_1 = 10 \text{ Hz}$  and  $f_2 = 25 \text{ Hz}$ ,

- (a) Using the DFT, compute and plot  $|W(f)|$  and  $\theta(f)$ .
- (b) Let  $\mathcal{P}_w(f)$  denote the PSD of  $w(t)$ . Using the DFT, compute and plot  $\mathcal{P}_w(f)$ .
- (c) Check your computed results obtained in (a) and (b) with known correct results that you have evaluated by using analytical methods.

- 2-87** Using the DFT, compute and plot  $|S(f)|$  for the periodic signal shown in Fig. P2-45, where  $A = 5$ .

- 2-88** Given the low-pass filter shown in Fig. 2-15,

- (a) Find the equivalent bandwidth in terms of  $R$  and  $C$ .
- (b) Find the first zero-crossing (null) bandwidth of the filter.
- (c) Find the absolute bandwidth of the filter.

- 2-89** Assume that the PSD of a signal is given by

$$\mathcal{P}_s(f) = \left[ \frac{\sin(\pi f/B_n)}{\pi f/B_n} \right]^2$$

where  $B_n$  is the null bandwidth. Find the expression for the equivalent bandwidth in terms of the null bandwidth.

- 2-90** Table 2-5 gives the bandwidths of a BPSK signal using six different definitions. Using the six definitions and (2-201), show that the results given in the table are correct.
- 2-91** Given a triangular pulse signal

$$s(t) = \Lambda(t/T_0)$$

- (a) Find the absolute bandwidth of this signal.
- (b) Find the 3-dB bandwidth in terms of  $T_0$ .
- (c) Find the equivalent bandwidth in terms of  $T_0$ .
- (d) Find the zero-crossing bandwidth in terms of  $T_0$ .

## CHAPTER 3

# BASEBAND PULSE AND DIGITAL SIGNALING

### 3-1 INTRODUCTION

This chapter shows how to encode analog waveforms (from analog sources) into baseband pulse signals and how to approximate analog signals with digital signals. As we will see, the digital approximation to the analog signal can be made very precise if we wish. In addition, we will learn how to process the digital baseband signals so that their bandwidth is minimized.

Digital signaling is popular because of the low cost of digital circuits and the flexibility of the digital approach. This flexibility arises, for example, because the digital data from digital sources may be merged with digitized data derived from analog sources to provide a general-purpose communication system.

The signals involved in the analog-to-digital conversion problem are *baseband* signals. We also realize that *bandpass* digital communication signals are produced by using baseband digital signals to modulate a carrier, as described in Chapter 1. For example, if a digital (baseband) signal phase modulates a carrier, the resulting digital bandpass signal is said to

be a *phase-shift-keyed* (PSK) signal. Bandpass digital communication systems such as PSK are discussed in more detail in Chapter 5.

The four main goals of this chapter are:

- To study how analog waveforms can be converted to digital waveforms. The most popular technique is called *pulse code modulation* (PCM).
- To learn how to compute the spectrum for digital signals.
- To examine how filtering of pulse signals affects our ability to recover the digital information at the receiver. This filtering can produce what is called *intersymbol interference* (ISI) in the recovered data signal.
- To study how we can *multiplex* (combine) data from several digital bit streams into one high-speed digital stream for transmission over a digital system. One such technique, called *time-division multiplexing* (TDM), will be studied in this chapter.<sup>†</sup>

There is another very important problem in digital communication systems: the effect of noise in causing the digital receiver to produce some bit errors at the output. This problem will be studied in Chapter 7 since it involves the use of statistical concepts that are emphasized in the second part of this book.

### 3-2 PULSE AMPLITUDE MODULATION

*Pulse amplitude modulation* (PAM) is an engineering term that is used to describe the conversion of the analog signal to a pulse-type signal where the amplitude of the pulse denotes the analog information. As we will see in Sec. 3-3, this PAM signal can be converted into a PCM digital signal (baseband), which in turn is modulated onto a carrier in bandpass digital communication systems. Consequently, the analog-to-PAM conversion process is the first step in converting an analog waveform to a PCM (digital) signal. (In some applications the PAM signal is used directly, and conversion to PCM is not required.)

The sampling theorem, as studied in Chapter 2, provides a way to reproduce an analog waveform by using sample values of that waveform and  $(\sin x)/x$  orthogonal functions. The purpose of PAM signaling is to provide *another* waveform that looks like pulses, yet contains the information that was present in the analog waveform. Because we are using pulses, we would expect the bandwidth of the PAM waveform to be wider than that of the analog waveform. However, the pulses are more practical to use in digital systems. We will see, that the pulse rate,  $f_s$ , for PAM is the same as that required by the sampling theorem, namely,  $f_s \geq 2B$ , where  $B$  is the highest frequency in the analog waveform and  $2B$  is called the *Nyquist rate*.

There are two classes of PAM signals: PAM that uses *natural sampling* (gating) and PAM that uses *instantaneous sampling* to produce a flat-top pulse. These signals are illustrated in Figs. 3-1 and 3-5, respectively. The flat-top type is more useful for conversion to

<sup>†</sup> Other techniques, frequency division multiplexing, and code division multiplexing are covered in Chapter 5 and 8.

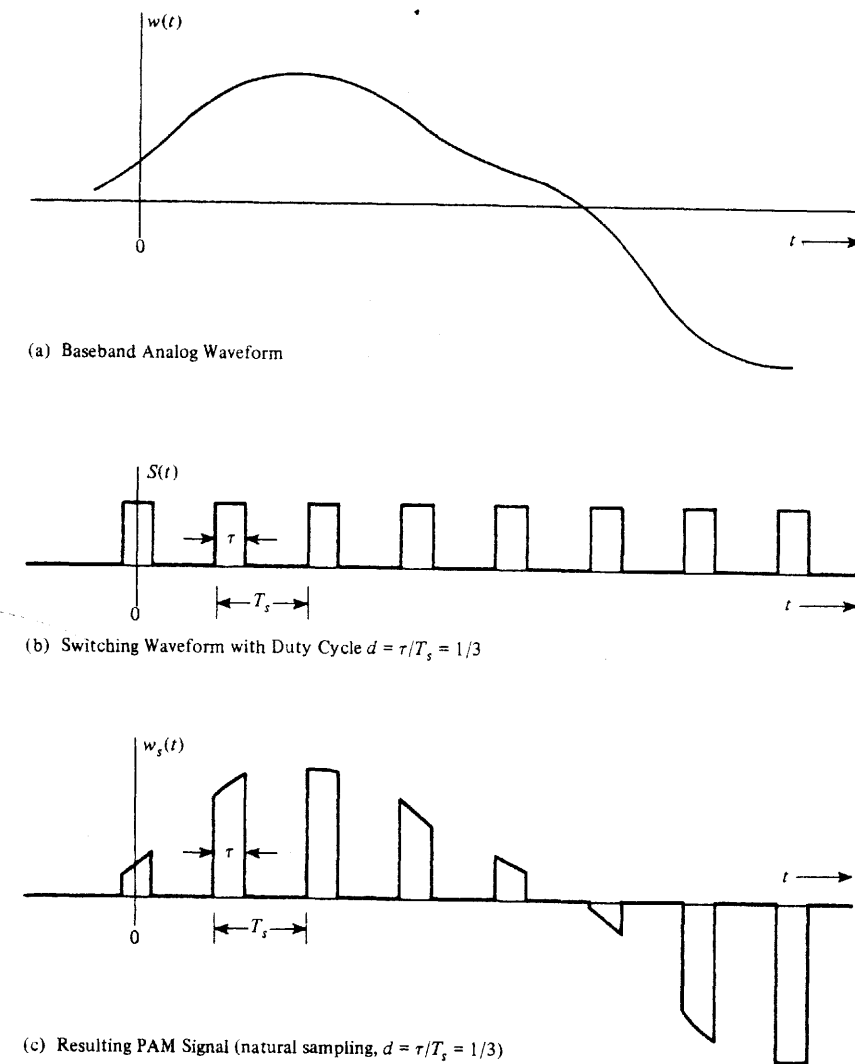


Figure 3-1 PAM signal with natural sampling.

PCM; however the naturally sampled type is easier to generate and is used in other applications.

#### Natural Sampling (Gating)

**DEFINITION.** If  $w(t)$  is an analog waveform bandlimited to  $B$  hertz, the *PAM* signal that uses *natural sampling* (gating) is

$$w_s(t) = w(t)s(t) \quad (3-1)$$

where

$$s(t) = \sum_{k=-\infty}^{\infty} \Pi\left(\frac{t - kT_s}{\tau}\right) \quad (3-2)$$

is a rectangular wave switching waveform and  $f_s = 1/T_s \geq 2B$ .

**THEOREM.** The spectrum for a naturally sampled PAM signal is



$$W_s(f) = \mathcal{F}[w_s(t)] = d \sum_{n=-\infty}^{\infty} \frac{\sin \pi n d}{\pi n d} W(f - nf_s) \quad (3-3)$$

where  $f_s = 1/T_s$ ,  $\omega_s = 2\pi f_s$ , the duty cycle of  $s(t)$  is  $d = \tau/T_s$ , and  $W(f) = \mathcal{F}[w(t)]$  is the spectrum of the original unsampled waveform.

**Proof.** Taking the Fourier transform of (3-1), we get

$$W_s(f) = W(f) * S(f) \quad (3-4)$$

Because  $s(t)$  is periodic, it may be represented by the Fourier series

$$s(t) = \sum_{n=-\infty}^{\infty} c_n e^{jn\omega_s t} \quad (3-5a)$$

where

$$c_n = d \frac{\sin n\pi d}{n\pi d} \quad (3-5b)$$

Thus

$$S(f) = \mathcal{F}[s(t)] = \sum_{n=-\infty}^{\infty} c_n \delta(f - nf_s) \quad (3-6)$$

and (3-4) becomes

$$W_s(f) = W(f) * \left( \sum_{n=-\infty}^{\infty} c_n \delta(f - nf_s) \right) = \sum_{n=-\infty}^{\infty} c_n W(f) * \delta(f - nf_s)$$

or

$$W_s(f) = \sum_{n=-\infty}^{\infty} c_n W(f - nf_s) \quad (3-7)$$

which becomes (3-3) upon substituting (3-5b).

The PAM waveform with natural sampling is relatively easy to generate since it only requires the use of an analog switch that is readily available in CMOS hardware (e.g., the

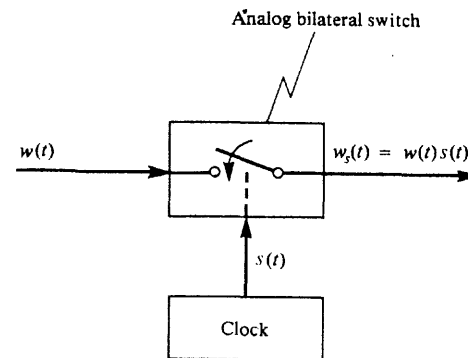
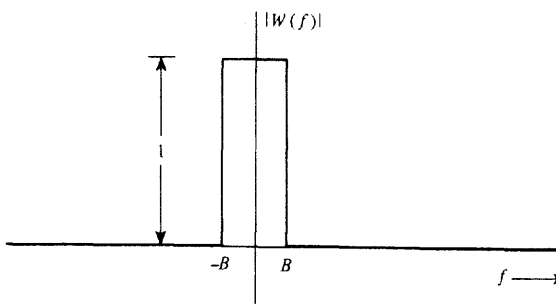
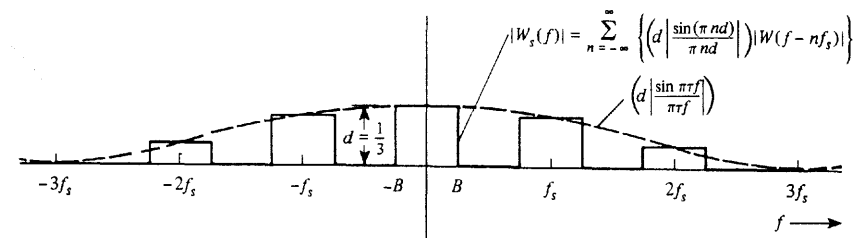


Figure 3-2 Generation of PAM with natural sampling (gating).



(a) Magnitude Spectrum of Input Analog Waveform



(b) Magnitude Spectrum of PAM (natural sampling) with  $d = 1/3$  and  $f_s = 4B$

Figure 3-3 Spectrum of a PAM waveform with natural sampling.

4016-quad bilateral switch). This is shown in Fig. 3-2, where the associated waveforms  $w(t)$ ,  $s(t)$ , and  $w_s(t)$  are as illustrated in Fig. 3-1.

The spectrum of the PAM signal with natural sampling is given by (3-3) in terms of the spectrum of the analog input waveform. This is illustrated in Fig. 3-3 for the case of an input waveform that has a rectangular spectrum where the duty cycle of the switching waveform is  $d = \tau/T_s = \frac{1}{3}$  and the sampling rate is  $f_s = 4B$ . For this example, where  $d = \frac{1}{3}$ , the PAM spectrum is zero for  $\pm 3f_s$ ,  $\pm 6f_s$ , and so on, because the spectrum in these harmonic

bands is nulled out by the  $(\sin x)/x$  function. From the figure, one sees that the bandwidth of the PAM signal is much larger than the bandwidth of the original analog signal. In fact, for the example illustrated in Fig. 3-3b, the null bandwidth of the PAM signal is  $3f_s = 12B$ ; that is the null bandwidth of this PAM signal is 12 times the bandwidth of the analog signal.

At the receiver, the original analog waveform,  $w(t)$ , can be recovered from the PAM signal,  $w_s(t)$ , by passing the PAM signal through a low-pass filter where the cutoff frequency is  $B < f_{cutoff} < f_s - B$ . This is seen by comparing Fig. 3-3b with 3-3a. Because the spectrum out of the low-pass filter would have the same shape as that of the original analog signal shown in Fig. 3-3a, the waveshape out of the low-pass filter would be identical to that of the original analog signal except for a gain factor of  $d$  (which could be compensated for by using an amplifier). From Fig. 3-3b, the spectrum out of the low-pass filter will have the same shape as the spectrum of the original analog signal only when  $f_s \geq 2B$ , because otherwise spectral components in harmonic bands (of  $f_s$ ) would overlap. This is another illustration of the Nyquist sampling rate requirement. If the analog signal is *undersampled* ( $f_s < 2B$ ), the effect of spectral overlapping is called *aliasing*. This results in a recovered analog signal that is distorted when compared to the original waveform. In practice, physical signals are usually considered to be time limited, so that (as we found in Chapter 2) they cannot be absolutely bandlimited. Consequently, there will be some aliasing in a PAM signal. Usually, we prefilter the analog signal before it is introduced to the PAM circuit so we do not have to worry about this problem; however, the effect of aliasing noise has been studied [Spilker, 1977].

It can also be shown (see Prob. 3-4) that the analog waveform may be recovered from the PAM signal by using *product detection*, as shown in Fig. 3-4. Here the PAM signal is multiplied with a sinusoidal signal of frequency  $\omega_o = n\omega_s$ . This shifts the frequency band of the PAM signal that was centered about  $n\omega_s$  to baseband (i.e.,  $f = 0$ ) at the multiplier output. We will study the product detector in Chapter 4. For  $n = 0$  this is identical to low-pass filtering, just discussed. Of course, you might ask: Why do you need to go to the trouble of using a product detector when a simple low-pass filter will work? The answer is: Because of noise on the PAM signal. Noise due to power supply hum or noise due to mechanical circuit vibration might fall in the band corresponding to  $n = 0$ , and other bands might be rel-

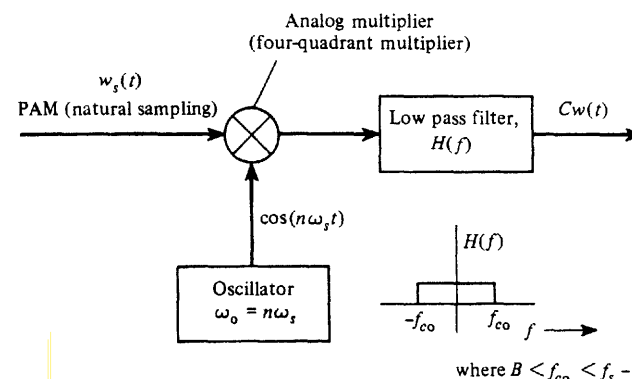


Figure 3-4 Demodulation of a PAM signal (naturally sampled).

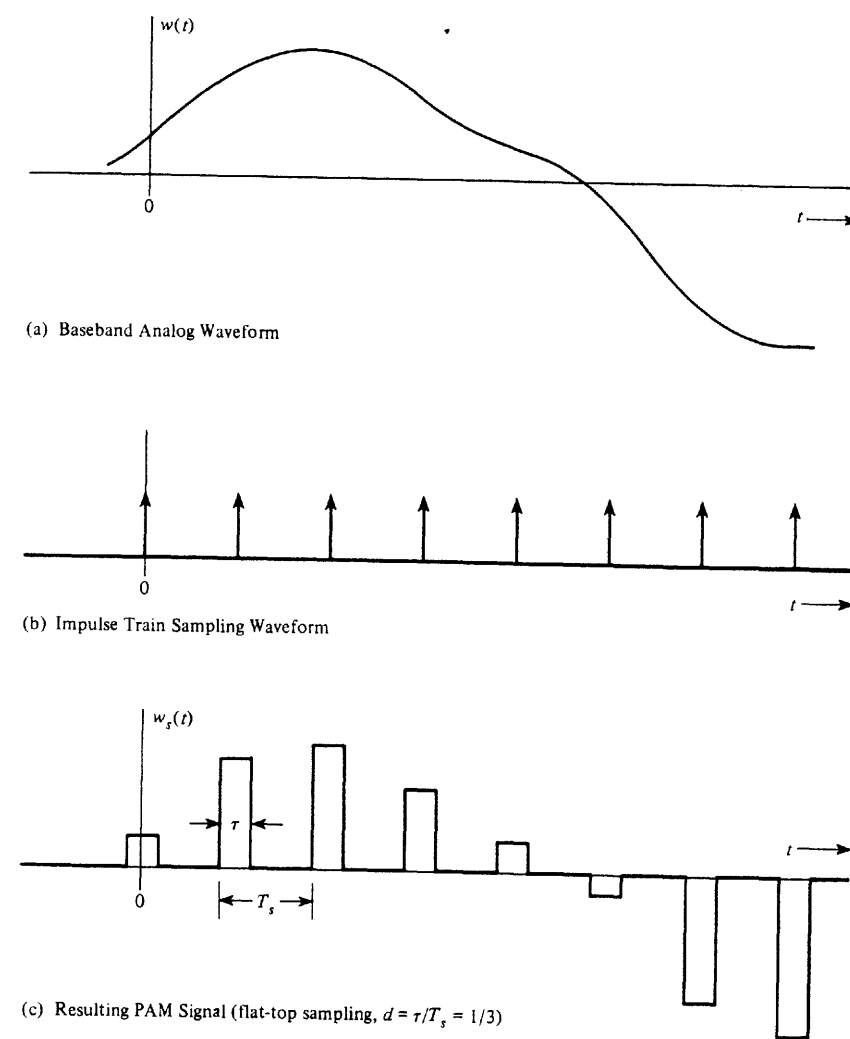


Figure 3-5 PAM signal with flat-top sampling.

atively noise free. In this case, a product detector might be used to get around the noise problem.

### Instantaneous Sampling (Flat-Top PAM)

Analog waveforms may also be converted to pulse signaling by the use of *flat-top* signaling with instantaneous sampling, as shown in Fig. 3-5. This is a generalization of the impulse train sampling technique that was studied in Sec. 2-7.

**DEFINITION.** If  $w(t)$  is an analog waveform bandlimited to  $B$  hertz, the *instantaneous sampled* PAM signal is given by

$$w_s(t) = \sum_{k=-\infty}^{\infty} w(kT_s)h(t - kT_s) \quad (3-8)$$

where  $h(t)$  denotes the sampling-pulse shape, and for flat-top sampling the pulse shape is

$$h(t) = \Pi\left(\frac{t}{\tau}\right) = \begin{cases} 1, & |t| < \tau/2 \\ 0, & |t| > \tau/2 \end{cases} \quad (3-9)$$

where  $\tau \leq T_s = 1/f_s$  and  $f_s \geq 2B$ .

**THEOREM.** *The spectrum for a flat-top PAM signal is*

$$W_s(f) = \frac{1}{T_s} H(f) \sum_{k=-\infty}^{\infty} W(f - kf_s) \quad (3-10)$$

where

$$H(f) = \mathcal{F}[h(t)] = \tau \left( \frac{\sin \pi \tau f}{\pi \tau f} \right) \quad (3-11)$$

This type of PAM signal is said to consist of instantaneous samples since  $w(t)$  is sampled at  $t = kT_s$  and the sample values  $w(kT_s)$  determine the amplitude of the flat-top rectangular pulses, as demonstrated in Fig. 3-5c. The flat-top PAM signal could be generated by using a sample-and-hold type of electronic circuit.

Another pulse shape, rather than the rectangular shape, could be used in (3-8), but in this case the resulting PAM waveform would not be flat-topped. Note that if the  $h(t)$  is of the  $(\sin x)/x$  type with overlapping pulses, then (3-8) becomes identical to the sampling theorem of (2-158).

**Proof.** The spectrum for flat-top PAM can be obtained by taking the Fourier transform of (3-8). First, rewrite (3-8), using a more convenient form involving the convolution operation.

$$w_s(t) = \sum_k w(kT_s)h(t) * \delta(t - kT_s)$$

$$= h(t) * \sum_k w(kT_s)\delta(t - kT_s)$$

or

$$w_s(t) = h(t) * \left[ w(t) \sum_k \delta(t - kT_s) \right]$$

The spectrum is

$$W_s(f) = H(f) \left[ W(f) * \sum_k e^{-j2\pi kfT_s} \right] \quad (3-12)$$

But the sum of the exponential functions is equivalent to a Fourier series expansion (in the frequency domain), where the periodic function is an impulse train. That is,

$$\frac{1}{T_s} \sum_k \delta(f - kf_s) = \frac{1}{T_s} \sum_{n=-\infty}^{\infty} c_n e^{j(2\pi n T_s)f} \quad (3-13a)$$

where

$$c_n = \frac{1}{f_s} \int_{-f_s/2}^{f_s/2} \left[ \sum_k \delta(f - kf_s) \right] e^{-j2\pi n T_s f} df = \frac{1}{f_s} \quad (3-13b)$$

Using (3-13a), we find that (3-12) becomes

$$\begin{aligned} W_s(f) &= H(f) \left[ W(f) * \frac{1}{T_s} \sum_k \delta(f - kf_s) \right] \\ &= \frac{1}{T_s} H(f) \left[ \sum_k W(f) * \delta(f - kf_s) \right] \end{aligned}$$

which reduces to (3-10).

The spectrum of the flat-topped PAM signal is illustrated in Fig. 3-6 for the case of an analog input waveform that has a rectangular spectrum. The analog signal may be recovered from the flat-topped PAM signal by the use of a lowpass filter. However, it is noted that there is some high-frequency loss in the recovered analog waveform due to the filtering effect,  $H(f)$ , caused by the flat-top pulse shape. This loss, if significant, can be reduced by decreasing  $\tau$  or by using some additional gain at the high frequencies in the low-pass filter transfer function. In this case, the low-pass filter would be called an *equalization filter* and have a transfer function of  $1/H(f)$ . The pulse width  $\tau$  is also called the *aperture* since  $\tau/T_s$  determines the gain of recovered analog signal, which is small if  $\tau$  is small relative to  $T_s$ . It is also possible to use product detection, similar to that shown in Fig. 3-4, except that now some prefilter might be needed before the multiplier (to make the spectrum flat in a band centered on  $f = nf_s$ ), to compensate for the spectral loss due to the aperture effect.

The transmission of either naturally or instantaneously sampled PAM over a channel requires a very wide frequency response because of the narrow pulse width. This imposes stringent requirements on the magnitude and phase response of the channel. The bandwidth required is much larger than that of the original analog signal, and the noise performance of the PAM system can never be better than that achieved by transmitting the analog signal directly. Consequently, PAM is not very good for long-distance transmission. It does provide a means for converting an analog signal to a PCM signal (as discussed in the next section).

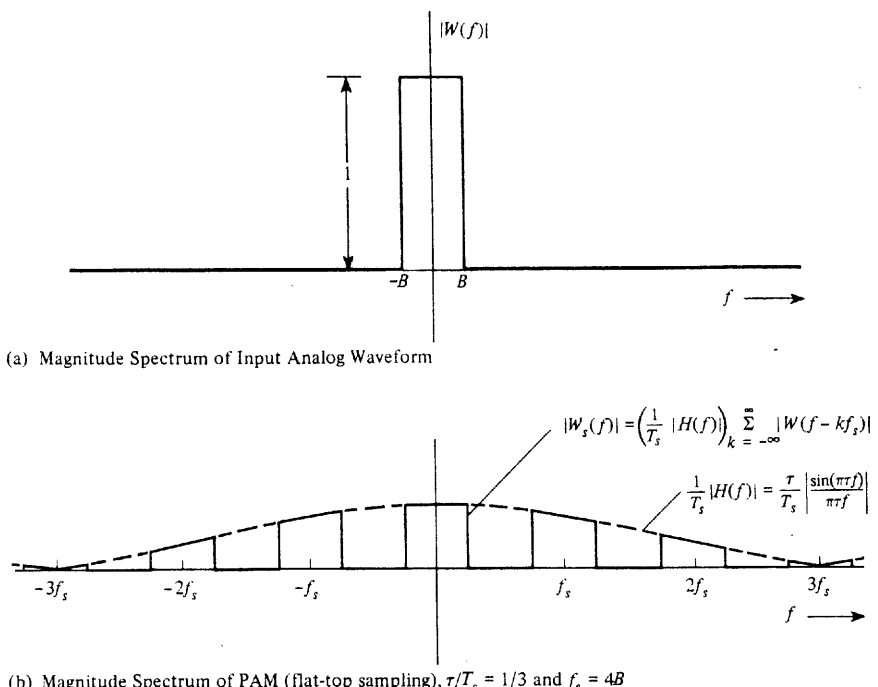


Figure 3-6 Spectrum of a PAM waveform with flat-top sampling.

PAM also provides a means for breaking a signal into time slots so that multiple PAM signals carrying information from different sources can be interleaved to transmit all of the information over a single channel. This is called time-division multiplexing and will be studied in Sec. 3-9.

### 3-3 PULSE CODE MODULATION

**DEFINITION.** *Pulse code modulation* (PCM) is essentially analog-to-digital conversion of a special type where the information contained in the instantaneous samples of an analog signal is represented by digital words in a serial bit stream.

If we assume that each of the digital words has  $n$  binary digits, there are  $M = 2^n$  unique code words that are possible, each code word corresponding to a certain amplitude level. However, each sample value from the analog signal can be any one of an infinite number of levels, so that the digital word that represents the amplitude closest to the actual sampled value is used. This is called *quantizing*. That is, instead of using the exact sample value of the analog waveform  $w(kT_s)$ , the sample is replaced by the closest allowed value, where

there are  $M$  allowed values, and each allowed value corresponds to one of the code words. Other popular types of analog-to-digital conversion, such as delta modulation (DM) and differential pulse code modulation (DPCM), are discussed in later sections.

PCM is very popular because of the many advantages it offers. Some of these advantages are as follows.

- Relatively inexpensive digital circuitry may be used extensively in the system.
- PCM signals derived from all types of analog sources (audio, video, etc.) may be merged with data signals (e.g., from digital computers) and transmitted over a common high-speed digital communication system. This merging is called time-division multiplexing and is discussed in detail in a later section.
- In long-distance digital telephone systems requiring repeaters, a *clean* PCM waveform can be regenerated at the output of each repeater, where the input consists of a noisy PCM waveform. However, the noise at the input may cause bit errors in the regenerated PCM output signal.
- The noise performance of a digital system can be superior to that of an analog system. In addition, the probability of error for the system output can be reduced even further by the use of appropriate coding techniques as discussed in Chapter 1.

These advantages usually outweigh the main disadvantage of PCM: a much wider bandwidth than that of the corresponding analog signal.

### Sampling, Quantizing, and Encoding

The PCM signal is generated by carrying out three basic operations: sampling, quantizing, and encoding (Fig. 3-7). The sampling operation generates a flat-top PAM signal.

The quantizing operation is illustrated in Fig. 3-8 for the  $M = 8$  level case. This quantizer is said to be *uniform* because all of the steps are of equal size. Because we are approximating the analog sample values by using a finite number of levels ( $M = 8$  in this illustration), *error* is introduced into the recovered output analog signal because of the quantizing effect. The error waveform is illustrated in Fig. 3-8c. The quantizing error consists of the difference between the analog signal at the sampler input and the output of the quantizer. Note that the peak value of the error ( $\pm 1$ ) is one half of the quantizer step size (2). If we sample at the Nyquist rate ( $2B$ ) or faster, and there is negligible channel noise, there will still be noise, called *quantizing noise*, on the recovered analog waveform due to this error. The quantizing noise can also be thought of as a round-off error. In Sec. 7-7 statistics of this quantizing noise are evaluated, and a formula for the PCM system signal-to-noise ratio is developed. The quantizer output is a *quantized* PAM signal.

The PCM signal is obtained from the quantized PAM signal by encoding each quantized sample value into a digital word. It is up to the system designer to specify the exact code word that will represent a particular quantized level. If a Gray code of Table 3-1 is used, the resulting PCM signal is shown in Fig. 3-8d, where the PCM word for each quan-

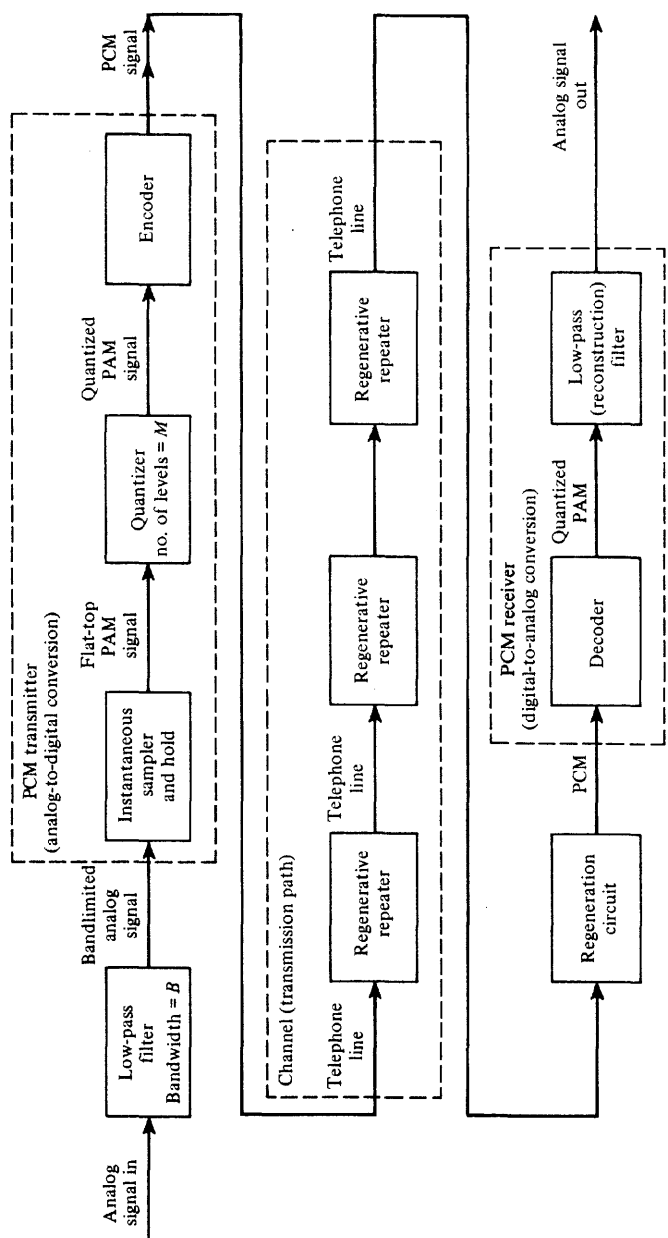


Figure 3-7 PCM transmission system.

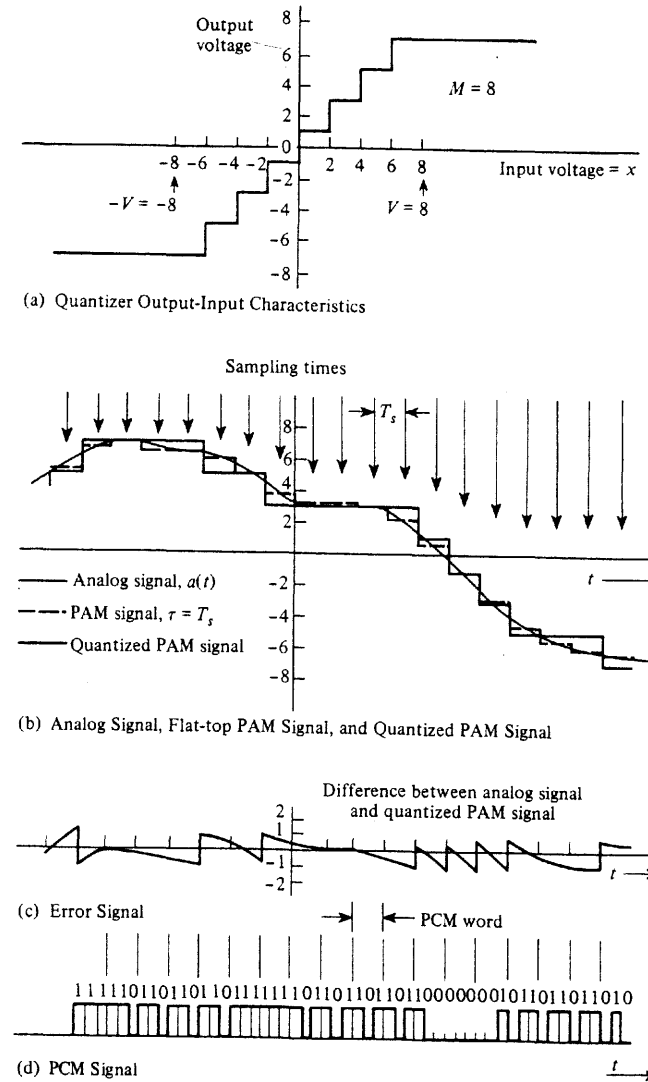


Figure 3-8 Illustration of waveforms in a PCM system.

tized sample is strobed out of the encoder by the next clock pulse. The Gray code was chosen because it has only one bit change for each step change in the quantized level. Consequently, single errors in the received PCM code word will cause minimum errors in the recovered analog level, provided that the sign bit is not in error.

Here we have described PCM systems that represent the quantized analog sample values by *binary* code words. In general, of course, it is possible to represent the quantized analog samples by digital words using other than base 2, or, equivalently, to convert the binary signal to a multilevel signal (as discussed in Sec. 3-4). Multilevel signals have the advantage

TABLE 3-1 THREE-BIT GRAY CODE FOR  $M = 8$  LEVELS

Quantized Sample Voltage	Gray Code Word (PCM Output)
+7	110
+5	111
+3	101
+1	100
Mirror image except for sign bit	
-1	000
-3	001
-5	011
-7	010

of much smaller bandwidth than binary signals but the disadvantage of requiring multilevel circuitry instead of binary circuitry.

### Practical PCM Circuits

Three popular techniques are used to implement the analog-to-digital converter (ADC) encoding operation. These are the *counting or ramp*, *serial or successive approximation*, and *parallel or flash* encoders.

In the counting encoder, at the same time that the sample is taken, a ramp generator is energized and a binary counter is started. The output of the ramp generator is continuously compared to the sample value; when the value of the ramp becomes equal to the sample value, the binary value of the counter is read. This count is taken to be the PCM word. The binary counter and the ramp generator are then reset to zero and are ready to be reenergized at the next sampling time. This technique requires only a few components, but the speed of this type of ADC is usually limited by the speed of the counter. The Intersil ICL7126 CMOS ADC integrated circuit uses this technique.

The serial encoder compares the value of the sample with trial quantized values. Successive trials depend on whether the past comparator outputs are positive or negative. The trial values are chosen first in large steps and then in small steps so that the process will converge rapidly. The trial voltages are generated by a series of voltage dividers that are configured by (on-off) switches. These switches are controlled by digital logic. After the process converges, the value of the switch settings is read out as the PCM word. This technique requires more precision components (for the voltage dividers) than the ramp technique. The speed of the feedback ADC technique is determined by the speed of the switches. The National Semiconductor ADC0804 8-bit ADC uses this technique.

The parallel encoder uses a set of parallel comparators with reference levels that are the permitted quantized values. The sample value is fed into all of the parallel comparators simultaneously. The high or low level of the comparator outputs determines the binary PCM

word with the aid of some digital logic. This is a fast ADC technique but requires more hardware than the other two methods. The RCA CA3318 8-bit ADC integrated circuit is an example of this technique.

All of the integrated circuits listed as examples above have parallel digital outputs that correspond to the digital word that represents the analog sample value. For generation of PCM, the parallel output (digital word) needs to be converted to serial form for transmission over a two-wire channel. This is accomplished by using a parallel-to-serial converter integrated circuit, which is also usually known as a *serial-input-output* (SIO) chip. The SIO chip includes a shift register that is set to contain the parallel data (from, usually, 8 or 16 input lines). Then the data are shifted out of the last stage of the shift register bit-by-bit onto a single output line to produce the serial format. Furthermore, the SIO chips are usually full duplex; that is, they have two sets of shift registers, one that functions for data flowing in each direction. One shift register converts parallel input data to serial output data for transmission over the channel, and, simultaneously, the other shift register converts received serial data from another input to parallel data that are available at another output. Three types of SIO chips are available: the *universal asynchronous receiver/transmitter* (UART), the *universal synchronous receiver/transmitter* (USRT), and the *universal synchronous/asynchronous receiver/transmitter* (USART). The UART transmits and receives asynchronous serial data, the USRT transmits and receives synchronous serial data, and the USART combines both a UART and a USRT on one chip. (See Sec. 3-9 for a discussion of asynchronous and synchronous serial data lines.)

At the receiving end the PCM signal is decoded back into an analog signal by using a digital-to-analog converter (DAC) chip. If the DAC chip has a parallel data input, the received serial PCM data are first converted to a parallel form using a SIO chip as described earlier. The parallel data are then converted to an approximation of the analog sample value by the DAC chip. This conversion is usually accomplished by using the parallel digital word to set the configuration of electronic switches on a resistive current (or voltage) divider network so that the analog output is produced. This is called a *multiplying DAC* because the "analog" output voltage is directly proportional to the divider reference voltage multiplied by the value of the digital word. The Motorola MC1408 and the National Semiconductor DAC0808 8-bit DAC chips are examples of this technique. The DAC chip outputs samples of the quantized analog signal that approximates the analog sample values. Consequently, as the DAC chip is clocked, it generates a quantized PAM signal. This may be smoothed by a low-pass reconstruction filter to produce the analog output as illustrated in Fig. 3-7.

The *Electrical Engineering Handbook* [Dorf, 1993, pp. 771-782] gives more details on ADC, DAC, and PCM circuits.

### Bandwidth of PCM

A good question to ask is: What is the spectrum of a PCM signal? For the case of PAM signaling, the spectrum of the PAM signal could be obtained as a function of the spectrum of the input analog signal because the PAM signal is a linear function of the analog signal. This is not the case for PCM. As shown in Figs. 3-7 and 3-8, the PCM is a *nonlinear* function of the input analog signal. Consequently, the spectrum of the PCM signal is not directly related to the spectrum of the input analog signal (as will be shown in Secs. 3-4 and 3-5).

The bandwidth of (serial) PCM signals depends on the bit rate and the pulse shape. From Fig. 3-8, the bit rate is

$$R = nf_s \quad (3-14)$$

where  $n$  is the number of bits in the PCM word ( $M = 2^n$ ) and  $f_s$  is the sampling rate. For no aliasing we require  $f_s \geq 2B$  where  $B$  is the bandwidth of the analog signal (that is to be converted to the PCM signal). In Sec. 3-4 we see that the dimensionality theorem shows that the bandwidth of the PCM waveform is bounded by

$$B_{PCM} \geq \frac{1}{2}R = \frac{1}{2}nf_s \quad (3-15a)$$

where equality is obtained if a  $(\sin x)/x$  type of pulse shape is used to generate the PCM waveform. The exact spectrum for the PCM waveform will depend on the pulse shape that is used as well as on the type of line encoding. This will be studied in Sec. 3-5. For example, if one uses a rectangular pulse shape with polar NRZ line coding, Fig. 3-16b shows that the first null bandwidth is simply

$$B_{PCM} = R = nf_s \quad (\text{first null bandwidth}) \quad (3-15b)$$

Table 3-2 presents a tabulation of this result for the case of the minimum sampling rate,  $f_s = 2B$ . Note that the dimensionality theorem of (3-15a) demonstrates that the bandwidth of the PCM signal has a lower bound given by

TABLE 3-2 PERFORMANCE OF A PCM SYSTEM WITH UNIFORM QUANTIZING AND NO CHANNEL NOISE

Number of Quantizer Levels Used, $M$	Length of the PCM Word, $n$ (bits)	Bandwidth of PCM Signal (First Null Bandwidth) <sup>a</sup>	Recovered Analog Signal Power-to-Quantizing Noise Power Ratios (dB)	
			(S/N) <sub>pk out</sub>	(S/N) <sub>out</sub>
2	1	2B	10.8	6.0
4	2	4B	16.8	12.0
8	3	6B	22.8	18.1
16	4	8B	28.9	24.1
32	5	10B	34.9	30.1
64	6	12B	40.9	36.1
128	7	14B	46.9	42.1
256	8	16B	52.9	48.2
512	9	18B	59.0	54.2
1,024	10	20B	65.0	60.2
2,048	11	22B	71.0	66.2
4,096	12	24B	77.0	72.2
8,192	13	26B	83.0	78.3
16,384	14	28B	89.1	84.3
32,768	15	30B	95.1	90.3
65,536	16	32B	101.1	96.3

<sup>a</sup>  $B$  is the absolute bandwidth of the input analog signal.

$$B_{PCM} \geq nB \quad (3-15c)$$

where  $f_s \geq 2B$  and  $B$  is the bandwidth of the corresponding analog signal. Thus, for reasonable values of  $n$ , the bandwidth of the PCM signal will be significantly larger than the bandwidth of the corresponding analog signal that it represents. For the example shown in Fig. 3-8 where  $n = 3$ , the PCM signal bandwidth will be at least three times wider than that of the corresponding analog signal. Furthermore, if the bandwidth of the PCM signal is reduced by improper filtering, or by passing the PCM signal through a system that has a poor frequency response, the filtered pulses will be elongated (stretched in width) so that pulses corresponding to any one bit will smear into adjacent bit slots. If this condition becomes too serious, it will cause errors in the detected bits. This pulse smearing effect is called *intersymbol interference* (ISI). The filtering specifications for no ISI are discussed in Sec. 3-6.

### Effects of Noise

The analog signal that is recovered at the PCM system output is corrupted by noise. Two main effects produce this noise or distortion:

- Quantizing noise that is caused by the  $M$ -step quantizer at the PCM transmitter.
- Bit errors in the recovered PCM signal. The bit errors are caused by *channel noise* as well as improper channel filtering, which causes ISI.

In addition, if the input analog signal that is sampled is not strictly bandlimited, there will be some aliasing noise on the recovered analog signal [Spilker, 1977]. In Chapter 7, under certain assumptions, it will be shown that the recovered analog *peak* signal power to total *average* noise power is given by<sup>†</sup>

$$\left(\frac{S}{N}\right)_{pk\ out} = \frac{3M^2}{1 + 4(M^2 - 1)P_e} \quad (3-16a)$$

and the *average* signal power to the *average* noise power is

$$\left(\frac{S}{N}\right)_{out} = \frac{M^2}{1 + 4(M^2 - 1)P_e} \quad (3-16b)$$

where  $M$  is the number of quantized levels used in the PCM system and  $P_e$  is the probability of bit error in the recovered binary PCM signal at the receiver DAC before it is converted back into an analog signal. In Chapter 7,  $P_e$  is evaluated for many different types of baseband and bandpass digital transmission systems. In Chapter 1 it was shown how channel coding could be used to correct some of the bit errors and, consequently, reduce  $P_e$ . Therefore, in many practical systems  $P_e$  is negligible. If we assume that there are no bit errors resulting from channel noise (i.e.,  $P_e = 0$ ) and no ISI, then, from (3-16a), the peak SNR resulting from only quantizing errors is

$$\left(\frac{S}{N}\right)_{pk\ out} = 3M^2 \quad (3-17a)$$

<sup>†</sup> This derivation is postponed until Chapter 7 because a knowledge of statistics is needed to carry it out.

and from (3-16b) the average SNR due only to quantizing errors is

$$\left(\frac{S}{N}\right)_{\text{out}} = M^2 \quad (3-17b)$$

Numerical values for these SNRs are given in Table 3-2.

To realize these SNRs, one critical assumption is that the peak-to-peak level of the analog waveform at the input to the PCM encoder is set to the design level of the quantizer. For example, referring to Fig. 3-8a, this corresponds to the input traversing the range  $-V$  to  $+V$  volts where  $V = 8$  volts is the design level of the quantizer. Equations (3-16) and (3-17) were derived for waveforms with equally likely values, such as a triangle waveshape, that have a peak-to-peak value of  $2V$  and an rms value of  $V/\sqrt{3}$ , where  $V$  is the design peak level of the quantizer.

From a practical viewpoint, the quantizing noise at the output of the PCM decoder can be categorized into four types depending on the operating conditions. The four types are overload noise, random noise, granular noise, and hunting noise. As discussed earlier, the level of the analog waveform at the input of the PCM encoder needs to be set so that its peak level does not exceed the design peak of  $V$  volts. If the peak input does exceed  $V$ , then the recovered analog waveform at the output of the PCM system will have flat-tops near the peak values. This produces *overload noise*. The flat-tops are easily seen on an oscilloscope, and the recovered analog waveform sounds distorted since the flat-topping produces unwanted harmonic components. For example, this type of distortion can be heard on a PCM telephone system (e.g., the AT&T and SLC lines as described in Chapter 8) when there are high levels such as dial tones, busy signals, or off-hook signals.

The second type of noise, *random noise*, is produced by the random quantization errors in the PCM system under normal operating conditions when the input level is properly set. This type of condition is assumed in (3-17). Random noise has a "white" hissing sound. If the input level is not sufficiently large, the SNR will deteriorate from that given by (3-17) to one that will be described later by (3-28a) and (3-28b); however, the quantizing noise will still be more or less random.

If the input level is reduced further to a relatively small value with respect to the design level, the error values are not equally likely from sample to sample, and the noise has a harsh sound resembling gravel being poured into a barrel. This is called *granular noise*. This type of noise can be randomized (noise power decreased) by increasing the number of quantization levels, and, consequently, increasing the PCM bit rate. Alternatively, granular noise can be reduced by using a nonuniform quantizer, such as the  $\mu$ -law or  $A$ -law quantizers that are described in the next section.

The fourth type of quantizing noise that may occur at the output of a PCM system is *hunting noise*. It can occur when the input analog waveform is nearly constant, including when there is no signal (i.e., zero level). For these conditions the sample values at the quantizer output (see Fig. 3-8) can oscillate between two adjacent quantization levels, causing an undesired sinusoidal type tone of frequency  $\frac{1}{2}f_s$  at the output of the PCM system. Hunting noise can be reduced by filtering out the tone or by designing the quantizer so that there is no vertical step at the "constant" value of the inputs—such as at zero volts input for the no signal case. For the no signal case, the hunting noise is also called *idle channel noise*. Idle

channel noise can be reduced by using a horizontal step at the origin of the quantizer output-input characteristic instead of a vertical step as shown in Fig. 3-8a.

Recalling that  $M = 2^n$ , we may express Eqs. (3-17a) and (3-17b) in decibels as

$$\left(\frac{S}{N}\right)_{\text{dB}} = 6.02n + \alpha \quad (3-18)$$

where  $n$  is the number of bits in the PCM word,  $\alpha = 4.77$  for the peak SNR, and  $\alpha = 0$  for the average SNR. This equation—called the *6 dB rule*—points out the significant performance characteristic for PCM: *an additional 6-dB improvement in SNR is obtained for each bit added to the PCM word*. This is illustrated in Table 3-2. Equation (3-18) is valid for a wide variety of assumptions (such as various types of input waveshapes and quantization characteristics), although the value of  $\alpha$  will depend on these assumptions [Jayant and Noll, 1984]. It is assumed that there are no bit errors and that the input signal level is large enough to range over a significant number of quantizing levels.

### Example 3-1 DESIGN OF A PCM SYSTEM

Assume that an analog voice-frequency signal, which occupies a band from 300 to 3400 Hz, is to be transmitted over a binary PCM system. The minimum sampling frequency would be  $2 \times 3.4 = 6.8$  kHz. In practice the signal would be oversampled, and in the United States a sampling frequency of 8 kHz is the standard used for voice-frequency signals in telephone communication systems. Assume that each sample value is represented by 7 information bits plus 1 parity bit; then the bit rate of the PCM signal is

$$\begin{aligned} R &= (f_s \text{ samples/s})(n \text{ bits/sample}) \\ &= (8 \text{ ksamples/s})(8 \text{ bits/sample}) = 64 \text{ kbits/s} \end{aligned} \quad (3-19)$$

Because the signaling is binary (i.e., two possible levels), each dimension<sup>†</sup> (or symbol) is carrying one bit of data, so that the baud rate is equal to the bit rate, or  $D = R = 64$  k symbols/s. Referring to the dimensionality theorem (3-15a), we realize that the theoretically minimum absolute bandwidth of the PCM signal is

$$(B)_{\min} = \frac{1}{2} D = 32 \text{ kHz} \quad (3-20)$$

and this is realized if the PCM waveform consists of  $(\sin x)/x$  pulse shapes. If rectangular pulse shaping is used, the absolute bandwidth is infinity and the first null bandwidth, as shown in Fig. 3-12b, is

$$(B)_{\text{null}} = R = \frac{1}{T_b} = 64 \text{ kHz} \quad (3-21)$$

That is, we require a bandwidth of 64 kHz to transmit this digital voice PCM signal where the bandwidth of the original analog voice signal was, at most, 4 kHz. (In Sec. 3-5 we will see that the bandwidth of this binary PCM signal may be reduced somewhat by filtering without introducing ISI.) Using (3-17a), we observe that the peak signal-to-quantizing noise power ratio is

<sup>†</sup> See Fig. 3-11 for an illustration of a three-dimensional signal expansion. In this example we have an eight-dimensional signal expansion.

$$\left(\frac{S}{N}\right)_{\text{pk out}} = 3(2^7)^2 = 46.9 \text{ dB} \quad (3-22)$$

where  $M = 2^7$ . Note that the inclusion of a parity bit does not affect the quantizing noise. However, coding (parity bits) may be used to decrease the decoded errors caused by channel noise or ISI. In this example, these effects were assumed to be negligible because  $P_e$  was assumed to be zero.

The performance of a PCM system for the most optimistic case (i.e.,  $P_e = 0$ ) can easily be obtained as a function of  $M$ , the number of quantizing steps used. The results are shown in Table 3-2. In obtaining the SNR, no parity bits were used in the PCM word.

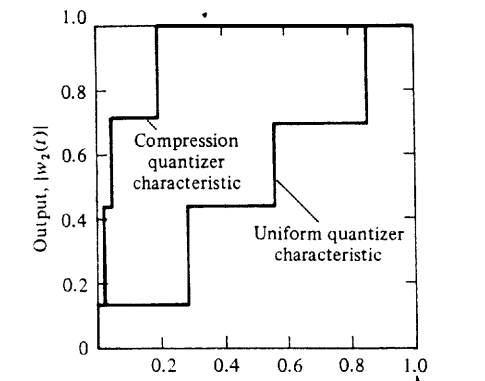
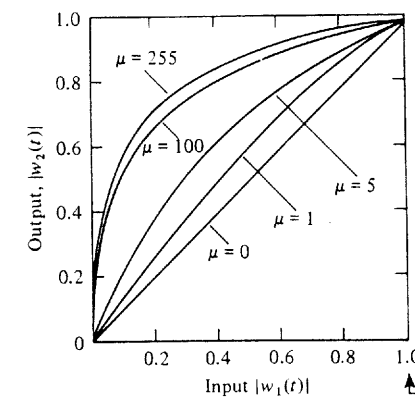
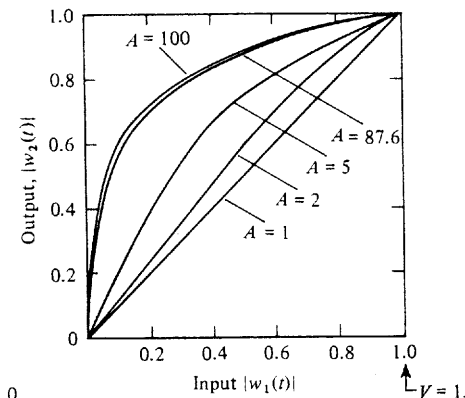
One might use this table to look at the design requirements in a proposed PCM system. For example, high-fidelity enthusiasts are turning to digital audio recording techniques. Here PCM signals are recorded instead of the analog audio signal to produce superb sound reproduction. For a dynamic range of 90 dB, it is seen that at least 15-bit PCM words would be required. Furthermore, if the analog signal had a bandwidth of 20 kHz, the first null bandwidth for rectangular bitshape PCM would be  $2 \times 20 \text{ kHz} \times 15 = 600 \text{ kHz}$ . With an allowance for some oversampling and a wider bandwidth to minimize ISI, the bandwidth needed would be around 1.5 MHz. Consequently, video-type tape recorders are needed to record and reproduce high-quality digital audio signals. Although this type of recording technique might seem ridiculous at first, it is realized that expensive high-quality analog recording devices are hard pressed to reproduce a dynamic range of 70 dB. Thus digital audio is one way to achieve improved performance. This is being proven in the marketplace with the popularity of the digital compact disk (CD). The CD uses a 16-bit PCM word and a sampling rate of 44.1 kHz on each stereo channel [Miyaoka, 1984; Peek, 1985]. Reed-Solomon coding with interleaving is used to correct burst errors that occur as a result of scratches and fingerprints on the compact disk.

### Nonuniform Quantizing: $\mu$ -Law and A-Law Companding

Voice analog signals are more likely to have amplitude values near zero than at the extreme peak values allowed. For example, when digitizing voice signals, if the peak value allowed is 1 V, weak passages may have voltage levels on the order of 0.1 V (20 dB down). For signals, such as these, with nonuniform amplitude distribution, the granular quantizing noise will be a serious problem if the step size is not reduced for amplitude values near zero and increased for extremely large values. This is called *nonuniform quantizing* since a variable step size is used. An example of a nonuniform quantizing characteristic is shown in Fig. 3-9a.

The effect of nonuniform quantizing can be obtained by first passing the analog signal through a compression (nonlinear) amplifier and then into the PCM circuit that uses a uniform quantizer. In the United States a  $\mu$ -law type of *compression* characteristic is used. It is defined [Smith, 1957] by

$$|w_2(t)| = \frac{\ln(1 + \mu |w_1(t)|)}{\ln(1 + \mu)} \quad (3-23)$$

(a)  $M = 8$  Quantizer Characteristic(b)  $\mu$ -law Characteristic

(c) A-law Characteristic

Figure 3-9 Compression characteristics (first quadrant shown).

where the allowed peak values of  $w_1(t)$  are  $\pm 1$  (i.e.,  $|w_1(t)| \leq 1$ ),  $\mu$  is a positive constant that is a parameter, and  $\ln$  is the natural logarithm. This compression characteristic is shown in Fig. 3-9b, for several values of  $\mu$ , and it is noted that  $\mu = 0$  corresponds to linear amplification (uniform quantization overall). In the United States, Canada, and Japan, the telephone companies use a  $\mu = 255$  compression characteristic in their PCM systems [Dammann, McDaniel, and Maddox, 1972]. In practice the smooth nonlinear characteristics of Fig. 3-9b are approximated by piecewise steps as shown in Fig. 3-9a. For example, to approximate the  $\mu = 255$  characteristic, let the height of all steps, be  $\Delta$ , then the first 16 steps have step width set to  $\Delta$ , the next 16 steps have width of  $2\Delta$ , followed by 80 steps of width  $4\Delta$ , and, finally, 16 steps of width  $128\Delta$ .

Another compression law, used mainly in Europe, is the *A*-law characteristic. It is defined [Cattermole, 1969] by

$$|w_2(t)| = \begin{cases} \frac{A|w_1(t)|}{1 + \ln A}, & 0 \leq |w_1(t)| \leq \frac{1}{A} \\ \frac{1 + \ln(A|w_1(t)|)}{1 + \ln A}, & \frac{1}{A} \leq |w_1(t)| \leq 1 \end{cases} \quad (3-24)$$

where  $|w_1(t)| \leq 1$  and  $A$  is a positive constant. The  $A$ -law compression characteristic is shown in Fig. 3-9c. The typical value for  $A$  is 87.6. In practice, to approximate the  $A = 87.6$  characteristic with steps, let the height of all steps be  $\Delta$ , then the first 32 steps have step width set to  $\Delta$ , the next 16 steps have width of  $2\Delta$ , followed by 64 steps of width  $4\Delta$ , and, finally, 16 steps of width  $64\Delta$ .

When compression is used at the transmitter, *expansion* (i.e., decompression) must be used at the receiver output to restore signal levels to their correct relative values. The *expandor* characteristic is the inverse of the compression characteristic, and the combination of a compressor and an expandor is called a *compandor*.

Once again, it can be shown that the output SNR follows the 6-dB law [Couch, 1993].

$$\left(\frac{S}{N}\right)_{\text{dB}} = 6.02n + \alpha \quad (3-25)$$

where

$$\alpha = 4.77 - 20 \log(V/x_{\text{rms}}) \quad \text{uniform quantizing} \quad (3-26a)$$

and for sufficiently large input levels

$$\alpha \approx 4.77 - 20 \log[\ln(1 + \mu)] \quad \mu\text{-law companding} \quad (3-26b)$$

and [Jayant and Noll, 1984]

$$\alpha \approx 4.77 - 20 \log[1 + \ln A] \quad A\text{-law companding} \quad (3-26c)$$

$n$  is the number of bits used in the PCM word,  $V$  is the peak design level of the quantizer, and  $x_{\text{rms}}$  is the rms value of the input analog signal. Notice that the output SNR is a function of the input level for the uniform quantizing (no companding) case but is relatively insensitive to input level for  $\mu$ -law and  $A$ -law companding as shown in Fig. 3-10. The ratio  $V/x_{\text{rms}}$  is called the *loading factor*. The input level is often set for a loading factor of 4, which is 12 dB, to ensure that the overload quantizing noise will be negligible. In practice this gives  $\alpha = -7.3$  for the case of uniform encoding as compared to  $\alpha = 0$  that was obtained for the ideal conditions associated with (3-17b). All of these results give a 6-dB increase in the signal to quantizing noise ratio for each bit added to the PCM code word.

### 3-4 DIGITAL SIGNALING

In this section, we will answer the question: How do we mathematically represent a digital signal, such as the PCM signal of Figure 3-8d, and how do we estimate its bandwidth?

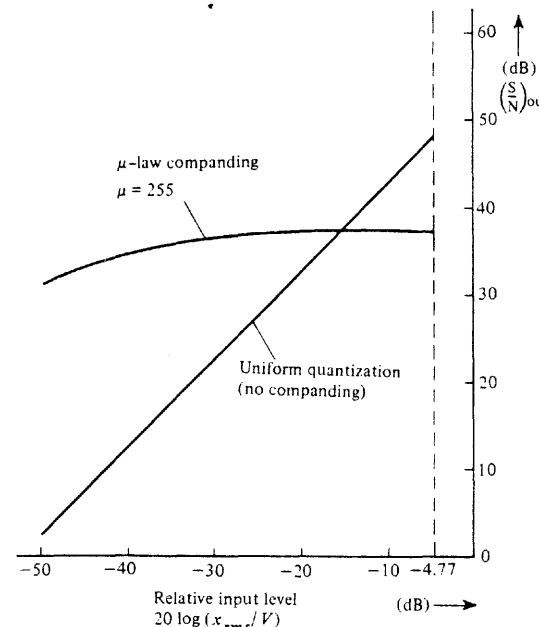


Figure 3-10 Output SNR of 8-bit PCM systems with and without companding.

The voltage (or current) waveforms for digital signals can be expressed as an orthogonal series with a finite number of terms,  $N$ . That is, the waveform can be written as

$$w(t) = \sum_{k=1}^N w_k \varphi_k(t), \quad 0 < t < T_0 \quad (3-27)$$

where  $w_k$  represents the digital data and  $\varphi_k(t)$ ,  $k = 1, 2 \dots N$ , are  $N$  orthogonal functions that give the waveform its waveshape. (This will be illustrated by examples that follow in the sections Binary Waveforms and Multilevel Waveforms.)  $N$  is the number of dimensions required to describe the waveform. The term *dimension* arises from the geometric interpretation as described in the next section on Vector Representation. The waveform  $w(t)$  as given by 3-27 to represent a PCM word or any message of the  $M$  message digital source, where each message is assigned a unique set of digital data  $\{w_k\}$ ,  $k = 1, 2 \dots N$  to represent that message. For example, for a binary source consisting of an ASCII computer keyboard, the letter  $X$  is assigned the code word 0001101. (See Appendix C, Table C-2.) Thus, in this case,  $w_1 = 0$ ,  $w_2 = 0$ ,  $w_3 = 0$ ,  $w_4 = 1$ ,  $w_5 = 1$ ,  $w_6 = 0$ ,  $w_7 = 1$ , and  $N = 7$ . In this message (i.e., the letter  $X$ ) is sent out over a time interval of  $T_0$  seconds, then the voltage (or current waveform) representing this message, as described by (3-27), would have a time span of  $T_0$  s and the data rate could be computed using the following definitions:

**DEFINITION.** The *baud (symbol rate)* is<sup>‡</sup>

$$D = N/T_0 \text{ symbols/s} \quad (3-28)$$

where  $N$  is the number of dimensions used in  $T_0$  s.

**DEFINITION.** The *bit rate* is

$$R = n/T_0 \text{ bits/s} \quad (3-29)$$

where  $n$  is the number of data bits sent in  $T_0$  s.

For the case when the  $w_k$ s have binary values,  $n = N$ , and  $w(t)$  is said to be a *binary signal*. When the  $w_k$ s are assigned more than two possible values (i.e., not binary),  $w(t)$  is said to be a *multilevel signal*. These two types of signaling are discussed in separate sections below.

A critical question is: If the waveform of (3-27) is transmitted over a channel and appears at the input to the receiver, how can a receiver be built to detect the data? Because  $w(t)$  is an orthogonal series, the formal way to detect the data is for the receiver to evaluate the orthogonal series coefficient. That is, using (2-84),

$$w_k = \frac{1}{K_k} \int_0^{T_0} w(t) \varphi_k^*(t) dt, k = 1, 2, \dots, N \quad (3-30)$$

where  $w(t)$  is the waveform at the receiver input and  $\varphi_k(t)$  is the known orthogonal function that was used to generate the received waveform. It can also be shown that (3-30) is the optimum way to detect data when the received signal is corrupted by white additive noise; this procedure is called *matched filter* detection using correlation processing as described in Sec. 6-8. Detection of data is illustrated in Examples 3-3 and 3-4.

### Vector Representation

The orthogonal function space representation of (3-27) corresponds to the orthogonal vector space represented by

$$\mathbf{w} = \sum_{j=1}^N w_j \varphi_j \quad (3-31a)$$

where the boldface type denotes a vector representing the waveform of (3-27), and  $\{\varphi_j\}$  is an orthogonal vector set.  $\mathbf{w}$  is an  $N$ -dimensional vector in Euclidean vector space, and  $\{\varphi_j\}$  is a set of  $N$  directional vectors that become a unit vector set if the  $K_j$ 's (2-78) are all unity. A shorthand notation for the vector  $\mathbf{w}$  of (3-52a) is given by a row vector:

$$\mathbf{w} = (w_1, w_2, w_3, \dots, w_N) \quad (3-31b)$$

<sup>‡</sup> In the technical literature, the term *baud rate* instead of baud is sometimes used even though baud rate is a misnomer, since the term *baud*, by definition, is the symbol rate (symbols/second).

### Example 3-2 VECTOR REPRESENTATION OF A BINARY SIGNAL

Examine the representation for the waveform of a 3-bit (binary) signal shown in Fig. 3-11a. This signal could be directly represented by

$$s(t) = \sum_{j=1}^{N=3} d_j p[t - (j - \frac{1}{2})T] = \sum_{j=1}^{N=3} d_j p_j(t)$$

where  $p(t)$  is shown in Fig. 3-11b and  $p_j(t) \triangleq p[t - (j - \frac{1}{2})T]$ .

The  $\{p_j(t)\}$  is a set of orthogonal functions that are not normalized.

$$\mathbf{d} = (d_1, d_2, d_3) = (1, 0, 1)$$

is the binary word with 1 representing a binary 1 and 0 representing a binary 0.  $p(t)$  is the pulse shape for each bit.

Using the orthogonal function approach, we can represent the waveform by

$$s(t) = \sum_{j=1}^{N=3} s_j \varphi_j(t)$$

Let  $\{\varphi_j(t)\}$  be the corresponding set of orthonormal functions. Then, using (2-78),

$$\varphi_j(t) = \frac{p_j(t)}{\sqrt{K_j}} = \frac{p_j(t)}{\sqrt{\int_0^{T_0} p_j^2(t) dt}} = \frac{p_j(t)}{\sqrt{25T}}$$

or

$$\varphi_j(t) = \begin{cases} \frac{1}{\sqrt{T}}, & (j-1)T < t < jT \\ 0, & \text{otherwise} \end{cases}$$

where  $j = 1, 2, \text{ or } 3$ . Using (2-84) where  $a = 0$  and  $b = 3T$ , we find that the orthonormal series coefficients for the digital signal shown in Fig. 3-11a are

$$\mathbf{s} = (s_1, s_2, s_3) = (5\sqrt{T}, 0, 5\sqrt{T})$$

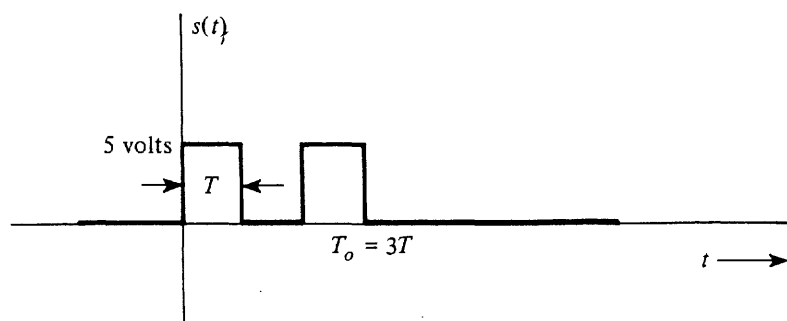
The vector representation for  $s(t)$  is shown in Fig. 3-11d. Note that for this  $N = 3$  dimensional case with binary signaling, only  $2^3 = 8$  different messages could be represented. Each message corresponds to a vector that terminates on a vertex of a cube.

### Bandwidth Estimation

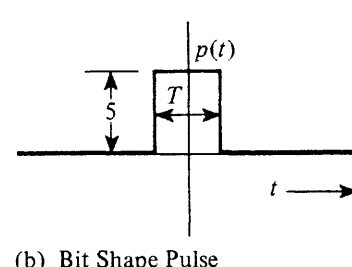
The lower bound for the bandwidth of the waveform representing the digital signal, (3-27), can be obtained from the dimensionality theorem. Thus, using (2-174) and (3-28), bandwidth of the waveform  $w(t)$  is

$$B \geq \frac{N}{2T_0} = \frac{1}{2} D \text{ Hz} \quad (3-32)$$

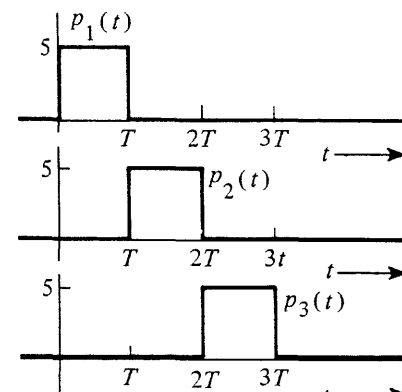
If the  $\varphi_k(t)$  are of the  $\sin(x)/x$  type, the lower bound absolute bandwidth of  $N/(2T_0) = D/2$  will be achieved; otherwise (i.e., for other pulse shapes), the bandwidth will be larger than this lower bound. Equation (3-32) is useful for predicting the bandwidth of digital signals, especially when the exact bandwidth of the digital signal is difficult (or impossible) to calculate. This point is illustrated in Examples 3-3 and 3-4.



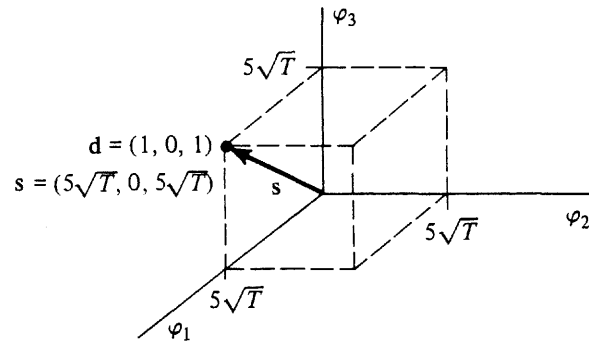
(a) A Three-Bit Signal Waveform



(b) Bit Shape Pulse



(c) Orthogonal Function Set



(d) Vector Representation of the Three-Bit Signal

Figure 3-11 Representation for a 3-bit binary digital signal.

### Binary Signaling

A waveform representing a binary signal can be described by the  $N$ -dimensional orthogonal series of (3-27) where the orthogonal series coefficients,  $w_k$ , take on binary values. More details about binary signaling including their waveforms, data rate, and waveform bandwidth are illustrated by the following example.

### Example 3-3 BINARY SIGNALING

Let us examine some properties of *binary signaling* from a digital source that can produce  $M = 256$  distinctly different messages. Each message could be represented by  $n = 8$ -bit binary words because  $M = 2^n = 2^8 = 256$ . Assume that it takes  $T_0 = 8$  ms to transmit one message, and that a particular message corresponding to the code word 01001110 is to be transmitted. Then,

$$w_1 = 0, w_2 = 1, w_3 = 0, w_4 = 0, w_5 = 1, w_6 = 1, w_7 = 1, w_8 = 0$$

**CASE 1. RECTANGULAR PULSE ORTHOGONAL FUNCTIONS** Assume that the orthogonal functions  $\varphi_k(t)$  are given by unity-amplitude rectangular pulses that are  $T_b = T_0/n = 8/8 = 1$  ms wide, where  $T_b$  is the time that it takes to send 1 bit of data. Then, with the use of (3-27) and MATLAB, the resulting waveform transmitted is given by Fig. 3-12a.

The data can be detected at the receiver by evaluating the orthogonal-series coefficients as given by (3-30). For the case of rectangular pulses, this is equivalent to sampling the waveform anywhere within each bit interval.<sup>†</sup> Referring to Fig. 3-12a, it is seen that sampling within each  $T_b = 1$ -ms interval results in detecting the correct 8-bit data word 01001110.

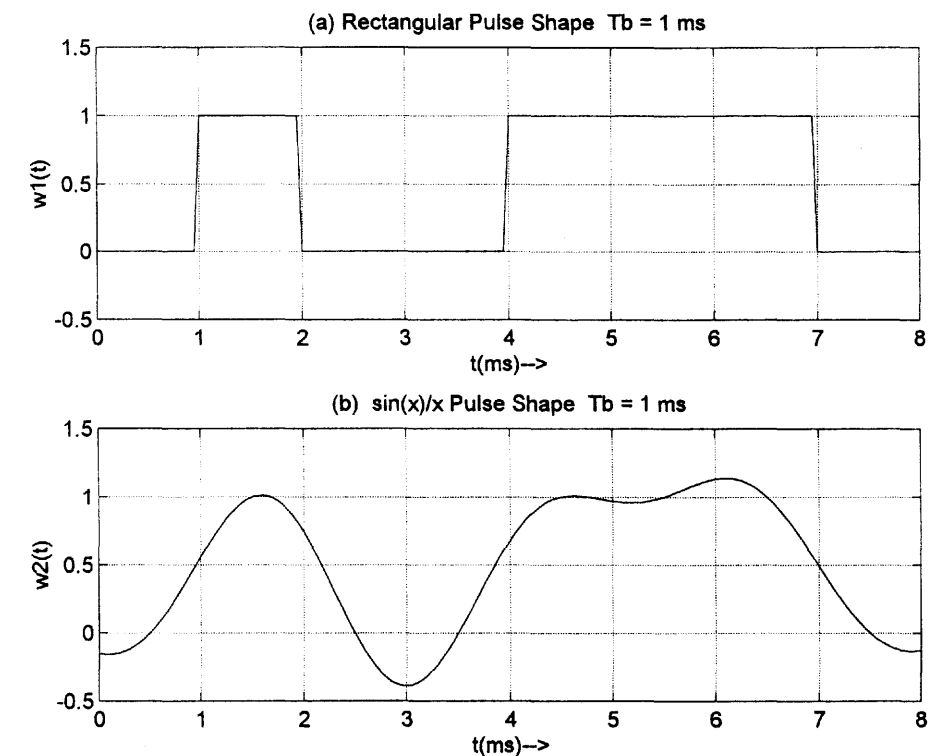


Figure 3-12 Binary signaling (computed).

<sup>†</sup> Sampling detection is optimum only if the received waveform is noise free. See the discussion following (3-30).

The bit rate and the baud (symbol rate) of the binary signal are  $R = n/T_0 = 1\text{-kbit/s}$  and  $D = N/T_0 = 1\text{ kbaud}$  because  $N = n = 8$  and  $T_0 = 8\text{ ms}$ . That is, the bit rate and the baud are equal for binary signaling.

What is the bandwidth for the waveform in Fig. 3-12a? Using (3-32), the lower bound for the bandwidth is  $\frac{1}{2}D = 500\text{ Hz}$ . In Sec. 3-5, it is shown that the actual null bandwidth of this binary signal with a rectangular pulse shape is  $B = 1/T_s = D = 1000\text{ Hz}$ . This is larger than the lower bound for the bandwidth, so the question arises: What is the waveshape that gives the lower bound bandwidth of 500 Hz? The answer is one with  $\sin(x)/x$  pulses as described in Case 2.

**CASE 2. SIN (X)/X PULSE ORTHOGONAL FUNCTIONS** From an intuitive viewpoint, we know that the sharp corners of the rectangular pulse need to be rounded to reduce the bandwidth of the waveform. Furthermore, recalling our study with the sampling theorem, (2-158), it is realized that the  $\sin(x)/x$  type pulse shape has the minimum bandwidth. Consequently, choose the  $\varphi_k(t)$  to be

$$\varphi_k(t) = \frac{\sin\left\{\frac{\pi}{T_s}(t - kT_s)\right\}}{\frac{\pi}{T_s}(t - kT_s)} \quad (3-33)$$

where  $T_s = T_b$  for the case of binary signaling. The resulting waveform that is transmitted is shown in Fig. 3-12b.

Once again, the data can be detected at the receiver by evaluating the orthogonal-series coefficients. Because  $\sin(x)/x$  orthogonal functions are used, (2-160) shows that the data can be recovered simply by sampling<sup>†</sup> the received waveform at the midpoint of each symbol interval. Referring to Fig. 3-12, and sampling at the midpoint of each  $T_s = 1\text{-ms}$  interval, the correct 8-bit word 01001110 is detected.

For Case 2, the bit rate and the baud are still  $R = 1\text{ kbit/s}$  and  $D = 1\text{ kbaud}$ . The absolute bandwidth of (3-33) can be evaluated with the help of Fig. 2-6b where  $2W = 1/T_s$ . That is,  $B = 1/(2T_s) = 500\text{ Hz}$ . Thus, the lower-bound bandwidth (as predicted by the dimensionality theorem) is achieved.

Note that when the rectangular pulse shape is used, as shown in Fig. 3-12a, the digital source information is transmitted via a binary *digital waveform*. That is, the digital signal is a digital waveform. However, when the  $\sin(x)/x$  pulse shape is used, as shown in Fig. 3-12b, the digital source information is transmitted via an *analog waveform* (i.e., an infinite number of voltage values ranging between  $-0.4$  and  $1.2\text{ V}$  are used).

## Multilevel Signaling

In the binary signaling example that was just completed, the lower-bound bandwidth of  $B = N/(2T_0)$  was achieved. That is, for Case 2,  $N = 8$  pulses were required and gave a bandwidth of 500 Hz for a message duration of  $T_0 = 8\text{ ms}$ . However, this bandwidth could be made smaller if  $N$  could be reduced.  $N$  (and, consequently, the bandwidth) can be reduced by letting the  $w_k$ s of (3-27) take on  $L > 2$  possible values (instead of 2 possible values that

<sup>†</sup> Sampling detection is optimum only if the received waveform is noise free. See the discussion following (3-30).

were used for binary signaling). When the  $w_k$ s have  $L > 2$  possible values, the resulting waveform obtained from (3-27) is called a *multilevel signal*.

### Example 3-4 $L = 4$ MULTILEVEL SIGNAL

Here, the  $M = 256$  message source of Example 3-3 will be encoded into a  $L = 4$  multilevel signal, and the message will be sent, once again, in  $T_0 = 8\text{ ms}$ . Multilevel data can be obtained by encoding the  $\ell$  bit binary data of the message source into  $L$ -level data by using a *digital-to-analog converter* (DAC),<sup>†</sup> as shown in Fig. 3-13. For example, one possible encoding scheme for a  $\ell = 2$ -bit DAC is shown in Table 3-3.  $\ell = 2$  bits are read in at a time to produce an output that is one of  $L = 4$  possible levels, where  $L = 2^\ell$ .

TABLE 3-3 A 2-BIT DIGITAL-TO-ANALOG CONVERTER

Binary Input ( $\ell = 2$ bits)	Output Level (V)
11	+3
10	+1
00	-1
01	-3

Thus, for the binary code word 01001110, the sequence of 4-level outputs would be  $-3, -1, +3, +1$ . Consequently, the  $w_k$ s of (3-27) would be  $w_1 = -3, w_2 = -1, w_3 = +3$ , and  $w_4 = +1$ , where  $N = 4$  dimensions are used. The corresponding  $L = 4$  multilevel waveform is shown in Fig. 3-14. Fig. 3-14a gives the multilevel waveform when rectangular pulses are used for  $\varphi_k(t)$  and Fig. 3-14b gives the multilevel waveform when  $\sin(x)/x$  pulses are used. For either case, the receiver could recover the 4-level data corresponding to the  $w_k$  values by sampling the received waveform at the middle of the  $T_s = 2\text{ ms}$  symbol intervals.<sup>‡</sup>

For these  $L = 4$  multilevel signals, the equivalent bit interval is  $T_b = 1\text{ ms}$  because each symbol carries  $\ell = 2$  bits of data (i.e., one of  $L = 4$  levels as shown in Table 3-3). The bit rate is  $R = n/T_0 = \ell/T_s = 1\text{ kbit/s}$  (same as for Example 3-3), and the baud rate is

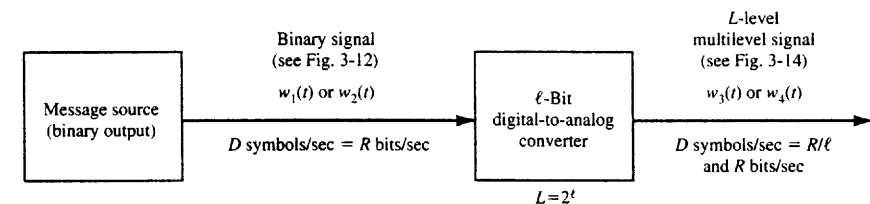
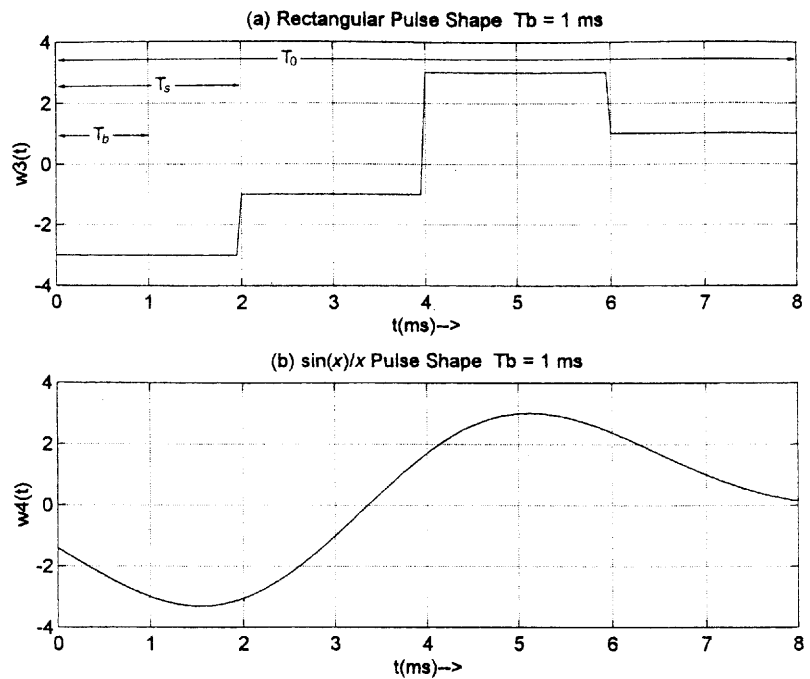


Figure 3-13 Binary-to-multilevel signal conversion.

<sup>†</sup> The term *analog* in digital-to-analog converter is a misnomer because the output is an  $L$ -level digital signal. However, these devices are called digital-to-analog converters in data manuals.

<sup>‡</sup> Sampling detection is optimum only if the received waveform is noise free. See the discussion following (3-30).



**Figure 3-14**  $L = 4$  Multilevel signaling (computed).

$D = N/T_0 = 1/T_s = 0.5 \text{ kbaud}$  (different from Example 3-3). The bit rate and the baud rate are related by

$$R = \ell D \quad (3-34)$$

where  $\ell = \log_2(L)$  is the number of bits read in by the DAC on each clock cycle.

The null bandwidth of the rectangular-pulse multilevel waveform, Fig. 3-14a, is  $B = 1/T_s = D = 500 \text{ Hz}$ . Using (3-32), the absolute bandwidth of the  $\sin(x)/x$ -pulse multilevel waveform, Fig. 3-14b, is  $B = N/(2T_0) = 1/(2T_s) = D/2 = 250 \text{ Hz}$ . Thus, each of these  $L = 4$  multilevel waveforms has  $1/2$  the bandwidth of the corresponding binary signal (with the same pulse shape). In general, an  $L$ -level multilevel signal would have  $1/\ell$  the bandwidth of the corresponding binary signal where  $\ell = \log_2(L)$ . This bandwidth reduction is achieved because the symbol duration of the multilevel signal is  $\ell$  times that of the binary signal. The bit rate,  $R$ , of the binary signal is  $\ell$  times the symbol rate of the multilevel signal.

In the next section, exact formulas are obtained for the power spectral density of binary and multilevel signals.

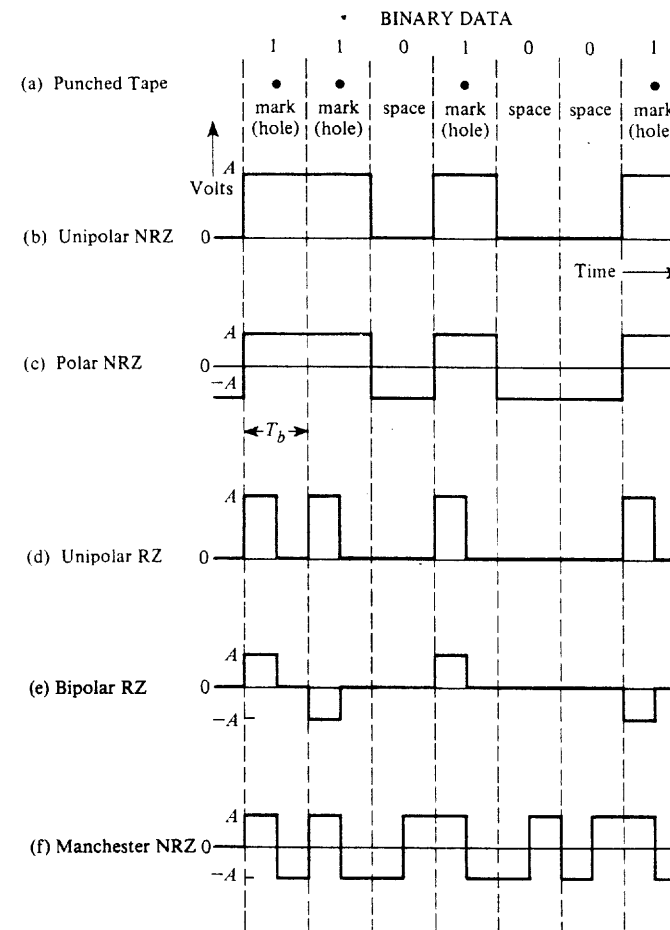


**Figure 3-15** Binary signaling formats.

### 3-5 LINE CODES AND SPECTRA

#### Binary Line Coding

Binary 1s and 0s, such as in PCM signaling, may be represented in various serial-bit signaling formats called *line codes*. Some of the more popular line codes are shown in Fig. 3-15.<sup>†</sup> There are two major categories: *return-to-zero* (RZ) and *nonreturn-to-zero*

<sup>†</sup> Strictly speaking, punched paper tape is a storage medium, not a line code. However, it is included for historical purposes to illustrate the origin of the terms *mark* and *space*. In punched paper tape the binary 1 corresponds to a hole (mark), and a binary 0 corresponds to no hole (space). In current loop signaling (see Appendix C), the presence of loop current denotes a mark and the absence of loop current denotes a space.

(NRZ). With RZ coding, the waveform returns to a zero-volt level for a portion (usually one half) of the bit interval. The waveforms for the line code may be further classified according to the rule that is used to assign voltage levels to represent the binary data. Some examples follow.

**Unipolar Signaling.** In positive logic unipolar signaling the binary 1 is represented by a high level (+A volts) and a binary 0 by a zero level. This type of signaling is also called *on-off keying*.

**Polar Signaling.** Binary 1's and 0's are represented by equal positive and negative levels.

**Bipolar (Pseudoternary) Signaling.** Binary 1's are represented by alternately positive or negative values. The binary 0 is represented by a zero level. The term *pseudoternary* refers to the use of three encoded signal levels to represent two-level (binary) data. This is also called *alternate mark inversion* (AMI) signaling.

**Manchester Signaling.** Each binary 1 is represented by a positive half-bit period pulse followed by a negative half-bit period pulse. Similarly, a binary 0 is represented by a negative half-bit period pulse followed by a positive half-bit period pulse. This type of signaling is also called *split-phase encoding*.

Later in this book we will often use shortened notations. *Unipolar NRZ* will be denoted simply by *unipolar*, *polar NRZ* by *polar*, and *bipolar RZ* as *bipolar*. It should also be pointed out that, unfortunately, the term *bipolar* has two different conflicting definitions as used in practice. The meaning is usually made clear by the context in which it is used: (1) In the space communication industry polar NRZ is sometimes called bipolar NRZ, or simply bipolar (this meaning will not be used in this book); and (2) in the telephone industry the term *bipolar* denotes pseudoternary signaling (used in this book) as in T1 bipolar RZ signaling described in Sec. 3-9.

The line codes shown in Fig. 3-15 are also known by alternate names [Deffebach and Frost, 1971; Sklar, 1988]. For example, polar NRZ is also called NRZ-L, where L denotes the normal logical level assignment. Bipolar RZ is also called RZ-AMI, where AMI denotes alternate mark (binary 1) inversion. Bipolar NRZ is called NRZ-M, where M denotes inversion on mark. Negative logic bipolar NRZ is called NRZ-S, where S denotes inversion on space. Manchester NRZ is called Bi- $\varphi$ -L for bi-phase with normal logic level.

Other line codes, too numerous to list here, can also be found in the literature. [Bylanski and Ingram, 1976; Bic, Dupontel, and Imbeaux, 1991]. For example, the bipolar (pseudoternary) type may be extended into several subclasses as briefly discussed following (3-45).

Each of the line codes shown in Fig. 3-15 has advantages and disadvantages. For example, the unipolar NRZ line code has the advantage of using circuits that require only one power supply (e.g., a single +5-V power supply for TTL circuits), but this line code has the disadvantage of requiring channels that are dc coupled (i.e., frequency response down to  $f = 0$ ) because the waveform has a nonzero dc value. The polar NRZ line code does not require a dc-coupled channel, provided that the data toggles between binary 1s and 0s often,

and equal numbers of binary 1s and 0s are sent. However, the circuitry that produces the polar NRZ signal requires a negative-voltage power supply as well as a positive-voltage power supply. The Manchester NRZ line code has the advantage of always having a 0 dc value, regardless of the data sequence, but it has twice the bandwidth of the unipolar NRZ or polar NRZ codes because the pulses are half the width (see Fig. 3-15).

Some of the desirable properties of a line code are as follows:

- *Self-synchronization.* There is enough timing information built into the code so that bit synchronizers can be designed to extract the timing or clock signal. A long series of binary 1s and 0s should not cause a problem in time recovery.
- *Low probability of bit error.* Receivers can be designed that will recover the binary data with a low probability of bit error when the input data signal is corrupted by noise or ISI. The ISI problem is discussed in Sec. 3-6, and the effect of noise is covered in Chapter 7.
- *A spectrum that is suitable for the channel.* For example, if the channel is ac coupled, the PSD of the line code signal should be negligible at frequencies near zero. In addition the signal bandwidth needs to be sufficiently small compared to the channel bandwidth so that ISI will not be a problem.
- *Transmission bandwidth.* It should be as small as possible.
- *Error detection capability.* It should be possible to implement this feature easily by the addition of channel encoders and decoders, or it should be incorporated into the line code.
- *Transparency.* The data protocol and line code are designed so that *every possible sequence of data* is faithfully and *transparently* received.

A protocol is not transparent if certain words are reserved for control sequences so that, for example, a certain word instructs the receiver to send all data that follows to the printer. This feature causes a problem when a random data file (such as a machine language file) is transferred over the link since some of the words in the file might be control character sequences. These sequences would be intercepted by the receiving system, and the defined action would be carried out, instead of passing the word on to the intended destination. In addition, a code is not transparent if some sequence will result in a loss of clocking signal out of the bit synchronizer at the receiver. The bipolar format is not transparent since a string of zeros will result in a loss of the clocking signal.

The particular type of waveform used for binary signaling depends on the application. For example, unipolar or polar signaling is usually found in most digital circuits, but these waveshapes may have a nonzero dc level; furthermore, the dc level depends on the exact data being represented. Conversely, bipolar and Manchester-type signaling will always have a zero dc level regardless of the data being represented. More discussion of the advantages and disadvantages of each signal format is given after their spectra have been derived.

### Power Spectra for Binary Line Codes

The PSD can be evaluated by using either deterministic or stochastic techniques. This was discussed first in Chapter 1 and later illustrated in Example 2-18. To evaluate the PSD us-

ing the deterministic technique, the waveform for a line code that results from a particular data sequence is used. The approximate PSD is then evaluated by using (2-66) or, if the line code is periodic, by (2-126). Work Prob. 3-22 to apply this deterministic approach. Alternatively, the PSD may be evaluated by using the stochastic approach that is developed in Chapter 6. The stochastic approach will be used to obtain PSD of line codes that are shown in Fig. 3-15. The stochastic approach is used because it gives the PSD for the line code with a random data sequence (instead of that for a particular data sequence).

As discussed and illustrated in Section 3-4, a digital signal (or line code) can be represented by

$$s(t) = \sum_{n=-\infty}^{\infty} a_n f(t - nT_s) \quad (3-35)$$

where  $f(t)$  is the symbol pulse shape, and  $T_s$  is the duration of one symbol. For binary signaling,  $T_s = T_b$ , where  $T_b$  is the time that it takes to send 1 bit. For multilevel signaling,  $T_s = \ell T_b$ .  $\{a_n\}$  is the set of random data. For example, for the unipolar NRZ line code,  $f(t) = \Pi\left(\frac{t}{T_b}\right)$ ; and  $a_n = +A$  V when a binary 1 is sent and  $a_n = 0$  V when a binary 0 is sent.

As proven in Sec. 6-2, using (6-70), the general expression for the PSD of a digital signal

$$\mathcal{P}_s(f) = \frac{|F(f)|^2}{T_s} \sum_{k=-\infty}^{\infty} R(k) e^{j2\pi kfT_s} \quad (3-36a)$$

where  $F(f)$  is the Fourier transform of the pulse shape,  $f(t)$ , and  $R(k)$  is the autocorrelation of the data. This autocorrelation is given by

$$R(k) = \sum_{i=1}^I (a_n a_{n+k})_i P_i \quad (3-36b)$$

where  $a_n$  and  $a_{n+k}$  are the (voltage) levels of the data pulses at the  $n$ th and  $n+k$ th symbol positions, respectively, and  $P_i$  is the probability of having the  $i$ th  $a_n a_{n+k}$  product. Note that (3-36a) shows that the spectrum of the digital signal depends on two things: (1) the pulse shape used and (2) statistical properties of the data.

Using (3-36), which is the stochastic approach, the PSD for the various line codes shown in Fig. 3-15 will now be evaluated.

**Unipolar NRZ Signaling.** For unipolar signaling, the possible levels for the  $a_n$ s are  $+A$  and  $0$  V. Assume that these values are equally likely to occur and that the data are independent. Now, evaluate  $R(k)$  as defined by (3-36b). For  $k = 0$  the possible products of  $a_n a_n$  are  $A \times A = A^2$  and  $0 \times 0 = 0$ , and consequently,  $I = 2$ . For random data, the probability of having  $A^2$  is  $\frac{1}{2}$  and the probability of having  $0$  is  $\frac{1}{2}$ , so that

$$R(0) = \sum_{i=1}^2 (a_n a_n)_i P_i = A^2 \cdot \frac{1}{2} + 0 \cdot \frac{1}{2} = \frac{1}{2} A^2$$

For  $k \neq 0$  there are  $I = 4$  possibilities for the product values:  $A \times A$ ,  $A \times 0$ ,  $0 \times A$ ,  $0 \times 0$ . They all occur with a probability of  $\frac{1}{4}$ . Thus, for  $k \neq 0$ ,

$$R(k) = \sum_{i=1}^4 (a_n a_{n+k})_i P_i = A^2 \cdot \frac{1}{4} + 0 \cdot \frac{1}{4} + 0 \cdot \frac{1}{4} + 0 \cdot \frac{1}{4} = \frac{1}{4} A^2$$

Thus,

$$R_{\text{unipolar}}(k) = \begin{cases} \frac{1}{2} A^2, & k = 0 \\ \frac{1}{4} A^2, & k \neq 0 \end{cases} \quad (3-37a)$$

For rectangular NRZ pulse shapes, the Fourier transform pair is

$$f(t) = \Pi\left(\frac{t}{T_b}\right) \leftrightarrow F(f) = T_b \frac{\sin \pi f T_b}{\pi f T_b} \quad (3-37b)$$

Using (3-36a) with  $T_s = T_b$ , the PSD for the unipolar NRZ line code is

$$\mathcal{P}_{\text{unipolar NRZ}}(f) = \frac{A^2 T_b}{4} \left( \frac{\sin \pi f T_b}{\pi f T_b} \right)^2 \left[ 1 + \sum_{k=-\infty}^{\infty} e^{j2\pi k f T_b} \right]$$

But<sup>†</sup>

$$\sum_{k=-\infty}^{\infty} e^{j2\pi k f T_b} = \frac{1}{T_b} \sum_{n=-\infty}^{\infty} \delta\left(f - \frac{n}{T_b}\right) \quad (3-38)$$

Thus,

$$\mathcal{P}_{\text{unipolar NRZ}}(f) = \frac{A^2 T_b}{4} \left( \frac{\sin \pi f T_b}{\pi f T_b} \right)^2 \left[ 1 + \frac{1}{T_b} \sum_{n=-\infty}^{\infty} \delta\left(f - \frac{n}{T_b}\right) \right] \quad (3-39a)$$

But because  $[\sin(\pi f T_b)/(\pi f T_b)] = 0$  at  $f = n/T_b$ ,  $n \neq 0$ ; this reduces to

$$\mathcal{P}_{\text{unipolar NRZ}}(f) = \frac{A^2 T_b}{4} \left( \frac{\sin \pi f T_b}{\pi f T_b} \right)^2 \left[ 1 + \frac{1}{T_b} \delta(f) \right] \quad (3-39b)$$

If  $A$  is selected so that the normalized average power of the unipolar NRZ signal is unity, then<sup>‡</sup>  $A = \sqrt{2}$ . This PSD is plotted in Fig. 3-16a, where  $1/T_b = R$ , the bit rate of the line code. The disadvantage of unipolar NRZ is the waste of power due to the dc level and the fact that the spectrum is not approaching zero near dc. Of course, dc coupled circuits are

<sup>†</sup> Equation (3-38) is known as the Poisson sum formula as derived in (2-115).

<sup>‡</sup> This can be demonstrated easily using a line code with periodic data 10101010. Then setting

$$P_s = \frac{1}{T_0} \int_0^{T_0} s^2(t) dt = \frac{1}{2T_b} A^2 T_b \text{ equal to unity, we get } A = \sqrt{2}.$$

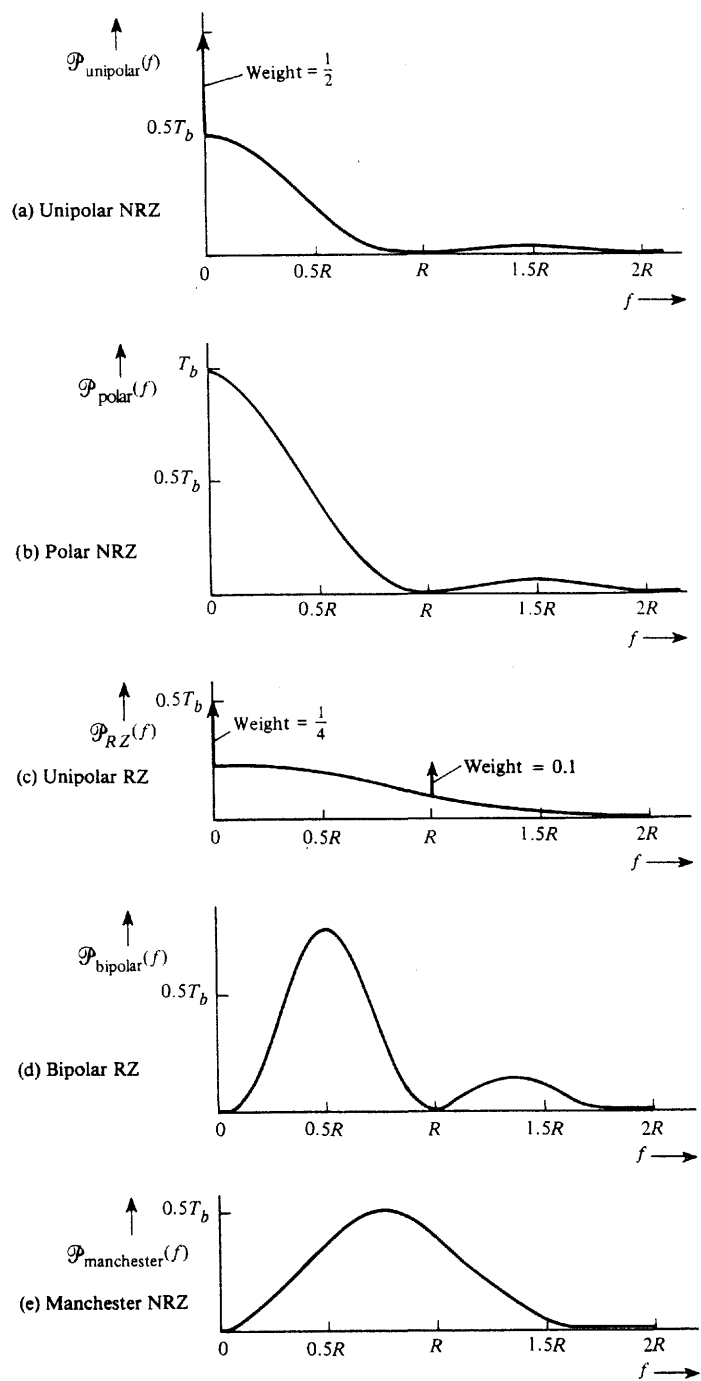


Figure 3-16 PSD for line codes (positive frequencies shown).

needed for this type of signaling. The advantages of unipolar signaling are that it is easy to generate (i.e., TTL and CMOS circuits) and it requires the use of only one power supply.

**Polar NRZ Signaling.** For polar NRZ signaling the possible levels for the  $a_i$ s are  $+A$  and  $-A$  V. For equally likely occurrences of  $+A$  and  $-A$  and assuming that the data are independent from bit-to-bit, we get

$$R(0) = \sum_{i=1}^2 (a_n a_{n+1})_i P_i = A^2 \frac{1}{2} + (-A)^2 \frac{1}{2} = A^2$$

For  $k \neq 0$ ,

$$R(k) = \sum_{i=1}^4 (a_n a_{n+k})_i P_i = A^2 \frac{1}{4} + (-A)(A) \frac{1}{4} + (A)(-A) \frac{1}{4} + (-A)^2 \frac{1}{4} = 0$$

Thus,

$$R_{\text{polar}}(k) = \begin{cases} A^2, & k = 0 \\ 0, & k \neq 0 \end{cases} \quad (3-40)$$

Then substituting (3-40) and (3-37a) in (3-36a), the PSD for the polar NRZ signal is

$$\mathcal{P}_{\text{polar NRZ}}(f) = A^2 T_b \left( \frac{\sin \pi f T_b}{\pi f T_b} \right)^2 \quad (3-41)$$

If  $A$  is selected so that the normalized average power of the polar NRZ signal is unity, then  $A = 1$ , and the resulting PSD is shown in Fig. 3-16b, where the bit rate is  $R = 1/T_b$ .

The polar signal has the disadvantage of having a large PSD near dc. On the other hand, polar signals are relatively easy to generate, although positive and negative power supplies are required unless special-purpose integrated circuits are used that generate dual supply voltages from a single supply. The probability of bit error performance is superior to that of other signaling methods (see Fig. 7-14).

**Unipolar RZ.** The autocorrelation for the unipolar data was calculated previously and is given by (3-37a). For RZ signaling, the pulse duration is  $T_b/2$  instead of  $T_b$  as used in NRZ signaling. That is, for RZ

$$F(f) = \frac{T_b}{2} \left( \frac{\sin(\pi f T_b/2)}{\pi f T_b/2} \right) \quad (3-42)$$

Then, referring to (3-37b) and (3-39a), the PSD for the unipolar RZ line code is

$$\mathcal{P}_{\text{unipolar RZ}}(f) = \frac{A^2 T_b}{16} \left( \frac{\sin(\pi f T_b/2)}{\pi f T_b/2} \right)^2 \left[ 1 + \frac{1}{T_b} \sum_{n=-\infty}^{\infty} \delta \left( f - \frac{n}{T_b} \right) \right] \quad (3-43)$$

If  $A$  is selected so that the normalized average power of the unipolar RZ signal is unity, then  $A = 2$ . The PSD for this unity power case is shown in Fig. 3-16c, where  $R = 1/T_b$ .

As expected, the first null bandwidth is twice that for unipolar or polar signaling since the pulse width is half as wide. Note that there is a discrete (impulse) term at  $f = R$ . Consequently, this periodic component can be used for recovery of the clock signal. One disadvantage of this scheme is that it requires 3 dB more signal power than polar signaling for the same probability of bit error (see Chapter 7). Moreover, the spectrum is not negligible for frequencies near dc.

**Bipolar RZ Signaling.** The PSD for a bipolar signal can also be obtained using (3-36a). The permitted values for  $a_n$  are  $+A$ ,  $-A$ , and 0 where binary 1s are represented by alternating  $+A$  and  $-A$  values and a binary 0 is represented by  $a_n = 0$ . For  $k = 0$  the products  $a_n a_{n+1}$  are  $A^2$  and 0 where each of these products occurs with a probability of  $\frac{1}{2}$ . Thus,

$$R(0) = \frac{A^2}{2}$$

For  $k = 1$  (the adjacent bit case) and the data sequences (1,1), (1,0), (0,1), and (0,0), the possible  $a_n a_{n+1}$  products are  $-A^2$ , 0, 0, 0. Each of these sequences occurs with a probability of  $\frac{1}{4}$ . Consequently,

$$R(1) = \sum_{i=1}^4 (a_n a_{n+1})_i P_i = -\frac{A^2}{4}$$

For  $k > 1$ , the bits being considered are not adjacent, and the  $a_n a_{n+k}$  products are  $\pm A^2$ , 0, 0, 0; these occur with a probability of  $\frac{1}{4}$ . Then

$$R(k > 1) = \sum_{i=1}^5 (a_n a_{n+k})_i P_i = A^2 \cdot \frac{1}{8} - A^2 \cdot \frac{1}{8} = 0$$

Thus,

$$R_{\text{bipolar}}(k) = \begin{cases} \frac{A^2}{2}, & k = 0 \\ -\frac{A^2}{4}, & |k| = 1 \\ 0, & |k| > 1 \end{cases} \quad (3-44)$$

Using (3-44) and (3-42) in (3-36a), where  $T_s = T_b$ , the PSD for the bipolar RZ line code is

$$\mathcal{P}_{\text{bipolar RZ}}(f) = \frac{A^2 T_b}{8} \left( \frac{\sin(\pi f T_b/2)}{\pi f T_b/2} \right)^2 (1 - \cos(2\pi f T_b))$$

or

$$\mathcal{P}_{\text{bipolar RZ}}(f) = \frac{A^2 T_b}{4} \left( \frac{\sin(\pi f T_b/2)}{\pi f T_b/2} \right)^2 \sin^2(\pi f T_b) \quad (3-45)$$

where  $A = 2$  if the normalized average power is unity. This PSD is plotted in Fig. 3-16d. Bipolar signaling has a spectral null at dc so that ac coupled circuits may be used in the transmission path.

The clock signal can be easily extracted from the bipolar waveform by converting the bipolar format to a unipolar RZ format by the use of full-wave rectification. The resulting (unipolar) RZ signal has a periodic component at the clock frequency (see Fig. 3-16c). Bipolar signals are not transparent. That is, a string of zeros will cause a loss in the clocking signal. This difficulty can be prevented by using *high-density bipolar n* (HDBn) signaling where a string of more than  $n$  consecutive zeros is replaced by a “filling” sequence that contains some pulses.<sup>†</sup> The calculation of the PSD for HDBn codes is difficult since the  $R(k)$  have to be individually evaluated for large values of  $k$  [Davis and Barber, 1973].

Bipolar signals also have single-error detection capabilities built in since a single error will cause a violation of the bipolar line code rule. Any violations can easily be detected by receiver logic.

Some disadvantages of bipolar signals are that the receiver has to distinguish between three levels ( $+A$ ,  $-A$ , and 0) instead of just two levels in the other signaling formats previously discussed. The bipolar signal also requires approximately 3 dB more signal power than a polar signal for the same probability of bit error. [It has  $\frac{3}{2}$  the error of unipolar signaling as described by (7-28).]

**Manchester NRZ Signaling.** The Manchester signal uses the pulse shape

$$f(t) = \Pi\left(\frac{t + T_b/4}{T_b/2}\right) - \Pi\left(\frac{t - T_b/4}{T_b/2}\right) \quad (3-46a)$$

and the resulting pulse spectrum is

$$F(f) = \frac{T_b}{2} \left[ \frac{\sin(\pi f T_b/2)}{\pi f T_b/2} \right] e^{j\omega T_b/4} - \frac{T_b}{2} \left[ \frac{\sin(\pi f T_b/2)}{\pi f T_b/2} \right] e^{-j\omega T_b/4}$$

or

$$F(f) = jT_b \left[ \frac{\sin(\pi f T_b/2)}{\pi f T_b/2} \right] \sin\left(\frac{\omega T_b}{4}\right) \quad (3-46b)$$

Substituting this and (3-40) into (3-36a), the PSD for Manchester NRZ becomes

$$\mathcal{P}_{\text{Manchester NRZ}}(f) = A^2 T_b \left( \frac{\sin(\pi f T_b/2)}{\pi f T_b/2} \right)^2 \sin^2(\pi f T_b/2) \quad (3-46c)$$

Where  $A = 1$  if the normalized average power is unity.

<sup>†</sup> For example, for HDB3, the filling sequences used to replace  $n + 1 = 4$  zeros are the alternating sequences 000V and 100V, where the 1 bit is encoded according to the bipolar rule and the V is a 1 pulse of such polarity as to violate the bipolar rule. The alternating filling sequences are designed so that consecutive V pulses alternate in sign. Consequently, there will be a 0 dc value in the line code and the PSD will have a null at  $f = 0$ . To decode the HDB3 code, the bipolar decoder has to detect the bipolar violations and to count the number of zeros preceding each violation so that the substituted 1s can be deleted.



This spectrum is plotted in Fig. 3-16e. The null bandwidth of the Manchester format is twice that of the bipolar bandwidth. However, the Manchester code has a zero dc level on a bit-by-bit basis. Moreover, a string of zeros will not cause a loss of the clocking signal.

In reviewing our study of PSD for digital signals, it should be emphasized that the spectrum is a function of the bit pattern (via the bit autocorrelation) as well as the pulse shape.

## Differential Coding

When serial data are passed through many circuits along a communication channel, the waveform is often unintentionally inverted (i.e., data complemented). This result can occur in a twisted-pair transmission line channel just by switching the two leads at a connection point when a polar line code is used. (Note that this would not affect the data on a bipolar signal.) To ameliorate this problem, *differential coding*, as illustrated in Fig. 3-17, is often employed. The encoded differential data are generated by

$$e_n = d_n \oplus e_{n-1} \quad (3-47)$$

where  $\oplus$  is a modulo 2 adder or exclusive OR gate (XOR) operation. The received encoded data are decoded by

$$\tilde{d}_n = \tilde{e}_n \oplus \tilde{e}_{n-1} \quad (3-48)$$

where the tilde denotes receiving-end data.

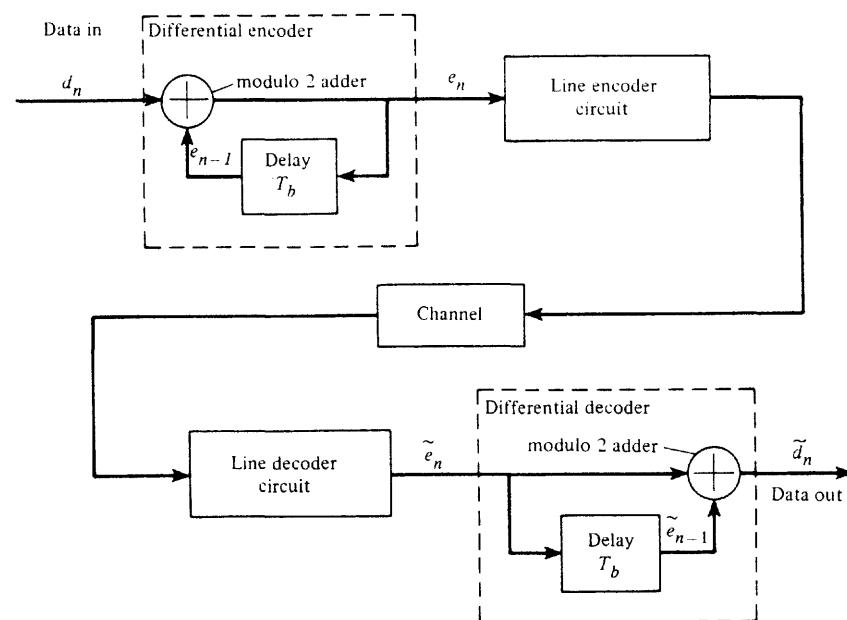


Figure 3-17 Differential coding system.

TABLE 3-4 EXAMPLE OF DIFFERENTIAL CODING

Encoding	$d_n$	1	1	0	1	0	0	1
Input sequence	$e_n$	1	0	1	1	0	0	1
Encoded sequence								
Reference digit								
Decoding (with correct channel polarity)								
Received sequence (correct polarity)	$\tilde{e}_n$	1	0	1	1	0	0	1
Decoded sequence	$\tilde{d}_n$		1	1	0	1	0	1
Decoding (with inverted channel polarity)								
Received sequence (inverted polarity)	$\tilde{e}_n$	0	1	0	0	1	1	0
Decoded sequence	$\tilde{d}_n$		1	1	0	1	0	1

Each digit in the encoded sequence is obtained by comparing the present input bit with the past encoded bit. A binary 1 is encoded if the present input bit and the past encoded bit are of opposite state, and a binary 0 is encoded if the states are the same. This is equivalent to the truth table of an XOR (exclusive OR) gate or a modulo 2 adder. An example of an encoded sequence is shown in Table 3-4, where the beginning reference digit is a binary 1. At the receiver the encoded signal is decoded by comparing the state of adjacent bits. If the present received encoded bit has the same state as the past encoded bit, a binary 0 is the decoded output. Similarly, a binary 1 is decoded for opposite states. As shown in the table, the polarity of the differentially encoded waveform may be inverted without affecting the decoded data. This is a great advantage when the waveform is passed through thousands of circuits in a communication system and the positive sense of the output is lost or changes occasionally as the network changes, such as switching between several data paths.

## Eye Patterns

The effect of channel filtering and channel noise can be seen by observing the received line code on an oscilloscope. The left side of Fig. 3-18 shows received corrupted polar NRZ waveforms for the cases of (a) ideal channel filtering, (b) filtering that produces intersymbol interference (ISI), and (c) noise plus ISI. (ISI is described in Sec. 3-6.) On the right side of the figure, corresponding oscilloscope presentations of the corrupted signal are shown with multiple sweeps where each sweep is triggered by a clock signal and the sweep width is slightly larger than  $T_b$ . These displays on the right are called *eye patterns* because they resemble the picture of a human eye. Under normal operating conditions (i.e., for no detected bit errors), the eye will be open. If there is a great deal of noise or ISI, the eye will close; this indicates that bit errors will be produced at the receiver output. The eye pattern provides an excellent way of assessing the quality of the received line code and the ability of the receiver to combat bit errors. As shown in the figure, the eye pattern provides the following information.

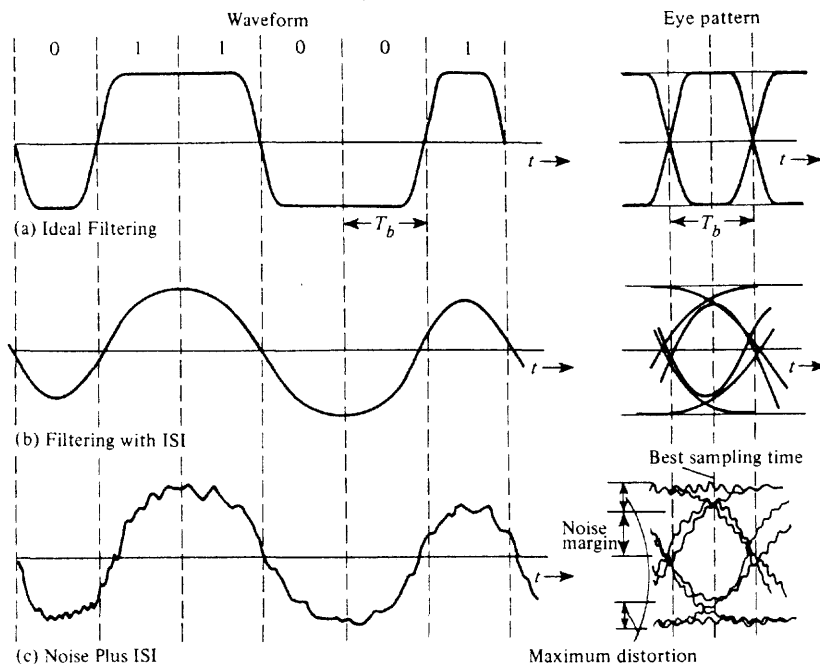


Figure 3-18 Distorted polar NRZ waveform and corresponding eye pattern.

- The *timing error* allowed on the sampler at the receiver is given by the width inside the eye, called the *eye opening*. Of course, the preferred time for sampling is at the point where the vertical opening of the eye is the largest.
- The *sensitivity* to timing error is given by the slope of the open eye (evaluated at, or near, the zero-crossing point).
- The *noise margin* of the system is given by the height of the eye opening.

### Regenerative Repeaters

When a line code digital signal (such as PCM) is transmitted over a hardwire channel (such as a twisted-pair telephone line), it is attenuated, filtered, and corrupted by noise. Consequently, for long lines, the data cannot be recovered at the receiving end unless repeaters are placed in cascade along the line and at the receiver as illustrated in Fig. 3-7. These repeaters amplify and “clean up” the signal periodically. If the signal was analog instead of digital, only linear amplifiers with appropriate filters could be used since relative amplitude values would need to be preserved. In this case in-band distortion would accumulate from linear repeater to linear repeater. This is one of the disadvantages of analog signaling. However, with digital signaling, nonlinear processing can be used to regenerate a “noise-free” digital signal. This type of nonlinear processing is called a *regenerative repeater*. A simplified block diagram of a regenerative repeater for unipolar NRZ signaling is shown in Fig. 3-19. The amplifying filter increases the amplitude of the low-level input signal to a level

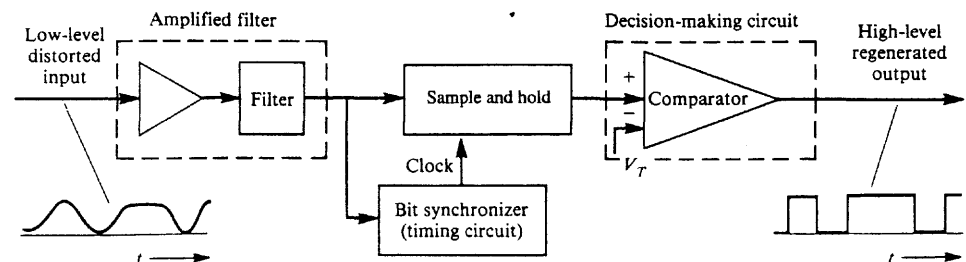


Figure 3-19 Regenerative repeater for unipolar NRZ signaling.

that is compatible with the remaining circuitry and filters the signal in such a way as to minimize the effects of channel noise and ISI. (The filter that reduces ISI is called an *equalizing filter* and is discussed in Sec. 3-6.) The bit synchronizer generates a clocking signal at the bit rate that is synchronized so that the amplified distorted signal is sampled at a point where the eye opening is at maximum. (Bit synchronizers are discussed in detail in the next section.) For each clock pulse, the sample and hold circuit produces the sample value that is held (for  $T_b$ , 1-bit interval) until the next clock pulse occurs. The comparator produces a high-level output only when the sample value is larger than the threshold level,  $V_T$ .  $V_T$  is usually selected to be one-half the expected peak-to-peak variation of the sample values.<sup>†</sup> If the input noise is small and there is negligible ISI, the comparator output will be high only when there is a binary 1 (i.e., a high level) on the corrupted unipolar NRZ line code at the input to the repeater. The comparator—a threshold device—acts as a decision-making device. Thus, the unipolar NRZ line code is regenerated “noise free” except for bit errors that are caused when the input noise and ISI alter the sample values sufficiently so that the sample values occur on the wrong side of  $V_T$ . Chapter 7 shows how the probability of bit error is influenced by the SNR at the input to the repeater, the filter that is used, and the value of  $V_T$  that is selected.<sup>‡</sup>

In long-distance digital communication systems, many repeaters may be used in cascade, as shown in Fig. 3-7. Of course, the spacing between the repeaters is governed by the path loss of the transmission medium and the amount of noise that is added. A repeater is required when the SNR at a point along the channel becomes lower than the value that is needed to maintain the overall probability-of-bit-error specification. Assume that the repeaters are spaced so that each of them has the same probability of bit error,  $P_e$ , and that there are  $m$  repeaters in the system, including the end receiver. Then, for  $m$  repeaters in cascade, the overall probability of bit error,  $P_{me}$ , can be evaluated by the use of the binomial distribution from Appendix B. Using (B-33), we see that the probability of  $i$  out of the  $m$  repeaters producing a bit error is

$$P_i = \binom{m}{i} P_e^i (1 - P_e)^{m-i} \quad (3-49)$$

<sup>†</sup> This is the optimum  $V_T$  when the binary 1s and 0s are equally likely.

<sup>‡</sup> For minimum probability of bit error, the sample-and-hold circuit of Fig. 3-19 is replaced by an optimum sample-detection circuit called a *matched filter* (MF), described in Sec. 6-8.

However, there is a bit error at the system output only when each of an *odd* number of the cascaded repeaters produces a bit error. Consequently, the overall probability of a bit error for  $m$  cascaded repeaters is

$$\begin{aligned} P_{me} &= \sum_{\substack{i=1 \\ i=\text{odd}}}^m P_i = \sum_{\substack{i=1 \\ i=\text{odd}}}^m \binom{m}{i} P_e^i (1 - P_e)^{m-i} \\ &= mP_e(1 - P_e)^{m-1} + \frac{m(m-1)(m-2)}{3!} P_e^3 (1 - P_e)^{m-3} + \dots \quad (3-50a) \end{aligned}$$

Under useful operating conditions,  $P_e \ll 1$ , so only the first term of this series is significant. Thus the overall probability of bit error is approximated by

$$P_{me} \approx mP_e \quad (3-50b)$$

where  $P_e$  is the probability of bit error for a single repeater.

### Bit Synchronization

Synchronization signals are clock-type signals that are necessary within a receiver (or repeater) for detection (or regeneration) of the data from the corrupted input signal. These clock signals have a precise frequency and phase relationship with respect to the *received* input signal, and they are delayed when compared to the clock signals at the transmitter since there is propagation delay through the channel.

Digital communications usually need at least three types of synchronization signals: (1) *bit sync* to distinguish one bit interval from another, as discussed in this section; (2) *frame sync* to distinguish groups of data, as discussed in Sec. 3-9 in regard to time-division multiplexing; and (3) *carrier sync* for bandpass signaling with coherent detection, as discussed in Chapters 4, 5 and 7. Systems are designed so that the sync is derived either directly from the corrupted signal or from a separate channel that is used only to transmit the sync information.

We will concentrate on systems with bit synchronizers that derive the sync directly from the corrupted signal because it is often not economically feasible to send sync over a separate channel. The complexity of the bit synchronizer circuit depends on the sync properties of the line code. For example, the bit synchronizer for a unipolar RZ code with a sufficient number of alternating binary 1's and 0's is almost trivial since the PSD of that code has a delta function at the bit rate,  $f = R$ , as shown in Fig. 3-16c. Consequently, the bit sync clock signal can be obtained by passing the received unipolar RZ waveform through a narrowband bandpass filter that is tuned to  $f_0 = R = 1/T_b$ . This is illustrated by Fig. 3-20 if the square-law device is deleted. Alternatively, as described in Sec. 4-3, a phase-locked-loop (PLL) can be used to extract the sync signal from the unipolar RZ line code by locking the PLL to the discrete spectral line at  $f = R$ . For a polar NRZ line code, the bit synchronizer is slightly more complicated as shown in Fig. 3-20. Here the filtered polar NRZ waveform (Fig. 3-20b) is converted to a unipolar RZ waveform (Fig. 3-20c) by using a square-law (or, alternatively, a full-wave rectifier) circuit. The clock signal is easily recovered by using a filter or a PLL since the unipolar RZ code has a delta function in its spectrum at  $f = R$ . All of

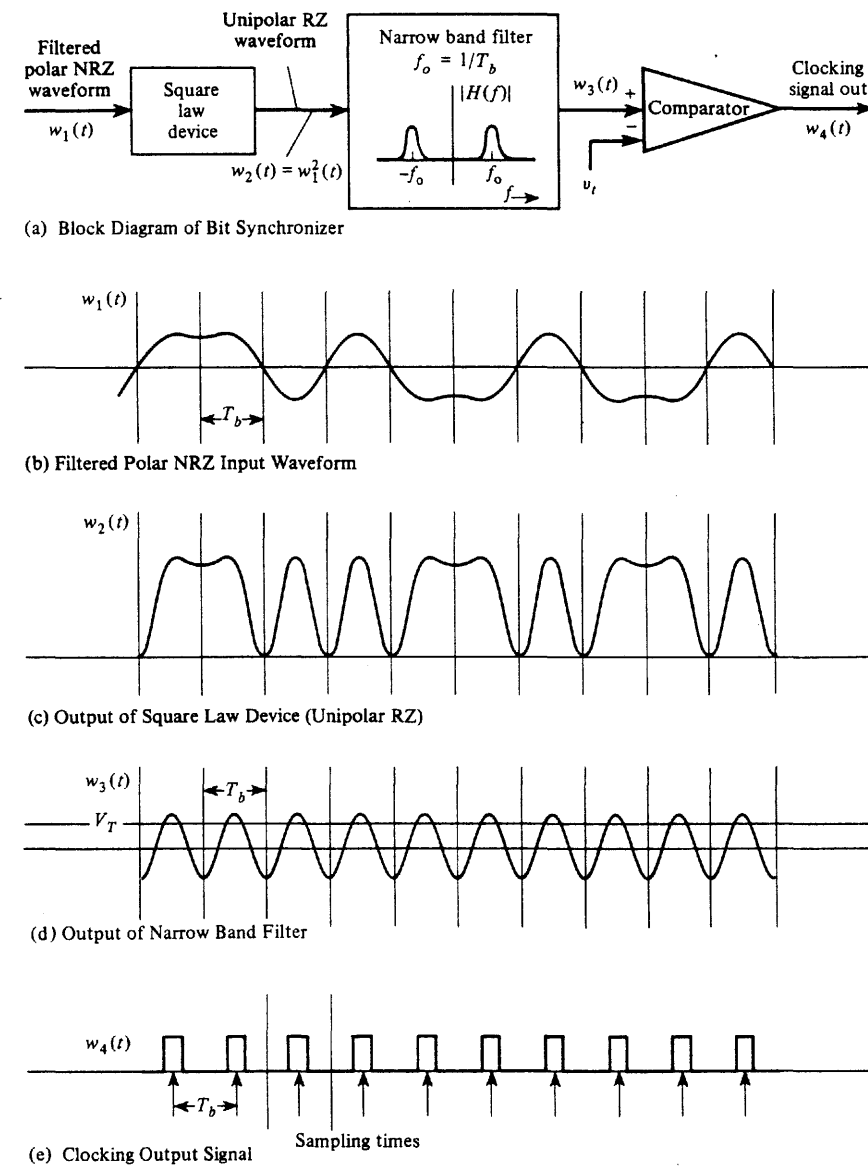


Figure 3-20 Square-law bit synchronizer for polar NRZ signaling.

the bit synchronizers discussed thus far use some technique for detecting the spectral line at  $f = R$ .

Another technique utilizes the symmetry property of the line code itself [Carlson, 1986]. Referring to Fig. 3-18 which illustrates the eye pattern for a polar NRZ code, we realize that a properly filtered line code has a pulse shape that is symmetrical about the optimum clocking (sampling) time, provided that the data are alternating between 1s and 0s. Referring to Fig. 3-21, let  $w_1(t)$  denote the filtered polar NRZ line code and let  $w_1(\tau_0 + nT_b)$  denote a sample value of the line code at the maximum (positive or negative) of the eye opening where  $n$  is an integer,  $R = 1/T_b$  is the bit rate,  $\tau$  is the relative clocking time (i.e., clock phase), and  $\tau_0$  is the optimum value corresponding to samples at the maximum of the eye opening. Because the pulse shape of the line code is approximately symmetrical about the optimum clocking time for alternating data,

$$|w_1(\tau_0 + nT_b - \Delta)| \approx |w_1(\tau_0 + nT_b + \Delta)|$$

where  $\tau_0$  is the optimum clocking phase and  $0 < \Delta < \frac{1}{2}T_b$ .  $w_1(\tau + nT_b - \Delta)$  is called the *early sample* and  $w_1(\tau + nT_b + \Delta)$  is called the *late sample*. These samples can be used to derive the optimum clocking signal as illustrated in the *early-late bit synchronizer* shown in Fig. 3-21. The control voltage,  $w_3(t)$ , for the voltage-controlled clock (VCC) is a smoothed (averaged) version of  $w_2(t)$ . That is,

$$w_3(t) = \langle w_2(t) \rangle \quad (3-51a)$$

where

$$w_2(t) = |w_1(\tau + nT_b - \Delta)| - |w_1(\tau + nT_b + \Delta)| \quad (3-51b)$$

(The averaging operation is needed so that the bit synchronizer will remain synchronized even if the data do not alternate for every bit interval.) If the VCC is producing clocking pulses with the optimum relative clocking time  $\tau = \tau_0$  so that samples are taken at the max-

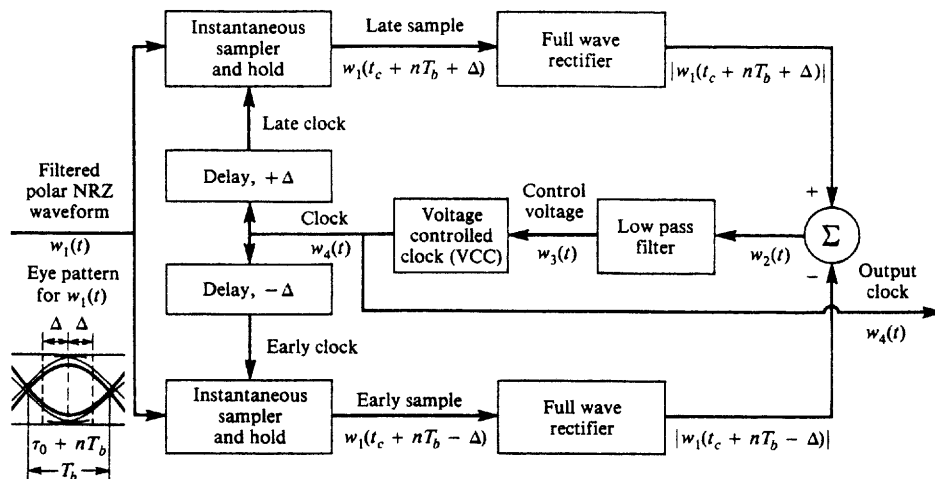


Figure 3-21 Early-late bit synchronizer for polar NRZ signaling.

imum of the eye opening, equation (3-51) demonstrates that the control voltage  $w_3(t)$  will be zero. If  $\tau$  is late  $w_3(t)$  will be a positive correction voltage, and if  $\tau$  is early  $w_3(t)$  will be negative. A positive (negative) control voltage will increase (decrease) the frequency of the VCC. Thus, the bit synchronizer will produce an output clock signal that is synchronized to the input data stream. That is,  $w_4(t)$  will be a pulse train with narrow clock pulses occurring at the time  $t = \tau + nT_b$ , where  $n$  is any integer and  $\tau$  approximates  $\tau_0$ , the optimum clock phase that corresponds to sampling at the maximum of the eye opening. It is interesting to realize that the early-late bit synchronizer of Fig. 3-21 has the same canonical form as the Costas carrier synchronization loop of Fig. 5-3.

Unipolar, polar, and bipolar bit synchronizers will work only when there are a sufficient number of alternating 1s and 0s in the data. The loss of synchronization because of strings of all 1s or all 0s can be prevented by adopting one of two possible alternatives. One alternative, as discussed in Chapter 1, is to use bit interleaving (i.e., scrambling). In this case, the source data with strings of 1s or 0s are scrambled to produce data with alternating 1s and 0s, which are transmitted over the channel using a unipolar, polar, or bipolar line code. At the receiving end scrambled data are first recovered using the usual receiving techniques with bit synchronizers as just described; then the scrambled data are unscrambled. The other alternative is to use a completely different type of line code that does not require alternating data for bit synchronization. For example, Manchester NRZ encoding can be used, but it will require a channel with twice the bandwidth of that needed for a polar NRZ code.

### Power Spectra for Multilevel Signals

Multilevel signaling provides reduced bandwidth when compared with binary signaling. This concept was introduced in Sec. 3-4. Here this concept will be extended and a general formula for the PSD of a multilevel signal will be obtained. To reduce the signaling bandwidth, Fig. 3-22 shows how a binary signal is converted to a multilevel signal, where an  $\ell$ -bit DAC is used to convert the binary signal with data rate  $R$  bits/sec to an  $L = 2^\ell$  level multilevel digital signal.

For example, assume that an  $\ell = 3$  bit DAC is used, so that  $L = 2^3 = 8$  levels. Fig. 3-22b illustrates a typical input waveform, and Fig. 3-22c shows the corresponding eight-level multilevel output waveform where  $T_s$  is the time it takes to send one multilevel symbol. To obtain this waveform, the code shown in Table 3-5 was used. From the figure, we see that  $D = 1/T_s = 1/(3T_b) = R/3$ , or, in general, the baud rate is

$$D = \frac{R}{\ell} \quad (3-52)$$

The relationship between the output baud rate  $D$  and the associated bit rate  $R$  is identical to that discussed in conjunction with the dimensionality theorem in Sec. 3-4, where it was found that the bandwidth was constrained by  $B \geq D/2$ .

The PSD of the multilevel waveform shown in Fig. 3-22c can be obtained by the use of (3-36a). Evaluating  $R(k)$  for the case of equally likely levels  $a_n$ , as shown in Table 3-5, for the  $k = 0$  case we have

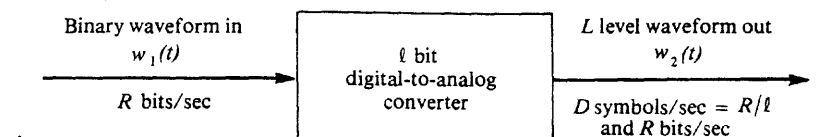
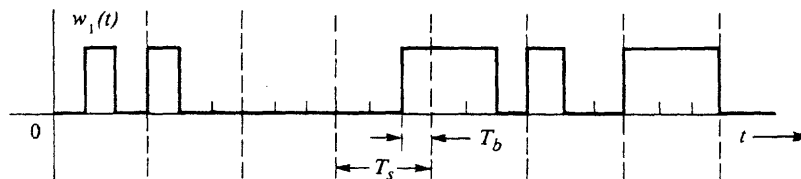
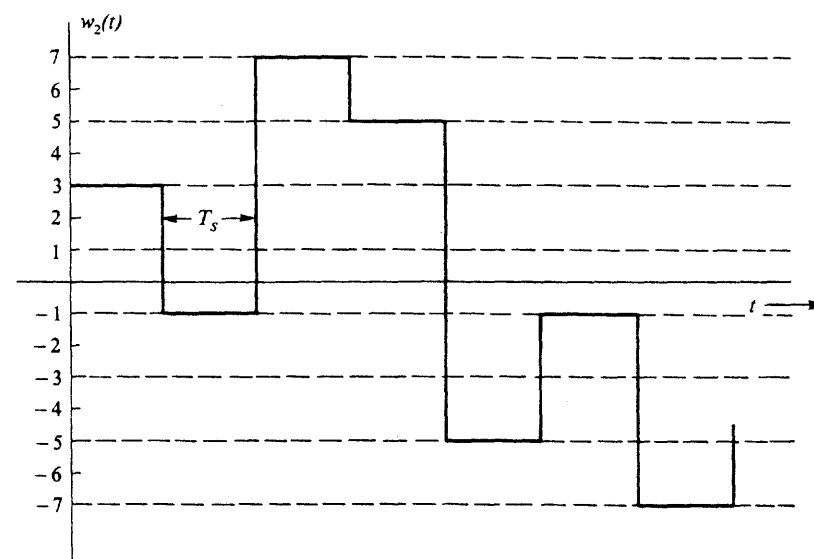
(a)  $\ell$  Bit Digital-to-Analog Converter(b) Input Binary Waveform,  $w_1(t)$ 

Figure 3-22 Binary-to-multilevel digital signal conversion.

$$R(0) = \sum_{i=1}^8 (a_n)_i^2 P_i = 21$$

where  $P_i = \frac{1}{8}$  for all of the eight possible values. For  $k \neq 0$ ,  $R(k) = 0$ . Then, from (3-36a), the PSD for  $w_2(t)$  is

$$\mathcal{P}_{w_2}(f) = \frac{|F(f)|^2}{T_s} (21 + 0)$$

TABLE 3-5 THREE-BIT DAC CODE

Digital Word	Output Level, $(a_n)_i$
000	+7
001	+5
010	+3
011	+1
100	-1
101	-3
110	-5
111	-7

where the pulse width (or symbol width) is now  $T_s = 3T_b$ . For the rectangular pulse shape of width  $3T_b$  this becomes

$$\mathcal{P}_{w_2}(f) = 63T_b \left( \frac{\sin 3\pi f T_b}{3\pi f T_b} \right)^2$$

for this case where  $\ell = 3$ . Consequently, the first null bandwidth for this multilevel signal is  $B_{\text{null}} = 1/(3T_b) = R/3$ , or one third the bandwidth of the input binary signal.

In general, for the case of  $L = 2^\ell$  levels, the PSD of a multilevel signal with rectangular pulse shapes is



$$\mathcal{P}_{\text{multilevel NRZ}}(f) = K \left( \frac{\sin \ell \pi f T_b}{\ell \pi f T_b} \right)^2 \quad (3-53)$$

where  $K$  is a constant and the null bandwidth is

$$B_{\text{null}} = R/\ell \quad (3-54)$$

In summary, multilevel signaling, where  $L > 2$ , is used to reduce the bandwidth of a digital signal when compared with the bandwidth required for binary signaling. In practice, filtered multilevel signals are often used to modulate a carrier for transmission of digital information over a communication channel. This provides a relatively narrowband digital signal.

### Spectral Efficiency

**DEFINITION.** The *spectral efficiency* of a digital signal is given by the number of bits per second of data that can be supported by each hertz of bandwidth:

$$\eta = \frac{R}{B} \text{ (bits/s)/Hz} \quad (3-55)$$

where  $R$  is the data rate and  $B$  is the bandwidth.

In applications where the bandwidth is limited by physical and regulatory constraints, the job of the communication engineer is to choose a signaling technique that gives the highest spectral efficiency while achieving given cost constraints and meeting specifications for low probability of bit error at the system output. Moreover, the maximum possible spectral efficiency is limited by the channel noise if the error is to be small. This maximum spectral efficiency is given by Shannon's channel capacity formula, (1-10),

$$\eta_{\max} = \frac{C}{B} = \log_2 \left( 1 + \frac{S}{N} \right) \quad (3-56)$$

Shannon's theory does not tell us how to achieve a system with this maximum theoretical spectral efficiency; however, practical systems that approach this spectral efficiency usually incorporate error correction coding and multilevel signaling.

The spectral efficiency for multilevel NRZ signaling is obtained by substituting (3-54) into (3-55):

$$\eta = \ell \text{ (bit/s)/Hz} \quad (\text{multilevel NRZ signaling}) \quad (3-57)$$

where  $\ell$  is the number of bits used in the DAC. Of course,  $\ell$  cannot be increased without limit to an infinite efficiency because it is limited by the signal-to-noise ratio as given in (3-56).

The spectral efficiencies for all the line codes studied in the previous sections can be easily evaluated from their PSDs. The results are shown in Table 3-6. Unipolar NRZ, polar NRZ, and bipolar RZ are twice as efficient as unipolar or Manchester NRZ.

All of these binary line codes have  $\eta \leq 1$ . Multilevel signaling can be used to achieve much greater spectral efficiency, but multilevel circuits are more costly. In practice, multilevel signaling is used in the T1G digital telephone lines as described in Sec. 3-9.

### 3-6 INTERSYMBOL INTERFERENCE

The absolute bandwidth of flat-top multilevel pulses is infinity. If these pulses are filtered improperly as they pass through a communication system, they will spread in time, and the pulse for each symbol may be smeared into adjacent time slots and cause *intersymbol interference* (ISI), as illustrated in Fig. 3-23. The question is: How can we restrict the bandwidth and still not introduce ISI? Of course, with restricted bandwidth, the pulses would have rounded tops (instead of flat tops). This problem was first studied by Nyquist [Nyquist, 1928]. He discovered three different methods for pulse shaping that could be used to eliminate ISI. Each of these methods will be studied in the sections that follow.

Consider a digital signaling system as shown in Fig. 3-24. In general, multilevel signaling will be assumed where the flat-topped multilevel signal at the input is

$$w_{in}(t) = \sum_n a_n h(t - nT_s) \quad (3-58)$$

TABLE 3-6 SPECTRAL EFFICIENCIES OF LINE CODES

Code Type	First-Null Bandwidth (Hz)	Spectral Efficiency $\eta = R/B$ [(bits/s)/Hz]
Unipolar NRZ	$R$	1
Polar NRZ	$R$	1
Unipolar RZ	$2R$	$\frac{1}{2}$
Bipolar RZ	$R$	1
Manchester NRZ	$2R$	$\frac{1}{2}$
Multilevel NRZ	$R/\ell$	$\ell$

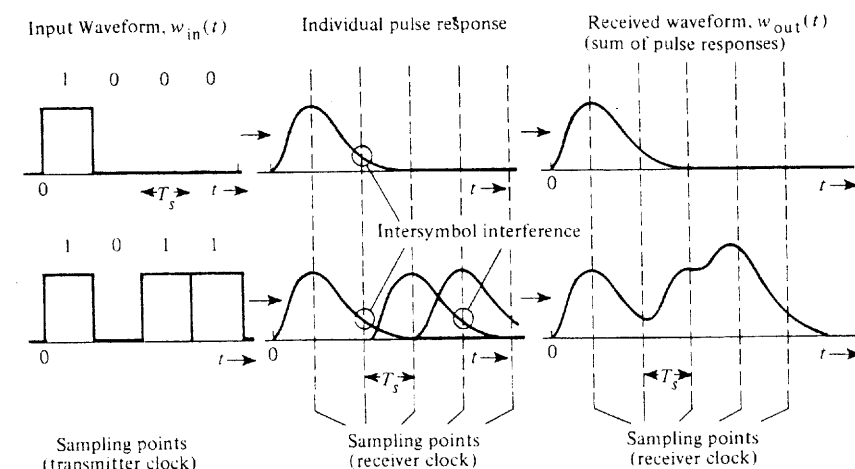


Figure 3-23 Examples of ISI on received pulses in a binary communication system.

where  $h(t) = \Pi(t/T_s)$  and  $a_n$  may take on any of the allowed  $L$  multilevels ( $L = 2$  for binary signaling). The symbol rate is  $D = 1/T_s$  pulses/s. Then (3-58) may be written as

$$\begin{aligned} w_{in}(t) &= \sum_n a_n h(t - nT_s) \\ &= \left[ \sum_n a_n \delta(t - nT_s) \right] * h(t) \end{aligned} \quad (3-59)$$

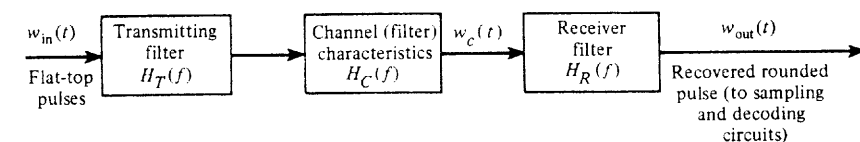


Figure 3-24 Baseband pulse transmission system.

The output of the linear system of Fig. 3-24 would be just the input impulse train convolved with the equivalent impulse response of the overall system

$$w_{\text{out}}(t) = \left[ \sum_n a_n \delta(t - nT_s) \right] * h_e(t) \quad (3-60)$$

where the equivalent impulse response is

$$h_e(t) = h(t) * h_T(t) * h_C(t) * h_R(t) \quad (3-61)$$

Note that  $h_e(t)$  is also the pulse shape that will appear at the output of the receiver filter when a single flat-top pulse is fed into the transmitting filter (Fig. 3-24).

The equivalent system transfer function is

$$H_e(f) = H(f)H_T(f)H_C(f)H_R(f) \quad (3-62)$$

where

$$H(f) = \mathcal{F} \left[ \Pi \left( \frac{t}{T_s} \right) \right] = T_s \left( \frac{\sin \pi f T_s}{\pi f T_s} \right) \quad (3-63)$$

Equation (3-63) is used so that flat-top pulses will be present at the input to the transmitting filter. The receiving filter,  $H_R(f)$ , is given by

$$H_R(f) = \frac{H_e(f)}{H(f)H_T(f)H_C(f)} \quad (3-64)$$

where  $H_e(f)$  is the overall filtering characteristic.

When  $H_e(f)$  is chosen to minimize the ISI, then  $H_R(f)$ , obtained from (3-64), is called an *equalizing filter*. The equalizing filter characteristic depends on  $H_C(f)$ , the channel frequency response, as well as on the required  $H_e(f)$ . When the channel consists of dial-up telephone lines, the channel transfer function changes from call to call and the equalizing filter may need to be an *adaptive filter*. In this case, the equalizing filter adjusts itself to minimize the ISI. In some adaptive schemes, each communication session is preceded by a test bit pattern that is used to adapt the filter electronically for the maximum eye opening (i.e., minimum ISI). Such sequences are called *learning* or *training sequences and preambles*.

If we rewrite (3-60), the rounded pulse train at the output of the receiving filter is

$$w_{\text{out}}(t) = \sum_n a_n h_e(t - nT_s) \quad (3-65)$$

The output pulse shape is affected by the input pulse shape (flat-topped in this case), the transmitter filter, the channel filter, and the receiving filter. Because, in practice, the channel filter is already specified, the problem is to determine the transmitting filter and the receiving filter that will minimize the ISI on the rounded pulse at the output of the receiving filter.

From an applications point of view, it is realized that when the required transmitter filter and/or receiving filter transfer functions are found, they can each be multiplied by

$Ke^{-j\omega T_d}$ , where  $K$  is a convenient gain factor and  $T_d$  is a convenient time delay. These parameters are chosen to make the filters easier to build. The  $Ke^{-j\omega T_d}$  factor(s) would not affect the zero ISI result but, of course, would modify the level and delay of the output waveform.

### Nyquist's First Method (Zero ISI)

*Nyquist's first method* for elimination of ISI is to use an equivalent transfer function,  $H_e(f)$ , such that the impulse response satisfies the following condition:

$$h_e(kT_s + \tau) = \begin{cases} C, & k = 0 \\ 0, & k \neq 0 \end{cases} \quad (3-66)$$

where  $k$  is an integer,  $T_s$  is the symbol (sample) clocking period,  $\tau$  is the offset in the receiver sampling clock times when compared with the clocking times of the input symbols, and  $C$  is a nonzero constant. That is, for a single flat-top pulse of level  $a$  present at the input to the transmitting filter at  $t = 0$ , the received pulse would be  $ah_e(t)$ . It would have a value of  $aC$  at  $t = \tau$  but would not cause interference at other sampling times because  $h_e(kT_s + \tau) = 0$  for  $k \neq 0$  (e.g., see Fig. 3-23).

Now suppose that we choose a  $(\sin x)/x$  function for  $h_e(t)$ . In particular, let  $\tau = 0$  and choose

$$h_e(t) = \frac{\sin \pi f_s t}{\pi f_s t} \quad (3-67)$$

where  $f_s = 1/T_s$ . This impulse response satisfies Nyquist's first criterion for zero ISI, (3-66). Consequently, if the transmit and received filters are designed so that the overall transfer function is

$$H_e(f) = \frac{1}{f_s} \Pi \left( \frac{f}{f_s} \right) \quad (3-68)$$

there will be no ISI. Furthermore, the absolute bandwidth of this transfer function is  $B = f_s/2$ . From our study of the sampling theorem and the dimensionality theorem in Chapter 2 and Sec. 3-4, we realize that this is the optimum filtering to produce a minimum bandwidth system. It will allow signaling at a baud rate of  $D = 1/T_s = 2B$  pulses/sec, where  $B$  is the absolute bandwidth of the system. However, the  $(\sin x)/x$  type of overall pulse shape has two practical difficulties.

- The overall amplitude transfer characteristic  $H_e(f)$  has to be flat over  $-B < f < B$  and zero elsewhere. This is physically unrealizable (i.e., the impulse response is noncausal and of infinite duration).  $H_e(f)$  is difficult to approximate because of the steep skirts in the filter transfer function at  $f = \pm B$ .
- The synchronization of the clock in the decoding sampling circuit has to be almost perfect since the  $(\sin x)/x$  pulse decays only as  $1/x$  and is zero in adjacent time slots only when  $t$  is at the exactly correct sampling time. Thus, inaccurate sync will cause ISI.

Because of these difficulties, we are forced to consider other pulse shapes that have a slightly wider bandwidth. The idea is to find pulse shapes that go through zero at adjacent sampling points and yet have an envelope that decays much faster than  $1/x$  so that clock jitter in the sampling times does not cause appreciable ISI. One solution for the equivalent transfer function, which has many desirable features, is the raised cosine-rolloff filter.

### Raised Cosine-Rolloff Filtering

**DEFINITION.** The *raised cosine-rolloff filter* has the transfer function



$$H_e(f) = \begin{cases} 1, & |f| < f_1 \\ \frac{1}{2} \left\{ 1 + \cos \left[ \frac{\pi(|f| - f_1)}{2f_\Delta} \right] \right\}, & f_1 < |f| < B \\ 0, & |f| > B \end{cases} \quad (3-69)$$

where  $B$  is the *absolute bandwidth* and the parameters  $f_1$  and  $f_\Delta$  are

$$f_\Delta = B - f_0 \quad (3-70)$$

$$f_1 \triangleq f_0 - f_\Delta \quad (3-71)$$

$f_0$  is the *6-dB bandwidth* of the raised cosine-rolloff filter. The *rolloff factor* is defined to be

$$r = \frac{f_\Delta}{f_0} \quad (3-72)$$

This filter characteristic is illustrated in Fig. 3-25. The corresponding impulse response is



$$h_e(t) = \mathcal{F}^{-1}[H_e(f)] = 2f_0 \left( \frac{\sin 2\pi f_0 t}{2\pi f_0 t} \right) \left[ \frac{\cos 2\pi f_\Delta t}{1 - (4f_\Delta t)^2} \right] \quad (3-73)$$

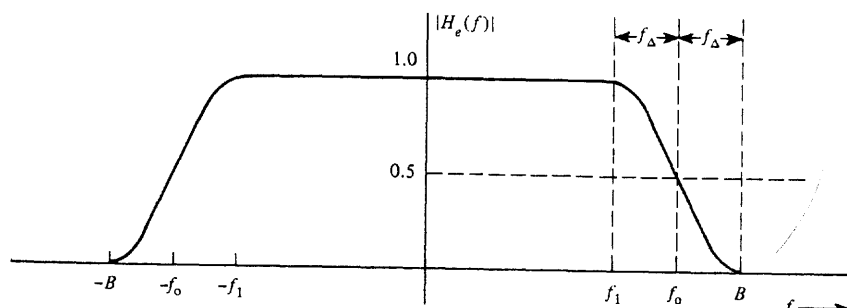
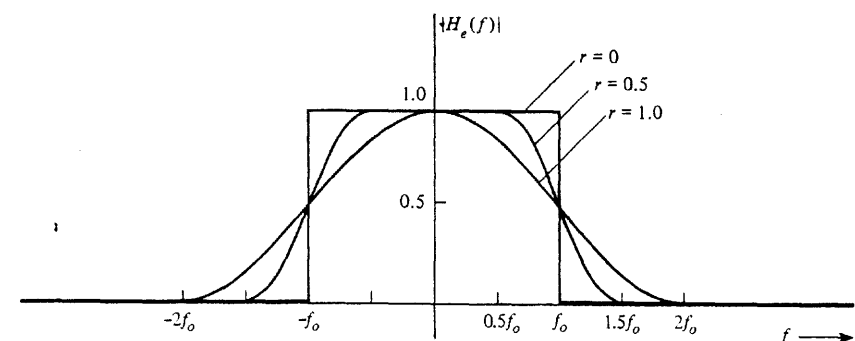
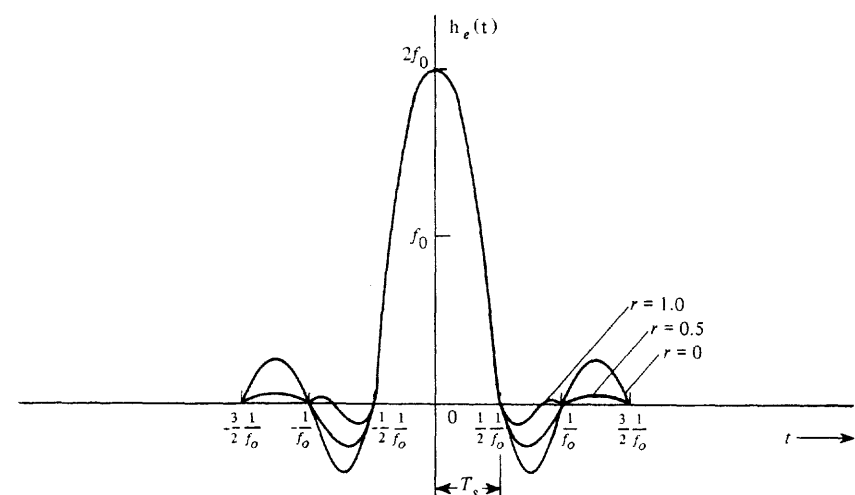


Figure 3-25 Raised cosine-rolloff filter characteristics.



(a) Magnitude Frequency Response



(b) Impulse Response

Figure 3-26 Frequency and time response for different rolloff factors.

Plots of the frequency response and the impulse response are shown in Fig. 3-26 for rolloff factors  $r = 0$ ,  $r = 0.5$ , and  $r = 1.0$ . The  $r = 0$  characteristic is the minimum bandwidth case where  $f_0 = B$  and the impulse response is the  $(\sin x)/x$  pulse shape. From this figure it is seen that as the absolute bandwidth is increased (e.g.,  $r = 0.5$  and  $r = 1.0$ ), (1) the filtering requirements are relaxed, although  $h_e(t)$  is still noncausal; and (2) the clock timing requirements are relaxed also since the envelope of the impulse response decays faster than  $1/|t|$  (on the order of  $1/|t|^3$  for large values of  $t$ ).

The baud rate that the communication system can support without ISI can be related to the absolute bandwidth of the system and the rolloff factor of the raised cosine-rolloff filter characteristic. From Fig. 3-26b, the zeros in the system impulse response occur at  $t = n/2f_0$ ,  $n \neq 0$ . Thus, the raised cosine-rolloff filter satisfies Nyquist's first criterion for no ISI as described by (3-66) if we use  $\tau = 0$  and sample with a period of  $T_s = 1/2f_0$ . The

corresponding baud rate is  $D = 1/T_s = 2f_0$  symbols/s. Using (3-70) and (3-72), we see that the baud rate that can be supported by the system is

$$D = \frac{2B}{1+r} \quad (3-74)$$

where  $B$  is the absolute bandwidth of the system and  $r$  is the system rolloff factor.

### Example 3-1 (CONTINUED)

Assume that a binary PCM signal, with polar NRZ signaling, is passed through a communication system with a raised cosine-rolloff filtering characteristic and that the rolloff factor is 0.25. The bit rate of the PCM signal is 64 kbit/s. Determine the absolute bandwidth of the filtered PCM signal.

Using (3-74), the absolute bandwidth is  $B = 40$  kHz, which is less than the unfiltered PCM signal null bandwidth of 64 kHz.

The raised cosine filter is only one of a more general class of filters that satisfy Nyquist's first criterion. This general class is described by the following theorem.

**THEOREM.** *The overall filter is said to be a Nyquist filter if the effective transfer function of a pulse system is*

$$H_e(f) = \begin{cases} \Pi\left(\frac{f}{2f_0}\right) + Y(f), & |f| < 2f_0 \\ 0, & \text{elsewhere} \end{cases} \quad (3-75)$$

where  $Y(f)$  is a real function that is even symmetric about  $f = 0$ ; that is,

$$Y(-f) = Y(f), \quad |f| < 2f_0 \quad (3-76a)$$

and odd symmetric about  $f = f_0$ ; that is,

$$Y(-f + f_0) = -Y(f + f_0), \quad |f| < f_0 \quad (3-76b)$$

Then there will be no intersymbol interference at the system output if the symbol rate is

$$D = f_s = 2f_0 \quad (3-77)$$

This theorem is illustrated in Fig. 3-27.  $Y(f)$  can be any real function that satisfies the symmetry conditions of (3-76). Thus, an infinite number of filter characteristics can be used to produce zero ISI.

**Proof.** We need to show that the impulse response of this filter is 0 at  $t = nT_s$ ,  $n \neq 0$ , where  $T_s = 1/f_s = 1/(2f_0)$ . Taking the inverse Fourier transform of (3-75), we have

$$h_e(t) = \int_{-2f_0}^{-f_0} Y(f) e^{j\omega_0 t} df + \int_{-f_0}^{f_0} [1 + Y(f)] e^{j\omega_0 t} df + \int_{-f_0}^{2f_0} Y(f) e^{j\omega_0 t} df$$

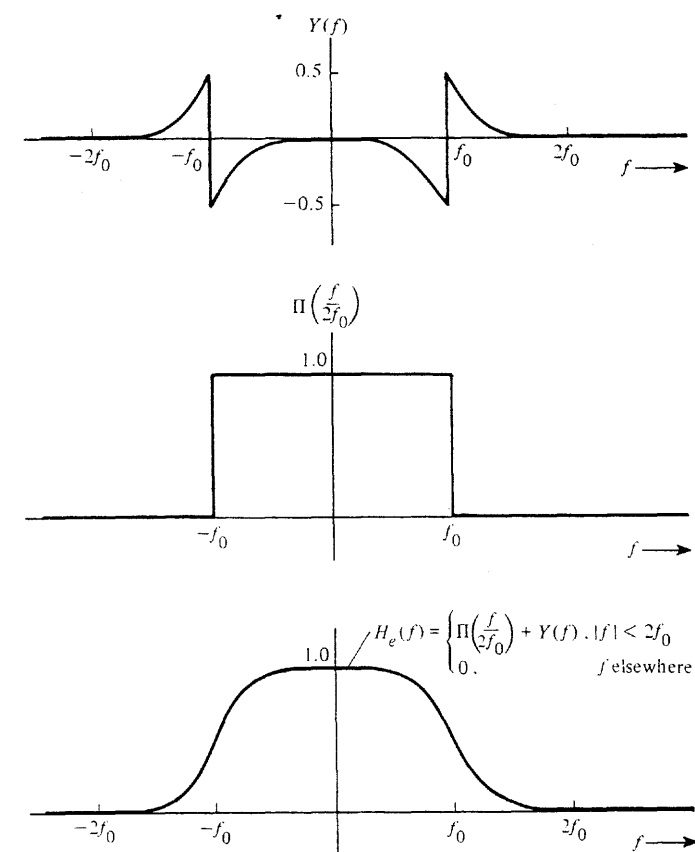


Figure 3-27 Nyquist filter characteristic.

or

$$\begin{aligned} h_e(t) &= \int_{-f_0}^{f_0} e^{j\omega_0 t} df + \int_{-2f_0}^{2f_0} Y(f) e^{j\omega_0 t} df \\ &= 2f_0 \left( \frac{\sin \omega_0 t}{\omega_0 t} \right) + \int_{-2f_0}^0 Y(f) e^{j\omega_0 t} df + \int_0^{2f_0} Y(f) e^{j\omega_0 t} df \end{aligned}$$

Making a change in variable in the integrals, letting  $f_1 = f + f_0$  in the first integral and  $f_1 = f - f_0$  in the second integral, we obtain

$$\begin{aligned} h_e(t) &= 2f_0 \left( \frac{\sin \omega_0 t}{\omega_0 t} \right) + e^{-j\omega_0 t} \int_{-f_0}^{f_0} Y(f_1 - f_0) e^{j\omega_0 t} df_1 \\ &\quad + e^{-j\omega_0 t} \int_{-f_0}^{f_0} Y(f_1 + f_0) e^{j\omega_0 t} df_1 \end{aligned}$$

From (3-76a) and (3-76b) we know that  $Y(f_1 - f_0) = -Y(f_1 + f_0)$ ; thus we have

$$h_e(t) = 2f_0 \left( \frac{\sin \omega_0 t}{\omega_0 t} \right) + j2 \sin \omega_0 t \int_{-f_0}^{f_0} Y(f_1 + f_0) e^{j\omega_0 t} df_1$$

This impulse response is real because  $H_e(-f) = H_e^*(f)$ ; furthermore, it satisfies Nyquist's first criterion. That is,  $h_e(t)$  is zero at  $t = n/(2f_0)$ ,  $n \neq 0$ , and  $\tau = 0$ .

Thus, if we sample at  $t = n/(2f_0)$ , there will be no ISI. However, the filter is noncausal.

In the preceding description of the Nyquist filter, we assumed that  $H_e(f)$  was real. Of course, we could use a filter with a linear phase characteristic [i.e.,  $H_e(f)e^{-j\omega T_d}$ ], and there would be no ISI if we delayed the clocking by  $T_d$  sec, since the  $e^{-j\omega T_d}$  factor is the transfer function of an ideal delay line. This would move the peak of the impulse response to the right (along the time axis), and then the filter would be approximately causal.

At the digital receiver, in addition to minimizing the ISI, we would like to minimize the effect of channel noise by proper receiver filtering. As will be shown in Chapter 6, the filter that minimizes the effect of channel noise is the *matched filter*. Unfortunately, if a matched filter is used for  $H_R(f)$  at the receiver, the overall filter characteristic,  $H_e(f)$ , will usually not satisfy the Nyquist characteristic for minimum ISI. However, it can be shown that for the case of Gaussian noise into the receiver, the effects of both ISI and channel noise are minimized if the transmitter and receiver filters are designed so that [Shanmugan, 1979; Sunde, 1969; Ziemer and Peterson, 1985]

$$|H_T(f)| = \frac{\sqrt{|H_e(f)| [\mathcal{P}_n(f)]^{1/4}}}{\alpha |H(f)| \sqrt{|H_c(f)|}} \quad (3-78a)$$

and

$$|H_R(f)| = \frac{\alpha \sqrt{|H_e(f)|}}{\sqrt{|H_c(f)| [\mathcal{P}_n(f)]^{1/4}}} \quad (3-78b)$$

where  $\mathcal{P}_n(f)$  is the PSD for the noise at the receiver input and  $\alpha$  is an arbitrary positive constant (e.g., choose  $\alpha = 1$  for convenience).  $H_e(f)$  is selected from any appropriate frequency response characteristic that satisfies Nyquist's first criterion as discussed previously and  $H(f)$  is given by (3-63). Any appropriate phase response can be used for  $H_T(f)$  and  $H_R(f)$  as long as the overall system phase response is linear. This results in a constant time delay versus frequency.

### Nyquist's Second and Third Methods for Control of ISI

Nyquist's *second method* of ISI control allows some ISI to be introduced in a *controlled* way so that it can be canceled out at the receiver and the data can be recovered without error if no noise is present [Couch, 1993]. This technique also allows for the possibility of doubling the bit rate or, alternatively, halving the channel bandwidth. This phenomenon was observed by telegraphers in the 1900s and is known as "doubling the dotting speed" [Bennett and Davy, 1965].

In Nyquist's *third method* of ISI control, the effect of ISI is eliminated by choosing  $h_e(t)$  so that the area under the  $h_e(t)$  pulse within the desired symbol interval,  $T_s$ , is not zero but the areas under  $h_e(t)$  in adjacent symbol intervals are zero. For data detection, the receiver evaluates the area under the receiver waveform over each  $T_s$  interval. Pulses have been found that satisfy Nyquist's third criterion, but their performance in the presence of noise is inferior to the examples that have been discussed previously [Sunde, 1969].

## 3-7 DIFFERENTIAL PULSE CODE MODULATION

When audio or video signals are sampled, it is usually found that adjacent samples are close to the same value. This means that there is a lot of redundancy in the signal samples and, consequently, that the bandwidth and the dynamic range of a PCM system are wasted when redundant sample values are retransmitted. One way to minimize redundant transmission and reduce the bandwidth is to transmit PCM signals corresponding to the difference in adjacent sample values. This, crudely speaking, is *differential pulse code modulation* (DPCM). At the receiver the present sample value is regenerated by using the past value plus the update differential value that is received over the differential system.

Moreover, the present value can be estimated from the past values by using a *prediction filter*. The filter may be realized by using a tapped delay line (bucket brigade device) to form a *transversal filter*, as shown in Fig. 3-28. When the tap gains  $\{a_l\}$  are set so that the filter output will predict the present value from past values, the filter is said to be a *linear prediction filter* [Spilker, 1977]. The optimum tap gains are a function of the correlation properties of the audio or video signal [Jayant and Noll, 1984]. The output samples are

$$z(nT_s) = \sum_{l=1}^K a_l y(nT_s - lT_s) \quad (3-79a)$$

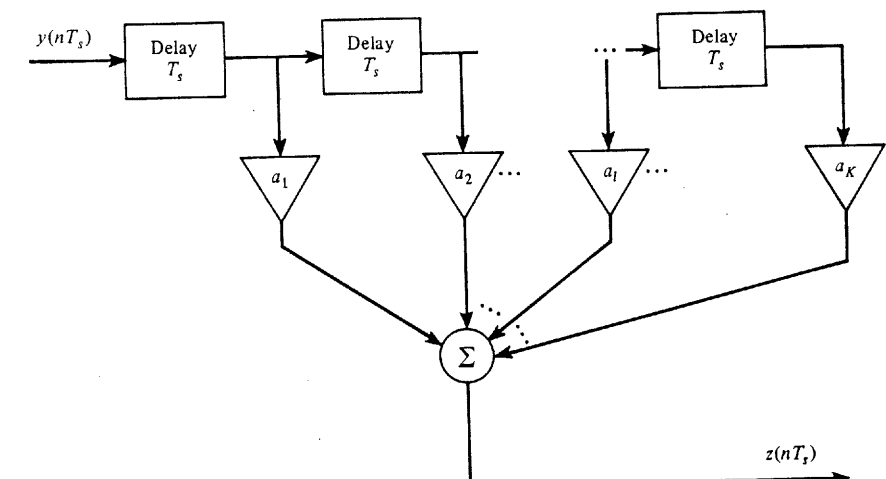


Figure 3-28 Transversal filter.

or, in simplified notation,

$$z_n = \sum_{l=1}^K a_l y_{n-l} \quad (3-79b)$$

where  $y_{n-l}$  denotes the sample value at the filter input at time  $t = (n - l)T_s$  and there are  $K$  delay devices in the transversal filter.

The linear prediction filter may be used in a differential configuration to produce DPCM. Two possible configurations will be examined.

The first DPCM configuration, shown in Fig. 3-29, uses the predictor to obtain a differential pulse amplitude modulated (DPAM) signal that is quantized and encoded to produce the DPCM signal. The recovered analog signal at the receiver output will be the same as that at the system input plus *accumulated* quantizing noise. We may eliminate the accumulation effect by using the transmitter configuration of Fig. 3-30.

In the second DPCM configuration shown in Fig. 3-30, the predictor operates on quantized values at the transmitter as well as at the receiver in order to minimize the quantization noise on the recovered analog signal. The analog output at the receiver is the same as the input analog signal at the transmitter except for quantizing noise; furthermore, the quantizing noise does not accumulate, as was the case in the first configuration.

It can be shown that DPCM, like PCM, follows the 6-dB rule [Jayant and Noll, 1984]

$$\left(\frac{S}{N}\right)_{\text{dB}} = 6.02n + \alpha \quad (3-80a)$$

where

$$-3 < \alpha < 15 \quad \text{for DPCM speech} \quad (3-80b)$$

and  $n$  is the number of quantizing bits ( $M = 2^n$ ). Unlike companded PCM, the  $\alpha$  for DPCM varies over a wide range depending on the properties of the input analog signal. Equation (3-80b) gives the range of  $\alpha$  for voice-frequency (300 to 3400 Hz) telephone-quality speech. This DPCM performance may be compared to that for PCM. Equation (3-26b) indicates that  $\alpha = -10$  dB for  $\mu$ -law companded PCM with  $\mu = 255$ . Thus there may be a SNR improvement as large as 25 dB when DPCM is used instead of  $\mu = 255$  PCM. Alternatively, for the same SNR, DPCM could require 3 or 4 fewer bits per sample than companded PCM. This is why telephone DPCM systems often operate at a bit rate of  $R = 32$  kbit/s or  $R = 24$  kbit/s instead of the standard 64 kbit/s as needed for companded PCM.

The CCITT has adopted a 32-kbit/s DPCM standard that uses 4-bit quantization at an 8-ksample/s rate for encoding 3.2-kHz bandwidth VF signals [Decina and Modena, 1988]. Moreover, a 64-kbit/s DPCM CCITT standard (4-bit quantization and 16 ksamples/s) has been adopted for encoding audio signals that have a 7-kHz bandwidth. A detailed analysis of DPCM systems is difficult and depends on the type of input signal present, the sample rate, the number of quantizing levels used, the number of stages in the prediction filter, and the predictor gain coefficients. This type of analysis is beyond the scope of this text, but for further study the reader is referred to published work on this topic [Flanagan et al., 1979; Jayant, 1974; Jayant and Noll, 1984; O'Neal, 1966b].

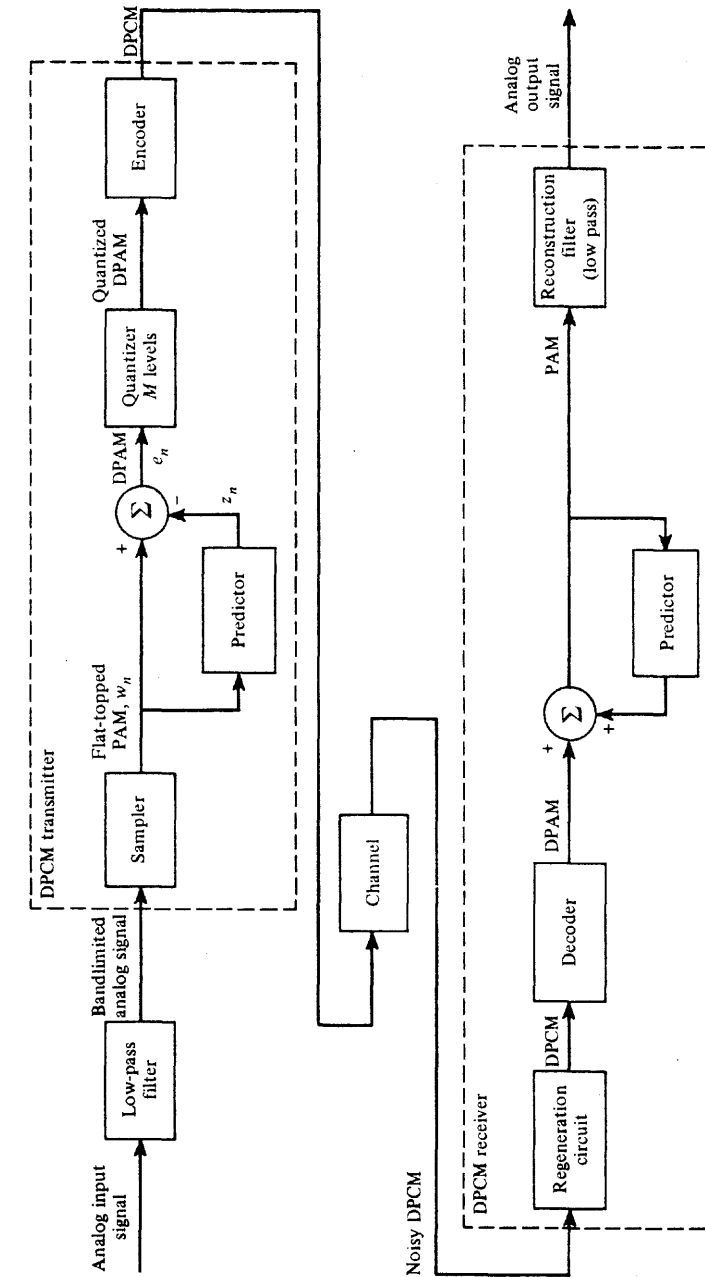


Figure 3-29 DPCM using prediction from samples of input signal.

### 3-8 DELTA MODULATION

From a block diagram point of view, *delta modulation* (DM) is a special case of DPCM where there are two quantizing levels. As shown in Fig. 3-30, for the case of  $M = 2$ , the quantized DPAM signal is *binary* and the encoder is not needed because the function of the encoder is to convert the multilevel DPAM signal to binary code words. For the case of  $M = 2$ , the DPAM signal is a DPCM signal where the code words are one bit long. The cost of a DM system is less than that of a DPCM system ( $M > 2$ ) because the analog-to-digital converter (ADC) and digital-to-analog converter (DAC) are not needed. This is the main attraction of the DM scheme—it is relatively inexpensive. In fact, the cost may be further reduced by replacing the predictor by a low-cost integration circuit (such as an RC low-pass filter), as shown in Fig. 3-31.

In the DM circuit shown in Fig. 3-31, the operations of the subtractor and two-level quantizer are implemented by using a comparator so that the output is  $\pm V_c$  (binary). In this case the DM signal is a polar signal. A set of waveforms associated with the delta modulator is shown in Fig. 3-32. In Fig. 3-32a an assumed analog input waveform is illustrated. If the instantaneous samples of the flat-topped PAM signal are taken at the beginning of each sampling period, the corresponding accumulator output signal is shown.<sup>†</sup> Here the integra-

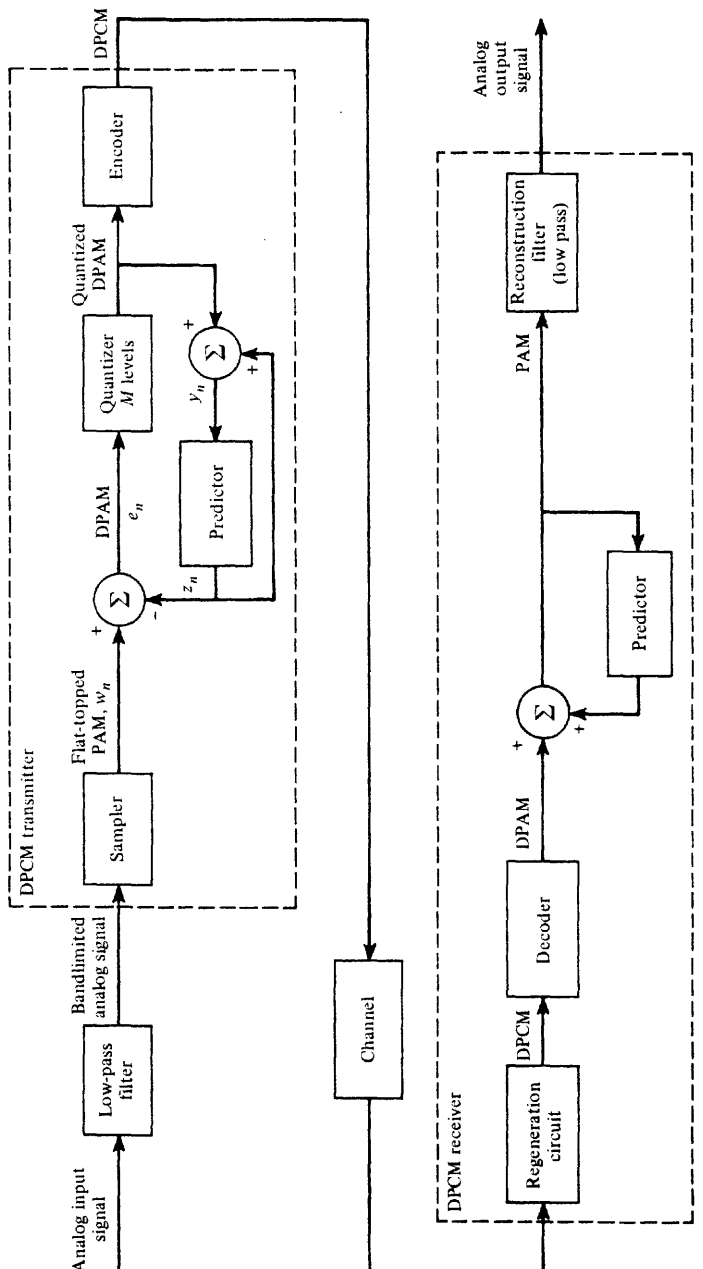


Figure 3-30 DPCM using prediction from quantized differential signal.

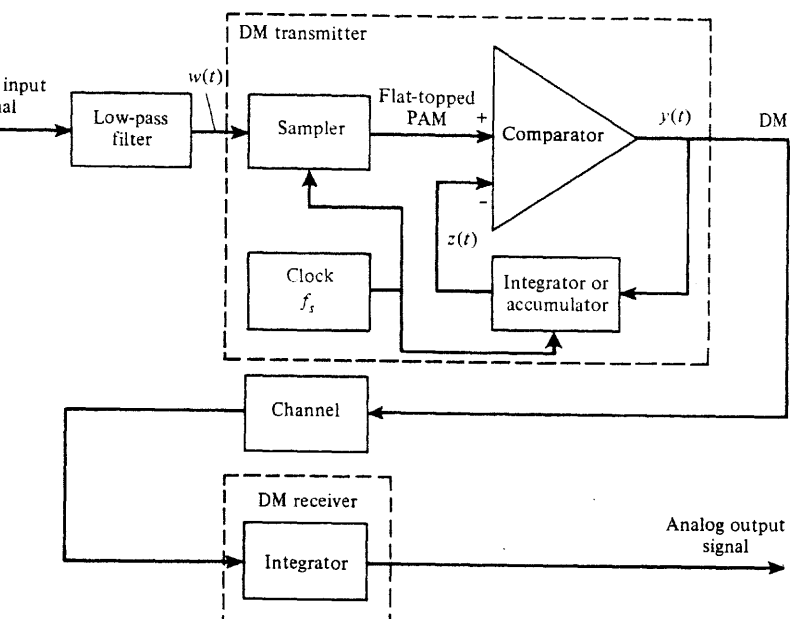
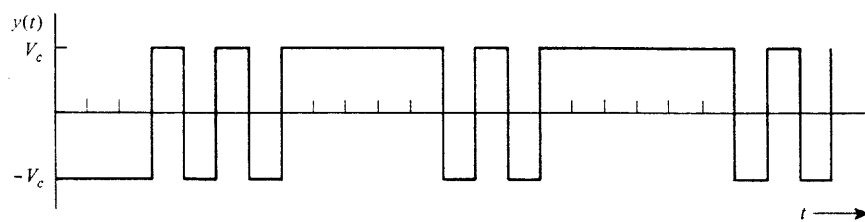
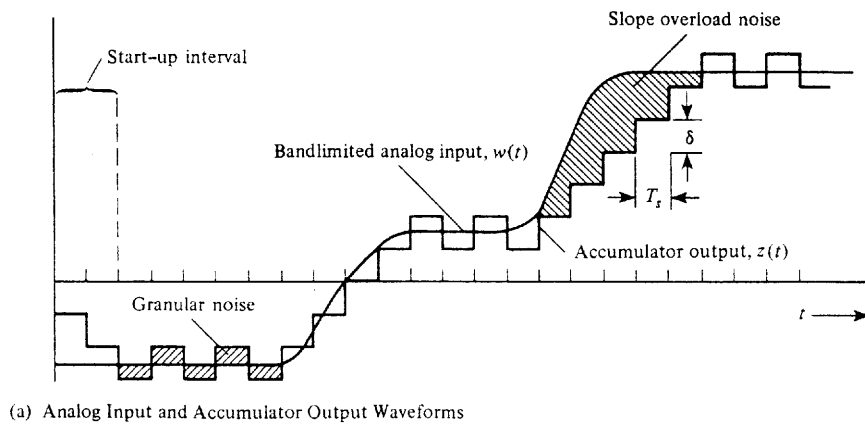


Figure 3-31 DM system.

<sup>†</sup> The sampling frequency,  $f_s = 1/T_s$ , is selected to be within the range  $2B_{in} < f_s < 2B_{channel}$ , where  $B_{in}$  is the bandwidth of the input analog signal and  $B_{channel}$  is the bandwidth of the channel. The lower limit prevents aliasing of the analog signal and the upper limit prevents ISI in the DM signal at the receiver. See Example 3-5 for further restrictions on the selection of  $f_s$ .



**Figure 3-32** DM system waveforms.

tor is assumed to act as an accumulator (such as integrating impulses) so that the integrator output at time  $t = nT_s$  is given by

$$z_n = \frac{1}{V_c} \sum_{i=0}^n \delta y_i \quad (3-81)$$

where  $y_i = y(iT_s)$  and  $\delta$  is the accumulator gain or step size. The corresponding DM output waveform is shown in Fig. 3-32b.

At the receiver the DM signal may be converted back to an analog signal approximation to the analog signal at the system input. This is accomplished by using an integrator for the receiver that produces a smoothed waveform corresponding to a smoothed version of the accumulator output waveform that is present in the transmitter (Fig. 3-32a).

### Granular Noise and Slope Overload Noise

From Fig. 3-32a it is seen that the accumulator output signal does not always track the analog input signal. The quantizing noise error signal may be classified into two types of noise—*slope overload noise* and *granular noise*. Slope overload noise occurs when the step size  $\delta$  is too small for the accumulator output to follow quick changes in the input waveform. Granular noise occurs for any step size but is smaller for a small step size. Thus we would like to have  $\delta$  as small as possible to minimize the granular noise. The granular noise in a DM system is similar to the granular noise in a PCM system, whereas slope overload noise

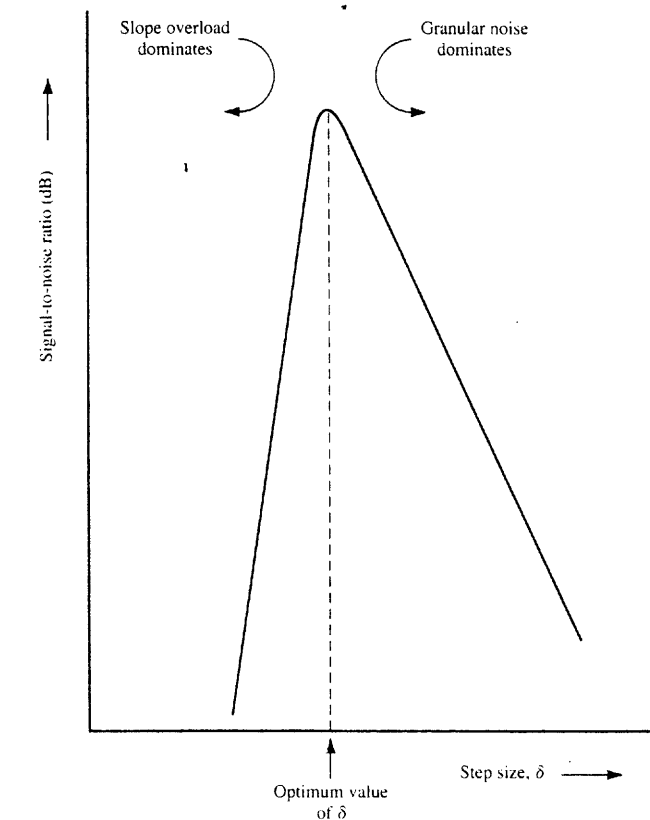


**Figure 3-33** Signal-to-noise out of a DM system as a function of step size.

is a new phenomenon due to a differential signal being encoded (instead of the original signal itself). Both phenomena are also present in the DPCM system discussed earlier.

It is clear that there should be an optimum value for the step size,  $\delta$ , because if  $\delta$  is increased, the granular noise will increase but the slope overload noise will decrease. This is illustrated in Fig. 3-33.

### Example 3-5 DESIGN OF A DM SYSTEM

Find the step size  $\delta$  required to prevent slope overload noise for the case when the input signal is a sine wave.

The maximum slope that can be generated by the accumulator output is

$$\frac{\delta}{T_s} = \delta f_s \quad (3-82)$$

For the case of the sine-wave input where  $w(t) = A \sin \omega_a t$ , the slope is

$$\frac{dw(t)}{dt} = A\omega_a \cos \omega_a t \quad (3-83)$$

and the maximum slope of the input signal is  $A\omega_a$ . Consequently, for no slope overload we require that  $\delta f_s > A\omega_a$ , or

$$\delta > \frac{2\pi f_a A}{f_s} \quad (3-84)$$

However, we do not want to make  $\delta$  too much larger than this value or the granular noise will become too large.

The resulting detected signal-to-noise ratio can also be calculated. It has been determined experimentally that the spectrum of the granular noise is uniformly distributed over the frequency band  $|f| \leq f_s$ . It can also be shown that the total granular quantizing noise is  $\delta^2/3$  (see Sec. 7-7, where  $\delta/2$  of PCM is replaced by  $\delta$  for DM). Thus the PSD for the noise is  $\mathcal{P}_n(f) = \delta^2/(6f_s)$ . The granular noise power in the analog signal band,  $|f| \leq B$ , is

$$N = \langle n^2 \rangle = \int_{-B}^B \mathcal{P}_n(f) df = \frac{\delta^2 B}{3f_s} \quad (3-85)$$

or, using (3-84), with equality

$$N = \frac{4\pi^2 A^2 f_a^2 B}{3f_s^3}$$

The signal power is

$$S = \langle w^2(t) \rangle = \frac{A^2}{2} \quad (3-86)$$

The resulting average signal to quantizing noise ratio out of a DM system with a sine-wave test signal is

$$\left( \frac{S}{N} \right)_{\text{out}} = \frac{3}{8\pi^2} \frac{f_s^3}{f_a^2 B} \quad (3-87)$$

where  $f_s$  is the DM sampling frequency,  $f_a$  is the frequency of the sinusoidal input, and  $B$  is the bandwidth of the receiving system. It is emphasized that (3-87) was shown to be valid only for sinusoidal-type signals.

For voice-frequency (VF) audio signals, it has been shown that (3-84) is too restrictive if  $f_a = 4$  kHz and that slope overload is negligible if [deJager, 1952]

$$\delta \geq \frac{2\pi 800 W_p}{f_s} \quad (3-88)$$

where  $W_p$  is the peak value of the input audio waveform,  $w(t)$ . (This is due to the fact that the midrange frequencies around 800 Hz dominate in the VF signal.) Combining (3-88) and (3-85), we obtain the S/N for the DM system with a VF-type signal

$$\left( \frac{S}{N} \right)_{\text{out}} = \frac{\langle w^2(t) \rangle}{N} = \frac{3f_s^3}{(1600\pi)^2 B} \left( \frac{\langle w^2(t) \rangle}{W_p^2} \right) \quad (3-89)$$

where  $B$  is the audio bandwidth and  $(\langle w^2(t) \rangle / W_p^2)$  is the average-audio-power to peak-audio-power ratio.

This result can be used to design a VF DM system. For example, suppose that we desire an SNR of at least 30 dB. Assume that the VF bandwidth is 4 kHz and the average-to-peak audio power is  $\frac{1}{2}$ . Then (3-89) gives a required sampling frequency of 40.7 kbits/s or  $f_s = 10.2B$ . It is also interesting to compare this DM system with a PCM system that has the same bandwidth (i.e., bit rate). The number of bits,  $n$ , required for each PCM word is determined by  $R = (2B)n = 10.2B$  or  $n \approx 5$ . Then the average-signal to quantizing-noise ratio of the comparable PCM system is 30.1 dB (see Table 3-5). Thus, under these conditions, the PCM system with a comparable bandwidth has about the same SNR performance as the DM system. Furthermore, repeating the preceding procedure, it can be shown that if an SNR larger than 30 dB was desired, the PCM system would have a larger SNR than that of a DM system with comparable bandwidth; on the other hand, if an SNR less than 30 dB was sufficient, the DM system would outperform (i.e., have a larger SNR than) the PCM system of the same bandwidth. Note that the SNR for DM increases as  $f_s^3$  or 9 dB per octave increase of  $f_s$ .

It is also possible to improve the SNR performance of a DM system by using double integration instead of single integration, as was studied here. With a double integration system the SNR increases as  $f_s^5$  or 15 dB per octave [Jayant and Noll, 1984].

### Adaptive Delta Modulation and Continuously Variable Slope Delta Modulation

To minimize the slope overload noise while holding the granular noise at a reasonable value, *adaptive delta modulation* (ADM) is used. Here the step size is varied as a function of time as the input waveform changes. The step size is kept small to minimize the granular noise until the slope overload noise begins to dominate. Then the step size is increased to reduce the slope overload noise. The step size may be adapted, for example, by examining the DM pulses at the transmitter output. When the DM pulses consist of a string of pulses with positive polarity, the step size is increased (see Fig. 3-32) until the DM pulses begin to alternate in polarity, then decreased, and so on. One possible algorithm for varying the step size is shown in Table 3-7, where the step size changes with discrete variation. Here the step size is normally set to a value  $\delta$  when the ADM signal consists of data with alternating 1s and 0s or when two successive binary 1s occur. However, if three successive binary 1s occur, the step size is increased to  $2\delta$ , and  $4\delta$  for four successive binary 1s. Figure 3-34 gives a block diagram for this ADM system.

Papers have been published with demonstration records that illustrate the quality of ADM and other digital techniques when voice signals are sent over digital systems and recovered [Flanagan et al., 1979; Jayant, 1974]. Another variation of ADM is *continuously*

TABLE 3-7 STEP-SIZE ALGORITHM

Data Sequence <sup>a</sup>				Number of Successive Binary 1s or 0s	Step-Size Algorithm, $f(d)$
X	X	0	1	1	$\delta$
X	0	1	1	2	$\delta$
0	1	1	1	3	$2\delta$
1	1	1	1	4	$4\delta$

<sup>a</sup> X, do not care.

variable slope delta modulation (CVSD). Here the step size is made continuously variable instead of stepped in discrete increments.

The Motorola MC3417 is a CVSD integrated circuit which varies the slope (step size) as a function of the last three bits of the encoded data sequence; the MC3418 has a similar 4-bit algorithm [Motorola, 1985]. Both of these CVSD codec chips can be connected either as modulators (encoders) or as demodulators (decoders) and may be operated with bit rates ranging from 9.4 to 64 kbit/s. A better SNR is obtained at the decoder output if a higher bit rate is used. For example, if MC3417 codecs are used for encoding and decoding in a 16-kbit/s CVSD system, the SNR at the output will be 16 dB. This is called "communication quality." If MC3418s are used in a 37.7-kbit/s system, the output SNR will be 30 dB. This performance is similar to that obtained for the DM and PCM systems discussed after equation (3-89).

The question might be asked: Which is better, PCM or DM? The answer, of course, depends on the criterion used for comparison and the type of message. If the objective is to have a relatively simple, low-cost system, delta modulation may be the best. However, the cost of ADCs is dropping, so this may not be a factor. If high output SNR is the criterion, PCM is probably the best [O'Neal, 1966a]. If one is interfacing to existing equipment, compatibility would be a prime consideration. In this regard, PCM has the advantage because it was adopted first and is widely used.

### Speech Coding

Digital speech coders can be classified into two categories: waveform coders and vocoders. *Waveform coders* use algorithms to encode and decode so that the system output is an approximation to the input waveform. *Vocoders* encode the speech by extracting a set of parameters. These parameters are digitized and transmitted to the receiver where they are used to set values for parameters in function generators and filters which, in turn, synthesize the output speech sound. Usually, the vocoder output waveform does not approximate the input waveform and has an artificial, unnatural sound. Although the words of the speaker may be clearly understandable, the speaker may not be identifiable. That is, the speaker may "sound like a robot." For this reason and because of space limitations, only waveform encoders (e.g., PCM, DPCM, DM, and CVSD) are covered in this book. It was demonstrated that VF-quality speech may be encoded at bit rates as low as 24 kbit/s. More advanced techniques reduce the required bit rate to 8 kbit/s, and researchers believe that speech coding may be

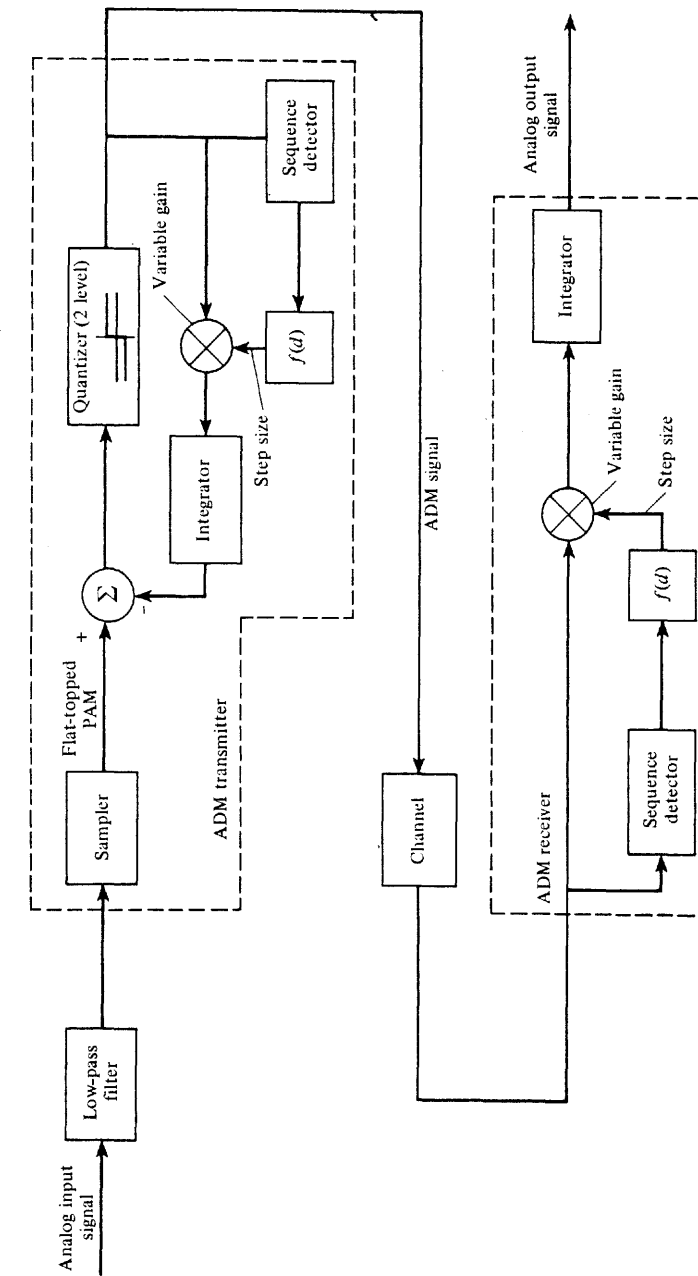


Figure 3-34 ADM system

possible even at 2 kbit/s. Some techniques that are available to achieve waveform coders at low bit rates are: linear prediction (already discussed as applied to DPCM), adaptive subband coding, and vector quantization. Adaptive subband coding allocates bits according to the input speech spectrum and the properties of hearing. With vector quantization, whole blocks of samples are encoded at a time instead of encoding on a sample-by-sample basis. An example is the vector sum excited linear prediction filter (VSELF) technique that is proposed for use in digital cellular telephones and described at the end of Sec. 8-8. Of course, these advanced techniques require more complex circuits and a larger delay while the output is being computed. For more details about this interesting topic of speech coders, the reader is referred to the literature [Aoyama, Daumer, and Modena, 1988; Flanagan et al., 1979; Jayant, 1986; Spanias, 1994].

### 3-9 TIME-DIVISION MULTIPLEXING<sup>†</sup>

**DEFINITION.** *Time-division multiplexing (TDM)* is the time interleaving of samples from several sources so that the information from these sources can be transmitted serially over a single communication channel.

Figure 3-35 illustrates the TDM concept as applied to three analog sources that are multiplexed over a PCM system. For convenience, natural sampling is shown together with the corresponding gated TDM PAM waveform. In practice, an electronic switch is used for the commutation (sampler). In this example the pulse width of the TDM PAM signal is  $T_s/3 = 1/(3f_s)$ , and the pulse width of the TDM PCM signal is  $T_s/(3n)$ , where  $n$  is the number of bits used in the PCM word. Here  $f_s = 1/T_s$  denotes the frequency of rotation for the commutator, and  $f_s$  satisfies the Nyquist rate for the analog source with the largest bandwidth. In some applications where the bandwidth of the sources is markedly different, the larger bandwidth sources may be connected to several switch positions on the sampler so that they will be sampled more often than the smaller bandwidth sources.

At the receiver the decommutator (sampler) has to be synchronized with the incoming waveform so that the PAM samples corresponding to source 1, for example, will appear on the channel 1 output. This is called frame synchronization. Low-pass filters are used to reconstruct the analog signals from the PAM samples. ISI resulting from poor channel filtering would cause PCM samples from one channel to appear on another channel, even though perfect bit and frame synchronization were maintained. This feedthrough of one channel's signal into another channel is called *crosstalk*.

#### Frame Synchronization

*Frame synchronization* is needed at the TDM receiver so that the received multiplexed data can be sorted and directed to the appropriate output channel. The frame sync can be provided to the receiver demultiplexer (demux) circuit either by sending a frame sync signal from the transmitter over a separate channel or by deriving the frame sync from the TDM

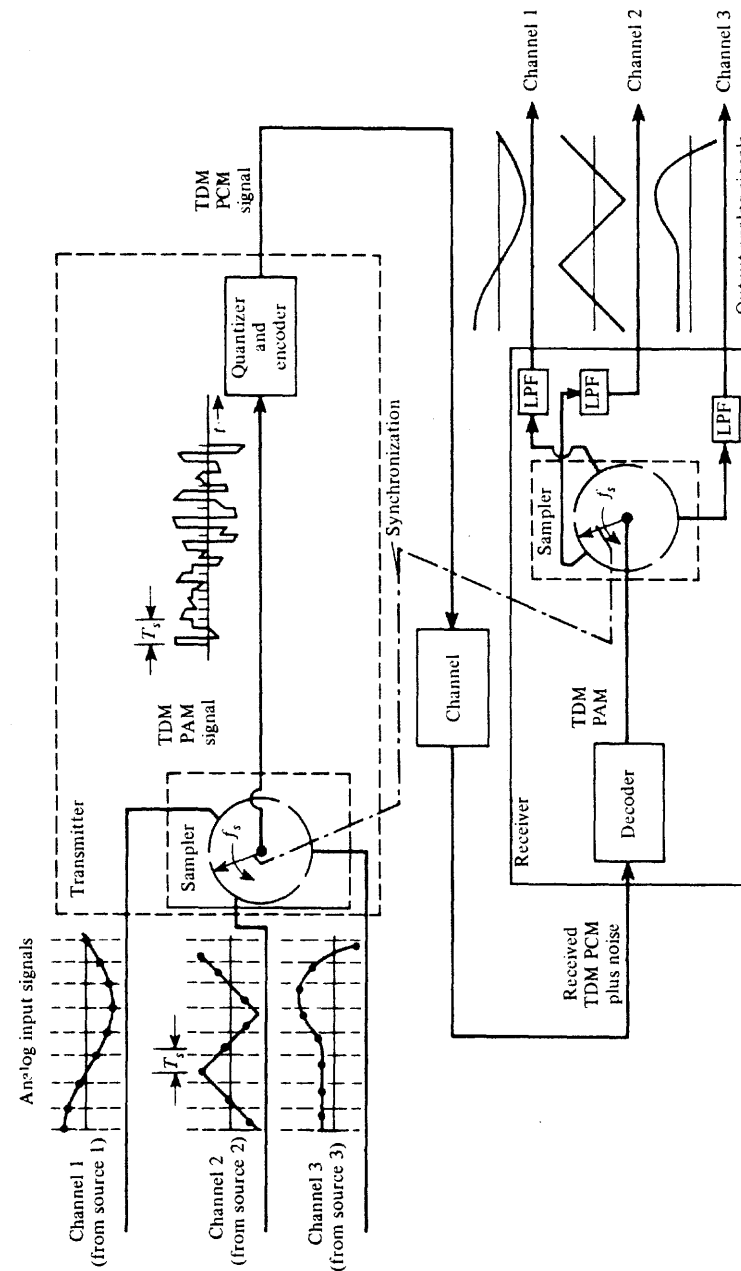


Figure 3-35 Three-channel TDM PCM system.

<sup>†</sup> This is a method in which a common channel or system is shared by many users. Other methods for sharing a common communication system are discussed under the topic of multiple access techniques in Sec. 8-5.

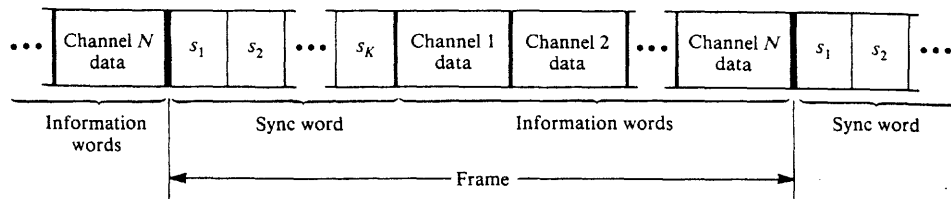


Figure 3-36 TDM frame sync format.

signal itself. Because the implementation of the first approach is obvious, we will concentrate on implementation of the latter approach. In addition, the latter approach is usually more economical since a separate sync channel is not needed. As illustrated in Fig. 3-36, frame sync may be multiplexed along with the information words in an  $N$  channel TDM system by transmitting a unique  $K$ -bit sync word at the beginning of each frame. As illustrated in Fig. 3-37, the frame sync is recovered from the corrupted TDM signal by using a frame synchronizer circuit which crosscorrelates the regenerated TDM signal with the expected unique sync word  $s = (s_1, s_2, \dots, s_K)$ . The elements of the unique sync word vector  $s$ , denoted by  $s_1, s_2, \dots, s_j, \dots, s_k$ , are binary 1s or 0s (which, for TTL logic would represent +5V or 0 V, respectively). The present bit of the regenerated TDM signal is clocked into the first stage of the shift register and then shifted to the next stage on the next clock pulse so that the most immediate  $K$  bits are always stored in the shift register. The  $s_j$ s within the triangles below the shift register denote the presence or absence of an inverter. That is, if the  $s_j$  is a binary 0, then there is an inverter in the  $j$ th leg. If  $s_j$  is a binary 1, there is no inverter. The coincident detector is a  $K$  input AND gate.

If the unique sync word happens to be present in the shift register, all the inputs to the coincident detector will be binary 1s and the output of the coincident detector will be a binary 1 (i.e., a high level). Otherwise, the output of the coincident detector is a binary 0 (i.e., a low level). Consequently, the coincident detector output will go high only during the  $T_b$ -s interval when the sync word is perfectly aligned in the shift register. Thus the frame synchronizer recovers the frame sync signal.

False sync output pulses will occur if  $K$  successive information bits happen to match the bits in the sync word. For equally likely TDM data the probability of this false sync occurring is equal to the probability of obtaining the unique sync word. This is

$$P_f = \left(\frac{1}{2}\right)^K = 2^{-K} \quad (3-90)$$

In frame synchronizer design, this equation may be used to determine the number of bits,  $K$ , needed in the sync word so that the false lock probability will meet specifications. Alternatively, more sophisticated techniques such as aperture windows can be used to suppress false lock pulses [Ha, 1986]. The information words may also be encoded so that they are not allowed to have the bit strings that match the unique sync word.

Since the output of the coincident detector is a digitized crosscorrelation of the sync word with the passing  $K$ -bit word stored in the shift register, the sync word needs to be chosen so that its autocorrelation function,  $R_s(k)$ , has the desirable properties:  $R_s(0) = 1$  and

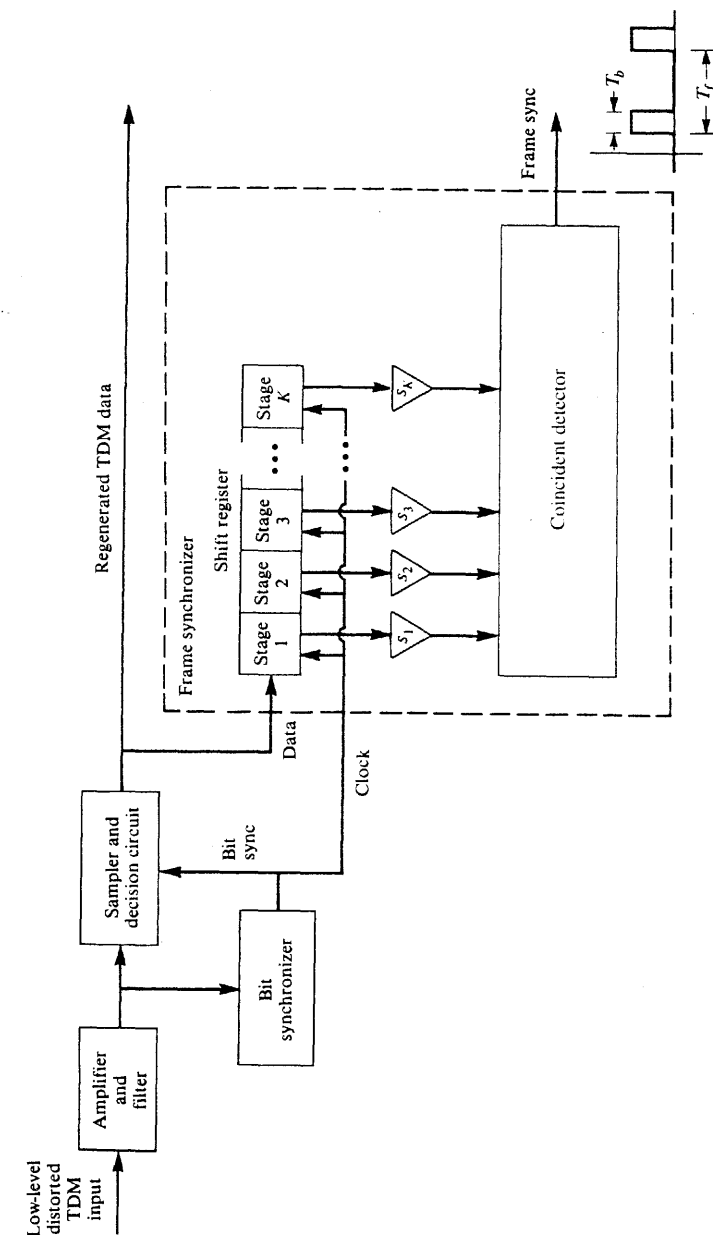


Figure 3-37 Frame synchronizer with TDM receiver front end.

$R(k) \approx 0$  for  $k \neq 0$ . The PN codes (studied in Sec. 5-12) are almost ideal in this regard. For example, if  $P_f = 4 \times 10^{-5}$  is the allowed probability of false sync, then from (3-90) a ( $K = 15$ )-bit sync word is required. Consequently, a 15-stage shift register is needed for the frame synchronizer in the receiver. The 15-bit PN sync word can be generated at the transmitter using a four-stage shift register. For further study of frame synchronizers the reader is referred to Ziemer and Peterson [1985] and Ha [1986].

### Synchronous and Asynchronous Lines

For bit sync, data transmission systems are designed to operate with either synchronous or asynchronous serial data lines. In a *synchronous* system, each device is designed so that its internal clock is relatively stable for a long period of time, and it is synchronized to a system master clock. Each bit of data is clocked in synchronization with the master clock. The synchronizing signal may be provided by a separate clocking line or may be embedded in the data signal (e.g., by the use of Manchester line codes). In addition, synchronous transmission requires a higher level of synchronization to allow the receiver to determine the beginning and end of blocks of data. This is achieved by the use of frame sync as discussed previously and data link protocols as described in Appendix C.

In *asynchronous* systems, the timing is precise only for the bits within each character (or word). This is also called *start-stop* signaling because each character consists of a “start bit” that starts the receiver clock and concludes with one or two “stop bits” that terminate the clocking. Usually, two stop bits are used with terminals that signal at rates less than 300 bits/s, and one stop bit is used if  $R \geq 300$  bits/s. Thus, with asynchronous lines, the receiver clock is started aperiodically and no synchronization with a master clock is required. This is ideal for keyboard terminals where the typist does not type at an even pace and the input rate is much slower than that of the data communication system. These asynchronous terminals often use a 7-bit ASCII code (see Appendix C), and the complete character consists of one start bit, 7 bits of the ASCII code, one parity bit, and one stop bit (for  $R \geq 300$  bits/s). This gives a total character length of 10 bits. In TDM of the asynchronous type, the different sources are multiplexed on a *character-interleaved* (i.e., character-by-character) basis instead of interleaving on a bit-by-bit basis. The synchronous transmission system is more efficient because start and stop bits are not required. However, the synchronous mode of transmission requires that the clocking signal be passed along with the data and that the receiver synchronize to the clocking signal.

“Intelligent” TDMs may be used to *concentrate* data arriving from many different terminals or sources. They are capable of providing speed, code, and protocol conversion. At the input to a large mainframe computer, these devices are called *front-end processors*. The hardware in the intelligent TDM consists of microprocessors or minicomputers. Usually, they connect “on the fly” to the input data lines that have data present and momentarily disconnect the lines that do not have data present. For example, the user of a keyboard terminal is disconnected from the system while he or she is thinking (although to the user it does not appear to be disconnected) but is connected as each character or block of data is sent. Thus the output data rate of the multiplexer is much less than the sum of the data capacities of the input lines. This technique is called *statistical* multiplexing; it allows many more terminals to be connected on line to the system.

Multiplexers can also be classified into three general types. The first TDM type consists of those that connect to synchronous lines. The second TDM type consists of those that connect to quasi-synchronous lines. In this case, the individual clocks of the input data sources are not exactly synchronized in frequency. Consequently, there will be some variation in the bit rates between the data arriving from different sources. In addition, in some applications the clock rates of the input data streams are not related by a rational number. In these cases, the TDM output signal will have to be clocked at an increased rate above the nominal value to accommodate those inputs that are not synchronous. When a new input bit is not available at the multiplexer clocking time (due to nonsynchronization), *stuff bits*, which are dummy bits, are inserted in the TDM output data stream. This is illustrated by the bit-interleaved multiplexer shown in Fig. 3-38. The stuff bits may be binary 1s, 0s, or some alternating pattern, depending on the choice of the system designer. The third TDM type consists of those that operate with asynchronous sources and produce a high-speed asynchronous output (no stuff bits required) or high-speed synchronous output (stuff bits required).

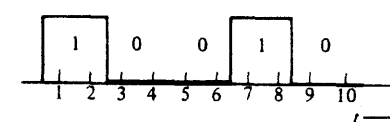
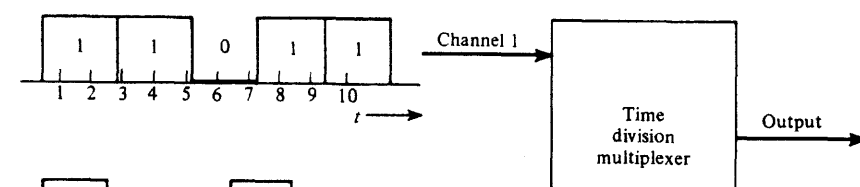
### Example 3-6 DESIGN OF A TIME-DIVISION MULTIPLEXER

Design a time-division multiplexer that will accommodate 11 sources. Assume that the sources have the following specifications.

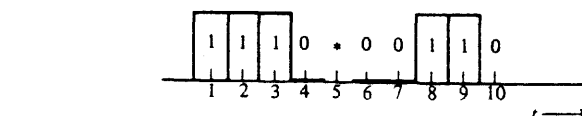
Source 1. Analog, 2-kHz bandwidth.

Source 2. Analog, 4-kHz bandwidth.

Digital input signals



Output TDM Signal



Input channel number → 1 2 1 2 1 2 1 2 1 2  
\* = stuffed bit

Figure 3-38 Two-channel bit-interleaved TDM with pulse stuffing.

Source 3. Analog, 2-kHz bandwidth.

Sources 4-11. Digital, synchronous at 7200 bits/s.

Also assume that the analog sources will be converted into 4-bit PCM words and, for simplicity, that frame sync will be provided via a separate channel and synchronous TDM lines are used. To satisfy the Nyquist rate for the analog sources, sources 1, 2, and 3 need to be sampled at 4, 8, and 4 kHz, respectively. As shown in Fig. 3-39, this can be accomplished by rotating the first commutator at  $f_1 = 4$  kHz and sampling source 2 twice on each revolution. This produces a 16-kilosamples/s TDM PAM signal on the commutator output. Each of the analog sample values is converted into a 4-bit PCM word, so that the rate of the TDM PCM signal on the ADC output is 64 kbit/s. The digital data on the ADC output may be merged with the data from the digital sources by using a second commutator rotating at  $f_2 = 8$  kHz and wired so that the 64-kbit/s PCM signal is present on 8 of 16 terminals. This provides an effective sampling rate of 64 kbit/s. On the other eight terminals the digital sources are connected to provide a data transfer rate of 8 kbit/s for each source. Since the digital sources are supplying a 7.2-kbit/s data stream, pulse stuffing is used to raise the source rate to 8 kbit/s.

This example illustrates the main advantage of TDM: it can easily accommodate both analog and digital sources. Unfortunately, when analog signals are converted to digital signals without redundancy reduction, they consume a great deal of digital system capacity.

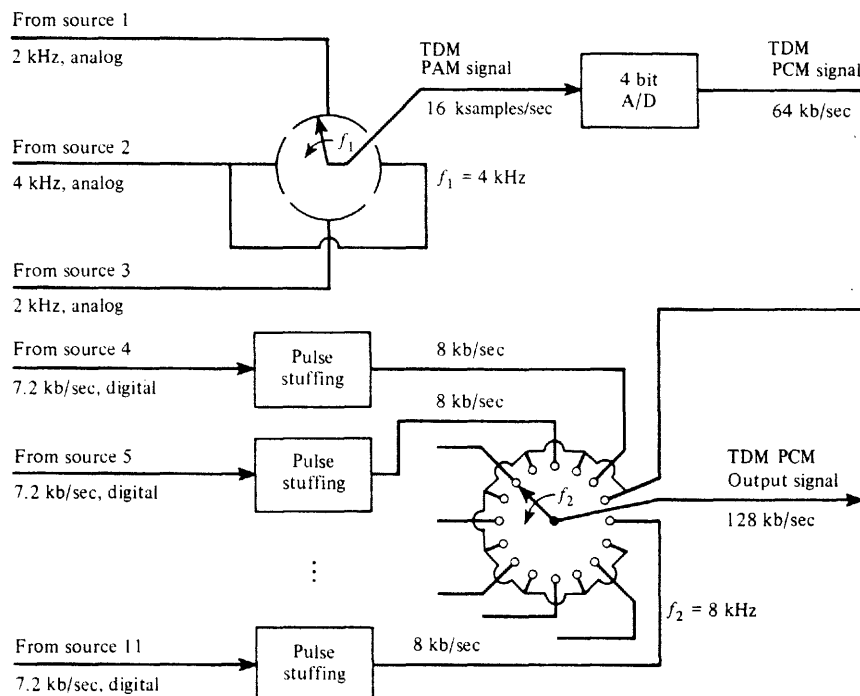


Figure 3-39 TDM with analog and digital inputs as described in Example 3-6.

### TDM Hierarchy

In practice, TDMS may be grouped into two categories. The first category consists of multiplexers used in conjunction with digital computer systems to merge digital signals from several sources for TDM transmission over a high-speed line to a digital computer. The output rate of these multiplexers has been standardized to 1.2, 2.4, 3.6, 4.8, 7.2, 9.6, 14.4, 19.2 and 28.8 kbit/s, and to 10 and 100 Mbit/s.

The second category of time-division multiplexers is used by the common carriers, such as the American Telephone and Telegraph Company (AT&T), to combine different sources into a high-speed digital TDM signal for transmission over toll networks. Unfortunately, the standards adopted by North America and Japan are different from those that have been adopted in other parts of the world. Of course, this leads to complications at the boundaries of two systems with different standards. The North America/Japan standards were first adopted by AT&T, and another set of standards has been adopted by CCITT under the auspices of ITU. The North American TDM hierarchy is shown in Fig. 3-40 [James and Muensch, 1972].<sup>†</sup> The telephone industry has standardized the bit rates to 1.544 Mbit/s, 6.312 Mbit/s, etc., and designates them as DS-1 for digital signal, type 1; DS-2 for digital signal, type 2; etc. as listed in Table 3-8. In Fig. 3-40 all input lines are assumed to be digital (binary) streams, and the number of voice-frequency (VF) analog signals that can be represented by these digital signals is shown in parentheses. The higher multiplexing level inputs are not always derived from lower level multiplexers. For example, one analog television signal can be converted directly to a DS-3 data stream (44.73 Mbit/s). Similarly, the DS streams can carry a mixture of information from a variety of sources such as video, VF, and computers.

The transmission medium that is used for the multiplex levels depends on the DS level involved and on the economics of using a particular type of medium at a particular location (Table 3-8). For example, higher DS levels may be transmitted over coaxial cables, fiber optic cable, microwave radio, or via satellite. A single DS-1 signal is usually transmitted over one pair of twisted wires. (One pair is used for each direction.) This type of DS-1 transmission over a twisted-pair medium is known (from its development in 1962 by AT&T) as the *T1 carrier system*. DS-1 signaling over a T1 system is very popular because of its relatively low cost and its excellent maintenance record. (T1 will be discussed in more detail in the following section.) Table 3-9 shows the specifications for the T-carrier digital baseband systems. Table 8-2 is a similar table for the capacity of common carrier bandpass systems. The corresponding CCITT TDM standard that is used throughout the world except for North America and Japan<sup>†</sup> is shown in Fig. 3-41 [Irmer, 1975].

With the development of high-bit-rate fiber optic systems, it has become apparent that the original TDM standards are not adequate. A new TDM standard called SONET (Synchronous Optical Network) was proposed by Bellcore (Bell Communications Research) around 1985 and has evolved into an international standard that was adopted by the CCITT in 1989. This SONET standard is shown in Table 3-10. The OC-1 signal is an optical (light) signal that is turned on and off (modulated) by an electrical binary signal that has a line rate

<sup>†</sup> The Japanese TDM hierarchy is the same as that for North America for multiplex levels 1 and 2, but differs for levels 3, 4, and 5. For level 3 the Japanese standard is 32.064 Mbit/s (480 VF), level 4 is 97.728 Mbit/s (1440 VF), and level 5 is 397.200 Mbit/s (5760 VF). Dissimilarities between standards used are briefly discussed and summarized by Jacobs [1986].

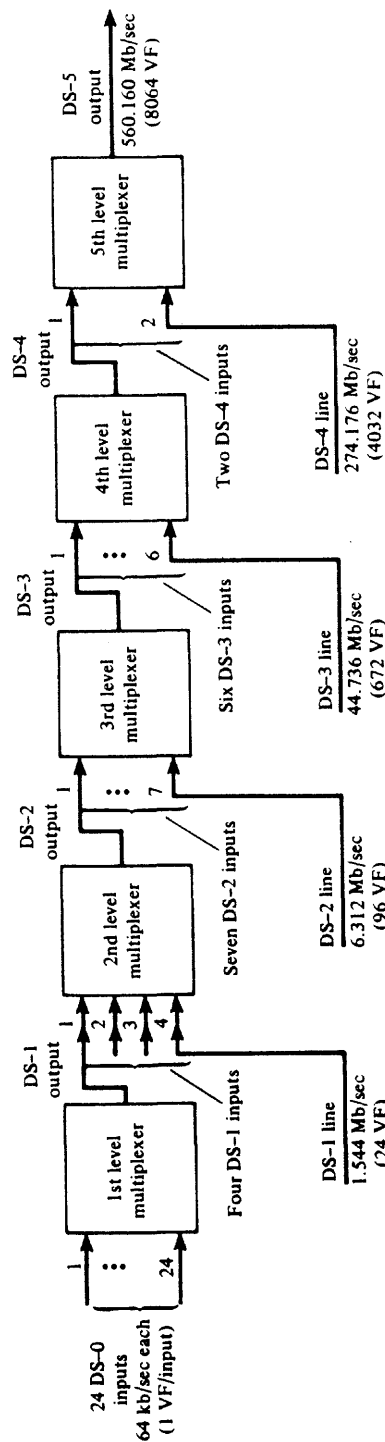


Figure 3-40 North American digital TDM hierarchy.

TABLE 3-8 TDM STANDARDS FOR NORTH AMERICA

Digital Signal Number	Bit Rate, $R$ (Mbits/sec)	No. of 64 kbits/sec PCM VF Channels	Transmission Media Used
DS-0	0.064	1	Wire pairs
DS-1	1.544	24	Wire pairs
DS-1C	3.152	48	Wire pairs
DS-2	6.312	96	Wire pairs, fiber
DS-3	44.736	672	Coax., radio, fiber
DS-3C	90.254	1344	Radio, fiber
DS-4E	139.264	2016	Radio, fiber, coax.
DS-4	274.176	4032	Coax., fiber
DS-432	432.00	6048	Fiber
DS-5	560.160	8064	Coax., fiber

of 51.84 Mbits/s. The electrical signal is called the STS-1 signal (Synchronous Transport Signal—level 1). Other OC-N signals have line rates of exactly  $N$  times the OC-1 rate and are formed by modulating a light signal with a STS-N electrical signal. The STS-N signal is obtained by byte-interleaving (scrambling)  $N$  STS-1 signals. (More details about fiber optic systems are given in Sec. 8-7.)

The telephone industry is moving toward an all-digital network that integrates voice and data over a single telephone line from each user to the telephone company equipment. This approach is called the *integrated service digital network* (ISDN). The standard implementation of *basic rate* ISDN service uses an overall data rate of 144 kbits/s which is broken down into two B channels (64 kbits/s each) and one D channel (16 kbits/s). The two B channels carry PCM-encoded telephone conversations or data and the D channel is used for signaling to set up calls, disconnect calls, and route data for the B channels [Pandhi, 1987]. Basic rate ISDN is also called *narrowband ISDN* (N-ISDN). The *primary rate* ISDN service is in the development stage, but one implementation has an aggregate data rate of 1536 kbits/s and consists of twenty-three 64-kbit/s B channels and one 64-kbit/s D channel. Primary rate ISDN is also called *broadband ISDN* (B-ISDN). A more detailed discussion of ISDN is given in Sec. 8-3 since material covered in the intervening chapters is useful for a better understanding of ISDN and its applications.

### The T1 PCM System

For telephone voice service the first-level TDM multiplexer in Fig. 3-40 is replaced by a TDM PCM system, which will convert 24-VF analog telephone signals to a DS-1 (1.544

TABLE 3-9 SPECIFICATIONS FOR T-CARRIER BASEBAND DIGITAL TRANSMISSION SYSTEMS

System	Rate (Mbits/s)	System Capacity			Medium	Line Code	Repeater Spacing (miles)	Maximum System Length (miles)	System Error Rate
		Digital Signal No.	Voice Channels	TV					
T1	1.544	DS-1	24	—	Wire pair	Bipolar RZ	1	50	$10^{-6}$
T1C	3.152	DS-1C	48	—	Wire pair	Bipolar RZ	1	—	$10^{-6}$
T1D	3.152	DS-1C	48	—	Wire pair	Duobinary NRZ	1	—	$10^{-6}$
T1G	6.443	DS-2	96	—	Wire pair	4-level NRZ	1	200	$10^{-6}$
T2	6.312	DS-2	96	—	Wire pair <sup>a</sup>	B6ZS <sup>b</sup> RZ	2.3	500	$10^{-7}$
T3	44.736	DS-3	672	1	Coax.	B3ZS <sup>b</sup> RZ	c	c	c
T4	274.176	DS-4	4032	6	Coax.	Polar NRZ	1	500	$10^{-6}$
T5	560.160	DS-5	8064	12	Coax.	Polar NRZ	1	500	$4 \times 10^{-7}$

<sup>a</sup> Special two-wire cable is required for 12,000-ft repeater spacing. Because T2 cannot use standard exchange cables, it is not as popular as T1.

<sup>b</sup> BnZS denotes *binary n-zero substitution*, where a string of *n* zeros in the bipolar line code is replaced with a special three-level code word so that synchronization can be maintained [Fike and Friend, 1984; Bic, Dupontel, and Imbeaux, 1991].

<sup>c</sup> Used in central telephone office for building multiplex levels; not used for transmission from office to office.

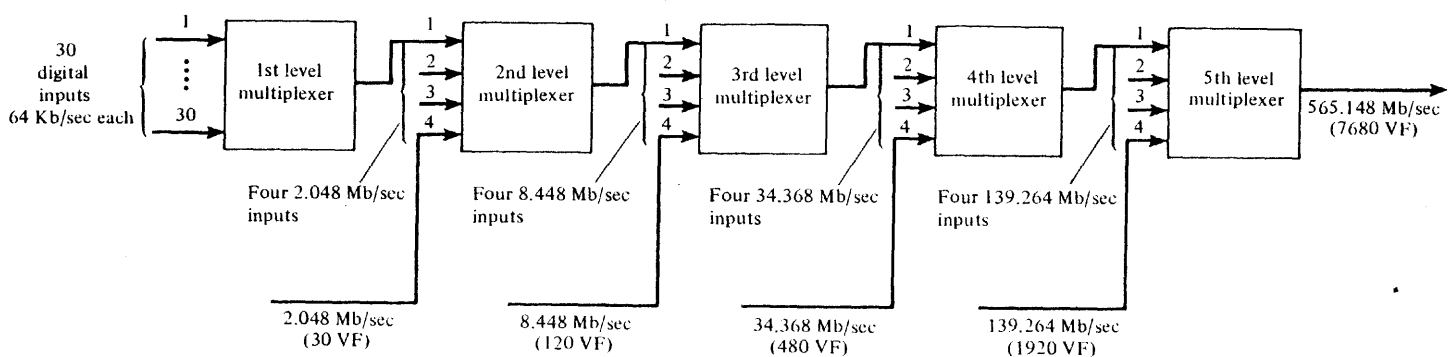


Figure 3-41 CCITT digital TDM hierarchy

TABLE 3-10 SONET SIGNAL HIERARCHY

OC Level	Line Rate (M Bits/s)	Equivalent Number of		
		DS-3s	DS-1s	DS-0s
OC-1	51.84	1	28	672
OC-3	155.52	3	84	2,016
OC-9	466.56	9	252	6,048
OC-12	622.08	12	336	8,064
OC-18	933.12	18	504	12,096
OC-24	1,244.16	24	672	16,128
OC-36	1,866.24	36	1,008	24,192
OC-48	2,488.32	48	1,344	32,256

Mbits/s) data stream. In AT&T terminology this is either a D-type channel bank or a digital carrier trunk (DCT) unit. A T1 line span is a twisted-pair telephone line that is used to carry the DS-1 (1.544 Mbit/s) data stream. Two lines, one for transmit and one for receive, are used in the system. If the T1 line is connecting telephone equipment at different sites, repeaters are required about every mile.

The T1 system was developed by Bell Laboratories for short-haul digital communication of VF traffic up to 50 mi. The sampling rate used on each of the 24 VF analog signals is 8 kHz, which means that one frame length is  $1/(8 \text{ kHz}) = 125 \mu\text{s}$ , as shown in Fig. 3-42. Presently, each analog sample is nominally encoded into an 8-bit PCM word so that there are  $8 \times 24 = 192$  bits of data, plus one bit that is added for frame synchronization, yielding a total of 193 bits per frame. The T1 data rate is then  $(193 \text{ bits/frame})(8000 \text{ frames/s}) = 1.544 \text{ Mbit/s}$ , and the corresponding duration of each bit is  $0.6477 \mu\text{s}$ . The signaling is incorporated into the T1 format by replacing the eighth bit (the least significant bit) in each of the 24 channels of the T1 signal by a signaling bit in every sixth frame. Thus the signaling data rate for each of the 24 input channels is  $(1 \text{ bit/6 frames})(8000 \text{ frames/s}) = 1.333 \text{ kbit/s}$ . The framing bit used in the even-numbered frames follows the sequence 001110, and in the odd-numbered frames it follows the sequence 101010, so that the frames with the signaling information in the eighth bit position (for each channel) may be identified. The digital signaling on the T1 line is represented by a bipolar RZ waveform format (see Fig. 3-15) with peak levels of  $\pm 3 \text{ V}$  across a  $100-\Omega$  load. Consequently, there is no dc component on the T1 line regardless of the data pattern. In encoding the VF PAM samples, a  $\mu = 255$  type

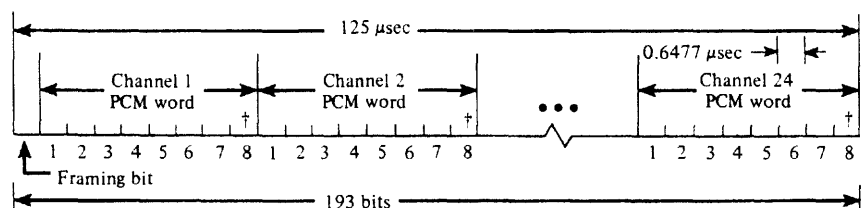


Figure 3-42 T1 TDM format for one frame.

compression characteristic is used, as described earlier in this chapter. Because the T1 data rate is 1.544 Mbit/s and the line code is bipolar, the first zero-crossing bandwidth is 1.544 MHz and the spectrum peaks at 772 kHz, as shown in Fig. 3-16d. If the channel filtering transfer function was of the raised cosine-rolloff type with  $r = 1$ , the absolute channel bandwidth would be 1.544 MHz. In the past, when twisted-pair lines were used for analog transmission only, loading coils (inductors) were used to improve the frequency (amplitude) response. However, they cause the line to have a phase response that is not linear with frequency, resulting in ISI. Thus they must be removed when the line is used for T1 service.

T1G carrier is described in Table 3-9. Instead of binary levels, it uses  $M = 4$  (quaternary) multilevel signaling, where +3 V represents the two binary bits 11, +1 V represents 01, -1 V represents 00, and -3 V represents 10 [Azaret et al., 1985]. Thus, a data rate of 6.443 Mbit/s is achieved via 3.221-Mbaud signaling. This gives a 3.221-MHz zero-crossing bandwidth, which is close to the 3.152 zero-crossing bandwidth of the T1C system. This bandwidth can be supported by standard twisted-pair wires (one pair for each direction) with repeaters spaced at one-mile intervals.

New fiber optic cable systems have phenomenal bandwidth and are relatively inexpensive on a perchannel basis. For example, the FT-2000 fiber optic TDM system (see Table 8-2 and 8-6) has a capacity of 32,256 VF channels.

### 3-10 PULSE TIME MODULATION: PULSE WIDTH MODULATION AND PULSE POSITION MODULATION

*Pulse time modulation* (PTM) is a class of signaling techniques that encodes the sample values of an analog signal onto the *time axis* of a digital signal, and it is analogous to angle modulation techniques, which are described in Chapter 5. (As we have seen, PAM, PCM, and DM techniques encode the sample values into the amplitude characteristics of the digital signal.)

The two main types of pulse time modulation are *pulse width modulation* (PWM) and *pulse position modulation* (PPM) (see Fig. 3-43). In PWM, which is also called *pulse duration modulation* (PDM), sample values of the analog waveform are used to determine the width of the pulse signal. Either *instantaneous* sampling or *natural* sampling can be used. Figure 3-44 shows a technique for generating PWM signals with instantaneous sampling, and Fig. 3-45 displays PWM with natural sampling. In PPM the analog sample value determines the *position* of a narrow pulse relative to the clocking time. Techniques for generating PPM are also shown in the figures, and it is seen that PPM is easily obtained from PWM by using a monostable multivibrator circuit. In the literature on PTM signals, the comparator level  $V_r$  is often called the *slicing level*.

PWM or PPM signals may be converted back to the corresponding analog signal by a receiving system (Fig. 3-46). For PWM detection the PWM signal is used to start and stop the integration of an integrator; that is, the integrator is reset to zero, and integration is begun when the PWM pulse goes from a low level to a high level and the integrator integrates until the PWM pulse goes low. If the integrator input is connected to a constant voltage source, the output will be a truncated ramp. After the PWM signal goes low, the amplitude of the truncated ramp signal will be equal to the corresponding PAM sample value. At clock-

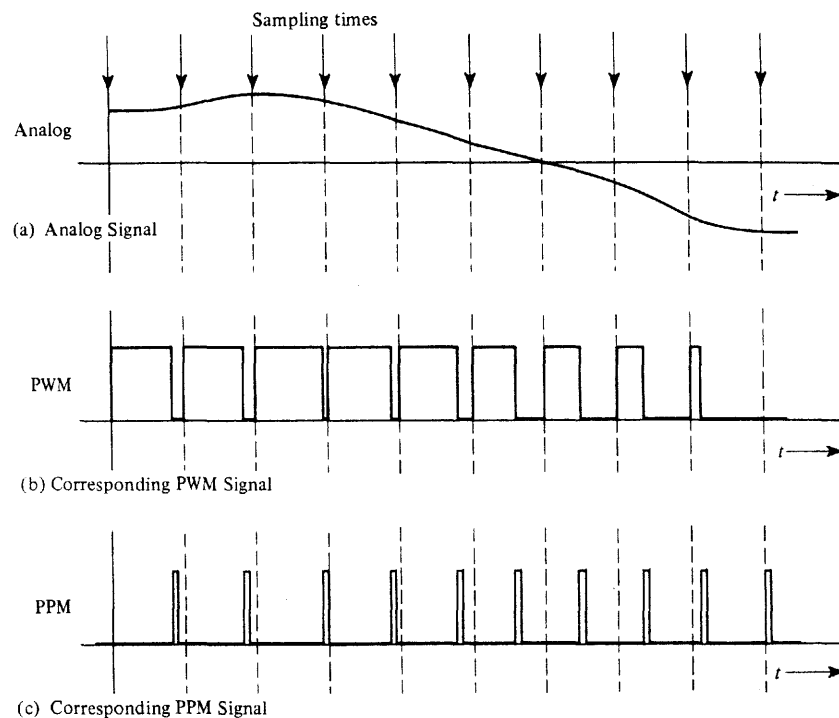


Figure 3-43 Pulse time modulation signaling.

ing time, the output of the integrator is then gated to a PAM output line (slightly before the integrator is reset to zero) using a sample-and-hold circuit. The PAM signal is then converted to the analog signal by low-pass filtering. In a similar way, PPM may be converted to PAM by using the clock pulse to reset the integrator to zero and start the integration. The PPM pulse is then used to stop the integration. The final value of the ramp is the PAM sample that is used to regenerate the analog signal.

Pulse time modulation signaling is not widely used to communicate across channels because a relatively wide bandwidth channel is needed, especially for PPM. However, PTM signals may be found internally in digital communications terminal equipment. The spectra of PTM signals are quite difficult to evaluate because of the nonlinear nature of the modulation [Rowe, 1965]. The main advantage of PTM signals is that they have a great immunity to additive noise when compared to PAM signaling, and they are easier to generate and detect than PCM, since PCM requires ADCs.

### 3-11 SUMMARY

In this study of baseband digital signaling we concentrated on four major topics: (1) how the information in analog waveforms can be represented by digital signaling; (2) how to compute the spectra for line codes; (3) how filtering of the digital signal, due to the communication channel, affects our ability to recover the digital information at the receiver [i.e., the

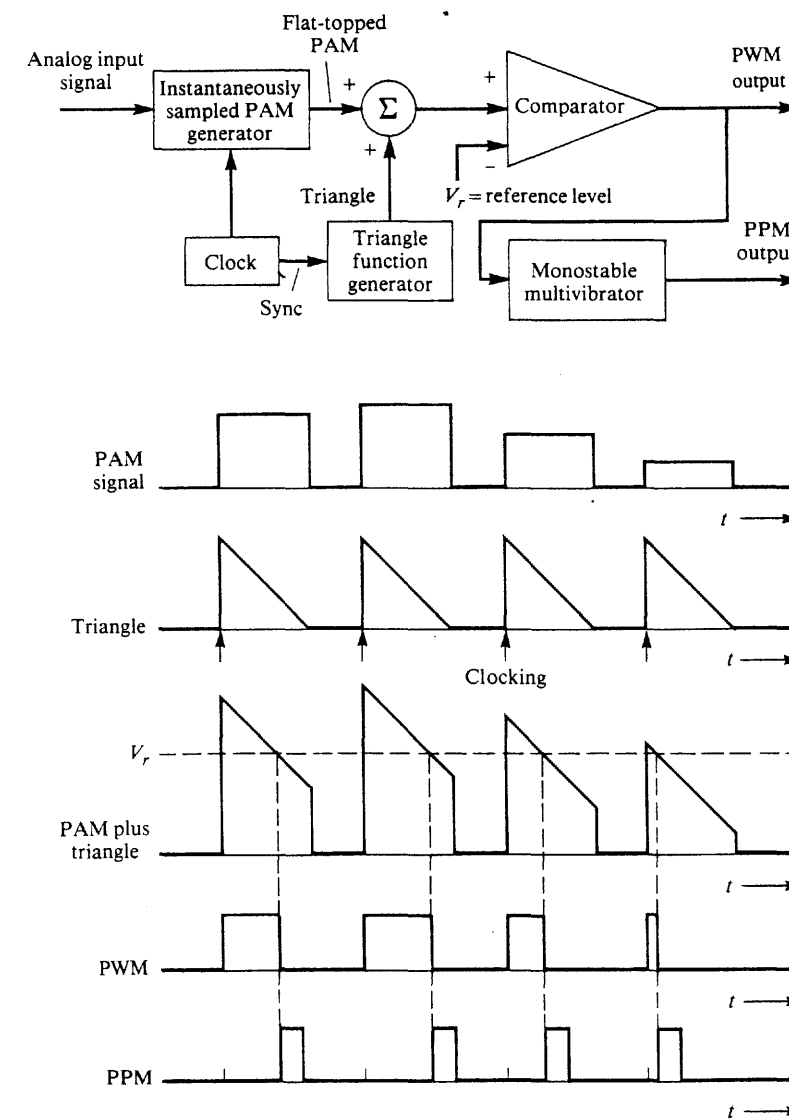


Figure 3-44 Technique for generating instantaneously sampled PTM signals.

intersymbol interference (ISI) problem]; and (4) how we can merge the information from several sources into one digital signal by using time-division multiplexing (TDM). U.S. and worldwide standards for TDM telecommunications systems were given.

PCM is an analog-to-digital conversion scheme that involves three basic operations: (1) *sampling* a bandlimited analog signal, (2) *quantizing* the analog samples into  $M$  discrete values, and (3) *encoding* each sample value into an  $n$ -bit word where  $M = 2^n$ . There are

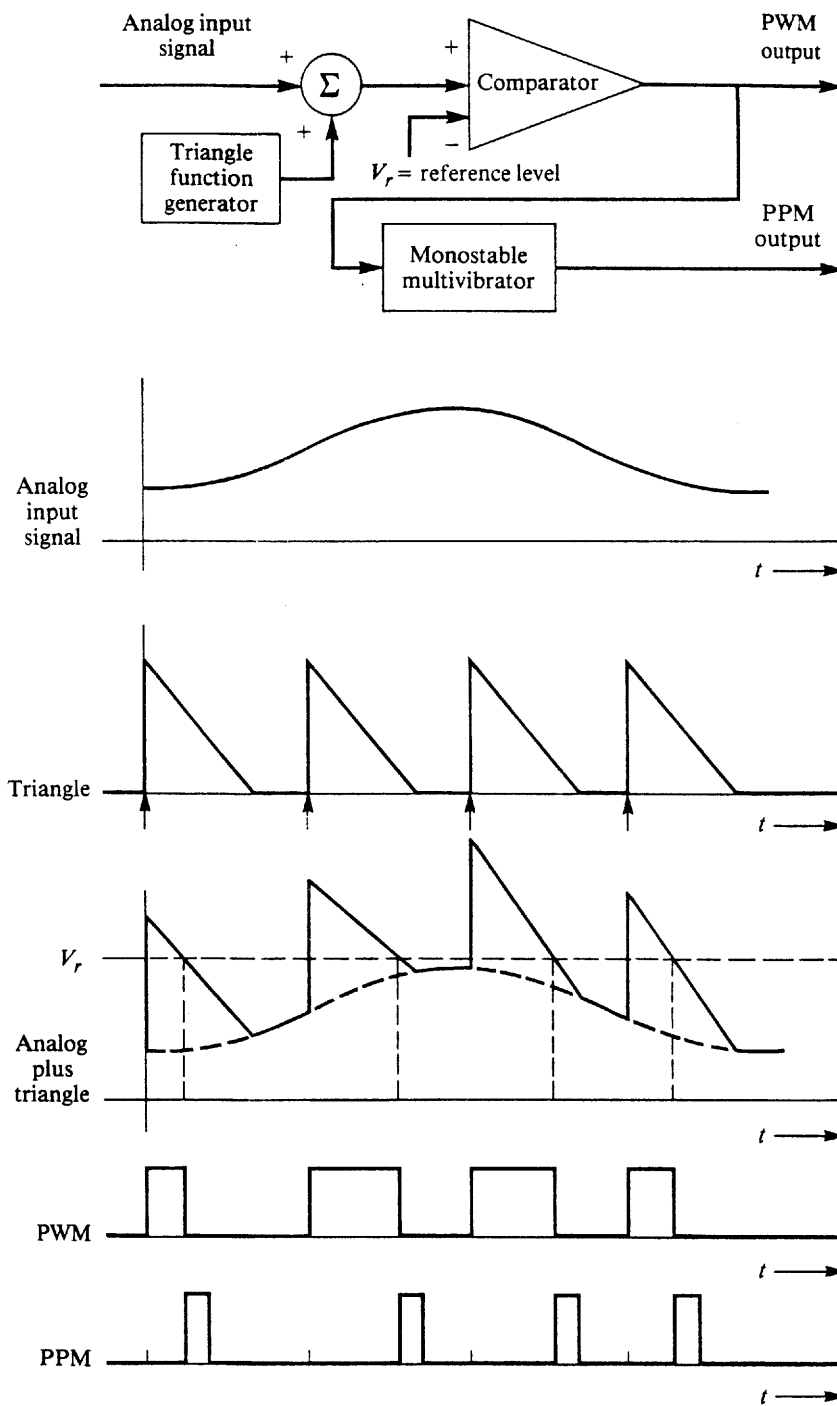


Figure 3-45 Technique for generating naturally sampled PAM signals.

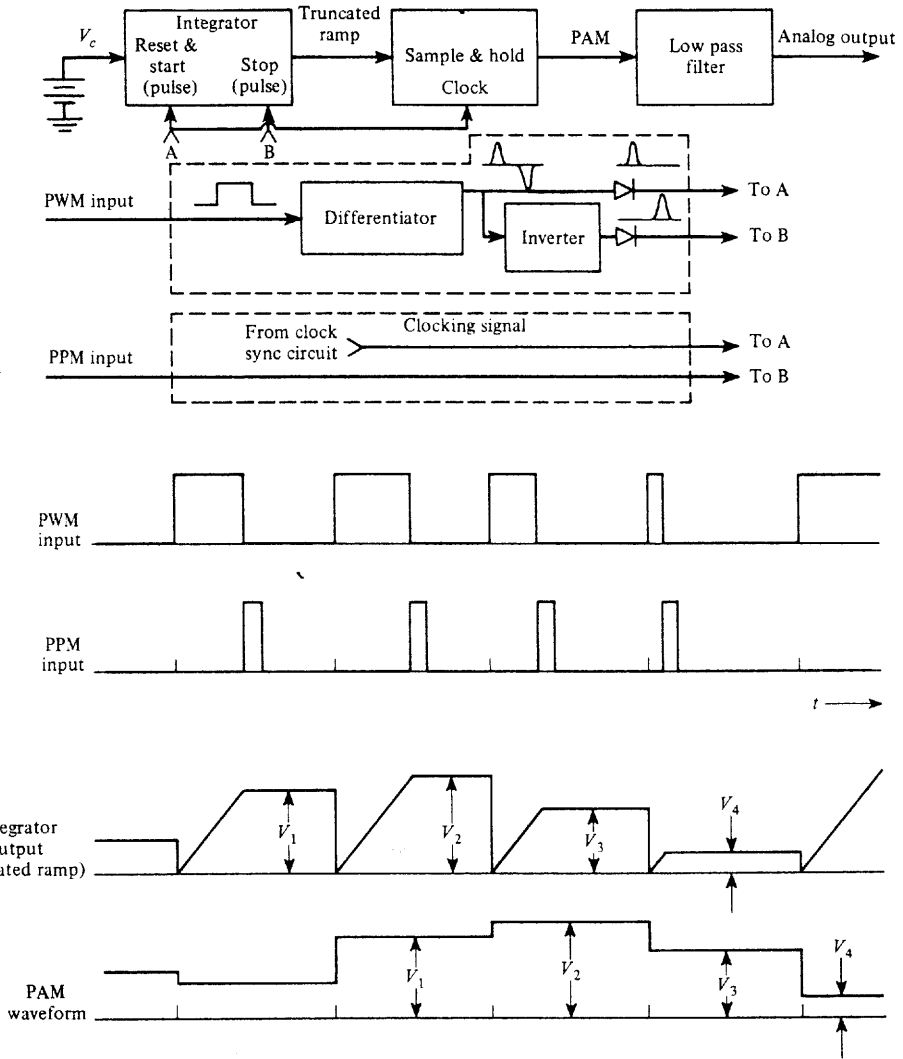


Figure 3-46 Detection of PWM and PPM signals.

two sources of noise in the signal that is recovered at the receiver output: (1) quantizing noise due to the approximation of the sample values using the  $M$  allowed values, and (2) noise due to receiver bit detection errors caused by channel noise or by ISI that arises because of improper channel frequency response. If the original analog signal is not strictly bandlimited, there will be a third noise component on the receiver output due to aliasing.

In studying the effect of improper channel filtering in producing ISI, the raised cosine-type rolloff filter was examined. Here it was found that the minimum bandwidth required to pass a PCM signal without ISI was equal to one half of the baud rate. However, this leads to technical difficulties since the overall filter characteristic is that for an ideal low-pass fil-

ter ( $r = 0$ ), which has an infinite number of poles. In addition, the sampling time at the receiver becomes very critical. A channel bandwidth equal to the baud rate ( $r = 1$ ), was found to be more realistic.

The channel bandwidth may be reduced if multilevel signal techniques are used (for a given data rate,  $R$ ) or if differential pulse code modulation (DPCM) is used. If equipment simplicity is of prime importance, delta modulation (DM) is the usual choice.

This chapter has focused on *baseband* signaling. In other words, the information is represented by a signal that has a spectrum concentrated about  $f = 0$ . In the next chapter we will be concerned with modulating baseband signals onto a carrier so that the spectrum will be concentrated about some desired frequency called the *carrier frequency*.

### 3-12 STUDY-AID EXAMPLES



**SA3-1** An analog waveform,  $w(t)$  is converted into a flat-topped PAM signal using a sampling rate of 8 kHz and a pulse width of 100  $\mu$ s. Assume that  $W(f) = 2\Lambda(f/B)$ , where  $B = 3$  kHz.

- Find and sketch the magnitude spectrum for the PAM signal.
- Find a numerical value for the first-null bandwidth of the PAM signal.

*Solution.*

(a) Using  $W(f) = 2\Lambda(f/B)$  in (3-10), MATLAB computes and plots the spectrum shown in Fig. 3-47. The plot shows how  $W(f)$  is repeated at harmonics of the sampling frequency and weighted by the  $\tau \left( \frac{\sin \pi \tau f}{\pi \tau f} \right)$  function (caused by the rectangular pulse shape).

(b) The spectrum first goes to zero at  $B = 3$  kHz. For this spectrum, 3 kHz is not a good measure of bandwidth because the spectral magnitude becomes large again at higher frequencies. In examples like this, engineers use the *envelope* of the spectrum to specify

the null bandwidth. Thus, the first null bandwidth of the spectral envelope,  $\tau \left| \frac{\sin \pi \tau f}{\pi \tau f} \right|$ , is  $B_{\text{null}} = 1/\tau = 1/100 \mu\text{s} = 10 \text{ kHz}$ .

**SA3-2** In a communications-quality audio system an analog voice-frequency (VF) signal with a bandwidth of 3200 Hz is converted into a PCM signal by sampling at 7000 samples/s and using a uniform quantizer with 64 steps. The PCM binary data is transmitted over a noisy channel to a receiver that has a bit error rate (BER) of  $10^{-4}$ .

- What is the null bandwidth of the PCM signal if a polar line code is used?
- What is the average SNR of the recovered analog signal at the receiving end?

*Solution.*

(a)  $M = 64$  quantizing steps generate 6-bit PCM words because  $M = 2^n$ . Using (3-15b), the null bandwidth is

$$B_{\text{null}} = n f_s = 6(7000) = 42 \text{ kHz}$$

*Note:* If  $\sin x/x$  pulse shapes were used, the bandwidth would be

$$B_{\text{null}} = \frac{1}{2} n f_s = 21 \text{ kHz}$$

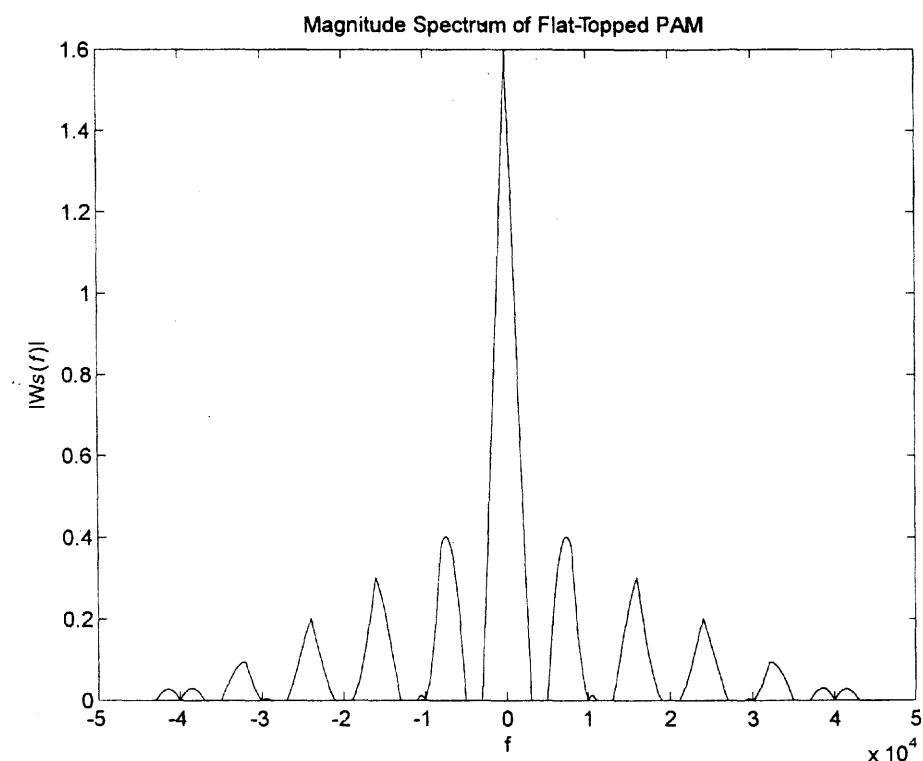


Figure 3-47 Solution for SA3-1.

- (b) Using (3-16b) with  $M = 64$  and  $P_e = 10^{-4}$

$$\left( \frac{S}{N} \right) = \frac{M^2}{1 + 4(M^2 - 1)P_e} = \frac{4096}{1 + 1.64} = 1552 = 31.9 \text{ dB}$$

*Note:* The 1 in the denominator represents quantization noise, and the 1.64 represents noise in the recovered analog signal caused by bit errors at the receiver. In this example, both noise effects contribute almost equally. For this case of  $M = 64$ , if the BER was less than  $10^{-5}$ , the quantizing noise would dominate or if the BER was larger than  $10^{-3}$ , noise resulting from receiver bit errors would dominate.

**SA3-3** A unipolar NRZ line code is converted to a multilevel signal for transmission over a channel as illustrated in Fig. 3-13. The number of possible values in the multilevel signal is 32, and the signal consists of rectangular pulses that have a pulse width of 0.3472 ms. For the multilevel signal

- What is the baud rate?
- What is the equivalent bit rate?
- What is the null bandwidth?
- Repeat (a) to (c) for the unipolar NRZ line code.

**Solution.**

(a) Using (3-28) where  $N = 1$  pulse occurs in  $T_0 = 0.3452$  ms, we get

$$D = N/T_0 = 1/0.3472 \text{ ms} = 2880 \text{ baud}$$

(b) Because  $L = 32 = 2^\ell$ ,  $\ell = 5$ . Using (3-34),

$$R = \ell D = 5(2880) = 14,400 \text{ bits/s}$$

(c) Using (3-54), the null bandwidth is

$$B_{\text{null}} = R/\ell = D = 2880 \text{ Hz}$$

(d) For the unipolar NRZ line code, there are  $N = 5$  pulses in  $T_0 = 0.3472$  ms or

$$D = 5/0.3472 \text{ ms} = 14400 \text{ baud}$$

**SA3-4** Because the unipolar NRZ line code is binary (i.e.,  $L = 2^\ell$  or  $\ell = 1$ ). Thus,  $R = 14,400$  bits/s. The null bandwidth is

$$B_{\text{null}} = R/\ell = D = 14,400 \text{ Hz}$$

The RS-232 serial port on a personal computer is transmitting data at a rate of 38,400 bits/s using a polar NRZ line code. Assume that binary 1s and 0s are equally likely to occur. Compute and plot the PSD for this RS-232 signal. Use a dB scale with the PSD being normalized so that 0 dB occurs at the peak of the PSD plot. Discuss the bandwidth requirements for this signal.

**Solution.** Referring to (3-41), set  $A^2 T_b$  equal to 1 so that 0 dB occurs at the peak. Then, the PSD in dB units is

$$P_{\text{dB}}(f) = 10 \log \left[ \left( \frac{\sin \pi f T_b}{\pi f T_b} \right)^2 \right]$$

where  $T_b = 1/R$  and  $R = 38,400$  bits/s.

This result is plotted in Fig. 3-48 using a dB scale. This plot reveals that the spectrum is broad for this case of digital signaling with rectangular pulse shapes. Although the null bandwidth is 38,000 Hz ( $B_{\text{null}} = R$ ), this gives a false sense that the spectrum is relatively narrow because the first sidelobe peak (at  $f = 57,600$  Hz =  $1.5R$ ) is down by only 13.5 dB from the main lobe, and the second sidelobe peak (at  $f = 96,000$  Hz =  $2.5R$ ) is down by only 17.9 dB. The power spectrum is falling off as  $1/f^2$ , which is only 6 dB per octave. Referring to Fig. 3-48 and knowing that the envelope of the PSD is described by  $(1/\pi f T_b)^2$ , it is found that a bandwidth of  $f = 386$  kHz =  $10.1R$  (i.e., 10 times the data rate) is needed to pass the frequency components that are not attenuated by more than 30 dB. Thus, the spectrum is broad when rectangular sampling pulses are used. (This was first illustrated in Fig. 2-24.)

Consequently, for applications of digital signaling over bandlimited channels, some sort of filtered pulse shape is required to provide good out-of-band spectral attenuation and yet not introduce ISI. For example, using (3-74), a filtered pulse corresponding to a  $r = 0.5$  raised cosine characteristic would have infinite attenuation at the frequency (absolute bandwidth) of  $B = \frac{1}{2}(1+r)D = (0.5)(1.5)(38,400) = 28,800$  Hz =  $0.75R$ . Referring to Fig. 3-26a and using (3-69), the  $r = 0.5$  raised cosine spectrum would be down by 30 dB at  $f = 20,070$  Hz =  $0.523R$  and 100 dB at  $f = 22,217$  Hz =  $0.579R$ . For the 30 dB down bandwidth criteria, this is a bandwidth (savings) of 19 times smaller than that required for rectangular pulse signaling.

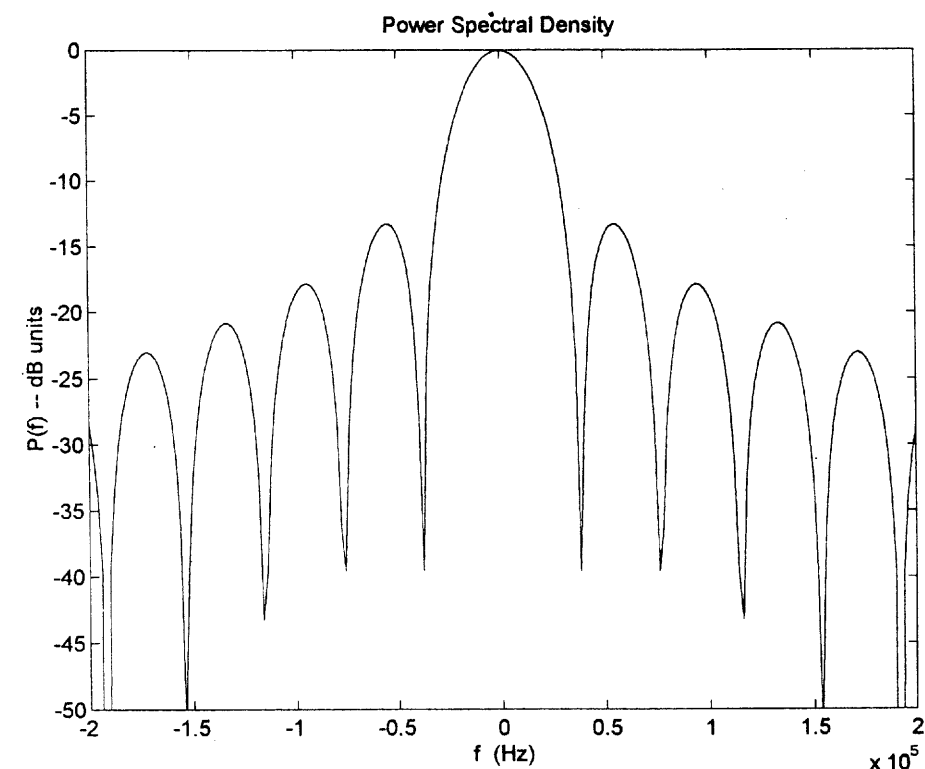


Figure 3-48 PSD of a RS-232 signal with a data rate of 38,400 bits/s.

**PROBLEMS**

**3-1** Demonstrate that the Fourier series coefficients for the switching waveform shown in Fig. 3-1b are given by (3-5b).

**3-2** (a) Sketch the naturally sampled PAM waveform that results from sampling a 1-kHz sine wave at a 4-kHz rate.

(b) Repeat part (a) for the case of a flat-topped PAM waveform.

**3-3** The spectrum of an analog audio signal is shown in Fig. P3-3. The wave form is to be sampled at a 10-kHz rate with a pulse width of  $\tau = 50 \mu\text{s}$ .

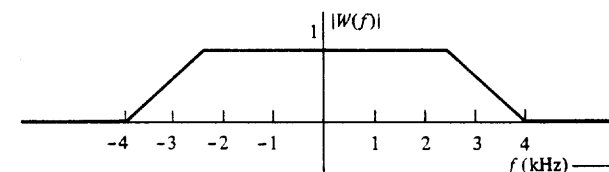


Figure P3-3

- (a) Find an expression for the spectrum of the naturally sampled PAM waveform. Sketch your result.
- (b) Find an expression for the spectrum of the flat-topped PAM waveform. Sketch your result.
- 3-4** (a) Show that an analog output waveform (which is proportional to the original input analog waveform) may be recovered from a naturally sampled PAM waveform using the demodulation technique shown in Fig. 3-4.
- (b) Find the constant of proportionality  $C$  that is obtained using this demodulation technique where  $w(t)$  is the original waveform and  $Cw(t)$  is the recovered waveform. Note that  $C$  is a function of  $n$  where the oscillator frequency is  $nf_s$ .
- 3-5** Figure 3-4 illustrates how a naturally sampled PAM signal can be demodulated to recover the analog waveform by use of a product detector. Show that the product detector can also be used to recover  $w(t)$  from an instantaneously sampled PAM signal provided that the appropriate filter,  $H(f)$ , is used. Find the required  $H(f)$  characteristic.
- 3-6** Starting with the PAM signal of Prob. 3-3:
- Design a PAM product demodulator with an oscillator operating at 30 kHz to recover the analog waveform from the naturally sampled PAM waveform.
  - Design a PAM product demodulator with an oscillator operating at 30 kHz to demodulate the flat-topped PAM waveform.
  - Discuss whether any synchronization signals are needed to operate these demodulators. Be sure to show the characteristics of any filters that are needed in your demodulator designs.
- 3-7** Assume that an analog signal with a spectrum shown in Fig. P3-3 is to be transmitted over a PAM system that has ac coupling. Thus a PAM pulse shape of the Manchester type as given by (3-46a) is used. The PAM sampling frequency is 10 kHz. Find the spectrum for the Manchester encoded flat-topped PAM waveform. Sketch your result.
- 3-8** In a binary PCM system, if the quantizing noise is not to exceed  $\pm P$  percent of the peak-to-peak analog level, show that the number of bits in each PCM word needs to be

$$n \geq \lceil \log_2 10 \rceil \left[ \log_{10} \left( \frac{50}{P} \right) \right] = 3.32 \log_{10} \left( \frac{50}{P} \right)$$

*Hint:* Look at Fig. 3-8c.

- 3-9** The information in an analog voltage waveform is to be transmitted over a PCM system with a  $\pm 0.1\%$  accuracy (full scale). The analog waveform has an absolute bandwidth of 100 Hz and an amplitude range of  $-10$  to  $+10$  V.
- Determine the minimum sampling rate needed.
  - Determine the number of bits needed in each PCM word.
  - Determine the minimum bit rate required in the PCM signal.
  - Determine the minimum absolute channel bandwidth required for transmission of this PCM signal.
- 3-10** A 850-Mbyte hard disk is used to store PCM data. Suppose that a VF (voice-frequency) signal is sampled at 8 ksamples/s and the encoded PCM is to have an average SNR of at least 30 dB. How many minutes of VF conversation (i.e., PCM data) can be stored on the hard disk?
- 3-11** An analog signal with a bandwidth of 4.2 MHz is to be converted into binary PCM and transmitted over a channel. The peak-signal/quantizing noise ratio at the receiver output must be at least 55 dB.
- If we assume  $P_e = 0$  and no ISI, what will be the word length and the number of quantizing steps needed?



- (b) What will be the equivalent bit rate?
- (c) What will be the channel null bandwidth required if rectangular pulse shapes are used?

- 3-12** Compact disk (CD) players use 16-bit PCM, including one parity bit with 8 times oversampling of the analog signal. The analog signal bandwidth is 20 kHz.
- What is the null bandwidth of this PCM signal?
  - Using (3-18), find the peak (SNR) in decibels.
- 3-13** Given an audio signal with spectral components in the frequency band 300 to 3000 Hz, assume that a sampling rate of 7 kHz will be used to generate a PCM signal. Design an appropriate PCM system, as follows.
- Draw a block diagram of the PCM system including the transmitter, channel, and receiver.
  - Specify the number of uniform quantization steps needed and the channel null bandwidth required, assuming that the peak signal-to-noise ratio at the receiver output needs to be at least 30 dB and that polar NRZ signaling is used.
  - Discuss how nonuniform quantization can be used to improve the performance.
- 3-14** The SNR as given by (3-17a) and (3-17b) assume no ISI and no bit errors due to channel noise (i.e.,  $P_e = 0$ ). How large can  $P_e$  become before (3-17a) and (3-17b) are in error by 0.1% if  $M = 4, 8$ , or 16.
- 3-15** In a PCM system the bit error rate due to channel noise is  $10^{-4}$ . Assume that the peak signal-to-noise ratio on the recovered analog signal needs to be at least 30 dB.
- Find the minimum number of quantizing steps that can be used to encode the analog signal into a PCM signal.
  - If the original analog signal had an absolute bandwidth of 2.7 kHz, what is the null bandwidth of the PCM signal for the polar NRZ signaling case?
- 3-16** Referring to Fig. 3-20 for a bit synchronizer using a square-law device, draw some typical waveforms that will appear in the bit synchronizer if a Manchester encoded PCM signal is present at the input. Discuss whether you would expect this bit synchronizer to work better for the Manchester encoded PCM signal or for a polar NRZ encoded PCM signal.
- 3-17** (a) Sketch the complete  $\mu = 10$  compressor characteristic that will handle input voltages over the range  $-5$  to  $+5$  V.
- Plot the corresponding expandor characteristic.
  - Draw a 16-level nonuniform quantizer characteristic that corresponds to the  $\mu = 10$  compression characteristic.
- 3-18** For a 4-bit PCM system, calculate and sketch a plot of the output SNR (in decibels) as a function of the relative input level,  $20 \log(x_{\text{rms}}/V)$  for
- A PCM system that uses  $\mu = 10$  law companding.
  - A PCM system that uses uniform quantization (no companding).
- Which of these systems is better to use in practice? Why?
- 3-19** The performance of a  $\mu = 255$  law companded PCM system is to be examined when the input consists of a sine wave having a peak value of  $V$  volts. Assume that  $M = 256$ .
- Find an expression that describes the output SNR for this companded PCM system.
  - Plot the  $(S/N)_{\text{out}}$  (in decibels) as a function of the relative input level,  $20 \log(x_{\text{rms}}/V)$ . Compare this result with that shown in Fig. 3-10.
- 3-20** A multilevel digital communication system sends one of 16 possible levels over the channel every 0.8 ms.
- What is the number of bits corresponding to each level?
  - What is the baud rate?
  - What is the bit rate?





- 3-21** A multilevel digital communication system is to operate at a data rate of 9600 bits/s.  
 (a) If 4-bit words are encoded into each level for transmission over the channel, what is the minimum required bandwidth for the channel?  
 (b) Repeat part (a) for the case of 8-bit encoding into each level.
- 3-22** Consider a deterministic test pattern consisting of alternating binary 1s and binary 0s. Determine the magnitude spectra (not the PSD) for the following types of signaling formats as a function of  $T_b$ , where  $T_b$  is the time needed to send one bit of data.  
 (a) Unipolar NRZ signaling.  
 (b) Unipolar RZ signaling where the pulse width  $\tau$  is  $\tau = \frac{1}{4} T_b$ .  
 How would each of these magnitude spectra change if the test pattern was changed to an alternating sequence of four binary 1s followed by four binary 0s?
- 3-23** Consider a random data pattern consisting of binary 1s and 0s, where the probability of obtaining either a binary 1 or a binary 0 is  $\frac{1}{2}$ . Calculate the PSD for the following types of signaling formats as a function of  $T_b$ , where  $T_b$  is the time needed to send one bit of data.  
 (a) Unipolar NRZ signaling.  
 (b) Unipolar RZ signaling where the pulse width  $\tau$  is  $\tau = \frac{1}{4} T_b$ .  
 How do these PSDs for the random data cases compare to the magnitude spectra for the deterministic case of Prob. 3-22? What is the spectral efficiency for each of these cases?
- 3-24** Consider a deterministic data pattern consisting of alternating binary 1s and 0s. Determine the magnitude spectra (not the PSD) for the following types of signaling formats as a function of  $T_b$ , where  $T_b$  is the time needed to send one bit of data.  
 (a) Polar NRZ signaling.  
 (b) Manchester NRZ signaling.  
 How would each of these magnitude spectra change if the test pattern was changed to an alternating sequence of four binary 1's followed by two binary 0s?
- 3-25** Consider a random data pattern consisting of binary 1s and 0s, where the probability of obtaining either a binary 1 or a binary 0 is  $\frac{1}{2}$ . Calculate the PSD for the following types of signaling formats as a function of  $T_b$ , where  $T_b$  is the time needed to send 1 bit of data.  
 (a) Polar RZ signaling where the pulse width is  $\tau = \frac{1}{2} T_b$ .  
 (b) Manchester RZ signaling where the pulse width is  $\tau = \frac{1}{4} T_b$ . What is the first-null bandwidth of these signals? What is the spectral efficiency for each of these signaling cases?
- 3-26** Obtain the equations for the PSD of the bipolar NRZ and bipolar RZ (pulse width  $\frac{1}{2} T_b$ ) line codes assuming peak values of  $\pm 3$  V. Plot these PSD results for the case of  $R = 1.544$  Mbit/s.
- 3-27** In Fig. 3-16 the PSDs for several line codes are shown. These PSDs were derived assuming unity power for each signal so that the PSDs could be compared on an equal transmission power basis. Rederive the PSDs for these line codes assuming that the peak level is unity (i.e.,  $A = 1$ ). Plot these PSDs so that the spectra can be compared on an equal peak-signal-level basis.
- 3-28** Using (3-36), determine the conditions required so that there are delta functions in the PSD for line codes. Discuss how this affects the design of bit synchronizers for these line codes. [Hint: Examine (3-43) and (6-70d).]
- 3-29** Consider a random data pattern consisting of binary 1s and 0s, where the probability of obtaining either a binary 1 or a binary 0 is  $\frac{1}{2}$ . Assume that these data are encoded into a polar-type waveform where the pulse shape of each bit is given by

$$f(t) = \begin{cases} \cos\left(\frac{\pi t}{T_b}\right), & |t| < T_b/2 \\ 0, & |t| \text{ elsewhere} \end{cases}$$

- $T_b$  is the time needed to send one bit.
- (a) Sketch a typical example of this waveform.  
 (b) Find the expression for the PSD of this waveform and sketch it.  
 (c) What is the spectral efficiency of this type of binary signal?
- 3-30** The data stream 01101000101 appears at the input of a differential encoder. Depending on the initial start-up condition of the encoder, find two possible differentially encoded data streams that can appear at the output.
- 3-31** Create a practical block diagram for a differential encoding and decoding system. Explain how it works by showing the encoding and decoding for the sequence 001111010001. Assume that the reference digit is a binary 1. Show that error propagation cannot occur.
- 3-32** Design a regenerative repeater with its associated bit synchronizer for a polar RZ line code. Explain how your design works. (Hint: See Fig. 3-19 and the discussion on bit synchronizers.)
- 3-33** Design a bit synchronizer for a Manchester NRZ line code by completing the following steps:  
 (a) Give a simplified block diagram.  
 (b) Explain how it works.  
 (c) Specify filter requirements.  
 (d) Explain the advantages and disadvantages of using this design for the Manchester NRZ line code as compared to using a polar NRZ line code and its associated bit synchronizer.
- 3-34** Figure 3-22c illustrates an eight-level multilevel signal. Assume that this line code is passed through a channel that filters this signal and adds some noise.  
 (a) Draw a picture of the eye pattern for the received waveform.  
 (b) Design a possible receiver with its associated symbol synchronizer for this line code.  
 (c) Explain how your receiver works.
- 3-35** The information in an analog waveform is first encoded into binary PCM and then converted to a multilevel signal for transmission over the channel. The number of multilevels is eight. Assume that the analog signal has a bandwidth of 2700 Hz and is to be reproduced at the receiver output with an accuracy of  $\pm 1\%$  (full scale).  
 (a) Determine the minimum bit rate of the PCM signal.  
 (b) Determine the minimum baud rate of the multilevel signal.  
 (c) Determine the minimum absolute channel bandwidth required for transmission of this PCM signal.
- 3-36** A binary waveform of 9600 bits/s is converted into an octal (multilevel) waveform that is passed through a channel with a raised cosine-rolloff filter characteristic. The channel has a conditioned (equalized) phase response out to 2.4 kHz.  
 (a) What is the baud rate of the multilevel signal?  
 (b) What is the rolloff factor of the filter characteristic?
- 3-37** Assume that the spectral properties of an  $L = 64$  level multilevel waveform with rectangular RZ-type pulse shapes are to be examined. The pulse shape is given by
- $$f(t) = \Pi\left(\frac{2t}{T_s}\right)$$
- $T_s$  is the time needed to send one of the multilevel symbols.
- (a) Determine the expression for the PSD for the case of equally likely levels where the peak signal levels for this multilevel waveform are  $\pm 10$  V.  
 (b) What is the null bandwidth?  
 (c) What is the spectral efficiency?



- 3-38** A binary communication system uses polar signaling. The overall impulse response is designed to be of the  $(\sin x)/x$  type as given by (3-67) so that there will be no ISI. The bit rate is  $R = f_s = 300$  bits/s.
- What is the bandwidth of the polar signal?
  - Plot the waveform of the polar signal at the system output when the input binary data is 01100101. Can you discern the data by looking at this polar waveform?

- 3-39** Equation (3-67) gives one possible noncausal impulse response for a communication system that will have no ISI. For a causal approximation, select

$$h_c(t) = \frac{\sin \pi f_s(t - 4 \times 10^{-3})}{\pi f_s(t - 4 \times 10^{-3})} \Pi\left(\frac{t - 4 \times 10^{-3}}{8 \times 10^{-3}}\right)$$

where  $f_s = 1000$ .

- Using a PC, calculate  $H_c(f)$  by use of the Fourier transform integral and plot  $|H_c(f)|$ .
  - What is the bandwidth of this causal approximation, and how does it compare to the bandwidth of the noncausal filter described by (3-67) and (3-68)?
- 3-40** Starting with (3-69), prove that the impulse response of the raised cosine rolloff filter is given by (3-73).

- 3-41** Consider the raised cosine-rolloff filter given by (3-69) and (3-73).
- Plot  $|H_c(f)|$  for the case of  $r = 0.75$ , indicating  $f_1, f_0$ , and  $B$  on your sketch, similar to Fig. 3-25.
  - Plot  $h_c(t)$  for the case of  $r = 0.75$  in terms of  $1/f_0$ , similar to Fig. 3-26.
- 3-42** Find the PSD of the waveform out of an  $r = 0.5$  raised cosine-rolloff channel when the input is a polar NRZ signal. Assume that equally likely binary signaling is used and the channel bandwidth is just large enough to prevent ISI.
- 3-43** Equation (3-66) gives the condition for no ISI (Nyquist's first method). Using (3-66) with  $C = 1$  and  $\tau = 0$ , show that Nyquist's first method for no ISI is also satisfied if

$$\sum_{k=-\infty}^{\infty} H_c\left(f + \frac{k}{T_s}\right) = T_s, \quad \text{for } |f| \leq \frac{1}{2T_s}$$

- 3-44** Using the results of Prob. 3-43, demonstrate that the following filter characteristics do or do not satisfy Nyquist's criterion for no ISI ( $f_s = 2f_0 = 2/T_0$ ).

$$(a) H_c(f) = \frac{T_0}{2} \Pi\left(\frac{1}{2} f T_0\right).$$

$$(b) H_c(f) = \frac{T_0}{2} \Pi\left(\frac{2}{3} f T_0\right).$$

- 3-45** Assume that a pulse transmission system has an overall raised cosine-rolloff filter characteristic as described by (3-69).
- Find the  $Y(f)$  Nyquist function of (3-75) corresponding to the raised cosine-rolloff filter characteristic.
  - Sketch  $Y(f)$  for the case of  $r = 0.75$ .
  - Sketch another  $Y(f)$  that is not of the raised cosine-rolloff type and determine the absolute bandwidth of the resulting Nyquist filter characteristic.
- 3-46** An analog signal is to be converted into a PCM signal that is a binary polar NRZ line code. This signal is transmitted over a channel that is absolutely bandlimited to 4 kHz. Assume that the

PCM quantizer has 16 steps and that the overall equivalent system transfer function is of the raised cosine-rolloff type with  $r = 0.5$ .

- Find the maximum PCM bit rate that can be supported by this system without introducing ISI.
- Find the maximum bandwidth that can be permitted for the analog signal.

- 3-47** Rework Prob. 3-46 for the case of a multilevel polar NRZ line code when the number of levels is four.

- 3-48** Multilevel data with an equivalent bit rate of 2400 bits/s is sent over a channel using a 4-level line code, which has a rectangular pulse shape at the output of the transmitter. The overall transmission system (i.e., the transmitter, channel, and receiver) has a  $r = 0.5$  raised cosine-rolloff filter characteristic.

- Find the baud rate of the received signal.
- Find the 6-dB bandwidth for this transmission system.
- Find the absolute bandwidth for this transmission system.

- 3-49** Assume that a PCM-type system is to be designed such that an audio signal can be delivered at the receiver output. This audio signal is to have a bandwidth of 3400 Hz and a SNR of at least 40 dB. Determine the bit rate requirements for a design that uses:

- $\mu = 255$  companded PCM signaling.
- DPCM signaling.

Discuss which of the preceding systems would be used in your design and why.

- 3-50** Refer to Fig. 3-32, which shows typical DM waveforms. Draw an analog waveform that is different from the one shown in the figure. Draw the corresponding DM and integrator output waveforms. Denote the regions where slope overload noise dominates and where granular noise dominates.

- 3-51** A DM system is tested with a 10-kHz sinusoidal signal, 1 V peak to peak, at the input. It is sampled at 10 times the Nyquist rate.

- What is the step size required to prevent slope overload and to minimize granular noise?
- What is the PSD for the granular noise?
- If the receiver input is bandlimited to 200 kHz, what is the average signal/quantizing-noise power ratio?

- 3-52** Assume that the input to a DM is  $0.1t^8 - 5t + 2$ . The step size of the DM is 1 V, and the sampler operates at 10 samples/s. Over a time interval of 0 to 2 s, sketch the input waveform, the delta modulator output, and the integrator output. Denote the granular noise and slope overload regions.

- 3-53** Rework Prob. 3-52 for the case of an adaptive delta modulator where the step size is selected according to the number of successive binary 1s or 0s on the DM output. Assume that the step size is 1.5 V when there are four or more binary digits of the same sign, 1 V for the case of three successive digits, and 0.5 V for the case of two or fewer successive digits.

- 3-54** A delta modulator is to be designed to transmit the information of an analog waveform that has a peak-to-peak level of 1 V and a bandwidth of 3.4 kHz. Assume that the waveform is to be transmitted over a channel where the frequency response is extremely poor above 1 MHz.

- Select the appropriate step size and sampling rate for a sine-wave test signal and discuss the performance of the system using the parameter values you have selected.
- If the DM system is to be used to transmit the information of a voice (analog) signal, select the appropriate step size when the sampling rate is 25 kHz. Discuss the performance of the system under these conditions.

- 3-55** One analog waveform  $w_1(t)$  is bandlimited to 3 kHz, and another,  $w_2(t)$ , is bandlimited to 9 kHz. These two signals are to be sent by TDM over a PAM-type system.



- (a) Determine the minimum sampling frequency for each signal and design a TDM commutator and decommutator to accommodate these signals.  
 (b) Draw some typical waveforms for  $w_1(t)$  and  $w_2(t)$ , and sketch the corresponding TDM PAM waveform.

- 3-56** Three waveforms are time-division multiplexed over a channel using instantaneously sampled PAM. Assume that the PAM pulse width is very narrow and that each of the analog waveforms are sampled every 0.15 s. Plot the (composite) TDM waveform when the input analog waveforms are

$$w_1(t) = 3 \sin(2\pi t)$$

$$w_2(t) = \Pi\left(\frac{t - 1}{2}\right)$$

$$w_3(t) = -\Lambda(t - 1)$$

- 3-57** Twenty-three analog signals, each with a bandwidth of 3.4 kHz, are sampled at an 8-kHz rate and multiplexed together with a synchronization channel (8 kHz) into a TDM PAM signal. This TDM signal is passed through a channel with an overall raised cosine-rolloff filter characteristic of  $r = 0.75$ .

- (a) Draw a block diagram for the system indicating the  $f_s$  of the commutator and the overall pulse rate of the TDM PAM signal.  
 (b) Evaluate the absolute bandwidth required for the channel.  
**3-58** Two flat-topped PAM signals are time-division multiplexed together to produce a composite TDM PAM signal that is transmitted over a channel. The first PAM signal is obtained from an analog signal that has a rectangular spectrum,  $W_1(f) = \Pi(f/2B)$ . The second PAM signal is obtained from an analog signal that has a triangular spectrum,  $W_2(f) = \Lambda(f/B)$  where  $B = 3$  kHz.

- (a) Determine the minimum sampling frequency for each signal and design a TDM commutator and decommutator to accommodate these signals.  
 (b) Calculate and sketch the magnitude spectrum for the composite TDM PAM signal.

- 3-59** Rework Prob. 3-57 for a TDM pulse code modulation system where an 8-bit quantizer is used to generate the PCM words for each of the analog inputs and an 8-bit synchronization word is used in the synchronization channel.

- 3-60** Design a TDM PCM system that will accommodate four 300-bit/s (synchronous) digital inputs and one analog input that has a bandwidth of 500 Hz. Assume that the analog samples will be encoded into 4-bit PCM words. Draw a block diagram for your design, analogous to Fig. 3-39, indicating the data rates at the various points on the diagram. Explain how your design works.

- 3-61** Design a TDM system that will accommodate two 2400-bit/s synchronous digital inputs and an analog input that has a bandwidth of 2700 Hz. Assume that the analog input is sampled at 1.11111 times the Nyquist rate and converted into 4-bit PCM words. Draw a block diagram for your design and indicate the data rate at various points on your diagram. Explain how your TDM scheme works.

- 3-62** Find the number of the following devices that could be accommodated by a T1-type TDM line if 1% of the line capacity were reserved for synchronization purposes.

- (a) 110-bit/s teleprinter terminals.
- (b) 300-bit/s computer terminals.
- (c) 1200-bit/s computer terminals.
- (d) 9600-bit/s computer output ports.
- (e) 64-kbit/s PCM VF lines.

How would these numbers change if each of the sources were operational an average of 10% of the time?

- 3-63** Assume that a sine wave is sampled at four times the Nyquist rate using instantaneous sampling.  
 (a) Sketch the corresponding PWM signal.  
 (b) Sketch the corresponding PPM signal.  
**3-64** Repeat Prob. 3-63, but assume that natural sampling is used.  
**3-65** Discuss why a PPM system requires a synchronizing signal, whereas PAM and PWM can be detected without the need for a synchronizing signal.  
**3-66** Compare the bandwidth required to send a message by using PPM and PCM signaling. Assume that the digital source sends out 8 bits/character, so that the digital source can send 256 different messages (characters). Assume that the source rate is 10 characters/s. Use the dimensionality theorem,  $N/T_0 = 2B$ , to determine the minimum bandwidth required,  $B$ .  
 (a) Determine the minimum bandwidth required for a PCM signal that will encode the source information.  
 (b) Determine the minimum bandwidth required for a PPM signal that will encode the source information.

## BANDPASS SIGNALING PRINCIPLES AND CIRCUITS

This chapter is concerned with *bandpass* signaling techniques. As indicated in Chapter 1, the bandpass communication signal is obtained by modulating a baseband analog or digital signal onto a carrier. Here the basic principles of bandpass signal representation and the modulation process are developed by use of the complex envelope. The complex envelope is then used to evaluate spectra and powers of bandpass signals.

The second half of this chapter, which begins with Sec. 5-8, uses this bandpass theory to analyze and design component blocks and circuits that are used in communication systems. These are filters, linear and nonlinear amplifiers, up-and-down converters, modulators, detectors, and phase-locked loops.

### 4-1 COMPLEX ENVELOPE REPRESENTATION OF BANDPASS WAVEFORMS

What is a general representation for bandpass digital and analog signals? How do we represent a modulated signal? How do we represent bandpass noise? These are some of the questions that are answered in this section.

#### Definitions: Baseband, Bandpass, and Modulation

**DEFINITION.** A *baseband* waveform has a spectral magnitude that is nonzero for frequencies in the vicinity of the origin (i.e.,  $f = 0$ ) and negligible elsewhere.

**DEFINITION.** A *bandpass* waveform has a spectral magnitude that is nonzero for frequencies in some band concentrated about a frequency  $f = \pm f_c$ , where  $f_c \gg 0$ . The spectral magnitude is negligible elsewhere.  $f_c$  is called the *carrier frequency*.

For bandpass waveforms the value of  $f_c$  may be arbitrarily assigned for mathematical convenience in *some* problems. In others, namely, modulation problems,  $f_c$  is the frequency of an oscillatory signal in the transmitter circuit and is the assigned frequency of the transmitter, such as, for example, 850 kHz for an AM broadcasting station.

In communication problems, the information source signal is usually a baseband signal: for example, a transistor-transistor logic (TTL) waveform from a digital circuit or an audio (analog) signal from a microphone. The communication engineer has the job of building a system that will transfer the information in this source signal  $m(t)$  to the desired destination. As shown in Fig. 4-1, this usually requires the use of a bandpass signal,  $s(t)$ , which has a bandpass spectrum that is concentrated at  $\pm f_c$ , where  $f_c$  is selected so that  $s(t)$  will propagate across the communication channel (either a softwire or a hardwire channel).

**DEFINITION.** *Modulation* is the process of imparting the source information onto a bandpass signal with a carrier frequency  $f_c$  by the introduction of amplitude and/or phase perturbations. This bandpass signal is called the *modulated* signal  $s(t)$ , and the baseband source signal is called the *modulating* signal  $m(t)$ .

Examples of exactly how modulation is accomplished are given later in this chapter. This definition indicates that modulation may be visualized as a mapping operation that maps the source information onto the bandpass signal  $s(t)$  that will be transmitted over the channel.

As the modulated signal passes through the channel, noise corrupts it. The result is a bandpass signal-plus-noise waveform that is available at the receiver input,  $r(t)$  (see Fig. 4-1). The receiver has the job of trying to recover the information that was sent from the source.  $\tilde{m}$  denotes the corrupted version of  $m$ .

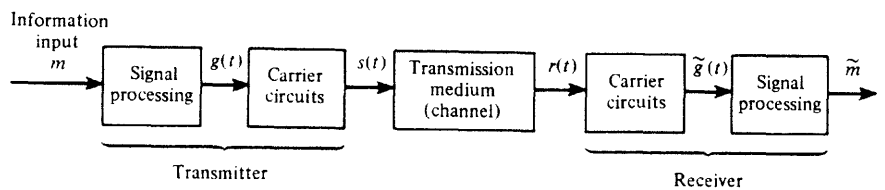


Figure 4-1 Communication system.

## Complex Envelope Representation

All bandpass waveforms, whether they arise from a modulated signal, interfering signals, or noise, may be represented in a convenient form given by the following theorem.  $v(t)$  will be used to denote the bandpass waveform canonically; specifically,  $v(t)$  can represent the signal when  $s(t) \equiv v(t)$ , the noise when  $n(t) \equiv v(t)$ , the filtered signal plus noise at the channel output when  $r(t) \equiv v(t)$ , or any other type of bandpass waveform.<sup>†</sup>

**THEOREM.** Any physical bandpass waveform can be represented by

$$v(t) = \operatorname{Re}\{g(t)e^{j\omega_c t}\} \quad (4-1a)$$

$\operatorname{Re}\{\cdot\}$  denotes the real part of  $\{\cdot\}$ ,  $g(t)$  is called the complex envelope of  $v(t)$ , and  $\omega_c$  is the associated carrier frequency (hertz) where  $\omega_c = 2\pi f_c$ . Furthermore, two other equivalent representations are

$$v(t) = R(t) \cos[\omega_c t + \theta(t)] \quad (4-1b)$$

and

$$v(t) = x(t) \cos \omega_c t - y(t) \sin \omega_c t \quad (4-1c)$$

where

$$g(t) = x(t) + jy(t) = |g(t)| e^{j\angle g(t)} \equiv R(t)e^{j\theta(t)} \quad (4-2)$$

$$x(t) = \operatorname{Re}\{g(t)\} \equiv R(t) \cos \theta(t) \quad (4-3a)$$

$$y(t) = \operatorname{Im}\{g(t)\} \equiv R(t) \sin \theta(t) \quad (4-3b)$$

$$R(t) \triangleq |g(t)| \equiv \sqrt{x^2(t) + y^2(t)} \quad (4-4a)$$

$$\theta(t) \triangleq \angle g(t) = \tan^{-1} \left( \frac{y(t)}{x(t)} \right) \quad (4-4b)$$

The waveforms  $g(t)$ ,  $x(t)$ ,  $y(t)$ ,  $R(t)$ , and  $\theta(t)$  are all baseband waveforms, and, except for  $g(t)$ , they are all real waveforms.  $R(t)$  is a nonnegative real waveform. Thus, (4-1) is a low-pass-to-bandpass transformation.

**Proof.** Any physical waveform (it does not have to be periodic) may be represented over all time,  $T_0 \rightarrow \infty$ , by the complex Fourier series:

$$v(t) = \sum_{n=-\infty}^{n=\infty} c_n e^{jn\omega_0 t}, \quad \omega_0 = 2\pi/T_0 \quad (4-5)$$

Furthermore, because the physical waveform is real  $c_{-n} = c_n^*$  and using  $\operatorname{Re}\{\cdot\} = \frac{1}{2}\{\cdot\} + \frac{1}{2}\{\cdot\}^*$ ,

$$v(t) = \operatorname{Re}\left\{c_0 + 2 \sum_{n=1}^{\infty} c_n e^{jn\omega_0 t}\right\} \quad (4-6)$$

<sup>†</sup> The symbol  $\equiv$  denotes an equivalence and the symbol  $\triangleq$  denotes a definition.

Furthermore, because  $v(t)$  is a bandpass waveform, the  $c_n$  have negligible magnitudes for  $n$  in the vicinity of 0 and, in particular,  $c_0 = 0$ . Thus, with the introduction of an arbitrary parameter  $f_c$ , (4-6) becomes<sup>†</sup>

$$v(t) = \operatorname{Re}\left\{ \left( 2 \sum_{n=1}^{n=\infty} c_n e^{jn(\omega_0 - \omega_c)t} \right) e^{j\omega_c t} \right\} \quad (4-7)$$

so that (4-1a) follows where

$$g(t) \equiv 2 \sum_{n=1}^{\infty} c_n e^{jn(\omega_0 - \omega_c)t} \quad (4-8)$$

Because  $v(t)$  is a bandpass waveform with nonzero spectrum concentrated near  $f = f_c$ , the Fourier coefficients  $c_n$  are nonzero only for values of  $n$  in the range  $\pm n_0 \approx f_c$ . Therefore, from (4-8)  $g(t)$  has a spectrum that is concentrated near  $f = 0$ . That is,  $g(t)$  is a baseband waveform. It is also obvious from (4-8) that  $g(t)$  may be a complex function of time. Representing the complex envelope in terms of two real functions in Cartesian coordinates, we have

$$g(t) \equiv x(t) + jy(t)$$

where  $x(t) = \operatorname{Re}\{g(t)\}$  and  $y(t) = \operatorname{Im}\{g(t)\}$ .  $x(t)$  is said to be the *in-phase modulation* associated with  $v(t)$ , and  $y(t)$  is said to be the *quadrature modulation* associated with  $v(t)$ . Alternatively, the polar form of  $g(t)$ , represented by  $R(t)$  and  $\theta(t)$ , is given by (4-2), where the identities between Cartesian and polar coordinates are given by (4-3) and (4-4).  $R(t)$  and  $\theta(t)$  are real waveforms and, in addition,  $R(t)$  is always nonnegative.  $R(t)$  is said to be the *amplitude modulation* (AM) on  $v(t)$ , and  $\theta(t)$  is said to be the *phase modulation* (PM) on  $v(t)$ . It is also realized that if  $v(t)$  is a deterministic waveform,  $x(t)$ ,  $y(t)$ ,  $R(t)$ , and  $\theta(t)$  are also deterministic. If  $v(t)$  is stochastic, for example, representing bandpass noise,  $x(t)$ ,  $y(t)$ ,  $R(t)$ , and  $\theta(t)$  are stochastic baseband processes. Thus, in general, bandpass noise includes both AM,  $R(t)$ , and PM,  $\theta(t)$ , noise components. This will be discussed further in Chapter 6. The usefulness of the complex envelope representation for bandpass waveforms cannot be overemphasized. In modern communication systems, the bandpass signal is often partitioned into two channels, one for  $x(t)$  called the *I* (in-phase) channel and one for  $y(t)$  called the *Q* (quadrature-phase) channel.

## 4-2 REPRESENTATION OF MODULATED SIGNALS

As defined earlier, modulation is the process of encoding the source information  $m(t)$  (modulating signal) into a bandpass signal  $s(t)$  (modulated signal). Consequently, the modulated signal is just a special application of the bandpass representation. The *modulated signal* is given by

<sup>†</sup> Because the frequencies involved in the argument of  $\operatorname{Re}\{\cdot\}$  are all positive, it can be shown that the complex function  $2 \sum_{n=1}^{\infty} c_n e^{jn\omega_0 t}$  is analytic in the upper-half complex  $t$  plane. Many interesting properties result because this function is an analytic function of a complex variable.

$$s(t) = \operatorname{Re}\{g(t)e^{j\omega_c t}\} \quad (4-9)$$

where  $\omega_c = 2\pi f_c$ .  $f_c$  is the carrier frequency. The complex envelope  $g(t)$  is a function of the modulating signal  $m(t)$ . That is,

$$g(t) = g[m(t)] \quad (4-10)$$

Thus  $g[\cdot]$  performs a mapping operation on  $m(t)$ . This was shown in Fig. 4-1.

Table 4-1 gives an overview on the *big picture* for the modulation problem. Examples of the mapping function  $g[m]$  are given for amplitude modulation (AM), double-sideband suppressed carrier (DSB-SC), phase modulation (PM), frequency modulation (FM), single-sideband AM suppressed carrier (SSB-AM- SC), single-sideband PM (SSB-PM), single-sideband FM (SSB-FM), single-sideband envelope detectable (SSB-EV), single-sideband square-law detectable (SSB-SQ), and quadrature modulation (QM). Modulated signals are discussed in detail in Chapter 5. Digitally modulated bandpass signals are obtained when  $m(t)$  is a digital baseband signal—for example, the output of a transistor transistor logic (TTL) circuit.

Obviously, it is possible to use other  $g[m]$  functions that are not listed in Table 4-1. The question is: Are they useful?  $g[m]$  functions are desired that are easy to implement and that will give desirable spectral properties. Furthermore, in the receiver the inverse function  $m[g]$  is required. The inverse should be single valued over the range used and should be easily implemented. The mapping should suppress as much noise as possible so that  $m(t)$  can be recovered with little corruption.

### 4-3 SPECTRUM OF BANDPASS SIGNALS

The spectrum of a bandpass signal is directly related to the spectrum of its complex envelope.

**THEOREM.** If a bandpass waveform is represented by

$$v(t) = \operatorname{Re}\{g(t)e^{j\omega_c t}\} \quad (4-11)$$

then the spectrum of the bandpass waveform is

$$V(f) = \frac{1}{2}[G(f - f_c) + G^*(-f - f_c)] \quad (4-12)$$

and the PSD of the waveform is

$$\mathcal{P}_v(f) = \frac{1}{4}[\mathcal{P}_g(f - f_c) + \mathcal{P}_g(-f - f_c)] \quad (4-13)$$

where  $G(f) = \mathcal{F}[g(t)]$  and  $\mathcal{P}_g(f)$  is the PSD of  $g(t)$ .

**Proof.**

$$v(t) = \operatorname{Re}\{g(t)e^{j\omega_c t}\} = \frac{1}{2}g(t)e^{j\omega_c t} + \frac{1}{2}g^*(t)e^{-j\omega_c t}$$

Thus,

$$V(f) = \mathcal{F}[v(t)] = \frac{1}{2}\mathcal{F}[g(t)e^{j\omega_c t}] + \frac{1}{2}\mathcal{F}[g^*(t)e^{-j\omega_c t}] \quad (4-14)$$

TABLE 4-1 COMPLEX ENVELOPE FUNCTIONS FOR VARIOUS TYPES OF MODULATION<sup>a</sup>

Type of Modulation	Mapping Functions $g(m)$	Corresponding Quadrature Modulation
	$x(t)$	$y(t)$
AM	$A_c[1 + m(t)]$ $A_c m(t)$	0 0
DSB-SC	$A_c e^{jD_p m(t)}$	$A_c \sin[D_p m(t)]$
PM	$A_c e^{jD_p m(t)}$ $A_c e^{j\int_{-\infty}^t m(\sigma) d\sigma}$	$A_c \sin\left[D_f \int_{-\infty}^t m(\sigma) d\sigma\right]$ $\pm A_c \hat{m}(t)$
FM	$A_c e^{j\int_{-\infty}^t m(\sigma) d\sigma}$	$A_c e^{j\tilde{D}_{pm}(t)} \sin[D_p m(t)]$
SSB-AM-SC <sup>b</sup>	$A_c [m(t) \pm j\hat{m}(t)]$	$A_c e^{\mp D_p m(t)} \cos[D_p m(t)]$
SSB-PM <sup>b</sup>	$A_c e^{jD_p [m(t) \pm j\hat{m}(t)]}$	$A_c e^{\mp D_p m(t)} \cos\left[D_f \int_{-\infty}^t m(\sigma) d\sigma\right]$
SSB-FM <sup>b</sup>	$A_c e^{jD_p \int_{-\infty}^t [m(\sigma) \pm j\hat{m}(\sigma)] d\sigma}$	$A_c e^{\mp D_p m(t)} \sin\left[D_f \int_{-\infty}^t m(\sigma) d\sigma\right]$
SSB-EV <sup>b</sup>	$A_c e^{j[m(t) + m(t)] \pm j\hat{m}(1+m(t))}$	$\pm A_c [1 + m(t)] \sin\{\ln[1 + m(t)]\}$
SSB-SQ <sup>b</sup>	$A_c e^{j(1/2)[m(t) + m(t)] \pm j\hat{m}(1+m(t))}$ $A_c m_1(t) + j m_2(t)$	$\pm A_c \sqrt{1 + m(t)} \sin\{\frac{1}{2} \ln[1 + m(t)]\}$ $A_c m_2(t)$
QM		

Type of Modulation	Corresponding Amplitude and Phase Modulation	$R(t)$	$\theta(t)$	Linearity	Remarks
AM	$A_c  1 + m(t) $	$\begin{cases} 0, & m(t) \geq -1 \\ 180^\circ, & m(t) < -1 \end{cases}$	L <sup>c</sup>	$m(t) > -1$ required for envelope detection	
DSB-SC	$A_c [m(t)]$	$\begin{cases} 0, & m(t) \geq 0 \\ 180^\circ, & m(t) < 0 \end{cases}$	L	Coherent detection required	
PM	$A_c$	$D_p m(t)$	NL	$D_p$ is the phase deviation constant (rad/volt)	
FM	$A_c$	$D_f \int_{-\infty}^t m(\sigma) d\sigma$	NL	$D_f$ is the frequency deviation constant (rad/volt-sec)	
SSB-AM-SC <sup>b</sup>	$A_c \sqrt{[m(t)]^2 + [\hat{m}(t)]^2}$	$\tan^{-1} [\pm \hat{m}(t)/m(t)]$	L		
SSB-PM <sup>b</sup>	$A_c e^{\pm D_p m(t)}$	$D_p m(t)$	NL		
SSB-FM <sup>b</sup>	$A_c e^{\pm D_f \int_{-\infty}^t m(\sigma) d\sigma}$	$D_f \int_{-\infty}^t m(\sigma) d\sigma$	NL	$m(t) > -1$ is required so that the ln(·) will have a real value	
SSB-EV <sup>b</sup>	$A_c  1 + m(t) $	$\pm \ln 1 + m(t) $	NL	$m(t) > -1$ is required so that the ln(·) will have a real value	
SSB-SQ <sup>b</sup>	$A_c \sqrt{ 1 + m(t) }$	$\pm \frac{1}{2} \ln 1 + m(t) $	NL	Used in NTSC color television; requires coherent detection	
QM	$A_c \sqrt{m_1^2(t) + m_2^2(t)}$	$\tan^{-1} [m_2(t)/m_1(t)]$	L		

<sup>a</sup>  $A_c > 0$  is a constant that sets the power level of the signal as evaluated by use of (4-17); L, linear; NL, nonlinear; [ $\cdot$ ] is the Hilbert transform (i.e.,  $-90^\circ$  phase-shifted version) of [ $\cdot$ ] (see Sec. 5-5 and Sec. A-7, Appendix A).

<sup>b</sup> Use upper signs for upper sideband signals and lower signs for lower sideband signals.

<sup>c</sup> In the strict sense, AM signals are not linear because the carrier term does not satisfy the linearity (superposition) condition.

#### Sec. 4-4 Evaluation of Power

If we use  $\mathcal{F}[g^*(t)] = G^*(-f)$  from Table 2-1 and the frequency translation property of Fourier transforms from Table 2-1, this equation becomes

$$V(f) = \frac{1}{2} \{G(f - f_c) + G^*[-(f + f_c)]\} \quad (4-15)$$

which reduces to (4-12).

The PSD for  $v(t)$  is obtained by first evaluating the autocorrelation for  $v(t)$ .

$$R_v(\tau) = \langle v(t)v(t + \tau) \rangle = \langle \text{Re}\{g(t)e^{j\omega_c t}\} \text{Re}\{g(t + \tau)e^{j\omega_c(t + \tau)}\} \rangle$$

Using the identity (see Prob. 2-66),

$$\text{Re}(c_2) \text{Re}(c_1) = \frac{1}{2} \text{Re}(c_2^* c_1) + \frac{1}{2} \text{Re}(c_2 c_1)$$

where  $c_2 = g(t)e^{j\omega_c t}$  and  $c_1 = g(t + \tau)e^{j\omega_c(t + \tau)}$ , we get

$$R_v(\tau) = \left\langle \frac{1}{2} \text{Re}\{g^*(t)g(t + \tau)e^{-j\omega_c t} e^{j\omega_c(t + \tau)}\} \right\rangle + \left\langle \frac{1}{2} \text{Re}\{g(t)g(t + \tau)e^{j\omega_c t} e^{j\omega_c(t + \tau)}\} \right\rangle$$

Realizing that both  $\langle \cdot \rangle$  and  $\text{Re}\{ \cdot \}$  are linear operators, we may exchange the order of the operators without affecting the result, and the autocorrelation becomes

$$R_v(\tau) = \frac{1}{2} \text{Re}\{\langle g^*(t)g(t + \tau)e^{j\omega_c t}\rangle\} + \frac{1}{2} \text{Re}\{\langle g(t)g(t + \tau)e^{j2\omega_c t} e^{j\omega_c t}\rangle\}$$

or

$$R_v(\tau) = \frac{1}{2} \text{Re}\{\langle g^*(t)g(t + \tau)\rangle e^{j\omega_c t}\} + \frac{1}{2} \text{Re}\{\langle g(t)g(t + \tau)e^{j2\omega_c t}\rangle e^{j\omega_c t}\}$$

But  $\langle g^*(t)g(t + \tau)\rangle = R_g(\tau)$ . The second term on the right is negligible because  $e^{j2\omega_c t} = \cos 2\omega_c t + j \sin 2\omega_c t$  oscillates much faster than variations in  $g(t)g(t + \tau)$ . In other words,  $f_c$  is much larger than the frequencies in  $g(t)$ , so the integral is negligible. This is an application of the Riemann-Lebesgue lemma from integral calculus [Olmsted, 1961]. Thus the autocorrelation reduces to

$$R_v(\tau) = \frac{1}{2} \text{Re}\{R_g(\tau)e^{j\omega_c t}\} \quad (4-16)$$

The PSD is obtained by taking the Fourier transform of (4-16) (i.e., applying the Wiener-Khintchine theorem). Note that (4-16) has the same mathematical form as (4-11) when  $t$  is replaced by  $\tau$ , so the Fourier transform has the same form as (4-12). Thus

$$\mathcal{P}_v(f) = \mathcal{F}[R_v(\tau)] = \frac{1}{4} [\mathcal{P}_g(f - f_c) + \mathcal{P}_g^*(-f - f_c)]$$

But  $\mathcal{P}_g^*(f) = \mathcal{P}_g(f)$  since the PSD is a real function. Thus the PSD is given by (4-13).

## 4-4 EVALUATION OF POWER

**THEOREM.** *The total average normalized power of a bandpass waveform,  $v(t)$ , is*

$$P_v = \langle v^2(t) \rangle = \int_{-\infty}^{\infty} \mathcal{P}_v(f) df = R_v(0) = \frac{1}{2} \langle |g(t)|^2 \rangle \quad (4-17)$$

where "normalized" implies that the load is equivalent to one ohm.

**Proof.** Substituting  $v(t)$  into (2-67), we get

$$P_v = \langle v^2(t) \rangle = \int_{-\infty}^{\infty} \mathcal{P}_v(f) df$$

But  $R_v(\tau) = \mathcal{F}^{-1}[\mathcal{P}_v(f)] = \int_{-\infty}^{\infty} \mathcal{P}_v(f) e^{j2\pi f\tau} df$ , so

$$R_v(0) = \int_{-\infty}^{\infty} \mathcal{P}_v(f) df$$

Also, from (4-16),

$$R_v(0) = \frac{1}{2} \operatorname{Re}\{R_g(0)\} = \frac{1}{2} \operatorname{Re}\{\langle g^*(t)g(t+0) \rangle\}$$

or

$$R_v(0) = \frac{1}{2} \operatorname{Re}\{\langle |g(t)|^2 \rangle\}$$

But  $|g(t)|$  is always real, so

$$R_v(0) = \frac{1}{2} \langle |g(t)|^2 \rangle$$

Another type of power rating, called the *peak envelope power* (PEP), is useful for transmitter specifications.

**DEFINITION.** The *peak envelope power* (PEP) is the average power that would be obtained if  $|g(t)|$  were to be held constant at its peak value.

This is equivalent to evaluating the average power in an unmodulated RF sinusoid that has a peak value of  $A_p = \max|v(t)|$ , as is readily seen from Fig. 5-1.

**THEOREM.** The normalized PEP is given by

$$P_{\text{PEP}} = \frac{1}{2} [\max|g(t)|]^2 \quad (4-18)$$

A proof of this theorem follows by applying the definition to (4-17). As described later in Chapters 5 and 8, the PEP is useful for specifying the power capability of AM, SSB, and television transmitters.

#### Example 4-1 AMPLITUDE-MODULATED SIGNAL

Evaluate the magnitude spectrum for an amplitude-modulated (AM) signal. From Table 4-1, the complex envelope of an AM signal is

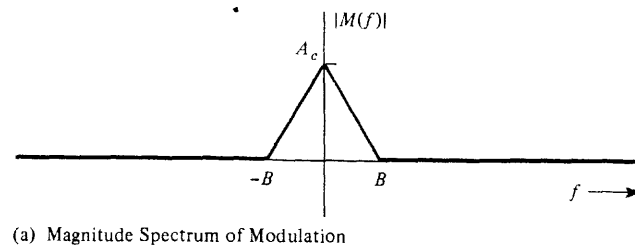
$$g(t) = A_c[1 + m(t)]$$

so that the spectrum of the complex envelope is

$$G(f) = A_c \delta(f) + A_c M(f) \quad (4-19)$$

Using (4-9), we obtain the AM signal waveform

$$s(t) = A_c[1 + m(t)] \cos \omega_c t$$



(a) Magnitude Spectrum of Modulation

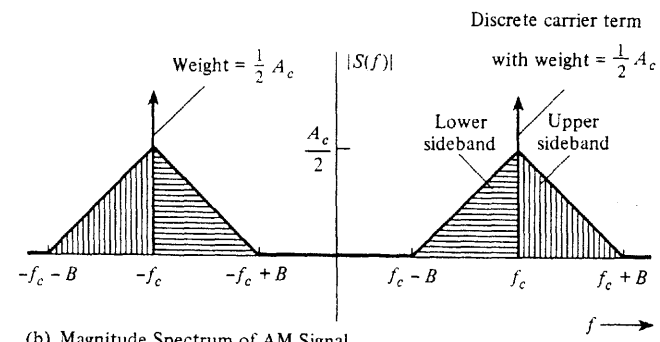


Figure 4-2 Spectrum of AM signal.

and, using (4-12), the AM spectrum

$$S(f) = \frac{1}{2} A_c [\delta(f - f_c) + M(f - f_c) + \delta(f + f_c) + M(f + f_c)] \quad (4-20a)$$

where, because  $m(t)$  is real,  $M^*(f) = M(-f)$ , and  $\delta(f) = \delta(-f)$  (the delta function was defined to be even) were used. Suppose that the magnitude spectrum of the modulation happens to be a triangular function, as shown in Fig. 4-2a. This spectrum might arise from an analog audio source where the bass frequencies are emphasized. The resulting AM spectrum, using (4-20a), is shown in Fig. 4-2b. Note that because  $G(f - f_c)$  and  $G^*(-f - f_c)$  do not overlap, the magnitude spectrum is

$$|S(f)| = \begin{cases} \frac{1}{2} A_c \delta(f - f_c) + \frac{1}{2} A_c |M(f - f_c)|, & f > 0 \\ \frac{1}{2} A_c \delta(f + f_c) + \frac{1}{2} A_c |M(-f - f_c)|, & f < 0 \end{cases} \quad (4-20b)$$

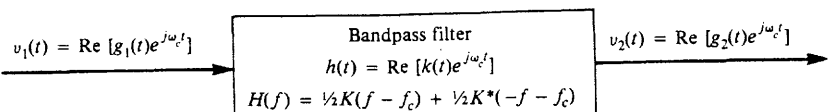
The 1 in  $g(t) = A_c[1 + m(t)]$  causes delta functions to occur in the spectrum at  $f = \pm f_c$ , where  $f_c$  is the assigned carrier frequency. Using (4-17), we obtain the total average signal power

$$\begin{aligned} P_s &= \frac{1}{2} A_c^2 \langle |1 + m(t)|^2 \rangle = \frac{1}{2} A_c^2 (1 + 2m(t) + m^2(t)) \\ &= \frac{1}{2} A_c^2 [1 + 2\langle m(t) \rangle + \langle m^2(t) \rangle] \end{aligned}$$

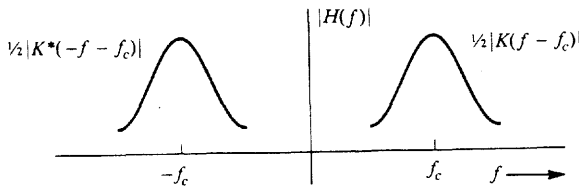
If we assume that the dc value of the modulation is zero, as shown in Fig. 4-2a, the average signal power becomes

$$P_s = \frac{1}{2} A_c^2 [1 + P_m] \quad (4-21)$$

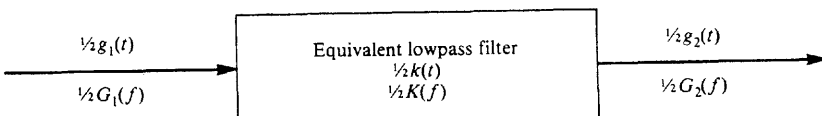
where  $P_m = \langle m^2(t) \rangle$  is the power in the modulation,  $m(t)$ ,  $\frac{1}{2} A_c^2$  is the carrier power, and  $\frac{1}{2} A_c^2 P_m$  is the power in the sidebands of  $s(t)$ .



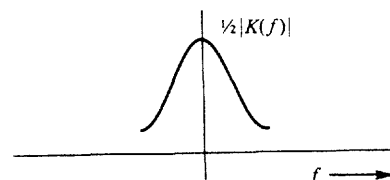
(a) Bandpass Filter



(b) Typical Bandpass Filter Frequency Response



(c) Equivalent (Complex Impulse Response) Lowpass Filter



(d) Typical Equivalent Lowpass Filter Frequency Response

Figure 4-3 Bandpass filtering.

## 4-5 BANDPASS FILTERING AND LINEAR DISTORTION

### Equivalent Low-Pass Filter

In Sec. 2-6 the general transfer function technique was described for the treatment of linear filter problems. Now a shortcut technique will be developed for modeling a bandpass filter by using an equivalent low-pass filter that has a complex valued impulse response (see Fig. 4-3a).  $v_1(t)$  and  $v_2(t)$  are the input and output bandpass waveforms with the corresponding complex envelopes  $g_1(t)$  and  $g_2(t)$ . The impulse response of the bandpass filter,  $h(t)$ , can also be represented by its corresponding complex envelope  $k(t)$ . In addition, as shown in Fig. 4-3a, the frequency domain description,  $H(f)$ , can be expressed in terms of  $K(f)$  with the help of (4-11) and (4-12). Figure 4-3b shows a typical bandpass frequency response characteristic  $|H(f)|$ .

**THEOREM.** *The complex envelopes for the input, output, and impulse response of a bandpass filter are related by*

$$\frac{1}{2}g_2(t) = \frac{1}{2}g_1(t) * \frac{1}{2}k(t) \quad (4-22)$$

where  $g_1(t)$  is the complex envelope of the input and  $k(t)$  is the complex envelope of the impulse response. It also follows that

$$\frac{1}{2}G_2(f) = \frac{1}{2}G_1(f) \frac{1}{2}K(f) \quad (4-23)$$

**Proof.** We know that the spectrum of the output is

$$V_2(f) = V_1(f) H(f) \quad (4-24)$$

Because  $v_1(t)$ ,  $v_2(t)$ , and  $h(t)$  are all bandpass waveforms, the spectra of these waveforms are related to the spectra of their complex envelopes by (4-15); thus, (4-24) becomes

$$\begin{aligned} & \frac{1}{2}[G_2(f - f_c) + G_2^*(-f - f_c)] \\ &= \frac{1}{2}[G_1(f - f_c) + G_1^*(-f - f_c)] \frac{1}{2}[K(f - f_c) + K^*(-f - f_c)] \quad (4-25) \\ &= \frac{1}{4}[G_1(f - f_c) K(f - f_c) + G_1(f - f_c) K^*(-f - f_c) \\ & \quad + G_1^*(-f - f_c) K(f - f_c) + G_1^*(-f - f_c) K^*(-f - f_c)] \end{aligned}$$

But  $G_1(f - f_c) K^*(-f - f_c) = 0$  because the spectrum of  $G_1(f - f_c)$  is zero in the region of frequencies around  $-f_c$ , where  $K^*(-f - f_c)$  is nonzero. That is, there is no spectral overlap of  $G_1(f - f_c)$  and  $K^*(-f - f_c)$  because  $G_1(f)$  and  $K(f)$  have nonzero spectra around only  $f = 0$  (i.e., baseband, as illustrated in Fig. 4-3d). Similarly,  $G_1^*(-f - f_c) K(f - f_c) = 0$ . Consequently, (4-25) becomes

$$\begin{aligned} & [\frac{1}{2}G_2(f - f_c)] + [\frac{1}{2}G_2^*(-f - f_c)] \\ &= [\frac{1}{2}G_1(f - f_c) \frac{1}{2}K(f - f_c)] + [\frac{1}{2}G_1^*(-f - f_c) \frac{1}{2}K^*(-f - f_c)] \quad (4-26) \end{aligned}$$

Thus,  $\frac{1}{2}G_2(f) = \frac{1}{2}G_1(f) \frac{1}{2}K(f)$ , which is identical to (4-23). Taking the inverse Fourier transform of both sides of (4-23), (4-22) is obtained.

This theorem indicates that any bandpass filter system may be described and analyzed by using an *equivalent low-pass filter* as shown in Fig. 4-3c. A typical equivalent low-pass frequency response characteristic is shown in Fig. 4-3d. Equations for equivalent low-pass filters are usually much less complicated than those for bandpass filters, so the equivalent low-pass filter system model is very useful. Because the highest frequency is much smaller in the equivalent low-pass filter, it is the basis for computer programs that simulate bandpass communication systems.

It is realized that the linear bandpass filter can produce variations in the phase modulation at the output,  $\theta_2(t)$ , where  $\theta_2(t) = \int g_2(t) dt$  as a function of the amplitude modulation on the input complex envelope,  $R_1(t)$ , where  $R_1(t) = |g_1(t)|$ . This is called *AM-to-PM conversion*. Similarly, the filter can also cause variations on the AM at the output,  $R_2(t)$ , because of the PM on the input,  $\theta_1(t)$ . This is called *PM-to-AM conversion*.

Because  $h(t)$  represents a linear filter,  $g_2(t)$  will be a linear filtered version of  $g_1(t)$ ; however,  $\theta_2(t)$  and  $R_2(t)$ —the PM and AM components of  $g_2(t)$ —will be a *nonlinear* fil-

tered version of  $g_1(t)$  since  $\theta_2(t)$  and  $R_2(t)$  are nonlinear functions of  $g_2(t)$ . The analysis of the nonlinear distortion is very complicated. Although many analysis techniques have been published in the literature, none has been entirely satisfactory. Panter [1965] gives a three-chapter summary of some of these techniques, and a classical paper is also recommended [Bedrosian and Rice, 1968]. Furthermore, nonlinearities that occur in a practical system will also cause nonlinear distortion and AM-to-PM conversion effects. Nonlinear effects can be analyzed by several techniques, including power-series analysis; this is discussed in the section on amplifiers that follows later in this chapter. If a nonlinear effect in a *bandpass* system is to be analyzed, a Fourier series technique that uses the Chebyshev transform has been found to be useful [Spilker, 1977].

### Linear Distortion

In Sec. 2-6 the general conditions were found for distortionless transmission. For linear *bandpass filters* (channels), a less restrictive set of conditions will now be shown to be satisfactory. For distortionless transmission of bandpass signals, the channel transfer function,  $H(f) = |H(f)|e^{j\theta(f)}$ , needs to satisfy the following requirements:

- The amplitude response is constant. That is,

$$|H(f)| = A \quad (4-27a)$$

where  $A$  is a positive (real) constant.

- The derivative of the phase response is a constant. That is,

$$-\frac{1}{2\pi} \frac{d\theta(f)}{df} = T_g \quad (4-27b)$$

where  $T_g$  is a constant called the complex *envelope delay* or, more concisely, the *group delay* and  $\theta(f) = \angle H(f)$ .

This is illustrated in Fig. 4-4. Note that (4-27a) is identical to the general requirement of (2-150a), but (4-27b) is less restrictive than (2-150b). That is, if (2-150b) is satisfied, (4-27b) is satisfied where  $T_d = T_g$ ; however, if (4-27b) is satisfied, (2-150b) is not necessarily satisfied because the integral of (4-27b) is

$$\theta(f) = -2\pi f T_g + \theta_0 \quad (4-28)$$

where  $\theta_0$  is a phase-shift constant, as shown in Fig. 4-4b. If  $\theta_0$  happens to be nonzero, (2-150b) is not satisfied.

Now it will be shown that (4-27a) and (4-27b) are sufficient requirements for distortionless transmission of bandpass signals. From (4-27a) and (4-28) the channel (or filter) transfer function is

$$H(f) = Ae^{j(-2\pi f T_g + \theta_0)} = (Ae^{j\theta_0})e^{-j2\pi f T_g} \quad (4-29)$$

over the bandpass of the signal. If the input to the bandpass channel is represented by

$$v_1(t) = x(t) \cos \omega_c t - y(t) \sin \omega_c t$$

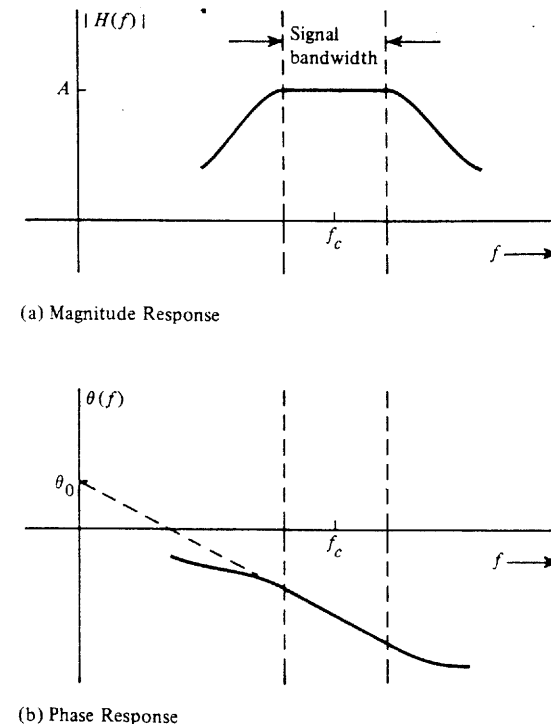


**Figure 4-4** Transfer characteristics of a distortionless bandpass channel.

then, using (4-29) and realizing that  $e^{-j2\pi f T_g}$  causes a delay of  $T_g$ , the output of the channel is

$$v_2(t) = Ax(t - T_g) \cos[\omega_c(t - T_g) + \theta_0] - Ay(t - T_g) \sin[\omega_c(t - T_g) + \theta_0]$$

Using (4-28), we obtain

$$v_2(t) = Ax(t - T_g) \cos[\omega_c t + \theta(f_c)] - Ay(t - T_g) \sin[\omega_c t + \theta(f_c)]$$

where, by use of (2-150b) evaluated at  $f = f_c$ ,

$$\theta(f_c) = -\omega_c T_g + \theta_0 = -2\pi f_c T_g$$

Thus, the output bandpass signal can be described by

$$v_2(t) = Ax(t - T_g) \cos[\omega_c(t - T_d)] - Ay(t - T_g) \sin[\omega_c(t - T_d)] \quad (4-30)$$

where the modulation on the carrier (i.e., the  $x$  and  $y$  components) has been delayed by the *group time delay*,  $T_g$ , and the carrier has been delayed by the *carrier time delay*,  $T_d$ . Because  $\theta(f_c) = -2\pi f_c T_d$ , where  $\theta(f_c)$  is the carrier phase shift,  $T_d$  is also called the *phase delay*. Equation (4-30) demonstrates that the bandpass filter delays the input complex envelope (i.e., the input information) by  $T_g$  seconds, whereas the carrier is delayed by  $T_d$  s. This is distortionless transmission, which is obtained when (4-27a) and (4-27b) are satisfied. Note that  $T_g$  will differ from  $T_d$  unless  $\theta_0$  happens to be zero.

In summary, the general requirements for distortionless transmission of either baseband or bandpass signals are given by (2-150a) and (2-150b). However, for the bandpass case (2-150b) is overly restrictive and may be replaced by (4-27b). (In this case  $T_d \neq T_g$  unless  $\theta_0 = 0$ .) That is, for distortionless *bandpass* transmission, it is only necessary to have a transfer function with a *constant amplitude* and a *constant phase derivative* over the bandwidth of the signal.

## 4-6 BANDPASS SAMPLING THEOREM

Computer simulation is often used to analyze the performance of complicated communication systems, especially when coding schemes are used. This requires that the RF signal and noise for the system under test be sampled so that the data can be obtained for processing by digital computer simulation. If the sampling were carried out at the Nyquist rate or larger ( $f_s \geq 2B$ , where  $B$  is the highest frequency involved in the spectrum of the RF signal), the sampling rate would be ridiculous. For example, consider a satellite communication system with a carrier frequency of  $f_c = 6$  GHz. The sampling rate required would be at least 12 GHz. Fortunately, for the signals of this type (bandpass signals), it can be shown that the sampling rate depends only on the *bandwidth* of the signal, not on the absolute frequencies involved. This is equivalent to saying that we can reproduce the signal from samples of the complex envelope.

**THEOREM. BANDPASS SAMPLING THEOREM:** *If a (real) bandpass waveform has a nonzero spectrum only over the frequency interval  $f_1 < |f| < f_2$  where the transmission bandwidth  $B_T$  is taken to be the absolute bandwidth given by  $B_T = f_2 - f_1$ , then the waveform may be reproduced from sample values, if the sampling rate is*

$$f_s \geq 2B_T \quad (4-31)$$

This theorem may be demonstrated by using the quadrature bandpass representation

$$v(t) = x(t) \cos \omega_c t - y(t) \sin \omega_c t \quad (4-32)$$

Let  $f_c$  be the center of the bandpass so that  $f_c = (f_2 + f_1)/2$ . Then, from (4-8) it is seen that both  $x(t)$  and  $y(t)$  are baseband signals and absolutely bandlimited to  $B = B_T/2$ . From the baseband sampling theorem the sampling rate required to represent these baseband signals is  $f_b \geq 2B = B_T$ . Equation (4-32) becomes

$$v(t) = \sum_{n=-\infty}^{n=\infty} \left[ x\left(\frac{n}{f_b}\right) \cos \omega_c t - y\left(\frac{n}{f_b}\right) \sin \omega_c t \right] \frac{\sin(\pi f_b [t - (n/f_b)])}{\pi f_b [t - (n/f_b)]} \quad (4-33)$$

For the general case, where the  $x(n/f_b)$  and  $y(n/f_b)$  samples are independent, two real samples are obtained for each value of  $n$  so that the overall sampling rate for  $v(t)$  is  $f_s = 2f_b \geq 2B_T$ . This is the bandpass sampling frequency requirement of (4-31). In most engineering applications,  $f_c \gg B_T$ . Thus the  $x$  and  $y$  samples can be obtained by sampling  $v(t)$  at  $t \approx (n/f_b)$ , but adjusting  $t$  slightly, so that  $\cos \omega_c t = 1$  and  $\sin \omega_c t = -1$  at the *exact* sampling time for  $x$  and  $y$ , respectively. That is, for  $t \approx n/f_s$ ,  $v(n/f_b) = x(n/f_b)$  when

$\cos \omega_c t = 1$  (i.e.,  $\sin \omega_c t = 0$ ) and  $v(n/f_b) = y(n/f_b)$  when  $\sin \omega_c t = -1$  (i.e.,  $\cos \omega_c t = 0$ ). If  $f_c$  is not large enough for the  $x$  and  $y$  samples to be obtained directly from  $v(t)$ , then  $x(t)$  and  $y(t)$  can first be obtained by the use of two quadrature product detectors as described by (4-76). The  $x(t)$  and  $y(t)$  baseband signals can then be individually sampled at a rate of  $f_b$ , and it is seen that the overall equivalent sampling rate is still  $f_s = 2f_b \geq 2B_T$ .

**THEOREM. BANDPASS DIMENSIONALITY THEOREM:** *Assume that a bandpass waveform has a nonzero spectrum only over the frequency interval  $f_1 < |f| < f_2$  where the transmission bandwidth  $B_T$  is taken to be the absolute bandwidth given by  $B_T = f_2 - f_1$  and  $B_T \ll f_1$ . The waveform may be completely specified over a  $T_0$ -second interval by*

$$N = 2B_T T_0 \quad (4-34)$$

independent pieces of information.  $N$  is said to be the number of dimensions required to specify the waveform.

Computer simulation is often used to analyze communication systems. The bandpass dimensionality theorem tells us that a bandpass signal  $B_T$  Hz wide can be represented over a  $T_0$ -s interval provided that at least  $N = 2B_T T_0$  samples are used. More details about the bandpass sampling theorem are discussed in study-aid problem SA4-5.

## 4-7 RECEIVED SIGNAL PLUS NOISE

Using the representation of bandpass signals and including the effects of channel filtering, a model for the received signal plus noise will now be obtained. Referring to Fig. 4-1, the signal out of the transmitter is

$$s(t) = \text{Re}[g(t)e^{j\omega_c t}]$$

where  $g(t)$  is the complex envelope for the particular type of modulation used (see Table 4-1).

A good mathematical model for the received signal plus noise,  $r(t)$ , may or may not be easy to obtain, depending on the complexity of the channel. If the channel is linear and time invariant, then

$$r(t) = s(t) * h(t) + n(t) \quad (4-35)$$

where  $h(t)$  is the impulse response of the channel and  $n(t)$  is the noise at the receiver input. Furthermore, if the channel is distortionless, its transfer function is given by (4-29), and consequently, the signal plus noise at the receiver input is

$$r(t) = \text{Re}[A g(t - T_g) e^{j(\omega_c t + \theta(f_c))} + n(t)] \quad (4-36)$$

where  $A$  is the gain of the channel (a positive number and usually less than 1),  $T_g$  is the channel group delay, and  $\theta(f_c)$  is the carrier phase shift caused by the channel. In practice, the values for  $T_g$  and  $\theta(f_c)$  are often not known, so that if values for  $T_g$  and  $\theta(f_c)$  are needed by the receiver to detect the information that was transmitted, receiver circuits are devised to recover (i.e., estimate) the received carrier phase  $\theta(f_c)$  and the group delay (e.g., a bit syn-

chronizer for the case of digital signaling). To carry out a detailed analysis of the receiver performance when there are errors due to poor estimates of received carrier phase and group delay is beyond the scope of this book. (These topics are appropriate for advanced graduate courses.) Consequently, we will assume that the receiver circuits are designed to make these effects negligible; therefore, we can consider the signal plus noise at the receiver input to be

$$r(t) = \operatorname{Re}[g(t)e^{j\omega_c t}] + n(t) \quad (4-37)$$

where the effects of channel filtering, if any, are included by some modification of the complex envelope,  $g(t)$ , and the constant  $A_c$  that is implicit within  $g(t)$  (see Table 4-1) is adjusted to reflect the effect of channel attenuation. Details of this approach are worked out in Sec. 8-6.

Given that (4-37) models the receiver input, the receiver output,  $\tilde{m}(t)$ , depends on the type of functional blocks used within the receiver, such as filters, limiters, and detectors. These blocks are described in Sects. 4-8 to 4-14 and their effects are summarized in Table 4-4.

## 4-8 CLASSIFICATION OF FILTERS AND AMPLIFIERS

### Filters

Filters are devices that take an input waveshape and modify the frequency spectrum to produce the output waveshape. Filters may be classified in several ways. One is by the type of construction used, such as  $LC$  elements or quartz crystal elements. Another is by the type of transfer function that is realized, such as the Butterworth or Chebyshev response (defined subsequently). These two topics of construction types and transfer function characteristics are discussed in this section.

Filters use energy storage elements to obtain frequency discrimination. In any physical filter the energy storage elements are imperfect. For example, a physical inductor has some series resistance as well as inductance, and a physical capacitor has some shunt (leakage) resistance as well as capacitance. A natural question, then, is: What is the quality,  $Q$ , of a circuit element or filter? Unfortunately, two different measures of filter quality are used in the technical literature. The first definition is concerned with the efficiency of *energy storage* in a circuit; it is [Ramo, Whinnery, and vanDuzer, 1967, 1984]

$$Q = \frac{2\pi(\text{maximum energy stored during one cycle})}{\text{energy dissipated per cycle}} \quad (4-38)$$

A larger value for  $Q$  corresponds to a more perfect storage element. That is, a perfect  $L$  or  $C$  element would have infinite  $Q$ . The second definition is concerned with the *frequency selectivity* of a circuit; it is

$$Q = \frac{f_0}{B} \quad (4-39)$$

where  $f_0$  is the resonant frequency and  $B$  is the 3-dB bandwidth. Here the larger the value of  $Q$ , the better the frequency selectivity, because for a given  $f_0$ , the bandwidth would be smaller.

In general, the value of  $Q$  as evaluated using (4-38) is different from the value of  $Q$  obtained from (4-39). However, these two definitions give identical values for an  $RLC$  series resonant circuit driven by a voltage source or for an  $RLC$  parallel resonant circuit driven by a current source [Nilsson, 1990]. For bandpass filtering applications, frequency selectivity is the desired characteristic, so (4-39) is used. Also, (4-39) is easy to evaluate from laboratory measurements. If we are designing a passive filter (not necessarily a single-tuned circuit) of center frequency  $f_0$  and 3-dB bandwidth  $B$ , the individual circuit elements will each need to have much larger  $Q$ s than  $f_0/B$ . Thus, for a practical filter design we first need to answer the question: What are the  $Q$ s needed for the filter elements, and what kind of elements will give these values of  $Q$ ? This question is answered in Table 4-2.

Table 4-2 lists filters as classified by the type of energy storage elements used in their construction and gives typical values for the  $Q$  of the elements. Filters that use lumped<sup>†</sup>  $L$  and  $C$  elements become impractical to build above 300 MHz because the parasitic capacitance and inductance of the leads significantly affect the frequency response at high frequencies. Active filters, which use operational amplifiers with  $RC$  circuit elements, are practical only below 500 kHz because the op amps need to have a large open-loop gain over the operating band. For very low-frequency filters,  $RC$  active filters are usually preferred to  $LC$  passive filters because the size of the  $LC$  components becomes large and the  $Q$  of the inductors becomes small in this frequency range. Active filters are difficult to implement within integrated circuits because the resistors and capacitors take up a significant portion of the chip area. This difficulty is reduced by using a switched capacitor design for IC implementation. In this case, resistors are replaced by an arrangement of electronic switches and capacitors that are controlled by a digital clock signal [Schaumann, et al., 1990].

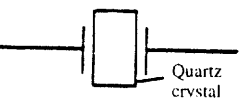
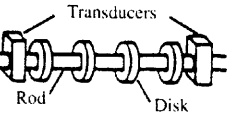
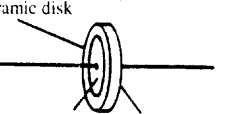
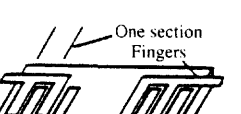
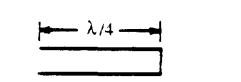
Crystal filters are manufactured from quartz crystal elements. These act as a series resonant circuit in parallel with a shunt capacitance caused by the holder (mounting). Thus a parallel resonant as well as a series resonant mode of operation is possible. Above 100 MHz the quartz element becomes physically too small to manufacture, and below 1 kHz the size of the element becomes prohibitively large. Crystal filters have excellent performance because of the inherently high  $Q$  of the elements, but they are more expensive than  $LC$  and ceramic filters.

Mechanical filters use the vibrations of a resonant mechanical system to obtain the filtering action. The mechanical system usually consists of a series of disks spaced along a rod. Transducers are mounted on each end of the rod to convert the electrical signals to mechanical vibrations at the input, and vice versa at the output. Each disk is the mechanical equivalent of a high- $Q$  electrical parallel resonant circuit. The mechanical filter usually has a high insertion loss resulting from the inefficiency of the input and output transducers.

Ceramic filters are constructed from piezoelectric ceramic disks with plated electrode connections on opposite sides of the disk. The behavior of the ceramic element is similar to that of the crystal filter element, as discussed earlier, except that the  $Q$  of the ceramic ele-

<sup>†</sup> A lumped element is a discrete  $R$ -,  $L$ -, or  $C$ -type element compared with a continuously distributed  $RLC$  element, such as that found in a transmission line.

TABLE 4-2 FILTER CONSTRUCTION TECHNIQUES

Construction Type	Description of Elements or Filter	Center Frequency Range	Unloaded Q (Typical)	Filter Application <sup>a</sup>
LC (passive)		dc-300 MHz	100	Audio, video, IF, and RF
Active and Switched Capacitor		dc-500 kHz	200 <sup>b</sup>	Audio
Crystal		1 kHz-100 MHz	100,000	IF
Mechanical		50-500 kHz	1,000	IF
Ceramic		10 kHz-10.7 MHz	1,000	IF
Surface acoustic waves (SAW)		10-800 MHz	<sup>c</sup>	IF and RF
Transmission line		UHF and microwave	1,000	RF
Cavity		Microwave	10,000	RF

<sup>a</sup> IF, intermediate frequency; RF, radio frequency (see Sec. 4-15).<sup>b</sup> Bandpass Q's.<sup>c</sup> Depends on design:  $N = f_0/B$ , where  $N$  is the number of sections,  $f_0$  is the center frequency, and  $B$  is the bandwidth. Loaded Qs of 18,000 have been achieved.

ment is much lower. The advantage of the ceramic filter is that it often provides adequate performance at a cost that is low when compared to that for crystal filters.

Surface acoustic wave (SAW) filters utilize acoustic waves that are launched and travel on the surface of a piezoelectric substrate (slab). Metallic interleaved "fingers" have been deposited on the substrate. The voltage signal on the fingers is converted to an acoustic signal (and vice versa) as the result of the piezoelectric effect. The geometry of the fingers determines the frequency response of the filter as well as providing the input and output coupling [Dorf, 1993, pp. 1073-1074]. The insertion loss is somewhat larger than that for crystal or ceramic filters. However, the ease of shaping the transfer function and the wide bandwidth that can be obtained with controlled attenuation characteristics make the SAW filters very attractive. This new technology is being used to provide excellent IF amplifier characteristics in modern television sets.

SAW devices can also be tapped so that they are useful for transversal filter configurations operating in the RF range. At lower frequencies, charge transfer devices (CTDs) can be used to implement transversal filters [Gersho, 1975].

Transmission line filters utilize the resonant properties of open-circuited or short-circuited transmission lines. These are useful at UHF and microwave frequencies where wavelengths are small enough so that filters of reasonable size can be constructed. Similarly, the resonant effect of cavities is useful in building filters for microwave frequencies where the cavity size becomes small enough to be practical.

Filters are also characterized by the type of transfer function that is realized. The transfer function of a linear filter with lumped circuit elements may be written as the ratio of two polynomials

$$H(f) = \frac{b_0 + b_1(j\omega) + b_2(j\omega)^2 + \cdots + b_k(j\omega)^k}{a_0 + a_1(j\omega) + a_2(j\omega)^2 + \cdots + a_n(j\omega)^n} \quad (4-40)$$

where the constants  $a_i$  and  $b_i$  are functions of the element values and  $\omega = 2\pi f$ . The parameter  $n$  is said to be the *order* of the filter. By adjusting the constants to certain values, desirable transfer function characteristics can be obtained. Table 4-3 lists three different filter characteristics and the optimization criterion that defines each one. The Chebyshev filter is used when a sharp attenuation characteristic is required when using a minimum number of circuit elements. The Bessel filter is often used in data transmission when the pulse shape is to be preserved since it attempts to maintain a linear phase response in the passband. The Butterworth filter is often used as a compromise between the Chebyshev and Bessel characteristics.

The topic of filters is immense, and all aspects of filtering cannot possibly be covered here. For example, with the advent of inexpensive microprocessors, *digital filtering* and *digital signal processing* is becoming very important [Oppenheim and Schafer, 1975, 1989]. Here the analog waveform is sampled, and the sample values are processed by using digital techniques. Difference equations (as opposed to differential equations) describe this type of filtering operation. By changing the software, different filter characteristics can be realized. This technique of filter realization by software programming instead of hardware programming has many advantages.

TABLE 4-3 SOME FILTER CHARACTERISTICS

Type	Optimization Criterion	Transfer Characteristic for the Low-Pass Filter <sup>a</sup>
Butterworth	Maximally flat: as many derivatives of $ H(f) $ as possible go to zero as $f \rightarrow 0$	$ H(f)  = \frac{1}{\sqrt{1 + (f/f_b)^{2n}}}$
Chebyshev	For a given peak-to-peak ripple in the passband of the $ H(f) $ characteristic, the $ H(f) $ attenuates the fastest for any filter of $n$ th order	$ H(f)  = \frac{1}{\sqrt{1 + \epsilon^2 C_n^2(f/f_b)}}$ $\epsilon$ = a design constant; $C_n(f)$ is the $n$ th-order Chebyshev polynomial defined by the recursion relation $C_n(x) = 2x C_{n-1}(x) - C_{n-2}(x)$ where $C_0(x) = 1$ and $C_1(x) = x$
Bessel	Attempts to maintain linear phase in the passband	$H(f) = \frac{K_n}{B_n(f/f_b)}$ $K_n$ is a constant chosen to make $H(0) = 1$ and the Bessel recursion relation is $B_n(x) = (2n - 1) B_{n-1}(x) - x^2 B_{n-2}(x)$ where $B_0(x) = 1$ and $B_1(x) = 1 + jx$

<sup>a</sup>  $f_b$  is the cutoff frequency of the filter.

For additional reading on analog filters with emphasis on communication system applications, the reader is referred to the literature [Bowron and Stephenson, 1979].

## Amplifiers

For analysis purposes, electronic circuits and, more specifically, amplifiers can be classified into two main categories:

- Nonlinear circuits
- Linear circuits

(Linearity was defined in Sec. 2-6.) In practice all circuits are nonlinear to some degree, even at low (voltage and current) signal levels, and become highly nonlinear for high signal levels. Linear circuit analysis is often used for the low signal level case since it greatly simplifies the mathematics and it gives accurate answers if the signal level is sufficiently small.

The main categories of nonlinear and linear analysis can be further classified into subcategories of circuits with

- Memory
- No memory

Circuits with memory contain inductive and capacitive effects which cause the present output value to be a function of previous input values as well as the present input value. If a circuit has no memory, its present output value is a function only of its present input value.

In introductory electrical engineering courses, it is first assumed that circuits are linear with no memory (resistive circuits) and, later, linear with memory (*RLC* circuits). It follows that linear amplifiers with memory may be described by a transfer function that is the ratio of the Fourier transform of the output signal divided by the Fourier transform of the input signal. As discussed in Sec. 2-6, the transfer function of a distortionless amplifier is given by  $Ke^{-j\omega T_d}$ , where  $K$  is the voltage gain of the amplifier and  $T_d$  is the delay between the output and input waveforms. If the transfer function of the linear amplifier is not of this form, the output signal will be a *linearly* distorted version of the input signal.

## 4-9 NONLINEAR DISTORTION

In addition to linear distortion, practical amplifiers also produce nonlinear distortion. To examine the effects of nonlinearity and yet keep a mathematical model that is tractable, we will assume that there is *no memory* in the following analysis. Thus, we will look at the present output as a function of the present input in the time domain. If the amplifier is linear, this relationship is

$$v_o(t) = Kv_i(t) \quad (4-41)$$

where  $K$  is the voltage gain of the amplifier. In practice, the output of the amplifier saturates at some value as the amplitude of the input signal is increased. This is illustrated by the nonlinear output-to-input characteristic shown in Fig. 4-5. The output-to-input characteristic may be modeled by a Taylor's expansion about  $v_i = 0$  (i.e., a Maclaurin series):

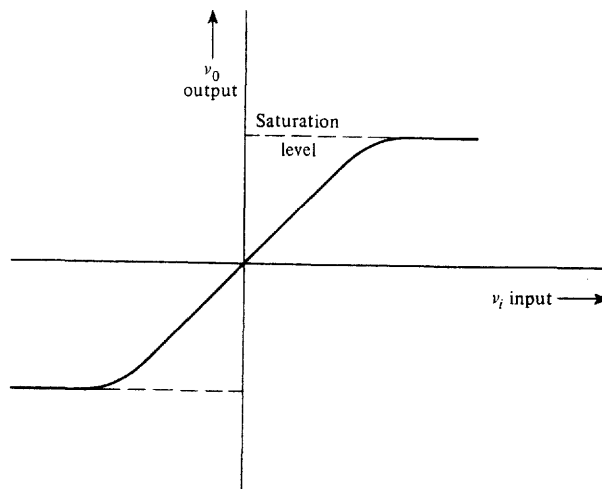


Figure 4-5 Nonlinear amplifier output-to-input characteristic.

$$v_0 = K_0 + K_1 v_i + K_2 v_i^2 + \dots = \sum_{n=0}^{\infty} K_n v_i^n \quad (4-42)$$

where

$$K_n = \frac{1}{n!} \left( \frac{d^n v_0}{dv_i^n} \right) \Big|_{v_i=0} \quad (4-43)$$

It is seen that there will be nonlinear distortion on the output signal if  $K_2, K_3, \dots$ , are not zero.  $K_0$  is the output dc offset level,  $K_1 v_i$  is the first-order (linear) term,  $K_2 v_i^2$  is the second-order (square-law) term, and so on. Of course,  $K_1$  will be larger than  $K_2, K_3, \dots$ , if the amplifier is anywhere near to being linear.

The *harmonic distortion* associated with the amplifier output is determined by applying a single sinusoidal test tone to the amplifier input. Let the input test tone be represented by

$$v_i(t) = A_0 \sin \omega_0 t \quad (4-44)$$

Then the second-order output term is

$$K_2(A_0 \sin \omega_0 t)^2 = \frac{K_2 A_0^2}{2} (1 - \cos 2\omega_0 t) \quad (4-45)$$

This indicates that the second-order distortion creates a dc level  $K_2 A_0^2/2$  (in addition to any dc bias) and second harmonic distortion with amplitude  $K_2 A_0^2/2$ . In general, for a single tone input the output will be

$$\begin{aligned} v_{\text{out}}(t) &= V_0 + V_1 \cos(\omega_0 t + \varphi_1) + V_2 \cos(2\omega_0 t + \varphi_2) \\ &\quad + V_3 \cos(3\omega_0 t + \varphi_3) + \dots \end{aligned} \quad (4-46)$$

where  $V_n$  is the peak value of the output at the frequency  $n f_0$  hertz. Then, the percentage of *total harmonic distortion* (THD) is defined by

$$\text{THD (\%)} = \frac{\sqrt{\sum_{n=2}^{\infty} V_n^2}}{V_1} \times 100 \quad (4-47)$$

The THD of an amplifier can be measured by using a distortion analyzer, or it can be evaluated by (4-47), with the  $V_n$ 's obtained from a spectrum analyzer.

The *intermodulation distortion* (IMD) of the amplifier is obtained by using a two-tone test. If the input (tone) signals are

$$v_i(t) = A_1 \sin \omega_1 t + A_2 \sin \omega_2 t \quad (4-48)$$

then the second-order output term is

$$K_2(A_1 \sin \omega_1 t + A_2 \sin \omega_2 t)^2 = K_2(A_1^2 \sin^2 \omega_1 t + 2A_1 A_2 \sin \omega_1 t \sin \omega_2 t + A_2^2 \sin^2 \omega_2 t)$$

The first and last terms on the right side of this equation produce harmonic distortion at frequencies  $2f_1$  and  $2f_2$ . The cross-product term produces IMD. This term is present only when

both input terms are present—thus, the name “intermodulation distortion.” Then the second-order IMD is

$$2K_2 A_1 A_2 \sin \omega_1 t \sin \omega_2 t = K_2 A_1 A_2 \{\cos[(\omega_1 - \omega_2)t] - \cos[(\omega_1 + \omega_2)t]\}$$

It is clear that IMD generates sum and difference frequencies.

The third-order term is

$$\begin{aligned} K_3 v_i^3 &= K_3(A_1 \sin \omega_1 t + A_2 \sin \omega_2 t)^3 \\ &= K_3(A_1^3 \sin^3 \omega_1 t + 3A_1^2 A_2 \sin^2 \omega_1 t \sin \omega_2 t \\ &\quad + 3A_1 A_2^2 \sin \omega_1 t \sin^2 \omega_2 t + A_2^3 \sin^3 \omega_2 t) \end{aligned} \quad (4-49)$$

The first and last terms on the right side of this equation will produce harmonic distortion and the second term, a cross product, becomes

$$\begin{aligned} 3K_3 A_1^2 A_2 \sin^2 \omega_1 t \sin \omega_2 t &= \frac{3}{2} K_3 A_1^2 A_2 \sin \omega_2 t (1 - \cos 2\omega_1 t) \\ &= \frac{3}{2} K_3 A_1^2 A_2 \{\sin \omega_2 t - \frac{1}{2} [\sin(2\omega_1 + \omega_2)t \\ &\quad - \sin(2\omega_1 - \omega_2)t]\} \end{aligned} \quad (4-50)$$

Similarly, the third term of (4-49) is

$$\begin{aligned} 3K_3 A_1 A_2^2 \sin \omega_1 t \sin^2 \omega_2 t &= \frac{3}{2} K_3 A_1 A_2^2 \{\sin \omega_1 t - \frac{1}{2} [\sin(2\omega_2 + \omega_1)t - \sin(2\omega_2 - \omega_1)t]\} \end{aligned} \quad (4-51)$$

The last two terms in (4-50) and (4-51) are intermodulation terms at nonharmonic frequencies. For the case of *bandpass* amplifiers where  $f_1$  and  $f_2$  are within the bandpass with  $f_1$  close to  $f_2$  (i.e.,  $f_1 \approx f_2 \gg 0$ ), the distortion products at  $2f_1 + f_2$  and  $2f_2 + f_1$  will usually fall outside the passband and, consequently, may not be a problem. However, the terms at  $2f_1 - f_2$  and  $2f_2 - f_1$  will fall inside the passband and will be close to the desired frequencies  $f_1$  and  $f_2$ . These will be the main distortion products for bandpass amplifiers, such as those used for RF amplification in transmitters and receivers.

As (4-50) and (4-51) show, if either  $A_1$  or  $A_2$  is increased sufficiently, the IMD will become significant since the desired output varies linearly with  $A_1$  or  $A_2$  and the IMD output varies as  $A_1^2 A_2$  or  $A_1 A_2^2$ . Of course, the exact input level required for the intermodulation products to be a problem depends on the relative values of  $K_3$  and  $K_1$ . This may be specified by the amplifier third-order *intercept point*, which is evaluated by applying two equal test tones (i.e.,  $A_1 = A_2 = A$ ). The desired linearly amplified outputs will have amplitudes of  $K_1 A$ , and each of the third-order intermodulation products will have amplitudes of  $3K_3 A^3/4$ . The ratio of the desired output to the IMD output is then

$$R_{\text{IMD}} = \frac{4}{3} \left( \frac{K_1}{K_3 A^2} \right) \quad (4-52)$$

The input intercept point is defined as the input level that causes  $R_{\text{IMD}}$  to be unity (see Fig. 4-6). The solid curves are obtained by measurement using two sinusoidal signal generators to generate the tones and measuring the level of the desired output (at  $f_1$  or  $f_2$ ) and the IMD products (at  $2f_1 - f_2$  or  $2f_2 - f_1$ ) using a spectrum analyzer. The intercept point is a fictitious

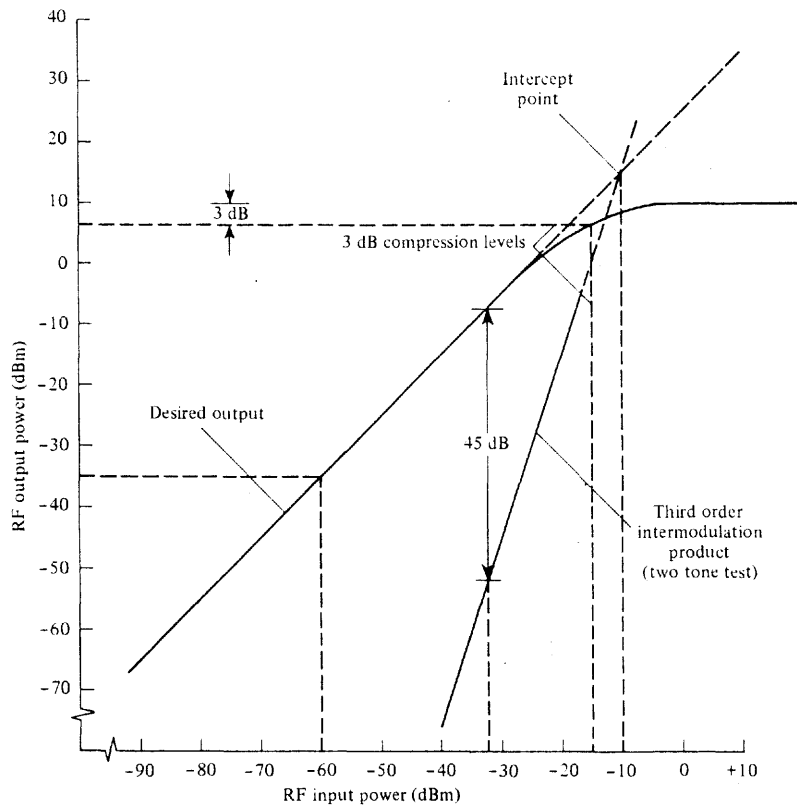


Figure 4-6 Amplifier output characteristics.

tious point that is obtained by extrapolation of the linear portion (decibel plot) of the desired output and IMD curves until they intersect. It is seen that the desired output (output at either  $f_1$  or  $f_2$ ) actually saturates when measurements are made since the higher-order terms in the Taylor series have components at  $f_1$  and  $f_2$  that subtract from the linearly amplified output. For example, with  $K_3$  being negative, the leading term in (4-51) occurs at  $f_1$  and will subtract from the linearly amplified component at  $f_1$ , thus producing a saturated characteristic for the sinusoidal component at  $f_1$ . For an amplifier that happens to have the particular nonlinear characteristic shown in Fig. 4-6, the intercept point occurs for an RF input level of  $-10$  dBm. Other properties of the amplifier are also illustrated in the figure. The gain of the amplifier is  $25$  dB in the linear region because a  $-60$ -dBm input produces a  $-35$  dBm output level. The desired output is compressed by  $3$  dB for an input level of  $-15$  dBm. Consequently, the amplifier might be considered to be linear only if the input level is less than  $-15$  dBm. Furthermore, if the third-order IMD products are to be down by at least  $45$  dBm, the input level will have to be kept lower than  $-32$  dBm.

Another term in the distortion products at the output of a nonlinear amplifier is called *cross-modulation*. Cross-modulation terms are obtained when examining the third-order products resulting from a two-tone test. As shown in (4-50) and (4-51), the terms

$\frac{3}{2}K_3A_1^2A_2 \sin \omega_2 t$  and  $\frac{3}{2}K_3A_1A_2^2 \sin \omega_1 t$  are cross-modulation terms. Let us examine the term  $\frac{3}{2}K_3A_1^2A_2 \sin \omega_2 t$ . If we allow some amplitude variation on the input signal  $A_1 \sin \omega_1 t$  so that it looks like an AM signal  $A_1[1 + m_1(t)] \sin \omega_1 t$ , where  $m_1(t)$  is the modulating signal, a third-order distortion product becomes

$$\frac{3}{2}K_3A_1^2A_2[1 + m_1(t)]^2 \sin \omega_2 t \quad (4-53)$$

Thus, the AM on the signal at carrier frequency  $f_1$  will produce a signal at frequency  $f_2$  with distorted modulation. That is, if two signals are passed through an amplifier having third-order distortion products in the output, and if either input signal has some AM, the amplified output of the *other* signal will be amplitude modulated to some extent by a distorted version of the modulation. This phenomenon is cross modulation.

Passive as well as active circuits may have nonlinear characteristics and, consequently, will produce distortion products. For example, suppose that two AM broadcast stations have strong signals in the vicinity of a barn or house that has a metal roof with rusted joints. The roof may act as an antenna to receive and reradiate the RF energy, and the rusted joints may act as a diode (a nonlinear passive circuit). Signals at harmonics and intermodulation frequencies may be radiated and cause interference to other communication signals. In addition, cross-modulation products may be radiated. That is, distorted modulation of one station is heard on radios (located in the vicinity of the rusted roof) that are tuned to the other station's frequency.

When amplifiers are used to produce high-power signals, such as in transmitters, it is desirable to have amplifiers with high efficiency in order to reduce the costs of power supplies, cooling equipment, and energy consumed. The efficiency is the ratio of the output signal power to the dc input power. Amplifiers may be grouped into several categories, depending on the biasing levels and circuit configurations used. Some of these are Class A, B, C, D, E, F, G, H, and S [Krauss, Bostian, and Raab, 1980; Smith, 1986]. For Class A operation, the bias on the amplifier stage is adjusted so that current flows all during the complete cycle of an applied input test tone. For Class B operation, the amplifier is biased so that current flows for  $180^\circ$  of the applied signal cycle. Therefore, if a Class B amplifier is to be used for a baseband linear amplifier, such as an audio power amplifier in a hi-fi system, two devices are wired in push-pull configuration so that each one alternately conducts current over half of the input signal cycle. In bandpass Class B linear amplification, where the bandwidth is a small percentage of the operating frequency, only one active device is needed since tuned circuits may be used to supply the output current over the other half of the signal cycle. For Class C operation, the bias is set so that (collector or plate) current flows in pulses, each one having a pulse width that is usually much less than half of the input cycle. Unfortunately, with Class C operation, it is not possible to have linear amplification even if the amplifier is a bandpass RF amplifier with tuned circuits providing current over the nonconducting portion of the cycle. If one tries to amplify an AM signal with a Class C amplifier or other types of nonlinear amplifiers, the AM on the output will be distorted. However, RF signals with a constant real envelope, such as FM signals, may be amplified without distortion since a nonlinear amplifier preserves the zero-crossings of the input signal.

The efficiency of a Class C amplifier is determined essentially by the conduction angle of the active device since poor efficiency is caused by signal power being wasted in the

device itself during the conduction time. The Class C amplifier is most efficient, having an efficiency factor of 100% for an ideal Class C amplifier. Class B amplifiers have an efficiency of  $\pi/4 \times 100 = 78.5\%$  or less, and Class A amplifiers have an efficiency of 50% or less [Krauss, Bostian, and Raab, 1980]. Because Class C amplifiers are the most efficient, they are generally used to amplify constant envelope signals, such as FM signals used in FM broadcasting. Class D, E, F, G, H, and S amplifiers usually employ switching techniques in specialized circuits to obtain high efficiency [Krauss, Bostian, and Raab, 1980; Smith, 1986].

Many types of microwave amplifiers, such as traveling-wave tubes (TWT), operate on the velocity modulation principle. The input microwave signal is fed into a slow-wave structure. Here the velocity of propagation of the microwave signal is reduced so that it is slightly below the velocity of the dc electron beam. This enables a transfer of kinetic energy from the electron beam to the microwave signal, thereby amplifying the signal. In this type of amplifier, the electron current is *not* turned on and off to provide the amplifying mechanism; thus it is not classified in terms of Class B or C operation. The TWT is a linear amplifier when operated at the appropriate drive level. If the drive level is increased, the efficiency (RF output/dc input) is improved, but the amplifier becomes nonlinear. In this case constant envelope signals, such as PSK or PM, need to be used so that the intermodulation distortion will not cause a problem. This is often the mode of operation for satellite transponders (transmitters in communication satellites), where solar cells are costly and have limited power output. This subject is discussed in more detail in Chapter 8 in the section on satellite communications.

#### 4-10 LIMITERS

A *limiter* is a nonlinear circuit with an output saturation characteristic. A soft saturating limiter characteristic is shown in Fig. 4-5. Figure 4-7 shows a hard (ideal) limiter characteristic, together with an illustration of the unfiltered output waveform obtained for an input waveform. The ideal limiter transfer function is essentially identical to the output-to-input characteristic of an ideal comparator with a zero reference level. The waveforms shown in Fig. 4-7 illustrate how amplitude variations on the input signal are eliminated on the output signal. A *bandpass limiter* is a nonlinear circuit with a saturating characteristic followed by a bandpass filter. For the case of an ideal bandpass limiter, the filter output waveform would be sinusoidal since the harmonics of the square wave would be filtered out. In general, any bandpass input (it might be a modulated signal plus noise) can be represented, using (4-1b), by

$$v_{in}(t) = R(t) \cos[\omega_c t + \theta(t)] \quad (4-54)$$

where  $R(t)$  is the equivalent real envelope and  $\theta(t)$  is the equivalent phase function. The corresponding output of an ideal bandpass limiter becomes

$$v_{out}(t) = KV_L \cos[\omega_c t + \theta(t)] \quad (4-55)$$

where  $K$  is the level of the fundamental component of the square wave,  $4/\pi$ , multiplied by the gain of the output (bandpass) filter. This equation indicates that any AM that was present on the limiter input does not appear on the limiter output but that the phase function is

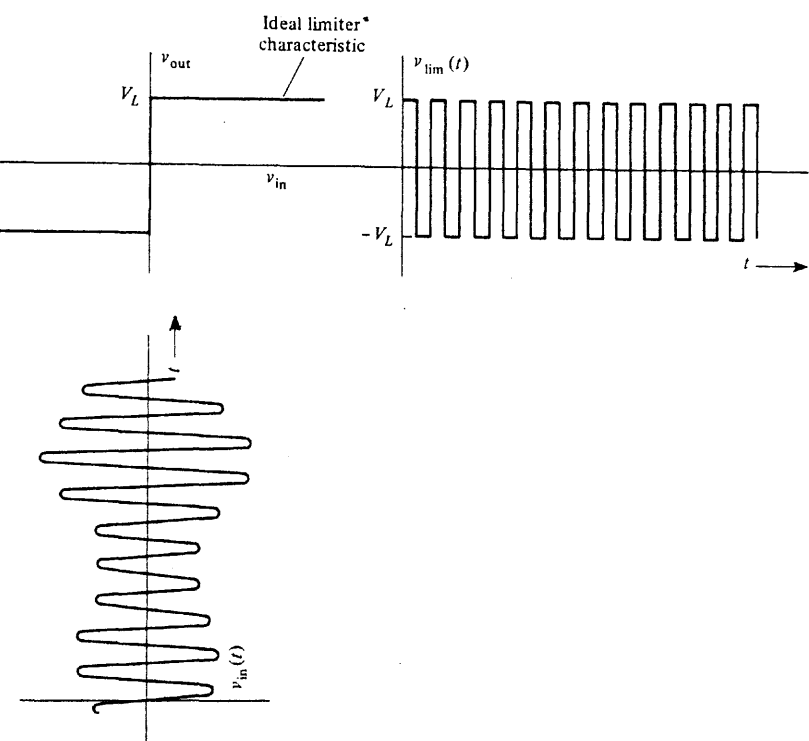


**Figure 4-7** Ideal limiter characteristic with illustrative input and unfiltered output waveforms.

preserved (i.e., the zero-crossings of the input are preserved on the limiter output). Limiters are often used in receiving systems designed for angle modulated signaling—such as PSK, FSK, and analog FM—to eliminate any variations in the real envelope of the receiver input signal that are caused by channel noise or signal fading.

#### 4-11 MIXERS, UP CONVERTERS, AND DOWN CONVERTERS

An *ideal mixer* is an electronic circuit that functions as a mathematical multiplier of two input signals. Usually one of these signals is a sinusoidal waveform produced by a local oscillator, as illustrated in Fig. 4-8.

Mixers are used to obtain frequency translation of the input signal. Assume that the input signal is a bandpass signal that has a nonzero spectrum in a band around or near  $f = f_c$ , then the signal is represented by

$$v_{in}(t) = \operatorname{Re}\{g_{in}(t)e^{j\omega_c t}\} \quad (4-56)$$

where  $g_{in}(t)$  is the complex envelope of the input signal. The signal out of the ideal mixer is then

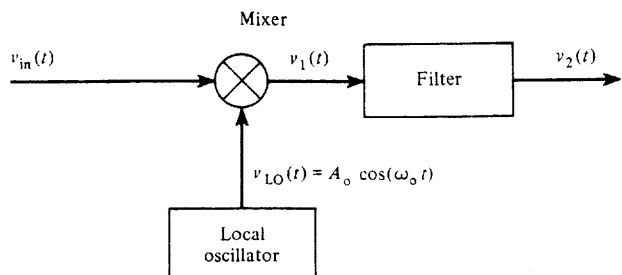


Figure 4-8 Mixer followed by a filter for either up or down conversion.

$$v_1(t) = [A_0 \operatorname{Re}\{g_{in}(t)e^{j\omega_0 t}\}] \cos \omega_0 t$$

$$\begin{aligned} &= \frac{A_0}{4} [g_{in}(t)e^{j\omega_c t} + g_{in}^*(t)e^{-j\omega_c t}] (e^{j\omega_0 t} + e^{-j\omega_0 t}) \\ &= \frac{A_0}{4} [g_{in}(t)e^{j(\omega_c + \omega_0)t} + g_{in}^*(t)e^{-j(\omega_c + \omega_0)t} + g_{in}(t)e^{j(\omega_c - \omega_0)t} + g_{in}^*(t)e^{-j(\omega_c - \omega_0)t}] \end{aligned}$$

or

$$v_1(t) = \frac{A_0}{2} \operatorname{Re}\{g_{in}(t)e^{j(\omega_c + \omega_0)t}\} + \frac{A_0}{2} \operatorname{Re}\{g_{in}(t)e^{j(\omega_c - \omega_0)t}\} \quad (4-57)$$

This equation illustrates that the input bandpass signal with a spectrum near  $f = f_c$  has been converted (i.e., frequency translated) into two output bandpass signals, one at the up-conversion frequency band, where  $f_u = f_c + f_0$ , and one at the down-conversion band, where  $f_d = f_c - f_0$ . A filter, as illustrated in Fig. 4-8, may be used to select either the up-conversion component or the down-conversion component. A *bandpass* filter is used to select the up-conversion component, but the down-conversion component is selected by either a *baseband* filter or a *bandpass* filter, depending on the location of  $f_c - f_0$ . For example, if  $f_c - f_0 = 0$ , a low-pass filter would be needed and the resulting output spectrum would be a baseband spectrum. If  $f_c - f_0 > 0$ , where  $f_c - f_0$  was larger than the bandwidth of  $g_{in}(t)$ , a bandpass filter would be used and the filter output would be

$$v_2(t) = \operatorname{Re}\{g_2(t)e^{j(\omega_c - \omega_0)t}\} = \frac{A_0}{2} \operatorname{Re}\{g_{in}(t)e^{j(\omega_c - \omega_0)t}\} \quad (4-58)$$

For this case of  $f_c > f_0$ , it is seen that the modulation on the mixer input signal  $v_{in}(t)$  is preserved on the mixer up- or down-converted signals.

If  $f_c < f_0$ , we rewrite (4-57), obtaining

$$v_1(t) = \frac{A_0}{2} \operatorname{Re}\{g_{in}(t)e^{j(\omega_c + \omega_0)t}\} + \frac{A_0}{2} \operatorname{Re}\{g_{in}^*(t)e^{j(\omega_c - \omega_0)t}\} \quad (4-59)$$

because the frequency in the exponent of the bandpass signal representation needs to be positive for easy physical interpretation of the location of spectral components. For this case of  $f_0 > f_c$ , the complex envelope of the down-converted signal has been conjugated when compared to the complex envelope of the input signal. This is equivalent to saying that the sidebands have been exchanged; that is, the upper sideband of the input signal spectrum becomes the lower sideband of the down-converted output signal, and so on. This is demonstrated mathematically by looking at the spectrum of  $g^*(t)$ . The spectrum is

$$\begin{aligned} \mathcal{F}[g_{in}^*(t)] &= \int_{-\infty}^{\infty} g_{in}^*(t)e^{-j\omega t} dt = \left[ \int_{-\infty}^{\infty} g_{in}(t)e^{-j(-\omega)t} dt \right]^* \\ &= G_{in}^*(-f) \end{aligned} \quad (4-60)$$

The  $-f$  indicates that the upper and lower sidebands have been exchanged, and the conjugate indicates that the phase spectrum has been inverted.

In summary, the complex envelope for the signal out of an *up converter* is

$$g_2(t) = \frac{A_0}{2} g_{in}(t) \quad (4-61a)$$

where  $f_u = f_c + f_0 > 0$ . Thus the same modulation is on the output signal as was on the input signal, but the amplitude has been changed by the  $A_0/2$  scale factor.

For the case of *down conversion* there are two possibilities. For  $f_d = f_c - f_0 > 0$  where  $f_0 < f_c$ ,

$$g_2(t) = \frac{A_0}{2} g_{in}(t) \quad (4-61b)$$

This is called *down conversion with low-side injection* because the LO frequency is below that of the incoming signal (i.e.,  $f_0 < f_c$ ). Here the output modulation is the same as that of the input except for the  $A_0/2$  scale factor. The other possibility is  $f_d = f_0 - f_c > 0$ , where  $f_0 > f_c$ , which produces the output complex envelope

$$g_2 = \frac{A_0}{2} g_{in}^*(t) \quad (4-61c)$$

This is *down conversion with high-side injection* because  $f_0 > f_c$ . This is the case where the sidebands on the down-converted output signal are reversed from those on the input (e.g., a LSSB input signal becomes a USSB output signal).

Ideal mixers act as linear time-varying circuit elements since

$$v_1(t) = (A \cos \omega_0 t) v_{in}(t)$$

where  $A \cos \omega_0 t$  is the time-varying gain of the linear circuit. It should also be recognized that mixers used in communication circuits are essentially mathematical multipliers. They should not be confused with the audio mixers that are used in radio and TV broadcasting studios. An *audio mixer* is a summing amplifier with multiple inputs so that several inputs from several sources—such as microphones, tape decks, and CD decks—can be “mixed” (added)

to produce one output signal. Unfortunately, the term *mixer* means entirely different things depending on the context used. As used in transmitters and receivers, it means a multiplying operation that produces a frequency translation of the input signal. In audio systems it means a summing operation to combine several inputs into one output signal.

In practice, the multiplying operation needed for mixers may be realized by using one of the following:

1. Continuously variable transconductance device, such as a dual-gate FET
2. Nonlinear device
3. Linear device with time-varying discrete gain

In the first method, when a dual-gate FET is used to obtain multiplication,  $v_{in}(t)$  is usually connected to gate 1 and the local oscillator is connected to gate 2. The resulting output is

$$v_1(t) = Kv_{in}(t)v_{LO}(t) \quad (4-62)$$

over the operative region, where  $v_{LO}(t)$  is the local oscillator voltage. The multiplier is said to be of a *single-quadrant* type if the multiplier action of (4-62) is obtained only when both the input waveforms,  $v_{in}$  and  $v_{LO}(t)$ , have either nonnegative or nonpositive values [i.e., a plot of the values of  $v_{in}(t)$  versus  $v_{LO}(t)$  falls within a single quadrant]. The multiplier is of the *two-quadrant* type if multiplier action is obtained when either  $v_{in}(t)$  or  $v_{LO}(t)$  is non-negative or nonpositive and the other is arbitrary. The multiplier is said to be of the *four-quadrant* type when multiplier action is obtained regardless of the signs of  $v_{in}(t)$  and  $v_{LO}(t)$ .

In the second technique, a nonlinear device can be used to obtain multiplication by summing the two inputs as illustrated in Fig. 4-9. Looking at the square-law component at the output, we have

$$\begin{aligned} v_1(t) &= K_2(v_{in} + v_{LO})^2 + \text{other terms} \\ &= K_2(v_{in}^2 + 2v_{in}v_{LO} + v_{LO}^2) + \text{other terms} \end{aligned} \quad (4-63)$$

The cross-product term gives the desired multiplier action:

$$2K_2v_{in}v_{LO} = 2K_2A_0v_{in}(t)\cos\omega_0t \quad (4-64)$$

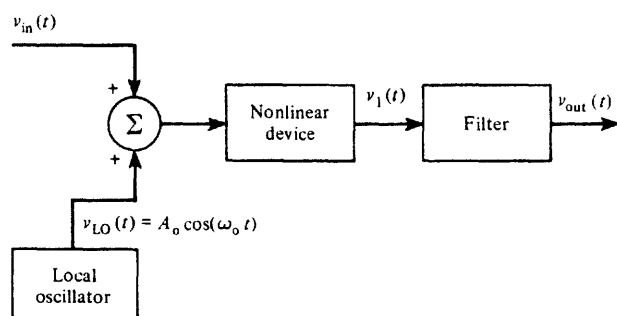


Figure 4-9 Nonlinear device used as a mixer.

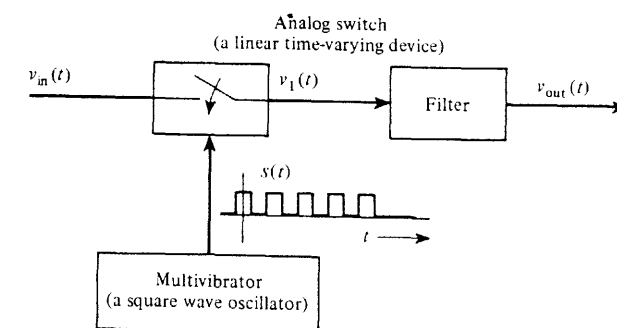


Figure 4-10 Linear time-varying device used as a mixer.

If we assume that  $v_{in}(t)$  is a bandpass signal, the filter can be used to pass either the up or down-conversion terms. However, some distortion products may also fall within the output passband if  $\omega_c$  and  $\omega_0$  are not chosen carefully.

In the third method, a linear device with time-varying discrete gain is used to obtain multiplier action. This is demonstrated in Fig. 4-10, where the time-varying device is an analog switch (such as a CMOS 4016 integrated circuit) that is activated by a square-wave oscillator signal,  $v_0(t)$ . The discrete gain of the switch is either unity or zero. The waveform at the output of the analog switch is

$$v_1(t) = v_{in}(t)s(t) \quad (4-65)$$

where  $s(t)$  is a unipolar switching square wave that has unity peak amplitude. (This is analogous to PAM with natural sampling that was studied in Chapter 3.) Thus, (4-65) becomes

$$v_1(t) = v_{in}(t) \left[ \frac{1}{2} + \sum_{n=1}^{\infty} \frac{2 \sin(n\pi/2)}{n\pi} \cos n\omega_0 t \right] \quad (4-66)$$

The multiplying action is obtained from the  $n = 1$  term, which is

$$\frac{2}{\pi} v_{in}(t) \cos \omega_0 t \quad (4-67)$$

This would generate up- and down-conversion signals at  $f_c + f_0$  and  $f_c - f_0$  if  $v_{in}(t)$  were a bandpass signal with a nonzero spectrum in the vicinity of  $f = f_c$ . However, (4-66) shows that other frequency bands are also present in the output signal, namely, at frequencies  $f = |f_c \pm nf_0|$ ,  $n = 3, 5, 7, \dots$  and, in addition, there is the feed-through term  $\frac{1}{2}v_{in}(t)$  appearing at the output. Of course, a filter may be used to pass either the up- or down-conversion component appearing in (4-66).

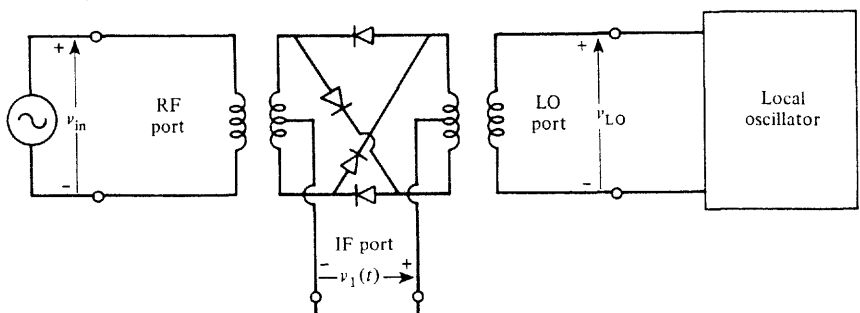
Mixers are often classified as being *unbalanced*, *single balanced*, or *double balanced*. That is, in general we obtain at the output of mixer circuits

$$v_1(t) = C_1v_{in}(t) + C_2v_0(t) + C_3v_{in}(t)v_0(t) + \text{other terms} \quad (4-68)$$

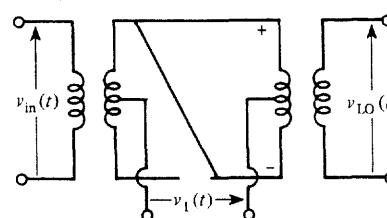
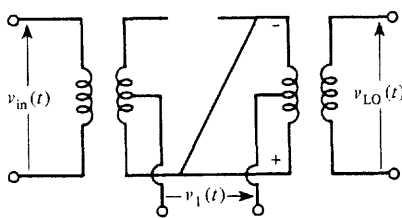
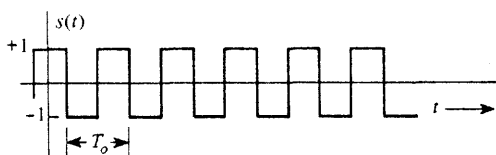
When  $C_1$  and  $C_2$  are not zero, the mixer is said to be *unbalanced* since  $v_{in}(t)$  and  $v_0(t)$  feed through to the output. An example of an unbalanced mixer was illustrated in Fig. 4-9, where

a nonlinear device was used to obtain mixing action. In the Taylor's expansion of the nonlinear device output-to-input characteristics, the linear term would provide feedthrough of both  $v_{in}(t)$  and  $v_0(t)$ . A *single-balanced mixer* has feedthrough for only one of the inputs; that is, either  $C_1$  or  $C_2$  of (4-68) is zero. An example of a single-balanced mixer is shown in Fig. 4-10, which uses sampling to obtain mixer action. In this example, (4-66) demonstrates that  $v_0(t)$  is balanced out (i.e.,  $C_2 = 0$ ) and  $v_{in}(t)$  feeds through with a gain of  $C_1 = \frac{1}{2}$ . A *double-balanced mixer* has no feedthrough from either input; that is, both  $C_1$  and  $C_2$  of (4-68) are zero. An example of a double-balanced mixer is discussed in the next paragraph.

Figure 4-11a exhibits the circuit for a double-balanced mixer. This circuit is popular because it is relatively inexpensive and it has excellent performance. The third-order IMD



(a) A Double-Balanced Mixer Circuit

(b) Equivalent Circuit When  $v_{LO}(t)$  Is Positive(c) Equivalent Circuit When  $v_{LO}(t)$  Is Negative

(d) Switching Waveform Due to the Local Oscillator Signal

Figure 4-11 Analysis of a double-balanced mixer circuit.

is typically down at least 50 dB compared with the desired output components. It is usually designed for source and load impedances of  $50 \Omega$  and has broadband input and output ports. The RF [i.e.,  $v_{in}(t)$ ] port and the LO (local oscillator) port are often usable over a frequency range of 1000:1, say 1 to 1000 MHz; and the IF (intermediate frequency) output port,  $v_1(t)$ , is typically usable from dc to 600 MHz. The transformers are made by using small toroidal cores, and the diodes are matched hot carrier diodes. The input signal level at the RF port is relatively small, usually less than  $-5 \text{ dBm}$ , and the local oscillator level at the LO port is relatively large, say  $+5 \text{ dBm}$ . The LO signal is large, so that this signal, in effect, turns the diodes on and off so that the diodes will act as switches. The LO provides the switching control signal. This circuit thus acts as a time-varying linear circuit (with respect to the RF input port), and the analysis is very similar to that used for the analog-switch mixer of Fig. 4-10. During the portion of the cycle when  $v_{LO}(t)$  has a positive voltage, the output voltage is proportional to  $+v_{in}(t)$  as seen from the equivalent circuit shown in Fig. 4-11b. When  $v_{LO}(t)$  is negative, the output voltage is proportional to  $-v_{in}(t)$ , as seen from the equivalent circuit shown in Fig. 4-11c. Thus the output of this double-balanced mixer is

$$v_1(t) = Kv_{in}(t)s(t) \quad (4-69)$$

where  $s(t)$  is a bipolar switching waveform as shown in Fig. 4-11d. Since the switching waveform arises from the LO signal, its period is  $T_0 = 1/f_0$ . The switching waveform is described by

$$s(t) = 4 \sum_{n=1}^{\infty} \frac{\sin(n\pi/2)}{n\pi} \cos n\omega_0 t \quad (4-70)$$

so that the mixer output is

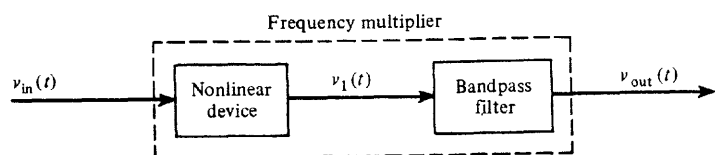
$$v_1(t) = [v_{in}(t)] \left[ 4K \sum_{n=1}^{\infty} \frac{\sin(n\pi/2)}{n\pi} \cos n\omega_0 t \right] \quad (4-71)$$

If the input is a bandpass signal with nonzero spectrum in the vicinity of  $f_c$ , this equation shows that the spectrum of the input will be translated to the frequencies  $|f_c \pm nf_0|$ , where  $n = 1, 3, 5, \dots$ . In practice, the value  $K$  is such that the conversion gain (which is defined as the desired output level divided by the input level) at the frequency  $|f_c \pm f_0|$  is about  $-6 \text{ dB}$ . Of course, an output filter may be used to select the up-converted or down-converted frequency band.

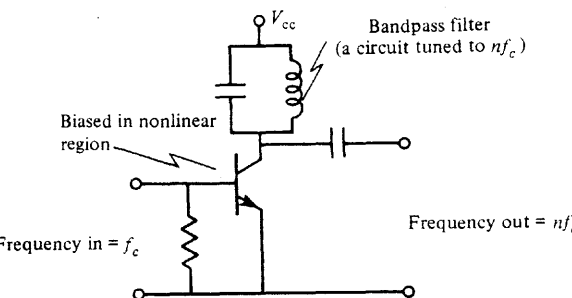
In addition to up- or down-conversion applications, mixers (i.e., multipliers) may be used for modulators to translate a baseband signal to an RF frequency band, and mixers may be used as product detectors to translate RF signals to baseband. These applications will be discussed in later sections that deal with transmitters and receivers.

## 4-12 FREQUENCY MULTIPLIERS

*Frequency multipliers* consist of a nonlinear circuit followed by a tuned circuit, as illustrated in Fig. 4-12. If a bandpass signal is fed into a frequency multiplier, the output will ap-



(a) Block Diagram of a Frequency Multiplier



(b) Circuit Diagram for a Frequency Multiplier

Figure 4-12 Frequency multiplier.

pear in a frequency band at the  $n$ th harmonic of the input frequency. Because the device is nonlinear, the bandwidth of the  $n$ th harmonic output is larger than that of the input signal. In general, the bandpass input signal is represented by

$$v_{in}(t) = R(t) \cos[\omega_c t + \theta(t)] \quad (4-72)$$

The transfer function of the nonlinear device may be expanded in a Taylor's series, so that the  $n$ th order output term is

$$v_1(t) = K_n v_{in}^n(t) = K_n R^n(t) \cos^n[\omega_c t + \theta(t)]$$

or<sup>†</sup>

$$v_1(t) = CR^n(t) \cos[n\omega_c t + n\theta(t)] + \text{other terms}$$

Because the bandpass filter is designed to pass frequencies in the vicinity of  $nf_c$ , the output is

$$v_{out}(t) = CR^n(t) \cos[n\omega_c t + n\theta(t)] \quad (4-73)$$

This illustrates that the input *amplitude* variation  $R(t)$  appears distorted on the output signal because the real envelope on the output is  $R^n(t)$ . The waveshape of the *angle* variation,  $\theta(t)$ , is *not distorted* by the frequency multiplier, but the frequency multiplier does increase the magnitude of the angle variation by a factor of  $n$ . Thus frequency multiplier circuits are

<sup>†</sup>  $m$ th-order output terms, where  $m > n$ , may also contribute to the  $n$ th harmonic output provided that  $K_m$  is sufficiently large with respect to  $K_n$ . This is illustrated by (A-18), where  $m = 4$  and  $n = 2$ .

not used on signals where the AM is to be preserved; but as we will see, the frequency multiplier is very useful in PM and FM problems since it effectively "amplifies" the angle variation waveform,  $\theta(t)$ . The  $n = 2$  multiplier is called a *doubler stage*, and the  $n = 3$  frequency multiplier is said to be a *tripler stage*.

The frequency multiplier should not be confused with a mixer. The frequency multiplier acts as a nonlinear device. The mixer circuit (which uses a mathematical multiplier operation) acts as a linear circuit with time-varying gain (caused by the LO signal). The bandwidth of the signal at the output of a frequency multiplier is larger than that of the input signal, and it appears in a frequency band located at the  $n$ th harmonic of the input. The bandwidth of a signal at the output of a mixer is the same as that of the input, but the input spectrum has been translated either up or down depending on the LO frequency and the bandpass of the output filter. Of course, it is realized that a frequency multiplier is essentially a nonlinear amplifier followed by a bandpass filter that is designed to pass the  $n$ th harmonic.

#### 4-13 DETECTOR CIRCUITS

As indicated in Fig. 4-1, the receiver contains carrier circuits that convert the input bandpass waveform into an output baseband waveform. These carrier circuits are called detector circuits. The following sections will show how detector circuits can be designed to produce  $R(t)$ ,  $\theta(t)$ ,  $x(t)$  or  $y(t)$  at their output for the corresponding bandpass signal that is fed into the detector input.

##### Envelope Detector

An *ideal envelope detector* is a circuit that produces a waveform at its output that is proportional to the real envelope,  $R(t)$ , of its input. From (4-1b) the bandpass input may be represented by  $R(t) \cos[\omega_c t + \theta(t)]$ , where  $R(t) \geq 0$ ; then the output of the ideal envelope detector is

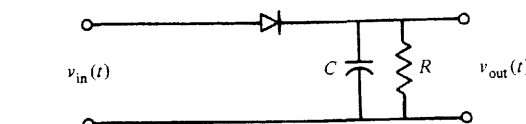
$$v_{out}(t) = KR(t) \quad (4-74)$$

where  $K$  is the proportionality constant.

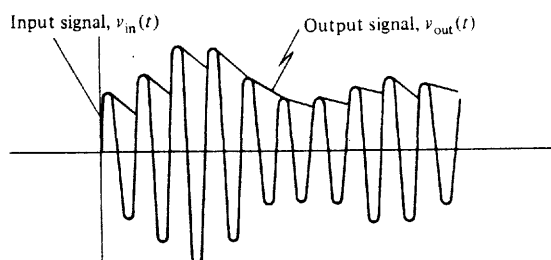
A simple diode detector circuit that approximates an ideal envelope detector is shown in Fig. 4-13a. The diode current occurs in pulses proportional to the positive part of the input waveform. The current pulses charge the capacitor to produce the output voltage waveform, as illustrated in Fig. 4-13b. The  $RC$  time constant is chosen so that the output signal will follow the real envelope,  $R(t)$ , of the input signal. Consequently, the cutoff frequency of the low-pass filter needs to be much smaller than the carrier frequency  $f_c$  and much larger than the bandwidth of the (detected) modulation waveform,  $B$ . That is,

$$B \ll \frac{1}{2\pi RC} \ll f_c \quad (4-75)$$

where  $RC$  is the time constant of the filter.



(a) A Diode Envelope Detector



(b) Waveforms Associated with the Diode Envelope Detector

Figure 4-13 Envelope detector.

The envelope detector is typically used to detect the modulation on AM signals. In this case,  $v_{in}(t)$  has the complex envelope  $g(t) = A_c[1 + m(t)]$ , where  $A_c > 0$  represents the signal strength of the received AM signal, and  $m(t)$  is the modulation. If  $|m(t)| < 1$ , then

$$v_{out} = KR(t) = K|g(t)| = KA_c[1 + m(t)] = KA_c + KA_c m(t)$$

$KA_c$  is a DC voltage that is used to provide *automatic gain control* (AGC) for the AM receiver. That is, for  $KA_c$  relatively small (weak received AM signal), the receiver gain is increased and vice versa.  $KA_c m(t)$  is the detected modulation. For the case of audio (not video) modulation, typical values for the components of the envelope detector are  $R = 10 \text{ k}\Omega$ , and  $C = 0.001 \mu\text{fd}$ . This provides a low-pass filter cutoff frequency (3 dB down) of  $f_{co} = 1/(2\pi RC) = 15.9 \text{ kHz}$ . This is much less than  $f_c$  and larger than the highest audio frequency,  $B$ , used in typical AM applications.

### Product Detector

A *product detector* (Fig. 4-14) is a mixer circuit that down-converts the input (bandpass signal plus noise) to baseband. The output of the multiplier is

$$\begin{aligned} v_1(t) &= R(t) \cos[\omega_c t + \theta(t)] A_0 \cos(\omega_c t + \theta_0) \\ &= \frac{1}{2} A_0 R(t) \cos[\theta(t) - \theta_0] + \frac{1}{2} A_0 R(t) \cos[2\omega_c t + \theta(t) + \theta_0] \end{aligned}$$

where the frequency of the oscillator is  $f_c$  and the phase is  $\theta_0$ . The low-pass filter passes only the down-conversion term, so that the output is

$$v_{out}(t) = \frac{1}{2} A_0 R(t) \cos[\theta(t) - \theta_0] = \frac{1}{2} A_0 \operatorname{Re}\{g(t)e^{-j\theta_0}\} \quad (4-76)$$

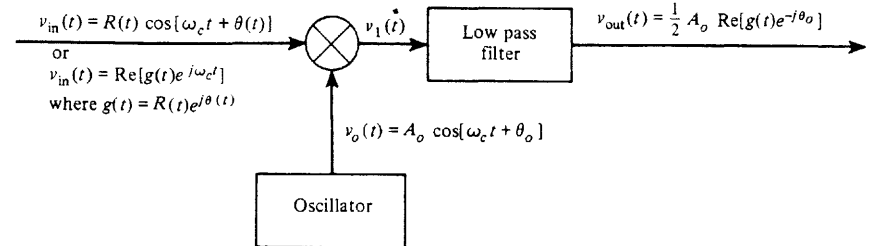


Figure 4-14 Product detector.

where the complex envelope of the input is denoted by

$$g(t) = R(t)e^{j\theta(t)} = x(t) + jy(t)$$

and  $x(t)$  and  $y(t)$  are the quadrature components [see (4-2)]. Because the frequency of the oscillator is the same as the carrier frequency of the incoming signal, the oscillator has been *frequency synchronized* with the input signal. Furthermore, if, in addition,  $\theta_0 = 0$ , the oscillator is said to be *phase synchronized* with the in-phase component and the output becomes

$$v_{out}(t) = \frac{1}{2} A_0 x(t) \quad (4-77a)$$

If  $\theta_0 = 90^\circ$ ,

$$v_{out} = \frac{1}{2} A_0 y(t) \quad (4-77b)$$

Equation (4-76) also indicates that a product detector is sensitive to AM and/or PM. For example, if the input contains no angle modulation so that  $\theta(t) = 0$  and if the reference phase is set to zero (i.e.,  $\theta_0 = 0$ ), then

$$v_{out}(t) = \frac{1}{2} A_0 R(t) \quad (4-78a)$$

which implies that  $x(t) \geq 0$  and the real envelope is obtained on the product detector output, just as for the case of the envelope detector discussed previously. However, if an angle-modulated signal  $A_c \cos[\omega_c t + \theta(t)]$  is present at the input and  $\theta_0 = 90^\circ$ , the product detector output is

$$v_{out}(t) = \frac{1}{2} A_0 \operatorname{Re}\{A_c e^{j[\theta(t) - 90^\circ]}\}$$

or

$$v_{out}(t) = \frac{1}{2} A_0 A_c \sin \theta(t) \quad (4-78b)$$

In this case, the product detector acts like a *phase detector* with a *sinusoidal characteristic* because the output voltage is proportional to the sine of the phase difference between the input signal and the oscillator signal. Phase detector circuits are also available that yield triangle and sawtooth characteristics [Krauss, Bostian, and Raab, 1980]. Referring to (4-78b) for the phase detector with a sinusoidal characteristic, and assuming that the phase difference is small [i.e.,  $|\theta(t)| \ll \pi/2$ ], we see that  $\sin \theta(t) \approx \theta(t)$  and

$$v_{out}(t) \approx \frac{1}{2} A_0 A_c \theta(t) \quad (4-79)$$

which is a linear characteristic (for small angles). Thus the output of this phase detector is directly proportional to the phase differences when the difference angle is small (see Fig. 4-20).

It should be realized that the product detector acts as a linear time-varying device with respect to the input  $v_{in}(t)$ , in contrast to the envelope detector, which is a nonlinear device. The property of being either linear or nonlinear significantly affects the results when two or more components, such as a signal plus noise, are applied to the input. This topic will be studied in Chapter 7.

Detectors may also be classified as being either coherent or noncoherent. A *coherent* detector has two inputs—one for a reference signal, such as the synchronized oscillator signal, and one for the modulated signal that is to be demodulated. The product detector is an example of a coherent detector. A *noncoherent* detector has only one input, namely, the modulated signal port. The envelope detector is an example of a noncoherent detector.

### Frequency Modulation Detector

An *ideal frequency modulation (FM) detector* is a device that produces an output that is proportional to the instantaneous frequency of the input. That is, if the bandpass input is represented by  $R(t) \cos[\omega_c t + \theta(t)]$ , the output of the ideal FM detector is

$$v_{out}(t) = \frac{Kd[\omega_c t + \theta(t)]}{dt} = K\left[\omega_c + \frac{d\theta(t)}{dt}\right] \quad (4-80)$$

Usually, the FM detector is *balanced*. This means that the dc voltage  $K\omega_c$  does not appear on the output if the detector is tuned to (or designed for) the carrier frequency  $f_c$ . In this case the output is

$$v_{out}(t) = K \frac{d\theta(t)}{dt} \quad (4-81)$$

There are many ways to build FM detectors, but almost all of them are based on one of three principles:

- FM-to-AM conversion
- Phase-shift or quadrature detection
- Zero-crossing detection

A *slope detector* is one example of the FM-to-AM conversion principle. A block diagram is shown in Fig. 4-15. A bandpass limiter is needed to suppress any amplitude varia-

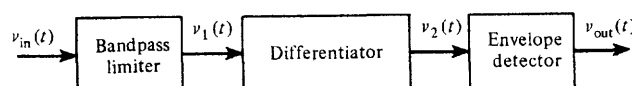


Figure 4-15 Frequency demodulation using slope detection.

tions on the input signal since these would distort (produce noise in) the desired output signal.

The slope detector may be analyzed as follows. Assume that the input is a fading signal with frequency modulation. From Table 4-1, this FM signal may be represented by

$$v_{in}(t) = A(t) \cos[\omega_c t + \theta(t)] \quad (4-82)$$

where

$$\theta(t) = K_f \int_{-\infty}^t m(t_1) dt_1 \quad (4-83)$$

$A(t)$  represents the envelope that is fading and  $m(t)$  is the modulation (e.g., audio) signal. It follows that the limiter output is

$$v_1(t) = V_L \cos[\omega_c t + \theta(t)] \quad (4-84)$$

and the output of the differentiator becomes

$$v_2(t) = -V_L \left[ \omega_c + \frac{d\theta(t)}{dt} \right] \sin[\omega_c t + \theta(t)] \quad (4-85)$$

The output of the envelope detector is the magnitude of the complex envelope for  $v_2(t)$ :

$$v_{out}(t) = \left| -V_L \left[ \omega_c + \frac{d\theta(t)}{dt} \right] \right|$$

and because  $\omega_c \gg d\theta/dt$  in practice, this becomes

$$v_{out}(t) = V_L \left[ \omega_c + \frac{d\theta(t)}{dt} \right]$$

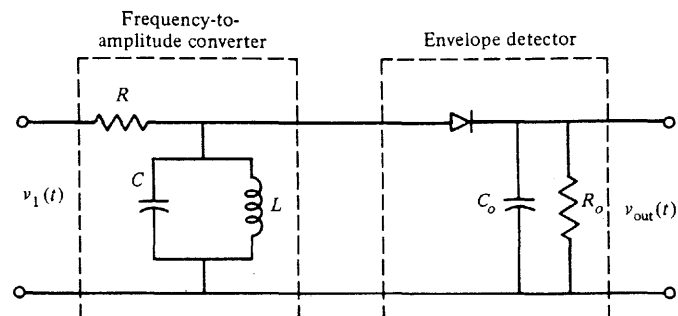
Using (4-83), we obtain

$$v_{out}(t) = V_L \omega_c + V_L K_f m(t) \quad (4-86)$$

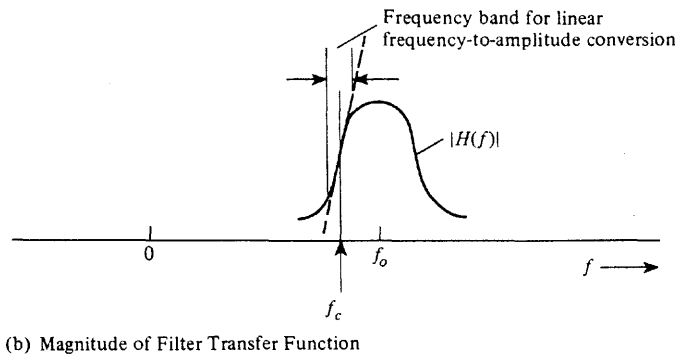
which indicates that the output consists of a dc voltage,  $V_L \omega_c$ , plus the ac voltage  $V_L K_f m(t)$ , which is proportional to the modulation on the FM signal. Of course, a capacitor could be placed in series with the output so that only the ac voltage would be passed to the load.

The differentiation operation can be obtained by any circuit that acts like a frequency-to-amplitude converter. For example, a single-tuned resonant circuit can be used as illustrated in Fig. 4-16, where the magnitude transfer function is  $|H(f)| = K_1 f + K_2$  over the linear (useful) portion of the characteristic. A balanced FM detector, which is also called a *balanced discriminator*, is shown in Fig. 4-17. Two tuned circuits are used to balance out the dc when the input has a carrier frequency of  $f_c$  and to provide an extended linear frequency-to-voltage conversion characteristic.

Balanced discriminators can also be built that function because of the phaseshift properties of a double-tuned RF transformer circuit with primary and secondary windings [Stark,



(a) Circuit Diagram of a Slope Detector



(b) Magnitude of Filter Transfer Function

**Figure 4-16** Slope detection using a single-tuned circuit for frequency-to-amplitude conversion.

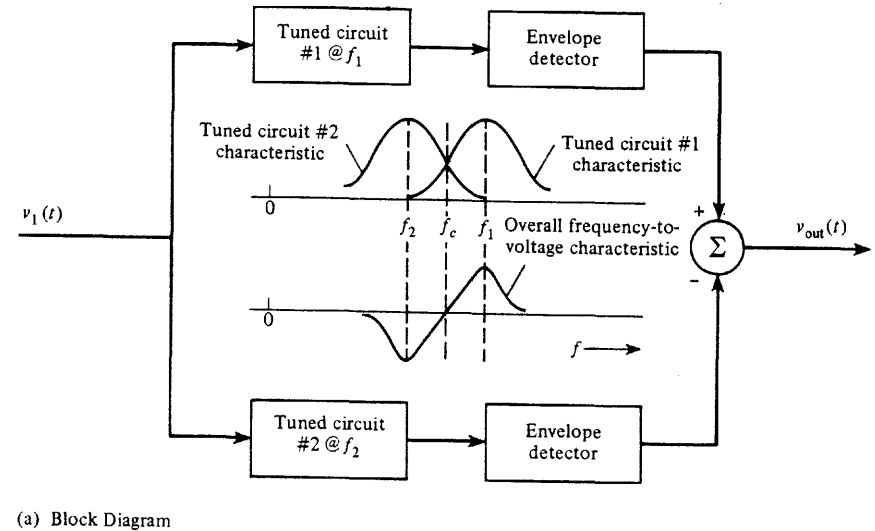
Tuteur, and Anderson, 1988]. In practice, discriminator circuits have been replaced by integrated circuits that operate on the quadrature principle.

The *quadrature detector* is described as follows: A quadrature signal is first obtained from the FM signal; then, using a product detector, the quadrature signal is multiplied with the FM signal to produce the demodulated signal,  $v_{out}(t)$ . The quadrature signal can be produced by passing the FM signal through a capacitor (large) reactance that is connected in series with a parallel resonant circuit which is tuned to  $f_c$ . The quadrature signal voltage appears across the parallel resonant circuit. The series capacitance provides a  $90^\circ$  phase shift and the resonant circuit provides an additional phase shift that is proportional to the instantaneous frequency deviation (from  $f_c$ ) of the FM signal. Using (4-84) and (4-83), the FM signal is

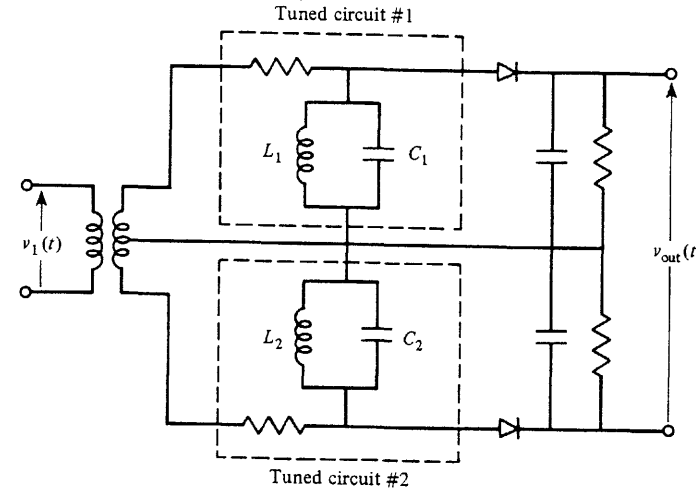
$$v_{in}(t) = V_L \cos[\omega_c t + \theta(t)] \quad (4-87)$$

and the quadrature signal is

$$v_{quad}(t) = K_1 V_L \sin\left[\omega_c t + \theta(t) + K_2 \frac{d\theta(t)}{dt}\right] \quad (4-88)$$



(a) Block Diagram



(b) Circuit Diagram

**Figure 4-17** Balanced discriminator.

where  $K_1$  and  $K_2$  are constants that depend on component values used for the series capacitor and in the parallel resonant circuit. These two signals, (4-87) and (4-88), are multiplied together by a product detector, for example, see Fig. 4-14, to produce the output signal

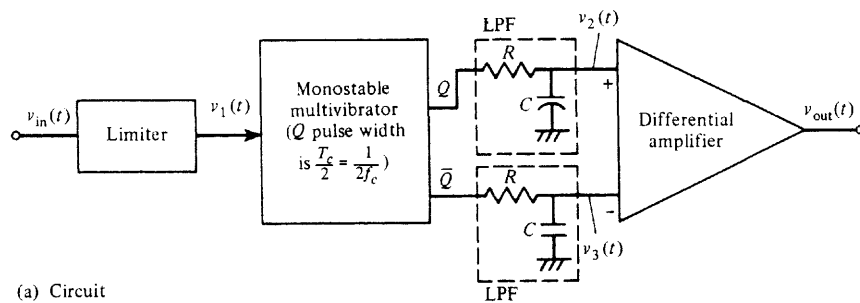
$$v_{out}(t) = \frac{1}{2} K_1 V_L^2 \sin\left[K_2 \frac{d\theta(t)}{dt}\right] \quad (4-89)$$

where the sum-frequency term is eliminated by the low-pass filter. For  $K_2$  sufficiently small,  $\sin x \approx x$ , and by use of (4-83), the output becomes

$$v_{\text{out}}(t) = \frac{1}{2} K_1 K_2 V_L^2 K_m(t) \quad (4-90)$$

This demonstrates that the quadrature detector detects the modulation on the input FM signal. The MC3363 VHF integrated circuit FM receiver uses a quadrature detector. The quadrature detector principle is also used by phase-locked loops that are configured to detect FM—see (4-110).

As indicated by (4-80), the output of an ideal FM detector is directly proportional to the instantaneous frequency of the input. This linear frequency-to-voltage characteristic may be obtained directly by counting the zero-crossings of the input waveform. An FM detector utilizing this technique is called a *zero-crossing detector*. A hybrid circuit (i.e., consisting of both digital and analog devices) that is a balanced FM zero-crossing detector is shown in Fig. 4-18. The limited (square-wave) FM signal, denoted by  $v_1(t)$ , is shown in Fig. 4-18b.



(a) Circuit

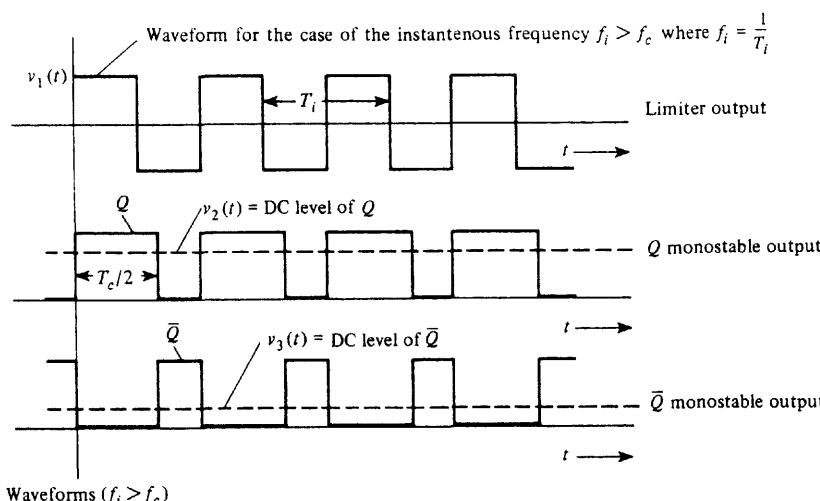


Figure 4-18 Balanced zero-crossing FM detector.

For illustration purposes, it is assumed that  $v_1(t)$  is observed over that portion of the modulation cycle when the instantaneous frequency

$$f_i(t) = f_c + \frac{1}{2\pi} \frac{d\theta(t)}{dt} \quad (4-91)$$

is larger than the carrier frequency,  $f_c$ . That is,  $f_i > f_c$  in the illustration. Since the modulation voltage varies slowly with respect to the input FM signal oscillation,  $v_1(t)$  appears (in the figure) to have a constant frequency, although it is actually varying in frequency according to  $f_i(t)$ . The monostable multivibrator (one shot) is triggered on the positive slope zero-crossings of  $v_1(t)$ . For balanced FM detection, the pulse width of the  $Q$  output is set to  $T_c/2 = 1/2f_c$ , where  $f_c$  is the carrier frequency of the FM signal at the input. Thus the differential amplifier output voltage is zero if  $f_i = f_c$ . For  $f_i > f_c$  [as illustrated by the  $v_1(t)$  waveform in the figure] the output voltage is positive and for  $f_i < f_c$  the output voltage will be negative. Thus a linear frequency-to-voltage characteristic,  $C[f_i(t) - f_c]$ , is obtained where, for an FM signal at the input,  $f_i(t) = f_c + (1/2\pi)K_m(t)$ .

Another circuit that can be used for FM demodulation as well as for other purposes is the phase-locked loop.

#### 4-14 PHASE-LOCKED LOOPS AND FREQUENCY SYNTHESIZERS

A phase-locked loop (PLL) consists of three basic components: (1) a phase detector, (2) a low-pass filter, and (3) a voltage-controlled oscillator (VCO) (see Fig. 4-19). The VCO is an oscillator that produces a periodic waveform, the frequency of which may be varied about some free-running frequency,  $f_0$ , according to the value of the applied voltage  $v_2(t)$ . The free-running frequency,  $f_0$ , is the frequency of the VCO output when the applied voltage  $v_2(t)$  is zero. The phase detector produces an output signal  $v_1(t)$  that is a function of the phase difference between the incoming signal  $v_{\text{in}}(t)$  and the oscillator signal  $v_0(t)$ . The filtered signal  $v_2(t)$  is the control signal that is used to change the frequency of the VCO output. The PLL configuration may be designed so that it acts as a narrowband tracking filter when the low-pass filter (LPF) is a narrowband filter. In this operating mode the frequency of the VCO will become that of one of the line components of the input signal spectrum, so

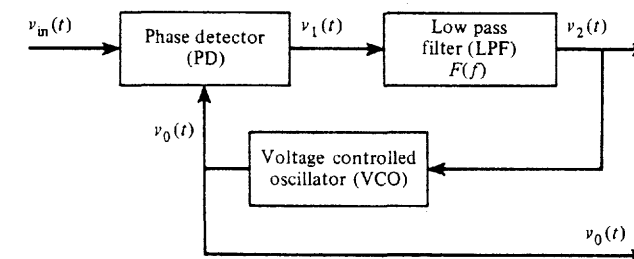


Figure 4-19 Basic PLL.

that, in effect, the VCO output signal is a periodic signal with a frequency equal to the average frequency of this input signal component. Once the VCO has acquired this frequency component, the frequency of the VCO will track this input signal component if it changes slightly in frequency. In another mode of operation, the bandwidth of the LPF is wider so that the VCO can track the instantaneous frequency of the input signal. When the PLL tracks the input signal in either of these ways, the PLL is said to be "locked."

If the applied signal has an initial frequency of  $f_0$ , the PLL will acquire lock and the VCO will track the input signal frequency over some range, provided that the input frequency changes slowly. However, the loop will remain locked only over some finite range of frequency shift. This range is called the *hold-in* (or *lock*) *range*. The hold-in range depends on the overall dc gain of the loop, which includes the dc gain of the LPF. On the other hand, if the applied signal has an initial frequency not equal to  $f_0$ , the loop may not acquire lock even though the input frequency is within the hold-in range. The frequency range over which the applied input will cause the loop to lock is called the *pull-in* (or *capture*) *range*. This range is primarily determined by the loop filter characteristics, and it is never greater than the hold-in range. (See Fig. 4-23.) Another important PLL specification is the *maximum locked sweep rate*. It is defined as the maximum rate of change of the input frequency for which the loop will remain locked. If the input frequency changes faster than this rate, the loop will drop out of lock.

If the PLL is realized using analog circuit techniques, it is said to be an *analog phase-locked loop* (APLL). Conversely, if digital circuits are used, it is said to be a *digital phase-locked loop* (DPLL). For example, the phase detection (PD) characteristic depends on the exact implementation used. Some PD characteristics are shown in Fig. 4-20. The sinusoidal characteristic is obtained if an (analog circuit) multiplier is used and the periodic signals are sinusoids. The multiplier may be implemented by using a double-balanced mixer. The triangle and sawtooth PD characteristics are obtained by using digital circuits. In addition to using digital VCO and PD circuits, the DPLL may incorporate a digital loop filter and signal processing techniques that use microprocessors. Gupta published a fine tutorial paper on analog phase-locked loops in the *IEEE Proceedings* [Gupta, 1975], and Lindsey and Chie followed with a survey paper on digital PLL techniques [Lindsey and Chie, 1981]. In addition, there are excellent books available [Blanchard, 1976; Gardner, 1979; Best, 1993]. A detailed discussion of PLLs is beyond the scope of this book, but some of the significant results will be developed here.

The PLL may be studied by examining the APLL, as shown in Fig. 4-21. In this figure a multiplier (sinusoidal PD characteristic) is used. Assume that the input signal is

$$v_{in}(t) = A_i \sin[\omega_0 t + \theta_i(t)] \quad (4-92)$$

and that the VCO output signal is

$$v_o(t) = A_0 \cos[\omega_0 t + \theta_0(t)] \quad (4-93)$$

where

$$\theta_0(t) = K_v \int_{-\infty}^t v_2(\tau) d\tau \quad (4-94)$$

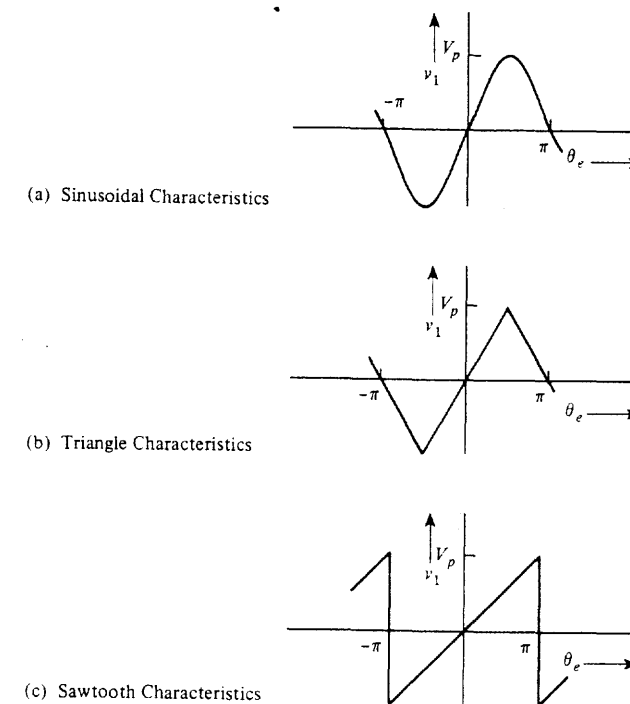


Figure 4-20 Some phase detector characteristics.

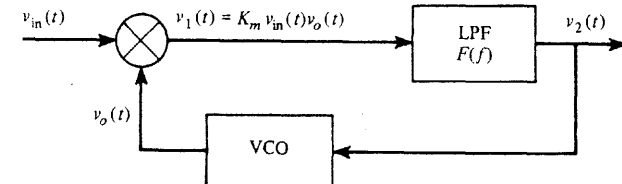


Figure 4-21 Analog PLL.

$K_v$  is the VCO gain constant (rad/V-s). The PD output is

$$\begin{aligned} v_1(t) &= K_m A_i A_0 \sin[\omega_0 t + \theta_i(t)] \cos[\omega_0 t + \theta_0(t)] \\ &= \frac{K_m A_i A_0}{2} \sin[\theta_i(t) - \theta_0(t)] + \frac{K_m A_i A_0}{2} \sin[2\omega_0 t + \theta_i(t) + \theta_0(t)] \end{aligned} \quad (4-95)$$

where  $K_m$  is the gain of the multiplier circuit. The sum frequency term does not pass through the LPF, so the LPF output is

$$v_2(t) = K_d [\sin \theta_e(t)] * f(t) \quad (4-96)$$

where

$$\theta_e(t) \triangleq \theta_i(t) - \theta_0(t) \quad (4-97)$$

$$K_d = \frac{K_m A_i A_0}{2} \quad (4-98)$$

and  $f(t)$  is the impulse response of the LPF.  $\theta_e(t)$  is called the *phase error*;  $K_d$  is the equivalent PD constant, which for the multiplier-type PD depends on the levels of the input signal,  $A_i$ , and the level of the VCO signal,  $A_0$ .

The overall equation describing the operation of the PLL may be obtained by taking the derivative of (4-94) and (4-97), and combining the result by use of (4-96). The resulting nonlinear equation that describes the PLL becomes

$$\frac{d\theta_e(t)}{dt} = \frac{d\theta_i(t)}{dt} - K_d K_v \int_0^t [\sin \theta_e(\lambda)] f(t - \lambda) d\lambda \quad (4-99)$$

where  $\theta_e(t)$  is the unknown and  $\theta_i(t)$  is the forcing function.

In general, this PLL equation is difficult to solve. However, it may be reduced to a linear equation if the gain  $K_d$  is large so that the error  $\theta_e(t)$  is small. In this case,  $\sin \theta_e(t) \approx \theta_e(t)$ , and the resulting linear equation is

$$\frac{d\theta_e(t)}{dt} = \frac{d\theta_i(t)}{dt} - K_d K_v \theta_e(t) * f(t) \quad (4-100)$$

A block diagram that follows from this linear equation is shown in Fig. 4-22. It should be realized that in this linear PLL model, the *phase* of the input signal and the *phase* of the VCO output signal are used instead of actual signals themselves. The closed-loop transfer function  $\Theta_0(f)/\Theta_i(f)$  is

$$H(f) = \frac{\Theta_0(f)}{\Theta_i(f)} = \frac{K_d K_v F(f)}{j2\pi f + K_d K_v F(f)} \quad (4-101)$$

where  $\Theta_0(f) = \mathcal{F}[\theta_0(t)]$  and  $\Theta_i(f) = \mathcal{F}[\theta_i(t)]$ . Of course, the design and analysis techniques used to evaluate linear feedback control systems, such as Bode plots, which will indicate phase gain and phase margins, are applicable. In fact, they are extremely useful in describing the performance of *locked* PLLs.

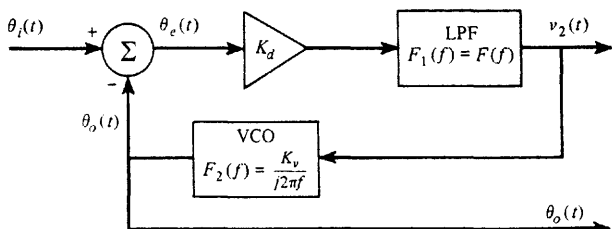


Figure 4-22 Linear model of the analog PLL.

The equation for the *hold-in range* may be obtained by examining the nonlinear behavior of the PLL. From (4-94) and (4-96), the instantaneous frequency deviation of the VCO from  $\omega_0$  is

$$\frac{d\theta_0(t)}{dt} = K_v v_2(t) = K_v K_d [\sin \theta_e(t)] * f(t) \quad (4-102)$$

To obtain the hold-in range, the input frequency is changed very slowly from  $f_0$ . Here the dc gain of the filter is the controlling parameter, and (4-102) becomes

$$\Delta\omega = K_v K_d F(0) \sin \theta_e \quad (4-103)$$

The maximum and minimum values of  $\Delta\omega$  give the hold-in range, and these are obtained when  $\sin \theta_e = \pm 1$ . Thus the maximum hold-in range (no noise case) is

$$\Delta f_h = \frac{1}{2\pi} K_v K_d F(0) \quad (4-104)$$

A typical lock-in characteristic is illustrated in Fig. 4-23. The solid curve shows the VCO control signal  $v_2(t)$  as the sinusoidal testing signal is swept from a low frequency to a high frequency (with the free-running frequency of the VCO,  $f_0$ , being within the swept band). The dashed curve shows the result when sweeping from high to low. The hold-in range  $\Delta f_h$  is related to the dc gain of the PLL as described by (4-104).

The *pull-in range*  $\Delta f_p$  is determined primarily by the loop filter characteristics. For example, assume that the loop has not acquired lock and that the testing signal is swept slowly toward  $f_0$ . At the PD output there will be a beat (oscillatory) signal, and its frequency  $|f_{in} - f_0|$  will vary from a large value to a small value as the test signal frequency sweeps toward  $f_0$ . As the testing signal frequency comes closer to  $f_0$ , the beat-frequency waveform will become nonsymmetrical so that it will have a nonzero dc value. This dc value tends to change the frequency of the VCO to that of the input signal frequency so that the loop will tend to lock. The pull-in range,  $\Delta f_p$ , where the loop acquires lock will depend on exactly how the loop filter  $F(f)$  processes the PD output to produce the VCO control signal. Furthermore,

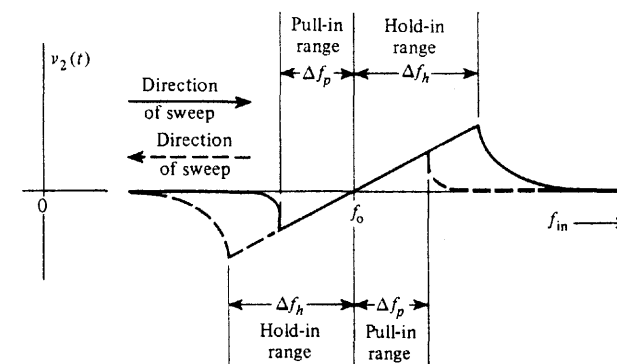


Figure 4-23 PLL VCO control voltage for a swept sinusoidal input signal.

be.

273

If the input signal is within the pull-in range, it may take a fair amount of time for the PLL to acquire lock since the LPF acts as an integrator and it takes some time for the charge (filter output) to build up to a value large enough for lock to occur. The analysis of the pull-in phenomenon is complicated. It is actually statistical in nature because it depends on the initial phase relationship of the input and VCO signals and on noise that is present in the circuit. Consequently, in the measurement of  $\Delta f_p$ , several repeated trials may be needed to obtain a typical value.

The locking phenomenon is not peculiar to PLL circuits but occurs in other types of circuits as well. For example, if an external signal is injected into the output port of an oscillator (i.e., a plain oscillator, not a VCO), the oscillator signal will tend to change frequency and will eventually lock onto the external signal frequency if the external signal is within the pull-in range of the oscillator. This phenomenon is called *injection locking* or *synchronization* of an oscillator. This injection-locking phenomenon may be modeled by a PLL model [Couch, 1971].

The PLL has numerous applications in communication systems. Some of these are (1) FM detection, (2) generation of highly stable FM signals, (3) coherent AM detection, (4) frequency multiplication, (5) frequency synthesis, and (6) use as a building block within complicated digital systems to provide bit synchronization and data detection.

Let us now find what conditions are required for the PLL to become an FM detector. Referring to Fig. 4-21, let the PLL input signal be an FM signal:

$$v_{\text{in}}(t) = A_c \sin \left[ \omega_c t + D_f \int_{-\infty}^t m(\lambda) d\lambda \right] \quad (4-105a)$$

where

$$\theta_i(t) = D_f \int_{-\infty}^t m(\lambda) d\lambda \quad (4-105b)$$

or

$$\Theta_i(f) = \frac{D_f}{j2\pi f} M(f) \quad (4-105c)$$

and  $m(t)$  is the baseband (e.g., audio) modulation that is to be detected. That is, we would like to find the conditions such that the PLL output,  $v_2(t)$ , is proportional to  $m(t)$ . Assume that  $f_c$  is within the capture (pull-in) range of the PLL; thus, for simplicity, let  $f_0 = f_c$ . Then the linearized PLL model, as shown in Fig. 4-22, can be used for analysis. Working in the frequency domain, we obtain the output

$$V_2(f) = \frac{\left( j \frac{2\pi f}{K_v} \right) F_1(f)}{F_1(f) + j \left( \frac{2\pi f}{K_v K_d} \right)} \Theta_i(f)$$

which becomes, using (4-105c),

$$V_2(f) = \frac{\frac{D_f}{K_v} F_1(f)}{F_1(f) + j \left( \frac{2\pi f}{K_v K_d} \right)} M(f) \quad (4-106)$$

We now need to find the conditions such that  $V_2(f)$  is proportional to  $M(f)$ . Assume that the bandwidth of the modulation is  $B$  hertz, and let  $F_1(f)$  be a low-pass filter. Thus

$$F(f) = F_1(f) = 1, \quad |f| < B \quad (4-107)$$

Also, let

$$\frac{K_v K_d}{2\pi} \gg B \quad (4-108)$$

Then (4-106) becomes

$$V_2(f) = \frac{D_f}{K_v} M(f) \quad (4-109)$$

or

$$v_2(t) = Cm(t) \quad (4-110)$$

where the constant of proportionality is  $C = D_f / K_v$ . Thus the PLL circuit of Fig. 4-21 will become a FM detector circuit where  $v_2(t)$  is the detected FM output when the conditions of (4-107) and (4-108) are satisfied.

In another application, the PLL may be used to supply the coherent oscillator signal for product detection of an AM signal (Fig. 4-24). Recall, from (4-92) and (4-93), that the VCO of a PLL locks 90° out of phase with respect to the incoming signal.<sup>†</sup> Then  $v_0(t)$  needs

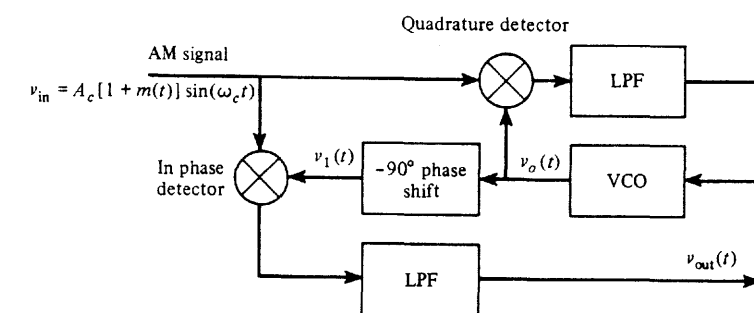


Figure 4-24 PLL used for coherent detection of AM.

<sup>†</sup> This results from the characteristic of the phase detector circuit. This statement is correct for a PD that produces a zero dc output voltage when the two PD input signals are 90° out of phase (i.e., a multiplier-type PD). However, if the PD circuit produced a zero dc output when the two PD inputs were in phase, the VCO of the PLL would lock in phase with the incoming PLL signal.

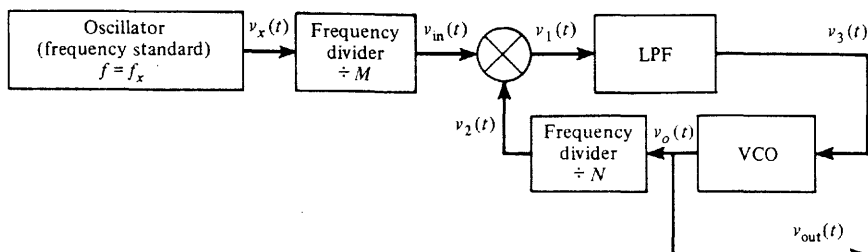


Figure 4-25 PLL used in a frequency synthesizer.

to be shifted by  $-90^\circ$  so that it will be in phase with the carrier of the input AM signal. This was found to be the requirement for coherent detection of AM as given by (4-77). In this application the bandwidth of the LPF needs to be just wide enough to provide the necessary pull-in range in order for the VCO to be able to lock onto the carrier frequency,  $f_c$ .

Figure 4-25 illustrates the use of a PLL in a frequency synthesizer. This frequency synthesizer generates a periodic signal of frequency

$$f_{\text{out}} = \left( \frac{N}{M} \right) f_x \quad (4-111)$$

where  $f_x$  is the frequency of the stable oscillator and  $N$  and  $M$  are the frequency-divider parameters. This result is verified by recalling that when the loop is locked, the dc control signal  $v_3(t)$  shifts the frequency of the VCO so that  $v_2(t)$  will have the same frequency as  $v_{\text{in}}(t)$ . Thus,

$$\frac{f_x}{M} = \frac{f_{\text{out}}}{N} \quad (4-112)$$

which is equivalent to (4-111). If programmable dividers are used, the synthesizer output frequency may be changed at will, according to (4-111), by selecting appropriate values of  $N$  and  $M$ . Of course, this could be carried out by using a microprocessor under software program control. It is noted that for the case of  $M = 1$ , this synthesizer configuration acts like a frequency multiplier. In addition, more complicated PLL synthesizer configurations can be built that incorporate mixers and additional oscillators.

#### 4-15 DIRECT DIGITAL SYNTHESIS

*Direct digital synthesis* (DDS) is a method for generating a desired waveform (such as a sine wave) by using the computer technique described in Fig. 4-26. To configure the DDS sys-

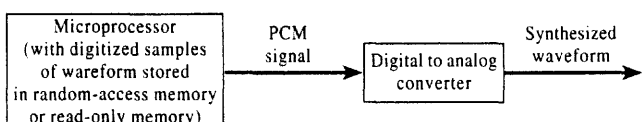


Figure 4-26 Direct digital synthesis (DDS).

tem to generate a waveform, samples of the desired waveform are converted into PCM words and stored in the memory (random access memory [RAM] or read-only memory [ROM]) of the microprocessor system. The DDS system can then generate the desired waveform by "playing back" the stored words into the digital-to-analog converter.

This DDS technique has many attributes. For example, if the waveform is periodic, such as a sine wave, only one cycle of samples need to be stored in memory. The continuous sine wave can be generated by repetitively cycling through the memory. The frequency of the generated sine wave is determined by the rate at which the memory is read out. If desired, the microprocessor can be programmed to generate a certain frequency during a certain time interval and then switch to a different frequency (and/or another waveshape) during a different time interval. Also, simultaneous sine and cosine (two phase) outputs can be generated by adding another DAC. The signal-to-quantizing noise can be designed to be as large as desired by selecting the appropriate number of bits that are stored for each PCM word, as described by (3-18).

The DDS technique is replacing analog circuits in many applications. For example, in higher-priced communications receivers, the DDS technique is used as a frequency synthesizer to generate local oscillator signals that tune the radio (see Sec. 4-16). In electronic pipe organs and music synthesizers, DDS can be used to generate authentic as well as weird sounds. Instrument manufacturers are using DDS to generate the output waveforms for function generators and arbitrary waveform generators. Telephone companies are using DDS to generate dial tones and busy signals (see Chapter 8).

#### 4-16 TRANSMITTERS AND RECEIVERS

##### Generalized Transmitters

Transmitters generate the modulated signal at the carrier frequency  $f_c$  from the modulating signal  $m(t)$ . In Sec. 4-1 and 4-2 it was demonstrated that any type of modulated signal could be represented by

$$v(t) = \operatorname{Re}\{g(t)e^{j\omega_c t}\} \quad (4-113)$$

or, equivalently,

$$v(t) = R(t) \cos[\omega_c t + \theta(t)] \quad (4-114)$$

and

$$v(t) = x(t) \cos \omega_c t - y(t) \sin \omega_c t \quad (4-115)$$

where the complex envelope



$$g(t) = R(t)e^{j\theta(t)} = x(t) + jy(t) \quad (4-116)$$

is a function of the modulating signal  $m(t)$ . The particular relationship that is chosen for  $g(t)$  in terms of  $m(t)$  defines the type of modulation that is used, such as AM, SSB, or FM (see Table 4-1). A generalized approach may be taken to obtain universal transmitter models that may be reduced to those used for a particular modulation type. We will also see that there

are equivalent models that correspond to different circuit configurations, yet they may be used to produce the same type of modulated signal at their outputs. It is up to the designer to select an implementation method that will maximize performance, yet minimize cost based on the state of the art in circuit development.

There are two canonical forms for the generalized transmitter, as indicated by (4-114) and (4-115). Equation (4-114) describes an AM-PM type circuit as shown in Fig. 4-27. The baseband signal processing circuit generates  $R(t)$  and  $\theta(t)$  from  $m(t)$ . The  $R$  and  $\theta$  are functions of the modulating signal  $m(t)$  as given in Table 4-1 for the particular modulation type desired. The signal processing may be implemented either by using nonlinear analog circuits or a digital computer that incorporates the  $R$  and  $\theta$  algorithms under software program control. In the implementation using a digital computer, one ADC will be needed at the input and two DACs will be needed at the output. The remainder of the AM-PM canonical form requires RF circuits, as indicated in the figure.

Figure 4-28 illustrates the second canonical form for the generalized transmitter. This uses in-phase and quadrature-phase (IQ) processing. Similarly, the formulas relating  $x(t)$  and  $y(t)$  to  $m(t)$  are shown in Table 4-1, and the baseband signal processing may be implemented

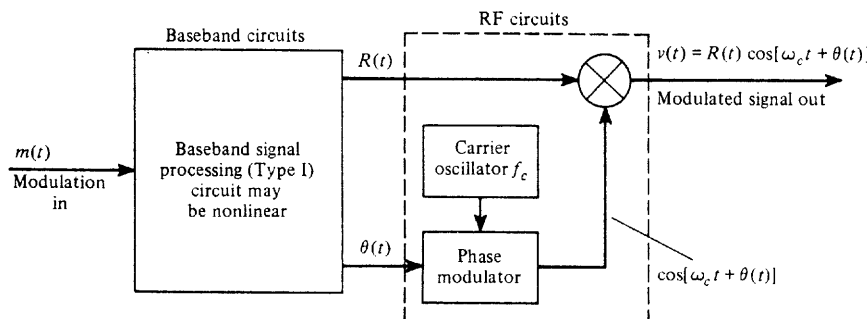


Figure 4-27 Generalized transmitter using the AM-PM generation technique.

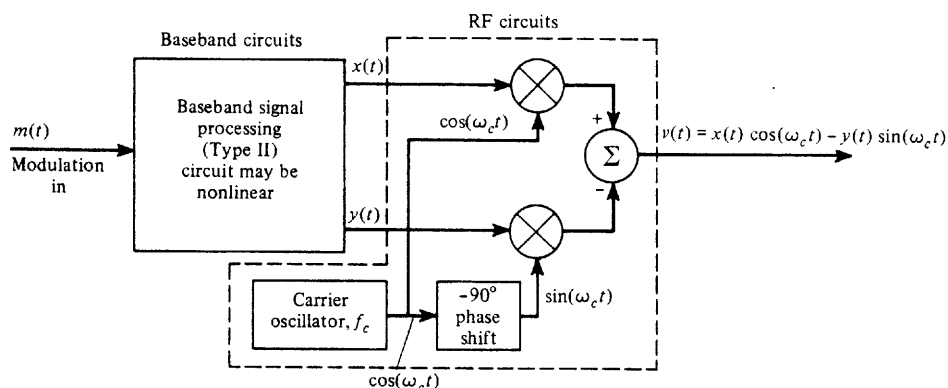


Figure 4-28 Generalized transmitter using the quadrature generation technique.

by using either analog hardware or digital hardware with software. The remainder of the canonical form uses RF circuits as indicated.

Once again, it is stressed that any type of signal modulation (AM, FM, SSB, QPSK, etc.) may be generated by using either of these two canonical forms. Both of these forms conveniently separate baseband processing from RF processing. Digital techniques are especially useful to realize the baseband processing portion. Furthermore, if digital computing circuits are used, any desired modulation type can be obtained by selecting the appropriate software algorithm.

Most of the practical transmitters in use today are special variations on these canonical forms. Practical transmitters may perform the RF operations at some convenient lower RF frequency and then up-convert to the desired operating frequency. In the case of RF signals that contain no AM, frequency multipliers may be used to arrive at the operating frequency. Of course, power amplifiers are usually required to bring the output power level up to the specified value. If the RF signal contains no amplitude variations, Class C amplifiers (relatively high efficiency) may be used; otherwise, Class B amplifiers are used.

### Generalized Receiver: The Superheterodyne Receiver

The receiver has the job of extracting the source information from the received modulated signal that may be corrupted by noise. Often it is desired that the receiver output be a replica of the modulating signal that was present at the transmitter input. There are two main classes of receivers: the *tuned radio frequency* (TRF) receiver and the *superheterodyne* receiver.

The TRF receiver consists of a number of cascaded high-gain RF bandpass stages that are tuned to the carrier frequency,  $f_c$ , followed by an appropriate detector circuit (envelope detector, product detector, FM detector, etc.). The TRF is not very popular because it is difficult to design tunable RF stages so that the desired station can be selected and yet have a narrow bandwidth so that adjacent channel stations are rejected. In addition, it is difficult to obtain high gain at radio frequencies and to have sufficiently small stray coupling between the output and input of the RF amplifying chain so that the chain will not become an oscillator at  $f_c$ . The "crystal set" that is built by the Cub Scouts is an example of a single-RF-stage TRF receiver that has no gain in the RF stage. TRF receivers are often used to measure time-dispersive (multipath) characteristics of radio channels [Rappaport, 1989].

Most receivers employ the *superheterodyne* receiving technique as shown in Fig. 4-29. This technique consists of either down-converting or up-converting the input signal to some convenient frequency band, called the *intermediate frequency* (IF) band, and then extracting the information (or modulation) by using the appropriate detector.<sup>†</sup> This basic receiver structure is used for the reception of all types of bandpass signals, such as television, FM, AM, satellite, and radar signals. The RF amplifier has a bandpass characteristic that passes the desired signal and provides amplification to override additional noise that is generated in the mixer stage. The RF filter characteristic also provides some rejection of adjacent channel signals and noise, but the main adjacent channel rejection is accomplished by the IF filter.

<sup>†</sup> Dual-conversion superheterodyne receivers can also be built. Here a second mixer and a second IF stage follow the first IF stage shown in Fig. 4-29. (The MC3363 is an example of a dual-conversion receiver.)

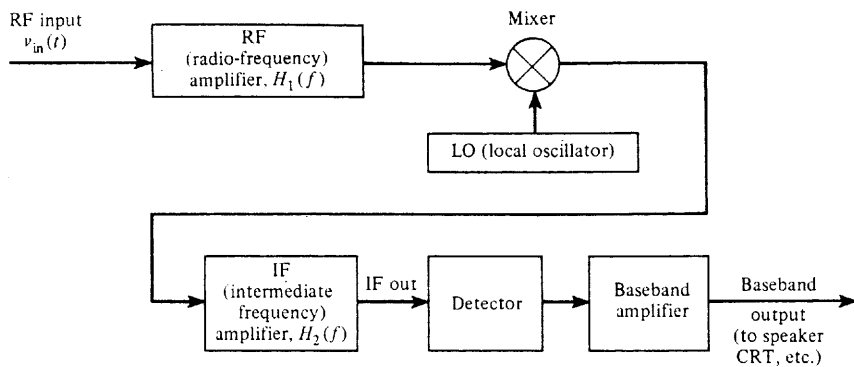


Figure 4-29 Superheterodyne receiver.

The IF filter is a bandpass filter that selects either the up-conversion or down-conversion component (whichever is chosen by the receiver designer). When up conversion is selected, the complex envelope of the IF (bandpass) filter output is the same as the complex envelope for the RF input, except for RF filtering,  $H_1(f)$ , and IF filtering  $H_2(f)$ . However, if down conversion is used with  $f_{LO} > f_c$ , the complex envelope at the IF output will be the conjugate of that for the RF input [see (4-59)]. This means that the sidebands of the IF output will be inverted (i.e., the upper sideband on the RF input will become the lower sideband, etc., on the IF output). If  $f_{LO} < f_c$ , the sidebands are not inverted. In some special applications the LO frequency is selected to be the carrier frequency ( $f_{LO} = f_c$ ), and then the superheterodyne receiver becomes a direct-conversion receiver.<sup>†</sup> In this case the IF filter is replaced by a low-pass filter so that the mixer-LPF combination becomes a product detector and the detector stage of Fig. 4-29 is deleted. Thus, the direct-conversion receiver is the same as a TRF receiver with product detection.

The center frequency selected for the IF amplifier is chosen based on three considerations.

- The frequency should be such that a stable high-gain amplifier can be economically attained.
- The frequency needs to be low enough so that with practical circuit elements in the IF filters, values of  $Q$  can be attained that will provide a steep attenuation characteristic outside the bandwidth of the IF signal. This decreases the noise and minimizes the interference from adjacent channels.
- The frequency needs to be high enough so that the receiver image response can be made acceptably small.

The *image response* is the reception of an unwanted signal located at the image frequency due to insufficient attenuation of the image signal by the RF amplifier filter. The image response is best illustrated by an example.

<sup>†</sup> A direct-conversion receiver is also called a *homodyne* or a *synchrodyne* receiver.

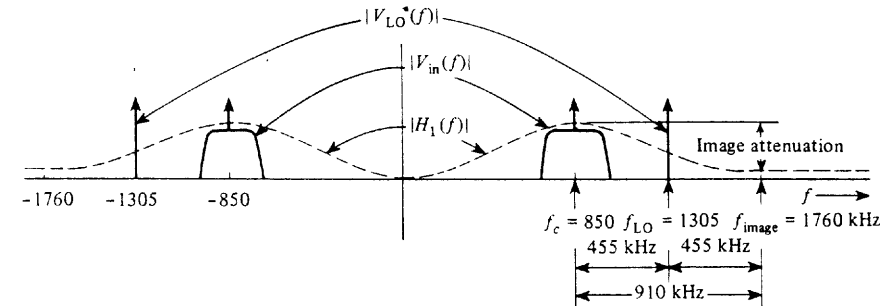


Figure 4-30 Spectra of signals and transfer function of an RF amplifier in a superheterodyne receiver.

### Example 4-2 AM BROADCAST SUPERHETERODYNE RECEIVER

Assume that an AM broadcast band radio is tuned to receive a station at 850 kHz and that the LO frequency is on the high side of the carrier frequency. If the IF frequency is 455 kHz, the LO frequency will be  $850 + 455 = 1305$  kHz (see Fig. 4-30). Furthermore, assume that other signals are present at the RF input of the radio and, particularly, that there is a signal at 1760 kHz; this signal will be down-converted by the mixer to  $1760 - 1305 = 455$  kHz. That is, the undesired (1760-kHz) signal will be translated to 455 kHz and will be added at the mixer output to the desired (850-kHz) signal, which was also down-converted to 455 kHz. This *undesired* signal that has been converted to the IF band is called the *image signal*. If the gain of the RF amplifier is down by, say, 25 dB at 1760 kHz as compared to 850 kHz, and if the undesired signal is 25 dB stronger at the receiver input than the desired signal, both signals will have the same level when translated to the IF. In this case the undesired signal will definitely interfere with the desired signal in the detection process.

For down converters (i.e.,  $f_{IF} = |f_c - f_{LO}|$ ) the image frequency is

$$f_{\text{image}} = \begin{cases} f_c + 2f_{\text{IF}}, & \text{if } f_{\text{LO}} > f_c \quad (\text{high-side injection}) \\ f_c - 2f_{\text{IF}}, & \text{if } f_{\text{LO}} < f_c \quad (\text{low-side injection}) \end{cases} \quad (4-117a)$$

where  $f_c$  is the desired RF frequency,  $f_{\text{IF}}$  is the IF frequency, and  $f_{\text{LO}}$  is the local oscillator frequency. For up converters (i.e.,  $f_{IF} = f_c + f_{LO}$ ) the image frequency is

$$f_{\text{image}} = f_c + 2f_{\text{LO}} \quad (4-117b)$$

From Fig. 4-30 it is seen that the image response will usually be reduced if the IF frequency is increased, since  $f_{\text{image}}$  will occur farther away from the main peak (or lobe) of the RF filter characteristic,  $|H_1(f)|$ .

Recalling our earlier discussion on mixers, we also realize that other spurious responses (in addition to the image response) will occur in practical mixer circuits. These must also be taken into account in good receiver design.

Table 4-4 illustrates some typical IF frequencies that have become de facto standards. For the intended application, the IF frequency is low enough that the IF filter will provide good adjacent channel signal rejection when circuit elements with realizable  $Q$  are used; yet

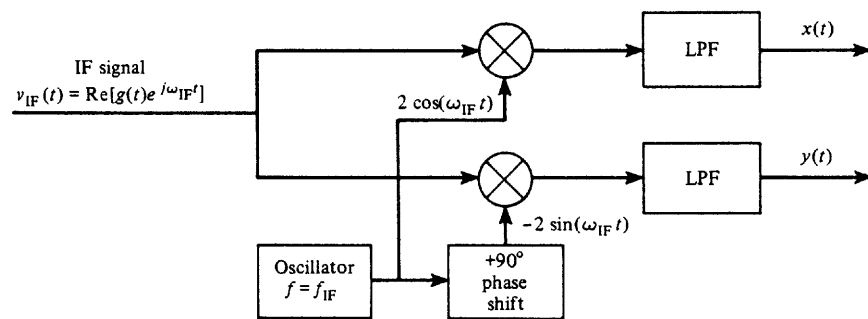
**TABLE 4-4** SOME POPULAR IF FREQUENCIES IN THE UNITED STATES.

IF Frequency	Application
262.5 kHz	AM broadcast radios (in automobiles)
455 kHz	AM broadcast radios
10.7 MHz	FM broadcast radios
21.4 MHz	FM two-way radios
30 MHz	Radar receivers
43.75 MHz (video carrier)	TV sets
60 MHz	Radar receivers
70 MHz	Satellite receivers

the IF frequency is large enough to provide adequate image-signal rejection by the RF amplifier filter.

The type of detector selected for use in the superheterodyne receiver depends on the intended application. For example, a product detector may be used in a PSK (digital) system, and an envelope detector is used in AM broadcast receivers. If the complex envelope  $g(t)$  is desired for generalized signal detection or for optimum reception in digital systems, the  $x(t)$  and  $y(t)$  quadrature components, where  $x(t) + jy(t) = g(t)$ , may be obtained by using quadrature product detectors, as illustrated in Fig. 4-31.  $x(t)$  and  $y(t)$  could be fed into a signal processor to extract the modulation information. Disregarding the effects of noise, the signal processor could recover  $m(t)$  from  $x(t)$  and  $y(t)$  (and, consequently, demodulate the IF signal) by using the inverse of the complex envelope generation functions given in Table 4-1.

The superheterodyne receiver has many advantages and some disadvantages. The main advantage is that extraordinarily high gain can be obtained without instability (self-oscillation). The stray coupling between the output of the receiver and the input does not cause oscillation because the gain is obtained in disjoint frequency bands—RF, IF, and baseband. The receiver is easily tunable to another frequency by changing the frequency of the LO signal (which may be supplied by a frequency synthesizer) and by tuning the bandpass of the RF amplifier to the desired frequency. Furthermore, high- $Q$  elements—which are need-

**Figure 4-31** IQ (in-phase and quadrature-phase) detector.

ed (to produce steep filter skirts) for adjacent channel rejection—are needed only in the fixed tuned IF amplifier. The main disadvantage of the superheterodyne receiver is the response to spurious signals that will occur if one is not careful with the design.

A discussion of receivers would not be complete without considering some of the causes of *interference*. Often the receiver owner thinks that a certain signal, such as an amateur radio signal, is causing the difficulty. This may or may not be the case. The origin of the interference may be at any of three locations.

- At the interfering signal *source*, the transmitter may generate out-of-band signal components (such as harmonics) that fall in the band of the desired signal.
- At the *receiver* itself, the front end may overload or produce spurious responses. Front-end overload occurs when the RF and/or mixer stage of the receiver is driven into the nonlinear range by the interfering signal and the nonlinearity causes cross modulation on the desired signal at the output of the receiver RF amplifier.
- In the *channel*, a nonlinearity in the transmission medium may cause undesired signal components in the band of the desired signal.

For more discussion of receiver design and examples of practical receiver circuits, the reader is referred to the *ARRL Handbook* [ARRL, 1994].

#### 4-17 SUMMARY

The basic techniques used for bandpass signaling have been studied in this chapter. The complex envelope technique for representing bandpass signals and filters was found to be very useful. A description of communication circuits with performance analysis was presented for filters, amplifiers, limiters, mixers, frequency multipliers, phase-locked loops, and detector circuits. Nonlinear as well as linear circuit analysis techniques were used. The results are summarized in Table 4-5, which gives the output of each device as a function of the complex envelope for the input to that device. The superheterodyne receiving circuit was found to be the fundamental technique used in communication receiver design, with the detector circuit determining whether the receiver is designed to detect digital or analog signals of a particular type. Generalized transmitters and receivers were developed, and practical aspects of their design, such as spurious signals, were evaluated.

#### 4-18 STUDY-AID EXAMPLES



**SA4-1** An AM voltage signal,  $s(t)$ , with a carrier frequency of 1150 kHz has a complex envelope  $g(t) = A_c[1 + m(t)]$ .  $A_c = 500$  V, and the modulation is a 1 kHz sinusoidal test tone described by  $m(t) = 0.8 \sin(2\pi 1000t)$ . Evaluate the voltage spectrum for this AM signal.

**Solution.** Using (A-1),

$$m(t) = \frac{0.8}{j2} [e^{j2\pi 1000t} - e^{-j2\pi 1000t}] \quad (4-118)$$

TABLE 4-5 EFFECT OF COMMUNICATION SYSTEM COMPONENTS

Device Name	Device Parameter(s) <sup>a</sup>	Output Complex Envelope <sup>b</sup>	Output Waveform
Linear bandpass amplifier	Gain = A	$\text{Re}\{Ag(t) e^{j\omega_0 t}\}$	$\text{Re}\{Ag(t) e^{j\omega_0 t}\}$
Linear bandpass filter	Impulse response = $\text{Re}\{k(t) e^{j\omega_0 t}\}$	$\frac{1}{2} \text{Re}\{g(t) * k(t) e^{j\omega_0 t}\}$	$\frac{1}{2} \text{Re}\{g(t) * k(t) e^{j\omega_0 t}\}$
Hard bandpass limiter	Limit level = $V_L$	$\text{Re}\{KV_L e^{j\theta(t)} e^{j\omega_0 t}\}$	$\text{Re}\{KV_L e^{j\theta(t)} e^{j\omega_0 t}\}$
Down converter <sup>c</sup>	Gain = $A$ ; $\omega_0 < \omega_c$	$\text{Re}\{Ag(t) e^{j(\omega_0 - \omega_c)t}\}$	$\text{Re}\{Ag(t) e^{j(\omega_0 - \omega_c)t}\}$
Up converter	Gain = $A$	$\text{Re}\{Ag^*(t) e^{j(\omega_0 + \omega_c)t}\}$	$\text{Re}\{Ag^*(t) e^{j(\omega_0 + \omega_c)t}\}$
Frequency multiplier	Input = $\text{Re}\{R(t) e^{j\theta(t)} e^{j\omega_0 t}\}$ ; multiply by $n$	$\text{Re}\{CR^n(t) e^{jn\theta(t)}\}$	$\text{Re}\{CR^n(t) e^{jn\theta(t)} e^{jn\omega_0 t}\}$
Envelope detector	Gain = A	NA	$AR(t)$
Phase detector	Gain = A	NA	$A\theta(t)$
Frequency modulation detector	Gain = A; reference = $K \cos(\omega_c t + \theta_0)$	NA	$A d\theta(t)/dt$
Product detector	Gain = A; in-phase ref. ( $\theta_0 = 0$ )	NA	$A \text{Re}\{g(t) e^{-j\theta_0}\}$
Product detector	Gain = A; quad-phase ref. ( $\theta_0 = 90^\circ$ )	NA	$Ax(t)$
Product detector		NA	$Ay(t)$

<sup>a</sup>  $\omega_0$ , LO frequency.<sup>b</sup> NA, not applicable.<sup>c</sup> For high-side injection (i.e.,  $\omega_c < \omega_0$ ), the upper and lower sidebands at the output are inverted compared to those at the input because  $\mathcal{F}[g^*(t)] = G^*(-f)$ .

## Sec. 4-18 Study-Aid Examples

Using (2-26) with the help of (A-86), the Fourier transform of  $m(t)$  is<sup>†</sup>

$$M(f) = -j 0.4 \delta(f - 1000) + j 0.4 \delta(f + 1000) \quad (4-119)$$

Substituting this into (4-20a), the voltage spectrum of the AM signal is

$$\begin{aligned} S(f) = & 250 \delta(f - f_c) - j100 \delta(f - f_c - 1000) + j100 \delta(f - f_c + 1000) \\ & + 250 \delta(f + f_c) - j100 \delta(f + f_c - 1000) + j100 \delta(f + f_c + 1000) \end{aligned} \quad (4-120)$$

## SA4-2 Compute the PSD for the AM signal that is described in SA4-1.

*Solution.* Using (2-71), the autocorrelation for the sinusoidal modulation,  $m(t)$  is

$$R_m(\tau) = \frac{A^2}{2} \cos \omega_0 \tau = \frac{A^2}{4} [e^{j\omega_0 \tau} + e^{-j\omega_0 \tau}] \quad (4-121)$$

where  $A = 0.8$  and  $\omega_0 = 2\pi 1000$ . Taking the Fourier transform by the use of (2-26) with the aid of (A-86), the PSD of  $m(t)$  is<sup>‡</sup>

$$\mathcal{P}_m(f) = \frac{A^2}{4} [\delta(f - f_0) + \delta(f + f_0)]$$

or

$$\mathcal{P}_m(f) = 0.16 [\delta(f - 1000) + \delta(f + 1000)] \quad (4-122)$$

The autocorrelation for the complex envelope of the AM signal is

$$\begin{aligned} R_g(\tau) &= \langle g^*(t) g(t + \tau) \rangle = A_c^2 \langle [1 + m(t)][1 + m(t + \tau)] \rangle \\ &= A_c^2 [\langle 1 \rangle + \langle m(t) \rangle + \langle m(t + \tau) \rangle + \langle m(t)m(t + \tau) \rangle] \end{aligned}$$

But  $\langle 1 \rangle = 1$ ,  $\langle m(t) \rangle = 0$ ,  $\langle m(t + \tau) \rangle = 0$  and  $\langle m(t)m(t + \tau) \rangle = R_m(\tau)$ . Thus,

$$R_g(\tau) = A_c^2 + A_c^2 R_m(\tau) \quad (4-123)$$

Taking the Fourier transform of both sides of (4-123), we get

$$\mathcal{P}_g(f) = A_c^2 \delta(f) + A_c^2 \mathcal{P}_m(f) \quad (4-124)$$

Substituting (4-124) into (4-13), with the aid of (4-122), we obtain the PSD for the AM signal

$$\begin{aligned} \mathcal{P}_s(f) = & 62,500 \delta(f - f_c) + 10,000 \delta(f - f_c - 1000) \\ & + 10,000 \delta(f - f_c + 1000) + 62,500 \delta(f + f_c) \\ & + 10,000 \delta(f + f_c - 1000) + 10,000 \delta(f + f_c + 1000) \end{aligned} \quad (4-125)$$

*Note:* We realize that this bandpass PSD for  $s(t)$  is obtained by translating (i.e., moving) the baseband PSD of  $g(t)$  up to  $f_c$  and down to  $-f_c$ . Furthermore, for the case of AM, the PSD of  $g(t)$  consists of the PSD for  $m(t)$  plus the superposition of a delta function at  $f = 0$ .SA4-3 Assume that the AM voltage signal,  $s(t)$ , as described in SA4-1, appears across a  $50\Omega$  resistive load. Compute the actual average power dissipated in the load.<sup>†</sup> Because  $m(t)$  is periodic, an alternative method for evaluating  $M(f)$  is given by (2-109) where  $c_{-1} = j0.4$ ,  $c_1 = -j0.4$  and the other  $c_n$ 's are zero.<sup>‡</sup> Because  $m(t)$  is periodic, (2-126) can be used as an alternate method to evaluate  $\mathcal{P}_m(f)$ . That is, using (2-126) with  $c_1 = c_{-1} = A/(2j) = -j0.8/2 = -j0.4$  (and the other  $c_n$ 's are zero), (4-122) is obtained.

**Solution.** Using (4-21), the normalized average power is

$$\begin{aligned}(P_s)_{\text{norm}} &= (V_s)^2_{\text{rms}} = \frac{1}{2} A_c^2 [1 + (V_m)^2_{\text{rms}}] \\ &= \frac{1}{2} (500)^2 \left[ 1 + \left( \frac{0.8}{\sqrt{2}} \right)^2 \right]^2 = 165 \text{ kW}\end{aligned}\quad (4-126a)$$

**Note:** An alternative method of computing  $(P_s)_{\text{norm}}$  is to calculate the area under the PDF for  $s(t)$ . That is, using (4-125),

$$(P_s)_{\text{norm}} = (V_s)^2_{\text{rms}} = \int_{-\infty}^{\infty} \mathcal{P}_s(f) df = 165 \text{ kW}\quad (4-126b)$$

Using (4-126a) or (4-126b), the actual average power dissipated in the  $50\Omega$  load is<sup>†</sup>

$$(P_s)_{\text{actual}} = \frac{(V_s)^2_{\text{rms}}}{R_L} = \frac{1.65 \times 10^5}{50} = 3.3 \text{ kW}\quad (4-127)$$

**SA4-4** If the AM voltage signal of SA4-1 appears across a  $50\Omega$  resistive load compute the actual peak envelope power (PEP).

**Solution.** Using (4-18), the normalized PEP is

$$\begin{aligned}(P_{\text{PEP}})_{\text{norm}} &= \frac{1}{2} [\max |g(t)|]^2 = \frac{1}{2} A_c^2 [\max m(t)]^2 \\ &= \frac{1}{2} (500)^2 [1 + 0.8]^2 = 405 \text{ kW}\end{aligned}\quad (4-128)$$

Then the actual PEP for this AM voltage signal with a  $50\Omega$  load is

$$(P_{\text{PEP}})_{\text{actual}} = \frac{(P_{\text{PEP}})_{\text{norm}}}{R_L} = \frac{4.05 \times 10^5}{50} = 8.1 \text{ kW}\quad (4-129)$$

**SA4-5** Assume that a bandpass signal,  $s(t)$ , is to be sampled and that the samples are to be stored for processing at a later time. As shown in Fig. 4-32a, this bandpass signal has a bandwidth of  $B_T$  centered about  $f_c$ , where  $f_c \gg B_T$  and  $B_T > 0$ .  $s(t)$  is to be sampled by using any one of three methods shown in Fig. 4-32.<sup>‡</sup> For each of these sampling methods, determine the minimum sampling frequency (i.e., minimum clock frequency) required and discuss the advantages and disadvantages of each method.

**Solution.**

**Method I** Referring to Fig. 4-32a, Method I uses direct sampling as described in Chapter 2. Using (2-168), the minimum sampling frequency is  $(f_s)_{\text{min}} = 2B$ , where  $B$  is the highest frequency in the signal. For this bandpass signal the highest frequency is  $B = f_c + B_T/2$ . Thus, for Method I, the minimum sampling frequency is

$$(f_s)_{\text{min}} = 2f_c + B_T \quad \text{Method I} \quad (4-130)$$

For example, if  $f_c = 100 \text{ MHz}$  and  $B_T = 1 \text{ MHz}$ , a minimum sampling frequency of  $(f_s)_{\text{min}} = 201 \text{ MHz}$  would be required.

<sup>†</sup> If  $s(t)$  were a current signal (instead of a voltage signal), then  $(P_s)_{\text{actual}} = (I_s)^2_{\text{rms}} R_L$ .

<sup>‡</sup> Thanks to Professor Christopher S. Anderson, Department of Electrical and Computer Engineering, University of Florida, for suggesting Method II.

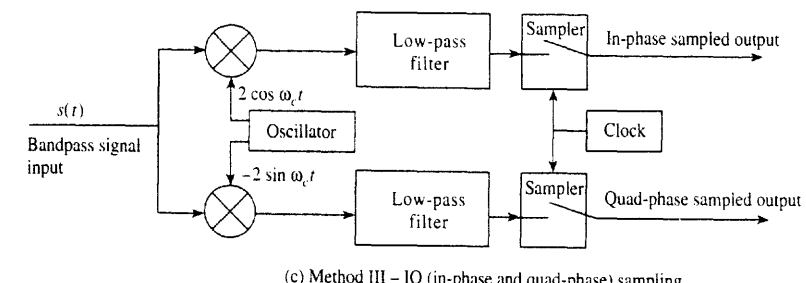
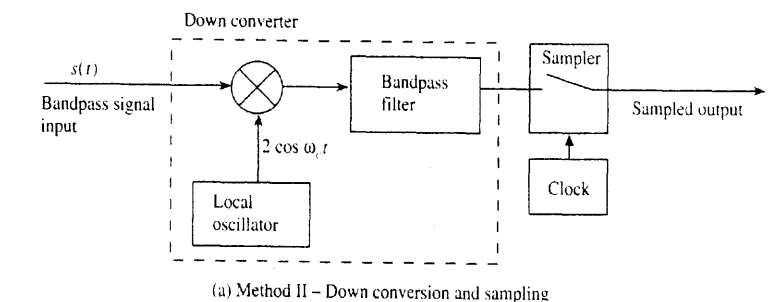
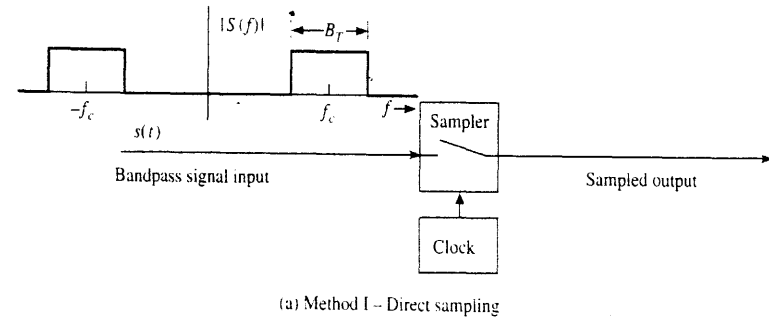


**Figure 4-32** Three methods for sampling bandpass signals.

**Method II** Referring to Fig. 4-32b, Method II down converts the bandpass signal so that the highest frequency that is to be sampled is drastically reduced. For maximum reduction of the highest frequency in the down-converted signal (at the sampler input) is  $B = (f_c + B_T/2) - f_0 = f_c + B_T/2 - f_c + B_T/2 = B_T$  and the lowest frequency (in the positive frequency part of the down converted signal) is  $(f_c - B_T/2) - f_0 = f_c - B_T/2 - f_c + B_T/2 = 0$ . Using (2-168), the minimum sampling frequency is

$$(f_s)_{\text{min}} = 2B_T \quad \text{Method II} \quad (4-131)$$

when the frequency of the LO is chosen to be  $f_0 = f_c - B_T/2$ . For this choice of LO frequency, the bandpass filter becomes a lowpass filter with a cutoff frequency of  $B_T$ . Also note that

<sup>†</sup> Low-side LO injection is used so that any asymmetry in the two sidebands of  $s(t)$  will be preserved in the same way in the down-converted signal.

Method II gives a drastic reduction of the sampling frequency (an advantage) when compared with Method I. For example, if  $f_c = 100$  MHz and  $B_T = 1$  MHz, then the minimum sampling frequency is now  $(f_s)_{\min} = 2$  MHz instead of 201 MHz required in Method I. However, Method II requires the use of a downconverter (a disadvantage). Also note, that  $(f_s)_{\min}$  of Method II, as specified by (4-131), satisfies the  $(f_s)_{\min}$  given by the *bandpass sampling theorem* as described by (4-31). Thus, Method II is one of the most efficient ways to obtain samples for a bandpass signal. However, when the bandpass signal is reconstructed from the sample values by use of (2-158) and (2-160), the *down-converted* bandpass signal is obtained. To obtain the original bandpass signal,  $s(t)$ , an upconverter is needed to convert the down-converted signal back to the original bandpass region of the spectrum. This disadvantage is eliminated when Method III is used.

**Method III** Referring to Fig. 4-32c, Method III uses in-phase ( $I$ ) and quadrature-phase ( $Q$ ) product detectors to produce the  $x(t)$  and  $y(t)$  quadrature components of  $s(t)$ . (This was discussed at the end of Sec. 4-16 and illustrated in Fig. 4-31). The highest frequencies in  $x(t)$  and  $y(t)$  are  $B = B_T/2$ . Thus, using (2-168), the minimum sampling frequency for the clock of the I and Q samplers are

$$(f_s)_{\min} = B_T \quad (\text{each sampler}) \quad \text{Method III} \quad (4-132)$$

Because there are two samplers, the combined sampling rate is  $(f_s)_{\min \text{ overall}} = 2B_T$ . This also satisfies the minimum sampling rate allowed for bandpass signals as described by (4-31). Thus, Method III (like Method II) gives one of the most efficient ways to obtain samples of bandpass signals. For the case of  $f_c = 100$  MHz and  $B_T = 1$  MHz, an overall sampling rate of 2 MHz is required for Method III, which is the same as that obtained by Method II. However, with Method III, samples of the  $x(t)$  and  $y(t)$  components are obtained (an advantage): That is, because IQ samples have been obtained, they may be processed using DSP algorithms to perform equivalent bandpass filtering as described by Sec. 4-5, or equivalent modulation of another type as described by Sec. 4-2. If desired, the original bandpass signal may be reconstructed by use of (4-32).

## PROBLEMS

- 4-1 If  $v(t) = \operatorname{Re}\{g(t)e^{j\omega_c t}\}$ , show that (4-1b) and (4-1c) are correct where  $g(t) = x(t) + jy(t) = R(t)e^{j\theta(t)}$ .
- 4-2 A double-sideband suppressed carrier (DSB-SC) signal,  $s(t)$ , with a carrier frequency of 3.8 MHz has a complex envelope  $g(t) = A_c m(t)$ .  $A_c = 50$  V, and the modulation is a 1-kHz sinusoidal test tone described by  $m(t) = 2 \sin(2\pi 1000t)$ . Evaluate the voltage spectrum for this DSB-SC signal.
- 4-3 Assume that the DSB-SC voltage signal,  $s(t)$ , as described in Prob. 4-2 appears across a  $50\Omega$  resistive load.
  - (a) Compute the actual average power dissipated in the load.
  - (b) Compute the actual PEP.
- 4-4 A bandpass filter is shown in Fig. P4-4.
  - (a) Find the mathematical expression for the transfer function of this filter  $H(f) = V_2(f)/V_1(f)$  as a function of  $R$ ,  $L$ , and  $C$ . Sketch the magnitude transfer function  $|H(f)|$ .
  - (b) Find the expression for the equivalent low-pass filter transfer function and sketch the corresponding low-pass magnitude transfer function.

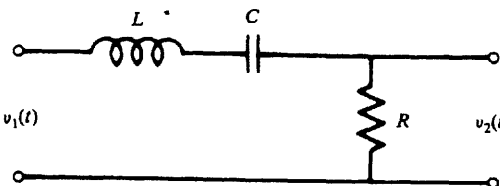


Figure P4-4

- 4-5 Let the transfer function of an ideal bandpass filter be given by

$$H(f) = \begin{cases} 1, & |f + f_c| < B_T/2 \\ 1, & |f - f_c| < B_T/2 \\ 0, & \text{elsewhere} \end{cases}$$

where  $B_T$  is the absolute bandwidth of the filter.

- (a) Sketch the magnitude transfer function,  $|H(f)|$ .
- (b) Find an expression for the waveform at the output,  $v_2(t)$ , if the input consists of the pulsed carrier:

$$v_1(t) = A\Pi(t/T) \cos(\omega_c t)$$

- (c) Sketch the output waveform,  $v_2(t)$ , for the case when  $B_T = 4/T$  and  $f_c \gg B_T$ .

*Hint:* Use the complex envelope technique and express the answer as a function of the sine integral where the sine integral is defined by

$$\operatorname{Si}(u) = \int_0^u \frac{\sin \lambda}{\lambda} d\lambda$$

The sketch can be obtained by looking up values for the sine integral from published tables [Abramowitz and Stegun, 1964] or by numerically evaluating  $\operatorname{Si}(u)$ .

- 4-6 Examine the distortion properties of an  $RC$  low-pass filter (shown in Fig. 2-15). Assume that the filter input consists of a bandpass signal that has a bandwidth of 1 kHz and a carrier frequency of 15 kHz. Let the time constant of the filter be  $\tau_0 = RC = 10^{-5}$  s.

- (a) Find the phase delay for the output carrier.
- (b) Determine the group delay at the carrier frequency.
- (c) Evaluate the group delay for frequencies around and within the frequency band of the signal. Plot this delay as a function of frequency.
- (d) Using the results of (a) through (c), explain why the filter does or does not distort the bandpass signal.

- 4-7 A bandpass filter as shown in Fig. P4-7 has the transfer function

$$H(s) = \frac{Ks}{s^2 + (\omega_0/Q)s + \omega_0^2}$$

where  $Q = R\sqrt{C/L}$ , the resonant frequency is  $f_0 = 1/(2\pi\sqrt{LC})$ ,  $\omega_0 = 2\pi f_0$ ,  $K$  is a constant, and values for  $R$ ,  $L$ , and  $C$  are given in the figure. Assume that a bandpass signal with  $f_c = 4$  kHz and a bandwidth of 200 Hz passes through the filter, where  $f_0 = f_c$ .

- (a) Using (4-39), find the bandwidth of the filter?
- (b) Plot the carrier delay as a function of  $f$  about  $f_0$ .

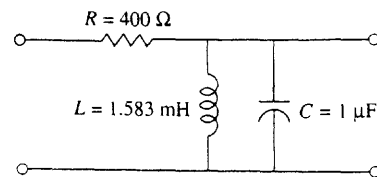


Figure P4-7

- (c) Plot the group delay as a function of  $f$  about  $f_0$ .  
 (d) Explain why the filter does or does not distort the signal.

**4-8** An FM signal is of the form

$$s(t) = \cos \left[ \omega_c t + D_f \int_{-\infty}^t m(\sigma) d\sigma \right]$$

where  $m(t)$  is the modulating signal and  $\omega_c = 2\pi f_c$ ,  $f_c$  being the carrier frequency. Show that the functions  $g(t)$ ,  $x(t)$ ,  $y(t)$ ,  $R(t)$ , and  $\theta(t)$  as given for FM in Table 4-1 are correct.

**4-9** Given a modulated signal

$$s(t) = 100 \sin(\omega_c + \omega_a)t + 500 \cos \omega_c t - 100 \sin(\omega_c - \omega_a)t$$

where the unmodulated carrier is  $500 \cos \omega_c t$ .

- (a) Find the complex envelope for the modulated signal. What type of modulation is it? What is the modulating signal?  
 (b) Find the quadrature modulation components,  $x(t)$  and  $y(t)$ , for this modulated signal.  
 (c) Find the magnitude and PM components,  $R(t)$  and  $\theta(t)$ , for this modulated signal.  
 (d) Find the total average power where  $s(t)$  is a voltage waveform that is applied across a  $50\text{-}\Omega$  load.  
**4-10** Find the spectrum for the modulated signal as given in Prob. 4-9 by two methods.  
 (a) By direct evaluation using the Fourier transform of  $s(t)$ .  
 (b) By the use of (4-12).  
**4-11** Given a pulse-modulated signal of the form

$$s(t) = e^{-at} \cos[(\omega_c + \Delta\omega)t] u(t)$$

where  $a$ ,  $\omega_c$ , and  $\Delta\omega$  are positive constants and  $\omega_c \gg \Delta\omega$  ( $\omega_c$  is the carrier frequency),

- (a) Find the complex envelope.  
 (b) Find the spectrum  $S(f)$ .  
 (c) Sketch the magnitude and phase spectra  $|S(f)|$  and  $\theta(f) = \angle S(f)$ .

- 4-12** In a digital computer simulation of a bandpass filter, the complex envelope of the impulse response is used where  $h(t) = \operatorname{Re}[k(t)e^{j\omega_c t}]$ , as shown in Fig. 4-3. The complex impulse response can be expressed in terms of quadrature components:  $k(t) = 2h_x(t) + j2h_y(t)$ , where  $h_x(t) = \frac{1}{2}\operatorname{Re}[k(t)]$  and  $h_y(t) = \frac{1}{2}\operatorname{Im}[k(t)]$ . The complex envelopes of the input and output are denoted, respectively, by  $g_1(t) = x_1(t) + jy_1(t)$  and  $g_2(t) = x_2(t) + jy_2(t)$ . The bandpass filter simulation can be carried out by using four *real baseband* filters (i.e., filters having real impulse responses), as shown in Fig. P4-12. Note that although there are four filters, there are only two distinctly different impulse responses,  $h_x(t)$  and  $h_y(t)$ .  
 (a) Using (4-22), show that Fig. P4-12 is correct.  
 (b) Show that  $h_y(t) \equiv 0$  (i.e., no filter needed) if the bandpass filter has a transfer function with Hermitian symmetry about  $f_c$ , that is, if  $H(-\Delta f + f_c) = H^*(\Delta f + f_c)$  where  $|\Delta f| < B_T/2$

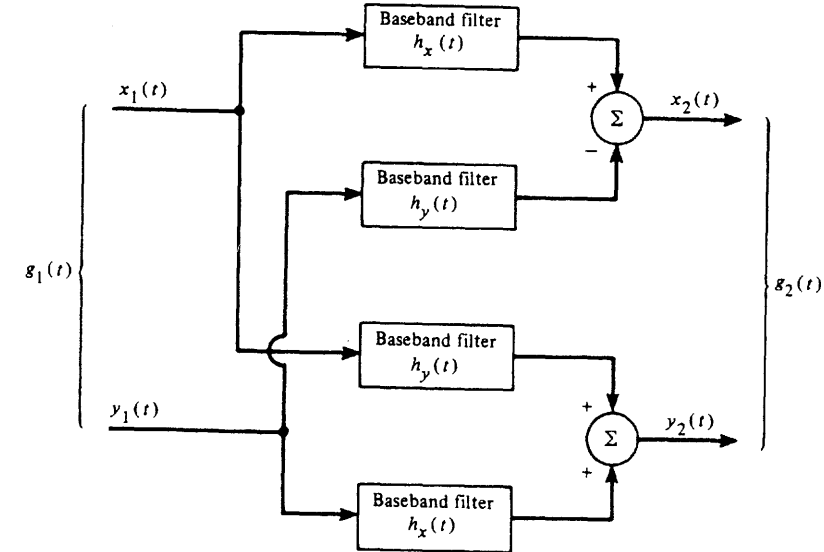


Figure P4-12

and  $B_T$  is the bounded spectral bandwidth of the bandpass filter. This Hermitian symmetry implies that the magnitude frequency response of the bandpass filter is even about  $f_c$  and the phase response is odd about  $f_c$ .

- 4-13** Evaluate and sketch the magnitude transfer function for (a) Butterworth, (b) Chebyshev, and (c) Bessel low-pass filters. Assume that  $f_b = 10$  Hz and  $\varepsilon = 1$ .  
**4-14** Plot the amplitude response, the phase response, and the phase delay as a function of frequency for the following low-pass filters where  $B = 100$  Hz. Also, compare your results for these two filters.  
 (a) Butterworth filter, second order:

$$H(f) = \frac{1}{1 + \sqrt{2}(jf/B) + (jf/B)^2}$$

- (b) Butterworth filter, fourth order:

$$H(f) = \frac{1}{[1 + 0.765(jf/B) + (jf/B)^2][1 + 1.848(jf/B) + (jf/B)^2]}$$

- 4-15** Assume that the output-to-input characteristic of a bandpass amplifier is described by (4-42) and that the linearity of the amplifier is being evaluated by using a two-tone test.  
 (a) Find the frequencies of the fifth-order intermodulation products that fall within the amplifier bandpass.  
 (b) Evaluate the levels for the fifth-order intermodulation products in terms of  $A_1$ ,  $A_2$ , and the  $K_s$ .  
**4-16** An amplifier is tested for total harmonic distortion (THD) by using a single-tone test. The output is observed on a spectrum analyzer. It is found that the peak values of the three measured harmonics decrease according to an exponential recursion relation,  $V_{n+1} = V_n e^{-n}$ , where  $n = 1, 2, 3$ . What is the THD?



- 4-17** The nonlinear output-input characteristic of an amplifier is

$$v_{\text{out}}(t) = 5v_{\text{in}}(t) + 1.5v_{\text{in}}^2(t) + 1.5v_{\text{in}}^3(t)$$

Assume that input signal consists of seven components

$$v_{\text{in}}(t) = \frac{1}{2} + \frac{4}{\pi^2} \sum_{k=1}^6 \frac{1}{(2k-1)^2} \cos[(2k-1)\pi t]$$

- (a) Plot the output signal and compare it with the linear output component  $5v_{\text{in}}(t)$ .  
 (b) Take the FFT of the output  $v_{\text{out}}(t)$  and compare it with the spectrum for the linear output component.

- 4-18** For a bandpass limiter circuit, show that the bandpass output is given by (4-55), where  $K = (4/\pi)A_0$ .  $A_0$  denotes the voltage gain of the bandpass filter, and it is assumed that the gain is constant over the frequency range of the bandpass signal.  
**4-19** Discuss whether or not the Taylor series nonlinear model is applicable for analysis of (a) soft limiters and (b) hard limiters.  
**4-20** Assume that an audio sine-wave testing signal is passed through an audio hard limiter circuit. Evaluate the total harmonic distortion (THD) on the signal at the limiter output.  
**4-21** Using the mathematical definition for linearity given in Chapter 2, show that the analog switch multiplier of Fig. 4-10 is a linear device.

- 4-22** An audio signal with a bandwidth of 10 kHz is transmitted over an AM transmitter with a carrier frequency of 1.0 MHz. The AM signal is received on a superheterodyne receiver with an envelope detector. What is the constraint on the  $RC$  time constant for the envelope detector?  
**4-23** Assume that an AM receiver with an envelope detector is tuned to an SSB-AM signal that has a modulation waveform given by  $m(t)$ . Find the mathematical expression for the audio signal that appears at the receiver output in terms of  $m(t)$ . Is the audio output distorted?

- 4-24** Evaluate the sensitivity of the zero-crossing FM detector shown in Fig. 4-18. Assume that the differential amplifier is described by  $v_{\text{out}}(t) = A[v_2(t) - v_3(t)]$ , where  $A$  is the voltage gain of the amplifier. In particular, show that  $v_{\text{out}} = Kf_d$ , where  $f_d = f_i - f_c$  and find the value of the sensitivity constant  $K$  in terms of  $A$ ,  $R$ , and  $C$ . Assume that the peak levels of the monostable outputs  $Q$  and  $\bar{Q}$  are 4 V (TTL circuit levels).

- 4-25** (a) Using (4-100), show that the linearized block diagram model for a PLL is given by Fig. 4-22.  
 (b) Show that (4-101) describes the linear PLL model as given in Fig. 4-22.

- 4-26** Using the Laplace transform and the final value theorem, find an expression for the steady-state phase error,  $\lim_{t \rightarrow \infty} \theta_e(t)$ , for a PLL as described by (4-100). [Hint: The final value theorem is  $\lim_{t \rightarrow \infty} f(t) = \lim_{s \rightarrow 0} sF(s)$ .]

- 4-27** Assume that the loop filter of a PLL is a low-pass filter, as shown in Fig. P4-27.

- (a) Evaluate the closed-loop transfer function  $H(f) = \frac{\Theta_0(f)}{\Theta_i(f)}$  for a linearized PLL.  
 (b) Sketch the Bode plot  $[|H(f)|]_{\text{dB}} \triangleq 20 \log |H(f)|$ , for this PLL.

- 4-28** Assume that the phase noise characteristic of a PLL is being examined. The internal phase noise of the VCO is modeled by the input  $\theta_n(t)$ , as shown in Fig. P4-28.  
 (a) Find an expression for the closed-loop transfer function  $\Theta_0(f)/\Theta_n(f)$ , where  $\theta_i(t) = 0$ .  
 (b) If  $F_1(f)$  is a low-pass filter given in Fig. P4-27, sketch the Bode plot  $[|\Theta_0(f)/\Theta_n(f)|]_{\text{dB}}$  for the phase noise transfer function.

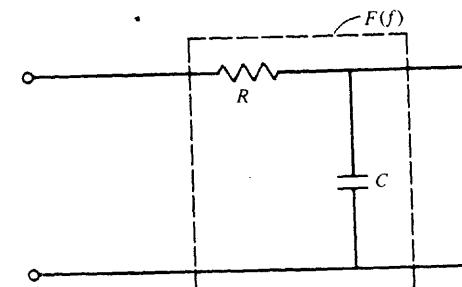


Figure P4-27

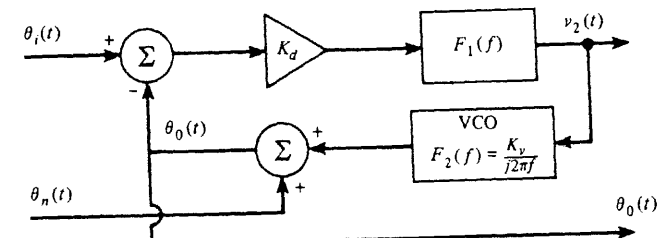


Figure P4-28

- 4-29** The input to a PLL is  $v_{\text{in}}(t) = A \sin(\omega_0 t + \theta_i)$ . The LPF has a transfer function  $F(s) = (s + a)/s$ .  
 (a) What is the steady-state phase error?  
 (b) What is the maximum hold-in range for the noiseless case?  
**4-30** (a) Refer to Fig. 4-25 for a PLL frequency synthesizer. Design a synthesizer that will cover a range of 144 to 148 MHz in 5-kHz steps starting at 144.000 MHz. Assume that the frequency standard operates at 5 MHz and that the  $M$  divider is fixed at some value and the  $N$  divider is programmable so that the synthesizer will cover the desired range. Sketch a diagram of your design, indicating the frequencies present at various points of the diagram.  
 (b) Modify your design so that the output signal can be frequency modulated with an audio-frequency input such that the peak deviation of the RF output is 5 kHz.  
**4-31** Assume that an SSB-AM transmitter is to be realized using the AM-PM generation technique, as shown in Fig. 4-27.  
 (a) Sketch a block diagram for the baseband signal processing circuit.  
 (b) Find expressions for  $R(t)$ ,  $\theta(t)$ , and  $v(t)$  when the modulation is  $m(t) = A_1 \cos \omega_1 t + A_2 \cos \omega_2 t$ .  
**4-32** Rework Prob. 4-31 for the case of generating an FM signal.  
**4-33** Assume that an SSB-AM transmitter is to be realized using the quadrature generation technique, as shown in Fig. 4-28.  
 (a) Sketch a block diagram for the baseband signal processing circuit.  
 (b) Find expressions for  $x(t)$ ,  $y(t)$ , and  $v(t)$  when the modulation is  $m(t) = A_1 \cos \omega_1 t + A_2 \cos \omega_2 t$ .  
**4-34** Rework Prob. 4-33 for the case of generating an FM signal.

- 4-35** An FM radio is tuned to receive an FM broadcasting station of frequency 96.9 MHz. The radio is of the superheterodyne type with the LO operating on the high side of the 96.9-MHz input and using a 10.7-MHz IF amplifier.
- Determine the LO frequency.
  - If the FM signal has a bandwidth of 180 kHz, determine the filter characteristics for the RF and IF filters.
  - Calculate the frequency of the image response.
- 4-36** A 4-GHz satellite downlink signal is received on an Earth station receiver. The IF frequency is 70 MHz. What is the image frequency for the case of:
- High-side injection?
  - Low-side injection?
- 4-37** A superheterodyne receiver is tuned to a station at 20 MHz. The local oscillator frequency is 80 MHz and the IF is 100 MHz.
- What is the image frequency?
  - If the LO has appreciable second-harmonic content, what two additional frequencies are received?
  - If the RF amplifier contains a single-tuned parallel resonant circuit with  $Q = 50$  tuned to 20 MHz, what will be the image attenuation in dB?
- 4-38** An SSB-AM receiver is tuned to receive a 7.225-MHz lower SSB (LSSB) signal. The LSSB signal is modulated by an audio signal that has a 3-kHz bandwidth. Assume that the receiver uses a superheterodyne circuit with an SSB IF filter. The IF amplifier is centered on 3.395 MHz. The LO frequency is on the high (frequency) side of the input LSSB signal.
- Draw a block diagram of the single-conversion superheterodyne receiver, indicating frequencies present and typical spectra of the signals at various points within the receiver.
  - Determine the required RF and IF filter specifications, assuming that the image frequency is to be attenuated by 40 dB.
- 4-39** (a) Draw a block diagram of a superheterodyne FM receiver that is designed to receive FM signals over a band from 144 to 148 MHz. Assume that the receiver is of the dual conversion type (i.e., a mixer and an IF amplifier followed by another mixer and a second IF amplifier) where the first IF frequency is 10.7 MHz and the second IF is 455 kHz. Indicate the frequencies of the signals at different points on the diagram and, in particular, show the frequencies involved when a signal at 146.82 MHz is being received.
- (b) Replace the first oscillator by a frequency synthesizer such that the receiver can be tuned in 5-kHz steps from 144.000 to 148.000 MHz. Show the diagram of your synthesizer design and the frequencies involved.
- 4-40** An AM broadcast-band radio is tuned to receive a 1080-kHz AM signal and uses high-side LO injection. The IF is 455 kHz.
- Sketch the frequency response for the RF and IF filters.
  - What is the image frequency?
- 4-41** Commercial AM broadcast stations operate in the 540- to 1700-kHz band with a transmission bandwidth limited to 10 kHz.
- What are the maximum number of stations that can be accommodated?
  - If stations are not assigned to adjacent channels (in order to reduce interference on receivers that have poor IF characteristics), how many stations can be accommodated?
  - For 455-kHz IF receivers, what band of image frequencies fall within the AM band for down-converter receivers with high-side injection?

## CHAPTER 5

# AM, FM, AND DIGITAL MODULATED SYSTEMS

This chapter is concerned with the classical bandpass techniques of amplitude modulation (AM), single-sideband (SSB), phase modulation (PM), and frequency modulation (FM); and with digital modulation techniques of on-off keying (OOK), binary-phase shift keying (BPSK), frequency-shift keying (FSK), quadrature phase-shift keying (QPSK), and quadrature amplitude modulation (QAM). All of these bandpass signaling techniques consist of modulating an analog or digital baseband signal onto a carrier. This was first introduced in Sec. 4-2. In particular, the modulated bandpass signal can be described by

$$s(t) = \operatorname{Re}\{g(t)^{j\omega_c t}\} \quad (5-1)$$

where  $\omega_c = 2\pi f_c$ , and  $f_c$  is the carrier frequency. The desired type of modulated signal,  $s(t)$ , is obtained by selecting the appropriate modulation mapping function  $g[m(t)]$  of Table 4-1 where  $m(t)$  is the analog or digital baseband signal.

The voltage (or current) spectrum of the bandpass signal is

$$S(f) = \frac{1}{2} [G(f - f_0) + G^*(-f - f_0)] \quad (5-2a)$$

and the PSD is

$$\mathcal{P}_s(f) = \frac{1}{4} [\mathcal{P}_g(f - f_c) + \mathcal{P}_g(-f - f_c)] \quad (5-2b)$$

where  $G(f) = \mathcal{F}[g(t)]$  and  $\mathcal{P}_g(f)$  is the PSD of the complex envelope  $g(t)$ .

The goals of this chapter are to

- Study  $g(t)$  and  $s(t)$  for various types of analog and digital modulations
- Evaluate the spectrum for various types of analog and digital modulations
- Examine some transmitter and receiver structures
- Study some adopted standards
- Learn about spread spectrum systems

## 5-1 AMPLITUDE MODULATION

From Table 4-1, the complex envelope of an AM signal is given by

$$g(t) = A_c[1 + m(t)] \quad (5-3)$$

where the constant  $A_c$  has been included to specify the power level and  $m(t)$  is the modulating signal (which may be analog or digital). These equations reduce to the representation for the AM signal:

$$s(t) = A_c[1 + m(t)] \cos \omega_c t \quad (5-4)$$

A waveform illustrating the AM signal, as seen on an oscilloscope, is shown in Fig. 5-1. For convenience it is assumed that the modulating signal  $m(t)$  is a sinusoid.  $A_c[1 + m(t)]$  corresponds to the in-phase component  $x(t)$  of the complex envelope; it also corresponds to the real envelope  $|g(t)|$  when  $m(t) \geq -1$  (the usual case).

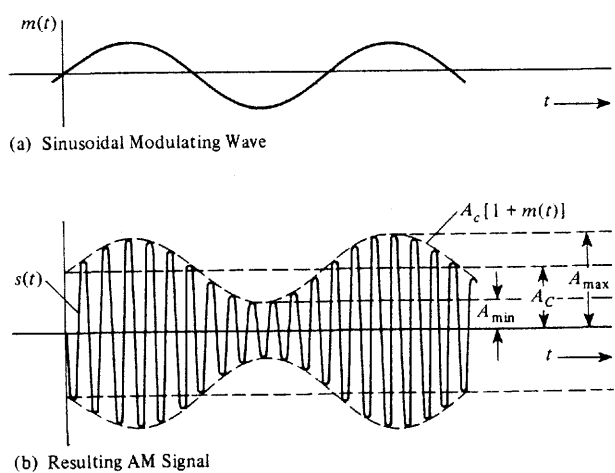


Figure 5-1 AM signal waveform.

## Sec. 5-1 Amplitude Modulation

If  $m(t)$  has a peak positive value of +1 and a peak negative value of -1, the AM signal is said to be 100% modulated.

**DEFINITION.** The *percentage of positive modulation* on an AM signal is

$$\% \text{ positive modulation} = \frac{A_{\max} - A_c}{A_c} \times 100 = \max[m(t)] \times 100 \quad (5-5a)$$

and the *percentage of negative modulation* is

$$\% \text{ negative modulation} = \frac{A_c - A_{\min}}{A_c} \times 100 = -\min[m(t)] \times 100 \quad (5-5b)$$

The overall modulation percentage is

$$\% \text{ modulation} = \frac{A_{\max} - A_{\min}}{2A_c} \times 100 = \frac{\max[m(t)] - \min[m(t)]}{2} \times 100 \quad (5-6)$$

where  $A_{\max}$  is the maximum value of  $A_c[1 + m(t)]$ ,  $A_{\min}$  is the minimum value, and  $A_c$  is the level of the AM envelope under the condition of no modulation [i.e.,  $m(t) = 0$ ].

Equation (5-6) may be obtained by averaging the positive and negative modulation as given by (5-5a) and (5-5b).  $A_{\max}$ ,  $A_{\min}$ , and  $A_c$  are illustrated in Fig. 5-1b, where, in this example,  $A_{\max} = 1.5A_c$  and  $A_{\min} = 0.5A_c$ , so that the percentages of positive and negative modulation are both 50% and the overall modulation is 50%.

The percentage of modulation can be over 100% ( $A_{\min}$  will have a negative value) provided that a four-quadrant multiplier is used to generate the product of  $A_c[1 + m(t)]$  and  $\cos \omega_c t$  so that the true AM waveform, as given by (5-4), is obtained.<sup>†</sup> However, if the transmitter uses a two-quadrant multiplier that produces a zero output when  $A_c[1 + m(t)]$  is negative, the output signal will be

$$s(t) = \begin{cases} A_c[1 + m(t)] \cos \omega_c t, & \text{if } m(t) \geq -1 \\ 0, & \text{if } m(t) < -1 \end{cases} \quad (5-7)$$

which is a distorted AM signal. The bandwidth of this signal is much wider than that of the undistorted AM signal, as is easily demonstrated by spectral analysis. This is the overmodulated condition that the FCC does not allow. An AM transmitter that uses plate modulation is an example of a circuit that acts as a two quadrant multiplier. Here, for high-power AM signal generation, the unmodulated carrier signal is applied to the grid of the tube, and the dc plate voltage is varied proportionally to  $A_c[1 + m(t)]$ , where  $A_c[1 + m(t)] \geq 0$ . This produces the product  $A_c[1 + m(t)] \cos \omega_c t$ , provided that  $m(t) \geq -1$ , but produces no output when  $m(t) < -1$ .

If the percentage of negative modulation is less than 100%, an envelope detector may be used to recover the modulation without distortion since the envelope,  $|g(t)| = |A_c[1 + m(t)]|$ , is identical to  $A_c[1 + m(t)]$ . If the percentage of negative modulation is over 100%,

<sup>†</sup> If the percentage of modulation becomes very large (approaching infinity), the AM signal becomes the double-sideband suppressed carrier signal that is described in the next section.

undistorted modulation can still be recovered provided that the proper type of detector—a product detector—is used. This is seen from (4-76) with  $\theta_0 = 0$ . Furthermore, the product detector may be used for any percentage of modulation. In Chapter 7 it will be found that a product detector is superior to an envelope detector when the input signal-to-noise ratio is small.

Using (4-17), we realize that the *normalized average power* of the AM signal is

$$\begin{aligned}\langle s^2(t) \rangle &= \frac{1}{2} \langle |g(t)|^2 \rangle = \frac{1}{2} A_c^2 \langle [1 + m(t)]^2 \rangle \\ &= \frac{1}{2} A_c^2 \langle 1 + 2m(t) + m^2(t) \rangle \\ &= \frac{1}{2} A_c^2 + A_c^2 \langle m(t) \rangle + \frac{1}{2} A_c^2 \langle m^2(t) \rangle\end{aligned}\quad (5-8)$$

If the modulation contains no dc level,  $\langle m(t) \rangle = 0$  and the *normalized power* of the AM signal is

$$\langle s^2(t) \rangle = \underbrace{\frac{1}{2} A_c^2}_{\text{discrete carrier power}} + \underbrace{\frac{1}{2} A_c^2 \langle m^2(t) \rangle}_{\text{sideband power}}\quad (5-9)$$

Note that this result is identical to that given by (4-21) if  $A_c = 1$ .

**DEFINITION.** The *modulation efficiency* is the percentage of the total power of the modulated signal that conveys information.

In AM signaling, only the sideband components convey information, so the modulation efficiency is

$$E = \frac{\langle m^2(t) \rangle}{1 + \langle m^2(t) \rangle} \times 100\% \quad (5-10)$$

The highest efficiency that could be obtained for a 100% AM signal would be 50%, which is attained only for square-wave modulation.

Using (4-18), we obtain the normalized peak envelope power (PEP) of the AM signal:

$$P_{\text{PEP}} = \frac{A_c^2}{2} \{1 + \max[m(t)]\}^2 \quad (5-11)$$

The voltage spectrum of the AM signal was obtained in (4-20a) of Example 4-1 and is

$$S(f) = \frac{A_c}{2} [\delta(f - f_c) + M(f - f_c) + \delta(f + f_c) + M(f + f_c)] \quad (5-12)$$

(The AM spectrum is given in Fig. 4-2.) The AM spectrum is relatively easy to obtain since it is just a translated version of the modulation spectrum plus delta functions that give the carrier line spectral component. The *bandwidth* is *twice* that of the modulation. As we will see shortly, the spectrum for an FM signal is much more complicated since the modulation mapping function  $g(m)$  is non-linear.

### Example 5-1 POWER OF AN AM SIGNAL

The FCC rates AM broadcast band transmitters by their average *carrier power*; this is common in other AM audio applications as well. Suppose that a 5000-W AM transmitter is connected to a  $50\Omega$  load; then the constant  $A_c$  is given by  $\frac{1}{2} A_c^2 / 50 = 5000$ . Thus the peak voltage across the load will be  $A_c = 707$  V during the times of no modulation. If the transmitter is then 100% modulated by a 1000-Hz test tone, the total (carrier plus sideband) average power will be, from (5-9),

$$1.5 \left[ \frac{1}{2} \left( \frac{A_c^2}{50} \right) \right] = (1.5) \times (5000) = 7500 \text{ W}$$

because  $\langle m^2(t) \rangle = \frac{1}{2}$  for a sinusoidal modulation waveshape of unity (100%) amplitude. Note that 7500 W is the actual power, not the normalized power. The peak voltage (100% modulation) is  $(2)(707) = 1414$  V across the  $50\Omega$  load. From (5-11), the PEP is

$$4 \left[ \frac{1}{2} \left( \frac{A_c^2}{50} \right) \right] = (4)(5000) = 20,000 \text{ W}$$

The modulation efficiency would be 33% since  $\langle m^2(t) \rangle = \frac{1}{2}$ .

There are many ways of building AM transmitters. One might first consider generating the AM signal at a low power level (by using a multiplier) and then amplifying it. This, however, requires the use of linear amplifiers (such as Class A or B amplifiers, as discussed in Sec. 4-9) so that the AM will not be distorted. Because these linear amplifiers are not very efficient in converting the power-supply power to an RF signal, much of the energy is wasted in heat.<sup>†</sup> Consequently, high-power AM broadcast transmitters are built by amplifying the carrier oscillator signal to a high power level with efficient Class C or Class D amplifiers and then amplitude modulating the last high-power stage. This is called *high-level* modulation, and an example is shown in Fig. 5-2a. For high conversion efficiency, a pulse width modulation (PWM) technique is used to achieve the AM [DeAngelo, 1982], as shown in this

<sup>†</sup> Do not confuse this conversion efficiency with modulation efficiency, which was defined by (5-10).

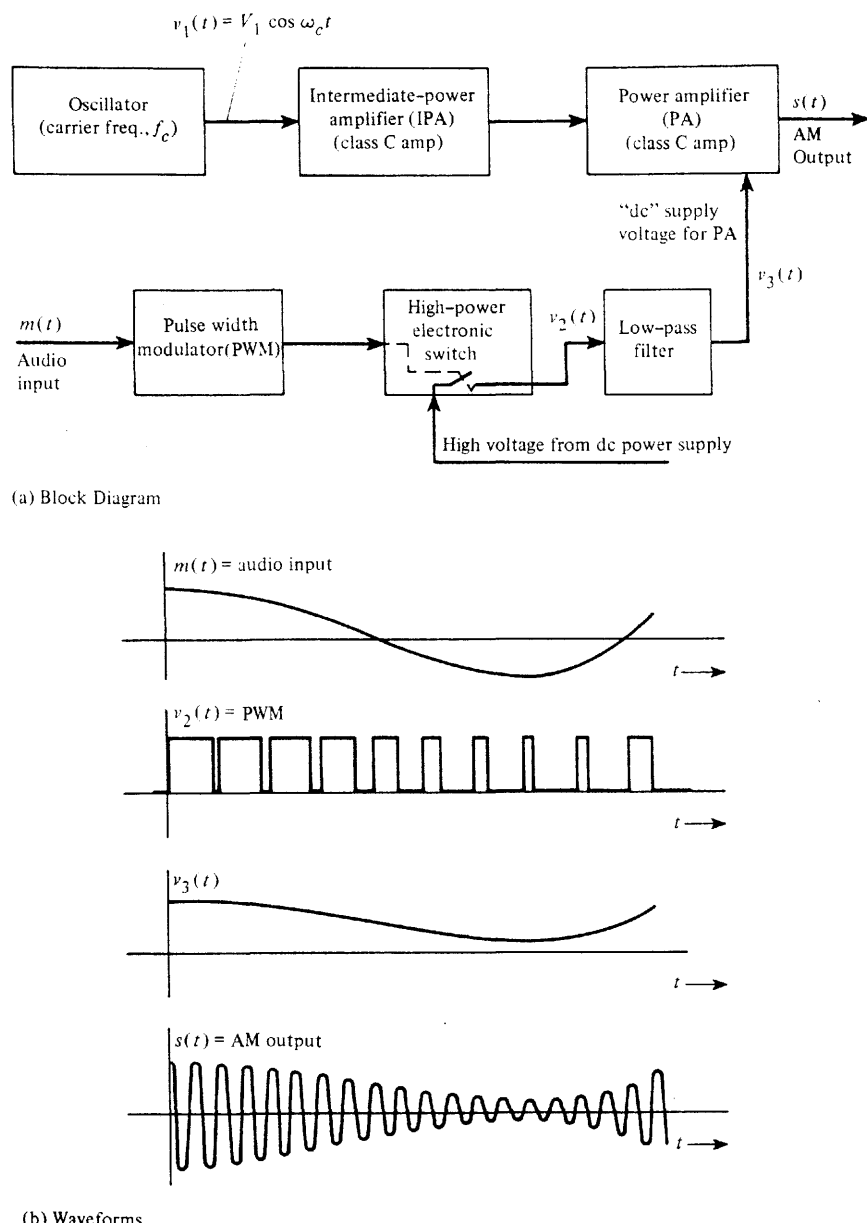


**Figure 5-2** Generation of high-power AM by the use of PWM.

figure. The audio input is converted to a PWM signal that is used to control a high-power switch (tube or transistor) circuit. The switch circuit output consists of a high-level PWM signal that is filtered by a low-pass filter to produce the “dc” component that is used as the power supply for the power amplifier (PA) stage. The PWM switching frequency is usually chosen in the range of 70 to 80 kHz so that the fundamental and harmonic components of

the PWM signal can be easily suppressed by the lowpass filter, and yet the “dc” can vary at an audio rate as high as 12 or 15 kHz for good AM audio frequency response. This technique provides excellent frequency response and low distortion since no high-power audio transformers are needed.

## 5-2 AM BROADCAST TECHNICAL STANDARDS

Some of the FCC technical standards for AM broadcast stations are shown in Table 5-1. In the United States, assigned carrier frequencies are classified according to the station’s intended coverage: clear-channel, regional, or local. Clear-channel stations, also called *Class I* or *Class II* stations, are licensed to operate with a carrier power as large as 50 kW. These stations are intended to cover large areas. Moreover, to accommodate as many stations as possible, nonclear-channel stations may be assigned to operate on clear-channel frequencies when they can be implemented without interfering with the dominant clear-channel station. Often, to prevent interference, these secondary stations have to operate with directional antenna patterns such that there is a null in the direction of the dominant station. This is especially true for nighttime operation when sky-wave propagation allows the clear-channel stations to cover most of the United States. Other secondary stations are allowed to operate only in the daytime since any nighttime operation would interfere with the clear-channel station. Other frequencies are set aside for regional stations, also called *Class III* stations, which are intended to cover medium-sized areas. These stations have allowed carrier power levels as large as 5 kW. A third class of frequencies is assigned to local (also called *Class IV*) stations, which are intended to cover one city or a county area and are licensed for a maximum power of 1 kW. Detailed listings of the frequency assignments for these four classes of stations and their licensed powers are available. International broadcast AM stations, which operate in the shortwave bands (3 to 30 MHz), generally operate with higher power levels. Some of these feed 500 kW of carrier power into directional antennas. These antennas pro-

**TABLE 5-1** AM BROADCAST STATION TECHNICAL STANDARDS

Item	FCC Technical Standard
Assigned frequency, $f_c$	In 10-kHz increments from 540 to 1700 kHz
Channel bandwidth	10 kHz
Carrier frequency stability	$\pm 20$ Hz of the assigned frequency
% modulation	Maintain 85-95%; max.: 100% neg., 125% pos.
Audio-frequency response <sup>a</sup>	$\pm 2$ dB from 100 Hz to 5 kHz with 1 kHz being the 0-dB reference
Harmonic distortion <sup>a</sup>	Less than 5% for up to 85% modulation; less than 7.5% for modulation between 85% and 95%
Noise and hum	At least 45 dB below 100% modulation in the band 30 Hz to 20 kHz
Maximum power licensed	50 kW

<sup>a</sup> Under the new FCC deregulation policy, these requirements are deleted from the FCC rules, although broadcasters still use them as guidelines for minimum acceptable performance.

duce effective radiated power levels in the megawatt range (i.e., when the gain of the directional antenna is included).

For many years, AM broadcasters have dreamed of offering stereo transmissions to their listeners. Technically, this advance has been possible for a long time, but for political reasons it was not implemented until the 1980's. In 1977 the FCC conducted evaluations of five different AM stereo systems that were proposed by the Kahn Communication/Hazeltine Corporation, Belar Electronics, the Magnavox Corporation, the Harris Corporation, and Motorola [Mennie, 1978; Murphy, 1988]. Each of these proposed systems had advantages and disadvantages, and the FCC decided to allow each AM broadcaster to implement any one of them. This led to confusion in the marketplace since each system required a different type of stereo decoding circuit in the AM receiver. However, it appears that the Motorola system is the choice of most broadcasters, and the FCC has now adopted the Motorola system for the AM stereo standard.

The Motorola C-QUAM<sup>†</sup> system uses quadrature modulation (QM) (see Table 4-1). The monaural audio, consisting of the sum of the left and right channels, is used to modulate a cosine carrier. That is,  $m_1(t) = V_0 + m_L(t) + m_R(t)$ , where  $V_0$  is the dc offset used to produce the discrete carrier term in the AM spectrum,  $m_L(t)$  is the left-channel audio, and  $m_R(t)$  is the right-channel audio. The quadrature carrier is modulated by  $m_2(t) = m_L(t) - m_R(t)$ . The resulting real envelope  $R(t)$  consists of a dc term and a distorted audio term. The distortion is reduced by using a limiter and a filter on the QM output and then amplitude modulating the resulting constant-amplitude signal with  $m_L(t) + m_R(t)$  [Mennie, 1978]. The resulting C-QUAM signal is compatible with a mono (conventional) AM receiver for mono reception. Stereo AM receivers use an envelope detector to recover  $m_L(t) + m_R(t)$  and a quadrature product detector to recover  $m_L(t) - m_R(t)$ . Sum and difference networks can then be used to obtain the left- and right-channel audio,  $m_L(t)$  and  $m_R(t)$ , respectively.

### 5-3 DOUBLE-SIDEBAND SUPPRESSED CARRIER

A double-sideband suppressed carrier (DSB-SC) signal is essentially an AM signal that has a suppressed discrete carrier. The DSB-SC signal is given by

$$s(t) = A_c m(t) \cos \omega_c t \quad (5-13)$$

where  $m(t)$  is assumed to have a zero dc level for the suppressed carrier case. The spectrum is identical to that for AM given by (5-12), except that the delta functions at  $\pm f_c$  are missing. That is, the spectrum for DSB-SC is

$$S(f) = \frac{A_c}{2} [M(f - f_c) + M(f + f_c)] \quad (5-14)$$

When compared with an AM signal, the percentage of modulation on a DSB-SC signal is infinite because there is no carrier line component. Furthermore, the modulation efficiency of a DSB-SC signal is 100% since no power is wasted in a discrete carrier. However, a product detector (which is more expensive than an envelope detector) is required for demodulation of the DSB-SC signal. If transmitting circuitry restricts the modulated signal to a certain

<sup>†</sup> C-QUAM is the acronym used by Motorola for compatible quadrature amplitude modulation.

peak value, say  $A_p$ , it can be demonstrated (see Prob. 5-8) that the sideband power of a DSB-SC signal is *four* times that of a comparable AM signal that has the same peak level. In this sense the DSB-SC signal has a fourfold power advantage over that of an AM signal.

It is also realized that if  $m(t)$  is a polar binary data signal (instead of an audio signal), then (5-13) is a BPSK signal, discussed in Example 2-18. As shown in Table 4-1, a QM signal can be generated by adding two DSB signals where there are two modulating signals,  $m_1(t)$  and  $m_2(t)$ , modulating cosine and sine carriers, respectively.

### 5-4 COSTAS LOOP AND SQUARING LOOP

The coherent reference for product detection cannot be obtained by the use of an ordinary phase-locked tracking loop since there are no spectral line components at  $\pm f_c$ . However, since the DSB-SC signal has a spectrum that is symmetrical with respect to the (suppressed) carrier frequency, either one of two types of carrier recovery loops shown in Fig. 5-3 may be used to demodulate the DSB-SC signal. Figure 5-3a shows the *Costas PLL* and Fig. 5-3b shows the *squaring loop*. It can be shown that the noise performance of these two loops are equivalent [Ziemer and Peterson, 1985], so the choice of which loop to implement depends on the relative cost of the loop components and the accuracy that can be realized when each component is built.

As shown in Fig. 5-3a, the Costas PLL is analyzed by assuming that the VCO is locked to the input suppressed carrier frequency,  $f_c$ , with a constant phase error of  $\theta_e$ . Then the voltages  $v_1(t)$  and  $v_2(t)$  are obtained at the output of the baseband low-pass filters as shown. Since  $\theta_e$  is small, the amplitude of  $v_1(t)$  is relatively large compared to that of  $v_2(t)$  (i.e.,  $\cos \theta_e \gg \sin \theta_e$ ). Furthermore,  $v_1(t)$  is proportional to  $m(t)$ , so it is the demodulated (product detector) output. The product voltage  $v_3(t)$  is

$$v_3(t) = \frac{1}{2} (\frac{1}{2} A_0 A_c)^2 m^2(t) \sin 2\theta_e$$

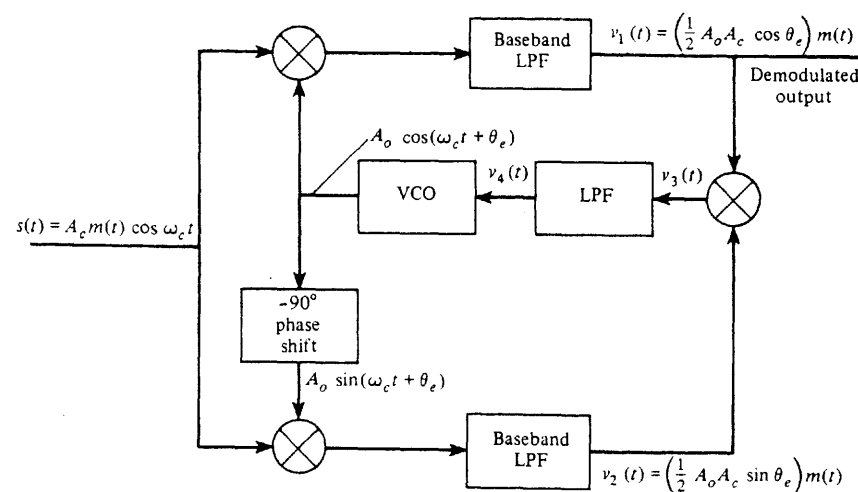
The voltage  $v_3(t)$  is filtered with a LPF that has a cutoff frequency near dc so that this filter acts as an integrator to produce the dc VCO control voltage

$$v_4(t) = K \sin 2\theta_e$$

where  $K = \frac{1}{2} (\frac{1}{2} A_0 A_c)^2 \langle m^2(t) \rangle$  and  $\langle m^2(t) \rangle$  is the dc level of  $m^2(t)$ . This dc control voltage is sufficient to keep the VCO locked to  $f_c$  with a small phase error,  $\theta_e$ .

The squaring loop, shown in Fig. 5-3b, is analyzed by evaluating the expression for the signal out of each component block as shown on this figure. As shown by Fig. 5-3, either the Costas PLL or the squaring loop can be used to demodulate a DSB-SC signal, since for each case the output is  $Cm(t)$ , where  $C$  is a constant. Furthermore, either of these loops can be used to recover (i.e., demodulate) a BPSK signal since the BPSK signal has the same mathematical form as a DSB-SC signal, where  $m(t)$  is a polar NRZ signal as given in Fig. 3-15c.

Both the Costas PLL and the squaring loop have one major disadvantage—a 180° phase ambiguity. For example, suppose that the input is  $-A_c m(t) \cos \omega_c t$  instead of  $+A_c m(t) \cos \omega_c t$ . Retracing the steps in the preceding analysis, we see that the output would be described by *exactly* the same equation that was obtained before. Then, whenever the loop is energized, it is just as likely to phase lock such that the demodulated output is proportional



(a) Costas Phase-Locked Loop

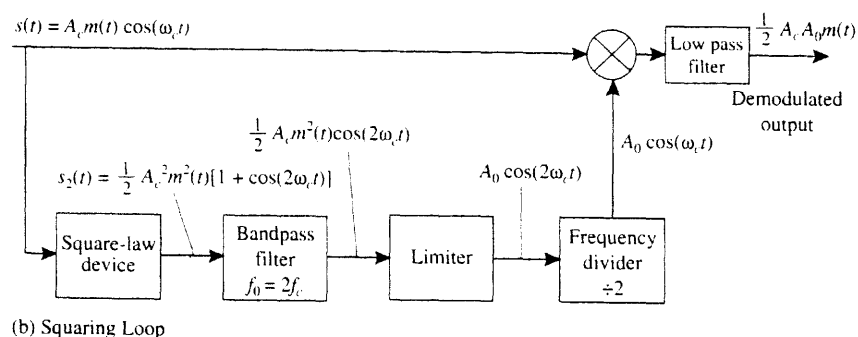


Figure 5-3 Carrier recovery loops for DSB-SC signals.

to  $-m(t)$  as it is to  $m(t)$ . Thus we cannot be sure of the polarity of the output. This is no problem if  $m(t)$  is a monaural audio signal since  $-m(t)$  sounds the same to our ears as  $m(t)$ . However, if  $m(t)$  is a polar data signal, binary 1s might come out as binary 0s after the circuit is energized, or vice versa. As we found in Chapter 3, there are two ways of abrogating this  $180^\circ$  phase ambiguity: (1) a known test signal can be sent over the system after the loop is turned on so that the sense of the polarity can be determined, or (2) differential coding and decoding may be used.

## 5-5 ASYMMETRIC SIDEBAND SIGNALS

### Single Sideband

**DEFINITION.** An *upper single sideband* (USSB) signal has a zero-valued spectrum for  $|f| < f_c$ , where  $f_c$  is the carrier frequency.

A *lower single sideband* (LSSB) signal has a zero-valued spectrum for  $|f| > f_c$ , where  $f_c$  is the carrier frequency.

There are numerous ways in which the modulation  $m(t)$  may be mapped into the complex envelope  $g[m]$  such that an SSB signal will be obtained. Table 4-1 lists some of these methods. SSB-AM is by far the most popular type. It is widely used by the military and by radio amateurs in high-frequency (HF) communication systems, and it is popular because the bandwidth is the same as that of the modulating signal (which is half the bandwidth of an AM or DSB-SC signal). For this reason, we will concentrate on this type of SSB signal. In the usual application, the term *SSB* refers to the SSB-AM type of signal unless otherwise denoted.

**THEOREM.** An SSB signal (i.e., SSB-AM type) is obtained by using the complex envelope

$$g(t) = A_c [m(t) \pm j\hat{m}(t)] \quad (5-15)$$

which results in the SSB signal waveform



$$s(t) = A_c [m(t) \cos \omega_c t \mp \hat{m}(t) \sin \omega_c t] \quad (5-16)$$

where the upper (−) sign is used for USSB and the lower (+) sign is used for LSSB.  $\hat{m}(t)$  denotes the Hilbert transform of  $m(t)$ , which is given by<sup>†</sup>

$$\hat{m}(t) \triangleq m(t) * h(t) \quad (5-17)$$

where

$$h(t) = \frac{1}{\pi t} \quad (5-18)$$

and  $H(f) = \mathcal{F}[h(t)]$  corresponds to a  $-90^\circ$  phase shift network:

$$H(f) = \begin{cases} -j, & f > 0 \\ j, & f < 0 \end{cases} \quad (5-19)$$

Figure 5-4 illustrates this theorem. Assume that  $m(t)$  has a magnitude spectrum that is of triangular shape, as shown in Fig. 5-4a. Then for the case of USSB (upper signs), the spectrum of  $g(t)$  is zero for negative frequencies, as shown in Fig. 5-4b, and  $s(t)$  has the USSB spectrum shown in Fig. 5-4c. This result is proved as follows.

**Proof.** We need to show that the spectrum of  $s(t)$  is zero on the appropriate sideband (depending on the sign chosen). Taking the Fourier transform of (5-15), we get

$$G(f) = A_c \{M(f) \pm j\mathcal{F}[\hat{m}(t)]\} \quad (5-20)$$

and using (5-17), this becomes

$$G(f) = A_c M(f) [1 \pm jH(f)] \quad (5-21)$$

<sup>†</sup> A table of Hilbert transform pairs is given in Sec. A-7 (Appendix A).

To prove the result for the USSB case, choose the upper sign. Then, using (5-19), (5-21) becomes

$$G(f) = \begin{cases} 2A_c M(f), & f > 0 \\ 0, & f < 0 \end{cases} \quad \text{USSB Case} \quad (5-22)$$

Substituting (5-22) into (4-15), the bandpass signal is

$$S(f) = A_c \begin{cases} M(f - f_c), & f > f_c \\ 0, & f < f_c \end{cases} + A_c \begin{cases} 0, & f > -f_c \\ M(f + f_c), & f < -f_c \end{cases} \quad (5-23)$$

which is indeed a USSB signal (see Fig. 5-4).

If the lower signs of (5-21) were chosen, an LSSB signal would have been obtained.

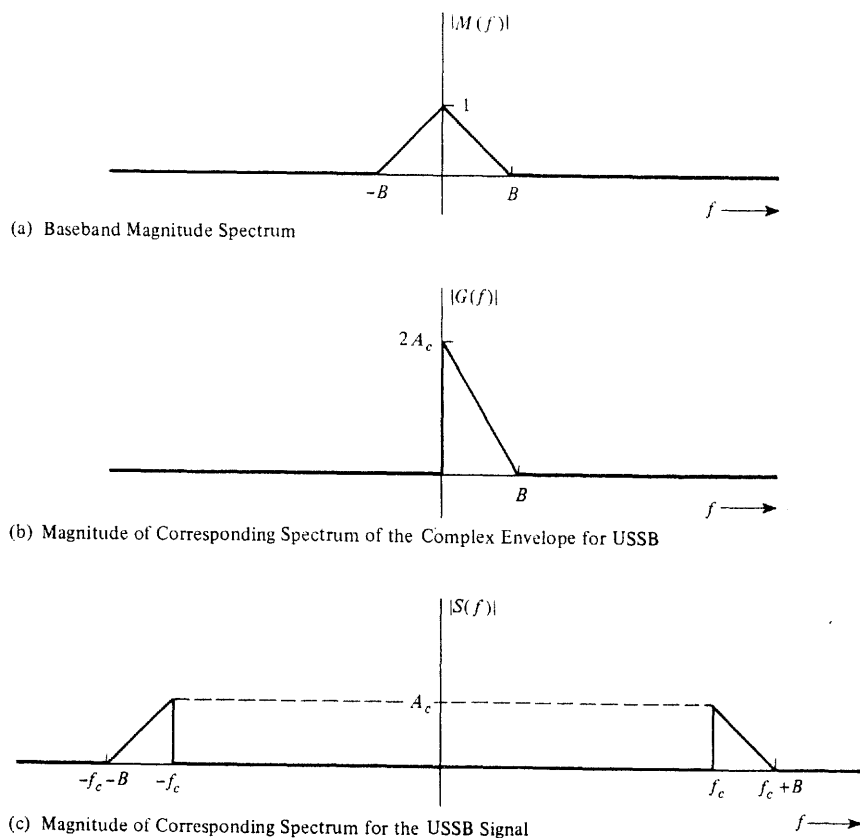


**Figure 5-4** Spectrum for a USSB signal.

The *normalized average power* of the SSB signal is

$$\langle s^2(t) \rangle = \frac{1}{2} \langle |g(t)|^2 \rangle = \frac{1}{2} A_c^2 \langle m^2(t) + [\hat{m}(t)]^2 \rangle \quad (5-24)$$

As shown in study-aid Example SA5-1,  $\langle \hat{m}(t)^2 \rangle = \langle m^2(t) \rangle$ , so that the SSB signal power is

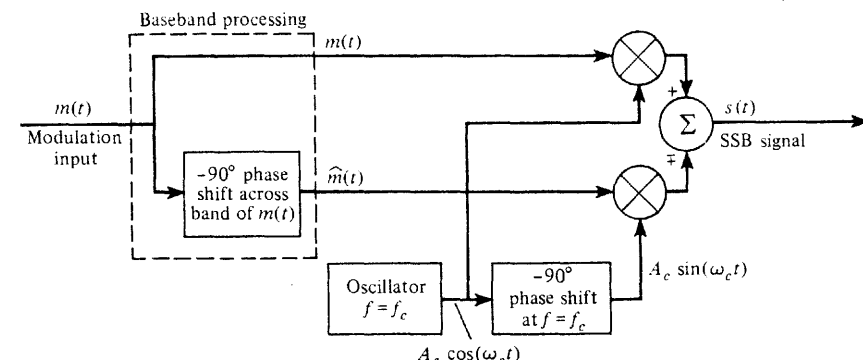
$$\langle s^2(t) \rangle = A_c^2 \langle m^2(t) \rangle \quad (5-25)$$

which is the power of the modulating signal  $\langle m^2(t) \rangle$  multiplied by the power gain factor  $A_c^2$ .

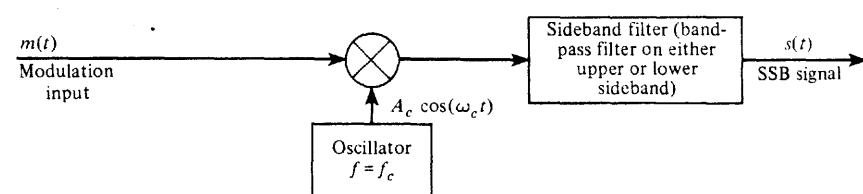
The *normalized peak envelope power (PEP)* is

$$\frac{1}{2} \max \{ |g(t)|^2 \} = \frac{1}{2} A_c^2 \max \{ m^2(t) + [\hat{m}(t)]^2 \} \quad (5-26)$$

Figure 5-5 illustrates two techniques for generating the SSB signal. The *phasing method* is identical to the IQ canonical form discussed earlier (Fig. 4-28) as applied to SSB signal generation. The *filtering method* is a special case where RF processing (by using the sideband filter) is used to form the equivalent  $g(t)$ , instead of using baseband processing to generate  $g[m]$  directly. The filter method is the most popular method used because excellent sideband suppression can be obtained when a crystal filter is used for the sideband fil-



(a) Phasing Method



(b) Filter Method

**Figure 5-5** Generation of SSB.

ter.<sup>†</sup> Crystal filters are relatively inexpensive when produced in quantity at standard IF frequencies. In addition to these two techniques for generating SSB, there is a third technique called *Weaver's method*. This is described by Fig. P5-12 and Prob. 5-12. The practical SSB transmitter would incorporate an up converter to translate the SSB signal to the desired operating frequency and use a Class B amplifier to amplify the signal to the desired power level.

SSB signals have both AM and PM. Using (5-15), we have for the AM component (real envelope)

$$R(t) = |g(t)| = A_c \sqrt{m^2(t) + [\hat{m}(t)]^2} \quad (5-27)$$

and for the PM component

$$\theta(t) = \angle g(t) = \tan^{-1} \left[ \frac{\pm \hat{m}(t)}{m(t)} \right] \quad (5-28)$$

SSB signals may be received by using a superheterodyne receiver that incorporates a product detector with  $\theta_0 = 0$ . Thus, the receiver output is

$$v_{\text{out}}(t) = K \operatorname{Re}\{g(t)e^{-j\theta_0}\} = KA_c m(t) \quad (5-29)$$

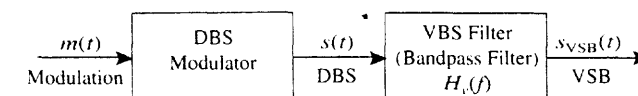
where  $K$  depends on the gain of the receiver and the loss in the channel. In detecting SSB signals with audio modulation, the reference phase  $\theta_0$  does not have to be zero because the same intelligence is heard regardless of the value of the phase used [although the  $v_{\text{out}}(t)$  waveform will be drastically different depending on the value of  $\theta_0$ ]. For digital modulation, the phase has to be exactly correct if the digital waveshape is to be preserved. Furthermore, SSB is a poor modulation technique to use if the modulating data signal consists of a line code with a rectangular pulse shape. The rectangular shape (zero rise time) causes the value of the SSB-AM signal to be infinite adjacent to the switching times of the data because of the Hilbert transform operation. (This result will be demonstrated in a homework problem.) Thus an SSB signal with this type of modulation cannot be generated by any practical device since a device can produce only finite peak value signals. However, if rolled-off pulse shapes are used in the line code, such as  $(\sin x)/x$  pulses, the SSB signal will have a reasonable peak value, and digital data transmission can then be accommodated via SSB.

SSB has many advantages such as the superior detected signal-to-noise ratio when compared to AM (see Chapter 7) and the fact that SSB has one half the bandwidth of AM or DSB-SC signals. Space limitations do not permit more discussion of SSB; for more information on this topic, the reader is referred to a book that is devoted wholly to SSB [Sabin and Schoenike, 1987].

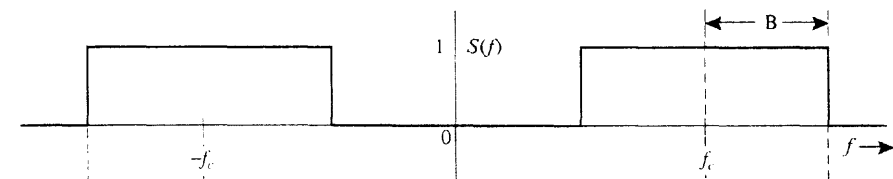
### Vestigial Sideband

In certain applications (such as television broadcasting) a DSB modulation technique takes too much bandwidth for the (television) channel and an SSB technique is too expensive to

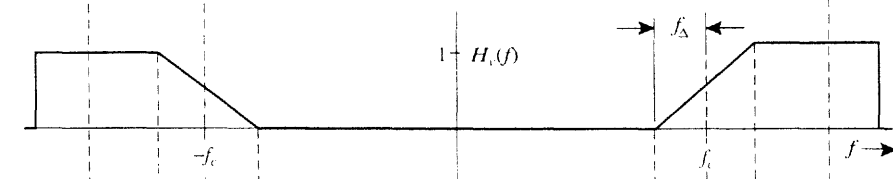
<sup>†</sup> Excellent sideband suppression is possible because communications-quality audio has negligible spectral content below 300 Hz. Thus, the sideband filter can be designed to provide the required sideband attenuation over a  $2 \times 300 = 600$  Hz transition band.



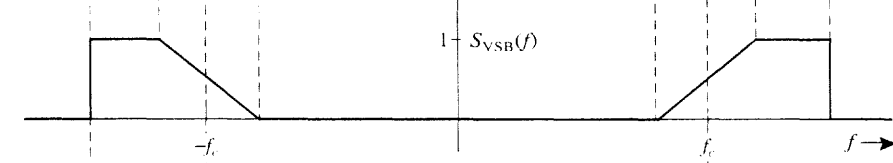
(a) Generation of VSB Signal



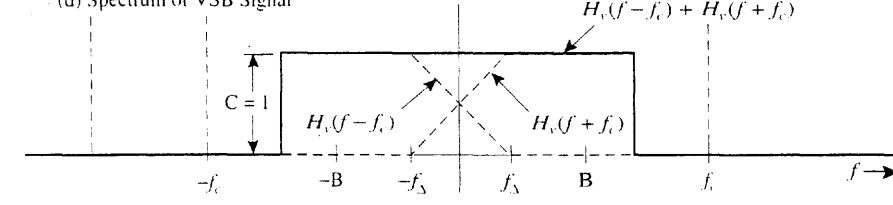
(b) Spectrum of DSB Signal



(c) Transfer Function of VSB Filter



(d) Spectrum of VSB Signal



(e) VSB Filter Constraint

Figure 5-6 VSB transmitter and spectra.

implement, although it takes only half the bandwidth. In this case a compromise between DSB and SSB, called *vestigial sideband* (VSB), is often chosen. VSB is obtained by partial suppression of one of the sidebands of a DSB signal. The DSB signal may be either an AM signal or a DSB-SC signal. This is illustrated by Fig. 5-6, where one sideband of the DSB signal is attenuated by using a bandpass filter, called a vestigial sideband filter, that has an asymmetrical frequency response about  $\pm f_c$ . The VSB signal is given by

$$s_{\text{VSB}}(t) = s(t) * h_v(t) \quad (5-30)$$

where  $s(t)$  is a DSB signal described by either (5-4) with carrier or (5-13) with suppressed carrier, and  $h_v(t)$  is the impulse response of the VSB filter. The spectrum of the VSB signal is

$$S_{\text{VSB}}(f) = S(f)H_v(f) \quad (5-31)$$

as illustrated in Fig. 5-6d.

The modulation on the VSB signal can be recovered by a receiver that uses product detection or, if a large carrier is present, by use of envelope detection. For recovery of undistorted modulation, the transfer function for the VSB filter must satisfy the constraint

$$H_v(f - f_c) + H_v(f + f_c) = C, \quad |f| \leq B \quad (5-32)$$

where  $C$  is a constant and  $B$  is the bandwidth of the modulation. Application of this constraint is shown in Fig. 5-6e, where it is seen that the condition specified by (5-32) is satisfied for the VSB filter characteristic shown in Fig. 5-6c.

The need for the constraint of (5-32) will now be proven. Assume that  $s(t)$  is a DSBSC signal. Then, by use of (5-14) and (5-31), the spectrum of the VSB signal is

$$S_{\text{VSB}}(f) = \frac{A_c}{2} [M(f - f_c)H_v(f) + M(f + f_c)H_v(f)]$$

Referring to Fig. 4-14, the product detector output is

$$v_{\text{out}}(t) = [A_0 s_{\text{VSB}}(t) \cos \omega_c t] * h(t)$$

where  $h(t)$  is the impulse response of the low-pass filter having a bandwidth of  $B$  hertz. In the frequency domain this becomes

$$V_{\text{out}}(f) = A_0 \{S_{\text{VSB}}(f) * [\frac{1}{2}\delta(f - f_c) + \frac{1}{2}\delta(f + f_c)]\} H(f)$$

where  $H(f) = 1$  for  $|f| < B$  and 0 for  $f$  elsewhere. Substituting for  $S_{\text{VSB}}(f)$  and using the convolutional property  $x(f) * \delta(f - u) = x(f - u)$ ,  $V_{\text{out}}(f)$  is

$$V_{\text{out}}(f) = \frac{A_c A_0}{4} [M(f)H_v(f - f_c) + M(f)H_v(f + f_c)], \quad |f| < B$$

or

$$V_{\text{out}}(f) = \frac{A_c A_0}{4} M(f)[H_v(f - f_c) + H_v(f + f_c)], \quad |f| < B$$

If  $H_v(f)$  satisfies the constraint of (5-32), this becomes

$$V_{\text{out}}(f) = K M(f)$$

or  $V_{\text{out}}(t) = K m(t)$  where  $K = A_c A_0 / 4$ . This shows that the output of the product detector is undistorted when (5-32) is satisfied.

As discussed in Chapter 8, Sec. 8-9, broadcast television uses VSB to reduce the required channel bandwidth to 6 MHz. In this application, as shown in Fig. 8-31c, the frequency response of the visual TV transmitter is flat over the upper sideband out to 4.2 MHz

above the visual carrier frequency and is flat over the lower sideband out to 0.75 MHz below the carrier frequency. The IF filter in the TV receiver has the VSB filter characteristic shown in Fig. 5-6c, where  $f_\Delta = 0.75$  MHz. This gives an overall frequency response characteristic that satisfies the constraint of (5-32) so that the video modulation on the visual VSB TV signal can be recovered at the receiver without distortion.

## 5-6 PHASE MODULATION AND FREQUENCY MODULATION

### Representation of PM and FM Signals

*Phase modulation* (PM) and *frequency modulation* (FM) are special cases of angle-modulated signaling. In angle modulated signaling the complex envelope is

$$g(t) = A_c e^{j\theta(t)} \quad (5-33)$$

Here the real envelope,  $R(t) = |g(t)| = A_c$ , is a constant, and the phase  $\theta(t)$  is a linear function of the modulating signal  $m(t)$ . However,  $g(t)$  is a *nonlinear* function of the modulation. Using (5-33), we find the resulting *angle-modulated signal* to be

$$s(t) = A_c \cos[\omega_c t + \theta(t)] \quad (5-34)$$

For PM the phase is directly proportional to the modulating signal:

$$\theta(t) = D_p m(t) \quad (5-35)$$

where the proportionality constant  $D_p$  is the phase sensitivity of the phase modulator, having units of radians per volt [assuming that  $m(t)$  is a voltage waveform].

For FM the phase is proportional to the integral of  $m(t)$ :

$$\theta(t) = D_f \int_{-\infty}^t m(\sigma) d\sigma \quad (5-36)$$

where the frequency deviation constant  $D_f$  has units of radians/volt-second.

By comparing the last two equations, it is seen that if we have a PM signal modulated by  $m_p(t)$ , there is *also* FM on the signal corresponding to a *different* modulation waveform that is given by

$$m_f(t) = \frac{D_p}{D_f} \left[ \frac{dm_p(t)}{dt} \right] \quad (5-37)$$

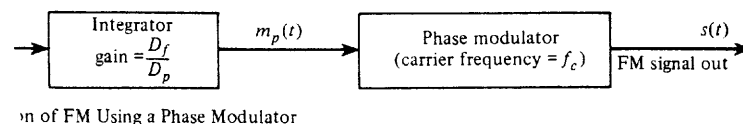
where the subscripts  $f$  and  $p$  denote frequency and phase, respectively. Similarly, if we have an FM signal modulated by  $m_f(t)$ , the corresponding phase modulation on this signal is

$$m_p(t) = \frac{D_f}{D_p} \int_{-\infty}^t m_f(\sigma) d\sigma \quad (5-38)$$

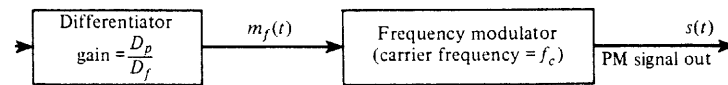
By using (5-38), a PM circuit may be used to synthesize an FM circuit by inserting an integrator in cascade with the phase modulator input (see Fig. 5-7a).

310 MHz  
characteristic  
val

311



Generation of FM Using a Phase Modulator



(b) Generation of PM Using a Frequency Modulator

Figure 5-7 Generation of FM from PM, and vice versa.

Direct PM circuits are realized by passing an unmodulated sinusoidal signal through a time-varying circuit that introduces a phase shift that varies with the applied modulating voltage (see Fig. 5-8a).  $D_p$  is the gain of the PM circuit (rad/V). Similarly, a direct FM circuit is obtained by varying the tuning of an oscillator tank (resonant) circuit according to the modulation voltage. This is shown in Fig. 5-8b, where  $D_f$  is the gain of the modulator circuit (which has units of radians per volt-second).

**DEFINITION.** If a bandpass signal is represented by

$$s(t) = R(t) \cos \psi(t)$$

where  $\psi(t) = \omega_c t + \theta(t)$ , then the *instantaneous* frequency (hertz) of  $s(t)$  is [Boashash, 1992]

$$f_i(t) = \frac{1}{2\pi} \omega_i(t) = \frac{1}{2\pi} \left[ \frac{d\psi(t)}{dt} \right]$$

or

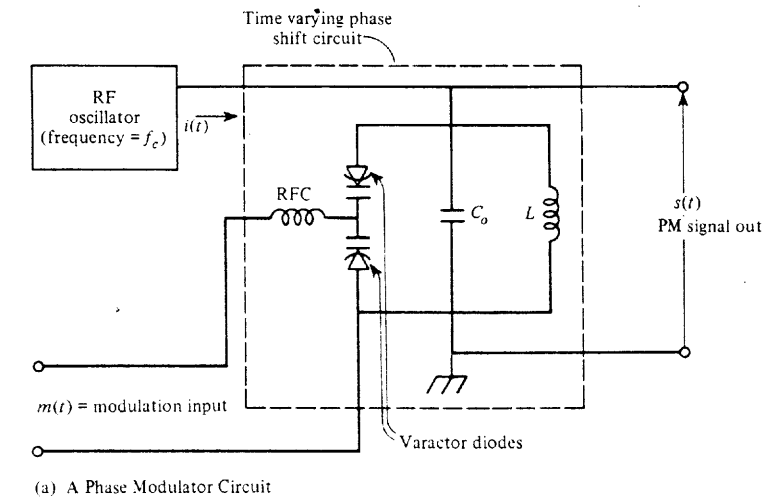
$$f_i(t) = f_c + \frac{1}{2\pi} \left[ \frac{d\theta(t)}{dt} \right] \quad (5-39)$$

For the case of FM, using (5-36), the instantaneous frequency is

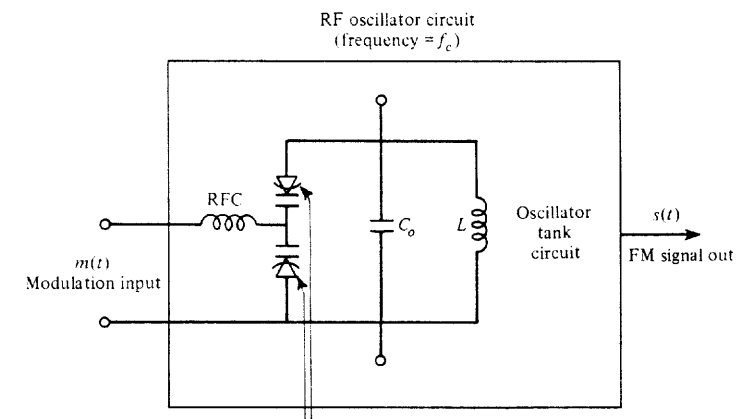
$$f_i(t) = f_c + \frac{1}{2\pi} D_f m(t) \quad (5-40)$$

Of course, this is the reason for calling this type of signaling *frequency modulation*—the instantaneous frequency varies about the assigned carrier frequency  $f_c$  directly proportional to the modulating signal  $m(t)$ . Figure 5-9b shows how the instantaneous frequency varies when a sinusoidal modulation (for illustrative purposes) is used. The resulting FM signal is shown in Fig. 5-9c.

The instantaneous frequency should not be confused with the term *frequency* as used in the spectrum of the FM signal. The spectrum is given by the Fourier transform of  $s(t)$  and is evaluated by looking at  $s(t)$  over the infinite time interval ( $-\infty < t < \infty$ ). Thus the spec-



(a) A Phase Modulator Circuit



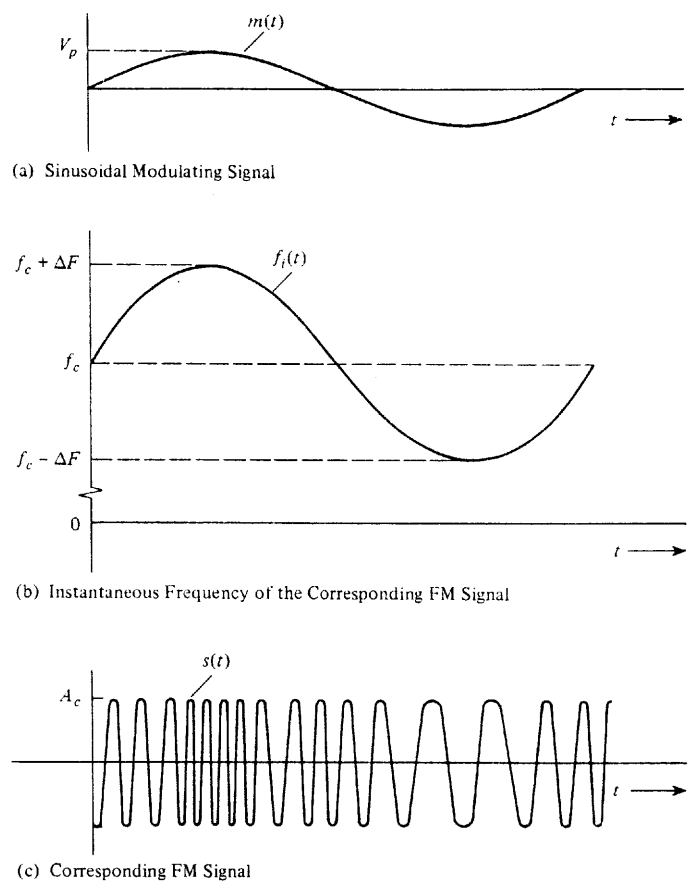
(b) A Frequency Modulator Circuit

Figure 5-8 Angle modulator circuits. RFC = radio-frequency choke.

trum tells us what frequencies are present in the signal (on the average) over all time. The instantaneous frequency is the frequency that is present at a particular instant of time.

The *frequency deviation* from the carrier frequency is

$$f_d(t) = f_i(t) - f_c = \frac{1}{2\pi} \left[ \frac{d\theta(t)}{dt} \right] \quad (5-41)$$



**Figure 5-9** FM with a sinusoidal baseband modulating signal.

and the *peak frequency deviation* is

$$\Delta F = \max \left\{ \frac{1}{2\pi} \left[ \frac{d\theta(t)}{dt} \right] \right\} \quad (5-42)$$

Note that  $\Delta F$  is a nonnegative number. In some applications, such as (unipolar) digital modulation, the peak-to-peak deviation is used. This is defined by

$$\Delta F_{pp} = \max \left\{ \frac{1}{2\pi} \left[ \frac{d\theta(t)}{dt} \right] \right\} - \min \left\{ \frac{1}{2\pi} \left[ \frac{d\theta(t)}{dt} \right] \right\} \quad (5-43)$$

For FM signaling the peak frequency deviation is related to the peak modulating voltage by

$$\Delta F = \frac{1}{2\pi} D_f V_p \quad (5-44)$$

where  $V_p = \max[m(t)]$ , as illustrated in Fig. 5-9a.

From Fig. 5-9 it is obvious that an increase in the amplitude of the modulation signal  $V_p$  will increase  $\Delta F$ . This will increase the bandwidth of the FM signal but will not affect the average power level of the FM signal, which is  $A_c^2/2$ . As  $V_p$  is increased, spectral components will appear farther and farther away from the carrier frequency, and the spectral components near the carrier frequency will decrease in magnitude since the total power in the signal remains constant (for specific details, see Example 5-2). This is distinctly different from AM signaling, where the level of the modulation affects the power in the AM signal but does not affect its bandwidth.

In a similar way, the *peak phase deviation* may be defined by

$$\Delta\theta = \max[\theta(t)] \quad (5-45)$$

and for PM this is related to the peak modulating voltage by

$$\Delta\theta = D_p V_p \quad (5-46)$$

where  $V_p = \max[m(t)]$ .

**DEFINITION.**<sup>†</sup> The *phase modulation index* is given by

$$\beta_p = \Delta\theta \quad (5-47)$$

where  $\Delta\theta$  is the peak phase deviation.

The *frequency modulation index* is given by

$$\beta_f = \frac{\Delta F}{B} \quad (5-48)$$

where  $\Delta F$  is the peak frequency deviation and  $B$  is the bandwidth of the modulating signal, which for the case of sinusoidal modulation is  $f_m$ , the frequency of the sinusoid.<sup>‡</sup>

For the case of PM or FM signaling with *sinusoidal* modulation such that the PM and FM signals have the same peak frequency deviation,  $\beta_p$  is identical to  $\beta_f$ .

### Spectra of Angle-Modulated Signals

Using (4-12), we find that the spectrum of an angle modulated signal is given by

$$S(f) = \frac{1}{2} [G(f - f_c) + G^*(-f - f_c)] \quad (5-49)$$

where

$$G(f) = \mathcal{F}[g(t)] = \mathcal{F}[A_c e^{j\theta(t)}] \quad (5-50)$$

<sup>†</sup> For digital signals, an alternative definition of modulation index is sometimes used and is denoted by  $h$  in the literature. This digital modulation index is given by  $h = 2\Delta\theta/\pi$ , where  $2\Delta\theta$  is the maximum peak-to-peak phase deviation change during the time that it takes to send one symbol,  $T_s$ , see (5-82).

<sup>‡</sup> Strictly speaking, the FM index is defined only for the case of single-tone (i.e., sinusoidal) modulation. However, it is often used for other waveshapes, where  $B$  is chosen to be the highest frequency or the dominant frequency in the modulating waveform.

When the spectra for AM, DSB-SC, and SSB were evaluated, we were able to obtain relatively simple formulas relating  $S(f)$  to  $M(f)$ . For angle modulation signaling this is not the case because  $g(t)$  is a nonlinear function of  $m(t)$ . Thus a general formula relating  $G(f)$  to  $M(f)$  cannot be obtained. This is unfortunate, but it is a fact of life. That is, to evaluate the spectrum for an angle-modulated signal, (5-50) must be evaluated on a case-by-case basis for the particular modulating waveshape of interest. Furthermore, since  $g(t)$  is a nonlinear function of  $m(t)$ , superposition does not hold and the FM spectrum for the sum of two modulating waveshapes is not the same as summing the FM spectra that were obtained when the individual waveshapes were used.

One example of the spectra obtained for an angle-modulated signal is given in Chapter 2 (see Example 2-18). There a carrier was phase-modulated by a square wave where the peak-to-peak phase deviation was  $180^\circ$ . In this example the spectrum was easy to evaluate because this was the very special case where the PM signal reduces to a DSB-SC signal. In general, of course, the evaluation of (5-50) into a closed form is not easy, and one often has to use numerical techniques to approximate this Fourier transform integral. An example for the case of a sinusoidal modulating waveshape will now be worked out.

### Example 5-2 SPECTRUM OF A PM OR FM SIGNAL WITH SINUSOIDAL MODULATION

Assume that the modulation on the PM signal is

$$m_p(t) = A_m \sin \omega_m t \quad (5-51)$$

Then

$$\theta(t) = \beta \sin \omega_m t \quad (5-52)$$

where  $\beta_p = D_p A_m = \beta$  is the phase modulation index.

The same phase function  $\theta(t)$ , as given by (5-52), could also be obtained if FM were used, where

$$m_f(t) = A_m \cos \omega_m t \quad (5-53)$$

and  $\beta = \beta_f = D_f A_m / \omega_m$ . The peak frequency deviation would be  $\Delta F = D_f A_m / 2\pi$ .

The complex envelope is

$$g(t) = A_c e^{j\theta(t)} = A_c e^{j\beta \sin \omega_m t} \quad (5-54)$$

which is periodic with period  $T_m = 1/f_m$ . Consequently,  $g(t)$  could be represented by a Fourier series that is valid over all time ( $-\infty < t < \infty$ ):

$$g(t) = \sum_{n=-\infty}^{n=\infty} c_n e^{jn\omega_m t} \quad (5-55)$$

where

$$c_n = \frac{A_c}{T_m} \int_{-T_m/2}^{T_m/2} (e^{j\beta \sin \omega_m t}) e^{-jn\omega_m t} dt \quad (5-56)$$

which reduces to

$$c_n = A_c \left[ \frac{1}{2\pi} \int_{-\pi}^{\pi} e^{j(\beta \sin \theta - n\theta)} d\theta \right] = A_c J_n(\beta) \quad (5-57)$$

This integral—known as the *Bessel function of the first kind of the nth order*,  $J_n(\beta)$ —cannot be evaluated in closed form, but it has been evaluated numerically. Some tabulated values for  $J_n(\beta)$  are given in Table 5-2. Extensive tables are available [Abramowitz and Stegun, 1964] or can be computed using MATLAB. The Bessel functions are standard function calls in mathematical personal computer programs such as MATLAB. Examination of the integral shows that (by making a change in variable)

$$J_{-n}(\beta) = (-1)^n J_n(\beta) \quad (5-58)$$

A plot of the Bessel functions for various orders,  $n$ , as a function of  $\beta$  is shown in Fig. 5-10.

Taking the Fourier transform of (5-55), we obtain

$$G(f) = \sum_{n=-\infty}^{n=\infty} c_n \delta(f - nf_m) \quad (5-59)$$

or

$$G(f) = A_c \sum_{n=-\infty}^{n=\infty} J_n(\beta) \delta(f - nf_m) \quad (5-60)$$

Using this result in (5-49), we obtain the spectrum of the angle modulated signal. The magnitude spectrum for  $f > 0$  is shown in Fig. 5-11 for the cases of  $\beta = 0.2, 1.0, 2.0, 5.0$ , and  $8.0$ . It is noted that the discrete carrier term (at  $f = f_c$ ) is proportional to  $|J_0(\beta)|$ ; consequently, the level (magnitude) of the discrete carrier depends on the modulation index. It will be zero if  $J_0(\beta) = 0$ , which occurs if  $\beta = 2.40, 5.52$ , and so on, as shown in Table 5-3.

Figure 5-11 also shows that the bandwidth of the angle modulated signal depends on  $\beta$  and  $f_m$ . In fact, it can be shown that 98% of the total power is contained in the bandwidth

$$B_T = 2(\beta + 1)B \quad (5-61)$$

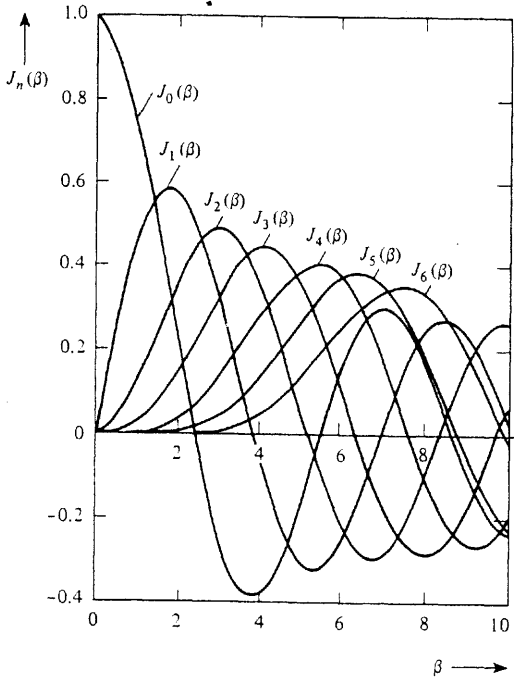
where  $\beta$  is either the phase modulating index or the frequency modulation index and  $B$  is the bandwidth of the modulating signal (which is  $f_m$  for sinusoidal modulation).<sup>†</sup> This formula gives a rule-of-thumb expression for evaluating the transmission bandwidth of PM and FM signals; it is called *Carson's rule*.  $B_T$  is shown in Fig. 5-11 for various values of  $\beta$ . Carson's rule, (5-61), is very important because it gives an easy way to compute the bandwidth of angle-modulated signals. Computation of the bandwidth using other definitions, such as 3-dB bandwidth, can be very difficult since the spectrum of the FM or PM signal must first be evaluated. This is a nontrivial task except for simple cases such as single-tone

<sup>†</sup> For the case of FM (not PM) with  $2 < B < 10$ , Carson's rule, (5-61), actually underestimates  $B_T$  somewhat. In this case a better approximation is  $B_T = 2(\beta + 2)B$ . Also, if the modulation signal contains discontinuities, such as square-wave modulation, both formulas may not be too accurate and the  $B_T$  should be evaluated by examining the spectrum of the angle-modulated signal. However, to avoid confusion in computing  $B_T$ , we will assume that (5-61) is approximately correct for all cases.

TABLE 5-2 FOUR-PLACE VALUES OF THE BESSEL FUNCTIONS  $I_n(\beta)$ 

$n \backslash \beta:$	0	0.5	1	2	3	4	5	6	7	8	9	10
0	0.9385	0.7652	0.2239	-0.2601	-0.3971	-0.1776	0.1506	0.3001	0.1717	-0.09033	-0.2459	
1	0.2423	0.4401	0.5767	0.3391	-0.06604	-0.3276	-0.2767	-0.004683	0.2346	0.2453	0.04347	
2	0.03060	0.1149	0.3528	0.4861	0.3641	0.04657	-0.2429	-0.3014	-0.1130	0.1448	0.2546	
3	0.002564	0.01956	0.1289	0.3091	0.4302	0.3648	0.1148	-0.1676	-0.2911	-0.1809	0.05838	
4	0.002477	0.03400	0.1320	0.2811	0.3912	0.3576	0.1578	-0.1054	-0.2655	-0.2196		
5		0.007040	0.04303	0.1321	0.2611	0.3621	0.3479	0.1858	-0.05504	-0.2341		
6		0.001202	0.01139	0.04909	0.1310	0.2458	0.3392	0.3376	0.2043	-0.01446		
7		0.002547	0.01518	0.05338	0.1296	0.1296	0.2336	0.3206	0.3275	0.2167		
8		0.004029	0.01841	0.05653	0.1280	0.1280	0.2235	0.3051	0.3179			
9		0.0001468	0.006964	0.02117	0.05892	0.1263	0.2149	0.2919				
10		0.0002048	0.008335	0.02354	0.06077	0.1247	0.2075					
11		0.002656	0.008335	0.02560	0.06222	0.1231						
12												
13												
14												
15												
16												

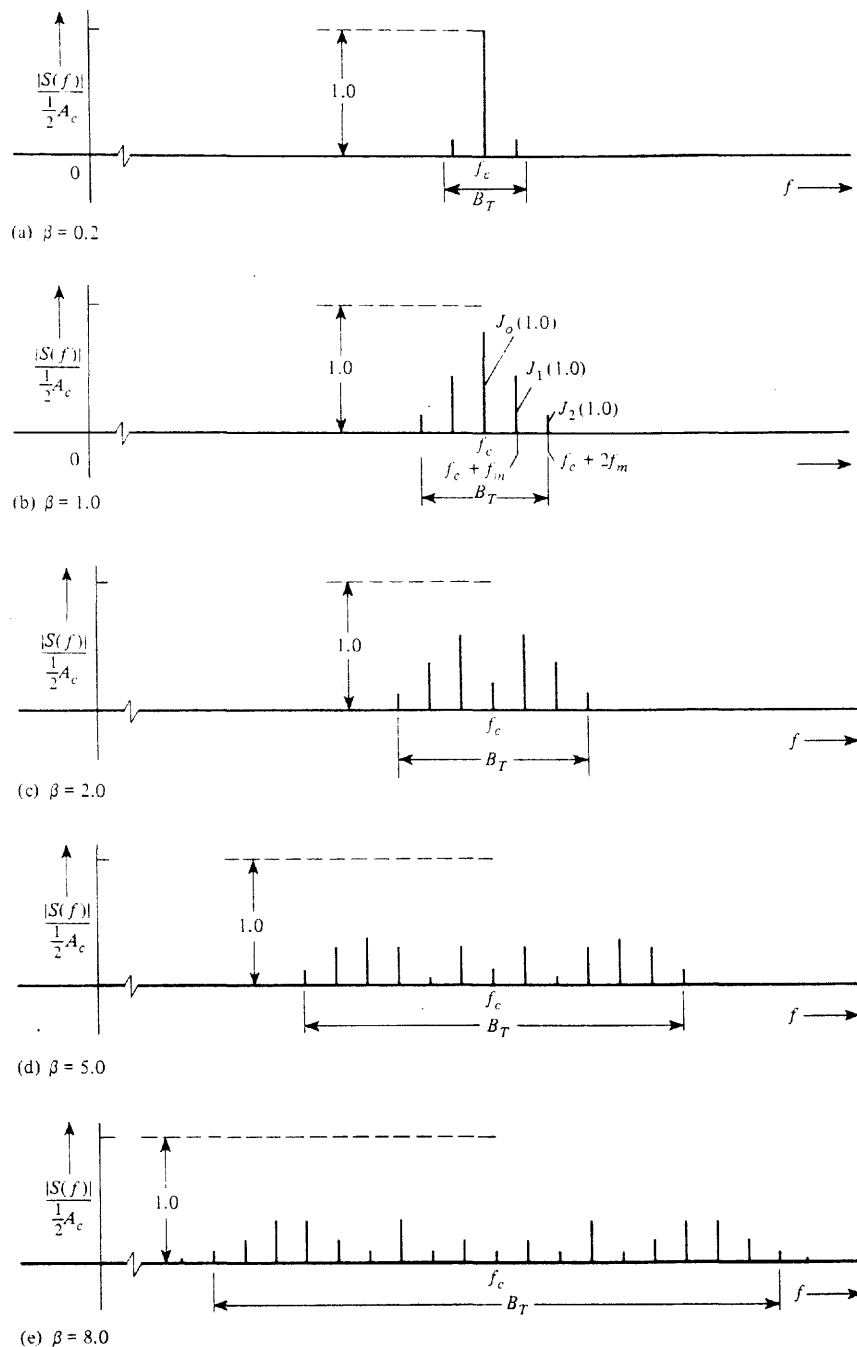
## Sec. 5-6 Phase Modulation and Frequency Modulation

Figure 5-10 Bessel functions for  $n = 0$  to  $n = 6$ .TABLE 5-3 ZEROS OF BESSSEL FUNCTIONS: VALUES FOR  $\beta$  WHEN  $J_n(\beta) = 0$ 

	Order of Bessel Function, $n$						
	0	1	2	3	4	5	6
$\beta$ for 1st zero	2.40	3.83	5.14	6.38	7.59	8.77	9.93
$\beta$ for 2nd zero	5.52	7.02	8.42	9.76	11.06	12.34	13.59
$\beta$ for 3rd zero	8.65	10.17	11.62	13.02	14.37	15.70	17.00
$\beta$ for 4th zero	11.79	13.32	14.80	16.22	17.62	18.98	20.32
$\beta$ for 5th zero	14.93	16.47	17.96	19.41	20.83	22.21	23.59
$\beta$ for 6th zero	18.07	19.61	21.12	22.58	24.02	25.43	26.82
$\beta$ for 7th zero	21.21	22.76	24.27	25.75	27.20	28.63	30.03
$\beta$ for 8th zero	24.35	25.90	27.42	28.91	30.37	31.81	33.23

(sinusoidal) modulation or unless a digital computer is used to compute the approximate spectrum.

Because the exact spectrum of angle modulated signals is difficult to evaluate in general, formulas for the approximation of the spectra are extremely useful. Some relatively simple approximations may be obtained when the peak phase deviation is small and when the modulation index is large. These topics are discussed in the following sections on narrowband angle modulation and wideband FM.



**Figure 5-11** Magnitude spectra for FM or PM with sinusoidal modulation for various modulation indexes.

### Narrowband Angle Modulation

When  $\theta(t)$  is restricted to a small value, say  $|\theta(t)| < 0.2$  rad, the complex envelope  $g(t) = A_c e^{j\theta}$  may be approximated by a Taylor's series where only the first two terms are used. Thus, because  $e^x \approx 1 + x$  for  $|x| \ll 1$ ,

$$g(t) \approx A_c [1 + j\theta(t)] \quad (5-62)$$

Using this approximation in (4-9) or (5-1), we obtain the expression for a *narrowband angle-modulated signal*

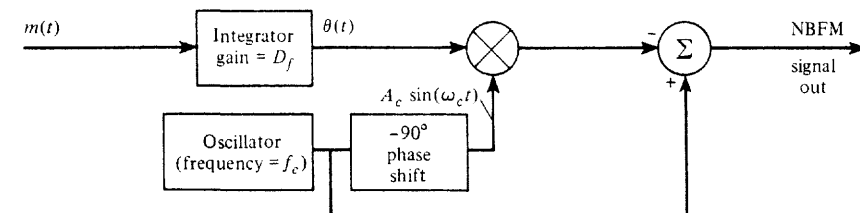


$$s(t) = \underbrace{A_c \cos \omega_c t}_{\text{discrete carrier term}} - \underbrace{A_c \theta(t) \sin \omega_c t}_{\text{sideband power}} \quad (5-63)$$

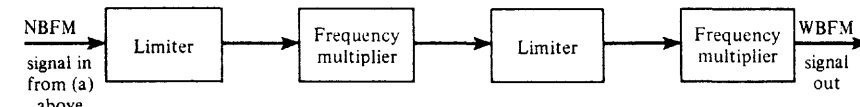
This result indicates that a narrowband angle modulated signal consists of two terms: a discrete carrier component (which does not change with modulating signal) and a sideband term. This is similar to AM-type signaling *except* that the sideband term is  $90^\circ$  out of phase with the discrete carrier term. The narrowband signal can be generated by using a balanced modulator (multiplier), as shown in Fig. 5-12a for the case of narrowband frequency modulation (NBFM). Furthermore, wideband frequency modulation (WBFM) may be generated from the NBFM signal by using frequency multiplication, as shown in Fig. 5-12b. Limiter circuits are needed to suppress the incidental AM [which is  $\sqrt{1 + \theta^2(t)}$  as the result of the approximation (5-62)] that is present in the NBFM signal. This method of generating WBFM is called the *Armstrong method* or *indirect method*.

From (5-62) and (5-49), the spectrum of the narrowband angle-modulated signal is

$$S(f) = \frac{A_c}{2} \{ [\delta(f - f_c) + \delta(f + f_c)] + j[\Theta(f - f_c) - \Theta(f + f_c)] \} \quad (5-64)$$



(a) Generation of NBFM Using a Balanced Modulator



(b) Generation of WBFM From a NBFM Signal

**Figure 5-12** Indirect method of generating WBFM (Armstrong method).

where

$$\Theta(f) = \mathcal{F}[\theta(t)] = \begin{cases} D_p M(f), & \text{for PM signaling} \\ \frac{D_f}{j2\pi f} M(f), & \text{for FM signaling} \end{cases} \quad (5-65)$$

### Wideband Frequency Modulation

A direct method of generating wideband frequency modulation (WBFM) is to use a voltage-controlled oscillator (VCO), as illustrated in Fig. 5-13b. However, for VCOs that are designed for wide frequency deviation ( $\Delta F$  large), the stability of the carrier frequency  $f_c = f_0$  is not very good, so the VCO is incorporated into a PLL arrangement where the PLL is locked to a stable frequency source, such as a crystal oscillator (see Fig. 5-13). The frequency divider is needed to lower the modulation index of the WBFM signal to produce an NBFM signal ( $\beta \approx 0.2$ ) so that a large discrete carrier term will always be present at frequency  $f_c/N$  to beat with the crystal oscillator signal and produce the dc control voltage [see Fig. 5-11a, (5-63), and (5-64)]. This dc control voltage holds the VCO on the assigned frequency with a tolerance determined by the crystal oscillator circuit.

The PSD of a WBFM signal may be approximated by using the probability density function (PDF) of the modulating signal. This is reasonable from an intuitive viewpoint, since the instantaneous frequency varies directly with the modulating signal voltage for the case of FM [ $D_f/(2\pi)$  being the proportionality constant]. If the modulating signal spends more time at one voltage value than another, the instantaneous frequency will dwell at the corresponding frequency, and the power spectrum will have a peak at this frequency. A discussion of the approximation involved—called the *quasi-static approximation*—is well documented [Rowe, 1965]. This result is stated in the following theorem.

**THEOREM.** For WBFM signaling, where

$$s(t) = A_c \cos \left[ \omega_c t + D_f \int_{-\infty}^t m(\sigma) d\sigma \right]$$

$$\beta_f = \frac{D_f \max[m(t)]}{2\pi B} > 1$$

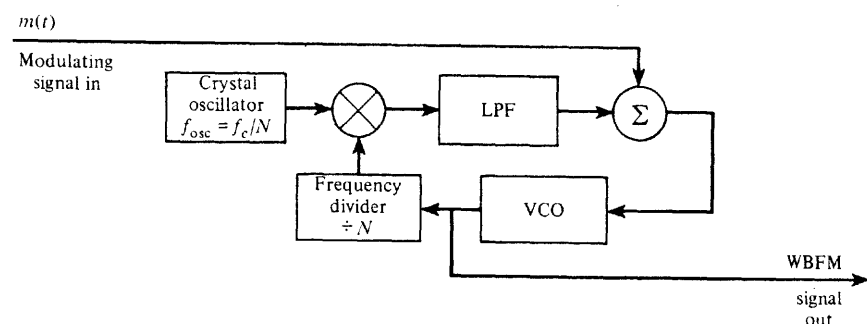


Figure 5-13 Direct method of generating WBFM.

and  $B$  is the bandwidth of  $m(t)$ , the normalized PSD of the WBFM signal is approximated by

$$\mathcal{P}(f) = \frac{\pi A_c^2}{2D_f} \left[ f_m \left( \frac{2\pi}{D_f} (f - f_c) \right) + f_m \left( \frac{2\pi}{D_f} (-f - f_c) \right) \right] \quad (5-66)$$

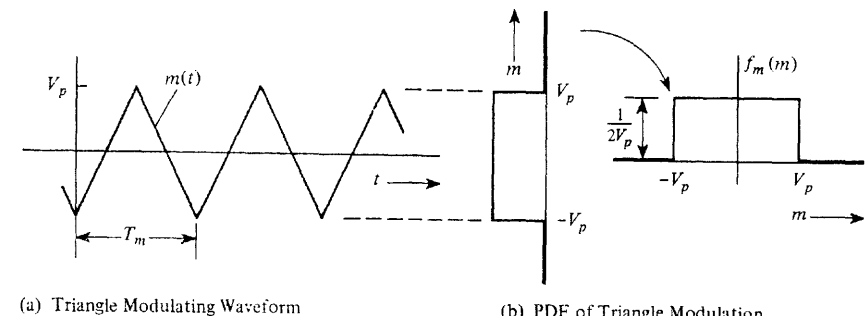
where  $f_m(\cdot)$  is the PDF of the modulating signal.<sup>+</sup>

This theorem is proved in Prob. 6-44.

### Example 5-3 SPECTRUM FOR WBFM WITH TRIANGULAR MODULATION

The spectrum for a WBFM signal with a triangular modulating signal (Fig. 5-14a) will be evaluated. The associated PDF for triangular modulation is shown in Fig. 5-14b. The PDF is described by

$$f_m(m) = \begin{cases} \frac{1}{2V_p}, & |m| < V_p \\ 0, & m \text{ otherwise} \end{cases} \quad (5-67)$$



(c) PSD of WBFM Signal with Triangle Modulation,  $\Delta F = D_f V_p / 2\pi$

Figure 5-14 Approximate spectrum of a WBFM signal with triangle modulation.

<sup>+</sup> See Appendix B for the definition of PDF and examples of PDFs for various waveforms. This topic may be deleted if the reader is not sufficiently familiar with PDFs. Do not confuse the PDF of the modulation,  $f_m(\cdot)$ , with the frequency variable,  $f$ .

where  $V_p$  is the peak voltage of the triangular waveform. Substituting this equation into (5-66), we obtain

$$\begin{aligned} \mathcal{P}(f) = & \frac{\pi A_c^2}{2D_f} \left[ \begin{cases} \frac{1}{2V_p}, & \left| \frac{2\pi}{D_f} (f - f_c) \right| < V_p \\ 0, & f \text{ otherwise} \end{cases} \right] \\ & + \left[ \begin{cases} \frac{1}{2V_p}, & \left| \frac{2\pi}{D_f} (f + f_c) \right| < V_p \\ 0, & f \text{ otherwise} \end{cases} \right] \end{aligned}$$

The PSD of the WBFM signal becomes

$$\begin{aligned} \mathcal{P}(f) = & \left\{ \begin{array}{ll} \frac{A_c^2}{8\Delta F}, & (f_c - \Delta F) < f < (f_c + \Delta F) \\ 0, & f \text{ otherwise} \end{array} \right\} \\ & + \left\{ \begin{array}{ll} \frac{A_c^2}{8\Delta F}, & (-f_c - \Delta F) < f < (f_c + \Delta F) \\ 0, & f \text{ otherwise} \end{array} \right\} \quad (5-68) \end{aligned}$$

where the peak frequency deviation is

$$\Delta F = \frac{D_f V_p}{2\pi} \quad (5-69)$$

This PSD is plotted in Fig. 5-14c. It is recognized that this result is an *approximation* to the actual PSD. In this example the modulation is periodic with period  $T_m$  so that the actual spectrum is a line spectrum with the delta functions spaced  $f_m = 1/T_m$  hertz apart from each other (like the spacing shown in Fig. 5-11 for the case of sinusoidal modulation). This approximation gives us the *approximate envelope* of the line spectrum. (If the modulation had been nonperiodic, the exact spectrum would be continuous and thus would not be a line spectrum.)

In the other example using sinusoidal (periodic) modulation, the exact PSD is known to contain line components with weights  $[A_c J_n(\beta)]^2/2$  located at frequencies  $f = f_c + nf_m$  (see Fig. 5-11). For the case of high index the envelope of these weights approximates the PDF of a sinusoid as given in Appendix B.

In summary, some important properties of angle modulated signals are

- It is a nonlinear function of the modulation, and, consequently, the bandwidth of the signal increases as the modulation index increases.
- The discrete carrier level changes, depending on the modulating signal, and is zero for certain types of modulating waveforms.
- The bandwidth of a narrowband angle modulated signal is twice the modulating signal bandwidth (same as that for AM signaling).
- The real envelope of an angle-modulated signal,  $R(t) = A_c$ , is constant and, consequently, does not depend on the modulating signal level.

### Preemphasis and Deemphasis in Angle-Modulated Systems

In angle-modulated systems the signal-to-noise ratio at the output of the receiver can be improved if the level of the modulation (at the transmitter) is boosted at the top end of the (e.g., audio) spectrum—this is called *preemphasis*—and attenuated at high frequencies on the receiver output—this is called *deemphasis*. This gives an overall baseband frequency response that is flat while improving the signal-to-noise ratio at the receiver output (see Fig. 5-15). In

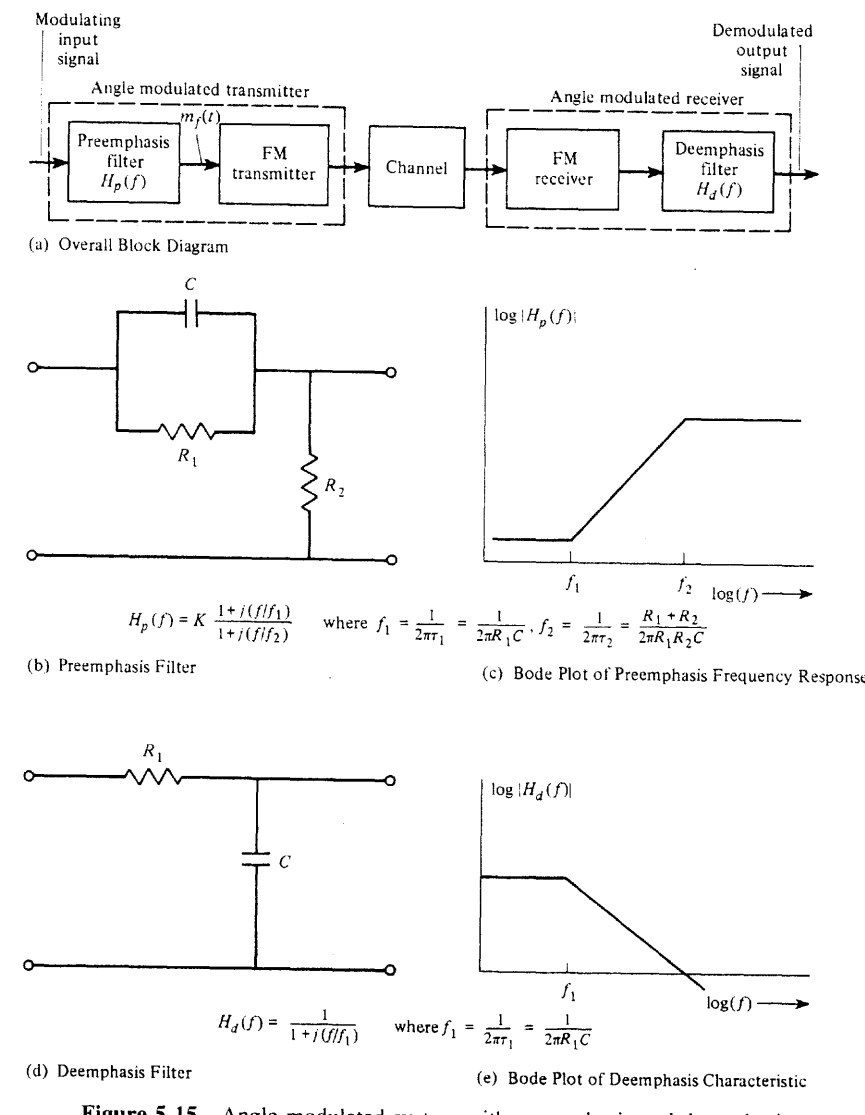


Figure 5-15 Angle-modulated system with preemphasis and deemphasis.

the preemphasis characteristic the second corner frequency  $f_2$  occurs much above the baseband spectrum of the modulating signal (say, 25 kHz for audio modulation). In FM broadcasting the time constant  $\tau_1$  is usually 75  $\mu\text{s}$  so that  $f_1$  occurs at 2.12 kHz. The resulting overall system frequency response using preemphasis at the transmitter and deemphasis at the receiver is flat over the band of the modulating signal. It is interesting to note that in FM broadcasting with 75- $\mu\text{s}$  preemphasis, the signal transmitted is an FM signal for modulating frequencies up to 2.1 kHz but a *phase-modulated* signal for audio frequencies above 2.1 kHz because the preemphasis network acts as a differentiator for frequencies between  $f_1$  and  $f_2$ . Hence, *preemphasized FM is actually a combination of FM and PM* and combines the advantages of both with respect to noise performance. In Chapter 7 it will be demonstrated that preemphasis-deemphasis improves the signal-to-noise ratio at the receiver output.

## 5-7 FREQUENCY-DIVISION MULTIPLEXING AND FM STEREO

*Frequency-division multiplexing* (FDM) is a technique for transmitting multiple messages simultaneously over a wideband channel by first modulating the message signals onto several subcarriers and forming a composite baseband signal that consists of the sum of these modulated subcarriers. This composite signal may then be modulated onto the main carrier, as shown in Fig. 5-16. Any type of modulation, such as AM, DSB, SSB, PM, FM, and so on, could be used. The modulation types used on the subcarriers, as well as the type used on the main carrier, may be different. However, as shown in Fig. 5-16b, the composite signal spectrum must consist of modulated signals that do not have overlapping spectra; otherwise, crosstalk will occur between the message signals at the receiver output. The composite baseband signal then modulates a main transmitter to produce the FDM signal that is transmitted over the wideband channel.

The received FDM signal is first demodulated to reproduce the composite baseband signal that is passed through filters to separate the individual modulated subcarriers. The subcarriers are then demodulated to reproduce the message signals  $m_1(t)$ ,  $m_2(t)$ , and so on.<sup>†</sup>

The FM stereo broadcasting system that has been adopted in the United States is an example of an FDM system. Furthermore, it is compatible with the monaural FM system that has existed since the 1940s. That is, a listener with a conventional monaural FM receiver will hear the monaural audio (which consists of the left- plus the right-channel audio), while the listener with a stereo receiver will receive the left-channel audio on the left speaker and the right-channel audio on the right speaker (Fig. 5-17). To obtain the compatibility feature, the left- and right-channel audios are combined (summed) to produce the monaural signal, and the difference audio is used to modulate a 38-kHz DSB-SC signal. A 19-kHz pilot tone is added to the composite baseband signal  $m_b(t)$  to provide a reference signal for coherent (product) subcarrier demodulation in the receiver. As seen from Fig. 5-17c, this system is compatible with existing FM monaural receivers. In Prob. 5-44 it will be found that a rela-

<sup>†</sup> Figure 8-1 shows a typical FDM hierarchy used by the telephone industry.

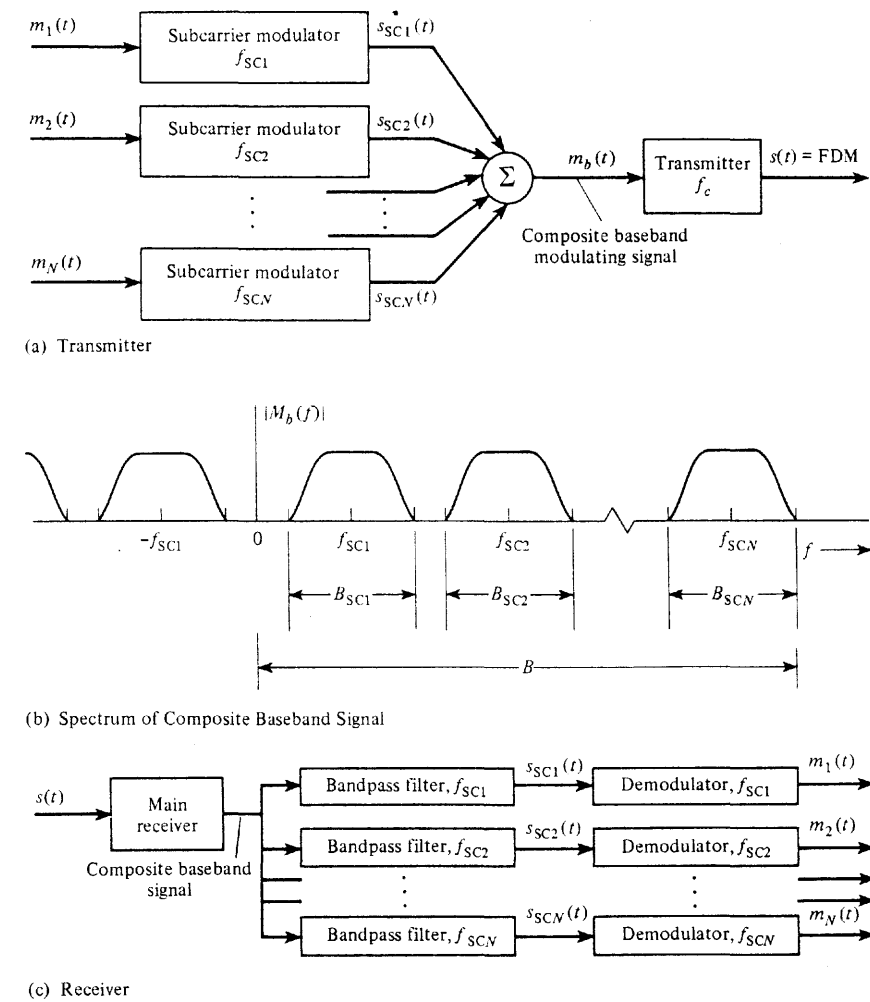


Figure 5-16 FDM system.

tively simple switching (sampling) technique may be used to implement the demodulation of the subcarrier and the separation of the left and right signals in one operation.

The FM station may also be given *subsidiary communications authorization* (SCA) by the FCC. This allows the station to add a FM subcarrier to permit the transmission of private background music to business subscribers for use in their store or office. The SCA FM subcarrier frequency is usually 67 kHz, although this frequency is not specified by FCC rules. Moreover, up to four SCA subcarriers are permitted by the FCC, and each may carry either data or audio material for private subscribers.

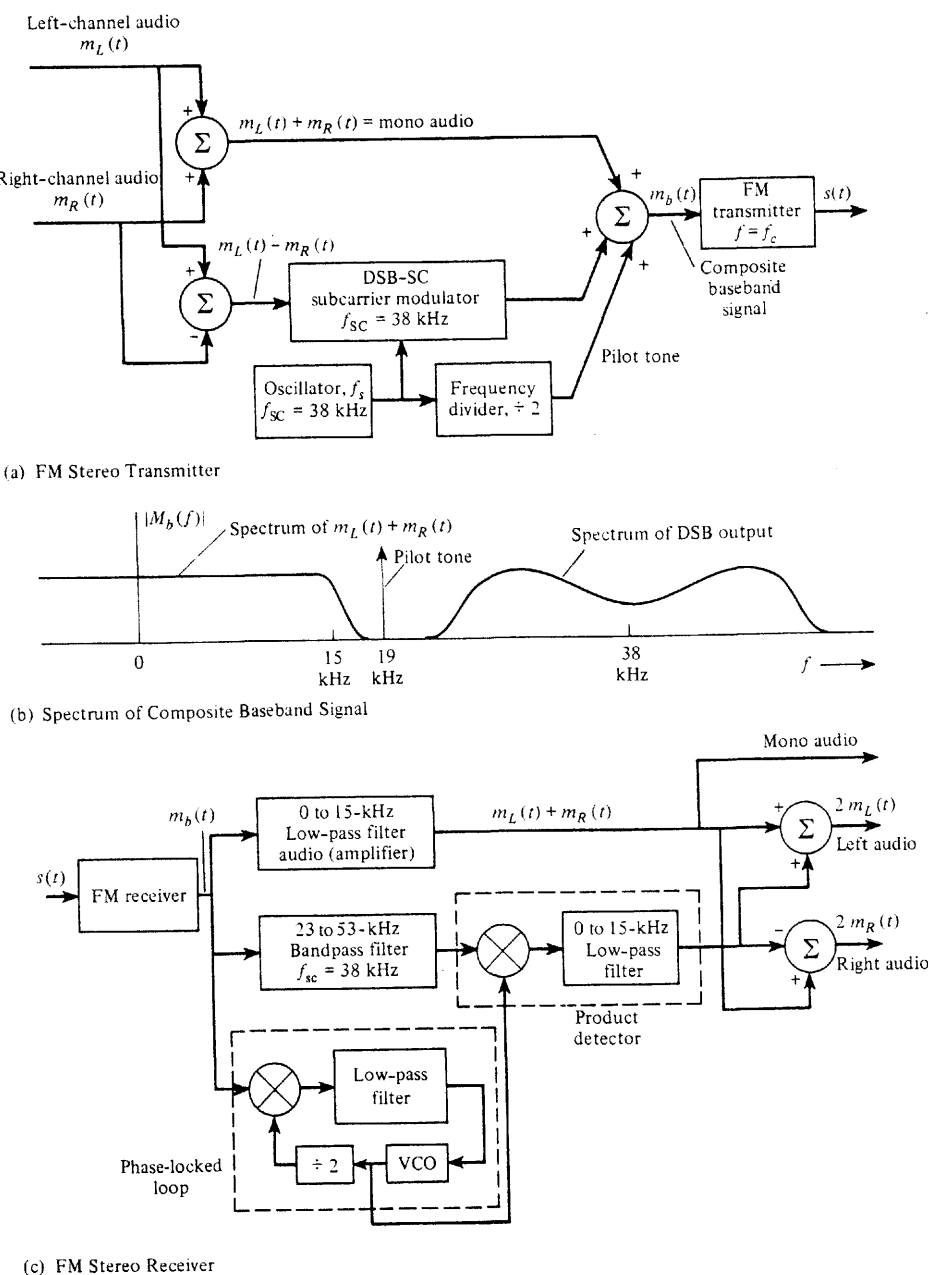


Figure 5-17 FM stereo system.

## 5-8 FM AND NOISE REDUCTION STANDARDS

### FM Broadcast Technical Standards

Table 5-4 gives some of the FCC technical standards that have been adopted for FM systems. In the United States, FM stations are classified into one of three major categories that depend on their intended coverage area. Class A stations are local stations. They have a maximum effective radiated power (ERP) of 6 kW and a maximum antenna height of 300 ft above average terrain. The ERP is the average transmitter output power multiplied by the power gains of both the transmission line (a number less than 1) and the antenna (see Sec. 8-9 for some TV ERP calculations). Class B stations have a maximum ERP of 50 kW, with a maximum antenna height of 500 ft above average terrain. Class B stations are assigned to the northeastern part of the United States, southern California, Puerto Rico, and the Virgin Islands. Class C stations are assigned to the remainder of the United States. They have a maximum ERP of 100 kW and a maximum antenna height of 2000 ft above average terrain. As shown in Table 5-4, FM stations are further classified as commercial or noncommercial. Noncommercial stations operate in the 88.1 to 91.9 MHz segment of the FM band and provide educational programs with no commercials. Class D stations are limited to 10-W transmitter output and are for noncommercial service only. In the commercial segment of the FM band, 92.1 to 107.9 MHz, certain frequencies are reserved for Class A stations and the remainder are for Class B or Class C station assignment. A listing of these frequencies and the specific station assignments for each city is available [Broadcasting, 1995].

### Dolby and DBX Noise Reduction Systems

As described previously, preemphasis and deemphasis are used in FM broadcasting for noise reduction. They are also used in audiotape recording for noise reduction. Other, more sophisticated noise reduction techniques have been developed in addition to companding (see Sec. 3-3). This section describes some of these techniques.

In audio cassette tape recording, noise occurs predominantly at the higher frequencies and is commonly called *hiss*. These noise reduction techniques use a combination of preemphasis filtering and dynamic range compression at the encoder before recording. The playback decoder circuit uses a combination of deemphasis and dynamic range expansion. If done properly, a high-quality audio signal can be recovered with low noise. However, if the encoder and decoders are not "matched," a "breathing" or "pumping" effect can result that can be more disturbing than the hiss on an unprocessed signal. Another disadvantage of these techniques is that if a tape with a processed signal is played back on a regular amplifier system without decoding, the reproduction is poor, with excessive high-frequency response.

Dolby Laboratories has developed a number of noise reduction techniques designated as Dolby-A, Dolby-B, and Dolby-C. *Dolby-A* is designed for commercial use and, consequently, is a relatively expensive system. The *Dolby-A* processor divides the audio spectrum into four frequency bands: low-pass, below 80 Hz; bandpass, 80 Hz to 3 kHz; high-pass, above 3 kHz; and high-pass, above 9 kHz. At the encoder, the gain in each of these bands is adaptively increased as the signal level in the associated band becomes lower. This pro-

TABLE 5-4 FCC FM STANDARDS

Class of Service	Item	FCC Standard
FM broadcasting	Assigned frequency, $f_c$	In 200-kHz increments from 88.1 MHz (FM Channel 201) to 107.9 MHz (FM Channel 300)
	Channel bandwidth	200 kHz
	Noncommercial stations	88.1 MHz (Channel 201) to 91.9 MHz (Channel 220)
	Commercial stations	92.1 MHz (Channel 221) to 107.9 MHz (Channel 300)
	Carrier frequency stability	$\pm 2000$ Hz of the assigned frequency
	100% modulation <sup>a</sup>	$\Delta F = 75$ kHz
	Audio frequency response <sup>b</sup>	50 Hz to 15 kHz following a 75- $\mu$ s preemphasis curve
	Modulation index	5 (for $\Delta F = 75$ kHz and $B = 15$ kHz)
	% harmonic distortion <sup>b</sup>	<3.5% (50–100 Hz) <2.5% (100–7500 Hz) <3.0% (7500–15,000 Hz)
	FM noise	At least 60 dB below 100% modulation at 400 Hz
Two-way FM mobile radio	AM noise	50 dB below the level corresponding to 100% AM in a band 50 Hz–15 kHz
	Maximum power licensed	100 kW in horizontal polarized plane plus 100 kW in vertical polarized plane
	100% modulation	$\Delta F = 5$ kHz
TV aural (FM) signal	Modulation index	1 (for $\Delta F = 5$ kHz and $B = 5$ kHz)
	Carrier frequencies are within the frequency bands:	32–50 MHz (low VHF band) 144–148 MHz (2-m amateur band) 148–174 MHz (high VHF band) 420–450 MHz ( $\frac{3}{4}$ -m amateur band) 450–470 MHz (UHF band) 470–512 MHz (UHF, T band) 806–928 MHz (900-MHz band)
	100% modulation	$\Delta F = 25$ kHz
	Modulation index	1.67 (for $\Delta F = 25$ kHz and $B = 15$ kHz)

<sup>a</sup> For stereo transmission the 19-kHz pilot tone may contribute as much as 10% of the total allowed 75-kHz peak deviation. If SCA is used, each SCA subcarrier may also contribute up to 10% and the total peak deviation may be 110% of 75 kHz provided that SCA subcarriers are present.

<sup>b</sup> Under the new FCC deregulation policy these requirements are deleted from the FCC rules, although broadcasters still use them as guidelines for minimum acceptable performance.

<sup>c</sup> Amplitude-compressed SSB is also permitted in the 150- to 170-MHz band in 5-kHz bandwidth channels.

vides an overall compression characteristic for the encoder. A maximum boost of 10 to 15 dB is used in each of the bands if the signal level is 45 dB below the maximum recording level (0 dB). For playback the decoder provides the appropriate expansion of the signal in each of the bands so that the overall frequency response is flat and the dynamic range of the original audio signal is preserved. If the recording and playback levels are properly set, the Dolby-A system provides a 10- to 15-dB increase in the signal-to-noise ratio.

The Dolby-B and Dolby-C systems are designed for consumer audio cassette and reel-to-reel tape recording. They are relatively inexpensive to implement and use a two-band instead of a four-band system, as in Dolby-A. As shown in Fig. 5-18, the Dolby-B encoder preemphasizes the higher frequencies and provides up to a 10-dB boost when the level in the high-frequency band is 45 dB below the reference level. The Dolby-C encoder provides as much as a 20-dB boost for the high-frequency components when their level is low. The Dolby-C encoder uses two cascaded stages of compression, one activated at high signal levels and another at low signal levels. Overall, the Dolby-B system reduces the tape hiss by about 10 dB for frequencies above 4 kHz, and the Dolby-C system reduces the hiss by about 20 dB for frequencies above 1 kHz. In FM broadcasting the Dolby-B system with a 6.4-kHz high-pass filter (25  $\mu$ s) is often used for additional signal-to-noise ratio improvement over the standard FM preemphasis-deemphasis system.

DBX, Inc. of Waltham, Massachusetts, has developed a noise reduction system that processes the whole audio signal in a single audio band. The DBX system uses voltage-controlled amplifiers with 130 dB of dynamic range at both the encoder and the decoder to provide the compression and expansion characteristics. The encoder also uses a 1.6-kHz preemphasis network that provides a 20-dB boost at the high end. The decoder has a matching deemphasis network. The DBX system provides a 20- to 30-dB signal-to-noise ratio im-

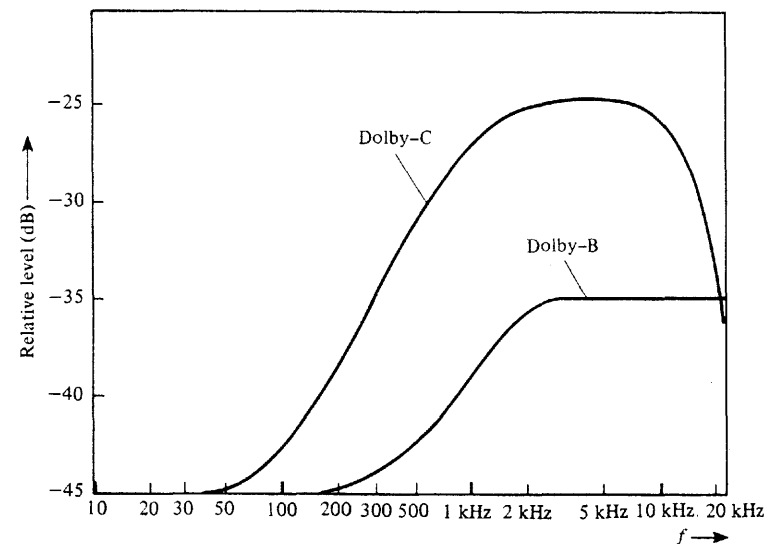


Figure 5-18 Low-level frequency response for Dolby-B and Dolby-C encoders.

provement and can handle large signal overloads (above the 0-dB level) without distortion. This system has the disadvantage, however, of single band processing. That is, a large-level component located anywhere within the frequency band will control the compression level of the whole signal.

## 5-9 BINARY MODULATED BANDPASS SIGNALING

Digitally modulated bandpass signals are generated by using the complex envelopes for AM, PM, FM, or QM (quadrature modulation) signaling that were first shown in Table 4-1 and studied in previous sections. For digital modulated signals, the modulating signal,  $m(t)$ , is a digital signal given by the binary or multilevel line codes that were developed in Chapter 3. In this section, details of binary modulated signals are given. In Sections 5-10 and 5-11, multilevel and minimum-shift-keyed (MSK) digitally modulated signals are described.

The most common binary bandpass signaling techniques are illustrated in Fig. 5-19. They are

- *On-off keying (OOK)*, also called *amplitude shift keying (ASK)*, which consists of keying (switching) a carrier sinusoid on and off with a unipolar binary signal. It is identical to *unipolar* binary modulation on a DSB-SC signal, (5-13). Morse code radio transmission is an example of this technique. Consequently, OOK was one of the first modulation techniques to be used and precedes analog communication systems.
- *Binary-phase shift keying (BPSK)*, which consists of shifting the phase of a sinusoidal carrier  $0^\circ$  or  $180^\circ$  with a unipolar binary signal. It is equivalent to PM signaling with a digital waveform and is also equivalent to modulating a DSB-SC signal with a polar digital waveform.
- *Frequency-shift keying (FSK)*, which consists of shifting the frequency of a sinusoidal carrier from a mark frequency (corresponding, for example, to sending a binary 1) to a space frequency (corresponding to sending a binary 0) according to the baseband digital signal. It is identical to modulating a FM carrier with a binary digital signal.

As indicated in Sec. 3-6, usually the bandwidth of the digital signal needs to be minimized to achieve spectral conservation as one transmits information over a channel. This may be accomplished by using a premodulation raised cosine-rolloff filter to minimize the bandwidth of the digital signal and yet not introduce ISI. The shaping of the baseband digital signal produces an analog baseband waveform that modulates the transmitter. Figure 5-19f illustrates the resulting DSB-SC signal when a premodulation filter is used. Thus the BPSK signal of Fig. 5-19d becomes a DSB-SC signal (Fig. 5-19f) when premodulation filtering is used.

### On-Off Keying (OOK)

The OOK signal is represented by

$$s(t) = A_c m(t) \cos \omega_c t \quad (5-70)$$

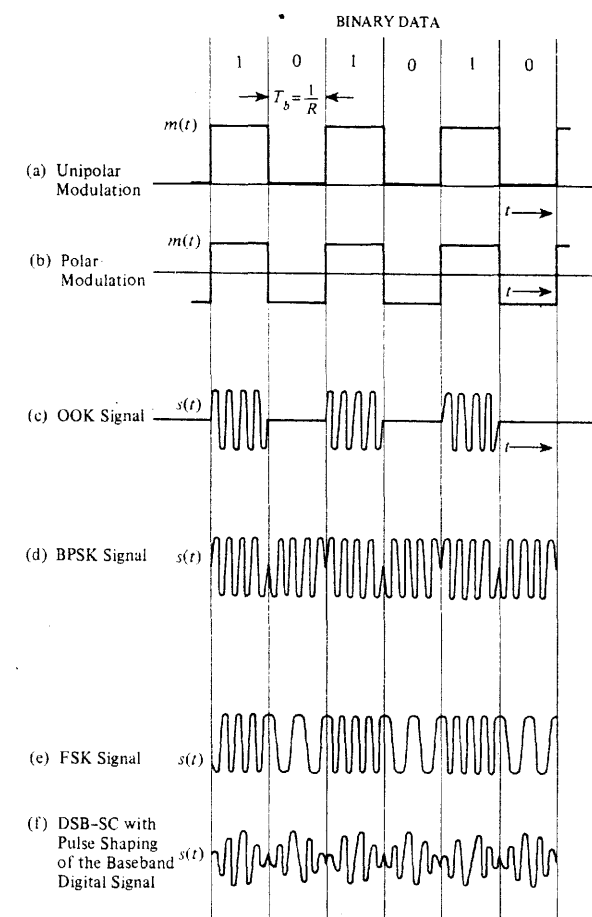


Figure 5-19 Bandpass digitally modulated signals.

where  $m(t)$  is a unipolar baseband data signal, as shown in Fig. 5-19a. Consequently, the complex envelope is simply

$$g(t) = A_c m(t) \quad \text{for OOK} \quad (5-71)$$

and the PSD of this complex envelope is proportional to that for the unipolar signal. Using (3-39b), we find that this PSD is

$$\mathcal{P}_g(f) = \frac{A_c^2}{2} \left[ \delta(f) + T_b \left( \frac{\sin \pi f T_b}{\pi f T_b} \right)^2 \right] \quad \text{for OOK} \quad (5-72)$$

where  $m(t)$  has a peak value of  $\sqrt{2}$  so that  $s(t)$  has an average normalized power of  $A_c^2/2$ . The PSD for the corresponding OOK signal is then obtained by substituting (5-72) into (5-2b). The result is shown for positive frequencies in Fig. 5-20a, where  $R = 1/T_b$  is the bit rate. It is seen that the null-to-null bandwidth is  $2R$ . That is, the transmission bandwidth of

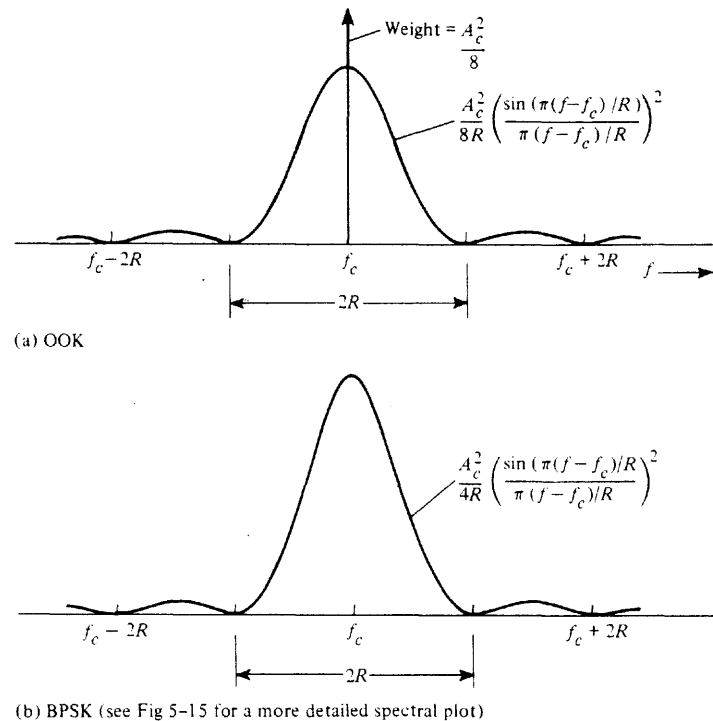


**Figure 5-20** PSD of bandpass digital signals (positive frequencies shown).

the OOK signal is  $B_T = 2B$  where  $B$  is the baseband bandwidth since OOK is AM-type signaling.

If raised cosine-rolloff filtering is used (to conserve bandwidth), the absolute bandwidth of the filtered binary signal is related to the bit rate  $R$  by (3-74), where  $D = R$  for binary digital signaling. Thus,

$$B = \frac{1}{2}(1+r)R \quad (5-73)$$

where  $r$  is the rolloff factor of the filter. This gives an absolute transmission bandwidth of

$$B_T = (1+r)R \quad (5-74)$$

for OOK signaling.

OOK may be detected using either an envelope detector (noncoherent detection) or a product detector (coherent detection) because it is a form of AM signaling. (In radio-frequency receiver applications where the input RF signal is small, a superheterodyne receiver circuit of Fig. 4-29 is used where one of these detector circuits are placed after the IF output stage.) These detectors are shown in Fig. 5-21a and 5-21b. For product detection the carrier reference,  $\cos(\omega_c t)$ , must be provided. This is usually obtained from a PLL circuit (studied in Sec. 4-14), where the PLL is locked onto a discrete carrier term (see Fig. 5-20a) of the OOK signal.

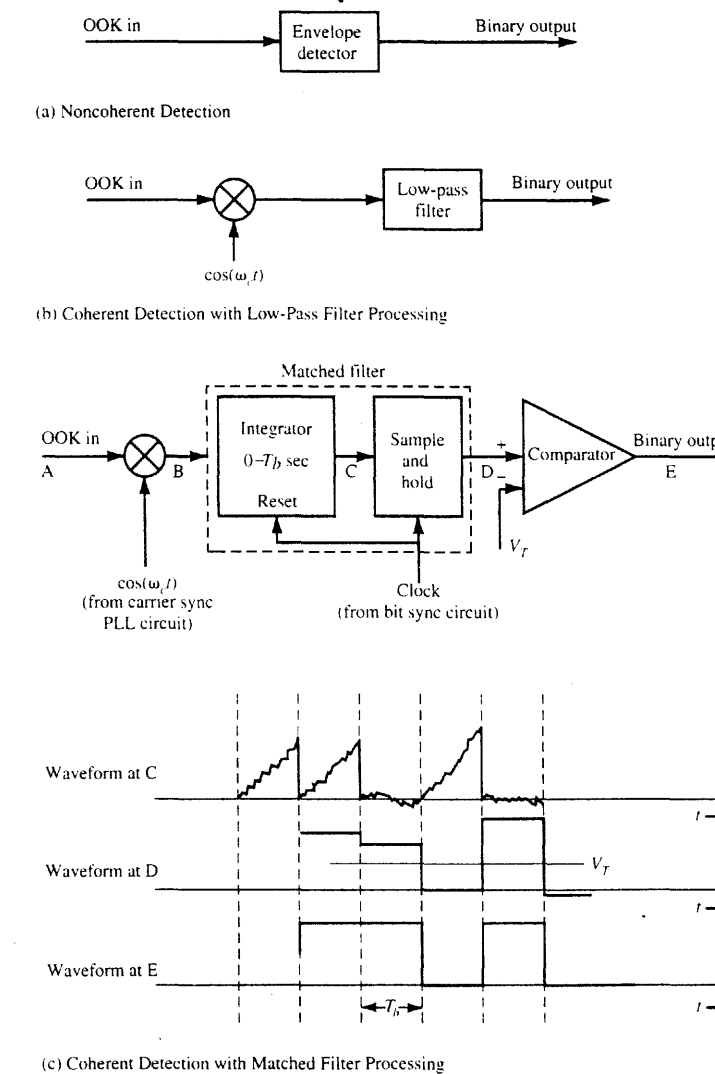


**Figure 5-21** Detection of OOK.

For optimum detection of OOK—that is, to obtain the lowest BER when the input OOK signal is corrupted by additive white Gaussian noise (AWGN)—product detection with matched filter processing is required. This is shown in Fig. 5-21c, where waveforms at various points of the circuit are illustrated for the case of receiving an OOK signal that corresponds to the binary data stream 1101. Details about the operation, the performance, and the realization of the matched filter are given in Sec. 6-8. Note that the matched filter also requires a clocking signal that is used to reset the integrator at the beginning of each bit in-

terval and to clock the sample-and-hold circuit at the end of each bit interval. This clock signal is provided by a bit synchronizer circuit (studied in Chapter 4).

The optimum coherent OOK detector of Fig. 5-21c is more costly to implement than the noncoherent OOK detector of Fig. 5-21a. If the input noise is small, the noncoherent receiver may be the best solution considering both cost and noise performance. The tradeoff in BER performance between optimum coherent detection and nonoptimum noncoherent detection is studied in Sec. 7-6.

### Binary-Phase Shift Keying (BPSK)

The BPSK signal is represented by

$$s(t) = A_c \cos[\omega_c t + D_p m(t)] \quad (5-75a)$$

where  $m(t)$  is a polar baseband data signal. For convenience, let  $m(t)$  have peak values of  $\pm 1$  and a rectangular pulse shape.

It will now be shown that BPSK is also a form of AM-type signaling. Expanding (5-75a), we get

$$s(t) = A_c \cos(D_p m(t)) \cos \omega_c t - A_c \sin(D_p m(t)) \sin \omega_c t$$

Recalling that  $m(t)$  has values of  $\pm 1$  and that  $\cos(x)$  and  $\sin(x)$  are even and odd functions of  $x$ , the representation of the BPSK signal reduces to

$$s(t) = \underbrace{(A_c \cos D_p) \cos \omega_c t}_{\text{pilot carrier term}} - \underbrace{(A_c \sin D_p)m(t) \sin \omega_c t}_{\text{data term}} \quad (5-75b)$$

The level of the pilot carrier term is set by the value of the peak deviation,  $\Delta\theta = D_p$ .

For digital angle modulated signals, the *digital modulation index*,  $h$ , is defined by

$$h = \frac{2\Delta\theta}{\pi} \quad (5-76)$$

where  $2\Delta\theta$  is the maximum peak-to-peak phase deviation (radians) during the time required to send one symbol,  $T_s$ . For binary signaling, the symbol time is equal to the bit time,  $T_s = T_b$ .

The level of the pilot carrier term is set by the value of the peak deviation, which is  $\Delta\theta = D_p$  for  $m(t) = \pm 1$ . If  $D_p$  is small, the pilot carrier term has a relatively large amplitude compared to the data term; consequently, there is very little power in the data term (which contains the source information). To maximize the signaling efficiency (low probability of error), the power in the data term needs to be maximized. This is accomplished by letting  $\Delta\theta = D_p = 90^\circ = \pi/2$  radians, which corresponds to a digital modulation index of  $h = 1$ . For this optimum case of  $h = 1$ , the BPSK signal becomes

$$s(t) = -A_c m(t) \sin \omega_c t \quad (5-77)$$

Throughout this text, we assume that  $\Delta\theta = 90^\circ$ ,  $h = 1$ , is used for BPSK signaling (unless otherwise stated). Equation (5-77) shows that BPSK is equivalent to DSB-SC signaling with a polar baseband data waveform. The complex envelope for this BPSK signal is

$$g(t) = jA_c m(t) \quad \text{for BPSK} \quad (5-78)$$

Using (3-41), we obtain the PSD for the complex envelope,

$$\mathcal{P}_g(f) = A_c^2 T_b \left( \frac{\sin \pi f T_b}{\pi f T_b} \right)^2 \quad \text{for BPSK} \quad (5-79)$$

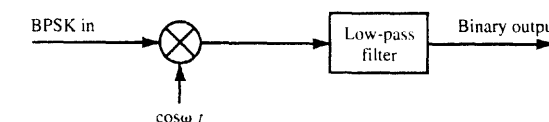
where  $m(t)$  has values of  $\pm 1$  so that  $s(t)$  has an average normalized power of  $A_c^2/2$ . The PSD for the corresponding BPSK signal is readily evaluated by translating the baseband spectrum to the carrier frequency, as specified by substituting (5-79) into (5-2b). The resulting BPSK spectrum is shown in Fig. 5-20b. The null-to-null bandwidth for BPSK is also  $2R$ , the same as that found for OOK.

To detect BPSK, synchronous detection must be used, as illustrated in Fig. 5-22a. Since there is no discrete carrier term in the BPSK signal, a PLL may be used to extract the carrier reference *only* if a low-level pilot carrier is transmitted together with this BPSK signal. Otherwise, a Costas loop or a squaring loop (Fig. 5-3) may be used to synthesize the carrier reference from this DSB-SC (i.e., BPSK) signal and to provide coherent detection. However, the  $180^\circ$  phase ambiguity must be resolved as discussed in Sec. 5-4. This can be accomplished by using differential coding at the transmitter input and differential decoding at the receiver output, as illustrated previously in Fig. 3-17.

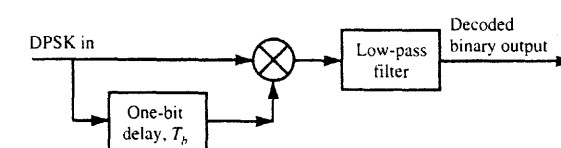
For optimum detection of BPSK (i.e. lowest BER for the case of AWGN) the low-pass filter in Fig. 5-22a is replaced by an integrate-and-dump matched filter processing that was illustrated in Fig. 5-21c where  $V_T$  is set to 0 V for the case of BPSK. The resulting probability of bit error is given in Sec. 7-3.

### Differential Phase-Shift Keying (DPSK)

Phase-shift-keyed signals cannot be detected incoherently. However, a partially coherent technique can be used whereby the phase reference for the present signaling interval is provided by a delayed version of the signal that occurred during the previous signaling inter-



(a) Detection of BPSK (Coherent Detection)



(b) Detection of DPSK (Partially Coherent Detection)

Figure 5-22 Detection of BPSK and DPSK.

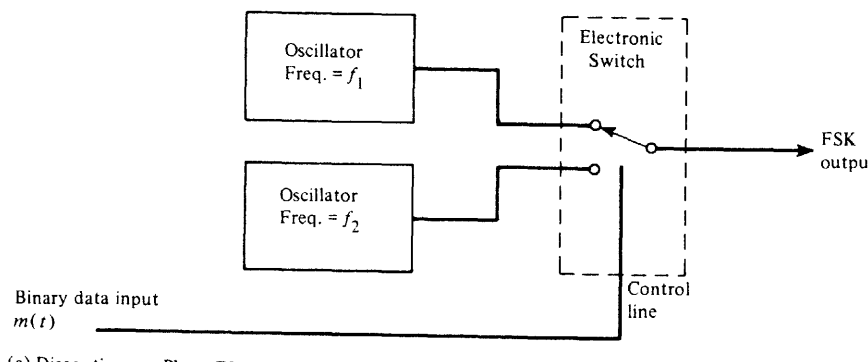
val. This is illustrated by the receivers shown in Fig. 5-22b, where differential decoding is provided by the (one-bit) delay and the multiplier. Consequently, if the data on the BPSK signal are differentially encoded (e.g., see the illustration in Table 3-4), the *decoded* data sequence will be recovered at the output of this receiver. This signaling technique consisting of transmitting a differentially encoded BPSK signal is known as DPSK.

For optimum detection of DPSK the low-pass filter of Fig. 5-22 is replaced by an integrate-and-dump matched filter and the DPSK input signal needs to be prefiltered by a bandpass filter that has an impulse response of  $h(t) = \Pi[(t - 0.5T_b)/T_b] \cos(\omega_c t)$ . For more details about this optimum receiver see Fig. 7-12. The resulting BER is given by (7-66) and (7-67).

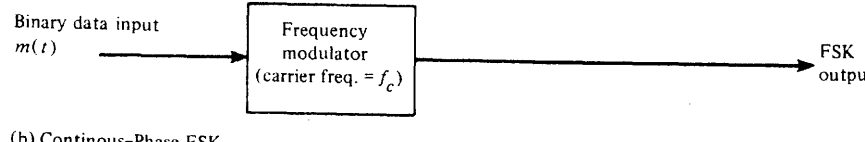
In practice, DPSK is often used instead of BPSK because the DPSK receiver does not require a carrier synchronizer circuit. An example is the Bell 212A modem (1200 bits/s) that is described in Appendix C, Table C-8.

### Frequency-Shift Keying (FSK)

The FSK signal can be characterized as one of two different types, depending on the method used to generate the FSK signal. One type is generated by switching the transmitter output line between two different oscillators, as shown in Fig. 5-23a. This type generates an output waveform that is discontinuous at the switching times. It is called *discontinuous-phase FSK* because  $\theta(t)$  is discontinuous at the switching times. The discontinuous phase FSK signal is represented by



(a) Discontinuous-Phase FSK



(b) Continuous-Phase FSK

Figure 5-23 Generation of FSK.

$$s(t) = \begin{cases} A_c \cos(\omega_1 t + \theta_1), & \text{for } t \text{ in the time interval when a binary 1 is being sent} \\ A_c \cos(\omega_2 t + \theta_2), & \text{for } t \text{ in the time interval when a binary 0 is sent} \end{cases} \quad (5-80)$$

where  $f_1$  is called the *mark* (binary 1) frequency and  $f_2$  is called the *space* (binary 0) frequency. Since FSK transmitters are not usually built this way, we will turn to the second type, shown in Fig. 5-23b.

The *continuous-phase FSK* signal is generated by feeding the data signal into a frequency modulator, as shown in Fig. 5-23b. This FSK signal is represented by (referring to Sec. 5-6)

$$s(t) = A_c \cos\left[\omega_c t + D_f \int_{-\infty}^t m(\lambda) d\lambda\right]$$

or

$$s(t) = \operatorname{Re}\{g(t)e^{j\omega_c t}\} \quad (5-81a)$$

where

$$g(t) = A_c e^{j\theta(t)} \quad (5-81b)$$

$$\theta(t) = D_f \int_{-\infty}^t m(\lambda) d\lambda \quad \text{for FSK} \quad (5-81c)$$

and  $m(t)$  is a baseband digital signal. Although  $m(t)$  is discontinuous at the switching time, the phase function  $\theta(t)$  is continuous because  $\theta(t)$  is proportional to the integral of  $m(t)$ . If the serial data input waveform is binary, such as a polar baseband signal, the resulting FSK signal is called a *binary FSK* signal. Of course, a multilevel input signal would produce a multilevel FSK signal. We will assume that the input is a binary signal in this section and examine the properties of binary FSK signals.

In general, the spectra of FSK signals are difficult to evaluate since the complex envelope,  $g(t)$ , is a nonlinear function of  $m(t)$ . However, the techniques that were developed in Sec. 5-6 are applicable, as we show in the following example.

### Example 5-4 SPECTRUM OF THE BELL-TYPE 103 FSK MODEM

Keyboard-type computer terminals are often used for communication with a remote computer via analog dial-up telephone lines. These telephone lines have a passband over the VF range of 300 to 3200 Hz. Because baseband digital signals (such as polar line code signals) do not have dominant frequencies in this band, they must be modulated onto a carrier to produce a bandpass signal that has dominant spectral components within the VF range. To accomplish this, modems (i.e., a modulator and demodulator) are connected to the phone line at each end. This is illustrated in Fig. 5-24 with an FSK-type modem. (In Appendix C, specifications are also given for modems with other types of modulation.) The Bell Telephone System was the first to adopt this technique, with their Model 103 modem, which uses FSK with a signaling speed of

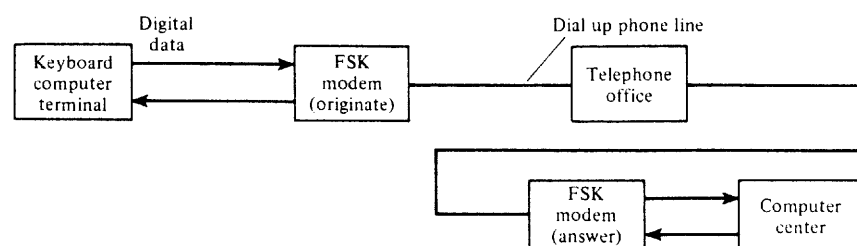


Figure 5-24 Computer communication using FSK signaling.

300 bits/s.<sup>†</sup> Each modem contains both an FSK transmitter and an FSK receiver so that the computer terminal can both "talk" and "listen." Two FSK frequency bands are used (one around 1 kHz and another around 2 kHz) so that it is possible to talk and listen simultaneously. This is called *full-duplex capability*. (In *half-duplex* one cannot listen while talking, and vice versa; in *simplex* one can only talk or only listen.) The standard mark and space frequencies for the two bands are shown in Table 5-5. From this table it is seen that the peak-to-peak deviation is  $2\Delta F = 200$  Hz.

The spectrum for a Bell-type 103 modem will now be evaluated for the case of the widest-bandwidth FSK signal. It is obtained when the input data signal consists of a deterministic (periodic) square wave corresponding to an alternating data pattern (i.e., 10101010).<sup>‡</sup> This is illustrated in Fig. 5-25a, where  $T_b$  is the time interval for one bit and  $T_0 = 2T_b$  is the period of the data modulation. The spectrum is obtained by using the Fourier series technique developed in Sec. 5-6 and Example 5-2. Since the modulation is periodic, we would expect the FSK spectrum to be a line spectrum (i.e., delta functions). Using (5-81c) and (5-42), we find that the peak frequency deviation is  $\Delta F = D_f/(2\pi)$  for  $m(t)$  having values of  $\pm 1$ . This results in the triangular phase function shown in Fig. 5-25b. From this figure the digital modulation index is

$$h = \frac{2\Delta\theta}{\pi} = \Delta FT_0 = \frac{2\Delta F}{R} \quad (5-82)$$

where the bit rate is  $R = 1/T_b = 2/T_0$ . In this application, note that the digital modulation index as given by (5-82) is identical to the FM modulation index as defined by (5-48) since

TABLE 5-5 MARK AND SPACE FREQUENCIES FOR THE BELL-TYPE 103 MODEM

	Originate Modem (Hz)	Answer Modem (Hz)
Transmit frequencies		
Mark (binary 1)	$f_1 = 1270$	$f_1 = 2225$
Space (binary 0)	$f_2 = 1070$	$f_2 = 2025$
Receive frequencies		
Mark (binary 1)	$f_1 = 2225$	$f_1 = 1270$
Space (binary 0)	$f_2 = 2025$	$f_2 = 1070$

<sup>†</sup> This example is included to illustrate the FSK technique. Popular 14.4- and 28.8-kbit/s modems use QAM signaling that is discussed in Sec. 5-10.

<sup>‡</sup> For the case of random data, the PSD for  $g(t)$  is given by the  $h = 0.7 \approx 0.67$  curve of Fig. 5-27.

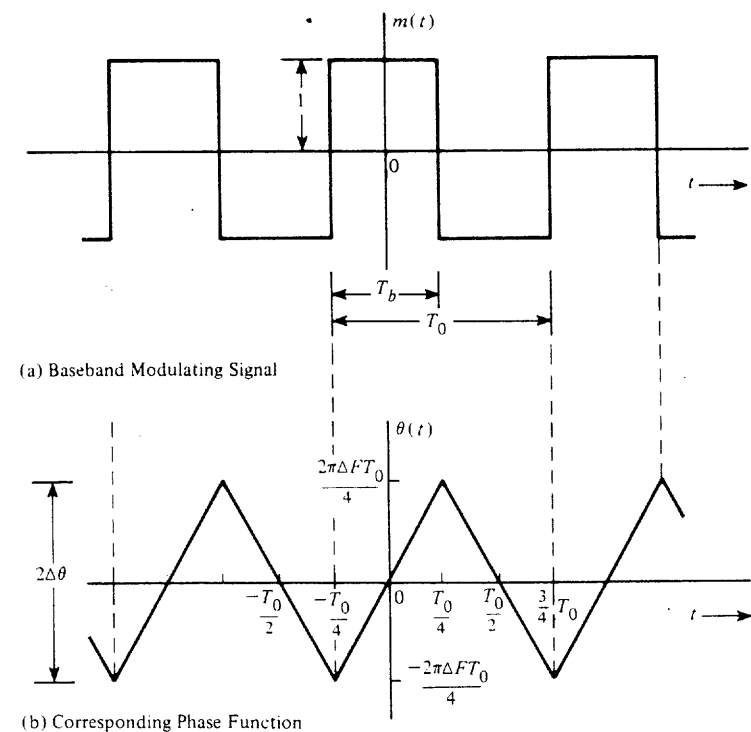


Figure 5-25 Input data signal and FSK signal phase function.

$$h = \frac{\Delta F}{1/T_0} = \frac{\Delta F}{B} = \beta_f$$

provided that the bandwidth of  $m(t)$  is defined as  $B = 1/T_0$ .

The Fourier series for the complex envelope is

$$g(t) = \sum_{n=-\infty}^{\infty} c_n e^{jn\omega_0 t} \quad (5-83)$$

where  $\omega_0 = 1/T_0 = R/2$  and

$$\begin{aligned} c_n &= \frac{A_c}{T_0} \int_{-T_0/2}^{T_0/2} e^{j\theta(t)} e^{-jn\omega_0 t} dt \\ &= \frac{A_c}{T_0} \left[ \int_{-T_0/4}^{T_0/4} e^{j\Delta\omega t} e^{-jn\omega_0 t} dt + \int_{T_0/4}^{3T_0/4} e^{-j\Delta\omega(t-(T_0/2))} e^{-jn\omega_0 t} dt \right] \end{aligned} \quad (5-84)$$

and  $\Delta\omega = 2\pi\Delta F = 2\pi h/T_0$ . This reduces to

$$c_n = \frac{A_c}{2} \left[ \left( \frac{\sin[(\pi/2)(h-n)]}{(\pi/2)(h-n)} \right) + (-1)^n \left( \frac{\sin[(\pi/2)(h+n)]}{(\pi/2)(h+n)} \right) \right] \quad (5-85)$$

where the digital modulation index is  $h = 2\Delta F/R$ .  $2\Delta F$  is the peak-to-peak frequency shift and  $R$  is the bit rate. Using (5-49) and (5-59), we see that the spectrum of this FSK signal with alternating data is

$$S(f) = \frac{1}{2} [G(f - f_c) + G^*(-f - f_c)] \quad (5-86a)$$

where

$$G(f) = \sum_{-\infty}^{\infty} c_n \delta(f - nf_0) = \sum_{-\infty}^{\infty} c_n \delta\left(f - \frac{nR}{2}\right) \quad (5-86b)$$

and  $c_n$  is given by (5-85).

FSK spectra can be evaluated easily for cases of different frequency shifts  $\Delta F$  and bit rates  $R$  if a personal computer is used. A summary of three computer runs using different sets of parameters is shown in Fig. 5-26. Figure 5-26a gives the FSK spectrum for the Bell 103. For this case, where the Bell 103 parameters are used, the digital modulation index is  $h = 0.67$ . Note that for this Bell 103 case there are no spectral lines at the mark and space frequencies,  $f_1$  and  $f_2$ . Figures 5-26b and 5-26c give the FSK spectra for  $h = 1.82$  and  $h = 3.33$ . Note that as the modulation index is increased, the spectrum concentrates about  $f_1$  and  $f_2$ . This is the same result predicted by the PSD theorem for wideband FM (5-66) since the PDF of the binary modulation consists of two delta functions (one for +1 and one for -1 of Fig. 5-25a).

The approximate transmission bandwidth  $B_T$  for the FSK signal is given by Carson's rule:  $B_T = 2(\beta + 1)B$ , where  $\beta = \Delta F/B$ . This is equivalent to

$$B_T = 2\Delta F + 2B \quad (5-87)$$

$B$  is the bandwidth of the digital (e.g., square-wave) modulation waveform. For our example of an alternating binary 1 and 0 test pattern waveform, the bandwidth of this square-wave modulating waveform (assuming that the first null type of bandwidth is used) is  $B = R$  and, using (5-87), the FSK transmission bandwidth becomes

$$B_T = 2(\Delta F + R) \quad (5-88)$$

This result is illustrated in Fig. 5-26. If a raised cosine-rolloff premodulation filter is used, the transmission bandwidth of the FSK signal becomes

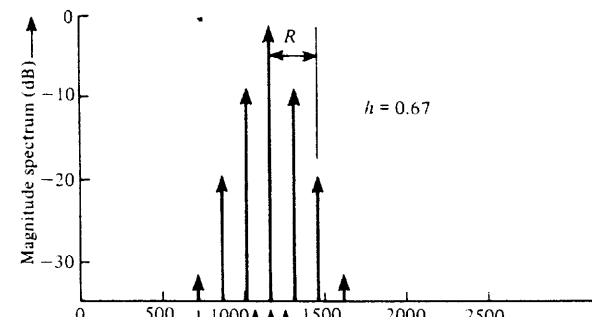
$$B_T = 2\Delta F + (1 + r)R \quad (5-89)$$

For wideband FSK, where  $\beta \gg 1$ ,  $\Delta F$  dominates in these equations and we have  $B_T = 2\Delta F$ . For narrowband FSK the transmission bandwidth is  $B_T = 2B$ .

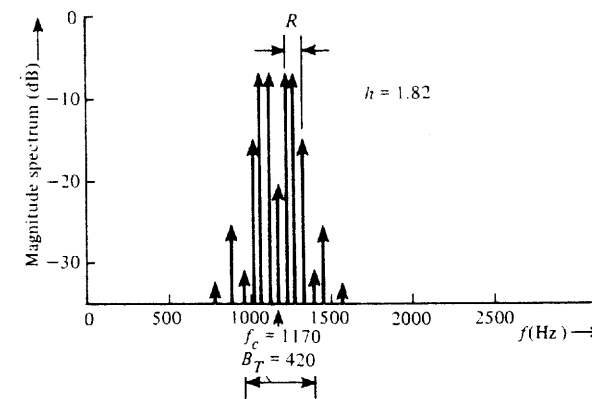
The exact PSD for continuous-phase FSK signals is difficult to evaluate for the case of random data modulation. However, it can be done by using some elegant statistical techniques [Proakis, 1995, pp. 209-215; Anderson and Salz, 1965; Bennett and Rice, 1963]. The resulting PSD for the complex envelope of the FSK signal is<sup>†</sup>

$$\begin{aligned} \mathcal{P}_g(f) &= \frac{A_c^2 T_b}{2} \\ &\times (A_1^2(f)[1 + B_{11}(f)] + A_2^2(f)[1 + B_{22}(f)] + 2B_{12}(f)A_1(f)A_2(f)) \end{aligned} \quad (5-90a)$$

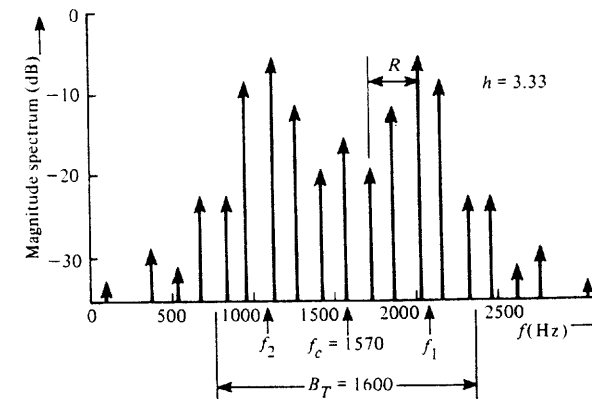
<sup>†</sup> It is assumed that  $h \neq 0, 1, 2, \dots$ . When  $h = 0, 1, 2, \dots$  there are also discrete terms (delta functions) in the spectrum.



(a) FSK Spectrum with  $f_2 = 1070$  Hz,  $f_1 = 1270$  Hz, and  $R = 300$  bits/sec  
(Bell 103 Parameters, Originate mode) for  $h = 0.67$



(b) FSK Spectrum with  $f_2 = 1070$  Hz,  $f_1 = 1270$  Hz, and  $R = 110$  bits/sec  
for  $h = 1.82$



(c) FSK Spectrum with  $f_2 = 1070$  Hz,  $f_1 = 2070$  Hz, and  $R = 300$  bits/sec  
for  $h = 3.33$

Figure 5-26 FSK spectra for alternating data modulation (positive frequencies shown with one-sided magnitude values).

where

$$A_n(f) = \frac{\sin[\pi T_b(f - \Delta F(2n - 3))]}{\pi T_b(f - \Delta F(2n - 3))} \quad (5-90b)$$

and

$$B_{nm}(f) = \frac{\cos[2\pi fT_b - 2\pi\Delta FT_b(n + m - 3)] - \cos(2\pi\Delta FT_b)\cos[2\pi\Delta FT_b(n + m - 3)]}{1 + \cos^2(2\pi\Delta FT_b) - 2\cos(2\pi\Delta FT_b)\cos(2\pi fT_b)} \quad (5-90c)$$

where  $\Delta F$  is the peak frequency deviation,  $R = 1/T_b$  is the bit rate, and the digital modulation index is  $h = 2\Delta F/R$ . The PSD is plotted in Fig. 5-27 for several values of the digital modulation index. The curves in this figure were obtained by using the MATLAB computation. The curve for  $h = 0.7 \approx 0.67$  corresponds to the PSD of  $g(t)$  for the 300 bits/s Bell 103 FSK modem of Example 5-4.

FSK can be detected by using either a frequency (noncoherent) detector or two product detectors (coherent detection), as shown in Fig. 5-28. A detailed study of coherent and noncoherent detection of FSK is given in Secs. 7-3 and 7-4, where the BER is evaluated. To obtain the lowest BER when the FSK signal is corrupted by AWGN, coherent detection with matched filter processing and a threshold device (comparator) is required (as shown in Fig. 7-8).

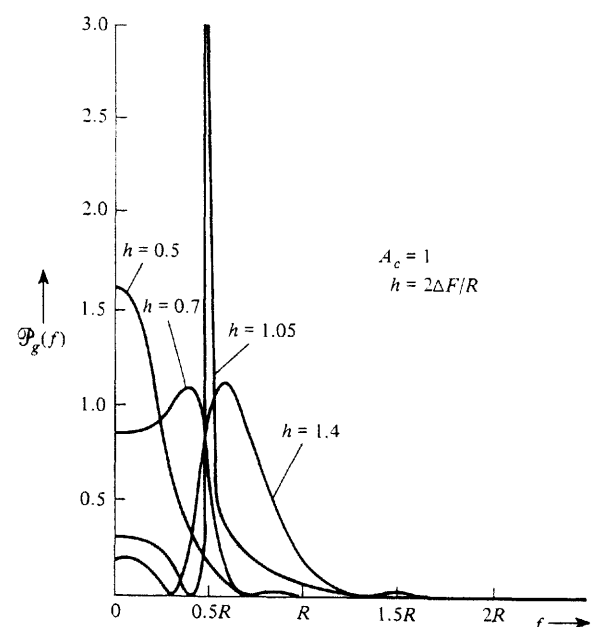


Figure 5-27 PSD for the complex envelope of FSK (positive frequencies shown).

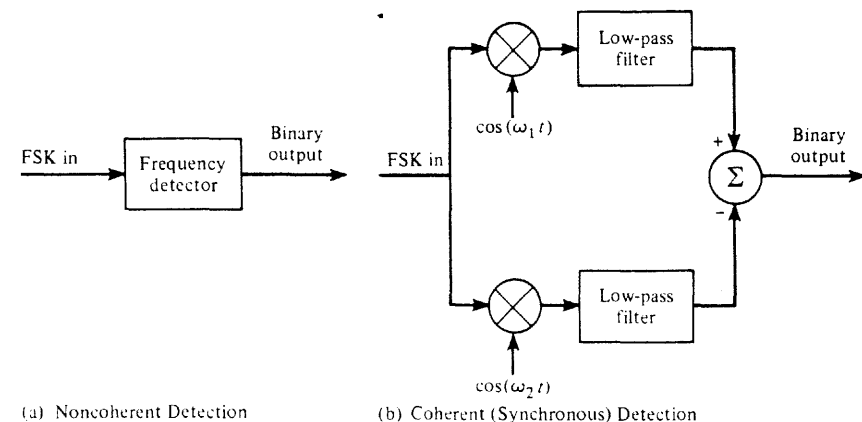


Figure 5-28 Detection of FSK.

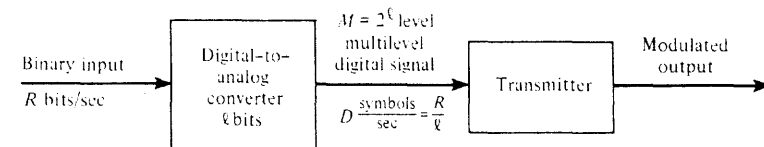


Figure 5-29 Multilevel digital transmission system.

## 5-10 MULTILEVEL MODULATED BANDPASS SIGNALING

With multilevel signaling, digital inputs with more than two modulation levels are allowed on the transmitter input. This is illustrated in Fig. 5-29, which shows how multilevel signals can be generated from a serial binary input stream using a digital-to-analog converter (DAC). For example, suppose that an  $\ell = 2$ -bit DAC is used. Then the number of levels (symbols) in the multilevel signal is  $M = 2^\ell = 2^2 = 4$ . The symbol rate (baud) of the multilevel signal is  $D = R/\ell = \frac{1}{2}R$ , where the bit rate is  $R = 1/T_b$  bits/s.

### Quadrature Phase-Shift Keying (QPSK) and $M$ -ary Phase-Shift Keying (MPSK)

If the transmitter is a PM transmitter with an  $M = 4$  level digital modulation signal,  $M$ -ary phase-shift keying (MPSK) is generated at the transmitter output. A plot of the permitted values of the complex envelope,  $g(t) = A_c e^{j\theta(t)}$ , would contain four points, one value of  $g$  (a complex number in general) for each of the four multilevel values, corresponding to the four phases that  $\theta$  is permitted to have. A plot of two possible sets of  $g(t)$  is shown in Fig. 5-30. For instance, suppose that the permitted multilevel values at the DAC are  $-3, -1, +1$ , and  $+3$  V; then in Fig. 5-30a these multilevel values might correspond to PSK phases of  $0, 90, 180$ , and  $270^\circ$ , respectively. In Fig. 5-30b these levels would correspond to carrier phases of  $45, 135, 225$ , and  $315^\circ$ , respectively. These two signal constellations are essentially

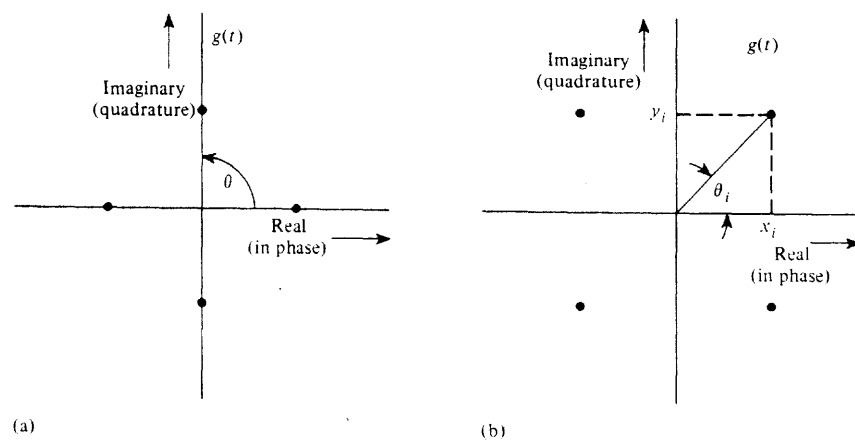


**Figure 5-30** QPSK signal constellations (permitted values of the complex envelope).

the same except for a shift in the carrier-phase reference.<sup>†</sup> This example of  $M$ -ary PSK where  $M = 4$  is called *quadrature-phase-shift-keyed* (QPSK) signaling.

MPSK can also be generated by using two quadrature carriers modulated by the  $x$  and  $y$  components of the complex envelope (instead of using a phase modulator)

$$g(t) = A_c e^{j\theta(t)} = x(t) + jy(t) \quad (5-91)$$

where the permitted values of  $x$  and  $y$  are

$$x_i = A_c \cos \theta_i \quad (5-92)$$

$$y_i = A_c \sin \theta_i \quad (5-93)$$

for the permitted phase angles  $\theta_i$ ,  $i = 1, 2, \dots, M$ , of the MPSK signal. This is illustrated by Fig. 5-31, where the signal processing circuit implements (5-92) and (5-93). Figure 5-30 gives the relationship between the permitted phase angles  $\theta_i$  and the  $(x_i, y_i)$  components for two QPSK signal constellations. Note that this is identical to the quadrature method of generating modulated signals presented in Fig. 4-28.

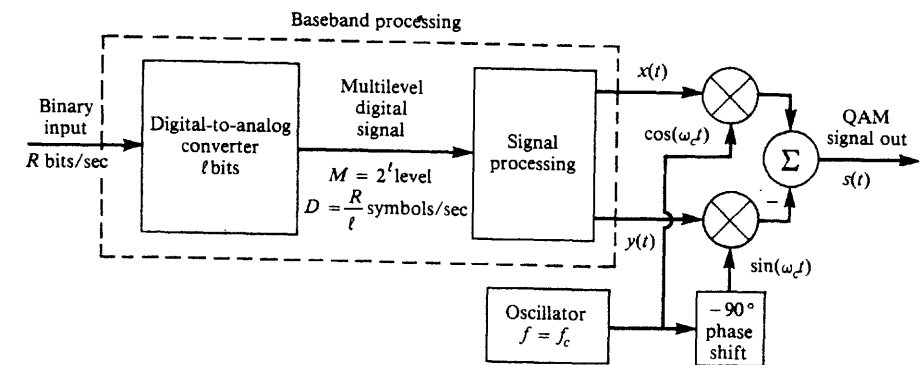
### Quadrature Amplitude Modulation (QAM)

Quadrature carrier signaling, as shown in Fig. 5-31, is called *quadrature amplitude modulation* (QAM). In general, QAM signal constellations are not restricted to having permitted signaling points only on a circle (of radius  $A_c$ , as was the case for MPSK). The general QAM signal is

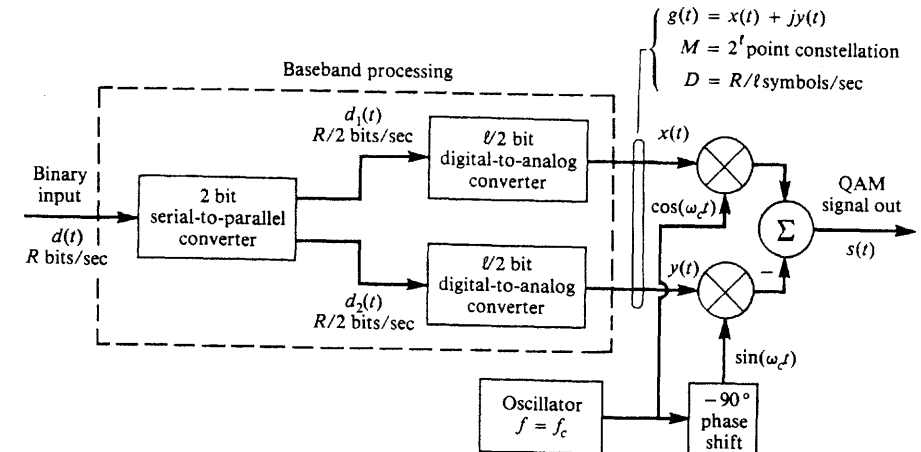
$$s(t) = x(t) \cos \omega_c t - y(t) \sin \omega_c t \quad (5-94)$$



<sup>†</sup> A constellation is an  $N$ -dimensional plot of the possible signal vectors corresponding to the possible digital signals (see Sec. 3-4).



**(a) Modulator for Generalized Signal Constellation**



**(b) Modulator for Rectangular Signal Constellation**

**Figure 5-31** Generation of QAM signals.

where

$$g(t) = x(t) + jy(t) = R(t) e^{j\theta(t)} \quad (5-95)$$

For example, a popular 16-symbol ( $M = 16$  levels) QAM constellation is shown in Fig. 5-32, where the relationship between  $(R_i, \theta_i)$  and  $(x_i, y_i)$  can readily be evaluated for each of the 16 signal values permitted. This type of signaling is used by 2400 bit/s V.22 bis computer modems (see Table C-7). Here  $x_i$  and  $y_i$  are each permitted to have four levels per dimension. This 16-symbol QAM signal may be generated by using two ( $\ell/2 = 2$ )-bit digital-to-analog converters and quadrature balanced modulators as shown in Fig. 5-31b. The waveforms of  $x$  and  $y$  are represented by

$$x(t) = \sum_n x_n h_1 \left( t - \frac{n}{D} \right) \quad (5-96)$$

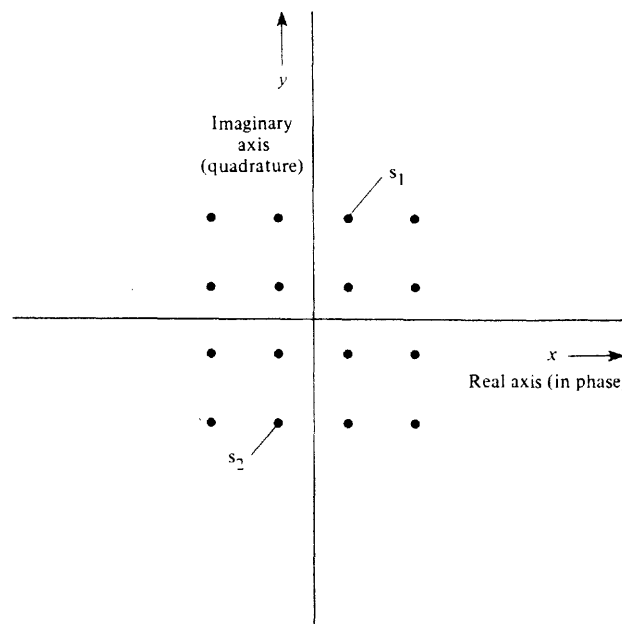


Figure 5-32 16-symbol QAM constellation (four levels per dimension).

and

$$y(t) = \sum_n y_n h_1 \left( t - \frac{n}{D} \right) \quad (5-97)$$

where  $D = R/\ell$  and  $(x_n, y_n)$  denotes one of the permitted  $(x_i, y_i)$  values during the symbol time that is centered on  $t = nT_s = n/D$  s. (It takes  $T_s$  s to send each symbol.)  $h_1(t)$  is the pulse shape that is used for each symbol. If the bandwidth of the QAM signal is not to be restricted, the pulse shape will be rectangular of  $T_s$ -s duration. In some applications the timing between the  $x(t)$  and  $y(t)$  components is offset by  $T_s/2 = 1/(2D)$  s. That is,  $x(t)$  would be described by (5-96), and the offset  $y(t)$  would be described by

$$y(t) = \sum_n y_n h_1 \left( t - \frac{n}{D} - \frac{1}{2D} \right) \quad (5-98)$$

One popular type of offset signaling is *offset QPSK (OQPSK)*, which is offset QAM when  $M = 4$ . A special case of OQPSK when  $h_1(t)$  has a sinusoidal type of pulse shape is called *minimum-shift keying (MSK)*. This type will be studied immediately after the next section. Furthermore, a QPSK signal is said to be *unbalanced* if the  $x(t)$  and  $y(t)$  components have unequal powers and/or unequal data rates.

### Power Spectral Density for MPSK and QAM

The PSD for MPSK and QAM signals is relatively easy to evaluate for the case of rectangular bit shape signaling. In this case, the PSD has the same spectral shape that was obtained for BPSK, *provided* that proper frequency scaling is used.

The PSD for the complex envelope,  $g(t)$ , of the MPSK or QAM signal can be obtained by using (6-70d). We know that

$$g(t) = \sum_{n=-\infty}^{\infty} c_n f(t - nT_s) \quad (5-99)$$

where  $c_n$  is a complex-valued random variable representing the multilevel value during the  $n$ th symbol pulse,  $f(t) = \Pi(t/T_s)$  is the rectangular symbol pulse with symbol duration  $T_s$ ,  $D = 1/T_s$  is the symbol (or baud) rate. The rectangular pulse has the Fourier transform

$$F(f) = T_s \left( \frac{\sin \pi f T_s}{\pi f T_s} \right) = \ell T_b \left( \frac{\sin \ell \pi f T_b}{\ell \pi f T_b} \right) \quad (5-100)$$

where  $T_s = \ell T_b$ . That is, there are  $\ell$  bits representing each allowed multilevel value. For symmetrical (polar type) signaling—for example, as illustrated in Fig. 5-32 for the  $M = 16$  case—with equally likely multilevels, the mean value of  $c_n$  is

$$m_c = \overline{c_n} = 0 \quad (5-101a)$$

and the variance is

$$\sigma_c^2 = \overline{c_n c_n^*} = \overline{|c_n|^2} = C \quad (5-101b)$$

where  $C$  is a real positive constant. Substituting (5-100) and (5-101) into (6-70d), the PSD for the complex envelope of MPSK or QAM signals with data modulation of rectangular bit shape is



$$\mathcal{P}_s(f) = K \left( \frac{\sin \pi f \ell T_b}{\pi f \ell T_b} \right)^2 \quad \text{for MPSK and QAM} \quad (5-102)$$

where  $K = C \ell T_b$ ,  $M = 2^\ell$  is the number of points in the signal constellation, and the bit rate is  $R = 1/T_b$ . For a total transmitted power of  $P$  watts the value of  $K$  is  $K = 2P\ell T_b$  since  $\int_{-\infty}^{\infty} \mathcal{P}_s(f) df = P$ . This PSD for the complex envelope is plotted in Fig. 5-33. The PSD of the MPSK or QAM signal is obtained by simply translating the PSD of Fig. 5-33 to the carrier frequency, as described by (5-2b). For  $\ell = 1$ , the figure gives the PSD for BPSK (i.e., compare Fig. 5-33,  $\ell = 1$ , with Fig. 5-20b). It is also realized that the PSD for the complex envelope of bandpass multilevel signals, as described by (5-102), is essentially the same as the PSD for baseband multilevel signals that was obtained in (3-53).

From Fig. 5-33 we see that the null-to-null transmission bandwidth of MPSK or QAM is

$$B_T = 2R/\ell \quad (5-103)$$

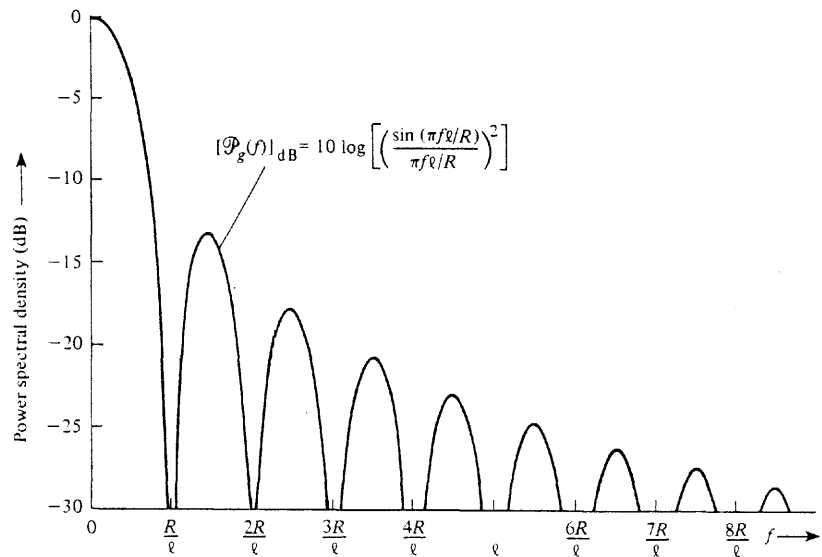


Figure 5-33 PSD for the complex envelope of MPSK and QAM where  $M = 2^\ell$ ,  $R$  is bit rate, and  $R/\ell = D$  is baud rate (positive frequencies shown).

When we use (3-55), the spectral efficiency of MPSK or QAM signaling with rectangular data pulses is

$$\eta = \frac{R}{B_T} = \frac{\ell}{2} \frac{\text{bits/s}}{\text{Hz}} \quad (5-104)$$

where  $M = 2^\ell$  is the number of points in the signal constellation. For example, for the  $M = 16$  QAM signal, the bandwidth efficiency is  $\eta = 2$  bits/s per hertz of bandwidth. For a 2400-bit/s V.22bis modem ( $M = 16$ , QAM, see Table C-7), the null-to-null transmission bandwidth is  $B_T = 1200$  Hz.

When QAM (or the QAM equivalent of MPSK) with a pulse shape of  $h_1(t)$ —see (5-96) and (5-97)—is transmitted over a bandlimited channel, the overall filter characteristic needs to be selected so that the intersymbol interference is negligible.  $h_1(t) = h(t) * h_T(t)$  corresponds to the transmitter pulse shape, as described in Sec. 3-6. If the overall pulse shape satisfies the raised cosine-rolloff filter characteristic, then, by use of (3-74), the absolute bandwidth of the  $M$ -level modulating signal is

$$B = \frac{1}{2}(1+r)D \quad (5-105)$$

where  $D = R/\ell$  from Fig. 5-31 and  $r$  is the rolloff factor of the filter characteristic. Furthermore, from our study of AM (and DSB-SC to be specific) we know that the transmission bandwidth is related to the modulation bandwidth by  $B_T = 2B$ , so that the overall absolute transmission bandwidth of the QAM signal is

$$B_T = \left(\frac{1+r}{\ell}\right)R \quad (5-106)$$

Because  $M = 2^\ell$ , which implies that  $\ell = \log_2 M = (\ln M)/(\ln 2)$ , the spectral efficiency of QAM-type signaling with raised cosine filtering is

$$\eta = \frac{R}{B_T} = \frac{\ln M}{(1+r)\ln 2} \frac{\text{bit/s}}{\text{Hz}} \quad (5-107)$$

This result is an extremely important one since it tells us how fast we can signal for a prescribed bandwidth. Of course, this result holds for MPSK since this is a special case of QAM. This formula is used to generate Table 5-6, which illustrates the allowable bit rate per hertz of transmission bandwidth for QAM signaling. For example, suppose that we want to signal over a telephone line that has an available bandwidth of 2.4 kHz. If we used BPSK ( $M = 2$ ) with a 50% rolloff factor, we could signal at a rate of  $B_T \times \eta = 2.4 \times 0.677 = 1.60$  kbit/s; but if we used QPSK ( $M = 4$ ) with a 25% rolloff factor, we could signal at a rate of  $2.4 \times 1.6 = 3.84$  kbit/s.

To conserve bandwidth, the number of levels  $M$  in (5-107) cannot be increased too much since, for a given peak envelope power (PEP), the spacing between the signal points in the signal constellation will decrease and noise on the received signal will cause errors (since the noise moves the received signal vector to a new location that might correspond to a different signal level). However, we know that  $R$  certainly has to be less than  $C$ , the channel capacity (Sec. 1-9) if the errors are to be kept small. Consequently, using (1-10), we require

$$\eta < \eta_{\max} \quad (5-108a)$$

where

$$\eta_{\max} = \log_2 \left(1 + \frac{S}{N}\right) \quad (5-108b)$$

TABLE 5-6 SPECTRAL EFFICIENCY FOR QAM SIGNALING WITH RAISED COSINE-ROLLOFF PULSE SHAPING

Number of Levels, $M$ (symbols)	Size of DAC, $\ell$ (bits)	$\eta = \frac{R}{B_T} \left(\frac{\text{bit/s}}{\text{Hz}}\right)$					
		$r = 0.0$	$r = 0.1$	$r = 0.25$	$r = 0.5$	$r = 0.75$	$r = 1.0$
2	1	1.00	0.909	0.800	0.667	0.571	0.500
4	2	2.00	1.82	1.60	1.33	1.14	1.00
8	3	3.00	2.73	2.40	2.00	1.71	1.50
16	4	4.00	3.64	3.20	2.67	2.29	2.00
32	5	5.00	4.55	4.0	3.33	2.86	2.50

## 5-11 MINIMUM-SHIFT KEYING (MSK)

Minimum-shift keying is another bandwidth conservation technique that has been developed. It has the advantage of being a constant-amplitude signal and, consequently, can be amplified with Class C amplifiers without distortion. As we will see, MSK is equivalent to OQPSK with sinusoidal pulse shaping [for  $h_i(t)$ ].

**DEFINITION.** *Minimum-shift keying (MSK) is continuous-phase FSK with a minimum modulation index ( $h = 0.5$ ) that will produce orthogonal signaling.*

First, let us show that  $h = 0.5$  is the minimum index allowed for orthogonal continuous-phase FSK. For a binary 1 to be transmitted over the bit interval  $0 < t < T_b$ , the FSK signal would be  $s_1(t) = A_c \cos(\omega_1 t + \theta_1)$ , and for a binary 0 to be transmitted, the FSK signal would be  $s_2(t) = A_c \cos(\omega_2 t + \theta_2)$ , where  $\theta_1 = \theta_2$  for the continuous-phase condition at the switching time  $t = 0$ . For orthogonal signaling, from (2-77), we require the integral of the product of the two signals over the bit interval to be zero. Thus we require that

$$\int_0^{T_b} s_1(t)s_2(t) dt = \int_0^{T_b} A_c^2 \cos(\omega_1 t + \theta_1) \cos(\omega_2 t + \theta_2) dt = 0 \quad (5-109a)$$

This reduces to the requirement

$$\begin{aligned} & \frac{A_c^2}{2} \left[ \frac{\sin[(\omega_1 - \omega_2)T_b + (\theta_1 - \theta_2)] - \sin(\theta_1 - \theta_2)}{\omega_1 - \omega_2} \right] \\ & + \frac{A_c^2}{2} \left[ \frac{\sin[(\omega_1 + \omega_2)T_b + (\theta_1 + \theta_2)] + \sin(\theta_1 + \theta_2)}{\omega_1 + \omega_2} \right] = 0 \end{aligned} \quad (5-109b)$$

The second term is negligible because  $\omega_1 + \omega_2$  is large,<sup>\*</sup> so the requirement is that

$$\frac{\sin[2\pi h + (\theta_1 - \theta_2)] - \sin(\theta_1 - \theta_2)}{2\pi h} = 0 \quad (5-110)$$

where  $(\omega_1 - \omega_2)T_b = 2\pi(2\Delta F)T_b$  and, from (5-82),  $h = 2\Delta F T_b$ . For the *continuous-phase* case  $\theta_1 = \theta_2$ , and (5-110) is satisfied for a minimum value of  $h = 0.5$  or a peak frequency deviation of

$$\Delta F = \frac{1}{4T_b} = \frac{1}{4} R \quad \text{for MSK} \quad (5-111)$$

Note that for *discontinuous-phase* FSK  $\theta_1 \neq \theta_2$  and the minimum value for orthogonality for that case is  $h = 1.0$ .

Now we will demonstrate that the MSK signal (which is  $h = 0.5$  continuous-phase FSK) is a form of OQPSK signaling with sinusoidal pulse shaping. First, consider the FSK signal over the signaling interval  $(0, T_b)$ . When we use (5-81), the complex envelope is

\* If  $\omega_1 + \omega_2$  is not sufficiently large to make the second term negligible, choose  $f_c = \frac{1}{2} m/T_b = \frac{1}{2} mR$  where  $m$  is a positive integer. This will make the second term zero ( $f_1 = f_c - \Delta F$  and  $f_2 = f_c + \Delta F$ ).

$$g(t) = A_c e^{j\theta(t)} = A_c e^{j2\pi\Delta F \int_0^t m(\lambda) d\lambda}$$

where  $m(t) = \pm 1$ ,  $0 < t < T_b$ . Using (5-111), we find that the complex envelope becomes

$$g(t) = A_c e^{\pm j\pi t/(2T_b)} = x(t) + jy(t), \quad 0 < t < T_b$$

where the  $\pm$  signs denote the possible data during the  $(0, T_b)$  interval. Thus

$$x(t) = A_c \cos \left( \pm 1 \frac{\pi t}{2T_b} \right), \quad 0 < t < T_b \quad (5-112a)$$

$$y(t) = A_c \sin \left( \pm 1 \frac{\pi t}{2T_b} \right), \quad 0 < t < T_b \quad (5-112b)$$

and the MSK signal is

$$s(t) = x(t) \cos \omega_c t - y(t) \sin \omega_c t \quad (5-112c)$$

A typical input data waveform,  $m(t)$ , and the resulting  $x(t)$  and  $y(t)$  quadrature modulation waveforms, are shown in Fig. 5-34. From (5-112a) and (5-112b), and realizing that  $\cos[\pm \pi t/(2T_b)] = \cos[\pi t/(2T_b)]$  and  $\sin[\pm \pi t/(2T_b)] = \pm \sin[\pi t/(2T_b)]$ , we see that the  $\pm 1$  sign of  $m(t)$  during the  $(0, T_b)$  interval affects only  $y(t)$  and not  $x(t)$  over the signaling interval of  $(0, 2T_b)$ . We also realize that the  $\sin[\pi t/(2T_b)]$  pulse of  $y(t)$  is  $2T_b$  s wide. Similarly, it can be seen that the  $\pm 1$  sign of  $m(t)$  over the  $(T_b, 2T_b)$  interval affects only  $x(t)$  and not  $y(t)$  over the interval  $(T_b, 3T_b)$ . In other words, the binary data of  $m(t)$  alternately modulates the  $x(t)$  and  $y(t)$  components, and the pulse shape for the  $x(t)$  and  $y(t)$  symbols (which are  $2T_b$  wide instead of  $T_b$ ) is a sinusoid, as shown in the figure. Thus MSK is equivalent to OQPSK with sinusoidal pulse shaping.

The  $x(t)$  and  $y(t)$  waveforms as shown in Fig. 5-34 illustrate the so-called Type II MSK [Bhargava, Haccoun, Matyas, and Nuspl, 1981], where the basic pulse shape is always a positive half-cosinusoid. For Type I MSK, the pulse shape [for both  $x(t)$  and  $y(t)$ ] alternates between a positive and a negative half-cosinusoid. For both Type I and Type II MSK, it can be shown that there is *not* a one-to-one relationship between the input data  $m(t)$  and the resulting mark and space frequencies,  $f_1$  and  $f_2$ , in the MSK signal. This can be demonstrated by evaluating the instantaneous frequency,  $f_i$ , as a function of the data presented by  $m(t)$  during the different bit intervals. The instantaneous frequency is  $f_i = f_c + (1/2\pi)[d\theta(t)/dt] = f_c \pm \Delta F$ , where  $\theta(t) = \tan^{-1}[y(t)/x(t)]$ . The  $\pm$  sign is determined by the encoding technique (Type I or II) that is used to obtain the  $x(t)$  and  $y(t)$  waveforms in each bit interval,  $T_b$ , as well as the sign of the data on  $m(t)$ . To get a one-to-one frequency relationship between a Type I MSK signal and the corresponding  $h = 0.5$  FSK signal, called a *fast frequency-shift keyed* (FFSK) signal, the data input to the Type I FSK modulator is first differentially encoded. Examples of the waveforms for MSK, Type I and II, and for FFSK can be found in the MATLAB solutions for Probs. 5-69, 5-70, and 5-71. Regardless of the differences noted, FFSK, MSK Type I, and MSK Type II are all constant-amplitude, continuous-phase FSK signals with a modulation index of  $h = 0.5$ .

The PSD for MSK (Type I and Type II) can be evaluated as follows. Because  $x(t)$  and  $y(t)$  have independent data and their dc value is zero, and since  $g(t) = x(t) + jy(t)$ , the PSD for the complex envelope is

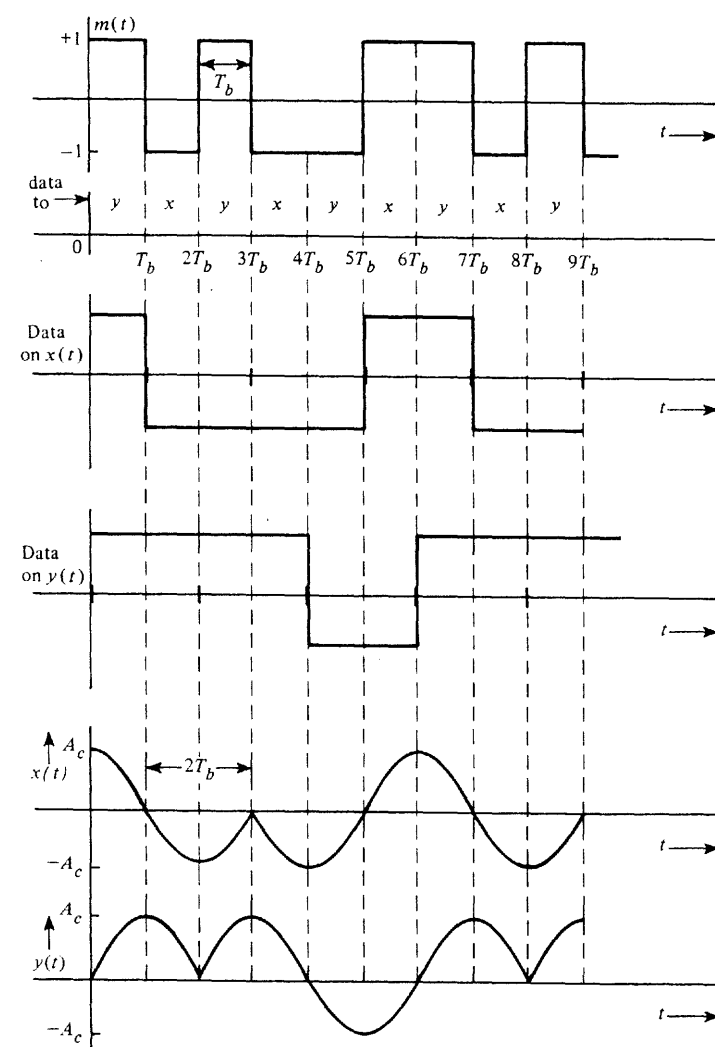


Figure 5-34 MSK quadrature component waveforms (Type II MSK).

$$\mathcal{P}_g(f) = \mathcal{P}_x(f) + \mathcal{P}_y(f) = 2\mathcal{P}_x(f)$$

where  $\mathcal{P}_x(x) = \mathcal{P}_y(f)$  because  $x(t)$  and  $y(t)$  have the same type of pulse shape. When we use (3-40) in (3-36a) with a pulse width of  $2T_b$ , this PSD becomes

$$\mathcal{P}_g(f) = \frac{2}{2T_b} |F(f)|^2 \quad (5-113)$$

where  $F(f) = \mathcal{F}[f(t)]$  and  $f(t)$  is the pulse shape. For the MSK half-cosinusoidal pulse shape, we have

$$f(t) = \begin{cases} A_c \cos\left(\frac{\pi t}{2T_b}\right), & |t| < T_b \\ 0, & t \text{ elsewhere} \end{cases} \quad (5-114a)$$

and the Fourier transform is

$$F(f) = \frac{4A_c T_b \cos 2\pi T_b f}{\pi [1 - (4T_b f)^2]} \quad (5-114b)$$

Thus, the PSD for the complex envelope of an MSK signal is

$$\mathcal{P}_g(f) = \frac{16A_c^2 T_b}{\pi^2} \left( \frac{\cos^2 2\pi T_b f}{[1 - (4T_b f)^2]^2} \right) \quad (5-115)$$

where the normalized power in the MSK signal is  $A_c^2/2$ . The PSD for MSK is readily obtained by translating this spectrum up to the carrier frequency, as described by (5-2b). This complex envelope PSD for MSK is shown by the solidline curve in Fig. 5-35. For compar-

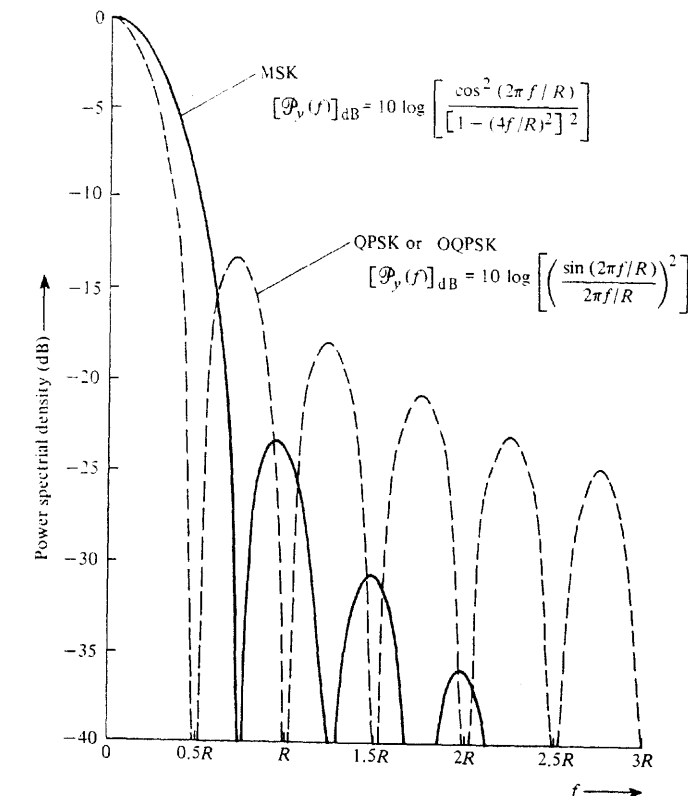


Figure 5-35 PSD for complex envelope of MSK, QPSK, and OQPSK where  $R$  is the bit rate (positive frequencies shown).

ison purposes, the corresponding PSD for OQPSK and QPSK complex envelopes is shown by the dashed-line curve. It is also known that there are other digital modulation techniques, such as *tamed frequency modulation* (TFM), that have even better spectral characteristics than MSK [DeJager and Dekker, 1978; Pettit, 1982; Taub and Schilling, 1986], and the optimum pulse shape for minimum spectral occupancy of FSK-type signals has been found [Campanella, LoFaso, and Mamola, 1984].

MSK signals can be generated by using any one of several methods, as illustrated in Fig. 5-36. Figure 5-36a shows the generation of FFSK (which is equivalent to Type I MSK with differential encoding of the input data). Here a simple FM-type modulator having a

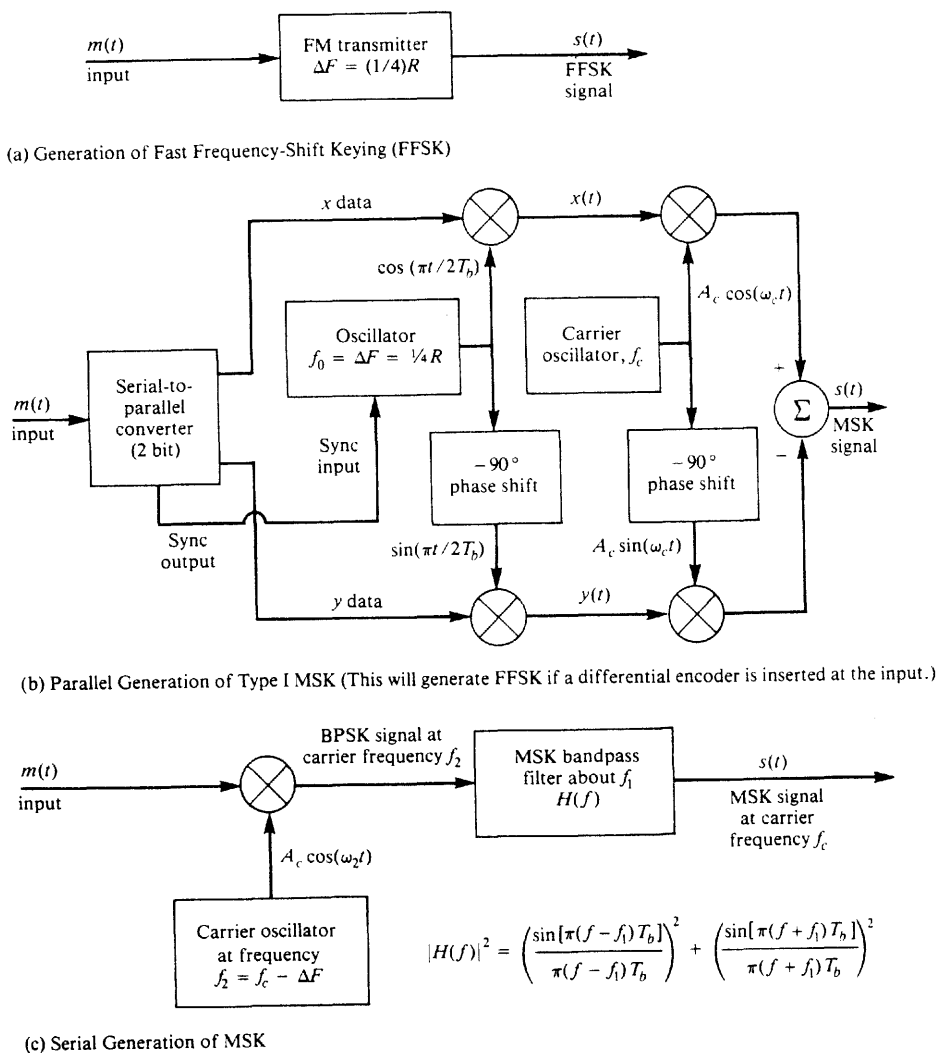


Figure 5-36 Generation of MSK signals.

peak deviation of  $\Delta F = 1/(4T_b) = (\Gamma/4)R$  is used. Figure 5-36b shows an MSK Type I modulator that is a realization of (5-112). This is called the *parallel* method of generating MSK since parallel in-phase (I) and quadrature-phase (Q) channels are used. Figure 5-36c shows the *serial* method of generating MSK. In this approach, BPSK is first generated at a carrier frequency of  $f_2 = f_c - \Delta F$  and the bandpass filtered about  $f_1 = f_c + \Delta F$  to produce an MSK signal with a carrier frequency of  $f_c$ . (See Prob. 5-72 to demonstrate that this technique is correct.) More properties of MSK are given [Leib and Pasupathy, 1993].

Sections 5-9, 5-10, and 5-11 on digital bandpass signaling techniques are summarized in Table 5-7. Here the spectral efficiencies of various types of digital signals are shown using two different bandwidth criteria—the null-to-null bandwidth and the 30-dB bandwidth. Of course, a larger value of  $\eta$  indicates better spectral efficiency. It is seen that MSK ranks better or worse than QPSK and 64 QAM depending on the bandwidth criteria used.

When designing a communication system, one is concerned with the cost and the error performance as well as the spectral occupancy of the signal. The topic of error performance is too immense to discuss in this section; it is covered in Chapter 7.

## 5-12 SPREAD SPECTRUM SYSTEMS

In our study of communication systems, we have been primarily concerned with the performance of communication systems in terms of bandwidth efficiency and energy efficiency (i.e., detected SNR or probability of bit error) with respect to natural noise. However, in some applications, we also need to consider multiple-access capability, antijam capability, interference rejection, and covert operation, or low-probability of intercept (LPI) capability. (The latter considerations are especially important to military applications.) These performance objectives can be optimized using spread spectrum techniques.

Multiple-access capability is needed in cellular telephone and personal communication applications where many users share a band of frequencies because there is not enough available bandwidth to assign a permanent frequency channel to each user. As we shall see, spread spectrum techniques can be used to provide simultaneous use of a wide frequency band by many users via *code-division multiple access* (CDMA) techniques. This is an alter-

TABLE 5-7 SPECTRAL EFFICIENCY OF DIGITAL SIGNALS

Type of Signal	Null-to-Null Bandwidth	30-dB Bandwidth
OOK and BPSK	0.500	0.052
QPSK and OQPSK	1.00	0.104
MSK	0.667	0.438
16 QAM	2.00	0.208
64 QAM	3.00	0.313

nate approach to band sharing. Two other approaches, time-division multiple access (TDMA) and frequency-division multiple access (FDMA), are studied in Sections 3-9, 5-7, and 8-5.

There are many types of *spread spectrum* (SS) systems. To be considered an SS system, a system must satisfy two criteria.

1. The bandwidth of the transmitted signal,  $s(t)$ , needs to be much greater than that of the message,  $m(t)$ .
2. The relatively wide bandwidth of  $s(t)$  must be caused by an independent modulating waveform,  $c(t)$ , called the *spreading signal*, and this signal must be known by the receiver in order for the message signal,  $m(t)$ , to be detected.

Consequently, the SS signal is

$$s(t) = \operatorname{Re}\{g(t)e^{j\omega_c t}\} \quad (5-116a)$$

where the complex envelope of the SS signal is a function of both  $m(t)$  and  $c(t)$ . In most cases, a product function is used, so that

$$g(t) = g_m(t)g_c(t) \quad (5-116b)$$

where  $g_m(t)$  and  $g_c(t)$  are the usual types of modulation complex envelope functions that generate AM, PM, FM, and so on, as given in Table 4-1. The SS signals are classified by the type of mapping functions that are used for  $g_c(t)$ .

Some of the most common types of SS signals are:

- *Direct Sequence* (DS). Here a DSB-SC type of spreading modulation is used [i.e.,  $g_c(t) = c(t)$ ] and  $c(t)$  is a polar waveform.
- *Frequency Hopping* (FH). Here  $g_c(t)$  is of the FM type where there are  $M = 2^k$  hop frequencies determined by the  $k$ -bit words obtained from the spreading code waveform,  $c(t)$ .
- *Hybrid* techniques that include both DS and FH.

We will illustrate exactly how DS and FH systems work in the following sections.

### Direct Sequence

Assume that the information waveform,  $m(t)$ , comes from a digital source and that  $m(t)$  is a polar waveform having values of  $\pm 1$ . Furthermore, let us examine the case of BPSK modulation where  $g_m(t) = A_c m(t)$ . Thus, for DS where  $g_c(t) = c(t)$  is used in (5-116b), the complex envelope for the SS signal becomes

$$g(t) = A_c m(t)c(t) \quad (5-117)$$

The resulting  $s(t) = \operatorname{Re}\{g(t)e^{j\omega_c t}\}$  is called a *binary-phase-shift keyed data, direct sequence spreading, spread spectrum signal* (BPSK-DS-SS) and  $c(t)$  is a polar spreading signal. Furthermore, let this spreading waveform be generated by using a *pseudonoise* (PN) code generator, as shown in Fig. 5-37b, where the values of  $c(t)$  are  $\pm 1$ . The pulse width of  $c(t)$  is

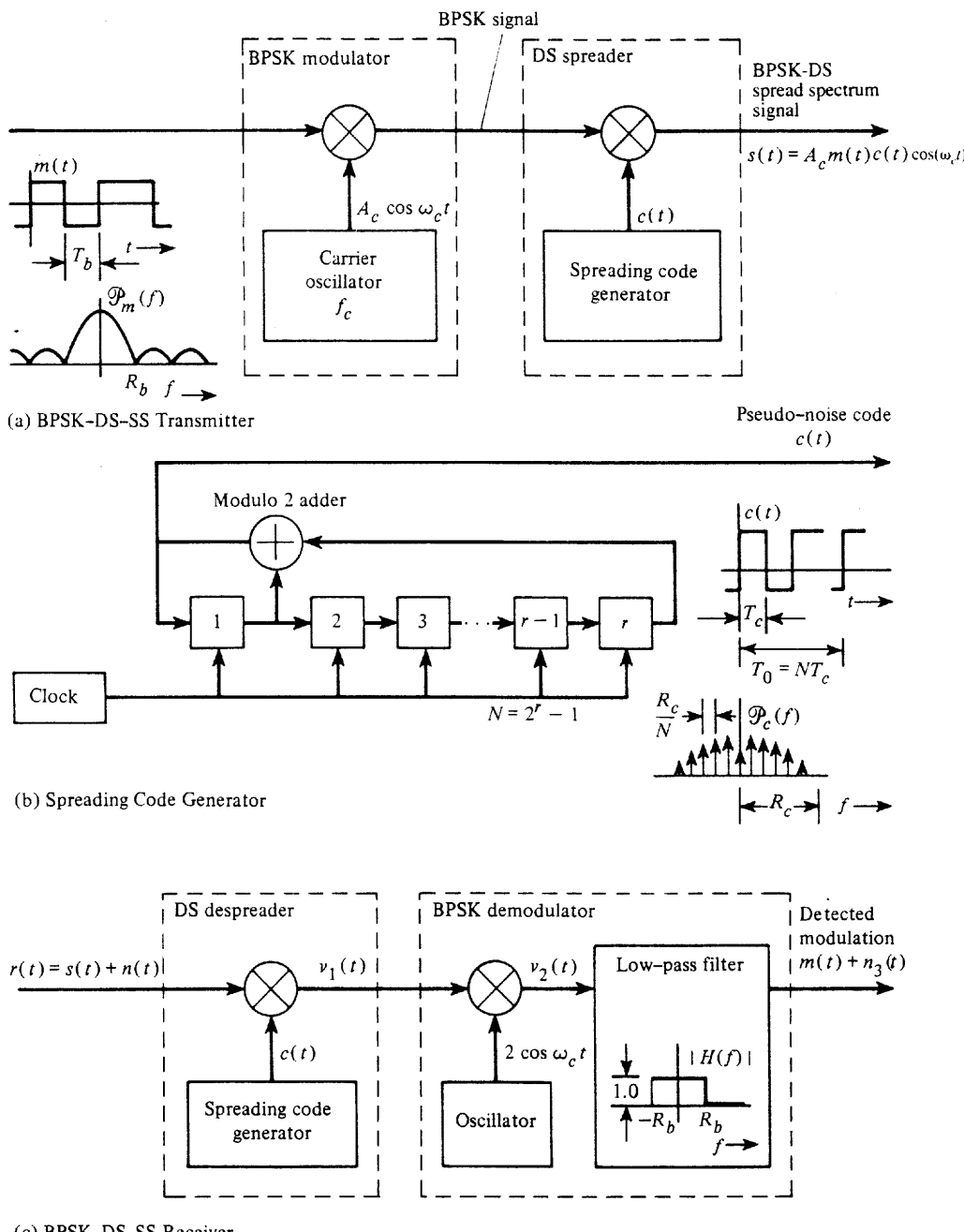


Figure 5-37 Direct sequence spread spectrum system (DS-SS).

denoted by  $T_c$  and is called a *chip* interval (as compared to a bit interval). The code generator uses a modulo 2 adder and  $r$  shift register stages that are clocked every  $T_c$  sec. It can be shown that  $c(t)$  is periodic. Furthermore, feedback taps from the stage of the shift registers and modulo 2 adders are arranged so that the  $c(t)$  waveform has a maximum period of  $N$  chips where  $N = 2^r - 1$ . This type of PN code generator is said to generate a *maximum-length sequence* or *m-sequence* waveform.

**Properties of Maximum-Length Sequences.** Some properties of *m*-sequences are [Peterson, Ziemer, and Borth, 1995]:

Property 1. In one period the number of 1s is always one more than the number of 0s.

Property 2. The modulo 2 sum of any *m*-sequence when summed chip by chip with a shifted version of the same sequence produces another shifted version of the same sequence.

Property 3. If a window of width  $r$  (where  $r$  is the number of stages in the shift register) is slid along the sequence for  $N$  shifts, then all possible  $r$ -bit words will appear exactly once, except for the all 0  $r$ -bit word.

Property 4. If the 0s and 1s are represented by  $-1$  and  $+1$  V, the autocorrelation of the sequence, denoted by  $R_c(k)$ , is

$$R_c(k) = \begin{cases} 1, & k = \ell N \\ -\frac{1}{N}, & k \neq \ell N \end{cases} \quad (5-118)$$

where  $R_c(k) \triangleq (1/N) \sum_{n=0}^{N-1} c_n c_{n+k}$  and  $c_n = \pm 1$ .

The autocorrelation of the *waveform*,  $c(t)$ , denoted by  $R_c(\tau)$ , is

$$R_c(\tau) = \left(1 - \frac{\tau_e}{T_c}\right) R_c(k) + \frac{\tau_e}{T_c} R_c(k+1) \quad (5-119)$$

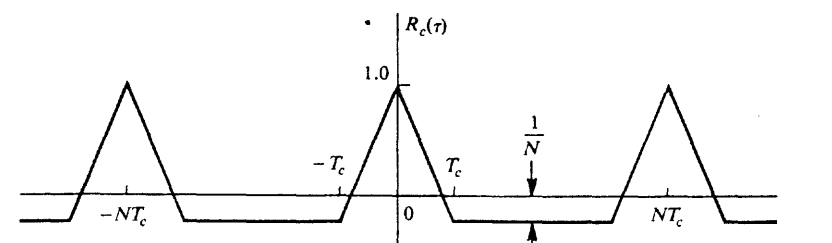
where  $R_c(\tau) = \langle c(t)c(t+\tau) \rangle$  and  $\tau_e$  is defined by

$$\tau = kT_c + \tau_e \quad \text{and} \quad 0 \leq \tau_e < T_c \quad (5-120)$$

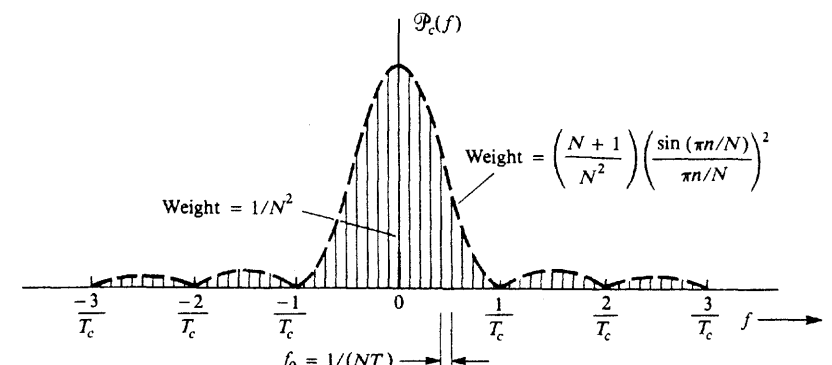
Equation (5-119b) reduces to

$$R_c(\tau) = \left[ \sum_{\ell=-\infty}^{\ell=\infty} \left(1 + \frac{1}{N}\right) \Lambda\left(\frac{\tau - \ell NT_c}{T_c}\right) \right] - \frac{1}{N} \quad (5-121)$$

This is plotted in Fig. 5-38a, where it is apparent that the autocorrelation function for the PN waveform is periodic with triangular pulses of width  $2T_c$  repeated every  $NT_c$  seconds and that a correlation level of  $-1/N$  occurs between these triangular pulses. Furthermore, since the autocorrelation function is periodic, the associated PSD is a line spectrum. That is, the autocorrelation is expressed as a Fourier series



(a) Autocorrelation Function



(b) Power Spectral Density (PSD)

Figure 5-38 Autocorrelation and PSD for an *m*-sequence PN waveform.

$$R_c(\tau) = \sum_{n=-\infty}^{\infty} r_n e^{j2\pi n f_0 t} \quad (5-122)$$

where  $f_0 = 1/(NT_c)$  and  $\{r_n\}$  is the set of Fourier series coefficients. Thus, using (2-109) yields

$$P_c(f) = \mathcal{F}[R_c(\tau)] = \sum_{n=-\infty}^{\infty} r_n \delta(f - nf_0) \quad (5-123)$$

where the Fourier series coefficients are evaluated and found to be

$$r_n = \begin{cases} \frac{1}{N^2}, & n = 0 \\ \left(\frac{N+1}{N^2}\right) \left(\frac{\sin(\pi n/N)}{\pi n/N}\right)^2, & n \neq 0 \end{cases} \quad (5-124)$$

This PSD is plotted in Fig. 5-38b.

Now let us demonstrate that the bandwidth of the SS signal is relatively large compared to the data rate,  $R_b$ , and is determined primarily by the spreading waveform,  $c(t)$ , and not by the data modulation,  $m(t)$ . Referring to Fig. 5-37, we see that the PSDs of both  $m(t)$  and  $c(t)$  are of the  $[(\sin x)/x]^2$  type, where the bandwidth of  $c(t)$  is much larger than that of  $m(t)$  because it is assumed that the chip rate,  $R_c = 1/T_c$  is much larger than the data rate,  $R_b = 1/T_b$ . That is,  $R_c \gg R_b$ . To simplify the mathematics, approximate these PSDs by rectangular spectra, as shown in Figs. 5-39a and 5-39b, where the heights of the PSD are selected so that the areas under the curves are unity because the powers of  $m(t)$  and  $c(t)$  are unity. (They both have only  $\pm 1$  values.) From (5-117),  $g(t)$  is obtained by multiplying  $m(t)$  and  $c(t)$  in the time domain, and  $m(t)$  and  $c(t)$  are independent. Thus the PSD for the complex envelope of the BPSK-DS-SS signal is obtained by a convolution operation in the frequency domain.

$$\mathcal{P}_m(f) = A_c^2 \mathcal{P}_m(f) * \mathcal{P}_c(f) \quad (5-125)$$

This result is shown in Fig. 5-39c for the approximate PSDs of  $m(t)$  and  $c(t)$ . The bandwidth of the BPSK-DS-SS signal is determined essentially by the chip rate,  $R_c$ , because  $R_c \gg R_b$ . For example, let  $R_b = 9.6$  kbits/s and  $R_c = 9.6$  Mchips/s. Then the bandwidth of the SS signal is  $B_T \approx 2R_c = 19.2$  MHz.

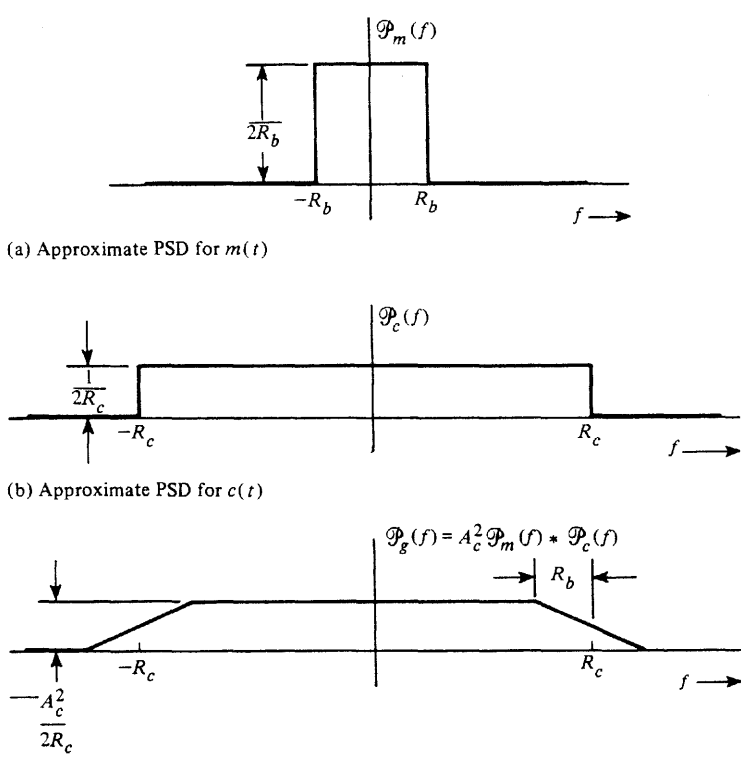


Figure 5-39 Approximate PSD of the BPSK-DS-SS signal.

From Fig. 5-39 we can also demonstrate that the spreading has made the signal less susceptible to detection by an eavesdropper. That is, this signal has LPI. Without spreading [i.e., if  $c(t)$  was unity], the level of the in-band PSD would be proportional to  $A_c^2/(2R_b)$ , as seen in Fig. 5-39a, but with spreading the in-band spectral level drops to  $A_c^2/(2R_c)$ , as seen in Fig. 5-39c. This is a reduction of  $R_c/R_b$ . For example, for the values of  $R_b$  and  $R_c$  just cited, the reduction factor would be  $(9.6 \text{ Mchips/s})/(9.6 \text{ kbits/s}) = 1000$  or 30 dB. Often the eavesdropper detects the presence of a signal by using a spectrum analyzer, but when SS is used, this level will drop by 30 dB. This is often below the noise floor of the potential eavesdropper, and thus the SS signal will escape detection by the eavesdropper.

Figure 5-37c shows a receiver that recovers the modulation on the SS signal. The receiver has a despreading circuit that is driven by a PN code generator in synchronism with the transmitter spreading code. Assume that the input to the receiver consists of the SS signal plus a narrowband (sine wave) jammer signal. Then,

$$r(t) = s(t) + n(t) = A_c m(t) c(t) \cos \omega_c t + n_J(t) \quad (5-126)$$

where the jamming signal is

$$n_J(t) = A_J \cos \omega_c t \quad (5-127)$$

Here it is assumed that the jamming power is  $A_J^2/2$  relative to the signal power of  $A_c^2/2$  and that the jamming frequency is set to  $f_c$  for the worst-case jamming effect. Referring to Fig. 5-37c, we find that the output of the despread is

$$v_1(t) = A_c m(t) \cos \omega_c t + A_J c(t) \cos \omega_c t \quad (5-128)$$

since  $c^2(t) = (\pm 1)^2 = 1$ . The BPSK-DS-SS signal has become simply a BPSK signal at the output of the despread. That is, at the receiver input the SS signal has a bandwidth of  $2R_c$ , but at the despread output the bandwidth of the resulting BPSK signal is  $2R_b$ , a 1000:1 reduction for the figures previously cited. The data on the BPSK despread signal are recovered by using a BPSK detector circuit as shown.

Now it will be shown that this SS receiver provides an antijam capability of 30 dB for the case of  $R_b = 9.6$  kbits/s and  $R_c = 9.6$  Mchips/s. From (5-128) it is seen that the narrowband jammer signal that was present at the receiver input has been spread by the despread since it has been multiplied by  $c(t)$ . It is this spreading effect on the jamming signal that produces the antijam capability. Using (5-128) and referring to Fig. 5-37c, we obtain an input to the LPF of

$$v_2(t) = A_c m(t) + n_2(t) \quad (5-129)$$

where

$$n_2(t) = A_J c(t) \quad (5-130)$$

and the terms about  $f = 2f_c$  have been neglected since they do not pass through the LPF. Referring to Fig. 5-37c, we note that the jammer power at the receiver output is

$$P_{n_3} = \int_{-R_b}^{R_b} \mathcal{P}_{n_2}(f) df = \int_{-R_b}^{R_b} A_J^2 \frac{1}{2R_c} df = \frac{A_J^2}{R_c/R_b} \quad (5-131)$$

and the jammer power at the input to the LPF is  $A_J^2$ . [ $\mathcal{P}_{n_2}(f) = A_J^2/(2R_c)$  as seen from Fig. 5-39b and (5-130).] For a conventional BPSK system (i.e., no spread spectrum),  $c(t)$  would be unity and (5-130) would become  $n_2(t) = A_J$ , so the jamming power out of the LPF would be  $A_J^2$  instead of  $A_J^2/(R_c/R_b)$  for the case of an SS system. [The output signal should be  $A_c m(t)$  for both cases.] Thus, the SS receiver has reduced the effect of narrowband jamming by the factor of  $R_c/R_b$ . This factor,  $R_c/R_b$ , is called the *processing gain* of the SS receiver.<sup>†</sup> For our example of  $R_c = 9.6$  Mchips/s and  $R_b = 9.6$  kbits/s, the processing gain is 30 dB. This means that the narrowband jammer would have to have 30 dB more power to have the same jamming effect on this SS system, compared with the conventional BPSK system (no SS). Thus this SS technique provides 30 dB of antijam capability for the  $R_c/R_b$  ratio cited in the example.

SS techniques can also be used to provide multiple access. This is called *code division multiple access* (CDMA). Here each user is assigned a spreading code such that the signals are orthogonal. Thus multiple SS signals can be transmitted simultaneously in the same frequency band, and yet the data on a particular SS signal can be decoded by a receiver, *provided* that this receiver uses a PN code that is identical to that used on the particular SS signal that is to be decoded. Although CDMA provides a neat solution for the multiple access problem in an interference environment, it can be shown that TDMA and FDMA are more bandwidth efficient [Viterbi, 1985].

To accommodate more users in frequency bands that are now saturated with conventional narrowband users (such as the two-way radio bands), it is possible to assign in addition new SS stations. This is called *spread spectrum overlay*. The SS stations would operate with such a wide bandwidth that their PSD would appear to be negligible to narrowband receivers located sufficiently distant from the SS transmitters. On the other hand, to the SS receiver, the narrowband signals would have a minimal jamming effect because of the large coding gain of the SS receiver.

### Frequency Hopping

As indicated previously, a frequency-hopped (FH) SS signal uses a  $g_c(t)$  that is of the FM type where there are  $M = 2^k$  hop frequencies controlled by the spreading code where  $k$  chip words are taken to determine each hop frequency. An FH-SS transmitter is shown in Fig. 5-40a. The source information is modulated onto a carrier using conventional FSK or BPSK techniques to produce an FSK or a BPSK signal. The frequency hopping is accomplished by using a mixer circuit where the LO signal is provided by the output of a frequency synthesizer that is hopped by the PN spreading code. The serial-to-parallel converter reads  $k$  serial chips of the spreading code and outputs a  $k$  chip parallel word to the programmable dividers in the frequency synthesizer. (See Fig. 4-25 and the related discussion of frequency synthesizers.) The  $k$  chip word specifies one of the possible  $M = 2^k$  hop frequencies,  $\omega_1, \omega_2, \dots, \omega_M$ .

The FH signal is decoded as shown in Fig. 5-40b. Here the receiver has the knowledge of the transmitter,  $c(t)$ , so that the frequency synthesizer in the receiver can be hopped in

<sup>†</sup> The processing gain is defined as the ratio to the noise power out without SS divided by the noise power out with SS. This is equivalent to the ratio  $(S/N)_{out}/(S/N)_{in}$  when  $(S/N)_{in}$  is the signal-to-noise power into the receiver and  $(S/N)_{out}$  is the signal-to-noise power out of the LPF.

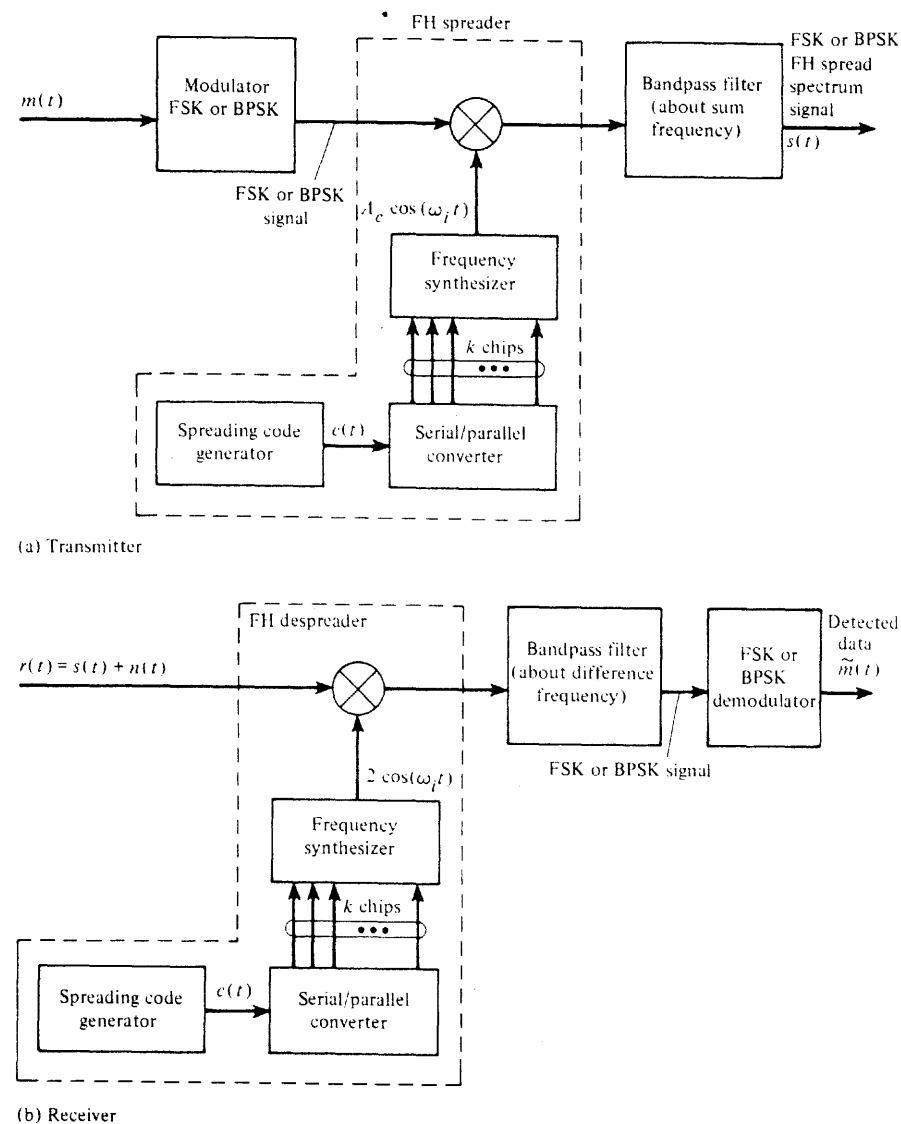


Figure 5-40 Frequency-hopped spread spectrum system (FH-SS).

synchronism with that at the transmitter. This despreads the FH signal, and the source information is recovered from the dehopped signal by use of a conventional FSK or BPSK demodulator, as appropriate.

In 1985 the FCC opened up three shared frequency bands—902 to 928 MHz, 2400 to 2483.5 MHz, and 5725 to 5850 MHz—for commercial SS use with unlicensed 1-W transmitters. This has led to the production and use of SS equipment for telemetry systems, personal communication networks (PCNs), wireless local area networks for personal computers,

and wireless fire and security systems [Schilling, Pickholtz, and Milstein, 1990]. Also, some commercial SS applications have advantages over other systems. For example, a digital SS cellular telephone system (i.e., CDMA) appears to be able to accommodate about 1000 users per cell as compared to the U.S. analog cellular system, which accommodates 55 users per cell [Schilling, Pickholtz, and Milstein, 1990]. See Sec. 8-8 for a CDMA cellular telephone standard that has been adopted. In another application, digital stereo broadcasting using SS techniques appears to accommodate up to 75 stations in a region using the U.S. FM band, 88 to 108 MHz [Schilling et al., 1991]. This is a larger number of stations than found with present analog FM stereo assignments; moreover, digital stereo SS broadcasting will provide a much larger audio signal-to-noise ratio for the listener.

Limited space does not permit further discussion of SS systems. For further study on this interesting topic, the reader is referred to books and papers that have been written on this subject [Cooper and McGillem, 1986; Dixon, 1994; MaGill, Natali, and Edwards, 1994; Peterson, Ziemer, and Borth, 1995].

### 5-13 SUMMARY

A wide range of analog and digital modulation systems were examined based on the theory developed in Chapters 1 to 4. AM, SSB, PM, and FM signaling techniques were developed in detail. Standards for AM and FM broadcasting signals were given. Digital signaling techniques such as OOK, BPSK, and FSK were developed from classical AM, PM, and FM theory. The spectra for these digital signals were evaluated in terms of the bit rate of the digital information source. Multilevel digital signaling techniques such as QPSK, MPSK, QAM, and MSK were also studied, and their spectra were evaluated.

Spread spectrum signaling was examined. It has multiple-access capability, antijam capability, interference rejection, and low probability of intercept that are applicable to personal communication systems and military systems. This study included the calculation of the spectrum for a spread spectrum signal and the examination of transmitter and receiver block diagrams for both direct sequence and frequency-hopped spread spectrum systems.

### 5-14 STUDY-AID EXAMPLES

**SA5-1** Prove that the normalized average power for a SSB signal is  $\langle s^2(t) \rangle = A_c^2 \langle m^2(t) \rangle$  as given by (5-25).

**Solution** For SSB,  $g(t) = A_c[m(t) \pm j\hat{m}(t)]$ . Using (4-17),

$$P_s = \langle s^2(t) \rangle = \frac{1}{2} \langle |g(t)|^2 \rangle = \frac{1}{2} A_c \langle m^2(t) + [\hat{m}(t)]^2 \rangle$$

or

$$P_s = \langle s^2(t) \rangle = \frac{1}{2} A_c \{ \langle m^2(t) \rangle + \langle [\hat{m}(t)]^2 \rangle \} \quad (5-132)$$

But,

$$\langle [\hat{m}(t)]^2 \rangle = \int_{-\infty}^{\infty} \mathcal{P}_{\hat{m}}(f) df = \int_{-\infty}^{\infty} |H(f)|^2 \mathcal{P}_m(f) df$$

### Sec. 5-14 Study-Aid Examples

where  $H(f)$  is the transfer function of the Hilbert transformer. Using (5-19), it is realized that  $|H(f)| = 1$ . Consequently,

$$\langle [\hat{m}(t)]^2 \rangle = \int_{-\infty}^{\infty} \mathcal{P}_{\hat{m}}(f) df = \langle m^2(t) \rangle \quad (5-133)$$

Substituting (5-133) into (5-132), we get

$$P_s = \langle s^2(t) \rangle = A_c^2 \langle m^2(t) \rangle$$

**SA5-2** A SSB transmitter with  $A_c = 100$  is being tested by modulating it with a triangular waveform that is shown in Fig. 5-14a, where  $V_p = 0.5$  V. This SSB transmitter is connected to a  $50\Omega$  resistive load. Calculate the actual power dissipated into the load.

**Solution** Using (5-25),

$$P_{\text{actual}} = \frac{(V_s)^2_{\text{rms}}}{R_L} = \frac{\langle s^2(t) \rangle}{R_L} = \frac{A_c^2}{R_L} \langle m^2(t) \rangle \quad (5-134)$$

For the waveform shown in Fig. 5-14a,

$$\langle m^2(t) \rangle = \frac{1}{T_m} \int_0^{T_m} m^2(t) dt = \frac{4}{T_m} \int_0^{T_m/4} \left( \frac{4V_p}{T_m} t - V_p \right)^2 dt$$

or

$$\langle m^2(t) \rangle = \frac{4V_p^2}{T_m} \frac{\left( \frac{4}{T_m} t - 1 \right)^3}{3 \left( \frac{4}{T_m} \right)} \Big|_0^{T_m/4} = \frac{V_p^2}{3} \quad (5-135)$$

Substituting (5-135) into (5-134), we get

$$P_{\text{actual}} = \frac{A_c^2 V_p^2}{3 R_L} = \frac{(100)^2 (0.5)^2}{3(50)} = 16.67 \text{ W}$$

**SA5-3** As shown in Fig. 5-41, a FM transmitter consists of a FM exciter stage, a  $\times 3$  frequency multiplier, an upconverter (with a bandpass filter), a  $\times 2$  frequency multiplier, and a  $\times 3$  frequency multiplier. The oscillator has a frequency of 80.0150 MHz, and the bandpass filter is centered around the carrier frequency that is located at approximately 143 MHz. The FM exciter has a carrier frequency 20.9957 MHz and a peak deviation of 0.694 kHz when the audio input is applied. The bandwidth of the audio input is 3 kHz. Calculate the carrier frequency and the peak deviation for the FM signals at points B, C, D, E and F. Also, calculate the bandwidth required for the bandpass filter and the exact center frequency for the bandpass filter.

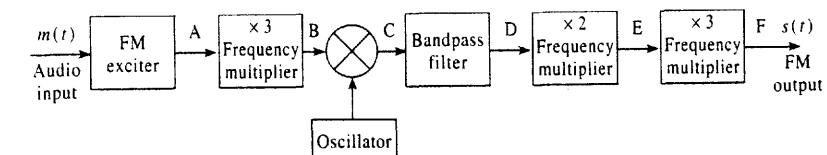


Figure 5-41 FM transmitter.

**Solution** As shown in Sec. 4-12, a frequency multiplier produces an output signal at the  $n$ th harmonic of the input, and it increases any PM/FM variation that is on the input signal by a factor of  $n$ . That is, if the input signal has an angle variation of  $\theta(t)$ , the output signal will have a variation of  $n\theta(t)$ , as shown by (4-73). Thus, the peak deviation at the output of a frequency multiplier is  $(\Delta F)_{\text{out}} = n(\Delta F)_{\text{in}}$  because  $\Delta F = (1/2\pi) d\theta(t)/dt$ . The FM exciter output has a carrier frequency  $(f_c)_A = 20.9957$  MHz and a peak deviation of  $(\Delta F)_A = 0.694$  kHz. Thus, the FM signal at point B has the parameters

$$(f_c)_B = 3(f_c)_A = 62.9871 \text{ MHz} \text{ and } (\Delta F)_B = 3(\Delta F)_A = 2.08 \text{ kHz}$$

The mixer (multiplier) produces two signals, a sum frequency term and a difference frequency term at point C, with the carrier frequencies

$$(f_c)_{C \text{ sum}} = f_0 + (f_c)_B = 143.0021 \text{ MHz}$$

$$(f_c)_{C \text{ diff}} = f_0 - (f_c)_B = 17.0279 \text{ MHz}$$

Because the mixer output signal has the same complex envelope as the complex envelope at its input (i.e., see Sec. 4-11), all the modulation output parameters at the mixer output are the same as those for the input. Thus, the sum and difference carrier frequencies are frequency modulated and the peak deviation for each is  $(\Delta F)_C = (\Delta F)_B = 2.08$  kHz. The bandpass filter passes the 143-MHz term. Consequently, the FM signal at point D has the parameters

$$(f_c)_D = (f_c)_{C \text{ sum}} = 143.0021 \text{ MHz} \text{ and } (\Delta F)_D = (\Delta F)_C = 2.08 \text{ kHz}$$

The FM signals at points E and F have the parameters

$$(f_c)_E = 2(f_c)_D = 286.0042 \text{ MHz} \text{ and } (\Delta F)_E = 2(\Delta F)_D = 4.16 \text{ kHz}$$

and

$$(f_c)_F = 3(f_c)_E = 858.0126 \text{ MHz} \text{ and } (\Delta F)_F = 3(\Delta F)_E = 12.49 \text{ kHz}$$

In summary, the circuit of Fig. 5-41 produces a FM signal at 858.0126 MHz that has a peak deviation of 12.49 kHz. The bandpass filter is centered at  $(f_c)_{C \text{ sum}} = 143.0021$  MHz and has a bandwidth sufficient to pass the FM signal with the deviation  $(\Delta F)_C = 2.08$  kHz. Using Carson's rule, (5-61), the required bandwidth for the bandpass filter is

$$B_T = 2[\beta_C + 1]B = 2[(\Delta F)_C + B]$$

or

$$B_T = 2[2.08 + 3.0] = 10.16 \text{ kHz}$$

**SA5-4** Data is sent by an amateur radio operator on the 40 meter band by using a SSB transceiver. To accomplish this, a modem of the Bell 103 type (described in Example 5-4) is connected to the audio (microphone) input of the SSB transceiver. Assume that the modem is set to the answer mode and the transceiver is set to transmit a lower SSB signal on a suppressed carrier frequency of  $(f_c)_{\text{SSB}} = 7.090$  MHz. Describe the type of digitally modulated signal that is emitted and determine its carrier frequency. For alternating 101010 data, compute the spectrum of the transmitted signal.

**Solution** Referring to Sec. 4-5, a LSSB transmitter just translates the spectrum of the audio input signal up to the suppressed carrier frequency and deletes the upper sideband. Referring to Table 5-5, the Bell 103 modem (answer mode) has a mark frequency of  $f_1 = 2225$  Hz, a space frequency of  $f_2 = 2025$  Hz, and a carrier frequency of  $(f_c)_{\text{Bell 103}} = 2125$  Hz. The LSSB transmitter translates these frequencies to a mark frequency (binary 1) of

$$(f_c)_{\text{SSB}} - f_1 = 7090 \text{ kHz} - 2.225 \text{ kHz} = 7087.775 \text{ kHz}$$

a space frequency (binary 0) of

$$(f_c)_{\text{SSB}} - f_2 = 7090 - 2.025 = 7087.975 \text{ kHz}$$

and a carrier frequency of

$$(f_c)_{\text{FSK}} = (f_c)_{\text{SSB}} - (f_c)_{\text{Bell 103}} = 7090 - 2.125 = 7087.875 \text{ kHz}$$

Consequently, the SSB transceiver would produce a FSK digital signal with a carrier frequency of 7087.875 kHz.

For the case of alternating data, the spectrum of this FSK signal is given by (5-85) and (5-86), where  $f_c = 7087.875$  kHz. The resulting spectral plot would be like that of Fig. 5-26a, where the spectrum is translated from  $f_c = 1170$  Hz to  $f_c = 7087.875$  kHz. It is also realized that this spectrum appears on the lower sideband of the SSB carrier frequency  $(f_c)_{\text{SSB}} = 7090$  kHz. If a DSB-SC transmitter had been used (instead of a LSSB transmitter), the spectrum would be replicated on the upper sideband as well as on the lower sideband, and two redundant FSK signals would be emitted.

For the case of random data, the PSD for the complex envelope is given by (5-90) and shown in Fig. 5-25 for the modulation index of  $h = 0.7$ . Using (5-2b), the PSD for the FSK signal is the translation of the PSD for the complex envelope to the carrier frequency of 7087.875 kHz.

## PROBLEMS

**5-1** An AM broadcast transmitter is tested by feeding the RF output into a  $50\Omega$  (dummy) load. Tone modulation is applied. The carrier frequency is 850 kHz and the FCC licensed power output is 5000 W. The sinusoidal tone of 1000 Hz is set for 90% modulation.

- (a) Evaluate the FCC power in dBk (dB above 1 kW) units.
- (b) Write an equation for the voltage that appears across the  $50\Omega$  load, giving numerical values for all constants.
- (c) Sketch the spectrum of this voltage as it would appear on a calibrated spectrum analyzer.
- (d) What is the average power that is being dissipated in the dummy load?
- (e) What is the peak envelope power?

**5-2** An AM transmitter is modulated with an audio testing signal given by  $m(t) = 0.2 \sin \omega_1 t + 0.5 \cos \omega_2 t$ , where  $f_1 = 500$  Hz,  $f_2 = 500\sqrt{2}$  Hz, and  $A_c = 100$ . Assume that the AM signal is fed into a  $50\Omega$  load.

- (a) Sketch the AM waveform.
- (b) What is the modulation percentage?
- (c) Evaluate and sketch the spectrum of the AM waveform.

**5-3** For the AM signal given in Prob. 5-2:

- (a) Evaluate the average power of the AM signal.
- (b) Evaluate the PEP of the AM signal.

**5-4** Assume that an AM transmitter is modulated with a video testing signal given by  $m(t) = -0.2 + 0.6 \sin \omega_1 t$  where  $f_1 = 3.57$  MHz. Let  $A_c = 100$ .

- (a) Sketch the AM waveform.
- (b) What is the percentage of positive and negative modulation?
- (c) Evaluate and sketch the spectrum of the AM waveform about  $f_c$ .

- 5-5** A 50,000-W AM broadcast transmitter is being evaluated by means of a two-tone test. The transmitter is connected to a  $50\Omega$  load and  $m(t) = A_1 \cos \omega_1 t + A_1 \cos 2\omega_1 t$  where  $\omega_1 = 500$  Hz. Assume that a perfect AM signal is generated.
- Evaluate the complex envelope for the AM signal in terms of  $A_1$  and  $\omega_1$ .
  - Determine the value of  $A_1$  for 90% modulation.
  - Find the values for the peak current and average current into the  $50\Omega$  load for the 90% modulation case.
- 5-6** An AM transmitter uses a two-quadrant multiplier so that the transmitted signal is described by (5-7). Assume that the transmitter is modulated by  $m(t) = A_m \cos \omega_m t$ , where  $A_m$  is adjusted so that 120% positive modulation is obtained. Evaluate the spectrum of this AM signal in terms of  $A_c$ ,  $f_c$ , and  $f_m$ . Sketch your result.
- 5-7** A DSB-SC signal is modulated by  $m(t) = \cos \omega_1 t + 2 \cos 2\omega_1 t$  where  $\omega_1 = 2\pi f_1$ ,  $f_1 = 500$  Hz, and  $A_c = 1$ .
- Write an expression for the DSB-SC signal and sketch a picture of this waveform.
  - Evaluate and sketch the spectrum for this DSB-SC signal.
  - Find the value of the average (normalized) power.
  - Find the value of the PEP (normalized).
- 5-8** Assume that transmitting circuitry restricts the modulated output signal to a certain peak value, say  $A_p$ , because of power-supply voltages that are used and the peak voltage and current ratings of the components. If a DSB-SC signal with a peak value of  $A_p$  is generated by this circuit, show that the sideband power of this DSB-SC signal is four times the sideband power of a comparable AM signal having the same peak value,  $A_p$ , that could also be generated by this circuit.
- 5-9** A DSB-SC signal can be generated from two AM signals as shown in Fig. P5-9. Using mathematics to describe signals at each point on the figure, prove that the output is a DSB-SC signal.

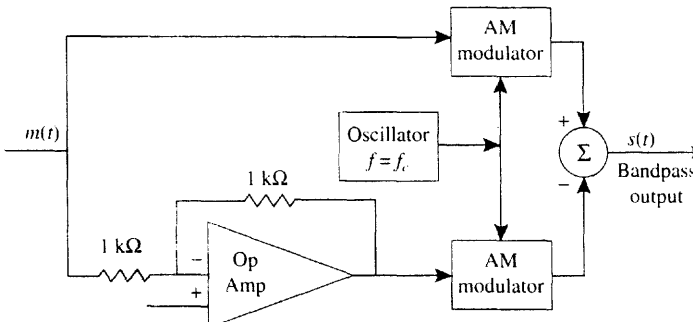


Figure P5-9

- 5-10** Show that the complex envelope  $g(t) = m(t) - j\hat{m}(t)$  produces a lower SSB signal, provided that  $m(t)$  is a real signal.
- 5-11** Show that the impulse response of a  $-90^\circ$  phase shift network (i.e., a Hilbert transformer) is  $1/\pi t$ . Hint:

$$H(f) = \lim_{\alpha \rightarrow 0} \begin{cases} -je^{-\alpha f}, & f > 0 \\ je^{\alpha f}, & f < 0 \end{cases}$$

- 5-12** SSB signals can be generated by the phasing method, Fig. 5-5a; the filter method, Fig. 5-5b; or by the use of Weaver's method as shown in Fig. P5-12. For Weaver's method (Fig. P5-12) where  $B$  is the bandwidth of  $m(t)$ :

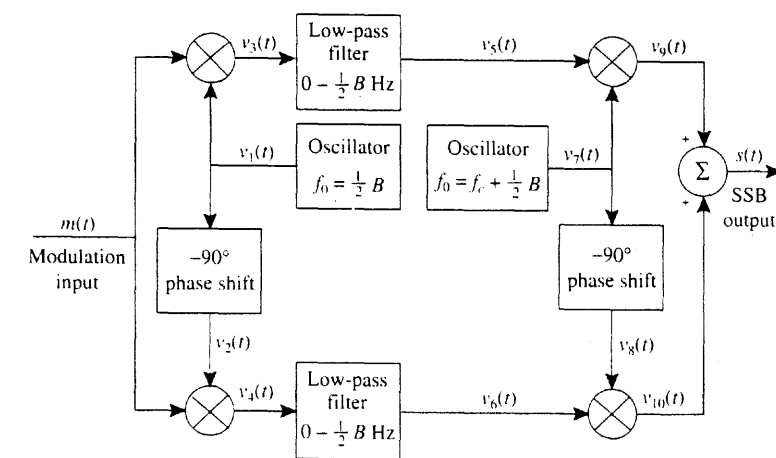


Figure P5-12 Weaver's method for generating SSB.

- Find a mathematical expression that describes the waveform out of each block on the block diagram.
  - Show that  $s(t)$  is an SSB signal.
- 5-13** An SSB-AM transmitter is modulated with a sinusoid  $m(t) = 5 \cos \omega_1 t$ , where  $\omega_1 = 2\pi f_1$ ,  $f_1 = 500$  Hz, and  $A_c = 1$ .
- Evaluate  $\hat{m}(t)$ .
  - Find the expression for a lower SSB signal.
  - Find the rms value of the SSB signal.
  - Find the peak value of the SSB signal.
  - Find the normalized average power of the SSB signal.
  - Find the normalized PEP of the SSB signal.
- 5-14** An SSB-AM transmitter is modulated by a rectangular pulse such that  $m(t) = \Pi(t/T)$  and  $A_c = 1$ .
- Prove that

$$\hat{m}(t) = \frac{1}{\pi} \ln \left| \frac{2t+T}{2t-T} \right|$$

as given in Table A-7.

- Find an expression for the SSB-AM signal,  $s(t)$ , and sketch  $s(t)$ .
  - Find the peak value of  $s(t)$ .
- 5-15** For Prob. 5-14:
- Find the expression for the spectrum of a USSB-AM signal.
  - Sketch the magnitude spectrum,  $|S(f)|$ .

**5-16** A USSB transmitter is modulated with the pulse

$$m(t) = \frac{\sin \pi a t}{\pi a t}$$

(a) Prove that

$$\hat{m}(t) = \frac{\sin^2[(\pi a/2)t]}{(\pi a/2)t}$$

(b) Plot the corresponding USSB signal waveform for the case of  $A_c = 1$ ,  $a = 2$ , and  $f_c = 20$  Hz.

**5-17** A USSB-AM signal is modulated by a rectangular pulse train:

$$m(t) = \sum_{n=-\infty}^{\infty} \Pi[(t - nT_0)/T]$$

where  $T_0 = 2T$ .

(a) Find the expression for the spectrum of the SSB-AM signal.

(b) Sketch the magnitude spectrum,  $|S(f)|$ .

**5-18** A phasing-type SSB-AM detector is shown in Fig. P5-18. This circuit is attached to the IF output of a conventional superheterodyne receiver to provide SSB reception.

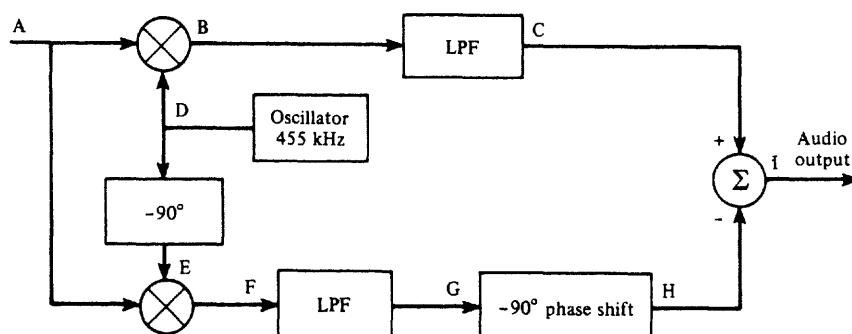


Figure P5-18

(a) Determine whether this detector is sensitive to LSSB or USSB signals. How would the detector be changed to receive SSB signals with alternate (opposite type of) sidebands?

(b) Assume that the signal at point A is a USSB signal with  $f_c = 455$  kHz. Find the mathematical expressions for the signals at points B through I.

(c) Repeat part (b) for the case of an LSSB-AM signal at point A.

(d) Discuss the IF and LP filter requirements if the SSB signal at point A has a 3-kHz bandwidth.

**5-19** Can a Costas loop, as shown in Fig. 5-3, be used to demodulate an SSB-AM signal? Demonstrate that your answer is correct by using mathematics.

**5-20** A modulated signal is described by the equation

$$s(t) = 10 \cos[(2\pi \times 10^8)t + 10 \cos(2\pi \times 10^3 t)]$$

Find each of the following.

(a) Percentage of AM.

(b) Normalized power of the modulated signal.

(c) Maximum phase deviation.

(d) Maximum frequency deviation.

**5-21** A sinusoidal signal,  $m(t) = \cos 2\pi f_m t$ , is the input to an angle-modulated transmitter where the carrier frequency is  $f_c = 1$  Hz and  $f_m = f_c/4$ .

(a) Plot  $m(t)$  and the corresponding PM signal where  $D_p = \pi$ .

(b) Plot  $m(t)$  and the corresponding FM signal where  $D_f = \pi$ .

**5-22** A sinusoidal modulating waveform of amplitude 4 V and a frequency of 1 kHz is applied to an FM exciter that has a modulator gain of 50 Hz/V.

(a) What is the peak frequency deviation?

(b) What is the modulation index?

**5-23** An FM signal has sinusoidal modulation with a frequency of  $f_m = 15$  kHz and modulation index of  $\beta = 2.0$ .

(a) Find the transmission bandwidth using Carson's rule.

(b) What percentage of the total FM signal power lies within the Carson rule bandwidth?

**5-24** An FM transmitter has a block diagram as shown in Fig. P5-24. The audio frequency response is flat over the 20-Hz to 15-kHz audio band. The FM output signal is to have a carrier frequency of 103.7 MHz and a peak deviation of 75 kHz.

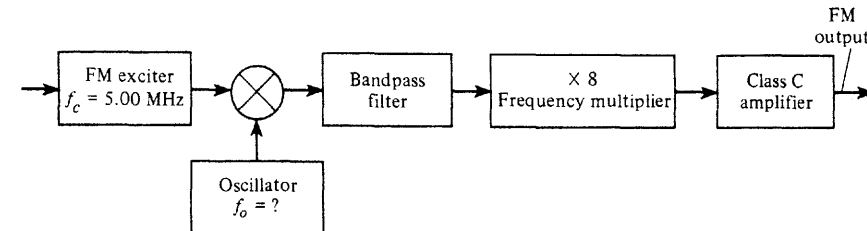


Figure P5-24

(a) Find the bandwidth and center frequency required for the bandpass filter.

(b) Calculate the frequency  $f_0$  of the oscillator.

(c) What is the required peak deviation capability of the FM exciter?

**5-25** Analyze the performance of the FM circuit of Fig. 5-8b. Assume that the voltage appearing across the reversed-biased diodes, which provide the voltage variable capacitance, is  $v(t) = 5 + 0.05m(t)$ , where the modulating signal is a test tone,  $m(t) = \cos \omega_1 t$ ,  $\omega_1 = 2\pi f_1$ , and  $f_1 = 1$  kHz. The capacitance of each of the biased diodes is  $C_d = 100/\sqrt{1 + 2v(t)}$  pF. Assume that  $C_0 = 180$  pF and that  $L$  is chosen to resonate at 5 MHz.

(a) Find the value of  $L$ .

(b) Show that the resulting oscillator signal is an FM signal. For convenience, assume that the peak level of the oscillator signal is 10 V. Find the parameter  $D_f$ .

**5-26** A modulated RF waveform is given by  $500 \cos[\omega_c t + 20 \cos \omega_1 t]$ , where  $\omega_1 = 2\pi f_1$ ,  $f_1 = 1$  kHz, and  $f_c = 100$  MHz.

(a) If the phase deviation constant is 100 rad/V, find the mathematical expression for the corresponding phase modulation voltage  $m(t)$ . What is its peak value and its frequency?

(b) If the frequency deviation constant is  $1 \times 10^6$  rad/V-s, find the mathematical expression for the corresponding FM voltage,  $m(t)$ . What is its peak value and its frequency?

(c) If the RF waveform appears across a  $50\Omega$  load, determine the average power and the PEP.

- 5-27** Given the FM signal  $s(t) = 10 \cos [\omega_c t + 100 \int_{-\infty}^t m(\sigma) d\sigma]$ , where  $m(t)$  is a polar square-wave signal with a duty cycle of 50%, a period of 1 s, and a peak value of 5 V.

- (a) Sketch the instantaneous frequency waveform and the waveform of the corresponding FM signal (see Fig. 5-9).  
 (b) Plot the phase deviation  $\theta(t)$  as a function of time.  
 (c) Evaluate the peak frequency deviation.

- 5-28** A carrier  $s(t) = 100 \cos(2\pi \times 10^9 t)$  of an FM transmitter is modulated with a tone signal. For this transmitter a 1-V (rms) tone produces a deviation of 30 kHz. Determine the amplitude and frequency of all FM signal components (spectral lines) that are greater than 1% of the unmodulated carrier amplitude for the following modulating signals:

- (a)  $m(t) = 2.5 \cos(3\pi \times 10^4 t)$ .  
 (b)  $m(t) = 1 \cos(6\pi \times 10^4 t)$ .

- 5-29** Referring to (5-58), show that

$$J_{-n}(\beta) = (-1)^n J_n(\beta)$$



- 5-30** Consider an FM exciter with the output  $s(t) = 100 \cos[2\pi 1000t + \theta(t)]$ . The modulation is  $m(t) = 5 \cos(2\pi 8t)$  and the modulation gain of the exciter is 8 Hz/V. The FM output signal is passed through an ideal (brickwall) bandpass filter which has a center frequency of 1000 Hz, a bandwidth of 56 Hz, and a gain of unity. Determine the normalized average power:

- (a) At the bandpass filter input.  
 (b) At the bandpass filter output.

- 5-31** A 1-kHz sinusoidal signal phase modulates a carrier at 146.52 MHz with a peak phase deviation of 45°. Evaluate the exact magnitude spectra of the PM signal if  $A_c = 1$ . Sketch your result. Using Carson's rule, evaluate the approximate bandwidth of the PM signal and see if it is a reasonable number when compared with your spectral plot.

- 5-32** A 1-kHz sinusoidal signal frequency modulates a carrier at 146.52 MHz with a peak deviation of 5 kHz. Evaluate the exact magnitude spectra of the FM signal if  $A_c = 1$ . Sketch your result. Using Carson's rule, evaluate the approximate bandwidth of the FM signal and see if it is a reasonable number when compared with your spectral plot.

- 5-33** The calibration of a frequency deviation monitor is to be verified by using a Bessel function test. An FM test signal with a calculated frequency deviation is generated by frequency modulating a sine wave onto a carrier. Assume that the sine wave has a frequency of 2 kHz and that the amplitude of the sine wave is slowly increased from zero until the discrete carrier term (at  $f_c$ ) of the FM signal reduces to zero, as observed on a spectrum analyzer. What is the peak frequency deviation of the FM test signal when the discrete carrier term is zero? Suppose that the amplitude of the sine wave is increased further until this discrete carrier term appears, reaches a maximum, and then disappears again. What is the peak frequency deviation of the FM test signal now?

- 5-34** A frequency modulator has a modulator gain of 10 Hz/V and the modulating waveform is

$$m(t) = \begin{cases} 0, & t < 0 \\ 5, & 0 < t < 1 \\ 15, & 1 < t < 3 \\ 7, & 3 < t < 4 \\ 0, & 4 < t \end{cases}$$



- (a) Plot the frequency deviation in hertz over the time interval  $0 < t < 5$ .  
 (b) Plot the phase deviation in radians over the time interval  $0 < t < 5$ .

- 5-35** A square-wave (digital) test signal of 50% duty cycle phase modulates a transmitter where  $s(t) = 10 \cos[\omega_c t + \theta(t)]$ . The carrier frequency is 60 MHz and the peak phase deviation is 45°. Assume that the test signal is of the unipolar NRZ type with a period of 1 ms and that it is symmetrical about  $t = 0$ . Find the exact spectrum for  $s(t)$ .

- 5-36** Two sinusoids,  $m(t) = A_1 \cos \omega_1 t + A_2 \cos \omega_2 t$ , phase modulate a transmitter. Derive a formula that gives the exact spectrum for the resulting PM signal in terms of the signal parameters  $A_c$ ,  $\omega_c$ ,  $D_p$ ,  $A_1$ ,  $A_2$ ,  $\omega_1$ , and  $\omega_2$ . [Hint: Use  $e^{ja(t)} = (e^{ja_1(t)})(e^{ja_2(t)})$  where  $a(t) = a_1(t) + a_2(t)$ .]

- 5-37** Plot the magnitude spectrum centered on  $f = f_c$  for an FM signal where the modulating signal is

$$m(t) = A_1 \cos 2\pi f_1 t + A_2 \cos 2\pi f_2 t$$



Assume that  $f_1 = 10$  Hz,  $f_2 = 17$  Hz, and that  $A_1$  and  $A_2$  are adjusted so that each tone contributes a peak deviation of 20 Hz.

- 5-38** For small values of  $\beta$ ,  $J_n(\beta)$  can be approximated by  $J_n(\beta) = \beta^n / (2^n n!)$ . Show that for the case of FM with sinusoidal modulation,  $\beta = 0.2$  is sufficiently small to give NBFM.

- 5-39** A polar square wave with a 50% duty cycle frequency modulates an NBFM transmitter such that the peak phase deviation is 10°. Assume that the square wave has a peak value of 5 V, a period of 10 ms, and a zero-crossing at  $t = 0$  with a positive-going slope.

- (a) Determine the peak frequency deviation of this NBFM signal.  
 (b) Evaluate and sketch the spectrum of this signal, using the narrowband analysis technique.  
 Assume that the carrier frequency is 30 MHz.

- 5-40** Design a wideband FM transmitter that uses the indirect method for generating a WBFM signal. Assume that the carrier frequency of the WBFM signal is 96.9 MHz and that the transmitter is capable of producing a high-quality FM signal with a peak deviation of 75 kHz when modulated by a 1-V (rms) sinusoid of frequency 20 Hz. Show a complete block diagram of your design, indicating the frequencies and peak deviations of the signals at various points.

- 5-41** An FM signal,  $100 \cos[\omega_c t + D_f \int_{-\infty}^t m(\sigma) d\sigma]$ , is modulated by the waveform shown in Fig. P5-41. Let  $f_c = 420$  MHz.

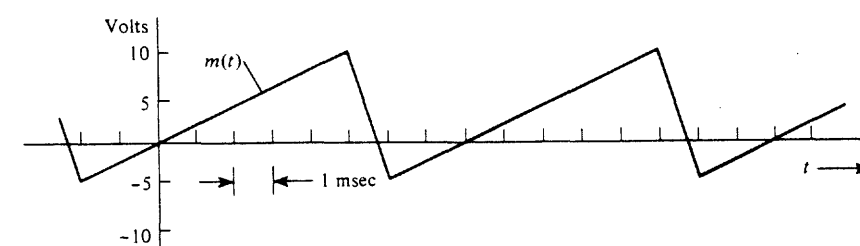


Figure P5-41

- (a) Determine the value of  $D_f$  so that the peak-to-peak frequency deviation is 25 kHz.  
 (b) Evaluate and sketch the approximate PSD.  
 (c) Determine the bandwidth of this FM signal such that spectral components are down at least 40 dB from the unmodulated carrier level for frequencies outside this bandwidth.

- 5-42** A multilevel digital test signal as shown in Fig. P5-42 modulates a WBFM transmitter. Evaluate and sketch the approximate power spectrum of this WBFM signal if  $A_c = 5$ ,  $f_c = 2$  GHz, and  $D_f = 10^5$ .

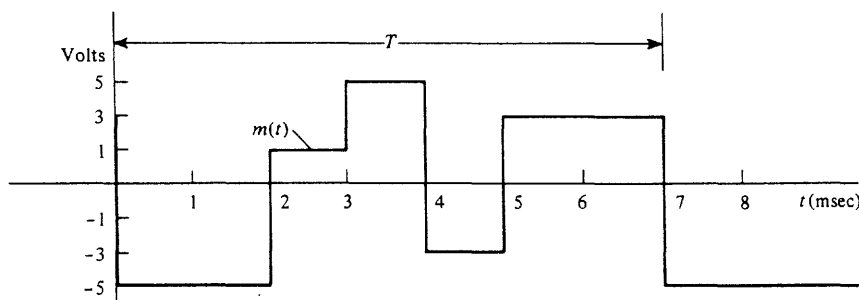


Figure P5-42

- 5-43 Refer to Fig. 5-15b, which displays the circuit diagram for a commonly used preemphasis filter network.  
 (a) Show that  $f_1 = 1/(2\pi R_1 C)$ .  
 (b) Show that  $f_2 = (R_1 + R_2)/(2\pi R_1 R_2 C) \approx 1/(2\pi R_2 C)$ .  
 (c) Evaluate  $K$  in terms of  $R_1$ ,  $R_2$ , and  $C$ .

- 5-44 The composite baseband signal for FM stereo transmission is given by

$$m_b(t) = [m_L(t) + m_R(t)] + [m_L(t) - m_R(t)] \cos(\omega_{sc}t) + K \cos(\frac{1}{2}\omega_{sc}t)$$

A stereo FM receiver using a switching type of demultiplexer for recovery of  $m_L(t)$  and  $m_R(t)$  is shown in Fig. P5-44.

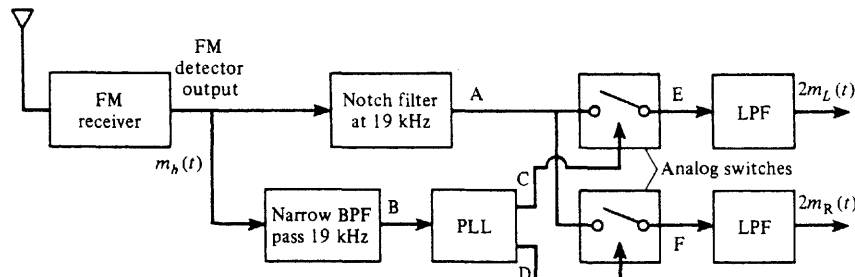


Figure P5-44

- (a) Determine the switching waveforms at points C and D that activate the analog switches. Be sure to specify the correct phasing for each one. Sketch these waveforms.  
 (b) Draw a more detailed block diagram showing the blocks inside the PLL.  
 (c) Write equations for the waveforms at points A through F and explain how this circuit works by sketching typical waveforms at each of these points.
- 5-45 In a communication system two baseband signals (they may be analog or digital) are transmitted simultaneously by generating the RF signal

$$s(t) = m_1(t) \cos \omega_c t + m_2(t) \sin \omega_c t$$

The carrier frequency is 7.250 MHz. The bandwidth of  $m_1(t)$  is 5 kHz and the bandwidth of  $m_2(t)$  is 10 kHz.

- (a) Evaluate the bandwidth of  $s(t)$ .

- (b) Derive an equation for the spectrum of  $s(t)$  in terms of  $M_1(f)$  and  $M_2(f)$ .  
 (c)  $m_1(t)$  and  $m_2(t)$  can be recovered (i.e., detected) from  $s(t)$  by using a superheterodyne receiver with two switching detectors. Draw a block diagram for the receiver and sketch the digital waveforms that are required to operate the samplers. Describe how they can be obtained. Show that the Nyquist sampling criterion is satisfied. (Hint: See Fig. P5-44).

- 5-46 A digital baseband signal consisting of rectangular binary pulses occurring at a rate of 2400 bits/s is to be transmitted over a bandpass channel.  
 (a) Evaluate the magnitude spectrum for OOK signaling that is keyed by a baseband digital test pattern consisting of alternating 1's and 0's.  
 (b) Sketch the magnitude spectrum and indicate the value of the first null-to-null bandwidth. Assume a carrier frequency of 50 kHz.  
 (c) For a random data pattern, find the PSD and plot the result. Compare this result with that obtained in parts (a) and (b) for alternating data.

- 5-47 Repeat Prob. 5-46 for the case of BPSK signaling.

- 5-48 A carrier is angle modulated with a polar baseband data signal to produce a BPSK signal,  $s(t) = 10 \cos[\omega_c t + D_p m(t)]$ , where  $m(t) = \pm 1$  corresponds to the binary data  $\{10010110\}$ .  $T_b = 0.0025$  sec and  $\omega_c = 1000\pi$ . Using MATLAB, plot the BPSK signal waveform and its corresponding FFT spectrum for the following digital modulation indices:  
 (a)  $h = 0.2$ .  
 (b)  $h = 0.5$ .  
 (c)  $h = 1.0$ .

- 5-49 Evaluate the magnitude spectrum for an FSK signal with alternating 1 and 0 data. Assume that the mark frequency is 50 kHz, the space frequency is 55 kHz, and the bit rate is 2400 bits/s. Find the first null-to-null bandwidth.

- 5-50 Assume that 4800-bits/s random data are sent over a bandpass channel by BPSK signaling. Find the transmission bandwidth  $B_T$  such that the spectral envelope is down at least 35 dB outside this band.

- 5-51 As indicated in Fig. 5-22a, a BPSK signal can be demodulated by using a coherent detector where the carrier reference is provided by a Costas loop for the case of  $h = 1.0$ . Alternatively, the carrier reference can be provided by a squaring loop that uses a  $\times 2$  frequency multiplier. A block diagram for a squaring loop is shown in Fig. P5-51.

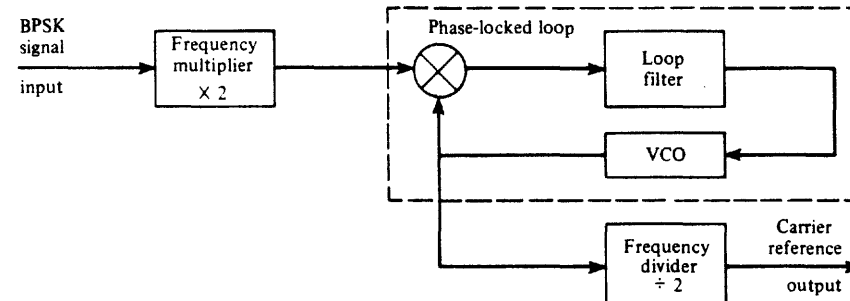


Figure P5-51

- (a) Draw an overall block diagram for a BPSK receiver using the squaring loop.

- (b) By using mathematics to represent the waveforms, show how the squaring loop recovers the carrier reference.
- (c) Demonstrate that the squaring loop does or does not have a  $180^\circ$  phase ambiguity problem.
- 5-52** A binary data signal is differentially encoded and modulates a PM transmitter to produce a differentially encoded phase-shift-keyed signal (DPSK). The peak-to-peak phase deviation is  $180^\circ$  and  $f_c$  is harmonically related to the bit rate  $R$ .
- (a) Draw a block diagram for the transmitter, including the differential encoder.
- (b) Show typical waveforms at various points on the block diagram if the input data sequence is 01011000101.
- (c) Assume that the receiver consists of a superheterodyne circuit. The detector that is used is shown in Fig. P5-52, where  $T = 1/R$ . If the DPSK IF signal  $v_1(t)$  has a peak value of  $A_c$  volts, determine the appropriate value for the threshold voltage setting  $V_T$ .

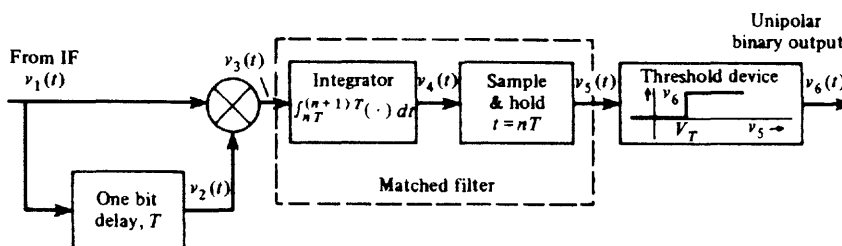


Figure P5-52

- (d) Sketch the waveforms that appear at various points of this detector circuit for the data sequence in part (b).
- 5-53** A binary baseband signal is passed through a raised cosine-rolloff filter with a 50% rolloff factor and is then modulated onto a carrier. The data rate is 2400 bits/s. Evaluate:
- (a) The absolute bandwidth of a resulting OOK signal.
- (b) The approximate bandwidth of a resulting FSK signal when the mark frequency is 50 kHz and the space frequency is 55 kHz.
- (Note: It is interesting to compare these bandwidths with those obtained in Probs. 5-46 and 5-49.)
- 5-54** Evaluate the exact magnitude spectrum of the FSK signal that is emitted by a Bell-type 103 modem operating in the answer mode at 300 bits/s. Assume that the data are alternating 1's and 0's.
- 5-55** Repeat Prob. 5-54 if the data have the periodic pattern 111000111000.
- 5-56** Starting with (5-84), work out all of the mathematical steps to derive the result given in (5-85).
- 5-57** When FSK signals are detected using coherent detection as shown in Fig. 5-28b, it is assumed that  $\cos \omega_1 t$  and  $\cos \omega_2 t$  are orthogonal functions. This is approximately true iff  $f_1 - f_2 = 2 \Delta f$  is sufficiently large. Find the exact condition required for the mark and space FSK signals to be orthogonal. (Hint: The answer relates  $f_1$ ,  $f_2$ , and  $R$ .)
- 5-58** Show that the approximate transmission bandwidth for FSK is given by  $B_T = 2R(1 + h/2)$ , where  $h$  is the digital modulation index and  $R$  is the bit rate.
- 5-59** Assume that a QPSK modem is used to send data at a rate of 3.6 kbit/s over a twisted pair telephone line. The line has a bandwidth of 2.4 kHz.

- (a) If the line is equalized to have an equivalent raised cosine filter characteristic, what is the rolloff factor,  $r$ , required?
- (b) Could a rolloff factor,  $r$ , be found so that a 4.8-kbit/s data rate could be supported?
- 5-60** Show that two BPSK systems can operate simultaneously over the same channel by using quadrature (sine and cosine) carriers. Give a block diagram for the transmitters and receivers. What is the overall aggregate data rate,  $R$ , for this quadrature carrier multiplex system as a function of the channel null bandwidth,  $B_T$ ? How does the aggregate data rate of this system compare to the data rate for a system that first time-division-multiplexes the two sources and transmits the TDM data via a QPSK carrier?
- 5-61** Assume that a telephone line channel is equalized to allow bandpass data transmission over a frequency range of 600 to 3000 Hz with raised cosine-rolloff filtering. The available channel bandwidth is 2400 Hz with a midchannel frequency of 1800 Hz.
- (a) Design a 2400-bit/s QPSK transmission system with  $f_c = 1800$  Hz. Show that the spectrum of this signal will fit into the channel when  $r = 1$ . Find the absolute and 6-dB bandwidths.
- (b) Repeat part (a) for the case of 4800-bit/s eight-phase PSK signaling.
- 5-62** Assume that a telephone line channel is equalized to allow bandpass data transmission over a frequency range of 400 to 3100 Hz so that the available channel bandwidth is 2700 Hz and the midchannel frequency is 1750 Hz. Design a 16-symbol QAM signaling scheme that will allow a data rate of 9600 bits/s to be transferred over the channel. In your design, choose an appropriate rolloff factor  $r$  and indicate the absolute and 6-dB QAM signal bandwidth. Discuss why you selected the particular value of  $r$  that you used.
- 5-63** Assume that  $R = 9600$  bits/s. Calculate the second null-to-null bandwidth of BPSK, QPSK, MSK, 64PSK, and 64QAM. Discuss the advantages and disadvantages of using each of these signaling methods.
- 5-64** Referring to Fig. 5-31b, sketch the waveforms that appear at the output of each block assuming that the input is a TTL level signal with data 110100101 and  $\ell = 4$ . Explain how this QAM transmitter works.
- 5-65** Design a receiver (i.e., determine the block diagram) that will detect the data on a QAM waveform having an  $M = 16$  point signal constellation as shown in Fig. 5-32. Explain how your receiver works. (Hint: Study Fig. 5-31b.)
- 5-66** Using MATLAB, plot the QPSK and OQPSK in-phase and quadrature modulation waveforms for the data stream

$$\{-1, -1, -1, +1, +1, -1, -1, -1, +1, -1, -1, +1, -1, -1\}$$



Use a rectangular pulse shape. For convenience let  $T_b = 1$ .

- 5-67** Calculate and plot the PSD for a CCITT V.22bis 2400-bit/s computer modem operating in the originate mode and sending random data. See Table C-7 for the modem specifications.
- 5-68** (a) Fig. 5-34 shows the  $x(t)$  and  $y(t)$  waveforms for Type II MSK. Redraw these waveforms for the case of Type I MSK.  
 (b) Show that (5-114b) is the Fourier transform of (5-114a).
- 5-69** Using MATLAB, plot the MSK Type I modulation waveforms  $x(t)$ ,  $y(t)$ , and the MSK signal  $s(t)$ . Assume that the input data stream is

$$\{+1, -1, -1, +1, -1, -1, +1, -1, +1, +1, -1, +1, -1\}$$



Assume that  $T_b = 1$  and that  $f_c$  has a value such that a good plot of  $s(t)$  is obtained for a reasonable amount of computer time.

- 5-70** Repeat Prob. 5-69 but use the data stream

$$\{-1, -1, -1, +1, +1, +1, -1, -1, -1, +1, -1, -1, +1, -1, -1\}$$



This data stream is the differentially encoded version of the data stream in Prob. 5-69. The generation of FFSK is equivalent to Type I MSK with differential encoding of the data input. FFSK has a one-to-one relationship between the input data and the mark and space frequencies.

- 5-71** Using MATLAB, plot the MSK Type II modulation waveforms  $x(t)$ ,  $y(t)$ , and the MSK signal  $s(t)$ . Assume that the input data stream is



$$\{-1, -1, -1, +1, +1, +1, -1, -1, -1, +1, -1, -1, +1, -1, -1\}$$

Assume that  $T_b = 1$  and  $f_c$  has a value such that a good plot of  $s(t)$  is obtained for a reasonable amount of computer time.

- 5-72** Show that MSK can be generated by the serial method of Fig. 5-36c. That is, show that the PSD for the signal at the output of the MSK bandpass filter is the MSK spectrum as described by (5-115) and (5-2b).

- 5-73** Recompute the spectral efficiencies for all of the signals shown in Table 5-7 using a 40-dB bandwidth criterion.

- 5-74** Prove that (5-104b)—the autocorrelation for an  $m$ -sequence PN code—is correct. *Hint:* Use the definition for the autocorrelation function,  $R_c(\tau) = \langle c(t)c(t + \tau) \rangle$  and (5-118) where

$$c(t) = \sum_{-\infty}^{\infty} c_n p(t - nT_c)$$

and

$$p(t) = \begin{cases} 1, & 0 < t < T_c \\ 0, & t \text{ elsewhere} \end{cases}$$

- 5-75** Find an expression for the PSD of an  $m$ -sequence PN code when the chip rate is 10 MHz and there are eight stages in the shift register. Sketch your result.

- 5-76** Referring to Fig. 5-38a, show that the complex Fourier series coefficients for the autocorrelation of an  $m$ -sequence PN waveform are given by (5-124).

- 5-77** Assume that the modulator and demodulator for the FH-SS system of Fig. 5-40 are of the FSK type.

- (a) Find a mathematical expression for the FSK-FH-SS signal,  $s(t)$ , at the transmitter output.  
 (b) Using your result for  $s(t)$  from part (a) as the receiver input in Fig. 5-40b [i.e.,  $r(t) = s(t)$ ], show that the output of the receiver bandpass filter is an FSK signal.

## CHAPTER 6

# RANDOM PROCESSES AND SPECTRAL ANALYSIS

The mathematics used to describe random signals and noise will be developed in this chapter. From Chapter 1 it is recalled that random signals (in contrast to deterministic signals) are used to convey information. Noise is also described in terms of statistics. Thus the description of random signals and noise is fundamental to the understanding of communication systems.

This chapter is written with the assumption that the reader has a basic understanding of probability, random variables, and ensemble averages as developed in Appendix B. If the reader is not familiar with these ideas, Appendix B should be studied now just like a regular chapter. For the reader who has had courses in this area, Appendix B can be used as a quick review.

Random processes are extensions of the concepts associated with random variables when the time parameter is brought into the problem. As we will see, this enables frequency response to be incorporated into the statistical description.

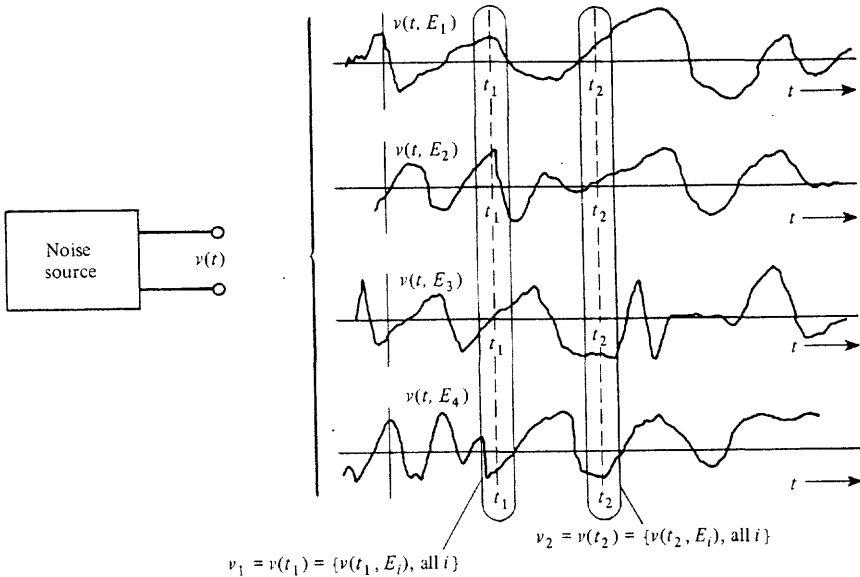


**Figure 6-1** Random noise source and some sample functions of the random noise process.

## 6-1 SOME BASIC DEFINITIONS

### Random Processes

**DEFINITION.** A *real random process* (or *stochastic process*) is an indexed set of real functions of some parameter (usually time) that has certain statistical properties.

Consider voltage waveforms that might be emitted from a noise source (see Fig. 6-1). One possible waveform is  $v(t, E_1)$ . Another is  $v(t, E_2)$ . In general,  $v(t, E_i)$  denotes the waveform that is obtained when the event  $E_i$  of the sample space occurs.  $v(t, E_i)$  is said to be a *sample function* of the sample space. The set of all possible sample functions  $\{v(t, E_i)\}$  is called the *ensemble* and defines the *random process*  $v(t)$  that describes the noise source. That is, the events  $\{E_i\}$  are mapped into a set of time functions  $\{v(t, E_i)\}$ . This collection of functions is the random process  $v(t)$ . When we observe the voltage waveform generated by the noise source, we see one of the sample functions.

Sample functions can be obtained by observing simultaneously the outputs of many identical noise sources. To obtain all of the sample functions in general, an infinite number of noise sources would be required.

The definition of a random process may be compared with that of a random variable. A random variable maps events into *constants*, whereas a random process maps events into *functions* of the parameter  $t$ .

**THEOREM.** A random process may be described by an indexed set of random variables.

## Sec. 6-1 Some Basic Definitions

Referring to Fig. 6-1, define a set of random variables  $v_1 = v(t_1)$ ,  $v_2 = v(t_2)$ , ..., where  $v(t)$  is the random process. Here the random variable  $v_j = v(t_j)$  takes on the values described by the set of constants  $\{v(t_j, E_i)\}$ , all  $i$ .

For example, suppose that the noise source has a Gaussian distribution. Then any of the random variables will be described by



$$f_{v_j}(v_j) = \frac{1}{\sqrt{2\pi}\sigma_j} e^{-(v_j - m_j)^2/(2\sigma_j^2)} \quad (6-1)$$

where  $v_j \triangleq v(t_j)$ . We realize that, in general, the probability density function (PDF) depends implicitly on time since  $m_j$  and  $\sigma_j$  correspond to the mean value and standard deviation measured at the time  $t = t_j$ . The  $N = 2$  joint distribution for the Gaussian source for  $t = t_1$  and  $t = t_2$  is the bivariate Gaussian PDF  $f_v(v_1, v_2)$  as given by (B-97), where  $v_1 = v(t_1)$  and  $v_2 = v(t_2)$ .

To describe a general random process  $x(t)$  completely, an  $N$ -dimensional PDF,  $f_x(\mathbf{x})$ , is required where  $\mathbf{x} = (x_1, x_2, \dots, x_j, \dots, x_N)$ ,  $x_j \triangleq x(t_j)$ , and  $N \rightarrow \infty$ . Furthermore, the  $N$ -dimensional PDF is an implicit function of  $N$  time constants  $t_1, t_2, \dots, t_N$  since

$$f_x(\mathbf{x}) = f_x(x(t_1), x(t_2), \dots, x(t_N)) \quad (6-2)$$

Random processes may be classified as being continuous or discrete. A *continuous random process* consists of a random process with associated continuously distributed random variables,  $v_j = v(t_j)$ . The Gaussian random process (described previously) is an example of a continuous random process. Noise in linear communication circuits is usually of the continuous type. (In many cases, noise in nonlinear circuits is also of the continuous type.) A *discrete random process* consists of random variables with discrete distributions. For example, the output of an ideal (hard) limiter is a binary (discrete with two levels) random process. Some sample functions of a binary random process are illustrated in Fig. 6-2.

### Stationarity and Ergodicity

**DEFINITION.** A random process  $x(t)$  is said to be *stationary to the order N* if, for any  $t_1, t_2, \dots, t_N$ ,

$$f_x(x(t_1), x(t_2), \dots, x(t_N)) = f_x(x(t_1 + t_0), x(t_2 + t_0), \dots, x(t_N + t_0)) \quad (6-3)$$

where  $t_0$  is any arbitrary real constant. Furthermore, the process is said to be *strictly stationary* if it is stationary to the order  $N \rightarrow \infty$ .

This definition implies that if a stationary process of order  $N$  is translated in time, then the  $N$ -th-order statistics do not change. Furthermore, the  $N$ -dimensional PDF depends on  $N - 1$  time differences  $t_2 - t_1, t_3 - t_1, \dots, t_N - t_1$  since  $t_0$  could be chosen to be  $-t_1$ .

### Example 6-1 FIRST-ORDER STATIONARITY

Examine a random process  $x(t)$  to determine if it is first-order stationary. From (6-3), the requirement for first-order stationarity is that the first-order PDF not be a function of time. Let the random process be

$$x(t) = A \sin(\omega_0 t + \theta_0) \quad (6-4)$$

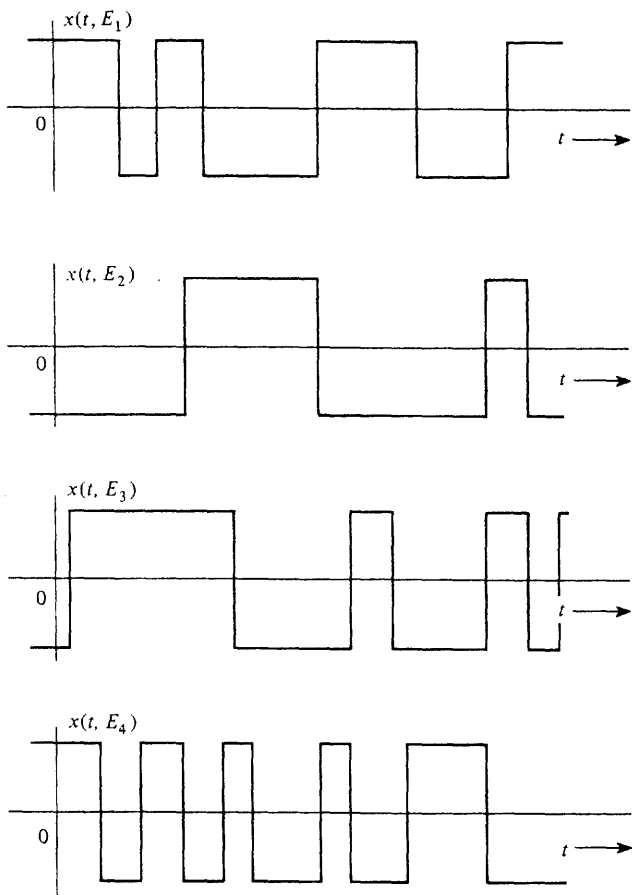


Figure 6-2 Sample functions of a binary random process.

**CASE 1: A STATIONARY RESULT.** First, assume that  $A$  and  $\omega_0$  are deterministic constants and  $\theta_0$  is a random variable.  $t$  is the time parameter. In addition, assume that  $\theta_0$  is uniformly distributed over  $-\pi$  to  $\pi$ . Then  $\psi \triangleq \theta_0 + \omega_0 t$  is a random variable uniformly distributed over the interval  $\omega_0 t - \pi < \psi < \omega_0 t + \pi$ . The first-order PDF for  $x(t)$  can be obtained by the transformation technique developed in Sec. B-8 of Appendix B. This is essentially the same problem as the one worked out in Example B-5. From (B-71), the first-order PDF for  $x(t)$  is

$$f(x) = \begin{cases} \frac{1}{\pi\sqrt{A^2 - x^2}}, & |x| \leq A \\ 0, & x \text{ elsewhere} \end{cases} \quad (6-5a)$$

Because this PDF is not a function of  $t$ ,  $x(t)$  is a first-order stationary process for the assumptions of Case 1 where  $\theta_0$  is a random variable. This result would be applicable to problems where  $\theta_0$  is the random start-up phase of an unsynchronized oscillator.

**CASE 2: A NONSTATIONARY RESULT.** Second, assume that  $A$ ,  $\omega_0$ , and  $\theta_0$  are deterministic constants. Then, at any time, the value of  $x(t)$  is known with a probability of 1. Thus the first-order PDF of  $x(t)$  is

$$f(x) = \delta(x - A \sin(\omega_0 t + \theta_0)) \quad (6-5b)$$

This PDF is a function of  $t$ ; consequently,  $x(t)$  is not first-order stationary for the assumption of Case 2, where  $\theta_0$  is a deterministic constant. This result will be applicable to problems where the oscillator is synchronized to some external source so that the oscillator start-up phase will have the known value  $\theta_0$ .

**DEFINITION.** A random process is said to be *ergodic* if all time averages of any sample function are equal to the corresponding ensemble averages (expectations).

Two important averages in electrical engineering are dc and rms values. These values are defined in terms of time averages, but if the process is ergodic, they may be evaluated by the use of ensemble averages. The dc value of  $x(t)$  is  $x_{dc} \triangleq \langle x(t) \rangle$ . When  $x(t)$  is ergodic, the time average is equal to the ensemble average, so we obtain

$$x_{dc} \triangleq \langle x(t) \rangle \equiv \overline{[x(t)]} = m_x \quad (6-6a)$$

where the time average is

$$\langle [x(t)] \rangle = \lim_{T \rightarrow \infty} \frac{1}{T} \int_{-T/2}^{T/2} [x(t)] dt \quad (6-6b)$$

the ensemble average is

$$\overline{[x(t)]} = \int_{-\infty}^{\infty} [x] f_x(x) dx = m_x \quad (6-6c)$$

and  $m_x$  denotes the mean value. Similarly, the rms value is obtained:

$$X_{rms} \triangleq \sqrt{\langle x^2(t) \rangle} \equiv \sqrt{\overline{x^2}} = \sqrt{\sigma_x^2 + m_x^2} \quad (6-7)$$

where  $\sigma_x^2$  is the variance of  $x(t)$ .

In summary, if a process is ergodic, all time and ensemble averages are interchangeable. The time average cannot be a function of time since the time parameter has been averaged out. Furthermore, the ergodic process must be stationary, since otherwise the ensemble averages (such as moments) would be a function of time. However, not all stationary processes are ergodic.

### Example 6-2 ERGODIC RANDOM PROCESS

Let the random process be given by

$$x(t) = A \cos(\omega_0 t + \theta) \quad (6-8)$$

where  $A$  and  $\omega_0$  are constants and  $\theta$  is a random variable that is uniformly distributed over  $(0, 2\pi)$ .

First, evaluate some ensemble averages. The mean and the second moment are

$$\bar{x} = \int_{-\infty}^{\infty} [x(\theta)] f_{\theta}(\theta) d\theta = \int_0^{2\pi} [A \cos(\omega_0 t + \theta)] \frac{1}{2\pi} d\theta = 0 \quad (6-9)$$

and

$$\overline{x^2(t)} = \int_0^{2\pi} [A \cos(\omega_0 t + \theta)]^2 \frac{1}{2\pi} d\theta = \frac{A^2}{2} \quad (6-10)$$

In this example the time parameter  $t$  disappeared when the ensemble averages were evaluated. This would not be the case unless  $x(t)$  was stationary.

Second, evaluate the corresponding time averages using a typical sample function of the random process. One sample function is  $x(t, E_1) = A \cos \omega_0 t$ , which occurs when  $\theta = 0$ .  $\theta = 0$  corresponds to one of the events (outcomes). The time average for any of the sample functions can be evaluated by letting  $\theta$  be the appropriate value between 0 and  $2\pi$ . The time averages for the first and second moments are

$$\langle x(t) \rangle = \frac{1}{T_0} \int_0^{T_0} A \cos(\omega_0 t + \theta) dt = 0 \quad (6-11)$$

and

$$\langle x^2(t) \rangle = \frac{1}{T_0} \int_0^{T_0} [A \cos(\omega_0 t + \theta)]^2 dt = \frac{A^2}{2} \quad (6-12)$$

where  $T_0 = 1/f_0$  and the time-averaging operator for a periodic function, (2-4), has been used. In this example  $\theta$  disappears when the time average is evaluated. This is a consequence of  $x(t)$  being an ergodic process. However, in a nonergodic example, the time average would be a random variable.

Comparing (6-9) with (6-11) and (6-10) with (6-12), we see that the time average is equal to the ensemble average for the first and second moments. Consequently, we suspect that this process might be ergodic. However, we have not proven that the process is ergodic because we have not evaluated all the possible time and ensemble averages or all the moments. However, it appears as if the other time and ensemble averages would be equal, so we will assume that the process is ergodic. In general, it is difficult to prove that a process is ergodic, so we will assume that this is the case if the process appears to be stationary and some of the time averages are equal to the corresponding ensemble averages. An ergodic process has to be stationary since the time averages cannot be functions of time. However, if a process is known to be stationary, it may or may not be ergodic.

In Prob. 6-2 it will be shown that the random process as described by (6-8) would not be stationary (and, consequently, would not be ergodic) if  $\theta$  were uniformly distributed over  $(0, \pi/2)$  instead of  $(0, 2\pi)$ .

### Correlation Functions and Wide-Sense Stationarity

**DEFINITION.** The autocorrelation function of a real process  $x(t)$  is

$$R_x(t_1, t_2) = \overline{x(t_1)x(t_2)} = \int_{-\infty}^{\infty} \int_{-\infty}^{\infty} x_1 x_2 f_x(x_1, x_2) dx_1 dx_2 \quad (6-13)$$

where  $x_1 = x(t_1)$  and  $x_2 = x(t_2)$ . If the process is stationary to the second order, the autocorrelation function is only a function of the time difference  $\tau = t_2 - t_1$ .

That is,

$$R_x(\tau) = \overline{x(t)x(t+\tau)} \quad (6-14)$$

if  $x(t)$  is second-order stationary.<sup>†</sup>

**DEFINITION.** A random process is said to be *wide-sense stationary* if

$$1. \overline{x(t)} = \text{constant} \quad (6-15a)$$

$$2. R_x(t_1, t_2) = R_x(\tau) \quad (6-15b)$$

where  $\tau = t_2 - t_1$ .

A process that is stationary to order 2 or greater is certainly wide-sense stationary. However, the converse is not necessarily true since only *certain* ensemble averages of second order or less, namely, those of (6-15), need to be satisfied for wide-sense stationarity.<sup>‡</sup> As indicated by (6-15), the mean and autocorrelation functions of a wide-sense stationary process do not change with a shift in the time origin. This implies that the associated circuit elements that generate the wide-sense stationary random process do not drift (age) with time.

The autocorrelation function gives us an idea of the frequency response that is associated with the random process. For example, if  $R_x(\tau)$  remains relatively constant as  $\tau$  is increased from zero to some positive number, it indicates that, on the average, sample values of  $x$  taken at  $t = t_1$  and  $t = t_1 + \tau$  are nearly the same. Consequently,  $x(t)$  does not change rapidly with time (on the average) and we would expect  $x(t)$  to have low frequencies present. On the other hand, if  $R_x(\tau)$  decreases rapidly as  $\tau$  is increased, we would expect  $x(t)$  to change rapidly with time and, consequently, high frequencies would be present. We formulate this result rigorously in Sec. 6-2, where it will be shown that the PSD, which is a function of frequency, is the Fourier transform of the autocorrelation function.

Properties of the autocorrelation function of a real wide-sense stationary process are as follows:

$$1. R_x(0) = \overline{x^2(t)} = \text{second moment} \quad (6-16)$$

$$2. R_x(\tau) = R_x(-\tau) \quad (6-17)$$

$$3. R_x(0) \geq |R_x(\tau)| \quad (6-18)$$

The first two properties follow directly from the definition of  $R_x(\tau)$  as given by (6-14). Furthermore, if  $x(t)$  is ergodic,  $R(0)$  is identical to the square of the rms value of  $x(t)$ . Property 3 is demonstrated as follows:  $[x(t) \pm x(t + \tau)]^2$  is a nonnegative quantity, so that

<sup>†</sup> The time average type of the autocorrelation function was defined in Chapter 2. The time average autocorrelation function, (2-68), is identical to the ensemble average autocorrelation function, (6-14), when the process is ergodic.

<sup>‡</sup> An exception occurs for the Gaussian random process. Here wide-sense stationarity does imply that the process is strict-sense stationary since the  $N \rightarrow \infty$ -dimensional Gaussian PDF is completely specified by the mean, variance, and covariance of  $x(t_1), x(t_2), \dots, x(t_N)$ .

$$[x(t) \pm x(t + \tau)]^2 \geq 0$$

or

$$\overline{x^2(t)} \pm 2\overline{x(t)x(t + \tau)} + \overline{x^2(t + \tau)} \geq 0$$

This is equivalent to

$$R_x(0) \pm 2R_{xy}(\tau) + R_y(0) \geq 0$$

which reduces to property 3.

The autocorrelation may be generalized to define an appropriate correlation function for two random processes.

**DEFINITION.** The *cross-correlation function* for two real processes  $x(t)$  and  $y(t)$  is

$$R_{xy}(t_1, t_2) = \overline{x(t_1)y(t_2)} \quad (6-19)$$

Furthermore, if  $x(t)$  and  $y(t)$  are jointly stationary,<sup>†</sup> the cross-correlation function becomes

$$R_{xy}(t_1, t_2) = R_{xy}(\tau)$$

where  $\tau = t_2 - t_1$ .Some *properties* of cross-correlation functions of jointly stationary real processes are

$$1. R_{xy}(-\tau) = R_{yx}(\tau) \quad (6-20)$$

$$2. |R_{xy}(\tau)| \leq \sqrt{R_x(0)R_y(0)} \quad (6-21)$$

$$3. |R_{xy}(\tau)| \leq \frac{1}{2}[R_x(0) + R_y(0)] \quad (6-22)$$

The first property follows directly from the definition, (6-19). Property 2 follows from the fact that

$$[x(t) + Ky(t + \tau)]^2 \geq 0 \quad (6-23)$$

for any real constant  $K$ . Expanding (6-23), we obtain an equation that is a quadratic in  $K$ .

$$[R_y(0)]K^2 + [2R_{xy}(\tau)]K + [R_x(0)] \geq 0 \quad (6-24)$$

For  $K$  to be real, it can be shown that the discriminant of (6-24) has to be nonpositive.<sup>‡</sup> That is,

$$[2R_{xy}(\tau)]^2 - 4[R_y(0)][R_x(0)] \leq 0 \quad (6-25)$$

<sup>†</sup> Similar to (6-3),  $x(t)$  and  $y(t)$  are said to be jointly stationary when

$$f_{xy}(x(t_1), x(t_2), \dots, x(t_N), y(t_{N+1}), y(t_{N+2}), \dots, y(t_{N+M}))$$

$$= f_{xy}(x(t_1 + t_0), x(t_2 + t_0), \dots, x(t_N + t_0), y(t_{N+1} + t_0), y(t_{N+2} + t_0), \dots, y(t_{N+M} + t_0))$$

$x(t)$  and  $y(t)$  are strict-sense jointly stationary if this equality holds for  $N \rightarrow \infty$  and  $M \rightarrow \infty$  and are wide-sense jointly stationary for  $N = 2$  and  $M = 2$ .

<sup>‡</sup> The parameter  $K$  is a root of this quadratic only when the quadratic is equal to zero. When the quadratic is positive, the roots have to be complex.

This is equivalent to property 2 as described by (6-21). Property 3 follows directly from (6-24), where  $K = \pm 1$ . Furthermore, it is seen that

$$|R_{xy}(\tau)| \leq \sqrt{R_x(0)R_y(0)} \leq \frac{1}{2}[R_x(0) + R_y(0)] \quad (6-26)$$

because the geometric mean of two positive numbers,  $R_x(0)$  and  $R_y(0)$ , does not exceed their arithmetic mean.

Note that the cross-correlation function of two random processes,  $x(t)$  and  $y(t)$ , is a generalization of the concept of the joint mean of two random variables as defined by (B-91). Here  $x_1$  is replaced by  $x(t)$  and  $x_2$  is replaced by  $y(t + \tau)$ . Thus two random processes  $x(t)$  and  $y(t)$  are said to be *uncorrelated* if

$$R_{xy}(\tau) = \overline{[x(t)][y(t + \tau)]} = m_xm_y \quad (6-27)$$

for all values of  $\tau$ . Similarly, two random processes  $x(t)$  and  $y(t)$  are said to be *orthogonal* if

$$R_{xy}(\tau) = 0 \quad (6-28)$$

for all values of  $\tau$ .

As mentioned previously, it is realized that if  $y(t) = x(t)$ , the cross-correlation function becomes an autocorrelation function. In this sense the autocorrelation function is a special case of the cross-correlation function. Of course, when  $y(t) \equiv x(t)$ , all the properties of the cross-correlation function reduce to those of the autocorrelation function.

If the random processes  $x(t)$  and  $y(t)$  are jointly ergodic, the time average may be used to replace the ensemble average. For correlation functions this becomes

$$R_{xy}(\tau) \triangleq \overline{x(t)y(t + \tau)} \equiv \langle x(t)y(t + \tau) \rangle \quad (6-29)$$

where

$$\langle [\cdot] \rangle = \lim_{T \rightarrow \infty} \frac{1}{T} \int_{-T/2}^{T/2} [\cdot] dt \quad (6-30)$$

when  $x(t)$  and  $y(t)$  are jointly ergodic. In this case, cross-correlation functions and autocorrelation functions of voltage and/or current waveforms may be measured by using an electronic circuit that consists of a delay line, a multiplier, and an integrator. This measurement technique is illustrated in Fig. 6-3.

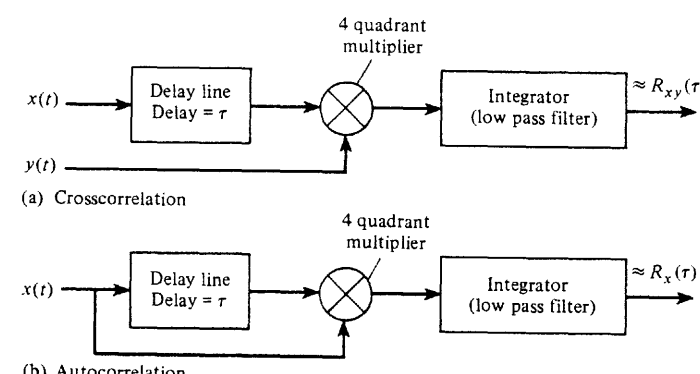


Figure 6-3 Measurement of correlation functions.

## Complex Random Processes

In previous chapters, the complex envelope  $g(t)$  was found to be extremely useful in describing bandpass waveforms. Bandpass *random* signals and noise can also be described in terms of the complex envelope, where  $g(t)$  is a *complex baseband random process*.

**DEFINITION.** A *complex random process* is

$$g(t) \triangleq x(t) + jy(t) \quad (6-31)$$

where  $x(t)$  and  $y(t)$  are real random processes and  $j = \sqrt{-1}$ .

A complex process is strict-sense stationary if  $x(t)$  and  $y(t)$  are jointly strict-sense stationary; that is,

$$\begin{aligned} f_g(x(t_1), y(t'_1), x(t_2), y(t'_2), \dots, x(t_N), y(t'_N)) \\ = f_g(x(t_1 + t_0), y(t'_1 + t_0), \dots, x(t_N + t_0), y(t'_N + t_0)) \end{aligned} \quad (6-32)$$

for any value of  $t_0$  and any  $N \rightarrow \infty$ .

The definitions for the correlation functions can be generalized to cover *complex* random processes.

**DEFINITION.** The *autocorrelation function* for a *complex* random process is

$$R_g(t_1, t_2) = \overline{g^*(t_1)g(t_2)} \quad (6-33)$$

where the asterisk denotes the complex conjugate.

Furthermore, the complex random process is stationary in the wide sense if  $\overline{g(t)}$  is a complex constant and  $R_g(t_1, t_2) = R_g(\tau)$ , where  $\tau = t_2 - t_1$ . The autocorrelation of a wide-sense stationary complex process has the Hermitian symmetry property

$$R_g(-\tau) = R_g^*(\tau) \quad (6-34)$$

**DEFINITION.** The *cross-correlation function* for two *complex* random processes  $g_1(t)$  and  $g_2(t)$  is

$$R_{g_1 g_2}(t_1, t_2) = \overline{g_1^*(t_1)g_2(t_2)} \quad (6-35)$$

When the complex random processes are jointly wide-sense stationary, the cross-correlation function becomes

$$R_{g_1 g_2}(t_1, t_2) = R_{g_1 g_2}(\tau)$$

where  $\tau = t_2 - t_1$ .

In Sec. 6-7 we use these definitions in the statistical description of bandpass random signals and noise.

## 6-2 POWER SPECTRAL DENSITY

### Definition

A definition for the PSD  $P_x(f)$  was given in Chapter 2 for the case of deterministic waveforms (2-66). Here we develop a more general definition that is applicable to spectral analysis of random processes.

Suppose that  $x(t, E_i)$  represents a sample function of a random process  $x(t)$ . A truncated version of this sample function can be defined:

$$x_T(t, E_i) = \begin{cases} x(t, E_i), & |t| < \frac{1}{2}T \\ 0, & t \text{ elsewhere} \end{cases} \quad (6-36)$$

where the subscript  $T$  denotes the truncated version. The corresponding Fourier transform is

$$\begin{aligned} X_T(f, E_i) &= \int_{-\infty}^{\infty} x_T(t, E_i) e^{-j2\pi ft} dt \\ &= \int_{-T/2}^{T/2} x(t, E_i) e^{-j2\pi ft} dt \end{aligned} \quad (6-37)$$

This indicates that  $X_T$  is itself a random process since  $x_T$  is a random process. We will now simplify the notation and denote these functions simply by  $X_T(f)$ ,  $x_T(t)$ , and  $x(t)$  since it is clear that they are all random processes.

The normalized<sup>†</sup> energy in the time interval  $(-T/2, T/2)$  is

$$E_T = \int_{-\infty}^{\infty} x_T^2(t) dt = \int_{-\infty}^{\infty} |X_T(f)|^2 df \quad (6-38)$$

Here Parseval's theorem was used to obtain the second integral. It is realized that  $E_T$  is a random variable because  $x(t)$  is a random process. Furthermore, the mean normalized energy is obtained by taking the ensemble average of (6-38).

$$\bar{E}_T = \int_{-T/2}^{T/2} \overline{x^2(t)} dt = \int_{-\infty}^{\infty} \overline{x_T^2(t)} dt = \int_{-\infty}^{\infty} \overline{|X_T(f)|^2} df \quad (6-39)$$

The normalized average power is the energy expended per unit time, so that the normalized average power is

$$P = \lim_{T \rightarrow \infty} \frac{1}{T} \int_{-T/2}^{T/2} \overline{x^2(t)} dt = \lim_{T \rightarrow \infty} \frac{1}{T} \int_{-\infty}^{\infty} \overline{x_T^2(t)} dt$$

or

$$P = \int_{-\infty}^{\infty} \left[ \lim_{T \rightarrow \infty} \frac{1}{T} \overline{|X_T(f)|^2} \right] df = \overline{\langle x^2(t) \rangle} \quad (6-40)$$

<sup>†</sup> If  $x(t)$  is a voltage or current waveform,  $E_T$  is the energy on a per-ohm (i.e.,  $R = 1$ ) normalized basis.

In the evaluation of the limit in (6-40), it is important that the ensemble average be evaluated *before* the limit operation is carried out because we want to ensure that  $X_T(f)$  is finite. [Because  $x(t)$  is a power signal,  $X(f) = \lim_{T \rightarrow \infty} X_T(f)$  may not exist.] Note that (6-40) indicates that for a random process, the average normalized power is given by the time average of the second moment. Of course, if  $x(t)$  is wide-sense stationary,  $\langle x^2(t) \rangle = x^2(t)$  because  $x^2(t)$  is a constant.

From the definition of the PSD in Chapter 2, we know that

$$P = \int_{-\infty}^{\infty} \mathcal{P}(f) df \quad (6-41)$$

Thus we see that the following definition of the PSD is consistent with that given in Chapter 2 (2-66).

**DEFINITION.** The *power spectral density* (PSD) for a random process  $x(t)$  is given by

$$\mathcal{P}_x(f) = \lim_{T \rightarrow \infty} \left( \frac{|X_T(f)|^2}{T} \right) \quad (6-42)$$

where

$$X_T(f) = \int_{-T/2}^{T/2} x(t) e^{-j2\pi f t} dt \quad (6-43)$$

### Wiener-Khintchine Theorem

Often the PSD is evaluated from the autocorrelation function for the random process by using the following theorem.

**WIENER-KHINTCHINE THEOREM<sup>†</sup>** When  $x(t)$  is a wide-sense stationary process, the PSD can be obtained from the Fourier transform of the autocorrelation function:

$$\mathcal{P}_x(f) = \mathcal{F}[R_x(\tau)] = \int_{-\infty}^{\infty} R_x(\tau) e^{-j2\pi f \tau} d\tau \quad (6-44)$$

and conversely,

$$R_x(\tau) = \mathcal{F}^{-1}[\mathcal{P}_x(f)] = \int_{-\infty}^{\infty} \mathcal{P}_x(f) e^{j2\pi f \tau} df \quad (6-45)$$

provided that  $R(\tau)$  becomes sufficiently small for large values of  $\tau$  so that

$$\int_{-\infty}^{\infty} |\tau R(\tau)| d\tau < \infty \quad (6-46)$$

<sup>†</sup> Named after the American mathematician Norbert Wiener (1894–1964) and the German mathematician A. I. Khintchine (1894–1959). Other spellings of the German name are Khinchine and Khinchin.

Furthermore, this theorem is also valid for a nonstationary process, provided that we replace  $R_x(\tau)$  by  $\langle R_x(t, t + \tau) \rangle$ .

**Proof.** From the definition of PSD,

$$\mathcal{P}_x(f) = \lim_{T \rightarrow \infty} \left( \frac{|X_T(f)|^2}{T} \right)$$

where

$$\begin{aligned} |X_T(f)|^2 &= \left| \int_{-T/2}^{T/2} x(t) e^{-j2\pi f t} dt \right|^2 \\ &= \int_{-T/2}^{T/2} \int_{-T/2}^{T/2} \overline{x(t_1)} x(t_2) e^{-j2\pi f t_1} e^{j2\pi f t_2} dt_1 dt_2 \end{aligned}$$

and  $x(t)$  is assumed to be real. But  $\overline{x(t_1)} x(t_2) = R_x(t_1, t_2)$ . Furthermore, let  $\tau = t_2 - t_1$  and make a change in variable from  $t_2$  to  $\tau + t_1$ . We get

$$\begin{aligned} |X_T(f)|^2 &= \int_{t_1=-T/2}^{t_1=T/2} \underbrace{\left[ \int_{\tau=-T/2-t_1}^{t_2=t_1+T/2-t_1} R_x(t_1, t_1 + \tau) e^{-j2\pi f \tau} d\tau \right]}_{\textcircled{1}} dt_1 \quad (6-47) \end{aligned}$$

The area of this two-dimensional integration is shown in Fig. 6-4. On the figure,  $\textcircled{1}$  denotes the area covered by the inner integral times the differential width  $dt_1$ . To evaluate this two-dimensional integral easily, the order of integration will be exchanged. As seen in the figure, this is accomplished by covering the total area by using  $\textcircled{2}$  when  $\tau < 0$  and  $\textcircled{3}$  when  $\tau \geq 0$ . Thus (6-47) becomes

$$\begin{aligned} |X_T(f)|^2 &= \int_{-T}^0 \underbrace{\left[ \int_{t_1=-T/2-\tau}^{t_1=T/2-\tau} R_x(t_1, t_1 + \tau) e^{-j2\pi f \tau} dt_1 \right]}_{\textcircled{2}} d\tau \\ &\quad + \int_0^T \underbrace{\left[ \int_{t_1=-T/2+\tau}^{t_1=T/2-\tau} R_x(t_1, t_1 + \tau) e^{-j2\pi f \tau} dt_1 \right]}_{\textcircled{3}} d\tau \quad (6-48) \end{aligned}$$

Assume that  $x(t)$  is stationary so that  $R_x(t_1, t_1 + \tau) = R_x(\tau)$ , and factor  $R_x(\tau)$  outside the inner integral. We get

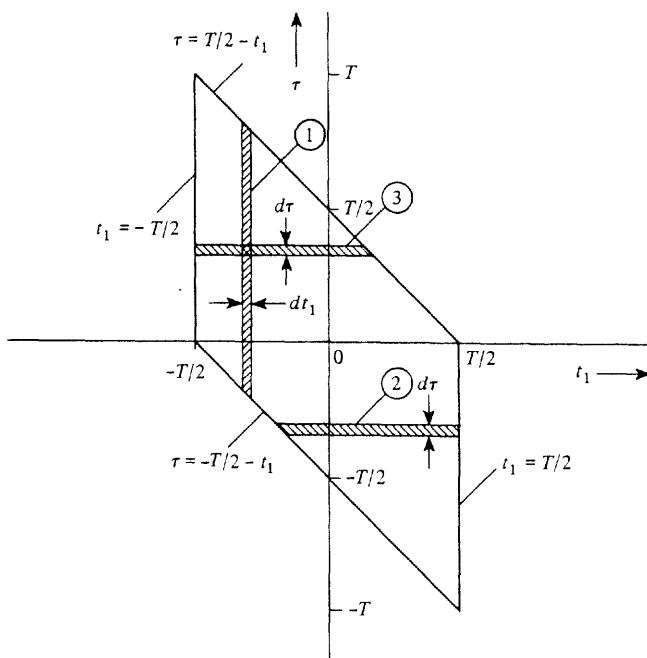


Figure 6-4 Region of integration for (6-47) and (6-48).

$$\begin{aligned} \overline{|X_T(f)|^2} &= \int_{-T}^0 R_x(\tau) e^{-j\omega\tau} \left[ t_1 \begin{vmatrix} T/2 \\ -T/2-\tau \end{vmatrix} \right] d\tau + \int_0^T R_x(\tau) e^{-j\omega\tau} \left[ t_1 \begin{vmatrix} T/2-\tau \\ -T/2 \end{vmatrix} \right] d\tau \\ &= \int_{-T}^0 (T+\tau) R_x(\tau) e^{-j\omega\tau} d\tau + \int_0^T (T-\tau) R_x(\tau) e^{-j\omega\tau} d\tau \end{aligned}$$

This equation can be written compactly as

$$\overline{|X_T(f)|^2} = \int_{-T}^T (T - |\tau|) R_x(\tau) e^{-j\omega\tau} d\tau \quad (6-49)$$

By substituting (6-49) into (6-42), we obtain

$$\mathcal{P}_x(f) = \lim_{T \rightarrow \infty} \int_{-T}^T \left( \frac{T - |\tau|}{T} \right) R_x(\tau) e^{-j\omega\tau} d\tau \quad (6-50a)$$

or

$$\mathcal{P}_x(f) = \int_{-\infty}^{\infty} R_x(\tau) e^{j\omega\tau} d\tau - \lim_{T \rightarrow \infty} \int_{-T}^T \frac{|\tau|}{T} R_x(\tau) e^{-j\omega\tau} d\tau \quad (6-50b)$$

Using the assumption of (6-46), we observe that the right-hand integral is zero and (6-50b) reduces to (6-44). Thus the theorem is proved. The converse relationship follows directly

from the properties of Fourier transforms. Furthermore, if  $x(t)$  is not stationary, (6-44) is still obtained if we replace  $R_x(t_1, t_1 + \tau)$  in (6-48) by  $\langle R_x(t_1, t_1 + \tau) \rangle = R_x(\tau)$ .

Comparing the definition of the PSD with results of the Wiener-Khintchine theorem, we see that there are two distinctly different methods that may be used to evaluate the PSD of a random process.

1. The PSD is obtained directly from the definition as given by (6-42).
2. The PSD is obtained by evaluating the Fourier transform of  $R_x(\tau)$ , where  $R_x(\tau)$  has to be obtained first.

Both methods will be demonstrated in Example 6-3.

### Properties of the PSD

Some properties of the PSD are:

$$1. \mathcal{P}_x(f) \text{ is always real.} \quad (6-51)$$

$$2. \mathcal{P}_x(f) \geq 0. \quad (6-52)$$

$$3. \text{When } x(t) \text{ is real, } \mathcal{P}_x(-f) = \mathcal{P}_x(f). \quad (6-53)$$

$$4. \int_{-\infty}^{\infty} \mathcal{P}_x(f) df = P = \text{total normalized power.} \quad (6-54a)$$

When  $x(t)$  is wide-sense stationary,

$$\int_{-\infty}^{\infty} \mathcal{P}_x(f) df = P = \overline{x^2} = R_x(0) \quad (6-54b)$$

$$5. \mathcal{P}_x(0) = \int_{-\infty}^{\infty} R_x(\tau) d\tau. \quad (6-55)$$

These properties follow directly from the definition and the use of the Wiener-Khintchine theorem.

### Example 6-3 EVALUATION OF THE PSD FOR A POLAR BASEBAND SIGNAL

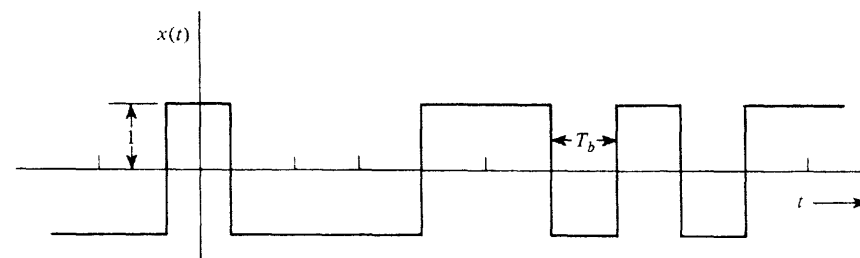
Let  $x(t)$  be a polar signal with random binary data. A sample function of this signal is illustrated in Fig. 6-5a. Assume that the data are independent from bit to bit and that the probability of obtaining a binary 1 during any bit interval is  $\frac{1}{2}$ . Find the PSD of  $x(t)$ .

The polar signal may be modeled by

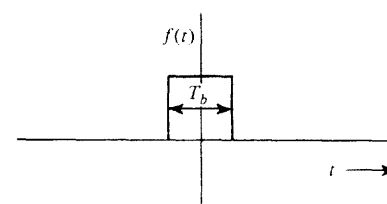
$$x(t) = \sum_{n=-\infty}^{\infty} a_n f(t - nT_b) \quad (6-56)$$

where  $f(t)$  is the signaling pulse shape, as shown in Fig. 6-5b, and  $T_b$  is the duration of one bit.  $\{a_n\}$  is a set of random variables that represent the binary data. It is given that the random variables are independent. It is realized that each one is discretely distributed at  $a_n = \pm 1$  and  $P(a_n = 1) = P(a_n = -1) = \frac{1}{2}$ , as described in the problem statement.

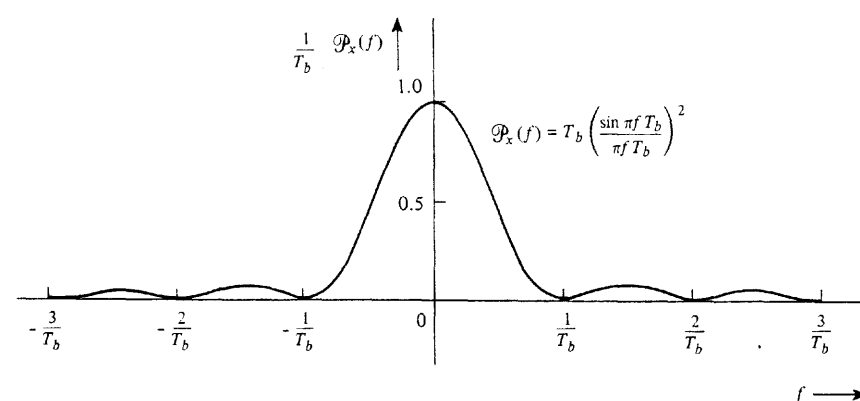
The PSD for  $x(t)$  will be evaluated first by using method 1, which requires that  $X_T(f)$  be obtained. We can obtain  $x_T(t)$  by truncating (6-56).



(a) Polar Signal



(b) Signaling Pulse Shape



(c) Power Spectral Density of a Polar Signal

**Figure 6-5** Random polar signal and its PSD.

where  $T/2 = (N + \frac{1}{2})T_b$ . Then

$$X_T(f) = \mathcal{F}[x_T(t)] = \sum_{n=-N}^N a_n \mathcal{F}[f(t - nT_b)] = \sum_{n=-N}^N a_n F(f) e^{-j\omega n T_b}$$

or

$$X_T(f) = F(f) \sum_{n=-N}^N a_n e^{-j\omega n T_b} \quad (6-57)$$

where  $F(f) = \mathcal{F}[f(t)]$ . When we substitute (6-57) into (6-42), the PSD is

$$\begin{aligned} P_x(f) &= \lim_{T \rightarrow \infty} \left( \frac{1}{T} |F(f)|^2 \left| \sum_{n=-N}^N a_n e^{-j\omega n T_b} \right|^2 \right) \\ &= |F(f)|^2 \lim_{T \rightarrow \infty} \left( \frac{1}{T} \sum_{n=-N}^N \sum_{m=-N}^N \overline{a_n a_m} e^{j(m-n)\omega T_b} \right) \end{aligned} \quad (6-58)$$

The average  $\overline{a_n a_m}$  now needs to be evaluated for the case of polar signaling ( $a_n = \pm 1$ ).

$$\overline{a_n a_m} = \begin{cases} \overline{a_n^2}, & n = m \\ \overline{a_n a_m}, & n \neq m \end{cases}$$

where  $\overline{a_n a_m} = \overline{a_n} \overline{a_m}$  for  $n \neq m$  since  $a_n$  and  $a_m$  are independent. Using the discrete distribution for  $a_n$ , we get

$$\overline{a_n} = (+1)^{\frac{1}{2}} + (-1)^{\frac{1}{2}} = 0$$

Similarly,  $\overline{a_m} = 0$ . Further,

$$\overline{a_n^2} = (+1)^2(\frac{1}{2}) + (-1)^2(\frac{1}{2}) = 1$$

Thus,

$$\overline{a_n a_m} = \begin{cases} 1, & n = m \\ 0, & n \neq m \end{cases} \quad (6-59)$$

With this result, (6-58) becomes

$$P_x(f) = |F(f)|^2 \lim_{T \rightarrow \infty} \left( \frac{1}{T} \sum_{n=-N}^N 1 \right)$$

and, with  $T = 2(N + \frac{1}{2})T_b$ ,

$$P_x(f) = |F(f)|^2 \lim_{N \rightarrow \infty} \left[ \frac{2N + 1}{(2N + 1)T_b} \right]$$

or

$$P_x(f) = \frac{1}{T_b} |F(f)|^2 \quad (\text{polar signaling}) \quad (6-60)$$

For the rectangular pulse shape shown in Fig. 6-5b,

$$F(f) = T_b \left( \frac{\sin \pi f T_b}{\pi f T_b} \right) \quad (6-61)$$

Thus the PSD for a polar signal with a rectangular pulse shape is

$$P_x(f) = T_b \left( \frac{\sin \pi f T_b}{\pi f T_b} \right)^2 \quad (6-62)$$

This PSD is plotted in Fig. 6-5c.<sup>†</sup> The null bandwidth is  $B = 1/T_b = R$ , where  $R$  is the bit rate. Note that (6-62) satisfies the properties for a PSD function as listed above.

Method 2 will now be used to evaluate the PSD of the polar signal. This involves calculating the autocorrelation function and then evaluating the Fourier transform of  $R_x(\tau)$  to obtain the PSD. When we use (6-56), the autocorrelation is

$$\begin{aligned} R_x(t, t + \tau) &= \overline{x(t)x(t + \tau)} \\ &= \overline{\sum_{n=-\infty}^{\infty} a_n f(t - nT_b) \sum_{m=-\infty}^{\infty} a_m f(t + \tau - mT_b)} \\ &= \sum_n \sum_m \overline{a_n a_m} f(t - nT_b) f(t + \tau - mT_b) \end{aligned}$$

By using (6-59), this equation reduces to

$$R_x(t, t + \tau) = \sum_{n=-\infty}^{\infty} f(t - nT_b) f(t + \tau - nT_b) \quad (6-63)$$

Obviously,  $x(t)$  is not a wide-sense stationary process since the autocorrelation function depends on absolute time,  $t$ . To reduce (6-63) a particular type of pulse shape needs to be designated. Assume, once again, the rectangular pulse shape

$$f(t) = \begin{cases} 1, & |t| \leq T_b/2 \\ 0, & \text{elsewhere} \end{cases}$$

The pulse product then becomes

$$f(t - nT_b) f(t + \tau - nT_b) = \begin{cases} 1, & \text{if } |t - nT_b| \leq T_b/2 \text{ and } |t + \tau - nT_b| \leq T_b/2 \\ 0, & \text{otherwise} \end{cases}$$

Working with the inequalities, we get a unity product only when

$$(n - \frac{1}{2})T_b \leq t \leq (n + \frac{1}{2})T_b$$

and

$$(n - \frac{1}{2})T_b - \tau \leq t \leq (n + \frac{1}{2})T_b - \tau$$

Assume that  $\tau \geq 0$ ; then we will have a unity product when

$$(n - \frac{1}{2})T_b \leq t \leq (n + \frac{1}{2})T_b - \tau$$

provided that  $\tau \leq T_b$ . Thus, for  $0 \leq \tau \leq T_b$ ,

$$R_x(t, t + \tau) = \sum_{n=-\infty}^{\infty} \begin{cases} 1, & (n - \frac{1}{2})T_b \leq t \leq (n + \frac{1}{2})T_b - \tau \\ 0, & \text{otherwise} \end{cases} \quad (6-64)$$

We know that the Wiener-Khintchine theorem is valid for nonstationary processes if we let  $R_x(\tau) = \langle R_x(t, t + \tau) \rangle$ . Using (6-64), we get

<sup>†</sup> The PSD of this polar signal is purely continuous since the positive and negative pulses are assumed to be of equal amplitude.

$$R_x(\tau) = \langle R_x(t, t + \tau) \rangle = \lim_{T \rightarrow \infty} \frac{1}{T} \int_{-T/2}^{T/2} \sum_{n=-\infty}^{\infty} \begin{cases} 1, & (n - \frac{1}{2})T_b \leq t \leq (n + \frac{1}{2})T_b - \tau \\ 0, & \text{elsewhere} \end{cases} dt$$

or

$$R_x(\tau) = \lim_{N \rightarrow \infty} \frac{1}{T} \sum_{n=-N}^N \left( \int_{(n+1/2)T_b}^{(n+1/2)T_b - \tau} 1 dt \right)$$

where  $T/2 = (N - \frac{1}{2})T_b$ . This reduces to

$$R_x(\tau) = \lim_{N \rightarrow \infty} \left[ \frac{1}{(2N+1)T_b} (2N+1) \begin{cases} (T_b - \tau), & 0 \leq \tau \leq T_b \\ 0, & \tau > T_b \end{cases} \right]$$

or

$$R_x(\tau) = \begin{cases} \frac{T_b - \tau}{T_b}, & 0 \leq \tau \leq T_b \\ 0, & \tau > T_b \end{cases} \quad (6-65)$$

Similarly, for  $\tau < 0$ , results can be obtained. However, we know that  $R_x(-\tau) = R_x(\tau)$ , so (6-65) can be generalized for all values of  $\tau$ . Thus

$$R_x(\tau) = \begin{cases} \frac{T_b - |\tau|}{T_b}, & |\tau| \leq T_b \\ 0, & \text{otherwise} \end{cases} \quad (6-66)$$

which shows that  $R_x(\tau)$  has a triangular shape. Evaluating the Fourier transform of (6-66), we obtain the PSD for the polar signal with a rectangular bit shape:

$$\mathcal{P}_x(f) = T_b \left( \frac{\sin \pi f T_b}{\pi f T_b} \right)^2 \quad (6-67)$$

This result, obtained by the use of method 2, is identical to (6-62), obtained by using method 1.

### General Formula for the PSD of Digital Signals

A general formula for the PSD of digital signals will now be obtained. The formulas for the PSD in Example 6-3 are valid only for polar signaling with  $a_n = \pm 1$  and no correlation between the bits. A more general result can be obtained by starting with (6-56) and obtaining a result in terms of the autocorrelation of the data,  $a_n$ . As illustrated in Figs. 3-12 and 3-14, the data may be binary or may be multilevel. The duration (width) of the symbol pulse,  $f(t)$ , is  $T_s$ . For binary data  $T_s = T_b$ , where  $T_b$  is the duration of 1 bit. Define the autocorrelation of the data by

$$R(k) = \overline{a_n a_{n+k}} \quad (6-68)$$

Make a change in the index in (6-58), letting  $m = n + k$ . Then, by using (6-68) and  $T = (2N+1)T_b$ , (6-58) becomes

$$\mathcal{P}_x(f) = |F(f)|^2 \lim_{N \rightarrow \infty} \left[ \frac{1}{(2N+1)T_s} \sum_{n=-N}^{n=N} \sum_{k=-N-n}^{k=N-n} R(k) e^{jk\omega T_s} \right]$$

Replacing the outer sum over the index  $n$  by  $2N + 1$ , we obtain the following expression. (This procedure is not strictly correct since the inner sum is also a function of  $n$ . The correct procedure would be to exchange the order of summation, similar to that used in (6-47) through (6-50) where the order of integration was exchanged. The result would be the same as that as obtained below when the limit is evaluated as  $N \rightarrow \infty$ .)

$$\begin{aligned} \mathcal{P}_x(f) &= \frac{|F(f)|^2}{T_s} \lim_{N \rightarrow \infty} \left[ \frac{(2N+1)}{(2N+1)T_s} \sum_{k=-N-n}^{k=N-n} R(k) e^{jk\omega T_s} \right] \\ &= \frac{|F(f)|^2}{T_s} \sum_{k=-\infty}^{k=\infty} R(k) e^{jk\omega T_s} \\ &= \frac{|F(f)|^2}{T_s} \left[ R(0) + \sum_{k=-\infty}^{-1} R(k) e^{jk\omega T_s} + \sum_{k=1}^{\infty} R(k) e^{jk\omega T_s} \right] \end{aligned}$$

or

$$\mathcal{P}_x(f) = \frac{|F(f)|^2}{T_s} \left[ R(0) + \sum_{k=1}^{\infty} R(-k) e^{-jk\omega T_s} + \sum_{k=1}^{\infty} R(k) e^{jk\omega T_s} \right] \quad (6-69)$$

But because  $R(k)$  is an autocorrelation function,  $R(-k) = R(k)$  and (6-69) becomes

$$\mathcal{P}_x(f) = \frac{|F(f)|^2}{T_s} \left[ R(0) + \sum_{k=1}^{\infty} R(k) (e^{jk\omega T_s} + e^{-jk\omega T_s}) \right]$$

In summary, the general expression for the PSD of a digital signal is

$$\mathcal{P}_x(f) = \frac{|F(f)|^2}{T_s} \left[ R(0) + 2 \sum_{k=1}^{\infty} R(k) \cos(2\pi k f T_s) \right] \quad (6-70a)$$

or, an equivalent expression is

$$\boxed{\mathcal{P}_x(f) = \frac{|F(f)|^2}{T_s} \left[ \sum_{k=-\infty}^{\infty} R(k) e^{jk\omega T_s} \right]} \quad (6-70b)$$

where the autocorrelation of the data is

$$R(k) = \overline{a_n a_{n+k}} = \sum_{i=1}^I (a_n a_{n+k})_i P_i \quad (6-70c)$$

$P_i$  is the probability of getting the product  $(a_n a_{n+k})_i$ , and there are  $I$  possible values for the  $a_n a_{n+k}$  product.  $F(f)$  is the spectrum of the pulse shape of the digital symbol.

Note that the quantity in the brackets of (6-70b) is similar to the discrete Fourier transform (DFT) of the data autocorrelation function,  $R(k)$ , except that the frequency variable,  $\omega$ , is continuous. Thus the PSD of the baseband digital signal is influenced by both the "spectrum" of the data and the spectrum of the pulse shape used for the line code. Furthermore, we will now demonstrate that the spectrum may also contain delta functions if the mean value of the data,  $\bar{a}_n$ , is nonzero. To do so, we first assume that the data symbols are uncorrelated; that is,

$$R(k) = \begin{cases} \overline{a_n^2}, & k = 0 \\ \overline{a_n a_{n+k}}, & k \neq 0 \end{cases} = \begin{cases} \sigma_a^2 + m_a^2, & k = 0 \\ m_a^2, & k \neq 0 \end{cases}$$

where, as defined in Appendix B, the mean and the variance for the data are  $m_a = \bar{a}_n$  and  $\sigma_a^2 = (a_n - m_a)^2 = \overline{a_n^2} - m_a^2$ . Substituting this into (6-70b), we get

$$\mathcal{P}_x(f) = \frac{|F(f)|^2}{T_s} \left[ \sigma_a^2 + m_a^2 \sum_{k=-\infty}^{\infty} e^{jk\omega T_s} \right]$$

From (2-115), recalling the Poisson sum formula,

$$\sum_{k=-\infty}^{\infty} e^{\pm jk\omega T_s} = D \sum_{n=-\infty}^{\infty} \delta(f - nD)$$

where  $D = 1/T_s$  is the baud (rate). We see that the PSD becomes

$$\mathcal{P}_x(f) = \frac{|F(f)|^2}{T_s} \left[ \sigma_a^2 + m_a^2 D \sum_{n=-\infty}^{\infty} \delta(f - nD) \right]$$

Thus, for the case of uncorrelated data, the PSD of the digital signal is

$$\mathcal{P}_x(f) = \underbrace{\sigma_a^2 D |F(f)|^2}_{\text{Continuous spectrum}} + \underbrace{(m_a D)^2 \sum_{n=-\infty}^{\infty} |F(nD)|^2 \delta(f - nD)}_{\text{Discrete spectrum}} \quad (6-70d)$$

For the general case where there is correlation between the data, let the data autocorrelation function,  $R(k)$ , be expressed in terms of the *normalized data* autocorrelation function,  $\rho(k)$ . That is, let  $\tilde{a}_n$  represent the corresponding data that have been normalized to have unity variance and zero mean. Thus

$$a_n = \sigma_a \tilde{a}_n + m_a$$

and, consequently,

$$R(k) = \sigma_a^2 \rho(k) + m_a^2$$

where

$$\rho(k) = \overline{[\tilde{a}_n \tilde{a}_{n+k}]}$$

Substituting this expression for  $R(k)$  into (6-70b) and using  $R(-k) = R(k)$ , we get

$$\mathcal{P}_x(f) = \frac{|F(f)|^2}{T_s} \left[ \sigma_u^2 \sum_{k=-\infty}^{\infty} \rho(k) e^{-jk\omega T_s} + m_d^2 \sum_{k=-\infty}^{\infty} e^{-jk\omega T_s} \right]$$

Thus, for the general case of correlated data, the PSD of the digital signal is

$$\mathcal{P}_x(f) = \underbrace{\sigma_u^2 D |F(f)|^2 W_p(f)}_{\text{Continuous spectrum}} + \underbrace{(m_d D)^2 \sum_{n=-\infty}^{\infty} |F(nD)|^2 \delta(f - nD)}_{\text{Discrete spectrum}} \quad (6-70e)$$

where

$$W_p(f) \sum_{k=-\infty}^{\infty} \rho(k) e^{-j2\pi kfT_s} \quad (6-70f)$$

is a spectral weight function obtained from the Fourier transform of the normalized autocorrelation impulse train

$$\sum_{k=-\infty}^{\infty} \rho(k) \delta(\tau - kT_s)$$

This demonstrates that the PSD of the digital signal consists of a continuous spectrum that depends on the pulse-shape spectrum,  $F(f)$ , and the data correlation. Furthermore, if  $m_d \neq 0$  and  $F(nD) \neq 0$ , the PSD will also contain spectral lines (delta functions) spaced at harmonics of the baud rate,  $D$ .

Examples of the application of these results are given in Sec. 3-5, where the PSD for unipolar RZ, bipolar, and Manchester line codes are evaluated. See Fig. 3-16 for a plot of the PSDs for these examples. Examples of bandpass digital signaling, such as OOK, BPSK, QPSK, MPSK, MPSK and QAM, are given in Sections 5-9 and 5-10.

## White Noise Processes

**DEFINITION.** A random process  $x(t)$  is said to be a *white noise process* if the PSD is constant over all frequencies:

$$\mathcal{P}_x(f) = \frac{N_0}{2} \quad (6-71)$$

where  $N_0$  is a positive constant.

The autocorrelation function for the white noise process is obtained by taking the inverse Fourier transform of (6-71). The result is

$$R_x(\tau) = \frac{N_0}{2} \delta(\tau) \quad (6-72a)$$

For example, the thermal noise process, as described in Sec. 8-6, can be considered to be a white noise process over the operating band where

$$N_0 = kT \quad (6-72b)$$

Thermal noise also happens to have a Gaussian distribution. Of course, it is also possible to have white noise with other distributions.

## Measurement of PSD

The PSD may be measured using analog or digital techniques. In either case, the measurement can only approximate the true PSD because the measurement is carried out over a finite time interval instead of the infinite interval as specified as (6-42).

**Analog Techniques.** The analog measurement technique consists of using either a bank of parallel narrowband bandpass filters with contiguous bandpass characteristics or by using a single bandpass filter that has a center frequency that is tunable. For the case of the filter bank, the waveform is fed simultaneously into the inputs of all the filters and the power at the output of each filter is evaluated. These output powers are divided (scaled) by the effective bandwidth of the corresponding filter so that an approximation for the PSD is obtained. That is, the PSD is evaluated for the frequency points corresponding to the center frequencies of the filters. Spectrum analyzers with this parallel type of analog processing are usually designed to cover the audio range of the spectrum where it is economically feasible to build a bank of bandpass filters.

RF spectrum analyzers are usually built using a single narrowband IF bandpass filter that is fed from the output of a mixer (up or down converter) circuit. The local oscillator (LO) of the mixer is swept slowly across an appropriate frequency band so that the RF spectrum analyzer is equivalent to a tunable narrowband bandpass filter where the center frequency of the tunable filter is swept across the desired spectral range. Once again, the PSD is obtained by evaluating the scaled power output of the narrowband filter as a function of the sweep frequency.

**Numerical Computation of the PSD.** The PSD is evaluated numerically in spectrum analyzers that use digital signal processing. One approximation for the PSD is

$$\mathcal{P}_T(f) = \frac{|X_T(f)|^2}{T} \quad (6-73a)$$

where the subscript  $T$  indicates that this approximation is obtained by viewing  $x(t)$  over a  $T$ -s interval.  $T$  is called the *observation interval* or *observation length*. Of course, (6-73a) is an approximation to the true PSD as defined in (6-42) because  $T$  is finite and because only a sample of the ensemble is used. In more sophisticated spectrum analyzers,  $\mathcal{P}_T(f)$  is evaluated for several  $x(t)$  records and the average value of  $\mathcal{P}_T(f)$  at each frequency is used to approximate the ensemble average required for a true  $\mathcal{P}_x(f)$  as defined in (6-42). In evaluating  $\mathcal{P}_T(f)$ , the DFT is generally used to approximate  $X_T(f)$ . This brings the pitfalls of DFT analysis into play, as described in Sec. 2-8.

It should be stressed that (6-73a) is an approximation or *estimate* of the PSD. This estimate is called a *periodogram* because it was used historically to search for periodicities in data records that appear as delta functions in the PSD. [Delta functions are relatively easy to find in the PSD, and thus the periodicities in  $x(t)$  are easily determined.] It is desirable that the estimate have an ensemble average that gives the true PSD. If this is the case, the estimator is said to be *unbiased*. We can easily check (6-73a) to see if it is unbiased.

$$\overline{\mathcal{P}_T(f)} = \left[ \frac{|X_T(f)|^2}{T} \right]$$

and, using (6-50a) for  $T$  finite, we obtain

$$\overline{\mathcal{P}_T(f)} = \mathcal{F} \left[ R_x(\tau) \Lambda \left( \frac{\tau}{T} \right) \right]$$

and then, referring to Table 2-2,

$$\overline{\mathcal{P}_T(f)} = T \mathcal{P}_x(f) * \left( \frac{\sin \pi f T}{\pi f T} \right)^2 \quad (6-73b)$$

Because  $\overline{\mathcal{P}_T(f)} \neq \mathcal{P}_x(f)$ , the periodogram is a *biased* estimate. The bias is caused by the triangular window function,  $\Lambda(\tau/T)$ , that arises from the truncation of  $x(t)$  to a  $T$ -second interval. Using (A-103) where  $a = \pi T$ , we see that  $\lim_{T \rightarrow \infty} [\overline{\mathcal{P}_T(f)}] = \mathcal{P}_x(f)$  so that the periodogram becomes unbiased as  $T \rightarrow \infty$ . Consequently, the periodogram is said to be *asymptotically unbiased*.

In addition to being unbiased, it is desirable that an estimator be *consistent*. This means that the variance of the estimator should become small as  $T \rightarrow \infty$ . In this regard, it can be shown that (6-73a) gives an *inconsistent* estimate of the PSD when  $x(t)$  is Gaussian [Bendat and Piersol, 1971].

Of course, window functions other than the triangle can be used to obtain different PSD estimators [Blackman and Tukey, 1958; Jenkins and Watts, 1968]. More modern techniques assume a mathematical model (i.e., form) for the autocorrelation function and estimate parameters for this model. The model is then checked to see if it is consistent with the data. Examples are the *moving average* (MA), *autoregressive* (AR), and the *autoregressive-moving average* (ARMA) models [Kay, 1986; Kay and Marple, 1981; Marple, 1986; Scharf, 1991; Shanmugan and Breipohl, 1988].

Spectrum analyzers that use microprocessor-based circuits often utilize numerical techniques to evaluate the PSD. These instruments can evaluate the PSD only for relatively low-frequency waveforms, say, over the audio or ultrasonic frequency range, since real-time digital signal-processing circuits cannot be built to process signals at RF rates.

## 6-3 DC AND RMS VALUES FOR ERGODIC RANDOM PROCESSES

In Chapter 2 the dc value, the rms value, and the average power were defined in terms of time average operations. For ergodic processes these time averages are equivalent to en-

semble averages. Thus the dc value, the rms value, and the average power (which are all fundamental concepts in electrical engineering) can be related to the moments of an ergodic random process. A summary of these relationships follows.  $x(t)$  is an ergodic random process that may correspond to either a voltage or a current waveform.

### 1. Dc value:

$$X_{dc} \triangleq \langle x(t) \rangle \equiv \bar{x} = m_x \quad (6-74)$$

### 2. Normalized dc power:

$$P_{dc} \triangleq [\langle x(t) \rangle]^2 \equiv (\bar{x})^2 \quad (6-75)$$

### 3. Rms value:

$$X_{rms} \triangleq \sqrt{\langle x^2(t) \rangle} \equiv \sqrt{\langle \bar{x}^2 \rangle} = \sqrt{R_x(0)} = \sqrt{\int_{-\infty}^{\infty} \mathcal{P}_x(f) df} \quad (6-76)$$

### 4. Rms value of the ac part:

$$\begin{aligned} (X_{rms})_{ac} &\triangleq \sqrt{\langle (x(t) - X_{dc})^2 \rangle} \equiv \sqrt{\langle \bar{x}^2 \rangle} \\ &= \sqrt{\bar{x}^2 - (\bar{x})^2} = \sqrt{R_x(0) - (\bar{x})^2} \\ &= \sqrt{\int_{-\infty}^{\infty} \mathcal{P}_x(f) df - (\bar{x})^2} = \sigma_x = \text{standard deviation} \end{aligned} \quad (6-77)$$

### 5. Normalized total average power:

$$P \triangleq \langle x^2(t) \rangle \equiv \bar{x}^2 = R_x(0) = \int_{-\infty}^{\infty} \mathcal{P}_x(f) df \quad (6-78)$$

### 6. Normalized average power of the ac part:

$$\begin{aligned} P_{ac} &\triangleq \langle (x(t) - X_{dc})^2 \rangle \equiv \bar{x}^2 \\ &= \bar{x}^2 - (\bar{x})^2 = R_x(0) - (\bar{x})^2 \\ &= \int_{-\infty}^{\infty} \mathcal{P}_x(f) df - (\bar{x})^2 = \sigma_x^2 = \text{variance} \end{aligned} \quad (6-79)$$

Furthermore, commonly available laboratory equipment may be used to evaluate the mean, second moment, and variance of an ergodic process. For example, if  $x(t)$  is a voltage waveform,  $\bar{x}$  can be measured by using a dc voltmeter and  $\sigma_x$  can be measured by using a

"true rms" (ac coupled) voltmeter.<sup>†</sup> Using the measurements, we easily obtain the second moment from  $\bar{x}^2 = \sigma_x^2 + (\bar{x})^2$ . At higher frequencies (e.g., radio, microwave, and optical),  $\bar{x}^2$  and  $\sigma_x^2$  can be measured by using a calibrated power meter. That is,  $\sigma_x^2 = \bar{x}^2 = RP$ , where  $R$  is the load resistance of the power meter (usually  $50\ \Omega$ ) and  $P$  is the reading obtained from the power meter.

## 6-4 LINEAR SYSTEMS

### Input-Output Relationships

As developed in Chapter 2, a linear time-invariant system may be described by its impulse response  $h(t)$  or, equivalently, by its transfer function  $H(f)$ . This is illustrated in Fig. 6-6, where  $x(t)$  is the input and  $y(t)$  is the output. The input-output relationships are

$$y(t) = h(t) * x(t) \quad (6-80)$$

The corresponding Fourier transform relationships are

$$Y(f) = H(f)X(f) \quad (6-81)$$

If  $x(t)$  and  $y(t)$  are random processes, these relationships are still valid (just as they were for the case of deterministic functions). In communication systems  $x(t)$  might be a random signal plus (random) noise, or  $x(t)$  might be noise alone when the signal is absent. For the case of random processes, autocorrelation functions and PSD functions may be used to describe the frequencies involved. Consequently, we need to address the question: What is the autocorrelation function and the PSD for the output process  $y(t)$  when the autocorrelation and PSD for the input  $x(t)$  are known?

**THEOREM.** If a wide-sense stationary random process,  $x(t)$ , is applied to the input of a time-invariant linear network with impulse response  $h(t)$ , the output autocorrelation is

$$R_y(\tau) = \int_{-\infty}^{\infty} \int_{-\infty}^{\infty} h(\lambda_1)h(\lambda_2)R_x(\tau - \lambda_2 + \lambda_1) d\lambda_1 d\lambda_2 \quad (6-82a)$$

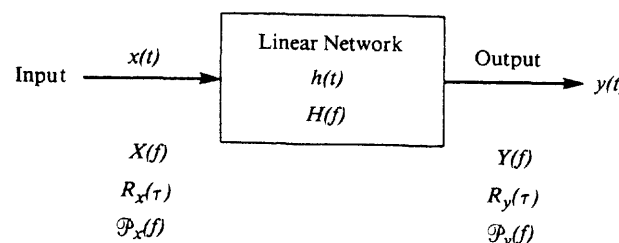


Figure 6-6 Linear system.

<sup>†</sup> Most "true rms" meters do not have a frequency response down to dc. Thus, they do not measure the true rms value  $\sqrt{\langle x^2(t) \rangle} = \sqrt{\bar{x}^2}$ ; instead, they measure  $\sigma$ .

or

$$R_y(\tau) = h(-\tau) * h(\tau) * R_x(\tau) \quad (6-82b)$$

The output PSD is

$$\mathcal{P}_y(f) = |H(f)|^2 \mathcal{P}_x(f) \quad (6-83)$$

where  $H(f) = \mathcal{F}[h(t)]$ .

It is also realized that (6-83) shows that the power transfer function of the network is

$$G_h(f) = \frac{\mathcal{P}_y(f)}{\mathcal{P}_x(f)} = |H(f)|^2 \quad (6-84)$$

as cited by (2-143).

**Proof.** From (6-80)

$$R_y(\tau) \triangleq \overline{y(t)y(t + \tau)}$$

$$\begin{aligned} &= \left[ \int_{-\infty}^{\infty} h(\lambda_1)x(t - \lambda_1) d\lambda_1 \right] \left[ \int_{-\infty}^{\infty} h(\lambda_2)x(t + \tau - \lambda_2) d\lambda_2 \right] \\ &= \int_{-\infty}^{\infty} \int_{-\infty}^{\infty} h(\lambda_1)h(\lambda_2)\overline{x(t - \lambda_1)x(t + \tau - \lambda_2)} d\lambda_1 d\lambda_2 \end{aligned} \quad (6-85)$$

But

$$\overline{x(t - \lambda_1)x(t + \tau - \lambda_2)} = R_x(t + \tau - \lambda_2 - t + \lambda_1) = R_x(\tau - \lambda_2 + \lambda_1)$$

so (6-85) is equivalent to (6-82a). Furthermore, (6-82a) may be written in terms of convolution operations as follows:

$$\begin{aligned} R_y(\tau) &= \int_{-\infty}^{\infty} h(\lambda_1) \left\{ \int_{-\infty}^{\infty} h(\lambda_2)R_x[(\tau + \lambda_1) - \lambda_2] d\lambda_2 \right\} d\lambda_1 \\ &= \int_{-\infty}^{\infty} h(\lambda_1) \{ h(\tau + \lambda_1) * R_x(\tau + \lambda_1) \} d\lambda_1 \\ &= \int_{-\infty}^{\infty} h(\lambda_1) \{ h[-((-\tau) - \lambda_1)] * R_x[-((-\tau) - \lambda_1)] \} d\lambda_1 \\ &= h(-\tau) * h[-(-\tau)] * R_x[-(-\tau)] \end{aligned}$$

which is equivalent to the convolution notation of (6-82b).

The PSD of the output is obtained by taking the Fourier transform of (6-82b).

$$\mathcal{F}[R_y(\tau)] = \mathcal{F}[h(-\tau)] \mathcal{F}[h(\tau) * R_x(\tau)]$$

or

$$\mathcal{P}_y(f) = H^*(f) H(f) \mathcal{P}_x(f)$$

where  $h(t)$  is assumed to be real. This equation is equivalent to (6-83).

This theorem may be applied to cascaded linear systems. For example, two cascaded networks are shown in Fig. 6-7.

This theorem may also be generalized to obtain the cross-correlation or cross-spectrum of two linear systems, as illustrated in Fig. 6-8.  $x_1(t)$  and  $y_1(t)$  are the input and output processes of the first system, which has the impulse response  $h_1(t)$ . Similarly,  $x_2(t)$  and  $y_2(t)$  are the input and output processes for the second system.

**THEOREM.** Let  $x_1(t)$  and  $x_2(t)$  be wide-sense stationary inputs for two time-invariant linear systems, as shown in Fig. 6-8; then the output cross-correlation function is

$$R_{y_1 y_2}(\tau) = \int_{-\infty}^{\infty} \int_{-\infty}^{\infty} h_1(\lambda_1) h_2(\lambda_2) R_{x_1 x_2}(\tau - \lambda_2 + \lambda_1) d\lambda_1 d\lambda_2 \quad (6-86a)$$

or

$$R_{y_1 y_2}(\tau) = h_1(-\tau) * h_2(\tau) * R_{x_1 x_2}(\tau) \quad (6-86b)$$

Furthermore, by definition the output cross power spectral density is the Fourier transform of the cross-correlation function; thus

$$\mathcal{P}_{y_1 y_2}(f) = H_1^*(f) H_2(f) \mathcal{P}_{x_1 x_2}(f) \quad (6-87)$$

where  $\mathcal{P}_{y_1 y_2}(f) = \mathcal{F}[R_{y_1 y_2}(\tau)]$ ,  $\mathcal{P}_{x_1 x_2}(f) = \mathcal{F}[R_{x_1 x_2}(\tau)]$ ,  $H_1(f) = \mathcal{F}[h_1(t)]$ , and  $H_2(f) = \mathcal{F}[h_2(t)]$ .

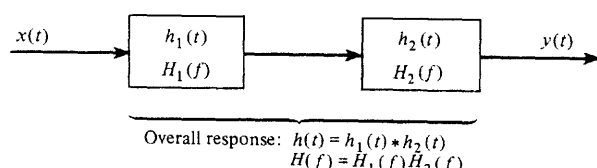


Figure 6-7 Two linear cascaded networks.

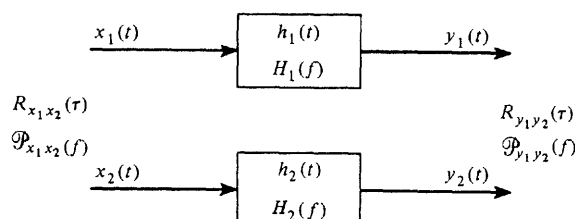


Figure 6-8 Two linear systems.

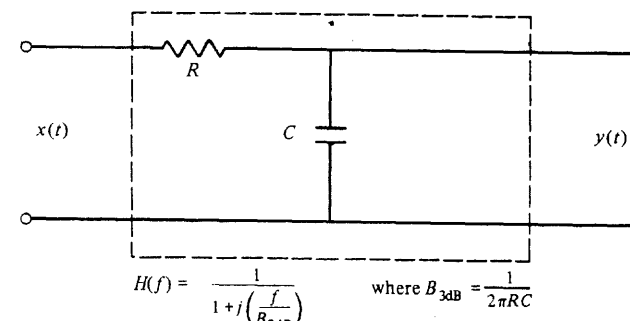


Figure 6-9 RC LPF

The proof of this theorem is similar to that for the preceding theorem and will be left to the reader as an exercise.

#### Example 6-4 OUTPUT AUTOCORRELATION AND PSD FOR AN RC LOW-PASS FILTER

An RC low-pass filter (LPF) is shown in Fig. 6-9. Assume that the input is an ergodic random process with a uniform PSD:

$$\mathcal{P}_x(f) = \frac{1}{2} N_0$$

Then the PSD of the output is

$$\mathcal{P}_y(f) = |H(f)|^2 \mathcal{P}_x(f)$$

which becomes

$$\mathcal{P}_y(f) = \frac{\frac{1}{2} N_0}{1 + (f/B_{3dB})^2} \quad (6-88)$$

where  $B_{3dB} = 1/(2\pi RC)$ . Note that  $\mathcal{P}_y(B_{3dB})/\mathcal{P}_y(0)$  is  $\frac{1}{2}$ , so  $B_{3dB} = 1/(2\pi RC)$  is indeed the 3-dB bandwidth. Taking the inverse Fourier transform of  $\mathcal{P}_y(f)$  as described by (6-88), we obtain the output autocorrelation function for the RC filter.

$$R_y(\tau) = \frac{N_0}{4RC} e^{-|\tau|/(RC)} \quad (6-89)$$

The normalized output power which is the second moment of the output is

$$P_y = \overline{y^2} = R_y(0) = \frac{N_0}{4RC} \quad (6-90)$$

Furthermore, the dc value of the output, which is the mean value, is zero since<sup>†</sup>

$$Y_{DC} = m_y = \sqrt{\lim_{\epsilon \rightarrow 0} \int_{-\epsilon}^{\epsilon} \mathcal{P}_y(f) df} = 0 \quad (6-91)$$

The variance of the output is also given by (6-90) since  $\sigma_y^2 = \overline{y^2} - m_y^2$ , where  $m_y = 0$ .

<sup>†</sup> When the integral is nonzero, the value obtained is equal or larger than the square of the mean value.

**Example 6-5 SIGNAL-TO-NOISE RATIO AT THE OUTPUT OF AN RC LOW-PASS FILTER**

Refer to Fig. 6-9 again and assume that  $x(t)$  consists of a sine-wave (deterministic) signal plus white ergodic noise. Thus

$$x(t) = s_i(t) + n_i(t)$$

and

$$s_i(t) = A_0 \cos(\omega_0 t + \theta_0)$$

where  $A_0$ ,  $\omega_0$ , and  $\theta_0$  are known constants and  $\mathcal{P}_{n_i}(f) = N_0/2$ . The input signal power is

$$\langle s_i^2(t) \rangle = \frac{A_0^2}{2}$$

and the input noise power is

$$\langle n_i^2(t) \rangle = \overline{n_i^2} = \int_{-\infty}^{\infty} \mathcal{P}_{n_i}(f) df = \int_{-\infty}^{\infty} \frac{N_0}{2} df = \infty$$

Thus the input signal-to-noise (SNR) ratio is

$$\left( \frac{S}{N} \right)_{\text{in}} = \frac{\langle s_i^2(t) \rangle}{\langle n_i^2(t) \rangle} = 0 \quad (6-92)$$

The output consists of the sum of the filtered input signal plus the filtered input noise since the system is linear.

$$y(t) = s_0(t) + n_0(t)$$

The output signal is

$$\begin{aligned} s_0(t) &= s_i(t) * h(t) \\ &= A_0 |H(f_0)| \cos[\omega_0 t + \theta_0 + \angle H(f_0)] \end{aligned}$$

and the output signal power is

$$\langle s_0^2(t) \rangle = \frac{A_0^2}{2} |H(f_0)|^2 \quad (6-93)$$

From (6-90) of Example 6-4, the output noise power is

$$\overline{n_0^2} = \frac{N_0}{4RC} \quad (6-94)$$

The output SNR is then

$$\left( \frac{S}{N} \right)_{\text{out}} = \frac{\langle s_0^2(t) \rangle}{\langle n_0^2(t) \rangle} = \frac{\langle s_0^2(t) \rangle}{\overline{n_0^2}} = \frac{2A_0^2 |H(f_0)|^2 RC}{N_0} \quad (6-95)$$

or

$$\left( \frac{S}{N} \right)_{\text{out}} = \frac{2A_0^2 RC}{N_0 [1 + (2\pi f_0 RC)^2]}$$

Using calculus, the reader is encouraged to find the value of  $RC$  that maximizes the SNR. It is  $RC = 1/(2\pi f_0)$ . Thus, for maximum SNR, the filter is designed to have a 3-dB bandwidth equal to  $f_0$ .

## 6-5 BANDWIDTH MEASURES

Several bandwidth measures were defined in Sec. 2-9, namely, absolute bandwidth, 3-dB bandwidth, equivalent bandwidth, null-to-null (zero-crossing) bandwidth, bounded bandwidth, power bandwidth, and the FCC bandwidth parameter. These definitions can be applied to evaluate the bandwidth of a wide-sense stationary process  $x(t)$ , where  $\mathcal{P}_x(f)$  replaces  $|H(f)|^2$  in the definitions. In this section we review the equivalent bandwidth and define a new bandwidth measure, rms bandwidth.

### Equivalent Bandwidth

For a wide-sense stationary process  $x(t)$ , the equivalent bandwidth, as defined by (2-192), becomes

$$B_{\text{eq}} = \frac{1}{\mathcal{P}_x(f_0)} \int_0^{\infty} \mathcal{P}_x(f) df = \frac{R_x(0)}{2\mathcal{P}_x(f_0)} \quad (6-96)$$

$f_0$  is the frequency where  $\mathcal{P}_x(f)$  is a maximum. This equation is valid for both bandpass and baseband processes (where  $f_0 = 0$  is used for baseband processes).

### Rms Bandwidth

The rms bandwidth is the square root of the second moment of the frequency with respect to a properly normalized PSD. In this case,  $f$ , although not random, may be *treated* as a random variable that has the “density function”  $\mathcal{P}_x(f)/\int_{-\infty}^{\infty} \mathcal{P}_x(\lambda) d\lambda$ . This is a nonnegative function in which the denominator provides the correct normalization so that the integrated value of this ratio is unity. Thus this function satisfies the properties of a PDF.

**DEFINITION.** If  $x(t)$  is a low-pass wide-sense stationary process, the *rms bandwidth* is

$$B_{\text{rms}} = \sqrt{\overline{f^2}} \quad (6-97)$$

where

$$\overline{f^2} = \int_{-\infty}^{\infty} f^2 \left[ \frac{\mathcal{P}_x(f)}{\int_{-\infty}^{\infty} \mathcal{P}_x(\lambda) d\lambda} \right] df = \frac{\int_{-\infty}^{\infty} f^2 \mathcal{P}_x(f) df}{\int_{-\infty}^{\infty} \mathcal{P}_x(\lambda) d\lambda} \quad (6-98)$$

The rms measure of bandwidth is often used in theoretical comparisons of communication systems since the mathematics involved in the rms calculation is often easier to carry out

than that for other bandwidth measures. However, the rms bandwidth is not easily measured with laboratory instruments.

**THEOREM.** For a wide-sense stationary process  $x(t)$ , the mean-squared frequency  $\bar{f}^2$  is

$$\bar{f}^2 = \left[ -\frac{1}{(2\pi)^2 R(0)} \right] \frac{d^2 R_x(\tau)}{d\tau^2} \Big|_{\tau=0} \quad (6-99)$$

**Proof.** We know that

$$R_x(\tau) = \int_{-\infty}^{\infty} \mathcal{P}_x(f) e^{j2\pi f\tau} dt$$

Taking the second derivative of this equation with respect to  $\tau$ , we obtain

$$\frac{d^2 R_x(\tau)}{d\tau^2} = \int_{-\infty}^{\infty} \mathcal{P}_x(f) e^{j2\pi f\tau} (j2\pi f)^2 df$$

Evaluating both sides of this equation at  $\tau = 0$  yields

$$\frac{d^2 R_x(\tau)}{d\tau^2} \Big|_{\tau=0} = (j2\pi)^2 \int_{-\infty}^{\infty} f^2 \mathcal{P}_x(f) df$$

Substituting this for the integral in (6-98), (6-98) becomes

$$\bar{f}^2 = \frac{\int_{-\infty}^{\infty} f^2 \mathcal{P}_x(f) df}{\int_{-\infty}^{\infty} \mathcal{P}_x(\lambda) d\lambda} = \frac{-\frac{1}{(2\pi)^2} \left[ \frac{d^2 R_x(\tau)}{d\tau^2} \right]_{\tau=0}}{R_x(0)}$$

which is identical to (6-99).

The rms bandwidth for a *bandpass* process can also be defined. Here we are interested in the square root of the second moment about the mean frequency of the *positive* frequency portion of the spectrum.

**DEFINITION.** If  $x(t)$  is a *bandpass* wide-sense stationary process, the *rms bandwidth* is

$$B_{\text{rms}} = 2\sqrt{(\bar{f} - f_0)^2} \quad (6-100)$$

where

$$\bar{f} = \int_0^{\infty} (f - f_0)^2 \left( \frac{\mathcal{P}_x(f)}{\int_0^{\infty} \mathcal{P}_x(\lambda) d\lambda} \right) df \quad (6-101)$$

and

$$f_0 \triangleq \bar{f} = \int_0^{\infty} f \left( \frac{\mathcal{P}_x(f)}{\int_0^{\infty} \mathcal{P}_x(\lambda) d\lambda} \right) df \quad (6-102)$$

As a sketch of a typical bandpass PSD will verify, the quantity given by the radical in (6-100) is analogous to  $\sigma_f$ . Consequently, the factor of 2 is needed to give a reasonable definition for the bandpass bandwidth.

### Example 6-6 EQUIVALENT BANDWIDTH AND RMS BANDWIDTH FOR AN RC LPF

To evaluate the equivalent bandwidth and the rms bandwidth for a filter, white noise may be applied to the input. The bandwidth of the output PSD is the bandwidth of the filter since the input PSD is a constant.

For the *RC LPF* (Fig. 6-9) the output PSD, for white noise at the input, is given by (6-88). The corresponding output autocorrelation function is given by (6-89). When we substitute these equations into (6-96), the equivalent bandwidth for the *RC LPF* is

$$B_{\text{eq}} = \frac{R_y(0)}{2\mathcal{P}_y(0)} = \frac{N_0/4RC}{2(\frac{1}{2} N_0)} = \frac{1}{4RC} \text{ hertz} \quad (6-103)$$

Consequently, for an *RC LPF*,

$$B_{\text{eq}} = \frac{\pi}{2} B_{3\text{dB}} \quad (6-104)$$

The rms bandwidth is obtained by substituting (6-88) and (6-90) into (6-98).

$$B_{\text{rms}} = \sqrt{\frac{\int_{-\infty}^{\infty} f^2 \mathcal{P}_y(f) df}{R_y(0)}} = \sqrt{\frac{1}{2\pi^2 RC} \int_{-\infty}^{\infty} \frac{f^2}{(B_{3\text{dB}})^2 + f^2} df} \quad (6-105)$$

Examining the integral, we note that the integrand becomes *unity* as  $f \rightarrow \pm\infty$ , so that the value of the integral is infinity. Thus  $B_{\text{rms}} = \infty$  for an *RC LPF*. For the rms bandwidth to be finite, the PSD needs to decay faster than  $1/|f|^2$  as the frequency becomes large. Consequently, for the *RC LPF*, the rms definition is not very useful.

## 6-6 THE GAUSSIAN RANDOM PROCESS

**DEFINITION.** A random process  $x(t)$  is said to be Gaussian if the random variables

$$x_1 = x(t_1), x_2 = x(t_2), \dots, x_N = x(t_N) \quad (6-106)$$

have an  $N$ -dimensional Gaussian PDF for any  $N$  and any  $t_1, t_2, \dots, t_N$ .

The  $N$ -dimensional Gaussian PDF can be written compactly by using matrix notation. Let  $\mathbf{x}$  be the *column* vector denoting the  $N$  random variables,

$$\mathbf{x} = \begin{bmatrix} x_1 \\ x_2 \\ \vdots \\ x_N \end{bmatrix} = \begin{bmatrix} x(t_1) \\ x(t_2) \\ \vdots \\ x(t_N) \end{bmatrix} \quad (6-107)$$

The  $N$ -dimensional Gaussian PDF is

$$f_{\mathbf{x}}(\mathbf{x}) = \frac{1}{(2\pi)^{N/2} |\text{Det } \mathbf{C}|^{1/2}} e^{-(1/2)[(\mathbf{x} - \mathbf{m})^T \mathbf{C}^{-1} (\mathbf{x} - \mathbf{m})]} \quad (6-108)$$

where the mean vector is

$$\mathbf{m} = \bar{\mathbf{x}} = \begin{bmatrix} \bar{x}_1 \\ \bar{x}_2 \\ \vdots \\ \bar{x}_N \end{bmatrix} = \begin{bmatrix} m_1 \\ m_2 \\ \vdots \\ m_N \end{bmatrix} \quad (6-109)$$

$(\mathbf{x} - \mathbf{m})^T$  denotes the transpose of the column vector  $(\mathbf{x} - \mathbf{m})$ .

$\text{Det } \mathbf{C}$  is the determinant of the matrix  $\mathbf{C}$ , and  $\mathbf{C}^{-1}$  is the inverse of the matrix  $\mathbf{C}$ . The covariance matrix  $\mathbf{C}$  is defined by

$$\mathbf{C} = \begin{bmatrix} c_{11} & c_{12} & \cdots & c_{1N} \\ c_{21} & c_{22} & \cdots & c_{2N} \\ \vdots & \vdots & & \vdots \\ c_{N1} & c_{N2} & \cdots & c_{NN} \end{bmatrix} \quad (6-110)$$

where the elements of the matrix are

$$c_{ij} = \overline{(x_i - m_i)(x_j - m_j)} = \overline{[x(t_i) - m_i][x(t_j) - m_j]} \quad (6-111)$$

For a wide-sense stationary process  $m_i = \overline{x(t_i)} = m_j = \overline{x(t_j)} = m$ . The elements of the covariance matrix become

$$c_{ij} = R_x(t_j - t_i) - m^2 \quad (6-112)$$

If, in addition, the  $x_i$  happen to be uncorrelated,  $\overline{x_i x_j} = \overline{x_i} \overline{x_j}$  for  $i \neq j$ , and the covariance matrix becomes

$$\mathbf{C} = \begin{bmatrix} \sigma^2 & 0 & \cdots & 0 \\ 0 & \sigma^2 & \cdots & 0 \\ \vdots & \ddots & \ddots & \vdots \\ 0 & 0 & \cdots & \sigma^2 \end{bmatrix} \quad (6-113)$$

where  $\sigma^2 = \overline{x^2} - m^2 = R_x(0) - m^2$ . That is, the covariance matrix becomes a diagonal matrix if the random variables are uncorrelated. Using (6-113) in (6-108), we can conclude that the Gaussian random variables are independent when they are uncorrelated.

### Properties of Gaussian Processes

Some properties of Gaussian processes are now given.

1.  $f_{\mathbf{x}}(\mathbf{x})$  depends only on  $\mathbf{C}$  and on  $\mathbf{m}$ , which is another way of saying that the  $N$ -dimensional Gaussian PDF is completely specified by the first- and second-order moments (i.e., means, variances, and covariances).
2. Since the  $\{x_i = x(t_i)\}$  are jointly Gaussian, the  $x_i = x(t_i)$  are individually Gaussian.
3. When  $\mathbf{C}$  is a diagonal matrix, the random variables are uncorrelated. Furthermore, the Gaussian random variables are independent when they are uncorrelated.
4. A linear transformation of a set of Gaussian random variables produces another set of Gaussian random variables.
5. A wide-sense stationary Gaussian process is also strict-sense stationary<sup>†</sup> [Papoulis, 1984, p. 222; Shanmugan and Breipohl, 1988, p. 141].

Property 4 is very useful in the analysis of linear systems. This property, as well as the following theorem, will be proved subsequently.

**THEOREM.** *If the input to a linear system is a Gaussian random process, the system output is also a Gaussian process.*

**Proof.** The output of a linear network having an impulse response  $h(t)$  is

$$y(t) = h(t) * x(t) = \int_{-\infty}^{\infty} h(t - \lambda)x(\lambda) d\lambda$$

This can be approximated by

$$y(t) = \sum_{j=1}^N h(t - \lambda_j)x(\lambda_j) \Delta\lambda \quad (6-114)$$

which becomes exact as  $N \rightarrow$  large, and  $\Delta\lambda \rightarrow 0$ .

The output random variables for the output random process are

$$y(t_1) = \sum_{j=1}^N [h(t_1 - \lambda_j) \Delta\lambda]x(\lambda_j)$$

$$y(t_2) = \sum_{j=1}^N [h(t_2 - \lambda_j) \Delta\lambda]x(\lambda_j)$$

⋮

$$y(t_N) = \sum_{j=1}^N [h(t_N - \lambda_j) \Delta\lambda]x(\lambda_j)$$

<sup>†</sup> This follows directly from (6-112) since the  $N$ -dimensional Gaussian PDF is a function only of  $\tau$  and not the absolute times.

In matrix notation this is

$$\begin{bmatrix} y_1 \\ y_2 \\ \vdots \\ y_N \end{bmatrix} = \begin{bmatrix} h_{11} & h_{12} & \cdots & h_{1N} \\ h_{21} & h_{22} & \cdots & h_{2N} \\ \vdots & \vdots & \ddots & \vdots \\ h_{N1} & h_{N2} & \cdots & h_{NN} \end{bmatrix} \begin{bmatrix} x_1 \\ x_2 \\ \vdots \\ x_N \end{bmatrix}$$

or

$$\mathbf{y} = \mathbf{H}\mathbf{x} \quad (6-115)$$

where the elements of the  $N \times N$  matrix  $\mathbf{H}$  are related to the impulse response of the linear network by

$$h_{ij} = [h(t_i - \lambda_j)] \Delta\lambda \quad (6-116)$$

We will now show that  $\mathbf{y}$  is an  $N$ -dimensional Gaussian PDF when  $\mathbf{x}$  is an  $N$ -dimensional Gaussian PDF. This may be accomplished by using the theory for a multivariate functional transformation as given in Appendix B. From (B-99) the PDF of  $\mathbf{y}$  is

$$f_y(\mathbf{y}) = \frac{f_x(\mathbf{x})}{|J(\mathbf{y}/\mathbf{x})|} \Big|_{\mathbf{x}=\mathbf{H}^{-1}\mathbf{y}} \quad (6-117)$$

The Jacobian is

$$J\left(\frac{\mathbf{y}}{\mathbf{x}}\right) = \text{Det} \begin{bmatrix} \frac{dy_1}{dx_1} & \frac{dy_1}{dx_2} & \cdots & \frac{dy_1}{dx_N} \\ \frac{dy_2}{dx_1} & \frac{dy_2}{dx_2} & \cdots & \frac{dy_2}{dx_N} \\ \vdots & \vdots & & \vdots \\ \frac{dy_N}{dx_1} & \frac{dy_N}{dx_2} & \cdots & \frac{dy_N}{dx_N} \end{bmatrix} = \text{Det}[\mathbf{H}] \triangleq K \quad (6-118)$$

where  $K$  is a constant. In this problem  $J(\mathbf{y}/\mathbf{x})$  is a *constant* (not a function of  $\mathbf{x}$ ) because  $\mathbf{y} = \mathbf{H}\mathbf{x}$  is a *linear* transformation. Thus

$$f_y(\mathbf{y}) = \frac{1}{|K|} f_x(\mathbf{H}^{-1}\mathbf{y})$$

or

$$f_y(\mathbf{y}) = \frac{1}{(2\pi)^{N/2} |K| |\text{Det } \mathbf{C}_x|^{1/2}} e^{-(1/2)[(\mathbf{H}^{-1}\mathbf{y} - \mathbf{m}_x)^T \mathbf{C}_x^{-1} (\mathbf{H}^{-1}\mathbf{y} - \mathbf{m}_x)]} \quad (6-119)$$

where the subscript  $x$  has been appended to the quantities that are associated with  $x(t)$ . But we know that  $\mathbf{m}_y = \mathbf{H}\mathbf{m}_x$  and from matrix theory we have the property  $[\mathbf{AB}]^T = \mathbf{B}^T \mathbf{A}^T$ , so that the exponent of (6-119) becomes

$$-\frac{1}{2}[(\mathbf{y} - \mathbf{m}_y)^T (\mathbf{H}^{-1})^T] \mathbf{C}_x^{-1} [\mathbf{H}^{-1}(\mathbf{y} - \mathbf{m}_y)] = -\frac{1}{2}[(\mathbf{y} - \mathbf{m}_y)^T \mathbf{C}_y^{-1} (\mathbf{y} - \mathbf{m}_y)] \quad (6-120)$$

where

$$\mathbf{C}_y^{-1} = (\mathbf{H}^{-1})^T \mathbf{C}_x^{-1} \mathbf{H}^{-1} \quad (6-121)$$

or

$$\mathbf{C}_y = \mathbf{H} \mathbf{C}_x \mathbf{H}^T \quad (6-122)$$

Thus the PDF for  $\mathbf{y}$  is

$$f_y(\mathbf{y}) = \frac{1}{(2\pi)^{N/2} |K| |\text{Det } \mathbf{C}_x|^{1/2}} e^{-(1/2)(\mathbf{y} - \mathbf{m}_y)^T \mathbf{C}_y^{-1} (\mathbf{y} - \mathbf{m}_y)} \quad (6-123)$$

which is an  $N$ -dimensional Gaussian PDF. This completes the proof of this theorem.

If a linear system acts like an integrator or LPF, the output random variables (of the output random process) tend to be proportional to the sum of the input random variables. Consequently, by applying the central limit theorem (see Appendix B), the output of the integrator or LPF will tend toward a Gaussian random process when the input random variables are independent with non-Gaussian PDFs.

### Example 6-7 WHITE GAUSSIAN NOISE PROCESS

Assume that a Gaussian random process  $n(t)$  is given that has a PSD of

$$P_n(f) = \begin{cases} \frac{1}{2} N_0, & |f| \leq B \\ 0, & f \text{ otherwise} \end{cases} \quad (6-124)$$

where  $B$  is a positive constant. This describes a *bandlimited white Gaussian* process as long as  $B$  is finite, but becomes a completely *white* (all frequencies present) *Gaussian process* as  $B \rightarrow \infty$ .

The autocorrelation function for the bandlimited white process is

$$R_n(\tau) = BN_0 \left( \frac{\sin 2\pi B\tau}{2\pi B\tau} \right) \quad (6-125)$$

The total average power is  $P = R_n(0) = BN_0$ . The mean value of  $n(t)$  is zero since there is no  $\delta$  function in the PSD at  $f = 0$ . Furthermore, the autocorrelation function is zero for  $\tau = k/(2B)$  when  $k$  is a nonzero integer. Therefore, the random variables  $n_1 = n(t_1)$  and  $n_2 = n(t_2)$  are uncorrelated when  $t_2 - t_1 = \tau = k/(2B)$ ,  $k \neq 0$ . For other values of  $\tau$ , the random variables are correlated. Since  $n(t)$  is assumed to be Gaussian,  $n_1$  and  $n_2$  are jointly Gaussian random variables. Consequently, by property 3, the random variables are independent when  $t_2 - t_1 = k/(2B)$ . They are dependent for other values of  $t_2$  and  $t_1$ . As  $B \rightarrow \infty$ ,  $R_n(\tau) \rightarrow \frac{1}{2} N_0 \delta(\tau)$ , and the random variables  $n_1$  and  $n_2$  become independent for all values of  $t_1$  and  $t_2$  provided that  $t_1 \neq t_2$ . Furthermore, as  $B \rightarrow \infty$ , the average power becomes infinite. Consequently, a white noise process is not physically realizable. However, it is a very useful mathematical idealization for system analysis, just as a deterministic impulse is useful for obtaining the impulse response of a linear system, although the impulse itself is not physically realizable.

## 6-7 BANDPASS PROCESSES<sup>†</sup>

### Bandpass Representations

In Sec. 4-1 it was demonstrated that any bandpass waveform could be represented by

$$v(t) = \operatorname{Re}\{g(t)e^{j\omega_c t}\} \quad (6-126a)$$

or, equivalently, by

$$v(t) = x(t) \cos \omega_c t - y(t) \sin \omega_c t \quad (6-126b)$$

and

$$v(t) = R(t) \cos[\omega_c t + \theta(t)] \quad (6-126c)$$

where  $g(t)$  is the complex envelope,  $R(t)$  is the real envelope,  $\theta(t)$  is the phase, and  $x(t)$  and  $y(t)$  are the quadrature components. Thus the complex envelope is

$$g(t) = |g(t)| e^{j\angle g(t)} = R(t) e^{j\theta(t)} = x(t) + jy(t) \quad (6-127a)$$

This gives the relationships

$$R(t) = |g(t)| = \sqrt{x^2(t) + y^2(t)} \quad (6-127b)$$

$$\theta(t) = \angle g(t) = \tan^{-1} \left[ \frac{y(t)}{x(t)} \right] \quad (6-127c)$$

$$x(t) = R(t) \cos \theta(t) \quad (6-127d)$$

$$y(t) = R(t) \sin \theta(t) \quad (6-127e)$$

Furthermore, the spectrum of  $v(t)$  is related to that of  $g(t)$  by (4-12), which is

$$V(f) = \frac{1}{2}[G(f - f_c) + G^*(-f - f_c)] \quad (6-128)$$

In Chapters 4 and 5, the bandpass representation was used to analyze communication systems from a *deterministic* viewpoint. Here we extend the representation to random processes. In communication systems the random processes may be random signals, noise, or signals corrupted by noise.

When  $v(t)$  is a bandpass random process containing frequencies in the vicinity of  $\pm f_c$ , then  $g(t)$ ,  $x(t)$ ,  $y(t)$ ,  $R(t)$ , and  $\theta(t)$  will be baseband processes. In general,  $g(t)$  is a complex process (as described in Sec. 6-1), and  $x(t)$ ,  $y(t)$ ,  $R(t)$ , and  $\theta(t)$  are always real processes. This is readily seen from a Fourier series expansion of  $v(t)$ , as demonstrated by (4-5) through (4-8), where the Fourier series coefficients form a set of random variables since  $v(t)$  is a random process. Furthermore, if  $v(t)$  is a Gaussian random process, the Fourier series coefficients consist of a set of *Gaussian* random variables since they are obtained by linear operations on  $v(t)$ . Similarly, when  $v(t)$  is a Gaussian process,  $g(t)$ ,  $x(t)$ , and  $y(t)$  are Gaussian processes since they are linear functions of  $v(t)$ . However,  $R(t)$  and  $\theta(t)$  are not Gaussian because they are nonlinear functions of  $v(t)$ . The first-order PDF for these processes will be evaluated in Example 6-10.

<sup>†</sup> In some other texts this is called a *narrowband noise process*, which is a misnomer because it may be wideband or narrowband.

We now need to address the topic of stationarity as applied to the bandpass representation.

**THEOREM.** *If  $x(t)$  and  $y(t)$  are jointly wide-sense stationary (WSS) processes, the real bandpass process*

$$v(t) = \operatorname{Re}\{g(t)e^{j\omega_c t}\} = x(t) \cos \omega_c t - y(t) \sin \omega_c t \quad (6-129a)$$

*will be WSS if and only if*

$$1. \overline{x(t)} = \overline{y(t)} = 0 \quad (6-129b)$$

$$2. R_x(\tau) = R_y(\tau) \quad (6-129c)$$

$$3. R_{xy}(\tau) = -R_{yx}(\tau) \quad (6-129d)$$

**Proof.** The requirements for WSS are that  $\overline{v(t)}$  be constant and  $R_v(t, t + \tau)$  be only a function of  $\tau$ . We see that  $\overline{v(t)} = \overline{x(t) \cos \omega_c t - y(t) \sin \omega_c t}$  is a constant for any value of  $t$  only if  $\overline{x(t)} = \overline{y(t)} = 0$ . Thus, condition 1 is required.

The conditions required to make  $R_v(t, t + \tau)$  only a function of  $\tau$  are found as follows:

$$\begin{aligned} R_v(t, t + \tau) &= \overline{v(t)v(t + \tau)} \\ &= \overline{[x(t) \cos \omega_c t - y(t) \sin \omega_c t][x(t + \tau) \cos \omega_c(t + \tau) - y(t + \tau) \sin \omega_c(t + \tau)]} \\ &= \overline{x(t)x(t + \tau)} \cos \omega_c t \cos \omega_c(t + \tau) - \overline{x(t)y(t + \tau)} \cos \omega_c t \sin \omega_c(t + \tau) \\ &\quad - \overline{y(t)x(t + \tau)} \sin \omega_c t \cos \omega_c(t + \tau) + \overline{y(t)y(t + \tau)} \sin \omega_c t \sin \omega_c(t + \tau) \end{aligned}$$

or

$$\begin{aligned} R_v(t, t + \tau) &= R_x(\tau) \cos \omega_c t \cos \omega_c(t + \tau) - R_{xy}(\tau) \cos \omega_c t \sin \omega_c(t + \tau) \\ &\quad - R_{yx}(\tau) \sin \omega_c t \cos \omega_c(t + \tau) + R_y(\tau) \sin \omega_c t \sin \omega_c(t + \tau) \end{aligned}$$

When we use trigonometric identities for products of sine and cosine, this equation reduces to

$$\begin{aligned} R_v(t, t + \tau) &= \frac{1}{2}[R_x(\tau) + R_y(\tau)] \cos \omega_c \tau + \frac{1}{2}[R_x(\tau) - R_y(\tau)] \cos \omega_c(2t + \tau) \\ &\quad - \frac{1}{2}[R_{xy}(\tau) - R_{yx}(\tau)] \sin \omega_c \tau - \frac{1}{2}[R_{xy}(\tau) + R_{yx}(\tau)] \sin \omega_c(2t + \tau) \end{aligned}$$

The autocorrelation for  $v(t)$  can be made to be a function of  $\tau$  only if the terms involving  $t$  are set equal to zero. That is,  $[R_x(\tau) - R_y(\tau)] = 0$  and  $[R_{xy}(\tau) + R_{yx}(\tau)] = 0$ . Thus conditions 2 and 3 are required.

If conditions 1 through 3 of (6-129) are satisfied so that  $v(t)$  is WSS, properties 1 through 5 of (6-133a) through (6-133e) are valid. Furthermore, the  $x(t)$  and  $y(t)$  components of  $v(t) = x(t) \cos \omega_c t - y(t) \sin \omega_c t$  satisfy properties 6 through 14, as described by

(6-133f) through (6-133n), when conditions 1 through 3 are satisfied. These properties are very useful in analyzing the random processes at various points in communication systems.

For a given bandpass waveform, the description of the complex envelope,  $g(t)$ , is not unique. This is easily seen in (6-126), where the choice of the value for the parameter  $f_c$  is left to our discretion. Consequently, for representation of a given bandpass waveform,  $v(t)$ , the frequency components that are present in the corresponding complex envelope,  $g(t)$ , depend on the value of  $f_c$  that is chosen in the model. Moreover, in representing random processes, one is often interested in having a representation for a WSS bandpass process with certain PSD characteristics. In this case, it can be shown that  $\text{Re}\{(-j)g(t)e^{j\omega_c t}\}$  gives the same PSD as  $\text{Re}\{g(t)e^{j\omega_c t}\}$  when  $v(t)$  is a WSS process [Papoulis, 1984, pp. 314-322]. Consequently,  $g(t)$  is not unique, and it can be chosen to satisfy some additional desired condition. Yet, properties 1 through 14 will still be satisfied when the conditions of (6-129) are satisfied.

In some applications, conditions 1 through 3 of (6-129) are not satisfied. This will be the case, for example, when the  $x(t)$  and  $y(t)$  quadrature components do not have the same power, as in an unbalanced quadrature modulation problem. Another example is the case in which  $x(t)$  and/or  $y(t)$  have a dc value. In these cases, the bandpass random process model described by (6-126) would be nonstationary. Consequently, one is faced with the question: Can another bandpass model be found that models a WSS  $v(t)$ , but yet does not require conditions 1 through 3 of (6-129)? The answer is, yes. Let the model of (6-126) be generalized to include a phase constant  $\theta_c$  that is a random variable. Then we have the following theorem.

**THEOREM.** *If  $x(t)$  and  $y(t)$  are jointly WSS processes, the real bandpass process*

$$v(t) = \text{Re}\{g(t)e^{j(\omega_c t + \theta_c)}\} = x(t)\cos(\omega_c t + \theta_c) - y(t)\sin(\omega_c t + \theta_c) \quad (6-130)$$

*will be WSS when  $\theta_c$  is an independent random variable uniformly distributed over  $(0, 2\pi)$ .*

This modification of the bandpass model should not worry us because we can argue that it is actually a better model for physically obtainable bandpass processes. That is, the constant  $\theta_c$  is often called the *random start-up phase* since it depends on the “initial conditions” of the physical process. Any noise source or signal source starts up with a random-phase angle when it is turned on unless it is synchronized by injecting some external signal.

**Proof.** Using (6-130) to model our bandpass process, we now demonstrate that this  $v(t)$  is wide-sense stationary when  $g(t)$  is wide-sense stationary even though the conditions of (6-129) may be violated. To show that (6-130) is WSS, the first requirement is that  $\bar{v}(t)$  be a constant.

$$\bar{v}(t) = \overline{\text{Re}\{g(t)e^{j(\omega_c t + \theta_c)}\}} = \text{Re}\{\overline{g(t)}e^{j\omega_c t}e^{j\theta_c}\}$$

But  $e^{j\theta_c} = 0$ , so we have  $\bar{v}(t) = 0$ , which is a constant. The second requirement is that  $R_v(t, t + \tau)$  be only a function of  $\tau$ .

$$\begin{aligned} R_v(t, t + \tau) &= \overline{v(t)v(t + \tau)} \\ &= \overline{\{g(t)e^{j(\omega_c t + \theta_c)}\}} \overline{\{g(t + \tau)e^{j(\omega_c t + \theta_c + \omega_c \tau + \theta_c)}\}} \end{aligned}$$

Using the identity  $\text{Re}(c_1)\text{Re}(c_2) = \frac{1}{2}\text{Re}(c_1c_2) + \frac{1}{2}\text{Re}(c_1^*c_2)$  and recalling that  $\theta_c$  is an independent random variable, we obtain

$$\begin{aligned} R_v(t, t + \tau) &= \frac{1}{2}\text{Re}\{\overline{g(t)g(t + \tau)}e^{j(2\omega_c t + \omega_c \tau)}e^{j2\theta_c}\} \\ &\quad + \frac{1}{2}\text{Re}\{\overline{g^*(t)g(t + \tau)}e^{j\omega_c \tau}\} \end{aligned}$$

But  $e^{j2\theta_c} = 0$  and  $R_g(\tau) = \overline{g^*(t)g(t + \tau)}$ , since  $g(t)$  is assumed to be wide-sense stationary. Thus

$$R_v(t, t + \tau) = \frac{1}{2}\text{Re}\{R_g(\tau)e^{j\omega_c \tau}\} \quad (6-131)$$

The right-hand side of (6-131) is not a function of  $t$ , so  $R_v(t, t + \tau) = R_v(\tau)$ . Consequently, (6-130) gives a model for a wide-sense stationary bandpass process.

Furthermore, for this model as described by (6-130), properties 1 through 5 of (6-133a) through (6-133e) are valid, but all the properties 6 through 14, (6-133f) through (6-133h) are not valid for the  $x(t)$  and  $y(t)$  components of  $v(t) = x(t)\cos(\omega_c t + \theta_c) - y(t)\sin(\omega_c t + \theta_c)$  unless all the conditions of (6-129) are satisfied. However, as will be proved later, the *detected*  $x(t)$  and  $y(t)$  components at the output of quadrature product detectors (see Fig. 6-11) satisfy properties 6 through 14, provided that the startup phase of the detectors,  $\theta_0$ , is independent of  $v(t)$ . [Note that the  $x(t)$  and  $y(t)$  components associated with  $v(t)$  at the input to the detector are not identical to the  $x(t)$  and  $y(t)$  quadrature output waveforms unless  $\theta_c = \theta_0$ ; however, the PSDs may be identical.]

The complex envelope representation of (6-130) is very useful for evaluating the output of detector circuits. For example, if  $v(t)$  is a signal plus noise process that is applied to a product detector,  $x(t)$  is the output process if the reference is  $2\cos(\omega_c t + \theta_c)$  and  $y(t)$  is the output process if the reference is  $-2\sin(\omega_c t + \theta_c)$  (see Chapter 4). Similarly,  $R(t)$  is the output process for an envelope detector, and  $\theta(t)$  is the output process for a phase detector.

### Properties of WSS Bandpass Processes

Theorems giving the relationships between the autocorrelation functions and the PSD of  $v(t)$ ,  $g(t)$ ,  $x(t)$ , and  $y(t)$  can be obtained. These and other theorems are listed subsequently as properties of bandpass random processes. These relationships assume that the bandpass process  $v(t)$  is real and WSS.<sup>†</sup> The bandpass nature of  $v(t)$  is described mathematically with the aid of Fig. 6-10a. Here

$$\mathcal{P}_v(f) = 0 \quad \text{for } f_1 < |f| < f_2 \quad (6-132)$$

where  $0 < f_1 \leq f_c \leq f_2$ . Furthermore, a positive constant  $B_0$  is defined such that  $B_0$  is the largest frequency interval between  $f_c$  and either band edge, as illustrated in Fig. 6-10a and  $B_0 < f_c$ .

The properties are:

1.  $g(t)$  is a complex wide-sense-stationary baseband process. (6-133a)

2.  $x(t)$  and  $y(t)$  are real jointly wide-sense stationary baseband processes. (6-133b)

3.  $R_v(\tau) = \frac{1}{2}\text{Re}\{R_g(\tau)e^{j\omega_c \tau}\}$ . (6-133c)

4.  $\mathcal{P}_v(f) = \frac{1}{4}[\mathcal{P}_g(f - f_c) + \mathcal{P}_g(-f - f_c)]$ . (6-133d)

5.  $\overline{v^2} = \frac{1}{2}\overline{|g(t)|^2} = R_v(0) = \frac{1}{2}\mathcal{P}_g(0)$ . (6-133e)

<sup>†</sup>  $v(t)$  also has zero mean value since it is a bandpass process.

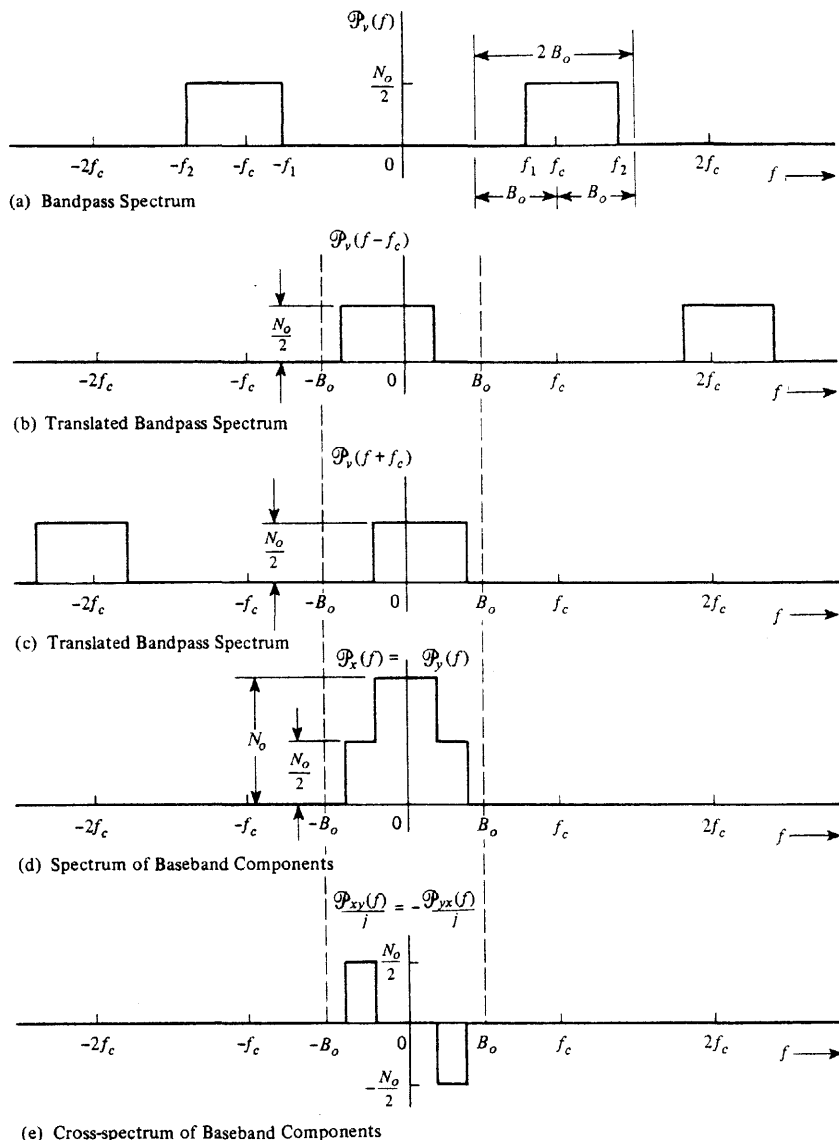


Figure 6-10 Spectra of random process for Example 6-8.

If the bandpass process  $v(t)$  is WSS and if conditions 1 through 3 of (6-129) are satisfied,  $v(t)$  can be represented by (6-129a), where the  $x(t)$  and  $y(t)$  components satisfy properties 6 through 14 listed below. On the other hand, if  $v(t)$  is WSS but does not satisfy all three conditions of (6-129), the representation of (6-129a) is not applicable because it will not be a WSS model, and consequently, properties 6 through 14 below are not applicable. However, for  $v(t)$  WSS, the representation of (6-130) is always applicable regardless of whether none, some, or all of conditions 1 through 3 of (6-129) are satisfied; and, consequently, none, some, or all of properties 6 through 14 listed below are satisfied by the  $x(t)$  and  $y(t)$  com-

ponents of (6-130). Furthermore, if the quadrature components of  $v(t)$  are recovered by product detector circuits, as shown in Fig. 6-11, where  $\theta_0$  is a uniformly distributed random variable that is *independent* of  $v(t)$ , the detected  $x(t)$  and  $y(t)$  quadrature components satisfy properties 6 through 14 listed below.<sup>†</sup>

$$6. \overline{x(t)} = \overline{y(t)} = 0 \quad (6-133f)$$

$$7. \overline{v^2(t)} = \overline{x^2(t)} = \overline{y^2(t)} = \frac{1}{2} |\overline{g(t)}|^2 \\ = R_v(0) = R_x(0) = R_y(0) = \frac{1}{2} R_g(0) \quad (6-133g)$$

$$8. R_x(\tau) = R_y(\tau) = 2 \int_0^\infty \mathcal{P}_v(f) \cos[2\pi(f - f_c)\tau] df \quad (6-133h)$$

$$9. R_{xy}(\tau) = 2 \int_0^\infty \mathcal{P}_v(f) \sin[2\pi(f - f_c)\tau] df \quad (6-133i)$$

$$10. R_{yy}(\tau) = -R_{xy}(-\tau) = -R_{yx}(\tau) \quad (6-133j)$$

$$11. R_{yy}(0) = 0 \quad (6-133k)$$

$$12. \mathcal{P}_x(f) = \mathcal{P}_y(f) = \begin{cases} [\mathcal{P}_v(f - f_c) + \mathcal{P}_v(f + f_c)], & |f| < B_0 \\ 0, & f \text{ elsewhere} \end{cases} \quad (6-133l)$$

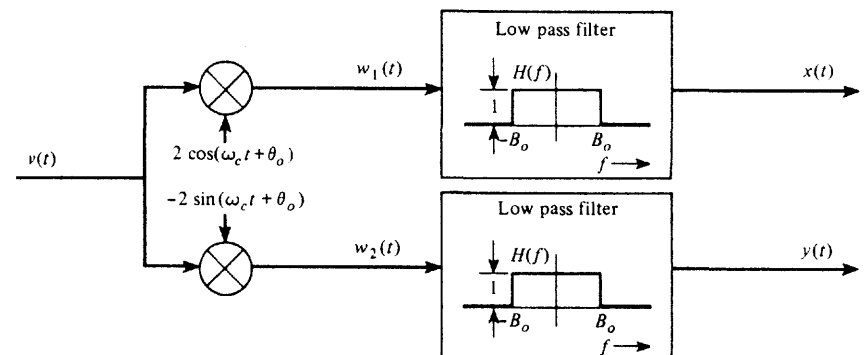
$$13. \mathcal{P}_{xy}(f) = \begin{cases} j[\mathcal{P}_v(f - f_c) - \mathcal{P}_v(f + f_c)], & |f| < B_0 \\ 0, & f \text{ elsewhere} \end{cases} \quad (6-133m)$$

$$14. \mathcal{P}_{xy}(f) = -\mathcal{P}_{xy}(-f) = -\mathcal{P}_{yx}(f) \quad (6-133n)$$

Additional properties can be obtained when  $v(t)$  is a wide-sense stationary *single-sideband (SSB) random process*. If  $v(t)$  is SSB about  $f = \pm f_c$ , from Chapter 5 we have

$$g(t) = x(t) \pm j\hat{x}(t) \quad (6-134)$$

where the upper sign is used for USSB and the lower sign is used for LSSB.  $\hat{x}(t)$  is the Hilbert transform of  $x(t)$ . Using (6-134), we obtain some additional properties.

Figure 6-11 Recovery of  $x(t)$  and  $y(t)$  from  $v(t)$ 

<sup>†</sup> Proofs of these properties will be given after Examples 6-8 and 6-9. Properties 6 through 14 also hold for the  $x(t)$  and  $y(t)$  components of (6-129a) provided that the conditions of (6-129b, c, and d) are satisfied.

15. When  $v(t)$  is a SSB process about  $f = \pm f_c$ ,

$$R_g(\tau) = 2[R_x(\tau) \pm j\hat{R}_x(\tau)] \quad (6-135a)$$

where  $\hat{R}_x(\tau) = [1/(\pi\tau)] * R_x(\tau)$

16. For USSB processes

$$\mathcal{P}_g(f) = \begin{cases} 4\mathcal{P}_x(f), & f > 0 \\ 0, & f < 0 \end{cases} \quad (6-135b)$$

17. For LSSB processes

$$\mathcal{P}_g(f) = \begin{cases} 0, & f > 0 \\ 4\mathcal{P}_x(f), & f < 0 \end{cases} \quad (6-135c)$$

From property 9 it is seen that if the PSD of  $v(t)$  is even about  $f = f_c$ ,  $f > 0$ , then  $R_{xy}(\tau) \equiv 0$  for all  $\tau$ . Consequently,  $x(t)$  and  $y(t)$  will be *orthogonal* processes when  $\mathcal{P}_v(f)$  is even about  $f = f_c$ ,  $f > 0$ . Furthermore, if in addition  $v(t)$  is Gaussian,  $x(t)$  and  $y(t)$  will be independent Gaussian random processes.

#### Example 6-8 SPECTRA FOR THE QUADRATURE COMPONENTS OF WHITE BANDPASS NOISE

Assume that  $v(t)$  is an independent bandlimited white noise process. Let the PSD of  $v(t)$  be  $N_0/2$  over the frequency band  $f_1 \leq |f| \leq f_2$ , as illustrated in Fig. 6-10a. Using property 12, we can evaluate the PSD for  $x(t)$  and  $y(t)$ . This is obtained by summing the translated spectra  $\mathcal{P}_v(f - f_c)$  and  $\mathcal{P}_v(f + f_c)$  as illustrated in Fig. 6-10b and c to obtain  $\mathcal{P}_x(f)$  shown in Fig. 6-10d. Note that the spectrum  $\mathcal{P}_x(f)$  is zero for  $|f| > B_0$ . Similarly, the cross-spectrum,  $\mathcal{P}_{xy}(f)$ , can be obtained by using property 13. This is shown in Fig. 6-10e. It is interesting to note that over the frequency range where the cross-spectrum is nonzero, it is completely imaginary since  $\mathcal{P}_v(f)$  is a real function. In addition, the cross-spectrum is always an odd function.

The total normalized power is

$$P = \int_{-\infty}^{\infty} \mathcal{P}_v(f) df = N_0(f_2 - f_1)$$

The same result is obtained if the power is computed from  $\mathcal{P}_x(f) = \mathcal{P}_y(f)$  by using property 7.

$$P = R_x(0) = R_y(0) = \int_{-\infty}^{\infty} \mathcal{P}_x(f) df = N_0(f_2 - f_1)$$

#### Example 6-9 PSD FOR A BPSK SIGNAL

The PSD for a BPSK signal that is modulated by random data will now be evaluated. In Chapters 2 and 5 it was demonstrated that the BPSK signal can be represented by

$$v(t) = x(t) \cos(\omega_c t + \theta_c) \quad (6-136)$$

where  $x(t)$  represents the polar binary data (see Example 2-18) and  $\theta_c$  is the random startup phase.

The PSD of  $v(t)$  is found by using property 4, where  $g(t) = x(t) + j0$ . Thus

$$\mathcal{P}_v(f) = \frac{1}{4} [\mathcal{P}_x(f - f_c) + \mathcal{P}_x(-f - f_c)] \quad (6-137)$$

Now we need to find the PSD for the polar binary modulation  $x(t)$ . This was calculated in Example 6-3, where the PSD of a polar baseband signal with equally likely binary data was evaluated. Substituting (6-62) or, equivalently, (6-67) into (6-137), we obtain the PSD for the BPSK signal.

$$\mathcal{P}_v(f) = \frac{T_b}{4} \left\{ \left[ \frac{\sin \pi(f - f_c) T_b}{\pi(f - f_c) T_b} \right]^2 + \left[ \frac{\sin \pi(f + f_c) T_b}{\pi(f + f_c) T_b} \right]^2 \right\} \quad (6-138)$$

A sketch of this result is shown in Fig. 6-12. This result was cited earlier in (2-200), where bandwidths were also evaluated.

#### Proofs of Some Properties

Proofs for all 17 properties listed previously would be a long task. We, therefore, present detailed proofs for some of them. Proofs that involve similar mathematics will be left to the reader as exercise problems.

Properties 1 through 3 have already been given in the discussion preceding (6-131). Property 4 follows readily from property 3 by taking the Fourier transform of (6-133c). The mathematics is identical to that used in obtaining (4-25). Property 5 also follows directly from property 3. Property 6 will be shown subsequently. Property 7 follows from properties 3 and 8. As we will see later, properties 8 through 11 follow from properties 12 and 13.

Properties 6 and 12 are obtained with the aid of Fig. 6-11. That is, as shown by (4-76) in Sec. 4-13,  $x(t)$  and  $y(t)$  can be recovered by using product detectors. Thus

$$x(t) = [2v(t) \cos(\omega_c t + \theta_0)] * h(t) \quad (6-139)$$

and

$$y(t) = -[2v(t) \sin(\omega_c t + \theta_0)] * h(t) \quad (6-140)$$

where  $h(t)$  is the impulse response of an ideal LPF that is bandlimited to  $B_0$  hertz.  $\theta_0$  is an independent random variable that is uniformly distributed over  $(0, 2\pi)$  and corresponds to the

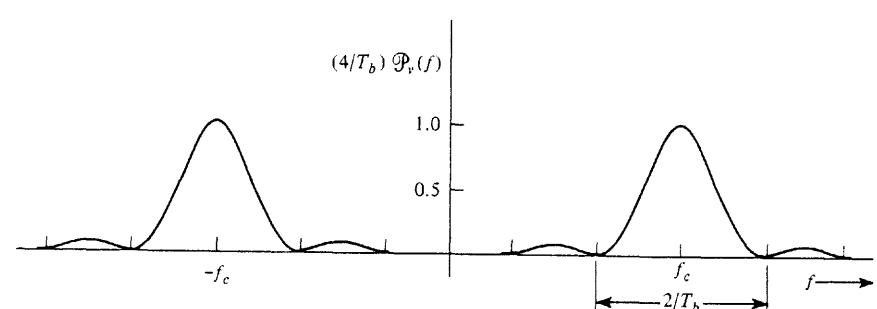


Figure 6-12 Power spectrum for a BPSK signal.

random startup phase of a phase-incoherent receiver oscillator. Property 6 follows from (6-139) by taking the ensemble average since  $\cos(\omega_c t + \theta_0) = 0$  and  $\sin(\omega_c t + \theta_0) = 0$ . Property 12, which is the PSD for  $x(t)$ , can be evaluated by first evaluating the autocorrelation for  $w_1(t)$  of Fig. 6-11.

$$w_1(t) = 2v(t) \cos(\omega_c t + \theta_0)$$

$$\begin{aligned} R_{w_1}(\tau) &= \overline{w_1(t)w_1(t+\tau)} \\ &= 4\overline{v(t)v(t+\tau)\cos(\omega_c t + \theta_0)\cos(\omega_c(t+\tau) + \theta_0)} \end{aligned}$$

But since  $\theta_0$  is an independent random variable, using a trigonometric identity, we have

$$R_{w_1}(\tau) = 4\overline{v(t)v(t+\tau)[\frac{1}{2}\cos\omega_c\tau + \frac{1}{2}\cos(2\omega_c t + \omega_c\tau + 2\theta_0)]}$$

But  $\overline{\cos(2\omega_c t + \omega_c\tau + 2\theta_0)} = 0$ , so

$$R_{w_1}(\tau) = 2R_v(\tau) \cos\omega_c\tau \quad (6-141)$$

The PSD of  $w_1(t)$  is obtained by taking the Fourier transform of (6-141).

$$\mathcal{P}_{w_1}(f) = 2\mathcal{P}_v(f) * [\frac{1}{2}\delta(f - f_c) + \frac{1}{2}\delta(f + f_c)]$$

or

$$\mathcal{P}_{w_1}(f) = \mathcal{P}_v(f - f_c) + \mathcal{P}_v(f + f_c)$$

Finally, the PSD of  $x(t)$  is

$$\mathcal{P}_x(f) = |H(f)|^2 \mathcal{P}_{w_1}(f)$$

or

$$\mathcal{P}_x(f) = \begin{cases} [\mathcal{P}_v(f - f_c) + \mathcal{P}_v(f + f_c)], & |f| < B_0 \\ 0, & \text{otherwise} \end{cases}$$

which is property 12.

Property 8 follows directly from property 12 by taking the inverse Fourier transform.

$$R_x(\tau) = \mathcal{F}^{-1}[\mathcal{P}_x(f)]$$

$$= \int_{-B_0}^{B_0} \mathcal{P}_v(f - f_c) e^{j2\pi f\tau} df + \int_{-B_0}^{B_0} \mathcal{P}_v(f + f_c) e^{j2\pi f\tau} df$$

Making changes in the variables, let  $f_1 = -f + f_c$  in the first integral and let  $f_1 = f + f_c$  in the second integral.

$$R_x(\tau) = \int_{f_c-B_0}^{f_c+B_0} \mathcal{P}_v(-f_1) e^{j2\pi(f_c-f_1)\tau} df_1 + \int_{f_c-B_0}^{f_c+B_0} \mathcal{P}_v(f_1) e^{j2\pi(f_1-f_c)\tau} df_1$$

But  $\mathcal{P}_v(-f) = \mathcal{P}_v(f)$  since  $v(t)$  is a real process. Furthermore, since  $v(t)$  is bandlimited, the limits on the integrals may be changed to integrate over the interval  $(0, \infty)$ . Thus

$$R_x(\tau) = 2 \int_0^\infty \mathcal{P}_v(f_1) \left[ \frac{e^{j2\pi(f_1-f_c)\tau} + e^{-j2\pi(f_1-f_c)\tau}}{2} \right] df_1$$

which is identical to property 8.

In a similar way, properties 13 and 9 can be shown to be valid. Properties 10 and 14 follow directly from property 9.

For SSB processes we know that  $y(t) = \pm \hat{x}(t)$ . Property 15 is then obtained as follows.

$$\begin{aligned} R_{gg}(\tau) &= \overline{g^*(t)g(t+\tau)} \\ &= \overline{[x(t) \mp j\hat{x}(t)][x(t+\tau) \pm j\hat{x}(t+\tau)]} \\ &= \overline{[x(t)x(t+\tau) + \hat{x}(t)\hat{x}(t+\tau)]} \\ &\quad \pm j[-\hat{x}(t)x(t+\tau) + \overline{x(t)\hat{x}(t+\tau)}] \end{aligned} \quad (6-142)$$

Using the definition for crosscorrelation functions and using property 10, we have

$$R_{x\bar{x}}(\tau) = \overline{x(t)\hat{x}(t+\tau)} = -R_{\hat{x}x}(\tau) = -\overline{\hat{x}(t)x(t+\tau)} \quad (6-143)$$

Furthermore, knowing that  $\hat{x}(t)$  is the convolution of  $x(t)$  with  $1/(\pi t)$ , we can demonstrate (see Prob. 6-35) that

$$R_{\hat{x}x}(\tau) = R_x(\tau) \quad (6-144)$$

and

$$R_{\hat{x}\bar{x}}(\tau) = \hat{R}_{xx}(\tau) \quad (6-145)$$

Thus (6-142) reduces to property 15. Taking the Fourier transform of (6-135a), we obtain properties 16 and 17.

As demonstrated by property 6, the detected mean values  $\overline{x(t)}$  and  $\overline{y(t)}$  are zero when  $v(t)$  is independent of  $\theta_0$ . However, from (6-139) and (6-140) we realize that a less restrictive condition is required. That is,  $\overline{x(t)}$  or  $\overline{y(t)}$  will be zero if  $v(t)$  is orthogonal to  $\cos(\omega_c t + \theta_0)$  or  $\sin(\omega_c t + \theta_0)$ , respectively; otherwise, they will be nonzero. For example, suppose that  $v(t)$  is

$$v(t) = 5 \cos(\omega_c t + \theta_c) \quad (6-146)$$

where  $\theta_c$  is a random variable uniformly distributed over  $(0, 2\pi)$ . If the reference  $2 \cos(\omega_c t + \theta_0)$  of Fig. 6-11 is phase coherent with  $\cos(\omega_c t + \theta_c)$  (i.e.,  $\theta_0 \equiv \theta_c$ ), the output of the upper LPF will have a mean value of 5. On the other hand, if the random variables  $\theta_0$  and  $\theta_c$  are independent, then  $v(t)$  will be orthogonal to  $\cos(\omega_c t + \theta_0)$  and  $\bar{x}$  of the output of the upper LPF of Fig. 6-11 will be zero. The output dc value (i.e., time average) will be  $5 \cos(\theta_0 - \theta_c)$  in either case.

No properties have been given pertaining to the autocorrelation or the PSD of  $R(t)$  and  $\theta(t)$  as related to the autocorrelation and PSD of  $v(t)$ . In general, this is a difficult problem because  $R(t)$  and  $\theta(t)$  are nonlinear functions of  $v(t)$ . This topic is discussed in more detail after Example 6-10.

As indicated previously,  $x(t)$ ,  $y(t)$ , and  $g(t)$  are Gaussian processes when  $v(t)$  is Gaussian. However,  $R(t)$  and  $\theta(t)$  are not Gaussian processes when  $v(t)$  is Gaussian, as we will demonstrate.

**Example 6-10 PDF FOR THE ENVELOPE AND PHASE FUNCTIONS OF A GAUSSIAN BANDPASS PROCESS**

Assume that  $v(t)$  is a wide-sense stationary *Gaussian* process with finite PSD that is symmetrical about  $f = \pm f_c$ . We want to find the one-dimensional PDF for the envelope process,  $R(t)$ . Of course, this is identical to the process that appears at the output of an envelope detector when the input is a Gaussian process, such as Gaussian noise. Similarly, the PDF for the phase,  $\theta(t)$  (the output of a phase detector), will also be obtained.

This problem is solved by evaluating the two-dimensional random variable transformation of  $x = x(t)$  and  $y = y(t)$  into  $R = R(t)$  and  $\theta = \theta(t)$ . This is illustrated in Fig. 6-13. Because  $v(t)$  is Gaussian, we know that  $x$  and  $y$  are jointly *Gaussian*. For  $v(t)$  having a finite PSD that is symmetrical about  $f = \pm f_c$ , the mean values for  $x$  and  $y$  are both zero and the variances of both are

$$\sigma^2 = \sigma_x^2 = \sigma_y^2 = R_v(0) \quad (6-147)$$

Furthermore,  $x$  and  $y$  are independent since they are uncorrelated Gaussian random variables [since the PSD of  $v(t)$  is symmetrical about  $f = \pm f_c$ ]. Therefore, the joint PDF of  $x$  and  $y$  is

$$f_{xy}(x, y) = \frac{1}{2\pi\sigma^2} e^{-(x^2+y^2)/(2\sigma^2)} \quad (6-148)$$

The joint PDF for  $R$  and  $\theta$  is obtained by the two-dimensional transformation of  $x$  and  $y$  into  $R$  and  $\theta$ .

$$\begin{aligned} f_{R\theta}(R, \theta) &= \frac{f_{xy}(x, y)}{|J[(R, \theta)/(x, y)]|} \Bigg|_{\substack{x=R \cos \theta \\ y=R \sin \theta}} \\ &= f_{xy}(x, y) \left| J\left(\frac{(x, y)}{(R, \theta)}\right) \right| \Bigg|_{\substack{x=R \cos \theta \\ y=R \sin \theta}} \end{aligned} \quad (6-149)$$

We will work with  $J[(x, y)/(R, \theta)]$  instead of  $J[(R, \theta)/(x, y)]$  because in this problem the partial derivatives in the former are easier to evaluate than those in the latter.

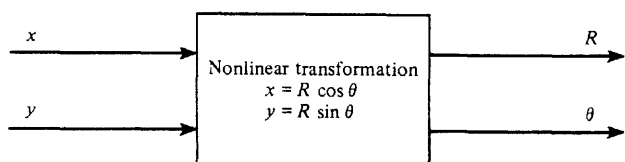


Figure 6-13 Nonlinear (polar) transformation of two Gaussian random variables.

$$J\left(\frac{(x, y)}{(R, \theta)}\right) = \text{Det} \begin{bmatrix} \frac{\partial x}{\partial R} & \frac{\partial x}{\partial \theta} \\ \frac{\partial y}{\partial R} & \frac{\partial y}{\partial \theta} \end{bmatrix}$$

where  $x$  and  $y$  are related to  $R$  and  $\theta$  as shown in Fig. 6-13. Of course,  $R \geq 0$ , and  $\theta$  falls in the interval  $(0, 2\pi)$ .

$$\begin{aligned} J\left(\frac{(x, y)}{(R, \theta)}\right) &= \text{Det} \begin{bmatrix} \cos \theta & -R \sin \theta \\ \sin \theta & R \cos \theta \end{bmatrix} \\ &= R[\cos^2 \theta + \sin^2 \theta] = R \end{aligned} \quad (6-150)$$

Substituting (6-148) and (6-150) into (6-149), the joint PDF of  $R$  and  $\theta$  is

$$f_{R\theta}(R, \theta) = \begin{cases} \frac{R}{2\pi\sigma^2} e^{-R^2/(2\sigma^2)}, & R \geq 0 \text{ and } 0 \leq \theta \leq 2\pi \\ 0, & R \text{ and } \theta \text{ otherwise} \end{cases} \quad (6-151)$$

The PDF for the envelope is obtained by calculating the marginal PDF:

$$f_R(R) = \int_{-\infty}^{\infty} f_{R\theta}(R, \theta) d\theta = \int_0^{2\pi} \frac{R}{2\pi\sigma^2} e^{-R^2/(2\sigma^2)} d\theta, \quad R \geq 0$$

or

$$f_R(R) = \begin{cases} \frac{R}{\sigma^2} e^{-R^2/(2\sigma^2)}, & R \geq 0 \\ 0, & R \text{ otherwise} \end{cases} \quad (6-152)$$

This is called a *Rayleigh* PDF. Similarly, the PDF of  $\theta$  is obtained by integrating out  $R$  in the joint PDF:

$$f_\theta(\theta) = \begin{cases} \frac{1}{2\pi}, & 0 \leq \theta \leq 2\pi \\ 0, & \text{otherwise} \end{cases} \quad (6-153)$$

This is called a *uniform* PDF. Sketches of these PDFs are shown in Fig. 6-14.

The random variables  $R = R(t_1)$  and  $\theta = \theta(t_1)$  are independent since it is seen that  $f_{R\theta}(R, \theta) = f_R(R)f_\theta(\theta)$ . However,  $R(t)$  and  $\theta(t)$  are *not* independent random processes since the random variables  $R = R(t_1)$  and  $\theta = \theta(t_1 + \tau)$  are not independent for all values of  $\tau$ . To verify this statement, a four-dimensional transformation problem consisting of transforming the random variables  $(x(t_1), x(t_2), y(t_1), y(t_2))$  into  $(R(t_1), R(t_2), \theta(t_1), \theta(t_2))$  needs to be worked out where  $t_2 - t_1 = \tau$  (Davenport and Root, 1958).

The evaluation of the autocorrelation function for the envelope  $R(t)$  generally requires that the two-dimensional density function of  $R(t)$  be known since  $R_R(\tau) = \overline{R(t)R(t+\tau)}$ .

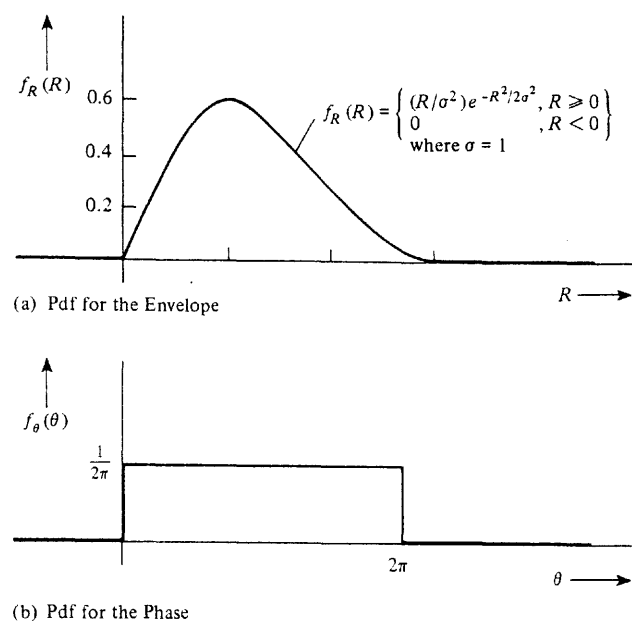


Figure 6-14 PDF for the envelope and phase of a Gaussian process.

However, to obtain this joint density function for  $R(t)$ , the four-dimensional density function of  $(R(t_1), R(t_2), \theta(t_1), \theta(t_2))$  must first be obtained by a four-dimensional transformation discussed in the preceding paragraph. A similar problem is worked to evaluate the autocorrelation function for the phase  $\theta(t)$ . These difficulties in evaluating the autocorrelation function for  $R(t)$  and  $\theta(t)$  arise because they are nonlinear functions of  $v(t)$ . The PSDs for  $R(t)$  and  $\theta(t)$  are obtained by taking the Fourier transform of the autocorrelation function.

## 6-8 MATCHED FILTERS

### General Results

In preceding sections of this chapter, we have developed techniques for describing random processes and analyzing the effect of linear systems on these processes. Here we develop a technique for designing a linear filter to minimize the effect of the noise while maximizing the signal.

A general representation for a matched filter is illustrated in Fig. 6-15. The input signal is denoted by  $s(t)$  and the output signal by  $s_0(t)$ . Similar notation is used for the noise. This filter is used in applications where the signal may or may not be present, but when the signal is present, its waveshape is known. (This has application to digital signaling and radar problems as will become clear in Examples 6-11 and 6-12.) The signal is assumed to be (absolutely) time limited to the interval  $(0, T)$  and is zero otherwise. The PSD,  $\mathcal{P}_n(f)$ , of the

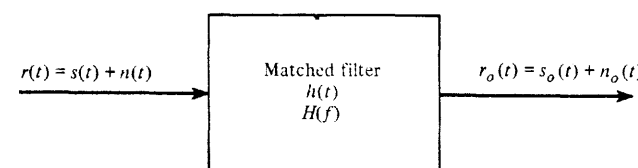


Figure 6-15 Matched filter.

additive input noise  $n(t)$  is also known. We wish to determine the filter characteristic such that the instantaneous output signal power is maximized at a sampling time  $t_0$ , when compared with the average output noise power. That is, we want to find  $h(t)$  or, equivalently,  $H(f)$ , so that

$$\left(\frac{S}{N}\right)_{\text{out}} = \frac{s_0^2(t)}{n_0^2(t)} \quad (6-154)$$

is a maximum. This is the matched filter design criterion.

The matched filter does not preserve the input signal waveshape. This is not the objective. The objective is to distort the input signal waveshape and filter the noise so that at the sampling time  $t_0$ , the output signal level will be as large as possible with respect to the rms (output) noise level. In Chapter 7 we demonstrate that, under certain conditions, this minimizes the probability of error when receiving digital signals.

**THEOREM.** The matched filter is the linear filter that maximizes  $(S/N)_{\text{out}} = \overline{s_0^2(t_0)/n_0^2(t)}$  of Fig. 6-15 and has a transfer function given by<sup>†</sup>

$$H(f) = K \frac{S^*(f)}{\mathcal{P}_n(f)} e^{-j\omega t_0} \quad (6-155)$$

where  $S(f) = \mathcal{F}[s(t)]$  is the Fourier transform of the known input signal  $s(t)$  of duration  $T$  sec.  $\mathcal{P}_n(f)$  is the PSD of the input noise,  $t_0$  is the sampling time when  $(S/N)_{\text{out}}$  is evaluated, and  $K$  is an arbitrary real nonzero constant.

**Proof.** The output signal at time  $t_0$  is

$$s_0(t_0) = \int_{-\infty}^{\infty} H(f) S(f) e^{j\omega t_0} df$$

The average power of the output noise is

$$\overline{n_0^2(t)} = R_{n_0}(0) = \int_{-\infty}^{\infty} |H(f)|^2 \mathcal{P}_n(f) df$$

<sup>†</sup> It appears that this formulation for the matched filter was first discovered independently by B. M. Dwork and T. S. George in 1950; the result for the white noise case was shown first by D. O. North in 1943 [Root, 1987].

Substituting these equations into (6-154), we get

$$\left(\frac{S}{N}\right)_{\text{out}} = \frac{\left| \int_{-\infty}^{\infty} H(f) S(f) e^{j\omega t_0} df \right|^2}{\int_{-\infty}^{\infty} |H(f)|^2 \mathcal{P}_n(f) df} \quad (6-156)$$

We wish to find the particular  $H(f)$  that maximizes  $(S/N)_{\text{out}}$ . This can be obtained with the aid of the Schwarz inequality,<sup>†</sup> which is

$$\left| \int_{-\infty}^{\infty} A(f) B(f) df \right|^2 \leq \int_{-\infty}^{\infty} |A(f)|^2 df \int_{-\infty}^{\infty} |B(f)|^2 df \quad (6-157)$$

where  $A(f)$  and  $B(f)$  may be complex functions of the real variable  $f$ . Furthermore, equality is obtained only when

$$A(f) = KB^*(f) \quad (6-158)$$

where  $K$  is any arbitrary real constant. The Schwarz inequality may be used to replace the numerator on the right-hand side of (6-156) by letting

$$A(f) = H(f) \sqrt{\mathcal{P}_n(f)}$$

and

$$B(f) = \frac{S(f) e^{j\omega t_0}}{\sqrt{\mathcal{P}_n(f)}}$$

Then (6-156) becomes

$$\left(\frac{S}{N}\right)_{\text{out}} \leq \frac{\int_{-\infty}^{\infty} |H(f)|^2 \mathcal{P}_n(f) df \int_{-\infty}^{\infty} \frac{|S(f)|^2}{\mathcal{P}_n(f)} df}{\int_{-\infty}^{\infty} |H(f)|^2 \mathcal{P}_n(f) df}$$

where it is realized that  $\mathcal{P}_n(f)$  is a nonnegative real function. Thus

$$\left(\frac{S}{N}\right)_{\text{out}} \leq \int_{-\infty}^{\infty} \frac{|S(f)|^2}{\mathcal{P}_n(f)} df \quad (6-159)$$

The maximum  $(S/N)_{\text{out}}$  is obtained when  $H(f)$  is chosen such that equality is attained. This occurs when  $A(f) = KB^*(f)$  or

$$H(f) \sqrt{\mathcal{P}_n(f)} = \frac{KS^*(f) e^{-j\omega t_0}}{\sqrt{\mathcal{P}_n(f)}}$$

which reduces to (6-155) of the theorem.

<sup>†</sup> A proof for the Schwarz inequality is given in the appendix at the end of this chapter.

From a practical viewpoint it is realized that the constant  $K$  is arbitrary since both the input signal and the input noise would be multiplied by  $K$  and  $K$  cancels out when  $(S/N)_{\text{out}}$  is evaluated. However, both the output signal and noise levels depend on the value of the constant.

In this proof, no constraint was applied to assure that  $h(t)$  would be causal. Thus the filter as specified by (6-155) may not be realizable (i.e., causal). However, the transfer function given by (6-155) can often be approximated by a realizable (causal) filter. If the causal constraint is included (in solving for the matched filter), the problem becomes more difficult. A linear integral equation is obtained that must be solved to obtain the unknown function  $h(t)$  [Thomas, 1969].

### Results for White Noise

For the case of white noise, the description of the matched filter is simplified as follows. For white noise  $\mathcal{P}_n(f) = N_0/2$ . Thus (6-155) becomes

$$H(f) = \frac{2K}{N_0} S^*(f) e^{-j\omega t_0}$$

From this equation we obtain the following theorem.

**THEOREM.** *When the input noise is white, the impulse response of the matched filter becomes*

$$h(t) = Cs(t_0 - t) \quad (6-160)$$

where  $C$  is an arbitrary real positive constant,  $t_0$  is the time of the peak signal output, and  $s(t)$  is the known input-signal waveshape.

*Proof.*

$$\begin{aligned} h(t) &= \mathcal{F}^{-1}[H(f)] = \frac{2K}{N_0} \int_{-\infty}^{\infty} S^*(f) e^{-j\omega t_0} e^{j\omega t} df \\ &= \frac{2K}{N_0} \left[ \int_{-\infty}^{\infty} S(f) e^{j2\pi f(t_0 - t)} df \right]^* \\ &= \frac{2K}{N_0} [s(t_0 - t)]^* \end{aligned}$$

But  $s(t)$  is a real signal and let  $C = 2K/N_0$ , so that the impulse response is equivalent to (6-160).

Equation (6-160) shows that the impulse response of the matched filter (white noise case) is simply the known signal waveshape that is “played backward” and translated by an amount  $t_0$  (as illustrated by Example 6-11). Thus the filter is said to be “matched” to the signal.

An important property is the actual value of  $(S/N)_{out}$  that is obtained from the matched filter. From (6-159), using Parseval's theorem as given by (2-41), we obtain

$$\left(\frac{S}{N}\right)_{out} = \int_{-\infty}^{\infty} \frac{|S(f)|^2}{N_0/2} df = \frac{2}{N_0} \int_{-\infty}^{\infty} s^2(t) dt$$

But  $\int_{-\infty}^{\infty} s^2(t) dt = E_s$  is the energy in the (finite-duration) input signal. Thus

$$\left(\frac{S}{N}\right)_{out} = \frac{2E_s}{N_0} \quad (6-161)$$

This is a very interesting result. It states that the  $(S/N)_{out}$  depends on the signal *energy* and PSD level of the noise and not on the particular signal waveshape that is used. Of course, the signal energy can be increased, to improve  $(S/N)_{out}$ , by increasing the signal amplitude, the signal duration, or both.

Equation (6-161) can also be written in terms of a time-bandwidth product and the ratio of the input average signal power (over  $T$  seconds) to average noise power. Assume that the input noise power is measured in a band that is  $W$  hertz wide. We also know that the signal has a duration of  $T$  seconds. Then, from (6-161),

$$\left(\frac{S}{N}\right)_{out} = 2TW \frac{(E_s/T)}{(N_0 W)} = 2(TW) \left(\frac{S}{N}\right)_{in} \quad (6-162)$$

where  $(S/N)_{in} = (E_s/T)/(N_0 W)$ . From (6-162), we see that an increase in the time-bandwidth product ( $TW$ ) does not change the output SNR because the input SNR decreases correspondingly. In radar applications, increased  $TW$  provides increased ability to resolve (distinguish) targets instead of seeing merged targets. Equation (6-161) clearly shows that it is the input-signal energy with respect to  $N_0$  that actually determines the  $(S/N)_{out}$  that is attained [Turin, 1976].

### Example 6-11 INTEGRATE-AND-DUMP (MATCHED) FILTER

Suppose that the known signal is the rectangular pulse, as shown in Fig. 6-16a.

$$s(t) = \begin{cases} 1, & t_1 \leq t \leq t_2 \\ 0, & \text{otherwise} \end{cases} \quad (6-163)$$

where the signal duration is  $T = t_2 - t_1$ . Then, for the case of white noise, the impulse response required for the matched filter is

$$h(t) = s(t_0 - t) = s(-(t - t_0)) \quad (6-164)$$

$C$  was chosen to be unity for convenience.  $s(-t)$  is shown in Fig. 6-16b. From this figure, it is obvious that for the impulse response to be causal we require

$$t_0 \geq t_2 \quad (6-165)$$

We will use  $t_0 = t_2$  because this is the smallest allowed value that satisfies the causal condition, and we would like to minimize the time that we have to wait before the maximum signal

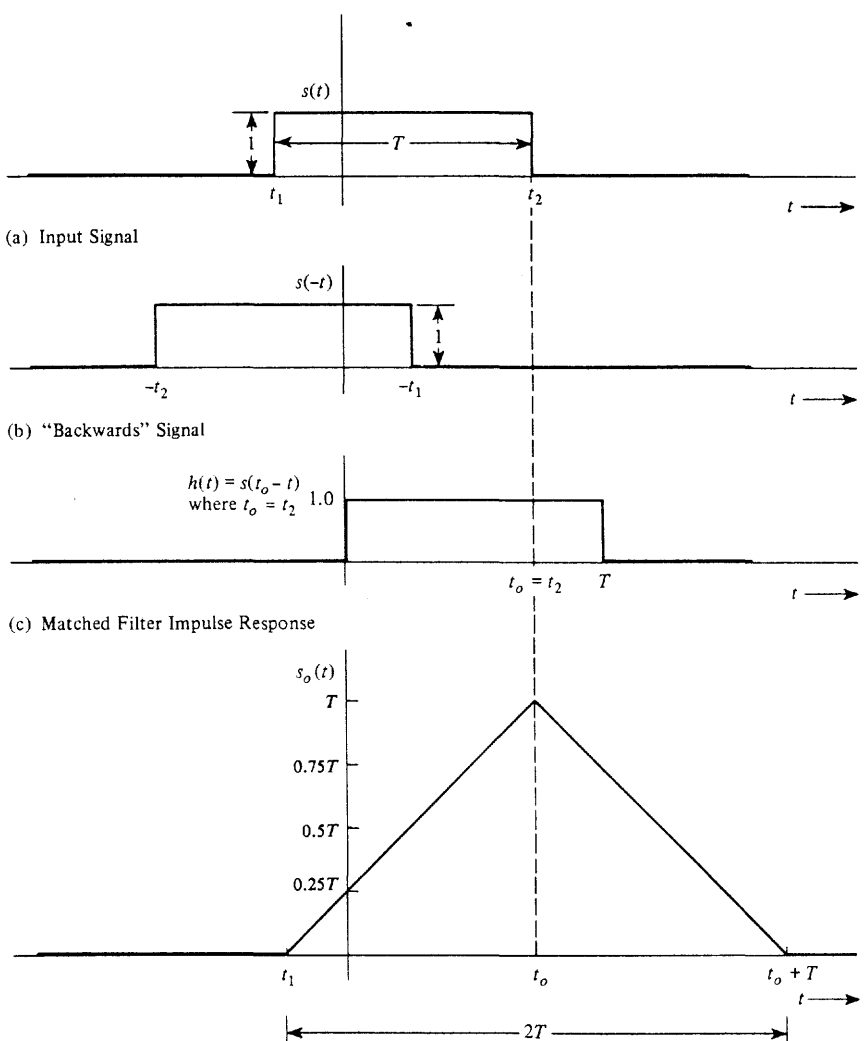


Figure 6-16 Waveforms associated with the matched filter of Example 6-11.

level occurs at the filter output (i.e.,  $t = t_0$ ). A sketch of  $h(t)$  for  $t_0 = t_2$  is shown in Fig. 6-16c. The resulting output signal is shown in Fig. 6-16d. Note that the peak output signal level does indeed occur at  $t = t_0$  and that the input signal waveshape has been distorted by the filter in order to peak up the output signal at  $t = t_0$ .

In applications to digital signaling with a rectangular bit shape, this matched filter is equivalent to an *integrate-and-dump filter*, as we now illustrate. Assume that we signal with one rectangular pulse and are interested in sampling the filter output when the signal level is maximum. Then the filter output at  $t = t_0$  is

$$r_0(t_0) = r(t_0) * h(t_0) = \int_{-\infty}^{\infty} r(\lambda)h(t_0 - \lambda) d\lambda$$

When we substitute for the matched-filter impulse response shown in Fig. 6-16c, this equation becomes

$$r_0(t_0) = \int_{t_0-T}^{t_0} r(\lambda) d\lambda \quad (6-166)$$

Thus we need to integrate the digital input signal plus noise over one symbol period  $T$  (which is the bit period for binary signaling) and "dump" the integrator output at the end of the symbol period. This is illustrated in Fig. 6-17 for binary signaling. Note that for proper operation of

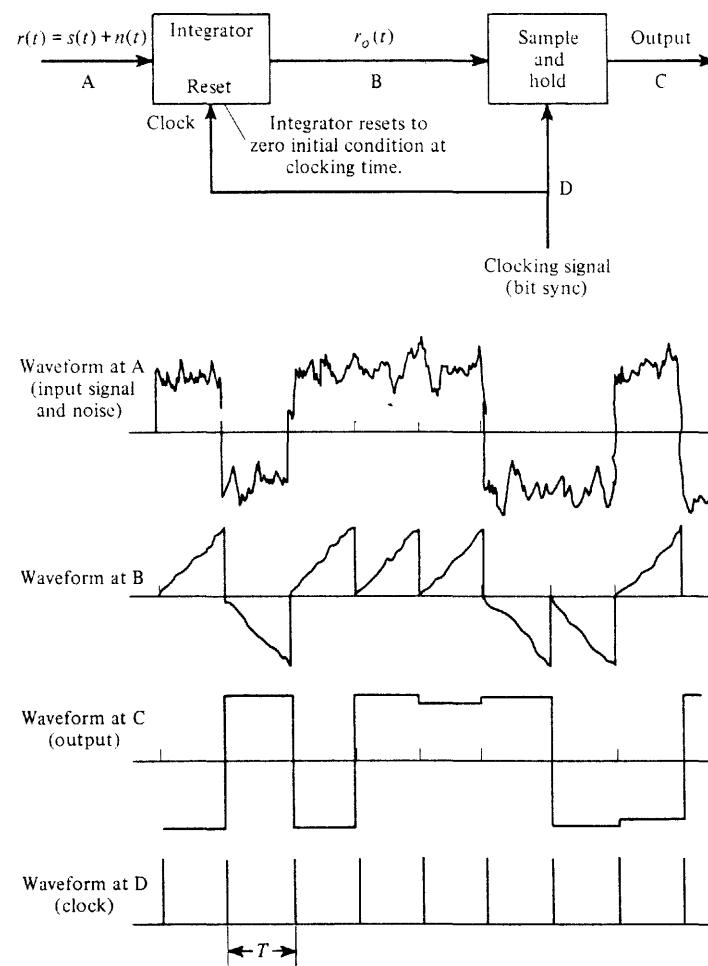


Figure 6-17 Integrate-and-dump realization of a matched filter.

this optimum filter, an external clocking signal called *bit sync* is required (see Chapter 3 for a discussion of bit synchronizers). In addition, the output signal is not binary since the output sample values are still corrupted by noise (although the noise has been minimized by the matched filter). The output could be converted into a binary signal by feeding it into a comparator. This is exactly what is done in digital receivers, as described in Chapter 7.

### Correlation Processing

**THEOREM.** *For the case of white noise, the matched filter may be realized by correlating the input with  $s(t)$ .*

$$r_0(t_0) = \int_{t_0-T}^{t_0} r(t)s(t) dt \quad (6-167)$$

where  $s(t)$  is the known signal waveshape and  $r(t)$  is the processor input, as illustrated in Fig. 6-18.

**Proof.** The output of the matched filter at time  $t_0$  is

$$r_0(t_0) = r(t_0) * h(t_0) = \int_{-\infty}^{t_0} r(\lambda)h(t_0 - \lambda) d\lambda$$

But from (6-160),

$$h(t) = \begin{cases} s(t_0 - t), & 0 \leq t \leq T \\ 0, & \text{elsewhere} \end{cases}$$

so

$$r_0(t_0) = \int_{t_0-T}^{t_0} r(\lambda)s[t_0 - (t_0 - \lambda)] d\lambda$$

which is identical to (6-167).

The correlation processor is often used as a matched filter for bandpass signals, as illustrated by Example 6-12.

### Example 6-12 MATCHED FILTER FOR DETECTION OF A BPSK SIGNAL

Referring to Fig. 6-18, let the filter input be a BPSK signal plus white noise. For example, this might be the IF output in a BPSK receiver. The BPSK signal can be written as

$$s(t) = \begin{cases} +A \cos \omega_c t, & nT < t \leq (n+1)T \text{ for a binary 1} \\ -A \cos \omega_c t, & nT < t \leq (n+1)T \text{ for a binary 0} \end{cases}$$

where  $f_c$  is the IF center frequency,  $T$  is the duration of one bit of data, and  $n$  is an integer. The reference input to the correlation processor should be either  $+A \cos \omega_c t$  or  $-A \cos \omega_c t$ ,

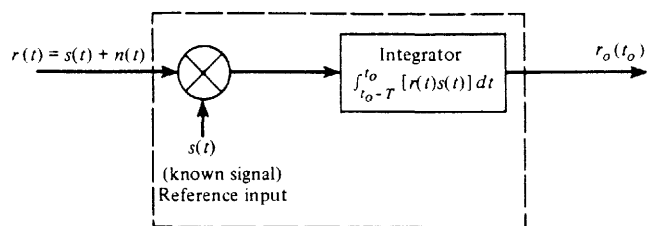


Figure 6-18 Matched-filter realization by correlation processing

depending on whether we are attempting to detect a binary 1 or a binary 0. Since these wave-shapes are identical except for the  $\pm 1$  constants, we could just use  $\cos \omega_c t$  for the reference and recognize that when a binary 1 BPSK signal is present at the input (no noise), a positive voltage,  $\frac{1}{2}AT$ , would be produced at the output. Similarly, a binary 0 BPSK signal would produce a negative voltage,  $-\frac{1}{2}AT$ , at the output. Thus, for BPSK signaling plus white noise, we obtain the matched filter shown in Fig. 6-19. Notice that this looks like the familiar product detector, except that the LPF has been replaced by a gated integrator that is controlled by the bit-sync clock. With this type of postdetection processing, the product detector becomes a matched filter. However, to implement this optimum detector, both bit sync and carrier sync are needed. It is also realized that this technique, shown in Fig. 6-19, could be classified as a more general form of an integrate-and-dump filter (first shown in Fig. 6-17).

### Transversal Matched Filter

A transversal filter can also be designed to satisfy the matched-filter criterion. Referring to Fig. 6-20, we wish to find the set of transversal filter coefficients  $\{a_i; i = 1, 2, \dots, N\}$  such that  $s_0^2(t_0)/n_0^2(t)$  is maximized.

The output signal at time  $t = t_0$  is

$$\begin{aligned}s_0(t_0) &= a_1 s(t_0) + a_2 s(t_0 - T) + a_3 s(t_0 - 2T) \\ &\quad + \dots + a_N s(t_0 - (N-1)T)\end{aligned}$$

or

$$s_0(t_0) = \sum_{k=1}^N a_k s(t_0 - (k-1)T) \quad (6-168)$$

Similarly, for the output noise,

$$n_0(t) = \sum_{k=1}^N a_k n(t - (k-1)T) \quad (6-169)$$

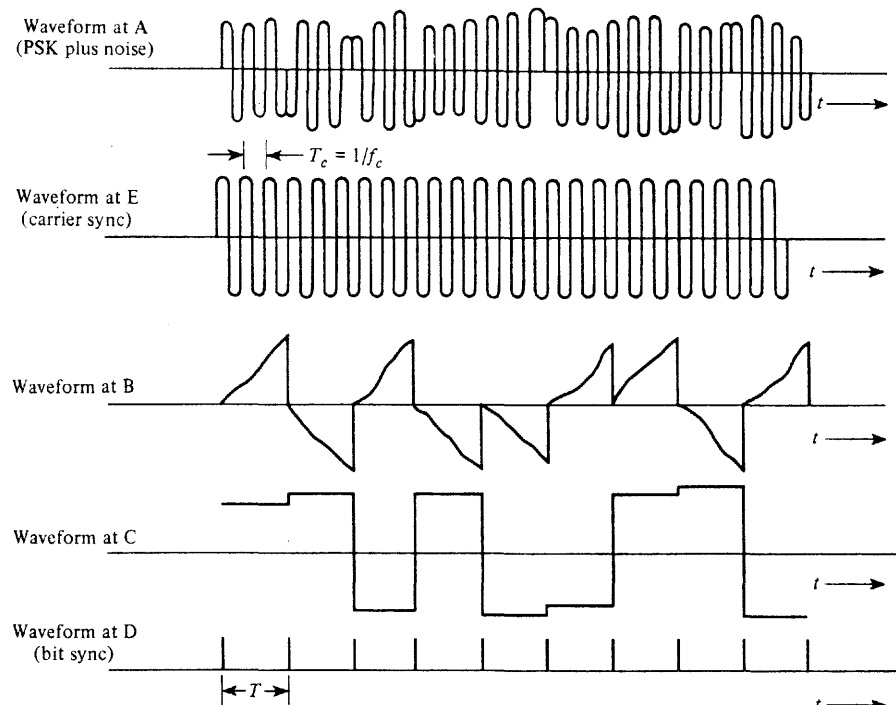
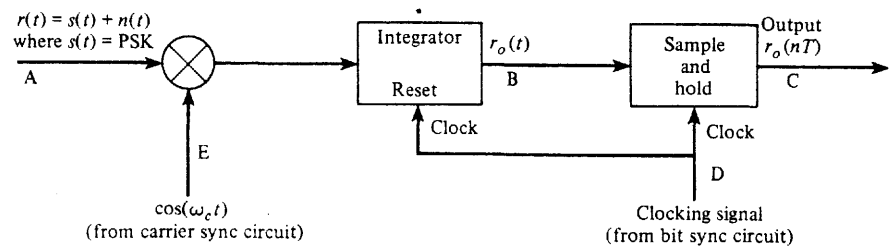


Figure 6-19 Correlation (matched-filter) detection for BPSK.

The average noise power is

$$\overline{n_0^2(t)} = \sum_{k=1}^N \sum_{l=1}^N a_k a_l n(t - (k-1)T) n(t - (l-1)T)$$

or

$$\overline{n_0^2(t)} = \sum_{k=1}^N \sum_{l=1}^N a_k a_l R_n(kT - lT) \quad (6-170)$$

where  $R_n(\tau)$  is the autocorrelation of the input noise. Thus the output peak signal to average noise power ratio is

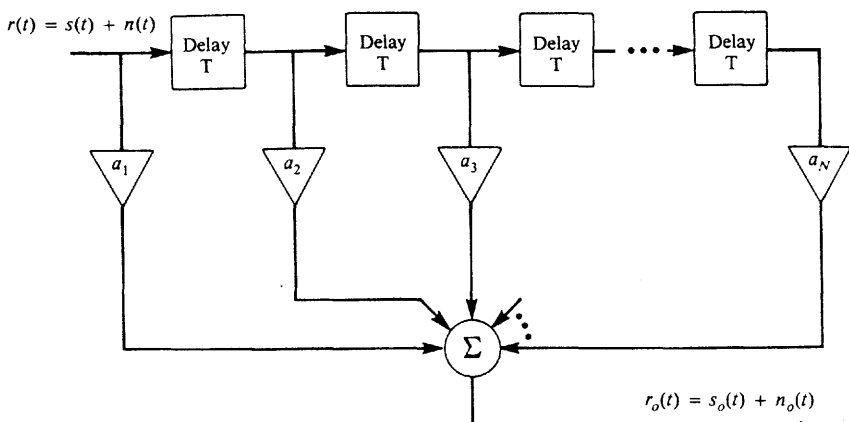


Figure 6-20 Transversal matched filter.

$$\frac{s_0^2(t_0)}{n_0^2(t)} = \frac{\left[ \sum_{k=1}^N a_k s(t_0 - (k-1)T) \right]^2}{\sum_{k=1}^N \sum_{l=1}^N a_k a_l R_n(kT - lT)} \quad (6-171)$$

We can find the  $a_i$ s that maximize this ratio by using Lagrange's method of maximizing the numerator while constraining the denominator to be a constant [Olmsted, 1961, p. 518]. Consequently, we need to maximize the function

$$M(a_1, a_2, \dots, a_N) = \left[ \sum_{k=1}^N a_k s(t_0 - (k-1)T) \right]^2 - \lambda \sum_{k=1}^N \sum_{l=1}^N a_k a_l R_n(kT - lT) \quad (6-172)$$

where  $\lambda$  is the Lagrange multiplier. The maximum occurs when  $\partial M / \partial a_i = 0$  for all the  $i = 1, 2, \dots, N$ . Thus

$$\begin{aligned} \frac{\partial M}{\partial a_i} &= 0 = 2 \left[ \sum_{k=1}^N a_k s(t_0 - (k-1)T) \right] s(t_0 - (i-1)T) \\ &\quad - 2\lambda \sum_{k=1}^N a_k R_n(kT - iT) \end{aligned} \quad (6-173)$$

for  $i = 1, 2, \dots, N$ . But  $\sum_{k=1}^N a_k s(t_0 - (k-1)T) = s_0(t_0)$ , which is a constant. Furthermore, let  $\lambda = s_0(t_0)$ . Then we obtain the required condition,

$$s(t_0 - (i-1)T) = \sum_{k=1}^N a_k R_n(kT - iT) \quad (6-174)$$

for  $i = 1, 2, \dots, N$ . This is a set of  $N$  simultaneous linear equations that must be solved to obtain the  $a_i$ s. We can obtain these coefficients conveniently by writing (6-174) in matrix form. Define the elements

$$s_i \triangleq s[t_0 - (i-1)T], \quad i = 1, 2, \dots, N \quad (6-175)$$

$$r_{ik} = R_n(kT - iT), \quad i = 1, \dots, N \quad (6-176)$$

In matrix notation (6-174) becomes

$$\mathbf{s} = \mathbf{R}\mathbf{a} \quad (6-177)$$

where the known signal vector is

$$\mathbf{s} = \begin{bmatrix} s_1 \\ s_2 \\ \vdots \\ s_N \end{bmatrix} \quad (6-178)$$

the known autocorrelation matrix for the input noise is

$$\mathbf{R} = \begin{bmatrix} r_{11} & r_{12} & \cdots & r_{1N} \\ r_{21} & r_{22} & \cdots & r_{2N} \\ \vdots & \vdots & & \vdots \\ r_{N1} & r_{N2} & \cdots & r_{NN} \end{bmatrix} \quad (6-179)$$

and the unknown transversal filter coefficient vector is

$$\mathbf{a} = \begin{bmatrix} a_1 \\ a_2 \\ \vdots \\ a_N \end{bmatrix} \quad (6-180)$$

The coefficients for the transversal matched filter are then given by

$$\mathbf{a} = \mathbf{R}^{-1} \mathbf{s} \quad (6-181)$$

where  $\mathbf{R}^{-1}$  is the inverse of the autocorrelation matrix for the noise and  $\mathbf{s}$  is the (known) signal vector.

## 6-9 SUMMARY

A random process is the extension of the concept of a random variable to random waveforms. A random process  $x(t)$  is described by an  $N$ -dimensional PDF where the random variables are  $x_1 = x(t_1), x_2 = x(t_2), \dots, x_N = x(t_N)$ . If this PDF is invariant for a shift in the time origin, as  $N \rightarrow \infty$ , the process is said to be *strict-sense stationary*.

The *autocorrelation function* of a random process  $x(t)$  is

$$R_x(t_1, t_2) = \overline{x(t_1)x(t_2)} = \int_{-\infty}^{\infty} \int_{-\infty}^{\infty} x_1 x_2 f_x(x_1, x_2) dx_1 dx_2$$

In general a two-dimensional PDF of  $x(t)$  is required to evaluate  $R_x(t_1, t_2)$ . If the process is stationary,

$$R_x(t_1, t_2) = \overline{x(t_1)x(t_1 + \tau)} = R_x(\tau)$$

where  $\tau = t_2 - t_1$ .

If  $\overline{x(t)}$  is a constant and if  $R_x(t_1, t_2) = R_x(\tau)$ , the process is said to be *wide-sense stationary*. If a process is strict-sense stationary, it is wide-sense stationary, but the converse is not generally true.

A process is *ergodic* when the time averages are equal to the corresponding ensemble averages. If a process is ergodic, it is also stationary, but the converse is not generally true. For ergodic processes, the dc value (a time average) is also  $X_{dc} = \overline{x(t)}$  and the rms value (a time average) is also  $X_{rms} = \sqrt{\overline{x^2(t)}}$ .

The *power spectral density* (PSD),  $\mathcal{P}_x(f)$ , is the Fourier transform of the autocorrelation function  $R_x(\tau)$  (Wiener-Khintchine theorem).

$$\mathcal{P}_x(f) = \mathcal{F}[R_x(\tau)]$$

The PSD is a nonnegative real function and is even about  $f = 0$  for real processes. The PSD can also be evaluated by the ensemble average of a function of the Fourier transforms of the truncated sample functions.

The autocorrelation function of a wide-sense stationary real random process is a real function, and it is even about  $\tau = 0$ . Furthermore,  $R_x(0)$  gives the total normalized average power, and this is the maximum value of  $R_x(\tau)$ .

For *white noise* the PSD is a constant, and the autocorrelation function is a Dirac delta function located at  $\tau = 0$ . White noise is not physically realizable because it has infinite power, but it is a very useful approximation for many problems.

The *cross-correlation* function of two jointly stationary real processes  $x(t)$  and  $y(t)$  is

$$R_{xy}(\tau) = \overline{x(t)y(t + \tau)}$$

and the cross-PSD is

$$\mathcal{P}_{xy}(f) = \mathcal{F}[R_{xy}(\tau)]$$

The two processes are said to be *uncorrelated* if

$$R_{xy}(\tau) = [\overline{x(t)}][\overline{y(t)}]$$

for all  $\tau$ . They are said to be orthogonal if

$$R_{xy}(\tau) = 0$$

for all  $\tau$ .

Let  $y(t)$  be the output process of a *linear system* and  $x(t)$  the input process, where  $y(t) = x(t) * h(t)$ . Then

$$R_y(\tau) = h(-\tau) * h(\tau) * R_x(\tau)$$

and

$$\mathcal{P}_y(f) = |H(f)|^2 \mathcal{P}_x(f)$$

where  $H(f) = \mathcal{F}[h(t)]$ .

The *equivalent bandwidth* of a linear system is defined by

$$B = \frac{1}{|H(f_0)|^2} \int_0^{\infty} |H(f)|^2 df$$

where  $H(f)$  is the transfer function of the system and  $f_0$  is usually taken to be the frequency, where  $|H(f_0)|$  is a maximum. Similarly, the equivalent bandwidth of a random process  $x(t)$  is

$$B = \frac{1}{\mathcal{P}_x(f_0)} \int_0^{\infty} \mathcal{P}_x(f) df = \frac{R_x(0)}{2\mathcal{P}_x(f_0)}$$

If the input to a linear system is a Gaussian process, the output is another *Gaussian* process.

A real stationary *bandpass random process* can be represented by

$$v(t) = \text{Re}\{g(t)e^{j(\omega_c t + \theta_c)}\}$$

where the complex envelope  $g(t)$  is related to quadrature processes  $x(t)$  and  $y(t)$ . Numerous properties of these random processes can be obtained as listed in Sec. 6-7. For example,  $x(t)$  and  $y(t)$  are independent Gaussian processes when the PSD of  $v(t)$  is symmetrical about  $f = f_c$ ,  $f > 0$ , and  $v(t)$  is Gaussian. Properties for SSB bandpass processes are also obtained.

The *matched filter* is a linear filter that maximizes the instantaneous output-signal power to the average output-noise power for a given input-signal waveshape. For the case of white noise, the impulse response of the matched filter is

$$h(t) = Cs(t_0 - t)$$

where  $s(t)$  is the known signal waveshape,  $C$  is a real constant, and  $t_0$  is the time that the output signal power is a maximum. The matched filter can be realized in many forms, such as the integrate-and-dump, the correlator, and the transversal filter configurations.

## 6-10 APPENDIX: PROOF OF SCHWARZ'S INEQUALITY

*Schwarz's inequality* is

$$\left| \int_{-\infty}^{\infty} f(t)g(t) dt \right|^2 \leq \int_{-\infty}^{\infty} |f(t)|^2 dt \int_{-\infty}^{\infty} |g(t)|^2 dt \quad (6-182)$$

and becomes an *equality* if and only if

$$f(t) = Kg^*(t) \quad (6-183)$$

where  $K$  is an arbitrary real constant.  $f(t)$  and  $g(t)$  may be complex valued. It is assumed that both  $f(t)$  and  $g(t)$  have finite energy. That is,

$$\int_{-\infty}^{\infty} |f(t)|^2 dt < \infty \quad \text{and} \quad \int_{-\infty}^{\infty} |g(t)|^2 dt < \infty \quad (6-184)$$

**Proof.** Schwarz's inequality is equivalent to the inequality.

$$\left| \int_{-\infty}^{\infty} f(t)g(t) dt \right| \leq \sqrt{\int_{-\infty}^{\infty} |f(t)|^2 dt} \sqrt{\int_{-\infty}^{\infty} |g(t)|^2 dt} \quad (6-185)$$

Furthermore, it is realized that

$$\left| \int_{-\infty}^{\infty} f(t)g(t) dt \right| \leq \int_{-\infty}^{\infty} |f(t)g(t)| dt = \int_{-\infty}^{\infty} |f(t)| |g(t)| dt \quad (6-186)$$

and equality holds if (6-183) is satisfied. Thus, if we can prove that

$$\int_{-\infty}^{\infty} |f(t)| |g(t)| dt \leq \sqrt{\int_{-\infty}^{\infty} |f(t)|^2 dt} \sqrt{\int_{-\infty}^{\infty} |g(t)|^2 dt} \quad (6-187)$$

then we have proved Schwarz's inequality. To simplify the notation, replace  $|f(t)|$  and  $|g(t)|$  by the real-valued functions  $a(t)$  and  $b(t)$  where

$$a(t) = |f(t)| \quad (6-188a)$$

$$b(t) = |g(t)| \quad (6-188b)$$

Then, we need to show that

$$\int_a^b a(t)b(t) dt \leq \sqrt{\int_{-\infty}^{\infty} a^2(t) dt} \sqrt{\int_{-\infty}^{\infty} b^2(t) dt} \quad (6-189)$$

This can easily be shown by using an orthonormal functional series to represent  $a(t)$  and  $b(t)$ . Let

$$a(t) = a_1 \varphi_1(t) + a_2 \varphi_2(t) \quad (6-190a)$$

$$b(t) = b_1 \varphi_1(t) + b_2 \varphi_2(t) \quad (6-190b)$$

where, as described in Chapter 2,  $\mathbf{a} = (a_1, a_2)$  and  $\mathbf{b} = (b_1, b_2)$  represent  $a(t)$  and  $b(t)$ . This is illustrated in Fig. 6-21.

Then, using the figure,

$$\cos \theta = \cos(\theta_a - \theta_b) = \cos \theta_a \cos \theta_b + \sin \theta_a \sin \theta_b = \frac{a_1}{|\mathbf{a}|} \frac{b_1}{|\mathbf{b}|} + \frac{a_2}{|\mathbf{a}|} \frac{b_2}{|\mathbf{b}|}$$

or

$$\cos \theta = \frac{\mathbf{a} \cdot \mathbf{b}}{|\mathbf{a}| |\mathbf{b}|} \quad (6-191)$$

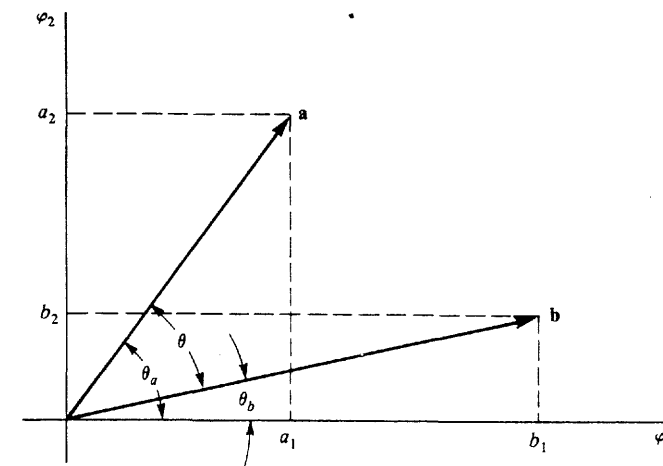


Figure 6-21 Vector representation for  $a(t)$  and  $b(t)$ .

Furthermore the dot product is equivalent to the inner product

$$\mathbf{a} \cdot \mathbf{b} = \int_{-\infty}^{\infty} a(t)b(t) dt \quad (6-192a)$$

(This may be demonstrated by substituting  $a(t) = \sum a_j \varphi_j(t)$  and  $b(t) = \sum b_k \varphi_k(t)$  into the integral, where  $\varphi_j(t)$  and  $\varphi_k(t)$  are real orthonormal functions.)

Using the Pythagorean theorem, the length (or norm) of the vector, is equivalent to

$$|\mathbf{a}| = \sqrt{a_1^2 + a_2^2} = \sqrt{\mathbf{a} \cdot \mathbf{a}} = \sqrt{\int_{-\infty}^{\infty} a^2(t) dt} \quad (6-192b)$$

and

$$|\mathbf{b}| = \sqrt{b_1^2 + b_2^2} = \sqrt{\mathbf{b} \cdot \mathbf{b}} = \sqrt{\int_{-\infty}^{\infty} b^2(t) dt} \quad (6-192c)$$

Because  $|\cos \theta| \leq 1$  we have

$$\left| \int_{-\infty}^{\infty} a(t)b(t) dt \right| \leq \sqrt{\int_{-\infty}^{\infty} a^2(t) dt} \sqrt{\int_{-\infty}^{\infty} b^2(t) dt} \quad (6-193)$$

where equality is obtained when we substitute

$$\mathbf{a} = K\mathbf{b} \quad (6-194)$$

Using (6-188), when  $f(t) = Kg^*(t)$ , we find that (6-194) is also satisfied so that equality is obtained. Thus the proof of (6-193) proves Schwarz's inequality.

**6-11 STUDY-AID EXAMPLES**

**SA6-1** Let  $y(t) = A \cos(10\pi t)$  be a random process, where  $A$  is a Gaussian random variable process with zero mean and variance  $\sigma_A^2$ . Find the PDF for  $y(t)$ . Is  $y(t)$  WSS?

**Solution**  $y(t)$  is a linear function of  $A$ . Thus,  $y(t)$  is Gaussian because  $A$  is Gaussian (see Sec. 6-6). Because  $\bar{A} = 0$ ,

$$m_y = \overline{y(t)} = \bar{A} \cos(10\pi t) = 0 \quad (6-195a)$$

and

$$\sigma_y^2 = \overline{y^2} - m_y^2 = \bar{A}^2 \cos^2(10\pi t) = \sigma_A^2 \cos^2(10\pi t) \quad (6-195b)$$

Thus, the PDF for  $y(t)$  is

$$f(y) = \frac{1}{\sqrt{2\pi \sigma_y^2}} e^{-y^2/2\sigma_y^2} \quad (6-195c)$$

where  $\sigma_y^2$  is given by (6-195b). Furthermore,  $y(t)$  is not WSS because

$$R_y(0) = \sigma_y^2 + m_y^2 = \sigma_A^2 \cos^2(10\pi t)$$

is a function of  $t$ .

**SA6-2** Derive an expression for the mean value of the output of a linear time-invariant filter if the input  $x(t)$  is a WSS random process.

**Solution** The output of the filter is

$$y(t) = h(t) * x(t)$$

where  $h(t)$  is the impulse response of the filter. Taking the expected value, we get

$$\begin{aligned} m_y &= \overline{y(t)} = \overline{h(t) * x(t)} = h(t) * \overline{x(t)} = h(t) * m_x \\ &= \int_{-\infty}^{\infty} h(\lambda) m_x d\lambda = m_x \int_{-\infty}^{\infty} h(\lambda) d\lambda \end{aligned} \quad (6-196)$$

However, the transfer function of the filter is

$$H(f) = \mathcal{F}[h(t)] = \int_{-\infty}^{\infty} h(t) e^{-j2\pi ft} dt$$

so that  $H(0) = \int_{-\infty}^{\infty} h(t) dt$ . Thus, (6-196) reduces to

$$m_y = m_x H(0) \quad (6-197)$$

**SA6-3** Let  $y(t) = dn(t)/dt$  where  $n(t)$  is a noise random process that has a PSD of  $\mathcal{P}_n(f) = N_0/2 = 10^{-6}$  W/Hz. Evaluate the normalized power of  $y(t)$  over a low-pass frequency band of  $B = 10$  Hz.

**Solution**  $\mathcal{P}_y(f) = |H(f)|^2 \mathcal{P}_n(f)$

where, from Table 2-1,  $H(f) = j2\pi f$  for a differentiator.

Thus,

$$\mathcal{P}_y = \int_{-B}^B \mathcal{P}_y(f) df = \int_{-B}^B (2\pi f)^2 \frac{N_0}{2} df = \frac{8\pi^2}{3} \left(\frac{N_0}{2}\right) B^3$$

or

$$\mathcal{P}_y = \frac{8\pi^2}{3} (10^{-6}) (10^3) = 0.0263 \text{ W} \quad (6-198)$$

**SA6-4** A bandpass process is described by

$$v(t) = x(t) \cos(\omega_c t + \theta_c) - y(t) \sin(\omega_c t + \theta_c)$$

where  $y(t) = x(t)$  is a WSS process with a PSD as shown in Fig. 6-22a.  $\theta_c$  is an independent random variable uniformly distributed over  $(0, 2\pi)$ . Find the PSD for  $v(t)$ .

**Solution** From (6-130), we know that  $v(t)$  is a WSS bandpass process with  $\mathcal{P}_v(f)$  given by (6-133d). Thus,  $\mathcal{P}_g(f)$  needs to be evaluated. Also,

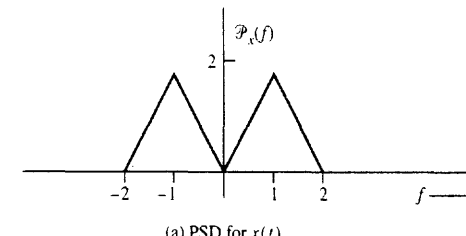
$$v(t) = \operatorname{Re}\{g(t)e^{j(\omega_c t + \theta_c)}\}$$

where  $g(t) = x(t) + jy(t) = x(t) + jx(t) = (1+j)x(t)$

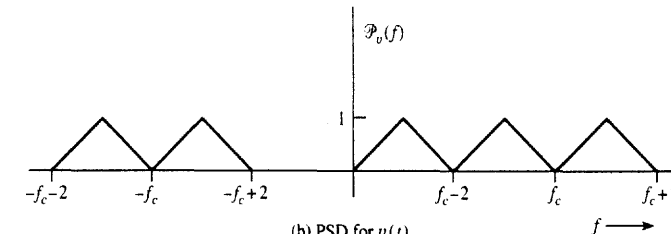
$$\begin{aligned} R_g(\tau) &= \overline{g^*(t)g(t+\tau)} = (1-j)(1+j)x(t)x(t+\tau) \\ &= (1+1)R_x(\tau) = 2R_x(\tau) \end{aligned}$$

Thus,

$$\mathcal{P}_y(f) = 2\mathcal{P}_x(f) \quad (6-199)$$



(a) PSD for  $x(t)$



(b) PSD for  $v(t)$

Figure 6-22 PSD for SA6-4.

Substituting (6-199) into (6-133d), we get

$$\mathcal{P}_v(f) = \frac{1}{2} [\mathcal{P}_x(f - f_c) + \mathcal{P}_x(-f - f_c)] \quad (6-200)$$

$\mathcal{P}_v(f)$  is plotted in Fig. 6-22b for the  $\mathcal{P}_x(f)$  of Fig. 6-22a.

## PROBLEMS

- 6-1 Let a random process  $x(t)$  be defined by

$$x(t) = At + B$$

- (a) If  $B$  is a constant and  $A$  is uniformly distributed between  $-1$  and  $+1$ , sketch a few sample functions.
- (b) If  $A$  is a constant and  $B$  is uniformly distributed between  $0$  and  $2$ , sketch a few sample functions.

- 6-2 Let a random process be given by

$$x(t) = A \cos(\omega_0 t + \theta)$$

where  $A$  and  $\omega_0$  are constants, and  $\theta$  is a random variable.

$$f(\theta) = \begin{cases} \frac{2}{\pi}, & 0 \leq \theta \leq \frac{\pi}{2} \\ 0, & \text{elsewhere} \end{cases}$$

- (a) Evaluate  $\overline{x(t)}$ .
- (b) From the result of part (a), what can be said about the stationarity of the process?
- 6-3 Using the random process described in Prob. 6-2:
  - (a) Evaluate  $\langle x^2(t) \rangle$ .
  - (b) Evaluate  $\overline{x^2(t)}$ .
  - (c) Using the results of parts (a) and (b), determine if the process is ergodic for these averages.
- 6-4 A conventional average reading ac voltmeter (volt-ohm multimeter) has a schematic diagram as shown in Fig. P6-4. The needle of the meter movement deflects proportionally to the average current flowing through the meter. The meter scale is marked to give the rms value of sine-wave voltages. Suppose that this meter is used to determine the rms value of a noise voltage. The noise voltage is known to be an ergodic Gaussian process having a zero mean value. What is the value of the constant that is multiplied by the meter reading to give the true rms value of the Gaussian noise? (Hint: The diode is a short circuit when the input voltage is positive and an open circuit when the input voltage is negative.)

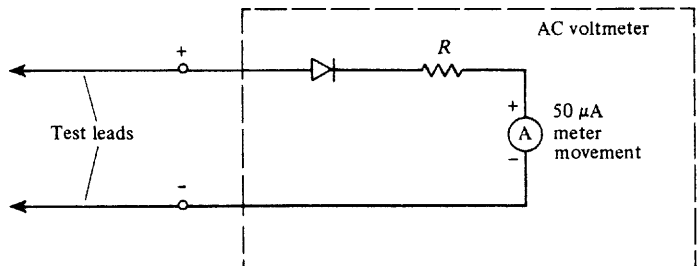


Figure P6-4

- 6-5 Let  $x(t) = A_0 \sin(\omega_0 t + \theta)$  be a random process where  $\theta$  is a random variable that is uniformly distributed between  $0$  and  $2\pi$ , and  $A_0$  and  $\omega_0$  are constants.

- (a) Find  $R_x(\tau)$ .
- (b) Show that  $x(t)$  is wide-sense stationary.
- (c) Verify that  $R_x(\tau)$  satisfies the appropriate properties.

- 6-6 Let  $r(t) = A_0 \cos \omega_0 t + n(t)$ , where  $A_0$  and  $\omega_0$  are constants. Assume that  $n(t)$  is a wide-sense stationary random noise process with a zero mean value and an autocorrelation of  $R_n(\tau)$ .

- (a) Find  $\overline{r(t)}$  and determine if  $r(t)$  is wide-sense stationary.
- (b) Find  $R_r(t_1, t_2)$ .
- (c) Evaluate  $\langle R_r(t, t + \tau) \rangle$  where  $t_1 = t$  and  $t_2 = t + \tau$ .

- 6-7 Let an additive signal plus noise process be described by  $r(t) = s(t) + n(t)$ .

- (a) Show that  $R_r(\tau) = R_s(\tau) + R_n(\tau) + R_{sn}(\tau) + R_{ns}(\tau)$ .
- (b) Simplify the result for part (a) for the case when  $s(t)$  and  $n(t)$  are independent and the noise has a zero mean value.

- 6-8 Consider the sum of two ergodic noise voltages

$$n(t) = n_1(t) + n_2(t)$$

The power of  $n_1(t)$  is  $5$  W, the power of  $n_2(t)$  is  $10$  W, the dc value of  $n_1(t)$  is  $-2$  V, and the dc value  $n_2$  is  $+1$  V. Find the power of  $n(t)$  if

- (a)  $n_1(t)$  and  $n_2(t)$  are orthogonal.
- (b)  $n_1(t)$  and  $n_2(t)$  are uncorrelated.
- (c) The cross-correlation of  $n_1(t)$  and  $n_2(t)$  is  $2$  for  $\tau = 0$ .

- 6-9 Assume that  $x(t)$  is ergodic and let  $x(t) = m_x + y(t)$ , where  $m_x = \overline{x(t)}$  is the dc value of  $x(t)$  and  $y(t)$  is the ac component of  $x(t)$ . Show that

- (a)  $R_x(\tau) = m_x^2 + R_y(\tau)$ .
- (b)  $\lim_{\tau \rightarrow \infty} R_x(\tau) = m_x^2$ .
- (c) If  $R_x(\tau)$  can be measured, how can the dc value of  $x(t)$  be determined from  $R_x(\tau)$ ?

- 6-10 Determine if the following functions satisfy the properties for autocorrelation functions.

- (a)  $\sin \omega_0 \tau$ .
- (b)  $(\sin \omega_0 \tau)/(\omega_0 \tau)$ .
- (c)  $\cos \omega_0 \tau + \delta(\tau)$ .
- (d)  $e^{-a|\tau|}$ , where  $a < 0$ .

(Note:  $\mathcal{F}[R(\tau)]$  must also be a nonnegative function.)

- 6-11 A random process  $x(t)$  has an autocorrelation function given by  $R_x(\tau) = 5 + 8e^{-3|\tau|}$ . Find:
- (a) The rms value for  $x(t)$ .
  - (b) The PSD for  $x(t)$ .



- 6-12 The autocorrelation of a random process is  $R_x(\tau) = 4e^{-\tau^2} + 3$ . Plot the PSD for  $x(t)$  and evaluate the rms bandwidth for  $x(t)$ .

- 6-13 Show that two random processes  $x(t)$  and  $y(t)$  are uncorrelated (i.e.,  $R_{xy}(\tau) = m_x m_y$ ) if the processes are independent.

- 6-14 If  $x(t)$  contains periodic components, show that:
- (a)  $R_x(\tau)$  contains periodic components.
  - (b)  $\mathcal{P}_x(f)$  contains delta functions.

- 6-15 Find the PSD for the random process described in Prob. 6-2.

- 6-16 Determine if the following functions can be valid PSD functions for a real process.
- (a)  $2e^{-2\pi|f-45|}$ .
  - (b)  $4e^{-2\pi|f^2-16|}$ .

- (c)  $25 + \delta(f - 16)$ .  
 (d)  $10 + \delta(f)$ .

6-17 The PSD of an ergodic random process  $x(t)$  is

$$\mathcal{P}_x(f) = \begin{cases} \frac{1}{B}(B - |f|), & |f| \leq B \\ 0, & f \text{ otherwise} \end{cases}$$

where  $B > 0$ . Find:

- (a) The rms value of  $x(t)$ .  
 (b)  $R_x(\tau)$ .

6-18 Referring to the techniques described in Example 6-3, evaluate the PSD for a PCM signal that uses Manchester NRZ encoding (see Fig. 3-11). Assume that the data have values of  $a_n = \pm 1$ , which are equally likely, and that the data are independent from bit to bit.

6-19 The *magnitude* frequency response of a linear time-invariant network is to be determined from a laboratory setup as shown in Fig. P6-19. Discuss how  $|H(f)|$  is evaluated from the measurements.

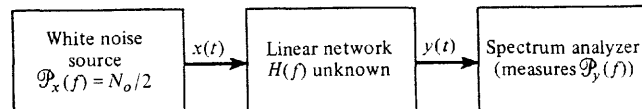


Figure P6-19

6-20 A linear time-invariant network with an unknown  $H(f)$  is shown in Fig. P6-20.

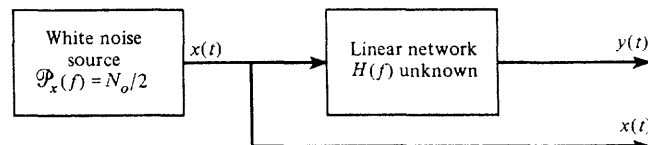


Figure P6-20

- (a) Find a formula for evaluating  $h(t)$  in terms of  $R_{xy}(\tau)$  and  $N_0$ .  
 (b) Find a formula for evaluating  $H(f)$  in terms of  $\mathcal{P}_{xy}(f)$  and  $N_0$ .  
 6-21 The output of a linear system is related to the input by  $y(t) = h(t) * x(t)$ , where  $x(t)$  and  $y(t)$  are jointly wide-sense stationary. Show that:

- (a)  $R_{xy}(\tau) = h(\tau) * R_x(\tau)$ .  
 (b)  $\mathcal{P}_{xy}(f) = H(f)\mathcal{P}_x(f)$ .  
 (c)  $R_{yx}(\tau) = h(-\tau) * R_x(\tau)$ .  
 (d)  $\mathcal{P}_{yx}(f) = H^*(f)\mathcal{P}_x(f)$ .

[Hint: Use (6-86) and (6-87).]

6-22 Ergodic white noise with a PSD of  $\mathcal{P}_n(f) = N_0/2$  is applied to the input of an ideal integrator with a gain of  $K$  (a real number) such that  $H(f) = K/(j2\pi f)$ .

- (a) Find the PSD for the output.  
 (b) Find the rms value of the output noise.

6-23 A linear system has a power transfer function  $|H(f)|^2$  as shown in Fig. P6-23. The input  $x(t)$  is a Gaussian random process with a PSD given by

$$\mathcal{P}_x(f) = \begin{cases} \frac{1}{2}N_0, & |f| \leq 2B \\ 0, & f \text{ elsewhere} \end{cases}$$

- (a) Find the autocorrelation function for the output  $y(t)$ .

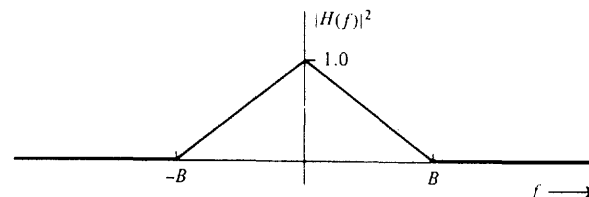


Figure P6-23

- (b) Find the PDF for  $y(t)$ .

- (c) When are the two random variables  $y_1 = y(t_1)$  and  $y_2 = y(t_2)$  independent?

6-24 A linear filter evaluates the  $T$ -second moving average of an input waveform where the filter output is

$$y(t) = \frac{1}{T} \int_{t-(T/2)}^{t+(T/2)} x(u) du$$

and  $x(t)$  is the input.

- (a) Show that the impulse response is  $h(t) = (1/T) \Pi(t/T)$ .

- (b) Show that

$$R_y(\tau) = \frac{1}{T} \int_{-T}^T \left(1 - \frac{|u|}{T}\right) R_x(\tau - u) du$$

- (c) If  $R_x(\tau) = e^{-|\tau|}$  and  $T = 1$  sec, plot  $R_y(\tau)$  and compare it with  $R_x(\tau)$ .

6-25 As shown in Example 6-5, the output signal-to-noise ratio of an RC LPF is given by (6-95) when the input is a sinusoidal signal plus white noise. Derive the value of the RC product such that the output signal-to-noise ratio will be a maximum.

6-26 Assume that a sine wave of peak amplitude  $A_0$  and frequency  $f_0$  plus white noise with  $\mathcal{P}_n(f) = N_0/2$  is applied to a linear filter. The transfer function of the filter is

$$H(f) = \begin{cases} \frac{1}{B}(B - |f|), & |f| < B \\ 0, & f \text{ elsewhere} \end{cases}$$

where  $B$  is the absolute bandwidth of the filter. Find the signal-to-noise power ratio for the filter output.

6-27 For the random process  $x(t)$  with the PSD shown in Fig. P6-27, determine

- (a) The equivalent bandwidth.  
 (b) The rms bandwidth.

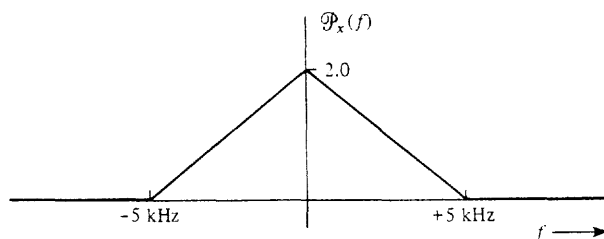


Figure P6-27

- 6-28 If  $x(t)$  is a real bandpass random process that is wide-sense stationary, show that the definition for rms bandwidth, (6-100), is equivalent to

$$B_{\text{rms}} = 2 \sqrt{\bar{f}^2 - (f_0)^2}$$

where  $\bar{f}^2$  is given by (6-98) or (6-99) and  $f_0$  is given by (6-102).

- 6-29 In the definition for the rms bandwidth of a *bandpass* random process,  $f_0$  is used. Show that

$$f_0 = \frac{1}{2\pi R_v(0)} \left( \frac{d\hat{R}_v(\tau)}{d\tau} \right) \Big|_{\tau=0}$$

where  $\hat{R}_v(\tau)$  is the Hilbert transform of  $R_v(\tau)$ .

- 6-30 Two identical  $RC$  LPFs are coupled in cascade by an isolation amplifier that has a voltage gain of 10.  
 (a) Find the overall transfer function of the network as a function of  $R$  and  $C$ .  
 (b) Find the 3-dB bandwidth in terms of  $R$  and  $C$ .
- 6-31 Let  $x(t)$  be a Gaussian process where two random variables are  $x_1 = x(t_1)$  and  $x_2 = x(t_2)$ . The random variables have variances of  $\sigma_1^2$  and  $\sigma_2^2$  and means of  $m_1$  and  $m_2$ . The correlation coefficient is

$$\rho = \overline{(x_1 - m_1)(x_2 - m_2)} / (\sigma_1 \sigma_2)$$

Using the matrix notation for the  $N = 2$  dimensional PDF, show that this reduces to the bivariate Gaussian PDF as given by (B-97).

- 6-32 A bandlimited white Gaussian random process has an autocorrelation function that is specified by (6-125). Show that as  $B \rightarrow \infty$ , the autocorrelation function becomes  $R_n(\tau) = \frac{1}{2} N_0 \delta(\tau)$ .
- 6-33 Let two random processes  $x(t)$  and  $y(t)$  be jointly Gaussian with zero-mean values. That is,  $(x_1, x_2, \dots, x_N, y_1, y_2, \dots, y_M)$  is described by an  $(N + M)$ -dimensional Gaussian PDF. The cross correlation is

$$R_{xy}(\tau) = \overline{x(t_1)y(t_2)} = 10 \sin(2\pi\tau)$$

- (a) When are the random variables  $x_1 = x(t_1)$  and  $y_2 = y(t_2)$  independent?  
 (b) Show that  $x(t)$  and  $y(t)$  are or are not independent random processes.

- 6-34 Starting with (6-121), show that

$$\mathbf{C}_y = \mathbf{H} \mathbf{C}_x \mathbf{H}^T$$

(Hint: Use the identity matrix property,  $\mathbf{A}\mathbf{A}^{-1} = \mathbf{A}^{-1}\mathbf{A} = \mathbf{I}$ , where  $\mathbf{I}$  is the identity matrix.)

- 6-35 Given the random process

$$x(t) = A_0 \cos(\omega_c t + \theta)$$

where  $A_0$  and  $\omega_0$  are constants and  $\theta$  is a random variable that is uniformly distributed over the interval  $(0, \pi/2)$ .

- (a) Determine if  $x(t)$  is wide-sense stationary.  
 (b) Find the PSD for  $x(t)$ .  
 (c) If  $\theta$  is uniformly distributed over  $(0, 2\pi)$ , is  $x(t)$  wide-sense stationary?

- 6-36 A bandpass WSS random process  $v(t)$  is represented by (6-129a) where the conditions of (6-129) are satisfied. The PSD of  $v(t)$  is shown in Fig. P6-36 where  $f_c = 1\text{ MHz}$ . Using MATLAB or MathCAD:

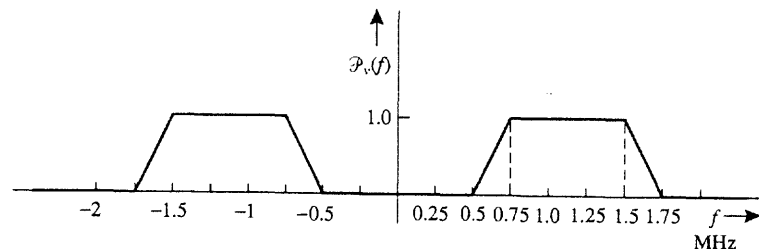


Figure P6-36

- (a) Plot  $\mathcal{P}_x(f)$ .  
 (b) Plot  $\mathcal{P}_{xy}(f)$ .

- 6-37 The PSD of a bandpass WSS process  $v(t)$  is shown in Fig. P6-37.  $v(t)$  is the input to a product detector and the oscillator signal (i.e., the second input to the multiplier) is  $5 \cos(\omega_c t + \theta_0)$ , where  $f_c = 1\text{ MHz}$  and  $\theta_0$  is an independent random variable with a uniform distribution over  $(0, 2\pi)$ . Using MATLAB or MathCAD, plot the PSD for the output of the product detector.

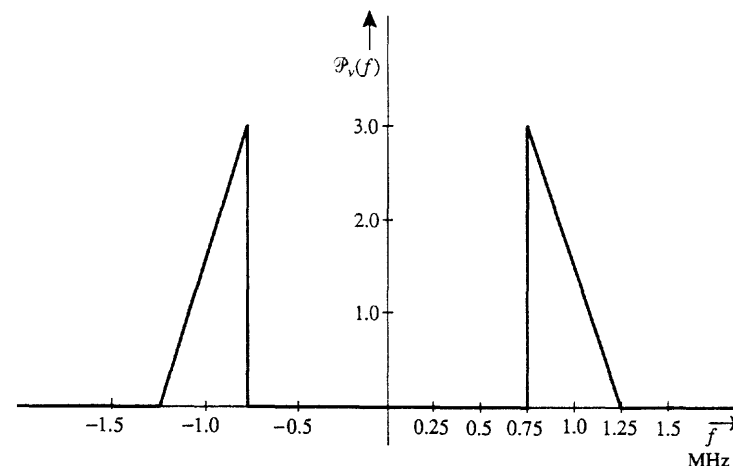


Figure P6-37

- 6-38 A WSS bandpass process  $v(t)$  is applied to a product detector as shown in Fig. 6-11 where  $\theta_c = 0$ .

- (a) Derive an expression for the autocorrelation of  $w_1(t)$  in terms of  $R_v(\tau)$ . Is  $w_1(t)$  WSS?  
 (b) Using  $R_{w_1}(\tau)$  obtained in part (a), to find an expression for  $\mathcal{P}_{w_1}(f)$ . (Hint: Use the Wiener-Khintchine theorem.)

**6-39** A USSB signal is

$$v(t) = 10 \operatorname{Re}\{[x(t) + j\hat{x}(t)]e^{j(\omega_c t + \theta_c)}\}$$

where  $\theta_c$  is a random variable that is uniformly distributed over  $(0, 2\pi)$ . The PSD for  $x(t)$  is given in Fig. P6-27. Find:

- (a) The PSD for  $v(t)$ .  
 (b) The total power of  $v(t)$ .

**6-40** Show that:

- (a)  $R_{\hat{x}}(\tau) = R_x(\tau)$   
 (b)  $R_{x,\hat{x}}(\tau) = \hat{R}_x(\tau)$ .

**6-41** A bandpass random signal can be represented by

$$s(t) = x(t) \cos(\omega_c t + \theta_c) - y(t) \sin(\omega_c t + \theta_c)$$

where the PSD of  $s(t)$  is shown in Fig. P6-41.  $\theta_c$  is an independent random variable that is uniformly distributed over  $(0, 2\pi)$ . Assume that  $f_3 - f_2 = f_2 - f_1$ . Find the PSD for  $x(t)$  and  $y(t)$  when

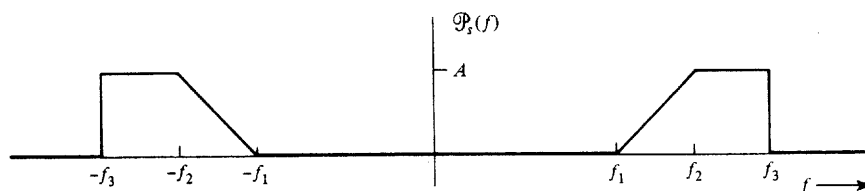


Figure P6-41

- (a)  $f_c = f_1$ . This is USSB signaling where  $y(t) = \hat{x}(t)$ .  
 (b)  $f_c = f_2$ . This represents independent USSB and LSSB signaling with two different modulations.  
 (c)  $f_1 < f_c < f_2$ . This is vestigial sideband signaling.  
 (d) For which, if any, of these cases are  $x(t)$  and  $y(t)$  orthogonal?
- 6-42** Referring to Prob. 6-41(b), how are the two modulations  $m_1(t)$  and  $m_2(t)$  for the independent sidebands related to  $x(t)$  and  $y(t)$ ? Give the PSD for  $m_1(t)$  and  $m_2(t)$ , where  $m_1(t)$  is the modulation on the USSB portion of the signal and  $m_2(t)$  is the modulation on the LSSB portion of  $s(t)$ .
- 6-43** For the bandpass random process, show that:  
 (a) Equation (6-133m) is valid (property 13).  
 (b) Equation (6-133i) is valid (property 9).
- 6-44** Referring to Example 6-9, find the PSD for a BPSK signal with Manchester-encoded data (see Fig. 3-15). Assume that the data have values of  $a_n = \pm 1$  that are equally likely and that the data are independent from bit to bit.
- 6-45** The input to an envelope detector is an ergodic bandpass Gaussian noise process. The rms value of the input is 2 V and the mean value is 0 V. The envelope detector has a voltage gain of 10. Find:

- (a) The dc value of the output voltage.  
 (b) The rms value of the output voltage.

**6-46** A narrowband signal plus noise process is

$$r(t) = A \cos(\omega_c t + \theta_c) + x(t) \cos(\omega_c t + \theta_c) - y(t) \sin(\omega_c t + \theta_c)$$

where  $A \cos(\omega_c t + \theta_c)$  is a sinusoidal carrier and the remaining terms are the bandpass noise. Let the noise have an rms value of  $\sigma$  and a mean of 0. This signal plus noise process appears at the input to an envelope detector. Show that the PDF for the output of the envelope detector is

$$f(R) = \begin{cases} \frac{R}{\sigma^2} e^{-[(R^2+A^2)/(2\sigma^2)]} I_0\left(\frac{RA}{\sigma^2}\right), & R \geq 0 \\ 0, & R < 0 \end{cases}$$

where

$$I_0(z) \triangleq \frac{1}{2\pi} \int_0^{2\pi} e^{z \cos \theta} d\theta$$

is the modified Bessel function of the first kind of zero order.  $f(R)$  is known as a *Rician PDF* in honor of the late S. O. Rice, who was an outstanding engineer at Bell Telephone Laboratories.

**6-47** Assume that a known signal is

$$s(t) = \begin{cases} \frac{A}{T} t \cos \omega_c t, & 0 \leq t \leq T \\ 0, & t \text{ otherwise} \end{cases}$$

This signal plus white noise is present at the input to a matched filter.

- (a) Design a matched filter for this signal. Sketch the waveforms for this problem analogous to those shown in Fig. 6-16.  
 (b) Sketch the waveforms for the correlation processor shown in Fig. 6-18.

**6-48** A baseband digital communication system uses polar signaling with a bit rate of  $R = 2000$  bits/s. The transmitted pulses are rectangular and the frequency response of channel filter is

$$H_c(f) = \frac{B}{B + jf}$$

where  $B = 6000$  Hz. The filtered pulses are the input to a receiver that uses integrate-and-dump processing as illustrated in Fig. 6-17. Examine the integrator output for ISI. In particular:

- (a) Plot the integrator output when a binary "1" is sent.  
 (b) Plot the integrator output for an all-pass channel and compare this result with that obtained in part (a).

**6-49** Refer to Fig. 6-19 for the detection of a BPSK signal. Suppose that the BPSK signal at the input is

$$r(t) = s(t) = \sum_{n=0}^7 d_n p(t - nT)$$

where

$$p(t) = \begin{cases} e^{-t} \cos(\omega_c t), & 0 < t < T \\ 0, & \text{elsewhere} \end{cases}$$

and the binary data  $d_n$  is the 8-bit string  $\{+1, -1, -1, +1, +1, -1, +1, -1\}$ . Use MATLAB or MathCAD to

- (a) Plot the input waveform  $r(t)$ .
- (b) Plot the integrator output waveform  $r_0(t)$ .

6-50 A matched filter is described in Fig. P6-50.

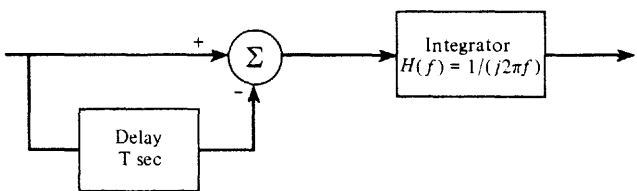


Figure P6-50

- (a) Find the impulse response of the matched filter.
- (b) Find the pulse shape to which this filter is matched (white noise case).

6-51 A FSK signal,  $s(t)$ , is applied to a matched-filter receiver circuit that is shown in Fig. P6-51. The FSK signal is

$$s(t) = \begin{cases} A \cos(\omega_1 t), & \text{when a binary 1 is sent} \\ A \cos(\omega_2 t), & \text{when a binary 0 is sent} \end{cases}$$

where  $f_1 = f_c + \Delta F$  and  $f_2 = f_c - \Delta F$ . Let  $\Delta F$  be chosen to satisfy the MSK condition, which is  $\Delta F = 1/(4T)$ .  $T$  is the time that it takes to send one bit and the integrator is reset every  $T$  seconds. Assume that  $A = 1$ ,  $f_c = 1000$  Hz, and  $\Delta F = 50$  Hz.

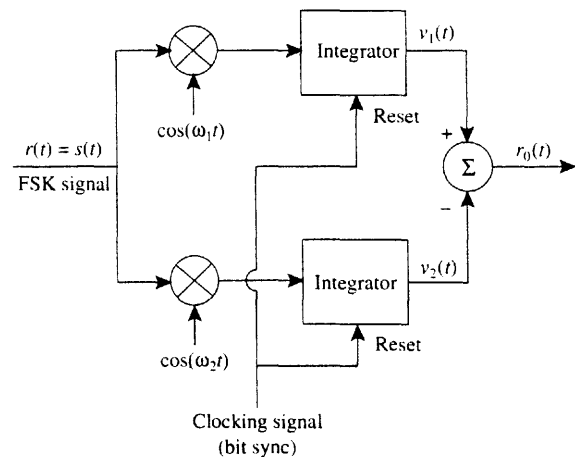


Figure P6-51

- (a) If a binary 1 is sent, plot  $v_1(t)$ ,  $v_2(t)$ , and  $r_0(t)$  over a  $T$ -second interval.
- (b) Referring to Fig. 6-16, find an expression that describes the output of a filter that is matched to the FSK signal when a binary 1 is sent. Plot it.
- (c) Discuss how the plots obtained for parts (a) and (b) agree or disagree.

6-52 Let

$$s(t) = \operatorname{Re}\{g(t)e^{j(\omega_c t + \theta_c)}\}$$

be a wideband FM signal where

$$g(t) = A_c e^{jD_f \int_{-\infty}^t m(\lambda) d\lambda}$$

and  $m(t)$  is a random modulation process.

- (a) Show that

$$R_g(\tau) = A_c^2 [\overline{e^{jD_f \tau m(t)}}]$$

when the integral  $\int_t^{t+\tau} m(\lambda) d\lambda$  is approximated by  $\tau m(t)$ .

- (b) Using the results of part (a), prove that the PSD of the wideband FM signal is given by (5-66). That is, show that

$$\mathcal{P}_s(f) = \frac{\pi A_c^2}{2D_f} \left[ f_m \left( \frac{2\pi}{D_f} (f - f_c) \right) + f_m \left( \frac{2\pi}{D_f} (-f - f_c) \right) \right]$$

## PERFORMANCE OF COMMUNICATION SYSTEMS CORRUPTED BY NOISE

As indicated in Chapter 1, the two primary considerations in the design of a communication system are:

1. The *performance* of the system when it is corrupted by noise. The performance measure for a digital system is the probability of error of the output signal. For analog systems, the performance measure is the output signal-to-noise ratio.
2. The channel *bandwidth* that is required for transmission of the communication signal. This bandwidth was evaluated for various types of digital and analog signals in the previous chapters.

There are numerous ways in which the information can be demodulated (recovered) from the received signal that has been corrupted by noise. Some receivers provide optimum performance, but most do not. Often a suboptimum receiver will be used in order to lower the cost. In addition, some suboptimum receivers perform almost as well as optimum ones for all practical purposes. Here we will analyze the performance of some suboptimum as well as some optimum receivers.

### 7-1 ERROR PROBABILITIES FOR BINARY SIGNALING

#### General Results

Figure 7-1 is a general block diagram for a binary communication system. The receiver input  $r(t)$  consists of the transmitted signal  $s(t)$  plus channel noise  $n(t)$ . For *baseband* signaling the processing circuits in the receiver consist of low-pass filtering with appropriate amplification. For *bandpass* signaling, such as OOK, BPSK, and FSK, discussed in Sec. 5-9, the processing circuits normally consist of a superheterodyne receiver containing a mixer, an IF amplifier, and a detector. These circuits produce a baseband analog output  $r_o(t)$ . (For example, when BPSK signaling is used, the detector might consist of a product detector and an integrator as described in Sec. 6-8 and illustrated in Fig. 6-19.)

The analog baseband waveform  $r_o(t)$  is sampled at the clocking time  $t = t_0 + nT$  to produce the samples  $r_o(t_0 + nT)$ , which are fed into a threshold device (a comparator). The threshold device produces the binary serial-data waveform  $\tilde{m}(t)$ .

In this subsection we develop a *general technique* for evaluating the probability of bit error, also called the *bit error rate* (BER), for binary signaling. In later sections, this technique will be used to obtain specific expressions for the BER of various binary signaling schemes such as OOK, BPSK, and FSK.

To develop a general formula for the BER of a detected binary signal, let  $T$  be the length of time that it takes to transmit one bit of data. The transmitted signal over a bit interval of  $(0, T)$  is represented by

$$s(t) = \begin{cases} s_1(t), & 0 < t \leq T \text{ for a binary 1} \\ s_2(t), & 0 < t \leq T \text{ for a binary 0} \end{cases} \quad (7-1)$$

where  $s_1(t)$  is the waveform that is used if a binary 1 is transmitted and  $s_2(t)$  is the waveform that is used if a binary 0 is transmitted. If  $s_1(t) = -s_2(t)$ ,  $s(t)$  is called an *antipodal*

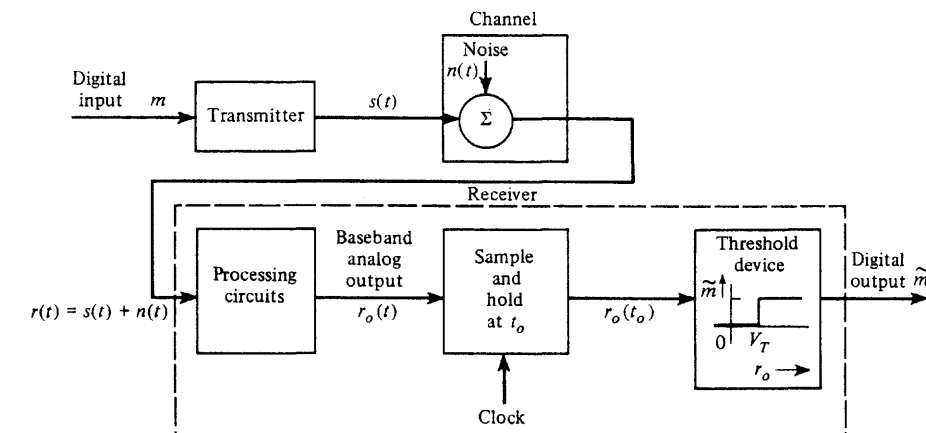


Figure 7-1 General binary communication system.

signal. The binary signal plus noise at the receiver input produces a baseband analog waveform at the output of the processing circuits that is denoted by

$$r_0(t) = \begin{cases} r_{01}(t), & 0 < t \leq T \text{ for a binary 1 sent} \\ r_{02}(t), & 0 < t \leq T \text{ for a binary 0 sent} \end{cases} \quad (7-2)$$

where  $r_{01}(t)$  is the output signal that is corrupted by noise for a binary 1 transmission and  $r_{02}(t)$  is the output for the binary 0 transmission. (Note that if the receiver uses nonlinear processing circuits, such as an envelope detector, the superposition of the signal plus noise outputs are not valid operations.) This analog voltage waveform  $r_0(t)$  is sampled at some time  $t_0$  during the bit interval. That is,  $0 < t_0 \leq T$ . For matched-filter processing circuits,  $t_0$  is usually  $T$ . The resulting sample is

$$r_0(t_0) = \begin{cases} r_{01}(t_0) & \text{for a binary 1 sent} \\ r_{02}(t_0) & \text{for a binary 0 sent} \end{cases} \quad (7-3)$$

It is realized that  $r_0(t_0)$  is a *random variable* that has a *continuous distribution* because the channel noise has corrupted the signal. To shorten the notation, we will denote  $r_0(t_0)$  simply by  $r_0$ . That is,

$$r_0 = r_0(t_0) = \begin{cases} r_{01} & \text{for a binary 1 sent} \\ r_{02} & \text{for a binary 0 sent} \end{cases} \quad (7-4)$$

$r_0 = r_0(t_0)$  is called the *test statistic*.

For the moment, let us assume that we can evaluate the PDFs for the two random variables  $r_0 = r_{01}$  and  $r_0 = r_{02}$ . These PDFs are actually *conditional PDFs* since they depend, respectively, on a binary 1 or a binary 0 being transmitted. That is, when  $r_0 = r_{01}$ , the PDF is  $f(r_0 | s_1 \text{ sent})$  and when  $r_0 = r_{02}$  the PDF is  $f(r_0 | s_2 \text{ sent})$ . These conditional PDFs are shown in Fig. 7-2. For illustrative purposes Gaussian shapes are shown. The actual shapes of the PDFs depend on the characteristics of the channel noise, the specific types of filter and detector circuits used, and the types of binary signals transmitted. (In later sections, we obtain specific PDFs using the theory developed in Chapter 6.)

In our development of a general formula for the BER, assume that the *polarity of the processing circuits* of the receiver is such that if the *signal only* (no noise) were present at

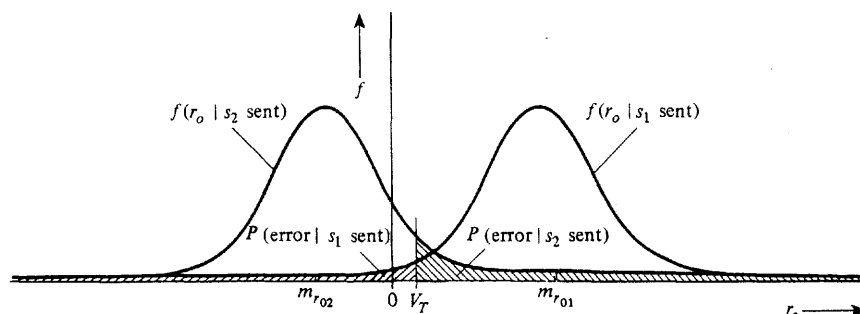


Figure 7-2 Error probability for binary signaling.

the receiver input,  $r_0 > V_T$  when a *binary 1* is sent and  $r_0 < V_T$  when a *binary 0* is sent;  $V_T$  is the threshold (voltage) setting of the comparator (threshold device).

When signal plus noise is present at the receiver input, errors can occur in two ways. An error occurs when  $r_0 < V_T$  if a binary 1 is sent:

$$P(\text{error} | s_1 \text{ sent}) = \int_{-\infty}^{V_T} f(r_0 | s_1) dr_0 \quad (7-5)$$

This is illustrated by a shaded area to the left of  $V_T$  in Fig. 7-2. Similarly, an error occurs when  $r_0 > V_T$  if a binary 0 is sent:

$$P(\text{error} | s_2 \text{ sent}) = \int_{V_T}^{\infty} f(r_0 | s_2) dr_0 \quad (7-6)$$

The bit error rate is then

$$P_e = P(\text{error} | s_1 \text{ sent})P(s_1 \text{ sent}) + P(\text{error} | s_2 \text{ sent})P(s_2 \text{ sent}) \quad (7-7)$$

This follows from probability theory (see Appendix B), where the probability of an event that consists of joint events is

$$P(E) = \sum_{i=1}^2 P(E, s_i) = \sum_{i=1}^2 P(E|s_i)P(s_i)$$

When we combine (7-5), (7-6), and (7-7), the general expression for the BER of any binary communication system is

$$P_e = P(s_1 \text{ sent}) \int_{-\infty}^{V_T} f(r_0 | s_1) dr_0 + P(s_2 \text{ sent}) \int_{V_T}^{\infty} f(r_0 | s_2) dr_0 \quad (7-8)$$

$P(s_1 \text{ sent})$  and  $P(s_2 \text{ sent})$  are known as the *source statistics* or *a priori statistics*. In most applications, the source statistics are considered to be equally likely. That is,

$$P(\text{binary 1 sent}) = P(s_1 \text{ sent}) = \frac{1}{2} \quad (7-9a)$$

$$P(\text{binary 0 sent}) = P(s_2 \text{ sent}) = \frac{1}{2} \quad (7-9b)$$

In the results that we obtain throughout the remainder of this chapter we will assume that the source statistics are equally likely. As indicated earlier, the conditional PDFs depend on the signaling waveshapes involved, the channel noise, and the receiver processing circuits used. These are obtained subsequently for the case of Gaussian channel noise and linear processing circuits.

### Results for Gaussian Noise

Assume that the channel noise is a zero-mean wide-sense stationary Gaussian process and that the receiver processing circuits, except for the threshold device, are linear. Then we know (see Chapter 6) that for Gaussian noise (only) at the input, the output of the linear processor,  $r_0(t) = n_0(t)$ , will also be a Gaussian process. For baseband signaling, the pro-

cessing circuits would consist of linear filters with some gain. For bandpass signaling, as we demonstrated in Chapter 4, a superheterodyne circuit (consisting of a mixer, IF stage, and product detector) is a linear circuit. However, if automatic gain control (AGC) or limiters are used, the receiver will be nonlinear and the results of this section will not be applicable. In addition, if a nonlinear detector such as an envelope detector is used, the output noise will not be Gaussian. For the case of a linear processing receiver circuit with a binary signal plus noise at the input, the sampled output is

$$r_0 = s_0 + n_0 \quad (7-10)$$

Here the shortened notation  $r_0(t_0) = r_0$  is used.  $n_0(t_0) = n_0$  is a zero-mean Gaussian random variable, and  $s_0(t_0) = s_0$  is a constant that depends on the signal being sent. That is,

$$s_0 = \begin{cases} s_{01} & \text{for a binary 1 sent} \\ s_{02} & \text{for a binary 0 sent} \end{cases} \quad (7-11)$$

where  $s_{01}$  and  $s_{02}$  are known constants for a given type of receiver with known input signaling waveshapes  $s_1(t)$  and  $s_2(t)$ . Since the output noise sample  $n_0$  is a zero-mean Gaussian random variable, the total output sample  $r_0$  is a Gaussian random variable with a mean value of either  $s_{01}$  or  $s_{02}$ , depending on whether a binary 1 or a binary 0 was sent. This is illustrated in Fig. 7-2, where the mean value of  $r_0$  is  $m_{r_{01}} = s_{01}$  when a binary 1 is sent and the mean value of  $r_0$  is  $m_{r_{02}} = s_{02}$  when a binary 0 is sent. Thus the two conditional PDFs are

$$f(r_0 | s_1) = \frac{1}{\sqrt{2\pi}\sigma_0} e^{-(r_0 - s_{01})^2/(2\sigma_0^2)} \quad (7-12)$$

and

$$f(r_0 | s_2) = \frac{1}{\sqrt{2\pi}\sigma_0} e^{-(r_0 - s_{02})^2/(2\sigma_0^2)} \quad (7-13)$$

$\sigma_0^2 = \overline{n_0^2} = \overline{n_0^2(t_0)} = \overline{n_0^2(t)}$  is the average power of the *output* noise from the receiver processing circuit where the output noise process is wide-sense stationary.

Using equally likely source statistics and substituting (7-12) and (7-13) into (7-8), we find that the bit error rate becomes

$$P_e = \frac{1}{2} \int_{-\infty}^{V_T} \frac{1}{\sqrt{2\pi}\sigma_0} e^{-(r_0 - s_{01})^2/(2\sigma_0^2)} dr_0 + \frac{1}{2} \int_{V_T}^{\infty} \frac{1}{\sqrt{2\pi}\sigma_0} e^{-(r_0 - s_{02})^2/(2\sigma_0^2)} dr_0 \quad (7-14)$$

This can be reduced to the  $Q(z)$  functions defined in Sec. B-7 (Appendix B) and tabulated in Sec. A-10 (Appendix A). Let  $\lambda = -(r_0 - s_{01})/\sigma_0$  in the first integral and  $\lambda = (r_0 - s_{02})/\sigma_0$  in the second integral; then

$$P_e = \frac{1}{2} \int_{-(V_T - s_{01})/\sigma_0}^{\infty} \frac{1}{\sqrt{2\pi}} e^{-\lambda^2/2} d\lambda + \frac{1}{2} \int_{(V_T - s_{02})/\sigma_0}^{\infty} \frac{1}{\sqrt{2\pi}} e^{-\lambda^2/2} d\lambda$$

or

$$P_e = \frac{1}{2} Q\left(\frac{-V_T + s_{01}}{\sigma_0}\right) + \frac{1}{2} Q\left(\frac{V_T - s_{02}}{\sigma_0}\right) \quad (7-15)$$

By using the appropriate value for the comparator threshold,  $V_T$ , this probability of error can be minimized. To find the  $V_T$  that minimizes  $P_e$ , we need to solve  $dP_e/dV_T = 0$ . Using Leibniz's rule, (A-36), for differentiating the integrals of (7-14), we obtain

$$\frac{dP_e}{dV_T} = \frac{1}{2} \frac{1}{\sqrt{2\pi}\sigma_0} e^{-(V_T - s_{01})^2/(2\sigma_0^2)} - \frac{1}{2} \frac{1}{\sqrt{2\pi}\sigma_0} e^{-(V_T - s_{02})^2/(2\sigma_0^2)} = 0$$

or

$$e^{-(V_T - s_{01})^2/(2\sigma_0^2)} = e^{-(V_T - s_{02})^2/(2\sigma_0^2)}$$

which implies the condition

$$(V_T - s_{01})^2 = (V_T - s_{02})^2$$

Consequently, for minimum  $P_e$ , the threshold setting of the comparator needs to be

$$V_T = \frac{s_{01} + s_{02}}{2} \quad (7-16)$$

Substituting (7-16) into (7-15), we obtain the expression for the minimum  $P_e$ . Thus, for binary signaling in Gaussian noise and with the optimum threshold setting as specified by (7-16), the BER is

$$P_e = Q\left(\frac{s_{01} - s_{02}}{2\sigma_0}\right) = Q\left(\sqrt{\frac{(s_{01} - s_{02})^2}{4\sigma_0^2}}\right) \quad (7-17)$$

where it is assumed that  $s_{01} > V_T > s_{02}$ .<sup>†</sup> So far, we have optimized only the threshold level, not the filters in the processing circuits.

### Results for White Gaussian Noise and Matched-Filter Reception

If the receiving filter (in the processing circuits of Fig. 7-1) is optimized, the BER as given by (7-17) can be reduced. To minimize  $P_e$  we need to maximize the argument of  $Q$ , as is readily seen from Fig. B-7. Thus we need to find the linear filter that maximizes

<sup>†</sup> If  $s_{01} < V_T < s_{02}$ , the result is

$$P_e = Q\left(\frac{s_{02} - s_{01}}{2\sigma_0}\right) = Q\left(\sqrt{\frac{(s_{02} - s_{01})^2}{4\sigma_0^2}}\right)$$

where the characteristic of the threshold device in Fig. 7-1 is altered so that a binary 0 is chosen when  $r_0 > V_T$  and a binary 1 is chosen when  $r_0 < V_T$ .

$$\frac{[s_{01}(t_0) - s_{02}(t_0)]^2}{\sigma_0^2} = \frac{[s_d(t_0)]^2}{\sigma_0^2}$$

$s_d(t_0) \triangleq s_{01}(t_0) - s_{02}(t_0)$  is the *difference signal sample value* that is obtained by subtracting the sample  $s_{02}$  from  $s_{01}$ . The corresponding instantaneous power of the difference output signal at  $t = t_0$  is  $s_d^2(t_0)$ . As derived in Sec. 6-8, the linear filter that maximizes the instantaneous output signal power at the sampling time  $t = t_0$  when compared to the average output noise power  $\sigma_0^2 = n_0^2(t)$  is the *matched filter*. For the case of *white noise* at the receiver input, the *matched filter needs to be matched to the difference signal*  $s_d(t) = s_1(t) - s_2(t)$ . Thus the impulse response of the matched filter for binary signaling is

$$h(t) = C[s_1(t_0 - t) - s_2(t_0 - t)] \quad (7-18)$$

where  $s_1(t)$  is the signal (only) that appears at the receiver input when a binary 1 is sent,  $s_2(t)$  is the signal that is received when a binary 0 is sent, and  $C$  is a real constant. Furthermore, by using (6-161) the output peak signal to average noise ratio that is obtained from the matched filter is

$$\frac{[s_d(t_0)]^2}{\sigma_0^2} = \frac{2E_d}{N_0}$$

$N_0/2$  is the PSD of the noise at the *receiver input*, and  $E_d$  is the difference signal energy at the *receiver input*, where

$$E_d = \int_0^T [s_1(t) - s_2(t)]^2 dt \quad (7-19)$$

Thus, for binary signaling corrupted by *white Gaussian noise*, *matched-filter reception*, and by using the optimum threshold setting, the bit error rate is

$$P_e = Q\left(\sqrt{\frac{E_d}{2N_0}}\right) \quad (7-20)$$

We will use this result to evaluate the  $P_e$  for various types of binary signaling schemes where matched-filter reception is used.

### Results for Colored Gaussian Noise and Matched-Filter Reception

The technique that we just used to obtain the BER for binary signaling in white noise can be modified to evaluate the BER for the colored noise case. The modification used is illustrated in Fig. 7-3. Here a *prewhitening filter* is inserted ahead of the receiver processing circuits. The transfer function of the prewhitening filter is

$$H_p(f) = \frac{1}{\sqrt{\mathcal{P}_n(f)}} \quad (7-21)$$

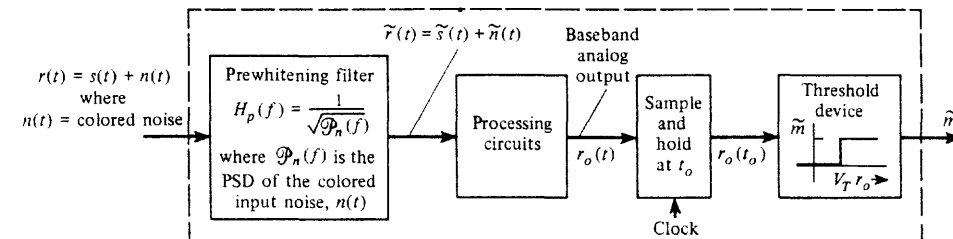


Figure 7-3 Matched-filter receiver for colored noise.

so that the noise that appears at the filter output,  $\tilde{n}(t)$ , is white. We have now converted the colored noise problem into a white noise problem, so that the design techniques presented in the preceding section are applicable. The matched filter in the processing circuits is now matched to the *filtered waveshapes*,

$$\tilde{s}(t) = \tilde{s}_1(t) = s_1(t) * h_p(t) \quad (\text{binary 1}) \quad (7-22a)$$

$$\tilde{s}(t) = \tilde{s}_2(t) = s_2(t) * h_p(t) \quad (\text{binary 0}) \quad (7-22b)$$

where  $h_p(t) = \mathcal{F}^{-1}[H_p(f)]$ . Since the prewhitening will produce signals  $\tilde{s}_1(t)$  and  $\tilde{s}_2(t)$ , which are spread beyond the  $T$ -sec signaling interval, two types of degradation will result.

- The signal energy of the filtered signal that occurs beyond the  $T$ -sec interval will not be used by the matched filter in maximizing the output signal.
- The portions of signals from previous signaling intervals that occur in the present signaling interval will produce ISI (see Chapter 3).

Both of these effects can be reduced if the duration of the original signal is made less than the  $T$ -s signaling interval so that almost all of the spread signal will occur within that interval.

## 7-2 PERFORMANCE OF BASEBAND BINARY SYSTEMS

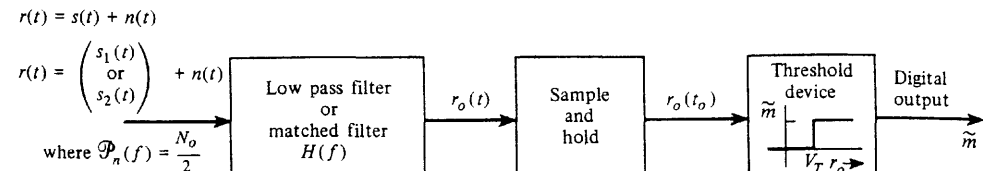
### Unipolar Signaling

As illustrated in Fig. 7-4b, the two baseband signaling waveforms are

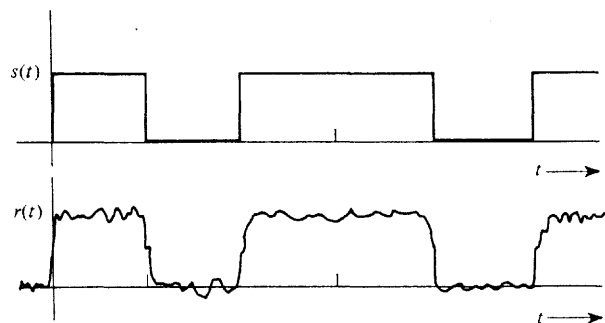
$$s_1(t) = +A, \quad 0 < t \leq T \quad (\text{binary 1}) \quad (7-23a)$$

$$s_2(t) = 0, \quad 0 < t \leq T \quad (\text{binary 0}) \quad (7-23b)$$

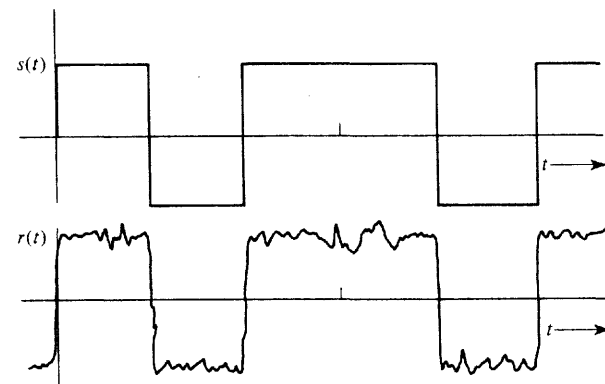
where  $A > 0$ . This unipolar signal plus white Gaussian noise is present at the receiver input.



(a) Receiver



(b) Unipolar Signaling



(c) Polar Signaling

Figure 7-4 Receiver for baseband binary signaling.

First, evaluate the performance of a receiver that uses an LPF,  $H(f)$ , with unity gain. Assume that the equivalent bandwidth of this LPF is  $B > 2/T$ , so that the unipolar signaling waveshape is preserved (approximately) at the filter output and yet the noise will be reduced by the filter.<sup>†</sup> Thus  $s_{01}(t_0) \approx A$  and  $s_{02}(t_0) \approx 0$ . The noise power at the output of the filter is  $\sigma_0^2 = (N_0/2)(2B)$ , where  $B$  is the equivalent bandwidth of the filter. The optimum threshold setting is then  $V_T = \frac{1}{2}A$ . When we use (7-17), the BER is

<sup>†</sup> From (3-39b), the PSD of a unipolar signal (rectangular pulse shape) is proportional to  $[\sin(\pi fT)/(\pi fT)]^2$  so that the second null bandwidth is  $2/T$ . Referring to study-aid examples SA7-1 and SA7-2, it is shown that if the equivalent bandwidth of the LPF is greater than  $2/T$ , the filtered signal will consist of pulses that are almost rectangular in shape and the peak values of the pulses are approximately equal to  $A$ .

$$P_e = Q\left(\sqrt{\frac{A^2}{4N_0B}}\right) \quad (\text{low-pass filter}) \quad (7-24a)$$

for a receiver that uses an LPF with an equivalent bandwidth of  $B$ .

The performance of a matched-filter receiver is obtained by using (7-20), where the sampling time is  $t_0 = T$ . The energy in the difference signal is  $E_d = A^2T$ , so that the BER is



$$P_e = Q\left(\sqrt{\frac{A^2T}{2N_0}}\right) = Q\left(\sqrt{\frac{E_b}{N_0}}\right) \quad (\text{matched filter}) \quad (7-24b)$$

where the average energy per bit is  $E_b = A^2T/2$  because the energy for a binary 1 is  $A^2T$  and the energy for a binary 0 is 0. For the rectangular pulse shape, the matched filter is an integrator. Consequently, the optimum threshold value is

$$V_T = \frac{s_{01} + s_{02}}{2} = \frac{1}{2}\left(\int_0^T A dt + 0\right) = \frac{AT}{2}$$

Often it is desirable to express the BER in terms of  $E_b/N_0$  because it indicates the average energy required to transmit one bit of data over a white (thermal) noise channel. By expressing the BER in terms of  $E_b/N_0$ , the performance of different signaling techniques can be easily compared.

A plot of (7-24b) is shown in Fig. 7-5.

### Polar Signaling

As shown in Fig. 7-4c, the baseband polar signaling waveform is

$$s_1(t) = +A, \quad 0 < t \leq T \quad (\text{binary 1}) \quad (7-25a)$$

$$s_2(t) = -A, \quad 0 < t \leq T \quad (\text{binary 0}) \quad (7-25b)$$

The polar signal is an antipodal signal since  $s_1(t) = -s_2(t)$ .

The performance of an LPF receiver system is obtained by using (7-17). Assuming that the equivalent bandwidth of the LPF is  $B \geq 2/T$ , we realize that the output signal samples are  $s_{01}(t_0) \approx A$  and  $s_{02}(t_0) \approx -A$  at the sampling time  $t = t_0$ . In addition,  $\sigma_0^2 = N_0B$ . The optimum threshold setting is now  $V_T = 0$ . Thus the BER for polar signaling is

$$P_e = Q\left(\sqrt{\frac{A^2}{N_0B}}\right) \quad (\text{low-pass filter}) \quad (7-26a)$$

where  $B$  is the equivalent bandwidth of the LPF.

The performance of the matched-filter receiver is obtained, once again, by using (7-20), where  $t_0 = T$ . (The integrate-and-dump matched filter for polar signaling was given in Fig. 6-17.) Since the energy of the difference signal is  $E_d = (2A)^2T$ , the BER is



$$P_e = Q\left(\sqrt{\frac{2A^2T}{N_0}}\right) = Q\left(\sqrt{2\left(\frac{E_b}{N_0}\right)}\right) \quad (\text{matched filter}) \quad (7-26b)$$

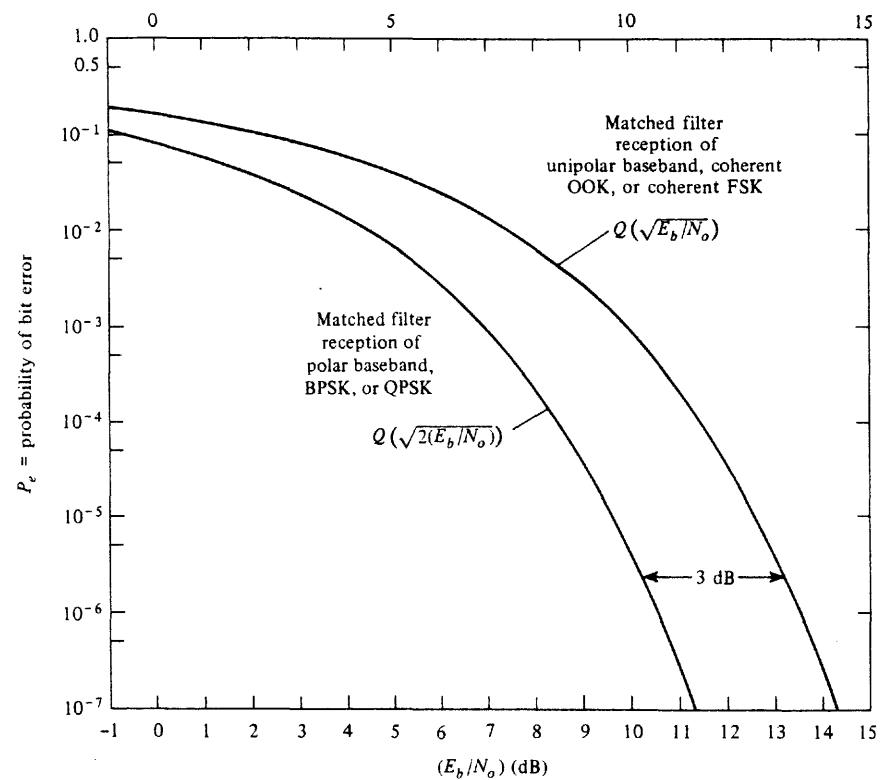


**Figure 7-5**  $P_e$  for matched-filter reception of several binary signaling schemes.



where the average energy per bit is  $E_b = A^2T$ . The optimum threshold setting is  $V_T = 0$ .

A plot of the BER for unipolar and polar baseband signaling is shown in Fig. 7-5. It is apparent that polar signaling has a 3-dB advantage over unipolar signaling since unipolar signaling requires a  $E_b/N_0$  that is 3 dB larger than that for polar signaling for the same  $P_e$ .

### Bipolar Signaling

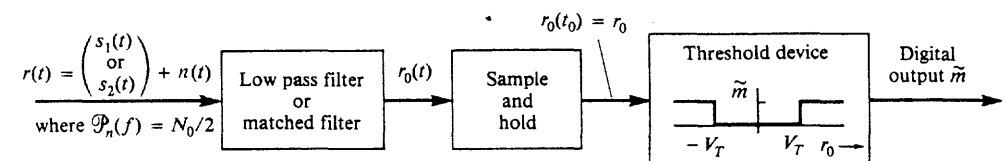
For bipolar NRZ signaling binary 1's are represented by alternating positive and negative values, and the binary 0's are represented by a zero level. Thus

$$s_1(t) = \pm A, \quad 0 < t \leq T \quad (\text{binary 1}) \quad (7-27a)$$

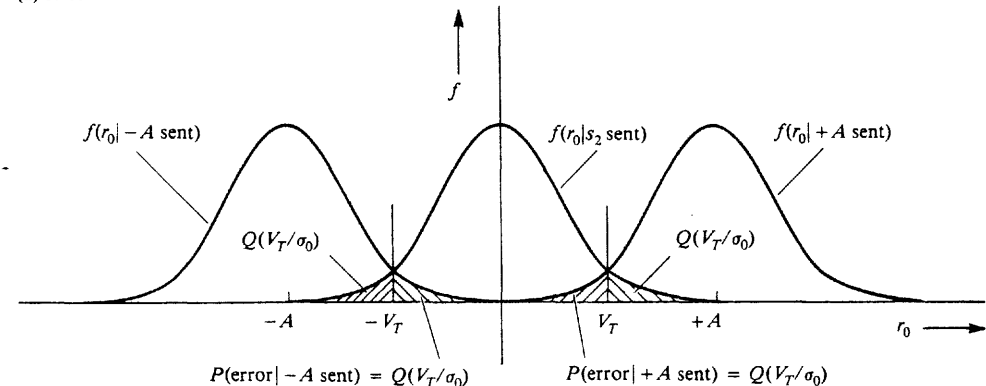
$$s_2(t) = 0, \quad 0 < t \leq T \quad (\text{binary 0}) \quad (7-27b)$$

where  $A > 0$ . This is similar to unipolar signaling except two thresholds,  $+V_T$  and  $-V_T$ , are needed as shown in Fig. 7-6. Figure 7-6b illustrates the error probabilities for the case of additive Gaussian noise. The BER is

$$\begin{aligned} P_e &= P(\text{error} | +A \text{ sent})P(+A \text{ sent}) + P(\text{error} | -A \text{ sent})P(-A \text{ sent}) \\ &\quad + P(\text{error} | s_2 \text{ sent})P(s_2 \text{ sent}) \end{aligned}$$



(a) Receiver



(b) Conditional PDFs

**Figure 7-6** Receiver for bipolar signaling.

and, by using Fig. 7-6b,

$$P_e \approx \left[ Q\left(\frac{V_T}{\sigma_0}\right) \right] \frac{1}{4} + \left[ Q\left(\frac{V_T}{\sigma_0}\right) \right] \frac{1}{4} + \left[ 2Q\left(\frac{V_T}{\sigma_0}\right) \right] \frac{1}{2}$$

which reduces to

$$P_e = \frac{3}{2} Q\left(\frac{V_T}{\sigma_0}\right)$$

or, by using the optimum threshold value,  $V_T = \frac{1}{2}A$ ,

$$P_e = \frac{3}{2} Q\left(\frac{A}{2\sigma_0}\right)$$

For the case of a receiver with a low-pass filter that has a bipolar signal plus white noise at its input,  $\sigma_0^2 = N_0 B$ . Thus the BER is

$$P_e = \frac{3}{2} Q\left(\sqrt{\frac{A^2}{4N_0 B}}\right) \quad (\text{low-pass filter}) \quad (7-28a)$$

where the PSD of the input noise is  $N_0/2$  and the equivalent bandwidth of the filter is  $B$  Hz. If a matched filter is used, its output SNR is, using (6-161),

$$\left(\frac{S}{N}\right)_{\text{out}} = \frac{A^2}{\sigma_0^2} = \frac{2E_d}{N_0}$$

For bipolar NRZ signaling the energy in the different signal is  $E_d = A^2 T = 2E_b$  where  $E_b$  is the average energy per bit. Thus for a matched-filter receiver, the BER is



$$P_e = \frac{3}{2} Q\left(\sqrt{\frac{E_b}{N_0}}\right) \quad (\text{matched filter}) \quad (7-28b)$$

For bipolar RZ signaling,  $E_d = A^2 T/4 = 2E_b$  so that the resulting BER formula is identical to (7-28b). These results show that the BER for bipolar signaling is just  $\frac{3}{2}$  that for unipolar signaling as described by (7-24b).

### 7-3 COHERENT DETECTION OF BANDPASS BINARY SIGNALS

#### On-Off Keying

From Fig. 5-1c, an OOK signal is represented by

$$s_1(t) = A \cos(\omega_c t + \theta_c), \quad 0 < t \leq T \quad (\text{binary 1}) \quad (7-29a)$$

or

$$s_2(t) = 0, \quad 0 < t \leq T \quad (\text{binary 0}) \quad (7-29b)$$

For coherent detection, a product detector is used as illustrated in Fig. 7-7. Actually, in RF applications a mixer would convert the incoming OOK signal to an IF so that stable high-gain amplification could be conveniently achieved and then a product detector would translate the signal to baseband. Figure 7-7, equivalently, represents these operations by converting the incoming signal and noise directly to baseband.

Assume that the OOK signal plus white (over the equivalent bandpass) Gaussian noise is present at the receiver input. As developed in Chapter 6, this bandpass noise may be represented by

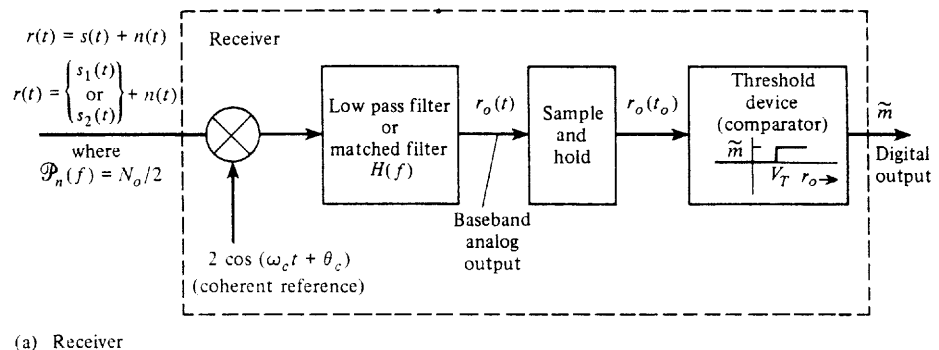
$$n(t) = x(t) \cos(\omega_c t + \theta_n) - y(t) \sin(\omega_c t + \theta_n)$$

where the PSD of  $n(t)$  is  $\mathcal{P}_n(f) = N_0/2$ , and  $\theta_n$  is a uniformly distributed random variable that is independent of  $\theta_c$ .

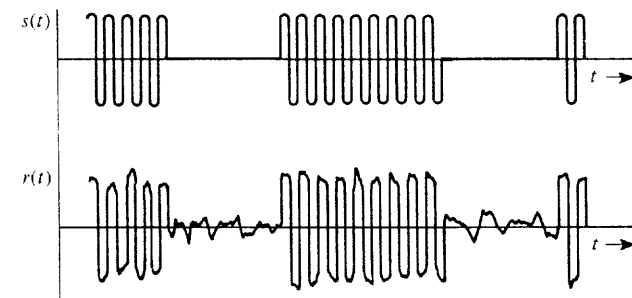
The receiving filter  $H(f)$  of Fig. 7-7 may be some convenient LPF or it may be a matched filter. Of course, the receiver would be optimized (for the lowest  $P_e$ ) if a matched filter were used.

First, evaluate the performance of a receiver that uses an LPF where the filter has a dc gain of unity. Assume that the equivalent bandwidth of the filter is  $B \geq 2/T$  so that the envelope of the OOK signal is (approximately) preserved at the filter output. The baseband analog output will be

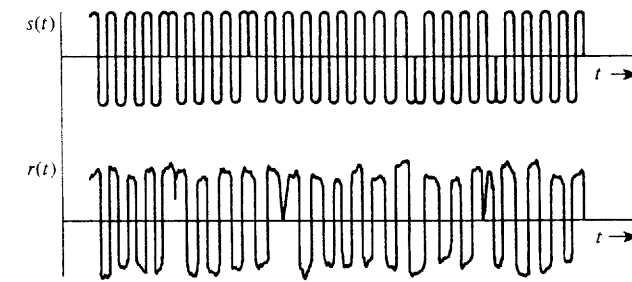
$$r_0(t) = \begin{cases} A, & 0 < t \leq T, \text{ binary 1} \\ 0, & 0 < t \leq T, \text{ binary 0} \end{cases} + x(t) \quad (7-30)$$



(a) Receiver



(b) OOK Signaling



(c) BPSK Signaling

Figure 7-7 Coherent detection of OOK or BPSK signals.

where  $x(t)$  is the baseband noise. The noise power is  $\overline{x^2(t)} = \sigma_0^2 = \overline{n^2(t)} = 2(N_0/2)(2B) = 2N_0B$ . Because  $s_{01} = A$  and  $s_{02} = 0$ , the optimum threshold setting is  $V_T = A/2$ . When we use (7-17), the BER is

$$P_e = Q\left(\sqrt{\frac{A^2}{8N_0B}}\right) \quad (\text{narrowband filter}) \quad (7-31)$$

$B$  is the equivalent bandwidth of the LPF. The equivalent bandpass bandwidth of this receiver is  $B_p = 2B$ .

The performance of a matched-filter receiver is obtained by using (7-20). The energy in the difference signal at the receiver input is<sup>†</sup>

$$E_d = \int_0^T [A \cos(\omega_c t + \theta_c) - 0]^2 dt = \frac{A^2 T}{2} \quad (7-32)$$

Consequently, the BER is

$$P_e = Q\left(\sqrt{\frac{A^2 T}{4N_0}}\right) = Q\left(\sqrt{\frac{E_b}{N_0}}\right) \quad (\text{matched filter}) \quad (7-33)$$

where the average energy per bit is  $E_b = A^2 T / 4$ . For this case, where  $s_1(t)$  has a rectangular (real) envelope, the matched filter is an integrator. Consequently, the optimum threshold value is

$$V_T = \frac{s_{01} + s_{02}}{2} = \frac{1}{2}s_{01} = \frac{1}{2}\left[\int_0^T 2A \cos^2(\omega_c t + \theta_c) dt\right]$$

which reduces to  $V_T = AT/2$  when  $f_c \gg R$ . Note that the performance of OOK is exactly the same as that for baseband unipolar signaling, as illustrated in Fig. 7-5.

### Binary-Phase-Shift Keying

Referring to Fig. 7-7 once again, we see that the BPSK signal is

$$s_1(t) = A \cos(\omega_c t + \theta_c), \quad 0 < t \leq T \quad (\text{binary 1}) \quad (7-34a)$$

and

$$s_2(t) = -A \cos(\omega_c t + \theta_c), \quad 0 < t \leq T \quad (\text{binary 0}) \quad (7-34b)$$

BPSK signaling is also called *phase reversal keying* (PRK). The BPSK signal is an antipodal signal because  $s_1(t) = -s_2(t)$ .

Once again, first evaluate the performance of a receiver that uses an LPF having a gain of unity and an equivalent bandwidth of  $B \geq 2/T$ . The baseband analog output is

$$r_0(t) = \begin{cases} A, & 0 < t \leq T \quad \text{binary 1} \\ -A, & 0 < t \leq T, \quad \text{binary 0} \end{cases} + x(t) \quad (7-35)$$

where  $\overline{x^2(t)} = \sigma_0^2 = \overline{n^2(t)} = 2N_0B$ . Because  $s_{01} = A$  and  $s_{02} = -A$ , the optimum threshold is  $V_T = 0$ . When we use (7-17), the BER is

$$P_e = Q\left(\sqrt{\frac{A^2}{2N_0B}}\right) \quad (\text{narrowband filter}) \quad (7-36)$$

When BPSK is compared with OOK on a *peak envelope power* (PEP) basis for a given value of  $N_0$ , 6 dB less (peak) signal power is required for BPSK signaling to give the same  $P_e$ .

<sup>†</sup> Strictly speaking,  $f_c$  needs to be an integer multiple of half the bit rate,  $R = 1/T$ , to obtain exactly  $A^2 T/2$  for  $E_d$ . However, because  $f_c \gg R$ , for all practical purposes  $E_d = A^2 T/2$  regardless of whether or not  $f_c = nR/2$ .

as that for OOK. However, if the two are compared on an average (signal) power basis, the performance of BPSK has a 3-dB advantage over OOK since the average power of OOK is 3 dB below its PEP (equally likely signaling), but the average power of BPSK is equal to its PEP.

The performance of the matched-filter receiver is obtained by using (7-20). Recall that the matched filter for BPSK signaling was illustrated in Fig. 6-19, where a correlation processor using an integrate-and-dump filter was shown. The energy in the difference signal at the receiver input is

$$E_d = \int_0^T [2A \cos(\omega_c t + \theta_c)]^2 dt = 2A^2 T \quad (7-37)$$

Thus, the BER is



$$P_e = Q\left(\sqrt{\frac{A^2 T}{N_0}}\right) = Q\left(\sqrt{2\left(\frac{E_b}{N_0}\right)}\right) \quad (\text{matched filter}) \quad (7-38)$$

where the average energy per bit is  $E_b = A^2 T / 2$  and  $V_T = 0$ . Note that the performance of BPSK is exactly the same as that for baseband polar signaling; however, it is 3 dB superior to OOK signaling (see Fig. 7-5).

### Frequency-Shift Keying

The FSK signal can be coherently detected by using two product detectors. This is illustrated in Fig. 7-8 where identical LPFs at the output of the product detectors have been replaced by only one of the filters since the order of linear operations may be exchanged without affecting the results. The mark (binary 1) and space (binary 0) signals are

$$s_1(t) = A \cos(\omega_1 t + \theta_c), \quad 0 < t \leq T \quad (\text{binary 1}) \quad (7-39a)$$

$$s_2(t) = A \cos(\omega_2 t + \theta_c), \quad 0 < t \leq T \quad (\text{binary 0}) \quad (7-39b)$$

where the frequency shift is  $2 \Delta F = f_1 - f_2$ , assuming that  $f_1 > f_2$ . This FSK signal plus white Gaussian noise is present at the receiver input. The PSD for  $s_1(t)$  and  $s_2(t)$  is shown in Fig. 7-8b.

First, evaluate the performance of a receiver that uses an LPF  $H(f)$  with a dc gain of 1. Once again, assume the equivalent bandwidth of the filter is  $2/T \leq B < \Delta F$ . The LPF, when combined with the frequency translation produced by the product detectors, acts as dual bandpass filters—one centered at  $f = f_1$  and the other at  $f = f_2$ , where each has an equivalent bandwidth of  $B_p = 2B$ . Thus the input noise that affects the output consists of two narrowband components  $n_1(t)$  and  $n_2(t)$ , where the spectrum of  $n_1(t)$  is centered at  $f_1$  and the spectrum of  $n_2(t)$  is centered at  $f_2$ , as shown in Fig. 7-8. Furthermore,  $n(t) = n_1(t) + n_2(t)$ , where

$$n_1(t) = x_1(t) \cos(\omega_1 t + \theta_c) - y_1(t) \sin(\omega_1 t + \theta_c) \quad (7-40a)$$

and

$$n_2(t) = x_2(t) \cos(\omega_2 t + \theta_c) - y_2(t) \sin(\omega_2 t + \theta_c) \quad (7-40b)$$

Assume that the frequency shift is  $2\Delta F > 2B$ , so that the mark and space signals may be separated by the filtering action. Then the input signal and noise that passes through the upper channel in Fig. 7-8a is

$$r_1(t) = \begin{cases} s_1(t), & \text{binary 1} \\ 0, & \text{binary 0} \end{cases} + n_1(t) \quad (7-41)$$

and the signal and noise that passes through the lower channel is

$$r_2(t) = \begin{cases} 0, & \text{binary 1} \\ s_2(t), & \text{binary 0} \end{cases} + n_2(t) \quad (7-42)$$

where  $r(t) = r_1(t) + r_2(t)$ . The noise power of  $n_1(t)$  and  $n_2(t)$  is  $\overline{n_1^2(t)} = \overline{n_2^2(t)} = (N_0/2)(4B) = 2N_0B$ . Thus the baseband analog output is

$$r_0(t) = \begin{cases} +A, & 0 < t \leq T, \text{ binary 1} \\ -A, & 0 < t \leq T, \text{ binary 0} \end{cases} + n_0(t) \quad (7-43)$$

where  $s_{01} = +A$ ,  $s_{02} = -A$  and  $n_0(t) = x_1(t) - x_2(t)$ . The optimum threshold setting is  $V_T = 0$ . Furthermore, the bandpass noise processes  $n_1(t)$  and  $n_2(t)$  are independent since they have spectra in nonoverlapping frequency bands (see Fig. 7-8) and they are white. (See Prob. 7-29 for the verification of this statement.) Consequently, the resulting baseband noise processes  $x_1(t)$  and  $x_2(t)$  are independent, and the output noise power is

$$\overline{n_0^2(t)} = \sigma_0^2 = \overline{x_1^2(t)} + \overline{x_2^2(t)} = \overline{n_1^2(t)} + \overline{n_2^2(t)} = 4N_0B \quad (7-44)$$

Substituting for  $s_{01}$ ,  $s_{02}$ , and  $\sigma_0$  into (7-17), we have

$$P_e = Q\left(\sqrt{\frac{A^2}{4N_0B}}\right) \quad (\text{bandpass filters}) \quad (7-45)$$

Comparing the performance of FSK with that of BPSK and OOK on a PEP basis, we see that FSK requires 3 dB more power than BPSK for the same  $P_e$  but 3 dB less power than OOK. Comparing the performance on an average power basis, we observe that FSK is 3 dB worse than BPSK but is equivalent to OOK (since the average power of OOK is 3 dB below its PEP).

The performance of FSK signaling with matched-filter reception is obtained from (7-20). The energy in the difference signal is

$$\begin{aligned} E_d &= \int_0^T [A \cos(\omega_1 t + \theta_c) - A \cos(\omega_2 t + \theta_c)]^2 dt \\ &= \int_0^T [A^2 \cos^2(\omega_1 t + \theta_c) - 2A^2 \cos(\omega_1 t + \theta_c) \\ &\quad \times \cos(\omega_2 t + \theta_c) + A^2 \cos^2(\omega_2 t + \theta_c)] dt \end{aligned}$$

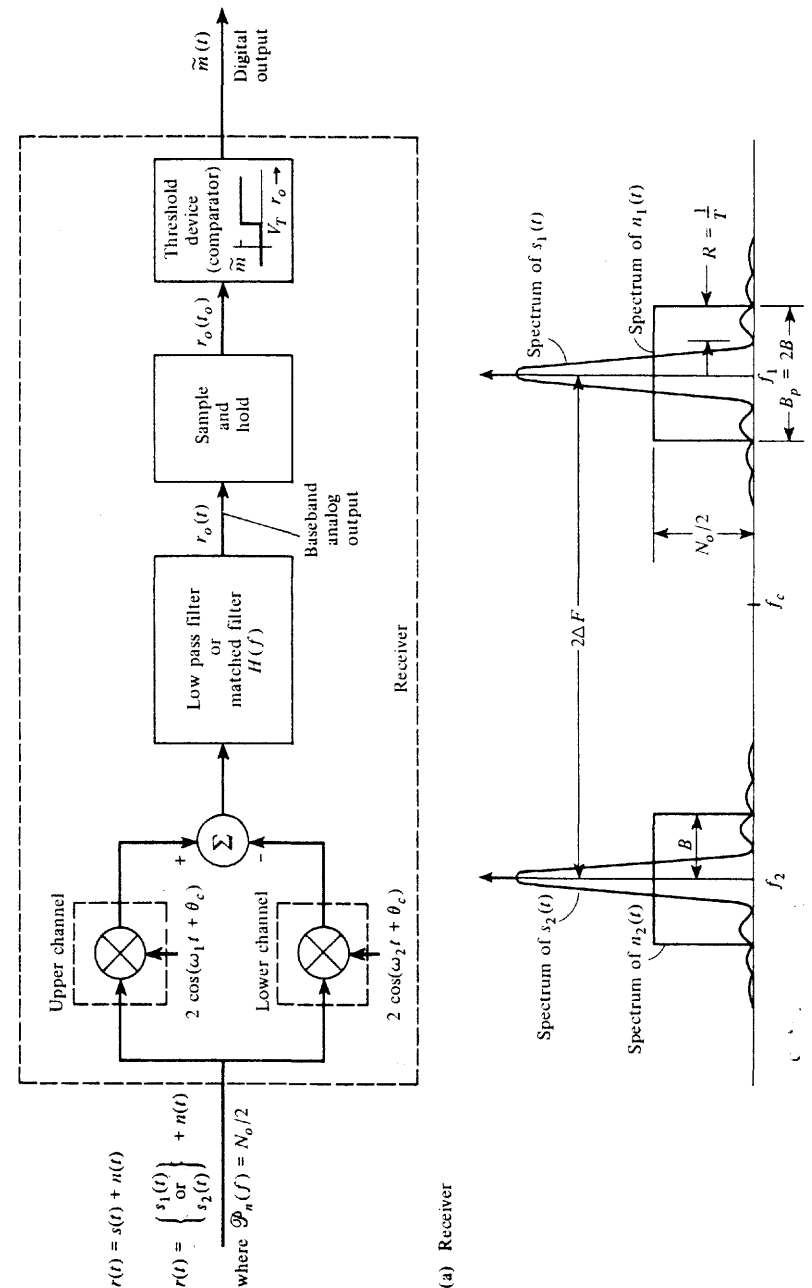


Figure 7-8 Coherent detection of an FSK signal.

or<sup>†</sup>

$$E_d = \frac{1}{2} A^2 T - A^2 \int_0^T [\cos(\omega_1 - \omega_2)t] dt + \frac{1}{2} A^2 T \quad (7-46)$$

Consider the case when  $2\Delta F = f_1 - f_2 = n/(2T) = nR/2$ . Under this condition the integral (i.e., the cross-product term) goes to zero. This condition is required for  $s_1(t)$  and  $s_2(t)$  to be orthogonal. Consequently,  $s_1(t)$  will not contribute an output to the lower channel (see Fig. 7-8), and vice versa. Furthermore, if  $(f_1 - f_2) \gg R$ ,  $s_1(t)$  and  $s_2(t)$  will be approximately orthogonal because the value of this integral will be negligible compared with  $A^2 T$ . Assuming that one or both of these conditions is satisfied, then  $E_d = A^2 T$ , and the BER for FSK signaling is



$$P_e = Q\left(\sqrt{\frac{A^2 T}{2N_0}}\right) = Q\left(\sqrt{\frac{E_b}{N_0}}\right) \quad (\text{matched filter}) \quad (7-47)$$

where the average energy per bit is  $E_b = A^2 T / 2$ . The performance of FSK signaling is equivalent to that of OOK signaling (matched-filter reception) and is 3 dB inferior to BPSK signaling (see Fig. 7-5).

As we demonstrate in the following section, coherent detection is superior to noncoherent detection. However, for coherent detection, the coherent reference must be available. This reference is often obtained from the noisy input signal so that the reference itself is also noisy. This, of course, increases  $P_e$  over those values given by the preceding formulas. The circuitry that extracts the carrier reference is usually complex and expensive. Often, one is willing to accept the poorer performance of a noncoherent system to simplify the circuitry and reduce the cost.

## 7-4 NONCOHERENT DETECTION OF BANDPASS BINARY SIGNALS

The derivation of the equations for the BER of noncoherent receivers is considerably more difficult than the derivation of the BER for coherent receivers. On the other hand, the circuitry for noncoherent receivers is *relatively simple* when compared to that used in coherent receivers. For example, OOK with noncoherent reception is the most popular signaling technique used in fiber optic communication systems.

In this section the BER will be computed for two noncoherent receivers—one for the reception of OOK signals and the other for the reception of FSK signals. As indicated in Chapter 5, BPSK cannot be detected noncoherently. However, as we will see, DPSK signals may be demodulated by using a partially (quasi) coherent technique.

<sup>†</sup> For integrals of the type  $\int_0^T A^2 \cos^2(\omega_1 t + \theta_c) dt = \frac{1}{2} A^2 [\int_0^T dt + \int_0^T \cos(2\omega_1 t + 2\theta_c) dt]$ , the second integral on the right is negligible compared to the first integral on the right because of the oscillation in the second integral (Riemann-Lebesgue lemma [Olmsted, 1961]).

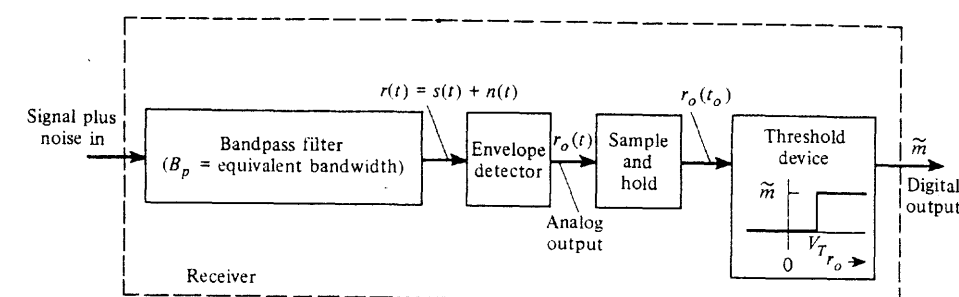


Figure 7-9 Noncoherent detection of OOK.

### On-Off Keying

A noncoherent receiver for detection of OOK signals is shown in Fig. 7-9. Assume that an OOK signal plus white Gaussian noise is present at the receiver input. Then the noise at the filter output  $n(t)$  will be bandlimited Gaussian noise, and the total filter output, consisting of signal plus noise, is

$$r(t) = \begin{cases} r_1(t), & 0 < t \leq T, \text{ binary 1 sent} \\ r_2(t), & 0 < t \leq T, \text{ binary 0 sent} \end{cases} \quad (7-48)$$

Let the bandwidth of the filter be  $B_p$ , where  $B_p$  is at least as large as the transmission bandwidth of the OOK signal so that the signal waveshape is preserved at the filter output. Then for the case of a binary 1,  $s_1(t) = A \cos(\omega_c t + \theta_c)$ , so

$$r_1(t) = A \cos(\omega_c t + \theta_c) + n(t), \quad 0 < t \leq T$$

or

$$r_1(t) = [A + x(t)] \cos(\omega_c t + \theta_c) - y(t) \sin(\omega_c t + \theta_c), \quad 0 < t \leq T \quad (7-49)$$

For a binary 0,  $s_2(t) = 0$  and

$$r_2(t) = x(t) \cos(\omega_c t + \theta_c) - y(t) \cos(\omega_c t + \theta_c), \quad 0 < t \leq T \quad (7-50)$$

The BER is obtained by using (7-8), which, for the case of equally likely signaling, is

$$P_e = \frac{1}{2} \int_{-\infty}^{V_r} f(r_0 | s_1) dr_0 + \frac{1}{2} \int_{V_r}^{\infty} f(r_0 | s_2) dr_0 \quad (7-51)$$

We need to evaluate the conditional PDFs for the output of the envelope detector,  $f(r_0 | s_1)$  and  $f(r_0 | s_2)$ .  $f(r_0 | s_1)$  is the PDF for  $r_0 = r_0(t) = r_{01}$  that occurs when  $r_1(t)$  is present at the input of the envelope detector, and  $f(r_0 | s_2)$  is the PDF for  $r_0 = r_0(t_0) = r_{02}$  that occurs when  $r_2(t)$  is present at the input of the envelope detector.

We will evaluate  $f(r_0 | s_2)$  first. When  $s_2(t)$  is sent, the input to the envelope detector,  $r_2(t)$ , consists of bandlimited bandpass Gaussian noise as seen from (7-50). In Example 6-10 we demonstrated that for this case, the PDF of the envelope is Rayleigh distributed. Of

course, the output of the envelope detector is the envelope, so  $r_0 = R = r_{02}$ . Thus the PDF for the case of noise alone is

$$f(r_0|s_2) = \begin{cases} \frac{r_0}{\sigma^2} e^{-r_0^2/(2\sigma^2)}, & r \geq 0 \\ 0, & r_0 \text{ otherwise} \end{cases} \quad (7-52)$$

The parameter  $\sigma^2$  is the variance of the noise at the input of the envelope detector. Thus,  $\sigma^2 = (N_0/2)(2B_p) = N_0B_p$ , where  $B_p$  is the effective bandwidth of the bandpass filter and  $N_0/2$  is the PSD of the white noise at the receiver input.

For the case of  $s_1(t)$  being transmitted, the input to the envelope detector is given by (7-49). Since  $n(t)$  is a Gaussian process (that has no delta functions in its spectrum at  $f = \pm f_c$ ) the in-phase baseband component,  $A + x(t)$ , is also a Gaussian process with a mean value of  $A$  instead of a zero mean, as in (7-50). The PDF for the envelope  $r_0 = R = r_{01}$  is evaluated using the same technique used in Example 6-10 and the result as cited in Prob. 6-46. Thus, for this case of a sinusoid plus noise at the envelope detector input,

$$f(r_0|s_1) = \begin{cases} \frac{r_0}{\sigma^2} e^{-(r_0^2+A^2)/(2\sigma^2)} I_0\left(\frac{r_0A}{\sigma^2}\right), & r_0 \geq 0 \\ 0, & r_0 \text{ otherwise} \end{cases} \quad (7-53)$$

which is a Rician PDF, where

$$I_0(z) \triangleq \frac{1}{2\pi} \int_0^{2\pi} e^{z \cos \theta} d\theta \quad (7-54)$$

is the modified Bessel function of the first kind of zero order.

The two conditional PDFs,  $f(r_0|s_2)$  and  $f(r_0|s_1)$ , are shown in Fig. 7-10. Actually,  $f(r_0|s_2)$  is a special case of  $f(r_0|s_1)$  when  $A = 0$  because for this condition we have noise

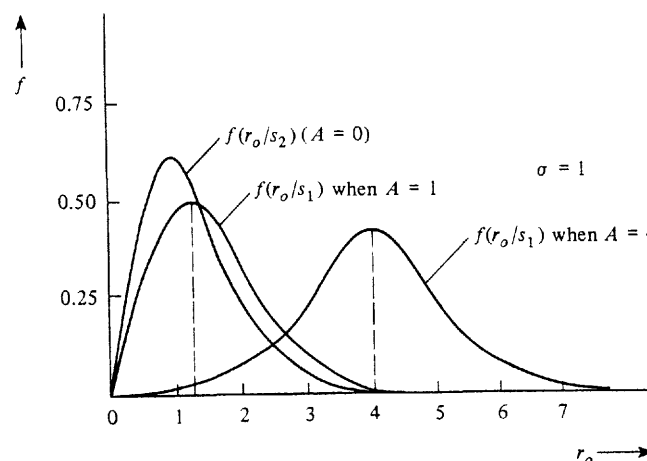


Figure 7-10 Conditional PDFs for noncoherent OOK reception.

only at the detector input and (7-53) becomes (7-52). Two other plots of (7-53) are also given, one for  $A = 1$  and another for  $A = 4$ . It is seen that for  $A/\sigma \gg 1$ , the mode of the distribution [i.e., where  $f(r_0|s_1)$  is a maximum] occurs at the value  $r_0 = A$ . In addition, note that for  $A/\sigma \gg 1$ ,  $f(r_0|s_1)$  takes on a Gaussian shape (as demonstrated subsequently).

The bit error rate for the noncoherent OOK receiver is obtained by substituting (7-52) and (7-53) into (7-51).

$$P_e = \frac{1}{2} \int_0^{V_T} \frac{r_0}{\sigma^2} e^{-(r_0^2+A^2)/(2\sigma^2)} I_0\left(\frac{r_0A}{\sigma^2}\right) dr_0 + \frac{1}{2} \int_{V_T}^{\infty} \frac{r_0}{\sigma^2} e^{-r_0^2/(2\sigma^2)} dr_0 \quad (7-55)$$

The optimum threshold level is the value of  $V_T$  for which  $P_e$  is a minimum. For  $A/\sigma \gg 1$ , the optimum threshold is close to  $V_T = A/2$ , so we will use this value to simplify the mathematics.<sup>†</sup> The integral involving the Bessel function cannot be evaluated in closed form. However,  $I_0(z)$  can be approximated by  $I_0(z) = e^z/\sqrt{2\pi z}$ , which is valid for  $z \gg 1$ . Then, for  $A/\sigma \gg 1$ , the left integral in (7-55) becomes

$$\frac{1}{2} \int_0^{V_T} \frac{r_0}{\sigma^2} e^{-(r_0^2+A^2)/(2\sigma^2)} I_0\left(\frac{r_0A}{\sigma^2}\right) dr_0 \approx \frac{1}{2} \int_0^{A/2} \sqrt{\frac{r_0}{2\pi\sigma^2 A}} e^{(r_0-A)^2/(2\sigma^2)} dr_0$$

Because  $A/\sigma \gg 1$ , the integrand is negligible except for values of  $r_0$  in the vicinity of  $A$ , so the lower limit may be extended to  $-\infty$  and  $\sqrt{r_0/(2\pi\sigma^2 A)}$  can be replaced by  $\sqrt{1/(2\pi\sigma^2)}$ . Thus

$$\frac{1}{2} \int_0^{V_T} \frac{r_0}{\sigma^2} e^{-(r_0^2+A^2)/(2\sigma^2)} I_0\left(\frac{r_0A}{\sigma^2}\right) dr_0 \approx \frac{1}{2} \int_{-\infty}^{V_T} \frac{1}{\sqrt{2\pi\sigma}} e^{-(r_0-A)^2/(2\sigma^2)} dr_0 \quad (7-56)$$

When we substitute (7-56) into (7-55), the BER becomes

$$P_e = \frac{1}{2} \int_{-\infty}^{A/2} \frac{1}{\sqrt{2\pi\sigma}} e^{-(r_0-A)^2/(2\sigma^2)} dr_0 + \frac{1}{2} \int_{A/2}^{\infty} \frac{r_0}{\sigma^2} e^{-r_0^2/(2\sigma^2)} dr_0$$

or

$$P_e = \frac{1}{2} Q\left(\frac{A}{2\sigma}\right) + \frac{1}{2} e^{-A^2/(8\sigma^2)} \quad (7-57)$$

Using  $Q(z) = e^{-z^2/2}/\sqrt{2\pi z^2}$  for  $z \gg 1$ , we have

$$P_e = \frac{1}{\sqrt{2\pi(A/\sigma)}} e^{-A^2/(8\sigma^2)} + \frac{1}{2} e^{-A^2/(8\sigma^2)}$$

Because  $A/\sigma \gg 1$ , the second term on the right dominates over the first term. Finally, we obtain the approximation for the BER for noncoherent detection of OOK. It is

<sup>†</sup> Most practical systems operate with  $A/\sigma \gg 1$ .

$$P_e = \frac{1}{2} e^{-A^2/(8\sigma^2)}, \quad \frac{A}{\sigma} \gg 1$$

or

$$P_e = \frac{1}{2} e^{-(1/(2TB_p))(E_b/N_0)}, \quad \frac{E_b}{N_0} \gg \frac{TB_p}{4} \quad (7-58)$$

where the average energy per bit is  $E_b = A^2T/4$  and  $\sigma^2 = N_0B_p$ .  $R = 1/T$  is the bit rate of the OOK signal and  $B_p$  is the equivalent bandwidth of the bandpass filter that precedes the envelope detector.

Equation (7-58) indicates that the BER depends on the bandwidth of the bandpass filter and that  $P_e$  becomes smaller as  $B_p$  is decreased. Of course, this result is valid only when the ISI is negligible. Referring to (3-74), we realize that the minimum bandwidth allowed (i.e., for no ISI) is obtained when the rolloff factor is  $r = 0$ . This implies that the minimum bandpass bandwidth that is allowed is  $B_p = 2B = R = 1/T$ . A plot of the BER is given in Fig. 7-14 for this minimum bandwidth case of  $B_p = 1/T$ .

### Frequency-Shift Keying

A noncoherent receiver for detection of frequency-shift-keyed (FSK) signals is shown in Fig. 7-11. The input consists of an FSK signal as described by (7-39) plus white Gaussian noise with a PSD of  $N_0/2$ . A sketch of the spectrum of the FSK signal and noise was given in Fig. 7-8b, where the bandpass filter bandwidth is  $B_p$ . It is assumed that the frequency shift,  $2\Delta F = f_1 - f_2$ , is sufficiently large so that the spectra of  $s_1(t)$  and  $s_2(t)$  have negligible overlap.

The BER for this receiver is obtained by evaluating (7-8). For signal alone at the receiver input, the output of the summing junction is  $r_0(t) = +A$  when a mark (binary 1) is transmitted and  $r_0(t) = -A$  when a space (binary 0) is transmitted. Because of this sym-

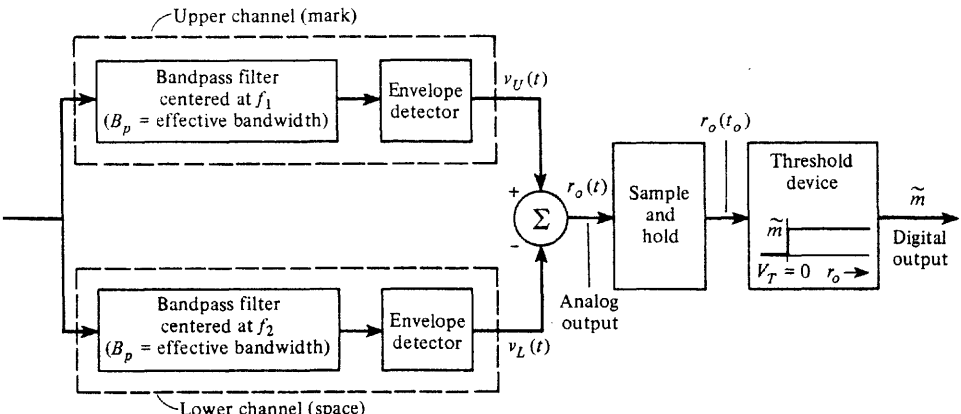


Figure 7-11 Noncoherent detection of FSK.

metry and because the noise out of the upper and lower receiver channels is similar, the optimum threshold is  $V_T = 0$ . Similarly, it is realized that the PDF of  $r_0(t)$  conditioned on  $s_1$  and the PDF of  $r_0(t)$  conditioned on  $s_2$  are similar. That is,

$$f(r_0|s_1) = f(-r_0|s_2) \quad (7-59)$$

Substituting (7-59) into (7-8), we find the BER to be

$$P_e = \frac{1}{2} \int_{-\infty}^0 f(r_0|s_1) dr_0 + \frac{1}{2} \int_0^{\infty} f(r_0|s_2) dr_0$$

or

$$P_e = \int_0^{\infty} f(r_0|s_2) dr_0 \quad (7-60)$$

As shown in Fig. 7-11,  $r_0(t)$  is positive when the upper channel output  $v_U(t)$  exceeds the lower channel output  $v_L(t)$ . Thus

$$P_e = P(v_U > v_L | s_2) \quad (7-61)$$

For the case of a space signal plus noise at the receiver input, we know that the output of the upper bandpass filter is only Gaussian noise (no signal). Thus the output of the upper envelope detector  $v_U$  is noise having a Rayleigh distribution

$$f(v_U|s_2) = \begin{cases} \frac{v_U}{\sigma^2} e^{-v_U^2/(2\sigma^2)}, & v_U \geq 0 \\ 0, & v_U < 0 \end{cases} \quad (7-62)$$

where  $\sigma^2 = N_0B_p$ . On the other hand,  $v_L$  has a Rician distribution since a sinusoid (the space signal) plus noise appears at the input to the lower envelope detector.

$$f(v_L|s_2) = \begin{cases} \frac{v_L}{\sigma^2} e^{-(v_L^2+A^2)/(2\sigma^2)} I_0\left(\frac{v_L A}{\sigma^2}\right), & v_L \geq 0 \\ 0, & v_L < 0 \end{cases} \quad (7-63)$$

where  $\sigma^2 = N_0B_p$  also. Using (7-62) and (7-63) in (7-61), we obtain

$$P_e = \int_0^{\infty} \frac{v_L}{\sigma^2} e^{-(v_L^2+A^2)/(2\sigma^2)} I_0\left(\frac{v_L A}{\sigma^2}\right) \left[ \int_{v_L}^{\infty} \frac{v_U}{\sigma^2} e^{-v_U^2/(2\sigma^2)} dv_U \right] dv_L$$

When we evaluate the inner integral, the BER becomes

$$P_e = e^{-A^2/(2\sigma^2)} \int_0^{\infty} \frac{v_L}{\sigma^2} e^{-v_L^2/\sigma^2} I_0\left(\frac{v_L A}{\sigma^2}\right) dv_L \quad (7-64)$$

This integral can be evaluated by using (A-81a) from the integral table in Appendix A. Thus for noncoherent detection of FSK, the BER is

$$P_e = \frac{1}{2} e^{-A^2/(4\sigma^2)}$$

or

$$P_e = \frac{1}{2} e^{-[1/(2B_p)](E_b/N_0)} \quad (7-65)$$

where the average energy per bit is  $E_b = A^2T/2$  and  $\sigma^2 = N_0B_p$ .  $N_0/2$  is the PSD of the input noise, and  $B_p$  is the effective bandwidth of each of the bandpass filters (see Fig. 7-11). Comparing (7-65) with (7-58), we see that OOK and FSK are equivalent on an  $E_b/N_0$  basis. A plot of (7-65) is given in Fig. 7-14 for the case of the minimum filter bandwidth allowed,  $B_p = R = 1/T$ , for no ISI. When comparing the error performance of noncoherently detected FSK with that of coherently detected FSK, it is seen that noncoherent FSK requires, at most, only 1 dB more  $E_b/N_0$  than that for coherent FSK if  $P_e$  is  $10^{-4}$  or less. The noncoherent FSK receiver is considerably easier to build since the coherent reference signals do not have to be generated. Thus, in practice, almost all of the FSK receivers use noncoherent detection.

### Differential Phase-Shift Keying

Phase-shift-keyed signals cannot be detected incoherently. However, a partially coherent technique can be used whereby the phase reference for the present signaling interval is provided by a delayed version of the signal that occurred during the previous signaling interval. This is illustrated by the receivers shown in Fig. 7-12, where differential decoding is provided by the (one-bit) delay and the multiplier. If a BPSK signal (no noise) were applied to the receiver input, the output of the sample-and-hold circuit,  $r_o(t_0)$ , would be positive (binary 1) if the present data bit and the previous data bit were of the same sense;  $r_o(t_0)$  would be negative (binary 0) if the two data bits were different. Consequently, if the data on the BPSK signal are differentially encoded (e.g., see the illustration in Table 3-4), the decoded data sequence will be recovered at the output of this receiver. This signaling technique consisting of transmitting a differentially encoded BPSK signal is known as DPSK.

The BER for these DPSK receivers can be derived under the following assumptions.

- The additive input noise is white and Gaussian.
- The phase perturbation of the composite signal plus noise varies slowly so that the phase reference is essentially a constant from the past signaling interval to the present signaling interval.
- The transmitter carrier oscillator is sufficiently stable so that the phase during the present signaling interval is the same as that from the past signaling interval.

The BER for the suboptimum demodulator of Fig. 7-12a has been obtained by J. H. Park for the case of a large input signal-to-noise ratio and for  $B_T > 2/T$  but yet not too large. The result is [Park, 1978]

$$P_e = Q \left( \sqrt{\frac{(E_b/N_0)}{1 + [(B_T T/2)/(E_b/N_0)]}} \right) \quad (7-66a)$$

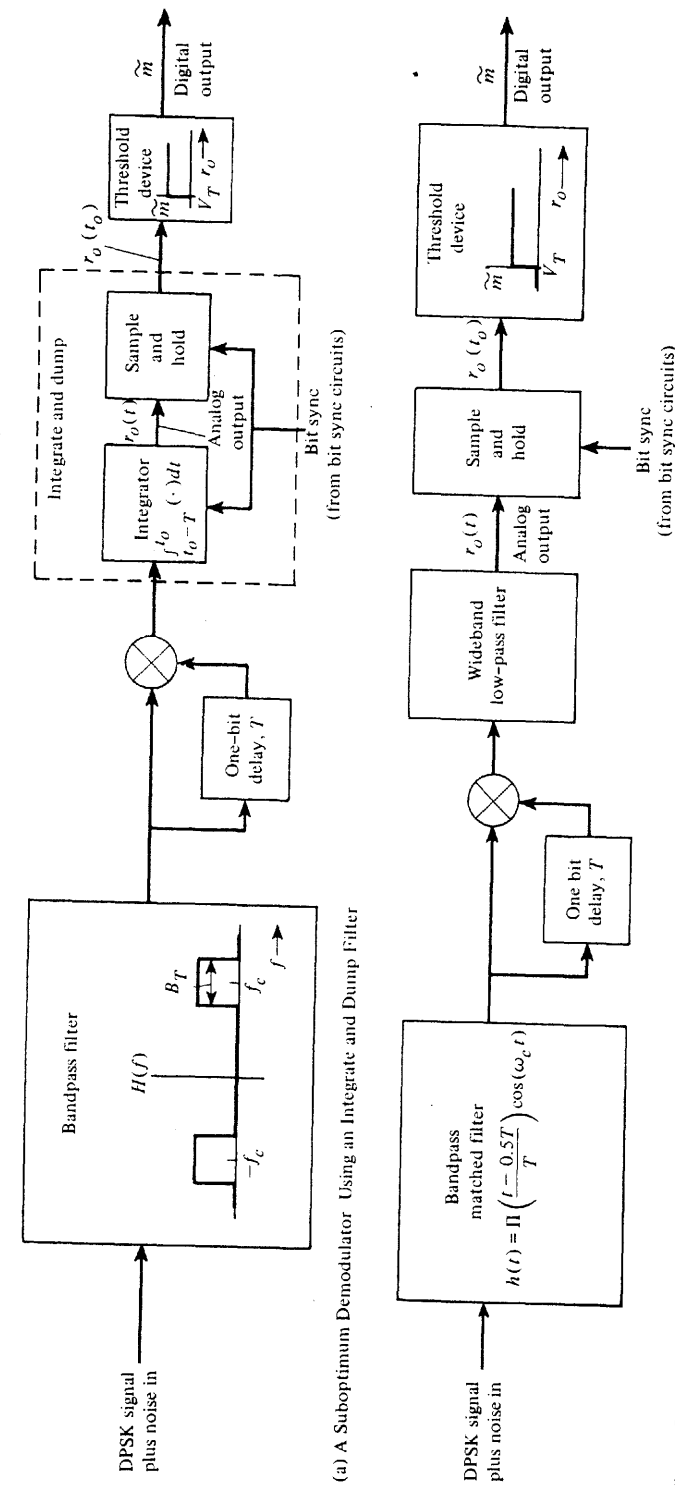


Figure 7-12 Demodulation of DPSK.

(a) A Suboptimum Demodulator Using an Integrate and Dump Filter

(from bit sync circuits)

(b) An Optimum Demodulator Using a Bandpass Matched Filter

(from bit sync circuits)

For typical values of  $B_T$  and  $E_b/N_0$  in the range of  $B_T = 3/T$  and  $E_b/N_0 = 10$ , this BER can be approximated by

$$P_e = Q\left(\sqrt{E_b/N_0}\right) \quad (7-66b)$$

Thus the performance of the suboptimum receiver of Fig. 7-12a is similar to that obtained for OOK and FSK as plotted in Fig. 7-14.

Figure 7-12b shows one form of an optimum DPSK receiver that can be obtained [Couch, 1993, Fig. 8-25]. The BER for optimum demodulation of DPSK is

$$P_e = \frac{1}{2} e^{-(E_b/N_0)} \quad (7-67)$$

Other alternative forms of optimum DPSK receivers are possible [Lindsey and Simon, 1973; Simon, 1978].

A plot of this error characteristic for the case of optimum demodulation of DPSK, (7-67), is shown in Fig. 7-14. In comparing the error performance of BPSK and DPSK with optimum demodulation, it is seen that for the same  $P_e$ , DPSK signaling requires, at most, 1 dB more  $E_b/N_0$  than BPSK provided that  $P_e = 10^{-4}$  or less. In practice, DPSK is often used instead of BPSK because the DPSK receiver does not require a carrier synchronization circuit.

## 7-5 QUADRATURE PHASE-SHIFT KEYING AND MINIMUM-SHIFT KEYING

As described in Sec. 5-10, quadrature phase-shift keying (QPSK) is a multilevel signaling technique that uses  $L = 4$  levels per symbol. Thus 2 bits are transmitted during each signaling interval ( $T$  seconds). The QPSK signal may be represented by

$$s(t) = (\pm A) \cos(\omega_c t + \theta_c) - (\pm A) \sin(\omega_c t + \theta_c), \quad 0 < t \leq T \quad (7-68)$$

where the  $(\pm A)$  factor on the cosine carrier is one bit of data and the  $(\pm A)$  factor on the sine carrier is another bit of data. The relevant input noise is represented by

$$n(t) = x(t) \cos(\omega_c t + \theta_n) - y(t) \sin(\omega_c t + \theta_n)$$

The QPSK signal is equivalent to two BPSK signals—one using a cosine carrier and the other using a sine carrier. The QPSK signal is detected by using the coherent receiver shown in Fig. 7-13. (This is an application of the IQ detector that was first given in Fig. 4-31.) Because both the upper and lower channels of the receiver are BPSK receivers, the BER is the same as that for a BPSK system. Thus from (7-38) the BER for the QPSK receiver is

$$P_e = Q\left(\sqrt{2}\left(\frac{E_b}{N_0}\right)\right) \quad (7-69)$$

This is also shown in Fig. 7-14. The BERs for the BPSK and QPSK signaling are identical, but for the same bit rate  $R$ , the bandwidths of the two signals are *not* the same. The band-

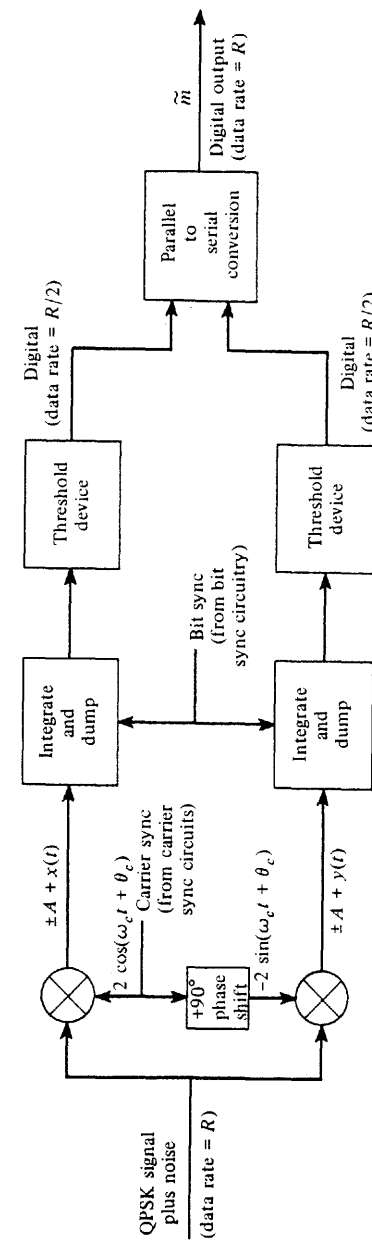
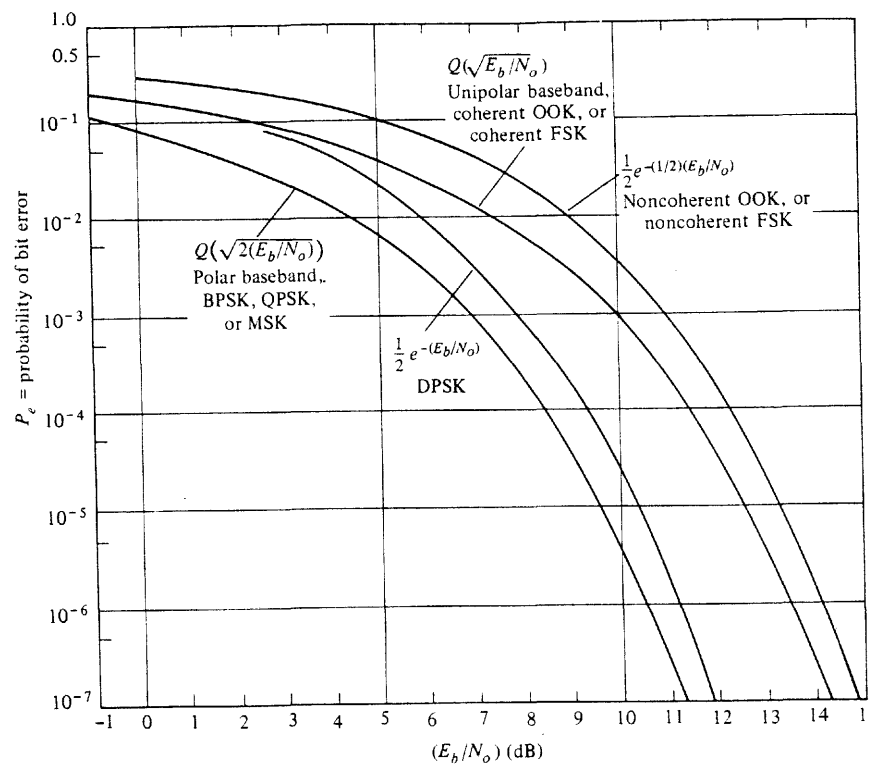


Figure 7-13 Matched-filter detection of QPSK.



**Figure 7-14** Comparison of the probability of bit error for several digital signaling schemes.

width of the QPSK signal is exactly one-half the bandwidth of the BPSK signal for a given bit rate. This result is given by (5-106), where the QPSK signal transmits one symbol for every 2 bits of data, whereas the BPSK signal transmits one symbol for each bit of data.

In Chapter 5 it was shown that MSK is essentially equivalent to QPSK except that the data on the  $x(t)$  and  $y(t)$  quadrature modulation components are offset and their equivalent data pulse shape is a positive part of a cosine function instead of a rectangular pulse. (This gives a PSD for MSK that rolls off faster than that for PSK.) The optimum receiver for detection of MSK is similar to that for QPSK (Fig. 7-13), except that a matched filter with a cosine pulse shape is used instead of the rectangular pulse shape that is synthesized by the integrate-and-dump circuit. Consequently, because the MSK and QPSK signal representations and the optimum receiver structures are identical except for the pulse shape, the probability of bit error for MSK and QPSK is identical, as described by (7-69). A plot of this BER is shown in Fig. 7-14.

If the data are properly encoded, the data on an MSK signal can also be detected by using FM-type detectors because the MSK signal is also an FSK signal with a minimum amount of frequency shift that makes  $s_1(t)$  and  $s_2(t)$  orthogonal signals. Thus, for suboptimal

mum detection of MSK, the BER is given by the BER for FSK, as described by (7-47) for coherent FM detection and (7-65) for noncoherent FM detection.

## 7-6 COMPARISON OF DIGITAL SIGNALING SYSTEMS

### Bit Error Rate and Bandwidth

A summary of the bit error rates that we obtained in the previous sections is given in Table 7-1. The minimum bandwidths for the signals are also tabulated using the equations developed in Chapter 5.

Zero-crossing bandwidths are not given in the table because they depend on the exact pulse shape used as well as the data statistics. The zero-crossing bandwidth can be evaluated from the PSD that describes the situation of interest. In Chapters 3 and 5 methods were given for evaluation of the PSD, and the PSD and corresponding zero-crossing bandwidth were worked out for many cases of practical interest.

In Fig. 7-14 the BER curves are plotted using the equations presented in Table 7-1. Except for the curves describing the noncoherent detection cases, all of these results assume that the optimum filter—the matched filter—is used in the receiver. In practice, simpler filters work almost as well as the matched filter. For example, in a computer simulation of a BPSK system with a threepole Butterworth receiving filter having a bandwidth equal to the bit rate, the  $E_b/N_0$  needs to be increased no more than 0.4 dB to obtain the same BER as that obtained when a matched filter is used (for error rates above  $10^{-12}$ ).

Comparing the various bandpass signaling techniques, we see that QPSK and MSK give the best overall performance in terms of the minimum bandwidth required for a given signaling rate and one of the smallest  $P_e$  for a given  $E_b/N_0$ . However, QPSK is relatively expensive to implement since it requires coherent detection. Figure 7-14 shows that for the same  $P_e$ , DPSK (using a noncoherent receiver) requires only about 1 dB more  $E_b/N_0$  than that for QPSK or BPSK, for error rates of  $10^{-4}$  or less. Because DPSK is much easier to receive than BPSK, it is often used in practice in preference to BPSK. Similarly, the BER performance of a noncoherent FSK receiver is very close to that of a coherent FSK receiver. Because noncoherent FSK receivers are simpler than coherent FSK receivers, they are often used in practice. In some applications there are multiple paths of different lengths between the transmitter and receiver (e.g., caused by reflection). This causes fading and noncoherence in the received signal (phase). In this case, it is very difficult to implement coherent detection, regardless of the complexity of the receiver, and one resorts to the use of noncoherent detection techniques.

Channel coding can be used to reduce the  $P_e$  below the values given in Fig. 7-14. This concept was developed in Chapter 1. By using Shannon's channel capacity formula, it was found that theoretically the BER would approach zero as long as  $E_b/N_0$  was above  $-1.59$  dB when optimum (unknown) coding was used on an infinite bandwidth channel. With practical coding it was found that coding gains as large as 9 dB could be achieved on BPSK and QPSK systems. That is, for a given BER the  $E_b/N_0$  requirements in Fig. 7-14 could be reduced by as much as 9 dB when coding was used.

TABLE 7-1 COMPARISON OF DIGITAL SIGNALING METHODS

Type of Digital Signaling	Minimum Transmission Bandwidth Required <sup>a</sup> (Where $R$ Is the Bit Rate)	Error Performance
<b>Baseband signaling</b>		
Unipolar	$\frac{1}{2}R$	(5-105)
Polar	$\frac{1}{2}R$	(5-105)
Bipolar	$\frac{1}{2}R$	(5-105)
<b>Bandpass signaling</b>		
OOK	$R$	(5-106)
BPSK	$R$	(5-106)
FSK	$2\Delta F + R$ where $2\Delta F = f_2 - f_1$ is the frequency shift	(5-89)
DPSK	$R$	(5-106)
QPSK	$\frac{1}{2}R$	(5-106)
MSK	$1.5R$ (null bandwidth)	(5-115)
•		

<sup>a</sup> Typical bandwidth specifications by ITU are larger than these minima [Jordan, 1985].

## Synchronization

As we have seen, three levels of synchronization are needed in digital communication systems.

1. Bit synchronization.
2. Frame or word synchronization.
3. Carrier synchronization.

Bit and frame synchronizations were discussed in Chapter 3.

Carrier synchronization is required in receivers that use coherent detection. If the spectrum of the digital signal has a discrete line at the carrier frequency, such as in equally likely OOK signaling, a PLL can be used to recover the carrier reference from the received signal. This was described in Chapter 4 and shown in Fig. 4-24. In BPSK signaling there is no discrete carrier term, but the spectrum is symmetrical about the carrier frequency. Consequently, a Costas loop or a squaring loop may be used for carrier sync recovery. These loops were illustrated in Figs. 5-3 and P5-51. As indicated in Sec. 5-4, these loops may lock up with a  $180^\circ$  phase error, which must be resolved to ensure that the recovered data will not be complemented. For QPSK signals, the carrier reference may be obtained by a more generalized Costas loop or, equivalently, by a fourth-power loop [Spilker, 1977]. These loops have a four-phase ambiguity of  $0^\circ$ ,  $\pm 90^\circ$ , or  $180^\circ$ , which must also be resolved to obtain correctly demodulated data. These facts illustrate once again why noncoherent reception techniques (which can be used for OOK, FSK, and DPSK) are so popular.

Bit synchronizers are needed at the receiver to provide the bit sync signal for clocking the sample-and-hold circuit and, if used, the matched filter circuit. The bit synchronizer was illustrated in Fig. 3-20.

All the BER formulas that we have obtained assume that noise-free bit sync and carrier sync (for coherent detection) are available at the receiver. Of course, if these sync signals are obtained from noisy signals that are present at the receiver input, the reference signals are also noisy. Consequently, the  $P_e$  will be larger than that given for the ideal case when noise-free sync is assumed.

The third type of synchronization that is required by most digital systems is frame sync or word sync. In some systems this sync is used simply to demark the serial data into digital words or *bytes*. In other systems, block coding or convolutional coding is used at the transmitter so that some of the bit errors at the output of the threshold device of the receiver can be detected and corrected by using decoding circuits. In these systems word sync is needed to clock the receiver decoding circuits. In addition, frame sync is required in time-division multiplex (TDM) systems. This was described in Fig. 3-37. Higher levels of synchronization, such as network synchronization, may be required when data are received from several sources. For example, multiple-access satellite communication systems require network synchronization, as illustrated in Chapter 8.

For further reading on the interesting topic of synchronization, the reader is referred to a special issue of the *IEEE Transactions on Communications*, which presents tutorial as well as in-depth papers on the different aspects of synchronization problems [Gardner and Lindsey, 1980].

## 7-7 OUTPUT SIGNAL-TO-NOISE RATIO FOR PCM SYSTEMS

In the previous sections we have analyzed how the  $P_e$  for various digital systems depends on the energy per bit  $E_b$  of the signal at the receiver input and on the level of the input noise spectrum  $N_0/2$ . Now suppose that we look at applications of these signaling techniques where an analog signal is encoded into a PCM signal that comprises the data that are transmitted over the digital system having a BER of  $P_e$ . This is illustrated in Fig. 7-15. The digital transmitter and receiver may be any one of those associated with the digital signaling systems studied in the previous sections. For example,  $s(t)$  might be an FSK signal and the receiver would be an FSK receiver. The recovered PCM signal has some bit errors (caused by channel noise). Consequently, the decoded analog waveform at the output of the PCM decoder will have noise because of these bit errors as well as quantizing noise. The question is: What is the peak signal to average noise ratio ( $S/N$ )<sub>out</sub> for the analog output? If the input analog signal has a uniform PDF over  $-V$  to  $+V$  and there are  $M$  steps in the uniform quantizer, the answer is

$$\left(\frac{S}{N}\right)_{\text{pk out}} = \frac{3M^2}{1 + 4(M^2 - 1)P_e} \quad (7-70)$$

Applications of this result were first studied in Sec. 3-3.

Equation (7-70) will now be derived. As shown in Fig. 7-15, the analog sample  $x_k$  is obtained at the sampling time  $t = kT_s$ . This sample is quantized to a value  $Q(x_k)$ , which is one of the  $M$  possible levels, as indicated in Fig. 7-15. The quantized sample  $Q(x_k)$  is encoded into an  $n$ -bit PCM word  $(a_{k1}, a_{k2}, \dots, a_{kn})$ , where  $M = 2^n$ . If polar signaling is used,

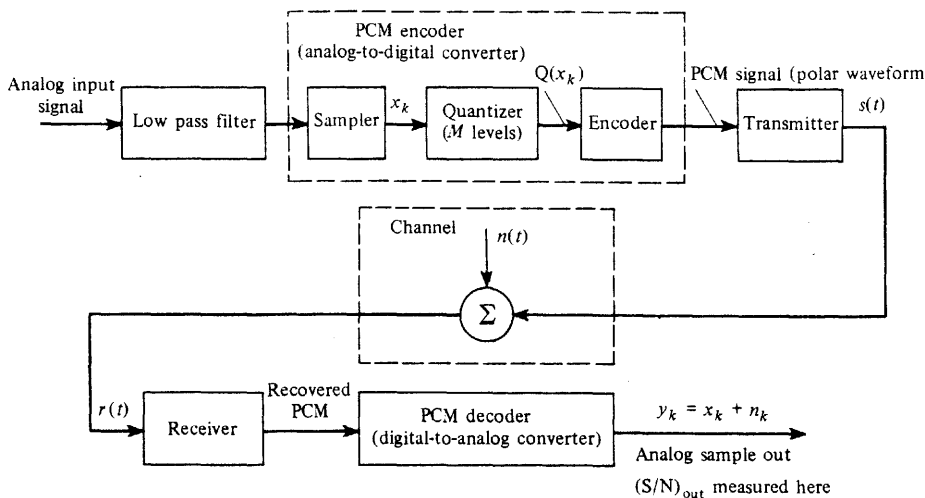


Figure 7-15 PCM communications system.

the  $a_k$ 's take on values of  $+1$  or  $-1$ . For simplicity, we assume that the PCM code words are related to the quantized values by<sup>†</sup>

$$Q(x_k) = V \sum_{j=1}^n a_{kj} \left(\frac{1}{2}\right)^j \quad (7-71)$$

For example, if the PCM word for the  $k$ th sample happens to be  $(+1, +1, \dots, +1)$ , then the value of the quantized sample will be

$$Q(x_k) = V \left( \frac{1}{2} + \frac{1}{2} + \dots + \frac{1}{2^n} \right) = \frac{V}{2} \left( 1 + \frac{1}{2} + \frac{1}{4} + \dots + \frac{1}{2^{n-1}} \right)$$

Using (A-90), we find that the sum of this finite series is

$$Q(x_k) = \frac{V}{2} \left[ \frac{\left(\frac{1}{2}\right)^n - 1}{\frac{1}{2} - 1} \right] = V - \frac{V}{2^n}$$

or, because  $V = (\delta/2)2^n$ ,

$$Q(x_k) = V - \frac{\delta}{2}$$

where  $\delta$  is the step size of the quantizer (Fig. 7-16). Thus the PCM word  $(+1, +1, \dots, +1)$  represents the maximum value of the quantizer, as illustrated in Fig. 7-16. Similarly, the level of the quantizer corresponding to the other code words can be obtained.

Referring to Fig. 7-15 again, we note that the analog sample output of the PCM system for the  $k$ th sampling time is

$$y_k = x_k + n_k$$

where  $x_k$  is the signal (same as the input sample) and  $n_k$  is noise. The output peak signal power to average noise power is then

$$\left(\frac{S}{N}\right)_{\text{pk out}} = \frac{[(x_k)_{\text{max}}]^2}{\overline{n_k^2}} = \frac{V^2}{\overline{n_k^2}} \quad (7-72)$$

where  $(x_k)_{\text{max}} = V$ , as is readily seen from Fig. 7-16. As indicated in Chapter 3, it is assumed that the noise  $n_k$  consists of two uncorrelated effects.

- Quantizing noise that is due to the quantizing error:

$$e_q = Q(x_k) - x_k \quad (7-73)$$

- Noise due to bit errors that are caused by the channel noise:

$$e_b = y_k - Q(x_k) \quad (7-74)$$

<sup>†</sup> For mathematical simplicity, natural binary coding levels are used in (7-71), not Gray coding of Table 3-1.

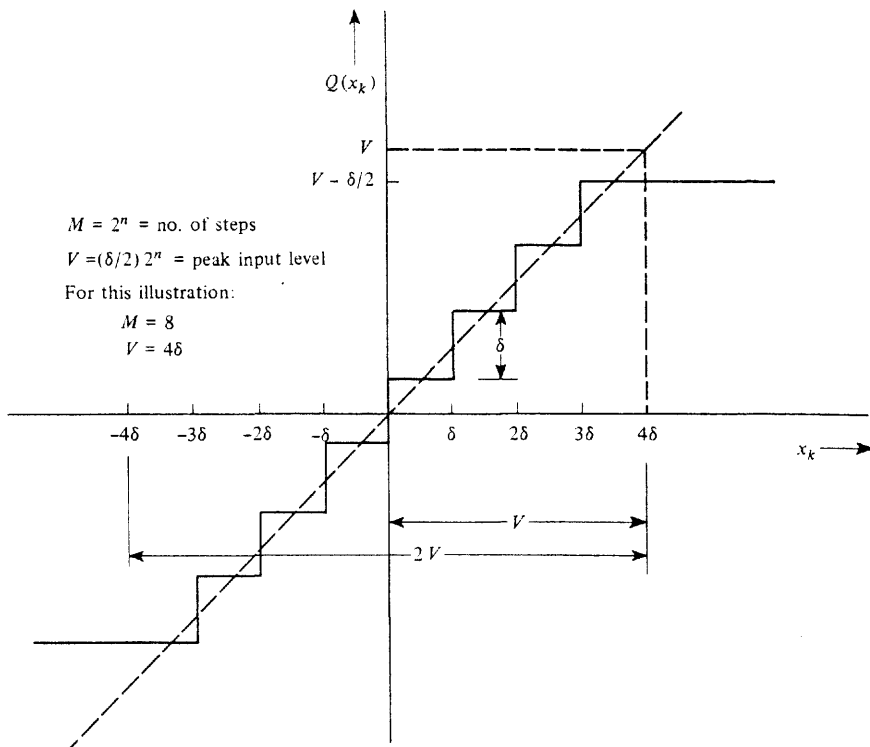


Figure 7-16 Uniform quantizer characteristic for  $M = 8$  ( $n = 3$  bits in each PCM word).

Thus

$$\overline{e_k^2} = \overline{e_q^2} + \overline{e_b^2} \quad (7-75)$$

First, evaluate the quantizing noise power. For a uniformly distributed signal, the quantizing noise is uniformly distributed. Furthermore, as indicated by Fig. 3-8c, the interval of the uniform distribution is  $(-\delta/2, \delta/2)$ , where  $\delta$  is the step size ( $\delta = 2$  in Fig. 3-8c). Thus, with  $M = 2^n = 2V/\delta$  (from Fig. 7-16),

$$\overline{e_q^2} = \int_{-\infty}^{\infty} e_q^2 f(e_q) de_q = \int_{-\delta/2}^{\delta/2} e_q^2 \frac{1}{\delta} de_q = \frac{\delta^2}{12} = \frac{V^2}{3M^2} \quad (7-76)$$

The noise power due to bit errors is evaluated by the use of (7-74),

$$\overline{e_b^2} = [\overline{y_k} - \overline{Q(x_k)}]^2 \quad (7-77)$$

where  $Q(x_k)$  is given by (7-71). The recovered analog sample  $y_k$  is reconstructed from the received PCM code word using the same algorithm as that of (7-71). Assuming that the received PCM word for the  $k$ th sample is  $(b_{k1}, b_{k2}, \dots, b_{kn})$ , then we see that

$$\overline{y_k} = V \sum_{j=1}^n b_{kj} \left(\frac{1}{2}\right)^j \quad (7-78)$$

The  $b$ 's will be different from the  $a$ 's whenever there is a bit error in the recovered digital (PCM) waveform. By using (7-78) and (7-71), (7-77) becomes

$$\begin{aligned} \overline{e_b^2} &= V^2 \left[ \sum_{j=1}^n (b_{kj} - a_{kj}) \left(\frac{1}{2}\right)^j \right]^2 \\ &= V^2 \sum_{j=1}^n \sum_{\ell=1}^n \left( \overline{b_{kj} b_{k\ell}} - \overline{a_{kj} b_{k\ell}} - \overline{b_{kj} a_{k\ell}} + \overline{a_{kj} a_{k\ell}} \right) 2^{-j-\ell} \end{aligned} \quad (7-79)$$

where  $b_{kj}$  and  $b_{k\ell}$  are two bits in the received PCM word that occur at different bit positions when  $j \neq \ell$ . Similarly,  $a_{kj}$  and  $b_{k\ell}$  are the transmitted (Tx) and received (Rx) bits in two different bit positions, where  $j \neq \ell$  (for the PCM word corresponding to the  $k$ th sample). The encoding process produces bits that are independent unless  $j = \ell$ . Furthermore, the bits have a zero-mean value. Thus  $\overline{b_{kj} b_{k\ell}} = \overline{b_{kj} b_{k\ell}} = 0$  for  $j \neq \ell$ . Similar results are obtained for the other averages on the right-hand side of (7-79). Equation (7-79) becomes

$$\overline{e_b^2} = V^2 \sum_{j=1}^n \left( \overline{b_{kj}^2} - 2\overline{a_{kj} b_{kj}} + \overline{a_{kj}^2} \right) 2^{-2j} \quad (7-80)$$

Evaluating the averages in (7-80), we obtain<sup>†</sup>

$$\begin{aligned} \overline{b_{kj}^2} &= (+1)^2 P(+1\text{Rx}) + (-1)^2 P(-1\text{Rx}) = 1 \\ \overline{a_{kj}^2} &= (+1)^2 P(+1\text{Tx}) + (-1)^2 P(-1\text{Tx}) = 1 \\ \overline{a_{kj} b_{kj}} &= (+1)(+1)P(+1\text{Tx}, +1\text{Rx}) + (-1)(-1)P(-1\text{Tx}, -1\text{Rx}) \\ &\quad + (-1)(+1)P(-1\text{Tx}, +1\text{Rx}) + (+1)(-1)P(+1\text{Tx}, -1\text{Rx}) \\ &= [P(+1\text{Tx}, +1\text{Rx}) + P(-1\text{Tx}, -1\text{Rx})] \\ &\quad - [P(-1\text{Tx}, +1\text{Rx}) + P(+1\text{Tx}, -1\text{Rx})] \\ &= [1 - P_e] - [P_e] = 1 - 2P_e \end{aligned}$$

Thus (7-80) reduces to

$$\overline{e_b^2} = 4V^2 P_e \sum_{j=1}^n \left(\frac{1}{4}\right)^j$$

which, by (A-90), becomes

$$\overline{e_b^2} = V^2 P_e \frac{\left(\frac{1}{4}\right)^n - 1}{\frac{1}{4} - 1} = \frac{4}{3} V^2 P_e \frac{(2^n)^2 - 1}{(2^n)^2}$$

<sup>†</sup> The notation  $+1\text{Tx}$  denotes a binary 1 transmitted,  $-1\text{Tx}$  denotes a binary 0 transmitted,  $+1\text{Rx}$  denotes a binary 1 received, and  $-1\text{Rx}$  denotes a binary 0 received.

or

$$\overline{e_b^2} = \frac{4}{3} V^2 P_e \frac{M^2 - 1}{M^2} \quad (7-81)$$

Substituting (7-76) and (7-81) into (7-72) with the help of (7-75), we have

$$\left( \frac{S}{N} \right)_{\text{pk out}} = \frac{V^2}{(V^2/3M^2) + (4V^2/3M^2)P_e(M^2 - 1)}$$

which reduces to (7-70).

Equation (7-70) is used to obtain the curves shown in Fig. 7-17. For a PCM system with  $M$  quantizing steps,  $(S/N)_{\text{out}}$  is given as a function of the BER of the digital receiver.

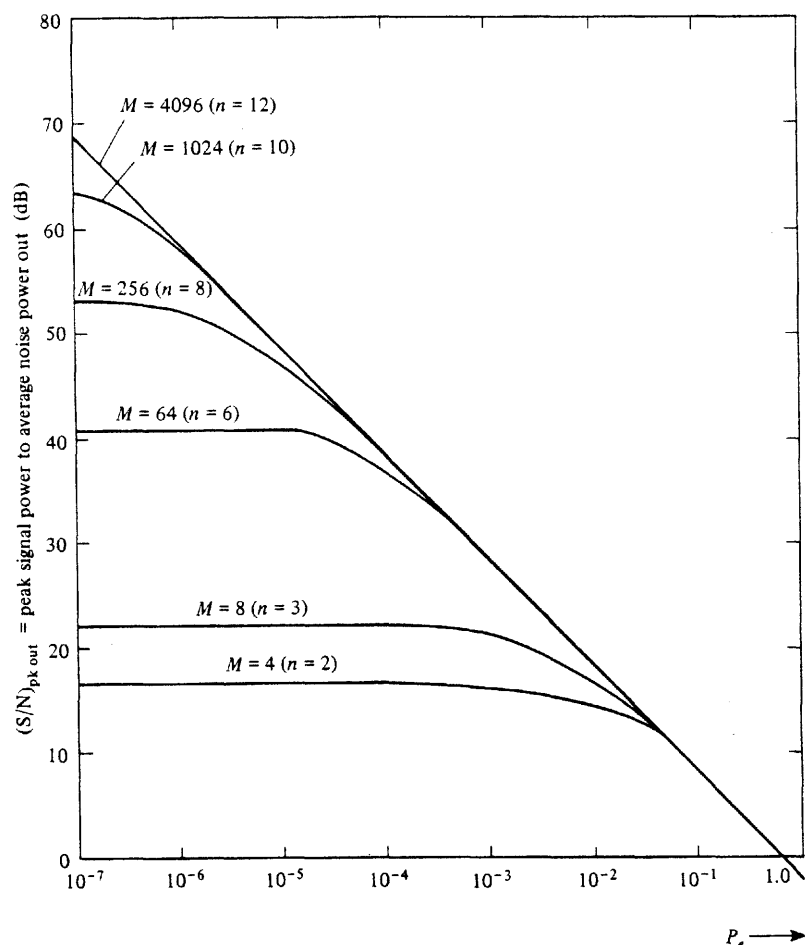


Figure 7-17  $(S/N)_{\text{out}}$  of a PCM system as a function of  $P_e$  and the number of quantizer steps,  $M$ .

For  $P_e < 1/(4M^2)$  the analog signal at the output is corrupted primarily because of quantizing noise. In fact, for  $P_e = 0$ ,  $(S/N)_{\text{out}} = 3M^2$ , where all the noise is quantizing noise. Conversely, for  $P_e > 1/(4M^2)$ , the output is corrupted primarily because of channel noise.

It is also stressed that (7-70) is the *peak* signal to average noise ratio. The *average* signal to average noise ratio is obtained easily from the results given above. The average signal to average noise ratio is

$$\left( \frac{S}{N} \right)_{\text{out}} = \frac{\overline{x_k^2}}{\overline{n_k^2}} = \frac{V^2}{3\overline{n_k^2}} = \frac{1}{3} \left( \frac{S}{N} \right)_{\text{pk out}}$$

where  $\overline{x_k^2} = V^2/3$  because  $x_k$  is uniformly distributed from  $-V$  to  $+V$ . Thus, using (7-72) and (7-70),

$$\left( \frac{S}{N} \right)_{\text{out}} = \frac{M^2}{1 + 4(M^2 - 1)P_e} \quad (7-82)$$

when  $(S/N)_{\text{out}}$  is the average signal to average noise power ratio at the output of the system.

## 7-8 OUTPUT SIGNAL-TO-NOISE RATIOS FOR ANALOG SYSTEMS

In Chapters 4 and 5 generalized modulation and demodulation techniques for analog and digital signals were studied. Specific techniques were shown for AM, DSB-SC, SSB, PM, and FM signaling, and the bandwidths of these signals were evaluated. Here we evaluate the output signal-to-noise ratios for these systems as a function of the input signal, noise, and system parameters. Once again, we will find that the mathematical analysis of noncoherent systems is more difficult than that for coherent systems and that approximations are often used to obtain simplified results. However, noncoherent systems are often found to be more prevalent in practice since the receiver cost is usually lower. This is certainly the case for overall system cost in applications involving one transmitter and thousands or millions of receivers such as FM, AM, and TV broadcasting.

For systems with additive noise channels the input to the receiver is

$$r(t) = s(t) + n(t)$$

For bandpass communication systems having a transmission bandwidth of  $B_T$ , this is

$$\begin{aligned} r(t) &= \operatorname{Re}\{ g_s(t) e^{j(\omega_c t + \theta_s)} \} + \operatorname{Re}\{ g_n(t) e^{j(\omega_c t + \theta_n)} \} \\ &= \operatorname{Re}\{ [g_s(t) + g_n(t)] e^{j(\omega_c t + \theta_n)} \} \end{aligned}$$

or

$$r(t) = \operatorname{Re}\{ g_T(t) e^{j(\omega_c t + \theta_n)} \} \quad (7-83a)$$

where

$$\begin{aligned}
 g_T(t) &\triangleq g_s(t) + g_n(t) \\
 &= [x_s(t) + x_n(t)] + j[y_s(t) + y_n(t)] \\
 &= x_T(t) + jy_T(t) \\
 &= R_T(t)e^{j\theta_T(t)}
 \end{aligned} \tag{7-83b}$$

$g_T(t)$  denotes the total (i.e., composite) complex envelope at the receiver input; it consists of the complex envelope of the signal plus the complex envelope of the noise. The properties of the total complex envelope, as well as those of Gaussian noise, were given in Chapter 6. The complex envelopes for a number of different types of modulated signals  $g_s(t)$  were given in Table 4-1.

### Comparison with Baseband Systems

The noise performance of the various types of bandpass systems is examined by evaluating the signal-to-noise power ratio at the receiver output,  $(S/N)_{out}$ , when a modulated signal plus noise is present at the receiver input. We would like to see if  $(S/N)_{out}$  is larger for an AM system, a DSB-SC system, or an FM system. For comparison of these SNRs, the power of the modulated signals at the inputs of these receivers is set to the same value and the PSD of the input noise is  $N_0/2$ . (That is, the input noise is white with a spectral level set to  $N_0/2$ .)

To compare the output signal-to-noise ratio  $(S/N)_{out}$  for various bandpass systems, we need a common measurement criterion for the receiver input. For example,  $E_b/N_0$  was used for digital systems. For analog systems the criterion is the received signal power  $P_s$  divided by the amount of power in the white noise that is contained in a bandwidth equal to the message (modulation) bandwidth. This is equivalent to the  $(S/N)_{out}$  of a baseband transmission system as illustrated in Fig. 7-18. That is,

$$\left(\frac{S}{N}\right)_{baseband} = \frac{P_s}{N_0 B} \tag{7-84}$$

We can compare the performance of different modulated systems by evaluating  $(S/N)_{out}$  for each system for a given value of  $(P_s/N_0 B) = (S/N)_{baseband}$ , where  $P_s$  is the power of the AM, DSB-SC, or FM signal (at the AM, DSB-SC, or FM receiver input).  $B$  is

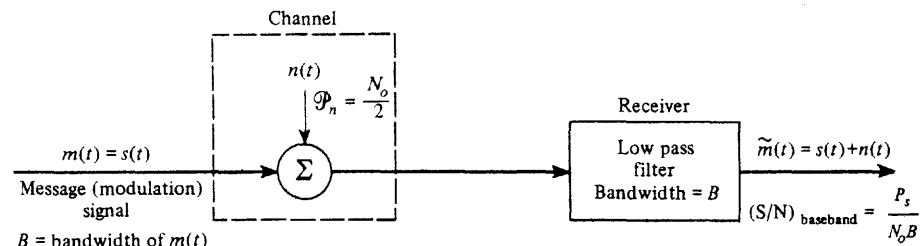


Figure 7-18 Baseband system.

chosen to be the bandwidth of the *baseband* (modulating) signal where the same baseband modulating signal is used for all cases so that the same basis of comparison will be realized. (If  $B$  were chosen to be the bandwidth of the input-modulated signal,  $B_T$ , the comparison would not be on an equal noise PSD basis of  $N_0/2$  for a fixed value of  $(S/N)_{baseband}$  because the  $B_T$  values for AM and FM signals are different.)

The SNR at the receiver input can also be obtained; it is

$$\left(\frac{S}{N}\right)_{in} = \frac{P_s}{N_0 B_T} = \left(\frac{S}{N}\right)_{baseband} \left(\frac{B}{B_T}\right) \tag{7-85}$$

where  $B_T$  is the bandwidth of the bandpass signal at the receiver input.

$(S/N)_{out}$  will now be evaluated for several different systems.

### AM Systems with Product Detection

Figure 7-19 illustrates the receiver for an AM system with coherent detection. From (4-107), the complex envelope of the AM signal is

$$g_s(t) = A_c[1 + m(t)]$$

The complex envelope of the composite received signal plus noise is

$$g_T(t) = [A_c + A_c m(t) + x_n(t)] + jy_n(t) \tag{7-86}$$

For product detection, using (4-71), we find that the output is

$$\tilde{m}(t) = \operatorname{Re}\{g_T(t)\} = A_c + A_c m(t) + x_n(t)$$

Here  $A_c$  is the dc voltage at the detector output that occurs because of the discrete AM carrier,<sup>†</sup>  $A_c m(t)$  is the detected modulation, and  $x_n(t)$  is the detected noise. The output SNR is

$$\left(\frac{S}{N}\right)_{out} = \frac{A_c^2 m^2(t)}{x_n^2(t)} = \frac{A_c^2 m^2(t)}{2N_0 B} \tag{7-87}$$

where, from (6-133g),  $\overline{x_n^2} = \overline{n^2} = 2(N_0/2)(2B)$ . The input signal power is

$$P_s = \frac{A_c^2}{2} \overline{[1 + m(t)]^2} = \frac{A_c^2}{2} [1 + \overline{m^2}]$$

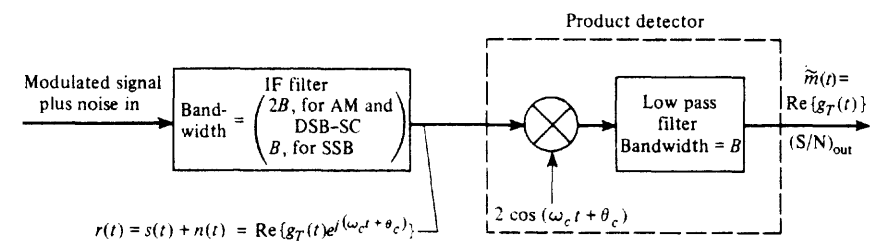


Figure 7-19 Coherent receiver.

<sup>†</sup> This dc voltage is often used to provide automatic gain control (AGC) of the preceding RF and IF stages.

where it is assumed that  $\overline{m(t)} = 0$  (i.e., no dc on the modulating waveform). Thus the input SNR is

$$\left(\frac{S}{N}\right)_{in} = \frac{(A_c^2/2)(1 + \overline{m^2})}{2N_0B} \quad (7-88)$$

Combining (7-87) and (7-88) yields

$$\frac{(S/N)_{out}}{(S/N)_{in}} = \frac{2\overline{m^2}}{1 + \overline{m^2}} \quad (7-89)$$

For 100% sine-wave modulation  $\overline{m^2} = \frac{1}{2}$  and  $(S/N)_{out}/(S/N)_{in} = \frac{2}{3}$ .

For comparison purposes, (7-87) can be evaluated in terms of  $(S/N)_{baseband}$  by substituting for  $P_s$ :

$$\frac{(S/N)_{out}}{(S/N)_{baseband}} = \frac{\overline{m^2}}{1 + \overline{m^2}} \quad (7-90)$$

For 100% sine-wave modulation,  $(S/N)_{out}/(S/N)_{baseband} = \frac{1}{3}$ . This illustrates that this AM system is 4.8 dB worse than a baseband system that uses the same amount of signal power. This is shown in Fig. 7-27.

### AM Systems with Envelope Detection

The envelope detector produces  $KR_T(t)$  at its output, where  $K$  is a proportionality constant. Then, for additive signal plus noise at the input, the output is

$$KR_T(t) = K|g_s(t) + g_n(t)|$$

Substituting (7-86) for  $g_s(t) + g_n(t)$  gives

$$KR_T(t) = K|[A_c + A_c m(t) + x_n(t)] + j[y_n(t)]| \quad (7-91)$$

The power is

$$[KR_T(t)]^2 = K^2 A_c^2 \left\{ \left[ 1 + m(t) + \frac{x_n(t)}{A_c} \right]^2 + \left[ \frac{y_n(t)}{A_c} \right]^2 \right\} \quad (7-92)$$

For the case of large  $(S/N)_{in}$ ,  $(y_n/A_c)^2 \ll 1$ , so we have

$$[KR_T(t)]^2 = (KA_c)^2 + K^2 A_c^2 \overline{m^2} + K^2 \overline{x_n^2} \quad (7-93)$$

where  $(KA_c)^2$  is the power of the AGC term,  $K^2 A_c^2 \overline{m^2}$  is the power of the detected modulation (signal), and  $K^2 \overline{x_n^2}$  is the power of the detected noise. Thus, for large  $(S/N)_{in}$ ,

$$\left(\frac{S}{N}\right)_{out} = \frac{A_c^2 \overline{m^2}}{\overline{x_n^2}} = \frac{A_c^2 \overline{m^2}}{2N_0B} \quad (7-94)$$

Comparing this with (7-87), we see that for large  $(S/N)_{in}$ , the performance of the envelope detector is identical to that of the product detector.

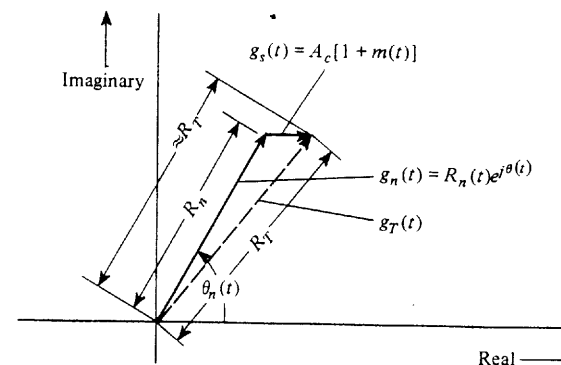


Figure 7-20 Vector diagram for AM,  $(S/N)_{in} \ll 1$ .

For small  $(S/N)_{in}$ , the performance of the envelope detector is much inferior to that of the product detector. Referring to (7-91), we note that the detector output is

$$KR_T(t) = K|g_T(t)| = K|A_c[1 + m(t)] + R_n(t)e^{j\theta_n(t)}|$$

For  $(S/N)_{in} < 1$ , as seen from Fig. 7-20, the magnitude of  $g_T(t)$  can be approximated by

$$KR_T(t) \approx K\{A_c[1 + m(t)] \cos \theta_n(t) + R_n(t)\} \quad (7-95)$$

Thus, for the case of a Gaussian noise channel, the output of the envelope detector consists of Rayleigh distributed noise  $R_n(t)$ , plus a signal term that is multiplied by a random noise factor  $\cos \theta_n(t)$ . This multiplicative effect corrupts the signal to a much larger extent than the additive Rayleigh noise. This produces a *threshold* effect. That is,  $(S/N)_{out}$  becomes very small when  $(S/N)_{in} < 1$ . In fact, it can be shown that  $(S/N)_{out}$  is proportional to the square of  $(S/N)_{in}$  for the case of  $(S/N)_{in} < 1$  [Schwartz, Bennett, and Stein, 1966]. Although the envelope detector is greatly inferior to the product detector for small  $(S/N)_{in}$ , this deficiency is seldom noticed in practice for AM broadcasting applications. This is because the AM listener is usually interested in listening to stations only if they have reasonably good  $(S/N)_{out}$ , say 25 dB or more. Under these conditions the envelope detector performance is equivalent to that of the product detector. Moreover, the envelope detector is inexpensive and does not require a coherent reference. For these reasons the envelope detector is used almost exclusively in AM broadcast receivers. For other applications, such as listening to weak AM stations or for AM data transmission systems, product detection may be required to eradicate the multiplicative noise that would occur with envelope detection of weak systems.

### DSB-SC Systems

As indicated in Chapter 5, the DSB-SC signal is essentially an AM signal in which the discrete carrier term has been suppressed (i.e., equivalent to infinite percent AM). The modulating waveform  $m(t)$  is recovered from the DSB-SC signal by using coherent detection, as shown in Fig. 7-19. For DSB-SC,

$$g_s(t) = A_c m(t) \quad (7-96)$$

Following the development leading to (7-89), the SNR for DSB-SC is

$$\frac{(S/N)_{\text{out}}}{(S/N)_{\text{in}}} = 2 \quad (7-97)$$

Using (7-90), we obtain

$$\frac{(S/N)_{\text{out}}}{(S/N)_{\text{baseband}}} = 1 \quad (7-98)$$

Thus the noise performance of a DSB-SC system is the same as that of baseband signaling systems, although the bandwidth requirement is twice as large (i.e.,  $B_T = 2B$ ).

### SSB Systems

The receiver for an SSB signal is also shown in Fig. 7-19, where the IF bandwidth is now  $B_T = B$ . The complex envelope for SSB is

$$g_s(t) = A_c[m(t) \pm j\hat{m}(t)] \quad (7-99)$$

where the upper sign is used for USSB and the lower sign is used for LSSB. The complex envelope for the (total) received SSB signal plus noise is

$$g_T(t) = [A_c m(t) + x_n(t)] + j[\pm A_c \hat{m}(t) + y_n(t)] \quad (7-100)$$

The output of the product detector is

$$\hat{m}(t) = \text{Re}\{g_T(t)\} = A_c m(t) + x_n(t) \quad (7-101)$$

The corresponding SNR is

$$\frac{(S/N)_{\text{out}}}{(S/N)_{\text{in}}} = \frac{A_c^2 \overline{\hat{m}^2(t)}}{\overline{x_n^2(t)}} = \frac{A_c^2 \overline{\hat{m}^2(t)}}{N_0 B} \quad (7-102)$$

where  $\overline{x_n^2} = \overline{n^2} = 2(N_0/2)(B)$ . Using (6-133g), we see that the input signal power is

$$P_s = \frac{1}{2} |g_s(t)|^2 = \frac{A_c^2}{2} [\overline{\hat{m}^2} + \overline{(\hat{m})^2}] = A_c^2 \overline{\hat{m}^2} \quad (7-103)$$

and the input noise power is  $P_n = \overline{n^2(t)} = N_0 B$ . Thus

$$\frac{(S/N)_{\text{out}}}{(S/N)_{\text{in}}} = 1 \quad (7-104)$$

Similarly,

$$\frac{(S/N)_{\text{out}}}{(S/N)_{\text{baseband}}} = 1 \quad (7-105)$$

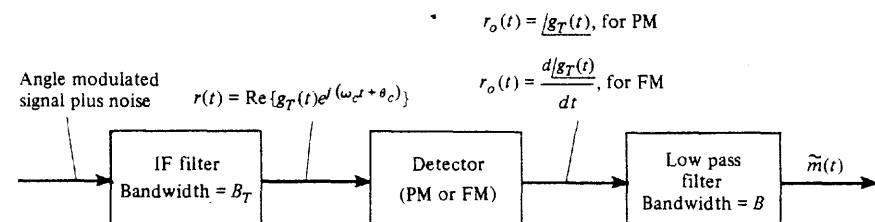


Figure 7-21 Receiver for angle-modulated signals.

SSB is exactly equivalent to baseband signaling, in terms of both the noise performance and the bandwidth requirements (i.e.,  $B_T = B$ ). Furthermore, (7-98) and (7-105) show that DSB, SSB, and baseband signaling systems are all equivalent in output SNR.

### PM Systems

As shown in Fig. 7-21, the modulation on a PM signal is recovered by a receiver that uses a (coherent) phase detector. (In Chapter 4 it was found that a phase detector could be realized by using a limiter that followed a product detector when  $\beta_p$  is small.) The PM signal has a complex envelope of

$$g_s(t) = A_c e^{j\theta_s(t)} \quad (7-106a)$$

where

$$\theta_s(t) = D_p m(t) \quad (7-106b)$$

The complex envelope of the composite signal plus noise at the detector input is

$$\begin{aligned} g_T(t) &= |g_T(t)| e^{j\theta_T(t)} = [g_s(t) + g_n(t)] \\ &= A_c e^{j\theta_s(t)} + R_n(t) e^{j\theta_n(t)} \end{aligned} \quad (7-107)$$

When the input is Gaussian noise (only),  $R_n(t)$  is Rayleigh distributed and  $\theta_n(t)$  is uniformly distributed as demonstrated in Example 6-10.

The phase detector output is proportional to  $\theta_T(t)$ :

$$r_0(t) = K / g_T(t) = K \theta_T(t)$$

where  $K$  is the gain constant of the detector. For large  $(S/N)_{\text{in}}$ , the phase angle of  $g_T(t)$  can be approximated with the help of a vector diagram for  $g_T = g_s + g_n$ . This is shown in Fig. 7-22. Then, for  $A_c \gg R_n(t)$ , the composite phase angle is approximated by

$$r_0(t) = K \theta_T(t) \approx K \left\{ \theta_s(t) + \frac{R_n(t)}{A_c} \sin[\theta_n(t) - \theta_s(t)] \right\} \quad (7-108)$$

For the case of no phase modulation (the carrier signal is still present), the equation reduces to

$$r_0(t) \approx \frac{K}{A_c} y_n(t), \quad \theta_s(t) = 0 \quad (7-109)$$

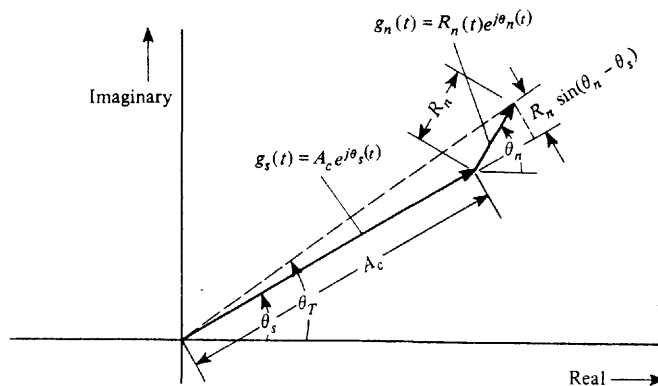


Figure 7-22 Vector diagram for angle modulation,  $(S/N)_{in} \gg 1$ .

where, using (6-127e),  $y_n(t) = R_n(t) \sin \theta_n(t)$ . This shows that the presence of an unmodulated carrier (at the input to the PM receiver) suppresses the noise on the output. This is called the *quieting effect*, and it occurs when the input signal power is above the *threshold* [i.e., when  $(S/N)_{in} \gg 1$ ]. Furthermore, when phase modulation is present and  $(S/N)_{in} \gg 1$ , we can replace  $R_n(t) \sin[\theta_n(t) - \theta_s(t)]$  by  $R_n(t) \sin \theta_n(t)$ . This can be done because  $\theta_s(t)$  can be considered to be deterministic, and, consequently,  $\theta_s(t)$  is a constant for a given value of  $t$ . Then  $\theta_n(t) - \theta_s(t)$  will be uniformly distributed over some  $2\pi$  interval since, from (6-153),  $\theta_n(t)$  is uniformly distributed over  $(0, 2\pi)$ . That is,  $\cos[\theta_n(t) - \theta_s(t)]$  will have the same PDF as  $\cos[\theta_n(t)]$  so that the replacement can be made. Thus, for large  $(S/N)_{in}$ , the relevant part of the PM detector output is approximated by

$$r_0(t) \approx s_0(t) + n_0(t) \quad (7-110)$$

where

$$s_0(t) = K\theta_s(t) = KD_p m(t) \quad (7-111a)$$

$$n_0(t) = \frac{K}{A_c} y_n(t) \quad (7-111b)$$

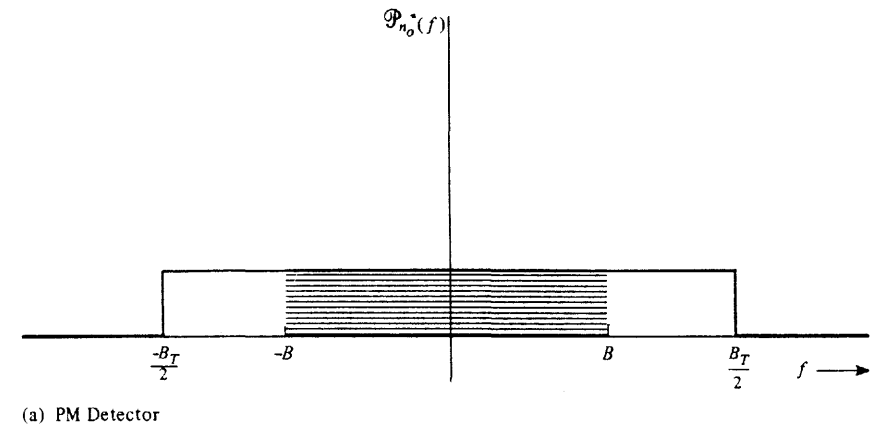
The PSD of this output noise,  $n_0(t)$ , is obtained by the use of (6-133l).

$$\mathcal{P}_{n_0}(f) = \begin{cases} \frac{K^2}{A_c^2} N_0, & |f| \leq B_T/2 \\ 0, & f \text{ otherwise} \end{cases} \quad (7-112)$$

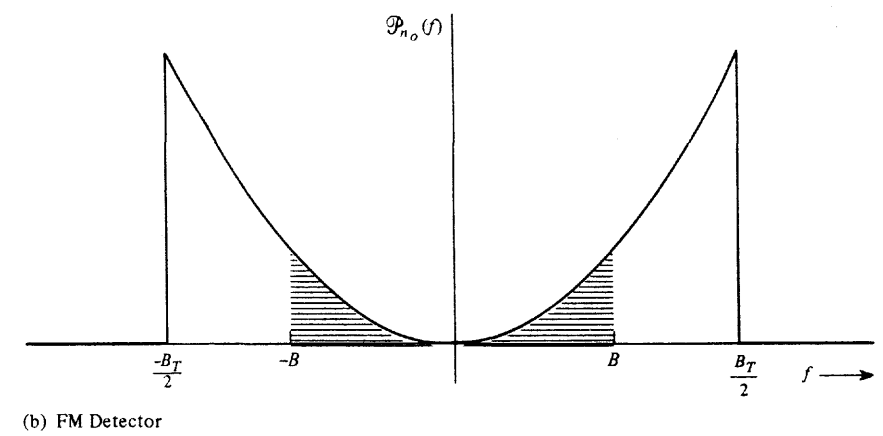
where the PSD of the bandpass input noise is  $N_0/2$  over the bandpass of the IF filter and zero outside the IF bandpass. Equation (7-112) is plotted in Fig. 7-23a, and the portion of the spectrum that is passed by the LPF is denoted by the hatched lines.

The receiver output consists of the low-pass filtered version of  $r_0(t)$ . However, the spectrum of  $s_0(t)$  is contained within the bandpass of the filter, so

$$\tilde{m}(t) = s_0(t) + \tilde{n}_0(t) \quad (7-113)$$



(a) PM Detector



(b) FM Detector

Figure 7-23 PSD for noise out of detectors for receivers of angle-modulated signals.

where  $\tilde{n}_0(t)$  is bandlimited white noise of the hatched portion of Fig. 7-23a. The noise power of the receiver is

$$\overline{[\tilde{n}_0(t)]^2} = \int_{-B}^B \mathcal{P}_{n_0}(f) df = \frac{2K^2 N_0 B}{A_c^2} \quad (7-114)$$

The output SNR is now easily evaluated with the help of (7-111a) and (7-114):

$$\left( \frac{S}{N} \right)_{out} = \frac{\overline{s_0^2}}{\overline{\tilde{n}_0^2}} = \frac{A_c^2 D_p^2 \overline{m^2}}{2N_0 B}$$

Using (5-46) and (5-47), we can write the sensitivity constant of the PM transmitter as

$$D_p = \frac{\beta_p}{V_p}$$

where  $\beta_p$  is the PM index and  $V_p$  is the peak value of  $m(t)$ . Thus the output SNR becomes

$$\left(\frac{S}{N}\right)_{\text{out}} = \frac{A_c^2 \beta_p^2 (m/V_p)^2}{2N_0 B} \quad (7-115)$$

The input SNR is

$$\left(\frac{S}{N}\right)_{\text{in}} = \frac{A_c^2/2}{2(N_0/2)B_T} = \frac{A_c^2}{2N_0 B_T} \quad (7-116)$$

where  $B_T$  is the transmission bandwidth of the PM signal (and also the IF filter bandwidth).

The transmission bandwidth of the PM signal is given by Carson's rule, (5-61),

$$B_T = 2(\beta_p + 1)B \quad (7-117)$$

where  $\beta_p$  is the PM index. The PM index is identical to the peak angle deviation of the PM signal, as indicated in (5-47). Thus

$$\left(\frac{S}{N}\right)_{\text{in}} = \frac{A_c^2}{4N_0(\beta_p + 1)B} \quad (7-118)$$

Combining (7-115) and (7-118), we obtain the ratio of output to input SNR.

$$\frac{(S/N)_{\text{out}}}{(S/N)_{\text{in}}} = 2\beta_p^2(\beta_p + 1) \overline{\left(\frac{m}{V_p}\right)^2} \quad (7-119)$$

The output SNR can also be expressed in terms of the equivalent baseband system by substituting (7-84) into (7-115), where  $P_s = A_c^2/2$ .

$$\frac{(S/N)_{\text{out}}}{(S/N)_{\text{baseband}}} = \beta_p^2 \overline{\left(\frac{m}{V_p}\right)^2} \quad (7-120)$$

This equation shows that the improvement of a PM system over a baseband signaling system depends on the amount of phase deviation that is used. It seems to indicate that we can make the improvement as large as we wish simply by increasing  $\beta_p$ . This depends on the types of circuits used. If the peak phase deviation exceeds  $\pi$  radians, special "phase unwrapping" techniques have to be used in some circuits to obtain the true value (as compared to the relative value) of the phase at the output. Thus the maximum value of  $\beta_p m(t)/V_p = D_p m(t)$  might be taken to be  $\pi$ . For sinusoidal modulation this would provide an improvement of  $D_p^2 \overline{m^2} = \pi^2/2$  or 6.9 dB over baseband signaling.

It is emphasized that the results obtained previously for  $(S/N)_{\text{out}}$  are valid only when the input signal is above the threshold [i.e.,  $(S/N)_{\text{in}} > 1$ ].

## FM Systems

The procedure that we will use to evaluate the output SNR for FM systems is essentially the same as that used for PM systems, except that the output of the FM detector is proportional to  $d\theta_T(t)/dt$ , whereas the output of the PM detector is proportional to  $\theta_T(t)$ . The detector in the angle modulated receiver of Fig. 7-21 is now an FM detector. The complex envelope of the FM signal (only) is

$$g_s(t) = A_c e^{j\theta_s(t)} \quad (7-121a)$$

where

$$\theta_s(t) = D_f \int_{-\infty}^t m(\lambda) d\lambda \quad (7-121b)$$

It is assumed that an FM signal plus white noise is present at the receiver input.

The output of the FM detector is proportional to the derivative of the composite phase at the detector input:

$$r_0(t) = \left(\frac{K}{2\pi}\right) \frac{d/g_s(t)}{dt} = \left(\frac{K}{2\pi}\right) \frac{d\theta_s(t)}{dt} \quad (7-122)$$

where  $K$  is the FM detector gain. Using the same procedure as that leading to (7-108), (7-110), and (7-111), we can approximate the detector output by

$$r_0(t) \approx s_0(t) + n_0(t) \quad (7-123)$$

where, for FM,

$$s_0(t) = \left(\frac{K}{2\pi}\right) \frac{d\theta_s(t)}{dt} = \left(\frac{KD_f}{2\pi}\right) m(t) \quad (7-124a)$$

and

$$n_0(t) = \left(\frac{K}{2\pi A_c}\right) \frac{dy_n(t)}{dt} \quad (7-124b)$$

This result is valid only when the input signal is above the threshold [i.e.,  $(S/N)_{\text{in}} \gg 1$ ]. The derivative of the noise, (7-124b), makes the PSD of the FM output noise different from that for the PM case. For FM we have

$$\mathcal{P}_{n_0}(f) = \left(\frac{K}{2\pi A_c}\right)^2 |j2\pi f|^2 \mathcal{P}_{y_n}(f)$$

or

$$\mathcal{P}_{n_0}(f) = \begin{cases} \left(\frac{K}{A_c}\right)^2 N_0 f^2, & |f| < B_T/2 \\ 0, & f \text{ otherwise} \end{cases} \quad (7-125)$$

This shows that the PSD for the noise out of the FM detector has a parabolic shape, as illustrated in Fig. 7-23b.

The receiver output consists of the low-pass filtered version of  $r_0(t)$ . The noise power for the filtered noise is

$$\overline{[\tilde{n}_0(t)]^2} = \int_{-B}^B \mathcal{P}_{n_0}(f) df = \frac{2}{3} \left( \frac{K}{A_c} \right)^2 N_0 B^3 \quad (7-126)$$

The output SNR is now easily evaluated using (7-124a) and (7-126):

$$\left( \frac{S}{N} \right)_{\text{out}} = \frac{\overline{s_0^2}}{\overline{[\tilde{n}_0]^2}} = \frac{3A_c^2 [D_f / (2\pi B)]^2 \overline{m^2}}{2N_0 B}$$

From (5-44) and (5-48), it is realized that

$$\frac{D_f}{2\pi B} = \frac{\beta_f}{V_p}$$

where  $V_p$  is the peak value of  $m(t)$ . Then the output SNR becomes

$$\left( \frac{S}{N} \right)_{\text{out}} = \frac{3A_c^2 \beta_f^2 (m/V_p)^2}{2N_0 B} \quad (7-127)$$

The input SNR is

$$\left( \frac{S}{N} \right)_{\text{in}} = \frac{A_c^2}{4N_0 (\beta_f + 1) B} \quad (7-128)$$

Combining (7-127) and (7-128), we obtain the ratio of output to input SNR,

$$\frac{(S/N)_{\text{out}}}{(S/N)_{\text{in}}} = 6\beta_f^2 (\beta_f + 1) \left( \frac{m}{V_p} \right)^2 \quad (7-129)$$

where  $\beta_f$  is the FM index and  $V_p$  is the peak value of the modulating signal  $m(t)$ .

The output SNR can be expressed in terms of the equivalent baseband SNR by substituting (7-84) into (7-127), where  $P_s = A_c^2/2$ ,

$$\frac{(S/N)_{\text{out}}}{(S/N)_{\text{baseband}}} = 3\beta_f^2 \left( \frac{m}{V_p} \right)^2 \quad (7-130)$$

For the case of sinusoidal modulation  $(m/V_p)^2 = \frac{1}{2}$ , and (7-130) becomes

$$\frac{(S/N)_{\text{out}}}{(S/N)_{\text{baseband}}} = \frac{3}{2} \beta_f^2 \quad (\text{sinusoidal modulation}) \quad (7-131)$$

At first glance, these results seem to indicate that the performance of FM systems can be increased without limit simply by increasing the FM index  $\beta_f$ . However, as  $\beta_f$  is increased, the transmission bandwidth increases, and, consequently,  $(S/N)_{\text{in}}$  decreases. These equations

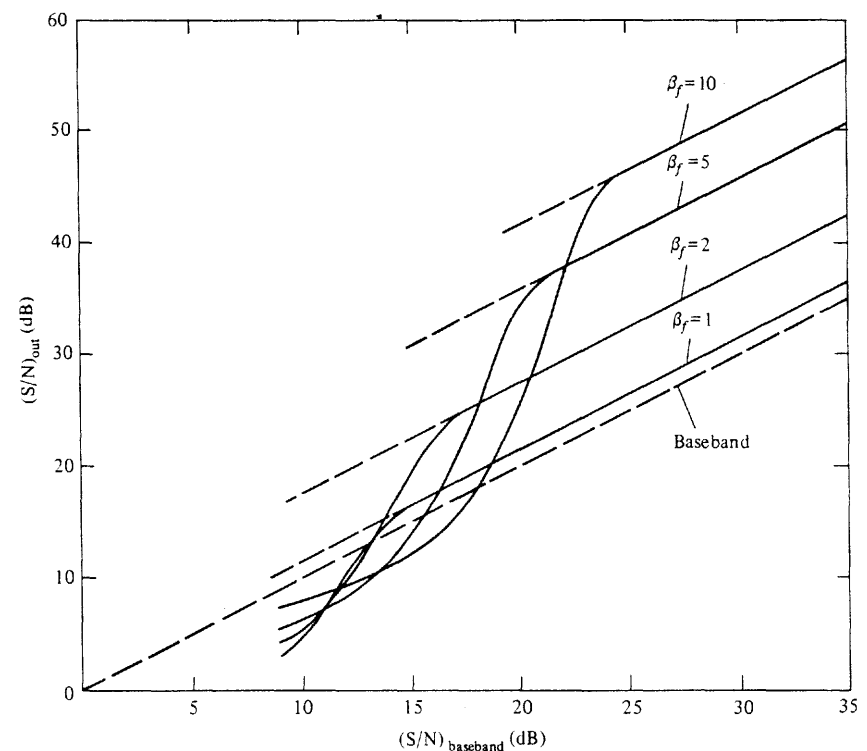


**Figure 7-24** Noise performance of an FM discriminator for a sinusoidal modulated FM signal plus Gaussian noise (no deemphasis).

for  $(S/N)_{\text{out}}$  are valid only when  $(S/N)_{\text{in}} \gg 1$  (i.e., input signal power above the threshold), so  $(S/N)_{\text{out}}$  does not increase to an excessively large value simply by increasing the FM index  $\beta_f$ . Plots of (7-131) are given by the dashed lines in Fig. 7-24.

The threshold effect was first analyzed in 1948 [Rice, 1948; Stumpers, 1948]. An excellent tutorial treatment has been given by Taub and Schilling [1986]. They have shown that (7-131) can be generalized to describe  $(S/N)_{\text{out}}$  near the threshold. For the case of sinusoidal modulation, the output SNR for a FM discriminator is shown to be

$$\left( \frac{S}{N} \right)_{\text{out}} = \frac{\frac{3}{2} \beta_f^2 (S/N)_{\text{baseband}}}{1 + \left( \frac{12}{\pi} \beta_f \right) \left( \frac{S}{N} \right)_{\text{baseband}} e^{-\left[ \frac{1}{2(\beta_f + 1)} \left( \frac{S}{N} \right)_{\text{baseband}} \right]}} \quad (7-132)$$

(No deemphasis is used in obtaining the result.) This output SNR characteristic showing the threshold effect of an FM discriminator is plotted by the solid lines in Fig. 7-24. This figure illustrates that the FM noise performance can be substantially better than baseband performance. For example, for  $\beta_f = 5$  and  $(S/N)_{\text{baseband}} = 25$  dB; the FM performance is 15.7 dB better than the baseband performance. The performance can be improved even further by the use of deemphasis, as we will demonstrate in a later section.

### FM Systems with Threshold Extension

Any one of several techniques may be used to lower the threshold below that provided by a receiver that uses only an FM discriminator. For example, a PLL FM detector could be used to extend the threshold below that provided by an FM discriminator. However, when the input SNR is large, all the FM receiving techniques provide the same performance—namely, that as predicted by (7-129) or (7-130).

An *FM receiver with feedback* (FMFB) is shown in Fig. 7-25. This is another threshold extension technique. The FMFB receiver provides threshold extension by lowering the modulation index for the FM signal that is applied to the discriminator input. That is, the modulation index of  $\tilde{e}(t)$  is smaller than that for  $v_{in}(t)$ , as we will show. Thus the threshold will be lower than that illustrated in Fig. 7-24. The calculation of the exact amount of threshold extension that is realized by an FMFB receiver is somewhat involved [Taub and Schilling, 1986]. However, we can easily show that the FMFB technique does indeed reduce the modulation index of the FM signal at the discriminator input. Referring to Fig. 7-25, we find that the FM signal at the receiver input is

$$v_{in}(t) = A_c \cos[\omega_c t + \theta_i(t)]$$

where

$$\theta_i(t) = D_f \int_{-\infty}^t m(\lambda) d\lambda$$

The output of the VCO is

$$v_0(t) = A_0 \cos[\omega_0 t + \theta_0(t)]$$

where

$$\theta_0(t) = D_v \int_{-\infty}^t \tilde{m}(\lambda) d\lambda$$

With these representations for  $v_{in}(t)$  and  $v_0(t)$ , the output of the multiplier (mixer) is

$$\begin{aligned} e(t) &= A_c A_0 \cos[\omega_c t + \theta_i(t)] \cos[\omega_0 t + \theta_0(t)] \\ &= \frac{1}{2} A_c A_0 \cos[(\omega_c - \omega_0)t + \theta_i(t) - \theta_0(t)] \\ &\quad + \frac{1}{2} A_c A_0 \cos[(\omega_c + \omega_0)t + \theta_i(t) + \theta_0(t)] \end{aligned}$$

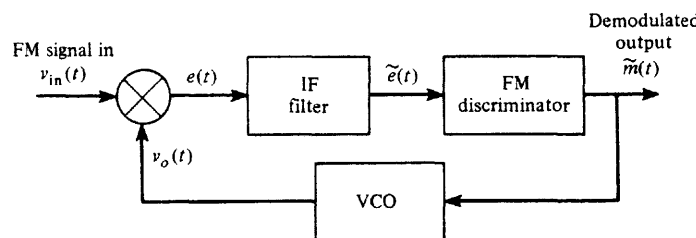


Figure 7-25 FMFB receiver.

If the IF filter is tuned to pass the band of frequencies centered about  $f_{if} \triangleq f_c - f_0$ , the IF output is

$$\tilde{e}(t) = \frac{A_c A_0}{2} \cos[\omega_{if} t + \theta_i(t) - \theta_0(t)] \quad (7-133a)$$

or

$$\tilde{e}(t) = \frac{A_c A_0}{2} \cos \left\{ \omega_{if} t + \int_{-\infty}^t [D_f m(\lambda) - D_v \tilde{m}(\lambda)] d\lambda \right\} \quad (7-133b)$$

The FM discriminator output is proportional to the derivative of the phase deviation.

$$\tilde{m}(t) = \frac{K}{2\pi} \frac{d}{dt} \left[ \int_{-\infty}^t [D_f m(\lambda) - D_v \tilde{m}(\lambda)] d\lambda \right]$$

Evaluating the derivative and solving the resulting equation for  $\tilde{m}(t)$ , we obtain

$$\tilde{m}(t) = \left( \frac{KD_f}{2\pi + KD_v} \right) m(t)$$

Substituting this expression for  $\tilde{m}(t)$  into (7-133), we get

$$\tilde{e}(t) = \frac{A_c A_0}{2} \cos \left[ \omega_{if} t + \left( \frac{1}{1 + (K/2\pi)D_v} \right) D_f \int_{-\infty}^t m(\lambda) d\lambda \right] \quad (7-134)$$

This demonstrates that the modulation index of  $\tilde{e}(t)$  is exactly  $1/[1 + (K/2\pi)D_v]$  of the modulation index of  $v_{in}(t)$ . The threshold extension provided by the FMFB receiver is on the order of 5 dB, whereas that of a PLL receiver is on the order of 3 dB (when both are compared to the threshold of an FM discriminator). Although this is not a fantastic improvement, it can be quite significant for systems that operate near the threshold, such as satellite communication systems. For example, a system that uses a threshold extension receiver instead of a conventional receiver with an FM discriminator may be much less expensive than the system that requires a doubled-size antenna to provide the 3-dB signal gain. Other threshold extension techniques have been described and analyzed in the literature [Klapper and Frankle, 1972].

### FM Systems with Deemphasis

In Chapter 5 (see Fig. 5-15) it was illustrated that the noise performance of an FM system could be improved by preemphasizing the higher frequencies of the modulation signal at the transmitter input and deemphasizing the output of the receiver. This improvement occurs because the PSD of the noise at the output of the FM detector has a parabolic shape, as shown in Fig. 7-23b.

Referring to Fig. 7-21, we incorporate deemphasis into the receiver by including a deemphasis response in the LPF characteristic. Assume that the transfer function of the LPF is

$$H(f) = \frac{1}{1 + j(f/f_1)} \quad (7-135)$$

over the low-pass bandwidth of  $B$  Hz. For standard FM broadcasting, a  $75\text{-}\mu\text{s}$  deemphasis filter is used so that  $f_1 = 1/[(2\pi)(75 \times 10^{-6})] = 2.1$  kHz. From (7-125) and (7-126), the noise power out of the receiver with deemphasis is

$$\overline{[\tilde{n}_0(t)]^2} = \int_{-B}^B |H(f)|^2 \mathcal{P}_{n_0}(f) df = \left(\frac{K}{A_c}\right)^2 N_0 \int_{-B}^B \left[ \frac{1}{1 + (f/f_1)^2} \right] f^2 df$$

or

$$\overline{[\tilde{n}_0(t)]^2} = 2 \left(\frac{K}{A_c}\right)^2 N_0 f_1^3 \left[ \frac{B}{f_1} - \tan^{-1} \left( \frac{B}{f_1} \right) \right] \quad (7-136)$$

In a typical application  $B/f_1 \gg 1$ , so  $\tan^{-1}(B/f_1) \approx \pi/2$ , which is negligible when compared to  $B/f_1$ . Thus (7-136) becomes

$$\overline{[\tilde{n}_0(t)]^2} = 2 \left(\frac{K}{A_c}\right)^2 N_0 f_1^2 B \quad (7-137)$$

for  $B/f_1 \gg 1$ .

The output signal power for the preemphasis-deemphasis system is the same as that when preemphasis-deemphasis is not used because the overall frequency response of the system to  $m(t)$  is flat (constant) over the bandwidth of  $B$  Hz.<sup>†</sup> Thus from (7-137) and (7-124a), the output SNR is

$$\left(\frac{S}{N}\right)_{\text{out}} = \frac{\overline{s_0^2}}{\overline{\tilde{n}_0^2}} = \frac{A_c^2 [D_f/(2\pi f_1)]^2 \overline{m^2}}{2N_0 B}$$

In addition,  $D_f/(2\pi B) = \beta_f/V_p$ , so the output SNR reduces to

$$\left(\frac{S}{N}\right)_{\text{out}} = \frac{A_c^2 \beta_f^2 (B/f_1)^2 (\overline{m/V_p})^2}{2N_0 B} \quad (7-138)$$

<sup>†</sup> For a fair comparison of FM systems with and without preemphasis, the peak deviation  $\Delta F$  needs to be the same for both cases. With typical audio program signals, preemphasis does not increase  $\Delta F$  appreciably because the low frequencies dominate in the spectrum of  $m(t)$ . Thus this analysis is valid. However, if  $m(t)$  is assumed to have a flat spectrum over the audio passband, the gain of the preemphasis filter needs to be reduced so that the peak deviation will be the same with and without preemphasis. In the latter case, there is less improvement in performance when preemphasis is used.

Using (7-128), we find that the output to input SNR is

$$\frac{(S/N)_{\text{out}}}{(S/N)_{\text{in}}} = 2 \beta_f^2 (\beta_f + 1) \left(\frac{B}{f_1}\right)^2 \left(\frac{m}{V_p}\right)^2 \quad (7-139)$$

where  $\beta_f$  is the FM index,  $B$  is the bandwidth of the baseband (modulation) circuits,  $f_1$  is the 3-dB bandwidth of the deemphasis filter,  $V_p$  is the peak value of the modulating signal  $m(t)$ , and  $(m/V_p)^2$  is the square of the rms value of  $m(t)/V_p$ .

The output SNR is expressed in terms of the equivalent baseband SNR by substituting (7-84) into (7-138).

$$\frac{(S/N)_{\text{out}}}{(S/N)_{\text{baseband}}} = \beta_f^2 \left(\frac{B}{f_1}\right)^2 \left(\frac{m}{V_p}\right)^2 \quad (7-140)$$

When a sinusoidal test tone is transmitted over this FM system,  $(m/V_p)^2 = \frac{1}{2}$  and (7-140) becomes

$$\frac{(S/N)_{\text{out}}}{(S/N)_{\text{baseband}}} = \frac{1}{2} \beta_f^2 \left(\frac{B}{f_1}\right)^2 \text{ (sinusoidal modulation)} \quad (7-141)$$

Of course, all of these results are valid only when the FM signal at the receiver input is above the threshold.

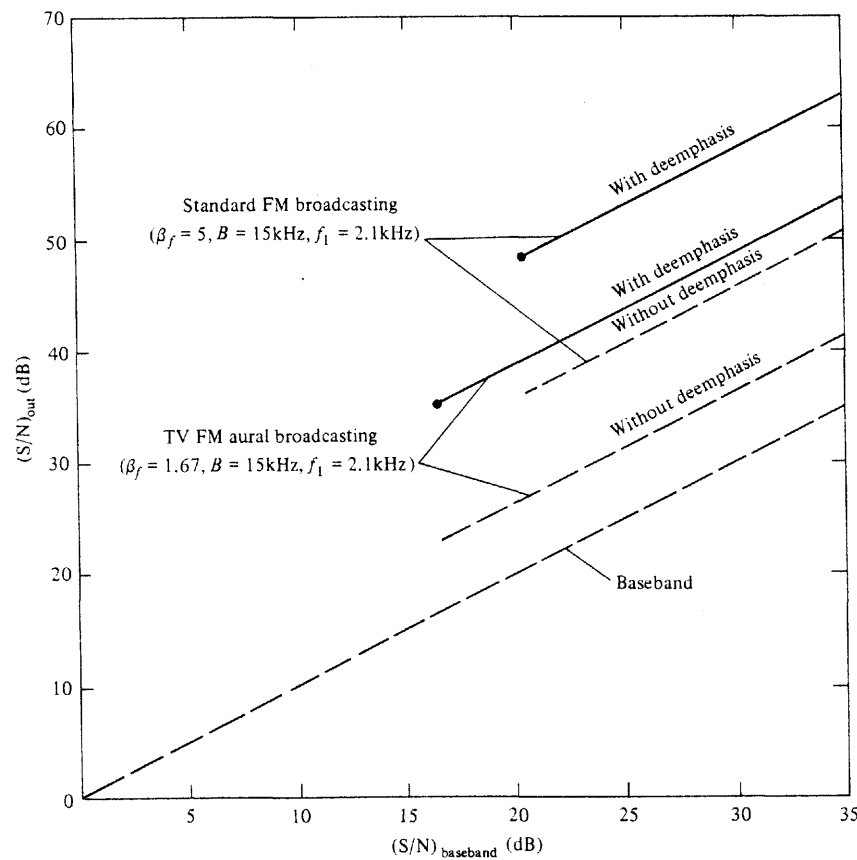
It is interesting to compare the noise performance of commercial FM systems. As shown in Table 5-4, for standard FM broadcasting  $\beta_f = 5$ ,  $B = 15$  kHz, and  $f_1 = 2.1$  kHz. Using these parameters in (7-141), we obtain the noise performance of an FM broadcasting system, as shown in Fig. 7-26 by a solid curve. The corresponding performance of the same system, but without preemphasis-deemphasis, is shown by a dashed curve [from (7-131)]. Similarly, results are shown for the performance of the TV FM aural transmission system where  $\beta_f = 1.67$ ,  $B = 15$  kHz, and  $f_1 = 2.1$  kHz.

Figure 7-26 also illustrates that the FM noise performance with deemphasis can be substantially better than that of FM without deemphasis. For example, for standard FM broadcasting ( $\beta_f = 5$ ,  $B = 15$  kHz, and  $f_1 = 2.1$  kHz) with  $(S/N)_{\text{baseband}} = 25$  dB, the FM performance is superior by 13.3 dB.

## 7-9 COMPARISON OF ANALOG SIGNALING SYSTEMS

Table 7-2 compares the analog systems that were analyzed in the previous sections. It is seen that the nonlinear modulation systems provide significant improvement in the noise performance, *provided* that the input signal is above the threshold. Of course, the improvement in the noise performance is obtained at the expense of having to use a wider transmission bandwidth. If the input SNR is very low, the linear systems outperform the nonlinear systems. SSB is best in terms of small bandwidth, and it has one of the best noise characteristics at low input SNR.

The selection of a particular system depends on the transmission bandwidth that is allowed and the available receiver input SNR. A comparison of the noise performance of these



**Figure 7-26** Noise performance of standard FM systems for sinusoidal modulation.

systems is given in Fig. 7-27, assuming that  $V_p = 1$ ,  $\overline{m^2} = \frac{1}{2}$  for the AM, PM, and FM systems. For the nonlinear systems a bandwidth spreading ratio of  $B_T/B = 12$  is chosen for system comparisons. This corresponds to a  $B_f = 5$  for the FM systems cited in the figure (which corresponds to commercial FM broadcasting).

Note that, except for the “wasted” carrier power in AM, all of the linear modulation methods have the same SNR performance as that for the baseband system. (SSB has the same performance as DSB because the coherence of the two sidebands in DSB compensates for the half noise power in SSB due to bandwidth reduction.) These comparisons are made on the basis of signals with equal *average* powers. If comparisons are made on equal *peak* powers (i.e., equal peak values for the signals), then SSB has a  $(S/N)_{out}$  that is 3 dB better than DSB and 9 dB better than AM with 100% modulation (as demonstrated by Prob. 7-34). Of course, when operating above threshold, all of the nonlinear modulation systems have better SNR performance than linear modulation systems because the nonlinear systems have larger transmission bandwidths.

**TABLE 7-2 COMPARISON OF ANALOG SIGNALING TECHNIQUES<sup>a</sup>**

Type	Linearity	Transmission Bandwidth Required <sup>b</sup>	$\frac{(S/N)_{out}}{(S/N)_{baseband}}$	Comments
Baseband	L	$B$	1	(7-84)
AM	L <sup>c</sup>	$2B$	$\frac{\overline{m^2}}{1 + \overline{m^2}}$	(7-90) Valid for all $(S/N)_{in}$ with coherent detection; valid above threshold for envelope detection and $ m(t)  \leq 1$
DSB-SC SSB	L	$2B$	1	(7-98) (7-105) Coherent detection required; performance identical to baseband system
PM		$2(\beta_p + 1)B$	$\beta_p^2 \left( \frac{m}{V_p} \right)^2$	(7-120) Coherent detection required; valid for $(S/N)_{in}$ above threshold
FM	NL	$2(\beta_f + 1)B$	$3\beta_f^2 \left( \frac{m}{V_p} \right)^2$	(7-130) Valid for $(S/N)_{in}$ above threshold
FM with deemphasis	NL	$2(\beta_f + 1)B$	$\beta_f^2 \left( \frac{B}{f_1} \right)^2 \left( \frac{m}{V_p} \right)^2$	(7-140) Valid for $(S/N)_{in}$ above threshold
PCM	NL	d	$M^2 / (S/N)_{baseband}$	(7-82) Valid for $(S/N)_{in}$ above threshold (i.e., $P_e \rightarrow 0$ )

<sup>a</sup>  $B$ , absolute bandwidth of the modulating signal;  $f_1$ , 3-dB bandwidth of the deemphasis filter; L, linear; m, m = m(t) is the modulating signal; M = 2<sup>n</sup>, number of quantizing steps where n is the number of bits in the PCM word; NL, nonlinear; V<sub>p</sub>, peak value of m(t); β<sub>p</sub>, PM index; β<sub>f</sub>, FM index.

<sup>b</sup> Typical bandwidth specifications by ITU are larger than these minimal [Jordan, 1985].

<sup>c</sup> In the strict sense, AM signaling is not linear because of the carrier term (see Table 4-1).

<sup>d</sup> The bandwidth depends on the type of digital system used (e.g., OOK, FSK).

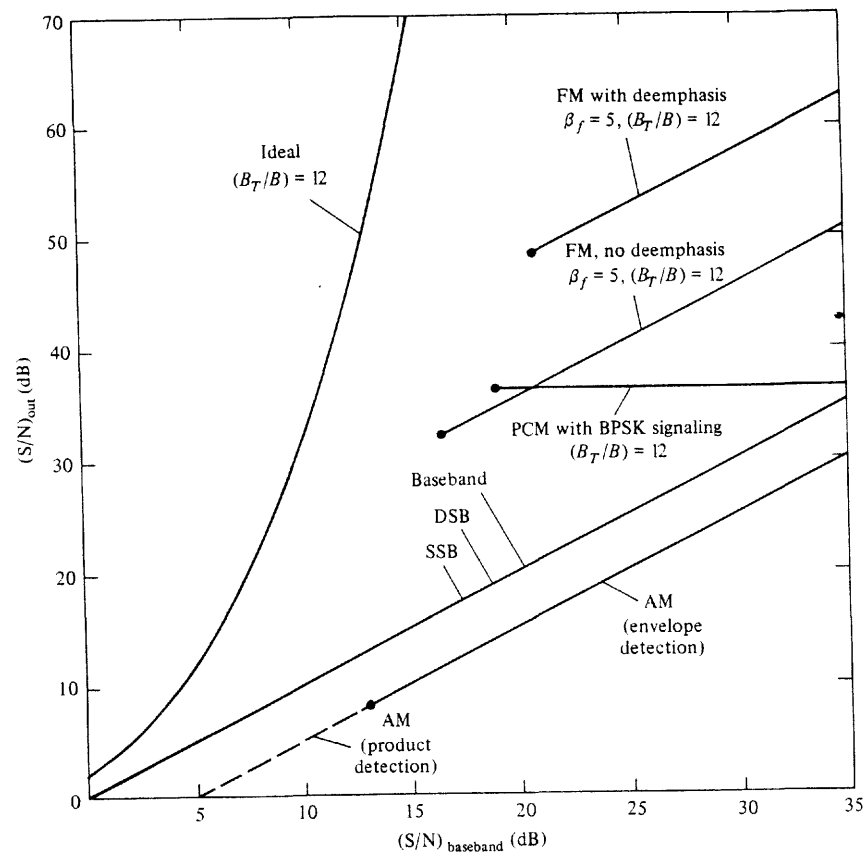


Figure 7-27 Comparison of the noise performance of analog systems.

### Ideal System Performance

It is interesting to ask the question: What is the best noise performance that is theoretically possible? Here a wide transmission bandwidth would be used to gain improved noise performance. The answer is given by Shannon's channel capacity theorem. The *ideal system* is defined as one that does not lose channel capacity in the detection process. Thus

$$C_{\text{in}} = C_{\text{out}} \quad (7-142)$$

where  $C_{\text{in}}$  is the bandpass channel capacity and  $C_{\text{out}}$  is the channel capacity after detection. Using (1-10) in (7-142), we have

$$B_T \log_2 [1 + (\text{S}/\text{N})_{\text{in}}] = B \log_2 [1 + (\text{S}/\text{N})_{\text{out}}} \quad (7-143)$$

where  $B_T$  is the transmission bandwidth of the bandpass signal at the receiver input and  $B$  is the bandwidth of the baseband signal at the receiver output. Solving for  $(\text{S}/\text{N})_{\text{out}}$ , we have

$$\left(\frac{\text{S}}{\text{N}}\right)_{\text{out}} = \left[1 + \left(\frac{\text{S}}{\text{N}}\right)_{\text{in}}\right]^{B_T/B} - 1 \quad (7-144)$$

But

$$\left(\frac{\text{S}}{\text{N}}\right)_{\text{in}} = \frac{P_s}{N_0 B_T} = \left(\frac{P_s}{N_0 B}\right) \left(\frac{B}{B_T}\right) = \left(\frac{B}{B_T}\right) \left(\frac{\text{S}}{\text{N}}\right)_{\text{baseband}} \quad (7-145)$$

where (7-84) was used. Thus (7-144) becomes

$$\left(\frac{\text{S}}{\text{N}}\right)_{\text{out}} = \left[1 + \left(\frac{B}{B_T}\right) \left(\frac{\text{S}}{\text{N}}\right)_{\text{baseband}}\right]^{B_T/B} - 1 \quad (7-146)$$

Equation (7-146), which describes the ideal system performance, is plotted in Fig. 7-27 for the case of  $B_T/B = 12$ . As expected, none of the practical signaling systems equals the performance of the ideal system. However, some of the nonlinear systems (near threshold) approach the performance of the ideal system.

### 7-10 SUMMARY

The performance of digital systems has already been summarized in Sec. 7-6, and the performance of analog systems has been summarized in Sec. 7-9. The reader is invited to review these sections for a summary of this chapter. However, to condense these sections, we will simply state that there is no "best system" that provides a universal solution to all problems. The solution depends on the noise performance required, the transmission bandwidth available, and the state of the art in electronics that might favor the use of one type of communication system over another. In addition, the performance has been evaluated for the case of an additive white Gaussian noise channel. For other types of noise distributions or for multiplicative noise, the results would be different.

### 7-11 STUDY-AID EXAMPLES



**SA7-1** Referring to Section 7-2 and parts (a) and (b) of Fig. 7-4, let a unipolar signal plus white Gaussian noise be the input to a receiver that uses a low-pass filter (LPF). Using the assumptions leading up to (7-24a), it is shown that the BER for the data out of a receiver that

uses a LPF (not the optimum matched filter) is approximately  $P_e = Q\left(\sqrt{\frac{A^2}{4N_0 B}}\right)$ , where  $A$  is

the peak value of the input unipolar signal,  $N_0/2$  is the PSD of the noise, and  $B$  is the equivalent bandwidth of the LPF. In obtaining this result, it is argued that the sample value for a filtered binary 1 signal,  $s_{01}(t_0)$ , is approximately  $A$ , provided that the equivalent bandwidth of the LPF is  $B > 2/T$ , where  $T$  is the width of the transmitted rectangular pulse when a binary 1 is sent.  $R = 1/T$  is the data rate. If the receiver uses an ideal LPF (i.e., a brickwall LPF) with

$$H(f) = \Pi\left(\frac{f}{2B}\right) \quad (7-147)$$

show that the approximation  $s_{01}(t_0) \approx A$  is valid for  $B \geq 2/T$ .

**Solution** The MATLAB solution is shown by the plots in Fig. 7-28. Fig. 7-28a shows the unfiltered rectangular pulse of amplitude  $A = 1$  and width  $T = 1$ . Fig. 7-28b, Fig. 7-28c, and Fig. 7-28d show the filtered pulse when the bandwidth of the brickwall LPF is  $B = 1/T$ ,  $B = 2/T$  or  $B = 3/T$ , respectively. For  $B \geq 2/T$ , it is seen that the sample value is approximately  $A$ , where  $A = 1$ , when the sample is taken near the middle of the bit interval. Also, note that there is negligible ISI provided that  $B \geq 2/T$ . Furthermore, as shown in Fig. 7-28b for  $B = 1/T$ , it is seen that  $s_{01}(t_0) \approx 1.2 \cdot 1 = 1.2A$ . Consequently, it is tempting to use  $s_{01}(t_0) \approx 1.2A$  (which will give a lower BER) in the formula for the BER and specify the filter equivalent bandwidth to be exactly  $B = 1/T$ . However, if this is done, the BER formula would not be correct for the cases when  $B > 1/T$ . In addition (as shown in SA7-2), if a RC LPF is used (instead of a brickwall LPF, which is impractical to build), we do not get  $s_{01}(t_0) = 1.2A$  for  $B = 1/T$ . That is, if  $s_{01}(t_0) = 1.2A$  is used to obtain the BER formula, the formula would not be valid for the RC LPF. Consequently, (7-24a), which assumes  $s_{01}(t_0) \approx A$  for  $B \geq 2/T$ , is approximately correct for all types of practical LPFs that might be used. Furthermore, if  $s_{01}(t_0)$  is not equal to  $A$  for a particular filter, then just replace  $A$  in (7-24a) by the correct sample value for that filter, and the exact (i.e., no approximation) result will be obtained.

**SA7-2** Rework SA7-1 for the case when the LPF is a RC filter with

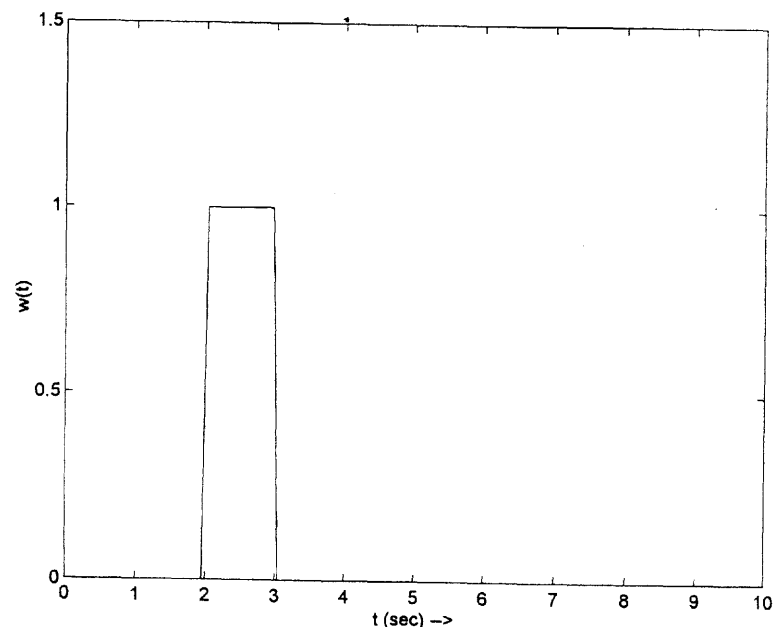
$$H(f) = \frac{1}{1 + j\left(\frac{f}{B_{3dB}}\right)} \quad (7-148)$$

where  $B_{3dB} = 1/(2\pi RC)$ . Note, using (6-104), the equivalent bandwidth of the RC LPF is  $B = (\pi/2)B_{3dB}$ .

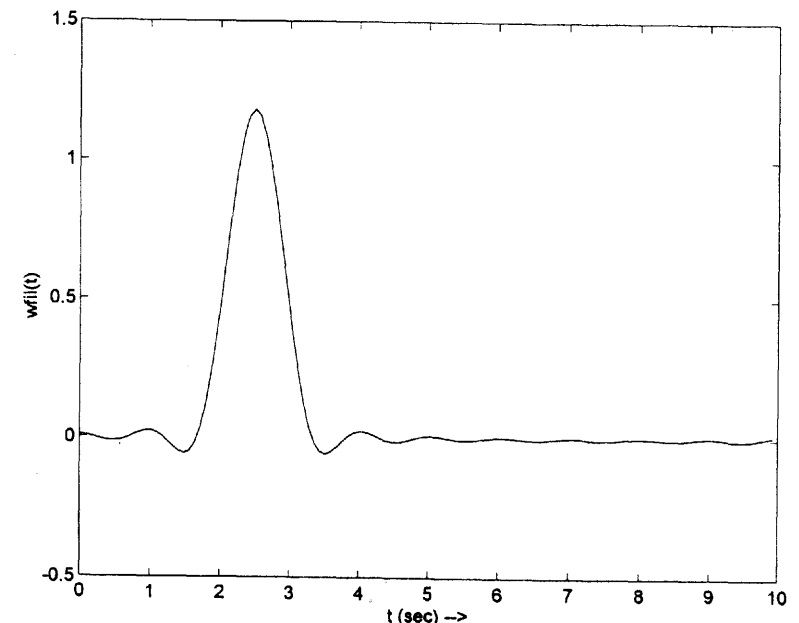
**Solution** The MATLAB solution is shown by the plots in Fig. 7-29. Fig. 7-29a shows the unfiltered rectangular pulse of amplitude  $A = 1$  and width  $T = 1$ . Fig. 7-29b, Fig. 7-29c and Fig. 7-29d show the filtered pulse when the equivalent bandwidth of the RC LPF is  $B = 1/T$ ,  $B = 2/T$ , or  $B = 3/T$ , respectively. For  $B = 1/T$ ,  $s_{01}(t_0) = 1 = A$  only if the sampling time,  $t_0$ , can be set near the end of the pulse precisely at the point where the filtered pulse is a maximum. This requires the use of an accurate bit synchronizer. For  $B \geq 2/T$  it is seen that  $s_{01}(t_0) = 1 = A$  and the sampling time,  $t_0$ , is not too critical because the filtered pulse is flat (with a value of  $A$ ) over a significant portion of the bit (pulse) interval. Also, the ISI is negligible when  $B \geq 2/T$ ; that is, the solution to homework Problem 7-7d demonstrates that the worst case signal to ISI ratio is about 70 dB. Consequently, (7-24a), which assumes  $s_{01}(t_0) \approx A$  is approximately correct for  $B \geq 1/T$  if the correct sampling time can be maintained precisely.

**SA7-3** Compare the performance of a digital receiver that uses a RC LPF with the performance of a receiver that uses a matched filter (MF). Referring to Fig. 7-4a, let the input to the receiver be a unipolar signal plus white Gaussian noise. Assume that the unipolar signal has a data rate of  $R = 9600$  bits/s and a peak value of  $A = 5$ . The noise has a PSD of  $\mathcal{P}_n(f) = 3 \times 10^{-5}$ .

(a) If the receiver filter is a RC LPF with an equivalent bandwidth of  $B = 2/T = 2R$ , evaluate the SNR at the RC filter input where the bandwidth of the noise is taken to be the



(a) Unfiltered Pulse with Amplitude  $A = 1$  and Pulse Width  $T = 1$



(b) Filtered Pulse with Equivalent Bandwidth  $B = 1/T = 1$  Hz

**Figure 7-28** Solution for SA7-1 showing the effect of brickwall low-pass filtering.

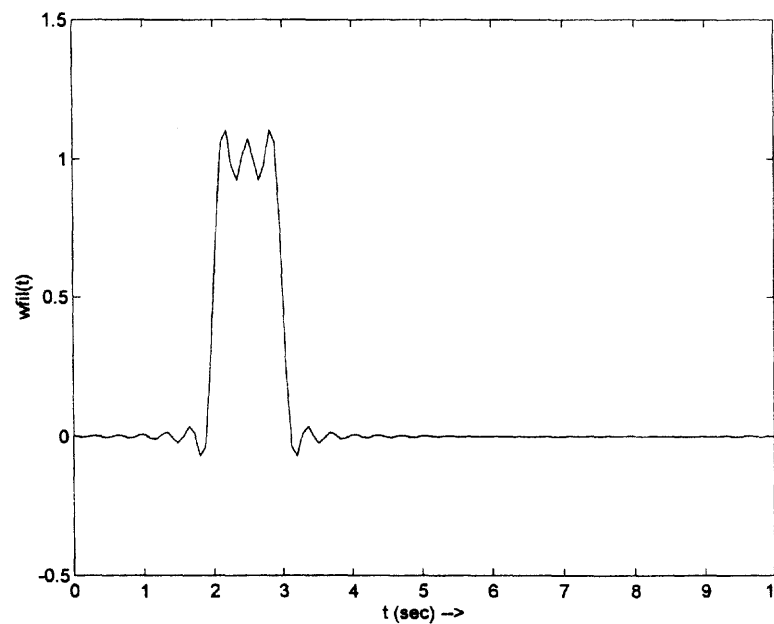
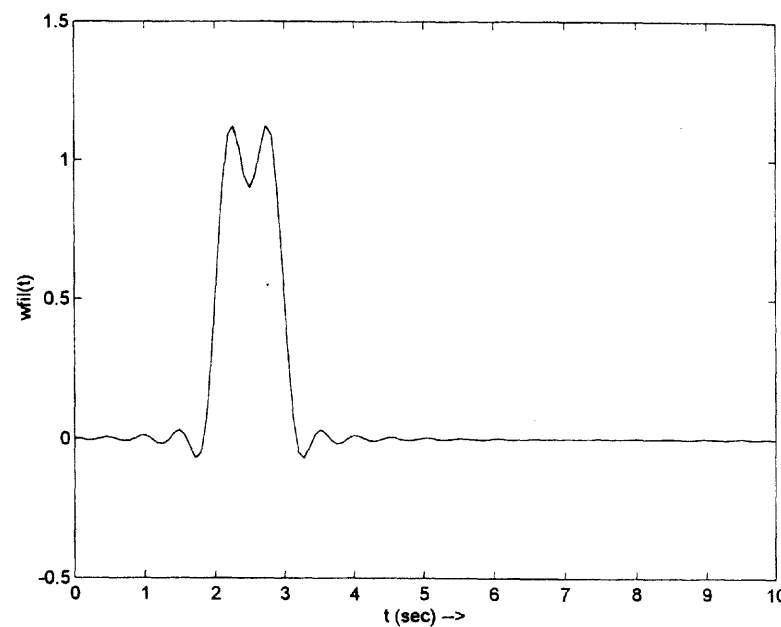


Figure 7-28 (continued)

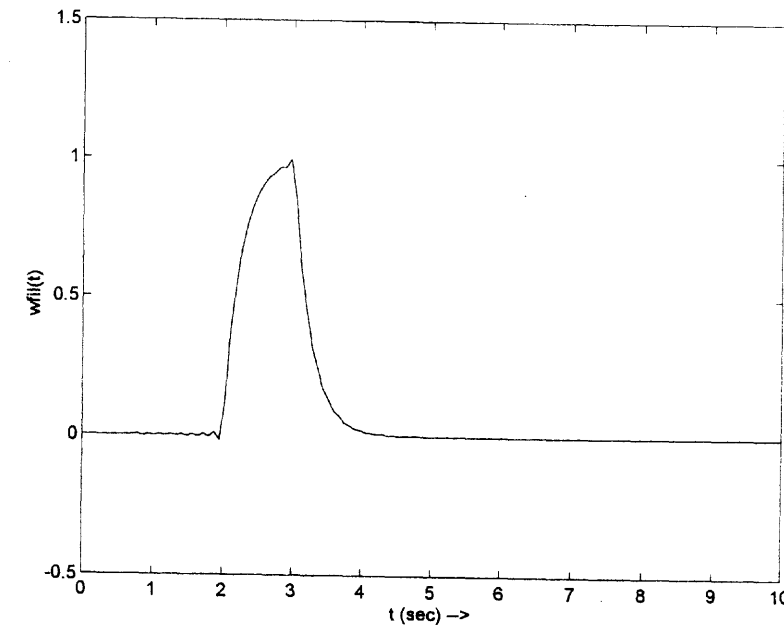
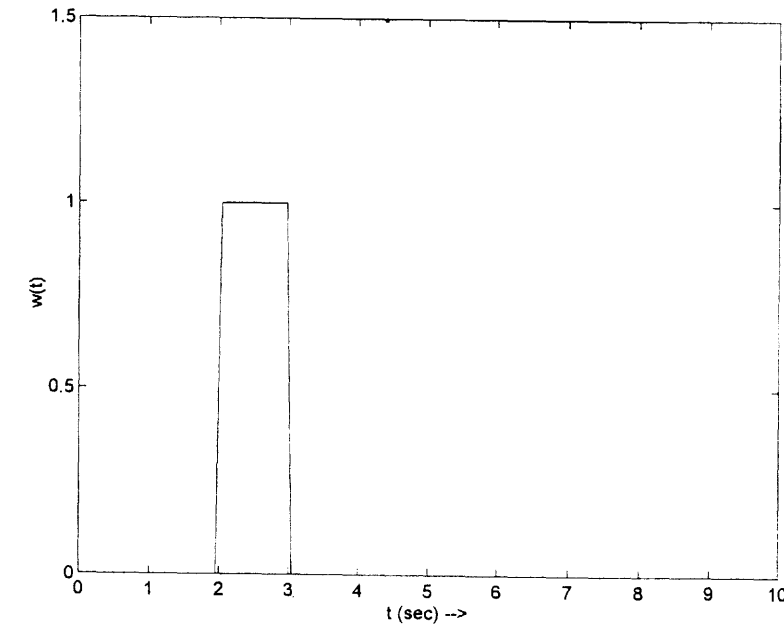


Figure 7-29 Solution for SA7-2 showing the effect of RC low-pass filtering.

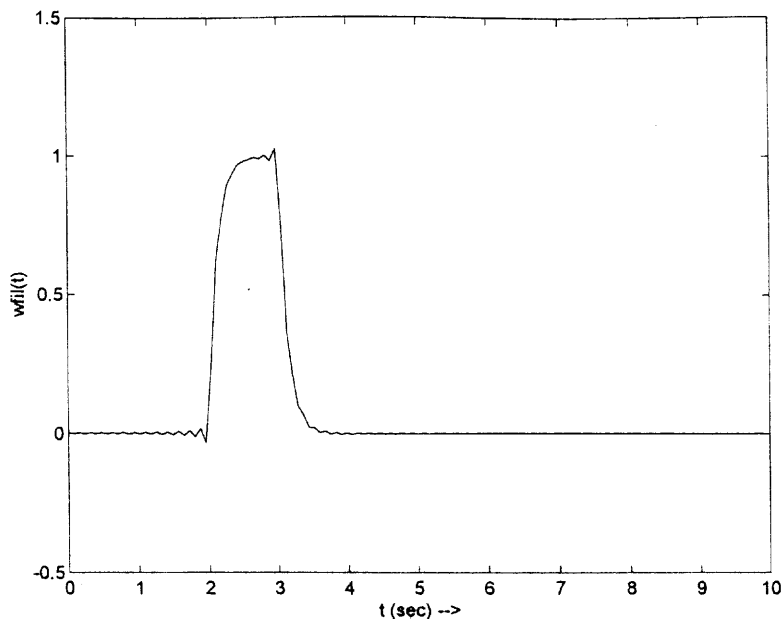
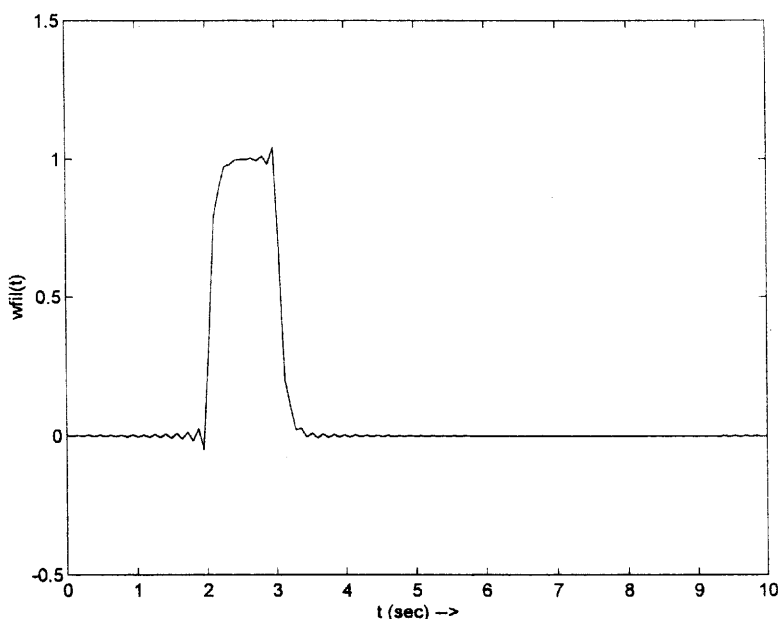
(c) Filtered Pulse with Equivalent Bandwidth  $B = 2/T = 2$  Hz(d) Filtered Pulse with Equivalent Bandwidth  $B = 3/T = 3$  Hz

Figure 7-29 (continued)

equivalent bandwidth of the RC LPF. Also, evaluate the BER for the data at the receiver output.

- (b) Repeat (a) for the case of  $B = 1/T = R$ .
- (c) If the receiver filter is a MF, evaluate the SNR at the MF input where the bandwidth of the noise is the equivalent bandwidth of the MF. Also, evaluate the BER for the data at the receiver output.
- (d) Compare the BER performance of the receiver that uses the RC LPF with the performance of the MF receiver.

**Solution** The average energy per bit for the signal at the receiver input is  $E_b = (A^2/2)T = A^2/(2R)$ .  $\mathcal{P}_n(f) = N_0/2 = 3 \times 10^{-5}$  so  $N_0 = 6 \times 10^{-5}$ . Thus,

$$\left(\frac{E_b}{N_0}\right)_{\text{dB}} = 10 \log\left(\frac{A^2}{2N_0R}\right) = 10 \log\left(\frac{(5)^2}{2(6 \times 10^{-5})(9600)}\right) = 13.4 \text{ dB} \quad (7-149)$$

- (a) For a receiver that uses a RC LPF with  $B = 2/T = 2R$ , the noise power in the bandwidth  $B$  is  $P_n = (N_0/2)(2B)$ . The rms signal or noise voltage is related to its average power by  $V_{\text{rms}}^2 = \langle v^2(t) \rangle = P$ . Because the average input signal power is  $P_s = A^2/2$ , the rms signal voltage at the receiver input is

$$V_s = \sqrt{A^2/2} = A/\sqrt{2} = 5/\sqrt{2} = 3.54 \text{ V rms signal}$$

The rms noise voltage (measured in a bandwidth of  $2R$ ) at the receiver input is

$$V_n = \sqrt{\frac{N_0}{2}(2B)} = \sqrt{2N_0R} = \sqrt{2(6 \times 10^{-5})(9600)} = 1.07 \text{ V rms noise}$$

Thus, the input SNR is

$$\left(\frac{S}{N}\right)_{\text{dB}} = 20 \log\left(\frac{V_s}{V_n}\right) = 20 \log\left(\frac{3.54}{1.07}\right) = 10.4 \text{ dB}$$

Also, the SNR can be evaluated by using

$$\left(\frac{S}{N}\right)_{\text{dB}} = 10 \log\left(\frac{P_s}{P_n}\right) = 10 \log\left(\frac{A^2}{2N_0B}\right) \quad (7-150)$$

which, for  $B = 2/T = 2R$ , becomes

$$\left(\frac{S}{N}\right)_{\text{dB}} = 10 \log\left(\frac{A^2}{4N_0R}\right) = 10.4 \text{ dB}$$

The BER is obtained by use of (7-24a) for the case of a RC LPF, where  $s_{01}(t_0) \approx A$  and  $B = 2/T = 2R$ . We get

$$P_e = Q\left(\sqrt{\frac{A^2}{8N_0R}}\right) = Q\left(\sqrt{\frac{(5)^2}{8(6 \times 10^{-5})(9600)}}\right) = 9.9 \times 10^{-3}$$

- (b) For a receiver that uses a RC LPF with  $B = 1/T = R$ , the rms noise voltage (measured in a bandwidth of  $R$ ) at the receiver input is

$$V_n = \sqrt{\frac{N_0}{2} (2B)} = \sqrt{N_0 R} = \sqrt{(6 \times 10^{-5}) (9600)} = 0.76 \text{ V rms noise}$$

Thus, the input SNR is

$$\left(\frac{S}{N}\right)_{\text{dB}} = 20 \log\left(\frac{V_s}{V_n}\right) = 20 \log\left(\frac{3.54}{0.54}\right) = 13.4 \text{ dB}$$

Also, using (7-150) with  $B = R$ , we get

$$\left(\frac{S}{N}\right)_{\text{dB}} = 10 \log\left(\frac{A^2}{2N_0 R}\right) = 13.4 \text{ dB}$$

The BER is obtained by the use of (7-24a) with  $B = 1/T = R$ . We get

$$P_e = Q\left(\sqrt{\frac{A^2}{4N_0 R}}\right) = Q\left(\sqrt{\frac{(5)^2}{4(6 \times 10^{-5}) (9600)}}\right) = 4.9 \times 10^{-4}$$

(c) To obtain the SNR for the MF receiver, we need to first evaluate the equivalent bandwidth of the MF. Using (6-155), the transfer function for the MF that is matched to the rectangular pulse  $s(t) = 5\Pi(t/T)$  is

$$H(f) = K \frac{S^*(f)}{\mathcal{P}_n(f)} e^{-j\omega t_0} = CT \left(\frac{\sin \pi T f}{\pi T f}\right) e^{-j\omega t_0}$$

where  $C = 5K/(N_0/2)$ . Using (2-192), the equivalent bandwidth of the MF is

$$B = \frac{1}{|H(0)|^2} \int_{-\infty}^{\infty} |H(f)|^2 df = \int_0^{\infty} \left(\frac{\sin \pi T f}{\pi T f}\right)^2 df$$

To evaluate this integral, make a change in variable. Let  $x = \pi T f$  so that with the aid of (A-83), we get

$$B = \frac{1}{\pi T} \int_0^{\infty} \left(\frac{\sin x}{x}\right) dx = \left(\frac{1}{\pi T}\right)\left(\frac{\pi}{2}\right) = \frac{1}{2T} = \frac{1}{2} R \quad (7-151)$$

Thus, the rms noise voltage (measured in a bandwidth of  $B = R/2$ ) at the receiver input is

$$V_n = \sqrt{\frac{N_0}{2} (2B)} = \sqrt{N_0 R/2} = \sqrt{(6 \times 10^{-5}) (9600)/2} = 0.54 \text{ V rms noise}$$

As obtained previously, the rms signal voltage is  $V_s = 3.54 \text{ V}$ . Then, the input SNR is

$$\left(\frac{S}{N}\right)_{\text{dB}} = 20 \log\left(\frac{V_s}{V_n}\right) = 20 \log\left(\frac{3.54}{0.54}\right) = 16.4 \text{ dB}$$

Also, using (7-150) with  $B = R/2$  we get

$$\left(\frac{S}{N}\right)_{\text{dB}} = 10 \log\left(\frac{A^2}{N_0 R}\right) = 16.4 \text{ dB}$$

The BER is obtained by using (7-24b).

$$\begin{aligned} P_e &= Q\left(\sqrt{\frac{E_b}{N_0}}\right) = Q\left(\sqrt{\frac{A^2 T}{2N_0}}\right) = Q\left(\sqrt{\frac{A^2}{2N_0 R}}\right) \\ &= Q\left(\sqrt{\frac{(5)^2}{2(6 \times 10^{-5}) (9600)}}\right) = 1.6 \times 10^{-6} \end{aligned}$$

This result may be verified by using Fig. 7-14 for the case of unipolar signaling with  $(E_b/N_0)_{\text{dB}} = 13.4 \text{ dB}$ .

(d) As discussed in the solution for SA7-2, if an inexpensive RC LPF is used with  $B = 2R$ , then an inexpensive bit synchronizer (with imprecise sampling times) is adequate for use in the receiver. As found in (a), this gives a BER of  $9.9 \times 10^{-3}$ .

If better performance (i.e., lower BER) is desired, the bandwidth of the LPF can be reduced to  $B = R$ , and a precise (more expensive) bit synchronizer is required. This lowers the BER to  $4.9 \times 10^{-4}$ , as found in part (b).

If even better performance is desired a MF (more expensive than a LPF) can be used. This is implemented by using an integrate and dump filter as shown previously in Fig. 6-17. This MF requires a precise bit synchronizer to provide the clocking signals which reset the integrator and dump the sampler. This MF receiver gives the optimum (lowest BER) performance. In this case, the BER is reduced to  $1.6 \times 10^{-6}$  as found in part (c). However, it is realized that in some applications, such as some fiber optic systems, the noise is negligible. In this case the simple LPF of part (a) with  $B = 2/T = 2R$  is adequate because the BER will be approach zero.

**SA7-4** In FM signaling systems preemphasis of the modulation at the transmitter input and deemphasis at the receiver output is often used to improve the output SNR. For  $75 \mu\text{s}$  emphasis, the 3-dB corner frequency of the receiver deemphasis LPF is  $f_1 = 1/(2\pi 75\mu\text{s}) = 2.12 \text{ kHz}$ . The audio bandwidth is  $B = 15 \text{ kHz}$ . Derive a formula for the improvement in dB,  $I_{\text{dB}}$ , for the SNR of a FM system with preemphasis-deemphasis when compared with the SNR for a FM system without preemphasis-deemphasis. Compute  $I_{\text{dB}}$  for  $f_1 = 2.12 \text{ kHz}$  and  $B = 15 \text{ kHz}$ .

**Solution** Refer to (7-121) through (7-127) for development of the  $(S/N)_{\text{out}}$  equation for FM with no deemphasis and to (7-135) through (7-138) for the development of the  $(S/N)_{\text{out}}$  equation for FM with deemphasis. Then,

$$I = \frac{(S/N)_{\text{with deemphasis}}}{(S/N)_{\text{no deemphasis}}} = \frac{\left(\frac{s_0^2}{n_0^2}\right)_{\text{with deemphasis}}}{\left(\frac{s_0^2}{n_0^2}\right)_{\text{no deemphasis}}} \quad (7-152)$$

From Sec. 5-6 and Fig. 5-15, it is seen that the inclusion of two filters—a deemphasis filter at the receiver,  $H_d(f)$ , and a preemphasis filter at the transmitter,  $H_p(f)$ —has no overall effect on the frequency response (and power) of the output audio signal,  $s_0(t)$ , because  $H_p(f)H_d(f) = 1$  over the audio bandwidth,  $B$ , where  $B < f_2$ . Thus,  $(\frac{s_0^2}{n_0^2})_{\text{with deemphasis}} = (\frac{s_0^2}{n_0^2})_{\text{no deemphasis}}$  and (7-152) reduces to

$$I = \frac{\left(\frac{n_0^2}{n_0^2}\right)_{\text{no deemphasis}}}{\left(\frac{n_0^2}{n_0^2}\right)_{\text{with deemphasis}}} \quad (7-153)$$

The output noise is different for the receiver with deemphasis (compared with a receiver without deemphasis) because the deemphasis filter attenuates the noise at the higher audio frequencies. (The transmitter preemphasis filter has no effect on the received noise.) Using (7-126) for  $(n_0^*)_{\text{no deemphasis}}$  and (7-136) for  $(n_0^*)_{\text{with deemphasis}}$ , (7-153) becomes

$$I = \frac{\frac{2}{3} \left( \frac{K}{A_c} \right)^2 N_0 B^3}{2 \left( \frac{K}{A_c} \right)^2 N_0 f_1^3 \left[ \frac{B}{f_1} - \tan^{-1} \left( \frac{B}{f_1} \right) \right]}$$

or

$$I = \frac{B^3}{3 f_1^3 \left[ \frac{B}{f_1} - \tan^{-1} \left( \frac{B}{f_1} \right) \right]} \quad (7-154)$$

Because  $I_{\text{dB}} = 10 \log(I)$ , we get

$$I_{\text{dB}} = 30 \log \left( \frac{B}{f_1} \right) - 10 \log \left[ 3 \left[ \frac{B}{f_1} - \tan^{-1} \left( \frac{B}{f_1} \right) \right] \right] \quad (7-155)$$

For  $f_1 = 2.1 \text{ kHz}$  and  $B = 15 \text{ kHz}$ , (7-155) gives

$$I_{\text{dB}} = 13.2 \text{ dB}$$

This checks with the value for  $I_{\text{dB}}$  that is obtained from Fig. 7-26.

## PROBLEMS

- 7-1** In a binary communication system the receiver test statistic,  $r_0(t_0) = r_0$ , consists of a polar signal plus noise. The polar signal has values  $s_{01} = +A$  and  $s_{02} = -A$ . Assume that the noise has a Laplacian distribution, which is

$$f(n_0) = \frac{1}{\sqrt{2} \sigma_0} e^{-\sqrt{2}|n_0|/\sigma_0}$$

where  $\sigma_0$  is the rms value of the noise.

- (a) Find the probability of error  $P_e$  as a function of  $A/\sigma_0$  for the case of equally likely signaling and  $V_T$  having the optimum value.
- (b) Plot  $P_e$  as a function of  $A/\sigma_0$  decibels. Compare this result with that obtained for Gaussian noise as given by (7-26a).
- 7-2** Using (7-8), show that the optimum threshold level for the case of antipodal signaling with additive white Gaussian noise is

$$V_T = \frac{\sigma_0^2}{2s_{01}} \ln \left[ \frac{P(s_1 \text{ sent})}{P(s_2 \text{ sent})} \right]$$

Here the receiver filter has an output with a variance of  $\sigma_0^2$ .  $s_{01}$  is the value of the sampled binary 1 signal at the filter output.  $P(s_1 \text{ sent})$  and  $P(s_2 \text{ sent})$  are the probabilities of transmitting a binary 1 and a binary 0, respectively.



- 7-3** A baseband digital communication system uses polar signaling with matched filter in the receiver. The probability of sending a binary 1 is  $p$  and the probability of sending a binary zero is  $1 - p$ .

- (a) For  $E_b/N_0 = 10 \text{ dB}$ , plot  $P_e$  as a function of  $p$  using a log scale.
- (b) Referring to (1-8), plot the entropy,  $H$ , as a function of  $p$ . Compare the shapes of these two curves.

- 7-4** A whole binary communication system can be modeled as an *information channel*, as shown in Fig. P7-4. Find equations for the four transition probabilities  $P(\tilde{m} | m)$ , where both  $\tilde{m}$  and  $m$  can be binary 1s or binary 0s. Assume that the test statistic is a linear function of the receiver input and that additive white Gaussian noise appears at the receiver input. [Hint: Look at (7-15).]

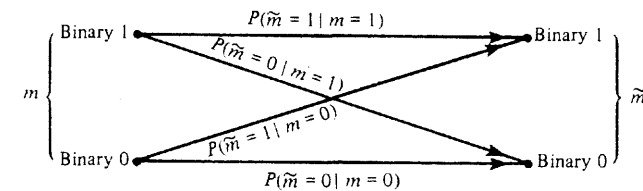


Figure P7-4



- 7-5** A baseband digital communication system uses unipolar signaling (rectangular pulse shape) with matched filter detection. The data rate is  $R = 9600 \text{ bits/sec}$ .

- (a) Find an expression for bit error rate (BER),  $P_e$ , as a function of  $(S/N)_{\text{in}}$ .  $(S/N)_{\text{in}}$  is the signal-to-noise power ratio at the receiver input where the noise is measured in a bandwidth corresponding to the equivalent bandwidth of the matched filter. [Hint: First find an expression of  $E_b/N_0$  in terms of  $(S/N)_{\text{in}}$ .]
- (b) Plot  $P_e$  vs.  $(S/N)_{\text{in}}$  in dB units on a log scale over a range of  $(S/N)_{\text{in}}$  from 0 to 15 dB.

- 7-6** Work Prob. 7-5 for the case of polar signaling.

- 7-7** Examine how the performance of a baseband digital communication system is affected by the receiver filter. Equation (7-26a) describes the BER when a low-pass filter is used and the bandwidth of the filter is sufficiently large so that the signal level at the filter output is  $s_{01} = +A$  or  $s_{02} = -A$ . Instead, suppose that a  $RC$  low-pass filter with a restricted bandwidth is used where  $T = 1/f_0 = 2\pi RC$ .  $T$  is the duration (pulse width) of one bit and  $f_0$  is the 3-dB bandwidth of the  $RC$  low-pass filter as described by (2-147). Assume that the initial conditions of the filter are reset to zero at the beginning of each bit interval.

- (a) Derive an expression for  $P_e$  as a function of  $E_b/N_0$ .
- (b) On a log scale, plot the BER obtained in part (a) for  $E_b/N_0$  over a range of 0 to 15 dB.
- (c) Compare this result with that for a matched-filter receiver (as shown in Fig. 7-5).

- 7-8** Consider a baseband digital communication system that uses polar signaling (rectangular pulse shape) where the receiver is shown in Fig. 7-4a. Assume that the receiver uses a second-order Butterworth filter with a 3-dB bandwidth of  $f_0$ . The filter impulse response and transfer function are

$$h(t) = \left[ \sqrt{2} \omega_0 e^{-(\omega_0/\sqrt{2})t} \sin \left( \frac{\omega_0}{\sqrt{2}} t \right) \right] u(t)$$

$$H(f) = \frac{1}{(jf/f_0)^2 + \sqrt{2}(jf/f_0) + 1}$$

where  $\omega_0 = 2\pi f_0$ . Let  $f_0 = 1/T$ , where  $T$  is the bit interval (i.e., pulse width) and assume that the initial conditions of the filter are reset to zero at the beginning of each bit interval.

- (a) Derive an expression for  $P_e$  as a function of  $E_b/N_0$ .
- (b) On a log scale, plot the BER obtained in part (a) for  $E_b/N_0$  over a range of 0 to 15 dB.
- (c) Compare this result with that for a matched-filter receiver (as shown in Fig. 7-5).

**7-9** Consider a baseband unipolar communication system with equally likely signaling. Assume that the receiver uses a simple  $RC$  LPF with a time constant of  $RC = \tau$  where  $\tau = T$  and  $1/T$  is the bit rate. (By "simple" it is meant that the initial conditions of the LPF are *not* reset to zero at the beginning of each bit interval.)

- (a) For signal alone at the receiver input, evaluate the approximate worst-case signal to ISI ratio (in decibels) out of the LPF at the sampling time  $t = t_0 = nT$ , where  $n$  is an integer.
- (b) Evaluate the signal to ISI ratio (in decibels) as a function of the parameter  $K$ , where  $t = t_0 = (n + K)T$  and  $0 < K \leq 1$ .
- (c) What is the optimum sampling time to use to maximize the signal-to-ISI power ratio out of the LPF?
- (d) Repeat (a) for the case when the equivalent bandwidth of the  $RC$  LPF is  $2/T$ .

**7-10** Consider a baseband polar communication system with equally likely signaling and no channel noise. Assume that the receiver uses a simple  $RC$  LPF with a time constant of  $\tau = RC$ . (By "simple" it is meant that the initial conditions of the LPF are *not* reset to zero at the beginning of each bit interval.) Evaluate the worst-case approximate signal to ISI ratio (in decibels) out of the LPF at the sampling time  $t = t_0 = nT$ , where  $n$  is an integer. This approximate result will be valid for  $T/\tau > \frac{1}{2}$ . Plot this result as a function of  $T/\tau$  for  $\frac{1}{2} \leq T/\tau \leq 5$ .

**7-11** Consider a baseband unipolar system described in Prob. 7-9d. Assume that white Gaussian noise is present at the receiver input.

- (a) Derive an expression for  $P_e$  as a function of  $E_b/N_0$  for the case of sampling at the times  $t = t_0 = nT$ .
- (b) Compare the BER obtained in part (a) with the BER characteristic that is obtained when a matched-filter receiver is used. Plot both of these BER characteristics as a function of  $(E_b/N_0)_{dB}$  over the range 0 to 15 dB.

**7-12** Work Prob. 7-11 for the case of *polar* baseband signaling.

**7-13** Work Prob. 7-9 for the case of *polar* baseband signaling.

**7-14** For unipolar baseband signaling as described by (7-23),

- (a) Find the matched-filter frequency response and show how the filtering operation can be implemented by using an integrate-and-dump filter.
- (b) Show that the equivalent bandwidth of the matched filter is  $B_{eq} = 1/(2T) = R/2$ .

**7-15** Equally likely polar signaling is used in a baseband communication system. Gaussian noise having a PSD of  $N_0/2$  W/Hz plus a polar signal with a peak level of  $A$  volts is present at the receiver input. The receiver uses a matched-filter circuit having a voltage gain of 1000.

- (a) Find the expression for  $P_e$  as a function of  $A$ ,  $N_0$ ,  $T$ , and  $V_T$ , where  $R = 1/T$  is the bit rate and  $V_T$  is the threshold level.
- (b) Plot  $P_e$  as a function of  $V_T$  for the case of  $A = 8 \times 10^{-3}$  V,  $N_0/2 = 4 \times 10^{-9}$  W/Hz, and  $R = 1200$  bits/sec.

**7-16** Consider a baseband polar communication system with matched-filter detection. Assume that the channel noise is white and Gaussian with a PSD of  $N_0/2$ . The probability of sending a binary 1 is  $P(1)$  and the probability of sending a binary 0 is  $P(0)$ . Find the expression for  $P_e$  as a function of the threshold level  $V_T$  when the signal level out of the matched filter is  $A$ , and the variance of the noise out of the matched filter is  $\sigma^2 = N_0/(2T)$  where  $R = 1/T$  is the bit rate.

**7-17** Design a receiver for detecting the data on a bipolar RZ signal that has a peak value of  $A = 5$  volts. In your design assume that an  $RC$  low-pass filter will be used and the data rate is 2400 b/sec.

- (a) Draw a block diagram of your design and explain how it works.
- (b) Give the values for the design parameters  $R$ ,  $C$ , and  $V_T$ .
- (c) Calculate the PSD level for the noise  $N_0$  that is allowed if  $P_e$  is to be less than  $10^{-6}$ .

**7-18** A BER of  $10^{-5}$  or less is desired for an OOK communication system where the bit rate is  $R = 2400$  bits/sec. The input to the receiver consists of the OOK signal plus white Gaussian noise.

- (a) Find the minimum transmission bandwidth required.
- (b) Find the minimum  $E_b/N_0$  required at the receiver input for coherent matched-filter detection.
- (c) Rework part (b) for the case of noncoherent detection.

**7-19** Rework Prob. 7-18 for the case when FSK signaling is used where  $2\Delta F = f_2 - f_1 = 1.5R$ .

**7-20** In this chapter the BER for a BPSK receiver was derived under the assumption that the coherent receiver reference (see Fig. 7-7) was exactly in phase with the received BPSK signal. Suppose that there is a phase error of  $\theta_e$  between the reference signal and the incoming BPSK signal. Obtain new equations that give the  $P_e$  in terms of  $\theta_e$  as well as the other parameters. In particular:

- (a) Obtain a new equation that replaces (7-36).
- (b) Obtain a new equation that replaces (7-38).
- (c) Plot results from part (b) where the log plot of  $P_e$  is given as a function of  $\theta_e$  over a range  $-\pi < \theta_e < \pi$  for the case when  $E_b/N_0 = 10$  dB.

**7-21** Digital data are transmitted over a communication system that uses nine repeaters plus a receiver. BPSK signaling is used. The  $P_e$  for each of the regenerative repeaters (see Sec. 3-5) is  $5 \times 10^{-8}$ , assuming additive Gaussian noise.

- (a) Find the overall  $P_e$  for the system.
- (b) If each repeater is replaced by an ideal amplifier (no noise or distortion), what is the  $P_e$  of the overall system?

**7-22** Digital data are to be transmitted over a toll telephone system using BPSK. Regenerative repeaters are spaced 50 miles apart along the system. The total length of the system is 600 miles. The telephone lines between the repeater sites are equalized over a 300- to 2700-Hz band and provide an  $E_b/N_0$  (Gaussian noise) of 15 dB to the repeater input.

- (a) Find the largest bit rate  $R$  that can be accommodated with no ISI.
- (b) Find the overall  $P_e$  for the system. (Be sure to include the receiver at the end of the system.)

**7-23** A BPSK signal is given by

$$s(t) = A \sin[\omega_c t + \theta_c + (\pm 1)\beta_p], \quad 0 < t \leq T$$

The binary data are represented by  $(\pm 1)$ , where  $(+1)$  is used to transmit a binary 1 and  $(-1)$  is used to transmit a binary 0.  $\beta_p$  is the phase modulation index as defined by (5-47).

- (a) For  $\beta_p = \pi/2$  show that this BPSK signal becomes the BPSK signal as described by (7-34).
- (b) For  $0 < \beta_p < \pi/2$  show that a discrete carrier term is present in addition to the BPSK signal as described by (7-34).

**7-24** Referring to the BPSK signal as described in Prob. 7-23, find  $P_e$  as a function of the modulation index  $\beta_p$ , where  $0 < \beta_p \leq \pi/2$ .

- (a) Find  $P_e$  as a function of  $A$ ,  $\beta_p$ ,  $N_0$ , and  $B$  for the receiver that uses a narrowband filter.

- (b) Find  $P_e$  as a function of  $E_b$ ,  $N_0$ , and  $\beta_p$  for the receiver that uses a matched filter. ( $E_b$  is the average BPSK signal energy that is received during one bit.)
- 7-25** Referring to the BPSK signal as described in Prob. 7-23, let  $0 < \beta_p < \pi/2$ .
- Show a block diagram for detection of the BPSK signal where a PLL is used to recover the coherent reference signal from the BPSK signal.
  - Explain why Manchester-encoded data are often used when the receiver uses a PLL for carrier recovery, as in part (a). (Hint: Look at the spectrum of the Manchester-encoded PSK signal.)
- 7-26** In obtaining the  $P_e$  for FSK signaling with coherent reception, the energy in the difference signal  $E_d$  was needed, as shown in (7-46). For *orthogonal* FSK signaling the cross-product integral was found to be zero. Suppose that  $f_1$ ,  $f_2$ , and  $T$  are chosen so that  $E_d$  is maximized.
- Find the relationship as a function of  $f_1$ ,  $f_2$ , and  $T$  for maximum  $E_d$ .
  - Find the  $P_e$  as a function of  $E_b$  and  $N_0$  for signaling with this FSK signal.
  - Sketch the  $P_e$  for this type of FSK signal and compare it with a sketch of the  $P_e$  for the orthogonal FSK signal that is given by (7-47).
- 7-27** An FSK signal with  $R = 110$  bits/sec is transmitted over an RF channel that has white Gaussian noise. The receiver uses a noncoherent detector and has a noise figure of 6 dB. The impedance of the antenna input of the receiver is  $50 \Omega$ . The signal level at the receiver input is  $0.05 \mu\text{V}$ , and the noise level is  $N_0 = kT_0$ , where  $T_0 = 290$  K and  $k$  is Boltzmann's constant (see Sec. 8-6). Find the  $P_e$  for the digital signal at the output of the receiver.
- 7-28** Work Prob. 7-27 for the case of DPSK signaling.
- 7-29** An analysis of the noise associated with the two channels of an FSK receiver precedes (7-44). It is stated that  $n_1(t)$  and  $n_2(t)$  are independent because they arise from a common white Gaussian noise process and since  $n_1(t)$  and  $n_2(t)$  have nonoverlapping spectra. Prove that this statement is correct. [Hint:  $n_1(t)$  and  $n_2(t)$  can be modeled as the outputs of two linear filters that have nonoverlapping transfer functions and the same white noise process,  $n(t)$ , at their inputs.]
- 7-30** In most applications, communication systems are designed to have a BER of  $10^{-5}$  or less. Find the minimum  $E_b/N_0$  decibels required to achieve an error rate of  $10^{-5}$  for the following types of signaling.
- Polar baseband.
  - OOK.
  - BPSK.
  - FSK.
  - DPSK.
- 7-31** Digital data are to be transmitted over a telephone line channel. Suppose that the telephone line is equalized over a 300- to 2700-Hz band and that the signal-to-Gaussian-noise (power) ratio at the output (receive end) is 25 dB.
- Of all the digital signaling techniques studied in this chapter, choose the one that will provide the largest bit rate for a  $P_e$  of  $10^{-5}$ . What is the bit rate  $R$  for this system?
  - Compare this result with the bit rate  $R$  that is possible when an ideal digital signaling scheme is used, as given by the Shannon channel capacity stated by (1-10).
- 7-32** An analog baseband signal has a uniform PDF and a bandwidth of 3500 Hz. This signal is sampled at an 8 ksamples/s rate, uniformly quantized, and encoded into a PCM signal having 8-bit words. This PCM signal is transmitted over a DPSK communication system that contains additive white Gaussian channel noise. The signal-to-noise ratio at the receiver input is 8 dB.
- Find the  $P_e$  of the recovered PCM signal.
  - Find the peak signal/average noise ratio (decibels) out of the PCM system.

- 7-33** A spread spectrum (SS) signal is often used to combat narrowband interference and for communication security. The SS signal with direct sequence spreading is (see Sec. 5-12)

$$s(t) = A_c c(t)m(t) \cos(\omega_c t + \theta_c)$$

where  $\theta_c$  is the start-up carrier phase,  $m(t)$  is the polar binary data baseband modulation, and  $c(t)$  is a polar baseband spreading waveform that usually consists of a pseudonoise (PN) code. The PN code is a binary sequence that is  $N$  bits long. The "bits" are called *chips* since they do not contain data and since many chips are transmitted during the time that it takes to transmit 1 bit of the data [in  $m(t)$ ]. The same  $N$ -bit code word is repeated over and over, but  $N$  is a large number, so the chip sequence in  $c(t)$  looks like digital noise. The PN sequence may be generated by using a clocked  $r$ -stage shift register having feedback so that  $N = 2^r - 1$ . The auto-correlation of a long sequence is approximately

$$R_c(\tau) = A \left( \frac{\tau}{T_c} \right)$$

where  $T_c$  is the duration of one chip (the time it takes to send one chip of the PN code).  $T_c \ll T_b$ , where  $T_b$  is the duration of a data bit.

- Find the PSD for the SS signal  $s(t)$ . [Hint: Assume that  $m(t)$ ,  $c(t)$ , and  $\theta_c$  are independent. In addition, note that the PSD of  $m(t)$  can be approximated by a delta function since the spectral width of  $m(t)$  is very small when compared to that for the spreading waveform  $c(t)$ .]
- Draw a block diagram for an optimum coherent receiver. Note that  $c(t)m(t)$  is first coherently detected and then the data,  $m(t)$ , are recovered by using a correlation processor.
- Find the expression for  $P_e$ .



- 7-34** Examine the performance of an AM communication system where the receiver uses a product detector. For the case of a sine wave modulating signal, plot the ratio of  $[(S/N)_{out}/(S/N)_{in}]$  as a function of the percent modulation.

- 7-35** An AM transmitter is modulated 40% by a sine-wave audio test tone. This AM signal is transmitted over an additive white Gaussian noise channel. Evaluate the noise performance of this system and determine by how many decibels this system is inferior to a DSB-SC system.

- 7-36** A phasing-type receiver for SSB signals is shown in Fig. P7-36. (This was the topic of Prob. 5-18.)

- Show that this receiver is or is not a linear system.
- Derive the equation for SNR out of this receiver when the input is an SSB signal plus white noise with a PSD of  $N_0/2$ .

- 7-37** Referring to Fig. P7-36, suppose that the receiver consists only of the upper portion of the figure, so that point C is the output. Let the input be an SSB signal plus white noise with a PSD of  $N_0/2$ . Find  $(S/N)_{out}$ .

- 7-38** Consider the receiver shown in Fig. P7-38. Let the input be a DSB-SC signal plus white noise with a PSD of  $N_0/2$ . The mean value of the modulation is zero.

- For  $A_0$  large, show that this receiver acts like a product detector.
- Find the equation for  $(S/N)_{out}$  as a function of  $A_c$ ,  $\bar{m^2}$ ,  $N_0$ ,  $A_0$ , and  $B_T$  when  $A_0$  is large.

- 7-39** Compare the performance of AM, DSB-SC, and SSB systems when the modulating signal  $m(t)$  is a Gaussian random process. Assume that the Gaussian modulation has a zero mean value and a peak value of  $V_p = 1$  where  $V_p \approx 4\sigma_m$ . Compare the noise performance of these three systems by plotting  $(S/N)_{out}/(S/N)_{baseband}$  for
- The AM system.

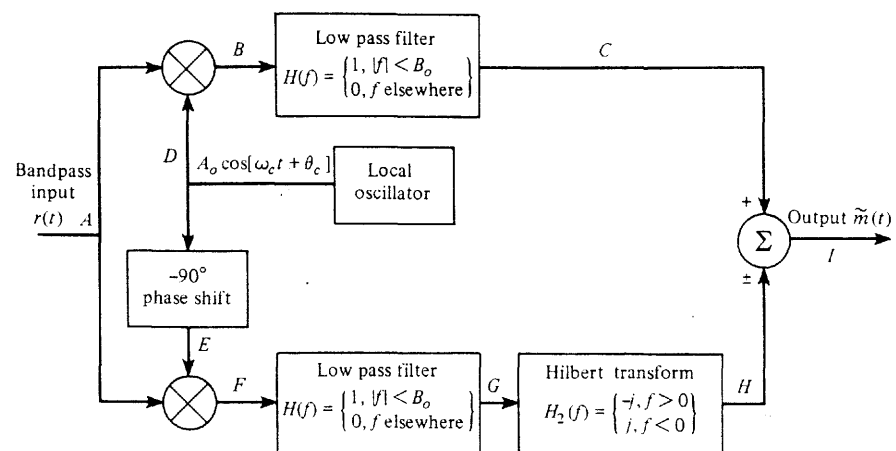


Figure P7-36

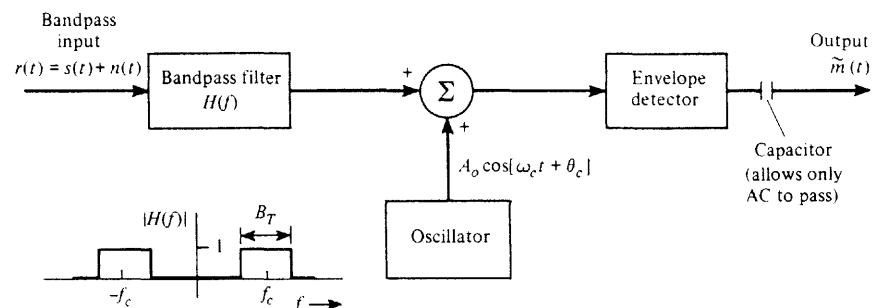


Figure P7-38

- (b) The DSB-SC system.  
(c) The SSB system.

- 7-40 If linear modulation systems are to be compared on an equal peak power basis (i.e., all have equal peak signal values), show that  
(a) SSB has a  $(S/N)_{out}$  that is 3 dB better than DSB.  
(b) SSB has a  $(S/N)_{out}$  that is 9 dB better than AM.  
(Hint: See Prob. 5-8.)
- 7-41 Using (7-132), plot the output SNR threshold characteristic of a discriminator for the parameters of a TV FM aural system. ( $\Delta F = 25$  kHz and  $B = 15$  kHz.) Compare the  $(S/N)_{out}$  versus  $(S/N)_{baseband}$  for this system with those shown in Fig. 7-24.
- 7-42 An FM receiver has an IF bandwidth of 25 kHz and a baseband bandwidth of 5 kHz. The noise figure of the receiver is 12 dB, and it uses a 75- $\mu$ sec deemphasis network. An FM signal plus white noise is present at the receiver input, where the PSD of the noise is  $N_0/2 = kT/2$ .  $T = 290$  K (see Sec. 8-6). Find the minimum input signal level (in dBm) that will give a SNR of 35 dB at the output when sine-wave test modulation is used.
- 7-43 Referring to Table 5-4, a two-way FM mobile radio system uses the parameters  $\beta_f = 1$  and  $B = 5$  kHz.

- (a) Find  $(S/N)_{out}$  for the case of no deemphasis.  
(b) Find  $(S/N)_{out}$  if deemphasis is used with  $f_l = 2.1$  kHz. It is realized that  $B$  is not much larger than  $f_l$  in this application.  
(c) Sketch the  $(S/N)_{out}$  versus  $(S/N)_{baseband}$  for this system and compare them with the result for FM broadcasting as shown in Fig. 7-26.

- 7-44 Compare the performance of two FM systems that use different deemphasis characteristics. Assume that  $\beta_f = 5$ ,  $(m/V_p)^2 = \frac{1}{2}$ ,  $B = 15$  kHz, and an additive white Gaussian noise channel is used. Find and sketch  $(S/N)_{out}/(S/N)_{baseband}$  for:  
(a) 25- $\mu$ sec deemphasis.  
(b) 75- $\mu$ sec deemphasis.

- 7-45 A baseband signal  $m(t)$  that has a Gaussian (amplitude) distribution frequency modulates a transmitter. Assume that the modulation has a zero-mean value and a peak value of  $V_p = 4\sigma_m$ . The FM signal is transmitted over an additive white Gaussian noise channel. Let  $\beta_f = 3$  and  $B = 15$  kHz. Find and sketch the  $(S/N)_{out}/(S/N)_{baseband}$  characteristic when:  
(a) No deemphasis is used.  
(b) 75- $\mu$ sec deemphasis is used.

- 7-46 In FM broadcasting, a preemphasis filter is used at the audio input of the transmitter and a deemphasis filter is used at the receiver output to improve the output SNR. For 75- $\mu$ sec emphasis, the 3-dB bandwidth of the receiver deemphasis LPF is  $f_l = 2.1$  kHz. The audio bandwidth is  $B = 15$  kHz. Define the improvement factor,  $I$ , as a function of  $B/f_l$ , as

$$I = \frac{(S/N)_{out} \text{ for system with preemphasis-deemphasis}}{(S/N)_{out} \text{ for system without preemphasis-deemphasis}}$$

For  $B = 15$  kHz, plot the decibel improvement that is realized as a function of the design parameter  $f_l$  where  $50$  Hz  $< f_l < 15$  kHz.

- 7-47 In FM broadcasting, preemphasis is used, and yet  $\Delta F = 75$  kHz is defined as 100% modulation. Examine the incompatibility of these two standards. For example, assume that the amplitude of a 1-kHz audio test tone is adjusted to produce 100% modulation (i.e.,  $\Delta F = 75$  kHz).  
(a) If the frequency is changed to 15 kHz, find the  $\Delta F$  that would be obtained ( $f_l = 2.1$  kHz). What is the percent modulation?  
(b) Explain why this phenomenon does not cause too much difficulty when typical audio program material (modulation) is broadcast.

- 7-48 Stereo FM transmission was studied in Sec. 5-6. At the transmitter, the left-channel audio,  $m_L(t)$ , and the right-channel audio,  $m_R(t)$ , are each preemphasized by an  $f_l = 2.1$ -kHz network. These preemphasized audio signals are then converted into the composite baseband modulating signal  $m_b(t)$ , as shown in Fig. 5-17. At the receiver, the FM detector outputs the composite baseband signal that has been corrupted by noise. (Assume that the noise comes from a white Gaussian noise channel.) This corrupted composite baseband signal is demultiplexed into corrupted left- and right-channel audio signals,  $\tilde{m}_L(t)$  and  $\tilde{m}_R(t)$ , each having been deemphasized by a 2.1-kHz filter. The noise on these outputs arises from the noise at the output of the FM detector that occurs in the 0- to 15-kHz and 23- to 53-kHz bands. The subcarrier frequency is 38 kHz. Assuming that the input SNR of the FM receiver is large, show that the stereo FM system is 22.2 dB more noisy than the corresponding monaural FM system.

- 7-49 An FDM signal,  $m_b(t)$ , consists of five 4-kHz-wide channels denoted by  $C_1, C_2, \dots, C_5$ , as shown in Fig. P7-49. The FDM signal was obtained by modulating five audio signals (each with 4-kHz bandwidth) onto USSB (upper single-sideband) subcarriers. This FDM signal,  $m_b(t)$ , modulates a DSB-SC transmitter. The DSB-SC signal is transmitted over an additive white

Gaussian noise channel. At the receiver the average power of the DSB-SC signal is  $P_s$ , and the noise has a PSD of  $N_0/2$ .

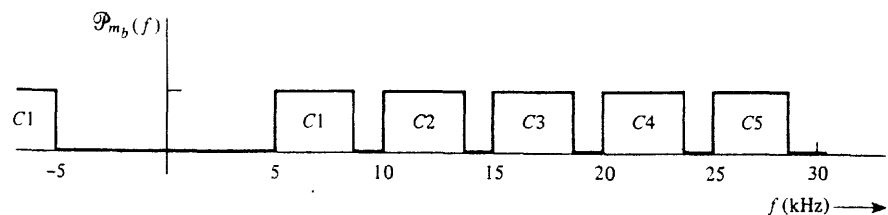


Figure P7-49

- (a) Draw a block diagram for a receiving system with five outputs, one for each audio channel.
- (b) Calculate the output SNR for each of the five audio channels.
- 7-50 Rework Prob. 7-49 when the FDM signal is frequency modulated onto the main carrier. Assume that the rms carrier deviation is denoted by  $\Delta F_{rms}$  and that the five audio channels are independent. No deemphasis is used.
- 7-51 Refer to Fig. 7-27 and
  - (a) Verify that the PCM curve is correct.
  - (b) Find the equation for the PCM curve for the case of QPSK signaling over the channel.
  - (c) Compare the performance of the PCM/QPSK system with that for PCM/BPSK and for the ideal case by sketching the  $(S/N)_{out}$  characteristic.

## CHAPTER 8

# CASE STUDIES OF COMMUNICATION SYSTEMS

The goal of this chapter is to examine the design of some practical communication systems. These systems are based on the communication principles that have been developed in previous chapters. Also, we see how modern designs are influenced by industry standards and how some sophisticated systems are the evolution of historical systems. This should be a “fun” chapter.

Case studies are presented for wire-line telephone systems, satellite systems, link budget system analysis, fiber optic systems, cellular telephone systems, and television systems. Link budget analysis is concerned with the design of a system to meet a required performance specification as a function of trade-off in the transmitted power, antenna gain, and noise figure of the receiving systems. This performance specification is the maximum allowed probability of error for digital systems, and the minimum allowed output SNR for analog systems.

## 8-1 TELECOMMUNICATION SYSTEMS

Telecommunication systems are designed to transmit voice, data, or visual information over some distance. (The prefix *tele* is derived from a Greek word meaning distance.) Modern telecommunication systems have evolved from the telegraph and telephone systems of the 1800s. Telecommunication companies that provide services for a large number of users over their *public switched telephone networks* (PSTN) on a for-hire basis are known as *common carriers*. The term is applied to widely diverse businesses such as mail, airline, trucking, telephone, and data services. The common carriers are usually regulated by the government for the general welfare of the public, and, in some countries, certain common carrier services are provided by the government. The information from multiple users is transmitted over these systems primarily by using TDM and frequency-division multiplexing (FDM).

### Time-Division Multiplexing

In Chapter 3, TDM techniques were first introduced. Examples of common carrier TDM techniques using digital signaling of the types DS-0, DS-1, DS-2, DS-3, DS-4, and DS-5 were studied. For a review of these techniques, the reader is referred to Sec. 3-9, specifically Figs. 3-39 and 3-40 and Tables 3-8 and 3-9. These figures and tables give the TDM standards that have been developed by the common carriers. For bandpass transmission, such as over microwave radio relay, fiber optic, or satellite systems, these TDM baseband signals are digitally modulated onto RF carriers using the OOK, QPSK, MPSK, or QAM techniques that were studied in Secs. 5-9 and 5-10. Fiber optic systems with OOK are described in Sec. 8-7.

TDM techniques are generally preferred to FDM techniques because of the ease of transmission of error-free data and voice information.

### Frequency-Division Multiplexing

FDM techniques were introduced in Chapter 5 (Fig. 5-16). This was followed by a discussion of the FDM technique used in FM stereo broadcasting, where the left and right audio signals are multiplexed onto one radio-frequency carrier. In toll telephone service, voice signals are transmitted over high-capacity channels using either TDM or FDM. The FDM technique was used historically; now TDM has become dominant and FDM is being phased out.

The telephone FDM technique is illustrated by the American Telephone and Telegraph Company (AT&T) FDM hierarchy, which is given in Fig. 8-1. Here, 12 analog (0- to 4-kHz voice frequency) telephone signals are frequency-division-multiplexed using lower SSB modulators to form one *group* signal. Five group signals are frequency-division-multiplexed to form one *supergroup* signal. The supergroup signal contains the information of 60 voice-frequency (VF) telephone signals. The bandwidth of the group signal is 48 kHz, and any 48-kHz signal (analog or digital) with spectrum centered in the group passband may replace a group input in the FDM hierarchy. Similarly, a supergroup signal may be replaced by any 240-kHz bandwidth signal when needed. Ten supergroup signals are frequency-division-multiplexed to form one *mastergroup* signal, which contains 600 VF signals. In Fig. 8-1 the carrier frequencies are given for the AT&T Type U600 mastergroup [Bell Telephone Laboratories, 1970]. Six mastergroup signals may be frequency-division-multiplexed to form a *jumbo-group* containing the information of 3600-VF signals.

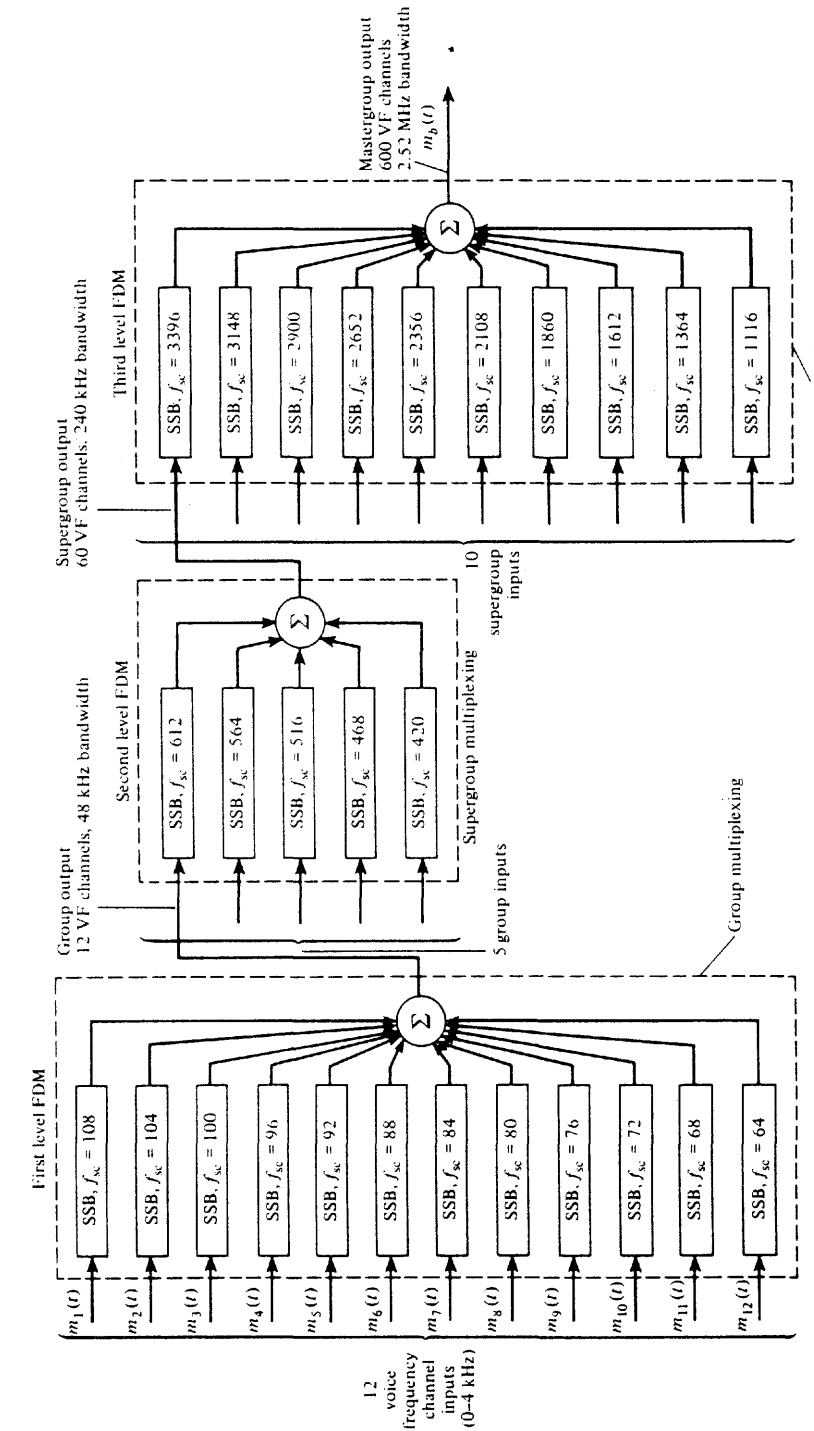


Figure 8-1 AT&T FDM hierarchy ( $f_{sc}$  given in kilohertz).

## 8-2 TELEPHONE SYSTEMS

Historically, telephone systems were designed only to reproduce voice signals that originated from a distant location. Today, modern telephone systems are very sophisticated. They use large digital computers at the *central office* (CO) to switch calls and to monitor the performance of the telephone system. The modern CO routes TDM PCM voice data, video data, and computer data to remote terminals and to other central offices.

### Historical Basis

As we shall see, modern telephone systems have evolved from the relatively simple analog circuit that was invented by Alexander Graham Bell in 1876. This circuit is shown in Fig. 8-2, where two telephone handsets are connected together by a twisted-pair (i.e., two-wire) telephone line and the telephone handsets are powered by a battery located at the CO. (Historically, the telephone-wire connection between the two parties was made by a telephone switchboard operator.) The battery produces a dc current around the telephone-wire loop. A carbon microphone element is used in each telephone handset. It consists of loosely packed carbon granules in a box that has one flexible side—the diaphragm. As sound pressure waves strike the diaphragm, the carbon granules are compressed and decompressed. This creates a variable resistance that causes the dc loop current to be modulated. Thus an ac audio current signal is produced, as shown in the figure. The handset earphone consists of an electromagnet with a paramagnetic diaphragm placed within the magnetic field. The ac current passing through the electromagnet causes the earphone diaphragm to vibrate and sound is reproduced.

The simple two-wire telephone system of Fig. 8-2 has three important advantages: (1) it is inexpensive; (2) the telephone sets are powered from the CO via the telephone line, so no power supply is required at the user's location; and (3) the circuit is full duplex.<sup>†</sup> The two-wire system has one main disadvantage—amplifiers cannot be used since they amplify the signal in only one direction. Consequently, for distant telephone connections, a more advanced technique—called a four-wire circuit—is required, as will be discussed subsequently. In summary, telephone circuits may be divided into two main categories:

- Two-wire or local loop circuits.
- Four-wire circuits.

### Modern Telephone Systems and Remote Terminals

A simplified diagram for a local loop system that is used today is shown in Fig. 8-3. The local switching office connects the two parties by making a hardwire connection between the two appropriate local loops. This is essentially a series connection, with the earphone and carbon microphone of each telephone handset wired in a series with a battery (located at the telephone plant). Figure 8-3 illustrates this analog local-loop system, which is said to supply *plain old telephone service* (POTS). The wire with positive voltage from the CO is called

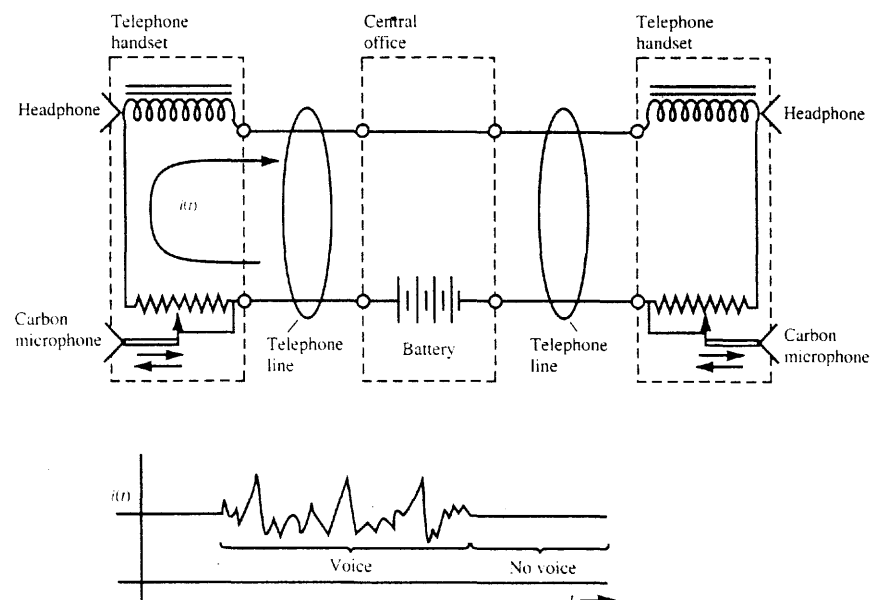


Figure 8-2 Historical telephone system.

the *tip* lead and it is color coded *green*. The wire with negative voltage is called the *ring* lead and is color coded *red*. The terms *tip* and *ring* are derived from the era when a plug switchboard was used at the CO and these leads were connected to a plug with tip and ring contacts. This jack is similar to a stereo headphone jack that has tip, ring, and sleeve contacts. The Earth ground lead was connected to the sleeve contact.

The sequence of events that occur when placing a local phone call will now be described with the aid of Fig. 8-3 and Table 8-1. The calling party—the upper telephone set in Fig. 8-3—removes the telephone handset; this action closes the switchhook contact (off-hook) so that dc current flows through the caller's telephone line. The current, about 40 mA, is sensed at the CO and causes the CO to place a dial-tone signal (approximately 400 Hz) on the calling party's line. The calling party dials the number by using either pulse or touch-tone dialing. If pulse dialing is used, the dc line current is interrupted for the number of times equal to the digit dialed (at a rate of 10 pulses/s). For example, there are five interruptions of the line current when the number 5 is dialed. Upon reception of the complete number sequence for the called party, the CO places the ringing generator (90 V rms, 20 Hz, on 2 s, off 4 s) on the line corresponding to the number dialed. This rings the phone. When the called party answers, dc current flows in that line to signal the CO to disconnect the ringing generator and to connect the two parties together via the CO circuit switch. Direct current is now flowing in the lines of both the called and the calling party, and there is a connection between the two parties via transformer coupling<sup>‡</sup> as shown in Fig. 8-3. When either person speaks, the sound vibrations cause the resistance of the carbon microphone element to

<sup>†</sup> With full-duplex circuits each person can talk and listen simultaneously to the other person.

<sup>‡</sup> The transformers are called "repeat coils" in telephone parlance.

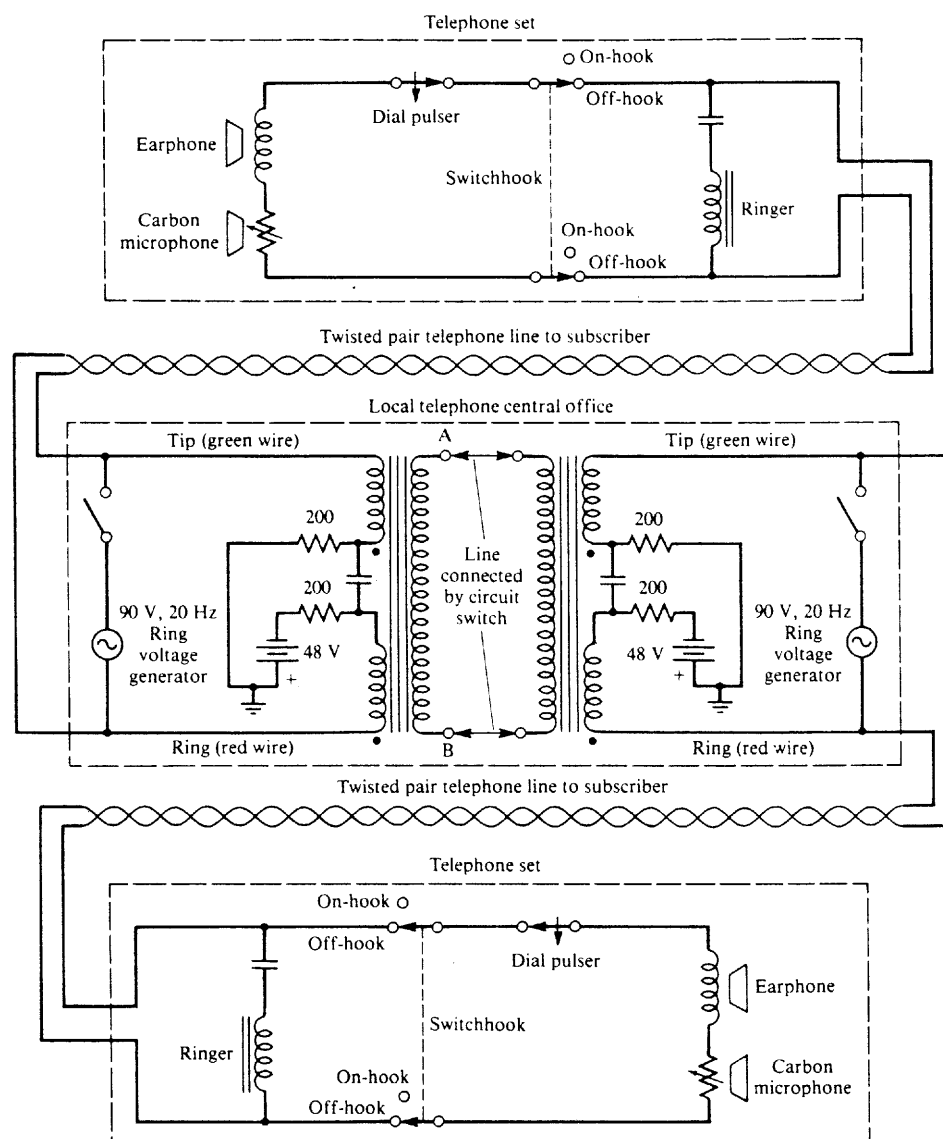


Figure 8-3 Local analog telephone system (simplified).

change in synchronization with the vibrations so that the dc line current is modulated (varied). This produces the ac audio signal that is coupled to the headphone of the other party's telephone. Note that both parties may speak and hear each other simultaneously. This is full-duplex operation.

In most modern telephone sets, the carbon microphone element is replaced with an electret or dynamic microphone element and an associated IC amplifier that is powered by

TABLE 8-1 TELEPHONE STANDARDS FOR THE SUBSCRIBER LOOP

Item	Standard
On-hook (idle status)	Line open circuit, minimum dc resistance 30 k $\Omega$
Off-hook (busy status)	Line closed circuit, maximum dc resistance 200 $\Omega$
Battery voltage	48 V
Operating current	20–80 mA, 40 mA typical
Subscriber-loop resistance	0–1300 $\Omega$ , 3600 $\Omega$ (max)
Loop loss	8 dB (typical), 17 dB (max)
Ringing voltage	90 V rms, 20 Hz (typical) (usually pulsed on 2 s, off 4 s)
Ringer equivalence number (REN) <sup>a</sup>	0.2 REN (minimum), 5.0 REN (maximum)
Pulse dialing	Momentary open-circuit loop
Pulsing rate	10 pulses/sec $\pm$ 10%
Duty cycle	58–64% break (open)
Time between digits	600 ms minimum
Pulse code	1 pulse = 1, 2 pulses = 2, ..., 10 pulses = 0
Touch-tone <sup>b</sup> dialing	Uses two tones, a low-frequency tone and a high-frequency tone, to specify each digit:
	High Tone (Hz)
Low Tone	1209      1336      1477
697 Hz	1      2      3
770	4      5      6
852	7      8      9
941	*      0      #
Level each tone	−6 to −4 dBm
Maximum difference in levels	4 dB
Maximum level (pair)	+2 dBm
Frequency tolerance	±1.5%
Pulse width	50 ms
Time between digits	45 ms minimum
Dial tone	350 plus 440 Hz
Busy signal	480 plus 620 Hz, with 60 interruptions per minute
Ringing signal tone	440 plus 480 Hz, 2 s on, 4 s off
Caller ID <sup>c</sup>	1.2-kbit/s FSK signal between first and second rings (Bell 202 modem standard; see Table C-8) <sup>d</sup>

<sup>a</sup> Indicates the impedance loading caused by the telephone ringer. An REN of 1.0 equals about 8 k $\Omega$ , 0.2 REN is 40 k $\Omega$ , and 5.0 REN is 1.6 k $\Omega$ .

<sup>b</sup> Touch-tone was a registered trademark of AT&T. It is also known as *dual-tone multiple frequency* (DTMF) signaling.

<sup>c</sup> Other display services are also proposed [Schwartz, 1993].

<sup>d</sup> [Lancaster, 1991].

the battery voltage from the CO, but the principle of operation is the same as previously described.

The telephone system of Fig. 8-3 is satisfactory as long as the resistance of the twisted-pair loops is  $1300\ \Omega$  or less. This limits the distance that telephones can be placed from this type of CO to about 15,000 ft for 26-gauge wire, 24,000 ft for 24-gauge, and 38,000 ft or about 7 miles if 22-gauge twisted-pair wire is used. Sometimes 19-gauge wire is used in rural areas so that phones may be located up to 20 miles from the CO.

Supplying a dedicated wire pair from each subscriber all the way to the CO is expensive. In applications where a large number of subscribers are clustered some distance from the CO, costs can be substantially reduced by using *remote terminals* (RT) (see Fig. 8-4). Remote terminals also allow telephones to be placed at any distance from the CO, as we will describe subsequently.

The circuit for a typical RT is illustrated in Fig. 8-5. The RT supplies battery voltage and ringing current to the subscriber's telephone. The *two-wire circuit* that carries the duplex VF signals to and from the subscriber is converted into a *four-wire circuit* that carries two one-way (simplex) transmit and receive signals by the use of a *hybrid* circuit. The hybrid is a balanced transformer circuit (or its equivalent electronic circuit) that provides isolation for the transmit and receive signals, so that self-oscillation will not occur if the amplified transmitted signal is fed back via the receive line. As shown in the figure, the transmit VF signal is converted to a DS-0 PCM signal, which is time-division-multiplexed with the PCM signals from other subscribers attached to the RT. The TDM signal is sent over a DS-1 trunk to the CO. Similarly, the received DS-1 signal from the CO is demultiplexed and decoded to obtain the received VF audio for the subscriber. In a popular RT sys-

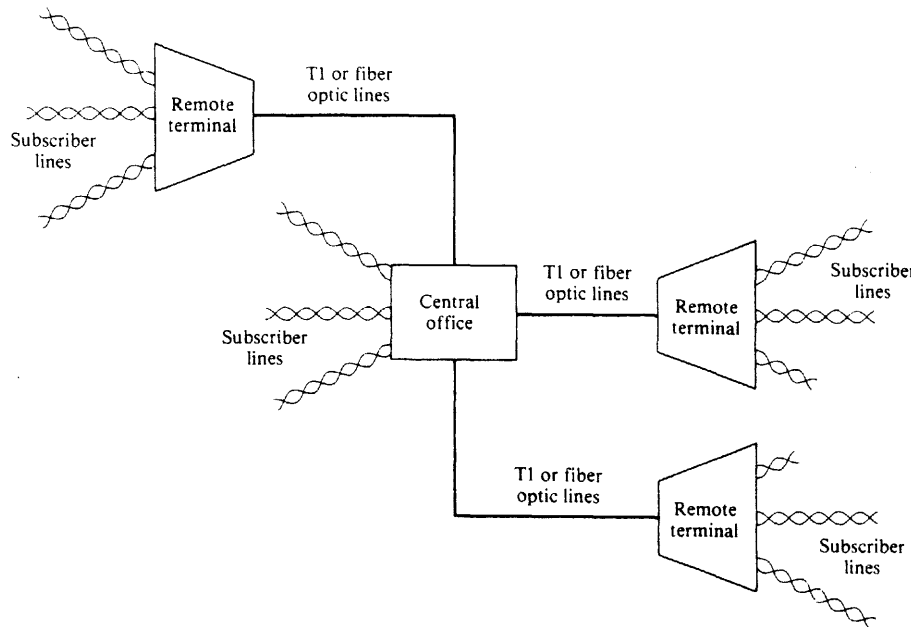


Figure 8-4 Telephone system with remote terminals.

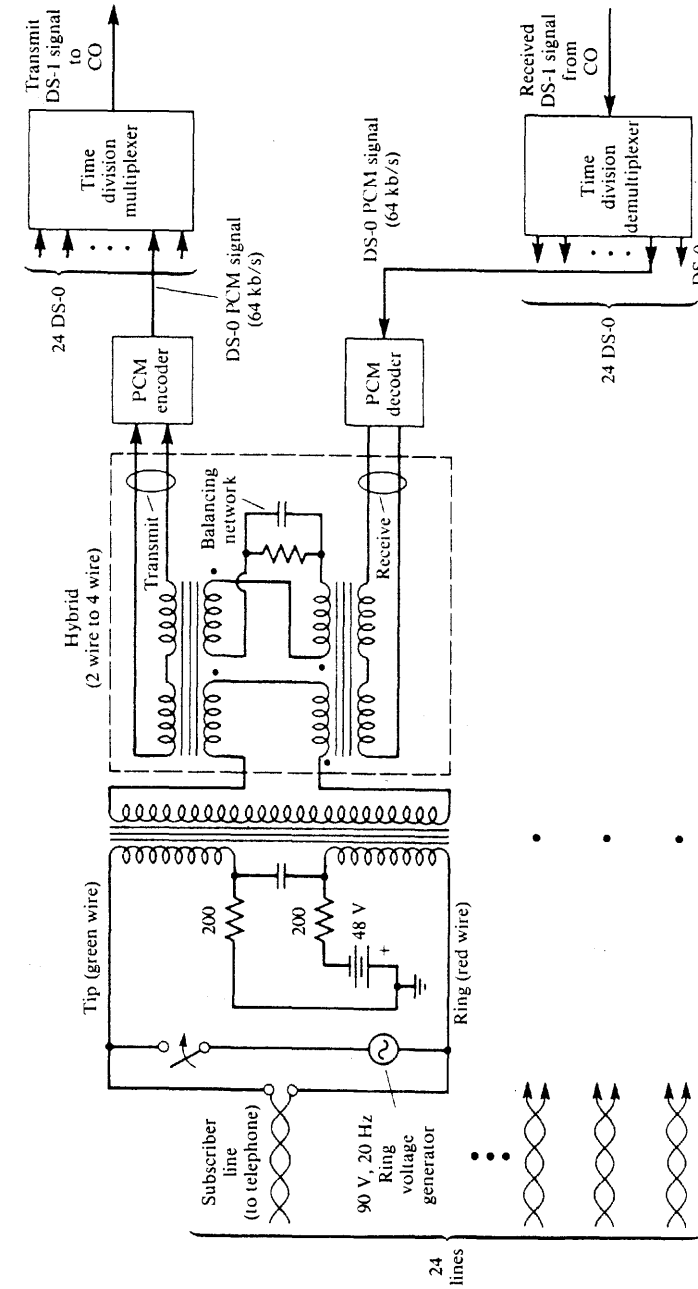


Figure 8-5 Remote terminal (RT).

tem manufactured by AT&T called SLC-96, 96 VF subscriber lines are digitized and multiplexed onto four T1 lines, and one additional T1 line is on standby in case one of the other T1 lines fails [Chapman, 1984]. From Chapter 3 it is recalled that a T1 line requires two twisted pairs (one for the transmit data and one for the receive data) and that each T1 line (1.544 Mbit/s) carries the equivalent of 24 VF signals.

Let us now compare the twisted-pair requirements for systems with and without RTs. If no RT is used, 96 pairs will be required to the CO for 96 subscribers, but if a SLC-96 RT is used, only 10 pairs (5 T1 lines) are needed to the CO. This provides a pair savings (also called pair gain) of 9.6 to 1. Furthermore, the RT may be located at any distance from the CO (there is no 1300- $\Omega$  limit) because the pairs are used for DS-1 signaling with repeaters spaced about every mile. Of course, fiber optic lines can also be used to connect the RT to the CO. For example, if two 560-Mbit/sec fiber optic lines are used (one for data sent in each direction), this has a capacity of 8064 VF channels for DS-5 signaling (see Table 3-8 and Fig. 3-40). Thus an RT with a 560-Mbit/s fiber optic link to the CO could serve 8064 subscribers. Furthermore, in Sec. 8-7 we see that no optical repeaters will be required if the RT is located within 35 miles (typically) of the CO.

Telephone companies are replacing their analog switches at the CO with digital switches. Historically, at the CO an analog circuit switch was used to connect the calling and the called party (as shown in Fig. 8-3). These switches were controlled by hardwired relay logic. Now, modern telephone offices use *electronic switching systems* (ESS). With ESS, a digital computer controls the switching operation as directed by software called *stored program control*. Moreover, the latest ESS switches use *digital switching* instead of *analog switching*. Examples are AT&T's No. 5 ESS (electronic switching system), and Northern Telcom's DMS-100 switches. In a digitally switched CO, the customer's VF signal is converted to PCM and time-division-multiplexed with other PCM signals onto a high-speed digital line. (When RTs are used, the conversion of the VF signal to PCM is carried out at the RT.) The digital CO switches a call by placing the PCM data of the calling party into the TDM time slot that has been assigned for the destination (called) party. This is called *time-slot interchange* (TSI). The digital switch is less expensive on a per customer basis than the analog switch (for a large number of customers), and it allows switching of data and digitized video as well as PCM audio. However, some analog switch COs remain since it is not cost effective to scrap existing analog facilities, and, of course, analog VF signals must be converted to TDM PCM signaling before a digital switch can be used. On the other hand, there is the incentive to upgrade analog telephone systems to digital switching with remote terminals since this allows the ISDN service, as introduced in Chapter 3 and described in more detail in the next section. That is, the use of RTs permits the subscriber line to be short (about 1 mile). With short subscriber lines, ISDN service, and, if needed, DS-1 (1.544-Mbit/s) service, can be provided directly over the existing twisted-pair lines that are already in place to the customer's premises.

For toll calls, the local CO switches the call to trunk lines that connect the local CO to a distant CO. The trunk lines usually carry either TDM or FDM signals, with TDM being the preferred technique. If the local CO uses analog switches, the two-wire circuit must be converted to a four-wire circuit (using a hybrid as described in Fig. 8-5) since unidirectional repeaters are used on the long-distance trunk lines. If the local CO uses a digital switch, it acts much like an RT with respect to the distant CO, and the two COs are con-

nected by high-speed TDM digital trunk lines. Interestingly, long-distance lines are less than 5% of the total cost of the telephone network; most of the cost is in the switching equipment.

In summary, the analog telephone subscriber is connected to a CO or a RT via a two-wire twisted-pair subscriber line. The CO or RT as a terminator of this subscriber loop provides the following functions for POTS:

1. Terminates the line with a 900- $\Omega$  ac load (balanced with respect to ground).
2. Supplies dc loop current from its battery through balanced 200- $\Omega$  resistors (for a total driven-point dc impedance of 400  $\Omega$ ).
3. Monitors loop current to determine on-hook and off-hook conditions.
4. Receives dialing information from the subscriber via touch-tone or dial pulse.
5. Applies ringing voltage and call progress signaling (i.e., dial tone, busy signal, ringing tone, etc.).
6. Converts the two-wire line to a four-wire line (transmit and receive path) for use by digital COs and RTs or for use on toll calls. Two-wire to four-wire conversion is usually not required for analog COs that switch local calls.
7. Provides analog-to-digital (i.e., PCM) and digital-to-analog conversion for digital systems.
8. Tests subscriber line and line termination (i.e., telephone loads connected to other end of the line).
9. Provide protective isolation of CO/RT equipment from unwanted line potentials such as lightning or cross connection to some ac power source.

Additional practical details are given in a book by Reeve [Reeve, 1995].

### 8-3 INTEGRATED SERVICE DIGITAL NETWORK

As indicated previously, the telephone industry is evolving from an analog network to a digital network. Presently, the trend is to provide a digital CO and a digital network out to the RT; the "last mile" from the RT to the subscriber is usually analog. A new approach called the *integrated service digital network* (ISDN) converts the "last mile" analog subscriber line (ASL) to a *digital subscriber line* (DSL) so that digital data can be delivered directly to the subscriber's premises. The ISDN subscriber can demultiplex the data to provide any one or all of the following applications simultaneously: (1) decode data to produce VF signals for telephone handsets, (2) decode data for a video display, or (3) process data for telemetry and/or PC applications.

As indicated in Chapter 3, there are two categories of ISDN: (1) *narrowband* or "*basic rate*" ISDN, denoted by N-ISDN, and (2) *broadband* or "*primary rate*" ISDN, denoted by B-ISDN. B-ISDN is in the process of being developed; consequently, there are many proposed protocols and data rates. One proposal has an aggregate data rate of 1.536 Mbit/s (approximately the same rate as for T1 lines) consisting of 23 B channels (64 kbit/s each) and one D channel (64 kbit/s). The B channels carry user (or bearer) data which may be PCM

for encoded video or audio. The D channel is used for signaling to set up calls, disconnect calls, and/or route data for the 23 B channels.

Since B-ISDN standards are not yet fully developed, B-ISDN will be discussed only briefly. It is clear that twisted-pair copper lines must be used (presently) to provide B-ISDN for the "last mile" to the subscriber since it is not financially feasible to replace all copper lines already installed (about a \$100 billion investment for U.S. copper line facilities) with fiber. Of course, fiber might be the economical solution for new installations. Furthermore, since 24-gauge copper lines have an attenuation of about 35 dB/mile at 1 MHz, the "last mile" copper line length from the RT to the subscriber will have to be limited to a mile or two, assuming that no repeaters are used. As discussed in Sec. 3-9, twisted-pair copper lines with repeaters spaced every mile can support a 1.5-Mbit/s data rate (T1 line, which has a bipolar line code), or 6.4-Mbit/s data rate (T1G line, which has a quarternary line code). Fiber optic (or coaxial) lines will be required for data rates on the order of 10 Mbit/s or larger. For further reading on the developing B-ISDN technology, the reader is referred to the literature [Hsing, Chen, Bellisio, 1993; Lin, Chen, Hsing, 1995; Saltzberg et al., 1991].

The standard implementation of N-ISDN is shown in Fig. 8-6. The N-ISDN subscriber is connected to the RT of the telephone company by a two-wire twisted pair (unloaded) telephone line. This allows existing copper pairs to be used for either POTS or N-ISDN simply by connecting the ends of the pairs to the appropriate terminating equipment. For N-ISDN service the line must be no longer than 18 kft (3.4 miles) for the 160-kbit/s N-ISDN aggregate data rate. (If the subscriber is located within 18 kft of the CO, an RT is not necessary.) The data rate available to the N-ISDN subscriber is 144 kbit/s, consisting of data partitioned into two B channels of 64 kbit/s each and one D channel of 16 kbit/s. In addition to the 2B + D data, the telephone company adds 12 kbit/s for framing/timing plus 4 kbit/s for overhead to support network operations. This gives an overall data rate of 160 kbit/s on the DSL in both the transmit and receive directions (simultaneously) for full-duplex operation. The DSL is terminated on the subscriber's end at the U interface as shown on Fig. 8-6. The NT1 (network termination) incorporates a hybrid circuit to convert the two-wire U interface to a four-wire T interface which has two two-wire buses, one for the transmit and one for the receive data signals. The NT1 is a slave transceiver that derives its clocking signals from the DSL signal that is transmitted from the RT. The NT1 passes the 2B + D data between the U and T interfaces and also processes additional bits that appear on the transmit and receive lines at the T interface. The additional bits are needed for addressing, control, and supervision of terminal equipment. The data rate on each transmit and receive T line is 192 kbit/s. The NT2 may or may not be needed. When used, it provides the appropriate higher-level protocols for a terminal cluster controller or for a local area network (LAN) access node. If not used, the NT1 four-wire interface becomes the S/T interface. The S and T interfaces are electrically identical and use a RJ45 8-pin modular connector. The S/T interface bus provided the connection medium for ISDN terminals (video, audio, and/or data) and/or a terminal adapter (TA). Up to eight terminals may be bridged onto the S/T bus. The TA allows non-ISDN terminals with RS-232 ports to be used on the ISDN network. For example, a personal computer (PC) can be connected to the N-ISDN network via its serial port and the R interface of the TA. Also, using an alternative approach, a PC adapter card with a built-in NT1 and a telephone codec can be used. That is, the DSL U interface modu-

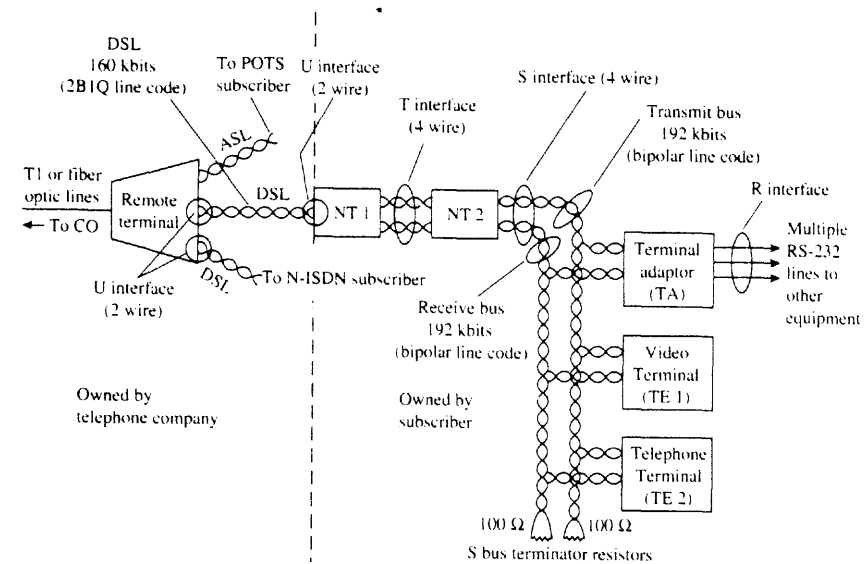


Figure 8-6 N-ISDN system with subscriber equipment attached.

lar connector is plugged directly into this adapter card on the PC. The PC then acts as an ISDN video terminal with a built-in telephone. For details on the protocols used at the U, S, and T interfaces, the reader is referred to application notes for ISDN chips such as Motorola's MC 145472 U interface transceiver, MC 145474 S/T interface, and MC 145554 telephone codec.

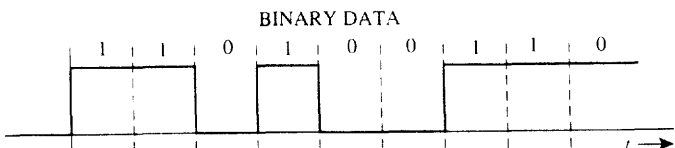
N-ISDN service to the subscriber via two-wire twisted-pair DSL up to 18 kft from a RT is made possible by the use of multilevel signaling. Referring to Fig. 5-33 with  $R = 160$  bits/s, a four-level (i.e.,  $\ell = 2$  bit) 80-kbaud line code has a null bandwidth of only 80 kHz instead of the 160-kHz null bandwidth for a binary ( $\ell = 1$ ) line code. The 80-kHz bandwidth is supported by 26-gauge twisted-pair cable if it is less than about 18 kft in length. The particular four-level signal used is the 2B1Q line code (for two binary digits encoded into one quadrenary symbol) as shown in Fig. 8-7. Note that the 2B1Q line code is a differential symbol code. Thus if (due to wiring error) the twisted pair is "turned over" so that the tip wire is connected to the ring terminal and the ring to the tip so that the 2B1Q signal polarity is inverted, the decoded binary data will still have the correct polarity (i.e., not complemented).

The primary advantage of ISDN is obvious—it provides TDM data channels directly to the subscriber. It also has disadvantages. For example, since the ISDN subscriber equipment is not powered by the DSL, it will not function when local ac power fails unless a backup power supply is provided by the subscriber. If only POTS is required, the conventional analog telephone is usually much cheaper and more reliable.

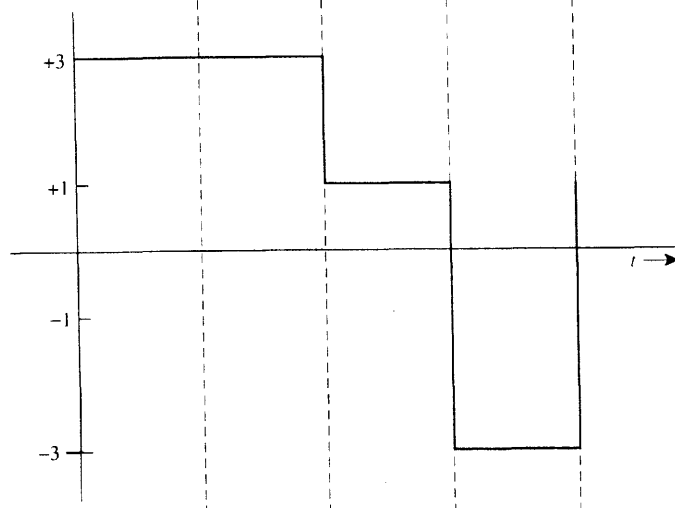
For study of additional N-ISDN topics, such as frame structure, timing recovery, synchronization, and echo cancellation, the reader is referred to a tutorial paper by [Huang and Valenti, 1991] and a book [Stallings, 1992].

Previous 2B1Q level	Current binary word	Present 2B1Q level
+1 or +3	{ 00 01 10 11	+1 +3 -1 -3
-1 or -3	{ 00 01 10 11	-1 -3 +1 +3

(a) 2B1Q differential code table



(b) Binary data waveform (160 kbit/sec)



(c) 2B1Q waveform (80 baud)

Figure 8-7 2B1Q Line code.

Because of government deregulations, the nature of telephone companies is changing at a fast pace. With the wireless and cellular telephone revolution, the telephone industry is becoming highly competitive. In the near future traditional telephone companies will be allowed to provide CATV-type video service to subscribers, and CATV companies will be allowed to provide telephone service. Consequently, the telephone industry is exploring cost-effective ways of delivering video service to the home. Installing a coaxial cable or fiber optic cable drop to the home would be very expensive, and, often, a twisted pair drop to the

home is already in place. One cost-effective solution is for the telephone company to provide *switched digital video* (SDV) to the home over the existing twisted pair copper wires. The copper wires do have the bandwidth to support the transmission of one to four TV channels of compressed digital video with data rates in the range of 1.5 to 6 Mbits/s [Lin, Chen, and Hsing, 1995]. In this SDV service, the intelligence of the telephone network is used. The subscriber selected TV channel is sent over his or her twisted pair line and the subscriber can instruct the SDV system to switch to a different TV channel whenever he or she wishes. Consequently, the SDV subscriber can have access to an almost unlimited number of TV channels and other video services.

#### 8-4. CAPACITIES OF PUBLIC SWITCHED TELEPHONE NETWORKS

The wideband channels used to connect the toll offices consist of three predominant types: fiber optic cable, microwave radio relay systems, and (buried) coaxial cable systems. Table 8-2 lists some of the wideband systems that are used, or have been used in the past, and indicates the capacity of these systems in terms of the number of VF channels they can handle and their bit rate.

Historically, open-wire pairs, which consist of individual bare wires supported by glass insulators on the cross arms of telephone poles provided "wideband" service via FDM/SSB signaling. Occasionally, some open-wire lines can still be seen along railroad tracks. Fiber cable with TDM/OOK signaling is now rapidly overtaking twisted pair cable, coaxial cable, and microwave relay because of its tremendous capacity and relatively low cost. For example, the capacity of the 6 fiber TAT-12 transoceanic cable is 200,000 VF channels. However, fiber cable provides service only from one fixed point to another. Conversely, communication satellites provide wideband connections to any point on the globe. Service to isolated locations can be provided almost instantaneously by the use of portable ground stations. This is described in more detail in the following section.

#### 8-5 SATELLITE COMMUNICATION SYSTEMS

The number of satellite communication systems has increased tremendously over the last few years. Satellite communications now relay the bulk of transoceanic telephone traffic. In addition, satellites have made transoceanic relaying of television signals possible. Satellite communications thus provide the relaying of data, telephone, and television signals, and it is now feasible to provide national direct-into-the-home television transmission via satellite.

Most communication satellites are placed in *geostationary orbit* (GEO). This is a circular orbit in Earth's equatorial plane. The orbit is located 22,300 miles above the equator so that the orbital period is the same as that of the Earth. Consequently, from Earth these satellites appear to be located at a stationary point in the sky, as shown in Fig. 8-8. This enables the Earth station antennas to be simplified since they are pointed in a fixed direction and do not have to track a moving object. (For communication to the polar regions of the Earth, satellites in polar orbits are used, which require Earth stations with tracking antennas.)

TABLE 8-2 CAPACITY OF PUBLIC SWITCHED TELEPHONE NETWORKS

Transmission Medium	Name	Developer	Year in Service	Number of Voice-Frequency Channels	Bit Rate (Mbits/sec)	Repeater Spacing (miles)	Operating Frequency (MHz)	D/A	Modulation <sup>a</sup>
Open-wire pair	A	Bell	1918	4			0.005–0.025	A	FDM/SSB
	C	Bell	1924	3		150	0.005–0.030	A	FDM/SSB
		CCITT		12		50	0.036–0.140		
	J	Bell	1938	12		50	0.036–0.143	A	FDM/SSB
		CCITT		28			0.003–0.300	A	FDM/SSB
Twisted-pair cable	K	Bell	1938	12		17	0.012–0.060	A	FDM/SSB
		CCITT		12		19	0.012–0.060	A	FDM/SSB
	N1	Bell	1950	12			0.044–0.260	A	FDM/SSB
	N3	Bell	1964	24			0.172–0.268	A	FDM/SSB
	T1 <sup>b</sup>	Bell	1962	24	1.544 (DS-1)	1		D	Bipolar
	T1G <sup>b</sup>	AT&T	1985	96	6.312 (DS-2)			D	Four-level
Coaxial cable	T2 <sup>b</sup>	Bell		96	6.312 (DS-2)	2.3		D	B6ZS
	L1	Bell	1941	600		8	0.006–2.79	A	FDM/SSB
	L3	Bell	1953	1,860		4	0.312–8.28	A	FDM/SSB
	L4	Bell	1967	3,600		2	0.564–17.55	A	FDM/SSB
	L5	Bell	1974	10,800		1	3.12–60.5	A	FDM/SSB
	T4 <sup>b</sup>	Bell		4,032	274.176 (DS-4)	1		D	Polar
Fiber optic	T5 <sup>b</sup>	Bell		8,064	560.16 (DS-5)	1		D	Polar
	FT3	Bell	1981	672	44.763 (DS-3)	4.4	0.82 μm	D	TDM/OOK
		Brit. Telcom	1984		140	6	1.3 μm	D	TDM/OOK
		Sask. Telcom	1985		45	6–18	0.84 and 1.3 μm	D	TDM/OOK
	F-400M	Nippon	1985		400	12	1.3 μm	D	TDM/OOK
	FT3C-90	AT&T	1985	1,344	90.254 (DS-3C)	16	1.3 μm	D	TDM/OOK
	FT4E-432	AT&T	1986	6,048	432 (DS-432)	16	1.3 μm	D	TDM/OOK
	LaserNet <sup>d</sup>	Microtel	1985	6,048	417.79 (9DS-3)	25	1.3 μm	D	TDM/OOK
	FTG1.7	AT&T	1987	24,192	1,668 (36DS-3)	29	1.3 μm	D	TDM/OOK
	FT-2000	AT&T	1995	32,256	2,488 (DC-48)	100	1.5 and 1.3 μm	D	TDM/OOK
Transoceanic	TAT-1 (SB)	Bell	1956	48		20	0.024–0.168	A	FDM/SSB
	TAT-3 (SD)	Bell	1963	138		11	0.108–1.05	A	FDM/SSB
	TAT-5 (SF)	Bell	1970	845		6	0.564–5.88	A	FDM/SSB
	TAT-6 (SG)	Bell	1976	4,200		3	0.5–30	A	FDM/SSB
	TAT-8 (3 fibers)		1988	8,000	280		1.3 μm	D	TDM/OOK
	TAT-9 (3 fibers)		1991	16,000	565		1.55 μm	D	TDM/OOK
	TAT-10 (6 fibers)		1992	80,000 <sup>e</sup>	565		1.55 μm	D	TDM/OOK
	TAT-12 (6 fibers)	Alcatel	1995	200,000	5,000	30	1.48 μm	D	TDM/OOK
Microwave relay	TD-2	Bell	1948	600 (1954)	plus 1.544 <sup>c</sup>	30	3700–4200	A	FDM/FM
	TH-1	Bell	1961	2,400 (1979)	plus 1.544 <sup>c</sup>	30	5925–6245	A	FDM/FM
	TD-3	Bell	1967	1,800 (1979)	plus 1.544 <sup>c</sup>	30	3700–4200	A	FDM/FM
	TN-1	Bell	1974	1,800	plus 1.544 <sup>c</sup>	30	K band, 18 GHz	A	FDM/FM
	AR6A	Bell	1980	6,000		30	5925–6425	A	FDM/SSB
	18G274	NEC	1974	4,032	274.176 (DS-4)	7	18 GHz	D	4 PSK
	6G90	NEC	1979	1,344	90 (2DS-3)	30	6 GHz	D	16 QAM
	11G135	NEC	1980	2,016	135 (3 DS-3)	30	11 GHz	D	16 QAM
	6G135	NEC	1983	2,016	135 (3 DS-3)	30	6 GHz	D	64 QAM
	MDR-2306	Collins	1983	2,016	135 (3 DS-3)	30	6 GHz	D	64 QAM
Communication satellite	RD-6A	Northern Tel.	1984	2,016	135 (3 DS-3)	30	6 GHz	D	64 QAM
	Intelsat IV	COMSAT	1970	8,000		22,300	6 GHz up/4 GHz down	A/D	FDM/FM, QPSK/SCPC
	Intelsat V	COMSAT	1980	25,000		22,300	6/4 and 14/11 GHz	A/D	FDM/FM, QPSK/SCPC
	Intelsat VI	COMSAT	1986	80,000		22,300	6/4 and 14/11 GHz	A/D	FDM/FM, QPSK/SCPC

<sup>a</sup> A-analog; D-digital plus modulation type.<sup>b</sup> See Table 3-9 for more details on the T-carrier system.<sup>c</sup> Since 1974 data under voice were added to give a 1.544-Mbit/sec (DS-1) data channel in addition to the stated VF FDM capacity.<sup>d</sup> See Example 8-5 in Sec. 8-7.<sup>e</sup> VF capacity with statistical multiplexing.

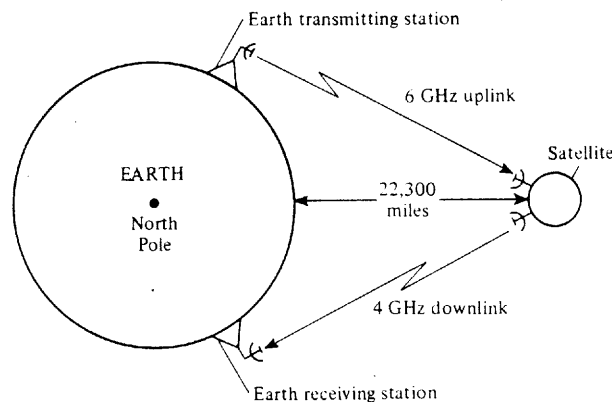


**Figure 8-8** Communications satellite in geosynchronous orbit.

To prevent the satellite from tumbling, one of two spin stabilization techniques—spin stabilization or three-axis stabilization—is used. For spin stabilization, the outside cylinder of the satellite is spun to create a gyroscopic effect that stabilizes the satellite. For three-axis stabilization, internal gyroscopes are used to sense satellite movement and the satellite is stabilized by firing appropriate thruster jets.

The most desired frequency band for satellite communication systems is 6 GHz on the uplink (Earth-to-satellite transmission) and 4 GHz on the downlink (satellite-to-Earth transmission). In this frequency range the equipment is relatively inexpensive, the cosmic noise is small, and the frequency is low enough so that rainfall does not appreciably attenuate the signals. Other losses, such as ionospheric scintillation and atmospheric absorption, are small at these frequencies [Spilker, 1977]. (Absorption occurs in specific frequency bands and is caused by the signal exciting atmospheric gases and water vapor.) However, existing terrestrial microwave radio relay links are already assigned to operate within the 6- and 4-GHz bands (see Table 8-2), so the FCC limits the power density on Earth from the satellite transmitters. One also has to be careful in locating the Earth station satellite receiving antennas so that they do not receive interfering signals from the terrestrial microwave radio links that are using the same frequency assignment. In the 6/4-GHz band, synchronous satellites are assigned an orbital spacing of  $2^\circ$  (U.S. standard).

Newer satellites operate in higher-frequency bands because there are so few vacant spectral assignments in the 6/4-GHz band (C band). The Ku band satellites use 14 GHz on the uplink and 12 GHz on the downlink with an orbital spacing of  $3^\circ$ . Some new Ku-band satellites have high-power amplifiers that feed 120 to 240 W into their transmitting antenna, as compared with 20 to 40 W for low- or medium-power satellites. High-power satellites—called direct broadcast satellites (DBS)—provide TV service directly to the homeowner that has a small receiving antenna (2 ft or less in diameter).

Each satellite has a number of *transponders* (receiver-to-transmitter) aboard to amplify the received signal from the uplink and to down-convert the signal for transmission on the downlink (Fig. 8-9). This figure shows a “bent pipe transponder” that does not demodulate the received signal and perform signal processing but acts as a high-power-gain down converter. Most transponders are designed for a bandwidth of 36, 54, or 72 MHz, with 36 MHz

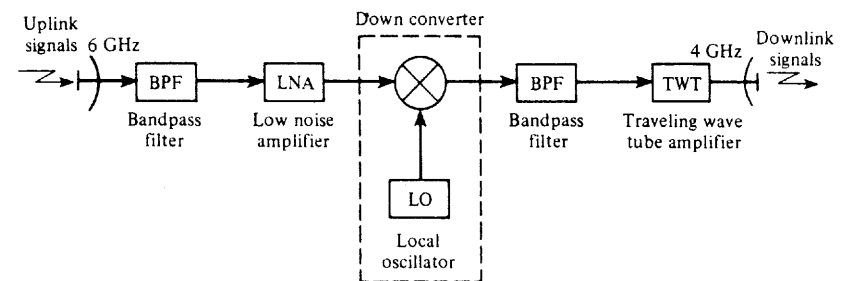


**Figure 8-9** Simplified block diagram of a communications satellite transponder.

being the standard used for C-band (6/4 GHz) television relay service. As technology permits, processing transponders will come into use since an improvement in error performance (for digital signaling) can be realized.

Each satellite is assigned a synchronous orbit position and a frequency band in which to operate. In the 6/4-GHz band, each satellite is permitted to use a 500-MHz-wide spectral assignment, and a typical satellite has 24 transponders aboard, with each transponder using 36 MHz of the 500-MHz bandwidth assignment. The satellites reuse the same frequency band by having 12 transponders operating with vertically polarized radiated signals and 12 transponders with horizontally polarized signals.<sup>†</sup> A typical 6/4-GHz frequency assignment for satellites is shown in Fig. 8-10. The transponders are denoted by C1 for channel 1, C2 for channel 2, and so on. These satellites are used mainly to relay signals for CATV systems.

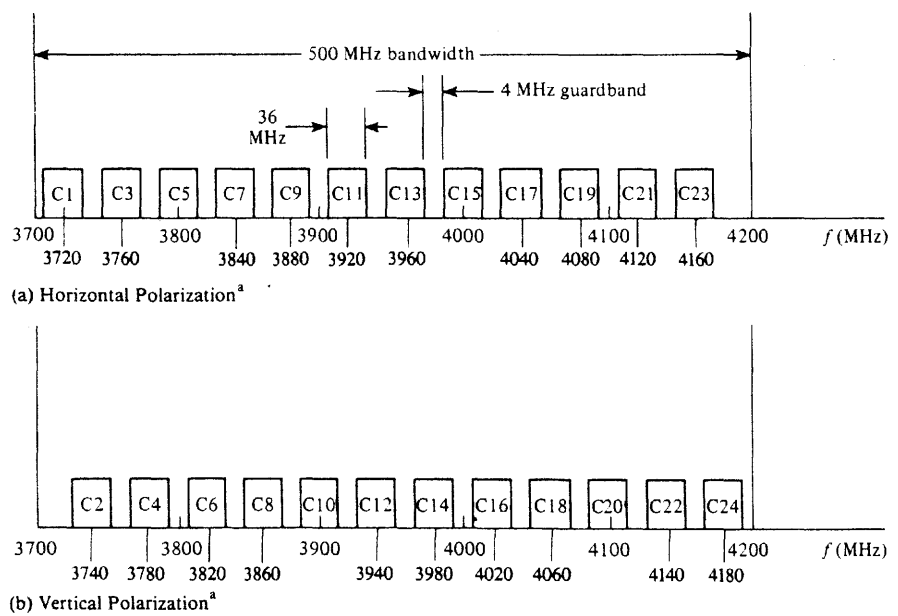
### Digital and Analog Television Transmission

TV may be relayed via satellite using either digital or analog transmission techniques.

For digital transmission, the baseband video signal is sampled and digitized. The data is usually compressed to conserve the bandwidth of the modulated satellite signal. The data are compressed by removing redundant video samples within each frame of the picture and removing redundant samples that occur frame to frame. For example, the Hughes Digital Satellite System (DSS)<sup>‡</sup> provides more than 200 channels directly to the home subscriber in the United States using two Hughes HS601 satellites. These geostationary satellites are located above the equator at  $101^\circ$  west longitude. Each DSS satellite contains 16-high-power (120 W) transponders operating in the Ku-band (12.2–12.7 GHz). The bandwidth of each transponder is 24 MHz; the effective radiated power of each transponder emitted from the satellite antenna is 48 to 53 dBw directed over the continental United States and southern Canada. Thus, a subscriber can receive the satellite signal using a relatively small receiving antenna consisting of an 18-in parabolic dish. The baseband video for each TV channel is digitized and compressed using the Motion Pictures Experts Group (MPEG) standard [Pancha and Zarki, 1994]. This compression gives an average video data rate of 3 to 6 Mbits/sec

<sup>†</sup> A vertically polarized satellite signal has an E field that is oriented vertically (parallel with the axis of rotation of the Earth). With horizontal polarization the E field is horizontal.

<sup>‡</sup> DSS is a trademark of DirecTV, Inc., a unit of GM Hughes Electronics, El Segundo, CA.



<sup>a</sup>These are the polarizations used for the Galaxy Satellites. Some of the other satellites use opposite polarization assignments.

**Figure 8-10** 6/4-GHz satellite transponder frequency plan for the downlink channels. (For the uplink frequency plan, add 2225 MHz to the numbers given above.)

for each channel, depending on the amount of motion in the video. Data for about six TV channels (video plus multichannel audio) are TDM for transmission over each satellite transponder using QPSK modulation [Thomson, 1994]. Furthermore, adaptive data compression is used to minimize the data rate of the TDM signal because the data for some of the TV channels in the TDM data stream may be encoded at a lower data rate than others depending on the amount of motion (and other properties) of each video source. More details about the DSS system are given in Study-Aid Examples SA8-1 and SA8-2. Digital encoding is also used for the U.S. high definition TV (HDTV) system. This is discussed in Sec. 8-9.

For analog TV transmission via satellite, the baseband video for a single TV channel is frequency modulated onto a carrier. For example, to relay TV signals to the head end of CATV systems, C-band satellites with 24 transponders are often used (as shown in Fig. 8-10). For each transponder, the 4.5-MHz bandwidth baseband composite video signal of a single TV channel is frequency modulated onto a 6-GHz carrier, as shown in Fig. 8-11. The composite visual signal consists of the black-and-white video signal, the color subcarrier signals, and the synchronizing pulse signal, as discussed in Sec. 8-9. The aural signal is also relayed over the same transponder by frequency modulating it onto a 6.8-MHz subcarrier that is frequency-division-multiplexed with the composite video signal. The resulting wideband signal frequency modulates the transmitter.

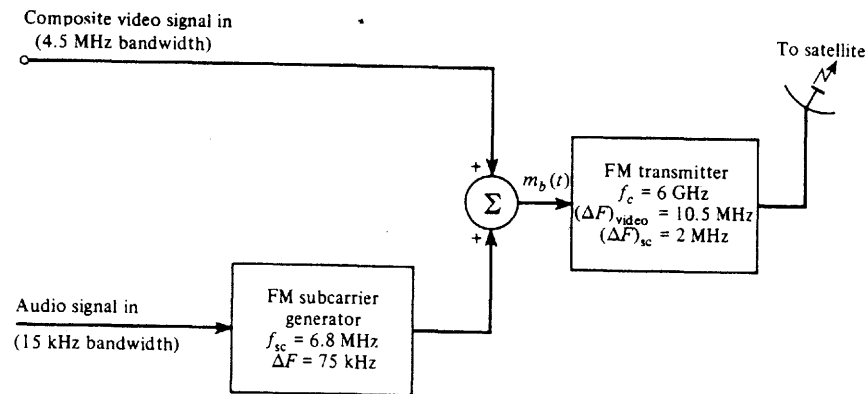


**Figure 8-11** Transmission of broadcast-quality TV signals from a ground station.

The bandwidth of the 6-GHz FM signal may be evaluated by using Carson's rule. The peak deviation of the composite video is 10.5 MHz and the peak deviation of the subcarrier is 2 MHz, giving an overall peak deviation of  $\Delta F = 12.5$  MHz. The baseband bandwidth is approximately 6.8 MHz. The transmission bandwidth is

$$B_T = 2(\Delta F + B) = 2(12.5 + 6.8) = 38.6 \text{ MHz} \quad (8-1)$$

which is accepted by the 36-MHz transponder. In addition, other wideband aural signals (0 to 15 kHz) can also be relayed by using FM subcarriers. Some typical subcarrier frequencies that are used are 5.58, 5.76, 6.2, 6.3, 6.48, 6.8, 7.38, and 7.56 MHz.

### Data and Telephone Signal Multiple Access

Satellite relays provide a channel for data and VF (telephone) signaling similar to conventional terrestrial microwave radio links. That is, data may be time-division-multiplexed into DS-1, DS-2, and so on, types of signals and (digitally) modulated onto a carrier for transmission via a satellite. The data may also be frequency-division-multiplexed. In this case, modems are used to convert the data into signals that are compatible with VF group, supergroup, or mastergroup bandwidths, which are (analog) modulated onto the carrier for transmission to the satellite.

Satellite communication systems do differ from terrestrial microwave links in the techniques used for *multiple access* of a single transponder by multiple uplink and multiple downlink stations. Four main methods are used for multiple access.

1. *Frequency-division multiple access* (FDMA), which is similar to FDM
2. *Time-division multiple access* (TDMA), which is similar to TDM<sup>†</sup>
3. *Code-division multiple access* (CDMA) or *spread-spectrum multiple access* (SSMA)

4. *Space-division multiple access* (SDMA) where narrow-beam antenna patterns are switched from one direction to another<sup>†</sup>

In addition, either of the following may be used:

1. A *fixed assigned multiple access* (FAMA) mode using either FDMA, TDMA, or CDMA techniques
2. A *demand assigned multiple access* (DAMA) mode using either FDMA, TDMA, or CDMA

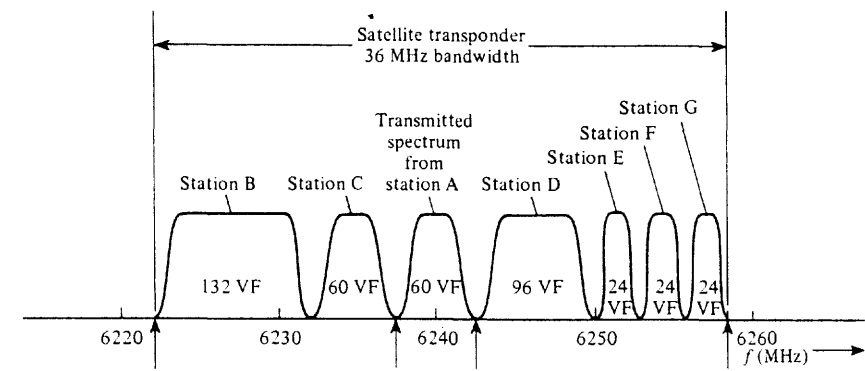
In the FAMA mode the FDMA, TDMA, or CDMA format does not change, even though the traffic load of various Earth stations changes. For example, there is more telephone traffic between Earth stations during daylight hours (local time) than between these stations in the hours after midnight. In the FAMA mode a large number of satellite channels would be idle during the early morning hours since they are fixed assigned. In the DAMA mode, the FDMA or TDMA formats are changed as needed depending on the traffic demand of the Earth stations involved. Consequently, the DAMA mode uses the satellite capacity more efficiently, but it usually costs more to implement and maintain.

In CDMA the different users share the same frequency band simultaneously in time, as opposed to FDMA and TDMA, where users are assigned different frequency slots or time slots. With CDMA each user is assigned a particular digitally encoded waveform  $\varphi_j(t)$  that is (nearly) orthogonal to the waveforms used by the others (see Secs. 2-4 and 5-12). Data may be modulated onto this waveform, transmitted over the communication system, and recovered. For example, if one bit of data,  $m_j$ , is modulated onto the waveform, the transmitted signal from the  $j$ th user might be  $m_j \varphi_j(t)$  and the composite CDMA signal from all users would be  $w(t) = \sum_j m_j \varphi_j(t)$ . The data from the  $j$ th user could be recovered from the CDMA waveform by evaluating  $\int_0^T w(t) \varphi_j(t) dt = m_j$ , where  $T$  is the length of encoded waveform  $\varphi_j(t)$ . Gold codes are often used to obtain the encoded waveforms.

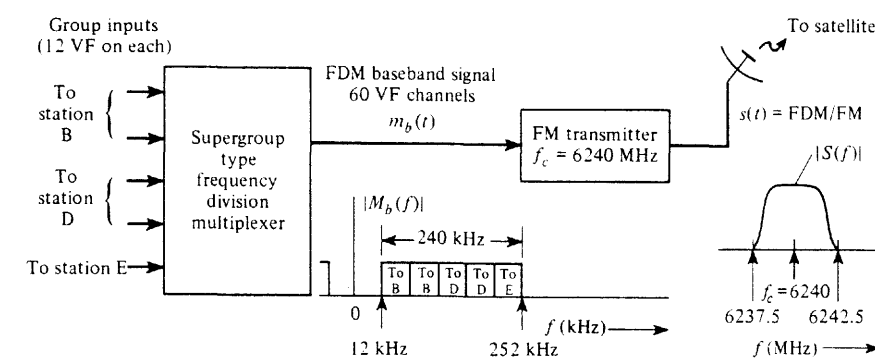
### Example 8-1 FIXED ASSIGNED MULTIPLE-ACCESS MODE USING AN FDMA FORMAT

A good example of the fixed assigned multiple-access technique is the FDM/FM format used with the *Intelsat IV* and *V* series satellites. Suppose that ground station A is sharing one 36-MHz transponder in the FDM mode with stations B, C, D, E, F, and G, which are all transmitting simultaneously through the transponder, as shown by their frequency assignments in Fig. 8-12a. Station A has an assigned band of 6237.5 to 6242.5 MHz in which it can transmit 60 VF channels using FDM/FM. This is the capacity of one supergroup. Suppose that station A has traffic as follows: 24 VF channels for station B, 24 VF channels for station D, and 12 VF channels for station E; then the equipment configuration would be as shown in Fig. 8-12b. In a similar way,

<sup>†</sup> Satellite-switched time-division multiple access (SS-TDMA) can also be used. With SS-TDMA satellites, different narrow-beam antennas are switched in at the appropriate time in the TDMA frame period to direct the transmit and receive beams to the desired direction. Thus, with multiple SS-TDMA beams the same transmit and receive frequencies may be reused simultaneously so that the capacity of the SS-TDMA satellite is much larger than that of a TDMA satellite. The *Intelsat VI* is a SS-TDMA satellite.



(a) Transponder Frequency Allocation



(b) Station A Ground Transmitting Equipment

Figure 8-12 Fixed assigned FDMA format for satellite communications.

the remaining spectrum of the 36-MHz transponder is divided among the other Earth stations according to their traffic needs on a fixed assignment basis.

### Example 8-2 SPADE SYSTEM

The *Intelsat IV* and *V* series satellites may also be operated in a DAMA mode using an FDMA format consisting of a single QPSK carrier for each telephone (VF) channel. This type of signaling is called *single channel per carrier* (SCPC), in which 800 QPSK signals may be accommodated in the 36-MHz bandwidth of the transponder, as shown in Fig. 8-13a. Thus 800 VF messages may be transmitted simultaneously through one satellite transponder, where each QPSK signal is modulated by a 64-kbit/s PCM (digitized) voice signal (studied earlier in Example 3-1 and used as inputs to the North American digital hierarchy shown in Fig. 3-40). This SCPC-DAMA technique, illustrated in Fig. 8-14, is called the *SPADE system*, which is an acronym for single channel per carrier, pulse code modulation, multiple access, demand assignment equipment [Edelson and Werth, 1972].

The demand assignment of the carrier frequency for the QPSK signal to a particular Earth station uplink is carried out by TDM signaling in the *common signaling channel* (CSC) (see Fig.

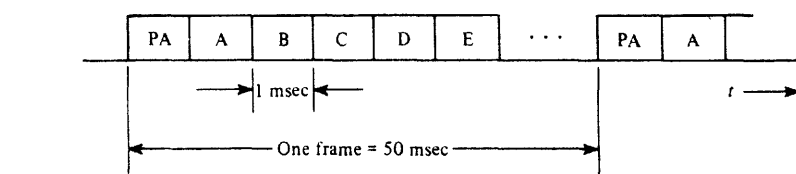
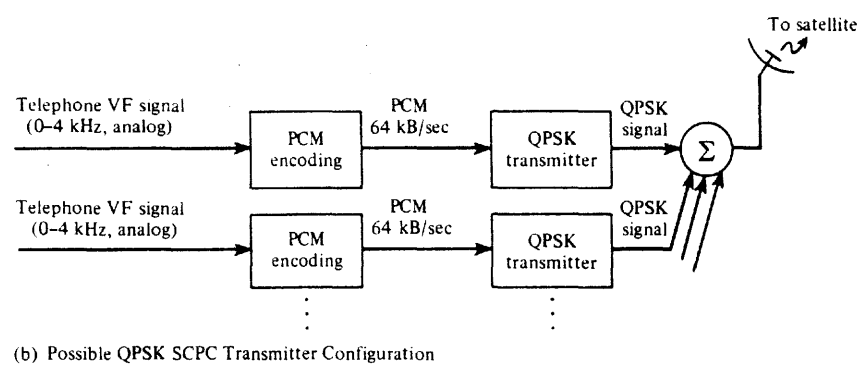
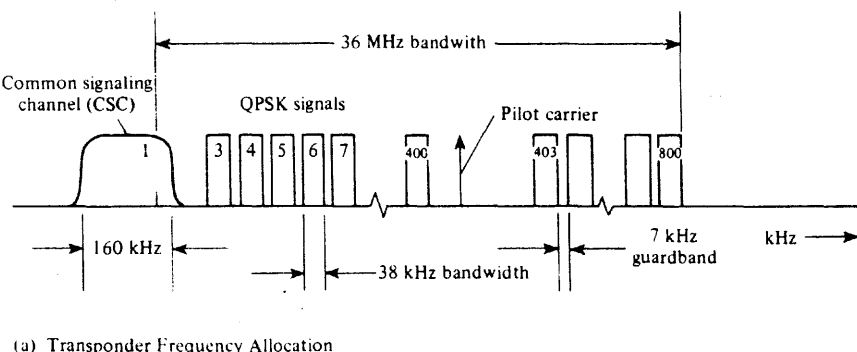


**Figure 8-13** SPADE satellite communication system for telephone VF message transmission.

(Fig. 8-13a), The CSC consists of a 128-kbit/s PSK signal that is time shared among the Earth stations by using a TDMA format, as shown in Fig. 8-13c. PA denotes the synchronizing preamble that occurs at the beginning of each frame, and A, B, C, and so on denote the 1-msec time slots that are reserved for transmission by Earth stations A, B, C, and so on. In this way 49 different Earth stations may be accommodated in the 50-msec frame. For example, if Earth station B wishes to initiate a call to Earth station D, station B selects a QPSK carrier frequency randomly from among the idle channels that are available and transmits this frequency information along the address of station D (the call destination) in the station B-TDMA time slot. If it is assumed that the frequency has not been selected by another station for another call station D will acknowledge the request in its TDMA time slot. This acknowledgement would be heard by station B about 600 msec after its TDMA signaling request since the round trip time delay to the

satellite is 240 ms, plus equipment delays and the delay to the exact time slot assigned to station D with respect to that of station B. If another station, say station C, had selected the same frequency during the request period, a busy signal would be received at station B, and station B would randomly select another available frequency and try again. When the call is over, disconnect signals are transmitted in the TDMA time slot and that carrier frequency is returned for reuse. Because the CSC signaling rate is 128 kbit/s and each time slot is 1 ms in duration, 128 bits are available for each accessing station to use for transmitting address information, frequency request information, and disconnect signaling.

In practice, because only 49 time slots are available for the TDMA mode, a number of the SCPC frequencies are assigned on a fixed basis.

In FDMA, such as the SPADE system, when the carriers are turned on and off on demand, there is amplitude modulation on the composite 36-MHz-wide signal that is being amplified by the transponder TWT. Consequently, the drive level of the TWT has to be "backed off" so that the amplifier is not saturated and will be sufficiently linear. Then the intermodulation products will be sufficiently low. On the other hand, if a single constant-amplitude signal (such as a single-wideband FM signal used in relaying television signals), had been used, IM products would not be a consideration and the amplifier could be driven harder to provide the full saturated power output level.

As indicated earlier, TDMA is similar to TDM, where the different Earth stations send up bursts of RF energy that contain packets of information. During the time slot designated for a particular Earth station, that station's signal uses the bandwidth of the whole transponder (see Fig. 8-14). Since the Earth stations use a constant envelope modulation technique, such as QPSK, and only one high-rate modulated signal is being passed through the

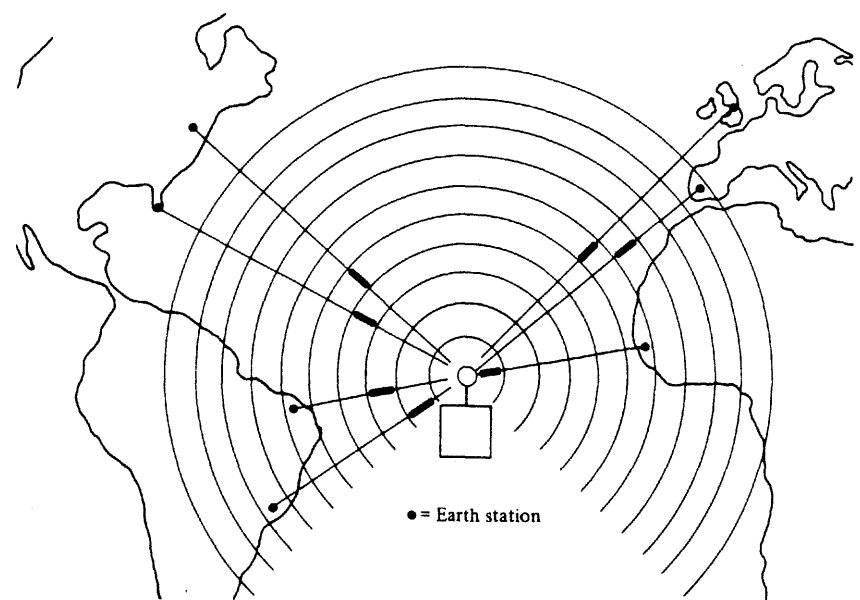


**Figure 8-14** Interleaving of bursts in a TDMA satellite.

transponder during any time interval, no inband IM products are generated (as in the FDMA technique described earlier). Thus the final TWT amplifier in the satellite may be driven into saturation for more power output. This advantage of TDMA over FDMA may be compared with the main disadvantage of the TDMA technique. The disadvantage of TDMA is that strict burst timing is required at the Earth station in order to prevent collision of the bursts at the satellite. In other words, the burst from a particular Earth station has to arrive at the satellite in the exact time slot designated for that station, so that its signal will not interfere with the bursts that are arriving from other Earth stations that are assigned adjacent time slots. Because the ground stations are located at different distances from the satellite and may use different equipment configurations, the time delay from each Earth station to the satellite will be different, and this must be taken into account when the transmission time for each Earth station is computed. In addition the satellite may be moving with respect to the Earth station, which means that the time delay is actually changing with time. Another disadvantage of TDMA is that the Earth stations are probably transmitting data that have arrived from synchronous terrestrial lines; consequently, the Earth station equipment must contain a large memory in which to buffer the data, which are read out at high speed when the packet of information is sent to the satellite.

A typical TDMA frame format for the data being relayed through a satellite is shown in Fig. 8-15. In this example, station B is sending data to stations A, E, G, and H. One frame consists of data arriving from each Earth station. At any time, only one Earth station provides the time reference signal for the other Earth stations to use for computation of their transmitting time for their data bursts (frame synchronization). The burst lengths from the various stations could be different depending on the traffic volume. The second part of the figure shows an exploded view of a typical burst format that is transmitted from station B. This consists of two main parts, the preamble and data that are being sent to other Earth stations from station B. The preamble includes a guard time before transmission is begun. Then

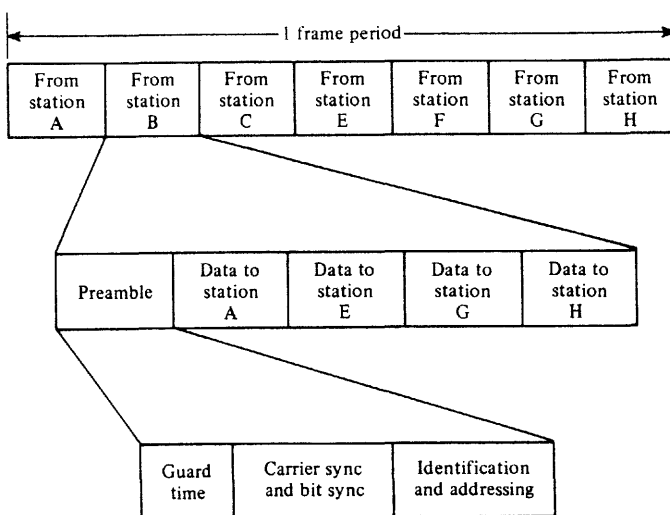


Figure 8-15 Typical TDMA frame format.

a string of synchronization characters is transmitted that give the carrier sync recovery loops and bit timing recovery loops (in the ground station receivers) time to lock onto this burst from station B. The end of the preamble usually contains a unique word that identifies the burst as coming from station B and might indicate the addresses (stations) for which the data are intended.

Another multiple access method which is similar to TDMA is the *ALOHA* technique [Lam, 1979]. Here the multiple users send bursts of data, called *packets*, whenever they wish. If two or more of the bursts overlap in time, called a *collision*, the users involved retransmit their packets after a random time delay. It is hoped that a second collision will not occur. If it does, the retransmission process is repeated until each party is successful. This technique has the advantage of being relatively inexpensive to implement, but it will not work if there is heavy traffic loading on the satellite. Then the satellite becomes saturated with colliding packets, and the collisions can be avoided only by stopping all new transmissions and increasing the random delay required before retransmission. A more elaborate technique is called *slotted ALOHA*. Here the packets are transmitted at random, but only in certain time slots. This avoids collisions due to partial packet overlap.

*Very small aperture terminals* (VSAT) have become popular with the availability of Ku-band satellites and with the recent advances that have made low-cost terminals possible. "Very small aperture" implies that these systems use Earth-terminal antennas that are relatively small, about 1 or 2 m in diameter. Solid-state power amplifiers (1 to 2 W), low-cost frequency converters, digital processing, and VLSI circuits have made VSATs feasible. The objective of VSAT systems is to provide low-cost data and voice transmission directly to users such as auto dealerships, banks (automatic teller machines), brokerage firms, pipeline companies (monitor and control), hotels and airlines (reservations), retail stores (data networks), and corporations (point-to-multipoint transmission). Typically, VSATs offer high-quality transmission (bit error rates of less than  $10^{-7}$  for 99.5% of the time) at data rates from 100 bits/sec to 64 kbytes/sec [Chakraborty, 1988; Maral, 1995]. Many users share a single satellite transponder via SCPC, TDMA, or CDMA so that the user's cost can be substantially less than that for the same type of service provided by the long-distance public telephone network [Dorf, 1993, p. 2201; Maral, 1995; Rana, McCoskey, and Check, 1990].

### Personal Communications via Satellite

Satellite systems are now being developed for communication directly to *personal communication system* (PCS) devices, such as hand-held portable telephones and mobile data terminals. In general, these PCS devices use small nondirectional antennas that have very little gain. Consequently, the signal from the satellite needs to be relatively strong at the user's location. Strong user signals can be achieved if the distance to the satellite is relatively small—around 400 to 1200 miles. Thus *low-Earth-orbit* (LEO) satellites, which are not geosynchronous, provide a solution to this problem. Other solutions are *medium-Earth-orbit* (MEO) satellites (5000-mile altitude) and *high-Earth-orbit* (HEO) satellites (10,000 mile altitude) with large high-gain antennas [Balduino, 1995; Wu, Miller, Pritchard, and Pickholtz, 1994]. Table 8-3 shows some of the LEO/MEO/HEO systems that are designed for use with hand-held PCS devices. These systems provide voice, data, and facsimile (FAX) service. The satellites are distributed around the globe in inclined (nonequatorial) orbits so

TABLE 8-3 PERSONAL COMMUNICATION SATELLITE SYSTEMS

	System			
	Globalstar	Immarstat P	Iridium	Odyssey
Owner(s)	Loral/Qualcomm	ICO Global Comm. Ltd.	Motorola	TRW
Development cost (billion \$)	1.6	2.6	3.4	1.3
Orbit	LEO	HEO	LEO	MEO
Orbit altitude (stat. miles)	880	11,895	485	6,450
No. of satellites	48	10	66	12
No. of orbit planes	8	2	6	3
Inclination of planes	52°	45°	86.4°	55°
Frequencies, up/down (GHz)	1.6/2.4	2.4/2.4	1.6/1.6	1.6/1.6
No. of VF channels	5,000		3,800	4,600
Cost of hand-held phones (\$)	750	500	2,500	300
Monthly service charge (\$)	25	30	50	24
Cost/min VF channel (\$)	0.30	2.00	3.00	0.65
Year in Service	1997	2000	1998	1998

that worldwide communication will be provided. These systems use cellular telephone technology (see Sec. 8-8) so that service can be provided to a large number of users. Most of the PCS devices are designed to seek local TELCO service first (via local cellular phone systems or local wireless systems) and, if local service is not available, connect to the satellite system for service.

More details about satellite systems can be obtained from literature devoted specifically to that subject [Gordon and Morgan, 1993; Ha, 1986; Ha, 1989; MaGill, Natali, and Edwards, 1994; Pratt and Bostian, 1986; Spilker, 1977; Xiong, 1994].

In the next section, a procedure is developed for calculating the signal strength of a received satellite signal and for evaluating the amount of noise that is present in a receiving system. This will be used to evaluate the BER at the output of the digital receivers and the SNR at the output of analog receivers.

## 8-6 LINK BUDGET ANALYSIS

In this section, formulas will be developed for the signal-to-noise ratio at the detector input as a function of the transmitted *effective isotropic radiated power* (EIRP), the free-space loss, the receiver antenna gain, and the receiver system noise figure. These results will allow us to evaluate the quality of the receiver output (as measured by the probability of bit error for digital systems and output signal-to-noise ratio for analog systems), provided that the noise characteristics of the receiver detector circuit are known.

### Signal Power Received

In communication systems the received signal power (as opposed to the voltage or current level) is the important quantity since it is the output signal power that ultimately drives the display device, which, for example, may be a loudspeaker. Consequently, it is the *power* of the received signal that is of prime importance while trying to *minimize* the effect of *noise sources* that feed into the system and get amplified. The voltage gain, current gain, and impedance levels have to be such that the required power gain is achieved. In FET circuits it is accomplished by using relatively large voltage levels and small currents (high-impedance circuitry). With bipolar transistors power gain is achieved with relatively small voltages and large currents (low-impedance circuitry).

A block diagram of a communication system with a free-space transmission channel is shown in Fig. 8-16. The overall power gain (or power transfer function) of the channel is

$$\frac{P_{Rx}}{P_{Tx}} = G_{AT} G_{FS} G_{AR} \quad (8-2)$$

where  $P_{Tx}$  is the signal power into the transmitting antenna,  $G_{AT}$  is the transmitting antenna power gain,  $G_{FS}$  is the free-space power gain<sup>†</sup> (which is orders of magnitude less than one in typical communication systems),  $G_{AR}$  is the receiving antenna power gain, and  $P_{Rx}$  is the signal power into the receiver.

To use this relationship, these gains should be expressed in terms of useful antenna and free-space parameters [Kraus, 1986]. Here  $G_{AT}$  and  $G_{AR}$  are taken to be the power gains with respect to an isotropic antenna.<sup>‡</sup> The EIRP is

$$P_{EIRP} = G_{AT} P_{Tx} \quad (8-3)$$

The antenna power gain is defined as

$$G_A = \frac{\text{radiation power density of the actual antenna in the direction of maximum radiation}}{\text{radiation power density of an isotropic antenna with the same power input}}$$

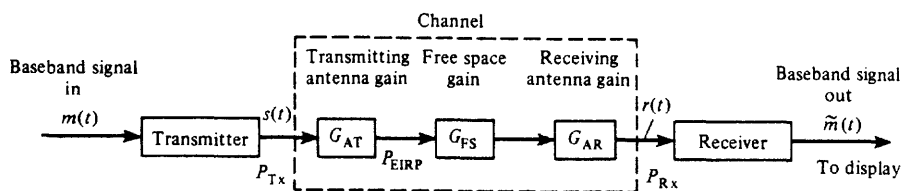


Figure 8-16 Block diagram of a communication system with a free-space transmission channel.

<sup>†</sup> A gain transfer function is the output quantity divided by the input quantity, whereas a loss transfer function is the input quantity divided by the output quantity.

<sup>‡</sup> An isotropic antenna is a nonrealizable theoretical antenna that radiates equally well in all directions and is a useful reference for comparing practical antennas.

TABLE 8-4 ANTENNA GAINS AND EFFECTIVE AREAS

Type of Antenna	Power Gain, $G_A$ (absolute units)	Effective Area, $A_e$ (m <sup>2</sup> )
Isotropic	1	$\lambda^2/4\pi$
Infinitesimal dipole or loop	1.5	$1.5\lambda^2/4\pi$
Half-wave dipole	1.64	$1.64\lambda^2/4\pi$
Horn (optimized), mouth area, $A$	$10A/\lambda^2$	$0.81A$
Parabola or "dish" with face area, $A$	$7.0A/\lambda^2$	$0.56A$
Turnstile (two crossed dipoles fed 90° out of phase)	1.15	$1.15\lambda^2/4\pi$

where the power density (W/m<sup>2</sup>) is evaluated at the same distance,  $d$ , for both antennas. The gain for some practical antennas is given in Table 8-4.

The power density (W/m<sup>2</sup>) of an isotropic antenna at a distance  $d$  from the antenna is

$$\text{power density at } d = \frac{\text{transmitted power}}{\text{area of a sphere with radius } d} = \frac{P_{\text{EIRP}}}{4\pi d^2} \quad (8-4)$$

The FCC and others often specify the strength of an electromagnetic field by the field intensity,  $E$  (V/m), instead of power density (W/m<sup>2</sup>). The two are related by

$$\text{power density} = \frac{E^2}{377} \quad (8-5)$$

where the power density and the field strength are evaluated at the same point in space and 377 Ω is the *free-space intrinsic impedance*. If the receiving antenna is placed at  $d$  meters from the transmitting antenna, it will act like a "catcher's mitt" and intercept the power in an effective area of  $(A_e)_{\text{Rx}}$  (m<sup>2</sup>), so that the received power will be

$$P_{\text{Rx}} = G_{\text{AT}} \left( \frac{P_{\text{Tx}}}{4\pi d^2} \right) (A_e)_{\text{Rx}} \quad (8-6)$$

where the gain of the transmitting antenna (with respect to an isotropic antenna),  $G_{\text{AT}}$ , has been included. Table 8-4 also gives the effective area for several types of antennas. The gain and the effective area of an antenna are related by

$$G_A = \frac{4\pi A_e}{\lambda^2} \quad (8-7)$$

where  $\lambda = c/f$  is the wavelength,  $c$  being the speed of light ( $3 \times 10^8$  m/s) and  $f$  the operating frequency (hertz). An antenna is a *reciprocal element*. That is, it has the same gain properties whether it is transmitting or receiving. Substituting (8-7) into (8-6), we obtain

$$\frac{P_{\text{Rx}}}{P_{\text{Tx}}} = G_{\text{AT}} \left( \frac{\lambda}{4\pi d} \right)^2 G_{\text{AR}} \quad (8-8)$$

where the free-space gain is

$$G_{\text{FS}} = \left( \frac{\lambda}{4\pi d} \right)^2 = \frac{1}{L_{\text{FS}}} \quad (8-9)$$

and  $L_{\text{FS}}$  is the free-space path loss (absolute units). The channel gain, expressed in decibel units, is obtained from (8-2):

$$(G_{\text{channel}})_{\text{dB}} = (G_{\text{AT}})_{\text{dB}} - (L_{\text{FS}})_{\text{dB}} + (G_{\text{AR}})_{\text{dB}} \quad (8-10)$$

where the free-space loss is<sup>†</sup>

$$(L_{\text{FS}})_{\text{dB}} = 20 \log \left( \frac{4\pi d}{\lambda} \right) \text{ dB} \quad (8-11)$$

For example, the free-space loss at 4 GHz for the shortest path to a synchronous satellite from Earth (22,300 miles) is 195.6 dB.

### Thermal Noise Sources

The noise power generated by a thermal noise source will be studied since the receiver noise is evaluated in terms of this phenomenon. A conductive element with two terminals may be characterized by its resistance,  $R$  ohms. This resistive or lossy element contains free electrons that have some random motion if the resistor has a temperature above absolute zero. This random motion causes a noise voltage to be generated at the terminals of the resistor. Although the noise is small, when the noise is amplified by a high-gain receiver it can become a problem. (If no noise were present, we could communicate to the edge of the universe with infinitely small power since the signal could always be amplified without having noise introduced.)

This physical lossy element, or physical resistor, can be modeled by an equivalent circuit that consists of a noiseless resistor in series with a noise voltage source (Fig. 8-17). From quantum mechanics, it can be shown that the (normalized) power spectrum corresponding to the voltage source is [Van der Ziel, 1986]

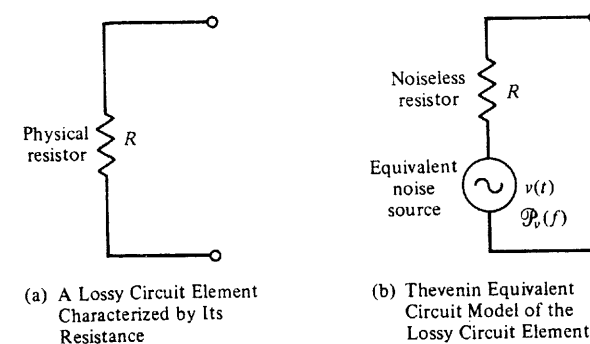


Figure 8-17 Thermal noise source.

<sup>†</sup>This free-space path loss expression can be modified to include effects of a multipath channel within an urban building environment—see (8-67).

$$\mathcal{P}_v(f) = 2R \left[ \frac{h|f|}{2} + \frac{h|f|}{e^{h|f|/(kT)} - 1} \right] \quad (8-12)$$

where

$R$  = value of the physical resistor (ohms)

$h = 6.2 \times 10^{-34}$  J-sec is Planck's constant

$k = 1.38 \times 10^{-23}$  J/K is Boltzmann's constant, where K is kelvin

$T = (273 + C)$  is the absolute temperature of the resistor (kelvin)

At room temperature for frequencies below 1000 GHz,  $[h|f|/(kT)] < 1/5$ , so that  $e^x = 1 + x$  is a good approximation. Then (8-12) reduces to

$$\mathcal{P}_v(f) = 2RkT \quad (8-13)$$

This equation will be used to develop other formulas in this text since the RF frequencies of interest are usually well below 1000 GHz and we are not dealing with temperatures near absolute zero.

If the open-circuit noise voltage that appears across a physical resistor is read by a true rms voltmeter that has a bandwidth of  $B$  hertz, then, using (2-67), the reading would be

$$V_{\text{rms}} = \sqrt{\langle v^2 \rangle} = \sqrt{2 \int_0^B \mathcal{P}_v(f) df} = \sqrt{4kTBR} \quad (8-14)$$

### Characterization of Noise Sources

Noise sources may be characterized by the maximum amount of noise power or PSD that can be passed to a load.

**DEFINITION.** The *available noise power* is the *maximum*<sup>†</sup> actual (i.e., not normalized) power that can be drawn from a source. The *available PSD* is the *maximum* actual (i.e., not normalized) PSD that can be obtained from a source.

For example, the available PSD for a thermal noise source is easily evaluated using Fig. 8-18 and (2-142).

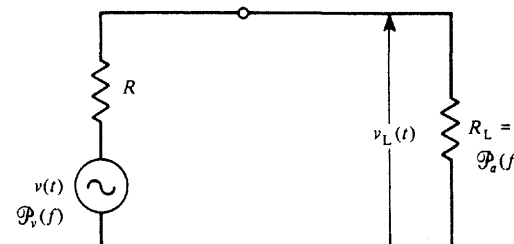


Figure 8-18 Thermal source with a matched load.

<sup>†</sup> The maximum or maximum PSD is obtained when  $Z_L(f) = Z_s^*(f)$ , where  $Z_L(f)$  is the load impedance and  $Z_s^*(f)$  is the conjugate of the source impedance.

$$\mathcal{P}_a(f) = \frac{\mathcal{P}_v(f)|H(f)|^2}{R} = \frac{1}{2}kT \text{ W/Hz} \quad (8-15)$$

where  $H(f) = \frac{1}{2}$  for the resistor divider network. The available power from a thermal source in a bandwidth of  $B$  hertz is

$$P_a = \int_{-B}^B \mathcal{P}_a(f) df = \int_{-B}^B \frac{1}{2} kT df$$

or

$$P_a = kTB \quad (8-16)$$

This equation indicates that the available noise power from a thermal source does *not* depend on the value of  $R$ , even though the open-circuit rms voltage does.

The available noise power from a source (it does not have to be a thermal source) can be specified by a number called the noise temperature.

**DEFINITION.** The *noise temperature* of a source is given by

$$T = \frac{P_a}{kB} \quad (8-17)$$

where  $P_a$  is the available power from the source in a bandwidth of  $B$  hertz.

In using this definition, it is noted that if the source happens to be of thermal origin,  $T$  will be the temperature of the device in kelvin, but if the source is not of thermal origin, the number obtained for  $T$  may have nothing to do with the physical temperature of the device.

### Noise Characterization of Linear Devices

A linear device with internal noise generators may be modeled as shown in Fig. 8-19. Any device that can be built will have some internal noise sources. As shown in the figure, the

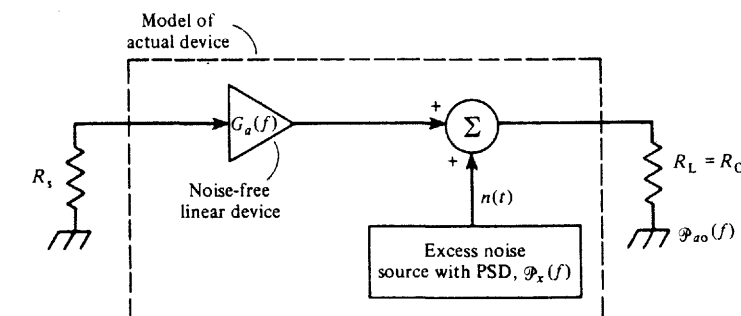


Figure 8-19 Noise model for an actual device.

device could be modeled as a noise-free device having a power gain  $G_a(f)$  and an excess noise source at the output to account for the internal noise of the actual device. Some examples of linear devices that have to be characterized in receiving systems are lossy transmission lines, RF amplifiers, down converters, and IF amplifiers.

The power gain of the devices is the available power gain.

**DEFINITION.** The *available power gain* of a linear device is

$$G_a(f) = \frac{\text{available PSD out of the device}}{\text{available PSD out of the source}} = \frac{\mathcal{P}_{ao}(f)}{\mathcal{P}_{as}(f)} \quad (8-18)$$

When  $\mathcal{P}_{ao}(f)$  is measured to obtain  $G_a(f)$ , the source noise power is made large enough so that the amplified *source noise* that appears at the output dominates any other noise. In addition, note that  $G_a(f)$  is defined in terms of actual (i.e., not normalized) PSD. In general,  $G_a(f)$  will depend on the driving source impedance as well as on elements within the device itself, but it does *not* depend on the load impedance. If the source impedance and the output impedance of the device are equal,  $G_a(f) = |H(f)|^2$ , where  $H(f)$  is the voltage or current transfer function of the linear device.

To characterize the goodness of a device, a figure of merit is needed that compares the actual (noisy) device with an ideal device (i.e., no internal noise sources). Two figures of merit, both of which tell us the same thing—namely, how bad the noise performance of the actual device is—are universally used. They are noise figure and effective input-noise temperature.

**DEFINITION.** The *spot noise figure* of a linear device is obtained by terminating the device with a thermal noise source of temperature  $T_0$  on the input and a matched load on the output as indicated in Fig. 8-19. The spot noise figure is

$$F_s(f) = \frac{\text{measured available PSD out of the actual device}}{\text{available PSD out of an ideal device with the same available gain}}$$

or

$$F_s(f) = \frac{\mathcal{P}_{ao}(f)}{(kT_0/2)G_a(f)} = \frac{(kT_0/2)G_a(f) + \mathcal{P}_x(f)}{(kT_0/2)G_a(f)} > 1 \quad (8-19)$$

The value of  $R_s$  is the same as the source resistance that was used when  $G_a(f)$  was evaluated. A standard temperature of  $T_0 = 290$  K is used as adopted by the IEEE [Haus, 1963].

$F_s(f)$  is called the *spot noise figure* because it refers to the noise characterization at a particular “spot” or frequency in the spectrum. Note that  $F_s(f)$  is always greater than unity for an actual device, but it is nearly unity if the device is almost an ideal device.  $F_s(f)$  is a function of the source temperature,  $T_0$ . Consequently, when the noise figure is evaluated, a standard temperature of  $T_0 = 290$  K is used. This corresponds to a room temperature of 62.3°F.

Often an average noise figure instead of a spot noise figure is desired. The average is measured over some bandwidth  $B$ .

**DEFINITION.** The *average noise figure* is

$$F = \frac{\mathcal{P}_{ao}}{kT_0 \int_{f_0-B/2}^{f_0+B/2} G_a(f) df} \quad (8-20)$$

where

$$\mathcal{P}_{ao} = 2 \int_{f_0-B/2}^{f_0+B/2} \mathcal{P}_{ao}(f) df$$

is the measured available output in a bandwidth  $B$  hertz wide centered on a frequency of  $f_0$  and  $T_0 = 290$  K.

If the available gain is constant over the band so that  $G_a(f) = G_a$  over the frequency interval  $(f_0 - B/2) \leq f \leq (f_0 + B/2)$ , the noise figure becomes

$$F = \frac{\mathcal{P}_{ao}}{kT_0 BG_a} \quad (8-21a)$$

The noise figure is often measured by using the Y-factor method. This technique is illustrated by Prob. 8-15. The Hewlett-Packard HP8970B noise figure meter uses the Y-factor method for measuring the noise figure of devices.

The noise figure can also be specified in decibel units,<sup>†</sup>

$$F_{dB} = 10 \log(F) = 10 \log\left(\frac{\mathcal{P}_{ao}}{kT_0 BG_a}\right) \quad (8-21b)$$

For example, suppose that the manufacturer of an RF preamplifier specifies that an RF preamp has a 2-dB noise figure. This means that the actual noise power at the output is 1.58 times the power that would occur because of amplification of noise from the input. The other figure of merit for evaluating the noise performance of a linear device is the effective input-noise temperature, which is illustrated in Fig. 8-20.

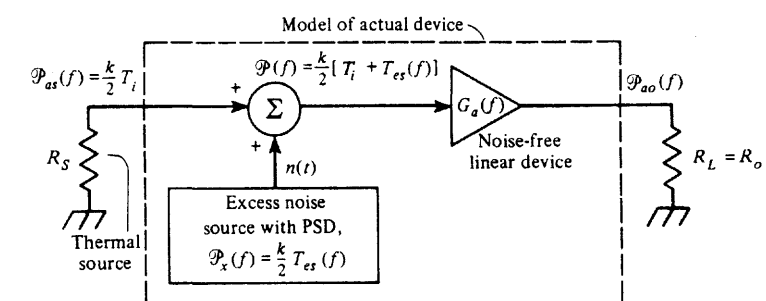


Figure 8-20 Another noise model for an actual device.

<sup>†</sup> Some authors call  $F$  the *noise factor* and  $F_{dB}$  the *noise figure*.

**DEFINITION.** The *spot effective input-noise temperature*,  $T_{es}(f)$ , of a linear device is the *additional* temperature required for an input source, which is driving an ideal (noise-free) device, to produce the same available PSD at the ideal device output as is obtained from the actual device when it is driven by the input source of temperature  $T_i$  kelvin. That is,  $T_{es}(f)$  is defined by

$$\mathcal{P}_{ao}(f) = G_a(f) \frac{k}{2} [T_i + T_{es}(f)] \quad (8-22)$$

where  $\mathcal{P}_{ao}(f)$  is the available PSD out of the actual device when driven by an input source of temperature  $T_i$ , and  $T_{es}(f)$  is the spot effective input-noise temperature.

The *average effective input-noise temperature*,  $T_e$ , is defined by the equation

$$P_{ao} = k(T_i + T_e) \int_{f_0 - B/2}^{f_0 + B/2} G_a(f) df \quad (8-23)$$

where the measured available noise power out of the device in a band  $B$  hertz wide is

$$P_{ao} = 2 \int_{f_0 - B/2}^{f_0 + B/2} \mathcal{P}_{ao}(f) df \quad (8-24)$$

Because  $G_a(f)$  depends on the source impedance as well as on the device parameters,  $T_e(f)$  will depend on the source impedance used as well as on the characteristics of the device itself, but it is independent of the value of  $T_i$  used. In the definition of  $T_e$ , note that the IEEE standards do not specify that  $T_i = T_0$  since the value of  $T_e$  obtained does not depend on the value of  $T_i$  that is used. However,  $T_i = T_0 = 290$  may be used for convenience. The effective input-noise temperature can also be evaluated by the Y-factor method, as illustrated by Prob. 8-15.

When the gain is flat (constant) over the frequency band,  $G_a(f) = G_a$ , the effective input-noise temperature is simply

$$T_e = \frac{P_{ao} - kT_i G_a B}{kG_a B} \quad (8-25)$$

Note that  $T_{es}(f)$  and  $T_e$  are greater than zero for an actual device, but if the device is nearly ideal (small internal noise sources), they will be very close to zero.

When  $T_e$  was evaluated by use of (8-23), an input source was used with some convenient value for  $T_i$ . However, when the device is used in a system, the available noise power from the source will be different if  $T_i$  is different. For example, suppose that the device is an RF preamplifier and the source is an antenna. The available power out of the amplifier when it is connected to the antenna is now<sup>†</sup>

$$P_{ao} = 2 \int_{f_0 - B/2}^{f_0 + B/2} \mathcal{P}_{as}(f) G_a(f) df + kT_e \int_{f_0 - B/2}^{f_0 + B/2} G_a(f) df \quad (8-26)$$

<sup>†</sup> The value of  $P_{ao}$ , in (8-26) and (8-27) is different from that in (8-23), (8-24), and (8-25).

## Sec. 8-6 Link Budget Analysis

where  $\mathcal{P}_{as}(f)$  is the available PSD out of the source (antenna).  $T_e$  is the average effective input temperature of the amplifier that was evaluated by using the input source  $T_i$ . If the gain of the amplifier is approximately constant over the band, this reduces to

$$P_{ao} = G_a P_{as} + kT_e B G_a \quad (8-27)$$

where the available power from the source (antenna) is

$$P_{as} = 2 \int_{f_0 - B/2}^{f_0 + B/2} \mathcal{P}_{as}(f) df \quad (8-28)$$

Furthermore, the available power from the source might be characterized by its noise temperature,  $T_s$ , so that, using (8-17),

$$P_{as} = kT_s B \quad (8-29)$$

In satellite Earth station receiving applications, the antenna (source) noise temperature might be  $T_s = 32$  K at 4 GHz for a parabolic antenna where the noise from the antenna is due to cosmic radiation and to energy received from the ground as the result of the sidelobe beam pattern of the antenna. (The Earth acts as a blackbody noise source with  $T = 280$  K.) Note that the  $T_s = 32$  K of the antenna is "caused" by *radiation resistance*, which is not the same as a loss resistance ( $I^2R$  losses) associated with a thermal source and  $T_s$  has no relation to the physical temperature of the antenna.

In summary, two figures of merit have been defined: noise figure and effective input-noise temperature. By combining (8-19) and (8-22) where  $T_i = T_0$ , a relationship between these two figures of merit for the spot measures is obtained:

$$T_{es}(f) = T_0 [F_s(f) - 1] \quad (8-30a)$$

Here  $T_i = T_0$  is required because  $T_i = T_0$  is used in the definition for the noise figure that precedes (8-19).

Using (8-21a) and (8-25) where  $T_i = T_0$ , we obtain the same relationship for the average measures:

$$T_e = T_0 (F - 1) \quad (8-30b)$$

### Example 8-3 $T_e$ AND $F$ FOR A TRANSMISSION LINE

The effective input-noise temperature,  $T_e$ , and the noise figure,  $F$ , for a lossy transmission line (a linear device) will now be evaluated.<sup>†</sup> This can be accomplished by terminating the transmission line with a source and a load resistance (all having the same physical temperature) that are both equal to the characteristic impedance of the line, as shown in Fig. 8-21. The gain of the transmis-

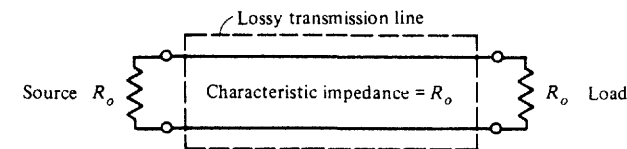


Figure 8-21 Noise figure measurement of a lossy transmission line.

<sup>†</sup> These results also hold for the  $T_e$  and  $F$  of (impedance) matched attenuators.

sion line is  $G_a = 1/L$ , where  $L$  is the transmission line loss (power in divided by power out) in absolute units (i.e., not dB units). Looking into the output port of the transmission line, one sees an equivalent circuit that is resistive (thermal source) with a value of  $R_0$  ohms since the input of the line is terminated by a resistor of  $R_0$  ohms (the characteristic impedance). Assume that the physical temperature of the transmission line is  $T_L$  as measured on the Kelvin scale. Since the line acts as a thermal source, the available noise power at its output is  $P_{ao} = kT_L B$ . Using (8-25) where the source is at the same physical temperature,  $T_e = T_L$  we get

$$T_e = \frac{kT_L B - kT_L G_a B}{kG_a B} = T_L \left( \frac{1}{G_a} - 1 \right)$$

Thus the effective input-noise temperature for the transmission line is

$$T_e = T_L(L - 1) \quad (8-31a)$$

where  $T_L$  is the physical temperature (Kelvin) of the line and  $L$  is the line loss.

If the physical temperature of the line happens to be  $T_0$ , this becomes

$$T_e = T_0(L - 1) \quad (8-31b)$$

The noise figure for the transmission line is obtained by using (8-30b) to convert  $T_e$  to  $F$ . Thus, substituting (8-31a) into (8-31b), we get

$$T_L(L - 1) = T_0(F - 1)$$

Solving for  $F$ , we obtain the noise figure for the transmission line

$$F = 1 + \frac{T_L}{T_0}(L - 1) \quad (8-32a)$$

where  $T_L$  is the physical temperature (Kelvin) of the line,  $T_0 = 290$ , and  $L$  is the line loss. If the physical temperature of the line is 290 K (63°F), (8-32a) reduces to

$$F = \frac{1}{G_a} = L \quad (8-32b)$$

In decibel measure, this is  $F_{dB} = L_{dB}$ . In other words, if a transmission line has a 3-dB loss, it has a noise figure of 3 dB provided that it has a physical temperature of 63°F. If the temperature is 32°F (273 K), the noise figure, using (8-32a), will be 2.87 dB. Thus  $F_{dB}$  is approximately  $L_{dB}$ , if the transmission line is located in an environment (temperature range) that is inhabitable by humans.

### Noise Characterization of Cascaded Linear Devices

In a communication system several linear devices, supplied by different vendors, are often cascaded together to form an overall system, as indicated in Fig. 8-22. In a receiving system these devices might be an RF preamplifier connected to a transmission line that feeds a down converter and an IF amplifier. (As discussed in Sec. 4-11, the down converter is a linear device and may be characterized by its conversion power gain and its noise figure.) For system performance calculations, we need to evaluate the overall power gain,  $G_a$ , and the overall noise characterization (which is given by the overall noise figure or the overall effec-

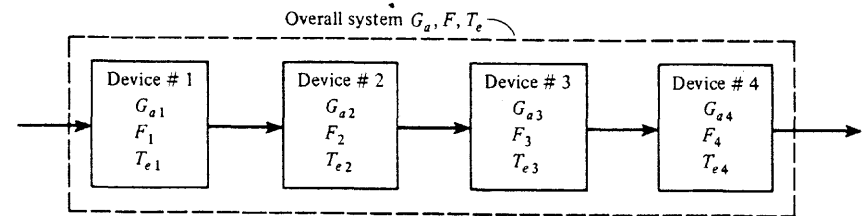


Figure 8-22 Cascade of four devices.

tive input-noise temperature) from the specifications for the individual devices provided by the vendors.

The overall available power gain is

$$G_a(f) = G_{a1}(f)G_{a2}(f)G_{a3}(f)G_{a4}(f) \dots \quad (8-33)$$

because, for example, for a four-stage system,

$$G_a(f) = \frac{\mathcal{P}_{ao4}}{\mathcal{P}_{as}} = \left( \frac{\mathcal{P}_{ao1}}{\mathcal{P}_{as}} \right) \left( \frac{\mathcal{P}_{ao2}}{\mathcal{P}_{ao1}} \right) \left( \frac{\mathcal{P}_{ao3}}{\mathcal{P}_{ao2}} \right) \left( \frac{\mathcal{P}_{ao4}}{\mathcal{P}_{ao3}} \right)$$

**THEOREM.** *The overall noise figure for cascaded linear devices is<sup>†</sup>*

$$F = F_1 + \frac{F_2 - 1}{G_{a1}} + \frac{F_3 - 1}{G_{a1}G_{a2}} + \frac{F_4 - 1}{G_{a1}G_{a2}G_{a3}} + \dots \quad (8-34)$$

as shown in Fig. 8-22 (for a four-stage system).

**Proof.** This result may be obtained by using an excess-noise model of Fig. 8-19 for each stage. We will prove the result for a two-stage system as modeled in Fig. 8-23. The overall noise figure is

$$F = \frac{P_{ao2}}{(P_{ao2})_{ideal}} = \frac{P_{x2} + P_{ao1}G_{a2}}{G_{a1}G_{a2}P_{as}}$$

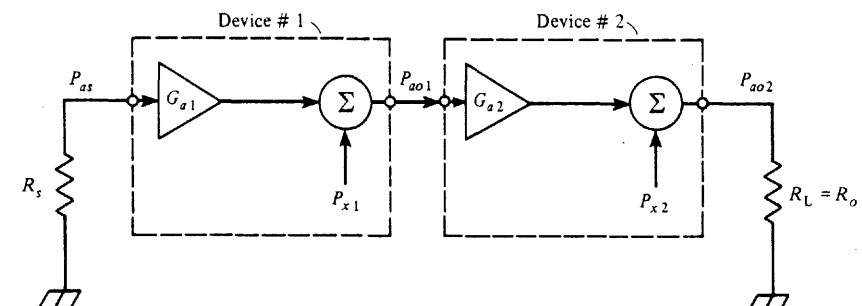


Figure 8-23 Noise model for two cascaded devices.

<sup>†</sup> This is known as Friis's noise formula.

which becomes

$$F = \frac{P_{x2} + G_{a2}(P_{x1} + G_{a1}P_{as})}{G_{a1}G_{a2}P_{as}} \quad (8-35)$$

where  $P_{as} = kT_0B$  is the available power from the thermal source.  $P_{x1}$  and  $P_{x2}$  can be obtained from the noise figures of the individual devices by using Fig. 8-19, so that for the  $i$ th device

$$F_i = \frac{P_{aoi}}{G_{ai}P_{as}} = \frac{P_{xi} + G_{ai}P_{as}}{G_{ai}P_{as}}$$

or

$$P_{xi} = G_{ai}P_{as}(F_i - 1) \quad (8-36)$$

Substituting this equation into (8-35) for  $P_{x1}$  and  $P_{x2}$ , we obtain

$$F = F_1 + \frac{F_2 - 1}{G_{a1}}$$

which is identical to (8-34) for the case of two cascaded stages. In a similar way (8-34) can be shown to be true for any number of stages.

Looking at (8-34), we see that if the terms  $G_{a1}$ ,  $G_{a1}G_{a2}$ ,  $G_{a1}G_{a2}G_{a3}$ , and so on, are relatively large,  $F_1$  will dominate the overall noise figure. Thus, in receiving system design, it is important that the first stage have a low noise figure and a large available gain so that the noise figure of the overall system will be as small as possible.

The overall effective input-noise temperature of several cascaded stages can also be evaluated.

**THEOREM.** *The overall effective input-noise temperature for cascaded linear devices is*

$$T_e = T_{e1} + \frac{T_{e2}}{G_{a1}} + \frac{T_{e3}}{G_{a1}G_{a2}} + \frac{T_{e4}}{G_{a1}G_{a2}G_{a3}} + \dots \quad (8-37)$$

as shown in Fig. 8-22.

A proof of this result is left for the reader as an exercise.

For further study concerning the topics of effective input-noise temperature and noise figure, the reader is referred to an authoritative monograph [Mumford and Scheibe, 1968].

### Link Budget Evaluation

The performance of a communication system depends on how large the SNR is at the detector input in the receiver. It is engineering custom to call the signal-to-noise ratio before

detection the *carrier-to-noise ratio* (CNR). Thus, in this section, we will use CNR to denote the signal-to-noise ratio before detection (bandpass case) and SNR to denote the signal-to-noise ratio after detection (baseband case). Here we are interested in evaluating the detector input CNR as a function of the communication link parameters, such as transmitted EIRP, space loss, receiver antenna gain, and the effective input-noise temperature of the receiving system. The formula that relates these system link parameters to the CNR at the detector input is called the *link budget*.

The communication system may be described by the block diagram shown in Fig. 8-24. In this model, the receiving system from the receiving-antenna output to the detector input is modeled by one linear block that represents the cascaded stages in the receiving system, such as a transmission line, a low-noise amplifier (LNA), a down converter, and an IF amplifier. This linear block describes the overall available power gain and effective input-noise temperature of these cascaded devices, as described in the preceding section and modeled in Fig. 8-21.

As shown in Fig. 8-24, the CNR at the ideal amplifier input (with gain  $G_a$ ) is identical to that at the detector input because the ideal amplifier adds no excess noise and it amplifies the signal and noise equally well in a bandwidth of  $B$  hertz (the IF bandwidth). Thus, denoting this simply by CNR,

$$\left(\frac{C}{N}\right) \triangleq \left(\frac{C}{N}\right)_{Rx} = \left(\frac{C}{N}\right)_{Det} \quad (8-38)$$

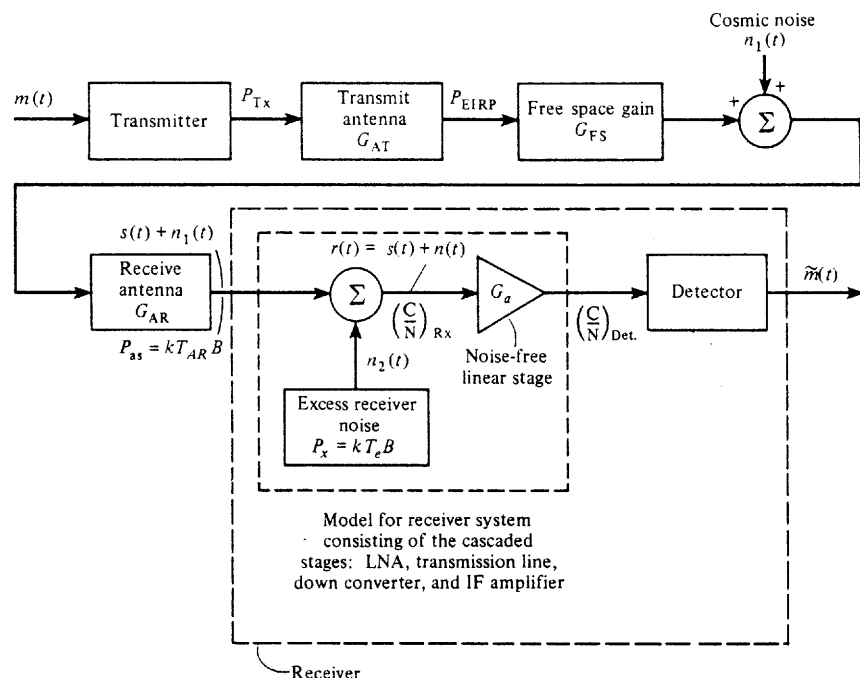


Figure 8-24 Communication system model for link budget evaluation.

where these carrier-to-noise power ratios are indicated on the figure.

Using (8-2) and (8-3), we obtain the received signal power

$$C_{\text{Rx}} = (P_{\text{EIRP}})G_{\text{FS}}G_{\text{AR}} \quad (8-39)$$

where  $P_{\text{EIRP}}$  is the EIRP from the transmitter,  $G_{\text{FS}}$  is the free-space gain, and  $G_{\text{AR}}$  is the receiving antenna power gain.

When we use (8-17), the available noise power at the input to the ideal amplifier in the model (Fig. 8-24) is

$$N = kT_{\text{syst}}B \quad (8-40)$$

where  $B$  is the IF bandwidth. The receiving system noise temperature is

$$T_{\text{syst}} = T_{\text{AR}} + T_e \quad (8-41)$$

where  $T_{\text{AR}}$  is the noise temperature of the antenna (due to received cosmic noise and Earth blackbody radiation) and  $T_e$  is the effective input-noise temperature of the overall receiving system.

When (8-39) and (8-40) are combined, the carrier-to-noise ratio at the detector input is

$$\frac{C}{N} = \frac{P_{\text{EIRP}}G_{\text{FS}}G_{\text{AR}}}{kT_{\text{syst}}B} \quad (8-42)$$

For engineering applications, this formula is converted to decibel units. Using (8-9) in (8-42), the received carrier-to-noise ratio at the detector input in decibels is

$$\left(\frac{C}{N}\right)_{\text{dB}} = (P_{\text{EIRP}})_{\text{dBW}} - (L_{\text{FS}})_{\text{dB}} + \left(\frac{G_{\text{AR}}}{T_{\text{syst}}}\right)_{\text{dB}} - k_{\text{dB}} - B_{\text{dB}} \quad (8-43)$$

where

$(P_{\text{EIRP}})_{\text{dBW}} = 10 \log(P_{\text{EIRP}})$  is the EIRP of the transmitter in dB above 1 W

$(L_{\text{FS}})_{\text{dB}} = 20 \log[(4\pi d)/\lambda]$  is the path loss<sup>†</sup>

$$k_{\text{dB}} = 10 \log(1.38 \times 10^{-23}) = -228.6$$

$$B_{\text{dB}} = 10 \log(B) \quad (B \text{ is the IF bandwidth in hertz})$$

For analog communication systems, the SNR at the detector output can be related to the CNR at the detector input. The exact relationship depends on the type of detector as well as the modulation used. These relationships were developed in Chapter 7. They are summarized in Table 7-2 and Fig. 7-27 with the use of (7-85), where  $C/N = (S/N)_{\text{in}}$ . Example 8-4 uses (8-43) to evaluate the performance of a CATV satellite receiving system.

### $E_b/N_0$ Link Budget for Digital Systems

In digital communication systems the probability of bit error  $P_e$  for the digital signal at the detector output describes the quality of the recovered data. The  $P_e$  is a function of the ratio of the energy per bit to the noise PSD,  $(E_b/N_0)$ , as measured at the detector input. The ex-

<sup>†</sup> This free-space path loss expression can be modified to include effects of a multipath channel within an urban building environment—see (8-67).

act relationship between  $P_e$  and  $E_b/N_0$  depends on the type of digital signaling used, as shown in Table 7-1 and Fig. 7-14. In this section we evaluate the  $E_b/N_0$  obtained at the detector input as a function of the communication link parameters.

The energy per bit is given by  $E_b = CT_b$ , where  $C$  is the signal power and  $T_b$  is the time required to send one bit. Using (8-17), we see that the noise PSD (one-sided) is  $N_0 = kT_{\text{syst}}$ . Thus,

$$\frac{C}{N} = \frac{E_b/T_b}{N_0 B} = \frac{E_b R}{N_0 B} \quad (8-44)$$

where  $R = 1/T_b$  is the data rate (bits/sec). Using (8-44) in (8-42), we have

$$\frac{E_b}{N_0} = \frac{P_{\text{EIRP}}G_{\text{FS}}G_{\text{AR}}}{kT_{\text{syst}}R} \quad (8-45)$$

In decibel units, the  $E_b/N_0$  received at the detector input in a digital communications receiver is related to the link parameters by



$$\left(\frac{E_b}{N_0}\right)_{\text{dB}} = (P_{\text{EIRP}})_{\text{dBW}} - (L_{\text{FS}})_{\text{dB}} + \left(\frac{G_{\text{AR}}}{T_{\text{syst}}}\right)_{\text{dB}} - k_{\text{dB}} - R_{\text{dB}} \quad (8-46)$$

where  $(R)_{\text{dB}} = 10 \log(R)$  and  $R$  is the data rate (bits/second).

For example, suppose that we have BPSK signaling and an optimum detector is used in the receiver; then  $(E_b/N_0)_{\text{dB}} = 8.4$  dB is required for  $P_e = 10^{-4}$  (see Fig. 7-14).<sup>†</sup> Using (8-46), the communication link parameters may be selected to give the required  $(E_b/N_0)_{\text{dB}}$  of 8.4 dB. Note that as the bit rate is increased, the transmitted power has to be increased or the receiving system performance—denoted by  $(G_{\text{AR}}/T_{\text{syst}})_{\text{dB}}$ —has to be improved to maintain the required  $(E_b/N_0)_{\text{dB}}$  of 8.4 dB.

### Example 8-4 LINK BUDGET EVALUATION FOR A TELEVISION RECEIVE-ONLY TERMINAL FOR SATELLITE SIGNALS

The link budget for a television receive-only (TVRO) terminal used for reception of TV signals from a satellite will be evaluated. It is assumed that this receiving terminal is located at Washington, D.C., and is receiving signals from a Hughes *Galaxy* satellite that is in a geostationary orbit at 134° W longitude above the equator. The specifications on the proposed receiving equipment are given in Table 8-5 together with the receiving site coordinates and satellite parameters. This TVRO terminal is typical of those used at the head end of CATV systems for reception of TV signals that are relayed via satellite. As discussed in Sec. 8-5, the composite NTSC baseband video signal is relayed via satellite by frequency-modulating this signal on a 6-GHz carrier that is radiated to the satellite. The satellite down-converts the FM signal to 4 GHz and retransmits this FM signal to the TVRO terminal.

The transmit antenna EIRP footprint for the *Galaxy I* satellite is shown in Fig. 8-25. From this figure it is seen that the EIRP directed toward Washington D.C., is approximately 36 dBW as obtained for inclusion in Table 8-5.

<sup>†</sup> If, in addition, coding were used with a coding gain of 3 dB (see Sec. 1-11), an  $E_b/N_0$  of 5.4 dB would be required for  $P_e = 10^{-4}$ .

TABLE 8-5 TYPICAL SATELLITE TELEVISION RELAY PARAMETERS

Item	Parameter Value
Hughes Galaxy I satellite	
Orbit	Geostationary
Location (above equator)	134° W longitude
Uplink frequency band	6 GHz
Downlink frequency band	4 GHz
$(P_{EIRP})_{dBW}$	36 dBW
TVRO terminal	
Site location	Washington, D.C., 38.8° N latitude, 77° W longitude
Antenna	
Antenna type	10 ft diameter parabola
Noise temperature	32 K (at feed output) for 16.8° elevation
Feedline gain	0.98
Low-noise amplifier	
Noise temperature	40 K
Gain	50 dB
Receiver	
Manufacturer	Microdyne Corp., Model 1100-TV (×24)
Noise temperature	2610 K
IF bandwidth	30 MHz
FM threshold	8 dB CNR

It can be shown that the *look angles* of the TVRO antenna can be evaluated using the following formulas [Davidoff, 1984, Chap. 9]. The elevation of the TVRO antenna is

$$E = \tan^{-1} \left[ \frac{1}{\tan \beta} - \frac{R}{(R + h) \sin \beta} \right] \quad (8-47)$$

where

$$\beta = \cos^{-1}[\cos \varphi \cos \lambda] \quad (8-48)$$

and  $\lambda$  is the difference between the longitude of the TVRO site and the longitude of the *substation point* (i.e., the point directly below the geostationary satellite along the equator).  $\varphi$  is the latitude of the TVRO site,  $R = 3963$  statute miles is the Earth radius, and  $h = 22,242$  statute miles is the altitude of the synchronous satellite. The distance between the TVRO site and satellite, called the *slant range*, is given by the cosine law:

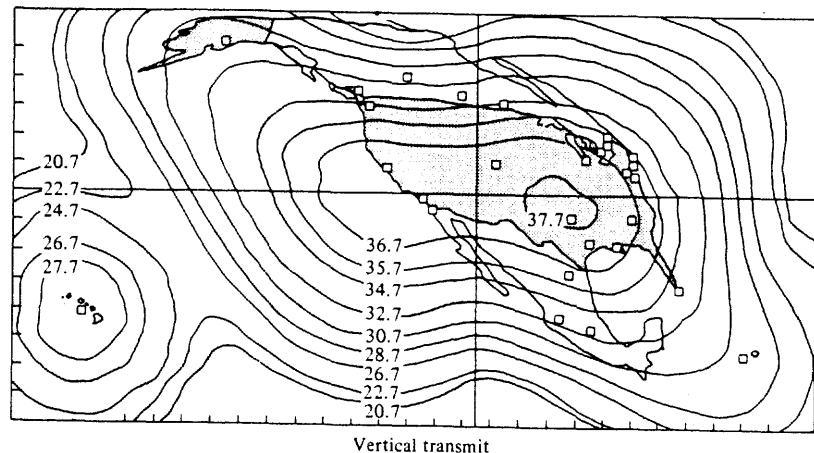
$$d = \sqrt{(R + h)^2 + R^2 - 2R(R + h) \cos \beta} \quad (8-49)$$

The azimuth of the TVRO antenna is

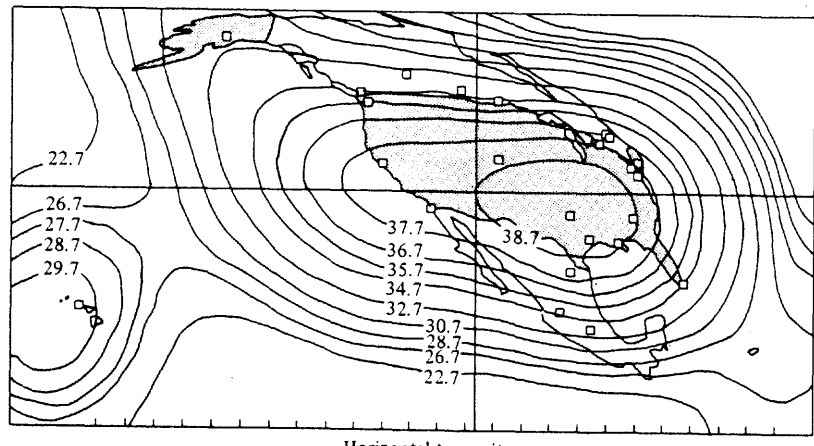
$$A = \cos^{-1} \left( -\frac{\tan \varphi}{\tan \beta} \right) \quad (8-50)$$

where the true azimuth as measured clockwise from the north is given by either  $A$  or  $360^\circ - A$ , as appropriate, since a calculator gives a value between 0 and  $180^\circ$  for  $\cos^{-1}(x)$ . Using these formulas for the Washington, D.C., TVRO site,<sup>†</sup> we get  $\lambda = 134^\circ - 77^\circ = 57^\circ$  and

<sup>†</sup> Here for convenience and for ease in interpretation of answers, the calculator is set to evaluate all trigonometric functions in degrees (not radians).



Vertical transmit



Horizontal transmit

Note: Actual values may vary  $\pm 1$  dB.

**Figure 8-25** Galaxy I (134° W longitude) antenna pattern EIRP footprint (contours given in dBw units). [Courtesy of Hughes Communications, Inc., a wholly owned subsidiary of Hughes Aircraft Company.]

$$\beta = \cos^{-1}[\cos(38.8) \cos(57)] = 64.9^\circ \quad (8-51)$$

The slant range is

$$\begin{aligned} d &= \sqrt{(26,205)^2 + (3963)^2 - 2(3963)(26,205) \cos 64.9^\circ} \\ &= 24,784 \text{ miles} \end{aligned} \quad (8-52)$$

The elevation angle of the TVRO antenna is

$$E = \tan^{-1} \left[ \frac{1}{\tan(64.9)} - \frac{3963}{(26,205) \sin(64.9)} \right] = 16.8^\circ \quad (8-53)$$

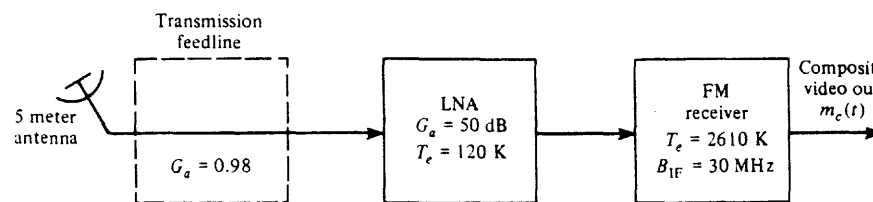


Figure 8-26 TVRO terminal.

The azimuth angle of the TVRO antenna is

$$A = \cos^{-1} \left[ \frac{-\tan(38.8)}{\tan(64.9)} \right] = 247.9^\circ \quad (8-54)$$

Thus, the look angles of the TVRO antenna at Washington, D.C., to the *Galaxy I* satellite are  $E = 16.8^\circ$  and  $A = 247.9^\circ$ .

A block diagram describing the receiving system is shown in Fig. 8-26. Using (8-43), the carrier-to-noise ratio at the detector input of the receiver is

$$\left( \frac{C}{N} \right)_{\text{dB}} = (P_{\text{EIRP}})_{\text{dBW}} - (L_{\text{FS}})_{\text{dB}} + \left( \frac{G_{\text{AR}}}{T_{\text{syst}}} \right)_{\text{dB}} - k_{\text{dB}} - B_{\text{dB}} \quad (8-55)$$

The corresponding path loss for  $d = 24,784$  mi at a frequency of 4 GHz is

$$(L_{\text{FS}})_{\text{dB}} = 20 \log \left( \frac{4\pi d}{\lambda} \right) = 196.5 \text{ dB}$$

For a 10-ft (3.05-m) parabola, using Table 8-4, the receiving antenna gain is

$$(G_{\text{AR}})_{\text{dB}} = 10 \log \left[ \frac{7\pi(3.05/2)^2}{\lambda^2} \right] = 10 \log(9085) = 39.6 \text{ dB}$$

Using (8-41) and (8-37), we obtain the system noise temperature

$$T_{\text{syst}} = T_{\text{AR}} + T_{\text{feed}} + \frac{T_{\text{LNA}}}{G_{\text{feed}}} + \frac{T_{\text{receiver}}}{G_{\text{feed}} G_{\text{LNA}}} \quad (8-56)$$

where the specified antenna noise temperature, including the feed, is  $T_A = (T_{\text{AR}} + T_{\text{feed}}) = 32$  K.

The  $T_{\text{AR}}$  is *not* the ambient temperature of the antenna (which is about 290 K) because the effective resistance of the antenna does not consist of a thermal resistor but of a radiation resistor. That is, if RF power is fed into the antenna, it will not be dissipated in the antenna but instead will be radiated into space. Consequently,  $T_{\text{AR}}$  is called the *sky noise temperature* and is a measure of the amount of cosmic noise power that is received from outer space and noise caused by atmospheric attenuation, where this power is  $P_{\text{AR}} = kT_{\text{AR}}B$ . Graphs giving the measured sky noise temperature as a function of the RF frequency and the elevation angle of the antenna are available [Jordan, 1985, Chap. 27; Pratt and Bostian, 1986].

Substituting the receive system parameters into (8-56). We have

$$T_{\text{syst}} = 32 + \frac{40}{0.98} + \frac{2610}{(0.98)(100,000)} = 72.8 \text{ K}$$

Thus,<sup>†</sup>

$$\left( \frac{G_{\text{AR}}}{T_{\text{syst}}} \right)_{\text{dB}} = 10 \log \left( \frac{9.085}{72.8} \right) = 21.0 \text{ dB/K}$$

Also,

$$(B)_{\text{dB}} = 10 \log(30 \times 10^6) = 74.8$$

Substituting these results into (8-55) yields

$$\left( \frac{C}{N} \right)_{\text{dB}} = 36 - 196.5 + 21.0 - (-228.6) - 74.8$$

Thus the carrier-to-noise ratio at the detector input (inside the FM receiver) is

$$\left( \frac{C}{N} \right)_{\text{dB}} = 14.3 \text{ dB} \quad (8-57)$$

A CNR of 14.3 dB does not seem to be a very good signal-to-noise ratio, does it? Actually, the question is: Does a CNR of 14.3 dB at the detector input give a high-quality video signal at the detector output? This question can be answered easily if we have some detector performance curves as shown in Fig. 8-27. Two curves are plotted in this figure. One is for the

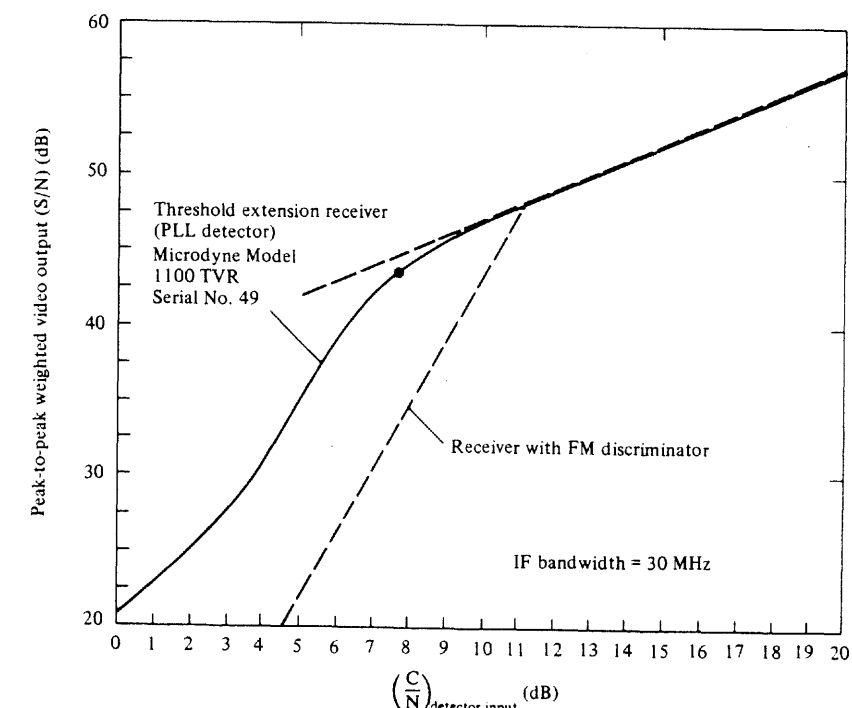


Figure 8-27 Output SNR as a function of FM detector input CNR. [Curve for the Microdyne receiver, Model 1100TVR, courtesy of the Microdyne Corporation, Ocala, FL, 1981.]

<sup>†</sup> Engineers specify dB/K as the units for  $(G/T)_{\text{dB}}$ , although it is a misnomer.

output of a receiver that uses an FM discriminator for the FM detector, and the other is for a receiver (Microdyne 1100TVR) that uses a PLL FM detector to provide threshold extension.<sup>†</sup> For a CNR of 14.3 dB on the input, both receivers will give a 51-dB output SNR, which corresponds to a high-quality picture. However, if the receive signal from the satellite fades because of atmospheric conditions, and so on, by, say, 6 dB, the output SNR of the receiver with an FM discriminator will be only about 36 dB, whereas the receiver with threshold extension detection will have an output SNR of about 45 dB.

## 8-7 FIBER OPTIC SYSTEMS

Since 1980 fiber optic cable transmission systems have become commercially viable. This is indicated in Table 8-2, which shows that common carriers have installed extensive fiber optic systems in the United States, Japan, Britain, and Canada. Fiber optic cable is the preferred underground transmission medium and is superseding twisted-pair cable and coaxial cable. Also, as shown in Table 8-2, transoceanic fiber optic cable systems are becoming popular. Digital fiber optic systems use simple OOK modulation of an optical source to produce a modulated light beam. The optical source has a wavelength in the range of 0.85 to 1.6  $\mu\text{m}$ , which is about 77,000 GHz. (Analog AM fiber optic systems can also be built.)

The optical sources can be classified into two categories: (1) light-emitting diodes (LED) that produce noncoherent light and (2) solid-state lasers that produce coherent (single-carrier-frequency) light. The LED source is popular because it is rugged and inexpensive. It has a relatively low power output, about  $-15 \text{ dBm}$  (including coupling loss), and a small modulation bandwidth of about 50 MHz. The laser diode has a relatively high power output, about  $+5 \text{ dBm}$  (including coupling loss), and a large modulation bandwidth of about 1 GHz. The laser diode is preferred over the LED since it produces coherent light and has high output power, but it is high in cost and has a short lifetime. OOK modulation is obtained simply by switching the bias current on and off.

The light source is coupled into the fiber optic cable, and this cable is the channel transmission medium. Fiber cables can be classified into two categories: (1) multimodal and (2) single-mode. Multimodal fiber has a core diameter of 50  $\mu\text{m}$  and a cladding diameter of 125  $\mu\text{m}$ . The light is reflected off the core-cladding boundary as it propagates down the fiber to produce multiple paths of different lengths. This causes pulse dispersion of the OOK signal at the receiving end and thus severely limits the transmission bit rate that can be accommodated. The single-mode fiber has a core diameter of approximately 8  $\mu\text{m}$  and propagates a single wave. Consequently, there is little dispersion of the received pulses of light. Because of its superior performance, single-mode fiber is preferred.

At the receiving end of the fiber, the receiver consists of a PIN diode, an avalanche photodiode (APD), or a GaAsMESFES transistor used as an optical detector. In 0.85- $\mu\text{m}$  systems any of these devices may be used as a detector. In 1.3- and 1.55- $\mu\text{m}$  systems the APD

<sup>†</sup> The threshold point is the point where the knee occurs in the  $(S/N)_{\text{out}}$  versus  $(C/N)_{\text{in}}$  characteristic. In the characteristic for threshold extension receivers, this knee is extended to the left (improved performance) when compared to the knee for the corresponding receiver that uses a discriminator as a detector.

is usually used. The PIN diode is low in cost and reliable but is used only in 0.85- $\mu\text{m}$  systems. These detectors act like a simple envelope detector. As shown in Fig. 7-14, better performance (lower probability of bit error) could be obtained by using a coherent detection system that has a product detector. This requires a coherent light source at the receiver that is mixed with the received OOK signal via the nonlinear action of the photodetector. Of course, it is possible to have coherent PSK and FSK systems [Basch and Brown, 1985], but they are usually not cost-effective.

### Example 8-5 LINK BUDGET FOR A FIBER OPTIC SYSTEM

Figure 8-28 shows the configuration of the AT&T FT-2000 fiber optic system. It consists of two bidirectional fiber optic rings with terminals located at service points (such as towns) within a given geographical area. The ring configuration is used to provide redundant data paths; if a cable cut occurs anywhere around the ring, service is still provided to the terminals by the remaining in-service fiber. The terminals are called add/drop terminals because they add/drop data from the ring for the subscribers that the terminal serves from its location. As shown in Fig. 8-28, two fibers are required in the ring for full duplex service. That is, one fiber provides for the transmitted (Tx) data and the other fiber provides the simultaneous received (Rx) data.

Specifications for the AT&T FT-2000 system are given in Table 8-6. This system has OC-48 capacity, which is equivalent to 48 DS-3 circuits or 32,256 full-duplex VF circuits as described in Sec. 3-9 (see Table 3-10).

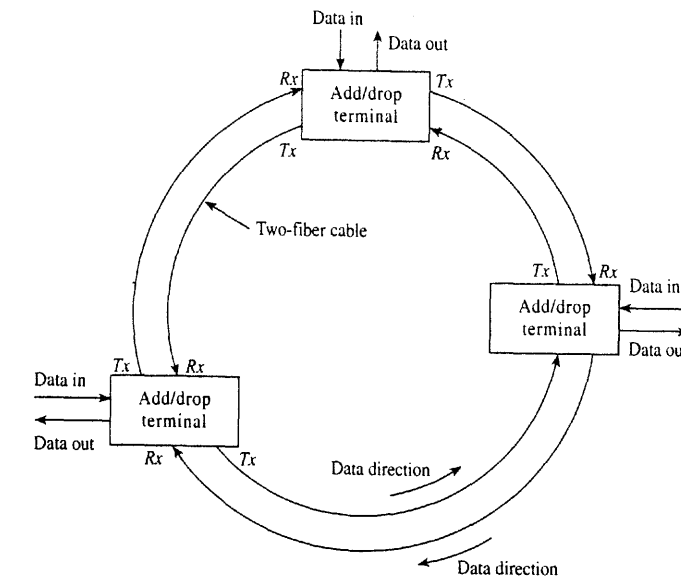


Figure 8-28 FT-2000 optical-fiber ring system.

**TABLE 8-6** SPECIFICATIONS FOR THE FT-2000 OC-48 LIGHTWAVE SYSTEM

Maximum capacity for 2-fiber bidirectional rings	24 DS-3 equivalents (16,128 full duplex VF circuits per fiber pair) per span 48 DS-3 equivalents (32,256 full duplex VF circuits per terminal)
Line rate	2.488 Gbits/sec
Line code	Scrambled unipolar NRZ
Wavelength	1310 nm $\pm$ 20 nm or 1550 nm $\pm$ 15 nm
Optical Source	Distributed feedback (DFB) laser
Optical detector	Avalanche photodiode (APD)
Optical fiber	Single mode
Transmitted power	
OC-48 1.31 $\mu\text{m}$ std. performance	Max: +2.5 dBm, Min: -2.0 dBm <sup>†</sup>
OC-48 1.3 $\mu\text{m}$ high performance	Max: +5.5 dBm, Min: +1.0 dBm <sup>†</sup>
OC-48 1.55 $\mu\text{m}$ std. performance	Max: +4.0 dBm, Min: -2.0 dBm <sup>†</sup>
Receiver sensitivity	-27.0 dBm
Maximum receiver power (no overload)	-10 dBm for 1.31 $\mu\text{m}$ , -9.0 dBm for 1.55 $\mu\text{m}$
Bit error rate (BER)	<10 <sup>-10</sup> for -27 dBm receiver input <10 <sup>-9</sup> accumulated BER for systems up to 400 km (250 miles)
Maximum repeater spacing	
OC-48 1.31 $\mu\text{m}$ high performance	60 km (0.45 dB/km loss fiber)
OC-48 1.55 $\mu\text{m}$ std. performance	92 km (0.25 dB/km loss fiber), dispersion limited

<sup>†</sup>Includes transmitter/receiver connector losses of 0.7 dB each (worst case) and system margins.

Source: AT&T 365-575-100 Manual, *FT-2000 OC-38 Lightwave System*, December 1994.

A link budget analysis for a FT-2000 line span operating at the 1.5  $\mu\text{m}$  wavelength is given in Table 8-7. It shows that a maximum line span of 92 km (57.5 miles) may be used between optical repeaters (or add/drop terminals). Moreover, an optional lightwave booster amplifier may be used at the transmitter end to increase the transmitted optical power to +16 dBm. This allows the maximum line span to be increased to 140 km (87.5 miles) using standard fiber or to 160 km (100 miles) if dispersion shifted fiber is used [AT&T, 1994].

## 8-8 CELLULAR TELEPHONE SYSTEMS

Since the invention of radio systems, the goal of telephone engineers has been to provide personal telephone service to individuals by using radio systems to link phone lines with persons in their cars or on foot. In the past this type of personal telephone service was not possible because limited spectrum space did not permit the assignment of a "private-line" radio channel for each subscriber. In addition, the existing radio equipment was bulky and expensive. However, with the development of the integrated circuit technology, radio equipment can now be miniaturized, and relatively sophisticated operations can be implemented at low cost. This development allows the sharing of a number of radio channels on demand (FDMA, TDMA, or CDMA) where a particular channel is assigned to a specific user only

**TABLE 8-7** LINK BUDGET ANALYSIS FOR A 1.55- $\mu\text{m}$  FT-2000 FIBER SPAN

Description	Value
Maximum transmitted power	+4.0 dBm
Receiver sensitivity	-27.0 dBm
Available margin	31.0 dB
Losses in a 57 mile fiber link	
Optical path penalty	2.0 dB
Transmitter/receiver connector loss (0.7 dB each)	1.4 dB
Fiber attenuation (92 km $\times$ 0.25 dB/km) <sup>†</sup>	23.0 dB
System margin	4.6 dB
Total loss	31.0 dB

<sup>†</sup>The 0.25 dB/km loss includes splicing losses.

when a telephone call is in progress. An example is *trunked mobile radio systems* in which a number of radio channels are shared with different groups of users (i.e., statistical multiplexing on a FDMA basis). In these trunked systems, relatively high-power transmitters are used so that each radio channel covers a whole city or county. Consequently, when a channel is being used by anyone in that area, it is not available for use by others. Many more users can be accommodated simultaneously if the coverage of each transmitter is reduced to some small geographical area (a cell) so that the same radio frequency channel can be reused by another individual a few miles away in a distant cell.

This *cellular radio* concept is illustrated in Fig. 8-29. Each user communicates via radio from a cellular telephone set to the cell-site base station. This base station is connected

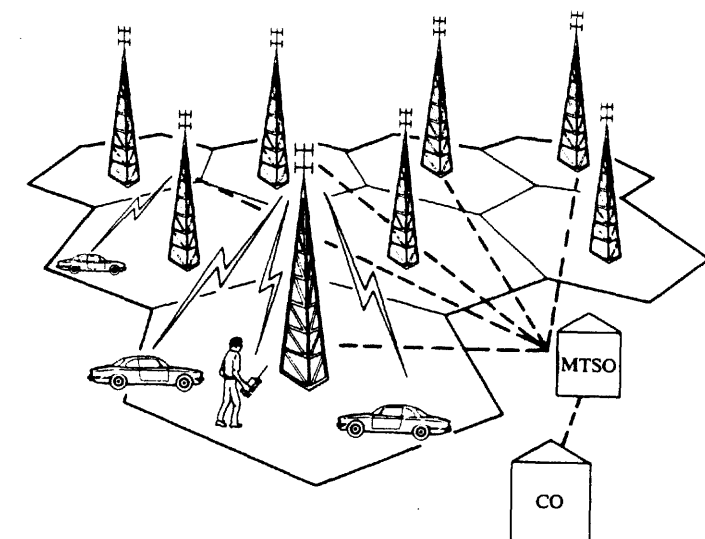


Figure 8-29 Cellular telephone system.

via telephone lines to the *mobile telephone switching office* (MTSO). The MTSO connects the user to the called party. If the called party is land based, the connection is via the central office (CO) to the terrestrial telephone network. If the called party is mobile, the connection is made to the cell site that covers the area in which the called party is located, using an available radio channel in the cell associated with the called party. Theoretically, this cellular concept allows any number of mobile users to be accommodated for a given set of radio channels. That is, if more channels are needed, the existing cell sizes are decreased and additional small cells are inserted so that the existing channels can be reused more efficiently. The critical consideration is to design the cells for acceptable levels of cochannel interference [Lee, 1986]. As the mobile user travels from one cell to another, the MTSO automatically switches the user to an available channel in the new cell and the telephone conversation continues uninterrupted.

The cellular concept has the following advantages.

- Large subscriber capacity.
- Efficient use of the radio spectrum.
- Nationwide compatibility.
- Service to hand-held portables as well as vehicles.
- High-quality telephone and data service to the mobile user at relatively low cost.

Unfortunately, there are many cellular standards used throughout the world [Dorf, 1996, pp. 1419–1420; Padgett, Gunther and Hattori, 1995]. For example, as many as 15 different types of cellular phones are needed to remain in communication as one travels around Europe. Table 8-8 shows three major analog standards that are used around the world. Moreover, since cellular telephones are so popular, it is clear that these wideband FM analog systems do not have the capacity to accommodate the expected new subscribers. Consequently, narrowband FM analog systems with higher capacity, as shown in Table 8-9, are replacing wideband systems on a channel-by-channel basis as needed. For example, one wideband 30-kHz AMPS channel can be replaced by three narrowband 10-kHz NAMPS channels to triple the capacity. For larger capacity, new digital cellular systems, as shown in Table 8-10, will be used. The GSM digital system is being placed into service in Europe to provide one uniform standard that replaces the numerous analog systems that are being phased out.

As shown in Table 8-8, the first generation cellular system used in the United States is the Advanced Mobile Phone System (AMPS), which was developed by AT&T and Motorola. To implement this cellular concept in the United States, the FCC had to find spectral space for assignment. It did so by using the 806- to 890-MHz band that was once assigned to TV channels 70 to 83 (see Table 8-12) but discontinued in 1974. Part of this band was assigned for cellular service as shown in Table 8-8. Furthermore, the FCC decided to license two competing call systems in each geographical area—one licensed to a conventional telephone company and another to a nontelephone company common carrier. The nontelephone system is called the *A service* or *nonwireline service*, and the telephone company system is called the *B service* or *wireline service*. Thus cell system subscribers have the option of renting service from the wireline company or the nonwireline company, or from both. In addition,

TABLE 8-8 MAJOR ANALOG FDMA CELLULAR TELEPHONE SYSTEMS

Item	System Name <sup>a</sup> and Where Used				
	AMPS		ETACS		JTACS
	North America		United Kingdom	Japan	
Year introduced	1983	1983	1985	1988	
Base cell station	869–880, 890–891.5	880–890, 891.5–894	917–933, 935–960	860–870	
Transmit bands (MHz)	824–835, 845–846.5	835–845, 846.5–849	872–888, 890–915	915–925	
Mobile station	3	3	3	2.8	
Transmit bands (MHz)	2–20	2–20	2–20	2–20	
Maximum power (watts)	416 <sup>b</sup>	416 <sup>b</sup>	1000	400	
Cell size, radius (km)	30	30	25	25	
Number of duplex channels					
Channel bandwidth (kHz)					
Modulation					
Voice	FM 12-kHz peak deviation	FM 12-kHz peak deviation	FM 9.5-kHz peak deviation	FM 9.5-kHz peak deviation	
Control signal	FSK	FSK	FSK	FSK	
(Voice and paging channels)	8-kHz peak deviation	8-kHz peak deviation	6.4-kHz peak deviation	6.4-kHz peak deviation	
	10 kbit/s	10 kbit/s	8 kbit/s	8 kbit/s	
	Manchester line code	Manchester line code	Manchester line code	Manchester line code	Manchester line code

<sup>a</sup>AMPS, advanced mobile phone system; ETACS, extended total access communication system; JTACS, Japan total access communication system.

<sup>b</sup>21 of the 416 channels are used exclusively for paging.

TABLE 8-9 NARROWBAND ANALOG FDMA CELLULAR TELEPHONE SYSTEMS

Item	System Name <sup>a</sup> and Where Used:	
	NAMPS North America	NTACS Japan
Year introduced	1992	1993
Base cell station		
Transmit band (MHz)	869–894	843–846, 860–870
Mobile station		
Transmit band (MHz)	824–849	898–901, 915–925
Maximum power (watts)	3	2.8
Number of duplex channels	2496	1040
Channel bandwidth		
Voice (kHz)	10	12.5
Paging (kHz)	30	25
Modulation		
Voice	FM 5-kHz peak deviation	FM 5-kHz peak deviation
Signaling (voice channel)	FSK 0.7-kHz peak deviation	FSK 0.7-kHz peak deviation
Signaling (paging channel)	100 bits/s, Manchester	100 bits/s, Manchester
	FSK 8-kHz peak deviation	FSK 6.4-kHz peak deviation
	10 kbytes/s, Manchester	8 kbytes/s, Manchester

<sup>a</sup>NAMPS, narrowband advanced mobile phone system; NTACS, narrowband total access communication system.

tion, as shown in the table, the standards provide for full duplex service. That is, one carrier frequency is used for mobile to cell base-station transmission, and another carrier frequency is used for base-station to mobile transmission. The telephone VF signals are frequency modulated onto the carriers, and control is provided by FSK signaling. Of the 416 channels that may be used by a cellular service licensee, 21 are used for paging and control with FSK signaling. FSK signaling is also used at the beginning and end of each call on a VF channel. When a cellular telephone is turned on, its receiver scans the paging channels looking for the strongest cell-site signal and then locks onto it. The cell site transmits FSK data continuously on a paging channel, and, in particular, it sends control information addressed to a particular cellular phone when a call comes in for it. That is, the FSK control signal tells the phone which voice-frequency (VF) channel to use for a call.

Each cellular telephone contains a PROM (programmable read-only memory) or EPROM (erasable programmable read only memory)—called a *numeric assignment module* (NAM)—that is programmed to contain

- The telephone number—also called the *electronic service number* (ESN)—of the phone.
- The serial number of the phone as assigned by the manufacturer.
- Personal codes that can be used to prevent unauthorized use of the phone.

TABLE 8-10 MAJOR DIGITAL CELLULAR TELEPHONE SYSTEMS

Item	System Name <sup>a</sup> and Where Used:	
	GSM Europe	IS-54, NADC North America
Year introduced	1990	1991
Base cell station		
Transmit bands (MHz)	935–960	869–894
Mobile station		
Transmit bands (MHz)	890–915	824–849
Maximum power (watts)	20	3
Number of duplex channels	125	832
Channel bandwidth (kHz)	200	30
Channel access method	TDMA	TDMA <sup>f</sup>
Users per channel	8	3
Modulation <sup>b</sup>		
Type	GMSK	$\pi/4$ DQPSK
Data rate	270.833 kbytes/s	48.6 kbytes/s
Filter	0.3R Gaussian <sup>c</sup>	$r = 0.35$ raised cosine <sup>d</sup>
Speech coding <sup>e</sup>	RPE-LTP	VSELP
	13 kbytes/sec	8 kbytes/sec
		8 kbytes/sec (variable)
		8 kbytes/sec

<sup>a</sup>GSM, group special mobile; NADC, North American digital cellular; JDC, Japan digital cellular.

<sup>b</sup>GMSK, Gaussian MSK (i.e.,  $h = 0.5$  FSK, also called FFSK, with Gaussian premodulation filter; see Sec. 5-11 and footnote c below);  $\pi/4$  DQPSK, differential QPSK with  $\pi/4$  rotation of reference phase for each symbol transmitted.

<sup>c</sup>Baseband Gaussian filter with 3 dB bandwidth equal to 0.3 of the bit rate.

<sup>d</sup>Square root of raised cosine characteristic at transmitter and receiver.

<sup>e</sup>RPE-LTP, regular pulse excitation—long term prediction; VSELP, Qualcomm's codebook excited linear prediction.

<sup>f</sup>The spread spectrum chip rate is 1.2288 Mcips/s for a spreading factor of 128 or 21-dB coding gain.

<sup>g</sup>For CDMA, channel frequencies may be reused in adjacent cells; other methods (TDMA and FDMA) require a seven-cell reuse pattern.

When the phone is "on-the-air" it automatically transmits its serial number to the MTSO. The serial number is used by the MTSO to lock out phone service to any phone that has been stolen. This feature, of course, discourages theft of the units. The MTSO uses the telephone number of the unit to provide billing information. When the phone is used in a remote city, it can be placed in the *roam* mode so that calls can be initiated or received and yet the service will be billed via the caller's "hometown" company.

To place a call the following sequence of events occurs.

1. The cellular subscriber initiates a call by keying in the telephone number of the called party and then presses the *send* key.
2. The MTSO verifies that the telephone number is valid and that the user is authorized to place a call.
3. The MTSO issues instructions to the user's cellular phone indicating which radio channel to use.
4. The MTSO sends out a signal to the called party to ring his or her phone. All of these operations occur within 10 sec of initiating the call.
5. When the called party answers, the MTSO connects the trunk lines for the two parties and initiates billing information.
6. When one party hangs up, the MTSO frees the radio channel and completes the billing information.

While a call is in progress, the cellular subscriber may be moving from one cell area to another, so the MTSO:

- Monitors the signal strength from the cellular telephone as received at the cell base station. If the signal drops below some designated level, the MTSO initiates a "hand-off" sequence.
- For "hand-off," the MTSO inquires about the signal strength as received at adjacent cell sites.
- When the signal level becomes sufficiently large at an adjacent cell site, the MTSO instructs the cellular radio to switch over to an appropriate channel for communication with that new cell site. This switching process takes less than 250 msec and usually is unnoticed by the subscriber.

As indicated by the tables, cellular systems and the standards for these systems are in a process of evolution throughout the world. The first commercial cellular service was implemented in the United States in 1983. There is a strong push for development of all digital cellular systems that have large user capacity, as illustrated by the TDMA-based IS-54<sup>†</sup> system and the CDMA based IS-95 system listed in Table 8-10. For bandwidth conservation, these systems use low-bit-rate encoding of the VF signal. For example, the vector sum excited linear prediction filter (VSELF) encoder used for the NADC and JDC systems is a

<sup>†</sup> Telecommunication Industry Association (TIA) Interium Standard 54 which is also called the North American Digital Cellular (NADC) system.

modified version of the codebook excited linear prediction (CELP) technique developed by B. Atal at the AT&T Bell Laboratories [Gerson and Jasiek, 1990]. This technique mimics the two main parts of the human speech system, the vocal cords and the vocal tract. The vocal tract is simulated by a time-varying linear prediction filter, and the vocal cord sounds used for the filter excitation are simulated with a database (i.e., a codebook) of possible excitations. The VSELF encoder (at the transmitter) partitions the talker's VF signal into 20-ms segments. The encoder sequences through the possible codebook excitation patterns and the possible values for the filter parameters to find the synthesized speech segment that gives the best match to the VF segment. The encoder parameters that specify this best match are then transmitted via digital data to the receiver, where the received data establish the parameters for the receiver speech synthesizer so that the VF signal may be reproduced for the listener.

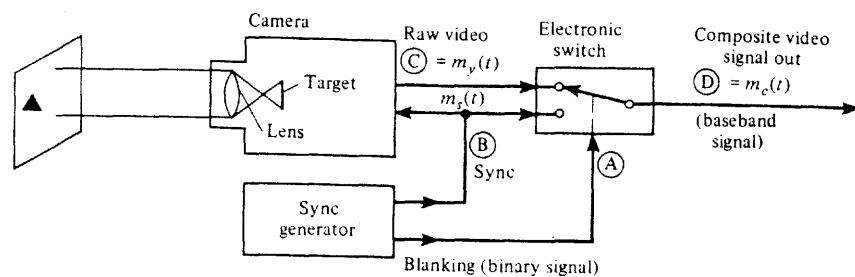
For more developments in digital cellular telephone and personal communication systems (PCS), the reader is referred to a summary paper in the *IEEE Proceedings* [Li and Qui, 1995] and to recent issues of the *IEEE Communication Magazine* and the *IEEE Personal Communications Magazine*. PCS via satellites was described in Table 8-3.

## 8-9 TELEVISION

Television (TV) is a method of reproducing fixed or moving visual images by the use of electronic signals. There are numerous kinds of TV systems and different standards have been adopted around the world. Moreover, as discussed subsequently, TV standards are in a state of flux since there is a worldwide push for digital *high-definition television* (HDTV). First we will concentrate on black-and-white broadcast TV as it has developed in the United States since the 1930s and then color television and digital HDTV will be examined.

### Black-and-White Television

The black-and-white image of a scene is essentially the intensity of the light as a function of the *x* and *y* coordinates of the scene and of time. However, an electrical waveform is only a function of time, so that some means of encoding the *x* and *y* coordinates associated with the intensity of light from a single point in the scene must be used. In broadcast TV this is accomplished by using *raster scanning*, as shown in Fig. 8-30. It is assumed that the whole scene is scanned before any object in the scene has moved appreciably. Thus moving images can be transmitted by sending a series of still images, just as in motion pictures. As the scene is scanned, its intensity is signified by the amplitude of the video signal. A synchronizing pulse is inserted at the end of each scan line by the electronic switch, as shown in Fig. 8-30, to tell the TV receiver to start another scan line. For illustrative purposes, a black triangle is located in the upper left portion of the scene. In Figs. 8-30b and 8-30c, numbers are used to indicate the corresponding times on the video waveform, with the location of the point being scanned in the scene at that instant. The composite video signal is actually a hybrid signal that consists of a digital waveform during the synchronizing interval and an analog waveform during the video interval. Operating personnel monitor the quality of the video by looking at a *waveform monitor*, which displays the composite video waveform as shown in Fig. 8-30c.



(a) Block Diagram of Camera System

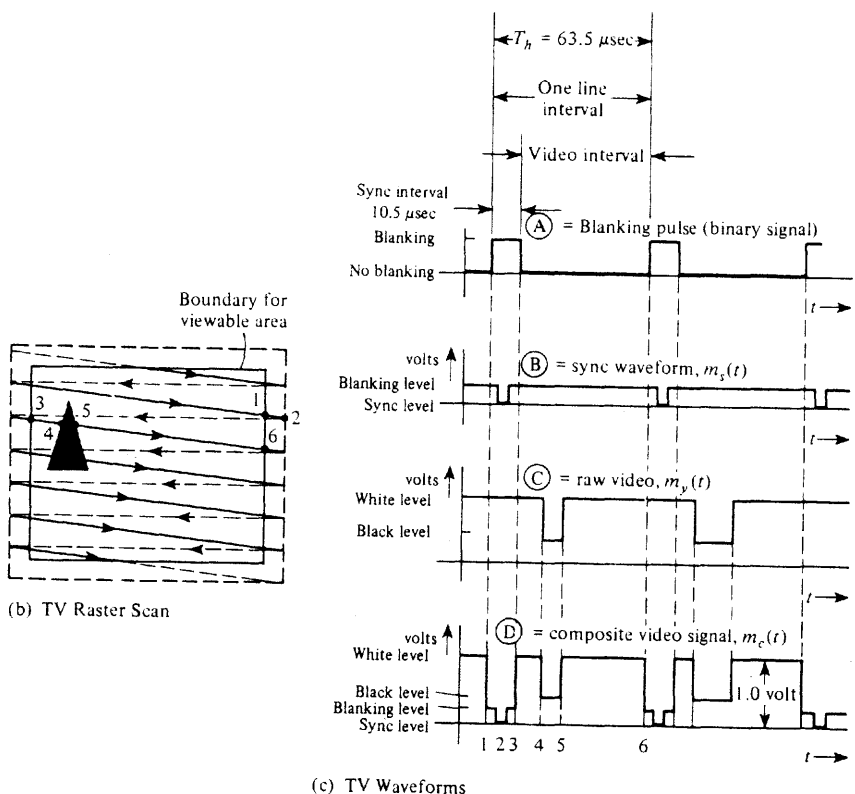


Figure 8-30 Generation of a composite black-and-white video signal.

The picture (as viewed) is generated by scanning left to right to create a line, and the lines move from the top to the bottom of the screen. During retrace, indicated by the dashed lines from right to left, the CRT is turned off by the video level that is "blacker than black" during the sync pulse interval.<sup>†</sup> The scene is actually covered by scanning alternate lines from the top to the bottom (one field) and returning to the top to scan the missed lines (the next field). This technique is called *interlacing* and reduces the flicker effect on moving

<sup>†</sup> In addition, most TV sets switch off the electron beam during retrace by using the sync pulse obtained from the horizontal output (flyback) transformer.

pictures, giving two fields (passes down the screen) for every frame. In the United States there are approximately 30 frames/s transmitted, which is equivalent to 60 fields/s for the 2:1 interlacing that is used. When the scan reaches the bottom of a field, the sync pulse is widened out to cover the whole video interval plus sync interval. This occurs for 21 lines, and, consequently, a black bar is seen across the screen if the picture is "rolled up" by misadjusting the vertical hold control. In the receiver, the vertical sync (wide pulse) can be separated from the horizontal sync (narrow pulse) by using a differentiator circuit to recover the horizontal sync and an integrator to recover the vertical sync. The vertical interval is also used to send special signals, such as testing signals that can be used by TV engineers to test the frequency response and linearity of the equipment on-line [Solomon, 1979]. In addition, some TV programs have closed-caption information that can be decoded on special TV sets used by deaf viewers. These sets insert subtitles across the bottom of the screen. As shown in Table 8-11, this closed-captioning information is transmitted during line 21 of the vertical interval by inserting a 16-bit code word. Details of the exact sync structure are rigorously specified by the FCC (see Fig. 8-37).

The composite baseband signal consisting of the *luminance* (intensity) video signal  $m_y(t)$  and the *synchronizing* signal  $m_s(t)$  is described by

$$m_c(t) = \begin{cases} m_s(t) & \text{during the sync interval} \\ m_y(t) & \text{during the video interval} \end{cases} \quad (8-58)$$

The spectrum of  $m_c(t)$  is very wide since  $m_c(t)$  contains rectangular synchronizing pulses. In fact, the bandwidth would be infinite if the pulses had perfect rectangular shapes. In order to reduce the bandwidth, the pulses are rounded as specified by FCC standards (see Fig. 8-37). This allows  $m_c(t)$  to be filtered to a bandwidth of  $B = 4.2$  MHz (U.S. standard). For a still picture, the exact spectrum can be calculated using Fourier series analysis (as shown in Sec. 2-5). For a typical picture all fields are similar, thus  $m_c(t)$  would be periodic with a period of approximately  $T_0 = 1/60$  s corresponding to the field rate of 60 fields/s (see Table 8-11 for exact values). Thus, for a still picture, the spectrum would consist of lines spaced at 60-Hz intervals. However, from Fig. 8-30, we can observe that there are dominant intervals of width  $T_h$  corresponding to scanned lines of the frame. Furthermore, the adjacent lines usually have similar waveshapes. Consequently,  $m_c(t)$  is quasiperiodic with period  $T_h$ , and the spectrum consists of clusters of spectral lines that are centered on harmonics of the scanning frequency,  $nf_h = n/T_h$  where the spacing of the lines within these clumps is 60 Hz. For moving pictures, the line structure of the spectrum "fuzzes out" to a continuous spectrum with spectral clusters centered about  $nf_h$ . Furthermore, between these clusters the spectrum is nearly empty. As we will see, these "vacant" intervals in the spectrum are used to transmit the color information for a color TV signal. This, of course, is a form of frequency-division multiplexing.

The resolution of TV pictures is often specified in terms of lines of resolution. The number of horizontal lines that can be distinguished from the top to the bottom of a TV screen for a horizontal line test pattern is called the *vertical line resolution*. The maximum number of distinguishable horizontal lines (vertical line resolution) is the total number of scanning lines in the raster less those not used for the image. That is, the vertical resolution is

$$n_v = (N_f - N_v) \quad \text{lines} \quad (8-59a)$$

TABLE 8-11 U.S. ANALOG TELEVISION BROADCASTING STANDARDS

Item	FCC Standard
Channel bandwidth	6 MHz
Visual carrier frequency	$1.25 \text{ MHz} \pm 1000 \text{ Hz}$ above the lower boundary of the channel
Aural carrier frequency	$4.5 \text{ MHz} \pm 1000 \text{ Hz}$ above the visual carrier frequency
Chrominance subcarrier frequency	$3.579545 \text{ MHz} \pm 10 \text{ Hz}$
Aspect (width-to-height) ratio	Four units horizontally for every three units vertically
Modulation-type visual carrier	AM with negative polarity (i.e., a decrease in light level causes an increased real envelope level)
Aural carrier	FM with 100% modulation being $\Delta f = 25 \text{ kHz}$ with a frequency response of 50 to 15,000 Hz using $75\text{-}\mu\text{s}$ preemphasis
Visual modulation levels	
Blanking level	$75\% \pm 2.5\%$ of peak real envelope level (sync tip level)
Reference black level	$7.5\% \pm 2.5\%$ (of the video range between blanking and reference white level) below blanking level; this is called the <i>setup</i> level by TV engineers <sup>a</sup>
Reference white level	$12.5\% \pm 2.5\%$ of sync tip level <sup>a</sup>
Scanning	
Number of lines	525 lines/frame, interlaced 2:1
Scanning sequence	Horizontally: left to right; vertically: top to bottom
Horizontal scanning frequency, $f_h$	$15,734.264 \pm 0.044 \text{ Hz}$ (2/455 of chrominance frequency); $15,750 \text{ Hz}$ may be used during monochrome transmissions
Vertical scanning frequency, $f_v$	$59.94 \text{ Hz}$ (2/525 of horizontal scanning frequency); 60 Hz may be used during monochrome transmissions; 21 equivalent horizontal lines occur during the vertical sync interval of each field
Vertical interval signaling	Lines 13, 14, 15, 16. Teletext Lines 17, 18. Vertical interval test signals (VITS) Line 19. Vertical interval reference (VIR) Line 20, Field 1. Station identification Line 21, Field 1. Captioning data Line 21, Field 2. Captioning framing code ( $\frac{1}{2}$ line)

<sup>a</sup> See Fig. 8-31 b.

where  $N_f$  is the total number of scanning lines per frame and  $N_v$  is the number of lines in the vertical interval (not image lines) for each frame. For U.S. standards (Table 8-11), the maximum vertical resolution is

$$n_v = 525 - 42 = 483 \text{ lines} \quad (8-59b)$$

The resolution in the horizontal direction is limited by the frequency response allowed for  $m_c(t)$ . For example, if a sine-wave test signal is used during the video interval, the highest sine-wave frequency that can be transmitted through the system will be  $B = 4.2 \text{ MHz}$  (U.S. standard) where  $B$  is the system video bandwidth. For each peak of the sine wave a

dot will appear along the horizontal direction as the CRT beam sweeps from left to right. Thus the horizontal resolution for 2:1 interlacing is

$$n_h = 2B(T_h - T_b) \text{ lines} \quad (8-60a)$$

where  $B$  is the video bandwidth,  $T_h$  is the horizontal interval, and  $T_b$  is the blanking interval (see Fig. 8-30). For U.S. standards,  $B = 4.2 \text{ MHz}$ ,  $T_h = 63.5 \mu\text{s}$ , and  $T_b = 10.5 \mu\text{s}$  so that the horizontal resolution is

$$n_h = 445 \text{ lines} \quad (8-60d)$$

Furthermore, because of poor video bandwidth and the poor interlacing characteristics of consumer TV sets, this horizontal resolution of 445 is usually not obtained in practice.<sup>†</sup> At best, the U.S. standard of  $445 \times 483$  does not provide very good resolution, and this poor resolution is especially noticeable on large-screen TV sets. [For comparison the super VGA computer monitor standard provides a resolution as large as  $1024 \times 768$ .]

For broadcast TV transmission (U.S. standard), the composite video signal of (8-58) is inverted and amplitude modulated onto an RF carrier so that the AM signal is

$$s_v(t) = A_c[1 - 0.875m_c(t)] \cos \omega_c t \quad (8-61)$$

This is shown in Fig. 8-31. The lower sideband of this signal is attenuated so that the spectrum will fit into the 6-MHz TV channel bandwidth. This attenuation can be achieved by using a vestigial sideband filter, which is a bandpass filter that attenuates most of the lower sideband. The resulting filtered signal is called a *vestigial sideband* (VSB) signal,  $s_{v0}(t)$  as described in Sec. 5-5. The discrete carrier term in the VSB signal changes when the picture is switched from one scene to another because the composite baseband signal has a non-zero dc level that depends on the particular scene being televised. The audio signal for the TV program is transmitted via a separate FM carrier located exactly 4.5 MHz above the visual carrier frequency.

The rated power of a TV visual signal is the effective isotropic radiated peak envelope power (EIRP, i.e., effective sync tip average power), and is usually called simply the *effective radiated power* (ERP). The EIRP is the power that would be required to be fed into an isotropic antenna to get the same field strength as that obtained from an antenna that is actually used as measured in the direction of its maximum radiation. The antenna pattern of an omnidirectional TV station is shaped like a doughnut with the tower passing through the hole. (The antenna structure is located at the top of the tower for maximum line-of-sight coverage.) The ERP of the TV station (visual or aural) signal is

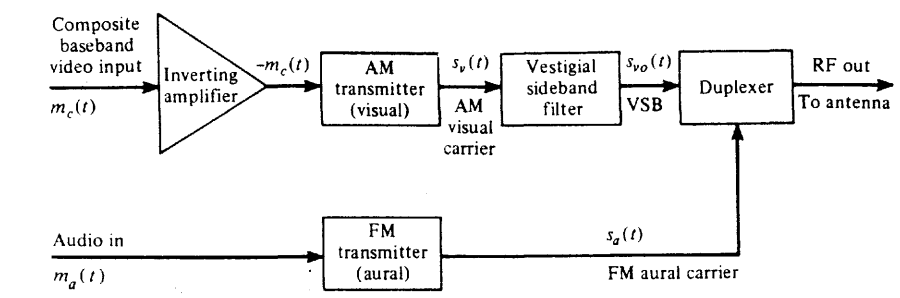
$$P_{\text{ERP}} = P_{\text{PEP}} G_A G_L \quad (8-62)$$

where

$P_{\text{PEP}}$  = peak envelope power out of the transmitter

$G_A$  = power gain of the antenna (absolute units as opposed to decibel units) with respect to an isotropic antenna

<sup>†</sup> Typically, a horizontal resolution of about 300 lines is obtained.



(a) Equipment Block Diagram

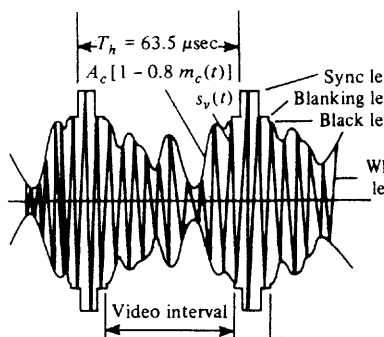
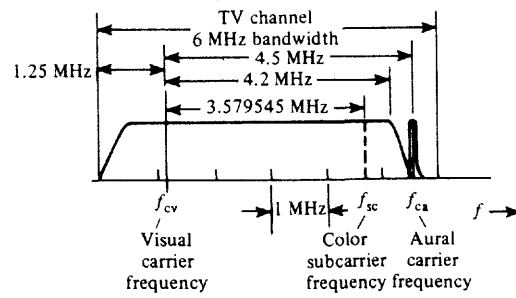
(b) AM Visual Carrier Waveform,  $s_v(t)$   
(Typical Video Modulation Illustrated)(c) Magnitude Spectrum of RF Output  
(Frequency Response Characteristic)

Figure 8-31 TV transmission system.

$G_L$  = total gain of the transmission line system from the transmitter output to the antenna (including the duplexer gain)

For a VHF TV station operating on channel 5, some typical values are  $G_A = 5.7$ ,  $G_L = 0.873$  (850 ft of transmission line plus duplexer), and a visual PEP of 20.1 kW. This gives an overall ERP of 100 kW, which is the maximum power licensed by the FCC for channels 2 to 6 (low-VHF band). For a UHF station operating on channel 20, some typical values are  $P_{PEP} = 21.7$  kW,  $G_A = 27$ ,  $G_L = 0.854$  (850 ft of transmission line), which gives an ERP of 500 kW.

A simplified block diagram of a black-and-white TV receiver is shown in Fig. 8-32. The composite video,  $m_c(t)$ , as described earlier, plus a 4.5-MHz FM carrier containing the audio modulation, appears at the output of the envelope detector. The 4.5-MHz FM carrier is present because of the nonlinearity of the envelope detector and because the detector input (IF signal) contains, among other terms, the FM aural carrier plus a discrete (i.e., sinusoidal) term, which is the video carrier, located 4.5 MHz away from the FM carrier signal. The intermodulation product of these two signals produces the 4.5-MHz FM signal, which is called the *intercarrier signal*, and contains the aural modulation. Of course, if either of these two input signal components disappears, the 4.5-MHz output signal will also disappear.

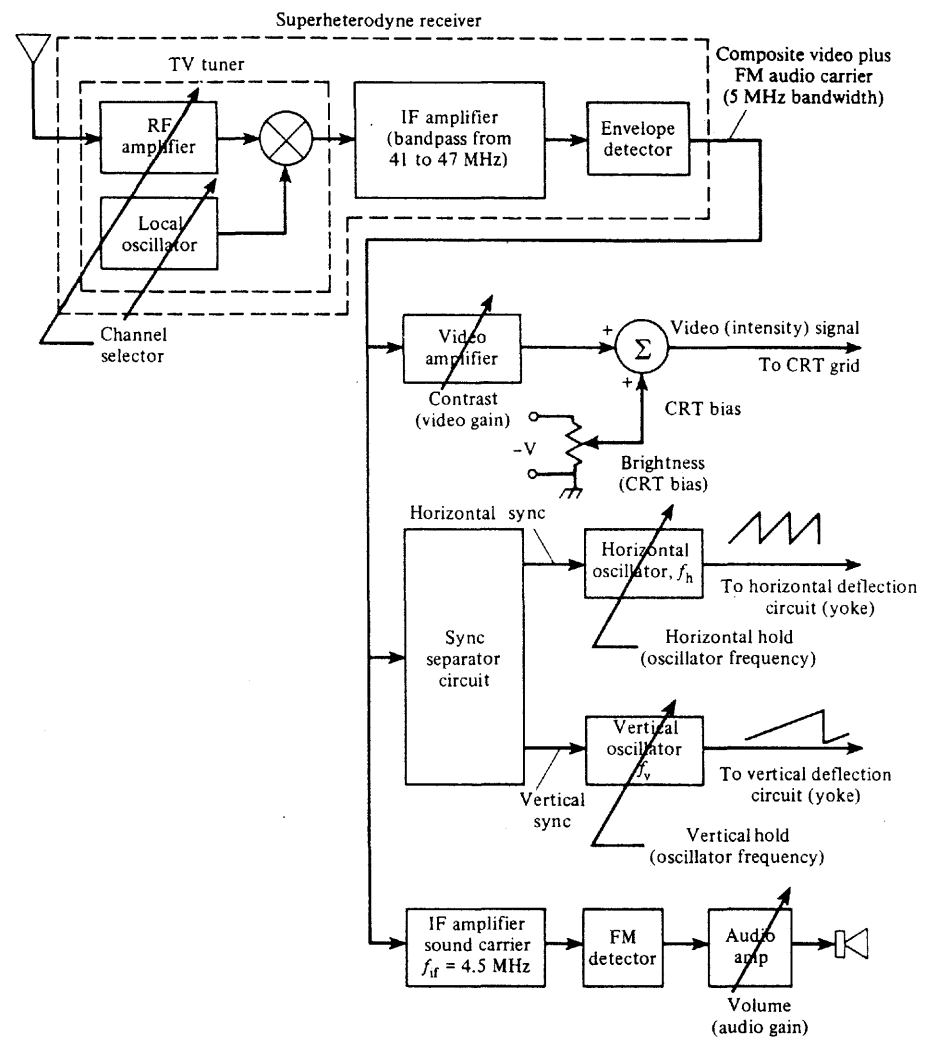
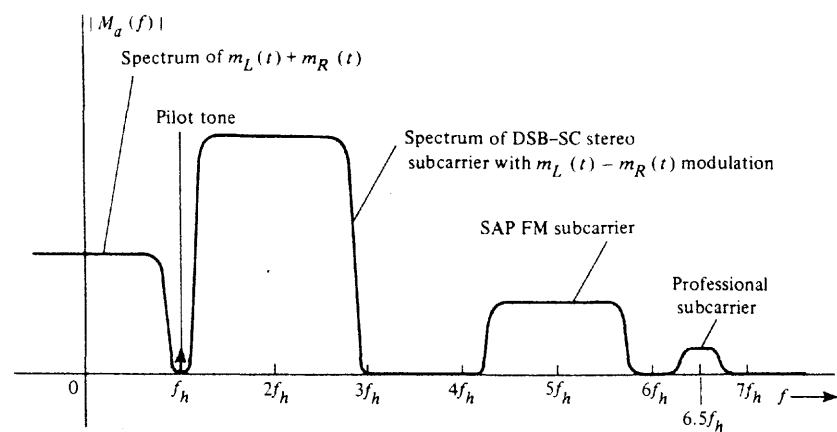


Figure 8-32 Black-and-white TV receiver.

This will occur if the white level of the picture is allowed to go below, say, 10% of the peak envelope level (sync tip level) of the AM visual signal. This is why the FCC specifies that the white level cannot be lower than  $(12.5 \pm 2.5)\%$  of the peak envelope level (see Table 8-11). When this occurs, a buzz will be heard in the sound signal since the 4.5-MHz FM carrier is disappearing at a 60-Hz (field) rate during the white portion of the TV scene. The sync separator circuit consists of a lossy integrator to recover the (wide) vertical sync pulses and a lossy differentiator to recover the (narrow) horizontal pulses. The remainder of the block diagram is self-explanatory. The user-available adjustments for a black-and-white TV are also shown.



**Figure 8-33** Spectrum of composite FDM baseband modulation on the FM aural carrier of U.S. TV stations.

### MTS Stereo Sound

Stereo audio, also known as *multichannel television sound* (MTS), is also available and is accomplished using the FDM technique shown in Fig. 8-33. This FDM technique is similar to that used in standard FM broadcasting, studied in Sec. 5-7 and illustrated by Fig. 5-17. For compatibility with monaural audio television receivers, the left plus right audio,  $m_L(t) + m_R(t)$ , is frequency modulated directly onto the aural carrier of the television station. Stereo capability is obtained by using a DSB-SC subcarrier with  $m_L(t) - m_R(t)$  modulation. The subcarrier frequency is  $2f_h$ , where  $f_h = 15.734$  kHz is the horizontal sync frequency for the video (see Table 8-11). Capability is also provided for a *second audio program* (SAP), such as audio in a second language. This is accomplished by using an FM subcarrier of frequency  $5f_h$ . DBX audio noise reduction processing is used on the audio on both the DSB-SC stereo subcarrier and the SAP subcarrier that is frequency modulated by the second audio signal. (See Sec. 5-8 for a discussion of the DBX noise reduction technique.) Furthermore, a *professional channel* subcarrier at  $6.5f_h$  is allowed for transmission of voice or data on a subscription service basis to paying customers. For further details on the FDM aural standards that have been adopted by television broadcasters and for other possible FDM formats, see a paper by Eilers [1985].

### Color Television

Color television pictures are synthesized by combining red, green, and blue light in the proper proportion to produce the desired color. This is done by using a color CRT that has three types of phosphors—one type that emits red light, one that emits green, and a third type that emits blue light when they are struck by electrons. Therefore, three electronic video signals— $m_R(t)$ ,  $m_G(t)$ , and  $m_B(t)$ —are needed to drive the circuits that create the red, green, and blue light. Furthermore, a compatible color TV transmission system is needed such that

black-and-white TV sets will receive the luminance video signal,  $m_y(t)$ , which corresponds to the gray scale of the scene. This compatibility between color and black-and-white transmission is accomplished by using a multiplexing technique analogous to that of FM stereo, except that three signals are involved in the problem instead of two.

The National Television System Committee (NTSC) compatible color TV system that was developed in the United States and adopted for U.S. transmissions in 1954 will be discussed. This technique is illustrated in Fig. 8-34. For compatible transmission, the waveforms that correspond to the intensity of the red, green, and blue components of the scene— $m_R(t)$ ,  $m_G(t)$ , and  $m_B(t)$ —are linearly combined to synthesize the equivalent black-and-white signal,  $m_y(t)$ , and two other independent video signals, called the *in-phase* and *quadrature* components,  $m_i(t)$  and  $m_q(t)$ . (The names of these components arise from the quadrature modulation technique that is used to modulate them onto a subcarrier.) The exact equations used for these signals can be expressed in matrix form:

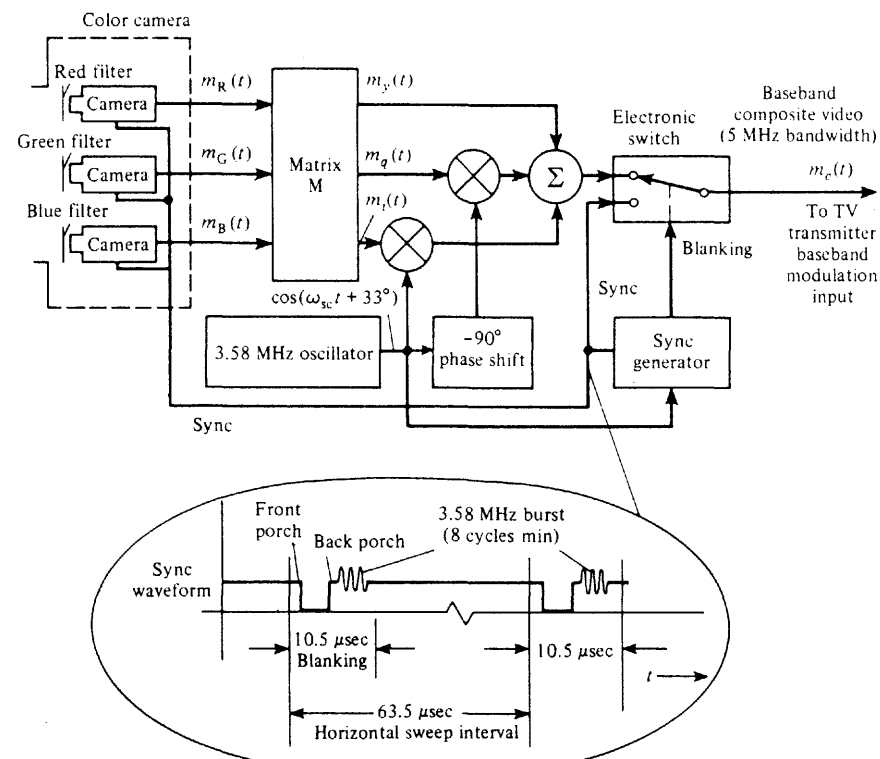


**Figure 8-34** Generation of the composite NTSC baseband video signal. [Technically,  $m_q(t)$  is low-pass filtered to an 0.5-MHz bandwidth and  $m_i(t)$  is low-pass filtered to a 1.5-MHz bandwidth.]

$$\begin{bmatrix} m_y(t) \\ m_i(t) \\ m_q(t) \end{bmatrix} = \underbrace{\begin{bmatrix} 0.3 & 0.59 & 0.11 \\ 0.6 & -0.28 & -0.32 \\ 0.21 & -0.52 & 0.31 \end{bmatrix}}_M \begin{bmatrix} m_R(t) \\ m_G(t) \\ m_B(t) \end{bmatrix} \quad (8-63)$$

where  $M$  is a  $3 \times 3$  matrix that translates the red, green, and blue signals to the brightness, in-phase, and quadrature phase video (baseband) signals. For example, from (8-63), the equation for the *luminance* (black-and-white) signal is

$$m_y(t) = 0.3m_R(t) + 0.59m_G(t) + 0.11m_B(t) \quad (8-64)$$

Similarly, the equations for  $m_i(t)$  and  $m_q(t)$ , which are called the *chrominance* signals, are easy to obtain. In addition, note that if  $m_R(t) = m_G(t) = m_B(t) = 1$ , which corresponds to maximum red, green, and blue, then  $m_y(t) = 1$ , which corresponds to the white level in the black-and-white picture.

The chrominance components are two other linearly independent components, and if they are transmitted to the color TV receiver together with the luminance signal, these three signals can be used to recover the red, green, and blue signals using an inverse matrix operation. The bandwidth of the luminance signal needs to be maintained at 4.2 MHz to preserve sharp (high-frequency) transition in the intensity of the light that occurs along edges of objects in the scene. However, the bandwidth of the chrominance signals does not need to be this large since the eye is not as sensitive to color transitions in a scene. In NTSC standards the bandwidth of the  $m_i(t)$  signal is 1.5 MHz and the bandwidth of  $m_q(t)$  is 0.5 MHz. When they are quadrature-modulated onto a subcarrier, the resulting composite baseband signal will then have a bandwidth of 4.2 MHz. (The upper sideband of the in-phase subcarrier signal is attenuated to keep a 4.2-MHz bandwidth.)

The composite NTSC baseband video signal is

$$m_c(t) = \begin{cases} m_s(t) & \text{during the sync interval} \\ m_y(t) + \operatorname{Re}\{g_{sc}(t)e^{j\omega_{sc}t}\} & \text{during the video interval} \end{cases} \quad (8-65)$$

where

$$g_{sc}(t) = [m_i(t) - jm_q(t)]e^{j33^\circ} \quad (8-66)$$

Equation (8-66) indicates that the chrominance information is quadrature modulated onto a subcarrier (as described in Table 4-1).  $m_s(t)$  is the sync signal,  $m_y(t)$  is the luminance signal, and  $g_{sc}(t)$  is the complex envelope of the subcarrier signal. The subcarrier frequency is  $f_{sc} = 3.579545 \text{ MHz} \pm 10 \text{ Hz}$ , which, as we will see later, is chosen so that the subcarrier signal will not interfere with the luminance signal even though both signals fall within the 4.2-MHz passband.

In broadcast TV, this composite NTSC baseband color signal is amplitude-modulated onto the visual carrier as described by (8-61) and shown in Fig. 8-31. In microwave relay applications and satellite relay applications, this NTSC baseband signal is frequency-modulated onto a carrier, as described in Sec. 8-5. These color baseband signals can be transmitted over communication systems that are used for black-and-white TV, although the

frequency response and linearity tolerances that are specified are tighter for color TV transmission.

As indicated before, the complex envelope for the subcarrier, as described by (8-66), contains the color information. The magnitude of the complex envelope,  $|g_{sc}(t)|$  is the *saturation* or amount of color in the scene as it is scanned with time. The angle of the complex envelope,  $\angle g_{sc}(t)$ , indicates hue or tint as a function of time. Thus  $g_{sc}(t)$  is a vector that moves about in the complex plane as a function of time as the lines of the picture are scanned. This vector may be viewed on an instrument called a *vectorscope*, which has a CRT that displays the vector  $g_{sc}(t)$ , as shown in Fig. 8-35. The vectorscope is a common piece of test equipment that is used to calibrate color TV equipment and to provide an on-line measure of the quality of the color signal being transmitted. The usual vectorscope presentation has the  $x$  axis located in the vertical direction, as indicated on the figure. Using (8-66), the positive axis directions for the  $m_i(t)$  and  $m_q(t)$  signals are also indicated on the vectorscope presentation, together with the vectors for the saturated red, green, and blue colors. For example, if saturated red is present, then  $m_R = 1$  and  $m_G = m_B = 0$ . Using (8-63), we get  $m_i = 0.6$  and  $m_q = 0.21$ . Thus, from (8-66), the saturated red vector is

$$(g_{sc})_{\text{red}} = (0.60 - j0.21)e^{j33^\circ} = 0.64 / 13.7^\circ$$

Similarly, the saturated green vector, is  $(g_{sc})_{\text{green}} = 0.59 / 151^\circ$ , and the saturated blue vector is  $(g_{sc})_{\text{blue}} = 0.45 / 257^\circ$ . These vectors are shown in Fig. 8-35. It is interesting to note that the complementary colors have the opposite polarity on the vectorscope, where cyan is the complement of red, magenta is the complement of green, and yellow is the complement of blue.

For color subcarrier demodulation at the receiver, a phase reference is needed. This is provided by keying in an eight-cycle (or more) burst of the 3.58-MHz subcarrier sinusoid on the "back porch" of the horizontal sync pulse, as shown in Fig. 8-34. The phase of the reference sinusoid is  $+90^\circ$  with respect to the  $x$  axis, as indicated on the vectorscope display (Fig. 8-35).

A color receiver is similar to a black-and-white TV receiver except that it has color demodulator circuits and a color CRT. This is shown in Fig. 8-36, where the color demodulator circuitry is indicated. The in-phase and quadrature signals,  $m_i(t)$  and  $m_q(t)$ , are recovered (demodulated) by using product detectors where the phase reference signal is obtained from a PLL circuit that is locked onto the color burst (which was transmitted on the back porch of the sync pulse).  $M^{-1}$  is the inverse matrix of that given in (8-63) so that the three video waveforms corresponding to the red, green, and blue intensity signals are recovered. It is realized that the hue control on the TV set adjusts the phase of the reference that sets the tint of the picture on the TV set. The color control sets the gain of the chrominance subcarrier signal. If the gain is reduced to zero, no subcarrier will be present at the input to the product detectors. Consequently, a black-and-white picture will be reproduced on the color TV CRT.

Of course, it is also possible to use different reference phases on the balanced detector inputs *provided* that the decoding matrix is changed to produce  $m_R$ ,  $m_G$ , and  $m_B$  at its output. For example, one popular technique uses the R-Y and B-Y phases on the input to the balanced modulators [Grob, 1975]. Here the reference phase out of the hue control circuit is  $0^\circ$  instead of  $33^\circ$ , as shown in Fig. 8-36. This corresponds to detecting the subcarrier

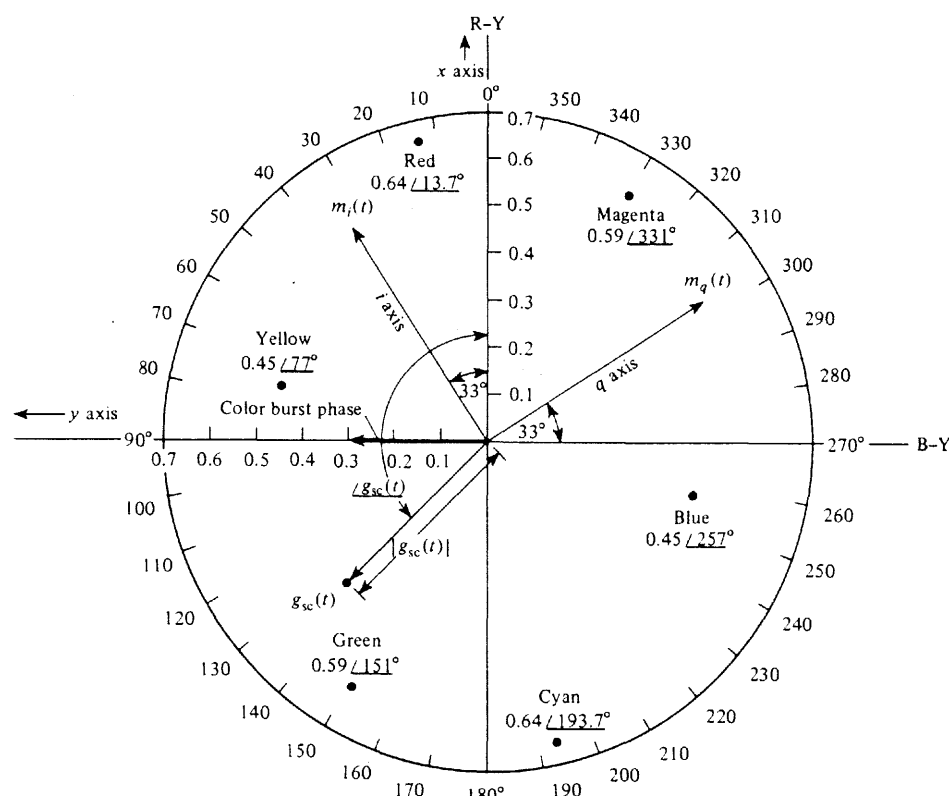


Figure 8-35 Vectorscope presentation of the complex envelope for the 3.58-MHz chrominance subcarrier.

along the R-Y and B-Y axes, as indicated on the vectorscope presentation (Fig. 8-35). In this case  $m_R(t) - m_Y(t)$  is obtained at the output of the upper product detector, and if a gain of two is used on the lower product detector,  $m_B(t) - m_Y(t)$  is obtained at its output. These two outputs may be added in the proper proportions to obtain  $m_G(t) - m_Y(t)$ . These three signals,  $m_R(t) - m_Y(t)$ ,  $m_G(t) - m_Y(t)$ , and  $m_B(t) - m_Y(t)$ , may be applied to the three control grids of a three-gun color CRT (one gun activating the red phosphor, one gun for the green, and one for the blue). The  $-m_Y(t)$  signal is applied to the common cathode of the three guns so that the effective signals on the guns are  $m_R(t)$ ,  $m_G(t)$ , and  $m_B(t)$ , respectively, which are the desired control signals. Furthermore, for black-and-white operation, it is only necessary to remove the three signals from the control grid since the luminance drive signal is applied at the cathode.

As stated earlier, both the luminance and chrominance subcarrier signals are contained in the 4.2-MHz composite NTSC baseband signal. This gives rise to interfering signals in the receiver video circuits. For example, in Fig. 8-36 there is an interfering signal on the input to the inverse matrix circuit. Here  $m_Y(t)$  plus interference is averaged out on a line-by-line scanning basis by the viewer's vision if the chrominance subcarrier frequency is an odd

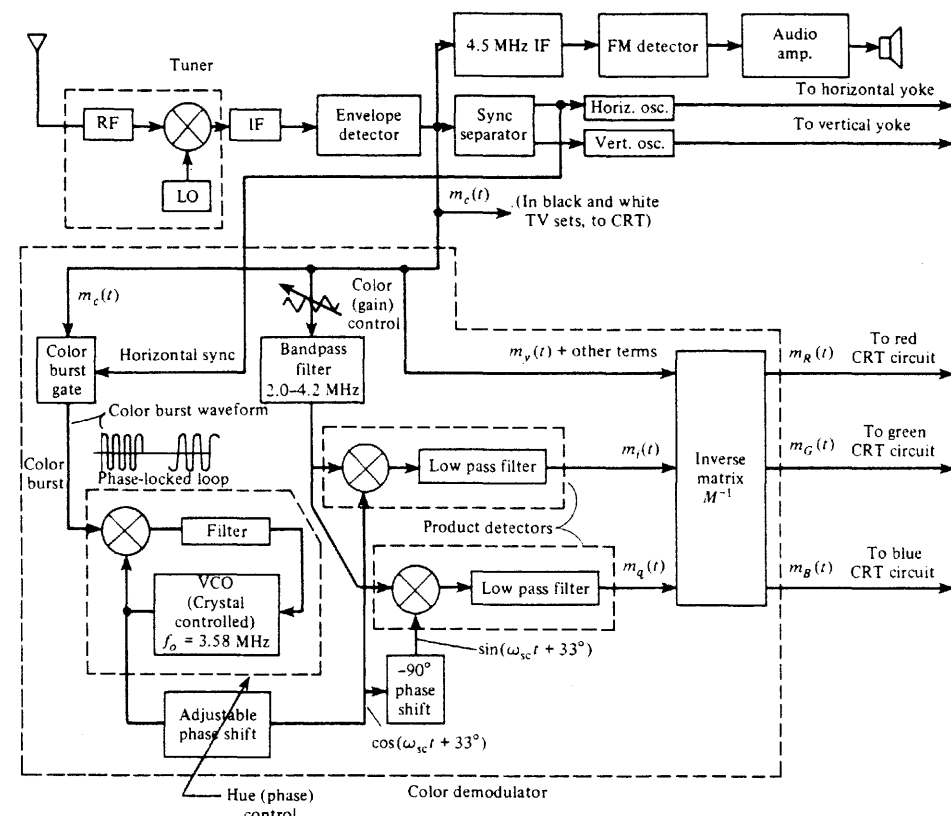


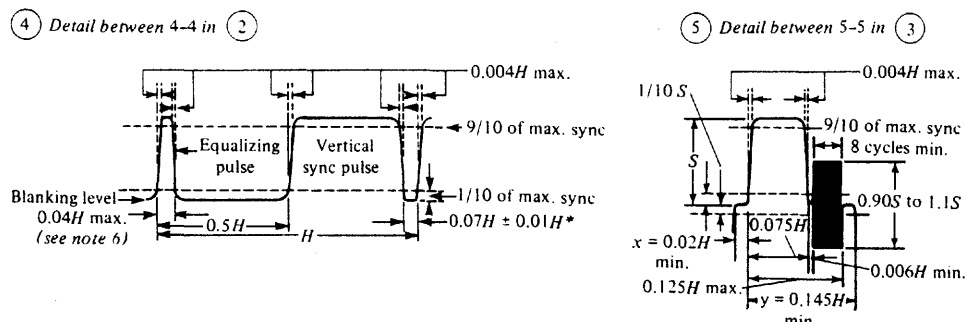
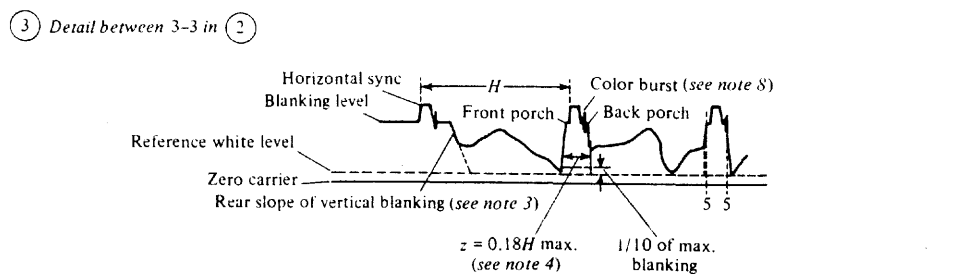
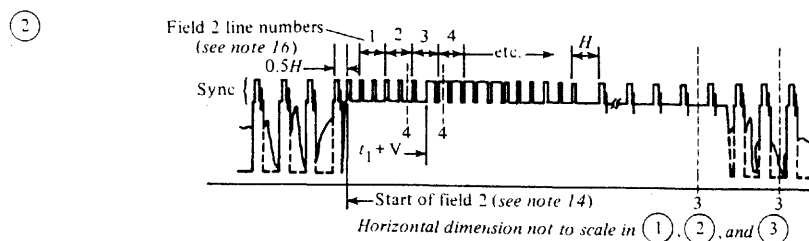
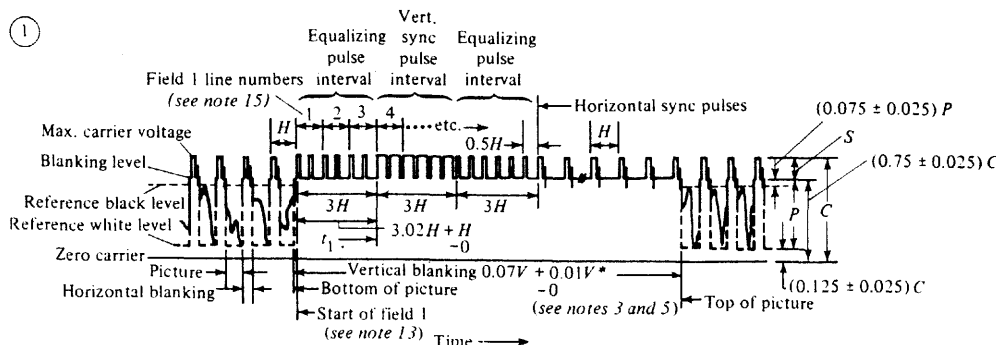
Figure 8-36 Color TV receiver with IQ demodulators.

multiple of half of the horizontal scanning frequency. For example, from Table 8-11,  $f_{sc} = 3,579,545$  Hz and  $f_h = 15,734$  Hz. Consequently, there are 227.5 cycles of the 3.58-MHz chrominance interference across one scanned line of the picture. Because there is a half cycle left over, the interference on the next scanned line will be *180° out of phase* with that of the present line and the interference will be *canceled out* by the eye when one views the picture.

As we have seen, the NTSC color system is an ingenious application of basic engineering principles, and this ingenuity is certainly not appreciated by the average color TV viewer.

### Standards for TV and CATV Systems

A summary of some of the U.S. analog TV transmission standards as adopted by the FCC is shown in Table 8-11, and details of the synchronizing waveform are given in Fig. 8-37.



A listing of the frequencies for the TV channels is given in Table 8-12. In addition, a comparison of some broadcast TV standards that are used by various countries is shown in Table 8-13. The CCIR system B standard, which is a 625-lines/frame, 25-frames/sec, negative modulation system is the dominant European TV standard [Dhake, 1980]. In addition to these standards for conventional TV as shown in this table, there are U.S. standards for HDTV as will be discussed in the next section. When TV signals are relayed from one country to another via satellite, the standards of the originating country are used, and, if needed, the signal is converted to the standards of the receiving country at the receiving ground station.

U.S. CATV channel standards are presented in Table 8-14. CATV systems use coaxial cable with amplifiers to distribute TV and other signals from the "head end" to the subscriber. Since the cable signals are not radiated, the frequencies that are normally assigned to two-way radio and other on-the-air services can be used for additional TV channels on the cable. Consequently, the CATV channel assignments have been standardized as shown in

#### NOTES TO FIGURE 8-37

1.  $H$  = time from start of one line to start of next line =  $1/f_h$  (see Table 8-11).
2.  $V$  = time from start of one field to start of next field =  $1/f_v$  (see Table 8-11).
3. Leading and trailing edges of vertical blanking should be complete in less than  $0.1 H$ .
4. Leading and trailing slopes of horizontal blanking must be steep enough to preserve minimum and maximum values of  $(x + y)$  and  $(z)$  under all conditions of picture content.
5. Dimensions marked with asterisk indicate that tolerances given are permitted only for long-time variations and not for successive cycles.
6. Equalizing pulse area shall be between 0.45 and 0.5 of area of a horizontal sync pulse.
7. Color burst follows each horizontal pulse, but is omitted following the equalizing pulses and during the broad vertical pulses.
8. Color bursts to be omitted during monochrome transmission.
9. The burst frequency shall be 3.579545 MHz. The tolerance on the frequency shall be  $\pm 10$  Hz with a maximum rate of change of frequency not to exceed  $1/10$  Hz/s.
10. The horizontal scanning frequency shall be  $2/455$  times the burst frequency.
11. The dimensions specified for the burst determine the times of starting and stopping the burst but not its phase. The color burst consists of amplitude modulation of a continuous sine wave.
12. Dimension  $P$  represents the peak excursion of the luminance signal from blanking level, but does not include the chrominance signal. Dimension  $S$  is the sync amplitude above blanking level. Dimension  $C$  is the peak carrier amplitude.
13. Start of field 1 is defined by a whole line between first equalizing pulse and preceding  $H$  sync pulses.
14. Start of field 2 is defined by a half line between first equalizing pulse and preceding  $H$  sync pulses.
15. Field 1 line numbers start with first equalizing pulse in field 1.
16. Field 2 line numbers start with second equalizing pulse in field 2.
17. Refer to Table 8-11 for further explanations and tolerances.

Figure 8-37 U.S. television synchronizing waveform standards for color transmission. (From Part 73 of FCC Rules and Regulations.)

TABLE 8-12 U.S. TELEVISION CHANNEL FREQUENCY ASSIGNMENTS

	Channel Number	Band (MHz)	UHF Channel Number	Band	UHF Channel Number	Band
Radio astronomy	2	54–60	29	560–566	57	728–734
Aeronautical	3	60–66	30	566–572	58	734–740
Two-way radio	4	66–72	31	572–578	59	740–746
	5	76–82	32	578–584	60	746–752
FM broadcasting	6	82–88	33	584–590	61	752–758
Aeronautical	7	174–180	34	590–596	62	758–764
Two-way radio	8	180–186	35	596–602	63	764–770
	9	186–192	36	602–608	64	770–776
	10	192–198	37	608–614	65	776–782
	11	198–204	38	614–620	66	782–788
VHF channels	12	204–210	39	620–626	67	788–794
	13	210–216	40	626–632	68	794–800
			41	632–638	69	800–806
UHF channels	14	470–476	42	638–644		
	15	476–482	43	644–650	70 <sup>a</sup>	806–812
	16	482–488	44	650–656	71 <sup>a</sup>	812–818
	17	488–494	45	656–662	72 <sup>a</sup>	818–824
	18	494–500	46	662–668	73 <sup>a</sup>	824–830
	19	500–506	47	668–674	74 <sup>a</sup>	830–836
	20	506–512	48	674–680	75 <sup>a</sup>	836–842
	21	512–518	49	680–686	76 <sup>a</sup>	842–848
	22	518–524	50	686–692	77 <sup>a</sup>	848–854
	23	524–530	51	692–698	78 <sup>a</sup>	854–860
	24	530–536	52	698–704	79 <sup>a</sup>	860–866
	25	536–542	53	704–710	80 <sup>a</sup>	866–872
	26	542–548	54	710–716	81 <sup>a</sup>	872–878
	27	548–554	55	716–722	82 <sup>a</sup>	878–884
	28	554–560	56	722–728	83 <sup>a</sup>	884–890

<sup>a</sup>These frequencies are now allocated to two-way radio and cellular telephone service but were allocated to UHF TV broadcasting before 1974.

this table. To receive these added channels, the subscriber has to have a TV set with CATV channel capability or use a down converter to convert the CATV channel to a standard channel such as channel 3 or channel 4. CATV systems can also be *bidirectional*, allowing some subscribers to transmit signals to the head end. In low-band split systems, frequencies below 50 MHz (T-band channels) are used for transmission to the head end. In mid-band, split system frequencies below 150 MHz are used for transmission to the head end.

Premium TV programs are often available to subscribers for an additional cost. The premium channels are usually scrambled by modifying the video sync or possibly by using digital encryption techniques. Subscribers to the premium services are provided with appropriate decoders that, in some systems, are addressable and remotely programmable by the CATV company. More details about TV standards and engineering practice can be found in the *Television Engineering Handbook* [Benson and Whitaker, 1992].

TABLE 8-13 COMPARISON OF SOME BROADCAST TELEVISION STANDARDS

Item	Where Used				
	North America, South America, Japan	Spain, Italy, England, Germany, CCIR System	France	USSR	
Lines/frame	525	625	625	819	625
Lines/second	15,750	15,625	15,625	20,475	15,625
Frames/second	30	25	25	25	25
Baseband video bandwidth (MHz)	4.2	5	6	10	6
Channel bandwidth (MHz)	6	7	8	14	8
Polarity of AM video modulation	Negative	Negative	Positive	Positive	Negative
Type of aural carrier	FM	FM	AM	AM	FM
Color system	NTSC <sup>b</sup>	PAL <sup>c</sup>	SECAM <sup>d</sup>	SECAM <sup>d</sup>	SECAM <sup>d</sup>
Color subcarrier frequency (MHz)	3.58	4.43	4.43	4.43	4.43

<sup>a</sup>The 625-line/frame, 25-frame/s system is the CCIR (International Radio Consultative Committee) system B standard and is the dominant TV standard used on the European continent.

<sup>b</sup>NTSC, National Television System Committee (United States).

<sup>c</sup>PAL, Phase Alternation Line (Europe).

<sup>d</sup>SECAM, Sequential Couleur à Mémoire (French).

## HDTV

Since 1987, the FCC has been encouraging the development of a *high definition television* (HDTV) system to replace the NTSC system. The HDTV system would have high resolution that approaches the quality of 35-mm film and a widescreen aspect ratio (width to height) of 16:9 instead of the narrow screen 4:3 aspect ratio of NTSC. Since 1987, more than 20 HDTV methods have been proposed [Jurgen, 1988; Jurgen, 1991]. Some of them are analog and some are digital. By 1993 the number of competing proposals had been reduced to four and all four of these were digital systems [Challapali et al., 1995; Harris, 1993; Zou, 1991]. In May 1993, the proponents of these four competing systems joined forces to develop a single digital HDTV system that used the best ideas of the four competing systems [Challapali et al., 1995; Hopkins, 1994; and Petajan, 1995]. This joint group is called the Grand Alliance (GA) and its members are: AT&T, General Instrument Corporation, Massachusetts Institute of Technology (MIT), Philips Electronics North America Corporation, David Sarnoff Research Center, Thomson Consumer Electronics, and Zenith Electronics

TABLE 8-14 CATV CHANNEL FREQUENCIES

CATV Channel Number	Band (MHz)	Letter Channel Designator	CATV Channel Number	UHF Band (MHz)
Sub-VHF	5.75–11.75	T–7	37	300–306
	11.75–17.75	T–8	38	306–312
	17.75–23.75	T–9	39	312–318
	23.75–29.75	T–10	40	318–324
	29.75–35.75	T–11	41	324–330
	35.75–41.75	T–12	42	330–336
	41.75–47.55	T–13	43	336–342
Low-VHF	2	54–60	44	342–348
	3	60–66	45	348–354
	4	66–72	46	354–360
	5	76–82	47	360–366
	6	82–88	48	366–372
	FM Broadcasting		49	372–378
High-VHF	88–108		50	378–384
	7	174–180	51	384–390
	8	180–186	52	390–396
	9	186–192	53	396–402
	10	192–198	54	402–408
	11	198–204	55	408–414
	12	204–210	56	414–420
Midband	13	210–216	57	420–426
	14	120–126	58	426–432
	15	126–132	59	432–438
	16	132–138	60	438–444
	17	138–144	61	444–450
	18	144–150		:
	19	150–156	89	612–618
	20	156–162	90	618–624
	21	162–168	91	624–630
	22	168–174	92	630–636
	23	216–222	93	636–642
	24	222–228	94	642–648
Superband	25	228–234	95	90–96
	26	234–240	96	96–102
	27	240–246	97	102–108
	28	246–252	98	108–114
	29	252–258	99	114–120
	30	258–264		
	31	264–270		
	32	270–276		
	33	276–282		
	34	282–288		
	35	288–294		
	36	294–300		
		W		

Corporation. This has resulted in the GA HDTV standard that was adopted by the FCC in 1995. This digital HDTV standard is described in Table 8-15.

The bit rate for uncompressed video data is tremendous. For example, referring to Table 8-15, for 1080 active lines, 1920 samples (pixels) per line, 8 bits per sample, 30 frames (pictures) per second and 3 primary colors (RGB), the bit rate is  $1080 \times 1920 \times 8 \times 30 \times 3 = 1,500$  Mbits/s. However, a TV channel with 6 MHz bandwidth can only support a data rate of about 20 Mbits/s if 8-level (3 bits/symbol) multilevel signaling is used (from Fig. 5-33,  $B_T \approx D = R/\ell = 20/3 = 6.67$  MHz). Consequently a data compression factor of about 75 (1,500/20) is needed. As shown in Table 8-15, this compression factor is achieved by using a *Motion Pictures Experts Group* (MPEG) encoding technique. This technique consists of taking the *discrete cosine transform* (DCT) of  $8 \times 8$  blocks of pixels within each frame and digitizing (using) only the significant DFT coefficients of each block for transmission. Furthermore, for each new frame, data is sent only when there is a change (motion) within the  $8 \times 8$  pixel block, frame to frame. As indicated in Table 8-15, this produces a payload (compressed) data rate of 19.39 Mbits/s. This payload data plus parity bits for the FEC codes are fed into a 3-bit digital-to-analog converter (DAC) to produce an 8-level baseband line code that has a symbol (baud) rate of 10.76 Msymbols/s. This 8-level line code is amplitude modulated onto a suppressed carrier and filtered to produce a vestigial sideband signal (8VSB). This 8VSB signal is transmitted to the TV receiver. Raised cosine filtering (square root raised cosine at the transmitter and square root raised cosine at the receiver) is used to produce a 6 MHz bandwidth 8VSB signal that has no ISI.

The digital HDTV standard has been adopted because digital TV has the following advantages:

- Use of digital signal processing (DSP) circuits.
- Error-free regeneration of relayed and recorded TV pictures since binary data represent the picture.
- Multiple sound channels (four to six) of CD quality for stereo multilingual capability via TDM of PCM signals.
- Data may be multiplexed for text captioning screen graphics and for control of TV recording and other equipment.
- Multipath (ghost) images and ignition noise can be canceled using DSP circuits.
- Lower TV transmitter power will be required because digital modulation is used.
- Co-channel digital HDTV signals will interfere less with each other than co-channel NTSC analog signals.

The FCC plans to implement the new HDTV system by assigning a new TV channel (for HDTV transmission) for each existing NTSC TV station. Thus each station will simultaneously broadcast a NTSC signal on their existing channel and a HDTV signal on their new channel. Channels 7 through 51 would be used for the new HDTV signals. By the year 2011, the FCC expects everyone to be using HDTV receivers, so the NTSC TV stations will cease transmission. This will free channels 2 through 6 and 52 through 69 for assignment to other uses.

In addition, the TV broadcasters are asking the FCC to allow them to have the option of substituting data for 4 or 5 *standard definition television* (SDTV) programs to replace the

TABLE 8-15 US HDTV SYSTEM

	Format 1	Format 2
<b>Video specifications</b>		
Aspect ratio	16:9	16:9
Active scan lines/frame	720	1080
Pixels/line	1280	1920
Frame rates (Hz) <sup>a</sup>	60P, 30P, 24P	60I, 30P, 24P
Compression standard <sup>b</sup>	MPEG-2	MPEG-2
Compression technique <sup>c</sup>	DCT, 8 × 8 block	DCT, 8 × 8 block
<b>Audio specifications</b>		
Method	Dolby AC-3	
Audio bandwidth	20 kHz	
Sampling frequency	48 kHz	
Dynamic range	100 dB	
Number of surround channels <sup>d</sup>	5.1	
Compressed data rate	384 kbit/s	
Multiple languages	Via multiple AC-3 data streams	
<b>Data transport system</b>		
Type	Packet	
TDM technique	MPEG-2, system layer	
Packet size	188 bytes	
Packet header size	4 bytes	
Encryption	Provision descrambling by authorized decoders	
Special features support	Closed captioning and private data	
<b>Transmission specifications for terrestrial mode broadcasting<sup>e</sup></b>		
Modulation <sup>f</sup>	8VSB	
Bits/symbol	3	
Channel bandwidth	6 MHz	
Channel filter	Raised cosine-rolloff, $r = 0.115$	
Symbol (baud) rate	10.76 Msymbols/s	
Payload data rate	19.39 Mbit/s	
Coding (FEC)	Rate 2/3 TCM and (207,187) Reed-Solomon	
CNR threshold	14.9 dB for a BER of $3 \times 10^{-6}$	
Pilot (for carrier sync)	310 kHz above lower band edge of RF channel	

<sup>a</sup>P = progressive scan, I = Interlace scan.

<sup>b</sup>MPEG = Moving Picture Experts Group of the International Standards Organization (ISO).

<sup>c</sup>DCT = Two-dimensional (horizontal and vertical) Discrete Cosine Transform taken over a  $8 \times 8$  block of pixels. The insignificant DCT values are ignored to provide data compression.

<sup>d</sup>Left, center, right, left surround, right surround, and subwoofer. The sixth (subwoofer) channel contains only low audio frequencies so it is considered to be a 0.1 channel.

<sup>e</sup>Terrestrial mode is for off-the-air broadcasting. For transmission via CATV, 16 VSB may be used. This allows a higher payload data rate of 38.6 Mbit/sec over a 6 MHz bandwidth channel. However, a minimum (CNR) of 28.3 dB is required.

<sup>f</sup>8VSB = 8 level Vestigial Sideband Modulation. That is, an 8 level baseband line code is amplitude modulated onto a suppressed carrier (DSB-SC) signal and the lower sideband is filtered off to produce the VSB signal.

data of one HDTV program. This is commercially attractive to the TV broadcasters because it would allow them to transmit 4 or 5 SDTV programs over their assigned (6MHz bandwidth) channel. If this is allowed, HDTV may or may not become a reality.

It will be interesting to see how this HDTV plan works out. It will require broadcasters to purchase expensive HDTV studio and transmission equipment. Initially, HDTV sets will cost much more than NTSC TV sets. Obviously, the economics of the marketplace will dictate how fast (or if) this transition to HDTV will occur.

## 8-10 SUMMARY

Case studies for a wide range of practical communication systems have been presented. Modern telephone systems that have large computer-controlled central offices and remote terminals have been studied. ISDN service was described. Specifications of PSTN systems were given for voice and data transmission via fiber-optic cable, twisted-pair wire, satellite and microwave radio relay. Digital and analog satellite systems for TV signal relay and data transmission with FDMA and TDMA were described. Noise figure and effective input-noise temperature of receiving systems were defined. Case studies of link budgets were presented. U.S. and worldwide standards for cellular telephone systems were examined. Finally, a case study of the U.S. NTSC TV system was presented with standards given for the United States, other countries, and for U.S. CATV channels. In addition, the U.S. digital HDTV system was discussed.

## 8-11 STUDY-AID EXAMPLES

**SA8-1** Compute the link budget for a digital TV satellite system that is similar to the GM Hughes DSS system that was described in Sec. 8-5. The DSS satellite is located in a geostationary orbit at 101° W longitude above the equator. Assume that the downlink receiving site is Gainesville, FL, located at 82.43° W longitude and 29.71° N latitude. The DSS satellite transmits downlink signals in the Ku band (12.2-12.7 GHz) using 16 transponders. Each transponder has a bandwidth of 24 MHz and an EIRP of 52 dBw in the direction of the U.S. and, in particular, to Gainesville, FL. Each transponder radiates a QPSK signal with a data rate of 40 Mbit/s. The receiving system consists of (1) an 18 inch diameter parabolic antenna with an attached (2) low-noise block downconverter (LNB) that converts the Ku band input down to 950 to 1450 MHz, (3) a transmission line that connects the LNB to (4) a receiver that is located on the top of the subscriber's TV set [Thomson, 1994]. The LNB has a gain of 40 dB and a noise figure (NF) of 0.6 dB. The RG6/U coaxial transmission line is 110 feet in length and has a loss of 8 dB/100 ft in the 950-1450 MHz band. The receiver detects the data packets, decodes them, and converts the data to analog video and audio signals using the built-in digital-to-analog converters. The receiver has a NF of 10 dB and an IF bandwidth of 24 MHz. Assume that the antenna source temperature is 20 K.

Compute the  $(C/N)_{dB}$ ,  $(E_b/N_0)_{dB}$ , and the BER for this receiving system.

**Solution.** The receiving antenna pointing parameters (azimuth and elevation) from Gainesville, FL, to the satellite are evaluated using Eqs. (8-47) to (8-54).

$$\beta = \cos^{-1} [\cos(29.71) \cos(101 - 82.43)] = 34.58^\circ$$

The azimuth is

$$A = 360 - \cos^{-1} \left( -\frac{\tan(29.71)}{\tan(34.58)} \right) = 214.13^\circ$$

The elevation is

$$E = \tan^{-1} \left[ \frac{1}{\tan(34.58)} - \frac{3963}{(26,205) \sin(34.58)} \right] = 49.82^\circ$$

Using (8-49), the slant range is

$$d = \sqrt{(26,205)^2 + (3963)^2 - 2(3693)(26,205) \cos(34.58)}$$

Thus,

$$d = 23,052 \text{ miles or } 3.709 \times 10^7 \text{ m}$$

The overall NF for the receiving system is evaluated using (8-34), where  $F_1 = 0.6 \text{ dB} = 1.15$ ,  $G_1 = 40 \text{ dB} = 10^4$ ,  $F_2 = 110 \text{ ft} \times 8 \text{ dB}/100 \text{ ft} = 8.8 \text{ dB} = 7.59$ ,  $G_2 = -8.8 \text{ dB} = 0.13$  and  $F_3 = 10 \text{ dB} = 10$ . Then,

$$F = F_1 + \frac{F_2 - 1}{G_{a1}} + \frac{F_3 - 1}{G_{a1} G_{a2}} = 1.15 + \frac{7.59 - 1}{10^4} + \frac{10 - 1}{(10^4)(0.13)}$$

or  $F = 1.15 + 6.59 \times 10^{-4} + 6.83 \times 10^{-3} = 1.15 = 0.6 \text{ dB}$ .

Thus,  $T_e = (F - 1)T_0 = (1.15 - 1)(290) = 43.18 \text{ K}$ .

*Note:* The gain of the LNB is designed to be sufficiently large so that the NF contributions of the transmission line and the receiver are negligible.

The receiving antenna is computed using Table 8-4 for an 18in = 0.46-m diameter parabola where  $\lambda = f/c = 3 \times 10^8/12.45 \times 10^9 = 0.0241 \text{ m}$ .

$$(G_{AR})_{\text{dB}} = 10 \log \left[ \frac{7\pi(0.46/2)^2}{(0.0241)^2} \right] = 32.96 \text{ dB}$$

$$(T_{\text{syst}})_{\text{dB}} = 10 \log(T_{AR} + T_e) = 10 \log(20 + 43.18) = 18.01 \text{ dB/K}$$

Thus,

$$\left( \frac{G_{AR}}{T_{\text{syst}}} \right)_{\text{dB}} = 32.96 - 18.01 = 14.96 \text{ dB/K}$$

The  $(C/N)_{\text{dB}}$  is evaluated using (8-55), where

$$(L_{FS})_{\text{dB}} = 20 \log \left( \frac{4\pi d}{\lambda} \right) = 20 \log \left( \frac{4\pi(3.709 \times 10^7)}{0.0241} \right) = 205.73 \text{ dB}$$

and

$$(B)_{\text{dB}} = 10 \log(B) = 10 \log(24 \times 10^6) = 73.8 \text{ dB}$$

Thus,

$$\begin{aligned} \left( \frac{C}{N} \right)_{\text{dB}} &= (P_{\text{EIRP}})_{\text{dBw}} - (L_{FS})_{\text{dB}} + \left( \frac{G_{AR}}{T_{\text{syst}}} \right)_{\text{dB}} - k_{\text{dB}} - B_{\text{dB}} \\ &= 52 - 205.73 + 14.96 - (-228.6) - 73.8 \end{aligned}$$

or

$$(C/N)_{\text{dB}} = 16.03 \text{ dB}$$

$(E_b/N_0)_{\text{dB}}$  may be evaluated using (8-44), where  $B = 24 \text{ MHz}$ , and  $R = 40 \text{ Mbits/s}$  or  $R = B$  for this problem. Then

$$\left( \frac{E_b}{N_0} \right)_{\text{dB}} = \left( \frac{C}{N} \right)_{\text{dB}} + \left( \frac{B}{R} \right)_{\text{dB}} = 16.03 - 2.22 = 13.81 \text{ dB}$$

An  $(E_b/N_0)_{\text{dB}}$  of 13.81 dB = 24.05 gives negligible errors for QPSK signaling. That is, if no coding is used, the QPSK BER is given by (7-69).

$$P_e = Q \left( \sqrt{2 \left( \frac{E_b}{N_0} \right)} \right) = Q(\sqrt{2(24.05)}) = 2.0 \times 10^{-12}$$

or one error every 3.4 hours. However, if there is signal fading (because of rain or other atmospheric conditions), significant errors may occur. This is examined in Example SA8-2.

**SA8-2** Repeat Example SA8-1, and assume that there is a 4-dB signal fade of the Ku band signal because of severe rain. Compute  $(C/N)_{\text{dB}}$ ,  $(E_b/N_0)_{\text{dB}}$  and the BER with and without coding. For the coding case, assume a 3-dB coding gain.

*Solution*

$$\left( \frac{C}{N} \right)_{\text{fade dB}} = \left( \frac{C}{N} \right)_{\text{dB}} - (L_{\text{fade}})_{\text{dB}} = 16.03 - 4.0 = 12.03 \text{ dB}$$

and

$$\left( \frac{E_b}{N_0} \right)_{\text{fade dB}} = 9.81 \text{ dB} = 9.57$$

Then, the BER with fading and no coding is

$$P_e = Q(\sqrt{2(9.57)}) = 6.04 \times 10^{-6}$$

or one error in 41 ms. This performance is not acceptable; consequently FEC coding is needed. Using coding with a coding gain of 3dB, compute the effective  $(E_b/N_0)$  by referring to Fig. 1-8,

$$\left( \frac{E_b}{N_0} \right)_{\text{dB}} = 9.81 + 3.0 = 12.81 \text{ dB} = 19.10$$

Then, using (7-69), the BER with fading and coding becomes

$$P_e = Q(\sqrt{2(19.10)}) = 3.20 \times 10^{-10}$$

or one error every 78s.

**SA8-3** Evaluate the BER performance of a wireless personal communication device (PCD). Assume that a portable computer/telephone/video terminal is connected to the outside world via a wireless link within a building. The wireless link operates between the PCD and a base station unit which is located within the building. The wireless link uses OOK signaling on a carrier frequency of 2.4 GHz and the data rate is 2 Mbits/s. The PCD transmit power on the uplink

(PCD to base station) is 0.5 mW. The base station receiver has a noise figure of 8 dB and an IF bandwidth of 4 MHz. It incorporates an envelope detector to detect the data. External noise at the receiver input is negligible when compared with the internal noise of the receiver. Assume that the transmit and receive antennas are simple dipoles; each has a gain of 2.15 dB. The path loss between the transmit and receive antenna within the building environment is modeled by [Rappaport, 1996, p. 126]

$$L_{\text{dB}}(d) = L_{\text{FSdB}}(d_0) + 10n \log\left(\frac{d}{d_0}\right) + X_{\text{dB}} \quad (8-67)$$

where  $L_{\text{dB}}(d)$  is the path loss in dB for a distance of  $d$  between the antennas,  $L_{\text{FSdB}}(d_0)$  is the free space loss for a distance  $d_0$  that is close to the transmitter but in the far field, and  $d > d_0$ .  $n$  is the path loss exponent and  $X_{\text{dB}}$  represents the loss margin due to variations in the path loss caused by multiple reflections. For this example, choose  $d_0 = 50$  feet,  $n = 3$ , and  $X_{\text{dB}} = 7$  dB. (The exponent,  $n$ , would be 2 for the free-space case and 4 for a 2-ray ground-reflection case.)

For a distance of 200 feet between the PCD and the base station, calculate the CNR at the detector input of the base station receiver and the BER for the detected data at the receiver output.

**Solution.** The CNR is obtained by using (8-67) to replace  $(L_{\text{FS}})_{\text{dB}}$  in (8-43). Using the values given above we get  $(P_{\text{EIRP}})_{\text{dBw}} = -30.86$  dBw,  $T_{\text{system}} = 1540$  K, and  $L_{\text{dB}}(200) = 88.18$  dB. From (8-43) with the PCD located 200 feet from the base station, the CNR is

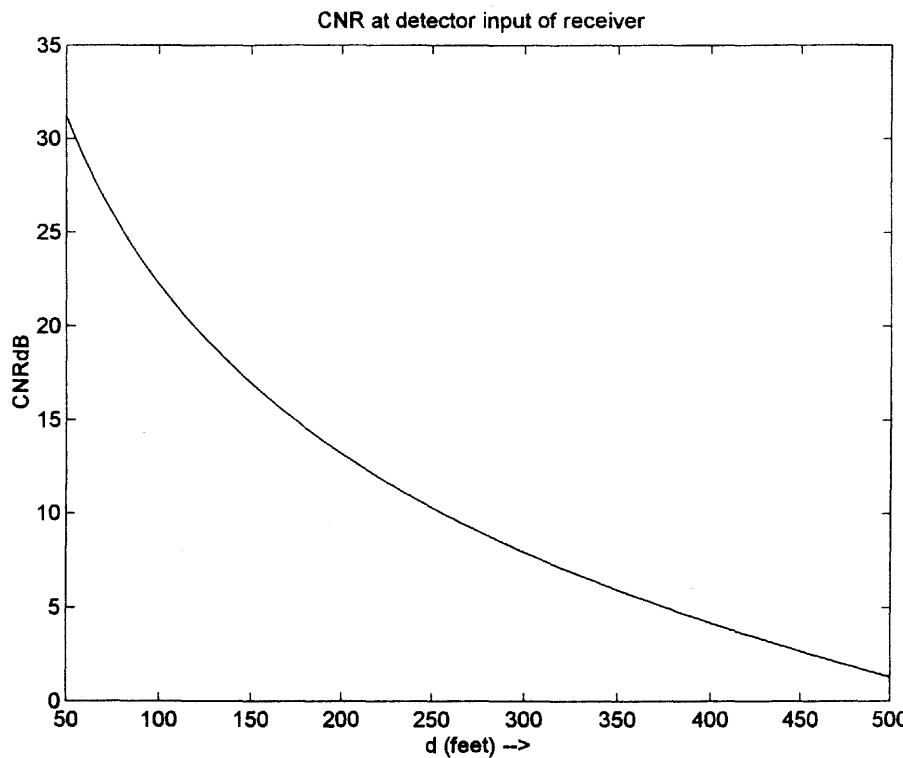


Figure 8-38 CNR for a PCD wireless link.

$$\left(\frac{C}{N}\right)_{\text{dB}} = 13.22 \text{ dB}, \quad 200 \text{ feet spacing}$$

Also, using (8-44),  $(E_b/N_0)_{\text{dB}} = 16.23$  dB. For this case of OOK with (noncoherent) envelope detection, the BER is obtained by using (7-58). The bit rate is  $R = 1/T = 2$  Mbit/s and the IF bandwidth is  $B_p = 4$  MHz. For a spacing of 200 feet between the PCD and the base station, the BER of the base station output data stream is

$$P_e = 1.36 \times 10^{-5}, \quad 200 \text{ feet spacing}$$

Using other values for  $d$  in these equations, MATLAB can compute the CNR and BER over a whole range of spacing from 50 feet to 500 feet. The MATLAB plots are shown in Figures 8-38 and 8-39.

The range of this PCD wireless link could be increased by increasing the transmit power, reducing the receiver noise figure, or implementing a spread spectrum (SS) system. If direct sequence SS is used with a  $r = 4$  stage shift register as shown in Figure 5-37, then the PN code length is  $N = 15$ . Assuming that code length spans one bit of data, then the chip rate is  $R_c = NR$ . From (5-131), this SS system would provide a processing gain of  $G_p = R_c/R = N = 15$  or  $G_p \text{dB} = 11.76$  dB. If despreading at the receiver is implemented after the IF stage (i.e. after the internal noise source of the receiver), this processing gain would increase the CNR at the detector input by 11.76 dB. This would increase the useful range to around 500 feet. That

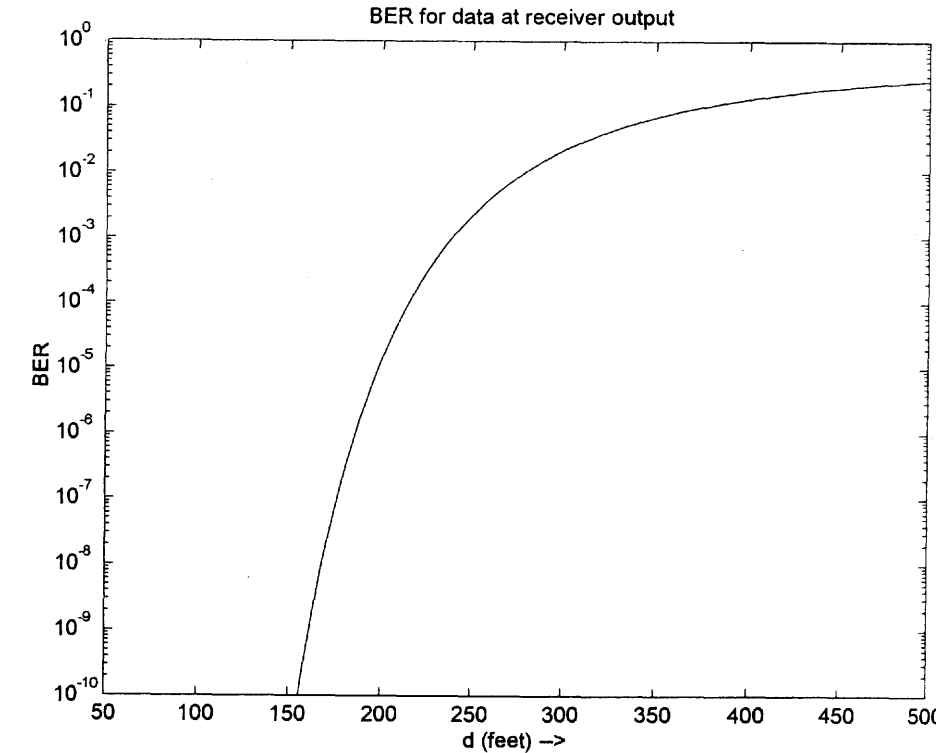


Figure 8-39 BER for a PCD wireless link.

is, referring to Fig. 8-38 at  $d = 500$  feet, a processing gain of 11.76 dB would result in a CNR of 13.0 dB which corresponds to a BER of  $2.1 \times 10^{-5}$ .

## PROBLEMS

- 8-1** A distant telephone subscriber is served by a twisted-pair line that is connected directly to the central office as shown in Fig. 8-3. The long telephone line has such a high resistance that the audio signals are weak. Suggest a way to modify the CO equipment so that the audio signal levels will be increased. (This modification is called a line extender and does not use a remote terminal.)
- 8-2** A 50-pair line provides telephone service to 50 subscribers in a rural subdivision via local loops to the CO. How many subscribers can be served if the 50 pairs are converted to T1 lines and a remote terminal is installed in the subdivision?
- 8-3** Assume that a telephone company has remote terminals connected to its CO via T1 lines. Draw a block diagram that illustrates how the T1 lines are interfaced with the CO switch if the CO uses:
- An analog switch.
  - An integrated digital switch.
- 8-4** Indicate whether a conference-call connection may be better or may be worse if a digital switch is used (at the CO) instead of an analog switch. Explain your answer.
- 8-5** Full-duplex data of 1200 bits/sec in each direction from a personal computer is sent via a twisted-pair telephone line having a bandpass from 300 to 2700 Hz. Explain why modems are needed at each end of the line.
- 8-6** A satellite with twelve 36-MHz bandwidth transponders operates in the 6/4-GHz bands with 500 MHz bandwidth and 4-MHz guardbands on the 4-GHz downlink, as shown in Fig. 8-10. Calculate the percentage bandwidth that is used for the guardbands.
- 8-7** An Earth station uses a 3-m-diameter parabolic antenna to receive a 4-GHz signal from a geosynchronous satellite. If the satellite transmitter delivers 10 W into a 3-m-diameter transmitting antenna and the satellite is located 36,000 km from the receiver, what is the power received?
- 8-8** Figure 8-12b shows an FDM/FM ground station for a satellite communication system. Find the peak frequency deviation needed to achieve the allocated spectral bandwidth for the 6240-MHz signal.
- 8-9** A microwave transmitter has an output of 0.1 W at 2 GHz. Assume that this transmitter is used in a microwave communication system where the transmitting and receiving antennas are parabolas, each 4 ft in diameter.
- Evaluate the gain of the antennas.
  - Calculate the EIRP of the transmitted signal.
  - If the receiving antenna is located 15 miles from the transmitting antenna over a free-space path, find the available signal power out of the receiving antenna in dBm units.
- 8-10** Using MATLAB or MathCAD, plot the PSD for a thermal noise source with a resistance of  $10\text{k}\Omega$  over a frequency range of 10 to 100,000 GHz where  $T = 300$  K.
- 8-11** Given the  $RC$  circuit of Fig. P8-11, where  $R$  is a physical resistor at temperature  $T$ , find the rms value of the noise voltage that appears at the output in terms of  $k$ ,  $T$ ,  $R$ , and  $C$ .
- 8-12** A receiver is connected to an antenna system that has a noise temperature of 100 K. Find the noise power that is available from the source over a 20-MHz band.

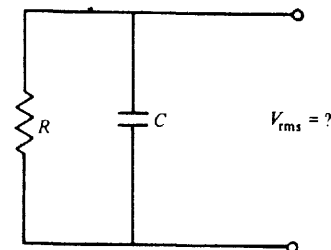


Figure P8-11

- 8-13** A bipolar transistor amplifier is modeled as shown in Fig. P8-13. Find a formula for the available power gain in terms of the appropriate parameters.

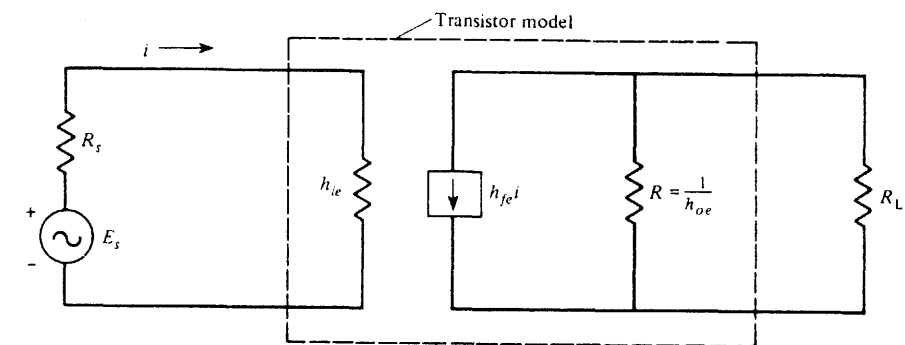


Figure P8-13

- 8-14** Using the definition for the available power gain,  $G_a(f)$ , as given by (8-18), show that  $G_a(f)$  depends on the driving source impedance as well as the elements of the device and that  $G_a(f)$  does not depend on the load impedance. [Hint: Calculate  $G_a(f)$  for a simple resistive network.]
- 8-15** Show that the effective input-noise temperature and the noise figure can be evaluated from measurements that use the Y-factor method. With this method the device under test (DUT) is first connected to a noise source that has a relatively large output denoted by its source temperature,  $T_h$ , where the subscript  $h$  denotes "hot," and then the available noise power at the output of the DUT,  $P_{aoh}$  is measured with a power meter. Next, the DUT is connected to a source that has relatively low source temperature,  $T_c$ , where the subscript  $c$  denotes "cold," and noise power at the output of the DUT is measured,  $P_{aoc}$ . Show that
- The effective input noise temperature of the DUT is

$$T_e = \frac{T_h - YT_c}{Y - 1}$$

- where  $Y = P_{aoh}/P_{aoc}$  is obtained from the measurements.
- The noise figure of the DUT is

$$F = \frac{[(T_h/T_0) - 1] + Y[(T_c/T_0) - 1]}{Y - 1}$$

where  $T_0 = 290$  K.

- 8-16 If a signal plus noise is fed into a linear device, show that the noise figure of that device is given by  $F = (S/N)_{\text{in}}/(S/N)_{\text{out}}$  (*Hint:* Start with the basic definition of noise figure that is given in this chapter.)
- 8-17 An antenna is pointed in a direction such that it has a noise temperature of 30 K. It is connected to a preamplifier that has a noise figure of 1.6 dB and an available gain of 30 dB over an effective bandwidth of 10 MHz.
- (a) Find the effective input noise temperature for the preamplifier.
  - (b) Find the available noise power out of the preamplifier.
- 8-18 A 10-MHz SSB-AM signal, which is modulated by an audio signal that is bandlimited to 5 kHz, is being detected by a receiver that has a noise figure of 10 dB. The signal power at the receiver input is  $10^{-10}$  mW and the PSD of the input noise,  $\mathcal{P}(f) = kT/2$ , is  $2 \times 10^{-21}$ . Evaluate:
- (a) The IF bandwidth needed.
  - (b) The signal-to-noise ratio at the receiver input.
  - (c) The signal-to-noise ratio at the receiver output, assuming that a product detector is used.
- 8-19 An FSK signal with  $R = 110$  bits/sec is transmitted over an RF channel that has white Gaussian noise. The receiver uses a noncoherent detector and has a noise figure of 6 dB. The impedance of the antenna input of the receiver is  $50 \Omega$ . The signal level at the receiver input is  $0.05 \mu\text{V}$ , and the noise level is  $N_0 = kT_0$ , where  $T_0 = 290$  K and  $k$  is Boltzmann's constant. Find the  $P_e$  for the digital signal at the output of the receiver.
- 8-20 Work Prob. 8-19 for the case of DPSK signaling.
- 8-21 Prove that the overall effective input-noise temperature for cascaded linear devices is given by (8-37).
- 8-22 A TV set is connected to an antenna system as shown in Fig. P8-22. Evaluate:
- (a) The overall noise figure.
  - (b) The overall noise figure if a 20-dB RF preamp with a 3-dB noise figure is inserted at point B.
  - (c) The overall noise figure if the preamp is inserted at point A.

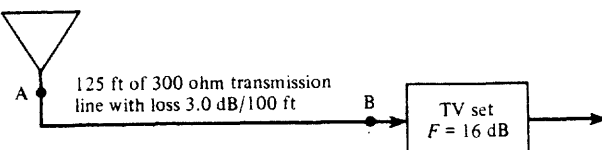


Figure P8-22

- 8-23 An Earth station receiving system consists of a 20-dB gain antenna with  $T_{\text{AR}} = 80$  K, an RF amplifier with  $G_a = 40$  dB and  $T_e = 200$  K, and a down converter with  $T_e = 15,000$  K. What is the overall effective input-noise temperature of this receiving system?
- 8-24 A low-noise amplifier (LNA), a down converter, and an IF amplifier are connected in cascade. The LNA has a gain of 40 dB and a  $T_e$  of 100 K. The down converter has a noise figure of

- 8 dB and a conversion gain of 6 dB. The IF amplifier has a gain of 60 dB and a noise figure of 14 dB. Evaluate the overall effective input-noise temperature for this system.
- 8-25 A geosynchronous satellite transmits 13.5 dBW EIRP on a 4-GHz downlink to an Earth station. The receiving system has a gain of 60 dB, an effective input-noise temperature of 80 K, an antenna source noise temperature of 60 K, and an IF bandwidth of 36 MHz. If the satellite is located 24,500 miles from the receiver, what is the  $(C/N)_{\text{dB}}$  at the input of the receiver detector circuit?
- 8-26 An antenna with  $T_{\text{AR}} = 160$  K is connected to a receiver by means of a waveguide that has a physical temperature of 290 K and a loss of 2 dB. The receiver has a noise bandwidth of 1 MHz, an effective input-noise temperature of 800 K, and a gain of 120 dB from its antenna input to its IF output. Using MATLAB or MathCAD, find:
- (a) The system noise temperature at the input of the receiver.
  - (b) The overall noise figure.
  - (c) The available noise power at the IF output.
- 8-27 The *Intelsat IV* satellite uses 36-MHz transponders with downlinks operating in the 4-GHz band. Each satellite transponder has a power output of 3.5 W and may be used with a  $17^\circ$  global coverage antenna that has a gain of 20 dB.
- (a) For users located at the subsatellite point (i.e., directly below the satellite), show that  $(C/N)_{\text{dB}} = (G_{\text{AR}}/T_{\text{syst}})_{\text{dB}} - 17.1$ , where  $(G_{\text{AR}}/T_{\text{syst}})_{\text{dB}}$  is the Earth receiving station figure of merit.
  - (b) Design a ground receiving station (block diagram) showing reasonable specifications for each block so that the IF output CNR will be 12 dB. Discuss the trade-offs that are involved.
- 8-28 The efficiency of a parabolic antenna is determined by the accuracy of the parabolic reflecting surface and other factors. The gain is  $G_A = 4\pi\eta A/\lambda^2$ , where  $\eta$  is the antenna efficiency. In Table 8-4 an efficiency of 56% was used to obtain the formula  $G_A = 7A/\lambda^2$ . In a ground receiving system for the *Intelsat IV* satellite, assume that a  $(G_{\text{AR}}/T_{\text{syst}})$  of 40 dB is needed. Using a 30-m antenna, give the required antenna efficiency if the system noise temperature is 85 K. How does the required antenna efficiency change if a 28-m antenna is used?
- 8-29 Evaluate the performance of a TVRO system. Assume that the TVRO terminal is located in Miami, Florida ( $26.8^\circ$  N latitude,  $80.2^\circ$  W longitude). A 10-ft-diameter parabolic receiving antenna is used and is pointed toward the *Galaxy I* satellite. Other TVRO parameters are given in Table 8-5, Fig. 8-25, and Fig. 8-27.
- (a) Find the TVRO antenna look angles to the satellite and find the slant range.
  - (b) Find the overall receiver system temperature.
  - (c) Find the  $(C/N)_{\text{dB}}$  into the receiver detector.
  - (d) Find the  $(S/N)_{\text{dB}}$  out of the receiver.
- 8-30 Repeat Prob. 8-29 if the TVRO terminal is located at Anchorage, Alaska ( $61.2^\circ$  N latitude,  $149.8^\circ$  W longitude), and a 8-m-diameter parabolic antenna is used.
- 8-31 A TVRO receive system consists of an 8-ft-diameter parabolic antenna that feeds a 50-dB, 85 K LNA. The sky noise temperature (with feed) is 32 K. The system is designed to receive signals from the *Galaxy I* satellite. The LNA has a post-mixer circuit that down-converts the satellite signal to 70 MHz. The 70-MHz signal is fed to the TVRO receiver via a 120-ft length of  $75\Omega$  coaxial cable. The cable has a loss of 3 dB/100 ft. The receiver has a bandwidth of 36 MHz and a noise temperature of 3800 K. Assume that the TVRO site is located in Los Angeles, California ( $34^\circ$  N latitude,  $118.3^\circ$  W longitude) and vertical polarization is of interest.
- (a) Find the TVRO antenna look angles to the satellite and find the slant range.
  - (b) Find the overall system temperature.
  - (c) Find the  $(C/N)_{\text{dB}}$  into the receiver detector.



- 8-32** An Earth station receiving system operates at 11.95 GHz and consists of a 20-m antenna with a gain of 65.53 dB and  $T_{AR} = 60$  K, a waveguide with a loss of 1.28 dB and a physical temperature of 290 K, a LNA with  $T_e = 150$  K and 60 dB gain, and a down converter with  $T_e = 11,000$  K. Using MATLAB or MathCAD, find  $(G/T)_{dB}$  for the receiving system evaluated at:
- The input to the LNA.
  - The input to the waveguide.
  - The input to the down converter.
- 8-33** Rework Example 8-4 for the case of reception of TV signals from a direct broadcast satellite (DBS). Assume that the system parameters are similar to those given in Table 8-5, except that the satellite power is 316 kW EIRP radiated in the 12-GHz band. Furthermore, assume that a 1-m parabolic receiving antenna is used and the LNA has a 240-K noise temperature.
- 8-34** The most distant planet from our sun is Pluto, which is located at a (greatest) distance from the Earth of  $7.5 \times 10^9$  km. Assume that an unmanned spacecraft with a 2-GHz, 10-W transponder is in the vicinity of Pluto. A receiving Earth station with a 64-m antenna is available that has a system noise temperature of 16 K at 2 GHz. Calculate the size of a spacecraft antenna that is required for a 300-bit/s BPSK data link to Earth that has a  $10^{-3}$  bit error rate (corresponding to  $E_b/N_0$  of 9.88 dB). Allow 2 dB for incidental losses.
- 8-35** Using MATLAB, MathCAD, or some spreadsheet program that will run on a personal computer (PC), design a spreadsheet that will solve Prob. 8-31. Run the spreadsheet on your PC and verify that it gives the correct answers. Print out your results. Also try other parameters, such as those appropriate for your location, and print out the results.
- 8-36** Assume that you want to analyze the overall performance of a satellite relay system that uses a "bent-pipe" transponder. Let  $(C/N)_{up}$  denote the carrier-to-noise ratio for the transponder as evaluated in the IF band of the satellite transponder. Let  $(C/N)_{dn}$  denote the IF carrier-to-noise ratio at the downlink receiving ground station when the satellite is sending a perfect (noise-free) signal. Show that the overall operating carrier-to-noise ratio at the IF of the receiving ground station,  $(C/N)_{ov}$ , is given by

$$\frac{1}{(C/N)_{ov}} = \frac{1}{(C/N)_{up}} + \frac{1}{(C/N)_{dn}}$$

- 8-37** Referring to Table 8-13, evaluate the maximum horizontal and vertical resolution (lines) for the CCIR System B TV standard. Assume that the horizontal blanking time is 10  $\mu s$ .
- 8-38** A VSB signal may be analyzed by using

$$g(t) = [m_1(t) + m_2(t)] + j[\hat{m}_2(t)]$$

- as a model for the complex envelope. Explain how this model may be used to represent U.S. TV signals.
- 8-39** A low-power TV station is licensed to operate on TV Channel 35 with an effective radiated visual power of 1000 W. The tower height is 400 ft and the transmission line is 450 ft long. Assume that a  $1\frac{3}{8}$ -in.-diameter semirigid 50- $\Omega$  coaxial transmission line will be used that has a loss of 0.6 dB/100 ft (at the operating frequency). The antenna has a gain of 5.6 dB and the duplexer loss is negligible. Find the PEP required at the visual transmitter output.
- 8-40** A TV visual transmitter is tested by modulating it with a periodic test signal. The envelope of the transmitter output is viewed on an oscilloscope as shown in Fig. P8-40, where  $K$  is an unknown constant. The output of the transmitter is connected to a 50- $\Omega$  dummy load that has a cal-

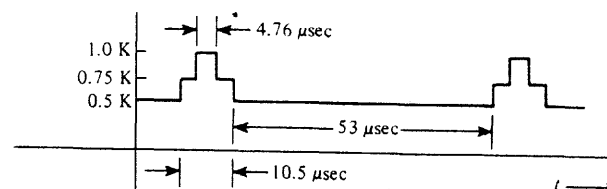


Figure P8-40

ibrated average reading wattmeter. The wattmeter reads 6.9 kW. Find the PEP of the transmitter output.

- 8-41** Specifications for the MTS stereo audio system for TV are given in Fig. 8-33. Using this figure:
- Design a block diagram for TV receiver circuitry that will detect the stereo audio signals and the second audio program (SAP) signal.
  - Describe how the circuit works. That is, give mathematical expressions for the signal at each point on your block diagram and explain in words. Be sure to specify all filter transfer functions, VCO center frequencies, and so on.
- 8-42** A TV broadcaster wants to send digital data to subscribers concerning the stock market using the professional aural subcarrier. Propose two digital signaling techniques that will satisfy the spectral requirements of Fig. 8-33 where the available bandwidth is  $0.5f_h$ . Specifically, design and draw block diagrams of transmit and receive modems and give the specifications for transmitting data at a rate of (a) 1200 bits/sec and (b) 9600 bits/sec. Discuss why you think you have a good design.
- 8-43** In the R-Y, B-Y color TV subcarrier demodulation system, the G-Y signal is obtained from the R-Y and B-Y signals. That is,
- $$[m_G(t) - m_Y(t)] = K_1[m_R(t) - m_Y(t)] + K_2[m_B(t) - m_Y(t)]$$
- Find the values for  $K_1$  and  $K_2$  that are required.
  - Draw a possible block diagram for a R-Y, B-Y system and explain how it works.

## MATHEMATICAL TECHNIQUES, IDENTITIES, AND TABLES

### A-1 TRIGONOMETRY

#### Definitions

$$\sin x = \frac{e^{jx} - e^{-jx}}{2j} \quad (\text{A-1})$$

$$\cos x = \frac{e^{jx} + e^{-jx}}{2} \quad (\text{A-2})$$

$$\tan x = \frac{\sin x}{\cos x} = \frac{e^{jx} - e^{-jx}}{j(e^{jx} + e^{-jx})} \quad (\text{A-3})$$

#### Trigonometric Identities

$$e^{\pm jx} = \cos x \pm j \sin x \quad (\text{Euler's theorem}) \quad (\text{A-4})$$

### Sec. A-2 Differential Calculus

$$\cos(x \pm y) = \cos x \cos y \mp \sin x \sin y \quad (\text{A-5})$$

$$\sin(x \pm y) = \sin x \cos y \pm \cos x \sin y \quad (\text{A-6})$$

$$\cos\left(x \pm \frac{\pi}{2}\right) = \mp \sin x \quad (\text{A-7})$$

$$\sin\left(x \pm \frac{\pi}{2}\right) = \pm \cos x \quad (\text{A-8})$$

$$\cos 2x = \cos^2 x - \sin^2 x \quad (\text{A-9})$$

$$\sin 2x = 2 \sin x \cos x \quad (\text{A-10})$$

$$2 \cos x \cos y = \cos(x - y) + \cos(x + y) \quad (\text{A-11})$$

$$2 \sin x \sin y = \cos(x - y) - \cos(x + y) \quad (\text{A-12})$$

$$2 \sin x \cos y = \sin(x - y) + \sin(x + y) \quad (\text{A-13})$$

$$2 \cos^2 x = 1 + \cos 2x \quad (\text{A-14})$$

$$2 \sin^2 x = 1 - \cos 2x \quad (\text{A-15})$$

$$4 \cos^3 x = 3 \cos x + \cos 3x \quad (\text{A-16})$$

$$4 \sin^3 x = 3 \sin x - \sin 3x \quad (\text{A-17})$$

$$8 \cos^4 x = 3 + 4 \cos 2x + \cos 4x \quad (\text{A-18})$$

$$8 \sin^4 x = 3 - 4 \cos 2x + \cos 4x \quad (\text{A-19})$$

$$A \cos x - B \sin x = R \cos(x + \theta) \quad (\text{A-20a})$$

$$\text{where } R = \sqrt{A^2 + B^2} \quad (\text{A-20b})$$

$$\theta = \tan^{-1}(B/A) \quad (\text{A-20c})$$

$$A = R \cos \theta \quad (\text{A-20d})$$

$$B = R \sin \theta \quad (\text{A-20e})$$

### A-2 DIFFERENTIAL CALCULUS

#### Definition

$$\frac{df(x)}{dx} = \lim_{\Delta x \rightarrow 0} \frac{f(x + (\Delta x/2)) - f(x - (\Delta x/2))}{\Delta x} \quad (\text{A-21})$$

#### Differentiation Rules

$$\frac{du(x)v(x)}{dx} = u(x)\frac{dv(x)}{dx} + v(x)\frac{du(x)}{dx} \quad (\text{products}) \quad (\text{A-22})$$

$$\frac{d\left(\frac{u(x)}{v(x)}\right)}{dx} = \frac{v(x)\frac{du(x)}{dx} - u(x)\frac{dv(x)}{dx}}{v^2(x)} \quad (\text{quotient}) \quad (\text{A-23})$$

$$\frac{du[v(x)]}{dx} = \frac{du}{dv} \frac{dv}{dx} \quad (\text{chain rule}) \quad (\text{A-24})$$

**Derivative Table**

$$\frac{d[x^n]}{dx} = nx^{n-1} \quad (\text{A-25})$$

$$\frac{d \sin ax}{dx} = a \cos ax \quad (\text{A-26})$$

$$\frac{d \cos ax}{dx} = -a \sin ax \quad (\text{A-27})$$

$$\frac{d \tan ax}{dx} = \frac{a}{\cos^2 ax} \quad (\text{A-28})$$

$$\frac{d \sin^{-1} ax}{dx} = \frac{a}{\sqrt{1 - (ax)^2}} \quad (\text{A-29})$$

$$\frac{d \cos^{-1} ax}{dx} = -\frac{a}{\sqrt{1 - (ax)^2}} \quad (\text{A-30})$$

$$\frac{d \tan^{-1} ax}{dx} = \frac{a}{1 + (ax)^2} \quad (\text{A-31})$$

$$\frac{d[e^{ax}]}{dx} = ae^{ax} \quad (\text{A-32})$$

$$\frac{d[a^x]}{dx} = a^x \ln a \quad (\text{A-33})$$

$$\frac{d(\ln x)}{dx} = \frac{1}{x} \quad (\text{A-34})$$

$$\frac{d(\log_a x)}{dx} = \frac{1}{x} \log_a e \quad (\text{A-35})$$

$$\begin{aligned} \frac{d \left[ \int_{a(x)}^{b(x)} f(\lambda, x) d\lambda \right]}{dx} &= f(b(x), x) \frac{db(x)}{dx} - f(a(x), x) \frac{da(x)}{dx} \\ &\quad + \int_{a(x)}^{b(x)} \frac{\partial f(\lambda, x)}{\partial x} d\lambda \quad (\text{Leibniz's rule}) \end{aligned} \quad (\text{A-36})$$

**A-3 INDETERMINATE FORMS**

If  $\lim_{x \rightarrow a} f(x)$  is of the form

$$\frac{0}{0}, \frac{\infty}{\infty}, 0 \cdot \infty, \infty - \infty, 0^0, \infty^0, 1^\infty$$

then

$$\lim_{x \rightarrow a} f(x) = \lim_{x \rightarrow a} \left[ \frac{N(x)}{D(x)} \right] = \lim_{x \rightarrow a} \left[ \frac{(dN(x)/dx)}{(dD(x)/dx)} \right] \quad (\text{L'Hospital's rule}) \quad (\text{A-37})$$

where  $N(x)$  is the numerator of  $f(x)$ ,  $D(x)$  is the denominator of  $f(x)$ ,  $N(a) = 0$ , and  $D(a) = 0$ .

**A-4 INTEGRAL CALCULUS****Definition**

$$\int f(x) dx = \lim_{\Delta x \rightarrow 0} \left\{ \sum_n [f(n \Delta x)] \Delta x \right\} \quad (\text{A-38})$$

**Integration Techniques**

1. Change in variable. Let  $v = u(x)$ :

$$\int_a^b f(x) dx = \int_{u(a)}^{u(b)} \left( \frac{f(x)}{dv/dx} \Big|_{x=u^{-1}(v)} \right) dv \quad (\text{A-39})$$

2. Integration by parts

$$\int u dv = uv - \int v du \quad (\text{A-40})$$

3. Integral tables

4. Complex variable techniques

5. Numerical methods

**A-5 INTEGRAL TABLES****Indefinite Integrals**

$$\int (a + bx)^n dx = \frac{(a + bx)^{n+1}}{b(n+1)}, \quad 0 < n \quad (\text{A-41})$$

$$\int \frac{dx}{a+bx} = \frac{1}{b} \ln|a+bx| \quad (A-42)$$

$$\int \frac{dx}{(a+bx)^n} = \frac{-1}{(n-1)b(a+bx)^{n-1}}, \quad 1 < n \quad (A-43)$$

$$\int \frac{dx}{c+bx+ax^2} = \begin{cases} \frac{2}{\sqrt{4ac-b^2}} \tan^{-1}\left(\frac{2ax+b}{\sqrt{4ac-b^2}}\right), & b^2 < 4ac \\ \frac{1}{\sqrt{b^2-4ac}} \ln\left|\frac{2ax+b-\sqrt{b^2-4ac}}{2ax+b+\sqrt{b^2-4ac}}\right|, & b^2 > 4ac \\ \frac{-2}{2ax+b}, & b^2 = 4ac \end{cases} \quad (A-44)$$

$$\int \frac{x \, dx}{c+bx+ax^2} = \frac{1}{2a} \ln|ax^2+bx+c| - \frac{b}{2a} \int \frac{dx}{c+bx+ax^2} \quad (A-45)$$

$$\int \frac{dx}{a^2+b^2x^2} = \frac{1}{ab} \tan^{-1}\left(\frac{bx}{a}\right) \quad (A-46)$$

$$\int \frac{x \, dx}{a^2+x^2} = \frac{1}{2} \ln(a^2+x^2) \quad (A-47)$$

$$\int \frac{x^2 \, dx}{a^2+x^2} = x - a \tan^{-1}\left(\frac{x}{a}\right) \quad (A-48)$$

$$\int \frac{dx}{(a^2+x^2)^2} = \frac{x}{2a^2(a^2+x^2)} + \frac{1}{2a^3} \tan^{-1}\left(\frac{x}{a}\right) \quad (A-49)$$

$$\int \frac{x \, dx}{(a^2+x^2)^2} = \frac{-1}{2(a^2+x^2)} \quad (A-50)$$

$$\int \frac{x^2 \, dx}{(a^2+x^2)^2} = \frac{-x}{2(a^2+x^2)} + \frac{1}{2a} \tan^{-1}\left(\frac{x}{a}\right) \quad (A-51)$$

$$\int \frac{dx}{(a^2+x^2)^3} = \frac{x}{4a^2(a^2+x^2)^2} + \frac{3x}{8a^4(a^2+x^2)} + \frac{3}{8a^5} \tan^{-1}\left(\frac{x}{a}\right) \quad (A-52)$$

$$\int \frac{x^2 \, dx}{(a^2+x^2)^3} = \frac{-x}{4(a^2+x^2)^2} + \frac{x}{8a^2(a^2+x^2)} + \frac{1}{8a^3} \tan^{-1}\left(\frac{x}{a}\right) \quad (A-53)$$

$$\int \frac{x^4 \, dx}{(a^2+x^2)^3} = \frac{a^2x}{4(a^2+x^2)^2} - \frac{5x}{8(a^2+x^2)} + \frac{3}{8a} \tan^{-1}\left(\frac{x}{a}\right) \quad (A-54)$$

$$\begin{aligned} \int \frac{dx}{(a^2+x^2)^4} = & \frac{x}{6a^2(a^2+x^2)^3} + \frac{5x}{24a^4(a^2+x^2)^2} \\ & + \frac{5x}{16a^6(a^2+x^2)} + \frac{5}{16a^7} \tan^{-1}\left(\frac{x}{a}\right) \end{aligned} \quad (A-55)$$

$$\begin{aligned} \int \frac{x^2 \, dx}{(a^2+x^2)^4} = & \frac{-x}{6(a^2+x^2)^3} + \frac{x}{24a^2(a^2+x^2)^2} \\ & + \frac{x}{16a^4(a^2+x^2)} + \frac{1}{16a^5} \tan^{-1}\left(\frac{x}{a}\right) \end{aligned} \quad (A-56)$$

$$\begin{aligned} \int \frac{x^4 \, dx}{(a^2+x^2)^4} = & \frac{a^2x}{6(a^2+x^2)^3} - \frac{7x}{24(a^2+x^2)^2} + \frac{x}{16a^2(a^2+x^2)} \\ & + \frac{1}{16a^3} \tan^{-1}\left(\frac{x}{a}\right) \end{aligned} \quad (A-57)$$

$$\begin{aligned} \int \frac{dx}{a^4+x^4} = & \frac{1}{4a^3\sqrt{2}} \ln\left(\frac{x^2+ax\sqrt{2}+a^2}{x^2-ax\sqrt{2}+a^2}\right) \\ & + \frac{1}{2a^3\sqrt{2}} \tan^{-1}\left(\frac{ax\sqrt{2}}{a^2-x^2}\right) \end{aligned} \quad (A-58)$$

$$\begin{aligned} \int \frac{x^2 \, dx}{a^4+x^4} = & -\frac{1}{4a\sqrt{2}} \ln\left(\frac{x^2+ax\sqrt{2}+a^2}{x^2-ax\sqrt{2}+a^2}\right) \\ & + \frac{1}{2a\sqrt{2}} \tan^{-1}\left(\frac{ax\sqrt{2}}{a^2-x^2}\right) \end{aligned} \quad (A-59)$$

$$\int \cos x \, dx = \sin x \quad (A-60)$$

$$\int x \cos x \, dx = \cos x + x \sin x \quad (A-61)$$

$$\int x^2 \cos x \, dx = 2x \cos x + (x^2 - 2) \sin x \quad (A-62)$$

$$\int \sin x \, dx = -\cos x \quad (A-63)$$

$$\int x \sin x \, dx = \sin x - x \cos x \quad (A-64)$$

$$\int x^2 \sin x dx = 2x \sin x - (x^2 - 2) \cos x \quad (A-65)$$

$$\int e^{ax} dx = \frac{e^{ax}}{a}, \quad a \text{ real or complex} \quad (A-66)$$

$$\int xe^{ax} dx = e^{ax} \left( \frac{x}{a} - \frac{1}{a^2} \right), \quad a \text{ real or complex} \quad (A-67)$$

$$\int x^2 e^{ax} dx = e^{ax} \left( \frac{x^2}{a} - \frac{2x}{a^2} + \frac{2}{a^3} \right), \quad a \text{ real or complex} \quad (A-68)$$

$$\int x^3 e^{ax} dx = e^{ax} \left( \frac{x^3}{a} - \frac{3x^2}{a^2} + \frac{6x}{a^3} - \frac{6}{a^4} \right), \quad a \text{ real or complex} \quad (A-69)$$

$$\int e^{ax} \sin x dx = \frac{e^{ax}}{a^2 + 1} (a \sin x - \cos x) \quad (A-70)$$

$$\int e^{ax} \cos x dx = \frac{e^{ax}}{a^2 + 1} (a \cos x - \sin x) \quad (A-71)$$

### Definite Integrals

$$\int_0^\infty \frac{x^{m-1}}{1+x^n} dx = \frac{\pi/n}{\sin(m\pi/n)}, \quad n > m > 0 \quad (A-72)$$

$$\int_0^\infty x^{\alpha-1} e^{-x} dx = \Gamma(\alpha), \quad \alpha > 0 \quad (A-73a)$$

$$\text{where } \Gamma(\alpha + 1) = \alpha \Gamma(\alpha) \quad (A-73b)$$

$$\Gamma(1) = 1; \Gamma(\frac{1}{2}) = \sqrt{\pi} \quad (A-73c)$$

$$\Gamma(n) = (n-1)! \quad \text{if } n \text{ is a positive integer} \quad (A-73d)$$

$$\int_0^\infty x^{2n} e^{-ax^2} dx = \frac{1 \cdot 3 \cdot 5 \cdots (2n-1)}{2^{n+1} a^n} \sqrt{\frac{\pi}{a}} \quad (A-74)$$

$$\int_{-\infty}^\infty e^{-a^2 x^2 + bx} dx = \frac{\sqrt{\pi}}{a} e^{b^2/(4a^2)}, \quad a > 0 \quad (A-75)$$

$$\int_0^\infty e^{-ax} \cos bx dx = \frac{a}{a^2 + b^2}, \quad a > 0 \quad (A-76)$$

$$\int_0^\infty e^{-ax} \sin bx dx = \frac{b}{a^2 + b^2}, \quad a > 0 \quad (A-77)$$

$$\int_0^\infty e^{-a^2 x^2} \cos bx dx = \frac{\sqrt{\pi} e^{-b^2/4a^2}}{2a}, \quad a > 0 \quad (A-78)$$

$$\int_0^\infty x^{\alpha-1} \cos bx dx = \frac{\Gamma(\alpha)}{b^\alpha} \cos \frac{1}{2}\pi\alpha, \quad 0 < \alpha < 1, b > 0 \quad (A-79)$$

$$\int_0^\infty x^{\alpha-1} \sin bx dx = \frac{\Gamma(\alpha)}{b^\alpha} \sin \frac{1}{2}\pi\alpha, \quad 0 < |\alpha| < 1, b > 0 \quad (A-80)$$

$$\int_0^\infty x e^{-ax^2} I_k(bx) dx = \frac{1}{2a} e^{b^2/4a} \quad (A-81a)$$

$$\text{where } I_k(bx) = \frac{1}{\pi} \int_0^\pi e^{b \cos \theta} \cos k\theta d\theta \quad (A-81b)$$

$$\int_0^\infty \frac{\sin x}{x} dx = \int_0^\infty \text{Sa}(x) dx = \frac{\pi}{2} \quad (A-82)$$

$$\int_0^\infty \left( \frac{\sin x}{x} \right)^2 dx = \int_0^\infty \text{Sa}^2(x) dx = \frac{\pi}{2} \quad (A-83)$$

$$\int_0^\infty \frac{\cos ax}{b^2 + x^2} dx = \frac{\pi}{2b} e^{-ab}, \quad a > 0, b > 0 \quad (A-84)$$

$$\int_0^\infty \frac{x \sin ax}{b^2 + x^2} dx = \frac{\pi}{2} e^{-ab}, \quad a > 0, b > 0 \quad (A-85)$$

$$\int_{-\infty}^\infty e^{\pm j2\pi yx} dx = \delta(y) \quad (A-86)$$

### A-6 SERIES EXPANSIONS

#### Finite Series

$$\sum_{n=1}^N n = \frac{N(N+1)}{2} \quad (A-87)$$

$$\sum_{n=1}^N n^2 = \frac{N(N+1)(2N+1)}{6} \quad (A-88)$$

$$\sum_{n=1}^N n^3 = \frac{N^2(N+1)^2}{4} \quad (A-89)$$

$$\sum_{n=0}^N a^n = \frac{a^{N+1} - 1}{a - 1} \quad (\text{A-90})$$

$$\sum_{n=0}^N \frac{N!}{n!(N-n)!} x^n y^{N-n} = (x+y)^N \quad (\text{A-91})$$

$$\sum_{n=0}^N e^{j(\theta+n\phi)} = \frac{\sin[(N+1)\phi/2]}{\sin(\phi/2)} e^{j[\theta+(N\phi/2)]} \quad (\text{A-92})$$

$$\sum_{k=0}^N \binom{N}{k} a^{N-k} b^k = (a+b)^N \quad (\text{A-93a})$$

$$\text{where } \binom{N}{k} = \frac{N!}{(N-k)! k!} \quad (\text{A-93b})$$

### Infinite Series

$$f(x) = \sum_{n=0}^{\infty} \left( \frac{f^{(n)}(a)}{n!} \right) (x-a)^n \quad (\text{Taylor's series}) \quad (\text{A-94})$$

$$f(x) = \sum_{n=-\infty}^{\infty} c_n e^{jn\omega_0 x} \quad \text{for } a \leq x \leq a+T \quad (\text{Fourier series}) \quad (\text{A-95a})$$

$$\text{where } c_n = \frac{1}{T} \int_a^{a+T} f(x) e^{-jn\omega_0 x} dx \quad (\text{A-95b})$$

$$\text{and } \omega_0 = \frac{2\pi}{T} \quad (\text{A-95c})$$

$$e^x = \sum_{n=0}^{\infty} \frac{x^n}{n!} \quad (\text{A-96})$$

$$\sin x = \sum_{n=0}^{\infty} \frac{(-1)^n x^{2n+1}}{(2n+1)!} \quad (\text{A-97})$$

$$\cos x = \sum_{n=0}^{\infty} \frac{(-1)^n x^{2n}}{(2n)!} \quad (\text{A-98})$$

### A-7 HILBERT TRANSFORM PAIRS<sup>†</sup>

$$\hat{x}(t) \triangleq x(t) * \frac{1}{\pi t} = \frac{1}{\pi} \int_{-\infty}^{\infty} \frac{x(\lambda)}{t - \lambda} d\lambda \quad (\text{A-99})$$

Function	Hilbert Transform
1. $x(at + b)$	$\hat{x}(at + b)$
2. $x(t) + y(t)$	$\hat{x}(t) + \hat{y}(t)$
3. $\frac{d^n x(t)}{dt^n}$	$\frac{d^n}{dt^n} \hat{x}(t)$
4. A constant	0
5. $\frac{1}{t}$	$-\pi\delta(t)$
6. $\sin(\omega_0 t + \theta)$	$-\cos(\omega_0 t + \theta)$
7. $\frac{\sin at}{at} = \text{Sa}(at)$	$-\frac{1}{2\pi} at \text{Sa}^2(at)$
8. $e^{\pm j\omega_0 t}$	$\mp j e^{\pm j\omega_0 t}$
9. $\delta(t)$	$\frac{1}{\pi t}$
10. $\frac{a}{\pi(t^2 + a^2)}$	$\frac{t}{\pi(t^2 + a^2)}$
11. $\Pi\left(\frac{t}{T}\right) \triangleq \begin{cases} 1, &  t  \leq T/2 \\ 0, & t \text{ elsewhere} \end{cases}$	$\frac{1}{\pi} \ln \left  \frac{2t+T}{2t-T} \right $

### A-8 THE DIRAC DELTA FUNCTION

**DEFINITION.** The Dirac *delta function*  $\delta(x)$ , also called the *unit impulse function*, satisfies *both* of the following conditions:

$$\int_{-\infty}^{\infty} \delta(x) dx = 1 \quad (\text{A-100})$$

$$\delta(x) = \begin{cases} \infty, & x = 0 \\ 0, & x \neq 0 \end{cases} \quad (\text{A-101})$$

<sup>†</sup> Fourier transform theorems are given in Table 2-1, and Fourier transform pairs are given in Table 2-2.

Consequently,  $\delta(x)$  is a "singular" function.<sup>†</sup>

### Properties of Dirac Delta Functions

- $\delta(x)$  can be expressed in terms of the limit of some ordinary functions such that (in the limit of some parameter) the ordinary function satisfies the definition for  $\delta(x)$ . For example,

$$\delta(x) = \lim_{\sigma \rightarrow 0} \left( \frac{1}{\sqrt{2\pi}\sigma} e^{-x^2/(2\sigma^2)} \right) \quad (\text{A-102})$$

$$= \lim_{a \rightarrow \infty} \left[ \frac{a}{\pi} \left( \frac{\sin ax}{ax} \right) \right] \quad (\text{A-103})$$

For these two examples,  $\delta(-x) = \delta(x)$ , so for these cases  $\delta(x)$  is said to be an *even-sided delta function*. The even-sided delta function is used throughout this text except when specifying the PDF of a discrete random variable.

$$\delta(x) = \begin{cases} \lim_{a \rightarrow \infty} (ae^{ax}), & x \leq 0 \\ 0, & x > 0 \end{cases} \quad (\text{A-104})$$

This is an example of a single-sided delta function; in particular, this is a *left-sided delta function*. This type of delta function is used to specify the PDF of a discrete point of a random variable (see Appendix B).

- Sifting property:

$$\int_{-\infty}^x w(x) \delta(x - x_0) dx = w(x_0) \quad (\text{A-105})$$

- For *even-sided* delta functions

$$\int_a^b w(x) \delta(x - x_0) dx = \begin{cases} 0, & x_0 < a \\ \frac{1}{2}w(a), & x_0 = a \\ w(x_0), & a < x_0 < b \\ \frac{1}{2}w(b), & x_0 = b \\ 0, & x_0 > b \end{cases} \quad (\text{A-106})$$

where  $b > a$ .

- For *left-sided* delta functions

$$\int_a^b w(x) \delta(x - x_0) dx = \begin{cases} 0, & x_0 \leq a \\ w(x_0), & a < x_0 \leq b \\ 0, & x_0 > b \end{cases} \quad (\text{A-107})$$

where  $b > a$ .

<sup>†</sup> The Dirac delta function is not an ordinary function since it is really undefined at  $x = 0$ . However, it is described by the mathematical theory of distributions [Bremermann, 1965].

$$5. \int_{-\infty}^{\infty} w(x) \delta^{(n)}(x - x_0) dx = (-1)^n w^{(n)}(x_0) \quad (\text{A-108})$$

where the superscript  $(n)$  denotes the  $n$ th derivative with respect to  $x$ .

- The Fourier transform of  $\delta(x)$  is unity. That is,

$$\mathcal{F}[\delta(x)] = 1 \quad (\text{A-109a})$$

Conversely,

$$\delta(x) = \mathcal{F}^{-1}[1] \quad (\text{A-109b})$$

- Scaling property:

$$\delta(ax) = \frac{1}{|a|} \delta(x) \quad (\text{A-110})$$

- For *even-sided* delta functions,

$$\delta(x) = \int_{-\infty}^{\infty} e^{\pm j2\pi xy} dy \quad (\text{A-111})$$

### A-9 TABULATION OF $\text{Sa}(x) = (\sin x)/x$



$x$	$\text{Sa}(x)$	$\text{Sa}^2(x)$	$x$	$\text{Sa}(x)$	$\text{Sa}^2(x)$
0.0	1.0000	1.0000	5.2	-0.1699	0.0289
0.2	0.9933	0.9867	5.4	-0.1431	0.0205
0.4	0.9735	0.9478	5.6	-0.1127	0.0127
0.6	0.9411	0.8856	5.8	-0.0801	0.0064
0.8	0.8967	0.8041	6.0	-0.0466	0.0022
1.0	0.8415	0.7081	6.2	-0.0134	0.0002
1.2	0.7767	0.6033	2 $\pi$	0.0000	0.0000
1.4	0.7039	0.4955	6.4	0.0182	0.0003
1.6	0.6247	0.3903	6.6	0.0472	0.0022
1.8	0.5410	0.2927	6.8	0.0727	0.0053
2.0	0.4546	0.2067	7.0	0.0939	0.0088
2.2	0.3675	0.1351	7.2	0.1102	0.0122
2.4	0.2814	0.0792	7.4	0.1214	0.0147
2.6	0.1983	0.0393	7.6	0.1274	0.0162
2.8	0.1196	0.0143	7.8	0.1280	0.0164
3.0	0.0470	0.0022	8.0	0.1237	0.0153
$\pi$	0.0000	0.0000	8.2	0.1147	0.0132
3.2	-0.0182	0.0003	8.4	0.1017	0.0104
3.4	-0.0752	0.0056	8.6	0.0854	0.0073
3.6	-0.1229	0.0151	8.8	0.0665	0.0044
3.8	-0.1610	0.0259	9.0	0.0458	0.0021
4.0	-0.1892	0.0358	9.2	0.0242	0.0006
4.2	-0.2075	0.0431	9.4	0.0026	0.0000
4.4	-0.2163	0.0468	3 $\pi$	0.0000	0.0000
4.6	-0.2160	0.0467	9.6	-0.0182	0.0003
4.8	-0.2075	0.0431	9.8	-0.0374	0.0014
5.0	-0.1918	0.0368	10.0	-0.0544	0.0030

A-10 TABULATION OF  $Q(z)$ 

$$Q(z) \triangleq \frac{1}{\sqrt{2\pi}} \int_z^{\infty} e^{-\lambda^2/2} d\lambda$$

(A-112)

For  $z \geq 3$ :

$$Q(z) \approx \frac{1}{\sqrt{2\pi} z} e^{-z^2/2} \quad (\text{see Fig. B-7})$$

(A-113)

Also,

$$Q(-z) = 1 - Q(z)$$

(A-114)

$$Q(z) = \frac{1}{2} \operatorname{erfc}\left(\frac{z}{\sqrt{2}}\right) = \frac{1}{2} \left[ 1 - \operatorname{erf}\left(\frac{z}{\sqrt{2}}\right) \right]$$

(A-115a)

where

$$\operatorname{erfc}(x) \triangleq \frac{2}{\sqrt{\pi}} \int_x^{\infty} e^{-\lambda^2} d\lambda$$

(A-115b)

$$\operatorname{erfc}(x) = \frac{2}{\sqrt{\pi}} \int_0^x e^{-\lambda^2} d\lambda$$

(A-115c)

For  $z \geq 0$ , a rational function approximation is [Ziemer and Tranter, 1990]

$$Q(z) = \frac{e^{-z^2/2}}{\sqrt{2\pi}} (b_1 t + b_2 t^2 + b_3 t^4 + b_4 t^4 + b_5 t^5) \quad (\text{A-116})$$

where  $t = 1/(1 + pz)$ , with  $p = 0.2316419$ ,

and

$$b_1 = 0.31981530$$

$$b_2 = -0.356563782$$

$$b_3 = 1.781477937$$

$$b_4 = -1.821255978$$

$$b_5 = 1.330274429$$

Another approximation for  $Q(z)$  for  $z \geq 0$  is [Börjesson and Sunberg, 1979; Peebles, 1993]:

$$Q(z) = \left[ \frac{1}{(1 - 0.339)z + 0.339\sqrt{z^2 + 5.510}} \right] \frac{e^{-z^2/2}}{\sqrt{2\pi}} \quad (\text{A-117})$$

This approximation has a maximum absolute error of 0.27% for  $z \geq 0$ .

$z$	$Q(z)$	$z$	$Q(z)$
0.0	0.50000	2.0	0.02275
0.1	0.46017	2.1	0.01786
0.2	0.42074	2.2	0.01390
0.3	0.38209	2.3	0.01072
0.4	0.34458	2.4	0.00820
0.5	0.30854	2.5	0.00621
0.6	0.27425	2.6	0.00466
0.7	0.24196	2.7	0.00347
0.8	0.21186	2.8	0.00256
0.9	0.18406	2.9	0.00187
1.0	0.15866	3.0	0.00135
1.1	0.13567	3.1	0.00097
1.2	0.11507	3.2	0.00069
1.3	0.09680	3.3	0.00048
1.4	0.08076	3.4	0.00034
1.5	0.06681	3.5	0.00023
1.6	0.05480	3.6	0.00016
1.7	0.04457	3.7	0.00011
1.8	0.03593	3.8	0.00007
1.9	0.02872	3.9	0.00005
		4.0	0.00003

Also see Fig. B-7 for a plot of  $Q(z)$ .

## PROBABILITY AND RANDOM VARIABLES

### B-1 INTRODUCTION

The need for probability theory arises in every scientific discipline since it is impossible to be exactly sure of values that are obtained by measurement. For example, we might say that we are 90% sure that a voltage is within  $\pm 0.1$  V of a 5-V level. This is a statistical description of the voltage parameter as opposed to a deterministic description whereby we might define the voltage as being exactly 5 V.

This appendix is intended to be a short course in probability and random variables. Numerous excellent books cover this topic in more detail [Papoulis, 1984 and 1991; Peebles, 1987 and 1993; Shanmugan and Breipohl, 1988]. However, this appendix will provide a good introduction to the topic for the new student or a quick review for the student who is already knowledgeable in this area.

If probability and random variables are new topics for you, you will soon realize that to understand them, you will need to master many new definitions that seem to be introduced all at once. It is important to memorize these definitions in order to have a vocabulary that

can be used when conversing with others about statistical results. In addition, you must develop a feeling for the engineering application of these definitions and theorems. If you accomplish this at the beginning, you can grasp more complicated statistical ideas easily.

### B-2 SETS

**DEFINITION.** A *set* is a collection (or class) of objects.

The largest set or the all-embracing set of objects under consideration in an experiment is called the *universal set*. All other sets under consideration in the experiment are subsets or *events* of the universal set. This is illustrated in Fig. B-1a, where a *Venn diagram* is given. For example,  $M$  might denote the set containing all types of milk shakes and  $B$  might denote the subset of blueberry milk shakes. Thus  $B$  is contained in  $M$ , which is denoted by  $B \subset M$ . In parts b and c of this figure two sets,  $A$  and  $B$ , are shown. There are two basic

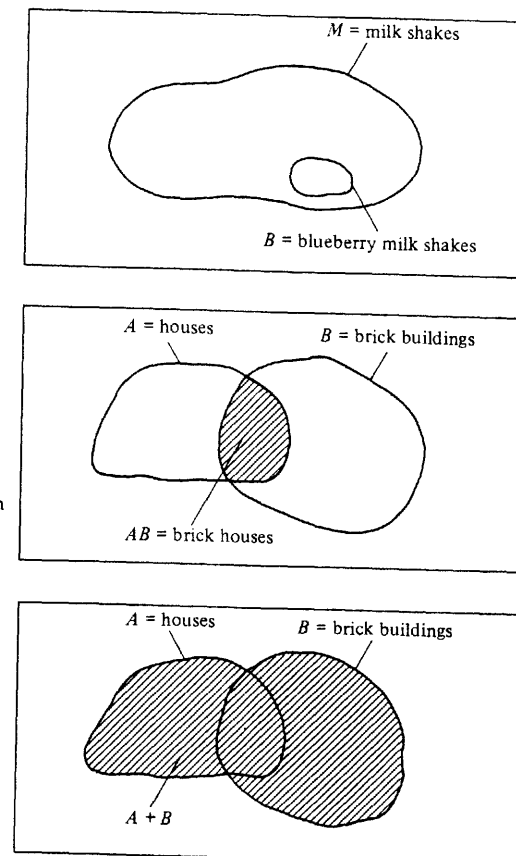


Figure B-1 Venn diagram.

ways of describing the combination of set  $A$  and set  $B$ . These are called *intersection* and *union*.

**DEFINITION.** The *intersection* of set  $A$  and set  $B$ , denoted by  $AB$ , is the set of elements that is common to  $A$  and  $B$ . (Mathematicians use the notation  $A \cap B$ .)

The intersection of  $A$  and  $B$  is analogous to the AND operation of digital logic. For example, if  $A$  denotes houses and  $B$  denotes brick buildings, then the event  $C = AB$  would denote only brick houses. This is illustrated by Fig. B-1b.

**DEFINITION.** The *union* of set  $A$  and set  $B$ , denoted by  $A + B$ , is the set that contains all the elements of  $A$  or all the elements of  $B$  or both. (Mathematicians use the notation  $A \cup B$ .)

The union of  $A$  and  $B$  is analogous to the OR operation of digital logic. Continuing with the example just given,  $D = A + B$  would be the set that contains all brick buildings, all houses, as well as all brick houses. This is illustrated in Fig. B-1c.

The events  $A$  and  $B$  are called *simple events*, and the events  $C = AB$  and  $D = A + B$  are called *compound events* since they are logical functions of simple events.

## B-3 PROBABILITY AND RELATIVE FREQUENCY

### Simple Probability

The probability of an event  $A$ , denoted by  $P(A)$ , may be defined in terms of the relative frequency of  $A$  occurring in  $n$  trials.

**DEFINITION.**<sup>†</sup>

$$P(A) = \lim_{n \rightarrow \infty} \left( \frac{n_A}{n} \right) \quad (\text{B-1})$$

where  $n_A$  is the number of times that  $A$  occurs in  $n$  trials.

In practice,  $n$  is taken to be some reasonable number such that a larger value for  $n$  would give approximately the same value for  $P(A)$ . For example, suppose that a coin is tossed 40 times and that the heads event, denoted by  $A$ , occurs 19 times. Then the probability of a head would be evaluated as approximately  $P(A) = \frac{19}{40}$ , where the true value of  $P(A) = 0.5$  would have been obtained if  $n = \infty$  had been used.

From the definition of probability, as given by (B-1), it is seen that all probability functions have the property

$$0 \leq P(A) \leq 1 \quad (\text{B-2})$$

<sup>†</sup> Here an engineering approach is used to define probability. Strictly speaking, statisticians have developed probability theory based on three axioms: (1)  $P(A) > 0$ , (2)  $P(S) = 1$  where  $S$  is the sure event, and (3)  $P(A + B) = P(A) + P(B)$  provided that  $AB$  is a null event (i.e.,  $AB = \emptyset$ ). Statisticians define  $P(A)$  as being any function of  $A$  that satisfies these axioms. The engineering definition is consistent with this approach since it satisfies these axioms.

where  $P(A) = 0$  if the event  $A$  is a *null event* (does not occur) and  $P(A) = 1$  if the event  $A$  is a *sure event* (always occurs).

### Joint Probability

**DEFINITION.** The probability of a *joint event*,  $AB$ , is

$$P(AB) = \lim_{n \rightarrow \infty} \left( \frac{n_{AB}}{n} \right) \quad (\text{B-3})$$

where  $n_{AB}$  is the number of times that the event  $AB$  occurs in  $n$  trials.

In addition, two events,  $A$  and  $B$ , are said to be *mutually exclusive* if  $AB$  is a null event, which implies that  $P(AB) = 0$ .

### Example B-1 EVALUATION OF PROBABILITIES

Let event  $A$  denote an auto accident blocking a certain street intersection during a 1-min interval. Let event  $B$  denote that it is raining at the street intersection during a 1-min period. Then event  $E = AB$  would be a blocked intersection while it is raining, as evaluated in 1-min increments.

Suppose that experimental measurements are tabulated continuously for 1 week, and it is found that  $n_A = 25$ ,  $n_B = 300$ ,  $n_{AB} = 20$ , and there are  $n = 10,080$  1-min intervals in the week of measurements. ( $n_A = 25$  does not mean that there were 25 accidents in a 1-week period, but that the intersection was blocked for 25 1-min periods because of car accidents; similarly for  $n_B$  and  $n_{AB}$ .) These results indicate that the probability of having a blocked intersection is  $P(A) = 0.0025$ , the probability of rain is  $P(B) = 0.03$ , and the probability of having a blocked intersection and it is raining is  $P(AB) = 0.002$ .

The probability of the union of two events may be evaluated by measuring the compound event directly, or it may be evaluated from the probabilities of simple events as given by the following theorem.

**THEOREM.** Let  $E = A + B$ ; then

$$P(E) = P(A + B) = P(A) + P(B) - P(AB) \quad (\text{B-4})$$

**Proof.** Let the event  $A$ -only occur  $n_1$  times out of  $n$  trials, the event  $B$ -only occur  $n_2$  times out of  $n$  trials, and the event  $AB$  occur  $n_{AB}$  times. Thus

$$P(A + B) = \lim_{n \rightarrow \infty} \left( \frac{n_1 + n_2 + n_{AB}}{n} \right)$$

$$= \lim_{n \rightarrow \infty} \left( \frac{n_1 + n_{AB}}{n} \right) + \lim_{n \rightarrow \infty} \left( \frac{n_2 + n_{AB}}{n} \right) - \lim_{n \rightarrow \infty} \left( \frac{n_{AB}}{n} \right)$$

which is identical to (B-4) since

$$P(A) = \lim_{n \rightarrow \infty} \left( \frac{n_1 + n_{AB}}{n} \right),$$

$$P(B) = \lim_{n \rightarrow \infty} \left( \frac{n_2 + n_{AB}}{n} \right), \text{ and } P(AB) = \lim_{n \rightarrow \infty} \left( \frac{n_{AB}}{n} \right)$$

### Example B-1 (Continued)

The probability of having a blocked intersection or rain occurring or both, is then

$$P(A + B) = 0.0025 + 0.03 - 0.002 \approx 0.03 \quad (\text{B-5})$$

### Conditional Probabilities

**DEFINITION.** The probability that an event  $A$  occurs, given that an event  $B$  has also occurred, is denoted by  $P(A|B)$  and is defined by

$$P(A|B) = \lim_{n_B \rightarrow \infty} \left( \frac{n_{AB}}{n_B} \right) \quad (\text{B-6})$$

### Example B-1 (Continued)

The probability of a blocked intersection when it is raining is approximately

$$P(A|B) = \frac{20}{300} = 0.066 \quad (\text{B-7})$$

**THEOREM.** Let  $E = AB$ ; then

$$P(AB) = P(A)P(B|A) = P(B)P(A|B) \quad (\text{B-8})$$

This is known as Bayes' theorem.

**Proof.**

$$P(AB) = \lim_{n \rightarrow \infty} \left( \frac{n_{AB}}{n} \right) = \lim_{\substack{n \rightarrow \infty \\ n_A \rightarrow \text{large}}} \left( \frac{n_{AB}}{n_A} \frac{n_A}{n} \right) = P(B|A)P(A) \quad (\text{B-9})$$

It is noted that the values obtained for  $P(AB)$ ,  $P(B)$ , and  $P(A|B)$  in Example B-1 can be verified by the use of (B-8).

**DEFINITION.** Two events,  $A$  and  $B$ , are said to be *independent* if either

$$P(A|B) = P(A) \quad (\text{B-10})$$

or

$$P(B|A) = P(B) \quad (\text{B-11})$$

Using this definition, we can easily demonstrate that events  $A$  and  $B$  of Example B-1 are not independent. Conversely, if event  $A$  had been defined as getting a head on a coin toss, while  $B$  was the event that it was raining at the intersection, then  $A$  and  $B$  would be independent. Why?

Using (B-8) and (B-10), we can show that if a set of events  $A_1, A_2, \dots, A_n$ , are independent; then a necessary condition is<sup>\*</sup>

$$P(A_1 A_2 \cdots A_n) = P(A_1)P(A_2) \cdots P(A_n) \quad (\text{B-12})$$

### B-4 RANDOM VARIABLES

**DEFINITION.** A real *random variable* is a real-valued function defined on the events (elements) of the probability system.

An understanding of why this definition is needed is fundamental to the topic of probability theory. So far we have defined probabilities in terms of events  $A$ ,  $B$ ,  $C$ , and so on. This method is awkward to use when the sets are objects (such as apples, oranges, etc.) instead of numbers. It is more convenient to describe sets by numerical values so that equations can be obtained as a function of numerical values instead of functions of alphanumeric parameters. This method is accomplished by using the random variable.

### Example B-2 RANDOM VARIABLE

Referring to Fig. B-2, we can show the mutually exclusive events  $A$ ,  $B$ ,  $C$ ,  $D$ ,  $E$ ,  $F$ ,  $G$ , and  $H$  by a Venn diagram. These are all the possible outcomes of an experiment, so the sure event is  $S = A + B + C + D + E + F + G + H$ . Each of these events is denoted by some convenient value of the random variable  $x$ , as shown in the table in this figure. The assigned values for  $x$  may be positive, negative, fractions, or integers as long as they are real numbers. Since all the events are mutually exclusive, using (B-4) yields

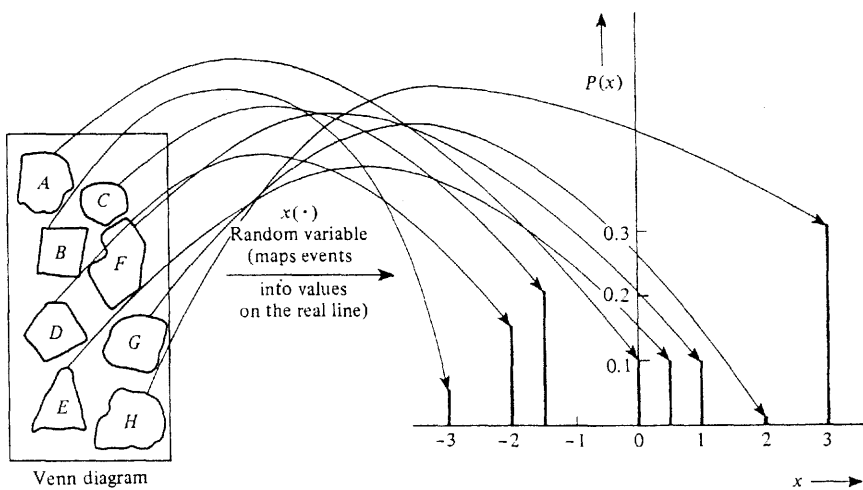
$$P(S) = 1 = P(A) + P(B) + P(C) + P(D) + P(E) + P(F) + P(G) + P(H) \quad (\text{B-13})$$

That is, the probabilities have to sum to unity (the probability of a sure event), as shown in the table, and the individual probabilities have been given or measured as shown. For example,  $P(C) = P(-1.5) = 0.2$ . These values for the probabilities may be plotted as a function of the random variable  $x$ , as shown in the graph of  $P(x)$ . This is a *discrete* (or *point*) distribution since the random variable takes on only discrete (as opposed to continuous) values.

### B-5 CUMULATIVE DISTRIBUTION FUNCTIONS AND PROBABILITY DENSITY FUNCTIONS

**DEFINITION.** The *cumulative distribution function* (CDF) of the random variable  $x$  is given by  $F(a)$ , where

<sup>\*</sup> Equation (B-12) is not a sufficient condition for  $A_1, A_2, \dots, A_n$  to be independent [Papoulis, 1984, p. 34].



Event [·]	Value of Random Variable $x[\cdot]$	Probability of Event $P(x)$
A	0.0	0.10
B	-3.0	0.05
C	-1.5	0.20
D	-2.0	0.15
E	+0.5	0.10
F	+1.0	0.10
G	+2.0	0.00
H	+3.0	0.30
Total =		1.00

Figure B-2 Random variable and probability functions for Example B-2.

$$F(a) \triangleq P(x \leq a) \equiv \lim_{n \rightarrow \infty} \left( \frac{n_{x \leq a}}{n} \right) \quad (\text{B-14})$$

where  $F(a)$  is a unitless function.

**DEFINITION.** The *probability density function* (PDF) of the random variable  $x$  is given by  $f(x)$ , where

$$f(x) = \frac{dF(a)}{da} \Big|_{a=x} = \frac{dP(x \leq a)}{da} \Big|_{a=x} = \lim_{\substack{n \rightarrow \infty \\ \Delta x \rightarrow 0}} \left[ \frac{1}{\Delta x} \left( \frac{n_{x \leq a}}{n} \right) \right] \quad (\text{B-15})$$

where  $f(x)$  has units of  $1/x$ .

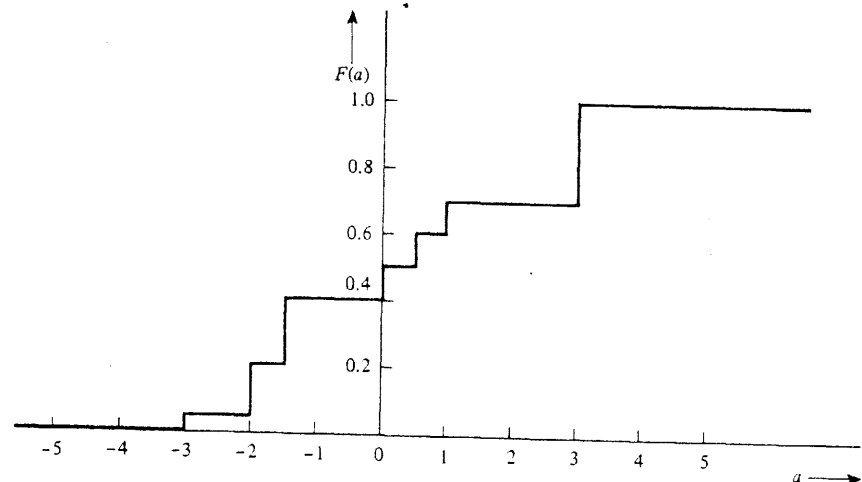


Figure B-3 CDF for Example B-2.

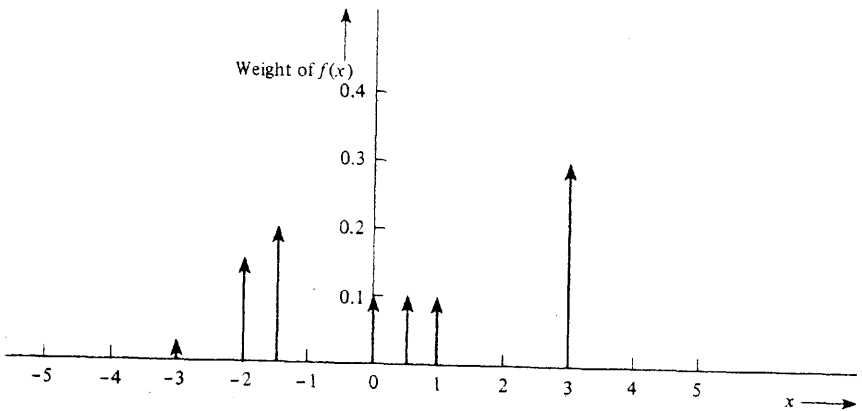


Figure B-4 PDF for Example B-2.

### Example B-2 (Continued)

The CDF for this example that was illustrated in Fig. B-2 is easily obtained using (B-14). The resulting CDF is shown in Fig. B-3. Note that the CDF starts at a zero value on the left ( $a = -\infty$ ), and the probability is accumulated until the CDF is unity on the right ( $a = +\infty$ ).

Using (B-15), we obtain the PDF by taking the derivative of the CDF. The result is shown in Fig. B-4. The PDF consists of Dirac delta functions located at the assigned (discrete) values of the random variable and having weights equal to the probabilities of the associated event.<sup>†</sup>

<sup>†</sup> Left-sided delta functions are used here so that if  $x = a$  happens to be a discrete point,  $F(a) = P(x \leq a)$  includes all the probability from  $x = -\infty$  up to and *including* the point  $x = a$ . See Sec. A-8 (Appendix A) for properties of Dirac delta functions.

## Properties of CDFs and PDFs

Some *properties of the CDF* are as follows:

1.  $F(a)$  is a nondecreasing function.
2.  $F(a)$  is *right-hand continuous*. That is,

$$\lim_{\substack{\epsilon \rightarrow 0 \\ \epsilon > 0}} F(a + \epsilon) = F(a)$$

3.

$$F(a) = \lim_{\substack{\epsilon \rightarrow 0 \\ \epsilon > 0}} \int_{-\infty}^{a+\epsilon} f(x) dx \quad (\text{B-16})$$

4.  $0 \leq F(a) \leq 1$ .
5.  $F(-\infty) = 0$ .
6.  $F(+\infty) = 1$ .

Note that the  $\epsilon$  is needed to account for a discrete point that might occur at  $x = a$ . If there is no discrete point at  $x = a$ , the limit is not necessary.

Some *properties of the PDF* are as follows.

1.  $f(x) \geq 0$ . That is,  $f(x)$  is a nonnegative function.
2.  $\int_{-\infty}^{\infty} f(x) dx = F(+\infty) = 1$ . (B-17)

As we will see later,  $f(x)$  may have values larger than unity; however, the area under  $f(x)$  is equal to unity. These properties of the CDF and PDF are very useful in checking results of problems. That is, if a CDF or a PDF violates any of these properties, you know that an error has been made in the calculations.

## Discrete and Continuous Distributions

Example B-2 was an example of a *discrete (or point) distribution*. That is, the random variable has  $M$  discrete values  $x_1, x_2, x_3, \dots, x_M = 7$  in this example. Consequently, the CDF increased only in jumps [i.e.,  $F(a)$  was discontinuous] as  $a$  increased, and the PDF consisted of delta functions located at the discrete values of the random variable. In contrast to this example of a discrete distribution, there are continuous distributions, one of which is illustrated in the following example. If a random variable is allowed to take on any value in some interval, it is a *continuously distributed* random variable in that interval.

### Example B-3 A CONTINUOUS DISTRIBUTION

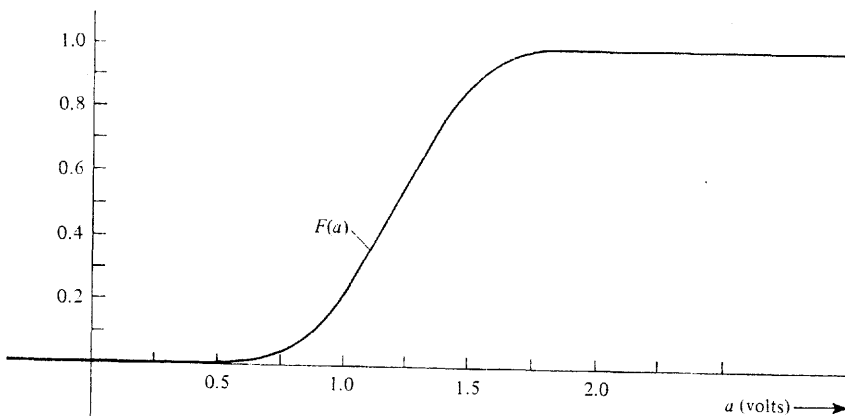
Let the random variable denote the voltages that are associated with a collection of a large number of flashlight batteries (1.5-V cells). If the number of batteries in the collection were infinite,

the number of different voltage values (events) that we could obtain would be infinite, so that the distributions (PDF and CDF) would be continuous functions. Suppose that, by measurement, the CDF is evaluated first by using  $F(a) = P(x \leq a) = \lim_{n \rightarrow \infty} (n_{x \leq a}/n)$ , where  $n$  is the number of batteries in the whole collection and  $n_{x \leq a}$  is the number of batteries in the collection with voltages less than or equal to  $a$  V, where  $a$  is a parameter. The CDF that might be obtained is illustrated in Fig. B-5a. The associated PDF is obtained by taking the derivative of the CDF, as shown in Fig. B-5b. Note that  $f(x)$  exceeds unity for some values of  $x$ , but that the area under  $f(x)$  is unity (a PDF property). (You might check to see that the other CDF and PDF properties are also satisfied.)

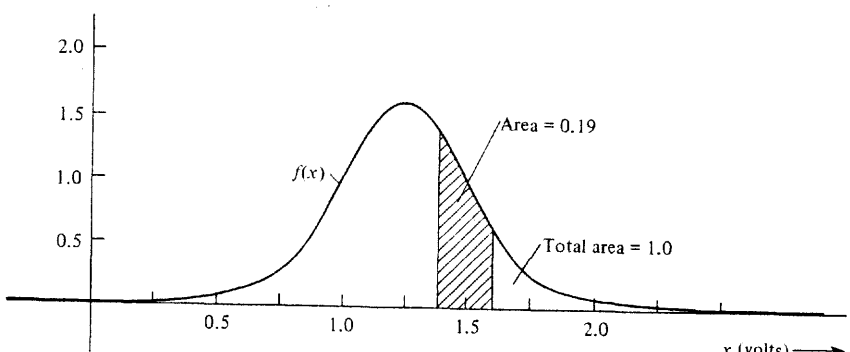
### THEOREM.

$$F(b) - F(a) = P(x \leq b) - P(x \leq a) = P(a < x \leq b)$$

$$= \lim_{\substack{\epsilon \rightarrow 0 \\ \epsilon > 0}} \left[ \int_{a+\epsilon}^{b+\epsilon} f(x) dx \right] \quad (\text{B-18})$$



(a) Cumulative Distribution Function



(b) Probability Density Function

Figure B-5 CDF and PDF for a continuous distribution (Example B-3).

*Proof.*

$$\begin{aligned} F(b) - F(a) &= \lim_{\substack{\epsilon \rightarrow 0 \\ \epsilon > 0}} \left[ \int_{-\infty}^{b+\epsilon} f(x) dx - \int_{-\infty}^{a+\epsilon} f(x) dx \right] \\ &= \lim_{\substack{\epsilon \rightarrow 0 \\ \epsilon > 0}} \left[ \int_{-\infty}^{a+\epsilon} f(x) dx + \int_{a+\epsilon}^{b+\epsilon} f(x) dx - \int_{-\infty}^{a+\epsilon} f(x) dx \right] \\ &= \lim_{\substack{\epsilon \rightarrow 0 \\ \epsilon > 0}} \left[ \int_{a+\epsilon}^{b+\epsilon} f(x) dx \right] \end{aligned}$$

### Example B-3 (Continued)

Suppose that we wanted to calculate the probability of obtaining a battery having a voltage between 1.4 and 1.6 V. Using this theorem, we compute

$$P(1.4 < x \leq 1.6) = \int_{1.4}^{1.6} f(x) dx = F(1.6) - F(1.4) = 0.19$$

(using Fig. B-5). We also realize that the probability of obtaining a 1.5-V battery is zero. Why? However, the probability of obtaining a  $1.5 \pm 0.1$  V battery is 0.19.

In communication systems we have digital signals that may have discrete distributions (one discrete value for each permitted level in a multilevel signal), and we have analog signals and noise that have continuous distributions. We may also have mixed distributions, which contain discrete as well as continuous values. These occur, for example, when a continuous signal and noise are clipped by an amplifier that is driven into saturation.

**THEOREM.** If  $x$  is discretely distributed, then

$$f(x) = \sum_{i=1}^M P(x_i) \delta(x - x_i) \quad (\text{B-19})$$

where  $M$  is the number of discrete events and  $P(x_i)$  is the probability of obtaining the discrete event  $x_i$ .

This theorem was illustrated by Example B-2, where the PDF of this discrete distribution is plotted in Fig. B-4.

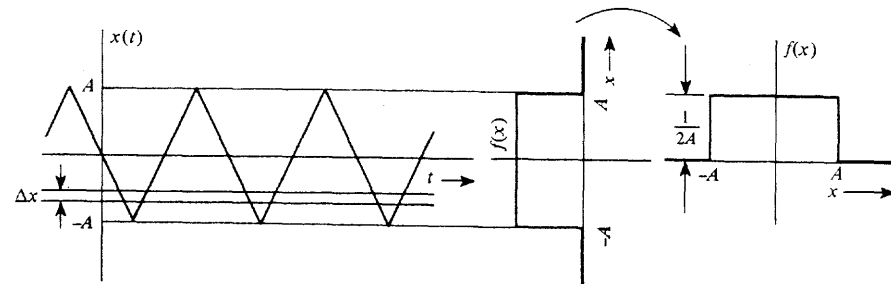
**THEOREM.** If  $x$  is discretely distributed, then<sup>†</sup>

$$F(a) = \sum_{i=1}^L P(x_i) \quad (\text{B-20})$$

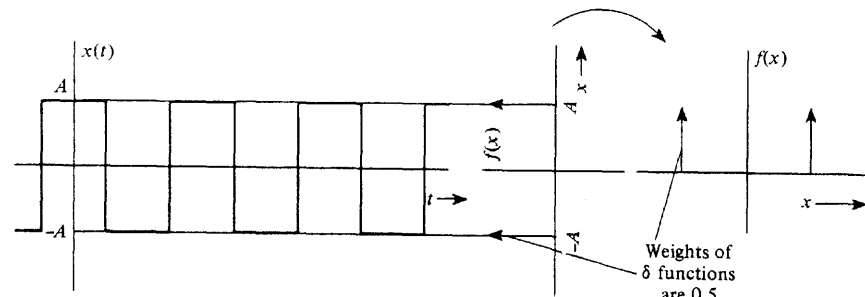
where  $L$  is the largest integer such that  $x_L \leq a$  and  $L \leq M$ , where  $M$  is the number of points in the discrete distribution. Here it is assumed that the discrete points  $x_i$  are indexed so that they occur in ascending order of the index. That is,  $x_1 < x_2 < x_3 < \dots < x_M$ .

This theorem was illustrated in Fig. B-3, which is a plot of (B-20) for Example B-2.

In electrical engineering problems, the CDFs or PDFs of waveforms are relatively easy to obtain by using the relative frequency approach, as described by (B-14) and (B-15). For example, the PDFs for triangular and square waves are given in Fig. B-6. These are obtained by sweeping a narrow horizontal window,  $\Delta x$  volts wide, vertically across the waveforms and measuring the relative frequency of occurrence of voltages in the  $\Delta x$  window. The time axis is divided into  $n$  intervals, and the waveform appears  $n_{\Delta x}$  times in these intervals in the  $\Delta x$  window. A rough idea of the PDF of a waveform can also be obtained by looking at the



(a) Triangular Waveform and Its Associated PDF



(b) Square Waveform and Its Associated PDF

Figure B-6 PDFs for triangular waves and square waves.

<sup>†</sup> Equation (B-20) is identical to  $F(a) = \sum_{i=1}^M P(x_i)u(a - x_i)$ , where  $u(y)$  is a unit step function [defined in (2-49)].

waveform on an oscilloscope. Using *no* horizontal sweep, the intensity of the presentation as a function of the voltage (*y* axis) gives the PDF. (This assumes that the intensity of the image is proportional to the time that the waveform dwells in the window  $\Delta y$  units wide.) The PDF is proportional to the intensity as a function of *y* (the random variable).

## B-6 ENSEMBLE AVERAGE AND MOMENTS

### Ensemble Average

One of the primary uses of probability theory is to evaluate the average value of a random variable (which represents some physical phenomenon) or to evaluate the average value of some function of the random variable. In general, let the function of the random variable be denoted by  $y = h(x)$ .

**DEFINITION.** The *expected value*, which is also called the *ensemble average*, of  $y = h(x)$  is given by

$$\bar{y} = \overline{[h(x)]} \triangleq \int_{-\infty}^{\infty} [h(x)] f(x) dx \quad (\text{B-21})$$

This definition may be used for discrete as well as continuous random variables. Note that it is a linear operator where the operator is

$$\overline{[\cdot]} = \int_{-\infty}^{\infty} [\cdot] f(x) dx \quad (\text{B-22})$$

Other authors denote the ensemble average of *y* by  $E[y]$  or  $\langle y \rangle$  as well as using this notation of  $\bar{y}$ . We will use the  $\bar{y}$  notation since it is easier to write and more convenient to use when long equations are being evaluated with a large number of averaging operators.

**THEOREM.** If *x* is a *discretely distributed random variable*, the expected value can be evaluated by using

$$\bar{y} = \overline{[h(x)]} = \sum_{i=1}^M h(x_i) P(x_i) \quad (\text{B-23})$$

where *M* is the number of discrete points in the distribution.

**Proof.** Using (B-19) in (B-21), we get

$$\begin{aligned} \overline{[h(x)]} &= \int_{-\infty}^{\infty} h(x) \left[ \sum_{i=1}^M P(x_i) \delta(x - x_i) \right] dx \\ &= \sum_{i=1}^M P(x_i) \int_{-\infty}^{\infty} h(x) \delta(x - x_i) dx \\ &= \sum_{i=1}^M P(x_i) h(x_i) \end{aligned}$$

### Example B-4 EVALUATION OF AN AVERAGE

We will now show that (B-23) and, consequently, the definition of expected value as given by (B-21) are consistent with the way in which we usually evaluate averages. Suppose that we have a class of *n* = 40 students who take a test. The resulting test scores are 1 paper with a grade of 100; 2 with scores of 95; 4, 90; 6, 85; 10, 80; 10, 75; 5, 70; 1, 65; and 1 paper with a score of 60. Then the class average will be

$$\begin{aligned} \bar{x} &= \frac{100(1) + 95(2) + 90(4) + 85(6) + 80(10) + 75(10) + 70(5) + 65(1) + 60(1)}{40} \\ &= 100\left(\frac{1}{40}\right) + 95\left(\frac{2}{40}\right) + 90\left(\frac{4}{40}\right) + 85\left(\frac{6}{40}\right) + 80\left(\frac{10}{40}\right) + 75\left(\frac{10}{40}\right) \\ &\quad + 70\left(\frac{5}{40}\right) + 65\left(\frac{1}{40}\right) + 60\left(\frac{1}{40}\right) \\ &= \sum_{i=1}^9 x_i P(x_i) = 79.6 \end{aligned} \quad (\text{B-24})$$

### Moments

*Moments* are defined as ensemble averages of some specific functions used for  $h(x)$ . For example, for the *r*th moment, defined subsequently, let  $y = h(x) = (x - x_0)^r$ .

**DEFINITION.** The *r*th moment of the random variable *x* taken about the point  $x = x_0$  is given by

$$\overline{(x - x_0)^r} = \int_{-\infty}^{\infty} (x - x_0)^r f(x) dx \quad (\text{B-25})$$

**DEFINITION.** The *mean m* is the first moment taken about the origin (i.e.,  $x_0 = 0$ ). Thus

$$m \triangleq \bar{x} = \int_{-\infty}^{\infty} x f(x) dx \quad (\text{B-26})$$

**DEFINITION.** The *variance  $\sigma^2$*  is the second moment taken about the mean. Thus

$$\sigma^2 = \overline{(x - \bar{x})^2} = \int_{-\infty}^{\infty} (x - \bar{x})^2 f(x) dx \quad (\text{B-27})$$

**DEFINITION.** The *standard deviation  $\sigma$*  is the square root of the variance. Thus

$$\sigma = \sqrt{\sigma^2} = \sqrt{\int_{-\infty}^{\infty} (x - \bar{x})^2 f(x) dx} \quad (\text{B-28})$$

As an engineer, you may recognize the integrals of (B-26) and (B-27) as related to applications in mechanical problems. The mean is equivalent to the center of gravity of a

mass that is distributed along a single dimension, where  $f(x)$  denotes the mass density as a function of the  $x$  axis. The variance is equivalent to the moment of inertia about the center of gravity. However, you might ask: What is the significance of the mean, variance, and other moments in electrical engineering problems? In Chapter 6 it is shown that if  $x$  represents a voltage or current waveform, the mean gives the dc value of the waveform. The second moment ( $r = 2$ ) taken about the origin ( $x_0 = 0$ ), which is  $\bar{x}^2$ , gives the normalized power  $\sigma^2$  gives the normalized power in the corresponding ac coupled waveform. Consequently,  $\sqrt{\bar{x}^2}$  is the rms value of the waveform and  $\sigma$  is the rms value of the corresponding ac coupled waveform.

In statistical terms,  $m$  gives the *center of gravity* of the PDF and  $\sigma$  gives us the *spread* of the PDF about this center of gravity. For example, in Fig. B-5 the voltage distribution for a collection of flashlight batteries is given. The mean is  $\bar{x} = 1.25$  V and the standard deviation is  $\sigma = 0.25$  V. This figure illustrates a Gaussian distribution that will be studied in detail in Sec. B-7. For this Gaussian distribution the area under  $f(x)$  from  $x = 1.0$  to  $1.5$  V, which corresponds to the interval  $\bar{x} \pm \sigma$ , is 0.68. Thus we conclude that 68% of the batteries have voltages within one standard deviation of the mean value (Gaussian distribution).

There are several ways to specify a number that is used to describe the typical or most common value of  $x$ . The *mean*  $m$  is one such measure that gives the center of gravity. Another measure is the *median*, which corresponds to the value  $x = a$ , where  $F(a) = \frac{1}{2}$ . A third measure is called the *mode*, which corresponds to the value of  $x$  where  $f(x)$  is a maximum, assuming that the PDF has only one maximum. For the Gaussian distribution, all these measures give the same number, namely,  $x = m$ . For other types of distributions, the values obtained for the mean, median, and mode will usually be nearly the same number. The variance is also related to the second moment about the origin and the mean, as described by the following theorem.

#### THEOREM.

$$\sigma^2 = \bar{x}^2 - (\bar{x})^2 \quad (B-29)$$

A proof of this theorem illustrates how the ensemble average operator notation is used.

#### Proof.

$$\begin{aligned} \sigma^2 &= \overline{(x - \bar{x})^2} \\ &= \overline{[x^2] - [2x\bar{x}] + [\bar{x}^2]} \end{aligned} \quad (B-30)$$

Because  $[\cdot]$  is a linear operator,  $[2x\bar{x}] = 2\bar{x}\bar{x} = 2(\bar{x})^2$ . Moreover,  $(\bar{x})^2$  is a constant and the average value of a constant is the constant itself. That is, for the constant  $c$ ,

$$\bar{c} = \int_{-\infty}^{\infty} c f(x) dx = c \int_{-\infty}^{\infty} f(x) dx = c \quad (B-31)$$

So, using (B-31) in (B-30), we obtain

$$\sigma^2 = \bar{x}^2 - 2(\bar{x})^2 + (\bar{x})^2$$

which is equivalent to (B-29).

Thus there are two ways to evaluate the variance: (1) by use of the definition as given by (B-27), or (2) by use of the theorem of (B-29).

## B-7 EXAMPLES OF IMPORTANT DISTRIBUTIONS

There are numerous types of distributions. Some of the more important ones used in communication and statistical problems are summarized in Table B-1. Here, the equations for their PDF and CDF, a sketch of the PDF, and the formula for the mean and variance are given. These distributions will be studied in more detail in the following paragraphs.

### Binomial Distribution

The binomial distribution is useful for describing digital as well as other statistical problems. Its application is best illustrated by an example.

Assume that we have a binary word that is  $n$  bits long and that the probability of sending a binary 1 is  $p$ . Consequently, the probability of sending a binary 0 is  $1 - p$ . We want to evaluate the probability of obtaining  $n$ -bit words that contain  $k$  binary 1s. One such word is  $k$  binary 1s followed by  $n - k$  binary 0s. The probability of obtaining this word is  $p^k(1 - p)^{n-k}$ . There are also other  $n$ -bit words that contain  $k$  binary 1s. In fact, the number of different  $n$ -bit words containing  $k$  binary 1s is

$$\binom{n}{k} = \frac{n!}{(n - k)!k!} \quad (B-32)$$

(This can be demonstrated by taking a numerical example such as  $n = 8$  and  $k = 3$ .) The symbol  $\binom{n}{k}$  is used in algebra to denote the operation described by (B-32) and is read "the combination of  $n$  things taken  $k$  at a time." Thus the probability of obtaining an  $n$ -bit word containing  $k$  binary 1s is

$$P(k) = \binom{n}{k} p^k (1 - p)^{n-k} \quad (B-33)$$

If we let the random variable  $x$  denote these discrete values, then  $x = k$ , where  $k$  can take on the values  $0, 1, 2, \dots, n$ , and we obtain the *binomial PDF*:

$$f(x) = \sum_{k=0}^n P(k) \delta(x - k) \quad (B-34)$$

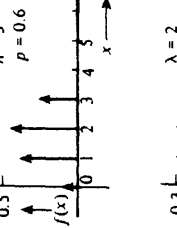
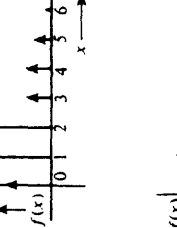
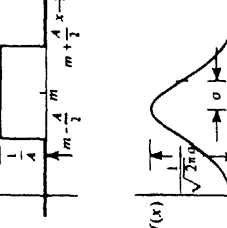
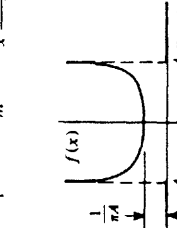
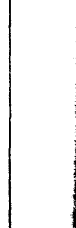
where  $P(k)$  is given by (B-33).

The name *binomial* comes from the fact that the  $P(k)$  are the individual terms in a binomial expansion. That is, letting  $q = 1 - p$ ,

$$(p + q)^n = \sum_{k=0}^n \binom{n}{k} p^k q^{n-k} = \sum_{k=0}^n P(k) \quad (B-35)$$

TABLE B-1 SOME DISTRIBUTIONS AND THEIR PROPERTIES

Equation for:

Name of Distribution	Type: $F(a)$ is:	Sketch of PDF	Cumulative Distribution Function (CDF)	Probability Density Function (PDF)	Mean	Variance
Binomial	Discrete		$F(a) = \sum_{k=0}^m P(k)$ where $P(k) = \binom{n}{k} p^k (1-p)^{n-k}$	$f(x) = \sum_{k=0}^n P(k) \delta(x - k)$ where $P(k) = \binom{n}{k} p^k (1-p)^{n-k}$	$np$	$np(1-p)$
Poisson	Discrete		$F(a) = \sum_{k=0}^m P(k)$ where $P(k) = \frac{\lambda^k e^{-\lambda}}{k!}$	$f(x) = \sum_{k=0}^x P(k) \delta(x - k)$ where $P(k) = \frac{\lambda^k e^{-\lambda}}{k!}$	$\lambda$	$\lambda$
Uniform	Continuous		$F(a) = \begin{cases} 0, & a < \left(\frac{2m-A}{2}\right) \\ \frac{1}{A} \left[ a - \left(\frac{2m-A}{2}\right) \right], &  a - m  \leq \frac{A}{2} \\ 1, & a \geq \left(\frac{2m+A}{2}\right) \end{cases}$	$f(x) = \begin{cases} 0, & x < \left(\frac{2m-A}{2}\right) \\ \frac{1}{A}, &  x - m  \leq \frac{A}{2} \\ 0, & x > \left(\frac{2m+A}{2}\right) \end{cases}$	$m$	$\frac{A^2}{12}$
Gaussian	Continuous		$F(a) = Q\left(\frac{m-a}{\sigma}\right)$ where $Q(\sigma) \triangleq \frac{1}{\sqrt{2\pi}} \int_a^\infty e^{-x^2/2} dx$	$f(x) = \frac{1}{\sqrt{2\pi\sigma^2}} e^{-(x-m)^2/2\sigma^2}$ where $Q(\sigma) \triangleq \frac{1}{\sqrt{2\pi}} \int_a^\infty e^{-x^2/2} dx$	$m$	$\sigma^2$
Sinusoidal	Continuous		$F(a) = \begin{cases} 0, & a \leq -A \\ \frac{1}{\pi} \left[ \frac{\pi}{2} + \sin^{-1} \left( \frac{a}{A} \right) \right], &  a  \leq A \\ 1, & a \geq A \end{cases}$	$f(x) = \begin{cases} 0, & x < -A \\ \frac{1}{\pi} \sqrt{A^2 - x^2}, &  x  \leq A \\ 0, & x > A \end{cases}$		

## Sec. B-7 Examples of Important Distributions

The combinations  $\binom{n}{k}$ , which are also the binomial coefficients, can be evaluated by using Pascal's triangle:

$n = 0$	1
$n = 1$	1 1
$n = 2$	1 2 1
$n = 3$	1 3 3 1
$n = 4$	1 4 6 4 1
$n = 5$	1 5 10 10 5 1
⋮	⋮

For a particular value of  $n$ , the combinations  $\binom{n}{k}$ , for  $k = 0, 1, \dots, n$ , are the elements in the  $n$ th row. For example, for  $n = 3$ ,

$$\binom{3}{0} = 1, \quad \binom{3}{1} = 3, \quad \binom{3}{2} = 3, \quad \text{and} \quad \binom{3}{3} = 1$$

The mean value of the binomial distribution is evaluated by the use of (B-23).

$$m = \bar{x} = \sum_{k=0}^n x_k P(x_k) = \sum_{k=0}^n k P(k)$$

or

$$m = \sum_{k=1}^n k \binom{n}{k} p^k q^{n-k} \quad (\text{B-36})$$

Using the identity

$$\begin{aligned} k \binom{n}{k} &= \frac{k n!}{(n-k)! k!} = \frac{n(n-1)!}{(n-k)!(k-1)!} \\ &= n \left[ \frac{(n-1)!}{((n-1)-(k-1))!(k-1)!} \right] \end{aligned}$$

or

$$k \binom{n}{k} = n \binom{n-1}{k-1} \quad (\text{B-37})$$

we have

$$m = \sum_{k=1}^n n \binom{n-1}{k-1} p^k q^{n-k} \quad (\text{B-38})$$

Making a change in the index, let  $j = k - 1$ . Thus,

$$\begin{aligned} m &= \sum_{j=0}^{n-1} n \binom{n-1}{j} p^{j+1} q^{n-(j+1)} \\ &= np \left[ \sum_{j=0}^{n-1} \binom{n-1}{j} p^j q^{(n-1)-j} \right] = np [(p+q)^{n-1}] \end{aligned} \quad (\text{B-39})$$

Recalling that  $p$  and  $q$  are probabilities and  $p + q = 1$ , then we see that  $(p+q)^{n-1} = 1$ . Thus (B-39) reduces to

$$m = np \quad (\text{B-40})$$

Similarly, it can be shown that the variance is  $np(1-p)$  by using  $\sigma^2 = \bar{x}^2 - (\bar{x})^2$ .

### Poisson Distribution

The Poisson distribution (Table B-1) is obtained as a limiting approximation of a binomial distribution when  $n$  is very large and  $p$  is very small, but the product  $np = \lambda$  is some reasonable size [Thomas, 1969].

### Uniform Distribution

The uniform distribution is

$$f(x) = \begin{cases} 0, & x < \frac{2m-A}{2} \\ \frac{1}{A}, & |x-m| \leq \frac{A}{2} \\ 0, & x > \frac{2m+A}{2} \end{cases} \quad (\text{B-41})$$

where  $A$  is the peak-to-peak value of the random variable. This is illustrated by the sketch in Table B-1. The mean of this distribution is

$$\int_{-\infty}^{\infty} x f(x) dx = \int_{m-(A/2)}^{m+(A/2)} x \frac{1}{A} dx = m \quad (\text{B-42})$$

and the variance is

$$\sigma^2 = \int_{m-(A/2)}^{m+(A/2)} (x-m)^2 \frac{1}{A} dx \quad (\text{B-43})$$

Making a change in variable, let  $y = x - m$ .

$$\sigma^2 = \frac{1}{A} \int_{-A/2}^{A/2} y^2 dy = \frac{A^2}{12} \quad (\text{B-44})$$

The uniform distribution is useful in describing quantizing noise that is created when an analog signal is converted into a PCM signal, as discussed in Chapter 3. In Chapter 6 it is shown that it also describes the noise out of a phase detector when the input is Gaussian noise (as described subsequently).

### Gaussian Distribution

The Gaussian distribution, which is also called the *normal distribution*, is one of the most important distributions, if not *the* most important. As discussed in Chapter 5, thermal noise has a Gaussian distribution. Numerous other phenomena can also be described by Gaussian statistics, and many theorems have been developed by statisticians that are based on Gaussian assumptions. It cannot be overemphasized that the Gaussian distribution is very important in analyzing both communication problems and problems in statistics. It can also be shown that the Gaussian distribution can be obtained as the limiting form of the binomial distribution when  $n$  becomes large, while holding the mean  $m = np$  finite, and letting the variance  $\sigma^2 = np(1-p)$  be much larger than unity [Feller, 1957; Papoulis, 1984].

**DEFINITION.** The Gaussian distribution is



$$f(x) = \frac{1}{\sqrt{2\pi}\sigma} e^{-(x-m)^2/(2\sigma^2)} \quad (\text{B-45})$$

where  $m$  is the mean and  $\sigma^2$  is the variance.

A sketch of (B-45) is given in Fig. B-5, together with the CDF for the Gaussian random variable where  $m = 1.25$  and  $\sigma = 0.25$ . The Gaussian PDF is symmetrical about  $x = m$ , with the area under the PDF being  $\frac{1}{2}$  for  $(-\infty \leq x \leq m)$  and  $\frac{1}{2}$  for  $(m \leq x \leq \infty)$ . The peak value of the PDF is  $1/(\sqrt{2\pi}\sigma)$  so that as  $\sigma \rightarrow 0$ , the Gaussian PDF goes into a  $\delta$  function located at  $x = m$  (since the area under the PDF is always unity).

We will now show that (B-45) is properly normalized; that is, the area under  $f(x)$  is unity. This can be accomplished by letting  $I$  represent the integral of the PDF:

$$I \triangleq \int_{-\infty}^{\infty} f(x) dx = \int_{-\infty}^{\infty} \frac{1}{\sqrt{2\pi}\sigma} e^{-(x-m)^2/(2\sigma^2)} dx \quad (\text{B-46})$$

Making a change in variable, let  $y = (x-m)/\sigma$ , then

$$I = \frac{1}{\sqrt{2\pi}\sigma} \int_{-\infty}^{\infty} e^{-y^2/2} (\sigma dy) = \frac{1}{\sqrt{2\pi}} \int_{-\infty}^{\infty} e^{-y^2/2} dy \quad (\text{B-47})$$

The integral  $I$  can be shown to be unity by showing that  $I^2$  is unity.

$$\begin{aligned} I^2 &= \left[ \frac{1}{\sqrt{2\pi}} \int_{-\infty}^{\infty} e^{-x^2/2} dx \right] \left[ \frac{1}{\sqrt{2\pi}} \int_{-\infty}^{\infty} e^{-y^2/2} dy \right] \\ &= \frac{1}{2\pi} \int_{-\infty}^{\infty} \int_{-\infty}^{\infty} e^{-(x^2+y^2)/2} dx dy \end{aligned} \quad (\text{B-48})$$

Make a change in the variables to polar coordinates from Cartesian coordinates. Let  $r^2 = x^2 + y^2$  and  $\theta = \tan^{-1}(y/x)$ ; then

$$I^2 = \frac{1}{2\pi} \int_0^{2\pi} \left[ \int_0^\infty e^{-r^2/2} r dr \right] d\theta = \frac{1}{2\pi} \int_0^{2\pi} d\theta = 1 \quad (\text{B-49})$$

Thus  $I^2 = 1$  and, consequently,  $I = 1$ .

Up to now, we have *assumed* that the parameters  $m$  and  $\sigma^2$  of (B-45) were the mean and the variance of the distribution. We need to *show* that indeed they are! This may be accomplished by writing the Gaussian form in terms of some arbitrary parameters  $\alpha$  and  $\beta$ .

$$f(x) = \frac{1}{\sqrt{2\pi}\beta} e^{-(x-\alpha)^2/(2\beta^2)} \quad (\text{B-50})$$

This function is still properly normalized, as demonstrated by (B-49). First, we need to show that the parameter  $\alpha$  is the mean.

$$m = \int_{-\infty}^{\infty} x f(x) dx = \frac{1}{\sqrt{2\pi}\beta} \int_{-\infty}^{\infty} x e^{-(x-\alpha)^2/(2\beta^2)} dx \quad (\text{B-51})$$

Making a change in variable, let  $y = (x - \alpha)/\beta$ ; then

$$m = \frac{1}{\sqrt{2\pi}} \int_{-\infty}^{\infty} (\beta y + \alpha) e^{-y^2/2} dy$$

or

$$m = \frac{\beta}{\sqrt{2\pi}} \int_{-\infty}^{\infty} (ye^{-y^2/2}) dy + \alpha \left( \int_{-\infty}^{\infty} \frac{1}{\sqrt{2\pi}} e^{-y^2/2} dy \right) \quad (\text{B-52})$$

The first integral on the right of (B-52) is zero because the integrand is an odd function and the integral is evaluated over symmetrical limits. The second integral on the right is the integral of a properly normalized Gaussian PDF, so the integral has a value of unity. Thus (B-52) becomes

$$m = \alpha \quad (\text{B-53})$$

and we have shown that the parameter  $\alpha$  is the mean value.

The variance is

$$\begin{aligned} \sigma^2 &= \int_{-\infty}^{\infty} (x - m)^2 f(x) dx \\ &= \frac{1}{\sqrt{2\pi}\beta} \int_{-\infty}^{\infty} (x - m)^2 e^{-(x-m)^2/(2\beta^2)} dx \end{aligned} \quad (\text{B-54})$$

Similarly, we need to show that  $\sigma^2 = \beta^2$ . This will be left as a homework exercise.

The next question to answer is: What is the CDF for the Gaussian distribution?

**THEOREM.** *The cumulative distribution function (CDF) for the Gaussian distribution is*

$$F(a) = Q\left(\frac{m-a}{\sigma}\right) = \frac{1}{2} \operatorname{erfc}\left(\frac{m-a}{\sqrt{2}\sigma}\right) \quad (\text{B-55})$$

where the  $Q$  function is defined by

$$Q(z) \triangleq \frac{1}{\sqrt{2\pi}} \int_z^{\infty} e^{-\lambda^2/2} d\lambda \quad (\text{B-56})$$

and the complementary error function ( $\operatorname{erfc}$ ) is defined as

$$\operatorname{erfc}(z) \triangleq \frac{2}{\sqrt{\pi}} \int_z^{\infty} e^{-\lambda^2} d\lambda \quad (\text{B-57})$$

It can also be shown that

$$\operatorname{erfc}(z) = 1 - \operatorname{erf}(z) \quad (\text{B-58})$$

where the error function is defined as

$$\operatorname{erf}(z) \triangleq \frac{2}{\sqrt{\pi}} \int_0^z e^{-\lambda^2} d\lambda \quad (\text{B-59})$$

The  $Q$  function and the complementary error function, as used in (B-55), give the same curve for  $F(a)$ . Because neither of the corresponding integrals, given by (B-56) and (B-57), can be evaluated in closed form, math tables (see Sec. A-10, Appendix A), numerical integration techniques, or closed-form approximations must be used to evaluate them. The equivalence between the two functions is

$$Q(z) = \frac{1}{2} \operatorname{erfc}\left(\frac{z}{\sqrt{2}}\right) \quad (\text{B-60})$$

Communication engineers often prefer to use the  $Q$  function as compared to the  $\operatorname{erfc}$  function since solutions to problems written in terms of the  $Q$  function do not require the writing of the  $\frac{1}{2}$  and  $1/\sqrt{2}$  factors. Conversely, the advantage of using the  $\operatorname{erf}(z)$  or  $\operatorname{erfc}(z)$  functions is that they are one of the standard functions in MATLAB and MathCAD, and these functions are also available on some hand calculators. However, textbooks in probability and statistics usually give a tabulation of the normalized CDF. This is a tabulation of  $F(a)$  for the case of  $m = 0$  and  $\sigma = 1$ , and it is equivalent to  $Q(-a)$  and  $\frac{1}{2} \operatorname{erfc}(-a/\sqrt{2})$ . Since  $Q(z)$  and  $\frac{1}{2} \operatorname{erfc}(z/\sqrt{2})$  are equivalent, which one is used is a matter of personal preference. We use the  $Q$ -function notation in this book.

**Proof.** Proof of a Theorem for the Gaussian CDF

$$F(a) = \int_{-\infty}^a f(x) dx = \frac{1}{\sqrt{2\pi}\sigma} \int_{-\infty}^a e^{-(x-m)^2/(2\sigma^2)} dx \quad (\text{B-61})$$

; a change in variable, let  $y = (m - x)/\sigma$ .

$$F(a) = \frac{1}{\sqrt{2\pi}\sigma} \int_{-\infty}^{(m-a)/\sigma} e^{-y^2/2} (-\sigma dy) \quad (\text{B-62})$$

or

$$F(a) = \frac{1}{\sqrt{2\pi}} \int_{(m-a)/\sigma}^{\infty} e^{-y^2/2} dy = Q\left(\frac{m-a}{\sigma}\right) \quad (\text{B-63})$$

Similarly,  $F(a)$  may be expressed in terms of the complementary error function.

As mentioned earlier, it is unfortunate that the integrals for  $Q(z)$  or  $\text{erfc}(z)$  cannot be evaluated in closed form. However, for large values of  $z$ , very good closed-form approximations can be obtained, and for small values of  $z$  numerical integration techniques can be applied easily. A plot of  $Q(z)$  is shown in Fig. B-7 for  $z \geq 0$  and a tabulation of  $Q(z)$  is given in Sec. A-10.

A relatively simple closed-form upper bound for  $Q(z)$ ,  $z > 0$ , is



$$Q(z) < \frac{1}{\sqrt{2\pi}z} e^{-z^2/2}, \quad z > 0 \quad (\text{B-64})$$

This is also shown in Fig. B-7. It is obtained by evaluating the  $Q(z)$  integral by parts.

$$Q(z) = \int_z^{\infty} \frac{1}{\sqrt{2\pi}} e^{-\lambda^2/2} d\lambda = \int_z^{\infty} u dv = uv \Big|_z^{\infty} - \int_z^{\infty} v du$$

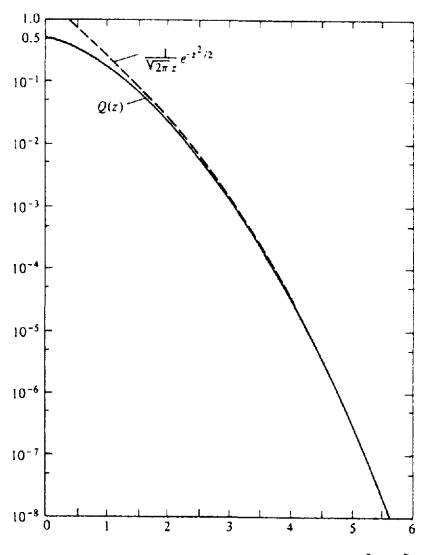


Figure B-7 The function  $Q(z)$  and an overbound,  $\frac{1}{\sqrt{2\pi}z} e^{-z^2/2}$ .

where  $u = 1/(\sqrt{2\pi}\lambda)$  and  $dv = \lambda e^{-\lambda^2/2} d\lambda$ . Thus

$$Q(z) = \left( \frac{1}{\sqrt{2\pi}\lambda} \right) \left( -e^{-\lambda^2/2} \right) \Big|_z^{\infty} - \int_z^{\infty} \left( -e^{-\lambda^2/2} \right) \left( -\frac{1}{\sqrt{2\pi}\lambda^2} d\lambda \right)$$

Dropping the integral, which is a positive quantity, we obtain the upper bound on  $Q(z)$  as given by (B-64). If needed, a lower bound may also be obtained [Wozencraft and Jacobs, 1965]. A rational function approximation for  $Q(z)$  is given by (A-116), and a closed-form approximation that has an error of less than 0.27% is given by (A-117).

For values of  $z \geq 3$  this upper bound has an error of less than 10% when compared to the actual value for  $Q(z)$ . That is,  $Q(3) = 1.35 \times 10^{-3}$  and the upper bound has a value of  $1.48 \times 10^{-3}$  for  $z = 3$ . This is an error of 9.4%. For  $z = 4$  the error is 5.6% and for  $z = 5$  the error is 3.6%. In evaluating the probability of error for digital systems, as discussed in Chapters 6, 7, and 8, the result is often found to be a  $Q$  function. Since most useful digital systems have a probability of error of  $10^{-3}$  or less, this upper bound becomes very useful for evaluating  $Q(z)$ . At any rate, if the upper bound approximation is used, we know that the value obtained indicates slightly poorer performance than is theoretically possible. In this sense, this approximation will give a worst-case result.

For the case of  $z$  negative,  $Q(z)$  can be evaluated by using the identity

$$Q(-z) = 1 - Q(z) \quad (\text{B-65})$$

where the  $Q$  value for positive  $z$  is used (as obtained from Fig. B-7) to compute the  $Q$  of the negative value of  $z$ .

### Sinusoidal Distribution

**THEOREM.** If  $x = A \sin \psi$ , where  $\psi$  has the uniform distribution,

$$f_{\psi}(\psi) = \begin{cases} \frac{1}{2\pi}, & |\psi| \leq \pi \\ 0, & \text{elsewhere} \end{cases} \quad (\text{B-66})$$

then the PDF for the sinusoid is given by

$$f_x(x) = \begin{cases} 0, & x < -A \\ \frac{1}{\pi \sqrt{A^2 - x^2}}, & |x| \leq A \\ 0, & x > A \end{cases} \quad (\text{B-67})$$

A proof of this theorem will be given in Sec. B-8.

A sketch of the PDF for a sinusoid is given in Table B-1, along with equations for the CDF and the variance. Note that the standard deviation, which is equivalent to the rms value as discussed in Chapter 6, is  $\sigma = A/\sqrt{2}$ . This should not be a surprising result.

The sinusoidal distribution can be used to model observed phenomena. For example,  $x$  might represent an oscillator voltage where  $\psi = \omega_0 t + \theta_0$ . Here the frequency of oscillation is  $f_0$ , and  $\omega_0$  and  $t$  are assumed to be deterministic values.  $\theta_0$  represents the random start-up phase of the oscillator. (When the power of an unsynchronized oscillator is turned on, the oscillation builds up from a noise voltage that is present in the circuit.) In another oscillator model, time might be considered to be a uniformly distributed random variable where  $\psi = \omega_0 t$ . Here, once again, we would have a sinusoidal distribution for  $x$ .

## B-8 FUNCTIONAL TRANSFORMATIONS OF RANDOM VARIABLES

As illustrated by the preceding sinusoidal distribution, we often need to evaluate the PDF for a random variable that is a function of another random variable for which the distribution is known. This is illustrated pictorially in Fig. B-8. Here the input random variable is denoted by  $x$ , and the output random variable is denoted by  $y$ . Because several PDFs are involved, subscripts (such as  $x$  in  $f_x$ ) will be used to indicate with which random variable the PDF is associated. The arguments of the PDFs may change, depending on what substitutions are made, as equations are reduced.

**THEOREM.** If  $y = h(x)$ , where  $h(\cdot)$  is the output-to-input (transfer) characteristic of a device without memory,<sup>†</sup> then the PDF of the output is

$$f_y(y) = \sum_{i=1}^M \frac{f_x(x)}{|dy/dx|} \Big|_{x=x_i=h^{-1}(y)} \quad (\text{B-68})$$

where  $f_x(x)$  is the PDF of the input,  $x$ .  $M$  is the number of real roots of  $y = h(x)$ . That is, the inverse of  $y = h(x)$  gives  $x_1, x_2, \dots, x_M$  for a single value of  $y$ .  $|\cdot|$  denotes the absolute value and the single vertical line denotes the evaluation of the quantity at  $x = x_i = h^{-1}(y)$ .

Two examples will now be worked out to demonstrate the application of this theorem, and then the proof will be given.

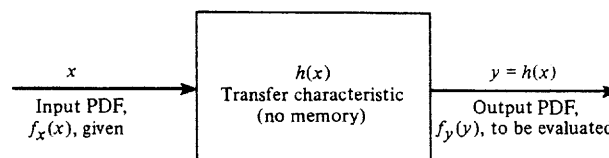


Figure B-8 Functional transformation of random variables.

<sup>†</sup> The output-to-input characteristic  $h(x)$  should not be confused with the impulse response of a linear network, which was denoted by  $h(t)$ .

### Example B-5 SINUSOIDAL DISTRIBUTION

Let

$$y = h(x) = A \sin x \quad (\text{B-69})$$

where  $x$  is uniformly distributed over  $-\pi$  to  $+\pi$ , as given by (B-66). This is illustrated in Fig. B-9. For a given value of  $y$ , say  $-A < y_0 < A$ , there are two possible inverse values for  $x$ , namely,  $x_1$  and  $x_2$ , as shown in the figure. Thus  $M = 2$ , provided that  $|y| < A$ . Otherwise,  $M = 0$ . Evaluating the derivative of (B-69), we obtain

$$\frac{dy}{dx} = A \cos x$$

and for  $0 \leq y \leq A$ ,

$$x_1 = \text{Sin}^{-1} \left( \frac{y}{A} \right)$$

and

$$x_2 = \pi - x_1$$

where the uppercase S in  $\text{Sin}^{-1}(\cdot)$  denotes the principal angle. A similar result is obtained for  $-A \leq y \leq 0$ . Using (B-68), we find that the PDF for  $y$  is

$$f_y(y) = \begin{cases} \frac{f_x(x_1)}{|A \cos x_1|} + \frac{f_x(x_2)}{|-A \cos x_2|}, & |y| \leq A \\ 0, & \text{y elsewhere} \end{cases} \quad (\text{B-70})$$

The denominators of these two terms are evaluated with the aid of the triangles shown in the insert of Fig. B-9. By using this result and substituting the uniform PDF for  $f_x(x)$ , (B-70) becomes

$$f_y(y) = \begin{cases} \frac{1/2\pi}{|\sqrt{A^2 - y^2}|} + \frac{1/2\pi}{|-\sqrt{A^2 - y^2}|}, & |y| \leq A \\ 0, & \text{y elsewhere} \end{cases}$$

or

$$f_y(y) = \begin{cases} 0, & y < -A \\ \frac{1}{\pi \sqrt{A^2 - y^2}}, & |y| \leq A \\ 0, & y > A \end{cases} \quad (\text{B-71})$$

which is the PDF for a sinusoid as given first by (B-67). This result is intuitively obvious since we realize that a sinusoidal waveform spends most of its time near its peak values and passes through zero relatively rapidly. Thus the PDF should peak up at  $+A$  and  $-A$  V.

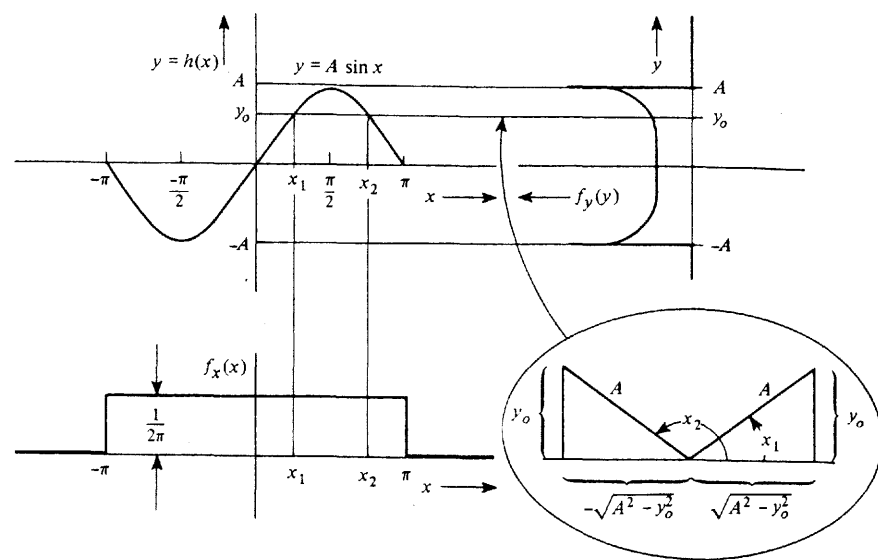


Figure B-9 Evaluation of the PDF of a sinusoid (Example B-5).

**Example B-6 PDF FOR THE OUTPUT OF A DIODE CHARACTERISTIC**

Assume that a diode current-voltage characteristic is modeled by the ideal characteristic shown in Fig. B-10, where  $y$  is the current through the diode and  $x$  is the voltage across the diode. This type of characteristic is also called *half-wave linear rectification*.

$$y = \begin{cases} Bx, & x > 0 \\ 0, & x \leq 0 \end{cases} \quad (\text{B-72})$$

where  $B > 0$ . For  $y > 0$ ,  $M = 1$ ; and for  $y < 0$ ,  $M = 0$ . However, if  $y = 0$ , there are an infinite number of roots for  $x$  (i.e., all  $x \leq 0$ ). Consequently, there will be a discrete point at  $y = 0$  if the area under  $f_x(x)$  is nonzero for  $x \leq 0$  (i.e., for the values of  $x$  that are mapped into  $y = 0$ ). Using (B-68), we get

$$f_y(y) = \begin{cases} \frac{f_x(y/B)}{B}, & y > 0 \\ 0, & y \leq 0 \end{cases} + P(y = 0) \delta(y) \quad (\text{B-73})$$

where

$$P(y = 0) = P(x \leq 0) = \int_{-\infty}^0 f_x(x) dx = F_x(0) \quad (\text{B-74})$$

Suppose that  $x$  has a Gaussian distribution with zero mean; then these equations reduce to

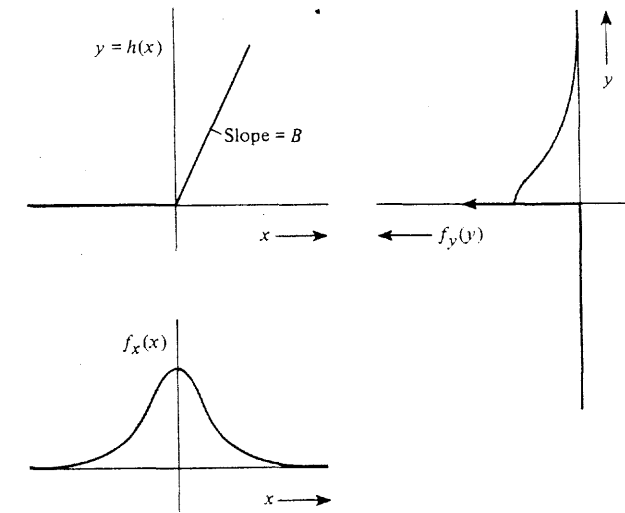


Figure B-10 Evaluation of the PDF out of a diode characteristic for Example B-6.

$$f_y(y) = \begin{cases} \frac{1}{\sqrt{2\pi} B\sigma} e^{-y^2/(2B^2\sigma^2)}, & y > 0 \\ 0, & y \leq 0 \end{cases} + \frac{1}{2} \delta(y) \quad (\text{B-75})$$

A sketch of this result is shown in Fig. B-10. For  $B = 1$ , note that the output is the same as the input for  $x$  positive (i.e.,  $y = x > 0$ ), so that the PDF of the output is the same as the PDF of the input for  $y > 0$ . For  $x < 0$ , the values of  $x$  are mapped into the point  $y = 0$ , so that the PDF of  $y$  contains a  $\delta$  function of weight  $\frac{1}{2}$  at the point  $y = 0$ .

*Proof.* We will demonstrate that (B-68) is valid by partitioning the  $x$  axis into intervals over which  $h(x)$  is monotonically increasing, monotonically decreasing, or a constant. As we have seen in Example B-6, when  $h(x)$  is a constant over some interval of  $x$ , a discrete point at  $y$  equal to that constant is possible. In addition, discrete points in the distribution of  $x$  will be mapped into discrete points in  $y$  even in regions where  $h(x)$  is not a constant.

Now we will demonstrate that the theorem, as described by (B-68), is correct by taking the case, for example, where  $y = h(x)$  is monotonically decreasing for  $x < x_0$  and monotonically increasing for  $x > x_0$ . This is illustrated in Fig. B-11. The CDF for  $y$  is then

$$\begin{aligned} F_y(y_0) &= P(y \leq y_0) = P(x_1 \leq x \leq x_2) \\ &= P[(x = x_1) + (x_1 < x \leq x_2)] \end{aligned} \quad (\text{B-76})$$

where the  $+$  sign denotes the union operation. Then using (B-4), we get

$$F_y(y_0) = P(x_1) + P(x_1 < x \leq x_2)$$

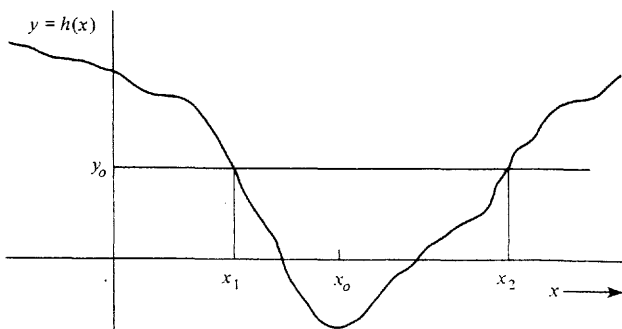


**Figure B-11** Example of a function  $h(x)$  that monotonically decreases for  $x < x_0$  and monotonically increases for  $x > x_0$ .

or

$$F_y(y_0) = P(x_1) + F_x(x_2) - F_x(x_1) \quad (\text{B-77})$$

The PDF of  $y$  is obtained by taking the derivative of both sides of this equation.

$$\frac{dF_y(y_0)}{dy_0} = \frac{dF_x(x_2)}{dx_2} \frac{dx_2}{dy_0} - \frac{dF_x(x_1)}{dx_1} \frac{dx_1}{dy_0} \quad (\text{B-78})$$

where  $dP(x_1)/dy_0 = 0$  was used since  $P(x_1)$  is a constant. Because

$$\frac{dF_x(x_2)}{dx_2} = f_x(x_2) \quad \text{and} \quad \frac{dF_x(x_1)}{dx_1} = f_x(x_1)$$

(B-78) becomes

$$f_y(y_0) = \frac{f_x(x_2)}{\frac{dx_2}{dy_0}} + \frac{f_x(x_1)}{-\frac{dx_1}{dy_0}} \quad (\text{B-79})$$

At the point  $x = x_1$ , the slope of  $y$  is negative because the function is monotonically decreasing for  $x < x_0$ ; thus  $\frac{dx_1}{dy_0} < 0$  and (B-79) becomes

$$f_y(y_0) = \sum_{i=1}^{M=2} \left. \frac{f_x(x)}{\frac{dx_i}{dy_0}} \right|_{x=x_i=h_i^{-1}(y_0)} \quad (\text{B-80})$$

When there are more than two intervals during which  $h(x)$  is monotonically increasing or decreasing, this procedure may be extended so that (B-68) is obtained.

In concluding this discussion on the functional transformation of a random variable, it should be emphasized that the description of the mapping function  $y = h(x)$  assumes that the output  $y$ , at any instant, depends on the value of the input  $x$  only at that same instant and not on previous (or future) values of  $x$ . Thus this technique is applicable to devices that contain no memory (i.e., no inductance or capacitance) elements; however, the device may be nonlinear, as we have seen in the preceding examples.

## B-9 MULTIVARIATE STATISTICS

In Sec. B-3 the probabilities of simple events, joint probabilities, and conditional probabilities were defined. In Secs. B-4 and B-5, using the probability of simple events, we developed the concepts of PDFs and CDFs. The PDFs and CDFs involved only one random variable, so these are one-dimensional problems. Similarly, the moments involved only one-dimensional integration.

In this section multiple-dimensional problems, also called *multivariate statistics*, will be developed. These involve PDFs and CDFs that are associated with probabilities of intersecting events and with conditional probabilities. In addition, multiple-dimensional moments will be obtained as an extension of one-dimensional moments that were studied in Sec. B-6. If the reader clearly understands the one-dimensional case (developed in the preceding sections), there will be little difficulty in generalizing those results to the  $N$ -dimensional case.

### Multivariate CDFs and PDFs

**DEFINITION.** The  $N$ -dimensional CDF is

$$F(a_1, a_2, \dots, a_N) = P[(x_1 \leq a_1)(x_2 \leq a_2) \cdots (x_N \leq a_N)] \\ = \lim_{n \rightarrow \infty} \left[ \frac{n_{(x_1 \leq a_1)(x_2 \leq a_2) \cdots (x_N \leq a_N)}}{n} \right] \quad (\text{B-81})$$

where the notation  $(x_1 \leq a_1)(x_2 \leq a_2) \cdots (x_N \leq a_N)$  is the intersection event consisting of the intersection of the events associated with  $x_1 \leq a_1$ ,  $x_2 \leq a_2$ , and so on.

**DEFINITION.** The  $N$ -dimensional PDF is

$$f(x_1, x_2, \dots, x_N) = \left. \frac{\partial^N F(a_1, a_2, \dots, a_N)}{\partial a_1 \partial a_2 \cdots \partial a_N} \right|_{\mathbf{a}=\mathbf{x}} \quad (\text{B-82})$$

where  $\mathbf{a}$  and  $\mathbf{x}$  are the row vectors;  $\mathbf{a} = (a_1, a_2, \dots, a_N)$  and  $\mathbf{x} = f(x_1, x_2, \dots, x_N)$ .

**DEFINITION.** The expected value of  $y = h(\mathbf{x})$  is

$$\begin{aligned} [y] &= \bar{h}(x_1, x_2, \dots, x_N) \\ &= \int_{-\infty}^{\infty} \int_{-\infty}^{\infty} \cdots \int_{-\infty}^{\infty} h(x_1, x_2, \dots, x_N) \\ &\quad \times f(x_1, x_2, \dots, x_N) dx_1 dx_2 \cdots dx_N \end{aligned} \quad (\text{B-83})$$

Some properties of  $N$ -dimensional random variables are

$$1. f(x_1, x_2, \dots, x_N) \geq 0 \quad (\text{B-84a})$$

$$2. \int_{-\infty}^{\infty} \int_{-\infty}^{\infty} \cdots \int_{-\infty}^{\infty} f(x_1, x_2, \dots, x_N) dx_1 dx_2 \cdots dx_N = 1 \quad (\text{B-84b})$$

$$3. F(a_1, a_2, \dots, a_N)$$

$$= \lim_{\epsilon \rightarrow 0} \int_{-\infty}^{a_1 + \epsilon} \int_{-\infty}^{a_2 + \epsilon} \cdots \int_{-\infty}^{a_N + \epsilon} f(x_1, x_2, \dots, x_N) dx_1 dx_2 \cdots dx_N \quad (\text{B-84c})$$

4.  $F(a_1, a_2, \dots, a_N) \equiv 0$  if any  $a_i = -\infty$ ,  $i = 1, 2, \dots, N$  (B-84d)
5.  $F(a_1, a_2, \dots, a_N) = 1$  when all  $a_i = +\infty$ ,  $i = 1, 2, \dots, N$  (B-84e)
6.  $P[(a_1 < x_1 \leq b_1)(a_2 < x_2 \leq b_2) \cdots (a_N < x_N \leq b_N)]$
- $$= \lim_{\epsilon \rightarrow 0} \int_{a_1 + \epsilon}^{b_1 + \epsilon} \int_{a_2 + \epsilon}^{b_2 + \epsilon} \cdots \int_{a_N + \epsilon}^{b_N + \epsilon} f(x_1, x_2, \dots, x_N) dx_1 dx_2 \cdots dx_N \quad (\text{B-84f})$$

The definitions and properties for multivariate PDFs and CDFs are based on the concepts of joint probabilities, as discussed in Sec. B-3. In a similar way, conditional PDFs and CDFs can be obtained [Papoulis, 1984]. Using the property  $P(AB) = P(A)P(B|A)$  of (B-8), we find that the joint PDF of  $x_1$  and  $x_2$  is

$$f(x_1, x_2) = f(x_1)f(x_2|x_1) \quad (\text{B-85})$$

where  $f(x_2|x_1)$  is the conditional PDF of  $x_2$  given  $x_1$ . Generalizing further, we obtain

$$f(x_1, x_2, x_3) = f(x_1|x_3)f(x_2|x_1, x_3) \quad (\text{B-86})$$

Many other expressions for relationships between multiple-dimensional PDFs should also be apparent. When  $x_1$  and  $x_2$  are *independent*,  $f(x_2|x_1) = f_{x_2}(x_2)$  and

$$f(x_1, x_2) = f_{x_1}(x_1)f_{x_2}(x_2) \quad (\text{B-87})$$

where the subscript  $x_1$  denotes the PDF associated with  $x_1$ , and the subscript  $x_2$  denotes the PDF associated with  $x_2$ . For  $N$  independent random variables this becomes

$$f(x_1, x_2, \dots, x_N) = f_{x_1}(x_1)f_{x_2}(x_2) \cdots f_{x_N}(x_N) \quad (\text{B-88})$$

**THEOREM.** If the  $N$ -dimensional PDF of  $\mathbf{x}$  is known, then the  $L$ -dimensional PDF of  $\mathbf{x}$  can be obtained when  $L < N$  by

$$\begin{aligned} & f(x_1, x_2, \dots, x_L) \\ &= \underbrace{\int_{-\infty}^{\infty} \int_{-\infty}^{\infty} \cdots \int_{-\infty}^{\infty}}_{N-L \text{ integrals}} f(x_1, x_2, \dots, x_N) dx_{L+1} dx_{L+2} \cdots dx_N \quad (\text{B-89}) \end{aligned}$$

This  $L$ -dimensional PDF, where  $L < N$ , is sometimes called the **marginal PDF** since it is obtained from a higher-dimensional ( $N$ th) PDF.

**Proof.** First, show that this result is correct if  $N = 2$  and  $L = 1$ .

$$\begin{aligned} \int_{-\infty}^{\infty} f(x_1, x_2) dx_2 &= \int_{-\infty}^{\infty} f(x_1)f(x_2|x_1) dx_2 \\ &= f(x_1) \int_{-\infty}^{\infty} f(x_2|x_1) dx_2 = f(x_1) \quad (\text{B-90}) \end{aligned}$$

since the area under  $f(x_2|x_1)$  is unity. This procedure is readily extended to prove the  $L$ -dimensional case of (B-89).

### Bivariate Statistics

Bivariate (or joint) distributions are the  $N = 2$  dimensional case. In this section the definitions from the previous section will be used to evaluate two-dimensional moments. As shown in Chapter 6, bivariate statistics have some very important applications to electrical engineering problems, and some additional definitions need to be studied.

**DEFINITION.** The *correlation* (or *joint mean*) of  $x_1$  and  $x_2$  is

$$m_{12} = \overline{x_1 x_2} = \int_{-\infty}^{\infty} \int_{-\infty}^{\infty} x_1 x_2 f(x_1, x_2) dx_1 dx_2 \quad (\text{B-91})$$

**DEFINITION.** Two random variables  $x_1$  and  $x_2$  are said to be *uncorrelated* if

$$m_{12} = \overline{x_1 x_2} = \overline{x_1} \overline{x_2} = m_1 m_2 \quad (\text{B-92})$$

If  $x_1$  and  $x_2$  are independent, it follows that they are also uncorrelated, but the converse is not generally true. However, as we will see, the converse is true for bivariate Gaussian random variables.

**DEFINITION.** Two random variables are said to be *orthogonal* if

$$m_{12} = \overline{x_1 x_2} \equiv 0 \quad (\text{B-93})$$

Note the similarity of the definition of orthogonal random variables to that of orthogonal functions given by (2-73).

**DEFINITION.** The *covariance* is

$$\begin{aligned} u_{11} &= \overline{(x_1 - m_1)(x_2 - m_2)} \\ &= \int_{-\infty}^{\infty} \int_{-\infty}^{\infty} (x_1 - m_1)(x_2 - m_2) f(x_1, x_2) dx_1 dx_2 \quad (\text{B-94}) \end{aligned}$$

It should be clear that if  $x_1$  and  $x_2$  are independent, the covariance is zero (and  $x_1$  and  $x_2$  are uncorrelated). The converse is not generally true, but it is true for the case of bivariate Gaussian random variables.

**DEFINITION.** The *correlation coefficient* is

$$\rho = \frac{u_{11}}{\sigma_1 \sigma_2} = \frac{\overline{(x_1 - m_1)(x_2 - m_2)}}{\sqrt{\overline{(x_1 - m_1)^2}} \sqrt{\overline{(x_2 - m_2)^2}}} \quad (\text{B-95})$$

This is also called the *normalized covariance*. The correlation coefficient is always within the range

$$-1 \leq \rho \leq +1 \quad (\text{B-96})$$

For example, suppose that  $x_1 = x_2$ ; then  $\rho = +1$ . If  $x_1 = -x_2$ , then  $\rho = -1$ ; and if  $x_1$  and  $x_2$  are independent,  $\rho = 0$ . Thus the correlation coefficient tells us, on the average, how likely a value of  $x_1$  is to be proportional to the value for  $x_2$ . This subject is discussed in more detail in Chapter 6, where these results are extended to include random processes (time functions). There the dependence of the value of a waveform at one time is compared to the value of the waveform that occurs at another time. This will bring the concept of frequency response into the problem.

### Gaussian Bivariate Distribution

A good example of a joint ( $N = 2$ ) distribution that is of great importance is the bivariate Gaussian distribution. The bivariate Gaussian PDF is

$$f(x_1, x_2) = \frac{1}{2\pi\sigma_1\sigma_2\sqrt{1-\rho^2}} e^{-\frac{1}{2(1-\rho^2)} \left[ \frac{(x_1 - m_1)^2}{\sigma_1^2} - 2\rho \frac{(x_1 - m_1)(x_2 - m_2)}{\sigma_1\sigma_2} + \frac{(x_2 - m_2)^2}{\sigma_2^2} \right]} \quad (\text{B-97})$$

where  $\sigma_1^2$  is the variance of  $x_1$ ,  $\sigma_2^2$  is the variance of  $x_2$ ,  $m_1$  is the mean of  $x_1$ , and  $m_2$  is the mean of  $x_2$ . Examining (B-97), we see that if  $\rho = 0$ ,  $f(x_1, x_2) = f(x_1)f(x_2)$ , where  $f(x_1)$  and  $f(x_2)$  are the one-dimensional PDFs of  $x_1$  and  $x_2$ . Thus if bivariate Gaussian random variables are uncorrelated (which implies that  $\rho = 0$ ), they are independent.

A sketch of the bivariate (two-dimensional) Gaussian PDF is shown in Fig. B-12.

### Multivariate Functional Transformation

Section B-8 will now be generalized for the multivariate case. Referring to Fig. B-13, we will obtain the PDF for  $\mathbf{y}$ , denoted by  $f_y(\mathbf{y})$  in terms of the PDF for  $\mathbf{x}$ , denoted by  $f_x(\mathbf{x})$ .

**THEOREM.** Let  $\mathbf{y} = \mathbf{h}(\mathbf{x})$  denote the transfer characteristic of a device (no memory) that has  $N$  inputs, denoted by  $\mathbf{x} = (x_1, x_2, \dots, x_N)$ ;  $N$  outputs, denoted by  $\mathbf{y} = (y_1, y_2, \dots, y_N)$ ; and  $y_i = h_i(\mathbf{x})$ . That is,

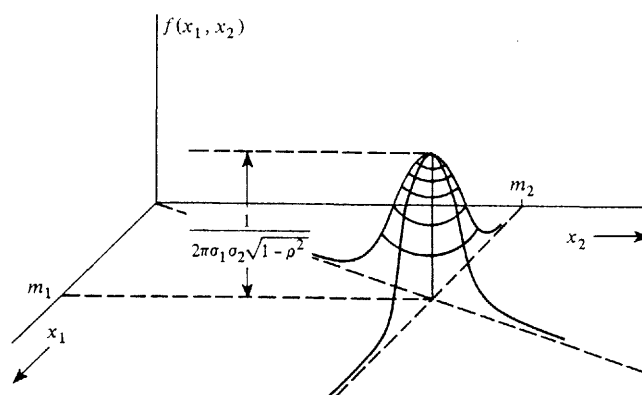


Figure B-12 Bivariate Gaussian PDF.

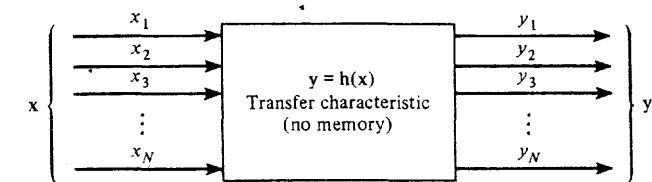


Figure B-13 Multivariate functional transformation of random variables.

$$\begin{aligned} y_1 &= h_1(x_1, x_2, \dots, x_N) \\ y_2 &= h_2(x_1, x_2, \dots, x_N) \\ &\vdots \\ y_N &= h_N(x_1, x_2, \dots, x_N) \end{aligned} \quad (\text{B-98})$$

Furthermore, let  $\mathbf{x}_i$ ,  $i = 1, 2, \dots, M$ , denote the real roots (vectors) of the equation  $\mathbf{y} = \mathbf{h}(\mathbf{x})$ . The PDF of the output is then

$$f_y(\mathbf{y}) = \sum_{i=1}^M \frac{f_x(\mathbf{x})}{|J(\mathbf{y}/\mathbf{x})|} \Big|_{\mathbf{x}=\mathbf{x}_i = \mathbf{h}_i^{-1}(\mathbf{y})} \quad (\text{B-99})$$

where  $|\cdot|$  denotes the absolute value operation and  $J(\mathbf{y}/\mathbf{x})$  is the Jacobian of the coordinate transformation to  $\mathbf{y}$  from  $\mathbf{x}$ . The Jacobian is

$$J\left(\frac{\mathbf{y}}{\mathbf{x}}\right) = \text{Det} \begin{bmatrix} \frac{\partial h_1(\mathbf{x})}{\partial x_1} & \frac{\partial h_1(\mathbf{x})}{\partial x_2} & \dots & \frac{\partial h_1(\mathbf{x})}{\partial x_N} \\ \frac{\partial h_2(\mathbf{x})}{\partial x_1} & \frac{\partial h_2(\mathbf{x})}{\partial x_2} & \dots & \frac{\partial h_2(\mathbf{x})}{\partial x_N} \\ \vdots & \vdots & \ddots & \vdots \\ \frac{\partial h_N(\mathbf{x})}{\partial x_1} & \frac{\partial h_N(\mathbf{x})}{\partial x_2} & \dots & \frac{\partial h_N(\mathbf{x})}{\partial x_N} \end{bmatrix} \quad (\text{B-100})$$

where  $\text{Det}[\cdot]$  denotes the determinant of the matrix  $[\cdot]$ .

A proof of this theorem will not be given, but it should be clear that it is a generalization of the theorem for the one-dimensional case that was studied in Sec. B-8. The coordinate transformation relates differentials in one coordinate system to those in another [Thomas, 1969]:

$$dy_1 dy_2 \cdots dy_N = J\left(\frac{\mathbf{y}}{\mathbf{x}}\right) dx_1 dx_2 \cdots dx_N \quad (\text{B-101})$$

### Example B-7 PDF FOR THE SUM OF TWO RANDOM VARIABLES

Suppose that we have a circuit configuration (such as an operational amplifier) that sums two inputs,  $x_1$  and  $x_2$ , to produce the output

$$y = A(x_1 + x_2) \quad (B-102)$$

where  $A$  is the gain of the circuit. Assume that  $f(x_1, x_2)$  is known and that we wish to obtain a formula for the PDF of the output in terms of the joint PDF for the inputs.

We can use theorem (B-99) to solve this problem. However, for two inputs we need two outputs in order to satisfy the assumptions of the theorem. This is achieved by defining an auxiliary variable for the output (say,  $y_2$ ). Thus

$$y_1 = h_1(\mathbf{x}) = A(x_1 + x_2) \quad (B-103)$$

$$y_2 = h_2(\mathbf{x}) = Ax_1 \quad (B-104)$$

The choice of the equation to use for the auxiliary variable, (B-104), is immaterial, provided that it is an independent equation so that the determinant,  $J(y/x)$ , is not zero. However, the equation is usually selected so that the ensuing mathematics will be relatively simple. Using (B-103) and (B-104), we get

$$J = \text{Det} \begin{bmatrix} A & A \\ A & 0 \end{bmatrix} = -A^2 \quad (B-105)$$

Substituting this into (B-99) yields

$$f_y(y_1, y_2) = \frac{f_x(x_1, x_2)}{|-A^2|} \Big|_{\mathbf{x}=h^{-1}(y)}$$

or

$$f_y(y_1, y_2) = \frac{1}{A^2} f_x \left( \frac{y_2}{A}, \frac{1}{A}(y_1 - y_2) \right) \quad (B-106)$$

We want to find a formula for  $f_{y_1}(y_1)$  since  $y_1 = A(x_1 + x_2)$ . This is obtained by evaluating the marginal PDF from (B-106).

$$f_{y_1}(y_1) = \int_{-\infty}^{\infty} f_y(y_1, y_2) dy_2$$

or

$$f_{y_1}(y_1) = \frac{1}{A^2} \int_{-\infty}^{\infty} f_x \left( \frac{y_2}{A}, \frac{1}{A}(y_1 - y_2) \right) dy_2 \quad (B-107)$$

This general result relates the PDF of  $y = y_1$  to the joint PDF of  $\mathbf{x}$  where  $y = A(x_1 + x_2)$ . If  $x_1$  and  $x_2$  are independent and  $A = 1$ , (B-107) becomes

$$f(y) = \int_{-\infty}^{\infty} f_{x_1}(\lambda) f_{x_2}(y - \lambda) d\lambda$$

or

$$f(y) = f_{x_1}(y) * f_{x_2}(y) \quad (B-108)$$

where  $*$  denotes the convolution operation. Similarly, if we sum  $N$  independent random variables, the PDF for the sum is the  $(N - 1)$ -fold convolution of the one-dimensional PDFs for the  $N$  random variables.

### Central Limit Theorem

If we have the sum of a number of independent random variables with arbitrary one-dimensional PDFs, the *central limit theorem* states that the PDF for the sum of these independent random variables approaches a Gaussian (normal) distribution under very general conditions. Strictly speaking, the central limit theorem does not hold for the PDF if the independent random variables are discretely distributed. In this case the PDF for the sum will consist of delta functions (not Gaussian, which is continuous); however, if the delta functions are "smeared out" (e.g., replace the delta functions with rectangles that have corresponding areas), the resulting PDF will be approximately Gaussian. Regardless, the CDF for the sum will approach that of a Gaussian CDF.

#### Example B-8 PDF FOR THE SUM OF THREE INDEPENDENT, UNIFORMLY DISTRIBUTED RANDOM VARIABLES

The central limit theorem will be illustrated by evaluating the exact PDF for the sum of three independent uniformly distributed random variables. This exact result will be compared with the Gaussian PDF, as predicted by the central limit theorem.

Let each of the independent random variables  $x_i$  have a uniform distribution, as shown in Fig. B-14a. The PDF for  $y_1 = x_1 + x_2$ , denoted by  $f(y_1)$ , is obtained by the convolution operation described by (B-108) and Fig. 2-7. This result is shown in Fig. B-14b. It is seen that after only one convolution operation the PDF for the sum (which is a triangle) is going toward the Gaussian shape. The PDF for  $y_2 = x_1 + x_2 + x_3, f(y_2)$ , is obtained by convolving the triangular PDF with another uniform PDF. The result is

$$f(y_2) = \begin{cases} 0, & y_2 \leq -\frac{3}{2}A \\ \frac{1}{2A^3} \left( \frac{3}{2}A + y_2 \right)^2, & -\frac{3}{2}A \leq y_2 \leq -\frac{1}{2}A \\ \frac{1}{2A^3} \left( \frac{3}{2}A^2 - 2y_2^2 \right), & |y_2| \leq \frac{1}{2}A \\ \frac{1}{2A^3} \left( \frac{3}{2}A - y_2 \right)^2, & \frac{1}{2}A \leq y_2 \leq \frac{3}{2}A \\ 0, & y_2 \geq \frac{3}{2}A \end{cases} \quad (B-109)$$

This curve is plotted by the solid line in Fig. B-14c. For comparison purposes, a matching Gaussian curve, with  $1/(\sqrt{2\pi}\sigma) = 3/(4A)$ , is also shown by the dashed line. It is seen that  $f(y_2)$  is very close to the Gaussian curve for  $|y_2| < \frac{3}{2}A$ , as predicted by the central limit theorem. Of course,  $f(y_2)$  is certainly not Gaussian for  $|y_2| > \frac{3}{2}A$  because  $f(y_2) = 0$  in this region, whereas the Gaussian curve is not zero except at  $y = \pm\infty$ . Thus we observe that the Gaussian approximation (as predicted by the central limit theorem) is not very good on the tails of the distribution. In Chapter 7 it is shown that the probability of bit error for digital systems is obtained by evaluating the area under the tails of a distribution. If the distribution is not known to be Gaussian, and the central limit theorem is used to approximate the distribution by a Gaussian PDF, the results are often not very accurate, as shown by this example. However, if the area

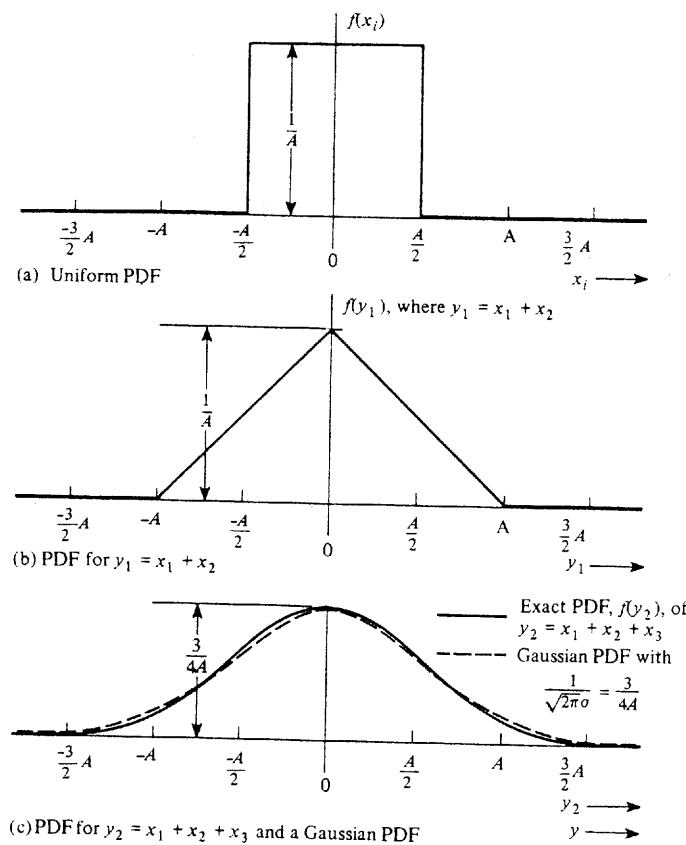


Figure B-14 Demonstration of the central limit theorem (Example B-8).

under the distribution is needed near the mean value, the Gaussian approximation may be very good.

## PROBLEMS

B-1 A long binary message contains 1428 binary 1's and 2668 binary 0's. What is the probability of obtaining a binary 1 in any received bit?

B-2 (a) Find the probability of getting an 8 in the toss of two dice.

(b) Find the probability of getting either a 5, 7, or 8 in the toss of two dice.

B-3 Show that

$$\begin{aligned} P(A + B + C) &= P(A) + P(B) + P(C) \\ &\quad - P(AB) - P(AC) - P(BC) + P(ABC) \end{aligned}$$

B-4 A die is tossed. The probability of getting any face is  $P(x) = \frac{1}{6}$ , where  $x = k = 1, 2, 3, 4, 5$ , or 6.

- (a) Find the probability of getting an odd-numbered face.  
(b) Find the probability of getting a 4 when an even-numbered face is obtained on a toss.

B-5 Which of the following functions satisfy the properties for a PDF. Why?

(a)  $f(x) = \frac{1}{\pi} \left( \frac{1}{1+x^2} \right)$

(b)  $f(x) = \begin{cases} |x|, & |x| < 1 \\ 0, & x \text{ otherwise} \end{cases}$

(c)  $f(x) = \begin{cases} \frac{1}{6}(8-x), & 4 \leq x \leq 10 \\ 0, & x \text{ otherwise} \end{cases}$

(d)  $f(x) = \sum_{k=0}^{\infty} \frac{3}{4} \left(\frac{1}{4}\right)^k \delta(x-k)$

B-6 Show that all cumulative distribution functions must satisfy the properties given in Sec. B-5.

B-7 Let  $f(x) = Ke^{-b|x|}$ , where  $K$  and  $b$  are positive constants. Find the mathematical expression for the CDF and sketch the results.

B-8 Find the probability that  $-\frac{1}{4}A \leq y_1 \leq \frac{1}{4}A$  for the triangular distribution shown in Fig. B-14b.

B-9 A triangular PDF is shown in Fig. B-14b.

(a) Find a mathematical expression that describes the CDF.

(b) Sketch the CDF.

B-10 Evaluate the PDFs for the two waveforms shown in Fig. PB-10.

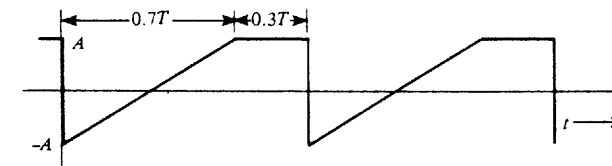
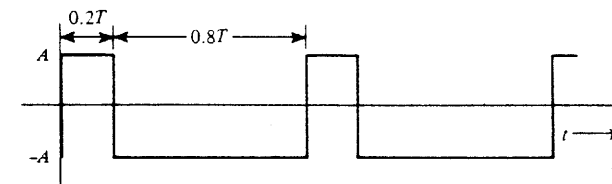


Figure PB-10

B-11 Let a PDF be given by  $f(x) = Ke^{-bx}$  for  $x \geq 0$  and zero for  $x$  negative where  $K$  and  $b$  are positive constants.

(a) Find the value required for  $K$  in terms of  $b$ .

(b) Find  $m$  in terms of  $b$ .

(c) Find  $\sigma^2$  in terms of  $b$ .



**B-12** A random variable  $x$  has a PDF

$$f(x) = \begin{cases} \frac{3}{32}(-x^2 + 8x - 12), & 2 \leq x \leq 6 \\ 0, & \text{elsewhere} \end{cases}$$

- (a) Demonstrate that  $f(x)$  is a valid PDF.
- (b) Find the mean.
- (c) Find the second moment.
- (d) Find the variance.

**B-13** Determine the standard deviation for the triangular distribution shown in Fig. B-14b.

**B-14** (a) Find the terms in a binomial distribution for  $n = 7$ , where  $p = 0.5$ .  
 (b) Sketch the PDF for this binomial distribution.  
 (c) Find and sketch the CDF for this distribution.  
 (d) Find  $x^3$  for this distribution.

**B-15** For a binomial distribution, show that  $\sigma^2 = np(1-p)$ .

**B-16** A binomial random variable  $x_k$  has values of  $k$  where

$$k = 0, 1, \dots, n; \quad P(k) = \binom{n}{k} p^k q^{n-k}; \quad q = 1 - p$$

Assume that  $n = 160$  and  $p = 0.1$ .

- (a) Plot  $P(k)$ .
- (b) Compare the plot of part (a) with a plot  $P(k)$  using the Gaussian approximation

$$\binom{n}{k} p^k q^{n-k} \approx \frac{1}{\sqrt{2\pi}\sigma} e^{-(k-m)^2/2\sigma^2}$$

which is valid when  $npq \gg 1$  and  $|k - np|$  is in the neighborhood of  $\sqrt{npq}$  where  $\sigma = \sqrt{npq}$  and  $m = np$ .

- (c) Also plot the Poisson approximation

$$\binom{n}{k} p^k q^{n-k} \approx \frac{\lambda^k}{k!} e^{-\lambda}$$

where  $\lambda = np$ ,  $n$  is large, and  $p$  is small.

**B-17** An order of  $n = 3000$  transistors is received. The probability that each transistor is defective is  $p = 0.001$ . What is the probability that the number of defective transistors in the batch is 6 or less? (Note: The Poisson approximation is valid when  $n$  is large and  $p$  is small.)

**B-18** In a fiber optic communication system, photons are emitted with a Poisson distribution as described in Table B-1.  $m = \lambda$  is the average number of photons emitted in an arbitrary time interval, and  $P(k)$  is the probability of  $k$  photons being emitted in the same interval.

- (a) Plot the PDF for  $\lambda = 0.5$ .
- (b) Plot the CDF for  $\lambda = 0.5$ .
- (c) Show that  $m = \lambda$ .
- (d) Show that  $\sigma = \sqrt{\lambda}$ .

**B-19** Let  $x$  be a random variable that has a Laplacian distribution. The Laplacian PDF is  $f(x) = (1/2b)e^{-|x-m|/b}$ , where  $b$  and  $m$  are real constants and  $b > 0$ .

- (a) Find the mean of  $x$  in terms of  $b$  and  $m$ .
- (b) Find the variance of  $x$  in terms of  $b$  and  $m$ .

**B-20** Given the Gaussian PDF

$$f(x) = \frac{1}{\sqrt{2\pi}\beta} e^{-(x-m)^2/(2\beta^2)}$$

show that the variance of this distribution is  $\beta^2$ .

**B-21** In a manufacturing process for resistors, the values obtained for the resistors have a Gaussian distribution where the desired value is the mean value. If we want 95% of the manufactured  $1\text{-k}\Omega$  resistors to have a tolerance of  $\pm 10\%$ , what is the required value for  $\sigma$ ?

**B-22** Assume that  $x$  has a Gaussian distribution. Find the probability that

- (a)  $|x - m| < \sigma$
- (b)  $|x - m| < 2\sigma$ .
- (c)  $|x - m| < 3\sigma$ .

Obtain numerical results by using MATLAB, MathCAD, or tables if necessary.

**B-23** Show that

- (a)  $Q(z) = \frac{1}{2} \operatorname{erfc}\left(\frac{z}{\sqrt{2}}\right)$ .
- (b)  $Q(-z) = 1 - Q(z)$ .
- (c)  $Q(z) = \frac{1}{2} \left[ 1 - \operatorname{erf}\left(\frac{z}{\sqrt{2}}\right) \right]$ .

**B-24** For a Gaussian distribution, show that

- (a)  $F(a) = \frac{1}{2} \operatorname{erfc}\left(\frac{m-a}{\sqrt{2}\sigma}\right)$ .
- (b)  $F(a) = \frac{1}{2} \left[ 1 + \operatorname{erfc}\left(\frac{a-m}{\sqrt{2}\sigma}\right) \right]$ .

**B-25** A noise voltage has a Gaussian distribution. The rms value is 5 V and the dc value is 1.0 V. Find the probability of the voltage having values between -5 and +5 V.

**B-26** Suppose that  $x$  is a Gaussian random variable with  $m = 5$  and  $\sigma = 0.6$ .

- (a) Find the probability that  $x \leq 1$ .
- (b) Find the probability that  $x \leq 6$ .

**B-27** The Gaussian random variable  $x$  has a zero mean and a variance of 2. Let  $A$  be the event such that  $|x| < 3$ .

- (a) Find an expression for the conditional PDF  $f(x|A)$ .
- (b) Plot  $f(x|A)$  over the range  $|x| < 5$ .
- (c) Plot  $f(x)$  over the range  $|x| < 5$  and compare these two plots.

**B-28** Let  $x$  have a sinusoidal distribution with a PDF as given by (B-67). Show that the CDF is

$$F(a) = \begin{cases} 0, & a \leq -A \\ \frac{1}{\pi} \left[ \frac{\pi}{2} + \sin^{-1}\left(\frac{a}{A}\right) \right], & |a| \leq A \\ 1, & a \geq A \end{cases}$$

**B-29** (a) If  $x$  has a sinusoidal distribution with the peak value of  $x$  being  $A$ , show that the rms value is  $\sigma = A/\sqrt{2}$ . [Hint: Use (B-67).]

- (b) If  $x = A \cos \psi$ , where  $\psi$  is uniformly distributed between  $-\pi$  and  $+\pi$ , show that the rms value of  $x$  is  $\sigma = A/\sqrt{2}$ .
- B-30** Given that  $y = x^2$  and  $x$  is a Gaussian random variable with mean value  $m$  and variance  $\sigma^2$ , find a formula for the PDF of  $y$  in terms of  $m$  and  $\sigma^2$ .
- B-31**  $x$  is a uniformly distributed random variable over the range  $-1 \leq x \leq 1$  plus a discrete point at  $x = \frac{1}{2}$  with  $P(x = \frac{1}{2}) = \frac{1}{4}$ .
- Find a mathematical expression for the PDF for  $x$  and plot your result.
  - Find the PDF for  $y$  where

$$y = \begin{cases} x^2, & x \geq 0 \\ 0, & x < 0 \end{cases}$$

Sketch your result.

- B-32** A saturating amplifier is modeled by

$$y = \begin{cases} Ax_0, & x > x_0 \\ Ax, & |x| \leq x_0 \\ -Ax_0, & x < -x_0 \end{cases}$$

Assume that  $x$  is a Gaussian random variable with mean value  $m$  and variance  $\sigma^2$ . Find a formula for the PDF of  $y$  in terms of  $A$ ,  $x_0$ ,  $m$ , and  $\sigma^2$ .



- B-33** A sinusoid with a peak value of 8 V is applied to the input of a quantizer. The quantizer characteristic is shown in Fig. 3-8a. Calculate and plot the PDF for the output.



- B-34** A voltage waveform that has a Gaussian distribution is applied to the input of a full-wave rectifier circuit. The full-wave rectifier is described by  $y(t) = |x(t)|$  where  $x(t)$  is the input and  $y(t)$  is the output. The input waveform has a dc value of 1 V and an rms value of 2 V.

- Plot the PDF for the input waveform.
- Plot the PDF for the output waveform.

- B-35** Refer to Example B-6 and (B-75), which describe the PDF for the output of an ideal diode (half-wave rectifier) characteristic. Find the mean (dc) value of the output.

- B-36** Given the joint density function,

$$f(x_1, x_2) = \begin{cases} e^{-(1/2)(4x_1 + x_2)}, & x_1 \geq 0, x_2 \geq 0 \\ 0, & \text{otherwise} \end{cases}$$

- Verify that  $f(x_1, x_2)$  is a density function.
- Show that  $x_1$  and  $x_2$  are either independent or dependent.
- Evaluate  $P(1 \leq x_1 \leq 2, x_2 \leq 4)$ .
- Find  $\rho$ .

- B-37** A joint density function is

$$f(x_1, x_2) = \begin{cases} K(x_1 + x_1 x_2), & 0 \leq x_1 \leq 1, 0 \leq x_2 \leq 4 \\ 0, & \text{elsewhere} \end{cases}$$

- Find  $K$ .
- Determine if  $x_1$  and  $x_2$  are independent.
- Find  $F_{x_1, x_2}(0.5, 2)$ .
- Find  $F_{x_2|x_1}(x_2|x_1)$ .

- B-38** Let  $y = x_1 + x_2$  where  $x_1$  and  $x_2$  are uncorrelated random variables. Show that

- (a)  $\bar{y} = m_1 + m_2$ , where  $m_1 = \bar{x}_1$  and  $m_2 = \bar{x}_2$ .

- (b)  $\sigma_y^2 = \sigma_1^2 + \sigma_2^2$ , where  $\sigma_1^2 = (\bar{x}_1 - m_1)^2$  and  $\sigma_2^2 = (\bar{x}_2 - m_2)^2$ .

[Hint: Use the ensemble operator notation similar to that used in the proof for (B-29).]

- B-39** Let  $x_1 = \cos \theta$  and  $x_2 = \sin \theta$ , where  $\theta$  is uniformly distributed over  $(0, 2\pi)$ . Show that
- $x_1$  and  $x_2$  are uncorrelated.
  - $x_1$  and  $x_2$  are not independent.



- B-40** Two random variables  $x_1$  and  $x_2$  are jointly Gaussian. The joint PDF is described by (B-97) where  $m_1 = m_2 = 0$ ,  $\sigma_{x_1} = \sigma_{x_2} = 1$  and  $\rho = 0.5$ . Plot  $f(x_1, x_2)$  for  $|x_1| < 5$  and  $x_2 = 0$ . Also give plots for  $f(x_1, x_2)$  for  $|x_1| < 5$  and  $x_2 = 0.4, 0.8, 1.2$ , and  $1.6$ .

- B-41** Show that the marginal PDF of a bivariate Gaussian PDF is a one-dimensional Gaussian PDF. That is, evaluate

$$f(x_1) = \int_{-\infty}^{\infty} f(x_1, x_2) dx_2$$

where  $f(x_1, x_2)$  is given by (B-97). [Hint: Factor some terms outside the integral containing  $x_1$  (but not  $x_2$ ). Complete the square on the exponent of the remaining integrand so that a Gaussianian PDF form is obtained. Use the property that the integral of a properly normalized Gaussian PDF is unity.]

- B-42** (a)  $y = A_1 x_1 + A_2 x_2$ , where  $A_1$  and  $A_2$  are constants and the joint PDF of  $x_1$  and  $x_2$  is  $f_x(x_1, x_2)$ . Find a formula for the PDF of  $y$  in terms of the (joint) PDF of  $x$ .
- If  $x_1$  and  $x_2$  are independent, how can this formula be simplified?



- B-43** Two independent random variables  $x$  and  $y$  have the PDFs  $f(x) = 5e^{-5x} u(x)$  and  $f(y) = 2e^{-2y} u(y)$ . Plot the PDF for  $w$  where  $w = x + y$ .



- B-44** Two Gaussian random variables  $x_1$  and  $x_2$  have a mean vector  $\mathbf{m}_x$  and a covariance matrix  $\mathbf{C}_x$  as shown. Two new random variables  $y_1$  and  $y_2$  are formed by the linear transformation  $\mathbf{y} = \mathbf{T}\mathbf{x}$ .

$$\mathbf{m}_x = \begin{bmatrix} 2 \\ -1 \end{bmatrix} \quad \mathbf{C}_x = \begin{bmatrix} 5 & -2/\sqrt{5} \\ -2/\sqrt{5} & 4 \end{bmatrix} \quad \mathbf{T} = \begin{bmatrix} 1 & 1/2 \\ 1/2 & 1 \end{bmatrix}$$

- (a) Find the mean vector for  $\mathbf{y}$ , which is denoted by  $\mathbf{m}_y$ .

- (b) Find the covariance matrix for  $\mathbf{y}$ , which is denoted by  $\mathbf{C}_y$ .

- (c) Find the correlation coefficient for  $y_1$  and  $y_2$ . (Hint: See Sec. 6-6.)



- B-45** Three Gaussian random variables  $x_1$ ,  $x_2$ , and  $x_3$  have zero mean values. Three new random variables  $y_1$ ,  $y_2$ , and  $y_3$  are formed by the linear transformation  $\mathbf{y} = \mathbf{T}\mathbf{x}$ , where

$$\mathbf{C}_x = \begin{bmatrix} 6.0 & 2.3 & 1.5 \\ 2.3 & 6.0 & 2.3 \\ 1.5 & 2.3 & 6.0 \end{bmatrix} \quad \mathbf{T} = \begin{bmatrix} 5 & 2 & -1 \\ -1 & 3 & 1 \\ 2 & -1 & 2 \end{bmatrix}$$

- (a) Find the covariance matrix for  $\mathbf{y}$ , which is denoted by  $\mathbf{C}_y$ .

- (b) Write an expression for the PDF  $f(y_1, y_2, y_3)$ . (Hint: See Sec. 6-6.)

- B-46** (a) Find a formula for the PDF of  $y = Ax_1 x_2$  where  $x_1$  and  $x_2$  are random variables having the joint PDF  $f_x(x_1, x_2)$ .
- If  $x_1$  and  $x_2$  are independent, reduce the formula obtained in part (a) to a simpler result.

**B-47**  $y_2 = x_1 + x_2 + x_3$ , where  $x_1$ ,  $x_2$ , and  $x_3$  are independent random variables. Each of the  $x_i$  has a one-dimensional PDF that is uniformly distributed over  $-(A/2) \leq x_i \leq (A/2)$ . Show that the PDF of  $y_2$  is given by (B-109).

**B-48** Use the built-in random number generator of MATLAB or MathCAD to demonstrate the central limit theorem. That is:

- Compute samples of the random variable  $y$  where  $y = \sum x_i$  and the  $x_i$  values are obtained from the random number generator.
- Plot the PDF for  $y$  by using the histogram function of MATLAB or MathCAD.



## APPENDIX C

# STANDARDS AND TERMINOLOGY FOR COMPUTER COMMUNICATIONS

### C-1 CODES

#### Baudot

In 1875, Emile Baudot developed a “multiplex telegraph” system. The Baudot code has evolved into what is now known as the *International Telegraph Alphabet (ITA) Number 2*. This Baudot code is given in Table C-1. The Baudot code is used for teleprinter service. It is used today for wire press and radio teletype press service, although it is being replaced by the ASCII code.

The Baudot code has two serious disadvantages: (1) it has no provisions for parity bits, and (2) it is a *sequential* code. That is, the Letters (down-shift) control character is sent to place the printer in the letter printing mode, and the Figure (up-shift) control character is used to shift the printer into the figures printing mode. If an error causes a control character to be received that shifts the printer into a false mode, the printer will print a wrong string of characters until a proper control-shift character is received.

TABLE C-1 BAUDOT CODE<sup>a</sup>

Character Case		Bit Pattern					Character Case		Bit Pattern				
Lower	Upper	5	4	3	2	1	Lower	Upper	5	4	3	2	1
A	-	0	0	0	1	1	Q	1	1	0	1	1	1
B	?	1	1	0	0	1	R	4	0	1	0	1	0
C	:	0	1	1	1	0	S	'	0	0	1	0	1
D	\$	0	1	0	0	1	T	5	1	0	0	0	0
E	3	0	0	0	0	1	U	7	0	0	1	1	1
F	!	0	1	1	0	1	V	;	1	1	1	1	0
G	&	1	1	0	1	0	W	2	1	0	0	1	1
H	#	1	0	1	0	0	X	/	1	1	1	0	1
I	8	0	0	1	1	0	Y	6	1	0	1	0	1
J	Bell	0	1	0	1	1	Z	"	1	0	0	0	1
K	(	0	1	1	1	1	Letters (shift) ↓		1	1	1	1	1
L	)	1	0	0	1	0	Figures (shift) ↑		1	1	0	1	1
M	.	1	1	1	0	0	Space (SP)		0	0	1	0	0
N	,	0	1	1	0	0	Carriage return		0	1	0	0	0
O	9	1	1	0	0	0	Line feed		0	0	0	1	0
P	0	1	0	1	1	0	Blank		0	0	0	0	0

<sup>a</sup> 1 = mark = punch hole, and 0 = space = no punch hole for paper tape.

## ASCII

The American National Standard Code for Information Interchange (ASCII) was first adopted in 1963 and updated in 1967. It was the first code specifically developed for computer communication systems. It is now the most popular code used by computer terminals. The code is shown in Table C-2. It has a total of 8 bits per character. Seven bits are completely specified as shown. The eighth bit is a parity bit that may be even or odd parity, depending on the choice selected for use in a particular installation.

## C-2 DTE/DCE AND ETHERNET INTERFACE STANDARDS

A general block diagram for a computer communication system is shown in Fig. C-1. To facilitate the use of equipment supplied by different vendors, interface standards have been adopted for connection of data terminal equipment (DTE) and data communications equipment (DCE). The DTE may be a digital computer, a printer, a keyboard, and so on, and the DCE may be a modem. In addition, one type of DTE, say a printer, may be connected to another type of DTE, say a keyboard, by the same type of interface.

Numerous organizations are concerned with advancement of practical standards. Internationally, the International Telegraph and Telephone Consultative Committee (CCITT) and the International Organization for Standardization (ISO) are the best known.

TABLE C-2 ASCII CODE<sup>a</sup>

Bit Position				7	0	0	0	0	1	1	1	1	1
4	3	2	1	5	0	1	0	1	0	1	0	1	0
0	0	0	0	0	0	0	0	0	0	0	0	0	0
0	0	0	1	0	0	1	1	1	1	1	1	1	1
0	0	1	0	0	0	1	1	1	1	1	1	1	1
0	1	0	0	0	0	1	1	1	1	1	1	1	1
0	1	1	0	0	0	1	1	1	1	1	1	1	1
0	1	1	1	0	0	1	1	1	1	1	1	1	1
0	1	1	1	1	0	1	1	1	1	1	1	1	1
1	0	0	0	0	0	0	0	0	0	0	0	0	0
1	0	0	0	0	1	0	0	0	0	0	0	0	0
1	0	0	1	0	0	1	0	0	0	0	0	0	0
1	0	1	0	0	0	1	0	0	0	0	0	0	0
1	1	0	0	0	0	1	0	0	0	0	0	0	0
1	1	0	1	0	0	1	0	0	0	0	0	0	0
1	1	1	0	0	0	1	0	0	0	0	0	0	0
1	1	1	1	0	0	1	0	0	0	0	0	0	0
1	1	1	1	1	0	1	0	0	0	0	0	0	0
1	1	1	1	1	1	0	0	0	0	0	0	0	0
1	1	1	1	1	1	1	0	0	0	0	0	0	0
1	1	1	1	1	1	1	1	0	0	0	0	0	0
1	1	1	1	1	1	1	1	1	0	0	0	0	0
1	1	1	1	1	1	1	1	1	1	0	0	0	0
1	1	1	1	1	1	1	1	1	1	1	0	0	0
1	1	1	1	1	1	1	1	1	1	1	1	0	0
1	1	1	1	1	1	1	1	1	1	1	1	1	0
1	1	1	1	1	1	1	1	1	1	1	1	1	1

ACK	Acknowledge	ENQ	Enquiry	RS	Record separator
BEL	Bell, or alarm	EOT	End of transmission	SI	Shift in
BS	Backspace	ESC	Escape	SO	Shift out
CAN	Cancel	ETB	End of transmission block	SOH	Start of heading
CR	Carriage return	ETX	End of text	SP	Space
DC1	Device control 1	FF	Form feed	STX	Start of text
DC2	Device control 2	FS	File separator	SUB	Substitute
DC3	Device control 3	GS	Group separator	SYN	Synchronous idle
DC4	Device control 4	HT	Horizontal tab	US	Unit separator
DEL	Delete	LF	Line feed	VT	Vertical tab
DLE	Data link escape	NAK	Negative acknowledge		
EM	End of medium	NUL	Null, or all zeros		

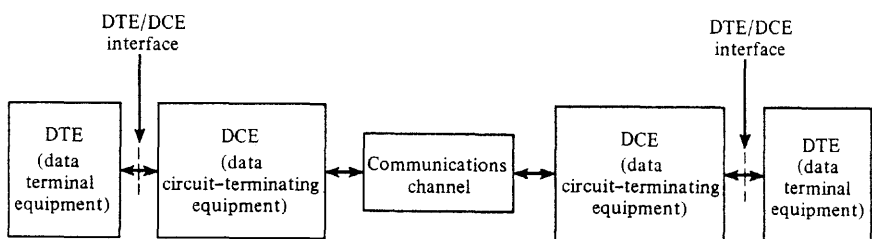


Figure C-1 Computer communication system.

In the United States, as well as internationally, four standards groups are the American National Standards Institute (ANSI), the Electronics Industries Association (EIA), the Institute of Electrical and Electronics Engineers (IEEE), and the National Communications System (NCS) of the federal government.

DTE/DCE standards are developed in terms of the following:

- The physical and electrical interface.
- The link control (software) interface that provides framing/synchronization and error detection/error correction functions.

Now several physical/electronic standards will be described.

### Current Loop

Since early in the twentieth century, when mechanical teleprinter systems were developed, the current loop has been a popular interface for transmission of asynchronous serial data (Fig. C-2). During the idle condition, the dc current in the local (interface) loop is specified to be some design value. In most teleprinters designed for computer terminal use, this value is 20 mA. To send an ASCII character, the current is interrupted at the transmitting device according to the binary word for that particular ASCII character. The presence of loop current denotes a mark, and the absence of loop current denotes a space. The interruption of the current is detected at the receiving point in the loop. If needed, a number of transmitting and receiving devices may be wired in series in this local loop (where only one transmits at a time).

### RS-232C, RS-422A, RS-449, and RS-530 Interfaces

The RS-232C serial interface (also known as the *EIA standard interface*) was developed in 1969 by the EIA in cooperation with the Bell System and independent computer and modem manufacturers. The CCITT has adopted an interface standard, called V.24, that is very similar to the RS-232C standard. The military MIL-188c is also similar. The RS-232C pin connections are given in Table C-3, where the EIA and CCITT circuit equivalents are listed. The standard provides for serial data transmission by using a voltage level of  $-V_0$  for a binary

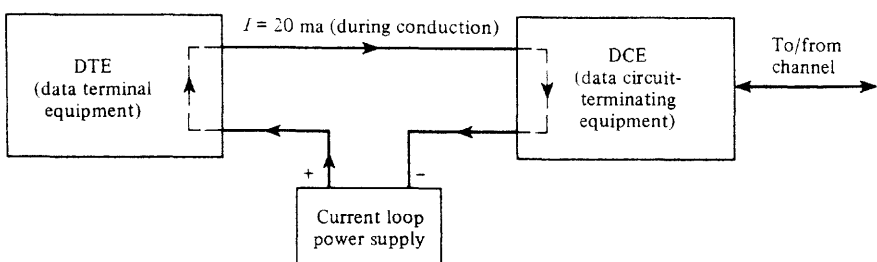


Figure C-2 20-mA current (local) loop interface.

1 (mark) and a level of  $+V_0$  for a binary 0 (space), where  $3 \leq V_0 \leq 25$  V. A typical value for  $V_0$  is 6 V. The voltage appears on the appropriate lead measured with respect to the common (signal) ground lead. This is called *unbalanced signaling* and is also known as single-ended signaling.

The RS-232C standard defines the electrical characteristics, the functional description of interchange circuits, and a list of standard applications. The type of physical connector is not specified, but a DB25 connector (25 pins) is generally used in practice.

The RS-232C interface is intended for data rates up to 20 kbits/sec and cable lengths up to 50 ft. Longer lengths are possible if twisted-pair cable is used and the loading capacitance is kept below 2500 pF. This interface is one of the most popular serial interfaces used in computer communication equipment today.

For higher data rates and longer cable lengths, the RS-422A interface was developed. This interface uses *balanced signaling* (also known as differential signaling), and, consequently, two wires are required for each circuit. This method gives greater noise and crosstalk immunity because a common signal return path is not used. The balanced-signaling technique allows the transition region between the mark and space voltage levels to be reduced so that the signal levels are  $\pm V_0$ , where  $0.2 \leq V_0 \leq 25$  V is used for balanced signaling. The RS-422A interface uses DB37 and DB9 connectors (37- and 9-pin) as specified in the ISO 4902 standard. The pin connections are given in Table C-3, where the two-wire connections for each balanced circuit are specified in columns A and B. The RS-422A standard allows for data rates up to 100 kbits/s at 4000 ft or 40 Mbits/s at 40 ft.

The RS-449 signal interface was intended to be the successor to the RS-232C interface. The RS-449 interface connections are also given in Table C-3. A 37-pin D connector is used for the primary channel and an auxiliary 9-pin D connector is used (when needed) for a secondary channel. The 37-pin connector allows for unbalanced or (optionally) balanced signaling where the signaling levels are those for RS-232C or RS-222A, respectively. Balanced signaling allows the RS-449 interface to support data rates up to 2 Mbits/s and cable lengths up to 667 ft.

The RS-530 interface supersedes the RS-449. It is a balanced signaling complement to the RS-232C (which uses unbalanced signaling). The RS-530 interface uses a DB-25 (25-pin) connector as described by Fig. C-3c and Table C-3. It accommodates data rates up to 2 Mbits/sec.

### Centronics Parallel Interface

Printers are often connected to computing equipment by either a RS-232C serial interface or a Centronics parallel interface. Figure C-4 and Table C-4 show the 36-pin connector for the Centronics parallel interface. This interface has eight data lines that provide eight bits of data in parallel. The data are controlled by the STROB pulse. This interface uses unbalanced signaling with TTL (transistor transistor logic) levels.

### IEEE-488 Interface

The IEEE-488 interface is designed to connect computer equipment with programmable instruments such as programmable voltmeters, signal sources, and power supplies. It allows programmable instruments to be easily connected together to create an *automatic test equipment*.

TABLE C-3 EIA RS-232C, RS-422A, RS-449, AND RS-530 INTERFACE STANDARDS<sup>a</sup>

RS-449/422						RS-530						
9 Pin Aux.	37 Pin		RS-449 Circuit	RS-449 Description	25 Pin		RS-530 Circuit	RS-530 Description				
	A	B			A	B						
1	1			Shield		1		Shield				
5	19		SG	Signal ground		7	AB	Signal ground				
9	37		SC	Send common								
6	20		RC	Receive common								
4	22		SD	Send data	2	14	BA	Transmitted data				
6	24		RD	Receive data	3	16	BB	Receive data				
7	25		RS	Request to send	4	19	CA	Request to send				
9	27		CS	Clear to send	5		CB	Clear to send				
11	29		DM	Data mode	6	22	CC	DCE ready				
12	30		TR	Terminal ready	20	23	CD	DTE ready				
15			IC	Incoming call								
13	31		RR	Receiver ready	8	10	CF	Receive line detector				
33			SQ	Signal quality								
16			SR	Signaling rate selector								
2			SI	Signaling rate indicator								
17	35		TT	Terminal timing	24	11	DA	Transmitter timing (DTE)				
5	23		ST	Send timing	15	12	DB	Transmitter timing (DCE)				
8	26		RT	Receive timing	17	9	DD	Receiver timing (DCE)				
3			SSD	Secondary send data			BA	Transmitted data				
4			SRD	Secondary receive data			BB	Receive data				
7			SRS	Secondary request to send								
8			SCS	Secondary clear to send	13		CB	Clear to send				
2			SRR	Secondary receiver ready			DB	Transmit timing (DCE)				
10			LL	Local loopback	18		LL	Local loopback				
14			RL	Remote loopback	21		RL	Remote loopback				
18			TM	Test mode	25		TM	Test mode				
32			SS	Select standby								
36			SB	Standby indicator								
16			SF	Select frequency								
28			IS	Terminal in service								
34			NS	New signal								

Source: Reproduced by permission of Black Box Corporation, Pittsburgh, PA. © Copyright, 1995. All rights reserved. Reprinted by permission.

<sup>a</sup>DB25 references the (25-pin) connector that is commonly used for RS-232 and V.24. Pins 9 and 10 are reserved for data set testing. Pins 11, 18, and 25 are undefined. Pins 3 and 21 of RS-449 interface connector are undefined. Lead 23 of RS232 connector may be defined as CH or CI.

TABLE C-3 (continued)

RS-232 Interface						Signal Type and Direction					
25 Pin	EIA-RS-232C Circuit	CCITT V.24 Circuit	Mnemonic Designation	RS-232 Description	GND	Data		Control		Timing	
	From DCE	To DCE	From DCE	To DCE	From DCE	To DCE	From DCE	To DCE	From DCE	To DCE	
1	AA	101	FG	Protective frame ground	×						
7	AB	102	SG	Signal ground/common return	×						
		102a		DTE common	×						
		102b		DCE common	×						
2	BA	103	TD	Transmitted data					×		
3	BB	104	RD	Received data					×		
4	CA	105	RTS	Request to send							×
5	CB	106	CTS	Clear to send							×
6	CC	107	DSR	Data set ready							×
20	CD	108.2	DTR	Data terminal ready							×
22	CE	125	RI	Ring indicator							×
8	CF	109	DCD	Received line carrier signal detector							×
21	CG	110	SQ	Signal quality detector							×
23	CH	111		Data signal rate selector (DTE)							×
23	CI	112		Data signal rate selector (DCE)							×
24	DA	113	TC	Transmitter clock signal element timing (DTE)							×
15	DB	114	TC	Transmitter clock signal element timing (DCE)							×
17	DD	115	RC	Receiver clock signal element timing (DCE)							×
14	SBA	118	STD	Second transmitter data							×
16	SBB	119	SRD	Secondary received data							×
19	SCA	120	SRTS	Secondary request to send							×
13	SCB	121	SCTS	Secondary clear to send							×
12	SCF	122	SDCD	Secondary received line signal detector							×
		141		Local loopback							×
		140		Remote loopback							×
		142		Test indicator							×
		116		Select standby							×
		117		Standby indicator							×
		126		Select transmit frequency							×

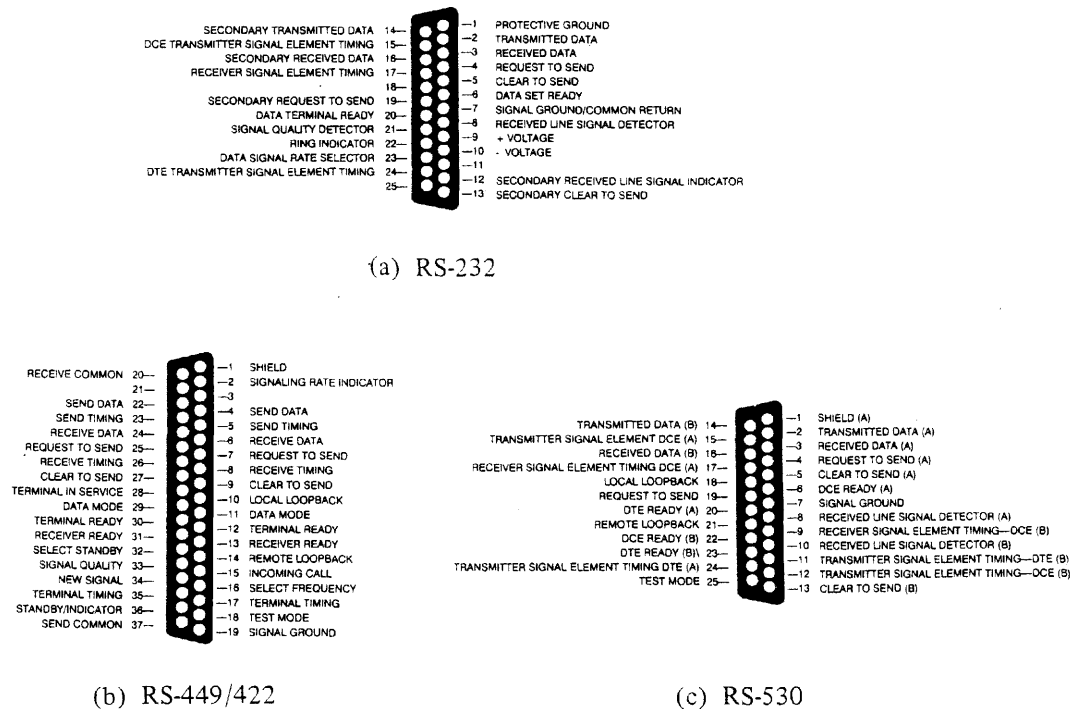
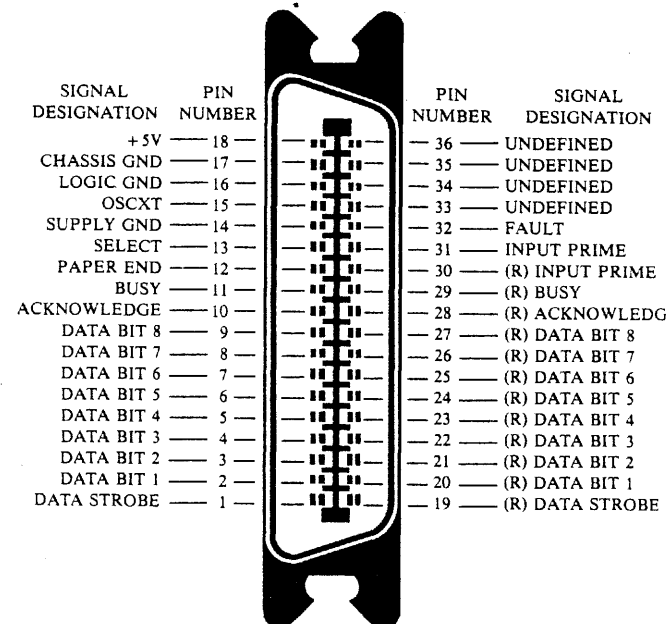


Figure C-3 RS-232C, RS-449/422, and RS-530 male connectors.

*ment* (ATE) system. This interface was first developed in 1965 by Hewlett Packard and was known as the HP Interface Bus (HP-IB) or the General Purpose Interface Bus (GPIB). In 1975 the IEEE adopted an evolved standard, which was named the IEEE-488 interface. Table C-5 presents some details on this parallel interface. The lines are held at +5 V for a binary 0 (false) and pulled to ground for a binary 1 (true). This standard allows the bus to extend over a distance of 67 ft. Every IEEE-488 device is a listener, a talker, or a controller. A *listener* is capable of receiving data from the bus, such as a printer or a programmable power supply. A *talker* is capable of transmitting data over the bus, such as a frequency counter or a voltmeter. There can be only one active talker on the bus at a time. A *controller* is a computer-type device that controls the network (including itself) and specifies which devices are active talkers or listeners. A 24-pin IEEE-488 connector is illustrated in Fig. C-5.

### Ethernet (IEEE 802.3) Interface

Ethernet is a method of connecting multiple computers, servers, and peripherals together to form a *local area network* (LAN). It was first developed by the Xerox Corporation in the 1970s and supported by Digital Equipment Corporation (DEC) and Intel in 1980. In 1988 the Ethernet concept was refined by the IEEE and the IEEE 802.3 standard was published.



(R) INDICATES SIGNAL GROUND RETURN

Figure C-4 Centronics connector.

As shown in Table C-6, this standard provides a 10-Mbit/sec serial data bus for a LAN using either coaxial cable or twisted-pair wire.

In the 10base5 (thick Ethernet) system, a 50- $\Omega$  coaxial backbone cable, up to 500 m in length, is used. The "10" in 10base5 indicates that a 10-Mbit/s data rate is supported, "base" indicates that baseband signaling (Manchester line code) is used, and "5" indicates that the maximum backbone length is 500 m unless repeaters are used. A DTE device with a Ethernet card is connected to the backbone cable by using a transceiver—also called a *medium attachment unit* (MAU)—in series with the backbone cable at the tap point. A cable drop then connects the transceiver to the DTE Ethernet card.

In the 10base2 (thin net or cheap net) system, a 50- $\Omega$  thin (0.25 in. diameter) coaxial cable, up to 200 m in length, is used. The DTE device is connected to this coaxial bus by inserting a BNC T-connector in series with the cable at the tap point. In this thin-net system the T-connector must be connected directly to the Ethernet card on the DTE (no drop cable allowed).

The 10base-T system uses twisted-pair wire, up to 100 m in length, to connect each DTE device with a 10base-T Ethernet card directly to a central hub. (There are no taps on the twisted-pair wire.)

Multiple 10base5, 10base2, or 10base-T systems (segments) may be connected together using a multiport repeater. A gateway may also connect the Ethernet LAN to a wide area network (WAN) which uses either coaxial cable or fiber optic cable to other networks.

TABLE C-4 CENTRONICS PARALLEL INTERFACE<sup>a</sup>

Signal Pin No.	Return Pin No.	Signal	Direction (with Reference to Printer)	Description
1	19	STROBE	In	STROBE pulse (negative going) enables reading data.
2	20	Data 1	In	1st to 8th bits of parallel data.
3	21	Data 2	In	Each signal is at "high" level
4	22	Data 3	In	when data are logical "1" and
5	23	Data 4	In	"low" when logical "0."
6	24	Data 5	In	
7	25	Data 6	In	
8	26	Data 7	In	
9	27	Data 8	In	
10	28	ACKNLG	Out	"Low" indicates that data have been received and that the printer is ready to accept other data.
11	29	BUSY	Out	"High" indicates that the printer cannot receive data.

Source: Reproduced by permission of Black Box Corporation, Pittsburgh, PA. © Copyright, 1988.

<sup>a</sup> Pins 12, 13, 14, 15, 18, 31, 32, 34, 35, and 36 vary in function depending on application; they are commonly used for printer auxiliary controls, and error handling and indication. Pins 16 and 17 are commonly used for logic ground and chassis ground, respectively.

### C-3 THE ISO OSI NETWORK MODEL

When users are connected together, many things must be considered for orderly, efficient data transmission. This complicated problem can be understood better and the network can be maintained more easily if the different tasks are divided into layered modules. These modules are implemented in both hardware and software. Most computer network designers and manufacturers follow the layered model recommended by the ISO in its Open System Interconnection (OSI) reference model. This model is shown in Fig. C-6. This figure presents an example of two end users (host A and host B) that are connected to a data communications network via the physical channel. The physical channel may be connections via telephone company (TELCO) lines, fiber optic link, microwave radio, or satellite links.

The layered approach has many attractive features [Stallings, 1994]. By adhering to the appropriate hardware and/or software specifications that define the layer boundaries, many different vendors can supply hardware/software that will work efficiently in the overall network. Furthermore, various parts of the system can be updated and maintained by replacing or modifying the hardware/software at each layer level instead of replacing the whole system.

The functions of the various layers may be described as follows:

TABLE C-5 IEEE-488 INTERFACE<sup>a</sup>

24-Pin				Data Line	Control Line	Handshake Line
A	B	Circuit	Description			
	24	GND	Logic ground	×		
1	24	D101	Data bit 1	×		
2	24	D102	Data bit 2	×		
3	24	D103	Data bit 3	×		
4	24	D104	Data bit 4	×		
13	24	D105	Data bit 5	×		
14	24	D106	Data bit 6	×		
15	24	D107	Data bit 7	×		
16	24	D108	Data bit 8	×		
9	21	IFC	Interface Clear—used by controller to place devices into quiescent state		×	
10	22	SRQ	Service Request—used by device to request service		×	
17	24	REN	Remote Enable—used by controller to override device front panel controls		×	
5	24	EOI	End of Identity—(a) used by talker to end message, or (b) used by controller with ATN for parallel pole		×	
11	23	ATN	Attention—used by controller to end its data and listen for a command		×	
6	18	DAV	Data Valid—used by controller to indicate a control byte on data bus		×	
7	19	NRFD	Not Ready For Data—used by listener to indicate it is not ready		×	
8	20	NDAC	No Data Accepted—used by listener to indicate it has not yet accepted last byte		×	
12		Shield				

<sup>a</sup> Column B pins are return leads to be grounded at the system ground point.

*Layer 1—Physical.* Concerned with bit transmission. Standards specify signal levels, cable connectors, and cable. For multiple-access packet transmission systems, the methods of carrier sense and collision detection are also specified.

*Layer 2—Data Link.* Concerned with beginning message transmission, error detection and correction, and ending message transmission.

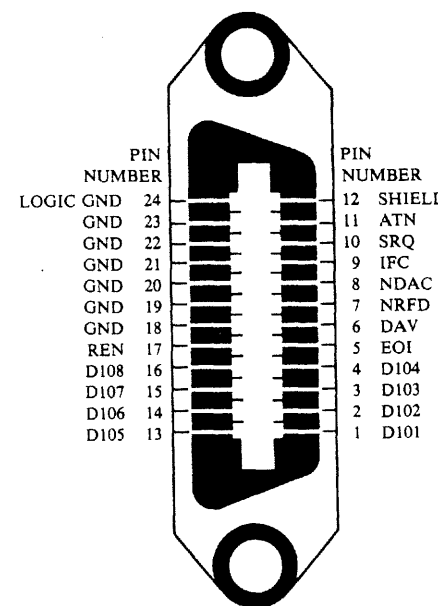


Figure C-5 IEEE-488 connector.

TABLE C-6 ETHERNET (IEEE 802.3) STANDARDS

Item	Thick (Standard) Ethernet	Thin Ethernet	Twisted-pair Ethernet <sup>a</sup>
IEEE designation	10base5	10base2	10base-T
Transmission medium	50- $\Omega$ coax	50- $\Omega$ coax	Twisted-pair wire
Cable diameter or wire size	0.4 in. diameter	0.25 in. diameter	22 to 26 AWG
Data rate	10 Mbits/sec	10 Mbits/sec	10 Mbits/sec
Maximum segment length	500 m <sup>b</sup>	200 m <sup>b</sup>	100 m
Maximum length with repeaters	4000 m	4000 m	NA
Minimum distance between taps	2.5 m	0.5 m	NA
Tap configuration	Transceiver	T-connector <sup>c</sup>	NA
Maximum number of taps	100	30	NA
Type of connectors used	N	BNC	NA

<sup>a</sup> NA, not applicable. Each device is connected to a central hub via an unshielded twisted-wire pair.

<sup>b</sup> Each end of the segment is terminated with a 50- $\Omega$  resistive load.

<sup>c</sup> T-connector must be connected directly to the Ethernet card on the DTE device.

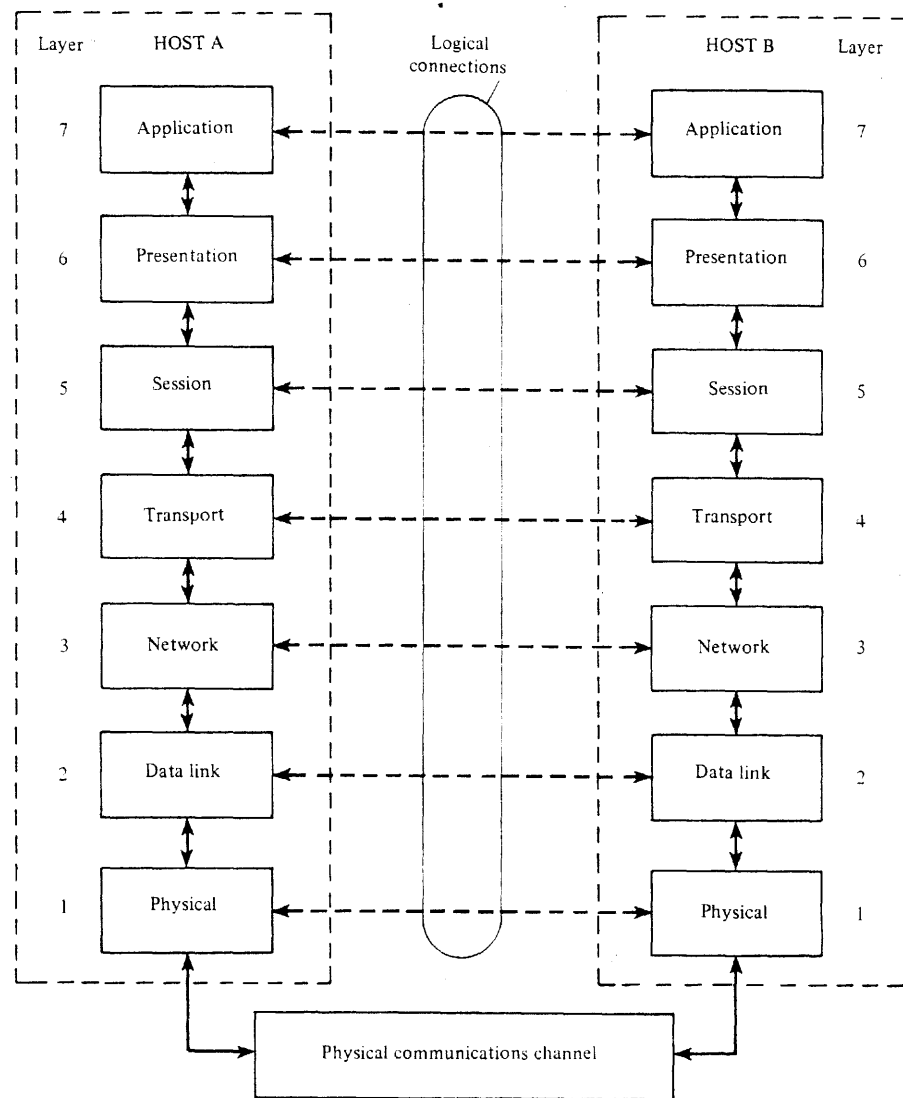


Figure C-6 ISO OSI reference model of physical and logical connections.

**Layer 3—Network.** Concerned with choosing the route taken by the message, flow control, and message priorities.

**Layer 4—Transport.** Concerned with end-to-end reliability (error detection and information recovery) and maps logical addresses to end-user devices.

**Layer 5—Session.** Starts and stops the communication session, transfers the user from one task to another, and provides recovery from communication problems (restart) without losing data.

*Layer 6—Presentation.* Converts data to the appropriate syntax for the display devices (character sets and graphics) and encodes/decodes compressed data.

*Layer 7—Application.* Provides a log-in procedure, checks passwords, allows file upload/download and remote job entry, and tabulates system resources used for billing purposes.

## C-4 DATA LINK CONTROL PROTOCOLS

*Data link control* (DLC) protocols, also called *line protocols*, are a set of rules for operating a computer network or a public switched telephone network (PSTN). They standardize the framing, addressing, and error control techniques used in the system.

### BISYNC

The Binary Synchronous Communication (BISYNC) protocol was developed in 1968 by IBM for synchronous transmission between two computers or between a computer and batch terminals. (It has been superseded by SDLC, which we will discuss subsequently.) BISYNC is a character-oriented protocol. That is, it uses characters (e.g. ASCII) to delineate the various fields of the message. It is also a half-duplex protocol, which means that the data flow in one direction at a time between two communication points. Periodically, an end-of-transmission-block (ETB) character is sent, which requires a response from the receiving station indicating acknowledgment of reception of error-free data (ACK) or error in the previous received block (NAK). If a NAK is received by the transmitter end, the whole block is retransmitted. This is automatic request for repeat (ARQ) error control. A typical BISYNC message is shown in Fig. C-7. The text portion is variable in length.

### SDLC

Synchronous Data Link Control (SDLC) is a bit-oriented protocol. That is, instead of control characters it uses a unique flag at the beginning and end of each frame. It was developed by IBM in 1974 to provide a more versatile protocol than BISYNC. It is a full-duplex protocol, which means that data can be transmitted in both directions simultaneously. Furthermore, SDLC permits the transmission to one remote location while receiving from a different remote location on a multidrop line. SDLC also uses ARQ error control, where a station has to acknowledge correct receipt of at least the eighth preceding frame if communication is to continue. The SDLC frame is shown in Fig. C-8.

### HDLC

High-Level Data Link Control (HDLC) was approved by ISO in 1975 (ISO 3309) and has been updated since then by other ISO standards. It is a packet protocol that has been adopted worldwide by many vendors. IBM's SDLC is a subset of HDLC, and ANSI's Advanced Data Communications Control Procedure (ADCCP) is equivalent to HDLC. As discussed in the next section, X.25 uses the HDLC protocol.

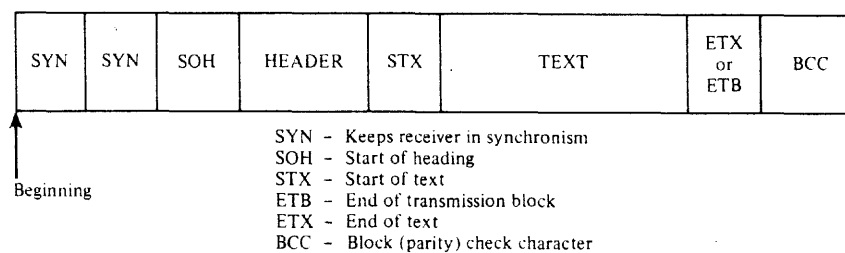


Figure C-7 BISYNC format.

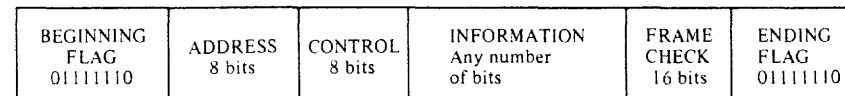


Figure C-8 SDLC and HDLC formats.

The general structure of the HDLC frame (packet) is shown in Fig. C-8. The address field may be extended recursively to allow more addresses. Two basic types of frames are allowed—control and information. In control frames there is no information field, and the control frame is used to set up, take down, or check a virtual link between users. In the information frame, the information field may be of any size. The information frames are numbered in sequence (by bits in the control field), so that the sending station does not have to wait for an acknowledgment of the frame just transmitted before sending another frame. The acknowledgment can be received at a later time (for error detection and recovery) since the frames are numbered. In addition, the packets may arrive out of sequence at the receiver, and the numbering allows the receiver to place the information in the correct order.

HDLC was originally developed for unbalanced operation (ISO 4335), in which one primary station controls secondary stations by sending command frames. The secondary stations respond only when polled in the normal response mode. In the asynchronous mode (not to be confused with asynchronous bit transmission), the secondary stations are allowed to send unsolicited response frames. Newer modes (ISO 6256) allow balanced operation, in which any station may initiate the setting up of a virtual call.

### CCITT X.25 Protocol

The CCITT X.25 standard is entitled "Interface Between a DTE and a DCE for Terminals Operating in the Packet Mode on Public Data Networks." It involves the use of data packets as the basis for creating a virtual circuit. With a virtual circuit, two users appear to have a private data connection between themselves, although they are actually sharing the same physical channel with other users. This is accomplished by breaking the serial data stream of each user into "packets" of data of a certain length. Each packet has a header attached, with the destination address for the packet and other control information. The packets from each user are interspersed with those of other users on the X.25 line.

The virtual circuits may be set up temporarily or permanently. A temporary virtual circuit consists of three operations: (1) setting up the call, (2) transferring the data, and (3)

TABLE C-7 MODEM STANDARDS

Type	Data Rate (bits/s)			Mode	Type of Line	Synch/ Asynch	Transmitting Frequencies (Hz) <sup>b</sup>			
	Normal	Fallback					Modulation <sup>a</sup>	Originate	Answer	
Bell 103/113	0-300			FDX	2W Dial-up	Async	FSK	1070S	1270M	2025S
CCITT V.21	0-300			FDX	2W Dial-up	Async	FSK	980M	1080S	1650M
Bell 202S	1,200			HDX	2W Dial-up	Async	FSK	1200M	2200S	
Bell 202T	1,200			FDX	4W Lease	Async	FSK	1200M	2200S	
CCITT V.23	1,200			HDX	2W Dial-up	Async	FSK	1300M	2100S	
		600		HDX	2W Dial-up	Async	FSK	1300M	1700S	
Bell 212A	1,200			FDX	2W Dial-up	Either	4DPSK	1200		2400
		300		FDX	2W Dial-up	Either	FSK			Same as Bell 103
CCITT V.22	1,200			FDX	2W Dial-up	Either	FSK			Same as Bell 212
		600		FDX	2W Dial-up	Either	2DPSK	1200		2400
Bell 201C	2,400			FDX	4W Lease	Sync	4DPSK	1800		
CCITT V.22bis	2,400			FDX	2W Dial-up	Either	16QAM	1200		2400
		1200		FDX	2W Dial-up	Either	4DPSK			Same as CCITT V.22
CCITT V.26	2,400			FDX	4W Lease	Sync	4DPSK	1800		(same as Bell 201C)
CCITT V.26bis	2,400			FDX	4W Lease	Sync	4DPSK	1800		
		1200		FDX	4W Lease	Sync	2DPSK	1800		
Bell 208A	4,800			FDX	4W Lease	Sync	8DPSK	1800		
Bell 208B	4,800			HDX	2W Dial-up	Sync	8DPSK	1800		
CCITT V.27bis	4,800			FDX	4W Lease	Sync	8DPSK	1800		
		2400		FDX	4W Lease	Sync	4DPSK	1800		
Bell 209	9,600			FDX	4W Lease D	Sync	16QAM	1700		
CCITT V.29	9,600	7200/4800		FDX	4W Lease D	Sync	16QAM	1700		
CCITT V.32	9,600	4800/2400		FDX	2W Dial-up	Either	32QAM <sup>c</sup>	1800		1800
CCITT V.32bis	14,400	12,000/9600		FDX	2W Dial-up	Either	128QAM <sup>c</sup>	1800		1800
CCITT V.33	14,400	9600/2400		FDX	4W Lease C2	Sync	128QAM <sup>c</sup>	1800		1800
CCITT V.34	28,800	26,400/24,000		FDX	2W Dial-up	Either	512QAM <sup>c</sup>			
Bell 301B	40,800			FDX	Group channel	Sync	BPSK			
Bell 303B	19,200			FDX	Half-group	Sync	VSB			
Bell 303C	50,000			FDX	Group channel	Sync	VSB			
Bell 303D	230,400			FDX	Supergroup	Sync	VSB			

<sup>a</sup> FSK, frequency-shift keying; BPSK, binary-phase-shift keying; MDPSK, *M*-ary differential phase-shift keying; VSB, vestigial sideband; MQAM, *M*-ary quadratic amplitude modulation.    <sup>b</sup> M, mark; S, space.    <sup>c</sup> Trellis-coded modulation is used.

TABLE C-8 POPULAR 300, 1200, AND 2400 BITS/S PERSONAL MODEMS<sup>a</sup>

Bell System Type				CCITT			
103/113		202		212A		V.22 bis	
Data	Serial binary Asynchronous Full duplex (two-wire line)	Dial-up or leased line Serial binary Asynchronous Half-duplex (two-wire line)	Serial binary Asynchronous or synchronous Full-duplex, dial-up lines (also contains a 103 type modem)	Serial binary Asynchronous or synchronous Full-duplex, dial-up (also usually contains a 212A-type modem)	Serial binary Asynchronous or synchronous Full-duplex, dial-up (also usually contains a 212A-type modem)	Serial binary Asynchronous or synchronous Full-duplex, dial-up (also usually contains a 212A-type modem)	Serial binary Asynchronous or synchronous Full-duplex, dial-up (also usually contains a 212A-type modem)
Data rate	0 to 300 bits/sec	0 to 1200 bits/s (dial-up) 0 to 1800 bits/s (leased C2)	1200 bits/sec 600 baud (symbols/s)	1200 bits/sec 600 baud (symbols/s)	2400 bits/s 600 baud (symbols/sec)	2400 bits/s 600 baud (symbols/sec)	2400 bits/s 600 baud (symbols/sec)
Modulation	FSK	FSK		QPSK ( <i>M</i> = 4 phases)		QAM (16-point rectangular-type signal constellation)	
Frequency/ phase assignment	Originate end Tx: Space 1070 Hz Mark 1270 Hz Rx: Space 2025 Hz Mark 2225 Hz	Answer end Mark: 1200 Hz Space: 2200 Hz		Carrier frequencies Originate end Answer end		Originate end Answer end	
				Tx: $f_c = 1200 \text{ Hz}$ $f_c = 2400 \text{ Hz}$		Tx: $f_c = 1200 \text{ Hz}$ $f_c = 2400 \text{ Hz}$	
				Rx: $f_c = 2400 \text{ Hz}$ $f_c = 1200 \text{ Hz}$		Rx: $f_c = 2400 \text{ Hz}$ $f_c = 1200 \text{ Hz}$	
Transmit level	0 to -12 dBm	0 to -12 dBm	Message (2 bits)	Phase Angle			
Receive level	0 to -50 dBm	0 to -50 dBm (dial-up line) 0 to -40 dBm (leased line)	00 01 10 11	90° 0° 180° 270°			

<sup>a</sup> Tx, Transmit; Rx, receive.

TABLE C-9 CCITT V.32 MODEM STANDARD

Item	Signal Constellation
Data	Serial binary, Asynchronous or synchronous Full duplex over two-wire line <sup>a</sup>
Carrier freq.	Transmit <sup>a</sup> : 1800 Hz Receive <sup>a</sup> : 1800 Hz
<i>Option 1</i>	9600 bits/s for high SNR 4800 bits/s for low SNR
DATA rate	32 QAM, 2400 baud, for high SNR using trellis-coded modulation (see Fig. 1-9, where $n = 3$ and $m - k = 2$ ) with 4 data bits plus 1 coding bit per symbol
Modulation	QPSK, 2400 baud (states A, B, C, D) for low SNR
<i>Option 2</i>	9600 bits/s for high SNR 4800 bits/s for low SNR
DATA rate	16 QAM, 2400 baud, for high SNR QPSK, 2400 baud (states A, B, C, D) for low SNR
Modulation	

<sup>a</sup> A two-wire to four-wire hybrid is used in this modem to obtain the transmit and receive lines.

TABLE C-10 CCITT V.32BIS AND V.33 MODEM STANDARDS

Item	128 QAM Signal Constellation
Data	Serial binary
V.32bis	Synchronous/asynchronous, full duplex over two-wire dial up line <sup>a</sup>
V.33	Synchronous, full duplex over four-wire leased line <sup>b</sup>
Carrier freq.	Transmit: 1800Hz Receive: 1800 Hz
Data rate	14,400 bits/s
Modulation	128 QAM, 2400 baud, using trellis-coded modulation (see Fig. 1-9, where $n = 3$ and $m - k = 4$ ) with 6 data bits plus 1 coding bit per symbol
Fallback mode	12,000 bits/s using 64 QAM, 2400 baud, (signal constellation not shown) and trellis-coded modulation with 5 data bits plus 1 coding bit per symbol

<sup>a</sup> The CCITT V.32bis modem uses a two-wire line and an internal two-wire to four-wire hybrid to obtain the transmit and receive lines.

<sup>b</sup> The CCITT V.33 modem uses two wires for transmit and two wires for receive.

fastrain stops the data transmission and renegotiates for the highest speed possible for reliable data transmission. (The highest speed may be lower if the noise increases or higher if the noise decreases.) The V.34 modem with a data rate of 28,800 bits/s uses almost all the available capacity of the typical VF TELCO system. That is, new TELCO terminal ADC equipments have more precise antialias filters that allow the bandwidth of the VF channel to be extended from 3200 to 3429 Hz. The typical twisted-pair subscriber analog line has a SNR of at least 30 dB. This gives a theoretical channel capacity of 34,178 bits/s (as computed by the method described in Study-Aid Example SA1-3). Because the V.34 modem almost achieves this maximum possible capacity, newer modem standards will not have data rates much faster than the 28,800-bit/s rate of the V.34. The V.34 modem will become the most popular modem as it becomes more inexpensive because of high-volume sales.

## C-6 BRIEF COMPUTER COMMUNICATIONS GLOSSARY

**Acoustic Coupler.** A method used to couple modem signals to the telephone line via sound transducers (microphone and headphone) that are positioned on the telephone handset.

**ACU** (automatic calling unit). A unit that dials up the telephone line connection on receipt of the proper data signal from a computer.

**Adaptive Equalizer.** An electronic circuit that automatically compensates for the changing envelope delay and frequency response of a telephone line.

**ARP** (Address Resolution Protocol). A TCP/IP (Transmission Control Protocol/Internet Protocol) process that maps the IP address to the Ethernet address as required by TCP/IP for use with Ethernet.

**ARQ** (automatic retransmission request). An error correction technique whereby the message is retransmitted when the receiver detects an error.

**ASCII** (American Standard Code for Information Interchange). A 7-bit plus 1-parity bit code; see Table C-2.

**ASR.** Automatic sending-receiving.

**Asynchronous Transmission.** The time intervals between transmitted characters may be of unequal length. Start and stop bits are transmitted before and after each character to synchronize the receiver clock.

**ATM** (asynchronous transfer mode). A new packet (or cell) protocol that is being implemented over the PSTN. See Sec. C-4.

**Baud.** The data transmission rate, in units of symbols per second, whereby one symbol is counted for each possible modulation level. Baud is sometimes used incorrectly by modem manufacturers to express bits per second. A baud is the same as a bit per second if each symbol represents one bit (i.e.,  $M = 2$  possible levels).

## Sec. C-6 Brief Computer Communications Glossary

**Baudot Code.** A 5-bit code set; see Table C-1. Also known as the *International Telegraph Alphabet (ITA) Number 2*.

**BISYNC** (Binary-Synchronous Communications Protocol). See Sec. C-4 and Fig. C-7.

**Bridge.** An electronic box that connects different local area networks at the data-link layer of the OSI model; see Fig. C-6 in Sec. C-3.

**Broadband Channel.** A channel that has a bandwidth much greater than that required to send one VF signal.

**CCITT.** The Consultative Committee for International Telephone and Telegraph, an international standards group.

**Circuit Switching.** A physically (or electronically) switched connection that connects the line of the calling party to that of the called party.

**Concentrator.** A device that connects a number of low-speed, usually asynchronous, devices to a high-speed, usually synchronous, device.

**Control Character.** A nonprinting functional character that provides some control function (e.g., see Table C-2 for the ASCII control characters).

**CRC** (cyclic redundancy check). Data are checked for errors by using a polynomial algorithm. The algorithm is used to compute a check field (usually 16 bits) that is appended to the frame of data at the transmitter and used by the receiver to verify the correctness of the data.

**CSMA/CD** (carrier sense multiple access/collision detection). Multiple users transmit data over a common channel. If two users transmit data at the same time, the resulting collision is detected and each tries to transmit again after a predetermined time interval.

**CTS.** Clear-to-send line on the RS-232C interface (see Table C-3).

**CXR.** Carrier.

**Data Set.** (1) A modem or (2) a collection of data records.

**DCE** (data communications equipment). A modem; see Fig. C-1.

**Dial-Up Line.** A switched-circuit telephone line connection (as opposed to a leased line).

**DTE** (data terminal equipment). The equipment that provides the data source or data sink; see Fig. C-1.

**EBCDIC** (Extended Binary-Coded Decimal Interchange Code). An 8-bit code used primarily in IBM equipment.

**Echo Check.** A method of checking for errors in a data system by looping the data at the receive site back to the transmitter site for comparison.

**Echo Suppressor.** A device that suppresses the echoes on toll lines that are caused by transmission line reflections (usually at the hybrid interface).

**Envelope Delay.** In the context of telephone lines, the measure of the delay through the circuit for a sinusoidal signal at a certain frequency as compared to the minimum delay, which usually occurs at a frequency of about 1800 Hz.

**Ethernet.** A coaxial cable local-area network that transmits data at 10 Mbits/sec with a CSMA/CD technique. It was first developed by Xerox Corporation and is now standardized by the IEEE (IEEE 802.3). See Table C-6.

**FDDI** (fiber distributed data interface). An ANSI standard for fiber optic computer data links with data rates up to 100 Mbits/s.

**Flow Control.** Ability to stop data flow from a transmitter so that receiver buffers do not overflow.

**Front-End Processor.** A communications computer connected between the main computer and the remote terminals; provides line control, code conversion, data concentration, and error control.

**Full Duplex.** (1) A protocol that provides for simultaneous transmission of data in both directions; also, or alternatively, (2) in the context of telephone data lines, a four-wire (two-pair) circuit.

**Gateway.** An electronic box or logical network device that interconnects incompatible networks or devices by performing protocol conversion.

**Half-Duplex.** (1) A protocol that allows data to be transmitted in only one direction at a time; also, or alternatively, (2) in the context of telephone data lines, a two-wire (one-pair) circuit.

**HDLC** (High-Level Data Link Control Protocol). See Sec. C-4 and Fig. C-8.

**Hybrid Network.** A circuit that couples a two-wire telephone line to a four-wire circuit. (See Fig. 8-5.)

**ISDN** (integrated services digital network). A PSTN service that provides a digital data link directly to the subscriber over a twisted-pair line. See Sec. 8-3.

**ISO.** International Organization for Standardization.

**ISO OSI Model.** See Fig C-6.

**LAN** (local-area network). A connection of office or campus computer facilities to each other by twisted-pair wire, coaxial cable, or fiber optic cable.

**Leased Line.** A permanent line between two or more communication sites (no exchange switching) for leasing customers.

**Message Switching.** See Store-and-Forward.

**Modem.** An acronym for modulator-demodulator. A modem converts the baseband data signal to a bandpass signal for transmission over an analog telephone line, and vice versa. The Bell System calls a modem a *data set*.

**Multipoint Line.** A line that connects two or more communication sites and requires the use of some type of polling and addressing mechanism for each site.

**Packet.** A group of bits with appended address bits, sender identification bits, and/or other control bits.

**Packet Switching.** The transfer of data by means of addressed packets. The channel is occupied only during the transmission of the packet. In this sense, there is a virtual circuit (no permanent circuit) between communication sites. See ATM, Sec. C-4.

**Parity Check.** The addition of an extra noninformation bit to the data group so that the number of 1's in the group is either even or odd; permits the detection of single errors.

**Polling.** In a multipoint network, the process of inquiring which sites have data to transmit.

**Protocol.** The rules for control of data transmission over the communication network.

**PSTN** (public switched telephone network). Common carrier facilities available for lease for transmission of audio, video, and data. See Table 8-2.

**Repeater.** An electronic device that receives an attenuated electrical or optical data signal with noise and regenerates a "noise-free" high-level signal (with, possibly, some bit errors) for retransmission.

**Reverse Channel.** A channel that allows the receiver in a modem to send slow-speed data to the transmitting modem for use in error control, circuit breaking, and network diagnostics.

**RS-232C.** A DCE/DTE interface. See Table C-3.

**RTS.** Request-to-send line on the RS-232C interface; see Table C-3.

**SDLC** (Synchronous Data Link Control Protocol). See Sec. C-4 and Fig. C-8.

**Server.** A computer with file storage for a LAN. The server may also link the LAN to other networks and provide protocol conversion.

**Simplex Mode.** The sending of data in one direction only.

**Slicing Level.** The threshold level of a comparator that determines whether the input level is converted into an output level corresponding to a binary 1 or a level corresponding to a binary 0.

**Statistical Multiplexer.** A time-division multiplexer that takes advantage of the fact that there is often "dead time" on the input data channels. Thus, by dynamically adapting

the time-division algorithm, a larger number of input channels can be serviced than with a fixed (nonadaptive) time-division multiplexer.

**Store-and-Forward.** The process by which messages are accepted into memory and forwarded at a convenient time according to the address on the header of the message.

**Switched Line.** The process by which lines from different sites are connected (switched) when a communication session is desired (e.g., the dial-up telephone network).

**Synchronous Transmission.** The process by which data characters are transmitted at a fixed rate, with the transmitter and receiver being in synchronism. There are no start and stop bits, so this transmission technique is much more efficient than asynchronous transmission.

**TCP/IP** (Transmission Control Protocol/Internet Protocol). A layered set of protocols to allow high-speed (e.g., Ethernet) network connection between PCs and other computers. Different types of vendor equipment can communicate with each other over the TCP/IP network. TCP/IP corresponds to Layers 3 and 4 of the OSI model as shown in Fig. C-6.

**Token Bus.** A LAN that uses a unique word (a token) to be passed to a device before it can place data on the LAN for transmission.

**Turnabout Time.** Time required for a modem to reverse the direction of transmission when connected to a half-duplex line.

**VF (Voice Frequency) Channel.** A channel with a frequency response over the range of 300 to 3200 Hz.

**X.25.** A packet protocol. See Sec. C-2.

**X Terminal.** A computer terminal with a video monitor and keyboard that runs X terminal software. The X terminal is connected to a RISC (reduced instruction set computing) UNIX workstation that provides the computation power and file server functions.

## REFERENCES

- ABRAMOWITZ, M., and I. A. STEGUN (Editors), *Handbook of Mathematical Functions*, National Bureau of Standards, Superintendent of Documents, U.S. Government Printing Office, Washington, DC, 1964. Also available in paperback from Dover Publications, New York, 1965.
- AMOROSO, F., "The Bandwidth of Digital Data Signals," *IEEE Communications Magazine*, vol. 18, no. 6, November 1980, pp. 13-24.
- ANDERSON, R. R. and J. SALZ, "Spectra of Digital FM," *Bell System Technical Journal*, vol. 44, July-August 1965, pp. 1165-1189.
- Aoyama, T., W. R. DAUMER, and G. MODENA (Editors), Special Issue on Voice Coding for Communications, *IEEE Journal on Selected Areas of Communications*, vol. 6, February 1988.
- ARRL, *The 1995 ARRL Handbook for Radio Amateurs*, 72nd Ed., 1994; *The 1994 ARRL Handbook for Radio Amateurs*, 1993; *The 1992 ARRL Handbook for Radio Amateurs*, 1991, American Radio Relay League, Newington, CT.
- AT&T, *FT-2000 OC-48 Lightwave System*, Publication No. AT&T 365-575-100, AT&T Regional Technical Assistance Center (800-432-6600), Holmdel, NJ, December 1994.
- BALDUINO, P. R. H., "Latin America Goes Wireless via Satellite," *IEEE Communications Magazine*, vol. 33, no. 9, September 1995, pp. 114-122.

- BASCH, E. E., and T. G. BROWN, "Introduction to Coherent Optical Fiber Transmission," *IEEE Communications Magazine*, vol. 23, May 1985, pp. 23-30.
- BEDROSIAN, E. B., and S. O. RICE, "Distortion and Crosstalk of Linearly Filtered Angle-Modulated Signals," *Proceedings of the IEEE*, vol. 56, January 1968, pp. 2-13.
- BELL TELEPHONE LABORATORIES, *Transmission Systems for Communications*, 4th ed., Western Electric Company, Winston-Salem, NC, 1970.
- BENDAT, J. S., and A. G. PIERSOL, *Random Data: Analysis and Measurement Procedures*, Wiley-Interscience, New York, 1971.
- BENEDETTO, S., E. BIGLIERI, and V. CASTELLANI, *Digital Transmission Theory*, Prentice Hall, Upper Saddle River, NJ, 1987.
- BENEDETTO, S., M. MONDIN, and G. MONTORSI, "Performance Evaluation of Trellis-Coded Modulation Schemes," *Proceedings of the IEEE*, vol. 82, no. 6, June 1994, pp. 833-855.
- BENNETT, W. R., and J. R. DAVEY, *Data Transmission*, McGraw-Hill Book Company, New York, 1965.
- BENNETT, W. R., and S. O. RICE, "Spectral Density and Autocorrelation Functions Associated with Binary Frequency Shift Keying," *Bell System Technical Journal*, vol. 42, September 1963, pp. 2355-2385.
- BENSON, K. B., and J. C. WHITAKER, *Television Engineering Handbook*, Rev. ed., McGraw-Hill Book Company, New York, 1992.
- BERGLAND, G. D., "A Guided Tour of the Fast Fourier Transform," *IEEE Spectrum*, vol. 6, July 1969, pp. 41-52.
- BEST, R. E., *Phase-Locked Loops*, 2nd ed., McGraw-Hill, Inc., New York, 1993.
- BHARGAVA, V. K., "Forward Error Correction Schemes for Digital Communications," *IEEE Communications Magazine*, vol. 21, January 1983, pp. 11-19.
- BHARGAVA, V. K., D. HACCONI, R. MATYAS, and P. P. NUSPL, *Digital Communications by Satellite*, Wiley-Interscience, New York, 1981.
- BIC, J. C., D. DUPONTEIL, and J. C. IMBEAUX, *Elements of Digital Communication*, John Wiley & Sons, New York, 1991.
- BIGLIERI, E., D. DIVSALAR, P. J. McLANE, and M. K. SIMON, *Introduction to Trellis-Coded Modulation with Applications*, Macmillan Publishing Company, New York, 1991.
- BLACKMAN, R. B., and J. W. TUKEY, *The Measurement of Power Spectra*, Dover, New York, 1958.
- BLAHUT, R. E., *Theory and Practice of Error Control Codes*, Addison-Wesley Publishing Company, Reading, MA, 1983.
- BLANCHARD, A., *Phase-Locked Loops*, Wiley-Interscience, New York, 1976.
- BOASHASH, B., "Estimating and Interpreting the Instantaneous Frequency of a Signal—Part 1: Fundamentals," and "Part 2: Algorithms and Applications," *Proceedings of the IEEE*, vol. 80, no. 4, April 1992, pp. 520-538, 540-568.
- BÖRJESSON P. O., and C. E. W. SUNDBERG, Simple Approximations for the Error Function Q(x) for Communication Applications," *IEEE Transactions on Communications*, vol. COM-27, March 1979, pp. 639-643.
- BOWRON, P., and F. W. STEPHENSON, *Active Filters for Communications and Instrumentation*, McGraw-Hill Book Company, New York, 1979.
- BREMERMANN, H., *Distributions, Complex Variables and Fourier Transforms*, Addison-Wesley Publishing Company, Reading, MA, 1965.
- BRILEY, B. E., *Introduction to Telephone Switching*, Addison-Wesley Publishing Company, Reading, MA, 1983.

- BROADCASTING, *Broadcasting and Cable Yearbook 1995*, R. R. Bowker, New Providence, NJ, 1995.
- BYLANSKI, P., and D. G. W. INGRAM, *Digital Transmission Systems*, Peter Peregrinus Ltd., Herts, England, 1976.
- CAMPANELLA, M., U. LoFASO, and G. MAMOLA, Optimum Pulse Shape for Minimum Spectral Occupancy in FSK Signals," *IEEE Transactions on Vehicular Technology*, vol. VT-33, May 1984, pp. 67-75.
- CARLSON, A. B., *Communication Systems*, 3rd ed., McGraw-Hill Book Company, New York, 1986.
- CATTERMOLE, K. W., *Principles of Pulse-Code Modulation*, American Elsevier, New York, 1969.
- CCITT STUDY GROUP XVII, "Recommendation V.32 for a Family of 2-Wire, Duplex Modems Operating on the General Switched Telephone Network and on Leased Telephone-Type Circuits," *Document AP VIII-43E*, May 1984.
- CHAKRABORTY, D., "VSAT Communication Networks—An Overview," *IEEE Communications Magazine*, vol. 26, no. 5, May 1988, pp. 10-24.
- CHALLAPALI, K., X. LEBEQUE, J. S. LIM, W. H. PAIK, R. SAINT GIBONS, E. PETAJAN, V. SATHE, P. A. SNOPKO, and J. ZDEPSKI, "The Grand Alliance System for US HDTV," *Proceedings of the IEEE*, vol. 83, no. 2, February 1995, pp. 158-173.
- CHAPMAN, R. C. (Editor), "The SLC96 Subscriber Loop Carrier System," *AT&T Bell Laboratories Technical Journal*, vol. 63, no. 10, Part 2, December 1984, pp. 2273-2437.
- CHILDERS, D., and A. DURLING, *Digital Filtering and Signal Processing*, West Publishing Company, New York, 1975.
- CHORAFAS, D. N., *Telephony, Today and Tomorrow*, Prentice Hall, Upper Saddle River, NJ, 1984.
- CLARK, G. C., and J. B. CAIN, *Error-Correction Coding for Digital Communications*, Plenum Publishing Corporation, New York, 1981.
- COOPER, G. R., and C. D. MCGILLEM, *Modern Communications and Spread Spectrum*, McGraw-Hill Book Company, New York, 1986.
- COUCH, L. W., "A Study of a Driven Oscillator with FM Feedback by Use of a Phase-Lock-Loop Model," *IEEE Transactions on Microwave Theory and Techniques*, vol. MTT-19, no. 4, April 1971, pp. 357-366.
- COUCH, L. W., *Digital and Analog Communication Systems*, 4th ed., Macmillan Publishing Company, New York, 1993.
- COUCH, L. W., *Modern Communications Systems*, Prentice Hall, Upper Saddle River, NJ, 1995.
- COURANT, R., and D. HILBERT, *Methods of Mathematical Physics*, Vol. 1, Wiley-Interscience, New York, 1953.
- DAMMANN, C. L., L. D. McDANIEL, and C. L. MADDOX, "D2 Channel Bank—Multiplexing and Coding," *Bell System Technical Journal*, vol. 51, October 1972, pp. 1675-1700.
- DAVENPORT, W. B., JR., and W. L. ROOT, *An Introduction to the Theory of Random Signals and Noise*, McGraw-Hill Book Company, New York, 1958.
- DAVIDOFF, M. R., *The Satellite Experimenter's Handbook*, American Radio Relay League, Newington, CT, 1984.
- DAVIS, D. W., and D. L. A. BARBER, *Communication Networks for Computers*, John Wiley & Sons, New York, 1973.
- DEANGELO, J., "New Transmitter Design for the 80's," *BM/E (Broadcast Management/Engineering)*, vol. 18, March 1982, pp. 215-226.
- DECINA, M., and G. MODENA, "CCITT Standards on Digital Speech Processing," *IEEE Journal on Selected Areas of Communications*, vol. 6, February 1988, pp. 227-234.

- DEFFEBACH, H. L., and W. O. FROST, "A Survey of Digital Baseband Signaling Techniques," *NASA Technical Memorandum NASATM X-64615*, June 30, 1971.
- DEJAGER, F., "Delta Modulation, A Method of PCM Transmission Using a 1-Unit Code," *Phillips Research Report*, no. 7, December 1952, pp. 442-466.
- DEJAGER, F., and C. B. DEKKER, "Tamed Frequency Modulation: A Novel Method to Achieve Spectrum Economy in Digital Transmission," *IEEE Transactions on Communications*, vol. COM-26, May 1978, pp. 534-542.
- DESHPANDE, G. S., and P. H. WITTKE, "Correlative Encoding of Digital FM," *IEEE Transactions on Communications*, vol. COM-29, February 1981, pp. 156-162.
- DHAKE, A. M., *Television Engineering*, McGraw-Hill Book Company, New Delhi, India, 1980.
- DIXON, R. C., *Spread Spectrum Systems*, 3rd ed., John Wiley & Sons, New York, 1994.
- DORF, R. C. (Editor-in-Chief), *The Electrical Engineering Handbook*, CRC Press, Boca Raton, FL, 1993.
- DORF, R. C. (Editor), *The Engineering Handbook*, CRC Press, Boca Raton, FL, 1996.
- EDELSON, B. I., and A. M. WERTH, "SPADE System Progress and Application," *COM-SAT Technical Review*, Spring 1972, pp. 221-242.
- EILERS, C. G., "TV Multichannel Sound—The BTSC System," *IEEE Transactions on Consumer Electronics*, vol. CE-31, February 1985, pp. 1-7.
- FASHANO, M., and A. L. STRODTBECK, "Communication System Simulation and Analysis with SYSTEM TID," *IEEE Journal on Selected Areas of Communications*, vol. SAC-2, January 1984, pp. 8-29.
- FEHER, K., *Digital Communications—Satellite/Earth Station Engineering*, Prentice Hall, Upper Saddle River, NJ, 1981.
- FELLER, W., *An Introduction to Probability Theory and Its Applications*, John Wiley & Sons, New York, 1957, p. 168.
- FIKE, J. L., and G. E. FRIEND, *Understanding Telephone Electronics*, 2nd ed., Texas Instruments, Dallas, 1984.
- FINK, D. G., and H. W. BEATY (Editors), *Standard Handbook for Electrical Engineers*, McGraw-Hill Book Company, New York, 1978.
- FLANAGAN, J. L., M. R. SCHROEDER, B. S. ATAL, R. E. CROCHIERE, N. S. JAYANT, and J. M. TRIBOLET, "Speech Coding," *IEEE Transactions on Communications*, vol. COM-27, April 1979, pp. 710-737.
- FOLEY, J., "Iridium: Key to World Wide Cellular Communications," *Telecommunications*, vol. 25, October 1991, pp. 23-28.
- FORNEY, G. D., "The Viterbi Algorithm," *Proceedings of the IEEE*, vol. 61, March 1973, pp. 268-273.
- GALLAGHER, R. G., *Information Theory and Reliable Communications*, John Wiley & Sons, New York, 1968.
- GARDNER, F. M., *Phaselock Techniques*, 2nd ed., John Wiley & Sons, New York, 1979.
- GARDNER, F. M., and W. C. LINDSEY (Guest Editors), Special Issue on Synchronization, *IEEE Transactions on Communications*, vol. COM-28, no. 8, August 1980.
- GERSHO, A., "Charge-Coupled Devices: The Analog Shift Register Comes of Age," *IEEE Communications Society Magazine*, vol. 13, November 1975, pp. 27-32.
- GERSON, I. A., and M. A. JASIU, "Vector Sum Excited Linear Prediction (VSELP) Speech Coding at 8kb/s," *International Conf. on Acoustics, Speech, and Signal Processing*, Albuquerque, NM, April 1990, pp. 461-464.
- GLISSON, T. L., *Introduction to System Analysis*, McGraw-Hill Book Company, New York, 1986.
- GOLDBERG, R. R., *Fourier Transforms*, Cambridge University Press, New York, 1961.

- GOLOMB, S. W. (Editor), *Digital Communications with Space Applications*, Prentice Hall, Upper Saddle River, NJ, 1964.
- GOODMAN, D. J., "Trends in Cellular and Cordless Communication," *IEEE Communications Magazine*, vol. 29, June 1991, pp. 31-40.
- GORDON, G. D., and W. L. MORGAN, *Principles of Communication Satellites*, Wiley-Interscience, New York, 1993.
- GRIFFITHS, J., *Radio Wave Propagation and Antennas*, Prentice Hall, Upper Saddle River, NJ, 1987.
- GROB, B., *Basic Television*, 4th ed., McGraw-Hill Book Company, New York, 1975.
- GRUBB, J. L., "The Traveller's Dream Come True," *IEEE Communications Magazine*, vol. 29, November 1991, pp. 48-51.
- GULSTAD, K., "Vibrating Cable Relay," *Electrical Review (London)*, vol. 42, 1898; vol. 51, 1902.
- GUPTA, S. C., "Phase Locked Loops," *Proceedings of the IEEE*, vol. 63, February 1975, pp. 291-306.
- HA, T. T., *Digital Satellite Communications*, Macmillan Publishing Company, New York, 1986.
- HA, T. T., *Digital Satellite Communications*, 2nd ed., John Wiley & Sons, New York, 1989.
- HAMMING, R. W., "Error Detecting and Error Correcting Codes," *Bell System Technical Journal*, vol. 29, April 1950, pp. 147-160.
- HÄNDEL, R., and M. N. HUBER, *Integrated Broadband Networks*, Addison-Wesley Publishing Company, Reading, MA, 1991.
- HARRIS, A., "The New World of HDTV," *Electronics Now*, vol. 64, May 1993, pp. 33-40 and p. 72.
- HARRIS, F. J., "On the Use of Windows for Harmonic Analysis with the Discrete Fourier Transform," *Proceedings of the IEEE*, vol. 66, January 1978, pp. 51-83.
- HARRIS, F. J., "The Discrete Fourier Transform Applied to Time Domain Signal Processing," *IEEE Communications Magazine*, vol. 20, May 1982, pp. 13-22.
- HARTLEY, R. V., "Transmission of Information," *Bell System Technical Journal*, vol. 27, July 1948, pp. 535-563.
- HAUS, H. A., Chairman IRE Subcommittee 7.9 on Noise, "Description of Noise Performance of Amplifiers and Receiving Systems," *Proceedings of the IEEE*, vol. 51, no. 3, March 1963, pp. 436-442.
- HAYKIN, S., *Communication Systems*, 2nd ed., John Wiley & Sons, New York, 1983.
- HOLMES, J. K., *Coherent Spread Spectrum Systems*, Wiley-Interscience, New York, 1982.
- HOPKINS, R., "Digital Terrestrial HDTV for North America: The Grand Alliance HDTV System," *IEEE Transactions on Consumer Electronics*, vol. 40, no. 3, August 1994, pp. 185-198.
- HSING, T. R., C. CHEN, and J. A. BELLISIO, "Video Communications and Services in the Copper Loop," *IEEE Communications Magazine*, vol. 31, January 1993, pp. 62-68.
- HUANG, D. T., and C. F. VALENTI, "Digital Subscriber Lines: Network Considerations for ISDN Basic Access Standard," *Proceedings of the IEEE*, vol. 79, February 1991, pp. 125-144.
- IRMER, T., "An Overview of Digital Hierarchies in the World Today," *IEEE International Conference on Communications*, San Francisco, June 1975, pp. 16-1 to 16-4.
- IRWIN, J. D., *Basic Engineering Circuit Analysis*, Macmillan Publishing Company, New York, 1st ed., 1984, 2nd ed., 1987, 3rd ed., 1993.
- JACOBS, I., "Design Considerations for Long-Haul Lightwave Systems," *IEEE Journal on Selected Areas of Communications*, vol. 4, December 1986, pp. 1389-1395.
- JAMES, R. T., and P. E. MUENCH, "A.T.& T. Facilities and Services," *Proceedings of the IEEE*, vol. 60, November 1972, pp. 1342-1349.
- JAYANT, N. S., "Digital Encoding of Speech Waveforms," *Proceedings of the IEEE*, May 1974, pp. 611-632.

- JAYANT, N. S., "Coding Speech at Low Bit Rates," *IEEE Spectrum*, vol. 23, August 1986, pp. 58-63.
- JAYANT, N. S., and P. NOLL, *Digital Coding of Waveforms*, Prentice Hall, Upper Saddle River, NJ, 1984.
- JENKINS, M. G., and D. G. WATTS, *Spectral Analysis and Its Applications*, Holden-Day, San Francisco, CA, 1968.
- JERRI, A. J., "The Shannon Sampling Theorem—Its Various Extensions and Applications: A Tutorial Review," *Proceedings of the IEEE*, vol. 65, no. 11, November 1977, pp. 1565-1596.
- JORDAN, E. C. (Editor), *Reference Data for Engineers: Radio, Electronics, Computer, and Communications*, 7th ed., Howard W. Sams & Company, Indianapolis, IN, 1985.
- JORDAN, E. C., and K. G. BALMAIN, *Electromagnetic Waves and Radiating Systems*, 2nd ed., Prentice Hall, Upper Saddle River, NJ, 1968.
- JURGEN, R. K., "High-Definition Television Update," *IEEE Spectrum*, vol. 25, April 1988, pp. 56-62.
- JURGEN, R. K., "The Challenges of Digital HDTV," *IEEE Spectrum*, vol. 28, April 1991, pp. 28-30 and 71-73.
- KAUFMAN, M., and A. H. SEIDMAN, *Handbook of Electronics Calculations*, McGraw-Hill Book Company, New York, 1979.
- KAY, S. M., *Modern Spectral Estimation—Theory and Applications*, Prentice Hall, Upper Saddle River, NJ, 1986.
- KAY, S. M., and S. L. MARPLE, "Spectrum-Analysis—A Modern Perspective," *Proceedings of the IEEE*, vol. 69, November 1981, pp. 1380-1419.
- KAZAKOS, D., and P. PAPANTONI-KAZAKOS, *Detection and Estimation*, Computer Science Press, New York, 1990.
- KLAPPER, J., and J. T. FRANKLE, *Phase-Locked and Frequency-Feedback Systems*, Academic Press, New York, 1972.
- KRAUS, J. D., *Radio Astronomy*, 2nd ed., Cygnus-Quasar Books, Powell, OH, 1986.
- KRAUSS, H. L., C. W. BOSTIAN, and F. H. RAAB, *Solid State Radio Engineering*, John Wiley & Sons, New York, 1980.
- KRETZMER, E. R., "Generalization of a Technique for Binary Data Communications," *IEEE Transactions on Communication Technology*, vol. COM-14, February 1966, pp. 67-68.
- LAM, S. S., "Satellite Packet Communications, Multiple Access Protocols and Performance," *IEEE Transactions on Communications*, vol. COM-27, October 1979, pp. 1456-1466.
- LANCASTER, D., "Hardware Hacker—Caller Number Delivery," *Radio-Electronics*, vol. 62, August 1991, pp. 69-72.
- LATHI, B. P., *Modern Digital and Analog Communication Systems*, Holt, Rinehart and Winston, New York, 1983 (2nd ed., 1989).
- LEE, W. C. Y., "Elements of Cellular Mobile Radio Systems," *IEEE Transactions on Vehicular Technology*, vol. VT-35, May 1986, pp. 48-56.
- LEE, W. C. Y., *Mobile Cellular Telecommunications Systems*, McGraw-Hill Book Company, New York, 1989.
- LEIB, H., and S. PASUPATHY, "Error-Control Properties of Minimum Shift Keying," *IEEE Communications Magazine*, vol. 31, January 1993, pp. 52-61.
- LENDER, A., "The Duobinary Technique for High Speed Data Transmission," *IEEE Transactions on Communication Electronics*, vol. 82, May 1963, pp. 214-218.
- LENDER, A., "Correlative Level Coding for Binary-Data Transmission," *IEEE Spectrum*, vol. 3, February 1966, pp. 104-115.

- LI, V. O. K., and X. QUI, "Personal Communication Systems (PCS)," *Proceedings of the IEEE*, vol. 83, no. 9, September 1995, pp. 1210-1243.
- LIN, D. W., C. CHEN, and T. R. HSING, "Video on Phone Lines: Technology and Applications," *Proceedings of the IEEE*, vol. 83, no. 2, February 1995, pp. 175-192.
- LIN, S., and D. J. COSTELLO, JR., *Error Control Coding*, Prentice Hall, Upper Saddle River, NJ, 1983.
- LINDSEY, W. C., and C. M. CHIE, "A Survey of Digital Phase-Locked Loops," *Proceedings of the IEEE*, vol. 69, April 1981, pp. 410-431.
- LINDSEY, W. C., and M. K. SIMON, *Telecommunication System Engineering*, Prentice Hall, Upper Saddle River, NJ, 1973.
- LUCKY, R. W., and H. R. RUDIN, "Generalized Automatic Equalization for Communication Channels," *IEEE International Communication Conference*, vol. 22, 1966.
- LUCKY, R. W., J. SALZ, and E. J. WELDON, *Principles of Data Communication*, McGraw-Hill Book Company, New York, 1968.
- MANASSEWITSCH, V., *Frequency Synthesizers*, 3rd ed., Wiley-Interscience, New York, 1987.
- MARAL, G., *VSAT Networks*, John Wiley & Sons, New York, 1995.
- MARKLE, R. E., "Single Sideband Triples Microwave Radio Route Capacity," *Bell Systems Laboratories Record*, vol. 56, no. 4, April 1978, pp. 105-110.
- MARKLE, R. E., "Prologue, The AR6A Single-Sideband Microwave Radio System," *Bell System Technical Journal*, vol. 62, December 1983, pp. 3249-3253. (The entire December 1983 issue deals with the AR6A system.)
- MARPLE, S. L., *Digital Spectral Analysis*, Prentice Hall, Upper Saddle River, NJ, 1986.
- MCELIECE, R. J., *The Theory of Information and Coding (Encyclopedia of Mathematics and Its Applications*, vol. 3), Addison-Wesley Publishing Company, Reading, MA, 1977.
- MCGILL, D. T., F. D. NATALI, and G. P. EDWARDS, "Spread-spectrum Technology for Commercial Applications," *Proceeding of the IEEE*, vol. 82, no. 4, April 1994, 572-584.
- MELSA, J. L., and D. L. COHN, *Decision and Estimation Theory*, McGraw-Hill Book Company, New York, 1978.
- MENNIE, D., "AM Stereo: Five Competing Options," *IEEE Spectrum*, vol. 15, June 1978, pp. 24-31.
- MIYAKO, S., "Digital Audio Is Compact and Rugged," *IEEE Spectrum*, vol. 21, March 1984, pp. 35-39.
- MOTOROLA, *Telecommunications Device Data*, Motorola Semiconductor Products, Austin, TX, 1985.
- MUMFORD, W. W., and E. H. SCHEIBE, *Noise Performance Factors in Communication Systems*, Horizon House-Microwave, Dedham, MA, 1968.
- MURPHY, E., "Whatever Happened to AM Stereo?" *IEEE Spectrum*, vol. 25, March 1988, p. 17.
- NILSSON, J. W., *Electric Circuits*, 3rd ed., Addison-Wesley Publishing Company, Reading, MA, 1990.
- NORTH, D. O., "An Analysis of the Factors Which Determine Signal/Noise Discrimination in Pulsed-Carrier Systems," *RCA Technical Report*, PTR-6-C, June 1943; reprinted in *Proceedings of the IEEE*, vol. 51, July 1963, pp. 1016- 1027.
- NYQUIST, H., "Certain Topics in Telegraph Transmission Theory," *Transactions of the AIEE*, vol. 47, February 1928, pp. 617-644.
- OKUMURA, Y., and M. SHINJI (Guest Editors) Special Issue on Mobile Radio Communications, *IEEE Communications Magazine*, vol. 24, February 1986.
- OLMSTED, J. M. H., *Advanced Calculus*, Appleton-Century-Crofts, New York, 1961.
- O'NEAL, J. B., "Delta Modulation and Quantizing Noise, Analytical and Computer Simulation Results for Gaussian and Television Input Signals," *Bell System Technical Journal*, vol. 45, January 1966 (a), pp. 117-141.

- O'NEAL, J. B., "Predictive Quantization (DPCM) for the Transmission of Television Signals," *Bell System Technical Journal*, vol. 45, May-June 1966(b), pp. 689-721.
- OPPENHEIM, A. V., and R. W. SCHAFER, *Digital Signal Processing*, Prentice Hall, Upper Saddle River, NJ, 1975.
- OPPENHEIM, A. V., and R. W. SCHAFER, *Discrete-Time Signal Processing*, Prentice Hall, Upper Saddle River, NJ, 1989.
- PADGETT, J. E., C. G. GUNTHER, and T. HATTORI, "Overview of Wireless Personal Communications," *IEEE Communications Magazine*, vol. 33, no. 1, January 1995, pp. 28-41.
- PANCHA, P., and M. EL ZARKI, "MPEG Coding of Variable Bit Rate Video Transmission," *IEEE Communications Magazine*, vol. 32, no. 5, May 1994, pp. 54-66.
- PANDHI, S. N., "The Universal Data Connection," *IEEE Spectrum*, vol. 24, July 1987, pp. 31-37.
- PANTER, P. F., *Modulation, Noise and Spectral Analysis*, McGraw-Hill Book Company, New York, 1965.
- PAPOULIS, A., *Probability, Random Variables and Stochastic Processes*, McGraw-Hill Book Company, New York, 2nd ed., 1984, 3rd ed., 1991.
- PARK, J. H., JR., "On Binary DPSK Detection," *IEEE Transactions on Communications*, vol. COM-26, April 1978, pp. 484-486.
- PASUPATHY, S., "Correlative Coding," *IEEE Communications Society Magazine*, vol. 15, July 1977, pp. 4-11.
- PEEBLES, P. Z., *Communication System Principles*, Addison-Wesley Publishing Company, Reading, MA, 1976.
- PEEBLES, P. Z., *Digital Communication Systems*, Prentice Hall, Upper Saddle River, NJ, 1987.
- PEEBLES, P. Z., *Probability, Random Variables, and Random Signal Principles*, 2nd ed., McGraw-Hill Book Company, New York, 1993.
- PEEK, J. B. H., "Communications Aspects of the Compact Disk Digital Audio System," *IEEE Communications Magazine*, vol. 23, February 1985, pp. 7-15.
- PERSONICK, S. D., "Digital Transmission Building Blocks," *IEEE Communications Magazine*, vol. 18, January 1980, pp. 27-36.
- PETAJAN, E., "The HDTV Grand Alliance System," *Proceedings of the IEEE*, vol. 83, no. 7, July 1995, pp. 1094-1105.
- PETERSON, R. L., R. E. ZIEMER, and D. E. BORTH, *Introduction to Spread-Spectrum Communications*, Prentice Hall, Upper Saddle River, NJ, 1995.
- PETERSON, W. W., and E. J. WELDON, *Error-Correcting Codes*, MIT Press, Cambridge, MA, 1972.
- PETTIT, R. H., *ECM and ECCM Techniques for Digital Communication Systems*, Lifetime Learning Publications (a division of Wadsworth, Inc.), Belmont, CA, 1982.
- PRATT, T., and C. W. BOSTIAN, *Satellite Communications*, John Wiley & Sons, New York, 1986.
- PRITCHARD, W. L., and C. A. KASE, "Getting Set for Direct-Broadcast Satellites," *IEEE Spectrum*, vol. 18, August 1981, pp. 22-28.
- PROAKIS, J. G., *Digital Communications*, 3rd ed., McGraw-Hill Book Company, New York, 1995.
- QURESHI, S., "Adaptive Equalization," *IEEE Communications Magazine*, vol. 20, March 1982, pp. 9-16.
- RAMO, S., J. R. WHINNERY, and T. VANDUZER, *Fields and Waves In Communication Electronics*, 2nd ed., John Wiley & Sons, Inc., New York, 1984.
- RANA, A. H., J. MCCOSKEY, and W. CHECK, "VSAT Technology, Trends and Applications," *Proceedings of the IEEE*, vol. 78, July 1990, pp. 1087-1095.

- RAPPAPORT, T. S., "Characteristics of UHF Multipath Radio Channels in Factory Buildings," *IEEE Transactions on Antennas and Propagation*, vol. 37, August 1989, pp. 1058-1069.
- RAPPAPORT, T. S., *Wireless Communications, Principles and Practice*, Prentice-Hall PTR, Upper Saddle River, NJ, 1996.
- REEVE, W. H., *Subscriber Loop Signaling and Transmission Handbook*, IEEE Press, New York, 1995.
- RHEE, S. B., and W. C. Y. LEE (Editors), Special Issue on Digital Cellular Technologies, *IEEE Transactions on Vehicular Technology*, vol. 40, May 1991.
- RICE, S. O., "Mathematical Analysis of Random Noise," *Bell System Technical Journal*, vol. 23, July 1944, pp. 282-333, and vol. 24, January 1945, pp. 46-156; reprinted in *Selected Papers on Noise and Stochastic Processes*, N. Wax (Editor), Dover Publications, New York, 1954.
- RICE, S. O., "Statistical Properties of a Sine-Wave Plus Random Noise," *Bell System Technical Journal*, vol. 27, January 1948, pp. 109-157.
- ROCKWELL DEFENSE ELECTRONICS, *Collins Prop Man High Frequency Propagation Software*, Rockwell, Collins Avionics and Communications Division, Cedar Rapids, IA, 1995.
- ROOT, W. L., "Remarks, Most Historical, on Signal Detection and Signal Parameter Estimation," *Proceedings of the IEEE*, vol. 75, November 1987, pp. 1446-1457.
- ROSE, R. B., "MIMIMUF: A Simplified MUF-Prediction Program for Microcomputers," *QST*, vol. 66, December 1982, pp. 36-38.
- ROSE, R. B., "Technical Correspondence—MIMIMUF Revisited," *QST*, vol. 68, March 1984, p. 46.
- ROWE, H. E., *Signals and Noise in Communication Systems*, D. Van Nostrand Company, Princeton, NJ, 1965.
- RYAN, J. S. (Editor), Special Issue on Telecommunications Standards, *IEEE Communications Magazine*, vol. 23, January 1985.
- SABIN, W. E., and E. O. SCHOENIKE, *Single-Sideband Systems and Circuits*, McGraw-Hill Book Company, New York, 1987.
- SALTZBERG, B. R., T. R. HSING, J. M. CIOFFI, and D. W. LIN (Editors), Special Issue on High-Speed Digital Subscriber Lines, *IEEE Journal on Selected Areas in Communications*, vol. 9, August 1991.
- SCHARF, L. L., *Statistical Signal Processing: Detection, Estimation, and Time Series Analysis*, Addison-Wesley Publishing Company, Reading, MA, 1991.
- SCHAUMANN, R., M. S. GHASI and K. R. LAKER, *Design of Analog Filters*, Prentice Hall, Upper Saddle River, NJ, 1990.
- SCHILLING, D. L., R. L. PICKHOLTZ, and L. B. MILSTEIN, "Spread Spectrum Goes Commercial," *IEEE Spectrum*, vol. 27, August 1990, pp. 40-45.
- SCHILLING, D. L., L. B. MILSTEIN, R. L. PICKHOLTZ, M. KULLBACK, and F. MILLER, "Spread Spectrum for Commercial Communications," *IEEE Communications Magazine*, vol. 29, April 1991, pp. 66-67.
- SCHWARTZ, B. K., "The Analog Display Services Interface," *IEEE Communications Magazine*, vol. 31, April 1993, pp. 70-75.
- SCHWARTZ, M., W. R. BENNETT, and S. STEIN, *Communication Systems and Techniques*, McGraw-Hill Book Company, New York, 1966.
- SHANMUGAN, K. S., *Digital and Analog Communication Systems*, John Wiley & Sons, New York, 1979.
- SHANMUGAN, K. S., and A. M. BREIPOHL, *Random Signals: Detection, Estimation and Data Analysis*, John Wiley & Sons, New York, 1988.
- SHANNON, C. E., "A Mathematical Theory of Communication," *Bell System Technical Journal*, vol. 27, July 1948, pp. 379-423, and October 1948, pp. 623-656.

- SHANNON, C. E., "Communication in the Presence of Noise," *Proceedings of the IRE*, vol. 37, January 1949, pp. 10-21.
- SIMON, M. K., "Comments on 'On Binary DPSK Detection,'" *IEEE Transactions on Communications*, vol. COM-26, October 1978, pp. 1477-1478.
- SINNEMA, W., and R. MCPHERSON, *Electronic Communications*, Prentice Hall Canada, Inc., Scarborough, Ontario, Canada, 1991.
- SIPERKO, C. M., "LaserNet—A Fiber Optic Intrastate Network (Planning and Engineering Considerations)," *IEEE Communications Magazine*, vol. 23, May 1985, pp. 31-45.
- SKLAR, B., *Digital Communications*, Prentice Hall, Upper Saddle River, NJ, 1988.
- SLEPIAN, D., "On Bandwidth," *Proceedings of the IEEE*, vol. 64, no. 3, March 1976, pp. 292-300.
- SMITH, B., "Instantaneous Companding of Quantized Signals," *Bell System Technical Journal*, vol. 36, May 1957, pp. 653-709.
- SMITH, J. R., *Modern Communication Circuits*, McGraw-Hill Book Company, New York, 1986.
- SOLOMON, L., "The Upcoming New World of TV Reception," *Popular Electronics*, vol. 15, no. 5, May 1979, pp. 49-62.
- SPANIAS, A. S., "Speech Coding: A Tutorial Review," *Proceedings of the IEEE*, vol. 82, no. 10, October 1994, pp. 1541-1582.
- SPILKER, J. J., *Digital Communications by Satellite*, Prentice Hall, Upper Saddle River, NJ, 1977.
- STALLINGS, W., *Data and Computer Communications*, 4th ed., Macmillan Publishing Company, New York, 1994.
- STALLINGS, W., *ISDN and Broadband ISDN*, Macmillan Publishing Company, New York, 1992.
- STARK, H., F. B. TUTEUR, and J. B. ANDERSON, *Modern Electrical Communications*, Prentice Hall, Upper Saddle River, NJ, 1988.
- STIFFLER, J. J., *Theory of Synchronous Communication*, Prentice Hall, Upper Saddle River, NJ, 1971.
- STUMPERS, F. L., "Theory of Frequency—Modulation Noise," *Proceedings of the IRE*, vol. 36, September 1948, pp. 1081-1092.
- SUNDE, E. D., *Communications Engineering Technology*, John Wiley & Sons, New York, 1969.
- SWEENEY, P., *Error Control Coding*, Prentice Hall, Upper Saddle River, NJ, 1991.
- TAUB, H., and D. L. SCHILLING, *Principles of Communication Systems*, 2nd ed., McGraw-Hill Book Company, New York, 1986.
- THOMAS, J. B., *An Introduction to Statistical Communication Theory*, John Wiley & Sons, New York, 1969.
- THOMSON CONSUMER ELECTRONICS, Inc., *RCA Self-Installer Manual (for DSS Receiver System)*, Thomson Consumer Electronics, Inc., Indianapolis, IN, 1994.
- TURIN, G., "An Introduction to Digital Matched Filters," *Proceedings of the IEEE*, vol. 64, no. 7, July 1976, pp. 1092-1112.
- UNGERBOECK, G., "Channel Coding with Multilevel/Phase Signals," *IEEE Transactions on Information Theory*, vol. IT-28, January 1982, pp. 55-67.
- UNGERBOECK, G., "Trellis-Coded Modulation with Redundant Signal Sets," Parts 1 and 2, *IEEE Communications Magazine*, vol. 25, no. 2, February 1987, pp. 5-21.
- VAN DER ZIEL, A., *Noise in Solid State Devices and Circuits*, Wiley-Interscience, New York, 1986.
- VITERBI, A. J., "When Not to Spread Spectrum—A Sequel," *IEEE Communications Magazine*, vol. 23, April 1985, pp. 12-17.

- VITERBI, A. J., and J. K. OMURA, *Principles of Digital Communication and Coding*, McGraw-Hill Book Company, New York, 1979.
- WEI, L., "Rotationally Invariant Convolutional Channel Coding with Expanded Signal Space—Part II: Nonlinear Codes," *IEEE Journal on Selected Areas in Communications*, vol. SAC-2, no. 2, September 1984, pp. 672-686.
- WHALEN, A. D., *Detection of Signals in Noise*, Academic Press, New York, 1971.
- WHITTAKER, E. T., "On Functions Which Are Represented by the Expansions of the Interpolation Theory," *Proceedings of the Royal Society (Edinburgh)*, vol. 35, 1915, pp. 181-194.
- WIENER, N., *Extrapolation, Interpolation, and Smoothing of Stationary Time Series with Engineering Applications*, MIT Press, Cambridge, MA, 1949.
- WOZENCRAFT, J. M., and I. M. JACOBS, *Principles of Communication Engineering*, John Wiley & Sons, New York, 1965.
- WU, W. W., E. F. MILLER, W. L. PRITCHARD, and R. L. PICKHOLTZ, "Mobile Satellite Communication," *Proceedings of the IEEE*, vol. 82, no. 9, September 1994, pp. 1431-1448.
- WYLIE, C. R., JR., *Advanced Engineering Analysis*, John Wiley & Sons, New York, 1960.
- YOUNG, P. H., *Electronic Communication Techniques*, Merrill Publishing Co., Columbus, OH, 1990.
- XIONG, F., "Modern Techniques in Satellite Communications," *IEEE Communications Magazine*, vol. 32, no. 8, August 1994, pp. 84-98.
- ZIEMER, R. E., and R. L. PETERSON, *Digital Communications and Spread Spectrum Systems*, Macmillan Publishing Company, New York, 1985.
- ZIEMER, R. E., and W. H. TRANTER, *Principles of Communications*, 3rd ed., Houghton Mifflin Company, Boston, 1990.
- ZIEMER, R. E., W. H. TRANTER, and D. R. FANNIN, *Signals and Systems*, Macmillan Publishing Company, New York, 1st ed., 1983, 2nd ed., 1989.
- ZOU, W. Y., "Comparison of Proposed HDTV Terrestrial Broadcasting Systems," *IEEE Transactions on Broadcasting*, vol. 37, December 1991, pp. 145-147.

# ANSWERS TO SELECTED PROBLEMS

## Chapter 1

**1-5** 1.97 bits

**1-9**  $H = 3.084$  bits

**1-11**  $H = 3.32$  bits,  $T = 1.66$  s

## Chapter 2

**2-9** 36 dB

**2-10** (a)  $4.08 \times 10^{-14}$  W      (b) -103.9 dBm      (c)  $1.75 \mu\text{V}$

**2-16**  $S(f) = -\frac{A}{\omega^2} + Ae^{-j\omega T_0} \left( \frac{1}{\omega^2} + j\frac{T_0}{\omega} \right)$ , where  $\omega = 2\pi f$ .

Note that  $S(0) = AT_0^2/2$ .

**2-40** (a)  $(\sin 4t)/(4t)$       (b) 7

**2-45** (a)  $-0.4545A$       (b)  $0.9129A$

- 2-47** (a)  $(A_1 + A_2)/\sqrt{2}$       (b)  $(\sqrt{A_1^2 + A_2^2})/\sqrt{2}$       (c)  $|A_2 - A_1|/\sqrt{2}$   
 (d)  $(\sqrt{A_1^2 + A_2^2})/\sqrt{2}$       (e)  $(\sqrt{A_1^2 + A_2^2})/\sqrt{2}$

$$\mathbf{2-56} \quad c_n = \begin{cases} \frac{AT^2}{2T_0}, & n = 0 \\ \frac{A\{e^{-j2\pi nT/T_0}[1 + j2\pi n(T/T_0)] - 1\}}{(2\pi n)^2/T_0}, & n \neq 0 \end{cases}$$

$$\mathbf{2-62} \quad c_n = \begin{cases} 0, & n = \text{even} \\ \frac{4}{n^2\pi^2}, & n = \text{odd} \end{cases}$$

- 2-82** (a) 6.28 msec      (b) 160

## Chapter 3

$$\mathbf{3-3} \quad \text{(a)} \quad W_s(f) = d \sum_{n=-\infty}^{\infty} \frac{\sin \pi n d}{\pi n d} \begin{cases} 1, & |f - nf_s| \leq 2500 \\ \frac{-1}{1500} (|f - nf_s| - 4000), & 2500 \leq |f - nf_s| \leq 4000 \\ 0, & f \text{ elsewhere} \end{cases}$$

where  $d = 0.5$  and  $f_s = 10,000$

$$\mathbf{3-3} \quad \text{(b)} \quad W_s(f) = 0.5 \left( \frac{\sin \pi \tau f}{\pi \tau f} \right) \sum_{k=-\infty}^{\infty} \begin{cases} 1, & |f - kf_s| \leq 2500 \\ \frac{-1}{1500} (|f - kf_s| - 4000), & 2500 \leq |f - kf_s| \leq 4000 \\ 0, & f \text{ elsewhere} \end{cases}$$

where  $\tau = 50 \times 10^{-6}$  and  $f_s = 10,000$

$$\mathbf{3-7} \quad W_s(f) = -j \left( \frac{1 - \cos(\pi f/f_s)}{\pi f/f_s} \right) \times \sum_{k=-\infty}^{\infty} \begin{cases} 1, & |f - kf_s| \leq 2500 \\ \frac{-1}{1500} (|f - kf_s| - 4000), & 2500 \leq |f - kf_s| \leq 4000 \\ 0, & f \text{ elsewhere} \end{cases}$$

- 3-9** (a) 200 samples/s      (b) 9 bits/word      (c) 1.8 kbits/s      (d) 900 Hz  
**3-15** (a) 5 bits      (b) 27 kHz

$$\mathbf{3-25} \quad \text{(a)} \quad \mathcal{P}(f) = \frac{A^2 T_b}{4} \left[ \frac{\sin(\frac{1}{2}\pi f T_b)}{\frac{1}{2}\pi f T_b} \right]^2$$

$$\text{(b)} \quad \mathcal{P}(f) = \frac{A^2 T_b}{4} \left[ \frac{\sin(\frac{1}{4}\pi f T_b)}{\frac{1}{4}\pi f T_b} \right]^2 [\sin(\frac{1}{4}\pi f T_b)]^2$$

- 3-35** (a) 32.4 kbit/s      (b) 10.8 ksymbols/s      (c) 5.4 kHz  
**3-36** (a) 3.2 ksymbols/s      (b) 0.5  
**3-46** (a) 5.33 kbit/s      (b) 667 Hz  
**3-47** (a) 10.7 kbit/s      (b) 1.33 kHz  
**3-54** (a) 0.00534      (b) 0.427  
**3-62** (a) 13.896      (b) 5095      (c) 1273      (d) 159      (e) 23  
**3-66** (a) 40 Hz      (b) 1280 Hz

**Chapter 4**

- 4-9** (a)  $g(t) = 500 + 200 \sin \omega_a t$ , AM,  $m(t) = 0.4 \sin \omega_a t$   
 (b)  $x(t) = 500 + 200 \sin \omega_a t$ ,  $y(t) = 0$   
 (c)  $R(t) = 500 + 200 \sin \omega_a t$ ,  $\theta(t) = 0$   
 (d) 2.7 kW  
**4-20** 48.3%  
**4-23**  $K \sqrt{m^2(t) + [\hat{m}(t)]^2}$ , yes  
**4-28** (a)  $(j2\pi f)/[j2\pi f + K_d K_v F_1(f)]$       (b)  $(j2\pi f)(f_1 + jf)/[j2\pi f(f_1 + jf) + K_d K_v f_1]$   
**4-35** (a) 107.6 MHz      (b) RF: At least 96.81-96.99 MHz; IF: 10.61-10.79 MHz  
 (c) 118.3 MHz

**Chapter 5**

- 5-1** (a) 6.99 dBk      (b) 707 V      (d) 7025 W      (e) 18,050 W  
**5-6**  $S(f) = \frac{1}{2} \left[ \sum_{n=-\infty}^{\infty} c_n \delta(f - f_c - nf_m) + \sum_{n=-\infty}^{\infty} c_n^* \delta(f + f_c + nf_m) \right]$   
 where  $c_n = \frac{A_c}{2\pi} \left[ 2\theta_1 \left( \frac{\sin n\theta_1}{n\theta_1} \right) + 2A_m \frac{\cos n\theta_1 \sin \theta_1 - n \sin n\theta_1 \cos \theta_1}{1 - n^2} \right]$ ,  
 $A_m = 1.2$ , and  $\theta_1 = 146.4^\circ$   
**5-7** (a)  $s(t) = (\cos \omega_1 t + 2 \cos 2\omega_1 t) \cos \omega_c t$ , where  $\omega_1 = 1000\pi$   
 (b)  $S(f) = \frac{1}{4} [\delta(f - f_c + f_1) + \delta(f + f_c - f_1) + \delta(f - f_c - f_1) + \delta(f + f_c + f_1)] + \frac{1}{2} [\delta(f - f_c + 2f_1) + \delta(f + f_c - 2f_1) + \delta(f - f_c - 2f_1) + \delta(f + f_c + 2f_1)]$   
 (c) 1.25 W      (d) 4.5 W

- 5-14** (b)  $s(t) = \Pi(t) \cos \omega_c t - \frac{1}{\pi} \ln \left( \frac{|t + \frac{1}{2}|}{|t - \frac{1}{2}|} \right) \sin \omega_c t$   
 (c)  $\max[s(t)] = \infty$   
**5-24** (a)  $f_{BPF} = 12.96$  MHz,  $B_{BPF} = 48.75$  kHz      (b) 7.96 or 17.96 MHz  
 (c) 9.38 kHz  
**5-26** (a)  $m(t) = 0.2 \cos(2000\pi t)$ ,  $M_p = 0.2$  V,  $f_m = 1$  kHz  
 (b)  $m(t) = -0.13 \sin(2000\pi t)$ ,  $M_p = 0.13$  V,  $f_m = 1$  kHz  
 (c)  $P_{AV} = 2500$  W,  $P_{PEP} = 2500$  W  
**5-31**  $S(f) = \frac{1}{2} [G(f - f_c) + G^*(-f - f_c)]$ , where  
 $G(f) = \sum_{n=-\infty}^{\infty} J_n(0.7854) \delta(f - nf_m)$ ,  $f_c = 146.52$  MHz,  
 and  $f_m = 1$  kHz.  $B = 3.57$  kHz

- 5-35**  $S(f) = \frac{1}{2} [\sum_{n=-\infty}^{\infty} c_n \delta(f - f_c - nf_m) + \sum_{n=-\infty}^{\infty} c_n^* \delta(f + f_c + nf_m)]$ , where  
 $c_n = 5(e^{j\beta} - 1) \left( \frac{\sin(n\pi/2)}{n\pi/2} \right)$ ,  $f_m = 1$  kHz,  $\beta = 0.7854$ , and  $f_c = 60$  MHz  
**5-39** (a) 5.5 Hz  
 (b)  $S(f) = \frac{A_c}{2} \left\{ \delta(f - f_c) + \delta(f + f_c) + \frac{D_f}{2\pi} \sum_{n=-\infty}^{\infty} \left( \frac{c_n}{nf_m} \right) \times [\delta(f - f_c - nf_m) - \delta(f + f_c - nf_m)] \right\}$ ,

- where  $c_n = 5e^{-jn\pi/2} \left( \frac{\sin(n\pi/2)}{n\pi/2} \right)$  ( $n \neq 0$ ),  
 $D_f = 6.98$  rads/V-sec,  $f_m = 100$  Hz, and  $f_c = 30$  MHz  
**5-42**  $\mathcal{P}(f) \approx 0.893 [2\delta(f - f_c + 5f_0) + \delta(f - f_c + 3f_0) + \delta(f - f_c - 5f_0) + 2\delta(f + f_c - 5f_0) + \delta(f + f_c - 3f_0) + \delta(f + f_c + f_0) + 2\delta(f + f_c + 3f_0) + \delta(f + f_c + 5f_0)]$

where  $f_0 \triangleq \frac{D_f}{2\pi} = 15.9$  kHz and  $f_c = 2$  GHz

- 5-45** (a) 20 kHz  
 (b)  $S(f) = \frac{1}{2} [M_1(f - f_c) + M_1(f - f_c)] + \frac{j}{2} [M_2(f + f_c) - M_2(f - f_c)]$   
**5-46** (a)  $S(f) = \frac{1}{2} [X(f - f_c) + X^*(-f - f_c)]$ ,  
 where  $X(f) = \frac{A_c}{2} \sum_{n=-\infty}^{\infty} \left( \frac{\sin(n\pi/2)}{n\pi/2} \right) \delta(f - \frac{1}{2}nR)$ ,  $R = 2400$   
 (b) 4.8 kHz  
**5-53** (a) 3.6 kHz      (b) 8.6 kHz

**Chapter 6**

- 6-2** (a)  $\bar{x} = (2\sqrt{2} A/\pi) \cos(\omega_0 t + \pi/4)$       (b)  $x(t)$  is not stationary  
**6-4**  $2/\sqrt{\pi} = 1.128$   
**6-8** (a) 15 W      (b) 11 W      (c) 19 W  
**6-10** (a) No      (b) Yes      (c) Yes      (d) No  
**6-17** (a)  $\sqrt{B}$       (b)  $R_x(\tau) = B[(\sin \pi B\tau)/(\pi B\tau)]^2$   
**6-22** (a)  $N_0 K^2/(8\pi^2 f^2)$       (b)  $\infty$   
**6-25**  $1/(2\pi f_0)$   
**6-30** (a)  $H(f) = 10 \left| \left[ \left( 1 + j \frac{f}{f_0} \right)^2 \right] \right|^2$   
 (b)  $0.690 f_0$ , where  $f_0 = 1/(2\pi RC)$

**6-35** (a) Not WSS      (b)  $\mathcal{P}_x(f) = \frac{A_0^2}{4} [\delta(f - f_0) + \delta(f + f_0)]$       (c) Yes

**6-42**  $x(t) = m_1(t) + m_2(t)$ ,  $y(t) = \hat{m}_1(t) - \hat{m}_2(t)$

$$\mathcal{P}_{m_1}(f) = A\Pi\left(\frac{f}{2(f_3 - f_c)}\right), \mathcal{P}_{m_2}(f) = A\Lambda\left(\frac{f}{f_c - f_1}\right)$$

**6-44**  $\mathcal{P}_v(f) = \frac{1}{4}[\mathcal{P}_x(f - f_c) + \mathcal{P}_x(-f - f_c)],$

where  $\mathcal{P}_x(f) = T_b \left( \frac{1 - \cos \pi f T_b}{\pi f T_b} \right)^2$

**6-50** (a)  $y(t) = \begin{cases} \frac{1}{2}, & t = 0 \\ 1, & 0 < t < T \\ \frac{1}{2}, & t = T \\ 0, & t \text{ elsewhere} \end{cases}$       (b) Same pulse shape answer for part (a)

## Chapter 7

**7-1**  $P_e = \frac{1}{2} e^{-\chi^2 A/\sigma_0}$

**7-11**  $P_e = Q(\sqrt{0.7992(E_b/N_0)})$

**7-14** (a)  $H(f) = T e^{-j\pi f T} \left( \frac{\sin \pi f T}{\pi f T} \right)$       (b)  $B_{eq} = 1/(2T)$

**7-16**  $P_e = P(1)Q\left(\sqrt{\frac{2(-V_T + A)^2 T}{N_0}}\right) + P(0)Q\left(\sqrt{\frac{2(V_T + A)^2 T}{N_0}}\right)$

**7-21** (a)  $5 \times 10^{-7}$       (b)  $4.42 \times 10^{-2}$

**7-22** (a) 2400 bits/s      (b)  $(P_e)_{\text{overall}} = 1.11 \times 10^{-14}$

**7-27**  $3.2 \times 10^{-7}$

**7-31** (a) 4800 bits/s      (b) 19,943 bits/s

**7-32** (a)  $9.09 \times 10^{-4}$       (b) 29.1 dB

**7-35** 11.3 dB inferior

**7-42**  $-100.9 \text{ dBm}$

**7-47** (a) 651%      (b) Low-frequency components predominate

**7-49**  $(S/N)_{\text{out}} = (5 \times 10^{-5})(P_s/N_0)$  for all five channels

## Chapter 8

**8-9** (a) 25.6 dB      (b) 36.3 W      (c)  $-54.9 \text{ dBm}$

**8-13**  $G_a = \frac{h_{re}^2 R_s}{h_{oe}(R_s + h_{ie})^2}$

**8-17** (a) 129 K      (b)  $-76.6 \text{ dBm}$

**8-19**  $3.2 \times 10^{-7}$

**8-22** (a) 19.8 dB      (b) 7.52 dB      (c) 4.67 dB

**8-34** 12.84-m diameter

**8-40** 20.6 kW

## Appendix B

**B-1** 0.3486

**B-2** (a) 5/36      (b) 15/36

**B-4** (a) 1/2      (b) 1/3

**B-8** 0.4375

**B-11** (a)  $b$       (b)  $1/b$       (c)  $1/b^2$

**B-21** 51.0

**B-26** (a)  $1.337 \times 10^{-11}$       (b) 0.9520

**B-30**  $f(y) = \begin{cases} \frac{1}{2\sigma\sqrt{2\pi y}} [e^{-(y-x-m)^2/(2\sigma^2)} + e^{-(y+x-m)^2/(2\sigma^2)}], & y \geq 0, \\ 0, & y < 0 \end{cases}$

**B-35**  $B\sigma/\sqrt{2\pi}$

**B-37** (a) 1/6      (b) Yes      (c) 1/12

(d)  $f(x_2|x_1) = \begin{cases} \frac{1}{12} (1 + x_2), & 0 \leq x_1 \leq 1, \quad 0 \leq x_2 \leq 4 \\ 0, & \text{otherwise} \end{cases}$

**B-46** (a)  $f_y(y) = \int_{-\infty}^{\infty} \frac{1}{|Ax|} f_i\left(\frac{y}{Ax}, x\right) dx$

(b)  $f_v(y) = \int_{-\infty}^{\infty} \frac{1}{|Ax|} f_{i_1}\left(\frac{y}{Ax}\right) f_{i_2}(x) dx$

# INDEX

## A

A priori probabilities, 461  
 Absolute bandwidth, 101  
 Acoustic coupler, 698  
 Active filter, 243–244  
 ACU, 698  
 Adaptive delta modulation, 193–194  
 Adaptive equalizing filter, 178, 698  
 Address resolution protocol (TCP/IP), 698  
 Advanced mobile phone system (AMPS), 584–585  
 Aliasing, 91  
     discrete Fourier transform, 96  
     PAM, 132  
 Allocations, frequency, 9–10.  
 ALOHA packet data transmission, 559  
 AM to PM conversion, 237  
 Amplifier, 246–247  
     bandpass, 249–252, 284

classes A,B,C,D,E,G,T, and S, 251–252  
 IF, 279–282  
     nonlinear, 247–252  
     output, 284  
 Amplitude modulation (AM), 296–302  
     broadcast standards, 301–302  
     complex envelope, 231–232, 296  
     detector. *See Envelope detector and Product detector*  
     generation of, 299–301  
     modulation efficiency, 298–299  
     power, 235, 298  
     signal-to-noise, 497–499  
     spectrum, 235, 298  
     stereo transmission, 302  
 Amplitude response, linear system, 80  
 Amplitude shift keying (ASK). *See On-off keying*  
 Amplitude spectrum, 44, 80  
     *See also Spectrum*

## Index

Analog:  
     cellular telephone, 584–586  
     source, 2  
     switching (telephone), 542  
     system, 5  
     waveform, 5  
 Analog subscriber loop, 537, 543  
 Analog-to-digital converter (ADC)  
     counting or ramp, 140–141  
     parallel or flash, 140–141  
     serial, 140  
     types, 140  
     *See also Pulse code modulation*  
 Analytic function, 86  
 Angle modulation, 311–326  
     *See also Frequency modulation*  
     *See also Phase modulation*  
 ANSI, 680  
 Answers to selected problems, 714–719  
 Antennas, 561–562  
     effective area, 562  
     gain, 561–562  
 Aperture  
     antenna, 562  
     PAM, 135  
 Aperiodic waveform, 36  
 Arbitrary waveform generator, 276–277  
 Armstrong FM method, 321  
 ASCII code, 679  
 Aspect ratio, 592, 608  
 ASR, definition, 698  
 Asymptotically unbiased estimate, 404  
 Asynchronous digital line, 200  
 Asynchronous transfer mode (ATM), 692  
 AT&T FT-2000 fiber optic system, 581–582  
 AT&T TDM hierarchy, 203–204  
 Attenuator:  
     effective input-noise temperature, 570  
     noise figure, 570  
 Audio mixer, 255  
 Autocorrelation function, 386, 390  
     bandpass process, 418–428  
     complex random process, 390  
     filter output, 406  
     for white process, 402, 417  
     properties, 387  
     time average, 63  
     Wiener-Khintchine theorem, 63, 392  
 Automatic gain control (AGC), 497–498  
 Automatic repeat request (ARQ), 19, 690, 698  
 Automatic test equipment (ATE), 683  
 Autoregressive-moving average (ARMA), 404  
 Available noise power, 564  
 Available power gain, 566, 571  
 Avalanche photodiode (APD), 580

Average:  
     dc value, 36  
     effective input-noise temperature, 568  
     ensemble, 385, 645  
     information, 17  
     noise figure, 567  
     power, 37, 63, 233, 405  
     time, 35  
 Average effective input-noise temperature, 568  
 Average noise figure, 567  
 Average power, 37, 63, 405  
     AM signal, 298–299  
     bandpass signal, 233  
     SSB signal, 306–307

## B

Balanced FM detector, 264  
     discriminator, 265, 267, 494  
 Balanced modulator, 258  
 Balanced signaling, 683  
 Bandlimited waveforms, 86  
 Bandlimited white process, 417  
 Bandpass:  
     channel, 8, 226–229  
     definition, 227  
     dimensionality theorem, 241  
     distortionless transmission, 238–240  
     filter, 236–240  
     limiter, 252–253  
     random process, 418–430  
     representation, 226–229  
     sampling theorem, 240–241  
     signal power, 233  
     spectrum, 230–233  
     waveform, 226–229  
 Bands, frequency, 11–12  
 Bandwidth, 101–109  
     absolute, 101  
     AM signal, 299  
     analog systems, 513  
     bounded spectrum, 105  
     BPSK signal, 107  
     coding, 27–30  
     digital systems, 488  
     equivalent, 103, 411  
     FCC, 105  
     FM, 317  
     multilevel signal, 175  
     noise, 103, 411  
     null-to-null, 103  
     PCM, 141–143  
     PM, 317  
     power, 105

Digital modulation:  
*See* Digital signaling  
 Digital modulation index, 336  
 Digital receivers:  
*See also* Probability of bit error  
 Digital satellite system (DSS), 551–552  
 Digital signaling, 148–156  
   bandwidth estimation, 151  
   baseband signal PSD, 400  
   binary, 152–154  
   bipolar, 157–158, 164  
   BPSK, 332, 336–337  
   cellular telephone, 587  
   condition for discrete spectra, 402  
   DPCM, 185–188  
   DPSK, 482–484  
   DS-1, DS-2, etc. data lines, 204–205  
   FSK, 332, 338–345  
   ISDN, 543–547  
   Manchester, 157–158, 165  
   MPSK, 345–346  
   MSK, 352–357  
   multilevel bandpass, 345–351  
   multilevel baseband, 154–157, 173–175  
   NRZ, 157–158  
   OOK, 332–336  
   OQPSK, 348  
   Polar, 157–158, 163  
   QAM, 346–348  
   QPSK, 345–346  
   RZ, 157  
   SONET, 208  
   telephone standards, 203–209, 543–547  
   unbalanced, 348  
   unipolar, 157–158, 161, 163  
   vector representation, 150–151  
 2B1Q, 545–546  
 8VSB, 608  
*See also* Pulse code modulation  
 Digital subscriber line, 543–547  
 Digital switching (telephone), 542  
 Digital-to-analog converter (DAC), 140–141  
   multilevel signaling, 345–346  
 Dimensionality theorem, 92–93  
   bandpass, 241  
 Dirac delta function, 51, 629–631  
   even-sided, 629–630  
   impulse response, 79, 81  
   left-sided, 630  
   properties of, 630–631  
   spectrum, 61  
 Direct broadcast satellite, 551–560  
 Direct digital synthesis (DDS), 276–277  
 Direct method for FM, 322  
 Direct sequence spread spectrum, 358–364  
*See also* Spread spectrum

Direct-conversion receiver, 280  
 Dirichlet conditions, 45  
 Discontinuous phase FSK, 338  
 Discrete cosine transform, 607  
 Discrete Fourier transform (DFT), 93–101  
   evaluation of PSD, 403–404  
   general result, 95  
   MathCAD, 94  
   MATLAB, 94, 98–99, 102–104  
   periodic waveforms, 100  
   selection of parameters, 97  
 Discrete random process, 383  
 Discrete random variables, 642  
 Discrete random variables  
   CDF of, 645  
   ensemble average of, 646  
   PDF of, 644  
 Discriminator, frequency, 265, 267, 494  
 Distortion:  
   cross modulation, 250–251  
   harmonic, 248  
   intermodulation, 248–250  
   linear, 83–84  
   nonlinear, 247–252  
   third-order, 249–251  
 Distortionless transmission, 83–84, 238–240  
   bandpass, 238–240  
   channel, 83  
 Distribution:  
   binomial, 649–652  
   continuous, 642  
   discrete, 642  
   Gaussian, bivariate, 666  
   Gaussian, N-dimensional, 413–417  
   Gaussian, one-dimensional, 653–657  
   Laplacian, 524  
   mixed, 644  
   N-dimensional, 663  
   Poisson, 652  
   Rayleigh, 429–430, 477–478  
   Rician, 455, 478  
   sinusoidal, 657  
   uniform, 652  
 Dolby noise reduction, 329–332  
 Double balanced mixer, 258  
 Double-sideband suppressed carrier (DSB-SC), 302–303  
   complex envelope, 231–232  
   demodulation of, 303–304  
   signal-to-noise, 499–500  
 Doubler stage, 261  
 Down converter, 253–259, 284  
   output, 284  
 DS-1, DS-2, DS-3, etc. lines, 204–205  
 DTE/DCE interface, 678–686, 699  
 Dual tone multiple frequency (DTMF), 539

Dual-conversion receiver, 279  
 Duplex, half and full, 700  
  
**E**  
 Early-late bit synchronizer, 172  
 $E_b$ , 467, 468, 470, 472, 473, 476, 480, 482  
 $E_b/N_0$ , 574–575  
   link budget evaluation, 574–575  
 Echo check, 699  
 Echo suppressor (hybrid), 700, 540–541  
 $E_s/N_0$ , 464  
 Effective input-noise temperature, 568  
   attenuator, 570  
   average, 568  
   cascaded linear devices, 572  
   spot, 568  
   transmission line, 570  
 Effective isotropic radiated power (EIRP), 560–561  
 Effective radiated power (ERP), 593–594  
 Efficiency:  
   conversion efficiency, 299  
   modulation, 298–299  
   spectral, 176, 350–351  
 EIA, 680  
 Electromagnetic spectrum, 11–12  
 Electromagnetic wave propagation, 10–16  
 Electronic service number (ESN), 586  
 Electronic switching system (ESS), 542  
 Encoder:  
   ADC, 140–141  
   DAC, 141  
 Energy calculation, from waveform, 40  
 Energy signal, 35, 40  
 Energy spectral density (ESD), 48  
 Ensemble average  
   autocorrelation, 386, 390  
   mean, 647, 665  
   N-dimensional, 663  
   one-dimensional, 385, 645  
   nth moment, 647  
   standard deviation, 647  
   variance, 647  
 Ensemble of events, 382–383  
*See also* Random processes  
 Entropy, 17  
 Envelope:  
   complex, 228, 231  
   real, 261–262, 428–430  
   *See also* Complex envelope  
 Envelope delay, 238–240, 700  
 Envelope detector, 261–262, 428–430  
   output, 284  
   PDF out, 429–430  
   with Gaussian input, 428–430

Equalizing filter, 178  
   adaptive, 178, 698  
   PAM, 135  
 Equally likely, 461  
 Equivalent bandwidth, 103, 411  
   RC low-pass filter, 413  
 Equivalent low-pass filter, 236–238, 290–291  
*erf(x) function, See Q(z) function*  
*erfc(x) function, See Q(z) function*  
 Ergodic random process, 385  
 Error, quantizing, 137  
 Error correction codes. *See Coding*  
 Error function, *See Q(z) function*  
 Error probability, *See Probability of bit error*  
 Error rate, *See Probability of bit error*  
 Estimation of PSD, 403–404  
 Ethernet, 684–685, 688  
 Euler's theorem, 620  
 Even-sided delta function, 629–630  
 Event:  
   compound, 636  
   independent, 638  
   null, 637  
   simple, 636  
   sure, 637  
 Expandor, 148  
*See also Companding*  
 Expected value  
   N-dimensional, 663  
   one-dimensional, 646  
*See also Ensemble average*  
 Extremely high frequency (EHF), 12  
 Eye pattern, 167–168  
  
**F**  
 Fading channels, 9  
 False frame sync, 198  
 Fast frequency-shift keying (FFSK), 353  
 FCC bandwidth, 105  
 FDDI, 700  
 Federal Communication Commission (FCC), 10  
*See also Standards*  
 Feedback communications, 21, 690, 698  
 Feedback demodulators:  
   Costas PLL, 303–304  
   FMFB receiver, 508–509  
   PLL, 269–276  
 Fiber optic systems, 580–582  
   FT-2000, 581–582  
   SONET, 208  
 Field intensity, 562  
 Field rate, television, 591, 592, 605, 608  
 Filter:  
   active, 243–244

Filter (*cont.*)  
 bandpass, 236–240  
 Bessel, 245–246  
 Butterworth, 245–246  
 cavity, 244–245  
 ceramic, 243–244  
 Chebyshev, 245–246  
 correlation, 437–438  
 crystal, 243–244  
 equalizing, 135, 178  
 integrate-and-dump, 436  
 intersymbol interference, 176–185  
 LC, 243–244  
 linear, 78–85  
 linear prediction, 185  
 matched, 430–441  
 mechanical, 243–244  
 nonlinear, 247–252  
 Nyquist, 182–184  
 passive, 243–244  
 PLL tracking, 269  
 prediction for DPCM, 185  
 prewhitening, 464–465  
 raised cosine-rolloff, 180–184  
 RC low pass, 81–82, 409  
 surface acoustic wave, 244–245  
 transmission line, 244–245  
*See also* Linear filter

Fixed assigned multiple access (FAMA), 554–557  
 Flash ADC, 140–141  
 Flat-top PAM, 133–136  
 Flow control, *See* CA of RS-232C circuit, 681–682, 700  
 FM detector, *See* Detector  
 FMFB receiver, 508–509  
 Formats, digital signal, 157–158  
 Forward error correction (FEC), 19, 21–30  
*See also* Coding  
 Four-quadrant multiplier, 256, 258  
 Four-wire circuit, 540–541  
 Fourier series, 68–78  
   complex, 68–70  
   MATLAB, 100–104  
   polar, 71–73  
   properties, 69–70  
   quadrature, 70–71  
   via DFT, 100–104  
 Fourier transform:  
   definition, 44  
   discrete, 93–104  
   discrete cosine, HDTV, 607  
   MATLAB, 94–99  
   properties, 46–47  
   table, 61  
   theorems, 50  
 Frame rate, television, 591, 592, 605, 608

Frame synchronization, 196–200, 489  
 Free space intrinsic impedance, 562  
 Free space loss, 563, 574  
 Frequency:  
   allocations, 11–12  
   carrier, 227, 228, 230  
   definition, 44, 312  
   IF, 279–282  
   instantaneous, 264, 312  
   spectrum, 44  
*See also* Standards  
 Frequency demodulation, *See* Detector  
 Frequency deviation, 313  
 Frequency-division multiple access (FDMA), 553  
 Frequency division multiplexing (FDM), 326–328, 534–536  
 Frequency hopped spread spectrum, 364–366  
*See also* Spread spectrum  
 Frequency modulation (FM), 311–326  
   bandwidth of, 317, 342  
   Bessel functions, 317–319  
   Carson's rule, 317, 342  
   circuit, 313, 321–322  
   complex envelope, 231–232, 311  
   detector, 264–269, 274–275, 494  
   direct generation, 322  
   FCC channels, 330  
   frequency multiplier, 259–261, 284  
   index, 315, 330  
   indirect generation, 321  
   narrowband, 321–322  
   preemphasis and deemphasis, 325–326, 509–511  
   properties, 324  
   quadrature detector, 266–268  
   receiver with feedback, 508–509  
   representation of, 229–233, 311–326  
   signal-to-noise, 509–511  
   standards, 329–330  
   stereo, 326–328, 596  
   threshold extension, 579–580  
   transmitter, 367, 373  
   TV audio, 592, 605, 608  
   wideband, 322–324  
*See also* Detector  
*See also* Digital signaling  
 Frequency multiplier, 259–261, 284  
   output, 284  
 Frequency response, linear system, 80  
 Frequency-shift keying (FSK), 332, 338–345  
   Bell 103 modem, 339–342, 695, 780  
   detector, 345  
   noncoherent detection, 480–482  
   orthogonal signaling, 476  
   probability of bit error, 474, 476, 482  
   spectrum, 343–344  
 Frequency synthesizer, 276–277

Frequency translation, 50, 253–259  
 Friis' theorem:  
   noise, 571  
   signal, 563  
 Front-end processor, 700  
 FT-2000 fiber optic system, 581–582  
 FTP files, 7  
 Full duplex, 700  
 Function:  
   analytic, 86  
   autocorrelation, 63, 386, 390  
   bandlimited, 86  
   Bessel, 317–319, 455  
   CDF, 639, 663  
   crosscorrelation, 388, 390  
   Dirac delta, 51, 629–631  
   frequency response, 80  
   impulse response, 79, 81  
   Kronecker delta, 65–66  
   linear system output, 80  
   orthogonal, 65  
   orthonormal, 66  
   PDF, 640, 663  
   power transfer, 81  
   Q(z), 632–633, 655–657  
   rectangular pulse, 54  
   Sa(x), 54, 631  
   sinc, 54  
   transfer, 80  
   triangular pulse, 54  
   unit step, 51  
 Function generator, 276–277  
 Functional transformation:  
   N-dimensional PDF, 666–667  
   one-dimensional, 658

**G**

Gain:  
   antenna, 561–562  
   coding, 25, 26, 28  
   dB, 41  
   power, 81, 407  
   processing, 364  
 Galaxy satellite, 575–580  
 Gateway, 700  
 Gating, 129–133  
 Gaussian:  
   area under PDF, 632–633, 655–657  
   bivariate PDF, 666  
   CDF, 655  
   mean, 654  
   N-dimensional PDF, 413–417  
   one-dimensional PDF, 653  
   properties, 415

random process, 413–417  
 random variable, 653–657, 666  
 variance, 654  
 General purpose interface bus (GPIB), 683, 687–688  
 Geosynchronous orbit (GEO), 547  
 Globalstar satellite, 560  
 Glossary, computer communications, 698–702  
 Granular noise, DM, 190–193  
 Graph, Q(z) function, 656  
 Gray code, 140  
 Ground wave propagation, 12–13,  
 Group delay, 239  
 Group FDM signal, 534–536  
 GSM cellular telephone, 587

**H**

Half duplex, 700  
 Half-power bandwidth, 101  
 Half-wave linear rectifier, 660  
 Hamming weight, 21  
 Hard decision, 23, 28  
 Hard limiter, 252–253, 284  
 Hardwire channel, 9  
 Harmonic distortion, 248  
 Hartley, 16  
 HDLC protocol, 690  
 High Earth orbit (HEO) satellites, 559–560  
 High-definition television (HDTV), 605–609  
 High-level modulation, 299  
 Hilbert transform, 305  
   table of, 629  
   used in SSB, 231–232, 305–308, 423–424  
 History of communication, 2–4  
 Hold-in range, PLL, 270  
 Horizontal resolution, television, 592, 593, 605, 608  
 HP interface bus, 683, 687–688  
 Hybrid (telephone) network, 540, 541, 562, 700

**I**

I channel, 229, 231, 278, 282  
 Ideal communication system, 18–19, 26, 514  
 Ideal envelope detector, 261–262, 428–430  
 Identities, trigonometric, 620–621  
 IEEE, 680, 683  
 IEEE 802.3 (Ethernet), 684–685, 688  
 IEEE-488 interface, 683, 687–688  
 Image response, 280–282  
 Immarstat satellite, 560  
 Impulse:  
   function, 51, 629–631  
   response, 79, 81  
   sampling, 89–92

In-phase component, 229, 231, 278, 282  
television, 597

Inconsistent estimate, 404

Indefinite integrals, 623–626

Independent:  
events, 638  
random variables, 664

Independent sideband (ISB), *See* Single sideband

Indeterminate forms, 623

**Index:**  
digital modulation, 336  
frequency modulation, 315, 330  
percent AM, 297  
phase modulation, 315

Indirect method for FM, 321

Information, 16–18  
analog, 2  
average, 17  
bits, 16  
capacity, 18, 514  
digital, 2, 16  
entropy, 17  
rate, 18  
sink, 2, 8  
source, 2, 8

Injection locking, 274

Input-noise temperature, cascaded devices, 572

Input-output relationships, linear systems, 406–411

Instantaneous frequency, 312

Instantaneous sample PAM, 133–136

Integral, 623  
calculus, 623–627  
evaluation by parts, 623  
evaluation techniques, 623  
table of, 623–627

Integrate-and-dump filter, 434–437

Integrated service digital network (ISDN), 543–547

Intelligent time-division multiplexer, 200

Intercarrier signal, 594

Intercept point, 249–250

Interface  
Centronics, 683, 685–686  
IEEE-488, 683, 687–688  
RS-232C, 680–683  
RS-422A, 680–683  
RS-449, 680–683  
RS-530, 680–683  
X.25, 691–692  
*See also* Data link control  
*See also* ISDN  
*See also* Standards

Interference, 283

Interlacing, television, 590, 605, 608

Interleaving, code, 23–24

Intermediate frequency (IF), 279–282

Intermodulation:

distortion, 248–250  
interference, 283

International Telecommunications Union (ITU), 10

Internet:  
ftp files, 7  
world wide web page, xix

Intersection of sets, 636

Intersymbol interference (ISI), 176–185

Intrinsic impedance, 562

Ionospheric scatter propagation, 15

IQ detector, 282

Iridium satellite system, 560

IS-54 cellular telephone standard, 587

IS-95 cellular telephone standard, 587

ISDN, 543–547  
broadband, 543  
narrowband, 543–547  
NT1, NT2, 544–547  
S interface, 544–547  
T interface, 544–547  
U interface, 544–547  
2B1Q line code, 545–546

ISO OSI computer network model, 686–690

ISO standard organization, 678, 686

Isotropic radiation, 561

**J**

Jacobian, 667

Joint:  
CDF and PDF, 663, 665  
mean, 665  
probability, 637,  
stationary process, 388

**K**

Kronecker delta function, 65–66

**L**

L'Hospital's rule, 623

LAN, 700

Laplacian distribution, 524

Laser diode, fiber optic, 580

LC filter, 243–244

Leakage, discrete Fourier transform, 96

Learning sequence, 178

Leased line, 700

Leibniz's rule, 622

Light-emitting diode (LED), fiber optics, 580

Limiter, 252–253, 284

Line coding, 157–159, 545–546

Line coding (*cont.*)  
advantages and disadvantages, 159  
power spectral density, 159–166  
spectral efficiency, 176, 350  
T1-carrier, 208  
T1G-carrier, 209  
2B1Q, 545–546

Line resolution, television, 591–593, 605, 608

Line spectra (delta functions), 73–78

Line-of-sight propagation, 14–15

Linear:  
amplifier, 246–247  
distortion, 83  
modulation, 231–232  
operator, 36  
system, 78

Linear filter, 78–85  
*See also* Filter

Linear systems:  
AM to PM conversion, 237  
amplitude response, 80  
autocorrelation of output, 407  
convolution integral, 79  
cross PSD of outputs, 408  
crosscorrelation of outputs, 408  
distortionless transmission, 83–84, 238–240  
impulse response, 79, 81  
output, 79  
phase response, 80  
PM to AM conversion, 237  
power transfer function, 81, 407  
PSD of output, 407  
random processes, 406–411  
spectrum of output, 80  
time-invariant, 78  
transfer function, 80  
with sinusoidal inputs, 80

Link budget, 572–582  
Carrier-to-noise (CNR), 572–574  
fiber optic, 581–582  
satellite, 575–580, 609–611

List of symbols, xxi–xxv

Loading coils, 209

Loading factor, companding, 148

Local area network, 684–685, 688

Local loop (telephone), 536–540, 543

Look angles to satellite, 576

Loop, *See* Phase-locked loop

Loss:  
free space, 563, 574  
multipath, 612

Low Earth orbit (LEO) satellites, 559–560

Low frequency (LF), 11

Low probability of intercept (LPI), 357

Lower single sideband (LSSB), 305

Luminance signal, television, 598

M-ary phase-shift keying (MPSK), 345–346

M-sequence waveform, 360–361

Magnitude response, linear system, 80

Magnitude spectrum, 44  
*See also* Spectrum

Manchester signaling, 157–158, 165

Marginal PDF, 664

Mark (binary signaling), 157, 339, 340

Mastergroup FDM signal, 534–536

Matched filter, 430–441  
colored noise case, 464–465  
correlation processing, 437–438  
integrate-and-dump, 434–437  
transfer function, 431  
transversal, 438–441  
white noise case, 433–448

Math tables, 620–633

MathCAD, 7  
DFT, 94  
ftp files, 7

MATLAB, 7  
binary signaling, 153  
DFT, 94, 98–99, 102–104  
FFT example, 98, 102  
filter response, 517–520  
ftp files, 7  
multilevel signaling, 156

Matrix, covariance, 414

Maximal-length codes, 21, 360–361

MC145472 ISDN U transceiver, 544–545

MC145474 ISDN S/T interface, 544–545

MC14554 telephone codec, 544–545

Mean value, 647, 665  
*See also* DC value

Measure, information, 16

Measurement of PSD, 403–404

Mechanical filter, 243–244

Median (statistics), 648

Medium attachment unit (MAU), 685

Medium Earth orbit (MEO) satellites, 559–560

Medium frequency (MF), 11

Message switching, 700

Microwave bands, 11–12

Millimeter band, 12

Minimum-shift keying (MSK), 352–357  
FFSK, 353  
probability of bit error, 486  
Type I, 353  
Type II, 353

Mixed distributions, 644

Mixer, 253–259  
audio, 255  
double balanced, 258  
output, 284

Mixer (*cont.*)  
 single balanced, 257  
 unbalanced, 257

Mobile radio:  
 cellular telephone, 582–589  
 FM, 330

Mobile telephone switching office (MTSO), 584

Mode (statistics), 648

Model:  
 communication system, 8  
 OSI computer network, 686–690

Modem, 693–698, 701  
 Bell 103, 339–342, 695, 780  
 Bell 202, 695  
 Bell 212A, 694, 695  
 standards, 693–698  
 V.22 bis, 347, 695  
 V.32, 696  
 V.32 bis, 697  
 V.33, 697  
 V.34, 693

Modified Bessel function, 455, 478

Modulation, 9  
 AM, 231–232, 296  
 complex envelope, 229–233  
 definition, 227, 229–233

DM, 189–196

DPCM, 185–188

DSB-SC, 302

efficiency, 292–299

FM, 311–326

negative AM, 297

PAM, 128–136

PCM, 136–148

percent AM, 297

PM, 311–326

positive AM, 297

PWM and PPM, 209–213

spectrum, 230–233

SSB-SC, 304–308

VSB, 308–311

*See also* Digital signaling

Moments:  
 mean, 647  
 one-dimensional, 647  
 r-th moment, 647  
 standard deviation, 647  
 two-dimensional, 665  
 variance, 647

Motion pictures experts group (MPEG), 607

Moving average (MA) estimation, 404

MTS stereo sound, 596

Multichannel television sound (MTS), 596

Multilevel signaling, 154–156  
 bandpass, 345–346  
 baseband, 154–157, 173–175

T1G-carrier, 209

Multimodal fiber optics, 580

Multipath propagation, 9, 612

Multiple access, 553–560  
 code division, 357, 554  
 demand assigned, 553, 555–557  
 fixed assigned, 554  
 frequency division, 554  
 time-division, 553, 557–559

Multiplexing  
 code division, 357, 554  
 frequency division, 326–328  
 time-division, 196–209, 534, 548–549

Multiplier:  
 four-quadrant, 256, 258  
 frequency, 259–261, 284  
 mixer, 253–259  
 product detector, 262–264, 423  
 single-quadrant, 256  
 two-quadrant, 256

Multipoint line, 701

Multivariate:  
 functional transformation, 666–667  
 statistics, 663–670

Mutually exclusive, 637

**N**

N-dimensional:  
 Gaussian PDF, 414  
 statistics, 663–670

N-order stationarity, 383

Narrowband angle modulation, 321–322

Narrowband ISDN, 543

Narrowband noise process, 418–430  
 properties of, 421–424

National Television System Committee (NTSC), 597

Nats, 16

Natural sample PAM, 129–133

Negative amplitude modulation, 297

Network, linear, 78–85

Noise:  
 available power, 564  
 bandpass, 418–430  
 bandwidth, 103, 411  
 definition, 33  
 effective input-noise temperature, 568  
 envelope-phase representation, 228, 428–430  
 equivalent bandwidth, 103, 411  
 eye pattern, 167–168  
 granular, 190–193  
 interference, 283  
 PCM, 143–148  
 power available, 564  
 quadrature-component representation, 229, 418–428

Noise (*cont.*)  
 quantizing, 137 ~  
 slope overload, 190–193  
 source temperature, 564  
 sources, 563–565  
 thermal, 563–564  
 white, 402, 417

*See also* Distributions  
*See also* Random processes  
*See also* Signal-to-noise

Noise figure:  
 attenuator, 571  
 average, 567  
 cascaded devices, 571  
 spot, 566  
 transmission line, 570

Noise reduction, Dolby and DBX, 329–332

Noise temperature, 563, 568–569  
 system, 574

Noncoherent detector, 264

Nonlinear:  
 amplifier, 247–252  
 channel, 283  
 distortion, 247–252

Nonreturn-to-zero signal, 157–158

Nonuniform quantizing, 146–148

Normalized covariance, 665

Normalized orthogonal functions, 66

Normalized power, 39, 405  
 bandpass signal, 233

North American TDM hierarchy, 203–204

NRZ signal, 157–158

NT1/2 ISDN network termination, 544–545

Null event, 637

Null-to-null bandwidth, 103

Numeric assignment module (NAM), 586

Numerical computation of PSD, 403–404

Nyquist filter, 182–184

Nyquist frequency, 88

Nyquist's:  
 first method (zero ISI), 179–180  
 second method, 184

**O**

Odyssey satellite system, 560

Offset quadrature phase-shift keying (OQPSK), 348

On-off keying (OOK), 332–336  
 bandwidth, 334  
 coherent detection, 470–472  
 detector, 335  
 fiber optics, 580

FT-2000 fiber optic system, 581–582

noncoherent detection, 477–480

probability of bit error, 471–472, 480

PSD, 333

One-sided delta function, 630

One-sided spectrum, 72

Open system interconnection (OSI) model, 686–690

Operator:  
 absolute value, 44  
 angle, 43, 71  
 conjugate, 46  
 convolution, 58  
 ensemble average, 646  
 Fourier transform, 44  
 Hilbert transform, 305, 629  
 imaginary part, 71  
 linear, 36, 78  
 real part, 71  
 time average, 35

Optimum code performance, 24–30

Optimum digital receivers  
*See also* Digital receivers

Optimum modulation, 515

Orthogonal:  
 FSK, 476, 352  
 functions, 65  
 random processes, 389  
 random variables, 665  
 series, 67

Orthonormal functions, 65

Oscillator:  
 DDS, 276–277  
 synchronization, 274  
 voltage-controlled, 269

Overload, receiver, 283

**P**

Packet data transmission, 559, 563, 701

Packet switching, 701

Packet transmission  
 ATM, 692  
 X.25, 691

Paley-Wiener criterion, 79

Parallel ADC, 140–141

Parity:  
 bits, 21  
 check, 701  
 CRC, 699

Parseval's theorem, 47

Pascal's triangle, 651

Path loss:  
 free space, 563, 574  
 multipath, 612

Peak envelope power (PEP), 234  
 AM signal, 298–299  
 SSB signal, 307

Peak frequency deviation, 314

Percent amplitude modulation, 297  
**Performance:**  
 analog systems, 511–515  
 coding, 24–30  
 digital systems, 488  
 ideal system, 26–27, 514  
 measures of, 458  
**Periodic:**  
 signal spectra, 73–78  
 waveform, 36  
**Periodogram,** 404  
**Personal communication systems:**  
 satellites, 559–560  
 wireless, 611–614  
**Personal computer solutions,** 7  
**Phase:**  
 peak deviation, 315  
 response, 80  
 spectrum, 44  
**Phase delay,** 239  
**Phase detector:**  
 sawtooth characteristic, 270–271  
 sinusoidal characteristic, 263, 270–271  
 triangle characteristic, 270–271  
**Phase error, PLL,** 272  
**Phase modulation (PM),** 311–326  
 circuit, 313  
 complex envelope, 231–232, 311  
 index, 315  
 signal-to-noise, 501–504  
*See also* Phase-shift keying  
**Phase reversal-keying (PRK),** *See* Binary phase-shift keying  
**Phase shift keying:**  
*See* Binary phase shift keying  
*See* Differential phase-shift keying  
*See* M-ary phase shift keying  
*See* Quadrature phase-shift keying  
**Phase spectrum,** 44  
**Phase-locked loop (PLL),** 269–276  
 analog, 270  
 as a tracking filter, 269  
 Costas, 303–304  
 digital, 270  
 for carrier synchronization, 337, 489  
 for coherent AM detection, 275–277  
 for FM or PM demodulation, 274–275  
 for frequency synthesizer, 276  
**Phasor,** 43  
**Physically realizable waveform,** 34–35  
**Picket-fence effect, DFT,** 96  
**Pilot signal,** 326–327, 596  
**PIN diode,** 580  
**Plank's constant,** 564  
**PM to AM conversion,** 237  
**Point distributions,** 642

**Poisson distribution,** 652  
**Polar Fourier series,** 71–73  
**Polar signaling,** 157–158, 163  
 probability of bit error, 467–468  
 spectrum, 163  
**Polling,** 701  
**Positive amplitude modulation,** 297  
**Power:**  
 AM signal, 238, 298  
 average, 37, 63, 405  
 bandpass signal, 233  
 decibel value, 42  
 instantaneous, 37  
 normalized, 39  
 peak envelope, 234  
 random process, 405  
 thermal noise, 563–564  
**Power bandwidth,** 105  
**Power density,** 562  
**Power efficiency,** 299–301  
**Power gain, available,** 566, 571  
**Power signal,** 35, 40  
**Power spectral density (PSD),** 62, 392  
 ASK, 333  
 bandpass process, 421–422  
 bandpass signal, 233  
 baseband digital signals, 399, 400  
 bipolar RZ signal, 164  
 BPSK, 337  
 condition for discrete spectra, 402  
 cross spectrum, 408  
 deterministic, 62  
 filter output, 408  
 FM noise, 503, 505  
 for white process, 402, 417  
 FSK, 343–344  
 line codes, 159–166  
 Manchester NRZ signal, 165  
 measurement of, 403–404  
 MPSK, 349–350  
 MSK, 355  
 multilevel signal, 175, 349–350  
 numerical computation, 403–404  
 periodic waveforms, 76  
 PM noise, 502–503  
 polar NRZ signal, 163  
 properties of, 395  
 QAM, 349–351  
 random processes, 391–404  
 spread spectrum, 361  
 thermal noise, 564  
 unipolar NRZ signal, 160–163  
 unipolar RZ signal, 162–164  
 WBFM, 323  
**Wiener-Khintchine theorem,** 392–394  
*See also* Spectrum

**Power transfer function,** 81, 407  
**Prediction filter, DPCM,** 185  
**Preemphasis and deemphasis in FM,** 325–326, 509–511  
**Preface, xvii–xx**  
**Prewhitening filter,** 464–465  
**Primary rate ISDN,** 543  
**Priori probabilities,** 461  
**Probability,** 636  
 conditional, 638  
 joint, 637  
 relative frequency, 636  
 simple, 636  
*See also* Distributions  
**Probability density function (PDF),** 640, 663  
 central limit theorem, 669  
 conditional, 664  
 discrete distribution, 641, 644  
 for envelope detector output, 429–430  
 for phase detector output, 429–430  
 for quadrature detector outputs, 428–430  
 for sum of two random variables, 669  
 joint, 664  
 marginal, 664  
 measurement of, 645  
 N-dimensional, 664, 383  
 properties of, 642, 663–664  
 table of, 650  
*See also* Distributions:  
**Probability distribution function**  
*See* Cumulative distribution function  
**Probability of bit error,** 9, 25, 459–488  
 bipolar signal, 468–470  
 BPSK, 472–473  
 BPSK with coding, 26, 28  
 calculation of, 459–488  
 comparison of systems, 487–488, 516–523  
 DPSK, 484  
 for additive Gaussian noise, 461–488  
 FSK, coherent detection, 474–476  
 FSK, noncoherent detection, 482  
 matched filter detection, 463–465  
 MSK, 486  
 OOK, coherent detection, 471–472  
 OOK, noncoherent detection, 480  
 optimum coding, 26–27  
 polar signal, 467–468  
 QPSK, 484  
 repeaters, 170  
 Shannon's limit, 27  
 unipolar signal, 465–467  
 with coding, 26, 28  
**Probability of error:**  
 Shannon's limit, 27  
*See also* Probability of bit error  
**Probability of false frame sync,** 198  
**Processing gain, spread spectrum,** 364  
**Product detector,** 262–264, 423  
 output, 284  
 random processes, 421–422  
**Professional carrier, television,** 596  
**Propagation:**  
 ground wave, 12–13  
 line-of-sight (LOS), 14–15  
 radio frequency, 10–16  
 sky-wave, 14  
**Properties:**  
 autocorrelation function, 387  
 bandpass random processes, 421–422  
 block codes, 21, 28  
 CDF, 642, 663–664  
 crosscorrelation function, 388  
 Dirac delta function, 630–631  
 Fourier series, 69–70  
 Fourier transform, 46–47  
 Gaussian random process, 415  
 PDF, 642, 663–664  
 power spectral density, 395  
 Q(z) function, 632  
 waveforms, 34  
**Protocol:**  
*See* Computer communications  
*See also* Data link control  
**Pseudonoise (PN) code,** 358–361  
**Pseudoternary signal,** 158, 164  
**Public switched telephone networks (PSTN),** 534, 548–549  
**Pull-in range, PLL,** 270, 273  
**Pulse amplitude modulation (PAM),** 128–136  
 flat-top, 133–136  
 instantaneous sampling, 133–136  
 natural sampling, 129–133  
**Pulse aperture,** 135  
**Pulse code modulation (PCM),** 136–148  
 bandwidth, 141–143  
 differential, 185–188  
 eye pattern of, 167–168  
 probability of bit error, 459–488  
 PSD of, 159–166  
 SNR, 143–148, 490–495  
 T1 PCM system, 205–209  
*See also* Time-division multiplexing  
**Pulse dialing,** 537–539  
**Pulse duration modulation (PDM)**  
*See* Pulse width modulation (PWM)  
**Pulse position modulation (PPM),** 209–213  
**Pulse resolution for no ISI,** 176–185  
**Pulse time modulation,** 209–213  
**Pulse width modulation (PWM),** 209–213  
 for generating high power AM, 299–301  
**Punched tape,** 157

## Index

231, 278, 282  
on for, 632  
55  
DF, 655  
6  
f, 632  
1, 656  
or, 242–243  
plitude modulation (QAM), 346–351  
49–350  
plitude-shift keying  
ture amplitude modulation (QAM)  
M detector, 266–268  
ourier series, 70–71  
odulation:  
ion, 597–600  
velope, 231–232  
351  
hase-shift keying (QPSK), 345–346  
of bit error, 484  
49–350  
, 348  
, 28  
hase component, 245, 231, 278, 282  
andom process, 418–428  
492  
, 146–148  
7, 492  
ct, FM systems, 502  
11  
istance, 569  
nny:  
–246  
propagation, 10–16  
e-rolloff filter, 180–184  
g-to-digital converter (ADC), 140–141  
cesses:  
wer, 405  
418–430  
231, 575–590, 600–611

## Index

ergodic, 386  
Gaussian, 413–417  
orthogonal, 389  
power spectral density, 391–404  
rms value, 405  
single sideband, 423–424  
stationary, 383  
strict-sense stationary, 383  
through linear systems, 406–411  
uncorrelated, 389  
white, 402, 417  
wide-sense stationary, 387  
Random start-up phase, 420  
Random variables:  
average value of, 646, 663  
CDF of, 639, 663  
central limit theorem, 669  
continuous, 642  
definition, 639  
functional transformation, 658, 666–667  
independent, 664  
N-dimensional, 664, 383  
PDF of, 640, 663  
sum of, 667–668  
*See also* Distributions  
Random waveform, 6, 382–383  
Raster scanning, 589  
Rate:  
baud, 150, 173  
bit, 150, 173  
code, 20  
information, 18  
source, 18  
Rayleigh PDF, 429–430, 477–478  
RC low-pass filter, 81–82, 409  
autocorrelation and PSD, 409  
equivalent bandwidth, 413  
output SNR, 410  
Received power, 562  
Received signal plus noise, 241–242  
Receiver, 8, 279–283  
black-and-white television, 595  
color television, 601  
direct-conversion, 280  
dual-conversion, 279  
fiber optic, 580  
FMFB, 508–509  
general, 279–283  
interference, 283  
overload, 283  
Receiver (*cont.*)  
TRF, 279  
*See also* Digital receivers  
*See also* Probability of bit error  
*See also* Signal-to-noise ratio  
Rectangular pulse:  
definition, 54  
spectrum, 54–55  
Reed-Solomon codes, 21, 28  
References, 703–713  
Regenerative repeater, *See* Repeater  
Relative frequency (probability), 636  
Remote (telephone) terminal (RT), 540–541  
Repeater, 168–170  
BER, 170  
Response:  
amplitude, 80  
frequency, 80  
image, 280–282  
impulse, 79, 81  
phase, 80  
Return-to-zero (RZ) signal, 157  
Reverse channel, 701  
Rician PDF, 455, 478  
Riemann-Lebesque lemma, 476  
Right-hand continuous, 642  
Ring (telephone) lead, 537  
Ringer equivalence number (REN), 539  
Rms bandwidth, 411  
Rms value, 39, 405  
RS-232C interface, 680–683  
RS-422A interface, 680–683  
RS-449 interface, 680–683  
RS-530 interface, 680–683  
Rth moment, 647  
RTS (request to send), 682, 701  
RZ signal, 157

## S

S interface, ISDN, 544–547  
Sa(x) function, 54, 56  
spectrum of, 55, 56  
table of, 631  
Sample space, 635–636  
Sampling theorem, 86–89  
bandpass, 240–241  
flat-top, 133–136  
three realizations, 287  
Satellite communications, 547–560, 575–580  
data transmission, 553–560

Hughes HS601, 551  
Immarstat, 560  
Iridium, 560  
link budget, 575–580, 609–611  
look angles, 576  
low Earth orbit (LEO), 559–560  
medium Earth orbit (MEO), 559–560  
Odyssey, 560  
packet transmission, 559  
satellite-switched TDMA (SS-TDMA), 554  
telephone transmission, 554–557, 559–560  
television transmission, 551–553, 575–580  
VSAT, 559  
Scatter propagation, 15  
Schwarz's inequality, 432  
proof of, 443–445  
Scrambling, 23–24  
SDLC protocol, 690  
Second audio program (SAP), television, 596  
Sequential code, 677  
Serial ADC, 140–141  
Series:  
cardinal, 87  
Fourier, 68–78  
orthogonal, 67  
table of, 627–628  
Taylor, 65  
Set, 635  
Shannon channel capacity, 18, 26, 514  
Shift-register sequences, 358–361  
Sifting property, 51  
Signal:  
antipodal, 459  
asynchronous, 200  
balanced, 683  
bandpass, 226–229  
baseband, 127–225  
chrominance, television, 598  
definition, 33  
deterministic, 6  
digital formats, 157–159  
energy, 35, 40  
fiber optic, 580–582  
image, 280–282  
luminance, television, 598  
modem, 693–698  
multilevel, 174  
periodic, 36  
phasor, 43  
pilot, 326–327, 596  
power, 35, 40

## Index

ope, 496

98

74

, 524

7

C), 555

SSB-EV, 231–232  
 SSB-FM, 231–232  
 SSB-PM, 231–232  
 SSB-SQ, 231–232  
 Weaver's method, 371  
 Single-balanced mixer, 257  
 Single-mode fiber optics, 580  
 Single-quadrant multiplier, 256  
 Sinusoidal, phasor notation, 43  
 Sinusoidal distribution, 657  
 Sky noise temperature, 578  
 Sky-wave propagation, 14  
 Slant range, satellite, 576  
 SLC-96 remote terminal, 542  
 Slicing level, 209, 701  
 Slope detector, 264, 266  
 Slope overload noise, DM, 190–193  
 Soft decision, 23, 28  
 Softwire channel, 8  
 SONET, 208  
 Source, 2  
 Source coding, 8  
 Source rate, 20  
 Source statistics, 461  
 Space (binary signaling), 157, 339, 340  
 SPADE system, 554–557  
 Spectral efficiency:  
     bandpass digital signals, 350–351, 357  
     multilevel signal, 176, 350–351  
     TCM, 27–30  
 Spectrum:  
     AM signal, 235, 298  
     amplitude, 44, 80  
     analyzers, 44, 403–404  
     bandpass signal, 230–233  
     current, 43  
     definition, 44  
     dirac delta function, 61  
     DSB-SC signal, 303  
     energy, 48  
     FM signal, 315–320  
     folded, 91  
     frequency variable, 44, 312  
     line, 73–78  
     magnitude, 44  
     MATLAB, 94–101  
     NBFM, 321–322  
     one-sided, 72  
     PAM, 130, 134  
     periodic waveform, 73–78

## Index

Spectrum (*cont.*)  
     television, 594, 604, 606  
     triangular pulse, 57  
     two-sided, 44  
     unit step, 61  
     voltage, 43  
     VSB signal, 310  
     *See also* Power spectral density  
 Speech coding, 194–196  
     cellular telephone, 558–559  
 Split-phase coding, 158, 165  
 Spot effective input-noise temperature, 568  
 Spot noise figure, 566  
 Spread spectrum (SS), 357–366  
     direct sequence, 358–364  
     effect of interference, 364  
     frequency hopping, 364–366  
     hybrid, 358  
     overlay, 364  
     PN sequence, 358–364  
     response to noise, 364  
     spreading signal, 358  
 Square-law bit synchronizer, 171  
 Squaring loop, 304  
 Standard deviation, 647  
 Standards:  
     AM broadcast, 301  
     CATV, 606  
     CCITT V.24 interface, 680–683  
     cellular telephone, 585–587  
     Centronics interface, 683, 685–686  
     computer communications, 677–702  
     Ethernet, 688  
     FM broadcast, 329–330  
     frequency allocations, 11–12  
     HDTV, 608  
     IEEE 802.3, 684–685, 688  
     IEEE-488 interface, 683, 687–688  
     intermediate frequencies, 282  
     ISDN, 543–547  
     ISO OSI model, 686–690  
     modems, 693–698  
     RS-232C interface, 680–683  
     RS-422A interface, 680–683  
     RS-449 interface, 680–683  
     SONET, 208  
     telephone, 203–209, 543–547  
     television, 592, 605–608  
     10base-T, 688  
     10base2, 688  
     10base5, 688  
     *See also* Modems

strict sense, 383  
 wide sense, 387  
 Statistical averages. *See* Ensemble average  
 Statistical independence, 638, 664  
 Statistical time-division multiplexer, 200, 701  
 Statistics:  
     bivariate, 665  
     N-dimensional, 663–670  
     one-dimensional, 639–649  
 Step size, delta modulation, 192  
 Stereo sound:  
     AM broadcasting, 302  
     Dolby & DBX noise reduction, 329–332  
     FM broadcast, 326–328  
     television, MTS, 596  
 Store and forward, 702  
 Stored program control, 542  
 Strict-sense stationary, 383  
 Stuff bits, 201  
 Subscriber (telephone) loop:  
     analog, 536–543  
     digital, 543–547  
 Successive approximation ADC, 140–141  
 Super high frequency (SHF), 11  
 Supergroup FDM signal, 534–536  
 Superheterodyne receiver, 279–283  
 Suppressed carrier, 302–303  
 Sure event, 637  
 Surface acoustic wave (SAW) filter, 244–245  
 Switched digital video, 547  
 Switched line, 702  
 Switching detector, FM stereo, 376  
 Switching modulator, 257–258  
 Synchronization  
     bit, 170–173, 489  
     carrier, 427  
     digital receivers, 489  
     frame or word, 196–200, 489  
     oscillator, 274  
     television, 591, 601, 605, 608  
 Synchronous detector, 262–264  
 Synchronous digital line, 200  
 Synchronous orbit, 547  
 Synchronous transmission, 702  
 Systematic block code, 21  
 Systems:  
     analog, 5  
     cellular telephone, 582–589  
     communication, 2, 8–9, 227–230  
     computer, 677–702  
     digital, 2

## Index

ature, 574.  
*See* Power spectral density  
 Telecommunication systems, 534–549  
 Telephone:  
   analog subscriber line, 536–543  
   analog switching, 542  
   caller ID, 539  
   capacities of PSTN, 547–549  
   cellular, 582–589  
   central office, 536–543  
   digital subscriber line, 543–547  
   digital switching, 542  
   DS type line standards, 203–204  
   FDM hierarchy, 535  
   hybrid, 540, 541, 562, 700  
   ISDN, 543–547  
   remote terminal, 540–541  
   ringer equivalence number (REN), 539  
   SLC-96, 542  
   SONET, 208  
   standards, 539  
   TDM hierarchy, 203–209  
   tip and ring, 537  
   TSI switching, 542  
   T1 PCM system, 205–209  
   via fiber optic cable, 580–582  
   via satellite, 554–560  
 Television, 589–609  
   black and white, 589–595  
   channels, 604, 606  
   chrominance signal, 598  
   color, 596–601, 605, 608  
   high-definition (HDTV), 605–609  
   line resolution, 591–593, 605, 608  
   luminance signal, 598  
   MTS stereo sound, 596  
   standard definition (SDTV), 607–609  
   standards, 592, 605, 608  
   switched digital video, 547  
   TVRO satellite terminal, 575–580, 609–611  
   vectorscope, 600  
   via satellite, 551–553, 575–580  
   waveform, sync pulses, 602  
 Temperature:  
   noise, 568  
   sky noise, 578  
 Test statistic, 460  
 Theorem  
   bandpass dimensionality, 241  
   bandpass sampling, 240–241  
   Bayes, 638  
   central limit, 669  
   dimensionality, 92  
   Euler's, 620  
   Fourier transforms, 50  
   Parseval's, 47  
   sampling, 86–87

## Index

Theorem (*cont.*)  
   sampling, 287  
   Shannon channel capacity, 18  
   Wiener-Khintchine, 63, 392  
 Theory of distributions, 51  
 Thermal noise, 563–564  
 Third-order distortion, 249–250  
 Three-decibel bandwidth, 101  
 Threshold extension for FM, 579–580  
 Time average operator, 35  
 Time-division multiple access (TDMA), 553, 557–559  
 Time-division multiplexing (TDM), 196–209, 534,  
   548–549  
   bandpass systems, 534, 548–549  
   bit interleaved, 200  
   CCITT hierarchy, 207  
   character interleaved, 200  
   North American hierarchy, 203–204  
   SONET, 208  
   stuff bits, 200  
 Time-invariant system, 78  
 Time-slot-interchange switching, 542  
 Timing, eye pattern, 167–168  
 Tip (telephone) lead, 537  
 Token bus, 702  
 Total harmonic distortion, 248  
 Touch-tone (telephone), 539  
 Tracking filter, PLL, 269  
 Transfer function:  
   linear system, 80  
   matched filter, 431  
   power, 81  
   RC filter, 81  
   voltage, 80  
 Transform:  
   DFT, 93–101  
   Fourier, 44  
   Hilbert, 305, 629  
 Transformation:  
   N-dimensional PDF, 666–667  
   one-dimensional PDF, 658  
 Transition probabilities, 525  
 Transmission line:  
   effective input-noise temperature, 570  
   filter, 244–245  
   noise figure, 570  
 Transmission, free space, 562  
 Transmitters, 8, 277–279  
   AM, 299–301  
   FM, 367, 373  
   SSB, 307  
   VSB, 309  
   *See also* Digital signaling  
 Transponder, 550  
 Transversal filter:  
   for DPCM, 185  
   matched, 438–441  
 Tree codes, 22, 25  
 Trellis-coded modulation (TCM), 27–30  
 TRF receiver, 279  
 Triangular pulse:  
   definition, 54  
   spectrum, 57  
 Trigonometry:  
   definitions, 620  
   identities, 620–621  
 Tripler stage, 261  
 Tropospheric scatter, 15  
 Trunked mobile radio, 583  
 Turnabout time (modem), 702  
 TVRO terminal, 575–580, 609–611  
 Two-quadrant multiplier, 256  
 Two-sided spectrum, 44  
 Two-tone test, 248–250  
 Two-way FM radio, 330  
   *See also* Cellular telephone, 582–589  
 Two-wire circuit, 536, 540  
 T1 PCM system, 205–209  
 T1G PCM system, 209

## U

U interface, ISDN, 544–547  
 UART, 141  
 Ultra high frequency (UHF), 11  
 Unbalanced mixer, 257  
 Unbalanced QPSK, 348  
 Unbalanced signaling, 683  
 Uncorrelated:  
   random processes, 389  
   random variables, 665  
 Uniform:  
   distribution, 652  
   PDF, 652  
   quantizer, 137  
 Union of sets, 636  
 Unipolar signal, 157–158, 161, 163  
   probability of bit error, 465–467  
   spectrum, 160–163  
 Unit step function:  
   definition, 51  
   spectrum, 61  
 Up converter, 253–259, 284  
   output, 284  
 Upper single sideband (USSB), 304  
 USART, 141

## V

V.22, 694  
 V.22 bis, 695

2, 696  
 2 bis, 697  
 3, 697  
 4, 693  
 ue:  
 c, 36, 405  
 ms, 39, 405  
 iable, random, 639, 663  
 iance, 647  
 :tor:  
 asis, 67, 150  
 hasors, 43  
 epresentation of waveforms, 150–152

:torscope, 600  
 in diagram, 635  
 critical resolution, television, 592, 605, 608  
 ry high frequency (VHF), 11  
 ry low frequency (VLF), 11  
 ry small scale aperture terminals (VSAT), 559  
 stigial sideband (VSB), 308–311, 593, 608  
 (voice frequency), 203, 540, 702  
 erbi decoding, 23  
 coders, 194  
 cellular telephone, 558–559  
 itage spectrum, 43  
 itage-controlled oscillator (VCO), 269

**W**

iveform:  
 analog, 5  
 bandlimited, 86  
 bandpass, 226–229  
 baseband, 227  
 deterministic, 6

device output, 284  
 digital, 5  
 dimensions, 91, 149–152  
 energy, 35, 40  
 m-sequence, 360–364  
 monitor, television, 589  
 noise, 33  
 periodic, 36  
 physically realizable, 34  
 power, 35, 40  
 random, 6, 382–383  
 signal, 33  
 Waveform coders, 194  
 Waveform monitor, 589  
 White Gaussian noise, 417  
 White noise process, 402, 417  
 Wide-sense stationarity, 387  
     properties of, 387  
 Wideband frequency modulation (WBFM), 322–324  
 Wiener-Khintchine theorem, 63, 392  
 Windowed waveform, 94  
 Wireless communications, 559–560, 611–614  
 Word synchronization, 196–200, 489

**X**

X.25 interface, 691–692

**Z**

Zero-crossing bandwidth, 103  
 Zero-crossing detector, 268–269  
 Zero-padding, 96  
 2B1Q line code, 545–546